frontiers | Research Topics

Immunotherapy with checkpoint inhibitors for non-small cell lung cancer, colon cancer and esophageal cancer

Edited by
Xuelei Ma, Hubing Shi, Udo S. Gaipl and Benjamin Frey

Published in
Frontiers in Immunology
Frontiers in Oncology

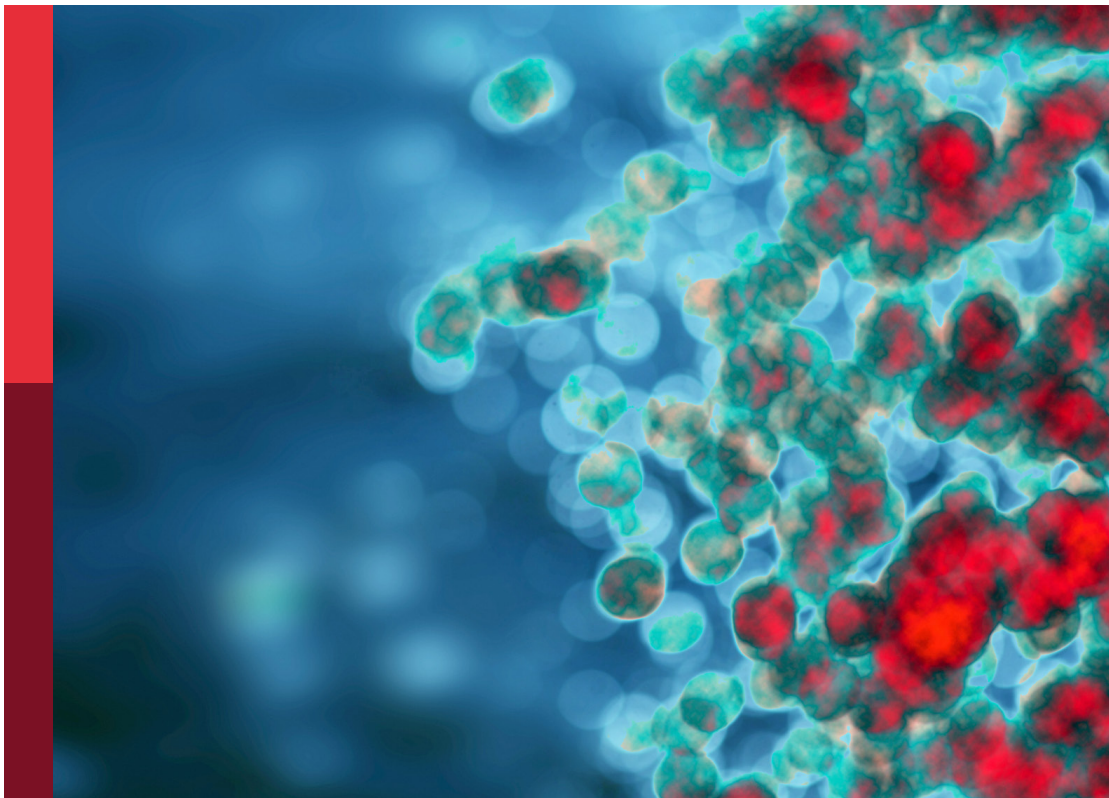

FRONTIERS EBOOK COPYRIGHT STATEMENT

The copyright in the text of individual articles in this ebook is the property of their respective authors or their respective institutions or funders. The copyright in graphics and images within each article may be subject to copyright of other parties. In both cases this is subject to a license granted to Frontiers.

The compilation of articles constituting this ebook is the property of Frontiers.

Each article within this ebook, and the ebook itself, are published under the most recent version of the Creative Commons CC-BY licence. The version current at the date of publication of this ebook is CC-BY 4.0. If the CC-BY licence is updated, the licence granted by Frontiers is automatically updated to the new version.

When exercising any right under the CC-BY licence, Frontiers must be attributed as the original publisher of the article or ebook, as applicable.

Authors have the responsibility of ensuring that any graphics or other materials which are the property of others may be included in the CC-BY licence, but this should be checked before relying on the CC-BY licence to reproduce those materials. Any copyright notices relating to those materials must be complied with.

Copyright and source acknowledgement notices may not be removed and must be displayed in any copy, derivative work or partial copy which includes the elements in question.

All copyright, and all rights therein, are protected by national and international copyright laws. The above represents a summary only. For further information please read Frontiers' Conditions for Website Use and Copyright Statement, and the applicable CC-BY licence.

ISSN 1664-8714
ISBN 978-2-83250-915-9
DOI 10.3389/978-2-83250-915-9

About Frontiers

Frontiers is more than just an open access publisher of scholarly articles: it is a pioneering approach to the world of academia, radically improving the way scholarly research is managed. The grand vision of Frontiers is a world where all people have an equal opportunity to seek, share and generate knowledge. Frontiers provides immediate and permanent online open access to all its publications, but this alone is not enough to realize our grand goals.

Frontiers journal series

The Frontiers journal series is a multi-tier and interdisciplinary set of open-access, online journals, promising a paradigm shift from the current review, selection and dissemination processes in academic publishing. All Frontiers journals are driven by researchers for researchers; therefore, they constitute a service to the scholarly community. At the same time, the *Frontiers journal series* operates on a revolutionary invention, the tiered publishing system, initially addressing specific communities of scholars, and gradually climbing up to broader public understanding, thus serving the interests of the lay society, too.

Dedication to quality

Each Frontiers article is a landmark of the highest quality, thanks to genuinely collaborative interactions between authors and review editors, who include some of the world's best academicians. Research must be certified by peers before entering a stream of knowledge that may eventually reach the public - and shape society; therefore, Frontiers only applies the most rigorous and unbiased reviews. Frontiers revolutionizes research publishing by freely delivering the most outstanding research, evaluated with no bias from both the academic and social point of view. By applying the most advanced information technologies, Frontiers is catapulting scholarly publishing into a new generation.

What are Frontiers Research Topics?

Frontiers Research Topics are very popular trademarks of the *Frontiers journals series*: they are collections of at least ten articles, all centered on a particular subject. With their unique mix of varied contributions from Original Research to Review Articles, Frontiers Research Topics unify the most influential researchers, the latest key findings and historical advances in a hot research area.

Find out more on how to host your own Frontiers Research Topic or contribute to one as an author by contacting the Frontiers editorial office: frontiersin.org/about/contact

Immunotherapy with checkpoint inhibitors for non-small cell lung cancer, colon cancer and esophageal cancer

Topic editors

Xuelei Ma — Sichuan University, China
Hubing Shi — Sichuan University, China
Udo S. Gaipl — University Hospital Erlangen, Germany
Benjamin Frey — University Hospital Erlangen, Germany

Citation

Ma, X., Shi, H., Gaipl, U. S., Frey, B., eds. (2022). *Immunotherapy with checkpoint inhibitors for non-small cell lung cancer, colon cancer and esophageal cancer*. Lausanne: Frontiers Media SA. doi: 10.3389/978-2-83250-915-9

Table of contents

09 Association of Dynamic Changes in Peripheral Blood Indexes With Response to PD-1 Inhibitor-Based Combination Therapy and Survival Among Patients With Advanced Non-Small Cell Lung Cancer
Yuzhong Chen, Shaodi Wen, Jingwei Xia, Xiaoyue Du, Yuan Wu, Banzhou Pan, Wei Zhu and Bo Shen

21 Corrigendum: Association of Dynamic Changes in Peripheral Blood Indexes With Response to PD-1 Inhibitor-Based Combination Therapy and Survival Among Patients With Advanced Non-Small Cell Lung Cancer
Yuzhong Chen, Shaodi Wen, Jingwei Xia, Xiaoyue Du, Yuan Wu, Banzhou Pan, Wei Zhu and Bo Shen

22 Association of *PTPRD/PTPRT* Mutation With Better Clinical Outcomes in NSCLC Patients Treated With Immune Checkpoint Blockades
Xiaoyan Wang, Bingchen Wu, Zhengqing Yan, Guoqiang Wang, Shiqing Chen, Jian Zeng, Feng Tao, Bichun Xu, Honggang Ke and Mei Li

32 The Impact of VEGF Inhibition on Clinical Outcomes in Patients With Advanced Non-Small Cell Lung Cancer Treated With Immunotherapy: A Retrospective Cohort Study
Keiko Tanimura, Tadaaki Yamada, Ayaka Omura, Shinsuke Shiotsu, Nobutaka Kataoka, Takayuki Takeda, Ryusuke Taniguchi, Takahiro Yamada, Mayumi Takeuchi, Yusuke Chihara, Yoshie Morimoto, Masahiro Iwasaku, Yoshiko Kaneko, Junji Uchino and Koichi Takayama

40 Atezolizumab Monotherapy or Plus Chemotherapy in First-Line Treatment for Advanced Non-Small Cell Lung Cancer Patients: A Meta-Analysis
Dan-Ni Li, Wen-Qing Lu, Bo-Wen Yang, Ling-Yun Zhang, Bo Jin, Shuo Wang, Xiao-Fang Che, Ce Li, Yun-Peng Liu and Xiu-Juan Qu

47 The Effectiveness and Safety of Immune Checkpoint Inhibitors in Non-Small Cell Lung Cancer Patients With Stage III/IV: A Multicenter Study
Jason C. Hsu, Phung-Anh Nguyen, Yen-Tzu Chen, Szu-Chun Yang, Chien-Chung Lin, Yi-Hsin Yang, Yu-Chao Lin, Te-Chun Hsia, Hsing-Chun Hsieh, Jia-Syuan Wu, Chi-Pei Chang, Yin-Hsun Feng, Peng-Chan Lin, Ping-Chih Hsu, Huey-En Tzeng, Shu-Chen Chien, Wei-Chiao Chang, Chih-Cheng Chang, Hsuan-Chia Yang, Chueh Ming Lee and Christine Y. Lu

57 Combination Therapy of Mithramycin A and Immune Checkpoint Inhibitor for the Treatment of Colorectal Cancer in an Orthotopic Murine Model
Rinku Dutta, Roukiah Khalil, Karthick Mayilsamy, Ryan Green, Mark Howell, Srinivas Bharadwaj, Shyam S. Mohapatra and Subhra Mohapatra

71 The Regulatory Network and Potential Role of LINC00973-miRNA-mRNA ceRNA in the Progression of Non-Small-Cell Lung Cancer
Qiang Guo, Dan Li, Xiangyu Luo, Ye Yuan, Tian Li, Huasong Liu and Xinju Wang

85 Targeted Immunotherapies in Gastrointestinal Cancer: From Molecular Mechanisms to Implications
Ding-Kang Wang, Qian Zuo, Qing-Yu He and Bin Li

100 Comparison of Efficacy and Safety of Single and Double Immune Checkpoint Inhibitor-Based First-Line Treatments for Advanced Driver-Gene Wild-Type Non-Small Cell Lung Cancer: A Systematic Review and Network Meta-Analysis
Qian Xu, Xue Zhang, Miao Huang, Xin Dai, Jing Gao, Song Li, Lei Sheng, Kai Huang, Jian Wang and Lian Liu

111 Predictive Value of Metabolic Parameters Derived From ^{18}F-FDG PET/CT for Microsatellite Instability in Patients With Colorectal Carcinoma
Hao Liu, Zheng Ye, Ting Yang, Hongjun Xie, Ting Duan, Mou Li, Min Wu and Bin Song

119 Case Report: A Rare Case of Pembrolizumab-Induced Bullous Pemphigoid
Xiaoyan Zhang, Dongjiang Sui, Dong Wang, Lina Zhang and Ruiyan Wang

125 Tumor-Infiltrating PD-1^{hi}CD8^{+}-T-Cell Signature as an Effective Biomarker for Immune Checkpoint Inhibitor Therapy Response Across Multiple Cancers
Zhenyu Yang, Yulan Deng, Jiahan Cheng, Shiyou Wei, Hao Luo and Lunxu Liu

140 The Prediction Potential of the Pretreatment Lung Immune Prognostic Index for the Therapeutic Outcomes of Immune Checkpoint Inhibitors in Patients With Solid Cancer: A Systematic Review and Meta-Analysis
Hui Liu, Xiao-Li Yang, Xiao-Yun Yang, Zhao-Ru Dong, Zhi-Qiang Chen, Jian-Guo Hong and Tao Li

149 Integrated Profiling Identifies *PLOD3* as a Potential Prognostic and Immunotherapy Relevant Biomarker in Colorectal Cancer
Junhong Shi, Meiyu Bao, Weifeng Wang, Xuan Wu, Yueying Li, Changdong Zhao and Weiwei Liu

161 Sanguisorbae Radix Suppresses Colorectal Tumor Growth Through PD-1/PD-L1 Blockade and Synergistic Effect With Pembrolizumab in a Humanized PD-L1-Expressing Colorectal Cancer Mouse Model
Eun-Ji Lee, Ji Hye Kim, Tae In Kim, Yeon-Ji Kim, Malk Eun Pak, Chang Hyun Jeon, Yeo Jin Park, Wei Li, Young Soo Kim, Jang-Gi Choi and Hwan-Suck Chung

172 Tumor Mutational Burden Predicting the Efficacy of Immune Checkpoint Inhibitors in Colorectal Cancer: A Systematic Review and Meta-Analysis
Yan Li, Yiqi Ma, Zijun Wu, Fanxin Zeng, Bin Song, Yanrong Zhang, Jinxing Li, Su Lui and Min Wu

183 Case Report: Immune and Genomic Characteristics Associated With Hyperprogression in a Patient With Metastatic Deficient Mismatch Repair Gastrointestinal Cancer Treated With Anti-PD-1 Antibody
Wenyue Zhou, Yuwen Zhou, Cheng Yi, Xinyao Shu, Guixia Wei, Xiaorong Chen, Xudong Shen and Meng Qiu

189 Immune Checkpoint Inhibitors With or Without Bone-Targeted Therapy in NSCLC Patients With Bone Metastases and Prognostic Significance of Neutrophil-to-Lymphocyte Ratio
Alberto Bongiovanni, Flavia Foca, Jessica Menis, Stefania Luigia Stucci, Fabrizio Artioli, Valentina Guadalupi, Maria Rosachiara Forcignanò, Manuela Fantini, Federica Recine, Laura Mercatali, Chiara Spadazzi, Marco Angelo Burgio, Valentina Fausti, Anna Miserocchi and Toni Ibrahim

200 Durable Complete Response to Pembrolizumab in Esophageal Squamous Cell Carcinoma With Divergent Microsatellite Status: A Case Report
Tian Zeng, Lei Zhang, Can Chen, Xiang Zhao, Xiaoqing Liu, Fengwei Ran, Tingting Yong, Ying Yang, Henghui Zhang and Yanling Zhang

206 A Network Comparison on Safety Profiling of Immune Checkpoint Inhibitors in Advanced Lung Cancer
Yi-Dan Yan, Jiu-Jie Cui, Jie Fu, Ying-Jie Su, Xiao-Yu Chen, Zhi-Chun Gu and Hou-Wen Lin

222 The Effects of Differentially-Expressed Homeobox Family Genes on the Prognosis and HOXC6 on Immune Microenvironment Orchestration in Colorectal Cancer
Lina Qi, Chenyang Ye, Ding Zhang, Rui Bai, Shu Zheng, Wangxiong Hu and Ying Yuan

237 Case Report: Glucocorticoid Effect Observation in a Ureteral Urothelial Cancer Patient With ICI-Associated Myocarditis and Multiple Organ Injuries
Xiajun Hu, Yumiao Wei and Xinxin Shuai

244 Good Tumor Response to Chemoradioimmunotherapy in dMMR/MSI-H Advanced Colorectal Cancer: A Case Series
Chengjing Zhou, Ting Jiang, Yajie Xiao, Qiaoxuan Wang, Zhifan Zeng, Peiqiang Cai, Yongtian Zhao, Zhikun Zhao, Dongfang Wu, Hanqing Lin, Chao Sun, Rong Zhang, Weiwei Xiao and Yuanhong Gao

251 Case Report: Clinical Management of a Patient With Metastatic Non-Small Cell Lung Cancer Newly Receiving Immune Checkpoint Inhibition During Symptomatic COVID-19
Sibylle C. Mellinghoff, Kanika Vanshylla, Christine Dahlke, Marylyn M. Addo, Oliver A. Cornely, Florian Klein, Thorsten Persigehl, Jan Rybniker, Henning Gruell and Paul J. Bröckelmann

257 Immune Checkpoint Inhibitor-Associated Colitis: From Mechanism to Management
Liansha Tang, Jialing Wang, Nan Lin, Yuwen Zhou, Wenbo He, Jiyan Liu and Xuelei Ma

281 A Combination of Biomarkers Predict Response to Immune Checkpoint Blockade Therapy in Non-Small Cell Lung Cancer
Zedong Jiang, Yao Zhou and Juan Huang

290 Camrelizumab-Related Myocarditis and Myositis With Myasthenia Gravis: A Case Report and Literature Review
Jing Bai, Dan Li, Peidan Yang, Kunyan Xu, Yingnan Wang, Qian Li, Jiang Liu, Wenli Du, Fengbin Zhang and Rui Feng

297 The Role of m6A Epigenetic Modification in the Treatment of Colorectal Cancer Immune Checkpoint Inhibitors
Huan Tong, He Wei, Alhaji Osman Smith and Juan Huang

310 Co-Mutation of FAT3 and LRP1B in Lung Adenocarcinoma Defines a Unique Subset Correlated With the Efficacy of Immunotherapy
Mingyu Zhu, Lu Zhang, Haiyan Cui, Qiang Zhao, Hao Wang, Baochao Zhai, Richeng Jiang and Zhansheng Jiang

322 Tumor-Infiltrating Lymphocytes in Colorectal Cancer: The Fundamental Indication and Application on Immunotherapy
Ziyi Bai, Yao Zhou, Zifan Ye, Jialong Xiong, Hongying Lan and Feng Wang

336 Case Report: Opportunities and Challenges of Immunotherapy in Heavily-Treated EGFR-Mutant Advanced Squamous Cell Lung Carcinoma After Progression on EGFR-TKIs and Chemotherapy
Wei Jin, Xin Wang, Jie Wang and Lin Lin

344 Safety and Feasibility of Esophagectomy Following Combined Immunotherapy and Chemotherapy for Locally Advanced Esophageal Squamous Cell Carcinoma: A Propensity Score Matching Analysis
Zhi-Nuan Hong, Lei Gao, Kai Weng, Zhixin Huang, Wu Han and Mingqiang Kang

353 Cost-Effectiveness Analysis of Pembrolizumab in Patients With Advanced Esophageal Cancer Based on the KEYNOTE-181 Study
Mei Zhan, Ting Xu, Hanrui Zheng and Zhiyao He

363 Neoadjuvant Immunotherapy for MSI-H/dMMR Locally Advanced Colorectal Cancer: New Strategies and Unveiled Opportunities
Xuan Zhang, Tao Wu, Xinyi Cai, Jianhua Dong, Cuifeng Xia, Yongchun Zhou, Rong Ding, Renfang Yang, Jing Tan, Lijuan Zhang, Ya Zhang, Yuqin Wang, Chao Dong and Yunfeng Li

376 A SIRPαFc Fusion Protein Conjugated With the Collagen-Binding Domain for Targeted Immunotherapy of Non-Small Cell Lung Cancer
Jiayang Liu, Zhefeng Meng, Tongyang Xu, Kudelaidi Kuerban, Songna Wang, Xuyao Zhang, Jiajun Fan, Dianwen Ju, Wenzhi Tian, Xuan Huang, Xiting Huang, Danjie Pan, Huaning Chen, Weili Zhao and Li Ye

388 Visual Analysis of Colorectal Cancer Immunotherapy: A Bibliometric Analysis From 2012 to 2021
Long Ma, Jixiang Ma, Muzhou Teng and Yumin Li

406 Nivolumab Combined With Ipilimumab Treatment Induced Hypophysitis and Immune-Mediated Liver Injury in Advanced Esophageal Squamous Cell Carcinoma: A Case Report
Yi Feng, Chengyang Li, Yuan Ji, Ying Liu, Lu Gan, Yiyi Yu and Tianshu Liu

413 What Is Long-Term Survival and Which First-Line Immunotherapy Brings Long-Term Survival for Advanced Wild-Type Non-Small Cell Lung Cancer: A Network Meta-Analysis Based on Integrated Analysis
Xue Zhang, Qian Xu, Xuejun Yu, Miao Huang, Song Li, Lei Sheng, Xin Dai, Kai Huang, Jian Wang and Lian Liu

424 Checkpoint Inhibitor Pneumonitis Induced by Anti-PD-1/PD-L1 Therapy in Non-Small-Cell Lung Cancer: Occurrence and Mechanism
Jianqiong Yin, Yuanjun Wu, Xue Yang, Lu Gan and Jianxin Xue

440 Non-Invasive Measurement Using Deep Learning Algorithm Based on Multi-Source Features Fusion to Predict PD-L1 Expression and Survival in NSCLC
Chengdi Wang, Jiechao Ma, Jun Shao, Shu Zhang, Jingwei Li, Junpeng Yan, Zhehao Zhao, Congchen Bai, Yizhou Yu and Weimin Li

451 TNF-α-Secreting Lung Tumor-Infiltrated Monocytes Play a Pivotal Role During Anti-PD-L1 Immunotherapy
Kirsten De Ridder, Hanne Locy, Elisa Piccioni, Miren Ibarra Zuazo, Robin Maximilian Awad, Stefaan Verhulst, Mathias Van Bulck, Yannick De Vlaeminck, Quentin Lecocq, Eva Reijmen, Wout De Mey, Lien De Beck, Thomas Ertveldt, Isabel Pintelon, Jean-Pierre Timmermans, David Escors, Marleen Keyaerts, Karine Breckpot and Cleo Goyvaerts

466 Predicting Durable Responses to Immune Checkpoint Inhibitors in Non-Small-Cell Lung Cancer Using a Multi-Feature Model
Lei Wang, Hongbing Zhang, Chaohu Pan, Jian Yi, Xiaoli Cui, Na Li, Jiaqian Wang, Zhibo Gao, Dongfang Wu, Jun Chen, Jizong Jiang and Qian Chu

474 The Comprehensive Analysis Identified an Autophagy Signature for the Prognosis and the Immunotherapy Efficiency Prediction in Lung Adenocarcinoma
Xizhe Li, Ziyu Dai, Xianning Wu, Nan Zhang, Hao Zhang, Zeyu Wang, Xun Zhang, Xisong Liang, Peng Luo, Jian Zhang, Zaoqu Liu, Yanwu Zhou, Quan Cheng and Ruimin Chang

492 Identification of a Novel Immune Landscape Signature for Predicting Prognosis and Response of Colon Cancer to Immunotherapy
Zheng Wang, Jingru Song, Nisma Lena Bahaji Azami and Mingyu Sun

506 Upper Gastrointestinal Tract IrAEs: A Case Report About Sintilimab-Induced Acute Erosive Hemorrhagic Gastritis
Qi Ai, Wen Chen, Yonggui Li and Guoqing Li

513 ASCL2 Affects the Efficacy of Immunotherapy in Colon Adenocarcinoma Based on Single-Cell RNA Sequencing Analysis
Lei Wu, Shengnan Sun, Fei Qu, Xiuxiu Liu, Meili Sun, Ying Pan, Yan Zheng and Guohai Su

528 Cost-Utility Analysis of Camrelizumab Plus Chemotherapy Versus Chemotherapy Alone as a First-Line Treatment for Advanced Nonsquamous Non-Small Cell Lung Cancer in China
Ting Chen, Ruixiang Xie, Qiuling Zhao, Hongfu Cai and Lin Yang

frontiers in Immunology

ORIGINAL RESEARCH
published: 14 May 2021
doi: 10.3389/fimmu.2021.672271

Association of Dynamic Changes in Peripheral Blood Indexes With Response to PD-1 Inhibitor-Based Combination Therapy and Survival Among Patients With Advanced Non-Small Cell Lung Cancer

Yuzhong Chen[1†], Shaodi Wen[1†], Jingwei Xia[1], Xiaoyue Du[1], Yuan Wu[1], Banzhou Pan[1], Wei Zhu[2] and Bo Shen[1]*

[1] The Affiliated Cancer Hospital of Nanjing Medical University, Jiangsu Cancer Hospital & Jiangsu Institute of Cancer Research, Nanjing, China, [2] Key Hematological of Medical Science and Hematological Medicine of Jiangsu Province, School of Medicine, Jiangsu University, Zhenjiang, China

OPEN ACCESS

Edited by:
Udo S. Gaipl,
University Hospital Erlangen, Germany

Reviewed by:
Lisa Sevenich,
Georg Speyer Haus, Germany
Jian-Guo Zhou,
University of Erlangen Nuremberg, Germany

***Correspondence:**
Bo Shen
shenbo987@126.com

[†]These authors have contributed equally to this work and share first authorship

Specialty section:
This article was submitted to Cancer Immunity and Immunotherapy, a section of the journal Frontiers in Immunology

Received: 25 February 2021
Accepted: 29 April 2021
Published: 14 May 2021

Citation:
Chen Y, Wen S, Xia J, Du X, Wu Y, Pan B, Zhu W and Shen B (2021) Association of Dynamic Changes in Peripheral Blood Indexes With Response to PD-1 Inhibitor-Based Combination Therapy and Survival Among Patients With Advanced Non-Small Cell Lung Cancer. Front. Immunol. 12:672271. doi: 10.3389/fimmu.2021.672271

Background: PD-1 inhibitors have been routinely used in the treatment of advanced non-small cell lung cancer (NSCLC), and have demonstrated to significantly improve survivorship when combining with other conventional therapies, such as chemotherapy and anti-angiogenesis therapy. PD-L1 is the most commonly used biomarker to select benefiting groups, while not all patients with high PD-L1 expression benefit from immunotherapy. Therefore, identifying other prognostic and predictive biomarkers, including peripheral blood indexes, is essential.

Methods: We retrospectively collected medical records and hematological data of 151 patients with advanced NSCLC treated with PD-1 inhibitor-based combination therapy in our hospital. The peripheral blood indexes of interest were NLR, PLR, PAR, Hb, LDH, CEA, and NSE. The association between peripheral blood indexes and treatment responses or survival outcomes was examined by multivariable logistic regression and Cox regression, respectively.

Results: The decreased CEA at week 6 (OR = 4.209, 95%CI: 1.287-13.758) or 12 (OR = 7.267, 95%CI: 1.508-35.006) post-treatment was related to a higher disease control rate. The decrease or NLR at week 6 (OR = 3.081, 95%CI: 1.464-6.483) or 12 (OR = 3.304, 95%CI: 1.560-7.001) post-treatment, or CEA at week 12 post-treatment (OR = 2.469, 95%CI: 1.134-5.375), was associated with a higher objective response rate. Patients whose NLR (HR = 0.610, 95%CI: 0.411-0.907) or CEA (HR = 0.477, 95%CI: 0.320-0.710) decreased at week 6 post-treatment tended to have longer progression-free survival, and similar results were found in those with decreased NLR (HR = 0.587, 95%CI: 0.388-0.886) or CEA (HR = 0.406, 95%CI: 0.270-0.609) at week 12 post-treatment. Patients whose CEA (HR = 0.543, 95%CI: 0.339-0.871) or NSE (HR = 0.619, 95%CI:

0.386-0.994) decreased after 6 weeks post-treatment appeared to have longer overall survival, and the same was found for those whoseCEA (HR = 0.620, 95%CI: 0.390-0.986) or NSE (HR = 0.578, 95%CI: 0.353-0.947) was decreased at 12 weeks after treatment.

Conclusion: Post-treatment NLR, CEA and NSE changes are suggestive indicators for the prognosis of NSCLC patients after immunotherapy.

Keywords: non-small cell lung cancer, PD-1 inhibitor, combination therapy, carcinoembryonic antigen, neutrophil-to-lymphocyte ratio, neuron-specific enolase

INTRODUCTION

Immunotherapy, especially immune checkpoint inhibitors (ICIs) represented by programmed cell death protein-1 (PD-1) inhibitors, has significantly improved the prognosis of patients with advanced non-small cell lung cancer (NSCLC). ICIs as a single agent or in combination with other treatments, such as chemotherapy and anti-angiogenic therapy, have become the standard treatment for driver gene-negative advanced NSCLC. However, approximately 50% of the patients showed no benefit from immunotherapy, and a proportion of them even experienced hyper-progression or fatal toxicity (1–4). Precise and reliable biomarkers are critical for identifying the patients who can potentially benefit from immunotherapy. Currently, programmed death-ligand 1 (PD-L1) and tumor mutation burden (TMB) remain as the most common biomarkers that are approved by the Food and Drug Administration (FDA) for predicting the efficacy of immunotherapy in NSCLC. Nevertheless, a certain percentage of patients with negative PD-L1 expression or low TMB can still benefit from immunotherapy. Oncogenic alterations, such as epidermal growth factor receptor (EGFR) and anaplastic lymphoma kinase (ALK), are usually associated with poor treatment response. Other potential predictive biomarkers, including microbiome, tumor infiltrating lymphocytes, gene signatures, multi-omics, etc. (5) are expensive, time-consuming for operation, and only tested on tissue specimens, which limit their clinical applications. Therefore, developing inexpensive and efficient biomarkers to select populations that can benefit from immunotherapy is urgently required.

In recent years, peripheral blood biomarkers representing tumor burden or inflammation have been increasingly studied for the purpose of predicting NSCLC treatment effect. The lower pre-treatment level or post-treatment declination of those biomarkers was previously shown to associate with the higher response rate and better prognosis in the patients (6–15). However, most studies were based on monotherapy, and the meaningfulness of baseline values remains controversial. Therefore, we conducted a retrospective study to further validate peripheral blood markers in predicting outcome and prognosis in patients with advanced NSCLC treated with PD-1 inhibitors-based combination therapy. The findings can serve as a designing reference for future stratified randomized controlled trials. In addition to the patient's baseline clinical characteristics, the explored peripheral blood markers are as follows: neutrophil-to-lymphocyte ratio (NLR), platelet-to-lymphocyte ratio (PLR), platelet-to-albumin ratio (PAR), hemoglobin (Hb), lactate dehydrogenase (LDH), carcinoembryonic antigen (CEA) and neuron-specific enolase (NSE).

MATERIALS AND METHODS

Study Design

We retrospectively identified and included 151 patients with advanced or relapsed NSCLC who received anti-PD-1-based combination therapy (pembrolizumab, sintilimab or toripalimab) at the Affiliated Cancer Hospital of Nanjing Medical University, China, from August 2018 to December 2019. Patients received 200mg pembrolizumab, 200mg sintilimab, or 240mg toripalimab intravenously once every 3 weeks. Combination chemotherapy was all based on platinum doublet chemotherapy, while the other drugs, including pemetrexed, docetaxel, paclitaxel/nab-paclitaxel, and gemcitabine was according to tumor histology. Bevacizumab was used as the combined anti-angiogenic drug. Patients who had inflammation or used steroids within 1 month were excluded.

Clinicopathological features of the patients, including age at the time of treatment, gender, pathology type, stage, Eastern Cooperative Oncology Group performance status (ECOG PS) score, smoking history, number of distant metastases, type of driver mutation, degree of tumor differentiation, treatment regimen, number of treatment lines, whether or not had received radiotherapy, and best response to treatment, were collected through electronic medical records or telephone follow-up. The peripheral blood indexes including NLR (absolute neutrophil count/absolute lymphocyte count), PLR (absolute platelet count/absolute lymphocyte count), PAR (absolute platelet count/albumin), hemoglobin (Hb), lactate dehydrogenase (LDH), and carcinoembryonic antigen (CEA), were collected before treatment, and 6 and 12 weeks after treatment ($_{0w}$, $_{6w}$, and $_{12w}$). All of the abovementioned indexes were considered as binary variables in the analysis: the first four were dichotomized based on the median value, and the last three were dichotomized from the upper or lower limit of hematological tests based on clinical significance. Whole-body computed tomography scans were performed every

6-8 weeks after treatment to assess patients' response to treatment according to The Response Evaluation Criteria in Solid Tumors (16). The last follow-up date was December 10th, 2020.

Treatment response was evaluated by objective response rate (ORR) and disease control rate (DCR), while survival was evaluated by progression-free survival (PFS) and overall survival (OS). Specifically, ORR was defined as the sum of complete response (CR) and partial response (PR), and DCR was defined as the sum of CR, PR, and stable disease (SD). PFS was defined as the time from initial treatment to clinical or imaging progression or death, and OS was defined as the time from initial treatment to the last follow-up or death, whichever came first.

This study was approved by the Institutional Review Board of Jiangsu Cancer Hospital. Patient's informed consent was not necessary because this study was a retrospective study.

Statistical Analysis

The baseline characteristics, peripheral blood indexes, and treatment response of the patients were reported as medians and interquartile ranges (IQRs) for continuous variables, or frequencies and percentages for categorical variables. For the response to treatment, we performed Chi-squared test (or Fisher's exact test if the expected frequency of any cell in the contingency table is smaller than 5) to compare the distributions of the clinical factors/peripheral blood indexes between patients with and without the best response. We explored the relationship between clinical factors/peripheral blood indexes and best treatment response through multivariable logistic regression. For the survival outcomes, we used the Kaplan–Meier method to generate the PFS and OS survival curves, and the Log-rank test to compare survival outcomes among patients separated by the factors of interest. Then, we constructed the Cox proportional hazards model to estimate the association between clinical factors/peripheral blood indexes and survival outcomes, and used concordance index (C-index) to evaluate the discriminative ability of models, with closer to 1.0 indicating a better ability to correctly discriminate the outcome. Variables included in the multivariable analysis were selected based on clinical relevance and statistical significance in the Chi-square test or univariable analysis ($P < 0.10$). The above analysis was carried out for data obtained at 3 different time points. $P < 0.05$ was considered statistically significant. All tests were two-sided. SPSS 25.0 and GraphPad Prism 9.0.0 were used for data analysis and graphing.

RESULTS

Patient Characteristics

A total of 151 patients were included in this study. **Table 1** shows detailed baseline clinicopathological characteristics. The median age of the patients was 63 years (IQR: 54-69), 76.2% of patients were male, 60.3% were smokers, and almost all patients were ECOG PS score 0-1, only four had PS 2. Most patients had distant metastasis (78.8%) and low degree of differentiation (76.8%). Among the 151 patients, 105 received anti-PD1 therapy combined with chemotherapy, 18 received anti-PD1 therapy combined with anti-angiogenesis therapy, and 28

TABLE 1 | Patients' characteristics at baseline and treatment response.

Characteristics	No. of patients(N = 151)	Percentage(%)
Age(years), median(IQR)	63(54-69)	
≥ 63	81	53.6
< 63	70	46.4
Gender		
Female	36	23.8
Male	115	76.2
Tumor histology		
Squamous	50	33.1
Non-Squamous	101	66.9
Adenocarcinoma	92	60.9
Others†	9	6.0
Stage		
Recurrence	29	19.2
Advanced	122	80.8
IIIB	29	19.2
IV	93	61.6
ECOG PS		
0-1	147	97.4
2	4	2.6
Smoking history		
Never	60	39.7
Now/ever	91	60.3
No. of metastasis sites		
0	32	21.2
1	72	47.4
2	33	21.9
≥ 3	14	9.3
Mutation type‡		
EGFR	28	18.5
KRAS	7	4.6
Wild-type	116	76.8
Degree of differentiation		
Low	116	76
Moderate/high	35	23.2
PD-1 inhibitor type		
Pembrolizumab	70	46.4
Sintilimab	66	43.7
Toripalimab	15	9.9
Combination regimen		
Chemotherapy	105	69.5
Anti-angiogenic therapy	18	11.9
Both	28	18.5
Lines of therapy		
1	61	40.4
2	49	32.5
≥ 3	41	27.2
Radiotherapy		
No	85	56.3
Yes	66	43.7
Best response		
CR	0	0.0
PR	46	30.5
SD	88	58.3
PD	17	11.3

†*adenosquamouscarcinoma(n = 3), Sarcomatoid carcinoma(n = 2), otherwise(n = 4).*
‡*ALK mutation(n = 0).*
ECOG, Eastern Cooperative Oncology Group; PS, performance status.

received both; 61 patients were untreated, while 90 patients were retreated (≥ 2). More than half of the patients received radiotherapy during immunotherapy. Their detailed peripheral blood indexes are shown in **Table 2** and **Supplementary Tables 1** and **2**. The median follow-up time was 20.4 months (95%CI: 14.5-26.3).

At the time of administrative censoring (Dec 10th, 2020), 83 patients have died, 48 were still receiving immunotherapy, 20 lost to follow-up or discontinued the therapy due to toxicity. Five patients failed to reach the fourth cycle of medication. No patient reached CR, 46 (30.5%) reached PR, 88 (58.3%) reached SD, and 17 (11.3%) reached "progressive disease (PD)". The ORR and DCR were 30.5% and 88.7%, respectively. Median PFS and OS were 8.0 (95%CI: 7.2-8.8) and 15.3 months (95%CI: 13.8-16.8), respectively (**Supplementary Figure 1**).

Associations Between PD-1 Inhibitor Type/Combination Regimen and Treatment Response/Survival Outcomes

We conducted a univariate analysis of PD-1 inhibitor type and combination regimen while no differences in DCR, ORR, PFS and OS were found(**Supplementary Table 3**).

Associations Between Clinical Factors/ Peripheral Blood Indexes and Treatment Response

As shown in **Supplementary Table 4**, age, lines of therapy, radiotherapy, LDH_{0w}, NLR_{6w}, LDH_{6w}, CER_{6w}, NLR_{12w} and CEA_{12w} was associated with DCR, while age, radiotherapy, Hb_{0w}, CEA_{0w}, NLR_{6w}, LDH_{6w}, NLR_{12w}, LDH_{12w} and CEA_{12w} were associated with ORR, without any adjustment. Considering that most of the patients received no radiotherapy at the early stage of treatment, "radiotherapy" was not included in the multivariable logistic regression analysis. Age ≤ 63 years (OR = 3.103, 95%CI: 1.035-9.306), CEA_{6w} Down (OR = 4.209, 95%CI: 1.287-13.758), and CEA_{12w} Down (OR = 7.267, 95%CI: 1.508-35.006) were significantly associated with higher DCR, while NLR_{12w} Down (OR = 4.682, 95%CI: 0.962-22.796) had marginal significance (P = 0.056). Age ≤ 63 years (OR = 2.273, 95%CI: 1.100-4.697), NLR_{6w} Down (OR = 3.081, 95%CI: 1.464-6.483), NLR_{12w} Down (OR = 3.304, 95%CI: 1.560-7.001) and CEA_{12w} Down (OR = 2.469, 95%CI: 1.134-5.375) were significantly associated with higher ORR (**Table 3** and **Figure 1**).

TABLE 2 | Patients' peripheral blood indexes before treatment (0 week).

Observation indexes	No. of patients(N = 151)	Percentage(%)
NLR, median(IQR)	2.96(2.13-4.54)	
> 2.96	75	49.7
≤ 2.96	76	50.3
PLR, median(IQR)	158.62(115.89-229.23)	
> 159	75	49.7
≤ 159	76	50.3
PAR(*10^9), median(IQR)	5.14 (3.98-6.42)	
≥ 5.15	75	49.7
< 5.15	76	50.3
Hb(g/L), median(IQR)	129.00(118.00-140.00)	
≥ 130	75	49.7
< 130	76	50.3
LDH(U/L), median(IQR)	206.00(181.00-258.00)	
> 245	42	27.8
≤ 245	109	72.2
CEA(ng/ml), median(IQR)	4.88(2.61-17.23)	
> 3.5	97	64.2
≤ 3.5	54	35.8
NSE[†] (ng/ml), median(IQR)	16.47(13.08-22.13)	
> 16.3	72	50.7
≤ 16.3	70	49.3

[†]*N = 142.*

NLR, neutrophil-to-lymphocyte ratio; PLR, platelet-to-lymphocyte ratio; PAR, platelet-to-albumin ratio; Hb, hemoglobin; LDH, lactate dehydrogenase; CEA, carcinoembryonic antigen; NSE, neuron-specific enolase.

Associations Between Clinical Factors/ Peripheral Blood Indexes and Survival Outcomes

Based on the Cox regression analysis (**Tables 4**, **5**, only significant variables from univariable analysis are shown), we found that ECOG PS (0 vs. 2: 11.2m vs. 4.1m, HR = 0.160, 95% CI: 0.050-0.515; 1 vs. 2: 7.9m vs. 4.1m, HR = 0.217, 95%CI: 0.077-0.612), radiotherapy (Yes vs. No: 11.2m vs. 7.2m, HR = 0.536, 95%CI: 0.359-0.800), NLR_{6w} (Down vs. Up: 11.2m vs. 7.2m, HR = 0.610, 95%CI: 0.411-0.907), CEA_{6w} (Down vs. Up: 10.5m vs. 6.6m, HR = 0.477, 95%CI: 0.320-0.710), NLR_{12w} (Down vs. Up: 10.8m vs. 5.9m, HR = 0.587, 95%CI: 0.388-0.886) and CEA_{12w} (Down vs. Up: 11.2m vs. 6.0m, HR = 0.406, 95%CI: 0.270-0.609) were independently associated with PFS (**Figure 2**). While CEA_{0w} (>3.5ng/ml vs. ≤ 3.5 ng/ml: 15.8m vs. 13.6m, HR = 0.611, 95%CI: 0.388-0.963), CEA_{6w} (Down vs. Up: 16.5m vs. 13.5m, HR = 0.543, 95%CI: 0.339-0.871), NSE_{6w} (Down vs. Up: 15.8m vs. 13.6m, HR = 0.619, 95%CI: 0.386-0.994), CEA_{12w} (Down vs. Up: 16.2m vs. 13.8m, HR = 0.620, 95%CI: 0.390-0.986) and NSE_{12w} (Down vs. Up: 15.3m vs. 15.3m, HR = 0.578, 95%CI: 0.353-0.947) were independently associated with OS (**Figure 3**). The C-index of $model_{6w}$ and $model_{12w}$ to predict PFS was 0.673 (95% CI: 0.623-0.724) and 0.691 (95% CI: 0.642-0.739), respectively. While the C-index of $model_{6w}$ and $model_{12w}$ to predict OS was 0.615 (95% CI: 0.553-0.677) and 0.614 (95% CI: 0.542-0.686), respectively.

Then, we grouped the patients according to the dynamic changes of NLR + CEA and CEA + NSE, and constructed the corresponding survival curve (**Figure 4** and **Supplementary Figure 3**). Patients with decreased NLR and CEA at week 6 post-treatment (median: 11.8m, 95%CI: 10.0-13.6) had a significantly longer PFS than those with increases in single (median: 7.2m, 95%CI: 5.4-9.0, P < 0.001) or both (median: 6.6m, 95%CI: 3.7-9.5, P < 0.001) indicators, while PFS was only numerically prolonged in "patients One up" compared to that in "patients Both up" (P = 0.172). Similarly, compared with the patients with increases in single (median: 7.2m, 95%CI: 6.1-8.3, P < 0.001) or both (median: 4.5m, 95%CI: 3.3-5.7, P < 0.001), those with decreased NLR and CEA at week 12 post-treatment (median: 11.3m, 95%CI: 10.5-12.1) had a significantly longer PFS, and "patients One up" had a significantly longer PFS than "patients Both up" (P = 0.015). Patients with decreased CEA

TABLE 3 | Multivariable Logistic regression models for DCR and ORR.

		Disease control rate				Objective response rate		
		Odds ratio	95%CI	*P*		Odds ratio	95%CI	*P*
0w	Age (years)				Age (years)			
	> 63	1			> 63	1		
	≤ 63	3.103	1.035-9.306	0.043	≤ 63	2.273	1.100-4.697	0.027
6w	Age (years)				Age (years)			
	> 63	1	0.976-9.162	0.055	> 63	1	1.122-5.028	0.024
	≤ 63	2.991			≤ 63	2.375		
	CEA				NLR			
	Up	1	1.287-13.758		Up	1	1.464-6.483	0.003
	Down	4.209		0.017	Down	3.081		
12w	NLR				NLR			
	Up	1	0.962-22.796	0.056	Up	1	1.560-7.001	0.002
	Down	4.682			Down	3.304		
	CEA				CEA			
	Up	1	1.		Up	1		0.023
	Down	7.267	508-35.006	0.013	Down	2.469	1.134-5.375	

NLR, neutrophil-to-lymphocyte ratio; CEA, carcinoembryonic antigen.

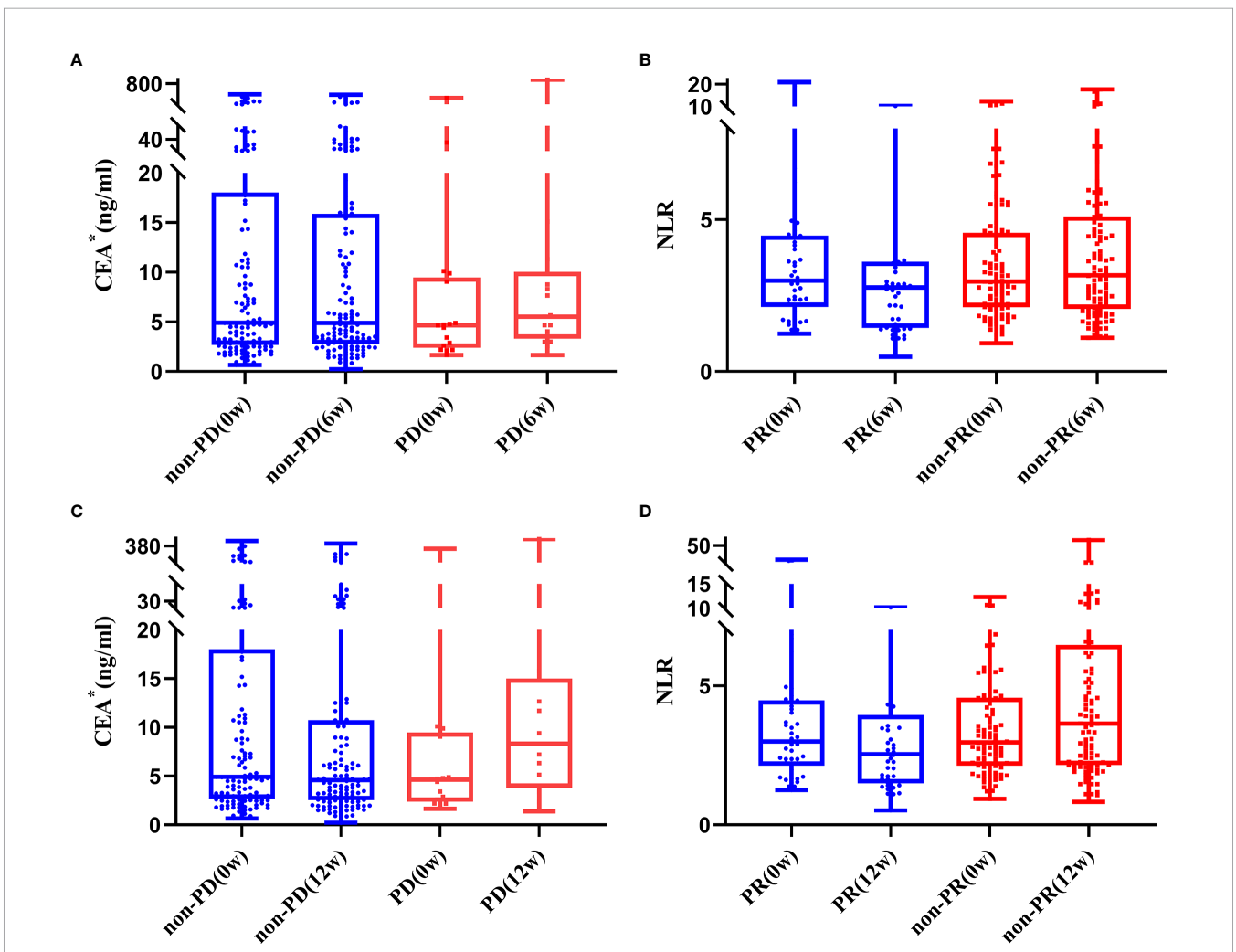

FIGURE 1 | Trend of CEA **(A, B)** and NLR **(C, D)** in patients with and without response to treatment (*one extreme value was removed).

TABLE 4 | Univariable Cox regression analysis for PFS and OS.

	Progression free survival				Overall survival		
	unadjusted HR	95%CI	*P*		unadjusted HR	95%CI	*P*
ECOG PS				Stage			
2	1			Recurrence	1		
0	0.165	0.051-0.528	0.002	IIIB	1.747	0.960-3.178	0.068
1	0.240	0.085-0.673	0.007	IV	1.153	0.678-1.961	0.599
NLR_{6w}				Mutation type			
Up	1			Wild-type	1		
Down	0.604	0.408-0.894	0.012	EGFR	1.779	0.993-3.189	0.053
Hb_{6w}				KRAS	1.145	0.416-3.146	0.793
Up	1			PLR_{0w}			
Down	0.682	0.446-1.045	0.079	Up	1		
CEA_{6w}				Down	0.679	0.439-1.052	0.083
Up	1			CEA_{0w}			
Down	0.510	0.344-0.756	0.001	Up	1		
NLR_{12w}				Down	0.620	0.393-0.977	0.039
Up	1			CEA_{6w}			
Down	0.536	0.357-0.802	0.002	Up	1		
CEA_{12w}				Down	0.497	0.320-0.771	0.002
Up	1			NSE_{6w}			
Down	0.413	0.276-0.618	0.000	Up	1		0.007
Radiotherapy				Down	0.537	0.340-0.846	
Up	1			CEA_{12w}			
Down	0.536	0.359-0.799	0.002	Up	1		
				Down	0.662	0.424-1.033	0.069
				NSE_{12w}			
				Up	1		
				Down	0.573	0.356-0.923	0.022

ECOG, Eastern Cooperative Oncology Group; PS, performance status; NLR, neutrophil-to-lymphocyte ratio; PLR, platelet-to-lymphocyte ratio; Hb, hemoglobin; CEA, carcinoembryonic antigen; NSE, neuron-specific enolase.

and NSE at week 6 post-treatment (median: 17.3m, 95%CI: 15.1-19.0) had a significantly longer OS than those with increases in single (median: 15.1m, 95%CI: 12.5-17.7, P = 0.012) or both (median: 13.5m, 95%CI: 11.2-15.8, $P < 0.001$), while the latter two groups of patients had only numerical differences in OS (P = 0.166). Similarly, compared to the patients with increased CEA and NSE at week 12 post-treatment (median: 13.8m, 95%CI: 10.3-17.3), those with decreases in single (median: 15.7m, 95%CI: 13.0-18.4, P = 0.015) or both (median: 15.8m, 95%CI: 13.3-18.3, P = 0.006) indicators had a significantly longer OS, while the latter two groups of patients had only numerical difference in OS (P = 0.139). We further divided all the patients into 4 groups according to CEA_{0w} (ng/ml) and CEA_{6w}: ≤ 3.5 and Down, ≤ 3.5 and Up, > 3.5 and Down, and > 3.5 and Up. The median OSs were 13.6m (13.2-14.0), 13.2m (11.4-15.0), 16.5m (15.5-17.5) and 13.6m (12.2-15.0), respectively. Pairwise comparison revealed that the OS of the third group (> 3.5 and Down) was significantly longer than that of the second group (≤ 3.5 and Up) (P = 0.005).

DISCUSSION

Compared with conventional chemotherapy, ICIs are highly effective on advanced NSCLC, especially in patients with PD-L1 TPS≥50%. However, ICIs alone may not be the best option for patients with PD-L1 TPS between 1-49% (1, 2). In addition, several studies on ICIs-based combination therapy have demonstrated its significant benefits regardless of PD-L1 expression status (3, 4, 17), without inducing concomitant side effects and financial burden for the patients. Efficient, convenient and inexpensive markers are needed to help characterize the patients who can potentially benefit from the ICIs treatment. To our knowledge, this is the first study to assess the association between peripheral blood markers and the outcome of PD-1 inhibitor-based combination therapy in a Chinese population, and our data can provide the basis for stratification in later RCTs. In our study, we found that the dynamic changes of NLR, CEA and NSE after treatment were strongly associated with the treatment outcomes and prognosis of the patients. Briefly, patients with decreased NLR or CEA at 6 or 12 weeks after treatment had better efficacy and longer PFS, and those with decreased CEA or NSE had longer OS.

Inflammation not only is critical at various stages of tumor development and progression, but also can either positively or negatively influence tumor immune-surveillance and therapeutic response. Therefore, inflammatory markers could be potential prognostic factors in immunotherapy for NSCLC. During the treatment of anti-PD-1/PD-L1 antibodies, the activation of lymphocytes is necessary for restoring the anti-tumor immune response (18). Such an immune response is the result of multiple interactions between T cells and other regulatory cells, including

TABLE 5 | Multivariable Cox regression analysis for PFS and OS.

		Progression free survival				Overall survival		
		adjusted HR	95%CI	*P*		adjusted HR	95%CI	*P*
0w	ECOG PS				CEA(ng/ml)			
	2	1			≤ 3.5	1		
	0	0.160	0.050-0.515	0.002	> 3.5	0.611	0.388-0.963	0.034
	1	0.217	0.077-0.612	0.004				
	Radiotherapy							
	No	1						
	Yes	0.536	0.359-0.800	0.002				
6w	ECOG PS				CEA			
	2	1			Up	1		
	0	0.126	0.038-0.415	0.001	Down	0.543	0.339-0.871	0.011
	1	0.207	0.072-0.592	0.003	NSE			
	Radiotherapy				Up	1		
	No	1			Down	0.619	0.386-0.994	0.047
	Yes	0.562	0.375-0.841	0.005				
	NLR							
	Up	1						
	Down	0.610	0.411-0.907	0.015				
	CEA							
	Up	1						
	Down	0.477	0.320-0.710	0.000				
12w	ECOG PS				CEA			
	2	1			Up	1		0.043
	0	0.129	0.038-0.437	0.001	Down	0.620	0.390-0.986	
	1	0.224	0.077-0.649	0.006	NSE			
	Radiotherapy				Up	1		0.029
	No	1			Down	0.578	0.353-0.947	
	Yes	0.569	0.375-0.865	0.008				
	NLR							
	Up	1						
	Down	0.587	0.388-0.886	0.011				
	CEA							
	Up	1						
	Down	0.406	0.270-0.609	0.000				

ECOG, Eastern Cooperative Oncology Group; PS, performance status; NLR, neutrophil-to-lymphocyte ratio; CEA, carcinoembryonic antigen; NSE, neuron-specific enolase.

neutrophils, which play a leading role in the immune environment of NSCLC. Tumor-associated neutrophils have diametrically opposite effects at different molecular levels, which can be divided as anti-tumor N1 type and tumor-promoting N2 type (19–21). A prospective study with 104 patients identified a predictive immune signature (LIPS) based on the peripheral blood immunophenotype, including $CD14^{high}$ monocytes, $CD8^+/PD\text{-}1^+$ T cells, plasmacytoid dendritic cells, neutrophils, and $CD3^+/CD56^+/CD16^+$ natural killer T cells (22). Based on LIPS, patients were categorized into low- and high-risk groups, and both PFS and OS were significantly longer for patients in the low-risk group than in the high-risk group, regardless of PD-L1 expression. This suggests that increased neutrophils counts in the peripheral blood were associated with less benefit from ICI. Another retrospective cohort study with 1714 patients examined the association between pretreatment NLR and TMB levels and survival among patients treated with ICI, and found that the patients with NLR-high/TMB-low had the worst prognosis, while those in the NLR-low/TMB-high group had the best prognosis (23). Other studies also found that patients with advanced NSCLC receiving immunotherapy with high NLR or PLR value (i.e., markers of chronic inflammation) usually showed poor prognosis (24–27). The nutritional status of patients is usually related to their prognosis, and serum albumin is considered a sensitive indicator of general nutritional status. A retrospective cohort study found that PAR is a potential prognostic biomarker for patients who underwent complete surgical resection for NSCLC (28). However, we found no correlation between treatment response or prognosis and PLR or PAR, regardless of their baseline values or changes after treatment. Moreover, no predictive significance of baseline values of NLR was identified, while patients with decreased NLR after treatment (whether at week 6 or 12) were more likely to achieve PR and had longer PFS.

Other peripheral blood indexes have also been proposed to be potential predictors for the effect of ICIs treatment. A recent prospective cohort study showed that normal pre-treatment level of Hbis a favorable prognostic factor for ICIs treatment in patients with advanced NSCLC (7). Furthermore, previous studies have shown that baseline level of LDH, a biomarker related to tumor burden, was associated with the poor treatment outcomes in NSCLC patients, which can also predict the prognosis of the patients treated with ICIs (29–31). However, our study did not find any association between Hb or LDH and

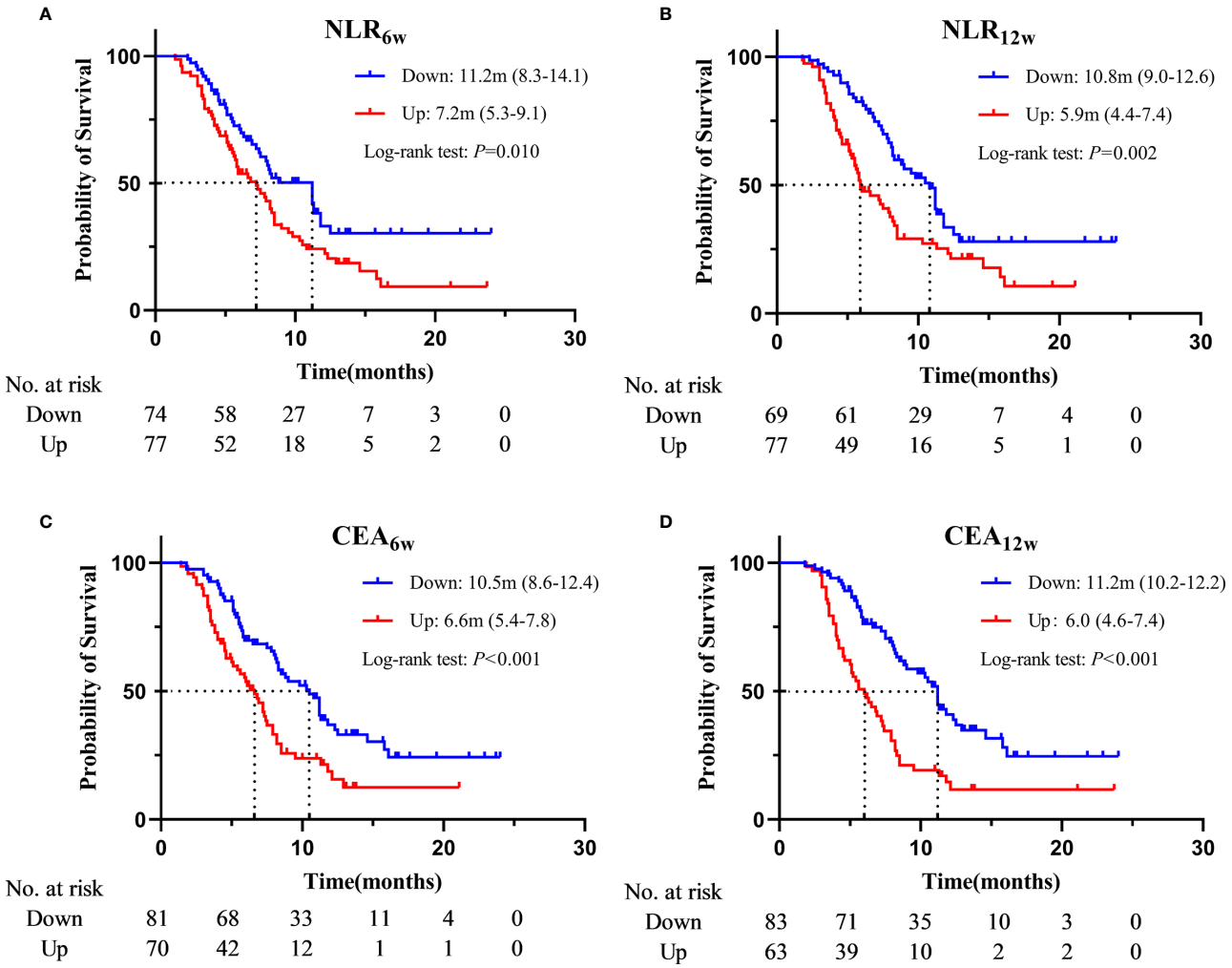

FIGURE 2 | Kaplan–Meier curves for PFS according to NLR_{6w} **(A)**, NLR_{12w} **(B)**, CEA_{6w} **(C)** and CEA_{12w} **(D)**.

treatment efficacy or prognosis. Several studies have shown that repeated measurements of serum tumor markers in patients with advanced NSCLC, especially CEA and NSE, may help clinicians assess the efficacy of anti-PD-1 monotherapy and predict the prognosis (8, 15, 32, 33), which supports our finding in the current study. Patients with decreased CEA after treatment had better outcomes and longer survival; CEA declination at week 6 and 12 post-treatment was associated with52.3% and 59.4% lower risk of tumor progression, respectively, and they were associated with 45.7% and 38.0% lower risk of death. These findings also reflect the significance of repeated measurements at different time points. However, prolongation of OS in patients with decreased NSE after treatment was identified, while it was not detected in those with decreased PFS. In addition, it is also noteworthy that the longer OS in patients with higher baseline CEA is due to that their CEA was decreased after treatment which may suggest that changes in indicators after treatment are more indicative than baseline values.

Recent studies suggest that the prognosis of immunotherapy is independent of age (34). We found better treatment outcomes in younger patients, while no significant difference in survival was observed between patients with different ages. Most immunotherapy-related RCTs excluded patients with ECOG PS ≥ 2, so data on selecting an effective population for immunotherapy based on ECOG PS status are scarce. Two retrospective studies demonstrated that NSCLC patients with ECOG PS ≥ 2 were not suitable for immunotherapy (35, 36), which is consistent with the results found in our study, though we only included 4 patients with PS = 2. The combination of radiotherapy and immunotherapy usually introduces synergistic treatment effects and increases the occurrence of the "abscopal effect" (37). Two previous clinical trials have confirmed that the combination of the two can significantly improve the efficiency of treatment (38, 39). In our study, patients who received radiotherapy during immunotherapy had better prognosis; their risk of progression was reduced by 43.1%, in comparison

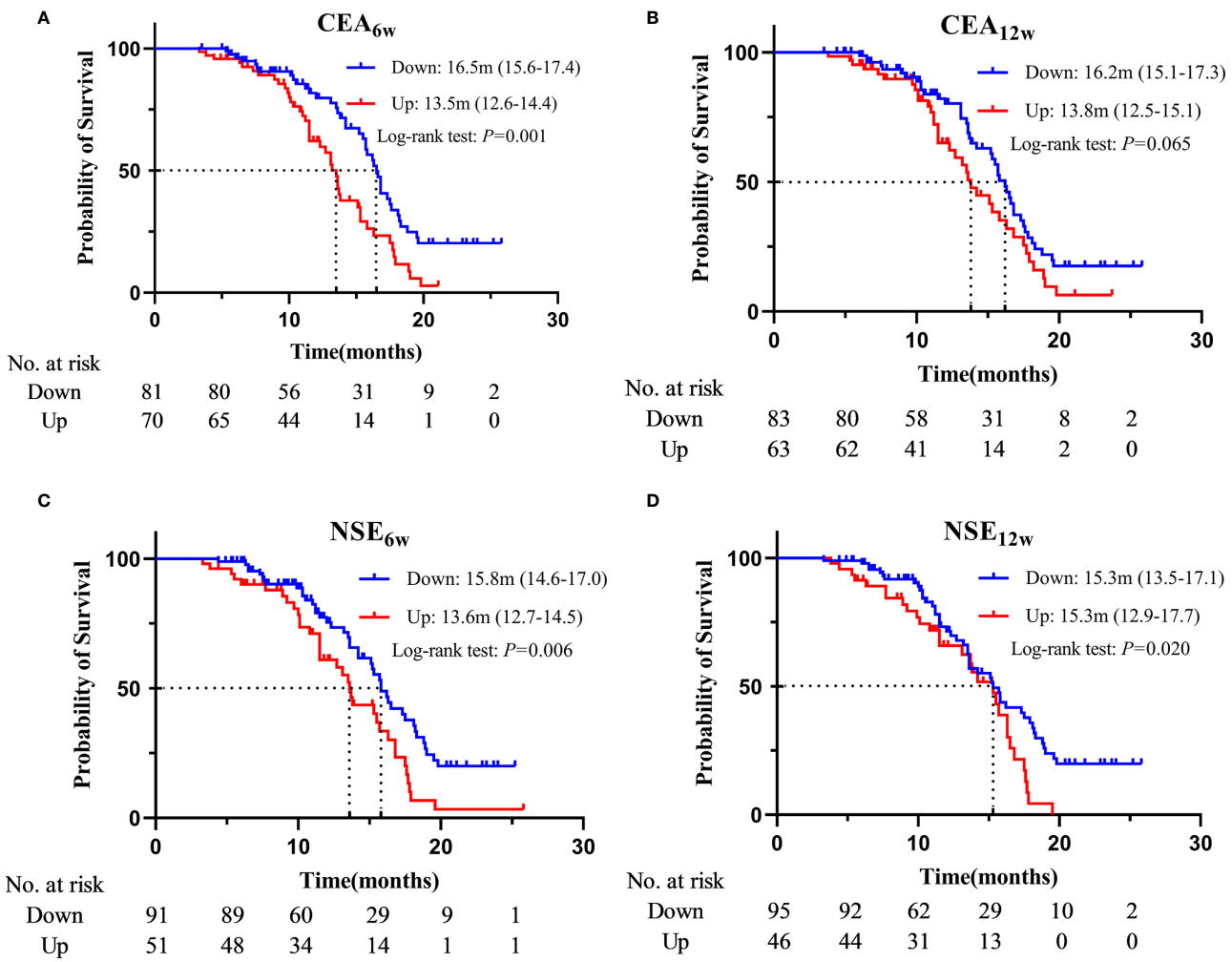

FIGURE 3 | Kaplan–Meier curves for OS according to CEA_{6w} **(A)**, CEA_{12w} **(B)**, NSE_{6w} **(C)** and NSE_{12w} **(D)**.

with those received no radiotherapy, though no differences in OS was observed.

In summary, we found that repeated measurements of NLR, CEA and NSE have greater value in assessing treatment efficacy and predicting prognosis, although the time point for repeated measurements cannot be fully determined. However, no significant results were found for the other parameters, attributed to: a). all the patients receive combined treatment, while chemotherapy only will affect these peripheral blood indexes; b). the best cut-off value was not optimal, which is currently uncertain; c). the follow-up time period was short, and several patients were lost because of COVID-2019. In addition, this study found a shorter median survival time than previous similar clinical trials, possibly due to that only 40.4% of the patients received initial treatment, and 48 patients still receive anti-PD-1 immunotherapy as of the follow-up time.

Our study has several limitations. First, it was a single-center retrospective study with a relatively small size, and Multi-center prospective cohort studies with larger sample sizes are warranted in the future. Second, the selection of peripheral blood indexes and time points for repeated measurement may have influence on the conclusion. Single indicators such as white blood cells, platelets, red blood cells and neutrophils were not included for analysis since most previous studies have shown that single blood parameters had no prognostic value; in addition C-reactive protein, cytokeratin-19-fragment and other tumor markers are not routinely tested in our institution. Moreover, the response to treatment may be reflected at various time points in different patients. In this study, 6 and 12 weeks' time points were selected to investigate the potential association between peripheral blood indexes at the early time of treatment and the treatment efficacy and prognosis of the patients. Third, the changes of peripheral blood indexes might be induced by single chemotherapy; therefore, a positive control group with patients treated with chemotherapy only would be optimal. However, we were unable to enroll a sufficient number of patients in this group, since chemotherapy alone is rare for current clinical practice.

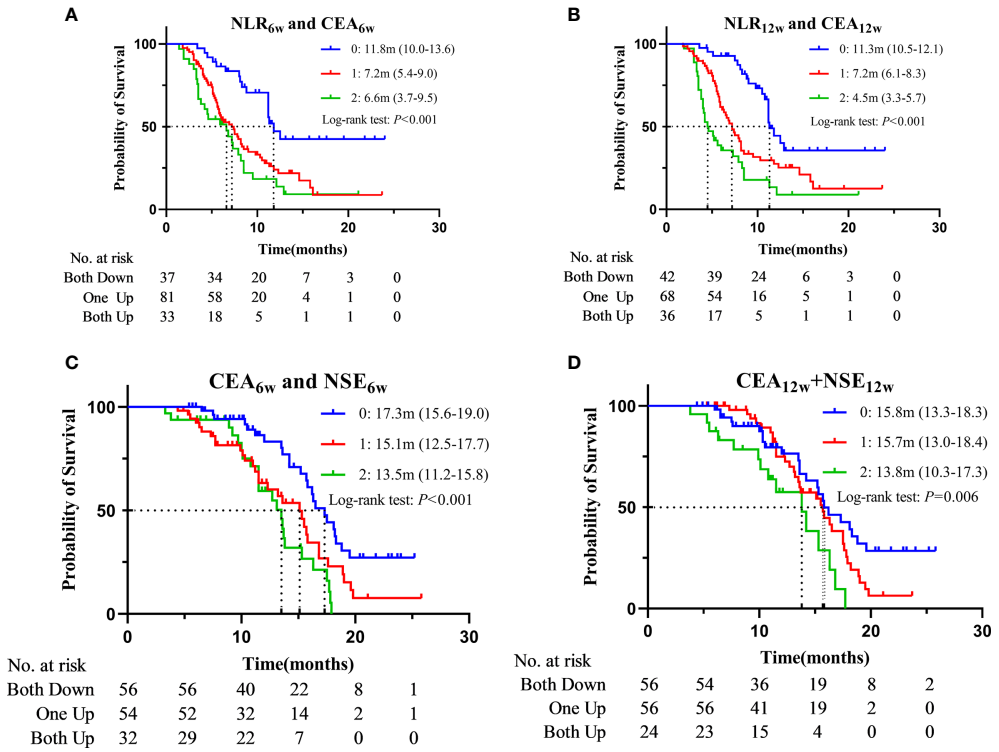

FIGURE 4 | Kaplan–Meier curves for PFS according to "NLR_{6w} and CEA_{6w}" **(A)** or "NLR_{12w} and CEA_{12w}" **(B)** and for OS according to "CEA_{6w} and NSE_{6w}" **(C)** or "CEA_{12w} and NSE_{12w}" **(D)** (0: Both Down, 1: One Up, 2: Both Up).

CONCLUSION

In conclusion, in advanced NSCLC patients, the decreased NLR and CEA after treatment are independent predictors of their response to combined immunotherapy, while the decreased CEA and NSE are associated with a better prognosis.

DATA AVAILABILITY STATEMENT

The raw data supporting the conclusions of this article will be made available by the authors, without undue reservation.

ETHICS STATEMENT

The study involving human participants was reviewed and approved by the Ethics Committee of Jiangsu Cancer Hospital. Patient's informed consent was not necessary because this study was a retrospective study.

AUTHOR CONTRIBUTIONS

YC and BS: idea & design. YC, SW, JX and BP: data collection & collation. YC, SW, XD, YW and WZ: data analysis & interpretation. YC, SW and BS: manuscript writing. All authors contributed to the article and approved the submitted version.

FUNDING

This work was supported by the National Natural Science Foundation of China (Grant No. 81972822, 81972313) and Wu Jieping Medical Foundation (Grant No.320.6750.19060).

ACKNOWLEDGMENTS

We thank for all the patients who were involved in this study. We acknowledge TopEdit LLC for the linguistic editing and proofreading during the preparation of this manuscript.

SUPPLEMENTARY MATERIAL

The Supplementary Material for this article can be found online at: https://www.frontiersin.org/articles/10.3389/fimmu.2021.672271/full#supplementary-material

Supplementary Figure 1 | Kaplan–Meier curves for PFS **(A)** and OS **(B)** in the overall population.

Supplementary Figure 2 | Kaplan–Meier curves for PFS according to ECOG **(A)**, Radiotherapy **(B)**.

Supplementary Figure 3 | Kaplan–Meier curves for OS according to "CEA0w and CEA6w".

REFERENCES

1. Reck M, Rodríguez-Abreu D, Robinson AG, Hui R, Csőszi T, Fülöp A, et al. Pembrolizumab Versus Chemotherapy for PD-L1–Positive Non–Small-Cell Lung Cancer. *N Engl J Med* (2016) 375:1823–33. doi: 10.1056/NEJMoa1606774
2. Mok TSK, Wu Y-L, Kudaba I, Kowalski DM, Cho BC, Turna HZ, et al. Pembrolizumab Versus Chemotherapy for Previously Untreated, PD-L1-expressing, Locally Advanced or Metastatic Non-Small-Cell Lung Cancer (Keynote-042): A Randomised, Open-Label, Controlled, Phase 3 Trial. *Lancet* (2019) 393:1819–30. doi: 10.1016/S0140-6736(18)32409-7
3. Gandhi L, Rodríguez-Abreu D, Gadgeel S, Esteban E, Felip E, De Angelis F, et al. Pembrolizumab Plus Chemotherapy in Metastatic Non–Small-Cell Lung Cancer. *N Engl J Med* (2018) 378:2078–92. doi: 10.1056/NEJMoa1801005
4. Langer CJ, Gadgeel SM, Borghaei H, Papadimitrakopoulou VA, Patnaik A, Powell SF, et al. Carboplatin and Pemetrexed With or Without Pembrolizumab for Advanced, Non-Squamous Non-Small-Cell Lung Cancer: A Randomised, Phase 2 Cohort of the Open-Label Keynote-021 Study. *Lancet Oncol* (2016) 17:1497–508. doi: 10.1016/S1470-2045(16)30498-3
5. Alex F, Alfredo A. Promising Predictors of Checkpoint Inhibitor Response in NSCLC. *Expert Rev Anticancer Ther* (2020) 20:931–7. doi: 10.1080/14737140.2020.1816173
6. Banna GL, Signorelli D, Metro G, Galetta D, Toma AD, Cantale O, et al. Neutrophil-to-Lymphocyte Ratio in Combination With PD-L1 or Lactate Dehydrogenase as Biomarkers for High Pd-L1 Non-Small Cell Lung Cancer Treated With First-Line Pembrolizumab. *Trans Lung Cancer Res* (2020) 9:12. doi: 10.21037/tlcr-19-583
7. Zhang Z, Zhang F, Yuan F, Li Y, Ma J, Ou Q, et al. Pretreatment Hemoglobin Level as a Predictor to Evaluate the Efficacy of Immune Checkpoint Inhibitors in Patients With Advanced Non-Small Cell Lung Cancer. *Ther Adv Med Oncol* (2020) 12:1–10.. doi: 10.1177/1758835920970049
8. Dall'Olio FG, Abbati F, Facchinetti F, Massucci M, Melotti B, Squadrilli A, et al. CEA and CYFRA 21-1 as Prognostic Biomarker and as a Tool for Treatment Monitoring in Advanced Nsclc Treated With Immune Checkpoint Inhibitors. *Ther Adv Med Oncol* (2020) 12:1–13. doi: 10.1177/1758835920952994
9. Petrova MP, Donev IS, Radanova MA, Eneva MI, Dimitrova EG, Valchev GN, et al. Sarcopenia and High NLR are Associated With the Development of Hyperprogressive Disease After Second-Line Pembrolizumab in Patients With Nonsmall-Cell Lung Cancer. *Clin Exp Immunol* (2020) 202:353–62. doi: 10.1111/cei.13505
10. Jiang M, Peng W, Pu X, Chen B, Li J, Xu F, et al. Peripheral Blood Biomarkers Associated With Outcome in Non-small Cell Lung Cancer Patients Treated With Nivolumab and Durvalumab Monotherapy. *Front Oncol* (2020) 10:913. doi: 10.3389/fonc.2020.00913
11. Simonaggio A, Elaidi R, Fournier L, Fabre E, Ferrari V, Borchiellini D, et al. Variation in Neutrophil to Lymphocyte Ratio (NLR) as Predictor of Outcomes inMetastatic Renal Cell Carcinoma (mRCC) and Non-Small Cell Lung Cancer (Mnsclc) Patients Treated With Nivolumab. *Cancer Immunol Immunother* (2020) 69:2513–22. doi: 10.1007/s00262-020-02637-1
12. Wang Z, Zhan P, Lv Y, Shen K, Wei Y, Liu H, et al. Prognostic Role of Pretreatment Neutrophil-to-Lymphocyte Ratio in Non-Small Cell Lung Cancer Patients Treated With Systemic Therapy: A Meta-Analysis. *Transl Lung Cancer Res* (2019) 8:214–26. doi: 10.21037/tlcr.2019.06.10
13. Zhang Z, Li Y, Yan X, Song Q, Wang G, Hu Y, et al. Pretreatment Lactate Dehydrogenase may Predict Outcome of Advanced Non Small-Cell Lung Cancer Patients Treated With Immune Checkpoint Inhibitors: A Meta-Analysis. *Cancer Med* (2019) 8:1467–73. doi: 10.1002/cam4.2024
14. Suh KJ, Kim SH, Kim YJ, Kim M, Keam B, Kim TM, et al. Post-Treatment Neutrophil-to-Lymphocyte Ratio at Week 6 is Prognostic in Patients With Advanced Non-Small Cell Lung Cancers Treated With anti-PD-1 Antibody. *Cancer Immunol Immunother* (2018) 67:459–70. doi: 10.1007/s00262-017-2092-x
15. Bello MGD. The Role of CEA, CYFRA21-1 and NSE in Monitoring Tumor Response to Nivolumab in Advanced Non-Small Cell Lung Cancer (NSCLC) Patients. *J Trans Med* (2019) 17:10. doi: 10.1186/s12967-019-1828-0
16. Lathrop K, Kaklamani V. The Response Evaluation Criteria in Solid Tumors (Recist). In: Badve S, Kumar GL, editors. *Predictive Biomarkers in Oncology: Applications in Precision Medicine*. Cham: Springer International Publishing. (2019). p. 501–11. doi: 10.1007/978-3-319-95228-4_46
17. Socinski MA, Jotte RM, Cappuzzo F, Orlandi F, Stroyakovskiy D, Nogami N, et al. Atezolizumab for First-Line Treatment of Metastatic Nonsquamous NSCLC. *N Engl J Med* (2018) 378:2288–301. doi: 10.1056/NEJMoa1716948
18. Grivennikov SI, Greten FR, Karin M. Immunityss, Inflammation, and Cancer. *Cell* (2010) 140:883–99. doi: 10.1016/j.cell.2010.01.025
19. Kargl J, Busch SE, Yang GHY, Kim K-H, Hanke ML, Metz HE, et al. Neutrophils Dominate the Immune Cell Composition in Non-Small Cell Lung Cancer. *Nat Commun* (2017) 8:14381. doi: 10.1038/ncomms14381
20. Gregory AD, Houghton AM. Tumor-Associated Neutrophils: New Targets for Cancer Therapy. *Cancer Res* (2011) 71:2411–6. doi: 10.1158/0008-5472.CAN-10-2583
21. Fridlender ZG, Sun J, Kim S, Kapoor V, Cheng G, Ling L, et al. Polarization of Tumor-Associated Neutrophil Phenotype by TGF-β: "N1" Versus "N2" Tan. *Cancer Cell* (2009) 16:183–94. doi: 10.1016/j.ccr.2009.06.017
22. Zhou J-G, Donaubauer A-J, Frey B, Becker I, Rutzner S, Eckstein M, et al. Prospective Development and Validation of a Liquid Immune Profile-Based Signature (LIPS) to Predict Response of Patients With Recurrent/Metastatic Cancer to Immune Checkpoint Inhibitors. *J Immunother Cancer* (2021) 9:e001845. doi: 10.1136/jitc-2020-001845
23. Valero C, Lee M, Hoen D, Weiss K, Kelly DW, Adusumilli PS, et al. Pretreatment Neutrophil-to-Lymphocyte Ratio and Mutational Burden as Biomarkers of Tumor Response to Immune Checkpoint Inhibitors. *Nat Commun* (2021) 12:729. doi: 10.1038/s41467-021-20935-9
24. Lalani A-KA, Xie W, Martini DJ, Steinharter JA, Norton CK, Krajewski KM, et al. Change in Neutrophil-to-Lymphocyte Ratio (NLR) in Response to Immune Checkpoint Blockade for Metastatic Renal Cell Carcinoma. *J Immunotherapy Cancer* (2018) 6:5. doi: 10.1186/s40425-018-0315-0
25. Russo A, Russano M, Franchina T, Migliorino MR, Aprile G, Mansueto G, et al. Neutrophil-to-Lymphocyte Ratio (Nlr), Platelet-to-Lymphocyte Ratio (PLR), and Outcomes With Nivolumab in Pretreated Non-Small Cell Lung Cancer (NSCLC): A Large Retrospective Multicenter Study. *Adv Ther* (2020) 37:1145–55. doi: 10.1007/s12325-020-01229-w
26. Zer A, Sung MR, Walia P, Khoja L, Maganti M, Labbe C, et al. Correlation of Neutrophil to Lymphocyte Ratio and Absolute Neutrophil Count With Outcomes With PD-1 Axis Inhibitors in Patients With Advanced Non–Small-Cell Lung Cancer. *Clin Lung Cancer* (2018) 19:426–34.e1. doi: 10.1016/j.cllc.2018.04.008
27. Takada K, Takamori S, Yoneshima Y, Tanaka K, Okamoto I, Shimokawa M, et al. Serum Markers Associated With Treatment Response and Survival in Non-Small Cell Lung Cancer Patients Treated With anti-PD-1 Therapy. *Lung Cancer* (2020) 145:18–26. doi: 10.1016/j.lungcan.2020.04.034
28. Guo M, Sun T, Zhao Z, Ming L. Preoperative Platelet to Albumin Ratio Predicts Outcome of Patients With Non-Small-Cell Lung Cancer. *ATCS* (2020) 27:84–90. doi: 10.5761/atcs.oa.20-00090
29. Petrelli F, Cabiddu M, Coinu A, Borgonovo K, Ghilardi M, Lonati V, et al. Prognostic Role of Lactate Dehydrogenase in Solid Tumors: A Systematic Review and Meta-Analysis of 76 Studies. *Acta Oncol* (2015) 54:961–70. doi: 10.3109/0284186X.2015.1043026
30. Tanizaki J, Haratani K, Hayashi H, Chiba Y, Nakamura Y, Yonesaka K, et al. Peripheral Blood Biomarkers Associated With Clinical Outcome in Non–Small Cell Lung Cancer Patients Treated With Nivolumab. *J Thoracic Oncol* (2018) 13:97–105. doi: 10.1016/j.jtho.2017.10.030
31. Kazandjian D, Gong Y, Keegan P, Pazdur R, Blumenthal GM. Prognostic Value of the Lung Immune Prognostic Index for Patients Treated for Metastatic Non–Small Cell Lung Cancer. *JAMA Oncol* (2019) 5:1481. doi: 10.1001/jamaoncol.2019.1747
32. Lang D, Horner A, Brehm E, Akbari K, Hergan B, Langer K, et al. Early Serum Tumor Marker Dynamics Predict Progression-Free and Overall Survival in Single Pd-1/Pd-L1 Inhibitor Treated Advanced Nsclc—a Retrospective Cohort Study. *Lung Cancer* (2019) 134:59–65. doi: 10.1016/j.lungcan.2019.05.033
33. Huang L, Li L, Zhou Y, Yang Z, Wang M, Gao Y, et al. Clinical Characteristics Correlate With Outcomes of Immunotherapy in Advanced Non-Small Cell Lung Cancer. *J Cancer* (2020) 11:7137–45. doi: 10.7150/jca.49213
34. Passaro A, Attili I, Morganti S, Del Signore E, GiaNoncelli L, Spitaleri G, et al. Clinical Features Affecting Survival in Metastatic Nsclc Treated With

Immunotherapy: A Critical Review of Published Data. *Cancer Treat Rev* (2020) 89:102085. doi: 10.1016/j.ctrv.2020.102085
35. Fujimoto D, Yoshioka H, Kataoka Y, Morimoto T, Kim YH, Tomii K, et al. Efficacy and Safety of Nivolumab in Previously Treated Patients With Non-Small Cell Lung Cancer: A Multicenter Retrospective Cohort Study. *Lung Cancer* (2018) 119:14–20. doi: 10.1016/j.lungcan.2018.02.017
36. Lobefaro R, Viscardi G, Di Liello R, Massa G, Iacovino ML, Sparano F, et al. Immunotherapy in Advanced Non-Small Cell Lung Cancer Patients With Poor Performance Status: The Role of Clinical-Pathological Variables and Inflammatory Biomarkers. *Lung Cancer* (2021) 152:165–73. doi: 10.1016/j.lungcan.2020.12.027
37. Weichselbaum RR, Liang H, Deng L, Fu Y-X. Radiotherapy and Immunotherapy: A Beneficial Liaison? *Nat Rev Clin Oncol* (2017) 14:365–79. doi: 10.1038/nrcliNonc.2016.211
38. Theelen WSME, Peulen HMU, Lalezari F, van der Noort V, de Vries JF, Aerts JGJV, et al. Effect of Pembrolizumab After Stereotactic Body Radiotherapy vs Pembrolizumab Alone on Tumor Response in Patients With Advanced Non–Small Cell Lung Cancer: Results of the PEMBRO-RT Phase 2 Randomized Clinical Trial. *JAMA Oncol* (2019) 5:1276. doi: 10.1001/jamaoncol.2019.1478
39. Gray JE, Villegas A, Daniel D, Vicente D, Murakami S, Hui R, et al. Three-Year Overall Survival With Durvalumab After Chemoradiotherapy in Stage Iii NSCLC—Update From Pacific. *J Thoracic Oncol* (2020) 15:288–93. doi: 10.1016/j.jtho.2019.10.002

Conflict of Interest: The authors declare that the research was conducted in the absence of any commercial or financial relationships that could be construed as a potential conflict of interest.

Copyright © 2021 Chen, Wen, Xia, Du, Wu, Pan, Zhu and Shen. This is an open-access article distributed under the terms of the Creative Commons Attribution License (CC BY). The use, distribution or reproduction in other forums is permitted, provided the original author(s) and the copyright owner(s) are credited and that the original publication in this journal is cited, in accordance with accepted academic practice. No use, distribution or reproduction is permitted which does not comply with these terms.

frontiers in Immunology

CORRECTION
published: 07 June 2021
doi: 10.3389/fimmu.2021.713268

Corrigendum: Association of Dynamic Changes in Peripheral Blood Indexes With Response to PD-1 Inhibitor-Based Combination Therapy and Survival Among Patients With Advanced Non-Small Cell Lung Cancer

Yuzhong Chen[1†], Shaodi Wen[1†], Jingwei Xia[1], Xiaoyue Du[1], Yuan Wu[1], Banzhou Pan[1], Wei Zhu[2] and Bo Shen[1]*

[1] The Affiliated Cancer Hospital of Nanjing Medical University, Jiangsu Cancer Hospital & Jiangsu Institute of Cancer Research, Nanjing, China, [2] Key Hematological of Medical Science and Hematological Medicine of Jiangsu Province, School of Medicine, Jiangsu University, Zhenjiang, China

OPEN ACCESS

Approved by:
Frontiers Editorial Office,
Frontiers Media SA, Switzerland

***Correspondence:**
Bo Shen
shenbo987@126.com

[†]These authors have contributed equally to this work and share first authorship

Specialty section:
This article was submitted to Cancer Immunity and Immunotherapy, a section of the journal Frontiers in Immunology

Received: 22 May 2021
Accepted: 24 May 2021
Published: 07 June 2021

Citation:
Chen Y, Wen S, Xia J, Du X, Wu Y, Pan B, Zhu W and Shen B (2021) Corrigendum: Association of Dynamic Changes in Peripheral Blood Indexes With Response to PD-1 Inhibitor-Based Combination Therapy and Survival Among Patients With Advanced Non-Small Cell Lung Cancer. Front. Immunol. 12:713268. doi: 10.3389/fimmu.2021.713268

Keywords: non-small cell lung cancer, PD-1 inhibitor, combination therapy, carcinoembryonic antigen, neutrophil-to-lymphocyte ratio, neuron-specific enolase

A Corrigendum on

Association of Dynamic Changes in Peripheral Blood Indexes With Response to PD-1 Inhibitor-Based Combination Therapy and Survival Among Patients With Advanced Non-Small Cell Lung Cancer

By Chen Y, Wen S, Xia J, Du X, Wu Y, Pan B, Zhu W and Shen B (2021). Front. Immunol. 12:672271. doi: 10.3389/fimmu.2021.672271

In the original article, there was an error in the Ethics Statement: "The studies involving human participants were reviewed and approved by the Ethics Committee of the First Hospital of Shanxi Medical University. The patients/participants provided their written informed consent to participate in this study."

A correction has been made:

"The study involving human participants was reviewed and approved by the Ethics Committee of Jiangsu Cancer Hospital. Patient's informed consent was not necessary because this study was a retrospective study."

The authors apologize for this error and state that this does not change the scientific conclusions of the article in any way. The original article has been updated.

Copyright © 2021 Chen, Wen, Xia, Du, Wu, Pan, Zhu and Shen. This is an open-access article distributed under the terms of the Creative Commons Attribution License (CC BY). The use, distribution or reproduction in other forums is permitted, provided the original author(s) and the copyright owner(s) are credited and that the original publication in this journal is cited, in accordance with accepted academic practice. No use, distribution or reproduction is permitted which does not comply with these terms.

frontiers in Oncology

ORIGINAL RESEARCH
published: 27 May 2021
doi: 10.3389/fonc.2021.650122

Association of *PTPRD/PTPRT* Mutation With Better Clinical Outcomes in NSCLC Patients Treated With Immune Checkpoint Blockades

Xiaoyan Wang[1†], Bingchen Wu[2†], Zhengqing Yan[3†], Guoqiang Wang[3], Shiqing Chen[3], Jian Zeng[4], Feng Tao[5], Bichun Xu[6], Honggang Ke[7] and Mei Li[8*]*

[1] Department of Respiratory Medicine, Affiliated Hospital of Nantong University, Nantong, China, [2] Department of Oncology, Hospital of Chinese Medicine of Changxing County, Huzhou, China, [3] The Medical Department, 3D Medicines Inc., Shanghai, China, [4] Department of Thoracic Surgery, Zhejiang Cancer Hospital, University of Chinese Academy of Sciences, Hangzhou, China, [5] Department of Respiratory Medicine, The Affiliated Hospital of Jiaxing University, Jiaxing, China, [6] Department of Radiotherapy, Second Affiliated Hospital of Soochow University, Suzhou, China, [7] Department of Cardiothoracic Surgery, Affiliated Hospital of Nantong University, Nantong, China, [8] Department of Medical Oncology, Affiliated Hospital of Nantong University, Nantong, China

OPEN ACCESS

Edited by:
Hubing Shi,
Sichuan University, China

Reviewed by:
Zhong-Yi Dong,
Southern Medical University, China
Jelena Stojsic,
University of Belgrade, Serbia

***Correspondence:**
Mei Li
13862901258@163.com
Honggang Ke
khg1220@163.com

[†]These authors have contributed equally to this work

Specialty section:
This article was submitted to Thoracic Oncology, a section of the journal Frontiers in Oncology

Received: *09 February 2021*
Accepted: *27 April 2021*
Published: *27 May 2021*

Citation:
Wang X, Wu B, Yan Z, Wang G, Chen S, Zeng J, Tao F, Xu B, Ke H and Li M (2021) Association of PTPRD/PTPRT Mutation With Better Clinical Outcomes in NSCLC Patients Treated With Immune Checkpoint Blockades. Front. Oncol. 11:650122. doi: 10.3389/fonc.2021.650122

The common gamma receptor–dependent cytokines and their JAK-STAT pathways play important roles in T cell immunity and have been demonstrated to be related with response to immune checkpoint blockades (ICBs). PTPRD and PTPRT are phosphatases involved in JAK-STAT pathway. However, their clinical significance for non-small cell lung cancer (NSCLC) treated with ICBs is still unclear. Genomic and survival data of NSCLC patients administrated with anti–PD-1/PD-L1 or anti–CTLA-4 antibodies (Rizvi2015; Hellmann2018; Rizvi2018 Samstein2019) were retrieved from publicly accessible data. Genomic, survival and mRNA data of 1007 patients with NSCLC were obtained from The Cancer Genome Atlas (TCGA). *PTPRD/PTPRT* mutation was significantly associated with better progression-free survival (PFS) in three independent Rizvi2015, Hellmann2018 and Rizvi2018 cohorts. The median PFS for *PTPRD/PTPRT* mutant-type *vs*. wild-type NSCLC patients were not reached *vs*. 6.3 months (Rizvi2015, HR = 0.16; 95% CI, 0.02-1.17; P=0.03), 24.0 *vs*. 5.4 months (Hellmann2018, HR, 0.49; 95% CI, 0.26-0.94; P=0.03), 5.6 *vs*. 3.0 months (Rizvi2018, HR = 0.64; 95% CI, 0.44-0.92; P=0.01) and 6.8 *vs*. 3.5 months (Pooled cohort, HR, 0.54; 95% CI, 0.39-0.73; P<0.0001) respectively. *PTPRD/PTPRT* mutation was an independent predictive factor for PFS in pooled cohort (P = 0.01). Additionally, *PTPRD/PTPRT* mutation associated with better overall survival (OS) in Samstein2019 cohort (19 *vs*. 10 months, P=0.03). While similar clinical benefits were not observed in patients without ICBs treatment (TCGA cohort, P=0.78). In the further exploratory analysis, *PTPRD/PTPRT* mutation was significantly associated with increased tumor mutation burden and higher mRNA expression of JAK1 and STAT1. Gene Set Enrichment Analysis revealed prominent

enrichment of signatures related to antigen processing and presentation in patients with *PTPRD/PTPRT* mutation. This work suggested that *PTPRD/PTPRT* mutation might be a potential positive predictor for ICBs in NSCLC. These results need to be further confirmed in future.

Keywords: *PTPRD*, *PTPRT*, JAK-STAT, immune checkpoint blockades, non-small cell lung cancer

INTRODUCTION

Lung cancer is the leading cause of cancer death worldwide with 1.6 million deaths per year (1). Approximately 85% of cases are non-small cell lung cancer (NSCLC), of which lung adenocarcinoma (LUAD) and lung squamous cell carcinoma (LUSC) are the common histological subtypes (2). With development of molecular diagnosis, tyrosine kinase inhibitors (TKIs) have become the standard therapy for NSCLC patients harboring EGFR or ALK alterations over the past two decades and brought great clinical benefit for NSCLC patients. However, as for patients without driver oncogenic gene, the improvement in survival was minimal before the appearance of immune checkpoint blockades (ICBs).

ICBs have demonstrated significant clinical benefit in NSCLC patients, including antibodies targeting programmed death receptor-1 (PD-1), its ligand (PD-L1) and cytotoxic T-lymphocyte antigen-4 (CTLA-4). Unfortunately, only a subset of patients could respond to current immunotherapy strategies. In order to increase the response rate to ICBs, identifying the patients who can benefit from ICBs and developing novel potential strategies are two common methods. Encouragingly, several biomarkers have been proposed as distinct positive predictor for ICBs therapy, such as MSI-H, PD-L1 expression (3, 4), tumor mutation burden (TMB) (5, 6), and the intensity of CD8+ T cell infiltrates (7). Additionally, several genomic alterations had been found to be correlated with the clinical outcomes in NSCLC patients who received ICBs. Dong et al. reported that *TP53* and *KRAS* mutations in NSCLC were associated with the increased PD-L1 expression and activated T-effector and interferon-γ signature (8). Zhang et al. uncovered significant correlation between *North1/2/3* mutation and better efficacy of ICBs (9). On the contrary, some negative predictors for ICBs therapy, including *JAK1/2*, *MDM2/4* and *EGFR* alternations were also reported in previous works (10, 11). Currently, exploring the role of gene alternations in the NSCLC patients who received ICBs remains valuable for precision therapies.

Common gamma receptor–dependent cytokines and their JAK-STAT pathways play important roles in T cell immunity (12). It was reported that IFNγ/STAT1/STAT3 signaling axis related to the upregulation expression of PD-L1 in lung tumors (13). Additionally, STAT1 activation could trigger IRF-1 expression and subsequent initiated MHC class I antigen presentation-associated gene expression (14). Noted that protein tyrosine phosphatase receptor type D or T (PTPRD or PTPRT) are two of receptor-protein tyrosine phosphatases (R-PTPs) in NSCLC, which were reported as the mediator of JAK-STAT signal pathway (15, 16). However, to our best knowledge, the clinical significance of *PTPRD* and *PTPRT* alterations for NSCLC treated with ICBs is still unclear. In the present work, we aimed to explore the relationship between *PTPRD/PTPRT* mutation and clinical outcomes of ICBs in NSCLC patients.

MATERIALS AND METHODS

Patients

Genomic and clinical data of NSCLC patients administrated with anti–PD-(L)1 or anti–CTLA-4 antibodies [Rizvi2015 (17), Hellmann2018 (18), Rizvi2018 (19) and Samstein 2019 (6)] were retrieved from publicly accessible data. The genomic, survival and mRNA data of 1226 patients with NSCLC were obtained from TCGA (www.cbioportal.org). As for the 3Dmed_NSCLC cohort, 1224 NSCLC patients were included from 22nd October 2019 to 15th April 2020 to explore the *PTPRD* and *PTPRT* mutation profiles in Chinese population. Their pathological diagnosis of the specimens was confirmed by hematoxylin and eosin (H&E) staining and the tumor tissue suffered to 733 cancer gene panel sequencing (3D Medicines Inc., Shanghai). All human sample collection and usage were in accordance with the principles of the Declaration of Helsinki and approved by Affiliated Hospital of Nantong University. All participated patients provided written consents.

Study Design

Any mutation including nonsense, frameshift and missense mutation in *PTPRD* or *PTPRT* was defined as *PTPRD/PTPRT* mutation. *PTPRD/PTPRT* wild-type suggested that both *PTPRD* and *PTPRT* were wild-type. TMB-high group was defined as TMB ≥ median. The primary outcome was progression-free survival (PFS), which was calculated from the date of first immunotherapy administration to disease progression. The secondary outcome was overall survival (OS), which was calculated from the date of first immunotherapy administrated until death due to any cause. We explored the association between *PTPRD*/PRPRT mutation and PFS or OS using univariable and multivariable regression analysis.

Statistical Analyses

Data analyses were performed using SPSS 20.0 (SPSS Inc., Chicago, IL). Survival description was illustrated by the Kaplan-Meier curves with P value determined by a log-rank test. Hazard's ratio (HR) was determined through a cox proportional hazards regression model. The associations between PFS and various variables were examined by

univariable and multivariable regression analysis. Continuous variables were compared by Mann-Whitney U test. False discovery rate (FDR) was used to adjust mRNA expression. Gene set enrichment analysis (GSEA) was used to determine potentially relevant gene expression signatures between patients harboring mutant-type or wild-type *PTPRD/PTPRT*. The java GSEA Desktop Application (GSEA 4.0.1) was downloaded from http://software.broadinstitute.org/gsea/index.jsp. The normalized enrichment score (NES) is the primary statistic for examining gene set enrichment results. The nominal P value estimates the statistical significance of the enrichment score. All reported P values were two-tailed, and P <0.05 or FDR <0.05 is considered statistically significant.

RESULTS

Association Between *PTPRD/PTPRT* Mutation and Better PFS in NSCLC Patients Who Received ICBs Therapy From Three Independent Cohorts

The detailed baseline characteristics of NSCLC patients in three independent cohorts (Rizvi2015; Hellmann2018 and Rizvi2018) were summarized in **Table 1**. (1) The Rizvi2015 cohort contains 34 advanced NSCLC patients and their tumor tissues were subjected to whole-exome sequencing (WES). (2) The Hellmann2018 cohort contains 75 patients with NSCLC as part of the CheckMate-012 study and WES was performed on tumor tissues. (3) The Rizvi2018 cohort contains 240 patients with advanced NSCLC and their tumor tissues were profiled with MSK-IMPACT gene panels (341-gene, 410-gene or 468-gene panel). All the three gene panels included *PTPRD* and *PTPRT* genes. In the pooled cohort, 349 advanced NSCLC patients were included. The overall frequency of *PTPRD/PTPRT* mutation in Rizvi2015, Hellmann2018, Rizvi2018 and pooled cohorts were 15%, 31%, 20% and 21% respectively.

The association between *PTPRD/PTPRT* mutation and PFS was analyzed in Rizvi2015, Hellmann2018, Rizvi2018 and pooled cohort respectively. As shown in **Figure 1**, *PTPRD/PTPRT* mutation was significantly associated with better PFS. The median PFS for *PTPRD/PTPRT* mutant-type *vs*. wild-type NSCLC patients were not reached *vs*. 6.3 months in Rizvi2015 cohort (HR = 0.16; 95% CI, 0.02-1.17; P=0.03), 24 *vs*. 5.4 months (HR, 0.49; 95% CI, 0.26-0.94; P=0.03) in Hellmann2018 cohort, 5.6 *vs*. 3.0 months (HR = 0.64; 95% CI, 0.44-0.92; P=0.01) in Rizvi2018 cohort and 6.8 *vs*. 3.5 months (HR, 0.54; 95% CI, 0.39-0.73; P<0.0001) in the pooled cohort respectively.

The association between *PTPRD* mutation and PFS was also explored in Rizvi2015, Hellmann2018, Rizvi2018 and pooled cohorts respectively. The corresponding results were shown in **Figure 2** respectively. In Rizvi2015 cohort, the median PFS in *PTPRD* mutant-type *vs*. wild-type NSCLC patients were not reached *vs*. 6.5 months (P=0.23). Although statistical significance was not obtained, *PTPRD* mutation tend to achieve longer PFS. In Hellmann2018 cohort, similar results also were observed, but with a marginal statistical significance. The median PFS in *PTPRD* mutant-type *vs*. wild-type NSCLC patients were not reached *vs*. 6.5 months (P=0.05). In Rizvi2018 cohort, *PTPRD* mutation were significantly associated with better PFS, and the median PFS in *PTPRD* mutant-type *vs*. wild-type NSCLC patients were 5.6 months *vs*. 3.1 months (P=0.04). In pooled cohort, significant association between *PTPRD* mutation and better PFS was also observed. The

TABLE 1 | Baseline characteristics of NSCLC patients in Rizvi2015, Hellmann2018, Rizvi2018 and pooled cohorts.

Characteristics	Rizvi2015	Hellmann2018	Rizvi2018	Pooled Cohort
Total n	34	75	240	349
Age, median (range)	62.5 (41-80)	66 (42-87)	66 (22-92)	65 (22-92)
Sex				
Male	16 (47%)	37 (49%)	118 (49%)	171 (49%)
Female	18 (53%)	38 (51%)	122 (51%)	178 (51%)
Cancer type n (%)				
Adenocarcinoma	34 (100%)	59 (79%)	186 (78%)	279 (80%)
Squamous	0 (0%)	16 (21%)	34 (14%)	50 (14%)
Others	0 (0%)	0 (%)	20 (8%)	20 (6%)
Agent				
PD-(L)1	34 (100%)	0 (0%)	206(86%)	240 (0%)
PD-(L)1+CTLA-4	0 (0%)	75 (100%)	34(14%)	109 (100%)
Smoking history, n (%)				
Current/former	28 (82%)	60 (80%)	193 (80%)	281 (80%)
Never	6 (18%)	15 (20%)	47 (20%)	68 (20%)
PDL1_expression				
≥1%	24 (70%)	45 (60%)	43 (18%)	112 (32%)
0%	6 (18%)	25 (33%)	41 (17%)	72 (21%)
Unknown	4 (12%)	5 (7%)	156 (65%)	165 (47%)
Gene, n (%)				
PTPRD mutation	3 (9%)	16 (21%)	30 (13%)	49 (14%)
PTPRT mutation	2 (6%)	9 (12%)	23 (10%)	34 (10%)
PTPRD/PTPRT mutation	5 (15%)	22 (29%)	47 (20%)	74 (21%)
PTPRD/PTPRT wild-type	29 (85%)	53 (71%)	193 (80%)	275 (79%)

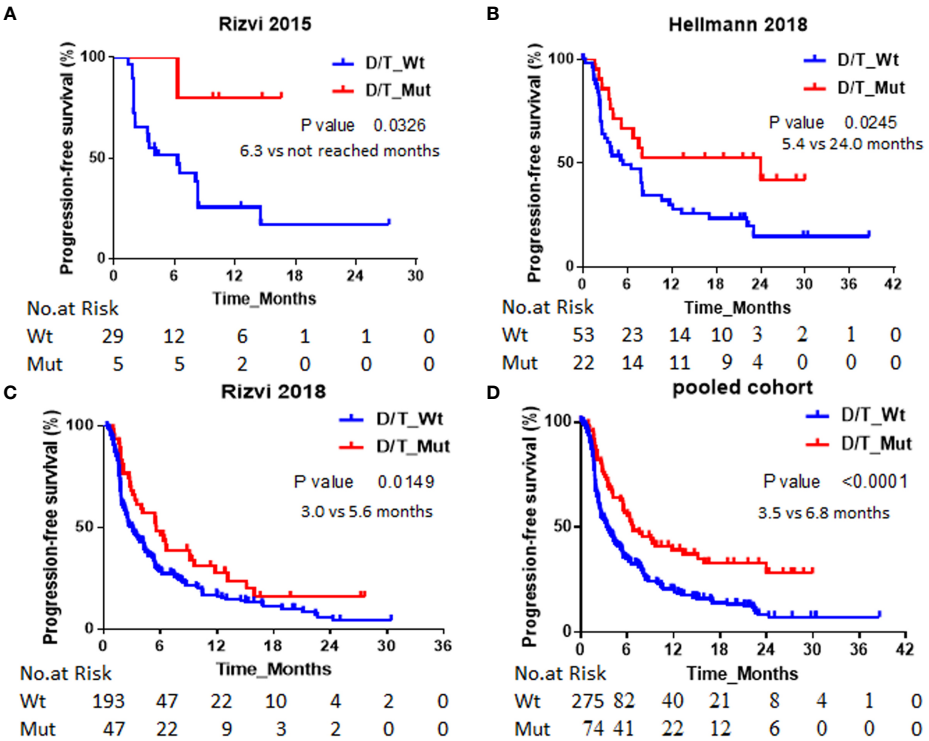

FIGURE 1 | Association between *PTPRD/PTPRT* mutation and PFS. Kaplan-Meier survival curves of PFS comparing NSCLC patients with *PTPRD/PTPRT* mutant-type and wild-type in of **(A)** Rizvi2015, **(B)** Hellmann2018, **(C)** Rizvi2018 and **(D)** pooled cohorts respectively. *PTPRD/PTPRT* mutation: D/T_Mut; *PTPRD/PTPRT* wild-type: D/T_Wt.

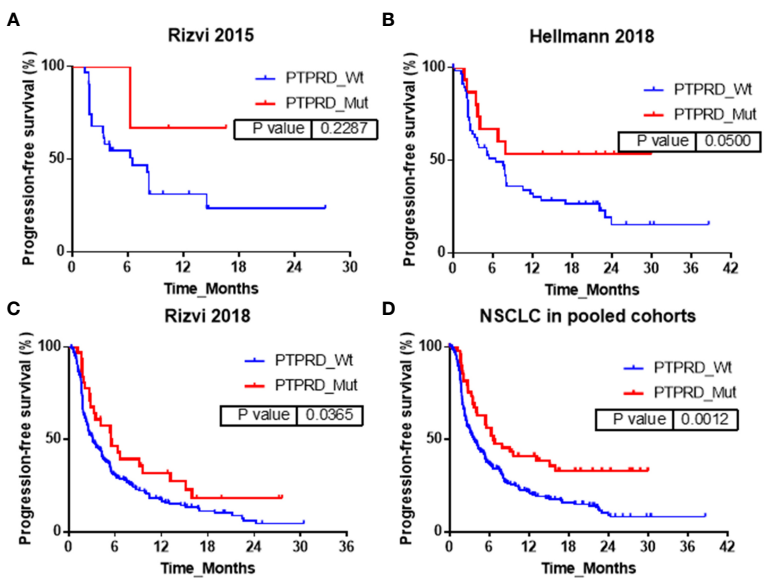

FIGURE 2 | Association between *PTPRD* mutation and PFS in **(A)** Rizvi2015, **(B)** Hellmann2018, **(C)** Rizvi2018 and **(D)** pooled cohorts.

median PFS in *PTPRD* mutant-type *vs*. wild-type NSCLC patients were 6.6 months *vs*. 3.6 months (P=0.001).

In addition, the influences of *PTPRT* mutation on PFS were also explored in Rizvi2015, Hellmann2018, Rizvi2018 and pooled cohorts respectively and the corresponding results were shown in **Figure 3**. In Rizvi2015 cohort, the median PFS in *PTPRT* mutant-type *vs*. wild-type NSCLC patients were not reached *vs*. 6.3 months respectively, with no statistically significant difference (P=0.10). In Hellmann2018 cohort similar results were also observed, but with a marginal statistical significance. The median PFS in *PTPRT* mutant-type *vs*. wild-type NSCLC patients were 24.0 months *vs*. 6.5 months (P=0.06). In Rizvi2018 cohort, *PTPRT* mutations were significantly associated with better PFS. The median PFS in *PTPRT* mutant-type *vs*. wild-type NSCLC patients was 6.0 months *vs*. 3.1 months (P=0.03). In pooled cohort, a significant association between *PTPRT* mutation and better PFS was also observed. The median PFS in *PTPRT* mutant-type *vs*. wild-type NSCLC patients were 9.2 months *vs*. 3.6 months (P=0.001).

The univariable and multivariable regression analysis of PFS the in Rizvi2015, Hellmann2018 and Rizvi2018 cohorts were summarized in **Table 2**. Several confounding factors were analyzed, including the age, sex and lines of therapy, PD-L1, TMB, smoker status, and *PTPRD/PTPRT* mutation. The multivariable analysis showed that *PTPRD/PTPRT* mutation was not significant associated with PFS in Rizvi2015 and Hellmann2018 cohort (HR 0.23, 95% CI, 0.03-2.04, p=0.18 and HR 0.59, 95% CI, 0.24-1.47, p=0.25, respectively). However, the multivariable analysis suggested that *PTPRD/PTPRT* mutation was an independent predictive factor for PFS in Rizvi2018 cohort (0.43, 95% CI, 0.20-0.92, p=0.03). The different outcomes between these independent cohorts might be due to the different size of patients. The deviation might exist in the conclusion of small cohorts (Rizvi2015, N=34 and Hellmann2018, N=75). In contrast, 240 NSCLC was included in the Rizvi2018 cohort. To further explore the influence of confounding factors on PFS, the univariable and multivariable regression analysis of PFS were also performed in pooled cohort. Notably, in the pooled cohort, the age (≥65 *vs*. <65 y), sex (male *vs*. female) and lines of therapy (lines of therapy ≥3 *vs*. <3), were not associated with PFS, no matter the univariable or multivariable regression analysis. In contrast, PD-L1, TMB, smoker status and *PTPRD/PTPRT* mutation were significantly associated with better PFS benefits. In the univariable analysis, PD-L1 status ≥1% *vs*. <1%, HR 0.60, 95% CI, 0.43-0.84, P =0.003; TMB≥ median *vs*. <median, HR 0.56, 95% CI, 0.44-0.72, P <0.001; Current or former *vs*. never smoker, HR 0.70, 95% CI, 0.52-0.93; P =0.01; *PTPRD/PTPRT* mutant-type *vs*. wild-type, HR 0.54, 95% CI, 0.39-0.73, p <0.001. In the multivariable analysis, PD-L1 status ≥1% *vs*. <1%, HR 0.67, 95% CI, 0.47-0.96, P =0.03; TMB≥ median *vs*. <median, HR 0.62, 95% CI, 0.42-0.92, P =0.02; Current or former *vs*. never smoker, HR 0.63, 95% CI, 0.41-0.97; P =0.04; *PTPRD/PTPRT* mutant-type *vs*. wild-type, HR 0.52, 95% CI, 0.31-0.87, p=0.01.

Association Between *PTPRD/PTPRT* Mutation and Better OS Benefit in NSCLC Patients Who Received ICBs Therapy

To explore whether *PTPRD/PTPRT* mutation is a predictive or prognostic biomarker for NSCLC, we retrieved the OS data from the Samstein2019 cohort and the Cancer Genome Atlas (TCGA) respectively. Samstein2019 cohort contains 350 advanced NSCLC patients treated with anti-PD- (L)1 monotherapy or combined therapy, and their tumor tissues were profiled with MSK-

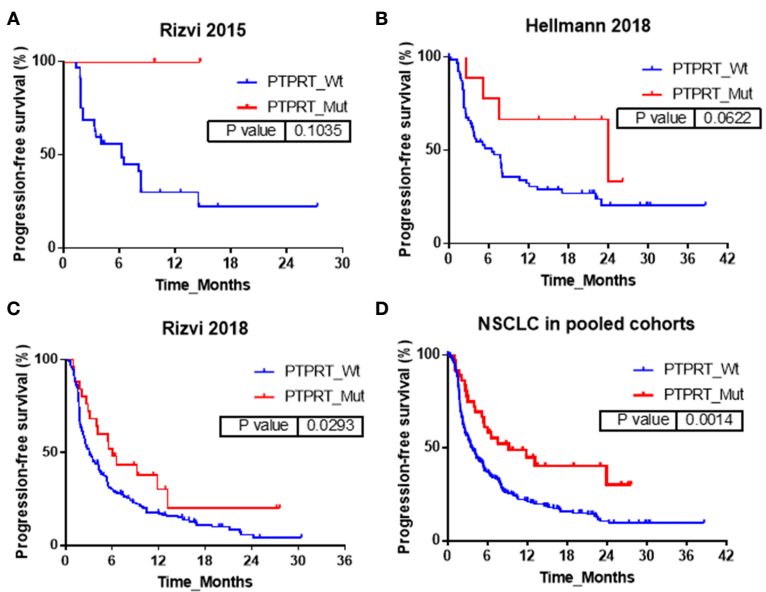

FIGURE 3 | Association between *PTPRT* mutation and PFS in **(A)** Rizvi2015, **(B)** Hellmann2018, **(C)** Rizvi2018 and **(D)** pooled cohorts.

TABLE 2 | Univariable and multivariable analyses of progression-free survival.

Rizvi2015				
Parameter	**Univariable Analysis**		**Multivariable Analysis**	
	HR (95%CI)	**P value**	**HR (95%CI)**	**P value**
Age ≥65 *vs*. <65 y	0.82 (0.33-2.01)	0.66	1.05 (0.33-3.38)	0.93
Male *vs*. female	1.75 (0.75-4.07)	0.20	1.09 (0.36-3.36)	0.88
Current or former *vs*. never smoker	0.60 (0.22-1.64)	0.32	0.67 (0.16-2.91)	0.60
TMB≥median *vs*. <median	0.21 (0.08-0.55)	0.002	0.20 (0.06-0.67)	0.01
PD-L1 status ≥1% *vs*. <1%	0.38 (0.14-1.01)	0.05	0.98 (0.33-2.98)	0.98
PTPRD/PTPRT mutant *vs*. wild	0.16 (0.02-1.17)	0.07	0.23 (0.03-2.04)	0.18
Lines of therapy ≥3 *vs*. <3	1.24 (0.53-2.91)	0.62	1.79 (0.46-6.93)	0.40
Hellmann2018				
Parameter	**Univariable Analysis**		**Multivariable Analysis**	
	HR (95%CI)	**P value**	**HR (95%CI)**	**P value**
Age ≥65 *vs*. <65 y	0.89 (0.51-1.55)	0.67	0.71 (0.37-1.36)	0.31
Male *vs*. female	1.03 (0.59-1.80)	0.92	1.03 (0.55-1.91)	0.94
Current or former *vs*. never smoker	0.70 (0.36-1.36)	0.29	0.78 (0.37-1.64)	0.51
TMB≥median *vs*. <median	0.49 (0.28-0.87)	0.02	0.59 (0.28-1.22)	0.16
PD-L1 status ≥1% *vs*. <1%	0.86 (0.47-1.59)	0.63	1.04 (0.52-2.07)	0.92
PTPRD/PTPRT mutant *vs*. wild	0.47 (0.24-0.92)	0.03	0.59 (0.24-1.47)	0.25
Rizvi2018				
Parameter	**Univariable Analysis**		**Multivariable Analysis**	
	HR (95%CI)	**P value**	**HR (95%CI)**	**P value**
Age ≥65 *vs*. <65 y	1.14 (0.86-1.52)	0.35	1.12 (0.69-1.81)	0.66
Male *vs*. female	1.09 (0.83-1.44)	0.54	0.88 (0.53-1.44)	0.60
Current or former *vs*. never smoker	0.69 (0.49-0.97)	0.03	0.59 (0.30-1.17)	0.13
TMB≥median *vs*. <median	0.65 (0.49-0.86)	0.003	0.94 (0.52-1.69)	0.84
PD-L1 status ≥1% *vs*. <1%	0.58 (0.36-0.92)	0.02	0.52 (0.31-0.88)	0.01
PTPRD/PTPRT mutant *vs*. wild	0.64 (0.44-0.92)	0.02	0.43 (0.20-0.92)	0.03
Lines of therapy ≥3 *vs*. <3	1.37 (1.00-1.88)	0.05	1.25 (0.70-2.20)	0.45
All NSCLC in pooled cohort				
Parameter	**Univariable Analysis**		**Multivariable Analysis**	
	HR (95%CI)	**P value**	**HR (95%CI)**	**P value**
Age ≥65 *vs*. <65 y	1.06 (0.83-1.35)	0.64	0.95 (0.67-1.35)	0.78
Male *vs*. female	1.13 (0.89-1.44)	0.31	1.00 (0.71-1.41)	0.99
Current or former *vs*. never smoker	0.70 (0.52-0.93)	0.01	0.63 (0.41-0.97)	0.04
TMB≥median *vs*. <median	0.56 (0.44-0.72)	<0.001	0.62 (0.42-0.92)	0.02
PD-L1 status ≥1% *vs*. <1%	0.60 (0.43-0.84)	0.003	0.67 (0.47-0.96)	0.03
PTPRD/PTPRT mutant *vs*. wild	0.54 (0.39-0.73)	<0.001	0.52 (0.31-0.87)	0.01
lines of therapy ≥3 *vs*. <3	0.88 (0.69-1.12)	0.30	0.80 (0.56-1.13)	0.21

IMPACT gene panels (341-gene or 410-gene panel). Forty-three (12%) patients harbored *PTPRD* mutation and thirty-five (10%) patients harbored *PTPRT* mutation. Eleven (3%) patients carried both *PTPRD* and *PTPRT* mutation. The overall frequency of *PTPRD/PTPRT* mutation was 19% (**Table S1**). Noted that 206 patients in Samstein2019 cohort were also contained in the Rizvi2018 cohort. **Figure 4A** showed that a significant OS benefit was observed in NSCLC patients with *PTPRD/PTPRT*

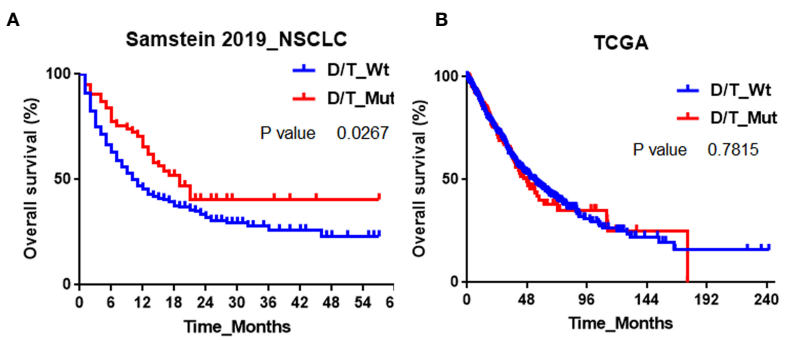

FIGURE 4 | Association between *PTPRD/PTPRT* mutation and OS in **(A)** Samstein2019 and **(B)** TCGA cohorts.

mutant-type compared to that with *PTPRD/PTPRT* wild-type in Samstein2019 cohort. The median OS in *PTPRD/PTPRT* mutant-type *vs.* wild-type NSCLC patients were 19 months *vs.* 10 months (P=0.03). As for *PTPRD* alone, the median OS in *PTPRD* mutant-type *vs.* wild-type NSCLC patients were 21 months *vs.* 11 months (P=0.01, **Figure S1A**). As for *PTPRT* alone, the median OS in *PTPRT* mutant-type *vs.* wild-type NSCLC patients were 19 months *vs.* 11 months (P=0.17, **Figure S1B**). The results of univariable and multivariable analysis in Samstein2019 cohort were summarized in **Table S2**. *PTPRD/PTPRT* mutation was significantly associated with better OS benefits in the univariable analysis (HR 0.66, 95% CI, 0.45-0.96, P =0.03) and in the multivariable analysis (HR 0.52, 95% CI, 0.31-0.87, P =0.045).

In contrast, for NSCLC patients who do not receive ICBs treatment (TCGA cohort), PTPRD/PTPRT mutation was not associated with a better OS benefit (**Figure 4B**). In TCGA, the *PTPRD* or *PTPRT* incidences are 13.7% and 10.7% in NSCLC respectively. The median OS in *PTPRD/PTPRT* mutant-type *vs.* wild-type NSCLC patients were 47.4 months *vs.* 53.3 months (P=0.78). As for *PTPRD*, the median OS in *PTPRD* mutant-type *vs.* wild-type NSCLC patients were 50.5 months *vs.* 54.1 months (P=0.67, **Figure S1C**). As for *PTPRT*, the median OS in *PTPRT* mutant-type *vs. PTPRT* wild-type NSCLC patients were 38.9 months *vs.* 54.1 months (P=0.22, **Figure S1D**). These results suggested that *PTPRD/PTPRT* mutation was a potential positive predictor for clinical benefit of anti-PD-(L)1 therapy in NSCLC instead of a prognosis factor for NSCLC.

Impact of *PTPRD/PTPRT* Mutation on TMB or Immune-Related Gene Signatures

To further understand the underlying mechanism of the association between *PTPRD/PTPRT* mutation and better clinical outcomes in NSCLC patients who received ICBs therapy, the impact of *PTPRD/PTPRT* mutation on TMB or immune-related gene signatures was explored. **Figures 5A–D** demonstrated that *PTPRD/PTPRT* mutation was associated with higher TMB in Rizvi2015, Hellmann2018, Rizvi2018 and TCGA cohorts (P<0.0001). We then analyzed the mRNA data from TCGA to compare mRNA expression of immune related genes between *PTPRD/PTPRT* mutant-type and wild-type NSCLC patients. The list of immune-related genes in **Table S3** was analyzed in this work. As shown in **Figure S2** and **Figures 5E, F**, the mRNA expressions of JAK1 and STAT1 were higher in *PTPRD/PTPRT* mutant-type than wild-type NSCLC patients ($p < 0.05$). What's more, GSEA was performed on gene sets in the Kyoto Encyclopedia of Genes and Genomes (KEGG) database. **Figure 5G** revealed enrichment of genes involved in antigen processing and presentation pathways were significantly enriched in NSCLC with *PTPRD/PTPRT* mutation (NES=2.35; FDR< 0.001).

Mutational Profiles of *PTPRD* or *PTPRT* in Chinese NSCLC 3DMed Cohort

To investigate the mutational profiles of *PTPRD* or *PTPRT* in Chinese NSCLC population, a total of 1224 cases of Chinese NSCLC who have undergone 733 cancer gene-panel *via* next-

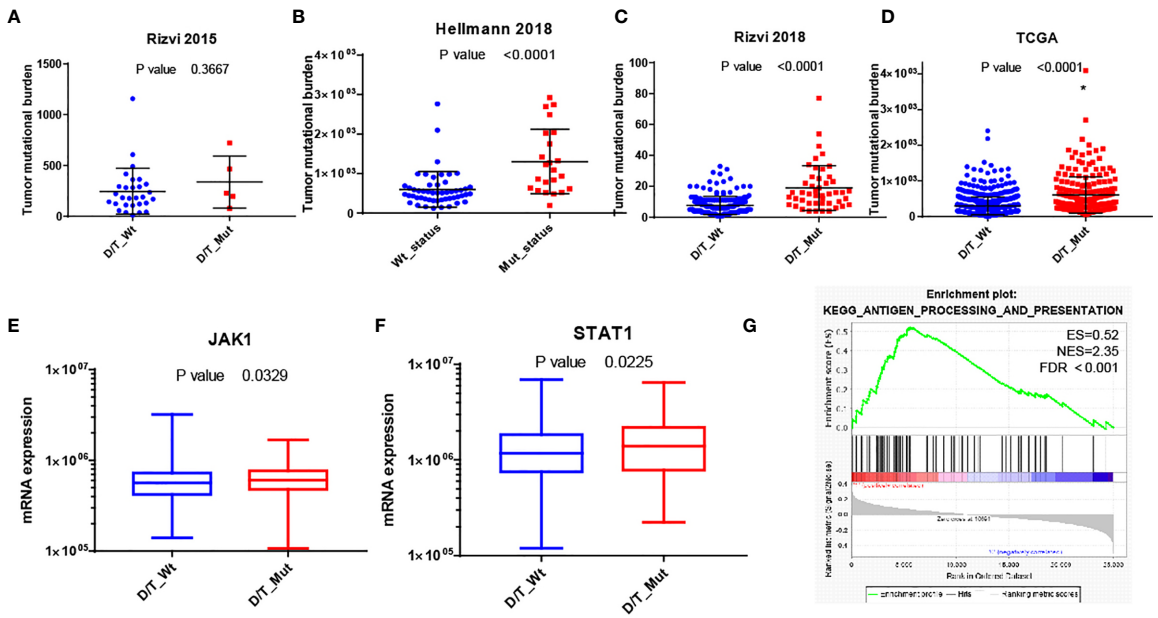

FIGURE 5 | Possible mechanism of the association of *PTPRD/PTPRT* mutation and better clinical outcomes of ICBs therapy. **(A–D)** Comparison of tumor mutational burden between *PTPRD/PTPRT* mutant-type and wild-type NSCLC patients in Rizvi2015, Hellmann2018, Rizvi2018 and TCGA cohorts respectively. **(E, F)** Comparing of mRNA expression of JAK1 and STAT1 between *PTPRD/PTPRT* mutant-type and wild-type NSCLC patients. **(G)** GSEA reveals prominent enrichment of signatures related to antigen processing and presentation in NSCLC patients with PTPRD/PTPRT mutation. *PTPRD/PTPRT* mutation: D/T_Mut; *PTPRD/PTPRT* wild-type: D/T_Wt.

generation sequencing (NGS) were included in this study, including 886 patients with lung adenocarcinoma and 188 patients with lung squamous cell carcinoma (**Table S4**). There were 768 male and 456 female patients. The median age was 63 (range 22-91). A total of 112 (9.2%) NSCLC patients with *PTPRD/PTPRT* mutation were identified. The incidences of patients with *PTPRD* or *PTPRT* mutation were 5.4% (N=66) and 4.7% (N=57) respectively, which was significantly lower than that of TCGA cohort (*PTPRD*: 5.4% *vs* 13.7%, p <0.0001; *PTPRT*: 4.7% *vs* 10.7%, p <0.0001). Such difference might result from the population. **Figure S3** described the graphical distribution of *PTPRD* and *PTPRT* mutation sites in Chinese NSCLC patients. No clear hotspot mutations and mutated codons were spread throughout *PTPRD* and *PTPRT*, including the phosphatase and extracellular domains, which was consistent with previous work (20).

DISCUSSION

In this work, *PTPRD/PTPRT* mutation was firstly identified as positive factor for better clinical benefit in NSCLC patients who received ICBs treatment. While no clinical benefits of OS were achieved in patients who do not receive ICBs treatment (TCGA cohort). Moreover, univariable and multivariable analysis further confirmed that *PTPRD/PTPRT* mutation was an independent positive predictor in pooled cohort. In the exploratory analysis, higher TMB and increased expression of genes related to JAK-STAT pathway activation served as potential mechanism underlying the predictive value of *PTPRD/PTPRT* mutation in NSCLC population. GSEA also revealed prominent enrichment of signatures related to antigen processing and presentation in patients with *PTPRD/PTPRT* mutation. Such results suggested that *PTPRD/PTPRT* mutation might be a potential positive predictor of NSCLC patients treated with ICBs.

Protein tyrosine phosphorylation is an important signaling event involved in a wide range of physiological processes in tumor development, whose level is balanced by antagonistic activities of protein tyrosine kinases and protein tyrosine phosphatases (PTPs) (21, 22). The classical PTPs are usually divided into two large groups according to their overall structure, including cytoplasmic non-receptor-type PTPs (NR-PTPs) and transmembrane R-PTPs. Noted that R-PTPs contain PTP domains and extracellular domains, which have intrinsic ability to transduce signals across the cell membrane (23). R-PTPs could not only antagonize tyrosine kinases but also engage extracellular ligands (24). Among R-PTPs, *PTPRD* and *PTPRT* belong to type IIa and IIb R-PTPs, respectively. *PTPRD* or *PTPRT* are identified as tumor suppressor, which is frequently inactivated and mutated in various human cancers. (25–30) For example, the reduced expression of *PTPRD* correlated with poor prognosis in gastric adenocarcinoma (31). Hsu et al. reported that deleterious mutations of *PTPRT* and *PTPRD* was significantly associated with bevacizumab resistance in metastatic colorectal cancer patients (16). Another study suggested that missense mutations in the catalytic domain of *PTPRT* or *PTPRD* were implicated in reducing its phosphatase activity, and mutations in the extracellular domain impair its function in cell adhesion (32, 33). Recently, Li et al. analyzed 2129 pan-cancer patients treated with ICBs, whose cancer genomic data are from the cBioPortal database (34). Compared with *PTPRT* wild-type, *PTPRT* nonsynonymous mutations were associated with better OS in melanoma (N=596) and in pan-cancer (N=2129), and was associated with better PFS in NSCLC (N=510). In the present work, we supposed that the association between *PTPRD/PTPRT* nonsynonymous mutation and good clinical outcomes of ICBs in NSCLC may partially on account of the up-regulation of JAK1 and STAT1 mRNA expression, which subsequently control the expression of chemokines with potent chemoattractant effect on T cells.

To our best knowledge, this is the first work to explore the relationship between *PTPRD/PTPRT* mutation and ICBs treatment in NSCLC patients. In view of the intrinsic property of retrospective study, several limitations exist in the present work. This analysis was based on public cohorts of NSCLC patients who underwent WES or multi-gene panel sequencing, which may yield selection bias. The possible mechanism of the association of *PTPRD/PTPRT* mutation and clinical outcomes of ICBs was performed in TCGA cohort. The application of these conclusions in the present study might be restricted by the limited quantity of patients. Such results should be confirmed in large cohorts.

CONCLUSION

Taken together, our results suggested that, in NSCLC patients receiving ICBs, *PTPRD/PTPRT* mutation was associated with better PFS and OS by increasing TMB and immune-related gene signatures. *PTPRD/PTPRT* mutation might be an important component of the immunogenetic landscape and should be integrated into predictive biomarker panels for ICBs therapy. In view of the intrinsic property of retrospective study, such conclusions should be validated in future prospective clinical trials.

DATA AVAILABILITY STATEMENT

The datasets presented in this study can be found in online repositories. The names of the repository/repositories and accession number(s) can be found in the article/**Supplementary Material**.

ETHICS STATEMENT

All human sample collection and usage were in accordance with the principles of the Declaration of Helsinki and approved by Affiliated Hospital of Nantong University. This study was approved by the Ethics Committee of Affiliated Hospital of Nantong University(2019-K065). All participated patients provided written consents.

AUTHOR CONTRIBUTIONS

HK, ML, XW, and BW designed and performed the experiments, prepared the figures and decided to publish. JZ, FT, and BX

collected clinical data. ZY and GW analyzed the clinical and TCGA data. ZY and SC prepared the manuscript. All authors contributed to the article and approved the submitted version.

ACKNOWLEDGMENTS

ZY, GW, and SC are employees of 3D Medicines Inc.

SUPPLEMENTARY MATERIAL

The Supplementary Material for this article can be found online at: https://www.frontiersin.org/articles/10.3389/fonc.2021.650122/full#supplementary-material

Supplementary Figure 1 | Association between **(A)** *PTPRD* or **(B)** *PTPRT* mutation and OS in Samstein 2019 cohort respectively. Association between **(C)** *PTPRD* or **(D)** *PTPRT* mutation and OS in TCGA cohort respectively.

Supplementary Figure 2 | Heatmap depicting the mRNA expression of immune-related genes between *PTPRD/PTPRT* mutant-type and wild-type NSCLC patients.

Supplementary Figure 3 | Graphical distribution of **(A)** *PTPRD* and **(B)** *PTPRT* mutations in Chinese 3Dmed_NSCLC cohort.

Supplementary Table 1 | Baseline characteristics of Samstein 2019.

Supplementary Table 2 | Univariable and multivariable analysis of OS in Samstein 2019.

Supplementary Table 3 | The list of immune-related genes analyzed in the work.

Supplementary Table 4 | Baseline characteristics of 3DMed NSCLC cohort.

REFERENCES

1. Torre LA, Bray F, Siegel RL, Ferlay J, Lortet-Tieulent J, Jemal A. Global Cancer Statistics, 2012. *CA: Cancer J Clin* (2015) 65(2):87–108. doi: 10.3322/caac.21262
2. Herbst RS, Morgensztern D, Boshoff C. The Biology and Management of non-Small Cell Lung Cancer. *Nature* (2018) 553(7689):446–54. doi: 10.1038/nature25183
3. Herbst RS, Baas P, Kim D-W, Felip E, Pérez-Gracia JL, Han J-Y, et al. Pembrolizumab Versus Docetaxel for Previously Treated, PD-L1-Positive, Advanced Non-Small-Cell Lung Cancer (KEYNOTE-010): A Randomised Controlled Trial. *The Lancet* (2016) 387(10027):1540–50. doi: 10.1016/s0140-6736(15)01281-7
4. Mok TSK, Wu Y-L, Kudaba I, Kowalski DM, Cho BC, Turna HZ, et al. Pembrolizumab Versus Chemotherapy for Previously Untreated, PD-L1-expressing, Locally Advanced or Metastatic non-Small-Cell Lung Cancer (KEYNOTE-042): A Randomised, Open-Label, Controlled, Phase 3 Trial. *Lancet* (2019) 393(10183):1819–30. doi: 10.1016/s0140-6736(18)32409-7
5. Wang Z, Duan J, Cai S, Han M, Dong H, Zhao J, et al. Assessment of Blood Tumor Mutational Burden as a Potential Biomarker for Immunotherapy in Patients With Non-Small Cell Lung Cancer With Use of a Next-Generation Sequencing Cancer Gene Panel. *JAMA Oncol* (2019) 5(5):696–702. doi: 10.1001/jamaoncol.2018.7098
6. Samstein RM, Lee CH, Shoushtari AN, Hellmann MD, Shen R, Janjigian YY, et al. Tumor Mutational Load Predicts Survival After Immunotherapy Across Multiple Cancer Types. *Nat Genet* (2019) 51(2):202–6. doi: 10.1038/s41588-018-0312-8
7. Sanmamed MF, Chen L. A Paradigm Shift in Cancer Immunotherapy: From Enhancement to Normalization. *Cell* (2018) 175(2):313–26. doi: 10.1016/j.cell.2018.09.035
8. Dong ZY, Zhong WZ, Zhang XC, Su J, Xie Z, Liu SY, et al. Potential Predictive Value of TP53 and KRAS Mutation Status for Response to PD-1 Blockade Immunotherapy in Lung Adenocarcinoma. *Clin Cancer Res* (2017) 23(12):3012–24. doi: 10.1016/j.jtho.2016.11.504
9. Zhang K, Hong X, Song Z, Xu Y, Li C, Wang G, et al. Identification of Deleterious Notch Mutation as Novel Predictor to Efficacious Immunotherapy in NSCLC. *Clin Cancer Res* (2020) 26(14):3649–61. doi: 10.1158/1078-0432.CCR-19-3976
10. Shin DS, Zaretsky JM, Escuin-Ordinas H, Garcia-Diaz A, Hu-Lieskovan S, Kalbasi A, et al. Primary Resistance to PD-1 Blockade Mediated by JAK1/2 Mutations. *Cancer Discovery* (2017) 7(2):188–201. doi: 10.1158/2159-8290.CD-16-1223
11. Kato S, Goodman A, Walavalkar V, Barkauskas DA, Sharabi A, Kurzrock R. Hyperprogressors After Immunotherapy: Analysis of Genomic Alterations Associated With Accelerated Growth Rate. *Clin Cancer Res* (2017) 23(15):4242–50. doi: 10.1158/1078-0432.CCR-16-3133
12. Waldmann TA, Chen J. Disorders of the JAK/STAT Pathway in T Cell Lymphoma Pathogenesis: Implications for Immunotherapy. *Annu Rev Immunol* (2017) 35:533–50. doi: 10.1146/annurev-immunol-110416-120628
13. Narayanapillai SC, Han YH, Song JM, Kebede ME, Upadhyaya P, Kassie F. Modulation of the PD-1/PD-L1 Immune Checkpoint Axis During Inflammation-Associated Lung Tumorigenesis. *Carcinogenesis* (2020) 41(11):1518–28. doi: 10.1093/carcin/bgaa059
14. Zhou F. Molecular Mechanisms of IFN-gamma to Up-Regulate MHC Class I Antigen Processing and Presentation. *Int Rev Immunol* (2009) 28(3-4):239–60. doi: 10.1080/08830180902978120
15. Xu D, Qu CK. Protein Tyrosine Phosphatases in the JAK/STAT Pathway. *Front Biosci* (2008) 13:4925–32. doi: 10.2741/3051
16. Hsu H-C, Lapke N, Chen S-J, Lu Y-J, Jhou R-S, Yeh C-Y, et al. PTPRT and PTPRD Deleterious Mutations and Deletion Predict Bevacizumab Resistance in Metastatic Colorectal Cancer Patients. *Cancers* (2018) 10(9). doi: 10.3390/cancers10090314
17. Rizvi NA, Hellmann MD, Snyder A, Kvistborg P, Makarov V, Havel JJ, et al. Cancer Immunology. Mutational Landscape Determines Sensitivity to PD-1 Blockade in non-Small Cell Lung Cancer. *Science* (2015) 348(6230):124–8. doi: 10.1126/science.aaa1348.
18. Hellmann MD, Nathanson T, Rizvi H, Creelan BC, Sanchez-Vega F, Ahuja A, et al. Genomic Features of Response to Combination Immunotherapy in Patients With Advanced non-Small-Cell Lung Cancer. *Cancer Cell* (2018) 33(5):843–52.e4. doi: 10.1016/j.ccell.2018.04.005
19. Rizvi H, Sanchez-Vega F, La K, Chatila W, Jonsson P, Halpenny D, et al. Molecular Determinants of Response to Anti-Programmed Cell Death (PD)-1 and Anti-Programmed Death-Ligand 1 (Pd-L1) Blockade in Patients With Non-Small-Cell Lung Cancer Profiled With Targeted Next-Generation Sequencing. *J Clin Oncol Off J Am Soc Clin Oncol* (2018) 36(7):633–41. doi: 10.1200/jco.2017.75.3384
20. Mitchell KA, Nichols N, Tang W, Walling J, Stevenson H, Pineda M, et al. Recurrent PTPRT/JAK2 Mutations in Lung Adenocarcinoma Among African Americans. *Nat Commun* (2019) 10(1):5735. doi: 10.1038/s41467-019-13732-y
21. Yu DJRG. Receptor Type Protein Tyrosine Phosphatases in Cancer. *Chin J Cancer* (2015) 34(2):61–9. doi: 10.5732/cjc.014.10146
22. Tonks NK. Protein Tyrosine Phosphatases: From Genes, to Function, to Disease. *Nat Rev Mol Cell Biol* (2006) 7(11):833–46. doi: 10.1038/nrm2039
23. Senis YA, Barr AJ. Targeting Receptor-Type Protein Tyrosine Phosphatases With Biotherapeutics: Is Outside-in Better Than Inside-Out? *Molecules* (2018) 23(3). doi: 10.3390/molecules23030569
24. Nikolaienko RM, Agyekum B, Bouyain S. Receptor Protein Tyrosine Phosphatases and Cancer: New Insights From Structural Biology. *Cell Adh Migr* (2012) 6(4):356–64. doi: 10.4161/cam.21242
25. Ortiz B, Fabius AW, Wu WH, Pedraza A, Brennan CW, Schultz N, et al. Loss of the Tyrosine Phosphatase PTPRD Leads to Aberrant STAT3 Activation and Promotes Gliomagenesis. *Proc Natl Acad Sci U.S.A.* (2014) 111(22):8149–54. doi: 10.1073/pnas.1401952111
26. Lui VW, Peyser ND, Ng PK, Hritz J, Zeng Y, Lu Y, et al. Frequent Mutation of Receptor Protein Tyrosine Phosphatases Provides a Mechanism for STAT3 Hyperactivation in Head and Neck Cancer. *Proc Natl Acad Sci U.S.A.* (2014) 111(3):1114–9. doi: 10.1073/pnas.1319551111

27. Zhang X, Guo A, Yu J, Possemato A, Chen Y, Zheng W, et al. Identification of STAT3 as a Substrate of Receptor Protein Tyrosine Phosphatase T. *Proc Natl Acad Sci United States America* (2007) 104:4060–4. doi: 10.1073/pnas.0611665104
28. Solomon DA, Kim JS, Cronin JC, Sibenaller Z, Ryken T, Rosenberg SA, et al. Mutational Inactivation of PTPRD in Glioblastoma Multiforme and Malignant Melanoma. *Cancer Res* (2008) 68(24):10300–6. doi: 10.1158/0008-5472.CAN-08-3272
29. Ortiz B, White JR, Wu WH, Chan TA. Deletion of Ptprd and Cdkn2a Cooperate to Accelerate Tumorigenesis. *Oncotarget* (2014) 5(16):6976–82. doi: 10.18632/oncotarget.2106
30. Veeriah C Brennan S, Meng S, Singh B, Fagin JA, Solit DB, Paty PB, et al. The Tyrosine Phosphatase PTPRD is a Tumor Suppressor That is Frequently Inactivated and Mutated in Glioblastoma and Other Human Cancers. *PNAS* (2009) 106(23)9435–40. doi: 10.1073/pnas.0900571106
31. Wang D, Wang L, Zhou J, Pan J, Qian W, Fu J, et al. Reduced Expression of PTPRD Correlates With Poor Prognosis in Gastric Adenocarcinoma. *PloS One* (2014) 9(11):e113754. doi: 10.1371/journal.pone.0113754
32. Kim M, Morales LD, Jang IS, Cho YY, Kim DJ. Protein Tyrosine Phosphatases as Potential Regulators of STAT3 Signaling. *Int J Mol Sci* (2018) 19(9):2708. doi: 10.3390/ijms19092708
33. Wang Z, Shen D, Parsons DW, Bardelli A, Sager J, Szabo S, et al. Mutational Analysis of the Tyrosine Phosphatome in Colorectal Cancers. *Science* (2004) 304(5674):1164–6. doi: 10.1126/science.1096096
34. Li A, Lin D, Yu Y, Gu Y, Ou Q, Zhang W, et al. Association of PTPRT Mutation With Survival of Immune Checkpoint Inhibitor in Patients With Cancer. *Ann Oncol* (2019) 30:xi52. doi: 10.1093/annonc/mdz452.014

Conflict of Interest: ZY, GW and SC were employed by 3D Medicines Inc.

The remaining authors declare that the research was conducted in the absence of any commercial or financial relationships that could be construed as a potential conflict of interest.

Copyright © 2021 Wang, Wu, Yan, Wang, Chen, Zeng, Tao, Xu, Ke and Li. This is an open-access article distributed under the terms of the Creative Commons Attribution License (CC BY). The use, distribution or reproduction in other forums is permitted, provided the original author(s) and the copyright owner(s) are credited and that the original publication in this journal is cited, in accordance with accepted academic practice. No use, distribution or reproduction is permitted which does not comply with these terms.

frontiers in Oncology

ORIGINAL RESEARCH
published: 28 May 2021
doi: 10.3389/fonc.2021.663612

The Impact of VEGF Inhibition on Clinical Outcomes in Patients With Advanced Non-Small Cell Lung Cancer Treated With Immunotherapy: A Retrospective Cohort Study

Keiko Tanimura[1], Tadaaki Yamada[1], Ayaka Omura[2], Shinsuke Shiotsu[2], Nobutaka Kataoka[3], Takayuki Takeda[3], Ryusuke Taniguchi[4], Takahiro Yamada[4], Mayumi Takeuchi[5], Yusuke Chihara[5], Yoshie Morimoto[1], Masahiro Iwasaku[1], Yoshiko Kaneko[1], Junji Uchino[1] and Koichi Takayama[1]*

[1] Department of Pulmonary Medicine, Graduate School of Medical Science, Kyoto Prefectural University of Medicine, Kyoto, Japan, [2] Department of Respiratory Medicine, Japanese Red Cross Kyoto Daiichi Hospital, Kyoto, Japan, [3] Department of Respiratory Medicine, Japanese Red Cross Kyoto Daini Hospital, Kyoto, Japan, [4] Department of Pulmonary Medicine, Matsushita Memorial Hospital, Osaka, Japan, [5] Department of Respiratory Medicine, Uji-Tokushukai Medical Center, Kyoto, Japan

OPEN ACCESS

Edited by:
Udo S. Gaipl,
University Hospital Erlangen, Germany

Reviewed by:
Jian-Guo Zhou,
University of Erlangen Nuremberg, Germany
Tiziana Schioppa,
University of Brescia, Italy

***Correspondence:**
Tadaaki Yamada
tayamada@koto.kpu-m.ac.jp

Specialty section:
This article was submitted to Cancer Immunity and Immunotherapy, a section of the journal Frontiers in Oncology

Received: 05 February 2021
Accepted: 16 April 2021
Published: 28 May 2021

Citation:
Tanimura K, Yamada T, Omura A, Shiotsu S, Kataoka N, Takeda T, Taniguchi R, Yamada T, Takeuchi M, Chihara Y, Morimoto Y, Iwasaku M, Kaneko Y, Uchino J and Takayama K (2021) The Impact of VEGF Inhibition on Clinical Outcomes in Patients With Advanced Non-Small Cell Lung Cancer Treated With Immunotherapy: A Retrospective Cohort Study. Front. Oncol. 11:663612. doi: 10.3389/fonc.2021.663612

Background: In recent years, immune checkpoint inhibitors (ICIs) in combination with chemotherapy have increased survival in patients with advanced non-small cell lung cancer (NSCLC). Vascular endothelial growth factor (VEGF), which plays a key role in tumor angiogenesis, is an immunological modulator; therefore, it is expected that anti-VEGF therapy in combination with ICIs enhances the antitumor effect of ICIs. In the present study, we investigated the impact of VEGF inhibition on clinical outcomes of NSCLC patients, including the efficacy of ICI treatment.

Methods: A total of 105 patients with advanced NSCLC who had been treated with ICIs were retrospectively analyzed to examine the relationship between the history of treatment with anti-VEGF agents and the clinical outcomes with ICI monotherapy.

Results: Patients who had received anti-VEGF therapy prior to ICIs showed shortened progression-free survival of ICI treatment and a decreased overall response rate to ICI treatment. By contrast, anti-VEGF therapy after ICI treatment was associated with increased survival, especially in patients who had also received anti-VEGF therapy prior to ICI therapy.

Conclusions: These retrospective observations suggest that anti-VEGF therapy prior to ICIs might be a negative predictor of response to ICIs. The sequence of anti-VEGF therapy might play a role in its ability to predict survival in NSCLC patients. Further investigation is warranted to identify the role of VEGF inhibition in altering clinical outcomes after immunotherapy.

Keywords: immune checkpoint inhibitors, immunotherapy, anti-VEGF therapy, non-small cell lung cancer, treatment response

INTRODUCTION

Lung cancer is the leading cause of cancer-related death worldwide (1). Novel strategies for treating advanced lung cancer have progressed in recent years. One strategy has been the successful treatment of non-small cell lung cancer (NSCLC) with angiogenesis inhibitors. In addition, cancer immunotherapies, including programmed cell death protein 1 (PD-1)/programmed death ligand 1 (PD-L1) and cytotoxic T lymphocyte-associated antigen 4 (CTLA-4) checkpoint inhibitors, are being developed as promising alternative strategies for treating patients with advanced NSCLC. Several phase III clinical trials have shown improved outcomes with these immune checkpoint inhibitors (ICIs), such as prolonged survival and a more durable treatment response (2–7). However, as with chemotherapy and molecular-targeted therapy, some patients show intrinsic resistance to ICIs, and a majority of patients treated with ICIs develop acquired resistance.

The tumor microenvironment (TME), which consists of blood vessels, stromal cells, fibroblasts, signaling molecules, immune cells, and extracellular matrix components, is controlled by extracellular signals released from tumors. Vascular endothelial growth factor (VEGF), which is produced by tumor cells and surrounding stromal cells, promotes angiogenesis by binding VEGF receptor (VEGFR) on vascular endothelial cells. VEGF is also a potential modulator of the innate immune response. VEGF/VEGFR signaling promotes evasion of the antitumor immune response through multiple mechanisms, including suppression of dendritic-cell maturation (8), reducing cytotoxic T lymphocyte activity *via* production of inflammatory cytokines and upregulation of immune checkpoint expression (9, 10), activation of regulatory T cells (Tregs) (11), and accumulation of myeloid-derived suppressor cells (MDSCs) (12). High levels of pretreatment serum VEGF are associated with poor response to immunotherapy in malignant melanoma (13). Further, in a preclinical model, VEGF/VEGFR blockade restores immunosuppressive alterations caused by VEGF production, and combination of VEGF/VEGFR blockade with immunotherapy improves the antitumor immune response (14).

Bevacizumab, which is a recombinant, humanized monoclonal antibody that binds all isoforms of VEGF-A, shows favorable outcomes in combination with chemotherapy in NSCLC patients (15). Additionally, a previous study demonstrated that combination of bevacizumab with the CTLA-4 inhibitor ipilimumab enhanced infiltration of CD8+ T-cells compared to ipilimumab monotherapy in malignant melanoma (16). In recent years, some clinical study demonstrated that combination of anti-VEGF agents and ICIs prolongs survival compared to anti-VEGF alone in multiple carcinomas such as renal cell carcinoma and hepatocellular carcinoma (17, 18). The IMpower150 trial demonstrated significant improvement in survival in non-squamous NSCLC patients receiving atezolizumab, bevacizumab, carboplatin, and paclitaxel compared to patients receiving bevacizumab, carboplatin, and paclitaxel (19). On the other hand, a previous study demonstrated that prior anti-VEGF therapy was a negative predictive factor for the treatment efficacy of ICIs in metastatic renal cell carcinoma (20). However, studies in NSCLC patients who had received immunotherapy indicated a survival benefit of ICIs following chemotherapy combined with an angiogenesis inhibitor (21–23). Therefore, the impact of anti-VEGF therapy on the efficacy of immunotherapy is not fully understood in NSCLC patients. In this study, we conducted a retrospective investigation focused on the impact of VEGF inhibition on clinical outcomes in patients with advanced NSCLC treated with ICIs.

Abbreviations: PD-1, programmed cell death 1; PD-L1, programmed death ligand 1; CTLA-4, cytotoxic T lymphocyte-associated antigen 4; NSCLC, non-small cell lung cancer; ICI, immune checkpoint inhibitor; TME, tumor microenvironment; VEGF: vascular endothelial growth factor; VEGFR, vascular endothelial growth factor receptor; Treg, regulator T cell; MDSC, myeloid-derived suppressor cell; OS, overall survival; PFS, progression-free survival; ORR, overall response rate; ECOG-PS, Eastern Cooperative Oncology Group-performance status; CI, confidence interval; HR, hazard ratio; FGF, fibroblast growth factor.

MATERIALS AND METHODS

Patients

We retrospectively analyzed the medical records of NSCLC patients who received ICIs from February 2016 to December 2017 at five institutions in Japan: the University Hospital Kyoto Prefectural University of Medicine (Kyoto, Japan), the Japanese Red Cross Kyoto Daiichi Hospital (Kyoto, Japan), the Japanese Red Cross Kyoto Daini Hospital (Kyoto, Japan), the Matsushita Memorial Hospital (Osaka, Japan), and the Uji-Tokushukai Medical Center (Kyoto, Japan). In total, 105 patients met the following inclusion criteria: 1) histologically or cytologically proven NSCLC; 2) age ≥ 20 years; 3) administered more than two cycles of anti-PD-1 antibodies (nivolumab or pembrolizumab); and 4) received systemic chemotherapy, including cytotoxic chemotherapy or molecular-targeted therapy, prior to ICI treatment. Patients were excluded if they met any of the following criteria: 1) patients who have uncontrolled serious infections, uncontrolled cardiovascular disease, and metabolic disorders, including diabetes mellitus; 2) patients who were pregnant or nursing; and 3) patients who were regarded as unsuitable for this study by the investigators.

The study was conducted in accordance with the Declaration of Helsinki. All patients provided written or electronic informed consent. The authors are accountable for all aspects of the work in ensuring that questions related to the accuracy or integrity of any part of the work are appropriately investigated and resolved. Each hospital study protocol was approved by the ethics committee of the respective hospital. We used the Response Evaluation Criteria in Solid Tumors version 1.1 for evaluation of treatment efficacy.

Statistical Analysis

Survival curves were calculated according to the Kaplan-Meier method. Gehan-Breslow-Wilcoxon method was used to compare survival. Overall survival (OS) was defined as the interval from the initial day of treatment to death from any cause. Progression-

free survival (PFS) was defined as the interval from the initial day of treatment to disease progression or death. Categorical variables, such as the overall response rate (ORR), were compared using Fisher's exact test. Cox proportional hazards models were used for multivariate analysis of PFS and OS, and logistic regression models were used for multivariate analysis of the ORR. For all analyses, a p-value less than 0.05 indicated statistical significance.

Software Tools

Statistical analyses were performed using GraphPad Prism8 (GraphPad Software, San Diego, CA, USA) and EZR statistical software version 1.50 (Saitama Medical Center, Jichi Medical University, Saitama, Japan), which is a graphical user interface for R (The R Foundation for Statistical Computing, Vienna, Austria). More precisely, it is a modified version of R commander designed to add statistical functions frequently used in biostatistics.

RESULTS

Patient Characteristics

The data cutoff date for the survival analysis was May 1, 2020. The median duration of follow-up for surviving participants was 36.8 months (range, 4.1-51.6 months). Of the 105 NSCLC patients treated with ICIs, 35 (33%) were treated with anti-VEGF agents before ICIs (pre-anti-VEGF) and 70 (67%) patients were not treated with anti-VEGF agents before ICIs (no pre-anti-VEGF) (**Figure 1**). The characteristics of the two groups are listed in **Table 1**. Non-squamous cell carcinoma was more common in the pre-anti-VEGF group than in the no pre-anti-VEGF group, and radiation therapy was less common in the pre-anti-VEGF group. Other factors, including the occurrence of immune related adverse events and peripheral blood findings, did not differ between the two groups (**Table 1**, **Supplementary Table 1**).

Efficacy and Survival Analysis for ICIs in Patients Previously Treated With Anti-VEGF Therapy

To investigate prognostic factors related to clinical outcomes, we conducted univariate and multivariate analyses for ORR, PFS and OS. The ORR of ICI treatment was significantly lower in the pre-anti-VEGF group than that in the no pre-anti-VEGF group in univariate analysis (17% and 33%, respectively; p = 0.014) (**Figure 2**). Multivariate analysis showed that a treatment history of anti-VEGF agents was independently associated with a poor response to ICI treatment [OR: odds ratio 0.30 (95% CI: 0.09-

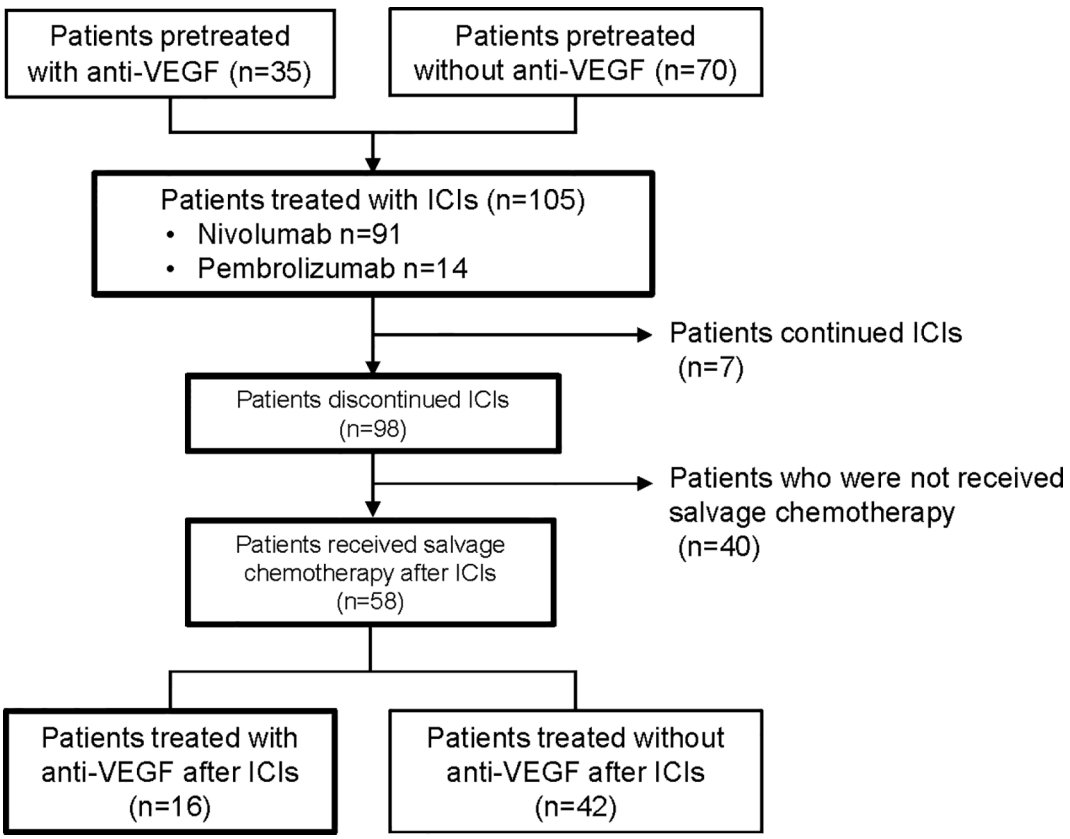

FIGURE 1 | Flow diagram of patients included in the analysis. VEGF, vascular endothelial growth factor; ICI, immune checkpoint inhibitor.

TABLE 1 | Characteristics of patients included in this study

	Pre-anti-VEGF (n=35)	No pre-anti-VEGF (n=70)	*p value*
Characteristics at Start of ICI			
Age-median (range), years	69 (41–83)	71 (46-83)	0.104
Sex-n. (%)			
Male	21 (60)	49 (70)	0.381
Female	14 (40)	21 (30)	
ECOG PS≥2 -2. (%)	3 (8.6)	14 (20)	0.167
Smoking history-2. (%)			
Current or former	26 (74.3)	54 (77.1)	0.81
Never	9 (25. 7)	16 (22.9)	
Histology-2. (%)			
Sq.	5.7 (26)	32 (45.7)	<0.001
Non-Sq.	94.3 (74)	38 (54.3)	
Driver oncogen-n. (%)			
With	28 (80)	47 (67.1)	0.069
Without	6 (17.1)	10 (14.3)	
Unknown	1 (2.9)	13 (18.6)	
PD-L 1 expression-n			
0%	4 (11.4)	3 (4.2)	0.347
<50%	5 (14.3)	12 (17.1)	
≥50%	5 (14.3)	14 (20)	
Unknown	21 (60)	41 (58.6)	
Corticosteroids and/or immunosuppressive agents -n. (%)	5 (14.3)	6 (8.6)	0.5
Autoimmune disease -n.(%)	3 (8.6)	3 (4.3)	0.398
ANC -(mean±SD, cells/rnrn^3)	4138 ± 1857	5095 ± 3014	0.088
ALC -(mean±SD, cells/rnrn^3)	1275 ± 518	1236 ± 573	0.23
AMC -(mean±SD, cells/rnrn^3)	536 ± 260	544 ± 301	0.89
Treatment history prior ICI therapy			
Platinum-based chemotherapy -n. (%)	34 (97.1)	66 (94.3)	0.663
Anti-angiogenic –n. (%)			
Bevacizurnab	31 (88.6)		
Ramucirumab	9 (25. 7)		
History of radiation -n.(%)	14 (40)	44 (62.9)	0.037
Information ofiCI therapy			
Information of ICI therapy			
Treatment line ofiCI-median (range)	3 (2-8)	3 (2-13)	0.346
ICI-n.(%)			
Nivolumab	30 (85.7)	61 (87.1)	1
Pembrolimmab	5 (14.3)	9 (12.9)	
irAE	12 (34.3)	30 (42.9)	0.527

VEGF, vascular endothelial growth factor; ICI, immune checkpoint inhibitor, ECOG PS, Eastern Cooperative Oncology Group performance status; Sq. squamous cell carcinoma; PD-L1, programmed death ligand 1; ANC, absolute neutrophil count; ALC, absolute lymphocyte count; AMC, absolute monicyte count.

0.96), p = 0.043] (**Table 2**). In the univariate analysis of PFS and OS, patients whose Eastern Cooperative Oncology Group-performance status (ECOG-PS) scores were ≥2 had significantly poorer PFS and OS than other patients (p = 0.039 and p < 0.001, respectively) (**Supplementary Table 2**). Multivariate analysis revealed that worse ECOG-PS and a treatment history of anti-VEGF agents were independently associated with poor PFS after immunotherapy [HR 2.26 (95% CI: 1.20-4.29), p = 0.012 and HR 1.83 (95% CI: 1.05-3.20), p = 0.033, respectively] (**Table 2**). By contrast, a treatment history of anti-VEGF agents was not significantly associated with OS [HR 1.47 (95% CI: 0.76-2.82), p = 0.249] (**Table 2**). Furthermore, propensity score matched analysis was performed to balance the characteristics between groups with or without anti-VEGF therapeutic history. After matching, the mean propensity scores for pre-anti-VEGF and no-anti-VEGF were 0.444 ± 0.162 and 0.444 ± 0.162, respectively (p = 1) (**Supplemnetary Table 3**). Pre-anti-VEGF group showed marginally shorten PFS of ICI treatment in the full cohort, however, this tendency was emphasized in the property score matched cohort (**Figure 3**).

Effect of Sequence of Anti-VEGF Agents With Regard to ICI Treatment on Patient Outcomes

To further reveal the impact of VEGF inhibition on patient outcomes, we examined the effect of the sequence of anti-VEGF therapy related to ICI treatment. Among the 98 patients who discontinued ICI treatment, previous treatment with anti-VEGF agents (n = 34) showed a trend toward prolonged OS compared to no previous treatment with anti-VEGF agents (n = 64) [median OS 20.1 months (95% CI 12.7-26.6) and 11.0 months (95% CI 6.6-15.5), respectively; p = 0.216] and post-ICI survival time [HR: 0.68 (95% CI: 0.42-1.09), p = 0.027] (**Figures 4A, B**). Patients who received anti-VEGF agents after ICIs tended to have longer post-ICI survival than those who did not receive anti-VEGF therapy after ICIs [HR 0.66 (95% CI 0.34-1.29), p = 0.195] (**Figure 4C**). Furthermore, a therapeutic history of anti-VEGF therapy prior to ICIs was associated with a favorable prognosis after ICIs among patients who received anti-VEGF therapy after ICIs [HR: 0.57 (95% CI: 0.14-2.24), p = 0.044) (**Figure 4D**).

DISCUSSION

This retrospective study revealed the impact of the sequence of anti-VEGF inhibition on clinical outcomes related to ICI treatment in NSCLC patients. Anti-VEGF therapy prior to ICIs was shown to be a negative predictor of response to ICI treatment. The sequence of anti-VEGF therapy might play a role in its ability to predict survival in NSCLC patients. Thus, it is important to establish a therapeutic strategy that maximizes the therapeutic effect of ICIs and anti-VEGF therapy.

Currently, immunotherapy is widely used in multiple cancers including lung cancer, and the multiple biomarkers related to the efficacy of ICI treatment have recently emerged, such as PD-L1 expression in tumor and/or immune cells and tumor mutation burden (5, 24, 25). Previous studies have reported that the profile of immune cells in the TME or circulating peripheral blood might be a predictor of the therapeutic effect of immunotherapy (26–30). Tumor-infiltrating CD8+T cells, which exert an effector function in the TME, are associated with favorable clinical outcomes in patients receiving immunotherapy, whereas accumulation of immunosuppressive cells, such as MDSCs and Tregs, which are major mediators of immune tolerance, correlates with poor prognosis (26–28). These immune-related cells are regulated by molecules secreted by TME components and negatively regulate

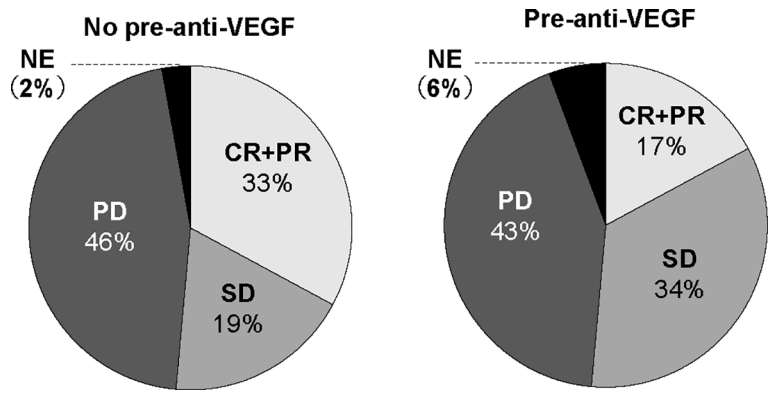

FIGURE 2 | ORR to ICIs according to anti-VEGF treatment prior to ICI treatment. ORR, overall response rate; ICI, immune checkpoint inhibitor; VEGF, vascular endothelial growth factor.

TABLE 2 | Multivariate analysis of ORR, PFS and OS.

	ORR		PFS		OS	
	OR (95%CI)	***P* value**	**HR (95%CI)**	***P* value**	**HR (95%CI)**	***P* value**
Age, < 70y	Reference		Reference		Reference	
≥70y	1.12 (0.45-2.79)	0.803	0.77 (0.49-1.19)	0.237	1.14 (0.70-1.86)	0.605
Gender						
Female	Reference		Reference		Reference	
Male	0.60 (0.17-2.09)	0.42	1.06 (0.58-1.92)	0.86	1.23 (0.59-2.57)	0.576
ECOG PS						
<2	Reference		Reference		Reference	
≥2	0.51 (0.13-1.97)	0.328	2.26 (1.20-4.29)	0.012	4.50 (2.22-9.11)	<0.001
Smoking history						
Never	Reference		Reference		Reference	
Current or former	1.60 (0.39-6.66)	0.516	0.83 (0.42-1.65)	0.599	1.03 (0.46-2.31)	0.948
Histology						
Sq.	Reference		Reference		Reference	
Non-Sq.	1.71 (0.60-4.91)	0.317	0.67 (0.39-1.17)	0.162	0.54 (0.29-1.02)	0.057
Corticosteroid and/or inunnosuppressive agents						
	2.01 (0.46-8.69)	0.352	1.13 (0.57-2.23)	0.734	1.24 (0.58-2.65)	0.584
History of radiation	1.00 (0.39-2.55)	0.993	0.76 (0.49-1.18)	0.228	0.98 (0.59-1.63)	0.934
History of anti- VEGF	0.30 (0.09-0.96)	0.043	1.83 (1.05-3.20)	0.033	1.47 (0.76-2.82)	0.249

PFS, progression free survival; OS, overall survivat ORR, overall response rate; HR, hazard ratio; OR, Odds Ratio; CI, confidence intervat ECOG PS, Eastern Cooperative Oncology Group performance status; Sq. squamous cell carcinoma; VEGF,vascular endothelial growth factor.

the function of effector T-cells. They can also inhibit the differentiation and maturation of dendritic cells (29, 30).

VEGF, a molecule secreted by tumor and stromal cells, plays pivotal roles in the TME. The TME is characterized by hypoperfusion, hypoxia, acidity, and high interstitial fluid pressure through tumor vascularization, which can lead to tumor growth and drug resistance. Anti-VEGF agents reverse these changes; therefore, combination treatment with anti-VEGF agents can be expected to enhance the therapeutic effect of ICIs. Previous studies have identified mechanisms of intrinsic resistance to immunotherapy related to previous treatment with anti-angiogenic therapies (31–33). One such mechanism is that anti-VEGF therapy induces compensatory upregulation of VEGF-independent angiogenic factors, which contribute to the production of an immunosuppressive TME. VEGF/VEGFR2 is a major signaling axis driving tumor angiogenesis, and blockade of this pathway induces upregulation of VEGF-independent compensatory pro-angiogenic factors, including fibroblast growth factor (FGF) 2, platelet-derived growth factor, and angiopoietin-1 and 2 (31). In preclinical models, bone marrow-derived fibrocyte-like cells, which are induced by anti-VEGF therapy, contribute to resistance to anti-VEGF therapy by upregulating FGF2, and the activated FGF/FGF receptor pathway is associated with non-T-cell inflamed tumors that show resistance to immunotherapy (32, 33). These previous studies suggest that multiple pro-angiogenic factors might be

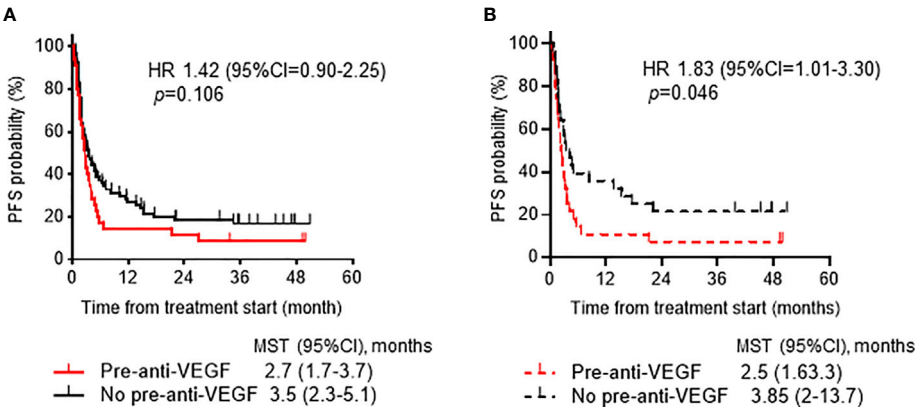

FIGURE 3 | Progression-free survival ICIs according to anti-VEGF treatment prior to ICI treatment. **(A)** Kaplan-Meier analysis of PFS after ICI treatment according to history of treatment with anti-VEGF agents in the full cohort. **(B)** Kaplan-Meier analysis of PFS in the propensity score-matched cohort (1:1, n=28 /group). ICI, immune checkpoint inhibitor; VEGF, vascular endothelial growth factor; PFS, progression-free survival.

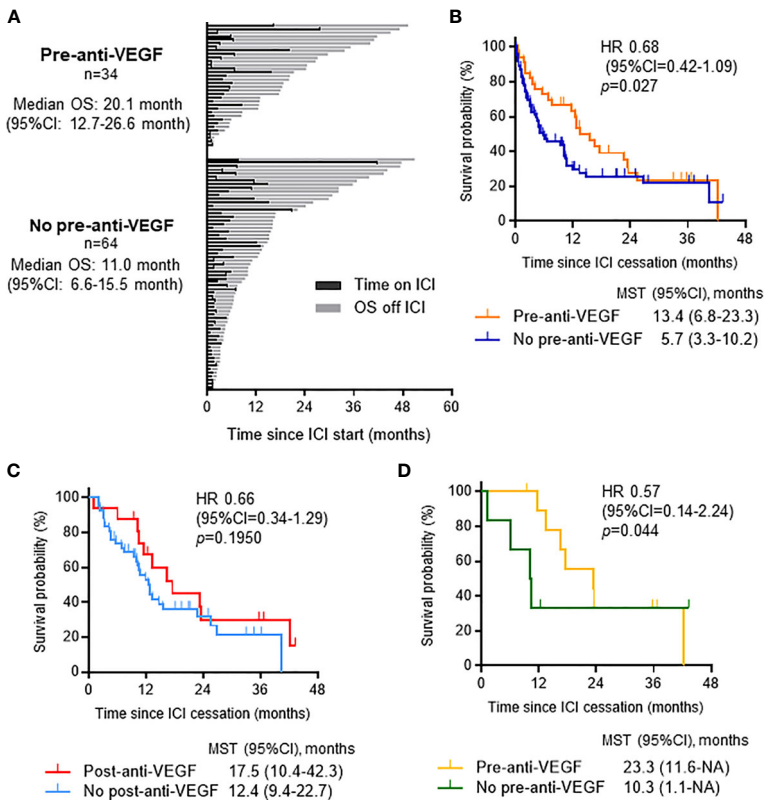

FIGURE 4 | Impact of anti-VEGF therapy on survival when administered pre- or post-ICI therapy. **(A)** Swimmer plot for patients who discontinued ICIs (n = 98) categorized by whether they received anti-VEGF therapy prior to ICIs. **(B)** Kaplan-Meier analysis of survival from ICI cessation according to history of treatment with anti-VEGF agents. Gehan-Breslow-Wilcoxon method was used to compare survival. **(C)** Kaplan-Meier analysis of survival from ICI cessation in patients who received salvage chemotherapy after ICIs (n = 58) according to post-ICI anti-VEGF treatment. **(D)** Kaplan-Meier analysis of survival from ICI cessation in patients who received post-ICI anti-VEGF therapy (n = 16) according to therapeutic history of anti-VEGF agents prior to ICIs. Gehan-Breslow-Wilcoxon method was used to compare survival. VEGF, vascular endothelial growth factor; OS, overall survival; CI, confidence interval; ICI, immune checkpoint inhibitor; HR, hazard ratio; MST, median survival time.

upregulated after VEGF inhibition, leading to attenuation of the antitumor immune response following ICI treatment. Another potential mechanism is that VEGF/VEGFR2 signaling, which is suppressed by anti-VEGF therapy, is immediately reactivated after withdrawal of anti-VEGF agents and returns to baseline, thereby inducing rapid revascularization (34).

In this study, anti-VEGF treatment prior to ICI treatment was associated with poor response to ICIs; however, salvage chemotherapy with anti-VEGF agents after ICI treatment increased survival. These observations support this second hypothesis and suggest that blockade of VEGF/VEGFR signaling might be reversible and that it is essential for patient survival after ICIs and prior anti-VEGF therapy. Additionally, pharmacodynamic analysis revealed that anti-PD-1 antibody remained bound even 2 months after infusion (35). Therefore, previous ICI treatment may improve the effect of any subsequent therapy, including anti-VEGF therapy. Further investigation is warranted to determine the optimal treatment strategy and sequence for ICIs and anti-VEGF therapy.

This study has several limitations. First, this was a retrospective study, so the cohort had a limited sample size and may be subject to patient selection bias. Second, additional analyses using peripheral blood or tumor samples, such as changes in secreted angiogenic factors and phenotypes of immune systems, were not performed, and the precise mechanisms of resistance to ICI were not elucidated. Third, PD-L1 expression, which is a predictive biomarker of ICI response, was measured in only some cases. Finally, the study does not examine the current standard regimens for advanced NSCLC: platinum-based chemotherapy combined with ICIs and angiogenesis inhibitors. Optimal treatment strategies that maximize the therapeutic effect of ICIs and anti-VEGF therapies should be investigated in future studies.

In conclusion, our study demonstrated poorer response to immunotherapy in patients previously treated with anti-VEGF agents than in patients not previously treated with anti-VEGF agents. However, salvage chemotherapy with anti-VEGF agents after ICI failure was associated with prolonged survival. These results suggest that the interventional sequence and maintenance of VEGF inhibition may be important and contribute to clinical outcomes in patients with advanced NSCLC. Further investigation is needed to determine the optimal treatment strategy for immunotherapy and anti-VEGF therapy.

DATA AVAILABILITY STATEMENT

The original contributions presented in the study are included in the article/**Supplementary Material**. Further inquiries can be directed to the corresponding author.

ETHICS STATEMENT

The studies involving human participants were reviewed and approved by Kyoto Prefectural University of Medicine. The patients/participants provided their written informed consent to participate in this study.

AUTHOR CONTRIBUTIONS

Conception and design: KeT and TadY. Administrative support: TakY and KoT. Provision of study materials or patients: SS, TT, TakY, YC, YM, MI, YK, and JU. Collection and assembly of data: KeT, AO, NK, RT, and MT. Data analysis and interpretation: KeT and TadY. All authors contributed to the article and approved the submitted version.

FUNDING

This work was supported by research grants from JSPS KAKENHI [Grant Numbers 20K22820 (to KeT) and 19K08608 (to TadY)].

ACKNOWLEDGMENTS

We would like to thank the patients, their families, and all investigators involved in this study. We would also like to thank Editage (www.editage.com) for English language editing.

SUPPLEMENTARY MATERIAL

The Supplementary Material for this article can be found online at: https://www.frontiersin.org/articles/10.3389/fonc.2021.663612/full#supplementary-material

REFERENCES

1. Miller KD, Sauer AG, Ortiz AP, Fedewa SA, Pinheiro PS, Tortolero-Luna G, et al. Cancer Statistics for Hispanics/Latinos, 2018. *CA Cancer J Clin* (2018) 68:425–45. doi: 10.3322/caac.21494
2. Antonia SJ, Villegas A, Daniel D, Vicente D, Murakami S, Hui R, et al. Durvalumab After Chemoradiotherapy in Stage III non-Small-Cell Lung Cancer. *N Engl J Med* (2017) 377:1919–29. doi: 10.1056/NEJMoa1709937
3. Borghaei H, Paz-Ares L, Horn L, Spigel DR, Steins M, Ready NE, et al. Nivolumab Versus Docetaxel in Advanced Nonsquamous non-Small-Cell Lung Cancer. *N Engl J Med* (2015) 373:1627–39. doi: 10.1056/NEJMoa1507643
4. Brahmer J, Reckamp KL, Baas P, Crinò L, Eberhardt WEE, Poddubskaya E, et al. Nivolumab Versus Docetaxel in Advanced Squamous-Cell non-Small-Cell Lung Cancer. *N Engl J Med* (2015) 373:123–35. doi: 10.1056/NEJMoa1504627
5. Herbst RS, Baas P, Kim DW, Felip E, Pérez-Gracia JL, Han JY, et al. Pembrolizumab Versus Docetaxel for Previously Treated, PD-L1-positive, Advanced non-Small-Cell Lung Cancer (KEYNOTE-010): A Randomised Controlled Trial. *Lancet* (2016) 387:1540–50. doi: 10.1016/S0140-6736(15)01281-7
6. Reck M, Rodríguez-Abreu D, Robinson AG, Hui R, Csőszi T, Fülöp A, et al. Pembrolizumab Versus Chemotherapy for PD-L1-positive non-Small-Cell Lung Cancer. *N Engl J Med* (2016) 375:1823–33. doi: 10.1056/NEJMoa1606774

7. Rittmeyer A, Barlesi F, Waterkamp D, Park K, Ciardiello F, von Pawel J, et al. Atezolizumab Versus Docetaxel in Patients With Previously Treated non-Small-Cell Lung Cancer (OAK): A Phase 3, Open-Label, Multicentre Randomised Controlled Trial. *Lancet* (2017) 389:255–65. doi: 10.1016/S0140-6736(16)32517-X
8. Oyama T, Ran S, Ishida T, Nadaf S, Kerr L, Carbone DP, et al. Vascular Endothelial Growth Factor Affects Dendritic Cell Maturation Through the Inhibition of Nuclear Factor-Kappa B Activation in Hemopoietic Progenitor Cells. *J Immunol* (1998) 160:1224–32.
9. Martino EC, Misso G, Pastina P, Costantini S, Vanni F, Gandolfo C, et al. Immune-Modulating Effects of Bevacizumab in Metastatic non-Small-Cell Lung Cancer Patients. *Cell Death Discov* (2016) 2:16025. doi: 10.1038/cddiscovery.2016.25
10. Voron T, Colussi O, Marcheteau E, Pernot S, Nizard M, Pointet AL, et al. VEGF-a Modulates Expression of Inhibitory Checkpoints on CD8+ T Cells in Tumors. *J Exp Med* (2015) 212:139–48. doi: 10.1084/jem.20140559
11. Terme M, Pernot S, Marcheteau E, Sandoval F, Benhamouda N, Colussi O, et al. VEGFA-VEGFR Pathway Blockade Inhibits Tumor-Induced Regulatory T-cell Proliferation in Colorectal Cancer. *Cancer Res* (2013) 73:539–49. doi: 10.1158/0008-5472.CAN-12-2325
12. Huang Y, Goel S, Duda DG, Fukumura D, Jain RK. Vascular Normalization as an Emerging Strategy to Enhance Cancer Immunotherapy. *Cancer Res* (2013) 73:2943–8. doi: 10.1158/0008-5472.CAN-12-4354
13. Yuan J, Zhou J, Dong Z, Tandon S, Kuk D, Panageas KS, et al. Pretreatment Serum VEGF is Associated With Clinical Response and Overall Survival in Advanced Melanoma Patients Treated With Ipilimumab. *Cancer Immunol Res* (2014) 2:127–32. doi: 10.1158/2326-6066.CIR-13-0163
14. Courau T, Nehar-Belaid D, Florez L, Levacher B, Vazquez T, Brimaud F, et al. TGF-β and VEGF Cooperatively Control the Immunotolerant Tumor Environment and the Efficacy of Cancer Immunotherapies. *JCI Insight* (2016) 1:e85974. doi: 10.1172/jci.insight.85974
15. Sandler A, Gray R, Perry MC, Brahmer J, Schiller JH, Dowlati A, et al. Paclitaxel-Carboplatin Alone or With Bevacizumab for non-Small-Cell Lung Cancer. *N Engl J Med* (2006) 355:2542–50. doi: 10.1056/NEJMoa061884
16. Hodi FS, Lawrence D, Lezcano C, Wu X, Zhou J, Sasada T, et al. Bevacizumab Plus Ipilimumab in Patients With Metastatic Melanoma. *Cancer Immunol Res* (2014) 2:632–42. doi: 10.1158/2326-6066.CIR-14-0053
17. Finn RS, Qin S, Ikeda M, Galle PR, Ducreux M, Kim TY, et al. Atezolizumab plus Bevacizumab in Unresectable Hepatocellular Carcinoma. *N Engl J Med* (2020) 382:1894–905. doi: 10.1056/NEJMoa1915745
18. Choueiri TK, Powles T, Burotto M, Escudier B, Bourlon MT, Zurawski B, et al. Nivolumab plus Cabozantinib versus Sunitinib for Advanced Renal-Cell Carcinoma. *N Engl J Med* (2021) 384:829–41. doi: 10.1056/NEJMoa2026982
19. Socinski MA, Jotte RM, Cappuzzo F, Orlandi F, Stroyakovskiy D, Nogami N, et al. Atezolizumab for First-Line Treatment of Metastatic Nonsquamous NSCLC. *N Engl J Med* (2018) 378:2288–301. doi: 10.1056/NEJMoa1716948
20. Jeyakumar G, Kim S, Bumma N, Landry C, Silski C, Suisham S, et al. Neutrophil Lymphocyte Ratio and Duration of Prior Anti-Angiogenic Therapy as Biomarkers in Metastatic RCC Receiving Immune Checkpoint Inhibitor Therapy. *J Immunother Cancer* (2017) 5:82. doi: 10.1186/s40425-017-0287-5
21. Yoshimura A, Yamada T, Okuma Y, Kitadai R, Takeda T, Kanematsu T, et al. Retrospective Analysis of Docetaxel in Combination With Ramucirumab for Previously Treated non-Small Cell Lung Cancer Patients. *Transl Lung Cancer Res* (2019) 8:450–60. doi: 10.21037/tlcr.2019.08.07
22. Harada D, Takata K, Mori S, Kozuki T, Takechi Y, Moriki S, et al. Previous Immune Checkpoint Inhibitor Treatment to Increase the Efficacy of Docetaxel and Ramucirumab Combination Chemotherapy. *Anticancer Res* (2019) 39:4987–93. doi: 10.21873/anticanres.13688
23. Shiono A, Kaira K, Mouri A, Yamaguchi O, Hashimoto K, Uchida T, et al. Improved Efficacy of Ramucirumab Plus Docetaxel After Nivolumab Failure in Previously Treated non-Small Cell Lung Cancer Patients. *Thorac Cancer* (2019) 10:775–81. doi: 10.1111/1759-7714.12998
24. Le DT, Uram JN, Wang H, Bartlett BR, Kemberling H, Eyring AD, et al. PD-1 Blockade in Tumors With Mismatch-Repair Deficiency. *N Engl J Med* (2015) 372:2509–20. doi: 10.1056/NEJMoa1500596
25. Rizvi NA, Hellmann MD, Snyder A, Kvistborg P, Makarov V, Havel JJ, et al. Cancer Immunology. Mutational Landscape Determines Sensitivity to PD-1 Blockade in non-Small Cell Lung Cancer. *Science* (2015) 348:124–8. doi: 10.1126/science.aaa1348
26. Donnem T, Hald SM, Paulsen EE, Richardsen E, Al-Saad S, Kilvaer TK, et al. Stromal CD8+ T-Cell Density—a Promising Supplement to TNM Staging in non-Small Cell Lung Cancer. *Clin Cancer Res* (2015) 21:2635–43. doi: 10.1158/1078-0432.CCR-14-1905
27. Martens A, Wistuba-Hamprecht K, Foppen MG, Yuan J, Postow MA, Wong P, et al. Baseline Peripheral Blood Biomarkers Associated With Clinical Outcome of Advanced Melanoma Patients Treated With Ipilimumab. *Clin Cancer Res* (2016) 22:2908–18. doi: 10.1158/1078-0432.CCR-15-2412
28. Martens A, Wistuba-Hamprecht K, Yuan J, Postow MA, Wong P, Capone M, et al. Increases in Absolute Lymphocytes and Circulating CD4+ and CD8+ T Cells are Associated With Positive Clinical Outcome of Melanoma Patients Treated With Ipilimumab. *Clin Cancer Res* (2016) 22:4848–58. doi: 10.1158/1078-0432.CCR-16-0249
29. Jain RK. Normalization of Tumor Vasculature: An Emerging Concept in Antiangiogenic Therapy. *Science* (2005) 307:58–62. doi: 10.1126/science.1104819
30. Pilon-Thomas S, Kodumudi KN, El-Kenawi AE, Russell S, Weber AM, Luddy K, et al. Neutralization of Tumor Acidity Improves Antitumor Responses to Immunotherapy. *Cancer Res* (2016) 76:1381–90. doi: 10.1158/0008-5472.CAN-15-1743
31. Gacche RN. Compensatory Angiogenesis and Tumor Refractoriness. *Oncogenesis* (2015) 4:e153. doi: 10.1038/oncsis.2015.14
32. Mitsuhashi A, Goto H, Saijo A, Trung VT, Aono Y, Ogino H, et al. Fibrocyte-Like Cells Mediate Acquired Resistance to Anti-Angiogenic Therapy With Bevacizumab. *Nat Commun* (2015) 6:8792. doi: 10.1038/ncomms9792
33. Sweis RF, Spranger S, Bao R, Paner GP, Stadler WM, Steinberg G, et al. Molecular Drivers of the non-T-cell-inflamed Tumor Microenvironment in Urothelial Bladder Cancer. *Cancer Immunol Res* (2016) 4:563–8. doi: 10.1158/2326-6066.CIR-15-0274
34. Yang Y, Zhang Y, Iwamoto H, Hosaka K, Seki T, Andersson P, et al. Discontinuation of anti-VEGF Cancer Therapy Promotes Metastasis Through a Liver Revascularization Mechanism. *Nat Commun* (2016) 7:12680. doi: 10.1038/ncomms12680
35. Brahmer JR, Drake CG, Wollner I, Powderly JD, Picus J, Sharfman WH, et al. Phase I Study of Single-Agent Anti-Programmed Death-1 (MDX-1106) in Refractory Solid Tumors: Safety, Clinical Activity, Pharmacodynamics, and Immunologic Correlates. *J Clin Oncol* (2010) 28:3167–75. doi: 10.1200/JCO.2009.26.7609

Conflict of Interest: TadY received commercial research grants from Pfizer, Ono Pharmaceutical, Chugai Pharmaceutical, and Takeda Pharmaceutical Company Limited. JU received research grants from Eli Lilly Japan K.K., AstraZeneca K.K., and Boehringer Ingelheim Japan. KoT received research grants from Chugai-Roche and Ono Pharmaceutical and personal fees from AstraZeneca, Chugai-Roche, MSD-Merck, Eli Lilly, Boehringer Ingelheim, and Daiichi Sankyo.

The remaining authors declare that the research was conducted in the absence of any commercial or financial relationships that could be construed as a potential conflict of interest.

Copyright © 2021 Tanimura, Yamada, Omura, Shiotsu, Kataoka, Takeda, Taniguchi, Yamada, Takeuchi, Chihara, Morimoto, Iwasaku, Kaneko, Uchino and Takayama. This is an open-access article distributed under the terms of the Creative Commons Attribution License (CC BY). The use, distribution or reproduction in other forums is permitted, provided the original author(s) and the copyright owner(s) are credited and that the original publication in this journal is cited, in accordance with accepted academic practice. No use, distribution or reproduction is permitted which does not comply with these terms.

frontiers in Immunology

ORIGINAL RESEARCH
published: 02 June 2021
doi: 10.3389/fimmu.2021.666909

Atezolizumab Monotherapy or Plus Chemotherapy in First-Line Treatment for Advanced Non-Small Cell Lung Cancer Patients: A Meta-Analysis

Dan-Ni Li[1,2,3], *Wen-Qing Lu*[1,2,3], *Bo-Wen Yang*[1,2,3], *Ling-Yun Zhang*[1,2,3], *Bo Jin*[1,2,3], *Shuo Wang*[1,2,3], *Xiao-Fang Che*[1,2,3], *Ce Li*[1,2,3], *Yun-Peng Liu*[1,2,3*] *and Xiu-Juan Qu*[1,2,3*]

[1] Department of Medical Oncology, The First Hospital of China Medical University, Shenyang, China, [2] Key Laboratory of Anticancer Drugs and Biotherapy of Liaoning Province, The First Hospital of China Medical University, Shenyang, China, [3] Liaoning Province Clinical Research Center for Cancer, Shenyang, China

OPEN ACCESS

Edited by:
Hubing Shi,
Sichuan University, China

Reviewed by:
Jie Liu,
Sichuan University, China
Lan Huiyin,
Zhejiang University, China

***Correspondence:**
Xiu-Juan Qu
xiujuanqu@yahoo.com
Yun-Peng Liu
ypliu@cmu.edu.cn

Specialty section:
This article was submitted to Cancer Immunity and Immunotherapy, a section of the journal Frontiers in Immunology

Received: 11 February 2021
Accepted: 27 April 2021
Published: 02 June 2021

Citation:
Li D-N, Lu W-Q, Yang B-W, Zhang L-Y, Jin B, Wang S, Che X-F, Li C, Liu Y-P and Qu X-J (2021) Atezolizumab Monotherapy or Plus Chemotherapy in First-Line Treatment for Advanced Non-Small Cell Lung Cancer Patients: A Meta-Analysis. Front. Immunol. 12:666909. doi: 10.3389/fimmu.2021.666909

Background: Atezolizumab plus chemotherapy has been recommended as a first-line treatment option for patients with advanced non-small cell lung carcinoma (NSCLC) irrespective of programmed cell death-ligand 1 (PD-L1) expression. Currently, little is known about the efficacy and treatment-related adverse effects (TRAEs) of subtracting chemotherapy from the combination for patients with high PD-L1 expression. Thus, we performed an indirect comparison between atezolizumab plus chemotherapy and atezolizumab alone.

Methods: A total of five eligible randomized controlled trials (RCTs) were identified from PubMed, EMBASE, and Cochrane Central controlled trial registries, using keywords including atezolizumab, PD-1, PD-L1, NSCLC, and RCT. The clinical outcomes of objective response rate (ORR), progression-free survival (PFS), OS, and TRAEs were extracted and evaluated. Using indirect analysis, the efficacy and TRAEs were compared between arm A (atezolizumab plus chemotherapy) and arm C (atezolizumab), linked by arm B (chemotherapy).

Results: Direct comparison revealed that both atezolizumab plus chemotherapy (HR 0.65, $P = 0.003$) and atezolizumab alone (HR 0.59, $P = 0.010$) significantly improved OS compared with chemotherapy. More importantly, the indirect comparison showed that atezolizumab plus chemotherapy was not superior to atezolizumab regarding OS (RR 1.10, $P = 0.695$) and ORR (RR 1.11, $P = 0.645$). However, patients who received atezolizumab combined with chemotherapy experienced more ≥ grade 3 TRAEs (RR 4.23, $P<0.001$) and TRAEs leading to drug discontinuation (RR 3.60, $P<0.001$) than those treated with atezolizumab monotherapy.

Conclusions: Atezolizumab monotherapy might be a better treatment option for patients with advanced NSCLC and high PD-L1 expression than atezolizumab plus chemotherapy.

Keywords: non-small cell lung cancer (NSCLC), programmed cell death-ligand 1 (PD-L1), atezolizumab, chemotherapy, first-line

INTRODUCTION

Lung cancer is the leading cause of cancer-related mortality (1). In recent years, immune checkpoint inhibitors, whether as a monotherapy or in combination with chemotherapy, have become the standard of care for first-line treatment of patients with advanced non-small cell lung cancer (NSCLC) that lack targetable driver mutations. Currently, pembrolizumab monotherapy, pembrolizumab plus chemotherapy, or atezolizumab monotherapy are the preferred options for patients with high programmed cell death ligand 1 (PD-L1) expression (2–4). Previous studies showed that for those with a PD-L1 tumor proportion score (TPS) of at least 50%, the addition of chemotherapy to pembrolizumab significantly improved objective response rate (ORR) and progression-free survival (PFS), though at the cost of increased treatment-related adverse effects (TRAEs). Overall survival (OS) was not different between these two treatment options (3). However, whether this conclusion is similar to atezolizumab, an anti-PD-L1 antibody, remains unknown.

With the IMpower150 study, atezolizumab plus bevacizumab, carboplatin, and paclitaxel has been approved by the Food and Drug Administration (FDA) and the European Medicines Agency (EMA) as a first-line treatment for patients with advanced non-squamous NSCLC, regardless of PD-L1 expression level (5). Similarly, atezolizumab in combination with nab-paclitaxel and carboplatin also showed a significant and meaningful improvement in OS compared with chemotherapy in the same population (6). For patients with advanced squamous cell lung cancer, atezolizumab plus nab-paclitaxel and carboplatin failed to prolong OS versus chemotherapy alone. However, there was a trend towards longer OS with atezolizumab plus nab-paclitaxel and carboplatin in the PD-L1-high subgroup (7). More recently, the phase III IMpower 110 trial showed that atezolizumab monotherapy outperforms chemotherapy for NSCLC patients with high PD-L1 expression, irrespective of histologic type (8). Therefore, both atezolizumab monotherapy or atezolizumab plus chemotherapy could be treatment options for patients with advanced NSCLC and high PD-L1 expression, defined as either greater than 50% PD-L1 expression in the tumor cells (TC) or greater than 10% PD-L1 expression in immune cells (IC) under SP142 PD-L1 immunohistochemistry (IHC) assay (PD-L1 TC3/IC3). Currently, whether the subtraction of chemotherapy from atezolizumab plus chemotherapy could be non-inferior is controversial owing to the lack of head-to-head comparisons.

Abbreviations: NSCLC, Non-small-cell lung carcinoma; PD-1, Programmed cell death 1; PD-L1, Programmed cell death-ligand 1; RCT, randomized controlled trials; PRISMA, Preferred Reporting Items for Systematic Reviews and Meta-Analyses; AACR, American Association for Cancer Research; ESMO, European Society of Medical Oncology; ASCO, American Society of Clinical Oncology; WCLC, World Conference on Lung Cancer; EMA, European Medicines Agency; FDA, drug administration; AEs, Adverse events; TRAEs, Treatment related adverse effects; CI, Confidence interval; HRs, Hazard ratios; RR, Relative risk; TC, tumor cells; IC, immune cells; DOR, Duration of response; ORR, Objective response rate; OS, Overall survival; PFS, Progression-free survival; ECOG, Eastern Cooperative Oncology Group; Immunohistochemistry, IHC.

As such, we estimated the efficacy and safety of atezolizumab plus chemotherapy versus atezolizumab alone for the first-line treatment of advanced NSCLC patients in a PD-L1 TC3/IC3 subgroup through an indirect comparison meta-analysis.

METHODS

Study Eligibility

This meta-analysis was prepared and written following the Preferred Reporting Items for Systematic Reviews and Meta-Analyses (PRISMA) statement. From the PubMed, EMBASE, and Cochrane Central controlled trial registries, we identified qualified randomized controlled trials that compared atezolizumab plus chemotherapy or atezolizumab alone with chemotherapy for first-line treatment of advanced NSCLC patients. We searched for studies using keywords including atezolizumab, PD-1, PD-L1, non-small cell lung cancer, and randomized controlled trial (**Supplemental Methods**). We also searched abstracts from major conferences of the American Society of Clinical Oncology (ASCO), the European Society of Medical Oncology (ESMO), the American Association for Cancer Research (AACR), and the World Congress on Lung Cancer (WCLC). These clinical studies were limited to those published in English before October 1, 2020.

Data Extraction

Data were extracted with a pre-determined information table. The primary results of this study included PFS, OS, ORR, and TRAEs. We derived the hazard ratios (HRs) and 95% confidence intervals (CIs) for OS and PFS, and the dichotomous data for ORR and TRAEs. Other items included the design of the trial, the number of patients registered, the year of publication or conference presentation, the median follow-up time, the clinical pathological characteristics of the patients, including histology, ECOG score, smoking status, and PD-L1 expression.

Data Analyses

Direct comparisons were conducted between arm A (atezolizumab plus chemotherapy) against arm B (chemotherapy), and arm C (atezolizumab) against arm B (chemotherapy). The pooled measurement of PFS and OS were shown with HRs, 95% Cis, and *P* values calculated by the inverse-variance-weighted method, while the estimation of ORR and TRAEs were pooled with the relative risks (RRs), 95% Cis, and *P* values *via* the Mantel Haenszel method. Fixed-effect or random-effect models were based on the heterogeneity between studies.

Indirect comparison between arm A and arm C was bridged by arm B. The adjusted indirect comparison was calculated by the following formula (9): $\log HR_{AB} = \log HR_{AC} - \log HR_{BC}$. The standard error (SE) for the log HR was $SE(logHRAB) = \sqrt{SE(logHRAC)^2 + SE(logHRBC)^2}$. RR was calculated similarly to the above method. HR < 1 or RR > 1 demonstrates that atezolizumab plus chemotherapy is superior to atezolizumab alone, and vice versa. All statistical analyses were performed using STATA (version 12.0). Statistical significance was defined as a two-sided $P < 0.05$.

RESULTS

The PRISMA flow diagram of our meta-analysis was shown in **Figure 1**. The quality assessment of risk of bias was presented in **Supplemental Table 1**. In total, five trials involving 616 patients fulfilled the predefined inclusion criteria. The principal characteristics and outcomes of the included trials were summarized in **Table 1**. In all clinical trials, patient characteristics between the experimental and control groups were well balanced. Patients with non-squamous NSCLC were recruited in three trials, one for squamous NSCLC and the other one for both histologies. Four trials compared atezolizumab plus chemotherapy versus chemotherapy and one trial compared atezolizumab alone versus chemotherapy. Additionally, IMpower130 study was a three-arm randomized trial that investigated atezolizumab with or without bevacizumab, an inhibition of vascular endothelial growth factor, plus chemotherapy versus chemotherapy alone. According to practice guidelines, all five trials were treated with standard-of-care chemotherapy regimens. The median follow-up time ranged from 15.7 to 28.4 months. PFS, OS, and AE information were provided for all five trials; however, ORR data was not reported in IMpower 130. The PD-L1 expression on tumor cells and tumor-infiltrating immune cells were measured by the SP142 IHC assay (Ventana Medical Systems). The safety summary was presented detailed in **Table 2**.

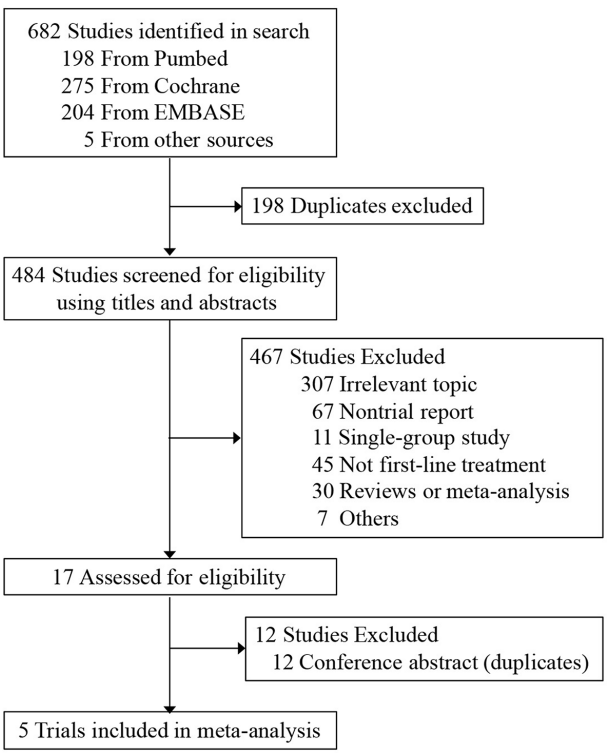

FIGURE 1 | PRISMA flow diagram of the meta-analysis.

Direct Meta-Analysis

Significant difference of ORR was observed in favor of atezolizumab plus chemotherapy versus chemotherapy ($RR_{atezo + chemo/chemo}$ 1.49, 95% CI 1.20–1.85; Z = 3.62, $P<0.001$). And in terms of atezolizumab versus chemotherapy, the pooled RR was 1.33 ($RR_{atezo + chemo/chemo}$ 1.34, 95% CI 0.90–1.99; Z = 1.46, $P = 0.145$) (**Figure 2A**). For PFS, atezolizumab plus chemotherapy significantly reduced the risk of disease progression or death compared with chemotherapy ($HR_{atezo + chemo/chemo}$, 0.42; 95% CI 0.33–0.54; Z = 7.09, $P = 0.001$). In addition, atezolizumab monotherapy was also correlated with longer PFS versus chemotherapy ($HR_{atezo/chemo}$ = 0.63; 95% CI, 0.45–0.88; Z = 2.70, $P = 0.007$) (**Figure 2B**). In terms of OS, compared with chemotherapy, both atezolizumab plus chemotherapy ($HR_{atezo+ chemo/chemo}$ = 0.65; 95% CI, 0.49–0.86; Z = 2.97, $P = 0.003$) and atezolizumab monotherapy ($HR_{atezo/chemo}$ = 0.59; 95% CI, 0.40–0.89; Z = 2.59, $P = 0.010$) significantly reduced the risk of death (**Figure 2C**).

Indirect Meta-Analysis

The correlation of indirect analysis was shown in **Figure 2D**. The results showed that the efficacy of the atezolizumab combined chemotherapy group was not superior to that of the atezolizumab monotherapy including ORR ($RR_{atezo + chemo/atezo}$ 1.11, $P = 0.645$) and OS ($HR_{atezo+ chemo/atezo}$ 1.10, $P = 0.695$). In addition, atezolizumab combined with chemotherapy did not show a significant difference in PFS compared with atezolizumab monotherapy in terms of PFS ($HR_{atezo + chemo/atezo}$ = 0.67, $P = 0.056$).

The rate of all grades (RR, 1.06; 95% CI, 1.29-1.61) and ≥ grade 3 (RR, 4.23; 95% CI, 3.02-5.91) TRAEs were both significantly higher in atezolizumab plus chemotherapy than those in the atezolizumab monotherapy group (**Figure 3**). Additionally, the rate of TRAEs leading to drug discontinuation occurred more frequently in those receiving atezolizumab plus chemotherapy than in those treated with atezolizumab monotherapy (RR, 3.60; 95% CI, 2.10-6.18). Treatment-related deaths were similar between atezolizumab alone and atezolizumab with chemotherapy groups (RR, 1.49; 95% CI, 0.62-3.58).

DISCUSSION

To the best of our knowledge, this is the first study to compare the efficacy and safety of atezolizumab plus chemotherapy and atezolizumab monotherapy in advanced NSCLC patients with high PD-L1 expression through indirect analysis. This hypothesis-generating meta-analysis showed that atezolizumab monotherapy was non-inferior to atezolizumab plus chemotherapy as a first-line treatment for patients with advanced NSCLC and PD-L1 TC3/IC3 expression. Unsurprisingly, patients receiving atezolizumab monotherapy experienced fewer TRAEs than those receiving combination therapy.

Currently, atezolizumab in combination with carboplatin plus nab-paclitaxel or with bevacizumab, carboplatin, and paclitaxel

TABLE 1 | Baseline characteristics and available endpoints of PD-L1 TC3/IC3 WT patients in included trials

Baseline Characteristics	IMpower110		IMpower130		IMpower131		IMpower132		IMpower150	
	Atezo	Chemo	Atezo+ Chemo	Chemo	Atezo+ Chemo	Chemo	Atezo+ Chemo	Chemo	Atezo+ Chemo	Chemo
All eligible patients	277	277	451	228	343	340	292	286	359	337
Median age-years	64	65	64	65	65	65	64	63	63	63
Male sex (%)	70.8	69.7	59	59	81.6	81.5	65.8	67.1	60.0	59.8
ECOG[a] score (%)										
0	35.0	36.8	42	40	33.5	32.4	43.2	40.1	40.1	45.1
1	65.0	63.2	58	60	66.2	67.4	NE	NE	59.9	54.9
Smoking status (%)										
Current/former	86.6	87.3	89	92	90.7	92.9	87.3	89.5	79.5	80.8
Never	13.4	12.6	11	7	9.3	6.8	12.7	10.5	20.5	19.2
Unknown	0	0	0	1	0	0.3	0	0	0	0
Histologic type (%)										
Squamous	30.7	30.3	0	0	100	100	0	0	0	0
Non-squamous	69.3	69.7	100	100	0	0	100	100	99.3	98.4
PD-L1 TC3/IC3 WT (%)	38.6	35.4	20.0	18.0	13.7	12.9	14.2	11.9	19.8	19.3
Endpoints	OS		PFS and OS		PFS and OS		PFS and OS		PFS and OS	
Interventions	Atezo[b]	Nsq: AP[c] Sq: GP[c]	Atezo+TC[d]	TC	Atezo+CP/CnP[e]	CnP	Atezo+TC/TP[f]	TC/TP	Atezo+Bev+CP	Bev+CP[g]
Follow-up time (m)	15.7		19.2		26.8		28.4		19.7	
OS (m), HR (95%CI)	20.2 vs. 13.1		17.3 vs. 16.9		23.4 vs. 10.2		NE vs. 26.9		25.2 vs. 13.2	
	0.59 (0.40, 0.89)		0.84 (0.51, 1.39)		0.48 (0.29, 0.81)		0.73 (0.31, 1.73)		0.67 (0.42–1.06)	
PFS (m), HR (95%CI)	8.1 vs. 5.0		6.4 vs. 4.6		10.1 vs. 5.1		10.8 vs. 6.5		15.4 vs. 6.9	
	0.63 (0.45, 0.88)		0.51 (0.34, 0.77)		0.41 (0.25, 0.68)		0.46 (0.22, 0.96)		0.33 (0·22–0·51)	
ORR (%)	38.3 vs. 28.6		NE		61.7 vs. 31.8		72.0 vs. 55.0		68.9 vs. 49.3	

[a]*Performance-status evaluation of the Eastern Cooperative Oncology Group.*

[b]*Atezolizumab (1200 mg intravenously).*

[c]*AP: pemetrexed (500 mg/m^2 Q3W) + cisplatin (75 mg/m^2 Q3W) /carboplatin (AUC=6 Q3W); GP: gemcitabine (1250/m^2) + cisplatin (75mg/m^2) or gemcitabine (1000 mg/m^2) + carboplatin (AUC=5 Q3W).*

[d]*Atezo+TC: Atezolizumab (1200 mg intravenously) + carboplatin (6 mg/mL/min Q3W) + nab-paclitaxel (100 mg/m2, every week).*

[e]*Atezo+CP: Atezolizumab (1200 mg intravenously) + carboplatin (6 mg/mL/min Q3W) + pemetrexed (200 mg/m^2 Q3W, 175 mg/m2 for Asian race), CnP : nab-paclitaxel (100 mg/m2, every week).*

[f]*Atezo+TC/TP: Atezolizumab (1200 mg intravenously) + carboplatin (6 mg/mL/min Q3W) or cisplatin (75mg/m^2) + pemetrexed (500 mg/m^2 Q3W).*

[g]*Bev+CP: bevacizumab (15mg/kg Q3W) + carboplatin (6 mg/mL/min Q3W)+ paclitaxel (200mg/m^2 Q3W, 175mg/m^2 for Asian patients) PD-L1, programmed cell death-ligand 1; TC, tumor cell; IC, immune cell; ECOG, Eastern Cooperative Oncology Group; OS, overall survival; PFS, progression-free survival; ORR, objective response rate; mDOR, median duration of response; 95%CI, 95% confidence interval (CI); m, months.*

have been officially approved as a first-line treatment for metastatic non-squamous NSCLC lacking EGFR mutation or ALK rearrangements, based on the OS benefit over their comparator chemotherapy alone (5, 6). For squamous cell lung cancer, atezolizumab plus chemotherapy was significantly associated with prolonged progression-free survival, though this was not translated into overall survival benefit. Yet, there was a tendency towards improved OS with the atezolizumab plus chemotherapy group for patients with high PD-L1 expression (HR, 0.56; 95% CI, 0.32-0.99) (7). These results indicate the atezolizumab plus chemotherapy might yield survival benefit for patients with advanced NSCLC and high PD-L1. We confirmed this observation by conducting a direct meta-analysis of randomized controlled trials. The results showed that

TABLE 2 | Safety summary.

	IMpower110		IMpower130		IMpower131		IMpower132		IMpower150	
	Atezo	Chemo	Atezo +Chemo	Chemo	Atezo +Chemo	Chemo	Atezo +Chemo	Chemo	Atezo +Chemo	Chemo
All cause AEs, n (%)	258 (90.2)	249 (94.7)	471 (99.6)	230 (99.1)	332 (99.4)	324 (97.0)	287 (98.6)	266 (97.1)	386 (98.2)	390 (99.0)
Grade 3–5 AEs, n (%)	97 (33.9)	149 (56.7)	406 (85.8)	177 (76.3)	277 (83.0)	235 (70.4)	208 (71.5)	166 (60.0)	274 (69.7)	251 (63.7)
AE leading to any treatment withdrawal, n (%)	18 (6.3)	43 (16.3)	125 (26.4)	51 (22.0)	102 (30.5)	58 (17.4)	83 (28.5)	50 (18.2)	133 (33.8)	98 (24.9)
AE related death, n (%)	2 (0.7)	3 (1.1)	8 (1.7)	1 (0.4)	4 (1.2)	3 (0.9)	11 (3.8)	8 (2.9)	11 (2.8)	9 (2.3)

Atezo, atezolizumab; Chemo, chemotherapy; AEs, adverse effects.

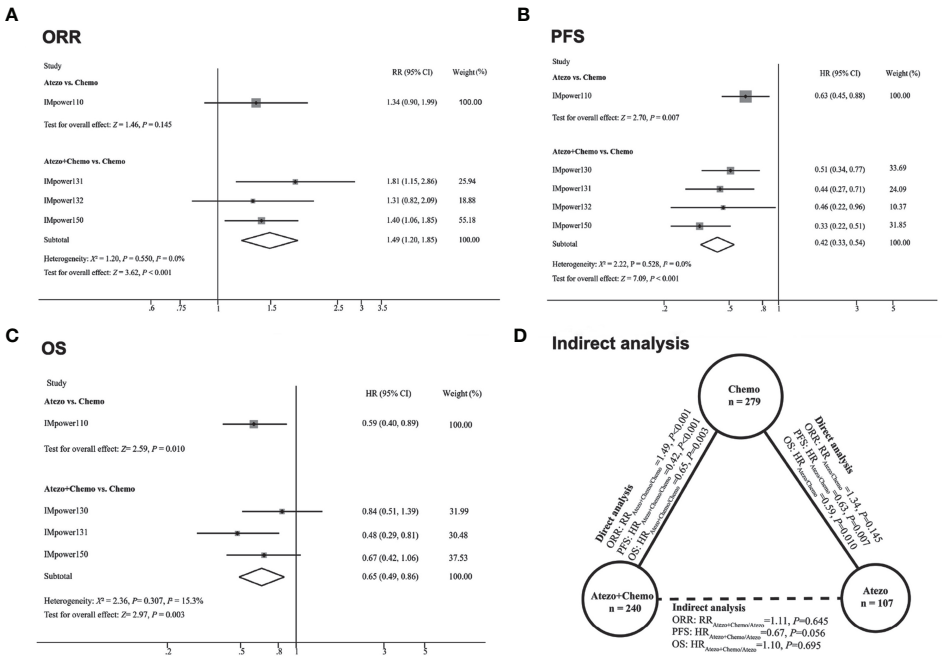

FIGURE 2 | Direct comparisons and indirect comparisons of efficacy between Atezolizumab (Atezo) plus chemotherapy versus Atezolizumab for patients with high PD-L1 expression. **(A–C)** showed the forest plot of RR and HR directly comparing ORR **(A)**, PFS **(B)**, and OS **(C)** between Atezo plus chemotherapy or Atezo alone. The size (square) of the data marker corresponds to the weight of the study in the meta-analysis. The horizontal line across the square represents 95% confidence interval (CI). Based on the meta-analysis, the diamond represents the overall effect of the estimation. **(D)** showed the results of indirect analysis for ORR, PFS, and OS between Atezo plus chemotherapy and Atezo. Solid lines represented the existence of direct comparisons between treatment regimens, while the dotted line represented the indirect comparison between Atezo plus chemotherapy versus Atezo. All statistical tests were two-sided.

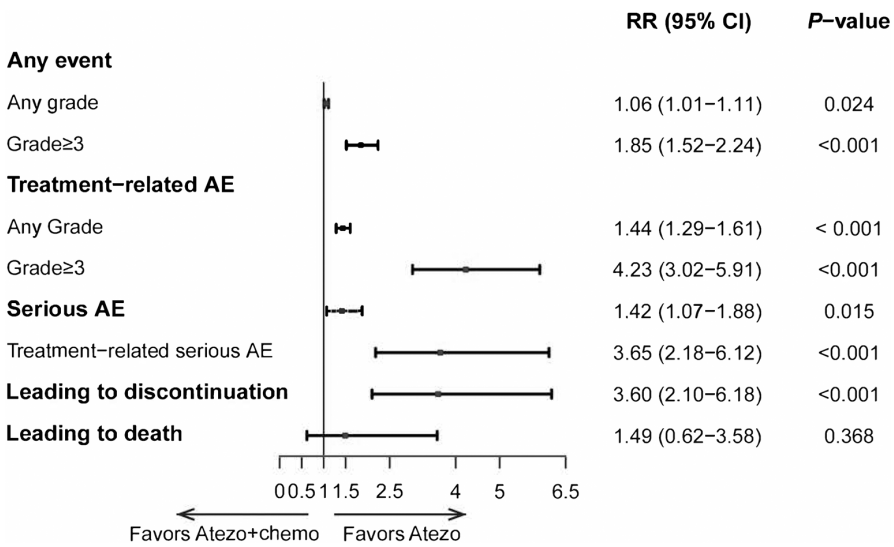

FIGURE 3 | Indirect comparisons of safety between Atezolizumab (Atezo) plus chemotherapy versus Atezolizumab for patients. The forest plot showed RRs for TRAEs between Atezo plus chemotherapy versus Atezo alone. The horizontal line crossing the square represents the 95% confidence interval (CI). The diamonds represent the estimated overall effect, based on the meta-analysis.

atezolizumab plus chemotherapy outperforms chemotherapy in terms of ORR (RR, 1.49; 95% CI, 1.20-1.85), PFS (HR, 0.42; 95% CI, 0.33-0.54), and OS (HR, 0.65; 95% CI, 0.49-0.86). Theoretically, combining immune checkpoint inhibitors with chemotherapy could achieve additive anti-tumor activity compared with ICIs alone: chemotherapy enhances the recognition and elimination of tumor cells by the host immune system; moreover, chemotherapy might optimize the tumor immune microenvironment (10–13). However, these combinatory strategies are challenged by their higher risks of TRAEs, discontinuation rates, and economic cost (14, 15). It is of important clinical significance to explore biomarkers to select the subgroup of NSCLC patients benefiting from chemotherapy-free treatment options. Among them, PD-L1 expression was the most extensively studied biomarker (2, 16, 17). A previous study found that, for patients whose tumoral PD-L1 expression stained by 22C3 clone was 50% or more, pembrolizumab plus chemotherapy produced better ORR and PFS than pembrolizumab alone. However, the OS was not different between pembrolizumab plus chemotherapy and pembrolizumab alone (3). This implies that the upfront application of chemotherapy for the combination with immunotherapy could lead to short-term clinical benefit but not OS benefit. For atezolizumab, the phase II clinical trial BIRCH has also demonstrated atezolizumab monotherapy was associated with good tolerability and efficacy in patients with PD-L1-selected advanced NSCLC across lines of therapy, especially in PD-L1 TC3/IC3 patients (16). Based on the promising results of BIRCH, the randomized controlled phase III IMpower110 study were conducted to evaluate the efficacy and safety of atezolizumab monotherapy as the first-line treatment in PD-L1 selected patients. Encouragingly, the final OS analysis of IMpower110 indicated atezolizumab monotherapy showed statistically significant and clinically meaningful OS, PFS, ORR, and duration of response (DOR) improvement in the TC3/IC3 population compared with platinum-based chemotherapy (4). Therefore, single-agent atezolizumab has been approved as one of the preferred first-line regimens for patients with metastatic NSCLC and a high PD-L1 expression. Considering these results, it is difficult to decide whether patients with high PD-L1 could benefit more from atezolizumab in combination with chemotherapy or atezolizumab alone. In light of the lack of such head-to-head comparisons and the urgent need for this evidence to guide clinical practice, we performed this indirect comparison for atezolizumab plus chemotherapy and atezolizumab as a single agent.

Our pooled analysis shows that the addition of chemotherapy to atezolizumab was not beneficial compared with atezolizumab alone in terms of OS (HR 1.10, P = 0.695). Additionally, the outcomes of ORR and PFS seem favorable in the combined treatment group, but the difference was not significant (ORR: RR, 1.11, P = 0.645; PFS: HR, 0.67, P = 0.056). However, the rate of all grades (RR, 1.06; 95% CI, 1.29-1.61) and ≥ grade 3 (RR, 4.23; 95% CI, 3.02-5.91) TRAEs were both obviously higher in the combination group. These results further provide support for the recommendation from NCCN that patients with advanced NSCLC and high PD-L1 could be treated preferentially by atezolizumab monotherapy rather than in combination with chemotherapy.

Our results support the predictive role of PD-L1 TC3/IC3 in the selection of advanced NSCLC patients who would benefit from single-agent atezolizumab to some extent. The underlying explanation of the lack of addictive benefit from the combination of chemotherapy to atezolizumab may include the following. Firstly, the subgroup of patients with PD-L1 TC3/IC3 possesses a specific tumor microenvironment where the tumor cells themselves and the surrounding immune cells collectively suppressed CD8+ cytotoxic T lymphocytes (CTLs)-mediated immune surveillance and attacked their high PD-L1 expression. Therefore, by removing the interaction between PD-1 and PD-L1, atezolizumab could induce anti-tumor immunity to a greater extent. Besides, it is likely that chemotherapy could not trigger further anti-tumor immunity in PD-L1 TC3/IC3 patients because they are a "hot tumor" by nature.

The advantage of our work lies on the quality of the evidence extracted and applied in the meta-analysis. The origin data were obtained from five prospective randomized controlled trials involving more than 2000 patients. The antibody of immunotherapy and method of detecting PD-L1 expression are the same. Therefore, the meta-analysis could obviously reduce the heterogeneity between studies by collecting data, thereby overcoming the problem of insufficient strength of multiple experiments, which makes indirect analysis feasible to a certain extent. In addition, several limitations of the study should also be considered. Firstly, our meta-analysis is based on study-level data, but not individual patients' data. The analyses could not be adjusted for patients' characteristics. Secondly, due to the absence of a head-to-head comparison between atezolizumab and atezolizumab plus chemotherapy, such a comparison could only be made *via* an indirect meta-analysis. Such an approach will face methodological challenges. However, we believe the quality of the included trials and the similarity between the comparative populations together make the indirect comparison more convincing (9). Finally, the data extracted in our meta-analysis are from subgroup analyses which means the sample is not large enough. Thus, the interpretation of our results requires extra caution. In view of these limitations, a randomized head-to-head trial will be urgently needed to directly compare the efficacy and safety between atezolizumab plus chemotherapy and atezolizumab alone.

Limitations aside, this study for the first time compared the efficacy and safety of atezolizumab plus chemotherapy with atezolizumab alone for advanced NSCLC. Atezolizumab monotherapy might be a preferred first-line treatment option for patients with advanced NSCLC and TC3/IC3 PD-L1 expression.

DATA AVAILABILITY STATEMENT

The raw data supporting the conclusions of this article will be made available by the authors, without undue reservation.

AUTHOR CONTRIBUTIONS

D-NL, W-QL, and B-WY contributed to data acquisition, data interpretation, statistical analysis, and drafting of the manuscript. Y-PL and X-JQ contributed to the study design, data acquisition, data interpretation, and statistical analysis. All authors contributed to the article and approved the submitted version.

FUNDING

This work was supported by grants from the National Natural Science Foundation of China under Grant (No.82003296), The Key Research and Development Program of Liaoning Province under Grant (2018225060), and the Technological Special Project of Liaoning Province of China under Grant (2019020176-JH1/103).

SUPPLEMENTARY MATERIAL

The Supplementary Material for this article can be found online at: https://www.frontiersin.org/articles/10.3389/fimmu.2021.666909/full#supplementary-material

REFERENCES

1. Siegel RL, Miller KD, Fuchs HE, Jemal A. Cancer Statistics, 2021. *CA Cancer J Clin* (2021) 71(1):7–33. doi: 10.3322/caac.21654
2. Reck M, Rodriguez-Abreu D, Robinson AG, Hui R, Csoszi T, Fulop A, et al. Pembrolizumab Versus Chemotherapy for PD-L1-Positive non-Small-Cell Lung Cancer. *N Engl J Med* (2016) 375(19):1823–33. doi: 10.1056/NEJMoa1606774
3. Zhou Y, Lin Z, Zhang X, Chen C, Zhao H, Hong S, et al. First-Line Treatment for Patients With Advanced non-Small Cell Lung Carcinoma and High PD-L1 Expression: Pembrolizumab or Pembrolizumab Plus Chemotherapy. *J Immunother Cancer* (2019) 7(1):120. doi: 10.1186/s40425-019-0600-6
4. Herbst RS, Giaccone G, de Marinis F, Reinmuth N, Vergnenegre A, Barrios CH, et al. Atezolizumab for First-Line Treatment of PD-L1-Selected Patients With NSCLC. *N Engl J Med* (2020) 383(14):1328–39. doi: 10.1056/NEJMoa1917346
5. Socinski MA, Jotte RM, Cappuzzo F, Orlandi F, Stroyakovskiy D, Nogami N, et al. Atezolizumab for First-Line Treatment of Metastatic Nonsquamous Nsclc. *N Engl J Med* (2018) 378(24):2288–301. doi: 10.1056/NEJMoa1716948
6. West H, McCleod M, Hussein M, Morabito A, Rittmeyer A, Conter HJ, et al. Atezolizumab in Combination With Carboplatin Plus Nab-Paclitaxel Chemotherapy Compared With Chemotherapy Alone as First-Line Treatment for Metastatic non-Squamous non-Small-Cell Lung Cancer (Impower130): A Multicentre, Randomised, Open-Label, Phase 3 Trial. *Lancet Oncol* (2019) 20(7):924–37. doi: 10.1016/S1470-2045(19)30167-6
7. Jotte R, Cappuzzo F, Vynnychenko I, Stroyakovskiy D, Rodriguez-Abreu D, Hussein M, et al. Atezolizumab in Combination With Carboplatin and Nab-Paclitaxel in Advanced Squamous NSCLC (Impower131): Results From a Randomized Phase III Trial. *J Thorac Oncol* (2020) 15(8):1351–60. doi: 10.1016/j.jtho.2020.03.028
8. Herbst R, Marinis FD, Giaccone G, Reinmuth N, Vergnenegre A, Barrios C, et al. O81 Impower110: Interim Overall Survival (OS) Analysis of a Phase III Study of Atezolizumab (ATEZO) Monotherapy vs Platinum-Based Chemotherapy (CHEMO) as First-Line (1L) Treatment in PD-L1–selected Nsclc. *J ImmunoTher Cancer* (2020) 8:A1–A. doi: 10.1136/LBA2019.1
9. Bucher HC, Guyatt GH, Griffith LE, Walter SD. The Results of Direct and Indirect Treatment Comparisons in Meta-Analysis of Randomized Controlled Trials. *J Clin Epidemiol* (1997) 50(6):683–91. doi: 10.1016/s0895-4356(97)00049-8
10. Chen DS, Mellman I. Oncology Meets Immunology: The Cancer-Immunity Cycle. *Immunity* (2013) 39(1):1–10. doi: 10.1016/j.immuni.2013.07.012
11. Zitvogel L, Apetoh L, Ghiringhelli F, Kroemer G. Immunological Aspects of Cancer Chemotherapy. *Nat Rev Immunol* (2008) 8(1):59–73. doi: 10.1038/nri2216
12. Emens LA, Middleton G. The Interplay of Immunotherapy and Chemotherapy: Harnessing Potential Synergies. *Cancer Immunol Res* (2015) 3(5):436–43. doi: 10.1158/2326-6066.CIR-15-0064
13. Leonetti A, Wever B, Mazzaschi G, Assaraf YG, Rolfo C, Quaini F, et al. Molecular Basis and Rationale for Combining Immune Checkpoint Inhibitors With Chemotherapy in non-Small Cell Lung Cancer. *Drug Resist Update* (2019) 46:100644. doi: 10.1016/j.drup.2019.100644
14. Reck M, Mok TSK, Nishio M, Jotte RM, Cappuzzo F, Orlandi F, et al. Atezolizumab Plus Bevacizumab and Chemotherapy in non-Small-Cell Lung Cancer (Impower150): Key Subgroup Analyses of Patients With EGFR Mutations or Baseline Liver Metastases in a Randomised, Open-Label Phase 3 Trial. *Lancet Respir Med* (2019) 7(5):387–401. doi: 10.1016/S2213-2600(19)30084-0
15. Kennedy LB, Salama AKS. A Review of Cancer Immunotherapy Toxicity. *CA Cancer J Clin* (2020) 70(2):86–104. doi: 10.3322/caac.21596
16. Peters S, Gettinger S, Johnson ML, Janne PA, Garassino MC, Christoph D, et al. Phase II Trial of Atezolizumab as First-Line or Subsequent Therapy for Patients With Programmed Death-Ligand 1-Selected Advanced non-Small-Cell Lung Cancer (Birch). *J Clin Oncol* (2017) 35(24):2781–9. doi: 10.1200/JCO.2016.71.9476
17. Mok TSK, Wu YL, Kudaba I, Kowalski DM, Cho BC, Turna HZ, et al. Pembrolizumab Versus Chemotherapy for Previously Untreated, PD-L1-expressing, Locally Advanced or Metastatic non-Small-Cell Lung Cancer (KEYNOTE-042): A Randomised, Open-Label, Controlled, Phase 3 Trial. *Lancet* (2019) 393(10183):1819–. doi: 10.1016/S0140-6736(18)32409-7

Conflict of Interest: The authors declare that the research was conducted in the absence of any commercial or financial relationships that could be construed as a potential conflict of interest.

Copyright © 2021 Li, Lu, Yang, Zhang, Jin, Wang, Che, Li, Liu and Qu. This is an open-access article distributed under the terms of the Creative Commons Attribution License (CC BY). The use, distribution or reproduction in other forums is permitted, provided the original author(s) and the copyright owner(s) are credited and that the original publication in this journal is cited, in accordance with accepted academic practice. No use, distribution or reproduction is permitted which does not comply with these terms.

frontiers in Oncology

ORIGINAL RESEARCH
published: 07 July 2021
doi: 10.3389/fonc.2021.671127

The Effectiveness and Safety of Immune Checkpoint Inhibitors in Non-Small Cell Lung Cancer Patients With Stage III/IV: A Multicenter Study

Jason C. Hsu[1], Phung-Anh Nguyen[2,3], Yen-Tzu Chen[4], Szu-Chun Yang[5], Chien-Chung Lin[5], Yi-Hsin Yang[6], Yu-Chao Lin[7], Te-Chun Hsia[7], Hsing-Chun Hsieh[5,8], Jia-Syuan Wu[8], Chi-Pei Chang[9], Yin-Hsun Feng[10], Peng-Chan Lin[5], Ping-Chih Hsu[11], Huey-En Tzeng[12], Shu-Chen Chien[13], Wei-Chiao Chang[14], Chih-Cheng Chang[15], Hsuan-Chia Yang[16], Chueh Ming Lee[17] and Christine Y. Lu[18]*

[1] International Ph.D. Program in Biotech and Healthcare Management, College of Management, Taipei Medical University, Taipei, Taiwan, [2] International Center for Health Information Technology, College of Medical Science & Technology, Taipei Medical University, Taipei, Taiwan, [3] Department of Healthcare Information & Management, Ming Chuan University, Taoyuan, Taiwan, [4] School of Pharmacy and Institute of Clinical Pharmacy and Pharmaceutical Sciences, College of Medicine, National Cheng Kung University, Tainan, Taiwan, [5] Department of Internal Medicine, National Cheng Kung University Hospital, College of Medicine, National Cheng Kung University, Tainan, Taiwan, [6] National Institute of Cancer Research, National Health Research Institutes, Tainan, Taiwan, [7] Department of Respiratory Therapy, China Medical University Hospital, Taichung, Taiwan, [8] Department of Pharmacy, Chi-Mei Medical Center, Tainan, Taiwan, [9] Department of Internal Medicine, Chi-Mei Medical Center, Tainan, Taiwan, [10] Division of Hematology and Oncology, Department of Internal Medicine, Chi-Mei Medical Center, Tainan, Taiwan, [11] Division of Thoracic Medicine, Department of Internal Medicine, Linkou Chang Gung Memorial Hospital, Chang Gung University College of Medicine, Taoyuan, Taiwan, [12] Division of Hematology and Oncology, Department of Medicine, Taipei Medical University Hospital, Taipei, Taiwan, [13] Department of Clinical Pharmacy, College of Pharmacy, Taipei Medical University, Taipei, Taiwan, [14] School of Pharmacy, College of Pharmacy, Taipei Medical University, Taipei, Taiwan, [15] Department of Internal Medicine, School of Medicine, College of Medicine, Taipei Medical University, Taipei, Taiwan, [16] Graduate Institute of Biomedical Informatics, College of Medical Science & Technology, Taipei Medical University, Taipei, Taiwan, [17] Department of Family Medicine, National Cheng Kung University Hospital, Tainan, Taiwan, [18] Department of Population Medicine, Harvard Medical School and Harvard Pilgrim Health Care Institute, Boston, MA, United States

OPEN ACCESS

Edited by:
Udo S Gaipl, University Hospital Erlangen, Germany

Reviewed by:
Sabine Semrau, University of Erlangen Nuremberg, Germany
Vishal Jindal, Beaumont Health, United States

***Correspondence:**
Jason C. Hsu
jasonhsu@tmu.edu.tw

Specialty section:
This article was submitted to Cancer Immunity and Immunotherapy, a section of the journal Frontiers in Oncology

Received: *23 February 2021*
Accepted: *22 June 2021*
Published: *07 July 2021*

Citation:
Hsu JC, Nguyen P-A, Chen Y-T, Yang S-C, Lin C-C, Yang Y-H, Lin Y-C, Hsia T-C, Hsieh H-C, Wu J-S, Chang C-P, Feng Y-H, Lin P-C, Hsu P-C, Tzeng H-E, Chien S-C, Chang W-C, Chang C-C, Yang H-C, Lee CM and Lu CY (2021) The Effectiveness and Safety of Immune Checkpoint Inhibitors in Non-Small Cell Lung Cancer Patients With Stage III/IV: A Multicenter Study. Front. Oncol. 11:671127. doi: 10.3389/fonc.2021.671127

Immune checkpoint inhibitors (ICIs) have been approved to treat patients with various cancer types, including lung cancer, in many countries. This study aims to investigate the effectiveness and safety of ICIs under different treatment conditions of non-small cell lung cancer patients. A population-based retrospective cohort study was conducted using the electronic health records of three medical centers in Taiwan. From January 01, 2016, to November 30, 2018, a total of 91 ICIs and 300 traditional chemotherapy users who had undergone stage III and IV lung cancer treatment were included in the study. We performed the randomized matched pair design by selecting a Chemotherapy subject for each ICI patient in the sample population. All subjects were monitored from the date of taking ICIs or chemotherapy drugs until the event of death, loss to follow-up, or were occurred with any defined adverse events. Kaplan-Meier estimators and cox proportional hazard regression models were used to compute the overall survival, efficacy, and safety of the ICIs group. The median overall survival (OS) in the ICI and Chemo groups after matching was 11.2 months and 10.5 months, respectively. However, the results showed

no significant OS differences between ICIs and chemo groups for both before and after matching (HR,1.30; 95%CI, 0.68-2.46; p=0.428 before matching and HR,0.96; 95CI%, 0.64-1.44; p=0.838 after matching). We observed that with the higher amount of PD-L1, the length of the patients' overall survival was (positive *vs.* negative PD-L1, HR,0.21; 95% CI, 0.05-0.80; p=0.022). The incidences of serious adverse drug events above grade 3 in the ICIs and traditional chemo groups were 12.7% and 21.5%, respectively. We also found that the number of AEs was less in ICIs than in the Chemo group, and the AEs that occurred after treatments were observed earlier in the ICIs compared to the Chemo group. ICIs drugs were observed to be safer than traditional chemotherapy as they had a lower risk of serious adverse drug events. It is necessary to pay attention to immune-related side effects and provide appropriate treatment. Furthermore, the patient's physical status and PD-L1 test can be used to evaluate the clinical effectiveness of ICIs.

Keywords: effectiveness, immune checkpoint inhibitors (ICI), non-small-cell lung cancer (NSCLA), observational study, Taiwan

INTRODUCTION

Lung cancer is the most leading cause of cancer death worldwide, including in Taiwan (1, 2). Non-small-cell lung cancer (NSCLC) accounts for 85% of overall lung cancer patients (3, 4). In recent years, immune checkpoint inhibitors (ICIs) have been approved to treat patients with various cancer types in many countries (5, 6). Immunotherapy drugs work by blocking checkpoint proteins from binding with their associated proteins. Thus, it targets cancer cells to slow cells' growth, prevent the cancer cell from spreading to other parts of the body, and increase the immune system's effectiveness (6, 7).

Recently, clinical trials studies have reported that ICIs drugs (e.g., pembrolizumab, atezolizumab, and nivolumab) used independently or its combination with traditional chemotherapies in NSCLC patients were significantly associated with 2 to 4 months longer of overall survival (OS) or progression-free survival (PFS) compared to those used only platinum-based chemotherapy (8–10). Studies also showed that ICIs drug users significantly improved the objective response rate (ORR, 63.5% *vs.* 48%) (11); It, however, increased the number of adverse events (AEs) (e.g., AE of grade 3 and over, 55.7% *vs.* 47%) compared to chemotherapy users (9, 11) (see **Table S1** in the appendix). Besides, NSCLC patients without EGFR/ALK mutations or patients with PD-L1 expression over 5% of tumor cells were observed with a significantly higher ORR and less AEs among ICIs drug patients than chemotherapy alone (12).

Furthermore, clinical trials had their limitations that could not be seen in clinical practice (e.g., patients with comorbidities, be short-time follow-up, analyze the long-term AEs associated with drugs, and patients with different genotypes, ethnic groups), may lead to being differences in the long-term effect and safety of drugs, especially for the immunotherapeutic results (5, 8, 9). Bagley et al. (13) showed NSCLC patients with nivolumab had a 19.4% ORR, the OS of 6.5 months, and the PFS of 2.1 months in the USA. Manrique et al. (14) and Oya et al. (15) conducted the study to observe the OS, SFS of patients treated with nivolumab in Spain and Japan, respectively. Lin et al. (16) and Hsu et al. (17) reported the studies in Taiwan among the patients with either pembrolizumab or nivolumab had 32% ORR, the OS ranged from 7.9 to 13 months, and the PFS ranged from 1.8 to 4.9 months. However, those studies reported with lack of information, such as no control group (i.e., chemotherapy), did not include new therapy 'atezolizumab'.

Therefore, this study aimed to address these gaps by examining the effectiveness and safety of ICIs under various treatment conditions and investigate the factors associated with their efficacy and safety. We also discuss the similarity and variations between our real-world empirical results and those obtained in previous clinical trials.

Abbreviation: NSCLC, Non-small-cell lung cancer; ICIs, Immune checkpoint inhibitors; OS, Overall survival; PFS, Progression-free survival; ORR, Objective response rate; AEs, Adverse events; ICD-10-CM, International Classification of Disease, Tenth Revision, Clinical Modification; ATC, Anatomical Therapeutic Chemical; HRs, Hazard ratios; Cis, Confidence intervals; IRBs, Institutional review boards.

METHOD

Study Design and Data Source

We conducted a retrospective cohort study by retrieving all patients were undergone treatments of non-small cell lung cancer (NSCLC) with stage III and IV from three medical centers in Taiwan, including National Cheng Kung University Hospital, Chi Mei Hospital, and China Medical University Hospital. We obtained the data of patients from three electronic medical records between 2016 and 2018. This study has been approved by the institutional review boards (IRBs) of the National Cheng Kung University Hospital. The data was anonymized and de-identified before the analysis.

Study Population

We identified patients diagnosed with lung cancer (International Classification of Disease, Tenth Revision, Clinical Modification [ICD-10-CM] codes C34), underwent treatments of NSCLC at stage III and IV from January 01, 2016, to November 30, 2018. We considered if patients had ever used immunological checkpoint inhibitors (ICIs) and those who had never used it in an analysis. Patients who had participated in any clinical trials and those who used more than two types of ICIs were excluded. Furthermore, patients with ages less than 20 years old were also excluded from the study.

Immunological checkpoint inhibitors (ICIs) drugs were classified as Anatomical Therapeutic Chemical (ATC) codes pembrolizumab (L01XC18), nivolumab (L01XC17), and atezolizumab (L01XC32) (see **Table S1** in the appendix). Cancer patients had received ICIs drugs for more than 14 days, defined as the ICIs group, compared with those who only used chemotherapy drugs.

To mimic the bias between two comparison groups, we performed the randomized matched-pair design. For each ICI patient, we selected a Chemo subject in the sample population; the randomized matched pair was matched for sex, age, EGFR/ALK mutation, daily performance status score (ECOG: 0-1 or 2-4 points), treatment situation (first-, second-, or third-line, or later).

Main Outcome Measurements

All subjects were monitored from the date of taking ICIs or chemotherapy drugs. Data were censored at the date of death or the date of any adverse events (AEs) that occurred (e.g., Skin rash, fatigue/asthenia, colitis, diarrhea, hepatitis, constipation, pneumonitis, anorexia/decreased appetite, hypothyroidism, nausea, hyperthyroidism, vomiting, adrenal insufficiency, mucositis, and myositis) (**Table S5** in the appendix), loss to follow-up, termination of insurance, or the end of the study at December 31, 2018.

Measurement of Covariates

We collected all information that might be associated with the mortality of studied patients. The data included demographic characteristics (e.g., age, sex, date of medical treatments, health performance status, smoking behavior status, HBsAg, and HCVAb), disease features (e.g., date of diagnosis, histology, stage, brain metastasis, EGFR/ALK mutation, and PD-L1 expression), and drug exposure information (e.g., line of treatments, drug types, a combination of chemotherapy, and baseline systemic steroid use). All covariates would include analyzing the effectiveness and safety of ICIs drugs in the study.

Statistical Analysis

We used the modified Kaplan-Meier and Gray methods (18) to compare the cumulative probabilities in competing for both ICIs and Chemo groups' overall survival in both samples, before and after matching. The log-rank test was used to estimate the differences in the time to event between patients using ICIs and Chemotherapy. In addition, hazard ratios (HRs) with 95% confidence intervals (CI) associated with the ICIs group were computed using Cox proportional hazard regression in competing for risk of death. Besides, we analyzed the factors related to the effectiveness and safety of ICI drugs.

All data management was performed using SAS v.9.3 software (SAS Institute Inc.). The statistical significance was considered with a p-value <0.05.

RESULTS

Basic Characteristics of Study Patients

We identified 391 potentially eligible NSCLC patients from three hospital datasets between 2016 to 2018, in which 91 patients were taken ICIs, and 300 patients were treated with chemotherapy drugs. After matching, 158 patients were included in the further analysis, in which 79 patients were in the ICIs, and another 79 patients were in the Chemo group (see **Figure 1**).

Basic characteristics of study groups after matching were presented in **Table 1**. The mean (SD, standard deviation) age of patients in ICIs and Chemo groups were 63.9 (10.2) and 64.2 (10.2) years, respectively. Male NSCLC patients were observed more than female in both groups (i.e., 65.8% *vs.* 34.2%). In this study, the histological type of NSCLC patients was non-squamous cell carcinoma (i.e., 84.8% for ICIs and 81% for the Chemo group). For both groups, patients were at stage IV (91.1% for ICIs *vs.* 88.6% for Chemo), and most patients did not have brain metastases at the initial cancer diagnosis. In addition, the positive PD-L1 expression was observed higher in both ICIs and Chemo groups for those who performed the PD-L1 gene test. The detailed demographic characteristics of both groups by various treatment lines before matching has shown in **Table S3** in the appendix.

Overall Survival Analysis of the Comparative Study Groups

Figure 2 showed the overall survival analysis between ICIs and Chemo group. The overall survival was observed no significantly in NSCLC patients with ICIs drugs compared to those with Chemotherapy drugs (HR, 0.96; 95% CI, 0.64 – 1.44; p=0.838) after matching (**Figure 2D**). Furthermore, we found that there were no statistically significant differences for overall survival between ICIs and Chemo groups by various treatment lines (first-, second-, third-line and over) before/after matching analysis (i.e., in the first-line, HR, 1.30; 95% CI, 0.68 – 2.46; p=0.428 before matching and HR, 1.11; 95% CI, 0.51-2.43; p=0.796 after matching) (**Figures 2A–C**, and **Table S4** in the appendix).

Multivariable Stratified Analysis for the Efficiency and Safety of ICIs Drugs

Table 2 showed the risk of death for the ICIs group after matching stratified by different factors. Patients with better performance status scores had a slightly reduced risk of death (i.e. 0-1 *vs.* 2-4, HR, 0.21; 95% CI, 0.05-1.01; p=0.051), while patients used steroid drugs had an increased risk of death (i.e.

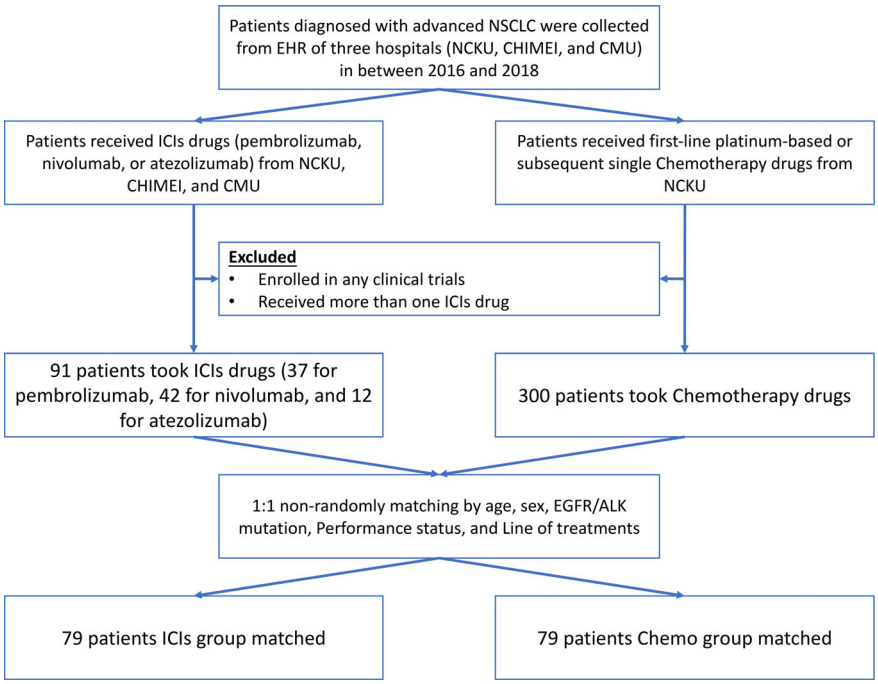

FIGURE 1 | Enrollment process of the study population.

used *vs.* non-use, HR, 2.88; 95% CI, 0.92-9.07; p=0.071). We found that patients with positive PD-L1 expression gene tests had a significantly decreased risk of death than those with negative test results (HR, 0.21; 95% CI, 0.05-0.80; p=0.022). The detailed information of patients with ICIs drugs had shown in **Table S2** in the appendix.

Figure 3 showed the adverse events (AEs) for the ICIs group stratified by different factors. We observed that patients who used ICIs combined with chemotherapy drugs had significantly higher adverse events than those who did not use combination drugs (HR, 7.16; 95% CI, 1.54-33.4; p=0.012). However, we also found that the number of AEs was less in ICIs than in the Chemo group, and the AEs that occurred after treatments were observed earlier in ICIs compared to the Chemo group (7 *vs.* 13 months) (**Table S5** and **Figure S1** in the appendix).

DISCUSSION

This study is the first observational study in Taiwan to compare the real-world effectiveness and safety of ICIs and traditional chemotherapy in the treatment of NSCLC. It considered NSCLC patients who used ICIs at three medical centers in Taiwan. The median overall survival in the first-line treatment setting was 14.4 months in the ICIs group and 17.4 months in the Chemo group. In the study, the median overall survival of the ICIs group was similar to the clinical trial results; the survival rate, however, was significantly longer in the Chemo group compared to those were in the clinical trial studies (17.4 *vs.* 11.3-14.7 months). The mortality risk ratio was 1.3 (95% CI, 0.68-2.46), with no significant between the comparative groups. The study subjects were Asian, with the proportion in the clinical trials was relatively low (1-19.4%) (19). Furthermore, studies have reported that Asian NSCLC patients have better survival prognoses and treatment responses than their non-Asian counterparts (20–22). A separate analysis of first-line chemotherapy among patients with NSCLC in Taiwan found that the median overall survival after treatment with different platinum-containing combined chemotherapy treatments ranged from 16.6 to 27.1 months (23), which is comparable to the results of the Chemo group in this study, suggesting that patients with NSCLC in Taiwan have reasonable survival rates with chemotherapy.

Furthermore, high PD-L1 expression (≥50%) is often used alone with pembrolizumab (9, 11), while low PD-L1 expression (<50%) has a better survival benefit when combined with pembrolizumab or atezolizumab and platinum-containing chemotherapy (24, 25). However, most of the drugs in the ICI group in this study were started before the relevant clinical trials were published; the treatment model was not consistent with the clinical trials, and the proportion of high PD-L1 expression (≥50%) was not as high as those in clinical trials.

Besides, we observed that it might take about three months or more from the start of ICIs to the response (10, 26–28), and the response pattern is different from that with chemotherapy. The immune system's particular mechanism induced by ICI causes the treatment response to persist until the drug is discontinued. It may even cause temporary deterioration of the tumor due to the temporary infiltration of immune cells. The tumor may begin

TABLE 1 | Demographic characteristics of study population after matching.

Characteristics	Immune checkpoint inhibitors n = 79 (%)	Chemotherapy n = 79 (%)	p-value[a]
Age			0.370
Mean (SD)	63.9 (10.2)	64.2 (10.2)	
Age group			0.983
30-39	1 (1.3)	1 (1.3)	
40-49	5 (6.3)	5 (6.3)	
50-59	22 (27.8)	19 (24.1)	
60-69	28 (35.4)	32 (40.5)	
70-79	18 (22.8)	16 (20.3)	
80-89	5 (6.3)	6 (7.6)	
Sex			1.000
Male	52 (65.8)	52 (65.8)	
Female	27 (34.2)	27 (34.2)	
Performance status			1.000
0-1	69 (87.3)	69 (87.3)	
2-4	10 (12.7)	10 (12.7)	
EGFR/ALK mutation			1.000
Positive	20 (25.3)	20 (25.3)	
Negative	59 (74.7)	59 (74.7)	
Treatment lines			1.000
First-line	30 (42.9)	30 (42.9)	
Second-line	13 (16.5)	13 (16.5)	
Third-line and over	36 (45.6)	36 (45.6)	
Histology			0.526
Squamous	12 (15.2)	15 (19)	
Non-squamous	67 (84.8)	64 (81)	
Tumor stage[b]			0.598
III	7 (8.9)	9 (11.4)	
IV	72 (91.1)	70 (88.6)	
Brain metastasis			0.602
Yes	25 (31.6)	22 (27.8)	
No	54 (68.4)	57 (72.2)	
PD-L1 expression			<0.001
Positive	42 (53.16)	18 (22.8)	
Negative	7 (8.86)	6 (7.6)	
Missing	30 (38)	55 (69.6)	

[a]*p-value was calculated using Student t test with continuous variables and chi-square or Fisher exact test with category variables.*
[b]*Tumor stage, represents the stage at the initial diagnosis of a cancer patient.*

to shrink after the disease has been observed to worsen (29, 30). However, the ICI group's median observation period in this study was only 3.94 months, which may not have been long enough to track the occurrence of treatment response.

Survival Trend in Different Treatment Lines

In the second-line and third-line treatment settings, the median overall survival in the ICI group was about two months longer than that in the Chemo group (second-line: 11.3 *vs.* 9.5 months, HR: 0.76, P = 0.46; third-line or later: 10.8 *vs.* 8.6 months, HR: 0.84, P = 0.39). Although there were no statistically significant differences, a better survival trend was observed in the ICI group. The second-and third-line subjects in this study were more likely to carry EGFR or ALK mutations, especially in third-line or later treatments. Studies have suggested that the use of second-line ICIs alone in treating lung cancer patients with EGFR mutations does not lead to good survival benefits (31, 32). Good outcomes might be achieved when combined ICIs with chemotherapy. Chemotherapy is generally considered to have only immunosuppressive effects, such as bone marrow suppression or hemocytopenia. However, recent studies have found that chemotherapy may have immunomodulatory properties, which can be induced by the tumor microenvironment from the immune desert or immune excluded to a state conducive to the role of immune cells (33). Even if the proportion of patients with EGFR or ALK mutations increases, chemotherapy may provide some survival benefits (34).

The Effectiveness and Safety of ICIs Drugs

Past clinical trials and observational studies have mentioned better physical performance status and high PD-L1 expression as factors that reduce death risk (16, 35, 36). In this study, PD-L1 expression was analyzed using stratification; Although there were no statistically significant differences, it was observed that the higher amount of PD-L1, the longer of the patient's overall survival was. In a past Taiwan cohort study (16), 74 patients with advanced NSCLC treated with pembrolizumab or nivolumab alone were analyzed by stratifying PD-L1. The median overall survival also showed the same increasing trend found in this study (PD-L1 ≥50%, not reached; PD-L11-49%, 10.5 months; PD-L1 <1%, 13.2 months; p = 0.217). The results confirmed that PD-L1 expression could be used as an evaluation index for the clinical selection of drugs. It is worth noting that this study included more patients with poor physical performance (PS≥2,

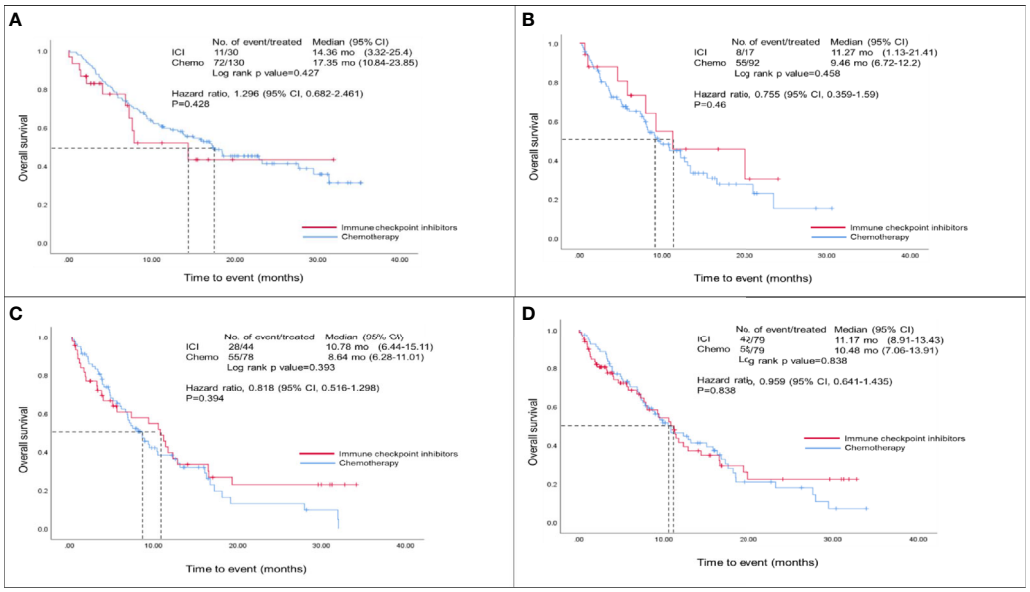

FIGURE 2 | Overall survival analysis of ICIs and Chemo groups. **(A)** Overall survival analysis of the first-line group before matching; **(B)** Overall survival analysis of the second-line group before matching; **(C)** Overall survival analysis of those patients at third-line and over before matching; **(D)** Overall survival analysis of both ICIs and Chemo groups after matching; Hazard ratios were adjusted for histological types, tumor stage, brain metastasis, and PD-L1 expression variables in the cox-regression model.

TABLE 2 | ICIs drugs use and its association with overall mortality by different covariates[a].

Variables	Univariate		Multivariate	
	HR (95% CI)	p-value	HR (95% CI)[b]	p-value
Sex				
Male *vs.* Female	1.04 (0.58-1.87)	0.890	1.39 (0.48-4.05)	0.542
Age				
≥65 *vs.* <65	1.12 (0.63-1.99)	0.706	0.48 (0.16-1.51)	0.210
Smoking status				
Never *vs.* Current	2.41 (0.86-6.74)	0.093	1.86 (0.41-8.34)	0.419
Performance status				
0-1 *vs.* 2-4	0.22 (0.1-0.51)	<0.001	0.21 (0.05-1.01)	0.051
Histology				
Squamous *vs.* Non-squamous	0.90 (0.38-2.13)	0.813	0.78 (0.15-4.05)	0.765
Brain metastasis				
Yes *vs.* No	1.70 (0.94-3.08)	0.079	0.94 (0.32-2.73)	0.905
PD-L1 expression				
Positive *vs.* Negative	0.46 (0.18-1.19)	0.111	**0.21 (0.05-0.80)**	**0.022**
EGFR/ALK mutation				
Positive *vs.* Negative	1.26 (0.68-2.33)	0.463	0.74 (0.21-2.64)	0.638
Treatment lines				
First-line *vs.* Subsequent-line	0.78 (0.39-1.54)	0.468	1.26 (0.26-6.03)	0.770
Steroid use				
Yes *vs.* No	2.97 (1.59-5.57)	0.001	2.88 (0.92-9.07)	0.071
Combined with chemotherapy				
Yes *vs.* No	0.60 (0.32-1.10)	0.100	0.38 (0.11-1.30)	0.123
Immune checkpoint inhibitors types				
Pembrolizumab *vs.* Nivolumab	0.90 (0.46-1.75)	0.748	–	
Pembrolizumab *vs.* Atezolizumab	0.63 (0.27-1.51)	0.304	–	
Nivolumab *vs.* Atezolizumab	0.58 (0.26-1.33)	0.198	–	

HR, hazard ratio; CI, confidence intervals.

[a]*Multivariable analysis is by Cox proportional hazards model.*

[b]*Adjusted for covariate factors, including in* ***Table S2*** *in the appendix.*

The bold values mean that it is a significant difference in the statistical analysis.

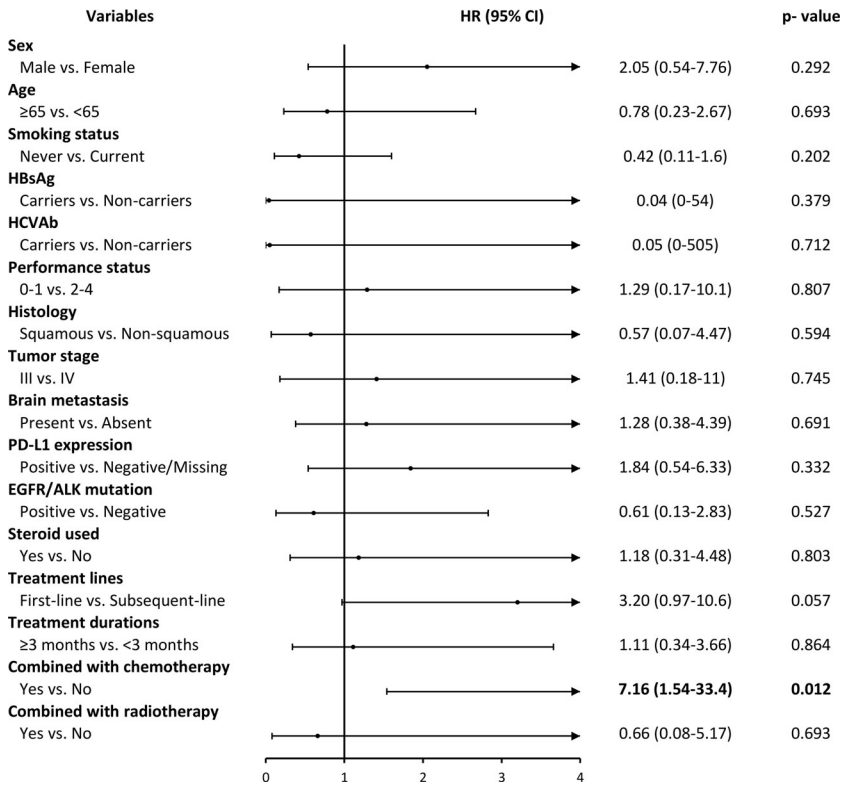

FIGURE 3 | ICIs drugs use and its association with grade 3 and over adverse events by different covariates. HR, hazard ratio; CI, confidence intervals.

36/74, 48.6%), where the ICI was third-line or later, accounting for 70%. The median overall survival of all patients was 7.9 months, which was worse than the overall survival of all patients in this study's ICI group (11.2 months).

Regarding the effects of steroids on ICIs, a real-world study of patients with NSCLC in the USA used pembrolizumab, nivolumab, atezolizumab, or durvalumab alone at two cancer centers compared the effectiveness of oral or injectable steroids in the first 30 days of use of ICIs. Steroids reduce not only overall patient survival but also treatment response and non-deteriorating survival (37).

Hepatitis patients are usually excluded from clinical ICI trials. However, Taiwan is a region with a high prevalence of hepatitis B. There is insufficient data on the effectiveness of ICI in patients with cancer and hepatitis B. According to the stratified survival analysis results in this study, the overall survival of patients with hepatitis B was significantly lower. Chronic infection may inhibit the role of T cells, thereby reducing the effect of drug-induced immunity (38). Thus, clinicians should carefully evaluate the suitability of immunotherapy for cancer patients with comorbid hepatitis.

Safety results reported in the clinical trials have shown that ICIs cause fewer serious adverse drug events than chemotherapy. This study confirmed this finding, but the between-group differences were not significant (ICIs: 10 patients, 12.7% *vs.* Chemo: 17 patients, 21.5%). The type of adverse events in the ICI group were mainly immune-related side effects. The common types were pneumonitis and skin rash, similar to past clinical trials and observational studies (39, 40). In addition, this study found that adverse events in the two groups occurred early in the treatment. Even the Chemo group had the most occurrences within one month of starting the treatment, with no significant between-group differences. Past literature indicates that most immune-related side effects occur within six months after medication (41). The adverse events observed in the ICI group in this study all happened within seven months after initiation of treatment and showed similar results. Besides, in terms of the type of immune-related side effects, in the past, the skin and gastrointestinal tract were found to be the earliest affected organs, followed by the liver, lungs, and endocrine system (41, 42). However, due to the small number of incidents and the short observation period, the same performance trend was not observed in this study. Therefore, we need to include more patients and extend the observation period to confirm the adverse event performance of ICIs.

There have been no published studies comparing the safety of ICI alone with concurrent chemotherapy in NSCLC. However, one network integration analysis included four Phase III clinical trials of the first-line pembrolizumab, which indirectly compared the adverse event risk of pembrolizumab with grade 3-5 combined with chemotherapy alone. The results also showed that the risk of concomitant use significantly increased the risk of

adverse events compared to a single-use (RR 2.14, 95% CI 1.50-3.05; P <0.001) (43).

Limitations

This study has the following limitations. First, the number of patients in the ICI group was less may affect the outcomes. The ICI was licensed as early as December 2015, Taiwan Health Insurance did not cover it until April 2019. All patients have to pay for ICIs at their own expense before payment is approved. These drugs are expensive and require continuous treatment until the disease worsens or severe intolerable side effects occur (44). Even if the patient is expected to experience an excellent therapeutic effect (such as high PD-L1 expression), the enormous economic burden makes the number of patients willing to accept treatment with ICIs low.

Second, the data source of this study was the electronic medical records from three medical centers. Some items had to be evaluated by a clinician, such as physical performance scores, adverse drug events, severity, etc. Data collection may have been incomplete because the patient did not report ultimately, or the medical records were not noted with this data. In addition, the PD-L1 detection rate of this research object was low, and more test data is needed further to verify the impact of performance on overall survival.

Third, this study's observation period was relatively short, especially in the ICI group, because nearly 41% of the patients started taking medication in 2018, and the median observation period was less than one year. Since most of the ICI clinical trials for NSCLC were published from 2016 to 2018 (10, 11, 45), the patients' treatment model in the ICI group did not fully follow the clinical trials' conclusion not show the actual effectiveness of the drug.

CONCLUSION

The overall survival of patients with advanced NSCLC in Taiwan using ICIs was not significantly better than that for patients undergoing traditional chemotherapy, regardless of where it was a first-line or subsequent treatment. It was also observed that ICIs drugs have a lower risk of serious adverse drug events than traditional chemotherapy, which indicated that they are safer. Nevertheless, ICI combined with chemotherapy may increase the risk of occurrence of adverse events. Therefore, it is still necessary to pay attention to immune-related side effects and provide appropriate treatment as soon as possible. Furthermore, the patient's physical status and PD-L1 test can be used to evaluate the clinical effectiveness of ICIs. Patients with hepatitis B receiving ICI and using systemic steroids at the beginning of treatment need to be carefully monitored for possible adverse reactions.

DATA AVAILABILITY STATEMENT

The raw data supporting the conclusions of this article will be made available by the authors, without undue reservation.

ETHICS STATEMENT

The studies involving human participants were reviewed and approved by National Cheng Kung University Hospital. Written informed consent for participation was not required for this study in accordance with the national legislation and the institutional requirements.

AUTHOR CONTRIBUTIONS

P-AN, JCH, Y-TC, S-CY, C-CL, and Y-HY conceptualized and designed the study. P-AN, Y-CL, T-CH, Y-HF, P-CL, P-CH, H-ET, S-CC, and W-CC provided suggestions for the research design from a clinical perspective. Y-TC, Y-CL, H-CH, J-SW, and CML collected data, performed the analyses, and drafted the manuscript. P-AN and CYL reviewed all data and revised the manuscript critically for intellectual content. All authors contributed to the article and approved the submitted version.

FUNDING

This work was supported by the Taiwan Ministry of Science and Technology grants [grant numbers: MOST 107-2320-B-006-040 and MOST 108-2314-B-006-039].

SUPPLEMENTARY MATERIAL

The Supplementary Material for this article can be found online at: https://www.frontiersin.org/articles/10.3389/fonc.2021.671127/full#supplementary-material

REFERENCES

1. Barta JA, Powell CA, Wisnivesky JP. Global Epidemiology of Lung Cancer. *Ann Global Health* (2019) 85(1):8. doi: 10.5334/aogh.2419
2. Reck M, Heigener DF, Mok T, Soria J-C, Rabe KF. Management of non-Small-Cell Lung Cancer: Recent Developments. *Lancet* (2013) 382 (9893):709–19. doi: 10.1016/S0140-6736(13)61502-0
3. Bray F, Ferlay J, Soerjomataram I, Siegel RL, Torre LA, Jemal A. Global Cancer Statistics 2018: GLOBOCAN Estimates of Incidence and Mortality Worldwide for 36 Cancers in 185 Countries. *CA Cancer J Clin* (2018) 68 (6):394–424. doi: 10.3322/caac.21492
4. Nguyen P-A, Chang C-C, Galvin CJ, Wang Y-C, An SY, Huang C-W, et al. Statins Use and its Impact in EGFR-TKIs Resistance to Prolong the Survival of Lung Cancer Patients: A Cancer Registry Cohort Study in Taiwan. *Cancer Sci* (2020) 111(8):2965–73. doi: 10.1111/cas.14493
5. Onoi K, Chihara Y, Uchino J, Shimamoto T, Morimoto Y, Iwasaku M, et al. Immune Checkpoint Inhibitors for Lung Cancer Treatment: A Review. *J Clin Med* (2020) 9(5):1362. doi: 10.3390/jcm9051362

6. Vaddepally RK, Kharel P, Pandey R, Garje R, Chandra AB. Review of Indications of FDA-Approved Immune Checkpoint Inhibitors Per NCCN Guidelines With the Level of Evidence. *Cancers (Basel)* (2020) 12(3):738. doi: 10.3390/cancers12030738
7. Picardo SL, Doi J, Hansen AR. Structure and Optimization of Checkpoint Inhibitors. *Cancers (Basel)* (2019) 12(1):38. doi: 10.3390/cancers12010038
8. Langer CJ, Gadgeel SM, Borghaei H, Papadimitrakopoulou VA, Patnaik A, Powell SF, et al. Carboplatin and Pemetrexed With or Without Pembrolizumab for Advanced, Non-Squamous Non-Small-Cell Lung Cancer: A Randomised, Phase 2 Cohort of the Open-Label KEYNOTE-021 Study. *Lancet Oncol* (2016) 17(11):1497–508. doi: 10.1016/s1470-2045(16)30498-3
9. Gandhi L, Rodríguez-Abreu D, Gadgeel S, Esteban E, Felip E, De Angelis F, et al. Pembrolizumab Plus Chemotherapy in Metastatic Non–Small-Cell Lung Cancer. *N Engl J Med* (2018) 378(22):2078–92. doi: 10.1056/NEJMoa1801005
10. Carbone DP, Reck M, Paz-Ares L, Creelan B, Horn L, Steins M, et al. First-Line Nivolumab in Stage IV or Recurrent Non–Small-Cell Lung Cancer. *N Engl J Med* (2017) 376(25):2415–26. doi: 10.1056/NEJMoa1613493
11. Socinski MA, Jotte RM, Cappuzzo F, Orlandi F, Stroyakovskiy D, Nogami N, et al. Atezolizumab for First-Line Treatment of Metastatic Nonsquamous NSCLC. *N Engl J Med* (2018) 378(24):2288–301. doi: 10.1056/NEJMoa1716948
12. Reck M, Rodríguez-Abreu D, Robinson AG, Hui R, Csőszi T, Fülöp A, et al. Pembrolizumab Versus Chemotherapy for PD-L1–Positive Non–Small-Cell Lung Cancer. *N Engl J Med* (2016) 375(19):1823–33. doi: 10.1056/NEJMoa1606774
13. Bagley SJ, Kothari S, Aggarwal C, Bauml JM, Alley EW, Evans TL, et al. Pretreatment Neutrophil-to-Lymphocyte Ratio as a Marker of Outcomes in Nivolumab-Treated Patients With Advanced Non-Small-Cell Lung Cancer. *Lung Cancer* (2017) 106:1–7. doi: 10.1016/j.lungcan.2017.01.013
14. Areses Manrique MC, Mosquera Martínez J, García González J, Afonso Afonso FJ, Lázaro Quintela M, Fernández Núñez N, et al. Real World Data of Nivolumab for Previously Treated Non-Small Cell Lung Cancer Patients: A Galician Lung Cancer Group Clinical Experience. *Transl Lung Cancer Res* (2018) 7(3):404–15. doi: 10.21037/tlcr.2018.04.03
15. Oya Y, Yoshida T, Kuroda H, Mikubo M, Kondo C, Shimizu J, et al. Predictive Clinical Parameters for the Response of Nivolumab in Pretreated Advanced Non-Small-Cell Lung Cancer. *Oncotarget* (2017) 8(61):103117–28. doi: 10.18632/oncotarget.21602
16. Lin SY, Yang CY, Liao BC, Ho CC, Liao WY, Chen KY, et al. Tumor PD-L1 Expression and Clinical Outcomes in Advanced-Stage Non-Small Cell Lung Cancer Patients Treated With Nivolumab or Pembrolizumab: Real-World Data in Taiwan. *J Cancer* (2018) 9(10):1813–20. doi: 10.7150/jca.24985
17. Hsu JC, Lin JY, Hsu MY, Lin PC. Effectiveness and Safety of Immune Checkpoint Inhibitors: A Retrospective Study in Taiwan. *PloS One* (2018) 13(8):e0202725. doi: 10.1371/journal.pone.0202725
18. Austin PC, Lee DS, Fine JP. Introduction to the Analysis of Survival Data in the Presence of Competing Risks. *Circulation* (2016) 133(6):601–9. doi: 10.1161/CIRCULATIONAHA.115.017719
19. Soo RA, Loh M, Mok TS, Ou SH, Cho BC, Yeo WL, et al. Ethnic Differences in Survival Outcome in Patients With Advanced Stage Non-Small Cell Lung Cancer: Results of a Meta-Analysis of Randomized Controlled Trials. *J Thorac Oncol* (2011) 6(6):1030–8. doi: 10.1097/JTO.0b013e3182199c03
20. Ahn MJ, Lee J, Park YH, Ahn JS, Ziogas A, Zell JA, et al. Korean Ethnicity as Compared With White Ethnicity is an Independent Favorable Prognostic Factor for Overall Survival in Non-Small Cell Lung Cancer Before and After the Oral Epidermal Growth Factor Receptor Tyrosine Kinase Inhibitor Era. *J Thorac Oncol* (2010) 5(8):1185–96. doi: 10.1097/JTO.0b013e3181e2f624
21. Gandara DR, Kawaguchi T, Crowley J, Moon J, Furuse K, Kawahara M, et al. Japanese-US Common-Arm Analysis of Paclitaxel Plus Carboplatin in Advanced Non-Small-Cell Lung Cancer: A Model for Assessing Population-Related Pharmacogenomics. *J Clin Oncol* (2009) 27(21):3540–6. doi: 10.1200/jco.2008.20.8793
22. Soo RA, Kawaguchi T, Loh M, Ou S-HI, Shieh MP, Cho B-C, et al. Differences in Outcome and Toxicity Between Asian and Caucasian Patients With Lung Cancer Treated With Systemic Therapy. *Future Oncol* (2012) 8(4):451–62. doi: 10.2217/fon.12.25
23. Liang YH, Shao YY, Liao BC, Lee HS, Yang JC, Chen HM, et al. Cytotoxic Chemotherapy as First-Line Therapy for Advanced Non-Small-Cell Lung Cancer in Taiwan: Daily Practice. *J Cancer* (2016) 7(11):1515–23. doi: 10.7150/jca.15180
24. Mok TSK, Wu YL, Kudaba I, Kowalski DM, Cho BC, Turna HZ, et al. Pembrolizumab Versus Chemotherapy for Previously Untreated, PD-L1-Expressing, Locally Advanced or Metastatic Non-Small-Cell Lung Cancer (KEYNOTE-042): A Randomised, Open-Label, Controlled, Phase 3 Trial. *Lancet* (2019) 393(10183):1819–30. doi: 10.1016/s0140-6736(18)32409-7
25. Rittmeyer A, Barlesi F, Waterkamp D, Park K, Ciardiello F, von Pawel J, et al. Atezolizumab Versus Docetaxel in Patients With Previously Treated Non-Small-Cell Lung Cancer (OAK): A Phase 3, Open-Label, Multicentre Randomised Controlled Trial. *Lancet* (2017) 389(10066):255–65. doi: 10.1016/s0140-6736(16)32517-x
26. Borghaei H, Paz-Ares L, Horn L, Spigel DR, Steins M, Ready NE, et al. Nivolumab Versus Docetaxel in Advanced Nonsquamous Non-Small-Cell Lung Cancer. *N Engl J Med* (2015) 373(17):1627–39. doi: 10.1056/NEJMoa1507643
27. Brahmer J, Reckamp KL, Baas P, Crinò L, Eberhardt WEE, Poddubskaya E, et al. Nivolumab Versus Docetaxel in Advanced Squamous-Cell Non–Small-Cell Lung Cancer. *N Engl J Med* (2015) 373(2):123–35. doi: 10.1056/NEJMoa1504627
28. Herbst RS, Baas P, Kim DW, Felip E, Pérez-Gracia JL, Han JY, et al. Pembrolizumab Versus Docetaxel for Previously Treated, PD-L1-Positive, Advanced Non-Small-Cell Lung Cancer (KEYNOTE-010): A Randomised Controlled Trial. *Lancet* (2016) 387(10027):1540–50. doi: 10.1016/s0140-6736(15)01281-7
29. Borcoman E, Kanjanapan Y, Champiat S, Kato S, Servois V, Kurzrock R, et al. Novel Patterns of Response Under Immunotherapy. *Ann Oncol* (2019) 30(3):385–96. doi: 10.1093/annonc/mdz003
30. Borcoman E, Nandikolla A, Long G, Goel S, Tourneau CL. Patterns of Response and Progression to Immunotherapy. *Am Soc Clin Oncol Educ Book* (2018) 38:169–78. doi: 10.1200/edbk_200643
31. Lee CK, Man J, Lord S, Cooper W, Links M, Gebski V, et al. Clinical and Molecular Characteristics Associated With Survival Among Patients Treated With Checkpoint Inhibitors for Advanced Non-Small Cell Lung Carcinoma: A Systematic Review and Meta-Analysis. *JAMA Oncol* (2018) 4(2):210–6. doi: 10.1001/jamaoncol.2017.4427
32. Garassino MC, Gelibter AJ, Grossi F, Chiari R, Soto Parra H, Cascinu S, et al. Italian Nivolumab Expanded Access Program In Nonsquamous Non-Small Cell Lung Cancer Patients: Results in Never-Smokers and EGFR-Mutant Patients. *J Thorac Oncol* (2018) 13(8):1146–55. doi: 10.1016/j.jtho.2018.04.025
33. Heinhuis KM, Ros W, Kok M, Steeghs N, Beijnen JH, Schellens JHM. Enhancing Antitumor Response by Combining Immune Checkpoint Inhibitors With Chemotherapy in Solid Tumors. *Ann Oncol* (2019) 30(2):219–35. doi: 10.1093/annonc/mdy551
34. Kuo CS, Wang CC, Huang YC, Pavlidis S, Liu CY, Ko HW, et al. Comparison of a Combination of Chemotherapy and Immune Checkpoint Inhibitors and Immune Checkpoint Inhibitors Alone for the Treatment of Advanced and Metastatic non-Small Cell Lung Cancer. *Thorac Cancer* (2019) 10(5):1158–66. doi: 10.1111/1759-7714.13057
35. Montana M, Garcia ME, Ausias N, Jeanpierre M, Meiffren M, Giorgi R, et al. Efficacy and Safety of Nivolumab in Patients With non-Small Cell Lung Cancer: A Retrospective Study in Clinical Practice. *J Chemother* (2019) 31(2):90–4. doi: 10.1080/1120009x.2018.1551753
36. Zhao Q, Xie R, Lin S, You X, Weng X. Anti-PD-1/PD-L1 Antibody Therapy for Pretreated Advanced or Metastatic Nonsmall Cell Lung Carcinomas and the Correlation Between PD-L1 Expression and Treatment Effectiveness: An Update Meta-Analysis of Randomized Clinical Trials. *BioMed Res Int* (2018) 2018:3820956. doi: 10.1155/2018/3820956
37. Arbour KC, Mezquita L, Long N, Rizvi H, Auclin E, Ni A, et al. Impact of Baseline Steroids on Efficacy of Programmed Cell Death-1 and Programmed Death-Ligand 1 Blockade in Patients With Non-Small-Cell Lung Cancer. *J Clin Oncol* (2018) 36(28):2872–8. doi: 10.1200/jco.2018.79.0006
38. Johnson DB, Sullivan RJ, Menzies AM. Immune Checkpoint Inhibitors in Challenging Populations. *Cancer* (2017) 123(11):1904–11. doi: 10.1002/cncr.30642
39. Nakaya A, Kurata T, Yoshioka H, Takeyasu Y, Niki M, Kibata K, et al. Neutrophil-To-Lymphocyte Ratio as an Early Marker of Outcomes in Patients

With Advanced Non-Small-Cell Lung Cancer Treated With Nivolumab. *Int J Clin Oncol* (2018) 23(4):634–40. doi: 10.1007/s10147-018-1250-2
40. Fujimoto D, Yoshioka H, Kataoka Y, Morimoto T, Kim YH, Tomii K, et al. Efficacy and Safety of Nivolumab in Previously Treated Patients With non-Small Cell Lung Cancer: A Multicenter Retrospective Cohort Study. *Lung Cancer* (2018) 119:14–20. doi: 10.1016/j.lungcan.2018.02.017
41. Martins F, Sofiya L, Sykiotis GP, Lamine F, Maillard M, Fraga M, et al. Adverse Effects of Immune-Checkpoint Inhibitors: Epidemiology, Management and Surveillance. *Nat Rev Clin Oncol* (2019) 16(9):563–80. doi: 10.1038/s41571-019-0218-0
42. Haanen J, Carbonnel F, Robert C, Kerr KM, Peters S, Larkin J, et al. Management of Toxicities From Immunotherapy: ESMO Clinical Practice Guidelines for Diagnosis, Treatment and Follow-Up. *Ann Oncol* (2017) 28 (suppl_4):iv119–42. doi: 10.1093/annonc/mdx225
43. Kim R, Keam B, Hahn S, Ock CY, Kim M, Kim TM, et al. First-Line Pembrolizumab Versus Pembrolizumab Plus Chemotherapy Versus Chemotherapy Alone in Non-Small-Cell Lung Cancer: A Systematic Review and Network Meta-Analysis. *Clin Lung Cancer* (2019) 20(5):331–8.e4. doi: 10.1016/j.cllc.2019.05.009
44. Planchard D, Popat S, Kerr K, Novello S, Smit EF, Faivre-Finn C, et al. Metastatic non-Small Cell Lung Cancer: ESMO Clinical Practice Guidelines for Diagnosis, Treatment and Follow-Up. *Ann Oncol* (2018) 29(Suppl 4): iv192–237. doi: 10.1093/annonc/mdy275
45. Paz-Ares L, Luft A, Vicente D, Tafreshi A, Gümüş M, Mazières J, et al. Pembrolizumab Plus Chemotherapy for Squamous Non–Small-Cell Lung Cancer. *N Engl J Med* (2018) 379(21):2040–51. doi: 10.1056/NEJMoa1810865

Conflict of Interest: The authors declare that the research was conducted in the absence of any commercial or financial relationships that could be construed as a potential conflict of interest.

Copyright © 2021 Hsu, Nguyen, Chen, Yang, Lin, Yang, Lin, Hsia, Hsieh, Wu, Chang, Feng, Lin, Hsu, Tzeng, Chien, Chang, Chang, Yang, Lee and Lu. This is an open-access article distributed under the terms of the Creative Commons Attribution License (CC BY). The use, distribution or reproduction in other forums is permitted, provided the original author(s) and the copyright owner(s) are credited and that the original publication in this journal is cited, in accordance with accepted academic practice. No use, distribution or reproduction is permitted which does not comply with these terms.

frontiers in Immunology

ORIGINAL RESEARCH
published: 26 July 2021
doi: 10.3389/fimmu.2021.706133

Combination Therapy of Mithramycin A and Immune Checkpoint Inhibitor for the Treatment of Colorectal Cancer in an Orthotopic Murine Model

Rinku Dutta[1,2,3], *Roukiah Khalil*[1,2,3], *Karthick Mayilsamy*[1,2,3], *Ryan Green*[1,3,4], *Mark Howell*[1,3,4], *Srinivas Bharadwaj*[4], *Shyam S. Mohapatra*[1,3,4] *and Subhra Mohapatra*[1,2,3]*

[1] James A. Haley Veterans' Hospital, Tampa, FL, United States, [2] Department of Molecular Medicine, Morsani College of Medicine, University of South Florida, Tampa, FL, United States, [3] Center for Research and Education in Nano-Bioengineering, Morsani College of Medicine, University of South Florida, Tampa, FL, United States, [4] Department of Internal Medicine, Morsani College of Medicine, University of South Florida, Tampa, FL, United States

OPEN ACCESS

Edited by:
Udo S. Gaipl,
University Hospital Erlangen, Germany

Reviewed by:
Stephanie Hehlgans,
Goethe University Frankfurt, Germany
Federica Facciotti,
European Institute of Oncology (IEO), Italy

***Correspondence:**
Subhra Mohapatra
smohapa2@usf.edu

Specialty section:
This article was submitted to Cancer Immunity and Immunotherapy, a section of the journal Frontiers in Immunology

Received: 06 May 2021
Accepted: 25 June 2021
Published: 26 July 2021

Citation:
Dutta R, Khalil R, Mayilsamy K, Green R, Howell M, Bharadwaj S, Mohapatra SS and Mohapatra S (2021) Combination Therapy of Mithramycin A and Immune Checkpoint Inhibitor for the Treatment of Colorectal Cancer in an Orthotopic Murine Model. Front. Immunol. 12:706133. doi: 10.3389/fimmu.2021.706133

The axis of Programmed cell death-1 receptor (PD-1) with its ligand (PD-L1) plays a critical role in colorectal cancer (CRC) in escaping immune surveillance, and blocking this axis has been found to be effective in a subset of patients. Although blocking PD-L1 has been shown to be effective in 5–10% of patients, the majority of the cohorts show resistance to this checkpoint blockade (CB) therapy. Multiple factors assist in the growth of resistance to CB, among which T cell exhaustion and immunosuppressive effects of immune cells in the tumor microenvironment (TME) play a critical role along with other tumor intrinsic factors. We have previously shown the polyketide antibiotic, Mithramycin-A (Mit-A), an effective agent in killing cancer stem cells (CSCs) *in vitro* and *in vivo* in a subcutaneous murine model. Since TME plays a pivotal role in CB therapy, we tested the immunomodulatory efficacy of Mit-A with anti-PD-L1 mAb (αPD-L1) combination therapy in an immunocompetent MC38 syngeneic orthotopic CRC mouse model. Tumors and spleens were analyzed by flow cytometry for the distinct immune cell populations affected by the treatment, in addition to RT-PCR for tumor samples. We demonstrated the combination treatment decreases tumor growth, thus increasing the effectiveness of the CB. Mit-A in the presence of αPD-L1 significantly increased $CD8^+$ T cell infiltration and decreased immunosuppressive granulocytic myeloid-derived suppressor cells and anti-inflammatory macrophages in the TME. Our results revealed Mit-A in combination with αPD-L1 has the potential for augmented CB therapy by turning an immunologically "cold" into "hot" TME in CRC.

Keywords: PD-L1, orthotopic tumor, colorectal cancer, Mithramycin-A, combination therapy

INTRODUCTION

Colorectal cancer (CRC) is the third most common cancer in men, the second most common in women, and the second most common cause of cancer-related deaths in the USA (1). With an estimated 5% lifetime risk, CRC is one of the malignant cancers whose 5-year survival rate is poor when patients are diagnosed at a late stage (2, 3). Microsatellite instability (MSI) plays a pivotal role in CRC stages and arises due to deficiencies in the DNA mismatch repair system, causing insertion, deletion, or misincorporation of nucleotides in the DNA (4). Recent advances in checkpoint blockade (CB) therapy for microsatellite instability (MSI) positive CRC patients have shown dramatic response for patients with high MSI (MSI-H) (5). Current FDA-approved combination immunotherapy drugs used for metastatic CRC are ipilimumab (Yervoy) and nivolumab (Opdivo) for patients with MSI-H (6, 7). However, single-agent checkpoint inhibitors do not show response in CRC patients with microsatellite stable (MSS) carcinomas, which comprise the majority of the aggressive CRCs with poor outcomes (5, 8).

Programmed death-1 (PD-1) is a checkpoint molecule that is highly expressed on tumor-infiltrating T cells. PD-1 ligand (PD-L1) is variably expressed on tumor cells and tumor-infiltrating antigen-presenting cells and is considered a negative prognostic marker (9). Engagement of PD-1 with PD-L1 suppresses T cell response and inhibits anti-tumor immunity (10). Hence, attempts are made to use checkpoint blocking antibodies against PD-1/PD-L1 as promising immunotherapy in CRC treatment. Unfortunately, patients with MSS showed 0% response to anti-PD-1 CB therapy (5, 11).

PD-L1 is a transmembrane protein belonging to the B7 family of the Ig superfamily and are expressed on lymphocytes (B and T), NK cells, dendritic cells, as well as IFN-γ stimulated monocytes, epithelial cells, and endothelial cells (12). Engagement of PD-L1 with PD-1 leads to inhibition of both T cell proliferation and cytokine production (8, 13). Thus, PD-L1 is thought to play an essential role in tumor immune evasion. Further, elevated PD-L1 expression has been found in some tumors resulting in increased resistance of tumor cells to $CD8^+$ T cell-mediated lysis (9). Thus, inhibiting PD-L1 with its antibody forms one of the bases of CB therapies. However, as the application of CB monotherapy has failed in MSS patients, combination approaches with chemo-drugs hold potential as a sensitizer to anti-tumor immune cells along with immune modulation (5). Also, combination therapies can lead to increased immune T-cell infiltration, which is generally found in MSI patients responsive to the treatment (4). As a result, combination chemotherapy strategies are evolving with CB for the treatment of metastatic CRC (14, 15).

The tumor microenvironment (TME) is infiltrated with immunosuppressive myeloid-derived suppressor cells (MDSCs) that constitute part of the myeloid regulatory network (16). In CRC, these cell types along with tumor-associated macrophages (TAMs) play a pivotal role in tumor immune evasion to cue the immune surveillance to bypass recognition of the tumor as foreign (16, 17). Therefore, they are often recruited to the TME, expanding and suppressing anti-tumor immunity (18).

Mithramycin A (Mit-A) is a polyketide antibiotic which is proven to bind to the minor groove of DNA and thus it inhibits the binding of the transcription factor SP1 with the DNA (19). Therefore, Mit-A potently inhibits the transcription factor, SP1, which is involved in chemoresistant cancers (20, 21). Moreover, it has been found to sensitize tumor cells to TRAIL-mediated apoptosis *via* XIAP-gene promoter downregulation *via* its SP1 sites (22). Recently, we have demonstrated Mit-A can specifically target cancer stem cells (CSCs) by inhibiting CSC proliferation when tested in mouse and human colon cancer tumor organoid (tumoroid) cultures (both *in vitro* and *ex vivo*) and *in vivo* (23).

We reasoned, that combining Mit-A with CB could increase the latter's effectiveness in the complex milieu of TME. Since immunosuppressive cells such as MDSCs and TAMs contribute to reduced T cell infiltration and activation (24), we reasoned that this combination might target the PD-L1 on the tumor cells and the MDSC and TAM and thus promote anti-tumor immune activation. Since the PDL1 promoter region has been found to serve as a binding site for SP1 in gastric cancer and rs10815225 polymorphism is related to the overexpression of PD-L1 (25), we reasoned Mit-A (an SP1 inhibitor) could influence the PD-L1 expression in TME. In this context, we were interested in studying the effects of Mit-A treatment on the immune cells such as for MDSC and macrophage-mediated immunosuppression in the TME. We hypothesized that treatment of tumor cells with Mit-A would lead to sensitization to αPD-L1 therapy, thus increasing the efficacy of the PD-L1 CB. To test our hypothesis, we used an MC38 (p-53 mutant, K-RAS wild-type, MSI-H) orthotopic tumor-bearing mouse model and treated it with Mit-A combined with αPD-L1 mAb. We demonstrated treatment with Mit-A significantly increases the latter's effectiveness by upregulating the PD-L1 of the granulocytic MDSCs and tumor cells, thus making them more susceptible to inhibition by anti-PD-L1 therapy. The inhibition of immunosuppressive cells leads to an increase of TME infiltration by anti-tumor T-cells. Based on these findings, we suggest that Mit-A can increase the efficacy of CB combination therapy.

MATERIALS AND METHODS

Antibodies and Reagents

All reagents and antibodies are listed in **Tables 2A, B**; **Supplementary Figure 4**. Gibco Dulbecco's Modified Eagle Medium (DMEM), L-glutamine, Fetal bovine serum (FBS) were purchased from Thermo Fischer Scientific. Mycoplasma kit was purchased from Lonza.

Cell Culture and Drug Treatments

MC38 cells (colon carcinoma epithelial cells derived from C57BL/6 mice; wt-KRAS, MSI-H, and p-53 mutant) were provided by Dr. Shari Pilon-Thomas (Moffitt Cancer Center) and were cultured in DMEM medium containing 2 mM L-glutamine, 0.1 mM nonessential amino acids, 1 mM sodium pyruvate, 100 U/ml penicillin, 100 mg/ml streptomycin, and 10% FBS. CT26 cells were maintained in complete RPMI media (100 U/ml penicillin, 100 mg/ml streptomycin, and 10% FBS). HT29 and HCT116 were maintained in McCoy's complete media as per ATCC. All cells were maintained in an atmosphere

containing 5% CO_2 and at 37°C. Besides, cells were routinely checked for mycoplasma contamination. MC38-Luc stable cells were created in-house following the standard transfection and G418 selection protocol. These cells were derived from MC38 cells as detailed earlier. Briefly, MC38 cells plated in 24-well cell culture-treated plates, grown to 70–80% confluency were transfected with the luciferase gene (Addgene) using Lipofectamine® 3000 (Invitrogen). Post 48 h of transfection, the cells were treated with selection antibiotic (G418) (Geneticin, Gibco, Invitrogen) (concentration—400 μg/ml obtained by antibiotic kill curve). Positive and negative control was maintained. Transfected cells were transferred to a 60 mm tissue culture plate. The cells were then plated in 96 well plates at 1 cell/well to form colonies from an individual cell. A suspension of 10 cells/ml was obtained by limiting dilution and forming colonies for 1–2 weeks. Single-cell colonies checked for luciferase activity. Next the clones were expanded to 6-well plates and then to tissue culture flasks. MC38-Luc clones were maintained in complete media with 400 μg/ml of G418 during cell culture.

For PD-L1 expressions analyses upon Mit-A treatment study, 1×10^5 and 0.75×10^5 HCT116 cells and 2×10^5 and 1.5×10^5 HT29 cells were grown as monolayer and tumoroids respectively. For monolayer, Mit-A was treated the next day (10 nM for HCT116 and 50 nM for HT29) and for tumoroid on Day 4 (25 nM for HCT116 and 100 nM for HT29). PD-L1 expressions were analyzed post 48 h of treatment with human PD-L1 and isotype control antibodies by Flow cytometry.

Tumoroid Culture

Polymeric nanofiber scaffold was prepared, sterilized in ethanol and used for tumoroid culture as previously described (22). Tumoroids were cultured in a humidified incubator at 37°C in a 5% CO_2 atmosphere. 3D Tumoroid formation was assessed using fluorescent microscopy (Olympus BX51) after nuclear staining with Nuc Blue dye (Thermo Scientific).

Cell Viability Assay

Cell growth was quantified using the CellTiter-Glo® Luminescent Cell Viability (Promega, G7572) assay. For MC38 monolayer culture, 4,000 cells were plated in a 96-well plate and treated the next day with Mit-A as indicated (n = 3). For scaffold culture, 3,000 cells from tumor biopsies were plated in a 96-well plate in 50 μl volume to stabilize cells on the scaffold (n = 3). The next day, 150 μl of fresh media was added. On day 4 of plating, cells were treated with Mit-A and αPD-L1 antibodies. According to the manufacturer's protocol for biopsy monolayers, 48 and 72 h after treatment, Cell Titer Glo reagent was added with media (1:1 ratio). The luminescence signal was read by an illuminometer (Synergy H4 hybrid reader; BioTek) in an opaque plate. For biopsy scaffolds, on Day 6, a CellTiter-Glo assay was performed.

Annexin V

Annexin V assay of a monolayer of MC38 cell line and biopsies from orthotopic tumor-bearing C57BL/6 mice was performed to measure the early and late apoptosis upon treatment with Mit-A w/o αPD-L1 antibody. As discussed earlier, biopsy tumors were dissociated into a single cell suspension and plated in 6-well plates at a cell density of 1.5×10^5/well in 2 ml of complete media. MC38 cell line was also plated similarly with the same cell density in complete media. The next day, diluted stock (DMSO) of Mit-A (300 and 600 nM) w/o αPD-L1 antibody (20 μg/ml) in complete media was added to the wells for both the monolayers (cell line and biopsies) and Annexin V (APC) assay was performed in 1× binding buffer with DAPI post 72 h of treatment. Similarly, for scaffolds also the same protocol was followed post 72 h of treatment.

Co-Culture Experiments: Tumoroid-T Cell Coculture

Orthotopic MC38 biopsies were collected, dissociated with Miltenyi tumor dissociation kit and collected as a single cell suspension. Approximately 1.2×10^5 cells were plated on pre-sterilized scaffolds in 1 ml media per well in non-treated 6-well plates as per our in-house protocol (23). The next day (Day 1), 3 ml of media was added. On Day 4, $CD8^+$T cells isolated from the spleen of naïve C57BL/6 female mice using $CD8a^+$ isolation kit were CFSE stained following manufacturer's protocol and activated with CD3/CD28 microbeads and added to the tumoroids in the ratio 1:1 and 1:6 in the presence of 30 U/ml of IL-2. Mit-A dissolved in DMSO was added to the scaffolds (600 and 800 nM) post T cell addition on the same day. Cells were collected post 72 h addition of Mit-A and stained with CD45, CD3, CD8 flow antibodies, and data collected in BD LSRII. Data analyzed by FlowJo software (version 10.). DAPI was used for live/dead staining. For positive and negative controls, activated and non-activated CFSE-stained $CD8^+$T cells were plated separately in 6 well plates and treated with IL-2 similar to the scaffold cultures and analyzed post 72 h along with the Mit-A treated samples.

MDSC-T Cell Co-Culture

Spleen collected from C57BL/6 orthotopic tumor-bearing mouse was dissociated, lysed with ACK (Ammonium Chloride-Potassium) lysis buffer, and collected into a single-cell suspension. Next, $CD11b^+$ cells were collected by positive selection using $CD11b^+$ microbeads and LS column in a MidiMACs separator, stained with $CD11b^+$ antibodies and sorted for $Ly6G^+$ and $Ly6G^-$ cells using Ly6G-antibody and DAPI for live/dead staining in the FACS Melody cell sorter. Spleen from naïve C57BL/6 mice was made. Next, the $CD8^+$ T cells were collected and stained with CFSE and activated using CD3/CD28 activation beads as mentioned earlier. Finally, the sorted granulocytes and monocytes were co-cultured in 96-well round-bottomed plates with the activated $CD8^+$ T (in the presence of IL-2 (30 U/ml)) cells in the ratio 1:3 (MDSC : $CD8^+$T cells) for the $CD8^+$T cell proliferation activity studies for immunosuppressive effects of MDSCs on $CD8^+$T cell activation/proliferation (26). On the same day, Mit-A (600 nM) w/o αPD-L1 mAb (20 μg/ml) was treated to the co-culture and cells collected post 72 h of treatment were analyzed by flow cytometry. For positive and negative controls,

activated and non-activated CFSE-stained $CD8^+$T cells were plated separately in 96-well round-bottomed plates and treated with IL-2 similar to the co-cultures and analyzed post 72 h with the Mit-A treated samples.

In Vivo Experiments

All experiments were performed in accordance with the IACUC of the University of South Florida. *Orthotopic tumor model:* Wild-type C57BL/6 mice (female, 6–8 weeks old; from Jackson Laboratory) mice were anesthetized with isoflurane inhalation and the cecum was exposed *via* a lower abdominal incision. Approximately 2×10^5 MC38-Luc cells suspended in 50 µl of PBS were injected subserosally using a 30-G BD insulin syringe under the microscope (Day 0). Mice were monitored regularly and surgical clips were removed on Day 7. Images captured every week post 1 week of tumor inoculation by *in vivo* imaging system (IVIS) (Xenogen; Perkin Elmer (Caliper Life Sciences) following intraperitoneal administration of D-Luciferin. The treatment regimen includes an equivalent amount of DMSO in PBS for vehicle control, 150 µg/mouse for IgG (isotype) and αPD-L1 mAb, 1 mg/kg of Mit-A with or without αPD-L1 in PBS. Initial and final mice body weights were taken.

Flow Cytometry

Spleens and tumors from *in vivo* experiments were harvested under sterile conditions. Tumors were sliced into 2–4 mm^3 pieces post collection and proceeded for enzymatic digestion using the Miltenyi tumor dissociation kit. Tumors were dissociated into single-cell suspensions, RBCs (Red Blood Cells) were removed using an ACK lysing buffer. Spleens were made into single-cell suspension in PBS followed by lyses with ACK lysing buffer. Approximately 1×10^6 tumor cells and splenocytes were incubated with Zombie in PBS for 20 min in the dark at RT (room temperature), followed by washing at 300*g* for 3 min and subsequently washed with FACS buffer (PBS with 10% heat-inactivated FBS and 2mM EDTA) and stained with relevant antibodies (Abs) for 30 min on ice in FACS buffer followed by washing. For intracellular staining of Foxp3, cells were labeled with all other Abs first except Foxp3, fixed (with 1× Mouse Foxp3 Fixation Buffer), permeabilized (with 1× Mouse Foxp3 Permeabilization Buffer using manufacturer's protocol). Next washed with FACS buffer and stained with Foxp3 Ab for 20 min at RT, followed by washing, re-suspending in FACS buffer and analyzing immediately using an LSRII flow cytometer (BD Biosciences) and data analyzed using FlowJo software (version 10).

Immunohistochemistry

Approximately 10-micron cryosectioned tumor samples were used for immunostaining. Sections were baked and boiled in antigen unmasking solution (Vector Laboratories Inc., Burlingame, CA; 1–100) for 45 min at 90°C. Post heat antigen retrieval, sections were treated with 3% hydrogen peroxide in water for 20 min, then the sections were blocked and permeabilized with 10% serum, 0.2% Triton X-100 in PBS for 1 h at RT. Following this, the sections were incubated with primary antibody solution (5% host serum, 0.1% Triton X-100 in PBS) at 4°C overnight. Following washing, sections were then sequentially incubated with biotinylated secondary antibody for 2 h at RT, avidin–biotin-peroxidase (ABC, 1:100 Vector Laboratories, Inc, Burlingame, CA) for 1 h at RT and DAB substrate solution (Vector Lab. Inc.) for 5 min. Finally, sections were washed, dried and cover-slipped with DPX mounting medium. All images including bright field ones were taken using a Keyence microscope (BZ-X710 Fluorescence microscope).

q-RT-PCR

Snap frozen tumor samples were homogenized in a lysis buffer and the total RNA was isolated using RNeasy Plus Mini kit (27) (Qiagen; Cat. no. 74134) followed by removing the residual DNA by treating with DNAse I. Using Maxima Enzyme and 5× Reaction Mix (Thermo Scientific), cDNA was prepared from 1 ug of RNA. With the cDNA, qRT-PCR was performed in CFX384 Touch Real-Time PCR Detection System (Bio-Rad). Reactions run in triplicates (n = 3) with cycles 95°C for 3 min, followed by 45 cycles of 95°C for 10 s, 60°C for 1 min and 72°C for 15 s with the reaction mixture containing 1 ul of 5× all-in-one SYBR-master mix, 2.5 ul of RNAse free water and 0.5 µl of primers (**Table 1**; **Supplementary Figure 3**) and 1 µl of cDNA. β-actin was run as an internal control for all the genes. Finally, $\Delta\Delta^{-Ct}$ values were calculated to measure each gene expression change.

Statistical Analysis

Data analyzed in Graphpad Prism (version 8). All quantitative data were analyzed through mean ± S.E.M (standard error of the mean) by Student's t-test and One-way ANOVA (Fischer's LSD test) as stated for each experiment.

RESULTS

Mit-A Causes Increased Early Apoptosis in Combination With CB by Sensitizing *Ex Vivo* Tumor Biopsy Cultures to CB *via* Enhancing PD-L1 Expression

We have previously reported Mit-A acts as an inhibitor of CRC by targeting the CSCs (23). We aimed to determine whether Mit-A along with αPD-L1 can cause increased cell apoptosis using orthotopic tumor biopsies grown as monolayer culture and compared with MC38 cell line. Firstly, the cytotoxic effect of Mit-A was evaluated with CellTiter-Glo assay and compared with the traditional colon cancer drug 5-FU (5-Fluorouracil) for MC38 monolayer cells. IC50 value for Mit-A and 5-FU was found to be 409.7 ± 8.06 nM and 2.55 ± 0.63 µM (**Supplementary Figure 1A**) respectively. For MC38 biopsies, the IC50 of Mit-A was found to be 1.27 ± 0.12 µM demonstrating the biopsies to be more resistant to Mit-A compared to immortalized cell line (**Figure 1A**). In our previous work, we have demonstrated that our in-house FiSS (Fiber-inspired smart scaffold system) forms tumoroids and expands CSCs (23, 28). We utilized these tumoroid cultures grown with orthotopic biopsies (**Supplementary Figure 1B**) recapitulating the *in vivo*

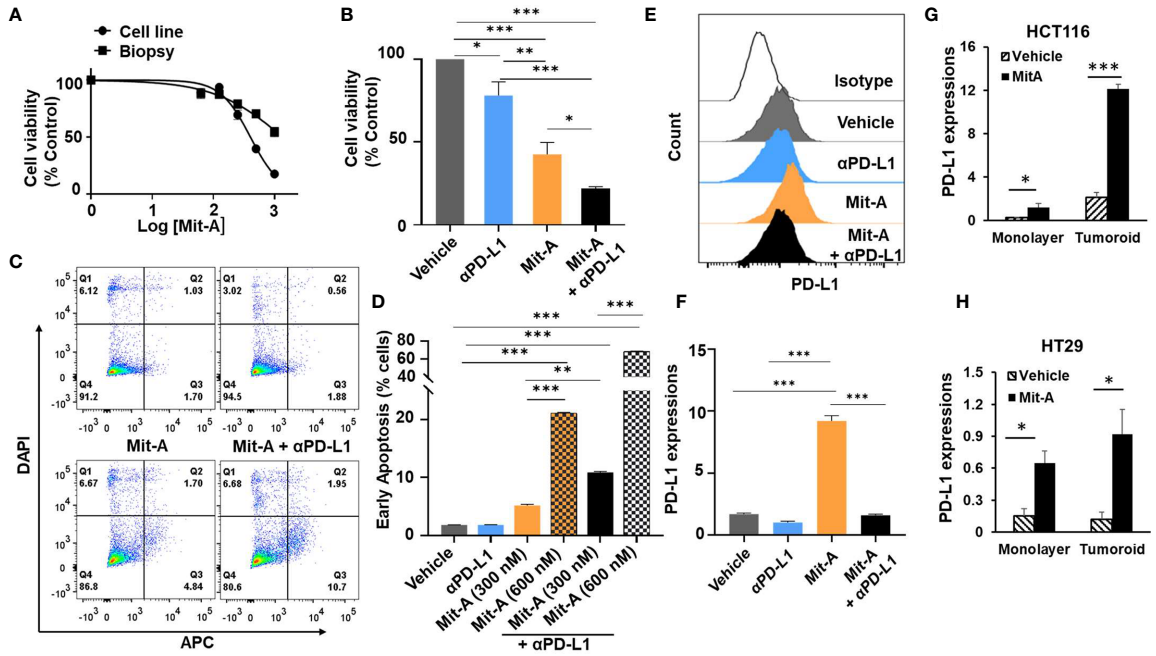

FIGURE 1 | Mit-A combined with CB causes increased early apoptosis by sensitizing the orthotopic tumor *via* increased PD-L1 expression. **(A)** Cell viability assay for monolayer cultures of MC38 cell line or biopsies from orthotopic tumors by CellTiter-Glo (Promega) post 48 h of Mit-A treatment. **(B)** Cell viability of MC38 tumoroids of orthotopic biopsies grown on scaffold. On Day 4 tumoroids were treated with Mit-A (250 nM) with or without αPD-L1 mAb (10 μg/ml) and Cell Titer Glo assay was performed 48 h post treatment. **(C, D)** Annexin V-binding assay of monolayer culture of MC38 tumor biopsies treated with vehicle, Mit-A with or without anti-PD-L1 (αPD-L1) mAb (20 μg/ml) (post 72 h of treatment) where **(C)** depicts the representative images of Annexin-V binding assay; **(D)** represents the percentage of cells from the Annexin V-binding assay undergoing early apoptosis (Q3). **(E, F)** Mit-A treatment sensitizes the MC38 biopsy leading to the increased expression of PD-L1 which was reversed upon addition of the αPD-L1 mAb treatment where **(E)** depicts the histogram from the flow analysis and **(F)** represents the bar graph plot of PD-L1 expression of MC38 biopsy monolayer cells treated with Mit-A (300 nM) and αPD-L1 mAb (20 μg/ml). **(G, H)** represent the PD-L1 expressions for HCT116 and HT29 cells grown as monolayer and tumoroids upon treatment with Mit-A (10 and 50 nM for HCT 116 and HT29 monolayer) and (25 and 100 nM for HCT116 and HT29 tumoroids), respectively. IC50 values were analyzed by non-linear regression analysis in Graphpad prism (version 8). Data analyzed as mean ± SEM by One-way ANOVA (Fischer's LSD test); *p < 0.05, **p < 0.01, ***p < 0.001. A representative of two experiments is shown.

microenvironment to test the efficacy of our combination treatment regimen (**Figure 1B**). CellTiter-Glo assay revealed a significantly higher decrease in cell viability for the combination compared to the Mit-A treatment in tumoroid cultures (**Figure 1B**).

In order to understand whether loss of cell viability is due to apoptosis, an Annexin V-binding assay was performed. We found that a monolayer of MC38 biopsies treated with Mit-A (300 and 600 nM) with or without αPD-L1 mAb (20 μg/ml) showed a significant increase in early apoptosis post 72 h of treatment in a dose-dependent manner (**Figures 1C, D**). Furthermore, the PD-L1 expression was measured post 72 h of 300 nM of Mit-A with or without αPD-L1 (20 μg/ml) and an increase of 7% was found with Mit-A treatment which was reversed in the presence of αPD-L1 treatment (**Figures 1E, F**). These results suggest Mit-A sensitizes the tumor biopsy in part by increasing the PD-L1 expression, and causes enhanced early apoptosis upon combination treatment.

In order to understand whether the PD-L1 modulation is specific for MC38 cells or a general feature of epithelial cell lines we checked the PD-L1 expressions with/without treatment of Mit-A on two human other epithelial cell lines, HT29 (p53 mutant, K-RAS wild type, MSS) and HCT116 (p53 wild-type, K-RAS mutant, MSI). We observed a significant increase in the PD-L1 expression in HCT116 monolayer and tumoroid cultures upon treatment with Mit-A (10 and 25 nM) respectively (**Figure 1G**). Although not as pronounced as HCT116, a significant increase was observed in HT29 monolayer and scaffold when treated with Mit-A for 50 and 100 nM respectively (**Figure 1H**). The drug concentrations were chosen based on IC50 studies post 48 h of treatment (23). Thus, the modulation of PD-L1 is not restricted to MC38; Mit-A is shown to modulate in the human epithelial cell lines, HT29 and HCT116 that have been tested. Experiments with other epithelial cell lines are needed to find whether the PD-L1 modulation is a general feature of epithelial cells or not.

Mit-A Promotes CD8$^+$T Cell Activation *Ex Vivo* in the Presence of Orthotopic Immunosuppressive Biopsy

Since the TME creates an immuno- suppressive effect on T cells, we aimed to determine whether Mit-A can reverse the immunosuppressive effects of the tumor milieu present in biopsy tumoroid-CD8$^+$T cell co-culture. Orthotopic biopsy tumoroids were co-cultured with activated CD8$^+$T cells

(isolated from the spleen of naïve mice) in the presence of IL-2 at the 1:1 and 1:6 (tumoroid: $CD8^+$T cell ratio) and the proliferation of the CFSE-stained $CD8^+$T cells were measured post 72 h of Mit-A treatment. The proliferation of the activated T cells was hindered in presence of tumoroid reflecting the immunosuppressive effects of the biopsies grown on scaffolds, thus mimicking the TME. This inhibition of proliferation was reversed with Mit-A treatment and the effect was more pronounced with a 1:6 ratio compared to a 1:1 ratio (**Figures 2A, B**). The differences in the $CD8^+$ T cell proliferation from the vehicle to the Mit-A (600 nM) treated groups for 1:1 and 1:6 ratio were 20.4 and 29.7%, respectively and that for 800 nM Mit-A were 18.7 and 27.3%, respectively. Thus, though there is significant increase in both the ratios, the change was more prominent in the 1:6 ratio compared to the 1:1 for both drug concentrations.

The Combination of Mit-A and αPD-L1 Suppresses the Immunosuppressive g-MDSCs and Reverses Their Suppressive Effect on T Cells

The TME becomes immunosuppressive through the activity of a diverse array of immunosuppressive immune cells, out of which MDSCs play a prominent role. Since MDSCs reprogram the tumor immunity by inhibiting T cell killing and other immunosurveillance (29), we reasoned that Mit-A would have an ameliorating effect in T cell activation. Since PD-L1 expression on MDSCs is known to have a suppressive effect on the immune response (17, 30), we tested whether the combination of αPD-L1 and Mit-A could reverse the mmunosuppressive effect leading to enhanced T cell proliferation. In this aspect, we performed a co-culture experiment where isolated $CD11b^+$ cells from the spleen of an orthotopic tumor-bearing mouse were sorted for $CD11b^+Ly6G^+Ly6C^{low}$ (granulocytic; g-MDSCs) and $CD11b^+Ly6G^-Ly6C^+$ (monocytic; m-MDSCs) (**Supplementary Figure 1C**) and co-cultured with CD3/CD28 microbeads activated $CD8^+$ T cells (from naïve mice spleen) in the ratio 1:3 (MDSC: T cell) and treated with Mit-A. Approximately 72 h post-treatment, T cell proliferation was found to be suppressed in the presence of the g-MDSCs which was reversed upon Mit-A treatment. The addition of αPD-L1 leads to a greater increase in T cell proliferation, thus revealing the effectiveness of the combination in tuning the T cell activation (**Figures 2C, D**). Mit-A was not found to increase the T cell proliferation in the presence of m-MDSCs (**Supplementary Figure 1D**), and neither the addition of αPD-L1 showed an increase in T cell proliferation (data not shown),

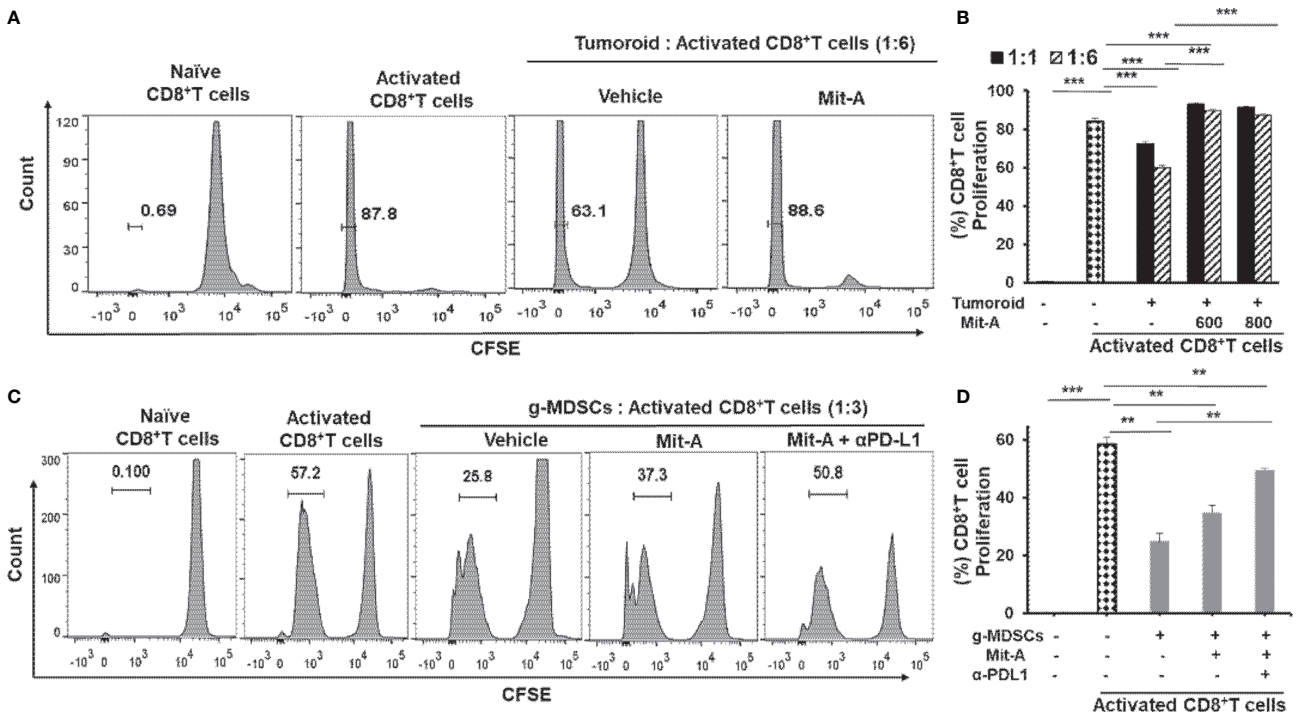

FIGURE 2 | Mit-A enhances proliferation of activated $CD8^+$ T cells and reverses the immunosuppression of tumoroid culture and g-MDSCs in combination with αPD-L1 mAb treatment. **(A, B)** $CD8^+$ T cells isolated from naïve C57BL/6 mouse spleen were stained with CFSE proliferation dye, stimulated using CD3/CD28 activation beads and co-cultured with biopsy tumoroid (on Day 4 of tumoroid culture) in presence of IL-2 (30 U/ml). Mit-A was added to the co-culture immediately post T cell addition at various ratios to tumoroid cultures and T cell proliferation assessed by flow cytometry 72 h post addition. CFSE plots are shown in **(A)** and percent T cell proliferation plotted in **(B)**. **(C, D)** The sorted g-MDSCs isolated from the spleen of orthotopic MC38 tumor bearing mice were co-cultured with CFSE-labelled activated $CD8^+$ T cells in 1:3 ratio (g-MDSC:T cells) in presence of Mit-A (600 nM) with or without αPD-L1 mAb (20 μg/ml). T cell proliferation was assessed by flow cytometry 72 h post treatment. CFSE plots are shown in **(C)** and percent T cell proliferation plotted in **(D)**. Data analyzed as mean ± SEM by Student's t-test. $^{**}p < 0.01$, $^{***}p < 0.001$. A representative of three experiments is shown.

suggesting that g-MDSCs are the potential targets for the proposed therapy.

The Combination of Mit-A and αPD-L1 Reduces the Tumor Burden in an Orthotopic Mouse Model and Arrests the Tumor Cell Proliferation

The therapeutic effect of Mit-A alone or in combination with αPD-L1 mAb was evaluated *in vivo*. To determine whether the combination of Mit-A with αPD-L1 mAb inhibits tumor growth and reduces the tumor burden, a luciferase reporter expressing MC38 (MC38-Luc) was injected subserosally in the cecum of the C57BL/6 mice in 50 µl of PBS. Treatment was initiated on Day 6 intraperitoneally and continued every alternate day where control group received vehicle (DMSO/PBS). Isotype and αPD-L1 groups received 150 ug/mouse of IgG and αPD-L1, respectively in PBS. Approximately 1 mg/kg of Mit-A was administered with or without αPD-L1 mAb in PBS (**Figure 3A**) (n = 4 mice per group). Tumor progression was monitored every week by bioluminescence using IVIS (**Figure 3B**). On Day 22, mice were sacrificed, tumors collected, weighed, and processed. No significant changes in the body weight were observed during the span of the experiment except for an increase in the weight of the control and IgG treated groups due to tumor growth. We found a significant decrease in tumor growth with Mit-A treatment. Combining it with αPD-L1 mAb resulted in a better tumor growth inhibition than the control and isotype. A reduction in the total flux of the IVIS images of the treatment groups demonstrated that the combination treatment led to higher tumor growth arrest compared to the rest of the groups (**Figure 3C**). We found significant decreases in the tumor growth in both the αPD-L1 mAb monotherapy and combination treatment groups compared to the isotype and vehicle controls. Although the combination group exhibited

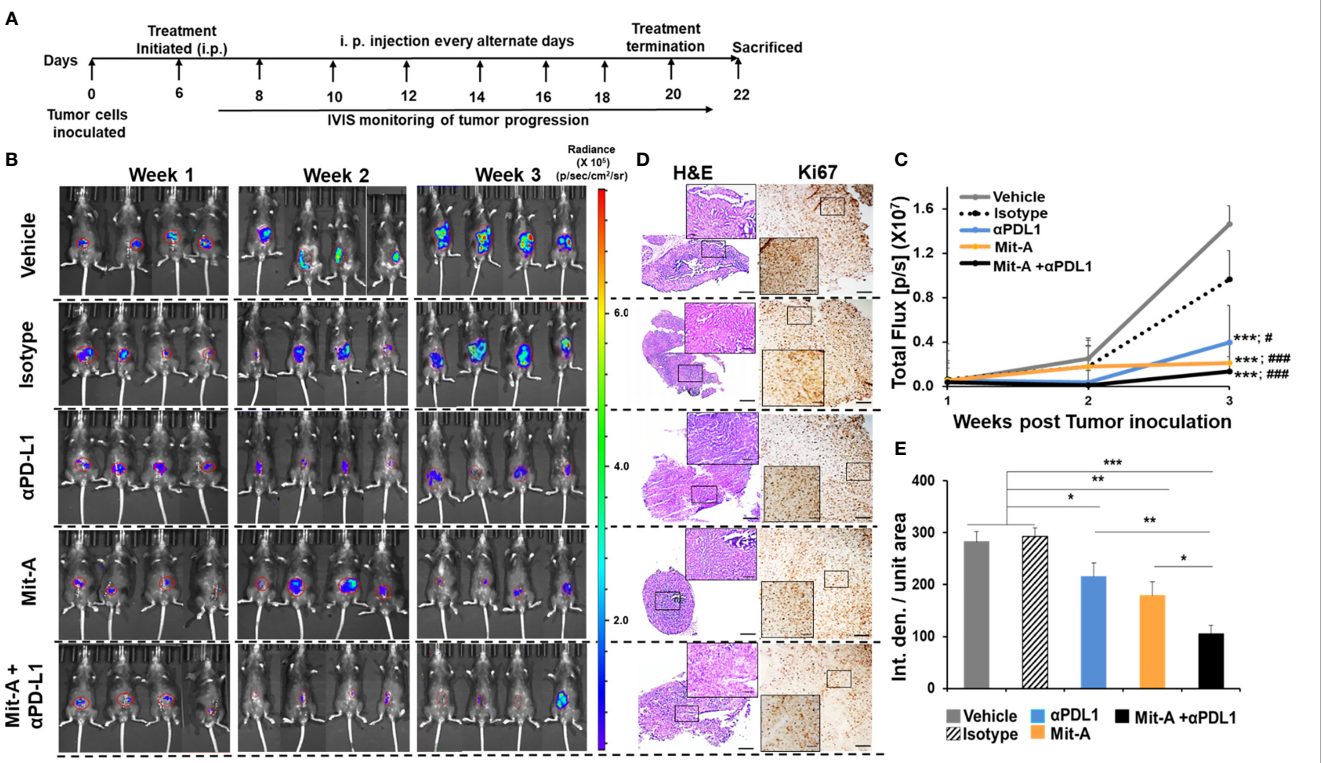

FIGURE 3 | Combination of Mit-A and αPD-L1 reduces the tumor burden in orthotopic MC38 tumor-bearing mice. **(A)** Treatment scheme. Approximately 6 to 8 weeks old (female) wild-type C57BL/6 mice were anesthesized with isoflurane inhalation and the cecum was exposed *via* a lower abdominal incision. Approximately 2×10^5 MC38-Luc cells suspended in 50 µl of PBS were injected subserosally using 30-G BD insulin syringe under the microscope (Day 0). On Day 6, the mice were divided into five groups and treatments were initiated (i.p.) every alternate day (n = 4/per group). The control group received the vehicle (PBS + DMSO), Mit-A group received 1.5 mg/kg/mice, isotype and anti-PD-L1 groups received 150 µg antibodies in PBS/mice and the combination groups got 1.5 mg/kg of the Mit-A + 150 µg of αPD-L1 mAb/mice. Treatment was continued until Day 21 after which the mice were sacrificed. **(B)** Tumor bioluminescence post 1, 2 and 3 week of MC38-Luc cell inoculation. Images captured by IVIS following i.p. injection of luciferin-D. IVIS images were quantified by Caliper Life Sciences Images software. **(C)** represents the total photon flux (p/s) measured by IVIS (* and # represent comparison with vehicle and isotype groups respectively for each group). **(D)** Representative images of the treated tumor sections showing H&E (left panel) and Ki67 (right panel), **(E)** Histograms showing Image J quantifications of Ki67 immunostaining. n = 3 mice/group. Scale bar 50 µm; inserts 10 µm. Data analyzed as mean ± SEM by Student's t-test. *p < 0.05, **p < 0.01, ***p < 0.001. where IVIS, *In vivo* imaging system; Luc, luciferase; p/s, photon/second; PBS, phosphate buffered saline; DMSO, dimethyl sulfoxide; Int. den., integrated density. The data is representative of three experiments. "###" denotes the significance between isotype and the other groups.

the most significant decrease in tumor growth, this difference between combination and αPD-L1 mAb treatment groups was not significant. The results aligned with the tumor growth images captured post sacrifice (data not shown). Histological (H & E) and immunohistochemical (Ki67) staining were performed in tumor sections following different treatments (**Figure 3D**). Tumors treated with the combination therapy were found to have the smallest tumors with significantly reduced Ki67 expression compared to the monotherapy treated groups and control (**Figure 3E**). We also tested our combination of Mit-A/αPD-L1 in CT26-bearing (murine colon cancer cell line (p53 wild-type, K-RAS mutant, MSS) subcutaneous tumor model in Balb/c mice. CT26 tumor model showed significantly decreased tumor growth compared to the control (vehicle) group and monotherapy groups (**Supplementary Figures 5A, B**).

PD-L1 Blockade in Combination With Mit-A Increases T Cell infiltration and Decreases Immunosuppressive Tregs

Both spleen and tumors from the five groups (vehicle control, IgG, αPD-L1, Mit-A, and Mit-A + αPD-L1) were processed, collected as single-cell suspension, and assessed by flow cytometry analysis. Out of live cells, $CD45^+$ cells were gated for $CD3^+CD8^+$ and $CD3^+CD4^+$ T cells and Tregs were analyzed from $CD4^+CD25^+FoxP3^+$ cells (**Supplementary Figure 2A**). A significant increase in $CD8^+$ T cell population for the combination-treated group was found compared to αPD-L1 treatment alone both in spleen and tumor (**Figure 4A**). Although an increase in $CD4^+$ T cell population was found in the spleen, no similar increase was found in the tumor (**Figure 4B**). When analyzed in tumor, although a significant decrease in Tregs was found for Mit-A compared to αPD-L1 treatment, the combination treatment showed no significant decrease (**Figure 4C**). However, a higher CD8:Tregs ratio was found for the Mit-A + αPD-L1 treatment group compared to the αPD-L1 monotherapy in both tumor and spleen (**Figure 4D**) suggesting that the combination treatment leads to higher T cell infiltration with suppression of the immunosuppressive Tregs cell population.

Mit-A in Combination With αPD-L1 Leads to a Decrease in the g-MDSCs and M2 Macrophages *In Vivo*

MDSCs were analyzed in both tumor and spleen from $CD45^+CD11b^+$ populations gated from $CD45^+$ live cells (**Supplementary Figure 2B**), and the granulocytic

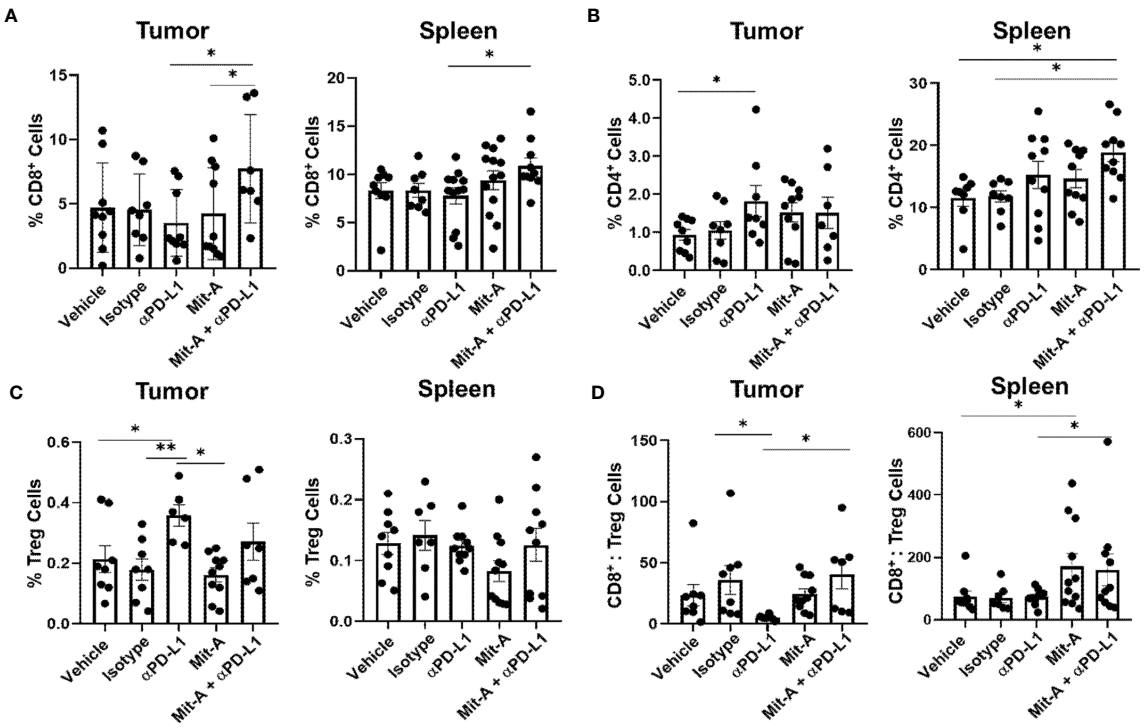

FIGURE 4 | PD-L1 blockade in combination with Mit-A increases T cell infiltration and decreases immunosuppressive Tregs. Flow cytometry analysis of tumor and spleen collected from the orthotopic tumor-bearing mice treated with vehicle, Isotype (IgG), Mit-A w/o αPD-L1 mAb. All cell populations were gated out of $CD45^+$ live cells. **(A)** Percentage of $CD8^+$ T cells ($CD3^+CD8^+$) for tumor (left) and spleen (right); **(B)** Percentages of $CD4^+$ T cells ($CD3^+CD4^+$) for tumor (left) and spleen (right); **(C)** Tregs representing percentage of $CD3^+CD4^+CD25^+FoxP3^+$ for tumor (left) and spleen (right) were analyzed and compared among the treatment groups. **(D)** $CD8^+$ T cells:Tregs ratio for tumor (left) and spleen (right), respectively shown. Each dot represents one individual mouse. Data pooled of two independent experiments (minimum n = 4 per group for each experiment) and analyzed as mean ± SEM by One-way ANOVA (Fischer's LSD test). *$p < 0.05$, **$p < 0.01$.

($CD11b^+Ly6G^+Ly6C^{low}$) and monocytic ($CD11b^+Ly6G^-Ly6C^+$) subpopulations were analyzed for the five treatment groups (**Figures 5A, B**). A significant decrease in the g-MDSC population was found for the combination group compared to the Mit-A alone group. Although a marginally significant increase was observed with the Mit-A single treatment compared to the control and αPD-L1 treatment groups, an overall decrease in the g-MDSC subpopulation was observed when αPD-L1 was combined with Mit-A (**Figure 5A**). No observable differences in the m-MDSC subpopulation were found in the tumor reflecting that the treatment did not impact m-MDSC subtypes in this model (**Figure 5B**). For the spleen, we observed a decrease in the g-MDSC cells in the combination and αPD-L1 treated groups compared to the IgG treated group (**Supplementary Figure 3A**). No significant difference between the Mit-A monotherapy and combination group was found in the spleen, thus emphasizing the combination treatment's effect on the g-MDSC population in the TME (decreasing its fraction and thus its immunosuppressive effects) (**Figure 5A**). However, a significant decrease in the splenic m-MDSCs was, observed with the combination and αPD-L1 treatment groups compared to the IgG group (**Supplementary Figure 3B**).

TAMs are also associated with immunosuppression, and their population is found to be increased in tumor growth and their release of anti-inflammatory cytokines. $CD11b^+F4/80^+$ cells representing the total macrophage population were significantly reduced with the combination treatment as compared to the single drug Mit-A, IgG-treated, and vehicle (control) groups (**Figure 5C**). However, no statistically significant difference was found between the αPD-L1 treated group and the combination-treated group predicting that the association of Mit-A with αPD-L1 was not able to suppress the M2 macrophage population ($CD11b^+CDF4/80^+CD206^+$) as compared to monotherapy. Although, the M2 population was suppressed in all treatments compared with the control and IgG groups (**Figure 5D**). Thus, although the combination suppressed the g-MDSCs and overall macrophage population, a robust decrease in the M2 subpopulation was not evident compared to the monotherapy.

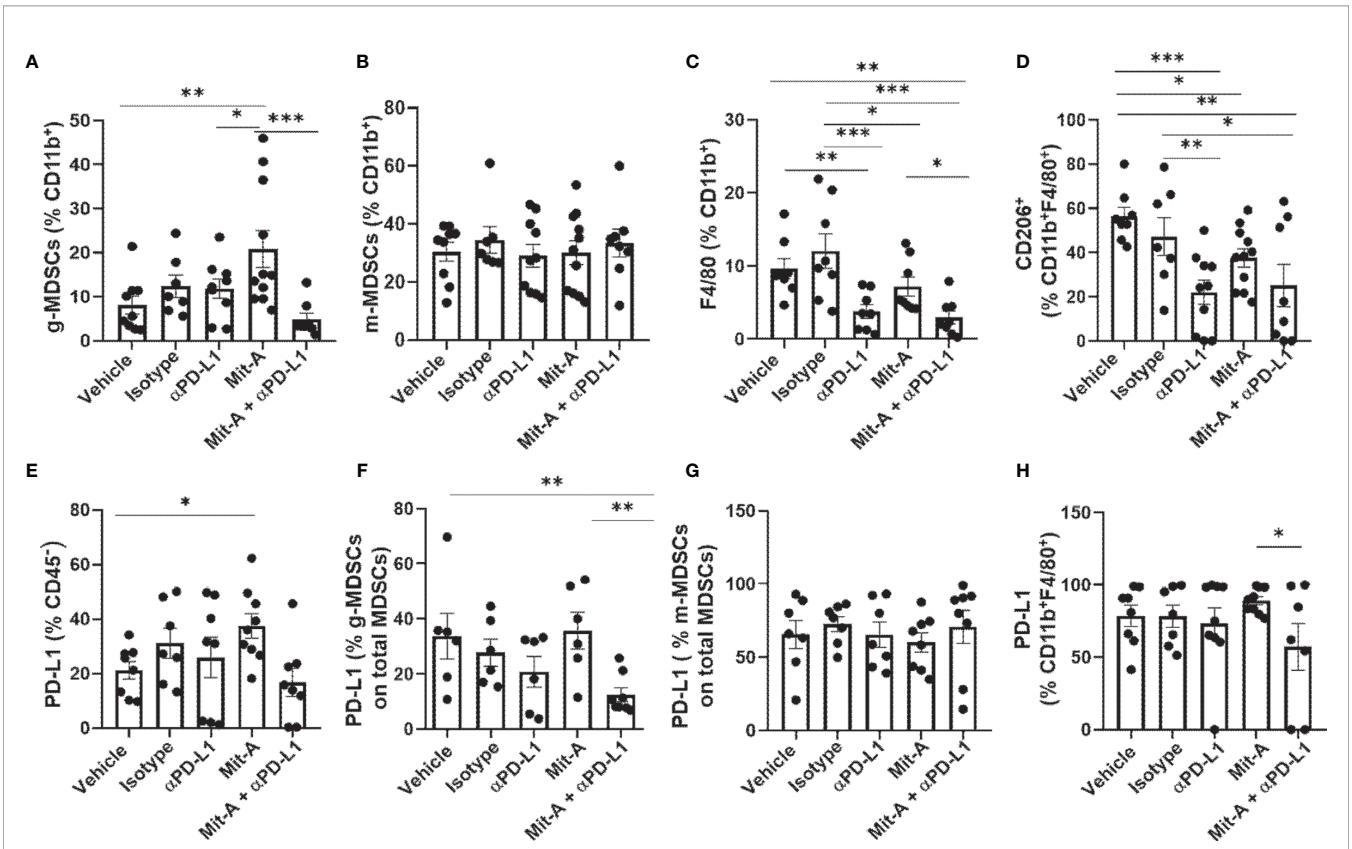

FIGURE 5 | Mit-A and anti-PD-L1 combination treatment decreases the immunosuppressive g-MDSCs population. Mit-A sensitizes orthotopic tumor and immune cells by modulating PD-L1 expression *in vivo*. Flow cytometry analyses of tumor from the MC38 orthotopic tumor bearing mice from the five groups treated with vehicle, IgG (isotype), αPD-L1 mAb, Mit-A and Mit-A + αPD-L1 mAb where all cell populations were gated out of $CD45^+$ live cells. **(A)** Percentage of g-MDSCs ($CD11b^+Ly6G^+Ly6C^{low}$ (granulocytic)) and **(B)** m-MDSCs (($CD11b^+LyG^-Ly6C^+$ (monocytic) populations from tumor of MC38 orthotopic-tumor bearing mice shown. **(C, D)** Percentage of $CD11b^+F4/80^+$ macrophage and $CD206^+CD11b^+F4/80^+$ anti-inflammatory M2-macrophage populations, respectively from tumor treated with the five treatment groups shown. **(E–H)** Percentages of PD-L1 expression on $CD45^-$ tumor cells **(E)**, g-MDSCs **(F)**, m-MDSCs **(G)** from tumor (calculated out of total MDSCs) and tumor $CD11b^+F4/80^+$ macrophage population **(H)**. Each dot represents one mouse in every group. Data pooled of two experiments (minimum of n = 3 per group for each experiment) and analyzed as mean ± SEM by One way ANOVA (Fischer's LSD test). *p < 0.05, **p < 0.01, ***p < 0.001.

Mit-A Sensitizes the Tumor and Immune Cells by Modulating the PD-L1 Expression

In our *ex vivo* studies, we observed an increased PD-L1 expression of the tumor cells upon treatment with Mit-A alone. A similar observation *in vivo* of PD-L1 expression on CD45- tumor cells revealed that Mit-A sensitizes the tumor cells by increasing its expression, which was decreased when, combined with αPD-L1 therapy (**Figure 5E**). Since we found the combination had a suppressive effect on the g-MDSCs population, the PD-L1 expression on tumor (**Figure 5F**) and spleen (**Supplementary Figure 3C**) g-MDCS was compared among the treatment groups. Percentage of PD-L1 expression on the g-MDSC when calculated among the total MDSCs ($CD11b^+Ly6G^+Ly6C^{low}$ + $CD11b^+Ly6G^-Ly6C^+$) in the tumor was found to be decreased with the combination treatment compared to the Mit-A alone. We did not observe any change in the PD-L1 expression for a similar population on the spleen (**Supplementary Figure 3C**). This data suggests that the combination therapy specifically targeted the tumor g-MDSCs, which are known to have suppressive effects. No change in the PD-L1 expression for tumor m-MDSCs was found (**Figure 5G**). However, although the PD-L1 expression on the tumor $CD11b^+F4/80^+$ macrophages was found to be decreased in the combination treatment compared to the Mit-A alone, no significant changes were observed when compared to the αPD-L1 mAb monotherapy (**Figure 5H**).

Since MDSCs migrate to the tumor site by C–C motif ligand 2 (CCL2) driven pathway and are involved in M2 macrophage polarization we analyzed CCL2 and IL-10 (which are anti-inflammatory cytokines released by M2 and also by MDSCs) (31) gene expression in the tumor sections collected from the treatment groups. A decrease in CCL2 and IL-10 expression was observed in the combination group compared to control and αPD-L1 treatment groups (**Figures 6A, B**). Since arginase-1 (ARG-1) and nitric oxide synthase 2 (NOS2) activation leads to the suppressive effects of MDSCs (26, 29), we next checked the expression of ARG1 and NOS2 in the tumor collected from the treatment groups. We found a significant decrease in the transcript level of *Arg1* compared to the control in the monotherapy and the combination group. We did not find any significant differences, however, in the *Nos2* transcript level (**Figures 6C, D**). This data suggested that Mit-A with/without αPD-L1 has a direct effect on the infiltrating g-MDSCs at least partially in terms of reversal of T cell proliferation. Furthermore, activation of STAT3 is associated with MDSC activation in CRC and its phosphorylation is correlated with tumor growth (29). A significant decrease in the STAT3 expression in the tumor with the combination treatment was found compared to the αPD-L1

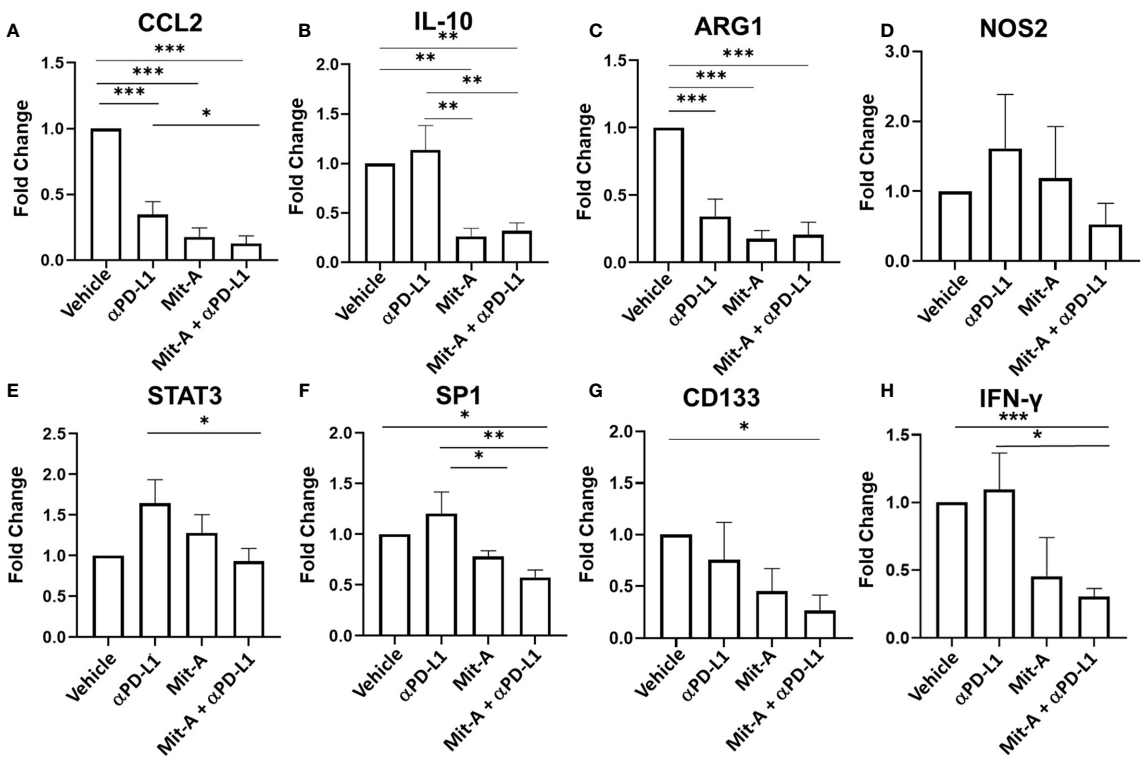

FIGURE 6 | Mit-A in combination with αPD-L1 mAb suppresses the g-MDSCs along with CSCs. Total RNA was isolated from the MC38 orthotopic tumors of the treatment groups (vehicle, isotype (IgG), Mit-A with or without αPD-L1 mAb), and subjected to qPCR analyses of **(A)** *CCL2*, **(B)** *IL-10*, **(C)** *ARG1*, **(D)** *NOS2*, **(E)** *STAT3*, **(F)** *SP1*, **(G)** *CD133* and **(H)** IFN-γ transcripts (n = 3). The vehicle and group was normalized and other groups were compared with the normalized control (vehicle) group. Gene expressions of vehicle and isotype were found to be similar. Data analyzed as mean ± SEM by One way ANOVA (Fischer's LSD test). *$p < 0.05$, **$p < 0.01$, ***$p < 0.001$. A representative of two experiments is shown.

therapy validating that MDSCs are suppressed by Mit-A in addition to αPD-L1 (**Figure 6E**). We have previously reported CSC as potential targets of Mit-A (23). In an attempt to test whether the combination therapy apart from targeting MDSCs and macrophages can foster the CSC killing, CD133 and SP1 gene expression was measured in the tumor sections revealing a significant decrease in both (**Figures 6F, G**). Thus, Mit-A which not only targets CSCs and inhibits SP1, continues to show these activities when used in combination with αPD-L1. Since IFN-γ produced by T cells is known to upregulate PD-L1 expression (32), we checked the IFN-γ expression in the tumor lysates of the treatment groups. We found a decrease of IFN-γ in the combination therapy group compared to the PD-L1 monotherapy treated group (**Figure 6H**).

DISCUSSION

In the majority of CRC patients, CB therapy has not been successful due to the presence of microsatellite stability and lower mismatch repair deficiencies (5). Although it has been proven to regress tumor growth in MSI-H patients, which comprise 5–10% of the patient population, most do not respond to the single therapy (7). As a result, the combination approach for superior clinical response holds potential for overall survival and progression-free survival (4, 33). While pre-clinical studies for various combination therapies are being tested in subcutaneous models, the lack of tissue-specific TME with its underlining heterogeneous immune profiles in these models makes them unsuitable for an accurate evaluation of these therapies (34). In this context, orthotopic tumors contain a native local tumor milieu enhancing the clinical relevance of this model for testing immunomodulatory agents and checkpoint blockers as combination approaches (35). While the MC38 orthotopic tumor model serves as a syngeneic murine model generated from wt-KRAS, MSI-H, and p-53 mutant MC38 cell line, we demonstrated as a proof-of-concept, the combination treatment could be effective in studying the mechanisms of immune modulation in response to CB (36). The effects of the combination treatment is not limited to MC38 orthotopic tumors. We also tested our Mit-A and αPD-L1 combination in CT26- bearing subcutaneous tumor model with MSS genetic mutations in Balb/c mice and found decrease in tumor growth in the combination groups compared to the control and monotherapy groups.

MC38 cells are known to express PD-L1 which gets up-regulated in the presence if IFN-γ *in vitro* (37, 38), and in our study, we found increased expression of PD-L1 on MC38 orthotopic tumor biopsies in response to the immunomodulatory drug, Mit-A. Chemoresistance due to significant upregulation of PD-L1 expressions in cancer cells by various drugs, such as doxorubicin (DOX), Oxaliplatin (OXA, a DNA alkylating agent), Paclitaxel (PACLI, a tubulin inhibitor), Irinotecan (IRI, a topoisomerase 1 inhibitor) has been found and the role of ERK activation increase has been correlated to the overexpression of PD-L1 (14, 39). These effects have been attributed to the sensitizing ability of cancer cells to αPD-L1 therapy, thus altering the "cold" TME to "hot" one (40, 41). The expression of PD-L1 on tumor and immune cells correlates to CB therapy's objective response and clinical outcome. Thus, the level of PD-L1 expressions and its regulation has become a predictive marker for personalized mono- or combination CB treatment (11). In cancer patients, where the PD-L1 level is low, the CB therapy fails. We found that Mit-A treatment increases in PD-L1 expression in cancer and immune cells, and sensitizes the tumor to anti-PD-L1 therapy. However, the mechanism of action is not clear.

Amongst several intrinsic and extrinsic factors that regulate PD-L1 expression in various cancers, DNA methylation of the PD-L1 promoter has been suggested recently in cancer malignancies (42). For instance, TGFβ1 has been shown to induce decrease expression of DNA-methyltransferase 1 (DNMT1) and PD-L1 promoter demethylation, leading to PD-L1 overexpression in lung cancer cells that were undergoing EMT (43). Thus, hypomethylating agents have a direct effect on the PD-L1 expression and thus the epigenetic hypomethylating agents are potential candidates for increasing the combination CB therapy (42).

It has been found that Mit-A reduces the CpG island methylation and inhibits 5'-cytosine-DNA-methyltransferase which is related to anti-metastatic tumor-suppressor genes in lung cancer cells (44). Additionally, Mit-A blocks SP1 from binding to DNA and acetylated SP1 is known to inhibit PTEN expression through binding to the PTEN core promoter (45). PTEN loss activates PI3K signaling that leads to an increase in PD-L1 expression (42). However, the precise mechanism of how Mit-A increases PD-L1 in MC38 tumor cells still remains to be elucidated. Thus, Mit-A which increases the PD-L1 expressions in various epithelial CRC cells, stands as an augmenting agent for CB therapy. Herein, we demonstrated that when orthotopic tumor-bearing mice were treated with Mit-A in addition to checkpoint-blocker αPD-L1, $CD8^+$ T cell infiltration in the tumor increased thereby arresting its growth. The resistance to αPD-L1 monotherapy thus could be overcome by combining Mit-A in the treatment regime.

Immature myeloid cells tend to differentiate into macrophages, granulocytes, and dendritic cells under normal physiological conditions (18). However, in cancer and other pathologic conditions, their differentiation is hampered resulting in the development and recruitment of MDSCs which are activated by suppressing the T cell infiltration locally thus aiding the tumor cells to evade immunosurveillance (46). The two subtypes of MDSCs, g-MDSCs and m-MDSCs hinder the effector T cell function by multiple pathways. Apart from MDSCs, the tumor stroma is infiltrated with TAMs, which also assist in abrogating the anti-tumor immunity (13). The co-inhibitory PD-1 receptors on the T cells with the association with its ligand PD-L1 helps in apoptosis, anergy, and exhaustion of T cells, thereby promoting tumor growth and metastasis (8). Not only on tumor cells, but PD-L1 expressions on immune cells (myeloid) have been reported to be responsible for $CD8^+$T cell suppression in the murine CRC model (37, 47). Therefore, blocking PD-L1 on these cells along with tumor cells with

checkpoint inhibitors holds potential for anti-tumor immunity (37). Our study demonstrated the reversal of the inhibition of immunosuppression of T cell proliferation by g-MDSC *via* Mit-A and αPD-L1 combination in monolayer co-culture platform *in vitro* as well as in the increase of CD8:Treg ratio *in vivo*. We showed that our tumoroid platform when co-cultured with T cells mimics an immunosuppressive environment for drug testing. As it has been found MSI-H patients who respond to CB therapy are infiltrated with increased $CD8^+$ T cells along with other factors such as elevated neoantigens and genetic mutations (48), increase in $CD8^+$ T cells as found in our model would aid in improved response to CB. Our data suggest that patients with MSS genetic mutations could respond to this combination therapy which likely to alter the TME *via* MDSC and TAMs inhibition.

As a monotherapy, Mit-A was unable to block PD-L1 expression within the TME. A dose-dependent increase in PD-L1 expression was observed with Mit-A treatment *in vitro* for tumor biopsies (data not shown) which reflected in the increased PD-L1 expression in the $CD45^-$ tumor cells from tumor-bearing mice treated with Mit-A, thus demonstrating the capacity of Mit-A to sensitize orthotopic tumor cells for improved checkpoint blocking therapy. Although the PD-L1 expression was found to be increased in tumor cells with Mit-A monotherapy, the effect was reversed in presence of the combination suggesting that the cytotoxicity of Mit-A on tumor cells is immunomodulating the TME for enhanced infiltration of T cells *via* application with the αPD-L1 mAb. The plausible mechanism could be through immunogenic cell death since Mit-A is known to increase tumor sensitivity due to DNA damage (49); this could affect in enhanced combination therapy with CB (50).

We checked the PD-1 on $CD8^+$, $CD4^+$ and Tregs cells (**Supplementary Figures 6A–C**). PD-1, which is a T cell inhibitory as well as activation marker, was found to be increased on $CD8^+$ T cells within the combination treated tumors compared to Mit-A treated group (**Supplementary Figure 6A**). However, Mit-A treatment alone led to a decrease in $CD8^+$ $PD\text{-}1^+$ cells compared to the control tumors. These data suggest that although the PD-L1 expression was decreased in tumor for combination treatment, PD-1 increased on $CD8^+$ T cells when Mit-A was combined with αPD-L1. This result is consistent with the activation of cytotoxic $CD8^+$ T cells. However, we currently do not know if these T cells remain activated persistently or proceed to an exhausted state. Further studies will be required to answer this question. No significant changes in the $PD\text{-}1^+$ $CD4^+$ T cells were observed amongst the treatment groups (**Supplementary Figure 6B**) suggesting a lack of helper T cell participation with these treatments. A significant decrease of $PD\text{-}1^+$ on Tregs (**Supplementary Figure 6C**) was observed for Mit-A treated group compared to the control group correlating with lesser activation of these immunosuppressive cell populations.

Intratumoral CCL2 expression levels have been reported in CRC patients and accumulation of MDSC induced by CCL2 correlated with the development and growth of colon adenoma (51). Mainly polymorphonuclear MDSCs which represent the granulocytic population are regulated by CCL2 in a STAT-3 dependent manner causing T cell suppression (31). Mit-A alone and in combination led to a decrease in the CCL2 gene expression *in vivo* as compared to the control tumors suggesting the g-MDSCs are the key targets for the therapy.

TAMS with M2 phenotype is responsible for angiogenesis, tumor promotion and adaptive immunity suppression (27). These M2 macrophages known for drug resistance in CSCs, act *via* STAT3 activation (52). Consistently, reduced expression of CD133, a marker for CSCs was observed both with Mit-A w/o αPD-L1 *in vivo*. As evidenced by the decrease in the M2 macrophages ($CD206^+$ $F4/80^+$) by Mit-A along with αPD-L1 treatment, our combination therapy was able to block the resistant CSCs *via* M2 suppression. Furthermore, tumor lysate IFN-γ measurement by RT-PCR (**Figure 6H**) was found to be decreased in the combination group compared to the controls. We argued this observation correlated with the decrease in the PD-L1 expressions in the tumor by combination treatment.

Herein, we have investigated the effect of Mit-A on the major tumor-infiltrating immune cells (T-cells, MDSCs, macrophages). Other populations (NK cells, DCs) have very low abundance in the MC38 tumor (53). Since we observed a decrease in the g-MDSCs with the combination treatment, the PD-L1 percentages in those subset populations were checked in particular. No significant change in the NK or dendritic cell population were observed among the treatment group. Granulocytic MDSCS and macrophages contribute to the immunosuppressive populations affecting the TME as observed in most cancer patients (29). Thus, we rationalized that these populations would be affected most compared to other cell populations and our findings largely corroborated this hypothesis.

CONCLUSION

Herein we have demonstrated the efficacy of Mit-A in overcoming the resistance of αPD-L1 monotherapy by sensitizing the tumor cells when treated in combination by targeting the immunosuppressive TME in the MC38-orthotopic mouse model. Our findings suggest that suppression of g-MDSCs by blocking their PD-L1 receptors and thus increasing the T cell infiltration with the combination strategy could be a potential therapeutic modality for MSS CRC patient cohorts.

DATA AVAILABILITY STATEMENT

The original contributions presented in the study are included in the article/**Supplementary Material**. Further inquiries can be directed to the corresponding author.

ETHICS STATEMENT

The animal study was reviewed and approved by Institutional Animal Care and Use Committee (IACUC) of the University of South Florida.

AUTHOR CONTRIBUTIONS

SM and SSM conceptualized the study and corrected the manuscript. RD executed *in vitro* and *in vivo* experiments, sample preparation, Flow cytometry and PCR studies, data analyses and writing the manuscript. RK, RG, and MH helped in flow cytometry studies. KM helped in immunohistochemistry and SB provided thoughtful suggestions. All authors contributed to the article and approved the submitted version.

FUNDING

This work was supported by Veterans Affairs Merit Review grant (BX003413) to SM, Research Career Scientist Awards to SM (IK6BX004212) and SSM (IK6BX003778), and Circle of Hope Research Initiative Grant Award to RD.

ACKNOWLEDGMENTS

We are thankful to Charles Szekeres at the University of South Florida's Flow cytometry core for assisting in cell sorting. We would also like to acknowledge Prateik Chopade, Payal Ghosh and Ishan Chaplot for helping in the development of the MC38-Luc cell line, flow cytometry, RT-PCR sample preparation and immunohistochemistry (staining), respectively.

SUPPLEMENTARY MATERIAL

The Supplementary Material for this article can be found online at: https://www.frontiersin.org/articles/10.3389/fimmu.2021.706133/full#supplementary-material

REFERENCES

1. Mohapatra SS, Batra SK, Bharadwaj S, Bouvet M, Cosman B, Goel A, et al. Precision Medicine for CRC Patients in the Veteran Population: State-of-the-Art, Challenges and Research Directions. *Dig Dis Sci* (2018) 63(5):1123–38. doi: 10.1007/s10620-018-5000-0
2. Siegel RL, Miller KD, Fedewa SA, Ahnen DJ, Meester RGS, Barzi A, et al. Colorectal Cancer Statistics, 2017. *CA Cancer J Clin* (2017) 67(3):177–93. doi: 10.3322/caac.21395
3. Qin J, Kunda N, Qiao G, Calata JF, Pardiwala K, Prabhakar BS, et al. Colon Cancer Cell Treatment With Rose Bengal Generates a Protective Immune Response Via Immunogenic Cell Death. *Cell Death Dis* (2017) 8(2):e2584. doi: 10.1038/cddis.2016.473
4. Kalyan A, Kircher S, Shah H, Mulcahy M, Benson A. Updates on Immunotherapy for Colorectal Cancer. *J Gastrointest Oncol* (2018) 9 (1):160–9. doi: 10.21037/jgo.2018.01.17
5. Overman MJ, Ernstoff MS, Morse MA. Where We Stand With Immunotherapy in Colorectal Cancer: Deficient Mismatch Repair, Proficient Mismatch Repair, and Toxicity Management. *Am Soc Clin Oncol Educ Book* (2018) 38:239–47. doi: 10.1200/EDBK_200821
6. Chu JN, Choi J, Ostvar S, Torchia JA, Reynolds KL, Tramontano A, et al. Cost-Effectiveness of Immune Checkpoint Inhibitors for Microsatellite Instability-High/Mismatch Repair-Deficient Metastatic Colorectal Cancer. *Cancer* (2019) 125(2):278–89. doi: 10.1002/cncr.31795
7. Overman MJ, Lonardi S, Wong KYM, Lenz HJ, Gelsomino F, Aglietta M, et al. Durable Clinical Benefit With Nivolumab Plus Ipilimumab in DNA Mismatch Repair-Deficient/Microsatellite Instability-High Metastatic Colorectal Cancer. *J Clin Oncol* (2018) 36(8):773–9. doi: 10.1200/JCO.2017.76.9901
8. Le DT, Uram JN, Wang H, Bartlett BR, Kemberling H, Eyring AD, et al. Pd-1 Blockade in Tumors With Mismatch-Repair Deficiency. *N Engl J Med* (2015) 372(26):2509–20. doi: 10.1056/NEJMoa1500596
9. Balar AV, Weber JS. PD-1 and PD-L1 Antibodies in Cancer: Current Status and Future Directions. *Cancer Immunol Immunother* (2017) 66(5):551–64. doi: 10.1007/s00262-017-1954-6
10. Azuma T, Yao S, Zhu G, Flies AS, Flies SJ, Chen L. B7-H1 Is a Ubiquitous Antiapoptotic Receptor on Cancer Cells. *Blood* (2008) 111(7):3635–43. doi: 10.1182/blood-2007-11-123141
11. Noh BJ, Kwak JY, Eom DW. Immune Classification for the PD-L1 Expression and Tumour-Infiltrating Lymphocytes in Colorectal Adenocarcinoma. *BMC Cancer* (2020) 20(1):58. doi: 10.1186/s12885-020-6553-9
12. Lynch D, Murphy A. The Emerging Role of Immunotherapy in Colorectal Cancer. *Ann Transl Med* (2016) 4(16):305. doi: 10.21037/atm.2016.08.29
13. Beyrend G, Gracht EVD, Yilmaz A, Duikeren SV, Camps M, Hollt T, et al. PD-L1 Blockade Engages Tumor-Infiltrating Lymphocytes to Co-Express Targetable Activating and Inhibitory Receptors. *J Immunother Cancer* (2019) 7(1):217. doi: 10.1186/s40425-019-0700-3
14. Bailly C, Thuru X, Quesnel B. Combined Cytotoxic Chemothrapy and Immunotherapy of Cancer: Modern Times. *NAR Cancer* (2020) 2(1):1–20. doi: 10.1093/narcan/zcaa002
15. Cubas R, Moskalenko M, Cheung J, Yang M, McNamara E, Xiong H, et al. Chemotherapy Combines Effectively With Anti-PD-L1 Treatment and Can Augment Antitumor Responses. *J Immunol* (2018) 201(8):2273–86. doi: 10.4049/jimmunol.1800275
16. Ding ZC, Munn DH, Zhou G. Chemotherapy-Induced Myeloid Suppressor Cells and Antitumor Immunity: The Janus Face of Chemotherapy in Immunomodulation. *Oncoimmunology* (2014) 3(8):e954471. doi: 10.4161/21624011.2014.954471
17. Yin K, Xia X, Rui K, Wang T, Wang S. Myeloid-Derived Suppressor Cells: A New and Pivotal Player in Colorectal Cancer Progression. *Front Oncol* (2020) 10:610104. doi: 10.3389/fonc.2020.610104
18. Gabrilovich DI, Nagaraj S. Myeloid-Derived Suppressor Cells as Regulators of the Immune System. *Nat Rev Immunol* (2009) 9(3):162–74. doi: 10.1038/nri2506
19. Schweer D, McCorkle JR, Rohr J, Tsodikov OV, Ueland F, Kolesr J. Mithramycin and Analogs for Overcoming Cisplatin Resistance in Ovarian Cancer. *Biomedicines* (2021) 9(1):1–11. doi: 10.3390/biomedicines9010070
20. Kormanec J, Novakova R, Csolleiova D, Feckova L, Rezuchova B, Sevcikova B, et al. The Antitumor Antibiotic Mithramycin: New Advanced Approaches in Modification and Production. *Appl Microbiol Biotechnol* (2020) 104 (18):7701–21. doi: 10.1007/s00253-020-10782-x
21. Duverger V, Murphy AM, Sheehan D, England K, Cotter TG, Hayes I, et al. The Anticancer Drug Mithramycin A Sensitises Tumour Cells to Apoptosis Induced by Tumour Necrosis Factor (TNF). *Br J Cancer* (2004) 90(10):2025–31. doi: 10.1038/sj.bjc.6601824
22. Lee TJ, Jung EM, Lee JT, Kim S, Park JW, Choi KS, et al. Mithramycin A Sensitizes Cancer Cells to TRAIL-Mediated Apoptosis by Down-Regulation of XIAP Gene Promoter Through Sp1 Sites. *Mol Cancer Ther* (2006) 5(11):2737–46. doi: 10.1158/1535-7163.MCT-06-0426
23. Quarni W, Dutta R, Green R, Katiri S, Patel B, Mohapatra SS, et al. Mithramycin A Inhibits Colorectal Cancer Growth by Targeting Cancer Stem Cells. *Sci Rep* (2019) 9(1):15202. doi: 10.1038/s41598-019-50917-3
24. Ugel S, De Sanctis F, Mandruzzato S, Bronte V. Tumor-Induced Myeloid Deviation: When Myeloid-Derived Suppressor Cells Meet Tumor-Associated Macrophages. *J Clin Invest* (2015) 125(9):3365–76. doi: 10.1172/JCI80006
25. Tao LH, Zhou XR, Li FC, Chen Q, Meng FY, Mao Y, et al. A Polymorphism in the Promoter Region of PD-L1 Serves as a Binding-Site for SP1 and Is Associated With PD-L1 Overexpression and Increased Occurrence of Gastric Cancer. *Cancer Immunol Immunother* (2017) 66(3):309–18. doi: 10.1007/s00262-016-1936-0
26. Youn JI, Nagaraj S, Collazo M, Gabrilovich DI. Subsets of Myeloid-Derived Suppressor Cells in Tumor-Bearing Mice. *J Immunol* (2008) 181(8):5791–802. doi: 10.4049/jimmunol.181.8.5791
27. Yahaya MAF, Lila MAM, Ismail S, Zainol M, Afizan N. Tumour-Associated Macrophages (Tams) in Colon Cancer and How to Reeducate Them. *J Immunol Res* (2019) 2019:2368249. doi: 10.1155/2019/2368249

28. Green R, Howell M, Khalil R, Nair R, Yan J, Foran E, et al. Actinomycin D and Telmisartan Combination Targets Lung Cancer Stem Cells Through the Wnt/Beta Catenin Pathway. *Sci Rep* (2019) 9(1):18177. doi: 10.1038/s41598-019-54266-z
29. Sieminska I, Baran J. Myeloid-Derived Suppressor Cells in Colorectal Cancer. *Front Immunol* (2020) 11:1526. doi: 10.3389/fimmu.2020.01526
30. Lu C, Redd PS, Lee JR, Savage N, Liu K. The Expression Profiles and Regulation of PD-L1 in Tumor-Induced Myeloid-Derived Suppressor Cells. *Oncoimmunology* (2016) 5(12):e1247135. doi: 10.1080/2162402X.2016.1247135
31. Chun E, Lavoie S, Michaud M, Gallini CA, Kim J, Soucy G, et al. Ccl2 Promotes Colorectal Carcinogenesis by Enhancing Polymorphonuclear Myeloid-Derived Suppressor Cell Population and Function. *Cell Rep* (2015) 12(2):244–57. doi: 10.1016/j.celrep.2015.06.024
32. Kim JM, Chen DS. Immune Escape to PD-L1/PD-1 Blockade: Seven Steps to Success (or failure). *Ann Oncol* (2016) 27(8):1492–1504. doi: 10.1093/annonc/mdw217
33. Llosa NJ, Cruise M, Tam A, Wicks EC, Hechenbleikner EM, Taube JM, et al. The Vigorous Immune Microenvironment of Microsatellite Instable Colon Cancer Is Balanced by Multiple Counter-Inhibitory Checkpoints. *Cancer Discovery* (2015) 5(1):43–51. doi: 10.1158/2159-8290.CD-14-0863
34. Zhao X, Li L, Starr TK, Subramanian S. Tumor Location Impacts Immune Response in Mouse Models of Colon Cancer. *Oncotarget* (2017) 8(33):54775–87. doi: 10.18632/oncotarget.18423
35. Burtin F, Mullins CS, Linnebacher M. Mouse Models of Colorectal Cancer: Past, Present and Future Perspectives. *World J Gastroenterol* (2020) 26 (13):1394–426. doi: 10.3748/wjg.v26.i13.1394
36. Zhong W, Myers JS, Wang F, Wang K, Lucas J, Rosfjord E, et al. Comparison of the Molecular and Cellular Phenotypes of Common Mouse Syngeneic Models With Human Tumors. *BMC Genomics* (2020) 21(1):2. doi: 10.1186/s12864-019-6344-3
37. Juneja VR, McGuire KA, Manguso RT, Lafleur MW, Collins N, Haining WN, et al. PD-L1 on Tumor Cells is Sufficient for Immune Evasion in Immunogenic Tumors and Inhibits CD8 T Cell Cytotoxicity. *J Exp Med* (2017) 214(4):895–904. doi: 10.1084/jem.20160801
38. Lau J, Cheung J, Navarro A, Lianoglou S, Haley B, Totpal K, et al. Tumour and Host Cell PD-L1 Is Required to Mediate Suppression of Anti-Tumour Immunity in Mice. *Nat Commun* (2017) 8:14572. doi: 10.1038/ncomms14572
39. Wu X, Li Y, Liu X, Chen C, Harrington SM, Cao S, et al. Targeting B7-H1 (PD-L1) Sensitizes Cancer Cells to Chemotherapy. *Heliyon* (2018) 4(12): e01039. doi: 10.1016/j.heliyon.2018.e01039
40. Haanen J. Converting Cold Into Hot Tumors by Combining Immunotherapies. *Cell* (2017) 170(6):1055–6. doi: 10.1016/j.cell.2017.08.031
41. van den Bulk J, Verdegaal EM, de Miranda NF. Cancer Immunotherapy: Broadening the Scope of Targetable Tumours. *Open Biol* (2018) 8(6):1–10. doi: 10.1098/rsob.180037
42. Shen X, Zhang L, Li J, Li Y, Wang Y, Xu ZX. Recent Findings in the Regulation of Programmed Death Ligand 1 Expression. *Front Immunol* (2019) 10:1337. doi: 10.3389/fimmu.2019.01337
43. Asgarova A, Asgarov K, Godet Y, Peixoto P, Nadaradjane A, Guittaut MB, et al. Pd-L1 Expression Is Regulated by Both DNA Methylation and NF-kB During EMT Signaling in Non-Small Cell Lung Carcinoma. *Oncoimmunology* (2018) 7(5):e1423170. doi: 10.1080/2162402X.2017.1423170
44. Lin RK, Hsu CH, Wang YC. Mithramycin A Inhibits DNA Methyltransferase and Metastasis Potential of Lung Cancer Cells. *Anticancer Drugs* (2007) 18 (10):1157–64. doi: 10.1097/CAD.0b013e3282a215e9
45. Li J, Gao H, Meng L, Yin L. Mithramycin Inhibits Epithelial-to-Mesenchymal Transition and Invasion by Downregulating SP1 and SNAI1 in Salivary Adenoid Cystic Carcinoma. *Tumour Biol* (2017) 39(6):1010428317708697. doi: 10.1177/1010428317708697
46. Kumar V, Patel S, Tcyganov E, Gabrilovich DI. The Nature of Myeloid-Derived Suppressor Cells in the Tumor Microenvironment. *Trends Immunol* (2016) 37(3):208–20. doi: 10.1016/j.it.2016.01.004
47. Zhang Y, Delgado AV, Mathew E, Li D, Mendez FM, Flannagan K, et al. Myeloid Cells are Required for PD-1/PD-L1 Checkpoint Activation and the Establishment of an Immunosuppressive Environment in Pancreatic Cancer. *Gut* (2017) 66(1):124–36. doi: 10.1136/gutjnl-2016-312078
48. Ganesh K, Stadler ZK, Cercek A, Mendelsohn RB, Shia J, Segal NH, et al. Immunotherapy in Colorectal Cancer: Rationale, Challenges and Potential. *Nat Rev Gastroenterol Hepatol* (2019) 16(6):361–75. doi: 10.1038/s41575-019-0126-x
49. Scroggins BT, Burkeen J, White AO, Chung EJ, Wei D, Chung SI, et al. Mithramycin A Enhances Tumor Sensitivity to Mitotic Catastrophe Resulting From DNA Damage. *Int J Radiat Oncol Biol Phys* (2018) 100(2):344–52. doi: 10.1016/j.ijrobp.2017.09.049
50. Brown JS, Sundar R, Lopez J. Combining DNA Damaging Therapeutics With Immunotherapy: More Haste, Less Speed. *Br J Cancer* (2018) 118(3):312–24. doi: 10.1038/bjc.2017.376
51. Itatani Y, Kawada K, Inamoto S, Yamamoto T, Ogawa R, Taketo MM, et al. The Role of Chemokines in Promoting Colorectal Cancer Invasion/Metastasis. *Int J Mol Sci* (2016) 17(5):643. doi: 10.3390/ijms17050643
52. Gupta R, Bhatt LK, Johnston TP, Prabhavalkar KS. Colon Cancer Stem Cells: Potential Target for the Treatment of Colorectal Cancer. *Cancer Biol Ther* (2019) 20(8):1068–82. doi: 10.1080/15384047.2019.1599660
53. Mosely SIS, Prime JE, Sainson RCA, Koopmann JO, Wang DYQ, Greenawalt DM, et al. Rational Selection of Syngeneic Preclinical Tumor Models for Immunotherapeutic Drug Discovery. *Cancer Immunol Res* (2017) 5(1):29–41. doi: 10.1158/2326-6066.CIR-16-0114

Author Disclaimer: Though this report is based upon work supported, in part, by the Department of Veterans Affairs, Veterans Health Administration, Office of Research and Development, the contents of this report do not represent the views of the Department of Veterans Affairs or the United States Government. This work has been supported in part by the Fred Wright Jr. Flow Cytometry Core at University of South Florida College of Medicine.

Conflict of Interest: SM (founder and scientific advisor) and SSM (founder and scientific advisor) have an equity interest in Transgenex Nanobiotech Inc. The terms of this arrangement have been reviewed and approved by the USF in accordance with its conflict of interest policies.

The remaining authors declare that the research was conducted in the absence of any commercial or financial relationships that could be construed as a potential conflict of interest.

Publisher's Note: All claims expressed in this article are solely those of the authors and do not necessarily represent those of their affiliated organizations, or those of the publisher, the editors and the reviewers. Any product that may be evaluated in this article, or claim that may be made by its manufacturer, is not guaranteed or endorsed by the publisher.

Copyright © 2021 Dutta, Khalil, Mayilsamy, Green, Howell, Bharadwaj, Mohapatra and Mohapatra. This is an open-access article distributed under the terms of the Creative Commons Attribution License (CC BY). The use, distribution or reproduction in other forums is permitted, provided the original author(s) and the copyright owner(s) are credited and that the original publication in this journal is cited, in accordance with accepted academic practice. No use, distribution or reproduction is permitted which does not comply with these terms.

frontiers in Immunology

ORIGINAL RESEARCH
published: 29 July 2021
doi: 10.3389/fimmu.2021.684807

The Regulatory Network and Potential Role of LINC00973-miRNA-mRNA ceRNA in the Progression of Non-Small-Cell Lung Cancer

Qiang Guo[1], Dan Li[2], Xiangyu Luo[1], Ye Yuan[1], Tian Li[3], Huasong Liu[1]* and Xinju Wang[1,4]**

[1] Department of Cardiothoracic Surgery, Taihe Hospital, Hubei University of Medicine, Shiyan, China, [2] Department of Oncology, Huanggang Central Hospital, Huanggang, China, [3] School of Basic Medicine, Fourth Military Medical University, Xi'an, China, [4] Department of Respiratory, Xinchang People's Hospital, Xinchang, China

OPEN ACCESS

Edited by:
Hubing Shi,
Sichuan University, China

Reviewed by:
Yanyang Liu,
Sichuan University, China
Virginia Tirino,
Università della Campania Luigi Vanvitelli, Italy

***Correspondence:**
Huasong Liu
huasong819@qq.com
Xinju Wang
xcwxj006@outlook.com
Tian Li
fmmult@foxmail.com

Specialty section:
This article was submitted to Cancer Immunity and Immunotherapy, a section of the journal Frontiers in Immunology

Received: *31 March 2021*
Accepted: *25 June 2021*
Published: *29 July 2021*

Citation:
Guo Q, Li D, Luo X, Yuan Y, Li T, Liu H and Wang X (2021) The Regulatory Network and Potential Role of LINC00973-miRNA-mRNA ceRNA in the Progression of Non-Small-Cell Lung Cancer. Front. Immunol. 12:684807. doi: 10.3389/fimmu.2021.684807

Background: The occurrence and development of cancer could be promoted by abnormally competing endogenous RNAs (ceRNA) network. This article aims to determine the prognostic biomarker of ceRNA for non-small-cell lung cancer (NSCLC) prognosis.

Methods: The expression and clinical significance of LINC00973 in NSCLC tissues were analyzed *via* the The Cancer Genome Atlas (TCGA), Gene Expression Profiling Interactive Analysis (GEPIA), lnCAR, and clinical samples in Taihe Hospital. The biological functions and signaling pathways involved in target genes of ceRNA network were analyzed *via* Gene Ontology (GO) and Kyoto Encyclopedia of Genes and Genomes (KEGG). Survival analysis, univariate and multivariate Cox regression analysis were used for prognostic-related mRNA.

Results: Expression of LINC00973 was increased in NSCLC tissues. High expression of LINC00973 was associated with poor prognosis of NSCLC patients. There were 15 miRNA and 238 differential mRNA in the INC00973-miRNA-mRNA ceRNA network, involving cell migration, endothelial cell proliferation, tumor growth factor (TGF)-β, cellular senescence, phosphatidylinositol 3-hydroxy kinase (PI3K)-Akt, Hippo, Rap1, mitogen-activated protein kinase (MAPK), cell cycle signaling pathway, etc. The expression levels of RTKN2, NFIX, PTX3, BMP2 and LOXL2 were independent risk factors for the poor prognosis of NSCLC patients.

Conclusions: LINC00973-miRNA-mRNA ceRNA network might be the basis for determining pivotal post-translational regulatory mechanisms in the progression of NSCLC. BMP2, LOXL2, NFIX, PTX3 and RTKN2 might be valuable prognostic markers and potential therapeutic targets.

Keywords: LINC00973, non-small cell lung cancer, prognosis, biomarker, ceRNA

INTRODUCTION

According to Global Cancer Statistics 2020, with an estimated 2.2 million new cancer cases and 1.8 million deaths, lung cancer was the second most commonly diagnosed cancer and the leading cause of cancer death in 2020, representing approximately one in 10 (11.4%) cancers diagnosed and one in 5 (18.0%) deaths (1–4). Lung cancer included non-small cell carcinoma (NSCLC) and small cell carcinoma. At present, surgery was the first choice for NSCLC patients at early-stage, and combined therapy was the main way for NSCLC patients at middle and advanced stage (5). With the improvement of treatment methods, the prognosis of cancer patients was improved, but the overall survival (OS) of NSCLC patients remained still frustrating. Recently, the researches had provided new insights into the molecular mechanisms of NSCLC in genomics and transcriptomics. For example, LCAT1, a member of long non-coding RNA (lncRNA), was an upregulated marker in lung cancer tissues. Elevated LCAT1 expression level was closely associated with poor prognosis of cancer patients (6). LncRNA MNX1-AS1 was upregulated in lung cancer tissues, and the prognosis of lung cancer patients with overexpression of MNX1-AS1 was often terrible. MNX1-AS1 promoted cell proliferation, migration and invasion of lung cancer. The MNX1-AS1/miR-527/BRF2 signaling axis was involved in the occurrence and development of lung cancer (7). The expression of LncRNA AFAP1-AS1 was increased in NSCLC tissues, and related to the TNM stage and tumor size of NSCLC patients. Interfering with the expression of AFAP1-AS1 could inhibit the growth of NSCLC cells *in vitro* and *in vivo* (8). Therefore, lncRNA played an essential role in the progression of lung cancer.

Studies have confirmed that non-coding RNA (ncRNA) played important roles in tumorigenesis and metastasis (6–8). microRNA (miRNA) and lncRNA belong to ncRNA, and both of which have miRNA recognition elements (MRE) (9, 10). miRNA could trigger degradation of downstream target genes by recognizing the MRE in the 3'non-transcribed region (11, 12). Therefore, when lncRNA and mRNA had the same MRE, both of them could competitively bind to miRNA, forming a competitive endogenous RNA (ceRNA) regulatory network (13, 14). When miRNA bound to the target mRNA, the stability of mRNA decreased and its translation was hindered, thereby affecting gene expression. When lncRNA bound to miRNA, the stability of competitive mRNA increases instead, so that transcription and translation were well performed. This was a competitive two-way gene expression regulation mechanism composed of endogenous RNA (15, 16).

The ceRNA network mechanism presents a significant role in the occurrence and development of cancer. For example, the expression of circ_0025033 and small nuclear ribonucleoprotein Sm-like4 (LSM4) increased in ovarian cancer tissues and cells. Interfered with circ_0025033 or LSM4 expression could inhibit colony formation, migration, invasion and glycolytic metabolism of ovarian cancer cells. Circ_0025033 acted as a ceRNA to regulate LSM4 expression by targeting miR-184. Overexpression of LSM4 promoted the expression of circ_0025033, thereby inducing colony formation, migration, invasion and glycolysis (17). This indicated that there were abnormalities in the ceRNA network mechanism in the development of cancer. It was recently discovered that lncRNA LINC00973 had a vital effect in cancer. For example, chemotherapy could upregulate the expression level of LINC00973 in normal cells and cancer cells, which might be related to the activation of DNA damage response pathways or mitotic arrest. LINC00973 could reduce p21 levels, activate cancer cell proliferation, and reduce the lethality of drugs (18). Siglec-15 was a tumor immunosuppressive molecule. LINC00973 was highly expressed in Siglec-15 positive clear cell renal cell carcinoma, and it could positively regulate the expression of Siglec-15, which was the direct target molecule of miR-7109. LINC00973 could regulate the expression of Siglec-15 by affecting the role of sponge miR-7109 and forming ceRNA. Therefore, the LINC00973-miR-7109-Siglec-15 ceRNA mechanism was involved in regulating the progression of renal cell carcinoma (19). Nowadays, there was no related literature report about the regulation mechanism of ceRNA network composed of LINC00973 in the progress of NSCLC. Therefore, this study aims to explore the role and potential value of LINC00973-miRNA-mRNA ceRNA in the progression of NSCLC, and to provide new target molecules and potential regulatory mechanisms for NSCLC diagnosis and treatment.

Abbreviation: NSCLC, Non-small cell lung cancer; miRNA, microRNAs; LUAD, lung adenocarcinoma; LUSC, lung squamous cell carcinoma; lncRNA, long non-coding RNA; MRE, miRNA recognition elements; OS, overall survival.

MATERIALS AND METHODS

NSCLC Tissue Sample

Cancer and normal adjacent tissues of 25 patients with NSCLC undergoing surgical treatment were collected at the Department of Thoracic Surgery, Taihe Hospital from December 2019 to April 2020. Inclusion criteria: (1) NSCLC was diagnosed pathologically; (2) Neoadjuvant chemotherapy or radiotherapy was not performed before surgery; (3) Immunosuppressant therapy, biological therapy, or targeted therapy were not performed. Exclusion criteria: 1) SCLC; 2) Patients voluntarily withdraw. This study was approved by the ethics committee of the Taihe Hospital, Hubei University of Medicine, and the patient has signed an informed consent. Among them, 11 cases were lung adenocarcinoma (LUAD) and 14 cases were lung squamous cell carcinoma (LUSC).

TCGA Database

In October 2020, 1145 samples were downloaded from the TCGA (https://portal.gdc.cancer.gov/) website (108 cases of normal lung tissue, including 59 cases of normal lung tissue from LUAD and 49 cases of normal lung tissue from LUSC; 1037 cases of NSCLC tissue samples, including 535 samples of LUAD Cases and 522 cases of LUSC samples) HTSeq-FPKM transcriptome data and TCGA clinical data of 1026 NSCLC patients. The clinical parameters and prognostic information of

NSCLC patients was sorted out. Patients with unknown or incomplete parameters to analyze the relationship between the expression level of LINC00973 and the prognosis was excluded. The limma package was used to analyze the differential expression genes in the tissues of NSCLC patients, and the screening conditions: fold change > 1 and $P < 0.05$.

Quantitative Real-Time PCR

According to the RNA kit (Invitrogen, USA) instructions, total RNA was extracted from NSCLC tissue, and the qualified RNA concentration was detected. Copying DNA (cDNA) was synthesized using a reverse transcription kit (Takara, Japan), and the expression of LINC00973 was detected by quantitative real-time PCR (qRT-PCR). Primers was supplied by Sangong Co Ltd. GAPDH was used as an internal control. Primer sequence (5'-3'): LINC00973: TTGAAGGCTTCCTGGTCTGAG (Forward), AGGCTTACATTCCAGCTGTGT (Reverse), GAPDH: AACGGATTTGGTCGTATTG (Forward), GGAAGATGGTGATGGGATT (Reverse). Experiments were performed in triplicate independently.

LNCAR and GEPIA Database

The LNCAR (http://lncar.renlab.org/) database data were acquired from the GEO database, which contained the cancer-related lncRNA expression database. The expression of LINC00973 in lung cancer tissues and its potential clinical value were analyzed in the LNCAR database. The screening criteria: $P < 0.05$. The GEPIA (http://gepia.cancer-pku.cn/) database was a reanalysis online database based on the TCGA and GTEx database data. The expression of LINC00973 and biomarkers in ceRNA network were explored. And the relationship between expression of LINC00973 and NSCLC overall survival (OS) and disease-free survival (DFS) were analyzed in the GEPIA database.

ceRNA Network

The miRNA of LINC00973 were predicted in the LncBase Predicted v.2 database, and the screening criteria: binding coefficient ≥ 0.6. In addition, the miRNA that predicting the differentially expressed genes of TCGA database were performed *via* the PITA, RNA22, miRmap, microT, miRanda, PicTar, and TargetScan databases, and the screening criteria: the number of databases with targeting relationships needed to be greater than 3. Screening for overlapping miRNA in the LINC00973 target miRNA and miRNA that differentially expressed genes of TCGA database, and the ceRNA network signaling mechanism was constructed *via* Cytoscape 3.6.1 software.

Gene Ontology (GO) and Kyoto Encyclopedia of Genes and Genomes (KEGG)

LncRNA competitively inhibited the mRNA binding to miRNA, and could maintain the stability of mRNA and promotes RNA transcription when LncRNA binds to miRNA. Therefore, the biological functions and signaling mechanisms involved in the ceRNA network was explored *via* the R clusterProfiler package. GO annotation included the biological process (BP), molecular function (MF) and cellular component (CC). The screening criteria: $P < 0.05$.

Prognostic Survival Analysis

Kaplan-Meier survival analysis was used to evaluate the role of differentially expressed genes in the prognosis of NSCLC patients to understand the important target molecules in the ceRNA mechanism. The screening criteria was $P < 0.05$. On this basis, univariate Cox and multivariate Cox regression analysis were performed, and a nomogram was constructed.

The Value of Poor Prognostic Factors in NSCLC Patients Were Verified

The GEPIA database was used to verify the expression of poor prognostic factors in the ceRNA network in NSCLC tissues. In addition, the Cbioportal database (http://www.cbioportal.org) was used to explore the relationship between poor prognostic factors and clinical pathological characteristics of patients with NSCLC. PrognoScan (http://www.abren.net/PrognoScan/) and Kaplan-Meier Plotter (http://kmplot.com/analysis/) databases were used to verify the value of poor prognostic factors in the prognosis of NSCLC patients, and the grouping standard was according to the best cutoff value.

Statistical Analysis

Data processing and statistical analysis adopt perl and R language. The expression level and prognostic value of LINC00973 and mRNA in the ceRNA network were analyzed by the wilcoxon signed-rank test and Kaplan-Meier survival analysis. In addition, the role of differentially expressed genes in NSCLC prognosis in the ceRNA network were explored *via* the univariate and multivariate Cox regression analysis. $P < 0.05$ was considered statistically significant.

RESULTS

LINC00973 Was Upregulated in NSCLC Tissues

In the TCGA database, the expression of LINC00973 was increased in unpaired NSCLC tissues (**Figure 1A**). The expression of LINC00973 was increased in unpaired LUAD and LUSC tissues (**Figures 1B, C**). The expression of LINC00973 in 106 paired NSCLC tissues was increased significantly (**Figure 1D**). The expression of LINC00973 was also increased in 57 paired LUAD and 49 paired LUSC significantly (**Figures 1E, F**).

In addition, the expression of LINC00973 was increased in NSCLC tissues in LNCAR database (**Figures 2A–F**). The GSE27262 and GSE89039 datasets showed that the expression of LINC00973 (LC_S148 and LC_S39) in lung cancer tissues was elevated, significantly (**Figures 2A, B**). The GSE101929 dataset revealed that the expression of LINC00973 (LC_S3) in NSCLC tissues was elevated (**Figure 2C**). The GSE40791 and GSE33532 datasets showed that the expression of LINC00973 (LC_S257 and

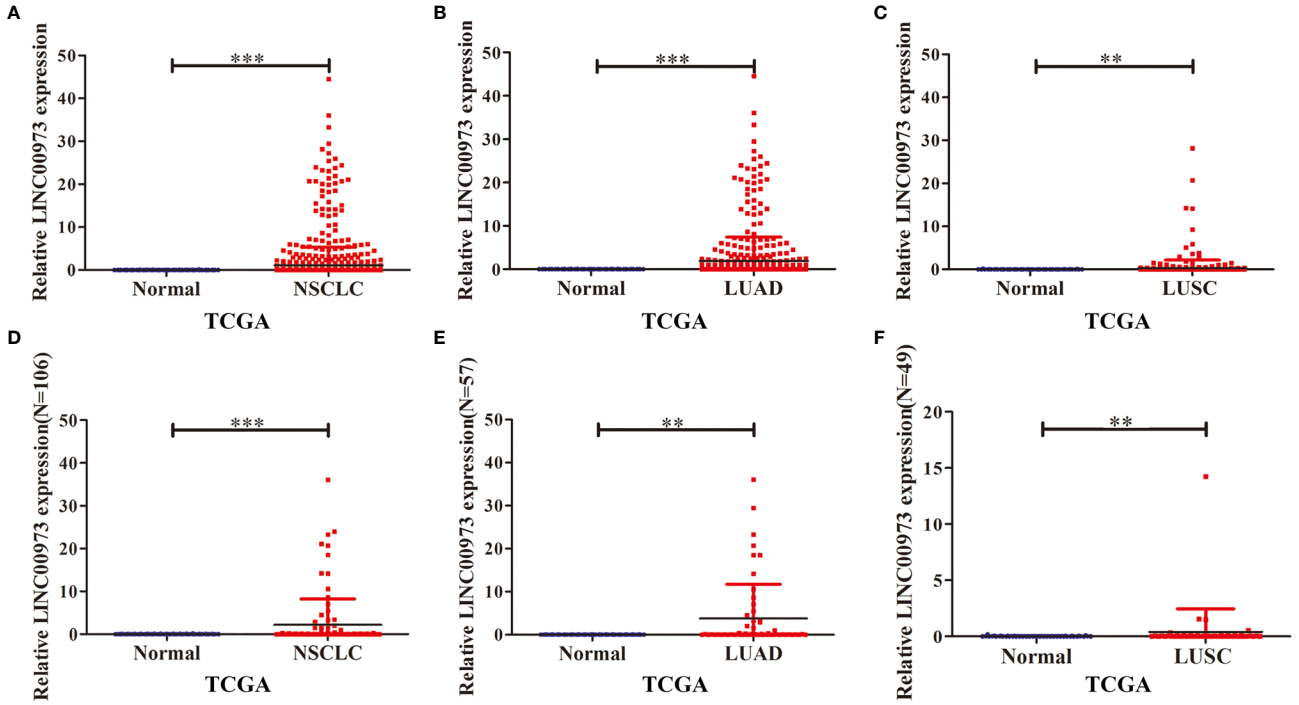

FIGURE 1 | LINC00973 expression was elevated in NSCLC tissue in the TCGA database. **(A–C)** Expression of LINC00973 in unpaired samples of NSCLC, LUAD and LUSC; **(D–F)** Expression of LINC00973 in paired samples of NSCLC, LUAD and LUSC. NSCLC, Non-small cell lung cancer; LUAD, lung adenocarcinoma; LUSC, lung squamous cell carcinoma; Normal, normal tissues; TCGA, The Cancer Genome Atlas; **P < 0.01; ***P < 0.001.

LC_S216) in LUAD tissues was increased, and it was statistically significant (**Figures 2D, E**). The GSE33532 dataset showed that the expression of LINC00973 (LC_S218) in LUSC tissues was increased. However, it was not statistically significant (**Figure 2E**).

Moreover, we collected 25 clinical NSCLC tissues and adjacent normal lung tissues. We found that the expression of LINC00973 was increased in NSCLC and its subtypes *via* qRT-PCR. However, it was not statistically significant (**Figures 2G–I**).

Elevated LINC00973 Expression Was Correlated With Poor Prognosis in NSCLC Patients

In the TCGA database, Kaplan-Meier survival curve suggested that increasing level of LINC00973 was closely associated with poor prognosis of NSCLC patients (**Figure 3A**). Subgroup analysis found that the prognosis of LUAD and LUSC patients with elevated LINC00973 expression levels were with poor prognosis, whereas there was no statistical significance between the LINC00973 expression levels and the prognosis of LUSC patients (**Figures 3B, C**). In addition, we found that increasing the expression levels of LINC00973 were with poor prognosis of NSCLC patients in the GEPIA database (**Figures 3D–F**). In detail, increasing levels of LINC00973 were negatively interrelated with OS and DFS in NSCLC patients, which indicated that LINC00973 might be a carcinogen. A consistent conclusion was reached in the LNCAR database. We found that anti-cancer drugs could inhibit the expression of LINC00973 in NSCLC PC9 and HCC827 cells (**Figure 4**). In detail, compared with the control group, GSE67051,GSE80316, and GSE51212 datasets showed that the expression of LINC00973 in the erlotinib treatment group was significantly decreased. The GSE38302 dataset showed that the expression of LINC00973 in the gefitinib group was significantly decreased.

Construction of LINC00973-miRNA-mRNA ceRNA Network

In the LncBase Predicted v.2 database, a total of 210 miRNA were screened with the binding coefficient ≥ 0.6 (**Table 1**). In the TCGA database, 5367 differentially expressed genes were found in NSCLC tissues. We use heat map and violin map to show the top 20 differentially expressed genes in TCGA *via* fold changes (**Figures S1A, B**). We predicted that there were 232 miRNAs for differentially expressed genes (**Table S1**). Further comparison suggested that there were 15 miRNA that were competitively bound, namely hsa-miR-374b-5p, hsa-miR-216b-5p, hsa-miR-196a-5p, hsa-miR-320c, hsa-miR-138 -5p, hsa-miR-150-5p, hsa-miR-196b-5p, hsa-miR-224-5p, hsa-miR-320a, hsa-miR-186-5p, hsa-miR-320b, hsa-miR -425-5p, hsa-miR-410-3p, hsa-miR-320d and hsa-miR-433-3p (**Figure S2**). There were 238 target genes for miRNA in the ceRNA network (**Table S2**), and the LINC0097-miRNA-mRNA ceRNA network signaling mechanism was constructed (**Figure 5**).

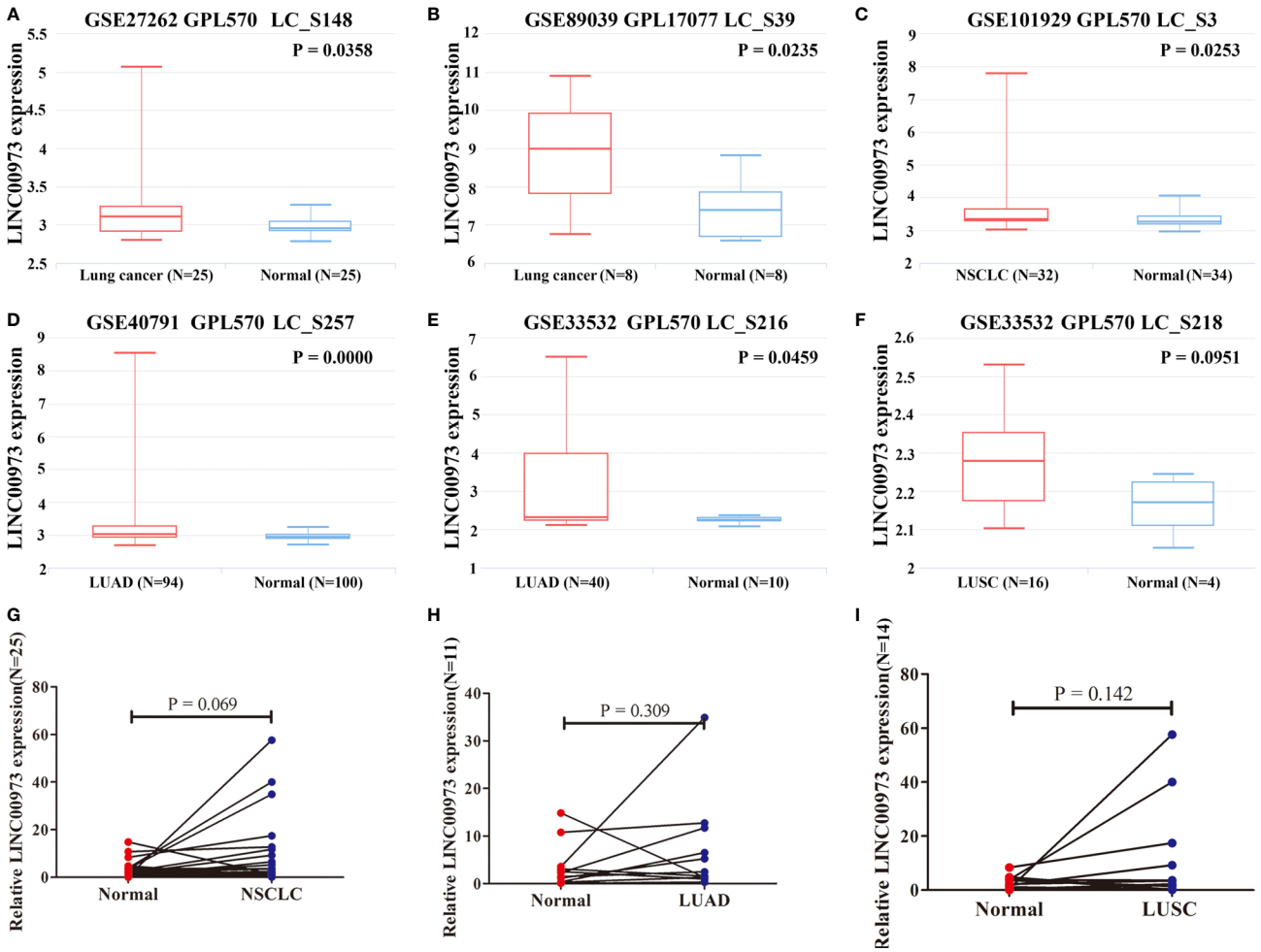

FIGURE 2 | LINC00973 expression was upregulated in the LNCAR database and clinical NSCLC tissues. **(A)** GSE27262 (LC_S148); **(B)** GSE89039 (LC_S39); **(C)** GSE101929 (LC_S3); **(D)** GSE40791 (LC_S257); **(E)** GSE33532 (LC_S216); **(F)** GSE33532 (LC_S218); **(G)** Clinical NSCLC samples; **(H)** Clinical LUSD samples; **(I)** Clinical LUSCsamples. NSCLC, Non-small cell lung cancer; LUAD, lung adenocarcinoma; LUSC, lung squamous cell carcinoma; Normal, normal tissues.

The Biological Functions and Signaling Pathways Involved in the ceRNA Network Mechanism

We performed GO annotation and KEGG on 238 mRNAs in the ceRNA network to explore the biological roles of LINC00973 of NSCLC. The GO annotation showed that LINC00973 might be involved in biological processes such as cell migration, response to oxygen levels, positive regulation of cell cycle process, and endothelial cell proliferation (**Figures 6A–C** and **Table S3**). KEGG showed that LINC00973 might be involved in the regulation of MicroRNAs in cancer, RNA transport, TGF β signaling pathway, Cellular senescence, PI3K-Akt signaling pathway, Hippo signaling pathway, Rap1 signaling pathway, Transcriptional misregulation in cancer, EGFR tyrosine kinase inhibitor resistance, MAPK signaling pathway, cell cycle and renin-angiotensin system and other signaling pathways (**Figure 6D** and **Table 2**).

Kaplan-Meier Survival Analysis Screens Prognostic Genes in the ceRNA Network

Kaplan-Meier survival analysis revealed that the expression levels of ANLN, BMP2, CALU, COL1A1, COL1A2, COL3A1, ERO1A, FSCN1, FZD3, LOXL2, MME, MSI2, NFIX, PTX3, RTKN2, SLC2A1, SLC16A1, and SNX30 were relevant with poor prognosis in NSCLC patients (**Figure 7**). In detail, NSCLC patients with elevated expression levels of ANLN, BMP2, CALU, COL1A1, COL1A2, COL3A1, LOXL2, MME, PTX3 and SLC2A1 had a poor prognosis. The prognosis of NSCLC patients with reduced expression levels of FZD3, MSI2, NFIX, RTKN2 and SNX30 were poor, respectively ($P < 0.05$).

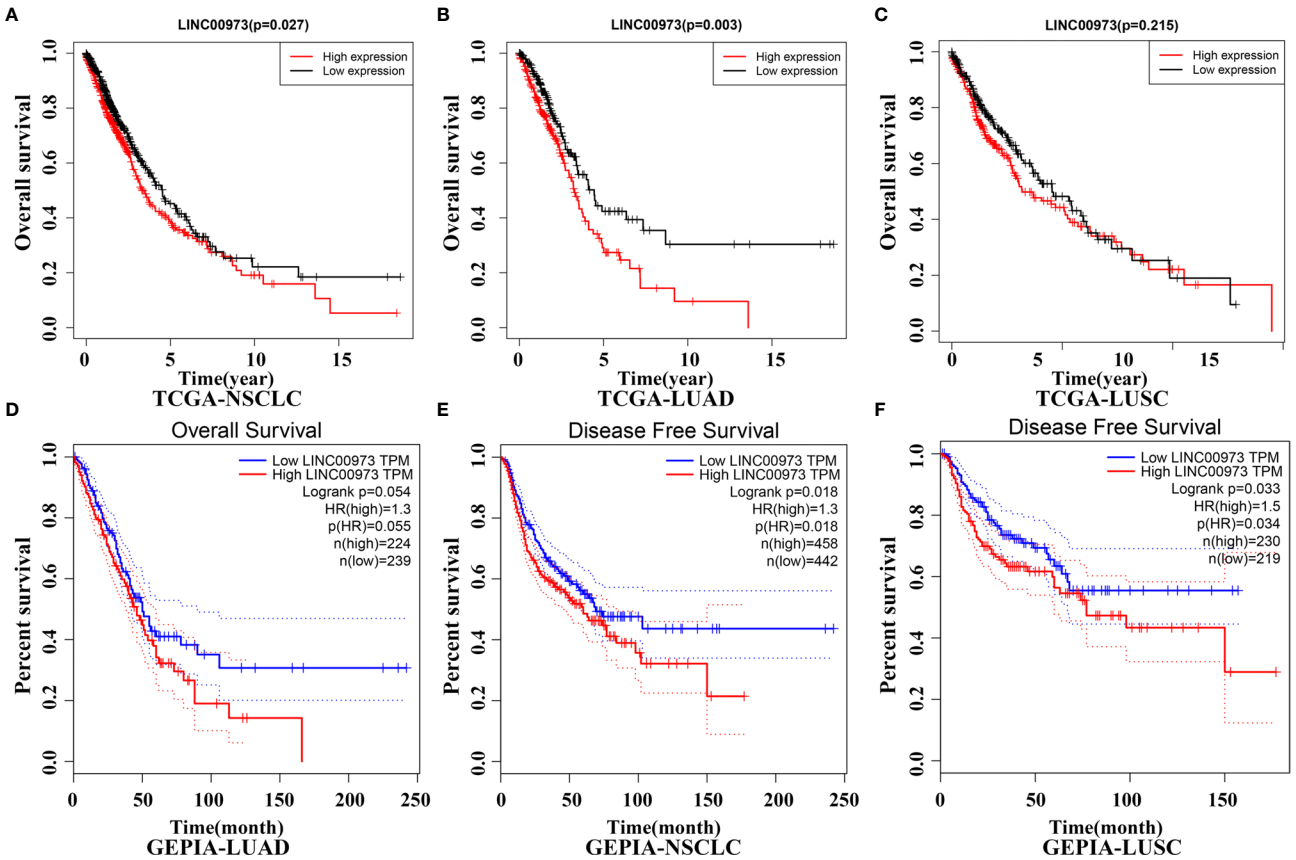

FIGURE 3 | NSCLC patients with elevated lncRNA expression have poor prognosis in TCGA and GEPIA databases. **(A)** TCGA-NSCLC-OS; **(B)** TCGA-LUAD-OS; **(C)** TCGA-LUSC-OS; **(D)** GEPIA-LUAD-OS; **(E)** GEPIA-NSCLC-DFS; **(F)** GEPIA-LUSC-DFS. NSCLC, Non-small cell lung cancer; LUAD, lung adenocarcinoma; LUSC, lung squamous cell carcinoma; TCGA, The Cancer Genome Atlas; GEPIA, Gene Expression Profiling Interactive Analysis.

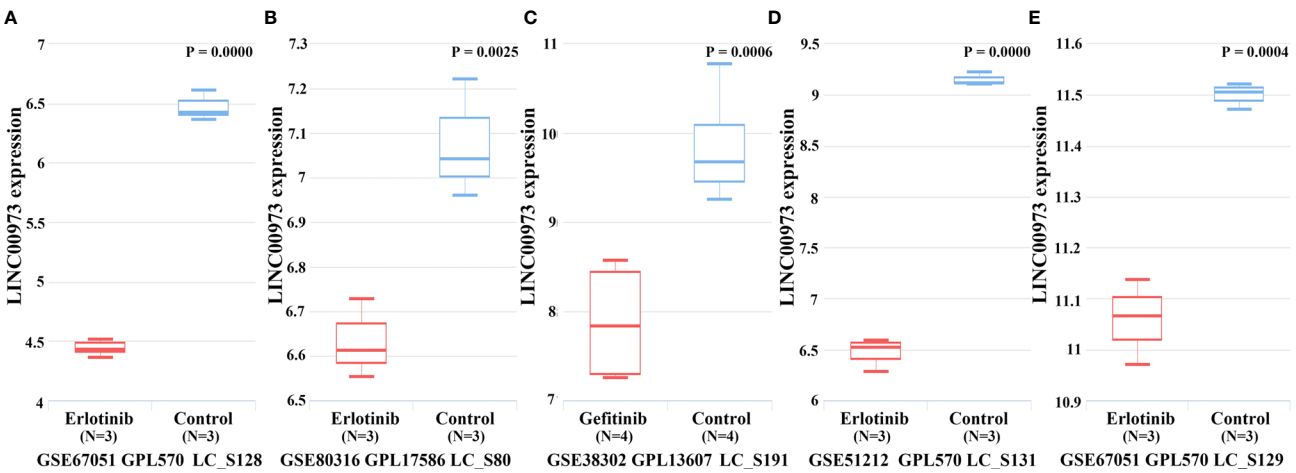

FIGURE 4 | Anti-cancer drugs could down-regulate the expression of LINC00973. **(A)** GSE67051-erlotinib; **(B)** GSE80316-erlotinib; **(C)** GSE38302-gefitinib; **(D)** GSE51212-erlotinib; **(E)** GSE67051-erlotinib.

TABLE 1 | LINC00973-bound miRNA in the LncBase Predicted v.2 database.

LINC00973-miRNA				
hsa-miR-6749-3p	hsa-miR-5088-3p	hsa-miR-4700-5p	hsa-miR-513a-3p	hsa-miR-4633-5p
hsa-miR-3127-3p	hsa-miR-1238-3p	hsa-miR-133a-5p	hsa-miR-609	hsa-miR-374b-5p
hsa-miR-3177-5p	hsa-miR-3160-5p	hsa-miR-3180-5p	hsa-miR-433-3p	hsa-miR-6832-3p
hsa-miR-6875-3p	hsa-miR-541-5p	hsa-miR-4666a-5p	hsa-miR-7162-5p	hsa-miR-3151-3p
hsa-miR-6831-5p	hsa-miR-559	hsa-miR-33a-3p	hsa-miR-4719	hsa-miR-4694-3p
hsa-miR-6739-5p	hsa-miR-4778-3p	hsa-miR-6821-3p	hsa-miR-3121-3p	hsa-miR-216b-5p
hsa-miR-6756-3p	hsa-miR-6823-5p	hsa-miR-4282	hsa-miR-518d-3p	hsa-miR-208b-5p
hsa-miR-7113-5p	hsa-miR-629-3p	hsa-let-7f-1-3p	hsa-miR-579-3p	hsa-miR-4510
hsa-miR-545-3p	hsa-miR-5703	hsa-miR-4667-5p	hsa-miR-100-3p	hsa-miR-1238-5p
hsa-miR-449b-3p	hsa-miR-3153	hsa-miR-4501	hsa-miR-3689f	hsa-miR-4496
hsa-miR-4469	hsa-miR-520f-5p	hsa-miR-150-5p	hsa-miR-4474-3p	hsa-miR-138-5p
hsa-miR-6733-5p	hsa-miR-3973	hsa-miR-3668	hsa-miR-1915-5p	hsa-miR-6130
hsa-miR-320a	hsa-miR-3919	hsa-miR-3927-3p	hsa-miR-942-5p	hsa-miR-6892-3p
hsa-miR-320b	hsa-miR-6077	hsa-miR-188-3p	hsa-miR-3606-3p	hsa-miR-548as-5p
hsa-miR-4429	hsa-miR-6834-5p	hsa-miR-7853-5p	hsa-miR-7113-3p	hsa-miR-548d-5p
hsa-miR-532-3p	hsa-miR-6867-3p	hsa-miR-676-5p	hsa-miR-3678-3p	hsa-miR-5587-5p
hsa-miR-320e	hsa-miR-4786-3p	hsa-miR-2355-3p	hsa-miR-664b-3p	hsa-miR-6792-3p
hsa-miR-320d	hsa-miR-6839-5p	hsa-miR-376a-5p	hsa-miR-1207-3p	hsa-miR-1273g-5p
hsa-miR-320c	hsa-miR-369-3p	hsa-miR-1277-5p	hsa-miR-518b	hsa-miR-6127
hsa-miR-675-3p	hsa-miR-4677-3p	hsa-miR-4760-3p	hsa-miR-3617-3p	hsa-miR-7843-3p
hsa-miR-4679	hsa-miR-2276-5p	hsa-miR-4455	hsa-miR-3123	hsa-miR-548a-5p
hsa-miR-3680-3p	hsa-miR-4434	hsa-let-7a-3p	hsa-miR-548b-5p	hsa-miR-6129
hsa-miR-493-5p	hsa-miR-7156-3p	hsa-miR-105-5p	hsa-miR-7154-5p	hsa-miR-4691-5p
hsa-miR-6780b-5p	hsa-miR-6772-5p	hsa-miR-520h	hsa-miR-224-5p	hsa-miR-6875-5p
hsa-miR-4725-3p	hsa-miR-509-5p	hsa-miR-5701	hsa-miR-4762-3p	hsa-miR-6133
hsa-miR-5692c	hsa-miR-3925-5p	hsa-miR-539-5p	hsa-miR-148b-5p	hsa-miR-548k
hsa-miR-5692b	hsa-miR-297	hsa-miR-3662	hsa-miR-516b-3p	hsa-miR-548j-5p
hsa-miR-3922-5p	hsa-miR-509-3-5p	hsa-miR-4753-5p	hsa-miR-516a-3p	hsa-miR-3126-5p
hsa-miR-3671	hsa-miR-4287	hsa-miR-2054	hsa-miR-517-5p	hsa-miR-378j
hsa-miR-1252-3p	hsa-miR-3646	hsa-miR-3149	hsa-miR-518c-3p	hsa-miR-4419a
hsa-miR-568	hsa-miR-4650-3p	hsa-miR-3942-3p	hsa-miR-425-5p	hsa-miR-548av-5p
hsa-miR-2115-5p	hsa-miR-6512-3p	hsa-miR-520g-3p	hsa-miR-612	hsa-miR-6854-5p
hsa-miR-513b-3p	hsa-miR-6720-5p	hsa-miR-8061	hsa-miR-4662a-3p	hsa-miR-548i
hsa-miR-4731-5p	hsa-miR-4685-3p	hsa-miR-2116-3p	hsa-miR-4775	hsa-miR-548ao-5p
hsa-miR-8070	hsa-miR-4713-5p	hsa-miR-196b-5p	hsa-miR-4311	hsa-miR-186-5p
hsa-miR-4659b-3p	hsa-miR-410-3p	hsa-miR-580-5p	hsa-miR-4745-5p	hsa-miR-548ab
hsa-miR-4659a-3p	hsa-miR-7114-5p	hsa-miR-4320	hsa-miR-548p	hsa-miR-330-3p
hsa-miR-4666b	hsa-miR-205-3p	hsa-miR-148a-5p	hsa-miR-4516	hsa-miR-545-5p
hsa-miR-6758-3p	hsa-miR-4495	hsa-miR-4306	hsa-miR-3689e	hsa-miR-6815-3p
hsa-miR-670-3p	hsa-miR-4267	hsa-miR-513c-3p	hsa-miR-3689a-5p	hsa-miR-548c-5p
hsa-miR-5692a	hsa-miR-4271	hsa-miR-671-5p	hsa-miR-3689b-5p	hsa-miR-548o-5p
hsa-miR-4799-5p	hsa-miR-8089	hsa-miR-196a-5p	hsa-miR-4758-5p	hsa-miR-548am-5p

Univariate and Multivariate Cox Regression Analysis to Screen Prognostic Factors in ceRNA Network

Univariate Cox regression analysis to screen 18 prognostic-related factors, it was found that LOXL2, PTX3, SLC2A1, RTKN2, ANLN, NFIX, CALU, ERO1A, BMP2, FSCN1, COL1A2, SLC16A1, COL3A1, MME, SNX30, COL1A1, and MSI2 might be prognostic risk factors of NSCLC patients (**Table 3**). Multivariate Cox regression analysis suggested that RTKN2, NFIX, PTX3, BMP2 and LOXL2 were independent risk factors for poor prognosis of NSCLC patients (**Figure 8**).

Verified the Expression and Potential Clinical Value of Independent Risk Factors in NSCLC Tissues

In the GEPIA database, we found that the expression levels of RTKN2, NFIX, PTX3 and BMP2 in NSCLC subtypes LUAD and LUSC tissues were significantly declined, while the expression of LOXL2 in NSCLC tissues increased (**Figure S3**). **Figure S4** showed the relationship between RTKN2, NFIX, PTX3, BMP2, and LOXL2 mutation status and clinicopathological characteristics of NSCLC patients. In addition, the expression levels of RTKN2, NFIX, PTX3, BMP2 and LOXL2 were correlated with poor prognosis of NSCLC patients in the PrognoScan and Kaplan-Meier Plotter databases (**Figure S5** and **Table 4**). Therefore, we grouped the median values of RTKN2, NFIX, PTX3, BMP2, and LOXL2 expression to construct a nomogram to assess the prognosis of patients (**Figure 9**).

DISCUSSION

Currently, it was urgent for us to improve the prognosis of NSCLC patients by finding novel and improved therapies.

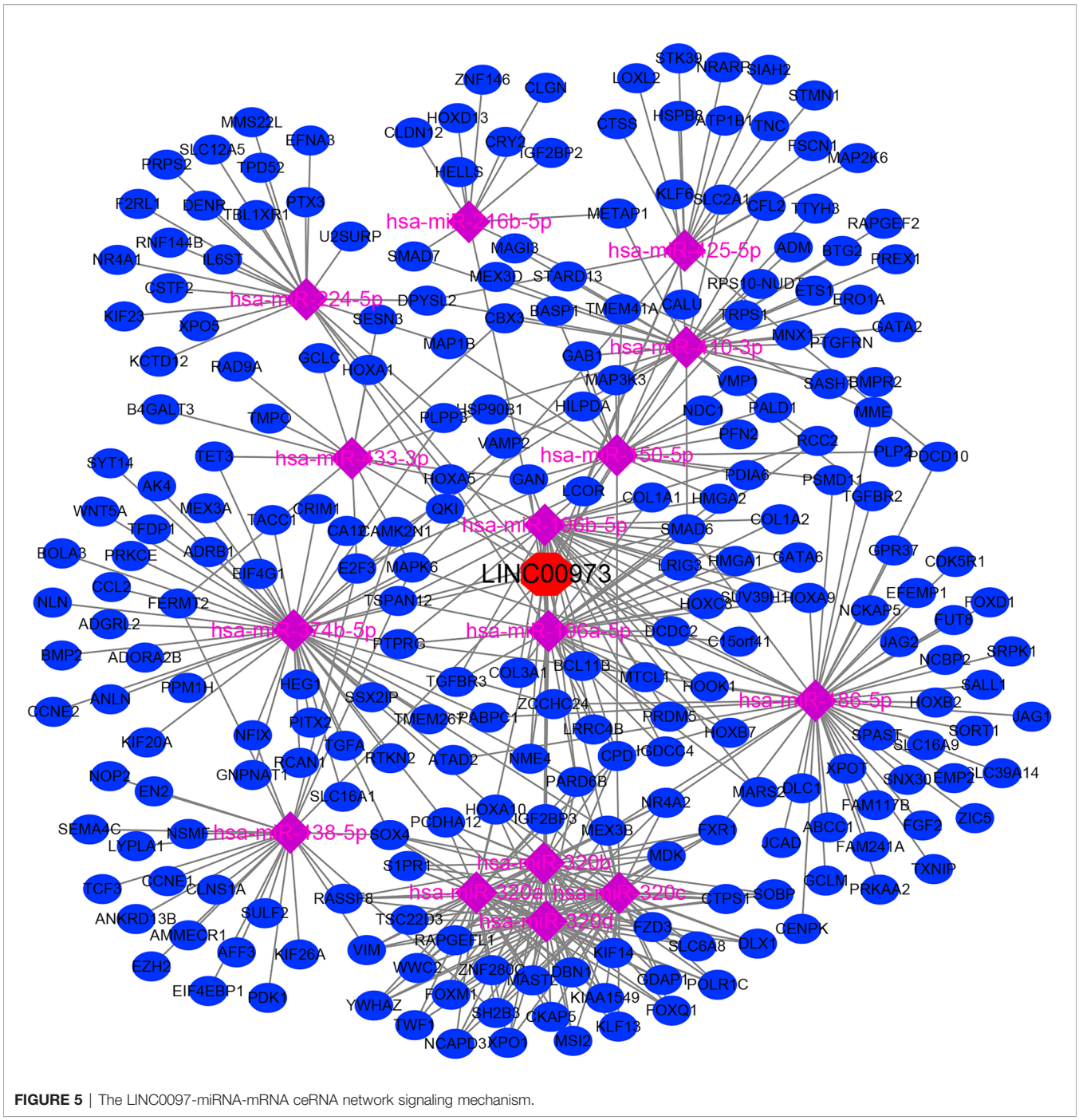
LINC00973
hsa-miR-224-5p
hsa-miR-133-3p
hsa-miR-374b-5p
hsa-miR-138-5p
hsa-miR-320b
hsa-miR-320a
hsa-miR-320c
hsa-miR-320d
hsa-miR-150-5p
hsa-miR-96a-5p
hsa-miR-486-5p
hsa-miR-425-5p
hsa-miR-410-3p
hsa-miR-16b-5p
hsa-miR-15b-5p
STK39
NRARP
SIAH2
LOXL2
STMN1
ZNF146
CLGN
HOXD13
CLDN12
CRY2
IGF2BP2
HELLS
CTSS
HSPB8
ATP1B1
TNC
FSCN1
MAP2K6
MMS22L
EFNA3
SLC12A5
PRPS2
TPD52
F2RL1
DENR
TBL1XR1
PTX3
U2SURP
RNF144B
NR4A1
IL6ST
CSTF2
KIF23
XPO5
KCTD12
RAD9A
GCLC
HOXA1
B4GALT3
TMPO
SYT14
AK4
WNT5A
MEX3A
TFDP1
BOLA3
PRKCE
ADRB1
CCL2
NLN
FERMT2
ADGRL2
BMP2
ADORA2B
ANLN
CCNE2
PPM1H
KIF20A
NOP2
EN2
SEMA4C
NSMF
LYPLA1
TCF3
CCNE1
CLNS1A
ANKRD13B
AMMECR1
EZH2
AFF3
KIF26A
EIF4EBP1
PDK1
SULF2
TET3
TACC1
CRIM1
CA12
CAMK2N1
QKI
E2F3
MAPK6
EIF4G1
TSPAN12
PTPRG
HEG1
SSX2IP
PITX2
NFIX
TGFA
RCAN1
GNPNAT1
SLC16A1
RASSF8
TSC22D3
VIM
RAPGEFL1
WWC2
ZNF280C
MAST1
DBN1
YWHAZ
FOXM1
SH2B3
CKAP5
TWF1
NCAPD3
XPO1
MSI2
KLF13
FOXQ1
KIAA1549
GDAP1
POLR1C
KIF14
SLC6A8
DLX1
CENPK
FZD3
GTPSP1
SOBP
GCLM
PRKAA2
TXNIP
FAM241A
FAM117B
ABCO1
FGF2
ZIC5
JCAD
MARS2
OLC1
XPOT
SNX30
EMP2
LC39A14
SPAST
SLC16A9
SORT1
JAG1
HOXB2
SALL1
HOOK1
HOXB7
LRRC4B
RRDM5
MTCL1
BCL11B
COL3A1
TGFBR3
ZCCHC24
PABPC1
TMEM267
HOXA10
IGF2BP3
PCDHA12
SOX4
S1PR1
NR4A2
MEX3B
FXR1
MDK
CPD
IGDCC4
ATAD2
NME4
RTKN2
PARD6B
BCDC2
C15orf41
HOXC8
SUV39H1
HOXA9
NCKAP5
EFEMP1
FOXD1
FUT8
JAG2
NCBP2
SRPK1
SALL4
HMGA1
LRIG3
GATA6
GPR37
CDK5R1
COL1A2
SMAD6
PDIA6
PSMD11
TGFBR2
PLP2
PDCD10
RCC2
PFN2
NDC1
PALD1
MME
VMP1
SASH1
BMPR2
MAP3K3
GAB1
MNX1
PTGFRN
GATA2
TRPS1
CALU
TMEM41A
BASP1
CBX3
SESN3
DPYSL2
MEX3D
STARD13
SMAD7
MAGI3
METAP1
KLF6
SLC2A1
CFL2
TTYH3
RAPGEF2
ADM
BTG2
PREX1
RPS10-NUDT3
ETS1
ERO1A
MAP1B
HSP90B1
HILPDA
PLPP3
VAMP2
HOXA5
GAN
LCOR
COL1A1
HMGA2
QKI
CAMK2N1
CA12
TACC1
CRIM1
MEX3A
TET3
SYT14
AK4
WNT5A
TFDP1
BOLA3
PRKCE
ADRB1
CCL2
NLN
FERMT2
ADGRL2
BMP2
ADORA2B
ANLN
CCNE2
PPM1H
KIF20A
NOP2
EN2
SEMA4C
NSMF
LYPLA1
TCF3
CCNE1
CLNS1A
ANKRD13B
AMMECR1
EZH2
AFF3
KIF26A
EIF4EBP1
PDK1
SULF2
HEG1
SSX2IP
PITX2
NFIX
TGFA
RCAN1
GNPNAT1
SLC16A1
TSPAN12
PTPRG
TGFBR3
TMEM267
ZCCHC24
PABPC1
COL3A1
BCL11B
MTCL1
HOOK1
HOXB7
LRRC4B
RRDM5
HOXB2
SALL1
JAG1
SORT1
SLC16A9
SPAST
SNX30
EMP2
LC39A14
XPOT
MARS2
OLC1
FAM117B
ZIC5
FGF2
ABCO1
FAM241A
TXNIP
PRKAA2
GCLM
JCAD
FXR1
MDK
NR4A2
MEX3B
HOXA10
IGF2BP3
PCDHA12
SOX4
S1PR

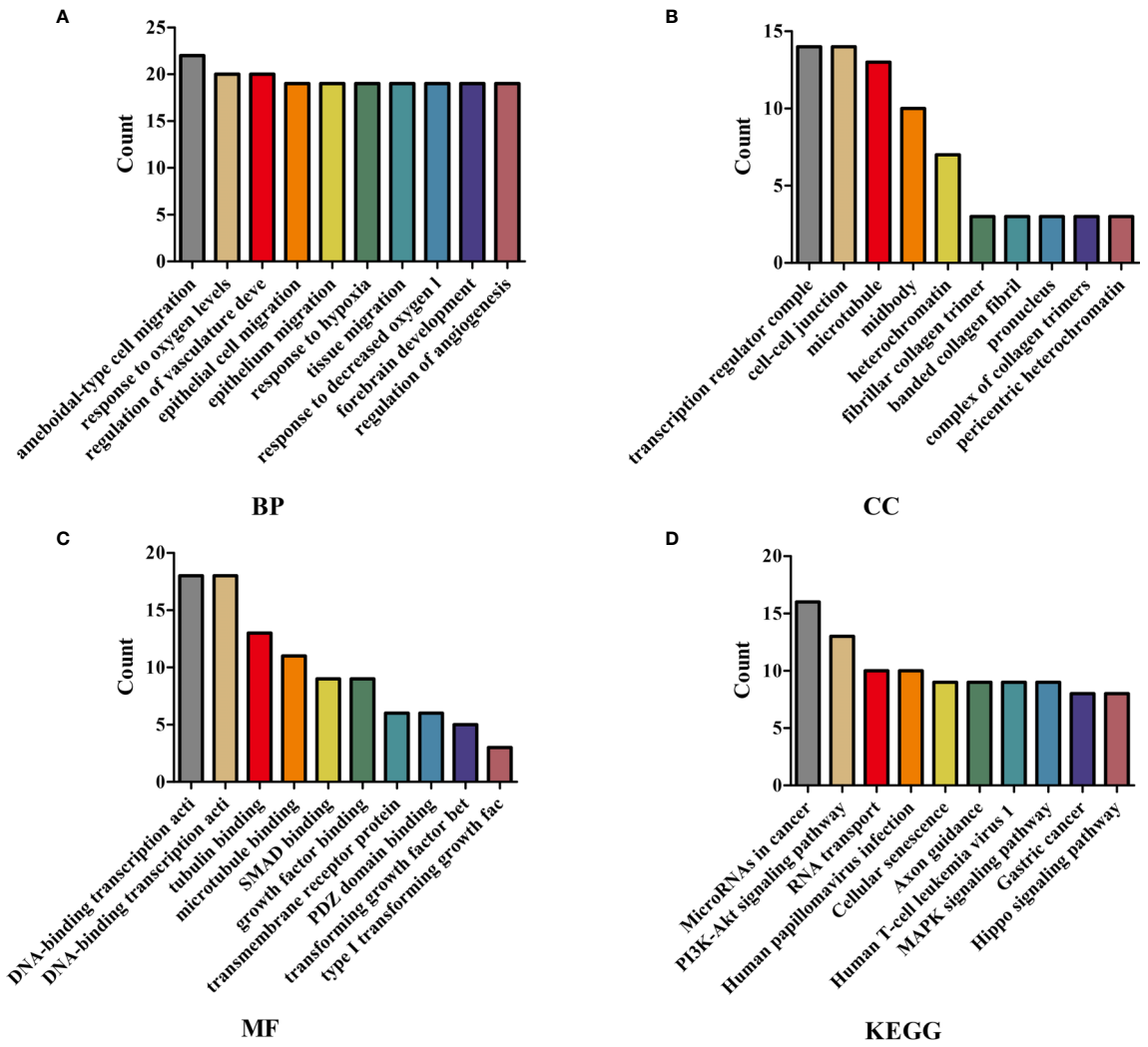

FIGURE 6 | GO and KEGG showed that the biological functions and signaling pathways involved in the ceRNA network mechanism. **(A)** BP; **(B)** CC; **(C)** MF; **(D)** KEGG. GO, Gene Ontology; KEGG, Kyoto Encyclopedia of Genes and Genomes; BP, Biological process; CC, Cellular components; MF, Molecular function.

carcinogen in the progression of NSCLC. As we all know, gefitinib and erlotinib were common anti-cancer drugs for lung cancer (26, 27), and Gefitinib and erlotinib could reduce the expression of carcinogenic LINC00973, which was expected to improve the prognosis of lung cancer patients. Therefore, LINC00973 might be a promising target for the development of new therapies for NSCLC.

lncRNAs could regulate the growth and migration behavior of cancer cells through a variety of mechanisms, including regulate expression of mRNA by ceRNA network, which could lead to its degradation (28, 29). For example, Cui et al. reported that the expression of lncRNA TRPM2-AS was significantly upregulated in NSCLC tissues and cells. Interfering with TRPM2-AS expression could inhibit cell proliferation, migration and invasion, and induce cell apoptosis. miR138-5p was the target downstream molecule of TRPM2-AS, and they showed a negative correlation. Interfering with TRPM2-AS expression could inhibit tumor formation, reduce the expression of EGFR and Ki67, and promote tumor cell apoptosis (28). At present, miR-374b-5p, miR-196a-5p, miR-138-5p, miR-150-5p, miR-196b-5p, miR-320a, miR-186-5p, etc. were related to the progress of NSCLC (30–38). For example, miR-138-5p could reduce the growth of NSCLC cells and increase the number of tumor-infiltrating dendritic cells (DCs). miR-138-5p down-regulates the expression of cyclin D3, CCD20, Ki67 and MCM in A549/3LL cells (37). The expression level of TSPAN12 was down-regulated in NSCLC tissues, and it was negatively correlated with the expression level of miR-196b-5p (35). However, LINC00973 was compatible with miR-374b-5p, miR-216b-5p, miR-196a-5p, miR-320c, miR-138-5p, miR-150-5p, miR-196b-5p, miR-224-5p. The relationship between miR-320a, miR-186-5p, miR-320b, miR-425-5p, miR-410-3p, miR-320d and miR-433-3p has not been reported yet, and we still need to conduct cell research to confirm.

TABLE 2 | KEGG showed that the signaling pathways involved in the ceRNA network mechanism.

ID	Description	Count	P value
hsa05206	MicroRNAs in cancer	16	1.13E-05
hsa03013	RNA transport	10	0.000399544
hsa04350	TGF-beta signaling pathway	7	0.00044901
hsa04218	Cellular senescence	9	0.000470354
hsa04360	Axon guidance	9	0.001362992
hsa05226	Gastric cancer	8	0.001552477
hsa04151	PI3K-Akt signaling pathway	13	0.002058027
hsa04390	Hippo signaling pathway	8	0.002161407
hsa04933	AGE-RAGE signaling pathway in diabetic complications	6	0.003489698
hsa05166	Human T-cell leukemia virus 1 infection	9	0.004929187
hsa04550	Signaling pathways regulating pluripotency of stem cells	7	0.005076892
hsa04015	Rap1 signaling pathway	8	0.012196648
hsa05215	Prostate cancer	5	0.014040933
hsa00533	Glycosaminoglycan biosynthesis - keratan sulfate	2	0.017456577
hsa04974	Protein digestion and absorption	5	0.017798661
hsa05211	Renal cell carcinoma	4	0.018587208
hsa05224	Breast cancer	6	0.02124233
hsa04216	Ferroptosis	3	0.022153401
hsa05202	Transcriptional misregulation in cancer	7	0.023095703
hsa05165	Human papillomavirus infection	10	0.023906377
hsa04934	Cushing syndrome	6	0.0267241
hsa01521	EGFR tyrosine kinase inhibitor resistance	4	0.028904446
hsa04010	MAPK signaling pathway	9	0.029244879
hsa05161	Hepatitis B	6	0.032232807
hsa04110	Cell cycle	5	0.035980455
hsa05225	Hepatocellular carcinoma	6	0.03750644
hsa04614	Renin-angiotensin system	2	0.044544163

KEGG, Kyoto Encyclopedia of Genes and Genomes.

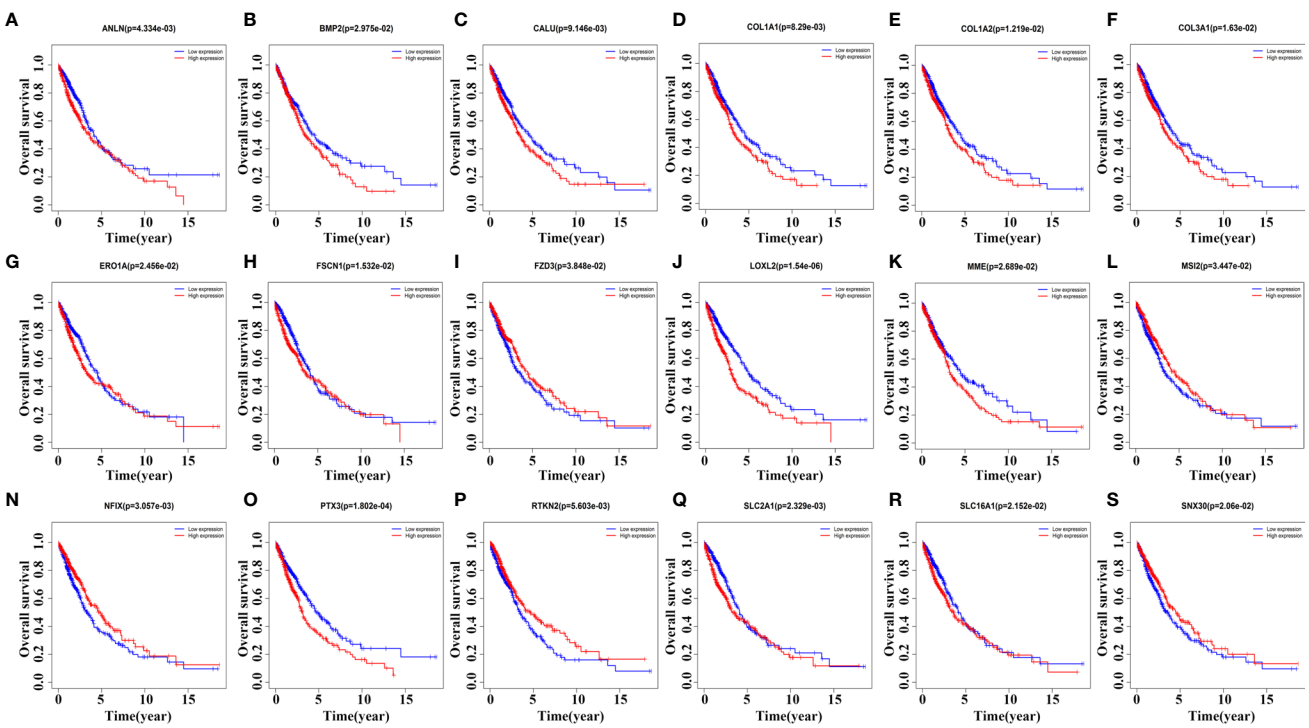

FIGURE 7 | Kaplan-Meier survival analysis screens prognostic factors in the ceRNA network. **(A)** ANLN; **(B)** BMP2; **(C)** CALU; **(D)** COL1A1; **(E)** COL1A2; **(F)** COL3A1; **(G)** ERO1A; **(H)** FSCN1; **(I)** FZD3; **(J)** LOXL2; **(K)** MME; **(L)** MSI2; **(N)** NFIX; **(O)** PTX3; **(P)** RTKN2; **(Q)** SLC2A1; **(R)** SLC16A1; **(S)** SNX30.

TABLE 3 | Univariate Cox regression analysis showed that the prognostic factors of NSCLC patients in ceRNA. network.

Gene	HR	HR.95L	HR.95H	P value
RTKN2	0.742284429	0.60197367	0.915299456	0.005305366
BMP2	1.288159834	1.044214828	1.589094231	0.018085515
ANLN	1.344766746	1.088990666	1.660618091	0.005923755
SLC2A1	1.389067051	1.124226954	1.716296931	0.002327596
COL1A2	1.281970754	1.040016495	1.580214374	0.019931627
CALU	1.301912007	1.055942536	1.60517719	0.013531776
MSI2	0.808993441	0.656396957	0.997064931	0.046864172
COL3A1	1.262426589	1.023801232	1.556670224	0.029256551
MME	1.253713201	1.017413308	1.544895058	0.033839712
SNX30	0.797756898	0.646015773	0.985140141	0.035812917
NFIX	0.74784094	0.606606233	0.921958993	0.006511941
PTX3	1.490910274	1.208082379	1.839951881	0.000198204
LOXL2	1.660877052	1.344818347	2.051215756	2.47E-06
SLC16A1	1.279724346	1.036424381	1.580138822	0.021876855
ERO1A	1.295617838	1.05112084	1.596986301	0.015214925
FZD3	0.81542587	0.661816109	1.004688976	0.055360497
FSCN1	1.285122696	1.04084388	1.586732051	0.019693861
COL1A1	1.309300819	1.061681099	1.614673781	0.011750581

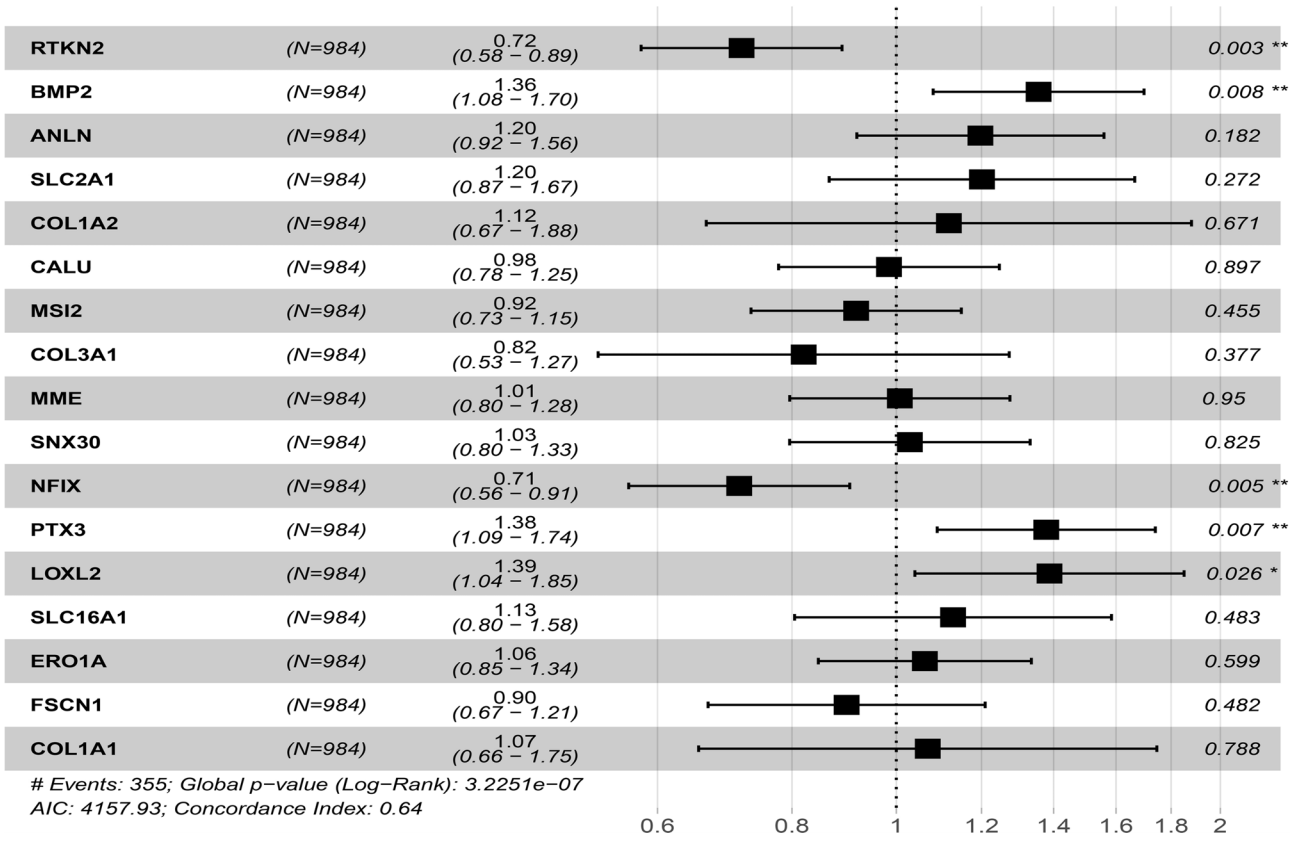

FIGURE 8 | Univariate and multivariate cox regression analysis showed that prognostic factors of NSCLC patients in ceRNA network. *P < 0.05; **P < 0.01.

RTKN2, NFIX, PTX3, BMP2 and LOXL2 of the ceRNA network play an important role in cancer progression (39–43). For instance, Ji et al. found that the expression level of RTKN2 in NSCLC tissues and cells was upregulated. Interfered with RTKN2 expression could induce NSCLC cell apoptosis and inhibit cell proliferation by increasing Bax levels and downregulating Bcl-2 levels. Interfered with RTKN2 expression could inhibit the migration and invasion of NSCLC cells by

TABLE 4 | The expression levels of RTKN2, NFIX, PTX3, BMP2 and LOXL2 were correlated with poor prognosis of NSCLC patients in the PrognoScan databases.

Gene	Dataset	Type	Endpoint	PROBE ID	N	COX P	HR [95% CI]
BMP2	GSE13213	LUAD	OS	A_23_P143331	117	2.69E-05	0.68 [0.57 - 0.81]
BMP2	GSE31210	LUAD	RFS	205290_s_at	204	0.0140761	0.67 [0.49 - 0.92]
BMP2	GSE31210	LUAD	RFS	205289_at	204	0.00186833	0.61 [0.45 - 0.83]
BMP2	GSE3141	NSCLC	OS	205289_at	111	0.0215927	1.34 [1.04 - 1.71]
NFIX	GSE13213	LUAD	OS	A_24_P858698	117	0.00181017	0.57 [0.40 - 0.81]
NFIX	GSE13213	LUAD	OS	A_23_P165295	117	0.0261232	0.71 [0.53 - 0.96]
NFIX	GSE31210	LUAD	RFS	209807_s_at	204	0.00254395	0.49 [0.31 - 0.78]
NFIX	GSE31210	LUAD	RFS	228278_at	204	0.000193836	0.51 [0.36 - 0.73]
NFIX	GSE31210	LUAD	OS	209807_s_at	204	0.00972759	0.45 [0.25 - 0.82]
NFIX	GSE31210	LUAD	OS	228278_at	204	0.0016013	0.48 [0.30 - 0.76]
NFIX	GSE8894	NSCLC	RFS	229834_at	138	0.040562	0.00 [0.00 - 0.59]
LOXL2	GSE31210	LUAD	OS	202998_s_at	204	0.0153133	1.78 [1.12 - 2.84]
LOXL2	GSE31210	LUAD	RFS	228808_s_at	204	0.044394	0.69 [0.48 - 0.99]
LOXL2	GSE31210	LUAD	RFS	202998_s_at	204	2.51E-05	2.12 [1.49 - 3.00]
LOXL2	GSE3141	NSCLC	OS	202998_s_at	111	0.00150164	1.95 [1.29 - 2.95]
LOXL2	GSE3141	NSCLC	OS	202997_s_at	111	0.0220928	1.41 [1.05 - 1.89]
LOXL2	GSE8894	NSCLC	RFS	202998_s_at	138	0.0103412	1.26 [1.06 - 1.49]
LOXL2	GSE8894	NSCLC	RFS	202997_s_at	138	0.000366017	2.21 [1.43 - 3.41]
PTX3	GSE31210	LUAD	OS	229760_at	204	0.0484883	0.76 [0.58 - 1.00]
PTX3	GSE31210	LUAD	RFS	229760_at	204	8.07E-05	0.67 [0.54 - 0.82]
PTX3	GSE31210	LUAD	RFS	229759_s_at	204	0.000904115	0.75 [0.63 - 0.89]
RTKN2	GSE31210	LUAD	RFS	230469_at	204	0.0162189	0.71 [0.54 - 0.94]
RTKN2	GSE3141	NSCLC	OS	230469_at	111	0.0421692	0.84 [0.70 - 0.99]

OS, Overall Survival; RFS, Relapse Free Survival; NSCLC, Non-small cell lung cancer; LUAD, lung adenocarcinoma; LUSC, lung squamous cell carcinoma.

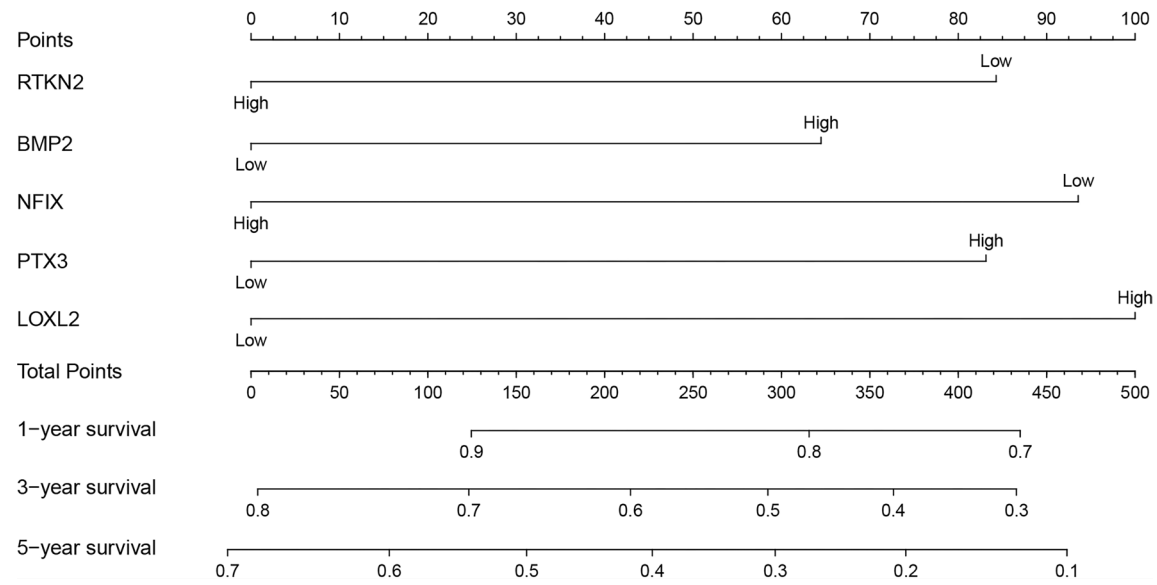

FIGURE 9 | Alignment to construct prognostic related models.

upregulating the expression of matrix metalloproteinase 9 (MMP9) and matrix metalloproteinase 2 (MMP2) (43). Huang et al. reported that elevated the levels of BMP2 were associated with short OS in NSCLC patients. BMP signaling was activated in the metastatic bone tumor of Lewis lung cancer in mice, and BMP2 signaling activation could enhance the bone metastasis of Lewis lung cancer, leading to poor prognosis. BMP2 secreted by mesenchymal fibroblasts could promote the migration and invasion of NSCLC cells (42). The expression of miR-504 in NSCLC tissues was significantly downregulated. The downregulation of miR-504 levels were positively correlated with lymph node metastasis and TNM stage. The overexpression of

miR-504 significantly inhibited the proliferation, invasion and EMT process of NSCLC cells. miR-504 could bind to the 3'UTR region of LOXL2 and regulate its expression. Overexpression of LOXL2 could rescue the miR-504-induced inhibition of NSCLC cell proliferation and invasion (41). In our study, Univariate and multivariate Cox analysis found that the target molecules RTKN2, NFIX, PTX3, BMP2 and LOXL2 in the ceRNA network were independent risk factors for poor prognosis of NSCLC patients. This further showed that they had an important biological role in the progression of NSCLC.

In our study, we found that the expression of LINC00973 in NSCLC tissues was increased, and that the increased expression levels of LINC00973 were associated with the poor prognosis of NSCLC patients, and constructed the LINC00973-miRNA-mRNA ceRNA network competition mechanism. Most of the miRNA and mRNA in the competitive ceRNA network have been confirmed to have important biological roles in the progression of NSCLC. There were few studies on LINC00973 in cancer, but we first formally formalize the expression of LINC00973 in NSCLC tissues, and explore the ceRNA network regulation mechanism of LINC00973 to provide new candidate markers for the treatment of NSCLC. Then, our research needs to be verified by *in vivo* and *in vitro* experiments to confirm the role and value of LINC00973-miRNA-mRNA ceRNA in the progression of NSCLC.

CONCLUSION

This study found that LINC00973-miRNA-mRNA ceRNA network might be the basis for determining important post-translational regulatory mechanisms in the progression of NSCLC. BMP2, LOXL2, NFIX, PTX3 and RTKN2 might be valuable prognostic markers and potential therapeutic targets in the progression of NSCLC.

DATA AVAILABILITY STATEMENT

The datasets presented in this study can be found in online repositories. The names of the repository/repositories and accession number(s) can be found in the article/**Supplementary Material**.

ETHICS STATEMENT

The studies involving human participants were reviewed and approved by Ethics committee of the Affiliated Taihe Hospital of Hubei University of Medicine. The patients/participants provided their written informed consent to participate in this study.

AUTHOR CONTRIBUTIONS

HL, TL, and XW conceived the research topic, made the research plan and directed the implementation of the whole research. QG drafted the manuscript together and processed the data. DL assisted to collect and analyze the data. XL and YY performed data checking and language polishing. All authors contributed to the article and approved the submitted version.

ACKNOWLEDGMENTS

We thank Home for Researchers editorial team (www.home-for-researchers.com) for language editing service.

SUPPLEMENTARY MATERIAL

The Supplementary Material for this article can be found online at: https://www.frontiersin.org/articles/10.3389/fimmu.2021.684807/full#supplementary-material

REFERENCES

1. Khan P, Siddiqui JA, Maurya SK, Lakshmanan I, Jain M, Ganti AK, et al. Epigenetic Landscape of Small Cell Lung Cancer: Small Image of a Giant Recalcitrant Disease. *Semin Cancer Biol* (2020). doi: 10.1016/j.semcancer.2020.11.006
2. Sung H, Ferlay J, Siegel RL, Laversanne M, Soerjomataram I, Jemal A, et al. Global Cancer Statistics 2020: GLOBOCAN Estimates of Incidence and Mortality Worldwide for 36 Cancers in 185 Countries. *CA Cancer J Clin* (2021) 71:209–49. doi: 10.3322/caac.21660
3. Woodman C, Vundu G, George A, Wilson CM. Applications and Strategies in Nanodiagnosis and Nanotherapy in Lung Cancer. *Semin Cancer Biol* (2021) 69:349–64. doi: 10.1016/j.semcancer.2020.02.009
4. Guo Q, Ke XX, Fang SX, Gao WL, Song YX, Chen C, et al. PAQR3 Inhibits Non-Small Cell Lung Cancer Growth by Regulating the NF-κb/P53/Bax Axis. *Front Cell Dev Biol* (2020) 8:581919. doi: 10.3389/fcell.2020.581919
5. Harrison PT, Vyse S, Huang PH. Rare Epidermal Growth Factor Receptor (EGFR) Mutations in Non-Small Cell Lung Cancer. *Semin Cancer Biol* (2020) 61:167–79. doi: 10.1016/j.semcancer.2019.09.015
6. Yang J, Qiu Q, Qian X, Yi J, Jiao Y, Yu M, et al. Long Noncoding RNA LCAT1 Functions as a ceRNA to Regulate RAC1 Function by Sponging miR-4715-5p in Lung Cancer. *Mol Cancer* (2019) 18:171. doi: 10.1186/s12943-019-1107-y
7. Liu H, Han L, Liu Z, Gao N. Long Noncoding RNA MNX1-AS1 Contributes to Lung Cancer Progression Through the miR-527/BRF2 Pathway. *J Cell Physiol* (2019) 234:13843–50. doi: 10.1002/jcp.28064
8. Yin D, Lu X, Su J, He X, De W, Yang J, et al. Long Noncoding RNA AFAP1-AS1 Predicts a Poor Prognosis and Regulates Non-Small Cell Lung Cancer Cell Proliferation by Epigenetically Repressing P21 Expression. *Mol Cancer* (2018) 17:92. doi: 10.1186/s12943-018-0836-7
9. McCabe EM, Rasmussen TP. lncRNA Involvement in Cancer Stem Cell Function and Epithelial-Mesenchymal Transitions. *Semin Cancer Biol* (2020). doi: 10.1016/j.semcancer.2020.12.012
10. Ferragut Cardoso AP, Banerjee M, Nail AN, Lykoudi A, States JC. miRNA Dysregulation Is an Emerging Modulator of Genomic Instability. *Semin Cancer Biol* (2021). doi: 10.1016/j.semcancer.2021.05.004
11. Fabian MR, Sonenberg N, Filipowicz W. Regulation of mRNA Translation and Stability by microRNAs. *Annu Rev Biochem* (2010) 79:351–79. doi: 10.1146/annurev-biochem-060308-103103
12. Jin X, Guan Y, Zhang Z, Wang H. Microarray Data Analysis on Gene and miRNA Expression to Identify Biomarkers in Non-Small Cell Lung Cancer. *BMC Cancer* (2020) 20:329. doi: 10.1186/s12885-020-06829-x
13. Yu H, Cheng Y, Li W, Li Z, Wu P, Qiu S, et al. A Novel lncRNA-miRNA-mRNA Competitive Endogenous RNA Network for Uveal Melanoma

Prognosis Constructed by Weighted Gene Co-Expression Network Analysis. *Life Sci* (2020) 260:118409. doi: 10.1016/j.lfs.2020.118409
14. Majed SO, Mustafa SA. MACE-Seq-Based Coding RNA and TrueQuant-Based Small RNA Profile in Breast Cancer: Tumor-Suppressive miRNA-1275 Identified as a Novel Marker. *BMC Cancer* (2021) 21:473. doi: 10.1186/s12885-021-08218-4
15. Smillie CL, Sirey T, Ponting CP. Complexities of Post-Transcriptional Regulation and the Modeling of ceRNA Crosstalk. *Crit Rev Biochem Mol Biol* (2018) 53:231–45. doi: 10.1080/10409238.2018.1447542
16. Cheng Y, Su Y, Wang S, Liu Y, Jin L, Wan Q, et al. Identification of circRNA-lncRNA-miRNA-mRNA Competitive Endogenous RNA Network as Novel Prognostic Markers for Acute Myeloid Leukemia. *Genes (Basel)* (2020) 11:8. doi: 10.3390/genes11080868
17. Hou W, Zhang Y. Circ_0025033 Promotes the Progression of Ovarian Cancer by Activating the Expression of LSM4 *via* Targeting miR-184. *Pathol Res Pract* (2021) 217:153275. doi: 10.1016/j.prp.2020.153275
18. Karpov DS, Spirin PV, Zheltukhin AO, Tutyaeva VV, Zinovieva OL, Grineva EN, et al. LINC00973 Induces Proliferation Arrest of Drug-Treated Cancer Cells by Preventing P21 Degradation. *Int J Mol Sci* (2020) 21:21. doi: 10.3390/ijms21218322
19. Liu Y, Li X, Zhang C, Zhang H, Huang Y. LINC00973 Is Involved in Cancer Immune Suppression Through Positive Regulation of Siglec-15 in Clear-Cell Renal Cell Carcinoma. *Cancer Sci* (2020) 111:3693–704. doi: 10.1111/cas.14611
20. Chen Z, Chen Q, Cheng Z, Gu J, Feng W, Lei T, et al. Long Non-Coding RNA CASC9 Promotes Gefitinib Resistance in NSCLC by Epigenetic Repression of DUSP1. *Cell Death Dis* (2020) 11:858. doi: 10.1038/s41419-020-03047-y
21. Li C, Zhao W, Pan X, Li X, Yan F, Liu S, et al. LncRNA KTN1-AS1 Promotes the Progression of Non-Small Cell Lung Cancer *via* Sponging of miR-130a-5p and Activation of PDPK1. *Oncogene* (2020) 39:6157–71. doi: 10.1038/s41388-020-01427-4
22. Zhu Y, Li J, Bo H, He D, Xiao M, Xiang L, et al. LINC00467 Is Up-Regulated by TDG-Mediated Acetylation in Non-Small Cell Lung Cancer and Promotes Tumor Progression. *Oncogene* (2020) 39:6071–84. doi: 10.1038/s41388-020-01421-w
23. Xue L, Li J, Lin Y, Liu D, Yang Q, Jian J, et al. M(6) A Transferase METTL3-Induced lncRNA ABHD11-AS1 Promotes the Warburg Effect of Non-Small-Cell Lung Cancer. *J Cell Physiol* (2021) 236:2649–58. doi: 10.1002/jcp.30023
24. Zinovieva OL, Grineva EN, Prokofjeva MM, Karpov DS, Zheltukhin AO, Krasnov GS, et al. Expression of Long Non-Coding RNA LINC00973 Is Consistently Increased Upon Treatment of Colon Cancer Cells With Different Chemotherapeutic Drugs. *Biochimie* (2018) 151:67–72. doi: 10.1016/j.biochi.2018.05.021
25. Jing C, Ma R, Cao H, Wang Z, Liu S, Chen D, et al. Long Noncoding RNA and mRNA Profiling in Cetuximab-Resistant Colorectal Cancer Cells by RNA Sequencing Analysis. *Cancer Med* (2019) 8:1641–51. doi: 10.1002/cam4.2004
26. Thomas P, Vincent B, George C, Joshua JM, Pavithran K, Vijayan M. A Comparative Study on Erlotinib & Gefitinib Therapy in Non-Small Cell Lung Carcinoma Patients. *Indian J Med Res* (2019) 150:67–72. doi: 10.4103/ijmr.IJMR_1896_17
27. Zhang Y, Fu F, Hu H, Wang S, Li Y, Hu H, et al. Gefitinib as Neoadjuvant Therapy for Resectable Stage II-IIIA Non-Small Cell Lung Cancer: A Phase II Study. *J Thorac Cardiovasc Surg* (2021) 161:434–442.e2. doi: 10.1016/j.jtcvs.2020.02.131
28. Cui D, Feng Y, Shi K, Zhang H, Qian R. Long Non-Coding RNA TRPM2-AS Sponges microRNA-138-5p to Activate Epidermal Growth Factor Receptor and PI3K/AKT Signaling in Non-Small Cell Lung Cancer. *Ann Transl Med* (2020) 8:1313. doi: 10.21037/atm-20-6331
29. Ren XY, Han YD, Lin Q. Long Non-Coding RNA MIR155HG Knockdown Suppresses Cell Proliferation, Migration and Invasion in NSCLC by Upregulating TP53INP1 Directly Targeted by miR-155-3p and miR-155-5p. *Eur Rev Med Pharmacol Sci* (2020) 24:4822–35. doi: 10.26355/eurrev_202005_21171
30. Wang J, Shi C, Wang J, Cao L, Zhong L, Wang D. MicroRNA-320a Is Downregulated in Non-Small Cell Lung Cancer and Suppresses Tumor Cell Growth and Invasion by Directly Targeting Insulin-Like Growth Factor 1 Receptor. *Oncol Lett* (2017) 13:3247–52. doi: 10.3892/ol.2017.5863
31. Bao M, Pan S, Yang W, Chen S, Shan Y, Shi H. Serum miR-10a-5p and miR-196a-5p as Non-Invasive Biomarkers in Non-Small Cell Lung Cancer. *Int J Clin Exp Pathol* (2018) 11(2):773–80.
32. Zhao W, Sun Q, Yu Z, Mao S, Jin Y, Li J, et al. MiR-320a-3p/ELF3 Axis Regulates Cell Metastasis and Invasion in Non-Small Cell Lung Cancer *via* PI3K/Akt Pathway. *Gene* (2018) 670:31–7. doi: 10.1016/j.gene.2018.05.100
33. Zeng Z, Zhao G, Rao C, Hua G, Yang M, Miao X, et al. Knockdown of lncRNA ZFAS1-Suppressed Non-Small Cell Lung Cancer Progression *via* Targeting the miR-150-5p/HMGA2 Signaling. *J Cell Biochem* (2019). doi: 10.1002/jcb.29542
34. Li J, Zhang X, Tang J, Gong C. MicroRNA-374b-5p Functions as a Tumor Suppressor in Non-Small Cell Lung Cancer by Targeting FOXP1 and Predicts Prognosis of Cancer Patients. *Oncol Targets Ther* (2020) 13:4229–37. doi: 10.2147/ott.S243221
35. Liang G, Meng W, Huang X, Zhu W, Yin C, Wang C, et al. miR-196b-5p-Mediated Downregulation of TSPAN12 and GATA6 Promotes Tumor Progression in Non-Small Cell Lung Cancer. *Proc Natl Acad Sci USA* (2020) 117:4347–57. doi: 10.1073/pnas.1917531117
36. Liu X, Zhou X, Chen Y, Huang Y, He J, Luo H. miR-186-5p Targeting SIX1 Inhibits Cisplatin Resistance in Non-Small-Cell Lung Cancer Cells (NSCLCs). *Neoplasma* (2020) 67:147–57. doi: 10.4149/neo_2019_190511N420
37. Song N, Li P, Song P, Li Y, Zhou S, Su Q, et al. MicroRNA-138-5p Suppresses Non-Small Cell Lung Cancer Cells by Targeting PD-L1/PD-1 to Regulate Tumor Microenvironment. *Front Cell Dev Biol* (2020) 8:540. doi: 10.3389/fcell.2020.00540
38. Wu Z, Li W, Li J, Zhang Y, Zhang X, Xu Y, et al. Higher Expression of miR-150-5p Promotes Tumorigenesis by Suppressing LKB1 in Non-Small Cell Lung Cancer. *Pathol Res Pract* (2020) 216:153145. doi: 10.1016/j.prp.2020.153145
39. Zhan P, Shen XK, Qian Q, Zhu JP, Zhang Y, Xie HY, et al. Down-Regulation of Lysyl Oxidase-Like 2 (LOXL2) Is Associated With Disease Progression in Lung Adenocarcinomas. *Med Oncol* (2012) 29:648–55. doi: 10.1007/s12032-011-9959-z
40. Infante M, Allavena P, Garlanda C, Nebuloni M, Morenghi E, Rahal D, et al. Prognostic and Diagnostic Potential of Local and Circulating Levels of Pentraxin 3 in Lung Cancer Patients. *Int J Cancer* (2016) 138:983–91. doi: 10.1002/ijc.29822
41. Ye MF, Zhang JG, Guo TX, Pan XJ. MiR-504 Inhibits Cell Proliferation and Invasion by Targeting LOXL2 in Non Small Cell Lung Cancer. *BioMed Pharmacother* (2018) 97:1289–95. doi: 10.1016/j.biopha.2017.11.005
42. Huang F, Cao Y, Wu G, Chen J, Lin W, Lan R, et al. BMP2 Signalling Activation Enhances Bone Metastases of Non-Small Cell Lung Cancer. *J Cell Mol Med* (2020) 24:10768–84. doi: 10.1111/jcmm.15702
43. Ji L, Huang Y, Zhang Y, Peng A, Qin J, Lu S, et al. RTKN2 Is Associated With Unfavorable Prognosis and Promotes Progression in Non-Small-Cell Lung Cancer. *Oncol Targets Ther* (2020) 13:10729–38. doi: 10.2147/ott.S260436

Conflict of Interest: The authors declare that the research was conducted in the absence of any commercial or financial relationships that could be construed as a potential conflict of interest.

Publisher's Note: All claims expressed in this article are solely those of the authors and do not necessarily represent those of their affiliated organizations, or those of the publisher, the editors and the reviewers. Any product that may be evaluated in this article, or claim that may be made by its manufacturer, is not guaranteed or endorsed by the publisher.

Copyright © 2021 Guo, Li, Luo, Yuan, Li, Liu and Wang. This is an open-access article distributed under the terms of the Creative Commons Attribution License (CC BY). The use, distribution or reproduction in other forums is permitted, provided the original author(s) and the copyright owner(s) are credited and that the original publication in this journal is cited, in accordance with accepted academic practice. No use, distribution or reproduction is permitted which does not comply with these terms.

frontiers in Immunology

REVIEW
published: 10 August 2021
doi: 10.3389/fimmu.2021.705999

Targeted Immunotherapies in Gastrointestinal Cancer: From Molecular Mechanisms to Implications

*Ding-Kang Wang†, Qian Zuo†, Qing-Yu He and Bin Li**

Ministry of Education (MOE), Key Laboratory of Tumor Molecular Biology and Key Laboratory of Functional Protein Research of Guangdong Higher Education Institutes, Institute of Life and Health Engineering, Jinan University, Guangzhou, China

OPEN ACCESS

Edited by:
Hubing Shi,
Sichuan University, China

Reviewed by:
Chu Lin,
Peking University People's Hospital, China
Navin Chintala,
Memorial Sloan Kettering Cancer Center, United States
Reem Saleh,
Peter MacCallum Cancer Centre, Australia

***Correspondence:**
Bin Li
libinjnu@163.com

†These authors have contributed equally to this work and share first authorship

Specialty section:
This article was submitted to Cancer Immunity and Immunotherapy, a section of the journal Frontiers in Immunology

Received: *06 May 2021*
Accepted: *26 July 2021*
Published: *10 August 2021*

Citation:
Wang D-K, Zuo Q, He Q-Y and Li B (2021) Targeted Immunotherapies in Gastrointestinal Cancer: From Molecular Mechanisms to Implications. Front. Immunol. 12:705999. doi: 10.3389/fimmu.2021.705999

Gastrointestinal cancer is a leading cause of cancer-related mortality and remains a major challenge for cancer treatment. Despite the combined administration of modern surgical techniques and chemoradiotherapy (CRT), the overall 5-year survival rate of gastrointestinal cancer patients in advanced stage disease is less than 15%, due to rapid disease progression, metastasis, and CRT resistance. A better understanding of the mechanisms underlying cancer progression and optimized treatment strategies for gastrointestinal cancer are urgently needed. With increasing evidence highlighting the protective role of immune responses in cancer initiation and progression, immunotherapy has become a hot research topic in the integrative management of gastrointestinal cancer. Here, an overview of the molecular understanding of colorectal cancer, esophageal cancer and gastric cancer is provided. Subsequently, recently developed immunotherapy strategies, including immune checkpoint inhibitors, chimeric antigen receptor T cell therapies, tumor vaccines and therapies targeting other immune cells, have been described. Finally, the underlying mechanisms, fundamental research and clinical trials of each agent are discussed. Overall, this review summarizes recent advances and future directions for immunotherapy for patients with gastrointestinal malignancies.

Keywords: gastrointestinal cancer, colorectal cancer, gastric cancer, esophageal cancer, immune checkpoint inhibitor, immunotherapy

INTRODUCTION

Gastrointestinal (GI) cancers are among the top 10 most prevalent and deadliest tumors worldwide, accounting for 26% of global cancer incidence and 35% of all cancer-related deaths (1). To date, surgical resection remains the primary treatment option for patients with colorectal cancer (CRC), gastric cancer (GC) and esophageal cancer (EC). Despite advances in adjuvant and neoadjuvant chemoradiotherapy (CRT), a fair number of patients still develop distant metastases and therapy resistance (2). To improve the prognosis of GI cancers, new therapeutic strategies are urgently needed. Over the last few decades, immune-targeted therapy has emerged as a revolutionary option for cancer treatment (3); however, the regulatory role of the immune system underlying GI cancers remains to be clarified. Fortunately, with the development of immunotherapy, cancer

immunotherapy mainly based on checkpoint inhibitors has shown great prospects in clinical research, which shows the importance of immunotherapy in cancer treatment.

In this review, we first provide an overview of GI in terms of the epidemiology, molecular pathogenesis and standard therapy regimens. In subsequent sections, we outline the functional and molecular basis of oncoimmunology, with an emphasis on novel immune checkpoint targets and examples of applications in both laboratory research and clinical trials. We hope that this review will bring new insight into cancer immunotherapy for oncologists and immunologists.

GASTROINTESTINAL CANCERS: A GENERAL OVERVIEW

Esophageal and Gastric Cancer

The esophagus and stomach are part of the upper GI tract, which is part of the digestive system. As two major types of EC, esophageal squamous cell carcinoma (ESCC) occurs more commonly in the upper or middle part of the esophagus, while esophageal adenocarcinoma (SCC) occurs in the lower part of the esophagus. GC can develop in any part of the stomach and can spread throughout the stomach and to other organs, such as the small intestines, lymph nodes, liver, pancreas and colon (4). EC and GC are listed as the seventh and fourth most prevalent cancers worldwide (5). Based on estimates from 2018, 36.4% of digestive cancers, including stomach, liver and esophageal cancers, in China have a very poor prognosis, and the 5-year overall survival (OS) rate is quite low (less than 35% from 2013 to 2015) (6).

In general, surgery plays a key role in the treatment of GC as well as EC at an early stage. Moreover, systemic therapy of advanced, metastatic esophageal and gastric cancer utilizes a combination of multiple cytotoxic chemotherapeutic agents. Combination chemotherapy with a platinum and fluoropyrimidine doublet, such as FOLFOX, CAPOX, cisplatin/5-fluorouracil (5-FU), or cisplatin/capecitabine, is a common regimen with the addition of trastuzumab for the treatment of HER2-positive disease (5, 7, 8). Other agents, such as irinotecan or taxanes, can be utilized with fluoropyrimidines, platinum and/or ramicurumab or applied as monotherapy for those unfit for combination regimens (9, 10).

Colorectal Cancer

In recent decades, the incidence rate of CRC has shown an upward trend worldwide, especially in developing countries. In China, CRC has an incidence rate exceeding 14.2/100,000, a mortality rate exceeding 7.4/100,000 and a 5-year prevalence exceeding 52/100,000. In addition, the prevalence rate of CRC is obviously higher in senior citizens aged over 60 (11). Currently, traditional therapies for CRC include endoscopic and surgical local excision, downstaging preoperative radiotherapy and systemic therapy, extensive surgery for locoregional and metastatic disease, local ablative therapies for metastases, palliative chemotherapy, targeted therapy, and immunotherapy. Although these new treatment options have doubled the OS for advanced disease to 3 years, the best survival rates still occur in patients without metastasis.

THE RATIONALE FOR IMMUNOTHERAPY IN GASTROINTESTINAL CANCER

The immune system exists within the body, and the execution of immune function is performed by the entire immune system. The immune system consists of immune organs, immune cells and immune molecules. These cell types surrounding cancer cells, including fibroblasts, endothelial cells, immune cells, and extracellular molecules, which include cytokines, hormones, cellular matrix, and growth factors, constitute the tumor microenvironment (TME) (12). According to relevant reports, some immune components in the TME can regulate the occurrence and development of tumors, and these components constitute the tumor immune microenvironment (TIME), which is expected to become a promising target for cancer immunotherapy (13–15) (**Figure 1**).

Components of the TME

Tumor Cells

Although many improvements in molecularly directed therapies have been achieved, the prognosis of GI cancers remains poor (12). Breakthroughs in the immune checkpoint blockade offer potential therapeutic avenues, particularly with tools to overcome the mechanisms of immunosuppression in the TME. Currently, extensive publications highlight critical roles of the TIME in GI cancers, including CRC and GC (16, 17). As an important determinant of tumor progression and outcome in GI cancers, the TIME can shape cancer cell phenotypes and therapy responses through interplay with cancerous cells *via* chemokine and cytokine signaling or direct contact (18–20). Several reports have revealed that tumor progression and metastasis are subjected to not only genetic alterations within tumor cells but also the TIME elements. In brief, CD4+ T helper cells, CD8+ CTLs, NK cells, M1 macrophages, and DCs have been shown to be associated with a good prognosis (21). Conversely, CD4+ FOXP3+ Th2 cells, M2 macrophages, and myeloid-derived suppressor cells (MDSCs) have been attributed to a poor outcome (18).

Immune Cells

Tumor-infiltrating lymphocytes (TILs) are immune cells that have migrated to tumor tissue and the local microenvironment. This population is indicative of an immune response generated by the patient against the malignancy. TIL populations across GI tumors generally contain T lymphocytes, particularly CD8+ cytotoxic T lymphocytes (CTLs) (12). In EC cells, blocking the programmed cell death 1 (PD-1)/programmed cell death ligand 1 (PD-L1) and TGF-β signaling pathways can synergistically restore the function of antigen-specific CD8+ T cells and the capacity of antitumor T cells (22). In addition, functional

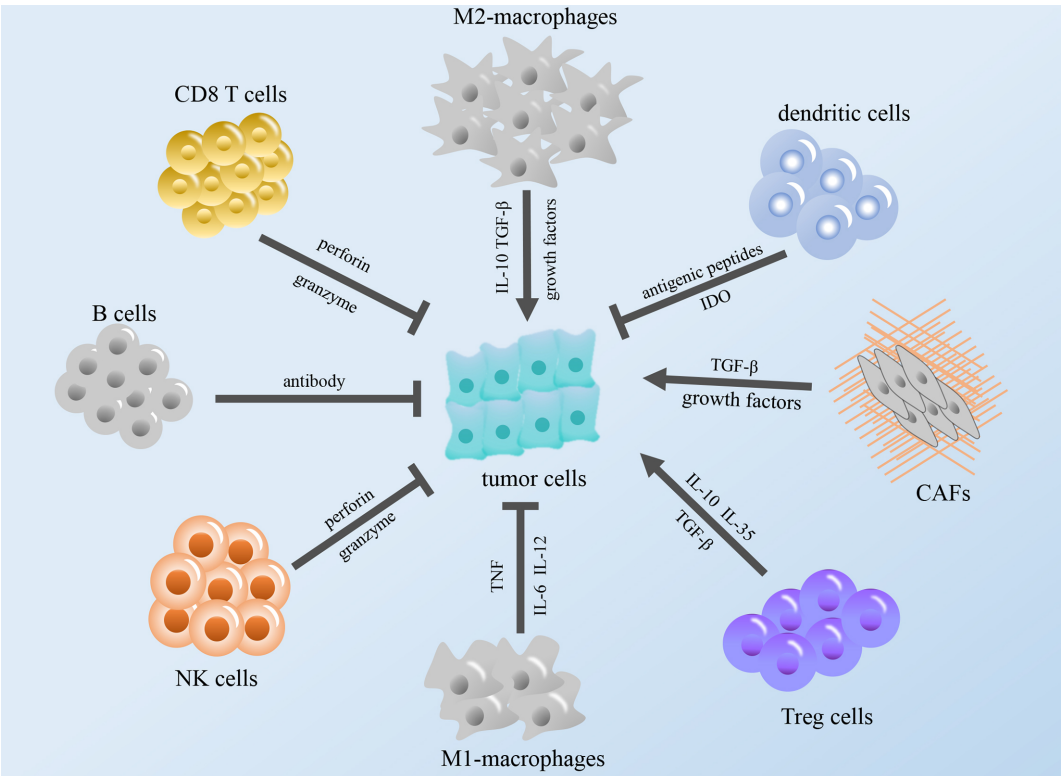

FIGURE 1 | Modulation of the tumor immune microenvironment. The figure shows that immune cells in TME regulate tumor growth through cytokines and other regulatory factors. TGF-β, transforming growth factor β; IL, interleukin; NK cells, natural killer cells; TNF, tumor necrosis factor; IDO, indoleamine 2,3-dioxygenase; CAFs, cancer-associated fibroblasts; Treg cells, regulatory T cells.

MAGE-A3-specific CD8+ T cells have an independent prognostic effect on the survival of patients with ESCC (22). Recent studies have demonstrated that higher numbers of CD3+, CD8+, or CD45RO+ T cells in tumor tissue are significantly correlated with a superior disease outcome in patients with GC, and an imbalance in Th1 and Th2 cells can lead to an immunosuppressive state dominated by Th2-type cells (23). The Th1/Th2 cell ratio in peripheral blood in GC can be used to predict postoperative prognosis (24). Similarly, the type, density, and location of immune cells in CRC also have prognostic value that is superior to and independent of those of the tumor node metastasis (TNM) classification (25). In addition to T cells, there are many other immune cell types that infiltrate GI cancers.

Tregs, as a subtype of CD4+ T cells, can inhibit effector T cells *via* a series of chemokine signaling (26). FOXP3+ Tregs, a subtype of Tregs, their roles are ambiguous. Some studies have shown that a high density of FOXP3+ Tregs is beneficial to the prognosis of CRC after undergoing chemo or chemoimmunotherapy (27). On the other hand, it has been shown that Tregs in the esophageal mucosa and peripheral blood of patients with esophageal cancer increase significantly (28).

DCs, on the one hand, express MHC Class II and can present their antigenic peptides to CD4+ T cells. They activate effector T cells to attack tumors and play a crucial role in shaping the host response to cancerous cells. GC patients with good DC infiltration had lower lymph node metastases and lymphatic invasion and better 5-year survival rates (78%) than patients with less DC infiltration (29). On the other hand, activated DCs help in the expansion of Tregs, consequently leading to regulation of immune responses and thereby tumor immune escape (30). Meanwhile, DCs also stimulate the formation of M2 macrophages, thereby increasing the secretion of IL-10 and TGF-β (31), which reduces the expression of IL-12 expressed by DCs and inhibits the activation of adaptive responses (32).

Tissue-resident macrophages are present prior to the development of any malignancy (33, 34). Tumor-associated macrophages (TAMs) can differentiate into two distinct subtypes, M1 and M2. M1 macrophages secrete IL-6 and IL-12 to mitigate resistance during tumor development; they can also be activated by IFN-γ to secrete TNF to kill cancer cells, while M2 macrophages secrete growth factors that promote neoangiogenesis and tumor proliferation (35). In various types of cancers, increased numbers of TAMs are often related to a poor prognosis. However, the roles of TAMs in CRC remain controversial. According to some reports, on the one hand, a high density of TAMs predicts a better postoperative outcome (36), and on the other hand, TAMs also secrete cytokines that

favor tumor development (37), which indicates that the impact of TAMs on CRC needs to be further explored. Additionally, in accordance with some studies, TGF-β and other growth factors secreted by cancer-associated fibroblasts (CAFs) promoted the proliferation of CRC cells through the Smad2/Smad4 pathway (38) and MAPK/PI3K/AKT pathway (39).

Neutrophils are similar to TAMs in classification. Neutrophils differentiate into N1 and N2 according to their polarization state. N1 has antitumor activity, which directly kill tumor cells by releasing reactive oxygen species (ROS) and reactive nitrogen species (RNS) (40, 41) and can also recruit M1 macrophages and promote T cell activation. In contrast, N2 has tumor-promoting activity, promoting angiogenesis and inhibiting the function of NK cells by releasing matrix metalloproteinase 9 (MMP9) (42). In addition, N2 recruits M2 macrophages and Treg cells and suppresses the function of CD8+ T cells, as well as other native neutrophils (43). Neutrophil extracellular traps (NETs) activate Toll-like receptor 9 on CRC cells through the MAPK pathway, which leads to the growth, migration and invasion of CRC cells (44).

B lymphocytes play an important role in tumor immunity and cancer biology. However, several studies have revealed that B lymphocytes can take part in carcinogenesis and tumor progression by producing antibodies to facilitate chronic inflammation in the TIME (45, 46). Moreover, regulatory B cells can also restrain antitumor responses mediated by T cells in cancer (47). Regulatory B cells (Breg cells), a novel subset of B lymphocytes, appear to facilitate tumor growth and progression *via* the production of IL-10 to suppress the activity of CD8+ T cells in squamous carcinoma (48). In CRC, the presence of B cells seems to be detrimental to prognostic outcome (49).

NK cells are unique in that they have both innate and adaptive immune properties. NK cells participate in the antitumor immune response through the production of proinflammatory cytokines, which recruit and induce the proliferation of other immune cells (12). Activated NK cells can directly kill some tumor cells and virus-infected cells. In EC, expanded NK cells had high cytotoxicity against ESCC cells, especially those with the epithelial-mesenchymal transition phenotype (50). In another investigation, a higher NK cell density was shown to be significantly related to a higher survival rate in GC, especially for advanced patients (51).

Cytokines/Chemokines

Cytokines are important players in the tumor microenvironment, and cytokines/chemokines are used to establish connections between various immune cells, such as IL-6 (52), IL-10 (53), IL-12 (54), IL-35 (55), epidermal growth factor (EGF), vascular endothelial growth factor (VEGF), tumor necrosis factor alpha (TNF-α) (56), interferon γ (IFN-γ) (57), indoleamine-2,3-dioxygenase (IDO) (58), and transforming growth factor beta (TGF-β) (59). For example, IL-10 and TGF-β switch macrophages from a M1-like (proinflammatory or classically activated) state to a M2-like (anti-inflammatory or alternatively activated) state. M1 macrophages induce antitumor immune signaling and correlate with tumor killing capacity. Conversely, M2 macrophages exhibit protumor effects and contribute to fibrosis and the production of matrix proteins (60) as well as angiogenesis, metastasis, and the suppression of adaptive immunity (61, 62). Human CRC cell lines cultured *in vitro* are able to polarize macrophages toward the M2 phenotype (63). In GC patient samples, M2 macrophages in the stroma may be correlated with the presence of a lesion (64). The CCL2-CCR2 axis in esophageal carcinogenesis contributes to immune evasion and tumor promotion through the PD-1 signaling pathway (65). At the same time, the activity of NK cells and effector T cells was suppressed due to the increased secretion of cytokines such as IL-10, TGF-β, EGF and VEGF (50).

Cells in the Extracellular Matrix (ECM)

Unlike strictly defined immune cells, fibroblasts are present within the stromal microenvironment and serve to produce extracellular matrix (ECM) proteins in particular collagen. They actively manufacture and respond to cytokines in cooperation with immune cells within the stromal microenvironment. Fibroblasts are also associated with epithelial cell polarity, proliferation, and, to some extent, tumorigenic potential. CAFs have been shown to drive increased tumor growth compared to normal fibroblasts (66). They contribute to cancer cell survival and progression *via* a series of nutrient-rich ECM proteins or ECM-degrading proteases, resulting in persistent chronic inflammation within the tumor microenvironment and enhanced epithelial mesenchymal transition (EMT) of tumor cells (67, 68).

Recent studies have demonstrated that CAFs have the capacity to produce proinflammatory cytokines, which disrupt the normal cytokine balance to stimulate tumor growth by initiating angiogenesis and inhibiting CTLs (69, 70). Additionally, CAFs have been shown to secrete high levels of the proinflammatory cytokines IL-1β, IL-8, IL-10, tumor necrosis factor-alpha (TNF-α), monocyte chemoattractant protein-1 (CCL2), stromal derived factor-1 (CXCL12) and interferon-beta (IFN-β) (71). The crucial role of CAFs in tumorigenesis has been addressed by genetic analyses showing that their gene expression profiles are very different from those of normal breast fibroblasts. Moreover, the expression profiles of CAFs obtained from tumors with poor versus good prognosis are also very different (72). Good-outcome fibroblasts were associated with immune modulators involved in the Th1 immune response. This includes the expression of T cell receptor complexes (CD8a, CD247, and CD3D), MHC class I protein binding and granzyme A/B activity. The poor-outcome stroma had increased levels of hypoxia and angiogenesis and decreased chemokines that stimulate NK migration and T cell survival (73).

Mechanisms of Tumor Immune Escape

One role of the immune system in mediating tumorigenesis is called "cancer immune editing", and it can be classified into 3 stages: elimination, stalemate, and escape. The elimination stage includes innate and adaptive immune responses to specific tumor-related antigens and is characterized by the effector functions of T cells, B cells and NK cells mediated by cytokines, including IFN-α, IFN-γ and IL-12. The stalemate stage of immune killing is mediated by the adaptive immune system and the persistence of a small number of

malignant clones. The escape stage involves malignant clones gaining the ability to evade surveillance carried out by the adaptive immune system.

The understanding of the mechanisms of tumor immune escape changes with each passing day, and the established mechanisms are as follows. First, there can be a lack of a specific antigen or an alteration in antigen processing. In a study of SCC cell lines and tumor tissues, levels of MIR125a-5p and MIR148a-3p were found to be increased, reducing levels of ATP binding cassette subfamily B member 3 (TAP2) and MHC I, both of which are required for antigen presentation (74). Tumor cells lack the expression of major MHC I molecules or lose the intracellular processing mechanism, enabling the transfer of tumor antigens to the surface of tumor cells for T cells to recognize (75). The high expression of MHC I molecules in SCC is related to markers of the adaptive immune response and significantly decreased OS time in patients (74). Second, tumors can promote the formation of an immune-tolerant microenvironment by affecting the levels of cytokines, such as by increasing the secretion of IL-6, IL-10 and TGF-β or by consuming IL-2. The changes in these cytokines in EC cells promote the infiltration of Treg cells, MDSCs and other types of cells, thus suppressing the function of cytotoxic T cells (76). Third, tumors can upregulate the expression of PD-1 and PD-L1 to induce peripheral T cell depletion (77). Finally, many oncogenic cell signaling pathways were originally thought to be used only to accelerate cell division and growth, but they are now thought to be factors mediating immune escape. For example, constitutively activated KIT signaling in GI tumors can lead to overexpression of indoleamine-2,3-dioxygenase (IDO), thus increasing Treg cell infiltration and promoting tumor growth; furthermore, melanoma cells activated by β-catenin/Wnt signaling can inhibit DC-mediated antigen presentation and prevent CD8+ T cell infiltration (78).

IMMUNOTHERAPEUTIC STRATEGIES IN GASTROINTESTINAL CANCER: THE CURRENT SCENARIO AND FUTURE PERSPECTIVES

Immunotherapy refers to the activation of the body's immune system to fight against tumor cells. It manipulates the immune system to target cancer antigens or break the barriers of T cell infiltration. Immunotherapy methods mainly include cytokines, immune checkpoint inhibitors, CAR T cell treatments, tumor vaccines, and treatments involving other immune cells in the TME.

Activating the Immune Response - Cytokines

Several cytokines impede cancer cell growth *via* direct antiproliferative or proapoptotic actions or by indirectly enhancing the cytotoxic effect of immune responses against cancer cells. For example, autocrine IL-10 activity on CD8+ T lymphocytes has been shown to be crucial for prolonging the effector activity of cytotoxic CD8+ T cells (79, 80). This concept has been evaluated in a phase I clinical trial in advanced treatment-refractory tumors (NCT02009449) using IL-10 conjugated with PEG to increase its half-life. The administration of PEGylated cytokines (termed pegilodecakin) resulted in partial responses in patients with uveal melanoma, renal cell carcinoma (RCC) and CRC (81). In addition, CCR5 is the receptor for both CCL3 and CCL5, while CCR2 binds to CCL2. In patients with metastatic CRC, CCR2/CCR5 inhibitors, coupled with either chemotherapy or nivolumab, suppressed myeloid cell recruitment by blocking the activity of these chemokines (82). Another paradigmatic case is IFN-α, first discovered in 1957, which induces antitumor efficacy by directly augmenting NK cell-mediated killing and acting on T and B lymphocytes to modulate their activity and/or survival.

Immune Checkpoint Inhibitors

Immune checkpoints play key roles in the innate immune system by ensuring that immune cells are capable of distinguishing self-antigens from exogenous antigens. In the TME, tumors often display self-antigens and escape immune surveillance. By blocking the interaction between immune cells and tumor cells expressing immune checkpoint molecules, checkpoint inhibitors allow the immune system to recognize tumor-associated antigens and consequently destroy malignant cells. As shown in **Figure 2**, when CTLA-4 and LAG-3 are bound by their corresponding monoclonal antibodies, T cells become activated and differentiate and proliferate; TIM-3 and PD-1 on T cells and PD-L1 on tumor cells are bound by their corresponding antibodies, which prevents T cell death, inhibits tumor cell evasion and promotes tumor cell apoptosis (**Figure 2**).

CTLA-4

As the first inhibitory receptor identified, CTLA-4 is mainly located on activated T lymphocytes and is also highly expressed in several types of cancer (83). There is a competitive interaction between CD28 and CTLA-4 in binding with CD80/CD86 molecules. CTLA-4 transmits an inhibitory signal to T cells, whereas CD28 transmits a stimulatory signal. A recent study revealed that the combined consideration of CTLA-4 expression and the platelet-lymphocyte ratio (PLR) has potential prognostic value for people suffering from ESCC (84). Therefore, it is not surprising that CTLA-4-targeted agents have shown great potential in the treatment of many cancers. In clinical trials, the tumor response rates of two anti-CTLA-4 agents, ipilimumab and tremelimumab, were approximately 10% (85). A large phase II clinical study explored the efficacy and safety of nivolumab (± ipilimumab) in the treatment of advanced CRC. The results revealed that most patients with microsatellite instability-high (MSI-H) metastatic CRC (mCRC) benefited from the nivolumab + ipilimumab regimen, and the regimen was well tolerated, but whether the combination therapy is superior to either drug as monotherapy therapy is still uncertain (86).

PD-1 and PD-L1/L2

PD-1 is one of the crucial immune checkpoint receptor proteins on T cells, B cells and NK cells and can bind to PD-L1 and/or PD-L2, which are located on the surface of multifarious tumor cells as well as hematopoietic cells. The combination of PD-1 and PD-L1/L2 expressed on tumor cells can dramatically inhibit the apoptosis of tumor cells, promoting the depletion of peripheral effector T cells and catalyzing the transformation of effector T cells into Treg cells (87).

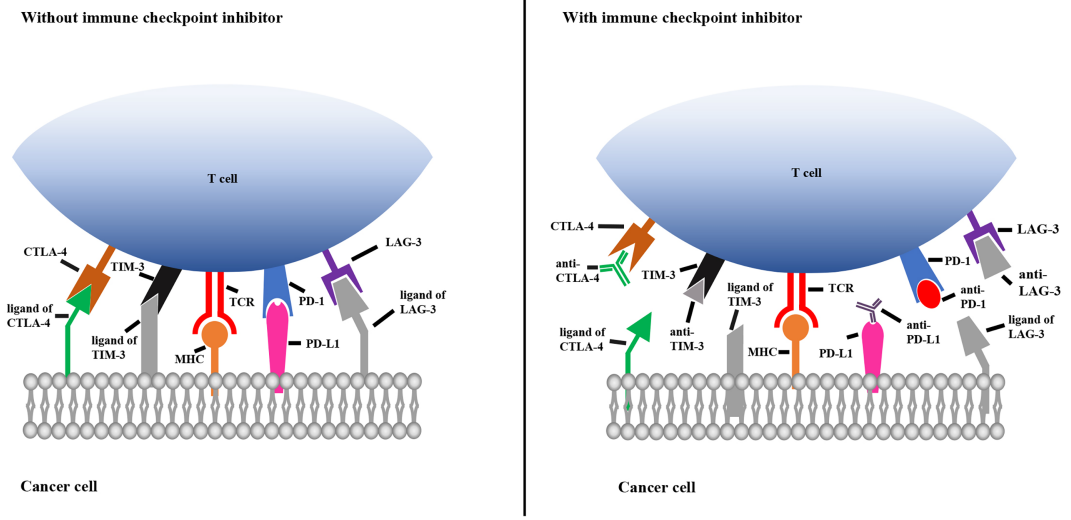

FIGURE 2 | Mechanisms of immune checkpoint inhibitors. The left picture shows that the immune checkpoint molecules on T cells combine with the corresponding ligands on cancer cells, resulting in immunosuppression of T cell. The right picture shows that immune checkpoint molecules bind to the corresponding antibody to prevent T cell death. TCR, T cell receptor; MHC, major histocompatibility complex; TIM-3, T cell immunoglobulin 3; CTLA-4, cytotoxic T-lymphocyte-associated protein 4; PD-1, programmed cell death 1; PD-L1, programmed cell death ligand 1; LAG-3, lymphocyte activation gene 3.

In 2017, the US Food and Drug Administration (FDA) approved pembrolizumab for the treatment of unresectable or metastatic MSI-H or mismatch repair deficient (dMMR) CRC that progressed following treatment with fluoropyrimidine, oxaliplatin, and irinotecan. This approval was based on results from the phase II CheckMate-142 trial (88), in which the objective response rate (ORR) was 28% in mCRC patients who received prior fluoropyrimidine, oxaliplatin, and irinotecan; in the trial, 1 patient had a complete response (CR), and 14 patients had partial responses (PRs). Furthermore, the expression of PD-L1 in cancer cells and the TME may contribute to the development of EBV-associated GC, and PD-L1 overexpression predicts large tumor size, lymph node metastasis, and poor prognosis in GC (89). A recent study presented at the American Society of Clinical Oncology (ASCO) meeting revealed that an anti-PD-1 monoclonal antibody could significantly prolong the OS of PD-L1-positive patients with advanced EC regardless of whether it was used alone or in combination with chemotherapy; furthermore, the antibody was highly safe (90, 91).

TIM-3

TIM-3 is a cell surface molecule expressed on DCs, monocytes, CD8 T cells and Th1 cells. The ligands of TIM-3 are frequently overexpressed in tumor cells. TIM-3 is a negative regulator of the antitumor immune response and has been proven to be associated with the occurrence and development of several malignant tumors. At both the mRNA and protein levels, the expression of TIM-3 in ESCC is remarkably higher than that in matched adjacent normal tissues; furthermore, researchers have found a close connection between the overexpression of TIM−3 and poor survival in patients with ESCC. Similarly, TIM-3 knockdown significantly inhibited the propagation, migration and invasion of ESCC cell lines. Further research explored whether the depletion of TIM-3 could restrain several signal transduction pathways, including the snail, p-GSK-3β and p-AKT pathways (92). In addition, some studies have suggested that the increased expression of TIM-3 on T cells may be partially responsible for the development of GC by inducing the secretion of IFN-γ and TNF-α (93). Another study has shown that reduced TIM-3 expression induced by genetic polymorphisms of TIM-3 may promote CRC invasion and metastasis (94). Taken together, these findings show that TIM-3 is a critical mediator in the progression of various cancers and may serve as a potential therapeutic target.

LAG-3

LAG-3 is another membrane protein expressed on B cells, some T cells, NK cells and TILs. LAG-3 can enhance the activation of Treg cells and prevent T cells from proliferating and differentiating into effector cells by binding with MHC II. In addition, some basic research has shown that dual blockade of LAG-3 and PD-1 can induce strong antitumor action (95). Furthermore, high expression of LAG-3 is associated with an improved survival rate in patients with ESCC or CRC and is being evaluated as a biomarker to predict response to antitumor treatment. These results indicate that LAG-3 can be used as a marker of the immune response for patients with ESCC or CRC (96, 97).

SIRPα

Signal regulatory protein-α (SIRPα) acts as an inhibitory receptor and is expressed on myeloid cells such as macrophages, DCs, mast cells and neutrophils. It interacts with the broadly expressed

transmembrane protein CD47, also called the "don't eat me" signal. In addition, the interaction between CD47 and SIRPα can help tumor cells avoid phagocytosis in the TME (98). The biological and preclinical relevance of the interaction of SIRPα and CD47 has been extensively investigated. A recent study showed that blocking SIRPα/CD47 signaling in ESCC cell lines could enhance the phagocytosis of ESCC cells in a dose-dependent manner (99). In addition, with the evolution of cancer immunotherapy, SIRPα/CD47 immunotherapy to stimulate the innate immune system as a cancer treatment has drawn increasing interest. Other reports have confirmed that the high expression of CD47 is an independent prognostic factor in GC, and the OS rate of patients with CD47-positive tumors was significantly lower than that of patients with CD47-negative tumors (100). Aberrant expression of CD47 has also been reported to strongly promote the proliferation of tumor cells (101).

CAR T Cell Treatments

Chimeric antigen receptor (CAR) T cell therapy includes T cell modifications that enable activated T cells to recognize specific tumor cell surface antigens independent of MHC and eventually eliminate malignant cells (102). After many years of medical and laboratory research as well as specific clinical trials, in 2017, the US FDA approved the use of two CAR T cell therapies (103, 104). In recent years, some laboratories have attempted to exploit EphA2. CAR T cells recognizing EphA2 have demonstrated the capacity to identify and attack ESCC cells *in vitro*. These findings open a new avenue for future immunotherapies for ESCC (105). Coincidentally, CAR T cell therapy has been widely used in the treatment of other GI cancers and liver cancers. The HER2 gene plays an important role in the occurrence and development of GC, which highly expresses the protein p185; p185 shows negative expression in healthy individuals, and thus, it could be used as an ideal target for antitumor therapy with CAR T cells (106). Carcinoembryonic antigen (CEA), a sensitive tumor biomarker, was found to be a potent target for CAR T cell therapy for GI cancers (106). Therefore, a great deal of research has been carried out on the treatment of different cancers, such as liver cancer, cholangiocarcinoma and pancreatic cancer. Combined treatment integrating CAR T cell therapy with targeted therapies, such as therapies targeting CEA, HER2, GPC3, MUC1, CD133, EpCAM or EGFR, has exhibited great potential (107–110).

Targeted Therapy Mediating Immune Cells

NK Cells

NK cells are innate lymphocytes and play a pivotal role in host immunity by killing virally infected and/or cancerous cells. Several clinical studies have suggested NK cell-based immunotherapy as a potential therapy for cancer. Inhibitory receptors, such as killer-cell immunoglobulin-like receptors (KIRs) and CD94/NK group 2 member A (NKG2A), recognize human leukocyte antigen (HLA) class I molecules on normal host cells. By lacking inhibitory receptor ligands, tumor cells that have downregulated surface MHC-I expression become susceptible to attack by NK cells. Current NK cell-based cancer immunotherapy aims to reverse tumor-induced NK cell dysfunction and sustain NK cell effector functions (111). To fight against tumors, NK cells can also be modulated to target the cell types responsible for maintaining the immunosuppressive TME, including M2-polarized macrophages, MDSCs, Treg cells, and fibroblasts (112). According to recent reports, adoptive cell therapy (ACT) has become a powerful tool to improve host antitumor activity (113), mainly including autologous NK cell transfer, allogeneic NK cell transfer and CAR-engineered NK cells (114). The three methods all artificially activate and expand NK cells *in vitro* and then transfer the modified NK cells to patients. Under the stimulation of some cytokines and costimulators, the antitumor ability of NK cells has been significantly improved (113, 115), and NK cells are expected to achieve staged success in the course of immunotherapy.

NKT Cells

Natural killer T cells (NKTs) are unique T lymphocytes that have the characteristics of conventional T cells and natural killer cells (116). They play an important role in connecting the natural immune system with the adaptive immune system and are also an important intermediary for mediating the immune response and tumor monitoring (117). It is usually composed of two parts, namely, the invariant TCRα chain and the semivariant TCRβ chain, recognizing the lipid antigen presented by the nonclassical MHC class I molecule CD1d (118). More importantly, the activation of CD1d-dependent invariant natural killer T cells (iNKT cells) can promote the release of cytokines such as IL-5, IL-6, IL-10, IL-17, IL-21, TNF-α, TGF-β and granulocyte-macrophage colony stimulating factor (GM-CSF) (116, 119, 120) and indirectly activate the antitumor mechanism. At present, several cancer immunotherapies based on iNKT cells have been developed, mainly including antigen-presenting cells (APCs) pulsed with α-GalCer, the transfer of *ex vivo*–expanded and/or activated iNKT cells, and iNKT cell–activating ligands (117). First, a clinical experimental study has not indicated any major toxicity or severe side effects in patients who have received repeated injection of the tumor immunity agonist α-GalCer (121), implying its clinical value in improving tumor immunity. In addition, patients with head and neck squamous cell carcinoma, who were treated with the combination of iNKT cells and α-GalCer-pulsed DCs, the antitumor immunity was greatly improved (122, 123)

Macrophages

Tumor-infiltrating immune cells play an ambiguous role in tumor development and progression. It has been extensively reported that TAMs promote or inhibit the expansion and dissemination of cancer cells depending on their functional states. Tumor-infiltrating macrophages are mainly recruited by CCL2 or CSF-1, and TAM depletion therapy (e.g., CCR2 or CSF1R antagonists) has already been tested in clinical trials for malignant solid tumors (124, 125). Some studies have also shown that CSF1R inhibitors represent a promising combination partner for T cell-enhancing immunotherapies (126, 127). Further investigation of the synergistic effects of these agents with immunotherapies will lead to the improvement of ongoing immunotherapeutic strategies. At the same time, some cancer immunotherapies targeting TAMs are on

the rise, and most of them follow the principle of directly reducing the formation of TAMs or polarizing TAMs from the pro-tumor phenotype (M2-like), which helps tumor development to an antitumor phenotype (M1-like) (128). By preventing the recruitment of TAMs or blocking the CSF1/CSF1R axis, the survival rate of TAMs can be significantly reduced (129, 130), as mentioned above. In addition, some studies have shown that the polarization of TAMs to M1 macrophages can be promoted by targeting antibody-dependent cellular phagocytosis (ADCP) induced by the SIRPα/CD47 axis, thus enhancing the tumor immune response (131). Finally, a possible strategy for cancer treatment is the use of natural living macrophages as drug delivery vehicles (128).

γδT Cells

As a subtype of T lymphocytes, γδT cells have a wide range of antigen recognition abilities and can be used to recognize a series of antigens, including mitochondrial ATPase, human mutS homolog 2 and nonpeptide phosphoantigens (132–134), without using traditional APC to mediate antigen recognition (135, 136). The mechanism of antigen recognition depends on its peptide sequence. Since the sequence of complementarity determining region 3 (CDR3) of the delta chain is longer and more varied, it is more important in the process of antigen recognition (137). In addition to expressing NK cell receptors such as NGG2D, it may be a bridge between the innate immune system and adaptive immunity (138). According to related reports, under certain conditions, γδT lymphocytes may be activated in the late stage of the immune response (139, 140), which shows cytotoxicity by secreting perforin and granzyme and can also regulate the secretion of IFN-γ and TNF-α (141). Conversely, some cytokines may drive γδT lymphocytes to remodel tumor-immunosuppressive functions; thus, there is an urgent need to optimize γδT lymphocytes to obtain new antitumor targets (142). A recent study demonstrated for the first time that CAR-γδT cells obtained by modification using CAR technology are able to migrate to tumor cells and cross-express antigens (143), which opens a new avenue for cancer immunotherapy research.

IDO1

IDO1 is the rate-limiting enzyme that participates in tryptophan metabolism by converting the amino acid L-tryptophan (Trp) into L-kynurenine (Kyn). This enzyme assists tumor cells in maximally utilizing essential amino acids such as tryptophan in the TME to support tumor growth. However, as immune cells lose tryptophan, they lose their ability to fight cancer cells. Overexpression of IDO1 in tumor cells inhibits T cell function and impairs immune surveillance, leading to immune escape (144). In addition, it has been verified that the expression of IDO1 is associated with prognosis in EC and could be used as a prognostic biomarker (145). In a multivariate analysis, IDO1 expression was proven to be an independent prognostic factor for developing recurrence (146). Chen et al. reported that the enzyme activity of IDO1 directly affected the radiosensitivity of CRC, and IDO1 inhibition made CRC cells more sensitive to radiation-induced cell death and protected the normal small intestinal epithelium from radiation toxicity, indicating that IDO1 inhibition enhances the radiotherapy effect in CRC (147). According to relevant studies, IDO1 can also cooperate with COL12A1 to promote GC metastasis. This new discovery suggests that IDO1 and COL12A1 may be promising targets for anticancer therapy in GC (148).

Tumor Vaccines

Tumor vaccines are a therapeutic method that can help educate the immune system to recognize cancer-related antigens and achieve antitumor effects. Tumor vaccines mainly include whole-cell vaccines, molecular vaccines and DC vaccines. DCs are one of the most effective APCs found in humans thus far. In addition, DC vaccines have achieved ideal results in clinical trials of malignant melanoma and prostate cancer (149). Due to the lack of MHC molecules and costimulatory molecules located on the surface of tumor cells, T lymphocyte immunity cannot be activated. Therefore, the immune response triggered by tumor vaccines mainly depends on the primary processing and further presentation of antigens by APCs, which is a key step in the development of effective adaptive immunity. As a new treatment strategy, immunotherapy based on tumor vaccines has received increasing attention in the treatment of advanced EC and other GI cancers (124, 150).

CLINICAL APPLICATION OF IMMUNOTHERAPIES IN GASTROINTESTINAL CANCERS

Colorectal Cancer

Immunotherapies have been studied extensively in CRC due to a better understanding of CRC subsets (particularly MSI/MMR status) and how they respond to immune modulation. Initial work on checkpoint inhibitors in CRC showed limited success. Neither the CTLA-4 inhibitor tremelimumab nor the PD-1 inhibitor nivolumab showed an objective response in CRC patients (151, 152). The Check-Mate-142 trial (phase II) evaluated single-agent nivolumab and nivolumab plus ipilimumab in patients with metastatic CRC with either MSI-H/dMMR or MSS/pMMR status. This study first investigated whether MSI-H tumors may be more responsive to immune checkpoint inhibitor therapy (88). Subsequent studies investigated targeting both CTLA-4 and PD-1 with ipilimumab/nivolumab in the pretreated population. The results were encouraging in that the ORR was 55%, the disease control rate for ≥ 12 weeks was 80%, and the progression-free survival (PFS) rates were 76 and 71% (9 and 12 months, respectively) (153). In the KEYNOTE-164 phase II trial, pembrolizumab monotherapy achieved an ORR of 28% and an excellent 1-year OS rate of 72% in heavily pretreated patients with MSI-H mCRC (154) responses to immune checkpoint inhibitors (155, 156).

Various regimens have been implemented to enhance immunogenicity in MSS/pMMR mCRC. The combination of atezolizumab and the MEK inhibitor conbimetinib showed limited effectiveness in CRC patients at advanced stages compared to regorafenib (157). A combination of FOLFOX

TABLE 1 | Landmark trials of immunotherapy in GI.

Name of trial	Title	Interventions	Phases
Colorectal Cancer			
KEYNOTE 028	Nivolumab in patients with metastatic DNA mismatch repair-deficient or microsatellite instability-high colorectal cancer	Drug: Pembrolizumab	Phase 2
CheckMate 142	Nivolumab + ipilimumab combination in patients with DNA mismatch repair-deficient/microsatellite instability-high metastatic colorectal cancer	Drug: Nivolumab	Phase 2
CheckMate 142 (further analysis of subgroup)	Mismatch repair deficiency predicts response of solid tumors to PD-1 blockade	Drug: Nivolumab+ Ipilumumab	Phase 2
Gastroesophageal Cancer			
ATTRACTION-2 CheckMate-032 KEYNOTE-012 KEYNOTE-059	A study of nivolumab by itself or nivolumab combined with ipilimumab in patients with advanced or metastatic solid tumors	Drug: Nivolumab	Phase 1-2
	A study of pembrolizumab in participants with recurrent or metastatic gastric or gastroesophageal junction adenocarcinoma	Drug: Pembrolizumab	Phase 2
NCT01585987	An efficacy study in gastric and gastroesophageal junction cancer comparing ipilimumab versus standard of care immediately following first line chemotherapy	Drug: Ipilimumab	Phase 2
NCT01693562	A phase I dose-escalation and cohort expansion study of lirilumab (anti-KIR; BMS-986015) administered in combination with nivolumab (anti-PD-1; BMS-936558; ONO-4538) in patients (Pts) with advanced refractory solid tumors.	Drug: MEDI4736	Phase 1-2

and PD-1/PD-L1 inhibitors achieved an ORR of up to 50% and increased PFS (from 14 to 16 months) (158, 159). Preliminary data from the AVETUX trial demonstrated that a combination of FOLFOX, cetuximab, and the PD-L1 antibody avelumab showed a 75% ORR in patients with treatment-naïve microsatellite stable (MSS) mCRC (160). In contrast, the combination of atezolizumab (anti-PD-L1) with maintenance therapy with fluoropyrimidines and bevacizumab failed to improve the PFS of mCRC patients (161). In conclusion, all mCRCs should be tested for their microsatellite status. In MSI-H/dMMR CRC, checkpoint inhibitors should be used after therapy with fluoropyrimidine, oxaliplatin, and irinotecan. Currently, the value of checkpoint inhibitors in MSS CRC is still unclear.

Gastroesophageal Cancer

Compared to CRC, the application of immunotherapy has been limited in gastroesophageal cancer due to tumor heterogeneity and complex immunosuppressive mechanisms. Checkpoint inhibition therapy showed some success in early trials, which is likely to be related to a specific phenotype of GC and its histopathology (162).

According to the outcomes of the KEYNOTE-059 trial, pembrolizumab has been approved by the FDA for the management of refractory GC. In addition, a series of KEYNOTE trials have been conducted in EC, including KEYNOTE-180, KEYNOTE-181, and KEYNOTE-590 (90, 163, 164). Nivolumab, based on the outcomes of ATTRACTION-2, was also approved in heavily pretreated tumors in Japan (165). Checkmate-032 confirmed that the combination of ipilimumab with nivolumab was superior to nivolumab monotherapy (166, 167). ATTRACTION-3 compared nivolumab to chemotherapy in refractory OC and demonstrated significant improvement in survival (median OS 10.9 months *vs.* 8.4 months; hazard ratio for death 0.77, p = 0.019) (168). Understanding the role of immunotherapy in GC has been improved with a shift in the classification of tumors, and four genomic subtypes of GC have been identified. Similar to CRC, the MSI-H population in GC has shown an encouraging response, as indicated by a subset analysis of trials (169). The EBV subtype is even more promising (170), with all patients of this subtype responding to pembrolizumab immunotherapy in a phase II trial (171). Meanwhile, there are still ongoing trials to evaluate the efficacy of different available immunotherapy agents, such as KEYNOTE-062 and KEYNOTE-061 (**Table 1**).

CONCLUDING REMARKS

In summary, this review systematically describes immunological aspects of GI cancer and discusses the latest progress in cancer immunotherapy. Although immune-targeted therapy has gradually become the mainstream strategy for cancer treatment, side effects, drug resistance and a low response rate still represent challenges for researchers and clinicians. In addition, because immunotherapy may not benefit all the cancer types, there are some patient populations who cannot receive immunotherapy. Based on the above, we should strive to improve the understanding of tumor immunology, and the curative effect should be emphasized in further research. Over the next few decades, we expect to see the advent of more effective immunotherapy, the development of predictive biomarkers or more personalized treatment to help patients who are less likely to respond to current treatments to improve the treatment effect.

AUTHOR CONTRIBUTIONS

D-KW and QZ drafted the manuscript. BL and Q-YH were involved in design of the study and revision of the manuscript. All authors contributed to the article and approved the submitted version.

FUNDING

This work was supported by National Natural Science Foundation of China (81973339, 31961160727, 81773085, 31770888) and the National Key Research and Development Program of China (2017YFA0505100).

REFERENCES

1. Arnold M, Abnet CC, Neale RE, Vignat J, Giovannucci EL, McGlynn KA, et al. Global Burden of 5 Major Types of Gastrointestinal Cancer. *Gastroenterology* (2020) 159:335–49.e315. doi: 10.1053/j.gastro.2020.02.068
2. Smyth EC, Moehler M. Late-Line Treatment in Metastatic Gastric Cancer: Today and Tomorrow. *Ther Adv Med Oncol* (2019) 11:1758835919867522. doi: 10.1177/1758835919867522
3. Daskivich TJ, Belldegrun A. Words of Wisdom. Re: Safety, Activity, and Immune Correlates of Anti-PD-1 Antibody in Cancer. *Eur Urol* (2015) 67:816–7. doi: 10.1016/j.eururo.2014.12.052
4. Pourhoseingholi MA, Vahedi M, Baghestani AR. Burden of Gastrointestinal Cancer in Asia; An Overview. *Gastroenterol Hepatol Bed Bench* (2015) 8:19–27. doi: 10.22037/ghfbb.v1i1.608
5. Lorenzen S, Schuster T, Porschen R, Al-Batran SE, Hofheinz R, Thuss-Patience P, et al. Cetuximab Plus Cisplatin-5-Fluorouracil Versus Cisplatin-5-Fluorouracil Alone in First-Line Metastatic Squamous Cell Carcinoma of the Esophagus: A Randomized Phase II Study of the Arbeitsgemeinschaft Internistische Onkologie. *Ann Oncol* (2009) 20:1667–73. doi: 10.1093/annonc/mdp069
6. Zeng H, Chen W, Zheng R, Zhang S, Ji JS, Zou X, et al. Changing Cancer Survival in China During 2003-15: A Pooled Analysis of 17 Population-Based Cancer Registries. *Lancet Glob Health* (2018) 6:e555–67. doi: 10.1016/S2214-109X(18)30127-X
7. Bang YJ, Van Cutsem E, Feyereislova A, Chung HC, Shen L, Sawaki A, et al. Trastuzumab in Combination With Chemotherapy Versus Chemotherapy Alone for Treatment of HER2-Positive Advanced Gastric or Gastro-Oesophageal Junction Cancer (ToGA): A Phase 3, Open-Label, Randomised Controlled Trial. *Lancet* (2010) 376:687–97. doi: 10.1016/S0140-6736(10)61121-X
8. Al-Batran SE, Hartmann JT, Probst S, Schmalenberg H, Hollerbach S, Hofheinz R, et al. Phase III Trial in Metastatic Gastroesophageal Adenocarcinoma With Fluorouracil, Leucovorin Plus Either Oxaliplatin or Cisplatin: A Study of the Arbeitsgemeinschaft Internistische Onkologie. *J Clin Oncol* (2008) 26:1435–42. doi: 10.1200/JCO.2007.13.9378
9. Albertsson M, Johansson B, Friesland S, Kadar L, Letocha H, Frykholm G, et al. Phase II Studies on Docetaxel Alone Every Third Week, or Weekly in Combination With Gemcitabine in Patients With Primary Locally Advanced, Metastatic, or Recurrent Esophageal Cancer. *Med Oncol* (2007) 24:407–12. doi: 10.1007/s12032-007-0028-6
10. Bouche O, Raoul JL, Bonnetain F, Giovannini M, Etienne PL, Lledo G, et al. Randomized Multicenter Phase II Trial of a Biweekly Regimen of Fluorouracil and Leucovorin (LV5FU2), LV5FU2 Plus Cisplatin, or LV5FU2 Plus Irinotecan in Patients With Previously Untreated Metastatic Gastric Cancer: A Federation Francophone De Cancerologie Digestive Group Study–FFCD 9803. *J Clin Oncol* (2004) 22:4319–28. doi: 10.1200/JCO.2004.01.140
11. Zhu J, Tan Z, Hollis-Hansen K, Zhang Y, Yu C, Li Y. Epidemiological Trends in Colorectal Cancer in China: An Ecological Study. *Dig Dis Sci* (2017) 62:235–43. doi: 10.1007/s10620-016-4362-4
12. Zhang Y, Xu J, Zhang N, Chen M, Wang H, Zhu D. Targeting the Tumour Immune Microenvironment for Cancer Therapy in Human Gastrointestinal Malignancies. *Cancer Lett* (2019) 458:123–35. doi: 10.1016/j.canlet.2019.05.017
13. Grizzi F, Basso G, Borroni EM, Cavalleri T, Bianchi P, Stifter S, et al. Evolving Notions on Immune Response in Colorectal Cancer and Their Implications for Biomarker Development. *Inflamm Res* (2018) 67:375–89. doi: 10.1007/s00011-017-1128-1
14. Sanmamed MF, Chen L. A Paradigm Shift in Cancer Immunotherapy: From Enhancement to Normalization. *Cell* (2018) 175:313–26. doi: 10.1016/j.cell.2018.09.035
15. Forde PM, Chaft JE, Smith KN, Anagnostou V, Cottrell TR, Hellmann MD, et al. Neoadjuvant PD-1 Blockade in Resectable Lung Cancer. *N Engl J Med* (2018) 378:1976–86. doi: 10.1056/NEJMoa1716078
16. Roelands J, Kuppen PJK, Vermeulen L, Maccalli C, Decock J, Wang E, et al. Immunogenomic Classification of Colorectal Cancer and Therapeutic Implications. *Int J Mol Sci* (2017) 18:2229. doi: 10.3390/ijms18102229
17. Yang L, Wang Y, Wang H. Use of Immunotherapy in the Treatment of Gastric Cancer. *Oncol Lett* (2019) 18:5681–90. doi: 10.3892/ol.2019.10935
18. Elinav E, Nowarski R, Thaiss CA, Hu B, Jin C, Flavell RA. Inflammation-Induced Cancer: Crosstalk Between Tumours, Immune Cells and Microorganisms. *Nat Rev Cancer* (2013) 13:759–71. doi: 10.1038/nrc3611
19. Topalian SL, Taube JM, Anders RA, Pardoll DM. Mechanism-Driven Biomarkers to Guide Immune Checkpoint Blockade in Cancer Therapy. *Nat Rev Cancer* (2016) 16:275–87. doi: 10.1038/nrc.2016.36
20. Nagarsheth N, Wicha MS, Zou W. Chemokines in the Cancer Microenvironment and Their Relevance in Cancer Immunotherapy. *Nat Rev Immunol* (2017) 17:559–72. doi: 10.1038/nri.2017.49
21. McAllister SS, Weinberg RA. The Tumour-Induced Systemic Environment as a Critical Regulator of Cancer Progression and Metastasis. *Nat Cell Biol* (2014) 16:717–27. doi: 10.1038/ncb3015
22. Chen X, Wang L, Li P, Song M, Qin G, Gao Q, et al. Dual TGF-Beta and PD-1 Blockade Synergistically Enhances MAGE-A3-Specific CD8(+) T Cell Response in Esophageal Squamous Cell Carcinoma. *Int J Cancer* (2018) 143:2561–74. doi: 10.1002/ijc.31730
23. Wang XC, Zhang JQ, Shen YQ, Miao FQ, Xie W. Loss of Heterozygosity at 6p21.3 Underlying HLA Class I Downregulation in Gastric Cancer. *J Exp Clin Cancer Res* (2006) 25:115–9. doi: 10.1111/j.1399-0039.2008.01078.x
24. Ubukata H, Motohashi G, Tabuchi T, Nagata H, Konishi S, Tabuchi T. Evaluations of Interferon-γ/Interleukin-4 Ratio and Neutrophil/Lymphocyte Ratio as Prognostic Indicators in Gastric Cancer Patients. *J Surg Oncol* (2010) 102:742–7. doi: 10.1002/jso.21725
25. Galon J, Costes A, Sanchez-Cabo F, Kirilovsky A, Mlecnik B, Lagorce-Pagès C, et al. Type, Density, and Location of Immune Cells Within Human Colorectal Tumors Predict Clinical Outcome. *Science* (2006) 313:1960–4. doi: 10.1126/science.1129139
26. van Herk EH, Te Velde AA. Treg Subsets in Inflammatory Bowel Disease and Colorectal Carcinoma: Characteristics, Role, and Therapeutic Targets. *J Gastroenterol Hepatol* (2016) 31:1393–404. doi: 10.1111/jgh.13342
27. Correale P, Rotundo MS, Del Vecchio MT, Remondo C, Migali C, Ginanneschi C, et al. Regulatory (FoxP3+) T-Cell Tumor Infiltration Is a Favorable Prognostic Factor in Advanced Colon Cancer Patients Undergoing Chemo or Chemoimmunotherapy. *J Immunother* (2010) 33:435–41. doi: 10.1097/CJI.0b013e3181d32f01
28. Ichihara F, Kono K, Takahashi A, Kawaida H, Sugai H, Fujii H. Increased Populations of Regulatory T Cells in Peripheral Blood and Tumor-Infiltrating Lymphocytes in Patients With Gastric and Esophageal Cancers. *Clin Cancer Res* (2003) 9:4404–8.
29. Ishigami S, Natsugoe S, Tokuda K, Nakajo A, Xiangming C, Iwashige H, et al. Clinical Impact of Intratumoral Natural Killer Cell and Dendritic Cell Infiltration in Gastric Cancer. *Cancer Lett* (2000) 159:103–8. doi: 10.1016/S0304-3835(00)00542-5
30. Yamazaki S, Iyoda T, Tarbell K, Olson K, Velinzon K, Inaba K, et al. Direct Expansion of Functional CD25+ CD4+ Regulatory T Cells by Antigen-Processing Dendritic Cells. *J Exp Med* (2003) 198:235–47. doi: 10.1084/jem.20030422
31. Dijkgraaf EM, Heusinkveld M, Tummers B, Vogelpoel LT, Goedemans R, Jha V, et al. Chemotherapy Alters Monocyte Differentiation to Favor Generation of Cancer-Supporting M2 Macrophages in the Tumor Microenvironment. *Cancer Res* (2013) 73:2480–92. doi: 10.1158/0008-5472.CAN-12-3542
32. Ruffell B, Chang-Strachan D, Chan V, Rosenbusch A, Ho CM, Pryer N, et al. Macrophage IL-10 Blocks CD8+ T Cell-Dependent Responses to Chemotherapy by Suppressing IL-12 Expression in Intratumoral Dendritic Cells. *Cancer Cell* (2014) 26:623–37. doi: 10.1016/j.ccell.2014.09.006
33. Coussens LM, Pollard JW. Leukocytes in Mammary Development and Cancer. *Cold Spring Harb Perspect Biol* (2011) 3:a003285. doi: 10.1101/cshperspect.a003285
34. Inman JL, Robertson C, Mott JD, Bissell MJ. Mammary Gland Development: Cell Fate Specification, Stem Cells and the Microenvironment. *Development* (2015) 142:1028–42. doi: 10.1242/dev.087643
35. Arango Duque G, Descoteaux A. Macrophage Cytokines: Involvement in Immunity and Infectious Diseases. *Front Immunol* (2014) 5:491. doi: 10.3389/fimmu.2014.00491
36. Larionova I, Cherdyntseva N, Liu T, Patysheva M, Rakina M, Kzhyshkowska J. Interaction of Tumor-Associated Macrophages and Cancer Chemotherapy. *Oncoimmunology* (2019) 8:1596004. doi: 10.1080/2162402X.2019.1596004

37. Barbera-Guillem E, Nyhus JK, Wolford CC, Friece CR, Sampsel JW. Vascular Endothelial Growth Factor Secretion by Tumor-Infiltrating Macrophages Essentially Supports Tumor Angiogenesis, and IgG Immune Complexes Potentiate the Process. *Cancer Res* (2002) 62:7042–9.
38. Peddareddigari VG, Wang D, Dubois RN. The Tumor Microenvironment in Colorectal Carcinogenesis. *Cancer Microenviron* (2010) 3:149–66. doi: 10.1007/s12307-010-0038-3
39. Torres S, Bartolomé RA, Mendes M, Barderas R, Fernandez-Aceñero MJ, Peláez-García A, et al. Proteome Profiling of Cancer-Associated Fibroblasts Identifies Novel Proinflammatory Signatures and Prognostic Markers for Colorectal Cancer. *Clin Cancer Res* (2013) 19:6006–19. doi: 10.1158/1078-0432.CCR-13-1130
40. Gershkovitz M, Caspi Y, Fainsod-Levi T, Katz B, Michaeli J, Khawaled S, et al. TRPM2 Mediates Neutrophil Killing of Disseminated Tumor Cells. *Cancer Res* (2018) 78:2680–90. doi: 10.1158/0008-5472.CAN-17-3614
41. Finisguerra V, Di Conza G, Di Matteo M, Serneels J, Costa S, Thompson AA, et al. MET Is Required for the Recruitment of Anti-Tumoural Neutrophils. *Nature* (2015) 522:349–53. doi: 10.1038/nature14407
42. Ardi VC, Kupriyanova TA, Deryugina EI, Quigley JP. Human Neutrophils Uniquely Release TIMP-Free MMP-9 to Provide a Potent Catalytic Stimulator of Angiogenesis. *Proc Natl Acad Sci USA* (2007) 104:20262–7. doi: 10.1073/pnas.0706438104
43. Giese MA, Hind LE, Huttenlocher A. Neutrophil Plasticity in the Tumor Microenvironment. *Blood* (2019) 133:2159–67. doi: 10.1182/blood-2018-11-844548
44. Tohme S, Yazdani HO, Al-Khafaji AB, Chidi AP, Loughran P, Mowen K, et al. Neutrophil Extracellular Traps Promote the Development and Progression of Liver Metastases After Surgical Stress. *Cancer Res* (2016) 76:1367–80. doi: 10.1158/0008-5472.CAN-15-1591
45. Berntsson J, Svensson MC, Leandersson K, Nodin B, Micke P, Larsson AH, et al. The Clinical Impact of Tumour-Infiltrating Lymphocytes in Colorectal Cancer Differs by Anatomical Subsite: A Cohort Study. *Int J Cancer* (2017) 141:1654–66. doi: 10.1002/ijc.30869
46. de Visser KE, Korets LV, Coussens LM. De Novo Carcinogenesis Promoted by Chronic Inflammation Is B Lymphocyte Dependent. *Cancer Cell* (2005) 7:411–23. doi: 10.1016/j.ccr.2005.04.014
47. He Y, Qian H, Liu Y, Duan L, Li Y, Shi G. The Roles of Regulatory B Cells in Cancer. *J Immunol Res* (2014) 2014:215471. doi: 10.1155/2014/215471
48. Schioppa T, Moore R, Thompson RG, Rosser EC, Kulbe H, Nedospasov S, et al. B Regulatory Cells and the Tumor-Promoting Actions of TNF-Alpha During Squamous Carcinogenesis. *Proc Natl Acad Sci USA* (2011) 108:10662–7. doi: 10.1073/pnas.1100994108
49. Berntsson J, Nodin B, Eberhard J, Micke P, Jirström K. Prognostic Impact of Tumour-Infiltrating B Cells and Plasma Cells in Colorectal Cancer. *Int J Cancer* (2016) 139:1129–39. doi: 10.1002/ijc.30138
50. Lim KS, Mimura K, Kua LF, Shiraishi K, Kono K. Implication of Highly Cytotoxic Natural Killer Cells for Esophageal Squamous Cell Carcinoma Treatment. *J Immunother* (2018) 41:261–73. doi: 10.1097/CJI.0000000000000227
51. Peng LS, Zhang JY, Teng YS, Zhao YL, Wang TT, Mao FY, et al. Tumor-Associated Monocytes/Macrophages Impair NK-Cell Function *Via* Tgfβ1 in Human Gastric Cancer. *Cancer Immunol Res* (2017) 5:248–56. doi: 10.1158/2326-6066.CIR-16-0152
52. Fisher DT, Appenheimer MM, Evans SS. The Two Faces of IL-6 in the Tumor Microenvironment. *Semin Immunol* (2014) 26:38–47. doi: 10.1016/j.smim.2014.01.008
53. Mannino MH, Zhu Z, Xiao H, Bai Q, Wakefield MR, Fang Y. The Paradoxical Role of IL-10 in Immunity and Cancer. *Cancer Lett* (2015) 367:103–7. doi: 10.1016/j.canlet.2015.07.009
54. Choi JN, Sun EG, Cho SH. IL-12 Enhances Immune Response by Modulation of Myeloid Derived Suppressor Cells in Tumor Microenvironment. *Chonnam Med J* (2019) 55:31–9. doi: 10.4068/cmj.2019.55.1.31
55. Turnis ME, Sawant DV, Szymczak-Workman AL, Andrews LP, Delgoffe GM, Yano H, et al. Interleukin-35 Limits Anti-Tumor Immunity. *Immunity* (2016) 44:316–29. doi: 10.1016/j.immuni.2016.01.013
56. Josephs SF, Ichim TE, Prince SM, Kesari S, Marincola FM, Escobedo AR, et al. Unleashing Endogenous TNF-Alpha as a Cancer Immunotherapeutic. *J Transl Med* (2018) 16:242. doi: 10.1186/s12967-018-1611-7
57. Burke JD, Young HA. IFN-γ: A Cytokine at the Right Time, Is in the Right Place. *Semin Immunol* (2019) 43:101280. doi: 10.1016/j.smim.2019.05.002
58. Munn DH, Mellor AL. IDO in the Tumor Microenvironment: Inflammation, Counter-Regulation, and Tolerance. *Trends Immunol* (2016) 37:193–207. doi: 10.1016/j.it.2016.01.002
59. Batlle E, Massagué J. Transforming Growth Factor-β Signaling in Immunity and Cancer. *Immunity* (2019) 50:924–40. doi: 10.1016/j.immuni.2019.03.024
60. Mills CD, Ley K. M1 and M2 Macrophages: The Chicken and the Egg of Immunity. *J Innate Immun* (2014) 6:716–26. doi: 10.1159/000364945
61. Siveen KS, Kuttan G. Role of Macrophages in Tumour Progression. *Immunol Lett* (2009) 123:97–102. doi: 10.1016/j.imlet.2009.02.011
62. Schmieder A, Michel J, Schonhaar K, Goerdt S, Schledzewski K. Differentiation and Gene Expression Profile of Tumor-Associated Macrophages. *Semin Cancer Biol* (2012) 22:289–97. doi: 10.1016/j.semcancer.2012.02.002
63. Popena I, Abols A, Saulite L, Pleiko K, Zandberga E, Jekabsons K, et al. Effect of Colorectal Cancer-Derived Extracellular Vesicles on the Immunophenotype and Cytokine Secretion Profile of Monocytes and Macrophages. *Cell Commun Signal* (2018) 16:17. doi: 10.1186/s12964-018-0229-y
64. Gambardella V, Castillo J, Tarazona N, Gimeno-Valiente F, Martinez-Ciarpaglini C, Cabeza-Segura M, et al. The Role of Tumor-Associated Macrophages in Gastric Cancer Development and Their Potential as a Therapeutic Target. *Cancer Treat Rev* (2020) 86:102015. doi: 10.1016/j.ctrv.2020.102015
65. Yang H, Zhang Q, Xu M, Wang L, Chen X, Feng Y, et al. CCL2-CCR2 Axis Recruits Tumor Associated Macrophages to Induce Immune Evasion Through PD-1 Signaling in Esophageal Carcinogenesis. *Mol Cancer* (2020) 19:41. doi: 10.1186/s12943-020-01165-x
66. Joshi RS, Kanugula SS, Sudhir S, Pereira MP, Jain S, Aghi MK. The Role of Cancer-Associated Fibroblasts in Tumor Progression. *Cancers (Basel)* (2021) 13:1399. doi: 10.3390/cancers13061399
67. Smith HA, Kang Y. The Metastasis-Promoting Roles of Tumor-Associated Immune Cells. *J Mol Med (Berl)* (2013) 91:411–29. doi: 10.1007/s00109-013-1021-5
68. Bonnans C, Chou J, Werb Z. Remodelling the Extracellular Matrix in Development and Disease. *Nat Rev Mol Cell Biol* (2014) 15:786–801. doi: 10.1038/nrm3904
69. Landskron G, de la Fuente M, Thuwajit P, Thuwajit C, Hermoso MA. Chronic Inflammation and Cytokines in the Tumor Microenvironment. *J Immunol Res* (2014) 2014:149185. doi: 10.1155/2014/149185
70. Chang CP, Hu MH, Hsiao YP, Wang YC. ST2 Signaling in the Tumor Microenvironment. *Adv Exp Med Biol* (2020) 1240:83–93. doi: 10.1007/978-3-030-38315-2_7
71. Unsworth A, Anderson R, Britt K. Stromal Fibroblasts and the Immune Microenvironment: Partners in Mammary Gland Biology and Pathology? *J Mammary Gland Biol Neoplasia* (2014) 19:169–82. doi: 10.1007/s10911-014-9326-8
72. Xing F, Saidou J, Watabe K. Cancer Associated Fibroblasts (CAFs) in Tumor Microenvironment. *Front Biosci (Landmark Ed)* (2010) 15:166–79. doi: 10.2741/3613
73. Freeman P, Mielgo A. Cancer-Associated Fibroblast Mediated Inhibition of CD8+ Cytotoxic T Cell Accumulation in Tumours: Mechanisms and Therapeutic Opportunities. *Cancers (Basel)* (2020) 12:2687. doi: 10.3390/cancers12092687
74. Mari L, Hoefnagel SJM, Zito D, van de Meent M, van Endert P, Calpe S, et al. microRNA 125a Regulates MHC-I Expression on Esophageal Adenocarcinoma Cells, Associated With Suppression of Antitumor Immune Response and Poor Outcomes of Patients. *Gastroenterology* (2018) 155:784–98. doi: 10.1053/j.gastro.2018.06.030
75. Zaretsky JM, Garcia-Diaz A, Shin DS, Escuin-Ordinas H, Hugo W, Hu-Lieskovan S, et al. Mutations Associated With Acquired Resistance to PD-1 Blockade in Melanoma. *N Engl J Med* (2016) 375:819–29. doi: 10.1056/NEJMoa1604958
76. Guo F, Wang Y, Liu J, Mok S, Xue F, Zhang W. CXCL12/CXCR4: A Symbiotic Bridge Linking Cancer Cells and Their Stromal Neighbors in Oncogenic Communication Networks. *Oncogene* (2016) 35:816–26. doi: 10.1038/onc.2015.139

77. Chen DS, Mellman I. Elements of Cancer Immunity and the Cancer-Immune Set Point. *Nature* (2017) 541:321–30. doi: 10.1038/nature21349
78. Spranger S, Gajewski TF. Impact of Oncogenic Pathways on Evasion of Antitumour Immune Responses. *Nat Rev Cancer* (2018) 18:139–47. doi: 10.1038/nrc.2017.117
79. Mumm JB, Emmerich J, Zhang X, Chan I, Wu L, Mauze S, et al. IL-10 Elicits IFNgamma-Dependent Tumor Immune Surveillance. *Cancer Cell* (2011) 20:781–96. doi: 10.1016/j.ccr.2011.11.003
80. Fioravanti J, Di Lucia P, Magini D, Moalli F, Boni C, Benechet AP, et al. Effector CD8(+) T Cell-Derived Interleukin-10 Enhances Acute Liver Immunopathology. *J Hepatol* (2017) 67:543–8. doi: 10.1016/j.jhep.2017.04.020
81. Naing A, Papadopoulos KP, Autio KA, Ott PA, Patel MR, Wong DJ, et al. Safety, Antitumor Activity, and Immune Activation of Pegylated Recombinant Human Interleukin-10 (AM0010) in Patients With Advanced Solid Tumors. *J Clin Oncol* (2016) 34:3562–9. doi: 10.1200/JCO.2016.68.1106
82. Zhao Q. Dual Targeting of CCR2 and CCR5: Therapeutic Potential for Immunologic and Cardiovascular Diseases. *J Leukoc Biol* (2010) 88:41–55. doi: 10.1189/jlb.1009671
83. Buchbinder E, Hodi FS. Cytotoxic T Lymphocyte Antigen-4 and Immune Checkpoint Blockade. *J Clin Invest* (2015) 125:3377–83. doi: 10.1172/JCI80012
84. Zhang C, Zhang J, Ma Y, Zhe H, Zhao R, Wang Y. Prognostic Value of Combined Analysis of CTLA-4 and PLR in Esophageal Squamous Cell Carcinoma (ESCC) Patients. *Dis Markers* (2019) 2019:1601072–1601072. doi: 10.1155/2019/1601072
85. Kim DW, Trinh VA, Hwu WJ. Ipilimumab in the Treatment of Advanced Melanoma - A Clinical Update. *Expert Opin Biol Ther* (2014) 14:1709–18. doi: 10.1517/14712598.2014.963053
86. Toh JWT, de Souza P, Lim SH, Singh P, Chua W, Ng W, et al. The Potential Value of Immunotherapy in Colorectal Cancers: Review of the Evidence for Programmed Death-1 Inhibitor Therapy. *Clin Colorectal Cancer* (2016) 15:285–91. doi: 10.1016/j.clcc.2016.07.007
87. Topalian SL, Taube JM, Pardoll DM. Neoadjuvant Checkpoint Blockade for Cancer Immunotherapy. *Science* (2020) 367:6477. doi: 10.1126/science.aax0182
88. Overman MJ, McDermott R, Leach JL, Lonardi S, Lenz HJ, Morse MA, et al. Nivolumab in Patients With Metastatic DNA Mismatch Repair-Deficient or Microsatellite Instability-High Colorectal Cancer (CheckMate 142): An Open-Label, Multicentre, Phase 2 Study. *Lancet Oncol* (2017) 18:1182–91. doi: 10.1016/S1470-2045(17)30422-9
89. Saito R, Abe H, Kunita A, Yamashita H, Seto Y, Fukayama M. Overexpression and Gene Amplification of PD-L1 in Cancer Cells and PD-L1(+) Immune Cells in Epstein-Barr Virus-Associated Gastric Cancer: The Prognostic Implications. *Mod Pathol* (2017) 30:427–39. doi: 10.1038/modpathol.2016.202
90. Kato K, Shah MA, Enzinger P, Bennouna J, Shen L, Adenis A, et al. KEYNOTE-590: Phase III Study of First-Line Chemotherapy With or Without Pembrolizumab for Advanced Esophageal Cancer. *Future Oncol* (2019) 15:1057–66. doi: 10.2217/fon-2018-0609
91. Metges JP, Francois E, Shah MA, Adenis A, Enzinger PC, Kojima T, et al. The Phase 3 KEYNOTE-181 Study: Pembrolizumab Versus Chemotherapy as Second-Line Therapy for Advanced Esophageal Cancer. *Ann Oncol* (2019) 30:iv130. doi: 10.1093/annonc/mdz154.011
92. Shan B, Man H, Liu J, Wang L, Zhu T, Ma M, et al. TIM-3 Promotes the Metastasis of Esophageal Squamous Cell Carcinoma by Targeting Epithelial-Mesenchymal Transition *Via* the Akt/GSK-3β/Snail Signaling Pathway. *Oncol Rep* (2016) 36:1551–61. doi: 10.3892/or.2016.4938
93. Yu J, Zhang H, Sun S, Sun S, Li L. The Effects of Tim-3 Activation on T-Cells in Gastric Cancer Progression. *Oncol Lett* (2019) 17:1461–6. doi: 10.3892/ol.2018.9743
94. Zhang P, Wang Y, Liu XR, Hong SR, Yao J. Downregulated Tim-3 Expression Is Responsible for the Incidence and Development of Colorectal Cancer. *Oncol Lett* (2018) 16:1059–66. doi: 10.3892/ol.2018.8697
95. Andrews LP, Marciscano AE, Drake CG, Vignali DA. LAG3 (CD223) as a Cancer Immunotherapy Target. *Immunol Rev* (2017) 276:80–96. doi: 10.1111/imr.12519
96. Zhang Y, Liu Y, Luo Y, Liu B, Huang Q, Wang F, et al. Prognostic Value of Lymphocyte Activation Gene-3 (LAG-3) Expression in Esophageal Squamous Cell Carcinoma. *J Cancer* (2018) 9:4287–93. doi: 10.7150/jca.26949
97. Saleh R, Taha RZ, Toor SM, Sasidharan Nair V, Murshed K, Khawar M, et al. Expression of Immune Checkpoints and T Cell Exhaustion Markers in Early and Advanced Stages of Colorectal Cancer. *Cancer Immunol Immunother* (2020) 69:1989–99. doi: 10.1007/s00262-020-02593-w
98. Zhang W, Huang Q, Xiao W, Zhao Y, Pi J, Xu H, et al. Advances in Anti-Tumor Treatments Targeting the CD47/SIRPalpha Axis. *Front Immunol* (2020) 11:18. doi: 10.3389/fimmu.2020.00018
99. Zhao CL, Yu S, Wang SH, Li SG, Wang ZJ, Han SN. Characterization of Cluster of Differentiation 47 Expression and Its Potential as a Therapeutic Target in Esophageal Squamous Cell Cancer. *Oncol Lett* (2017) 15:2017–23. doi: 10.3892/ol.2017.7447
100. Yoshida K, Tsujimoto H, Matsumura K, Kinoshita M, Takahata R, Matsumoto Y, et al. CD47 Is an Adverse Prognostic Factor and a Therapeutic Target in Gastric Cancer. *Cancer Med* (2015) 4:1322–33. doi: 10.1002/cam4.478
101. Tzatzarakis E, Hissa B, Reissfelder C, Schölch S. The Overall Potential of CD47 in Cancer Immunotherapy: With a Focus on Gastrointestinal Tumors. *Expert Rev Anticancer Ther* (2019) 19:993–9. doi: 10.1080/14737140.2019.1689820
102. Sadelain M, Brentjens R, Riviere I. The Basic Principles of Chimeric Antigen Receptor Design. *Cancer Discov* (2013) 3:388–98. doi: 10.1158/2159-8290.CD-12-0548
103. Sandlund JT, Martin MG. Non-Hodgkin Lymphoma Across the Pediatric and Adolescent and Young Adult Age Spectrum. *Hematology Am Soc Hematology Educ Program* (2016) 2016:589–97. doi: 10.1182/asheducation-2016.1.589
104. Al-Mansour M, Al-Foheidi M, Ibrahim E. Efficacy and Safety of Second-Generation CAR T-Cell Therapy in Diffuse Large B-Cell Lymphoma: A Meta-Analysis. *Mol Clin Oncol* (2020) 13:33. doi: 10.3892/mco.2020.2103
105. Shi H, Yu F, Mao Y, Ju Q, Wu Y, Bai W, et al. EphA2 Chimeric Antigen Receptor-Modified T Cells for the Immunotherapy of Esophageal Squamous Cell Carcinoma. *J Thorac Dis* (2018) 10:2779–88. doi: 10.21037/jtd.2018.04.91
106. Zhang Q, Zhang Z, Peng M, Fu S, Xue Z, Zhang R. CAR-T Cell Therapy in Gastrointestinal Tumors and Hepatic Carcinoma: From Bench to Bedside. *Oncoimmunology* (2016) 5:e1251539. doi: 10.1080/2162402X.2016.1251539
107. Holzinger A, Abken H. CAR T Cells Targeting Solid Tumors: Carcinoembryonic Antigen (CEA) Proves to be a Safe Target. *Cancer Immunol Immunother* (2017) 66:1505–7. doi: 10.1007/s00262-017-2045-4
108. Chi X, Yang P, Zhang E, Gu J, Xu H, Li M, et al. Significantly Increased Anti-Tumor Activity of Carcinoembryonic Antigen-Specific Chimeric Antigen Receptor T Cells in Combination With Recombinant Human IL-12. *Cancer Med* (2019) 8:4753–65. doi: 10.1002/cam4.2361
109. Zhou JT, Liu JH, Song TT, Ma B, Amidula N, Bai C. EGLIF-CAR-T Cells Secreting PD-1 Blocking Antibodies Significantly Mediate the Elimination of Gastric Cancer. *Cancer Manag Res* (2020) 12:8893–902. doi: 10.2147/CMAR.S260915
110. Tabernero J, Hoff PM, Shen L, Ohtsu A, Shah MA, Cheng K, et al. Pertuzumab Plus Trastuzumab and Chemotherapy for HER2-Positive Metastatic Gastric or Gastro-Oesophageal Junction Cancer (JACOB): Final Analysis of a Double-Blind, Randomised, Placebo-Controlled Phase 3 Study. *Lancet Oncol* (2018) 19:1372–84. doi: 10.1016/S1470-2045(18)30481-9
111. Chester C, Fritsch K, Kohrt HE. Natural Killer Cell Immunomodulation: Targeting Activating, Inhibitory, and Co-Stimulatory Receptor Signaling for Cancer Immunotherapy. *Front Immunol* (2015) 6:601. doi: 10.3389/fimmu.2015.00601
112. Hasmim M, Messai Y, Ziani L, Thiery J, Bouhris JH, Noman MZ, et al. Critical Role of Tumor Microenvironment in Shaping NK Cell Functions: Implication of Hypoxic Stress. *Front Immunol* (2015) 6:482. doi: 10.3389/fimmu.2015.00482
113. Alici E, Konstantinidis KV, Sutlu T, Aints A, Gahrton G, Ljunggren HG, et al. Anti-Myeloma Activity of Endogenous and Adoptively Transferred Activated Natural Killer Cells in Experimental Multiple Myeloma Model. *Exp Hematol* (2007) 35:1839–46. doi: 10.1016/j.exphem.2007.08.006

114. Lin C, Zhang J. Reformation in Chimeric Antigen Receptor Based Cancer Immunotherapy: Redirecting Natural Killer Cell. *Biochim Biophys Acta Rev Cancer* (2018) 1869:200–15. doi: 10.1016/j.bbcan.2018.01.005
115. Siegler U, Kalberer CP, Nowbakht P, Sendelov S, Meyer-Monard S, Wodnar-Filipowicz A. Activated Natural Killer Cells From Patients With Acute Myeloid Leukemia Are Cytotoxic Against Autologous Leukemic Blasts in NOD/SCID Mice. *Leukemia* (2005) 19:2215–22. doi: 10.1038/sj.leu.2403985
116. Bendelac A, Savage PB, Teyton L. The Biology of NKT Cells. *Annu Rev Immunol* (2007) 25:297–336. doi: 10.1146/annurev.immunol.25.022106.141711
117. McEwen-Smith RM, Salio M, Cerundolo V. The Regulatory Role of Invariant NKT Cells in Tumor Immunity. *Cancer Immunol Res* (2015) 3:425–35. doi: 10.1158/2326-6066.CIR-15-0062
118. Wolf BJ, Choi JE, Exley MA. Novel Approaches to Exploiting Invariant NKT Cells in Cancer Immunotherapy. *Front Immunol* (2018) 9:384. doi: 10.3389/fimmu.2018.00384
119. Coquet JM, Kyparissoudis K, Pellicci DG, Besra G, Berzins SP, Smyth MJ, et al. IL-21 Is Produced by NKT Cells and Modulates NKT Cell Activation and Cytokine Production. *J Immunol* (2007) 178:2827–34. doi: 10.4049/jimmunol.178.5.2827
120. Heczey A, Liu D, Tian G, Courtney AN, Wei J, Marinova E, et al. Invariant NKT Cells With Chimeric Antigen Receptor Provide a Novel Platform for Safe and Effective Cancer Immunotherapy. *Blood* (2014) 124:2824–33. doi: 10.1182/blood-2013-11-541235
121. Crowe NY, Uldrich AP, Kyparissoudis K, Hammond KJ, Hayakawa Y, Sidobre S, et al. Glycolipid Antigen Drives Rapid Expansion and Sustained Cytokine Production by NK T Cells. *J Immunol* (2003) 171:4020–7. doi: 10.4049/jimmunol.171.8.4020
122. Yamasaki K, Horiguchi S, Kurosaki M, Kunii N, Nagato K, Hanaoka H, et al. Induction of NKT Cell-Specific Immune Responses in Cancer Tissues After NKT Cell-Targeted Adoptive Immunotherapy. *Clin Immunol* (2011) 138:255–65. doi: 10.1016/j.clim.2010.11.014
123. Kunii N, Horiguchi S, Motohashi S, Yamamoto H, Ueno N, Yamamoto S, et al. Combination Therapy of *In Vitro*-Expanded Natural Killer T Cells and Alpha-Galactosylceramide-Pulsed Antigen-Presenting Cells in Patients With Recurrent Head and Neck Carcinoma. *Cancer Sci* (2009) 100:1092–8. doi: 10.1111/j.1349-7006.2009.01135.x
124. Nywening TM, Wang-Gillam A, Sanford DE, Belt BA, Panni RZ, Cusworth BM, et al. Targeting Tumour-Associated Macrophages With CCR2 Inhibition in Combination With FOLFIRINOX in Patients With Borderline Resectable and Locally Advanced Pancreatic Cancer: A Single-Centre, Open-Label, Dose-Finding, Non-Randomised, Phase 1b Trial. *Lancet Oncol* (2016) 17:651–62. doi: 10.1016/S1470-2045(16)00078-4
125. Cannarile MA, Weisser M, Jacob W, Jegg AM, Ries CH, Rüttinger D. Colony-Stimulating Factor 1 Receptor (CSF1R) Inhibitors in Cancer Therapy. *J Immunother Cancer* (2017) 5:53. doi: 10.1186/s40425-017-0257-y
126. Ruffell B, Coussens LM. Macrophages and Therapeutic Resistance in Cancer. *Cancer Cell* (2015) 27:462–72. doi: 10.1016/j.ccell.2015.02.015
127. Quail DF, Bowman RL, Akkari L, Quick ML, Schuhmacher AJ, Huse JT, et al. The Tumor Microenvironment Underlies Acquired Resistance to CSF-1R Inhibition in Gliomas. *Science* (2016) 352:aad3018. doi: 10.1126/science.aad3018
128. Li X, Liu R, Su X, Pan Y, Han X, Shao C, et al. Harnessing Tumor-Associated Macrophages as Aids for Cancer Immunotherapy. *Mol Cancer* (2019) 18:177. doi: 10.1186/s12943-019-1102-3
129. Ries CH, Cannarile MA, Hoves S, Benz J, Wartha K, Runza V, et al. Targeting Tumor-Associated Macrophages With Anti-CSF-1R Antibody Reveals a Strategy for Cancer Therapy. *Cancer Cell* (2014) 25:846–59. doi: 10.1016/j.ccr.2014.05.016
130. Pyonteck SM, Akkari L, Schuhmacher AJ, Bowman RL, Sevenich L, Quail DF, et al. CSF-1R Inhibition Alters Macrophage Polarization and Blocks Glioma Progression. *Nat Med* (2013) 19:1264–72. doi: 10.1038/nm.3337
131. Willingham SB, Volkmer JP, Gentles AJ, Sahoo D, Dalerba P, Mitra SS, et al. The CD47-Signal Regulatory Protein Alpha (SIRPa) Interaction Is a Therapeutic Target for Human Solid Tumors. *Proc Natl Acad Sci USA* (2012) 109:6662–7. doi: 10.1073/pnas.1121623109
132. Kabelitz D, Wesch D, He W. Perspectives of Gammadelta T Cells in Tumor Immunology. *Cancer Res* (2007) 67:5–8. doi: 10.1158/0008-5472.CAN-06-3069
133. Scotet E, Martinez LO, Grant E, Barbaras R, Jenö P, Guiraud M, et al. Tumor Recognition Following Vgamma9Vdelta2 T Cell Receptor Interactions With a Surface F1-ATPase-Related Structure and Apolipoprotein A-I. *Immunity* (2005) 22:71–80. doi: 10.1016/j.immuni.2004.11.012
134. Chen H, He X, Wang Z, Wu D, Zhang H, Xu C, et al. Identification of Human T Cell Receptor Gammadelta-Recognized Epitopes/Proteins *Via* CDR3delta Peptide-Based Immunobiochemical Strategy. *J Biol Chem* (2008) 283:12528–37. doi: 10.1074/jbc.M708067200
135. Hayday AC. [Gamma][Delta] Cells: A Right Time and a Right Place for a Conserved Third Way of Protection. *Annu Rev Immunol* (2000) 18:975–1026. doi: 10.1146/annurev.immunol.18.1.975
136. Lin C, Zhang J. Chimeric Antigen Receptor Engineered Innate Immune Cells in Cancer Immunotherapy. *Sci China Life Sci* (2019) 62:633–9. doi: 10.1007/s11427-018-9451-0
137. Rock EP, Sibbald PR, Davis MM, Chien YH. CDR3 Length in Antigen-Specific Immune Receptors. *J Exp Med* (1994) 179:323–8. doi: 10.1084/jem.179.1.323
138. Wu YL, Ding YP, Tanaka Y, Shen LW, Wei CH, Minato N, et al. γδ T Cells and Their Potential for Immunotherapy. *Int J Biol Sci* (2014) 10:119–35. doi: 10.7150/ijbs.7823
139. Khairallah C, Déchanet-Merville J, Capone M. γδ T Cell-Mediated Immunity to Cytomegalovirus Infection. *Front Immunol* (2017) 8:105. doi: 10.3389/fimmu.2017.00105
140. Mamedov MR, Scholzen A, Nair RV, Cumnock K, Kenkel JA, Oliveira JHM, et al. A Macrophage Colony-Stimulating-Factor-Producing γδ T Cell Subset Prevents Malarial Parasitemic Recurrence. *Immunity* (2018) 48:350–63.e357. doi: 10.1016/j.immuni.2018.01.009
141. Born WK, Reardon CL, O'Brien RL. The Function of Gammadelta T Cells in Innate Immunity. *Curr Opin Immunol* (2006) 18:31–8. doi: 10.1016/j.coi.2005.11.007
142. Morrow ES, Roseweir A, Edwards J. The Role of Gamma Delta T Lymphocytes in Breast Cancer: A Review. *Transl Res* (2019) 203:88–96. doi: 10.1016/j.trsl.2018.08.005
143. Capsomidis A, Benthall G, Van Acker HH, Fisher J, Kramer AM, Abeln Z, et al. Chimeric Antigen Receptor-Engineered Human Gamma Delta T Cells: Enhanced Cytotoxicity With Retention of Cross Presentation. *Mol Ther* (2018) 26:354–65. doi: 10.1016/j.ymthe.2017.12.001
144. Liu M, Wang X, Wang L, Ma X, Gong Z, Zhang S, et al. Targeting the IDO1 Pathway in Cancer: From Bench to Bedside. *J Hematol Oncol* (2018) 11:100. doi: 10.1186/s13045-018-0644-y
145. Kiyozumi Y, Baba Y, Okadome K, Yagi T, Ishimoto T, Iwatsuki M, et al. IDO1 Expression Is Associated With Immune Tolerance and Poor Prognosis in Patients With Surgically Resected Esophageal Cancer. *Ann Surg* (2019) 269:1101–8. doi: 10.1097/SLA.0000000000002754
146. Zhou S, Zhao L, Liang Z, Liu S, Li Y, Liu S, et al. Indoleamine 2,3-Dioxygenase 1 and Programmed Cell Death-Ligand 1 Co-Expression Predicts Poor Pathologic Response and Recurrence in Esophageal Squamous Cell Carcinoma After Neoadjuvant Chemoradiotherapy. *Cancers (Basel)* (2019) 11:169. doi: 10.3390/cancers11020169
147. Chen B, Alvarado DM, Iticovici M, Kau NS, Park H, Parikh PJ, et al. Interferon-Induced IDO1 Mediates Radiation Resistance and Is a Therapeutic Target in Colorectal Cancer. *Cancer Immunol Res* (2020) 8:451–64. doi: 10.1158/2326-6066.CIR-19-0282
148. Xiang Z, Li J, Song S, Wang J, Cai W, Hu W, et al. A Positive Feedback Between IDO1 Metabolite and COL12A1 *Via* MAPK Pathway to Promote Gastric Cancer Metastasis. *J Exp Clin Cancer Res* (2019) 38:314. doi: 10.1186/s13046-019-1318-5
149. Ozao-Choy J, Lee DJ, Faries MB. Melanoma Vaccines: Mixed Past, Promising Future. *Surg Clinics North Am* (2014) 94:1017–1030, viii. doi: 10.1016/j.suc.2014.07.005
150. Bouzid R, Peppelenbosch M, Buschow SI. Opportunities for Conventional and in Situ Cancer Vaccine Strategies and Combination With Immunotherapy for Gastrointestinal Cancers, A Review. *Cancers (Basel)* (2020) 12:1121. doi: 10.3390/cancers12051121
151. Topalian SL, Hodi FS, Brahmer JR, Gettinger SN, Smith DC, McDermott DF, et al. Safety, Activity, and Immune Correlates of Anti-PD-1 Antibody in Cancer. *N Engl J Med* (2012) 366:2443–54. doi: 10.1056/NEJMoa1200690

152. Chung KY, Gore I, Fong L, Venook A, Beck SB, Dorazio P, et al. Phase II Study of the Anti-Cytotoxic T-Lymphocyte-Associated Antigen 4 Monoclonal Antibody, Tremelimumab, in Patients With Refractory Metastatic Colorectal Cancer. *J Clin Oncol* (2010) 28:3485–90. doi: 10.1200/JCO.2010.28.3994
153. Overman MJ, Lonardi S, Wong KYM, Lenz HJ, Gelsomino F, Aglietta M, et al. Durable Clinical Benefit With Nivolumab Plus Ipilimumab in DNA Mismatch Repair-Deficient/Microsatellite Instability-High Metastatic Colorectal Cancer. *J Clin Oncol* (2018) 36:773–9. doi: 10.1200/JCO.2017.76.9901
154. Middha S, Zhang L, Nafa K, Jayakumaran G, Wong D, Kim HR, et al. Reliable Pan-Cancer Microsatellite Instability Assessment by Using Targeted Next-Generation Sequencing Data. *JCO Precis Oncol* (2017) 1:1–17. doi: 10.1200/PO.17.00084
155. Asaoka Y, Ijichi H, Koike K. PD-1 Blockade in Tumors With Mismatch-Repair Deficiency. *N Engl J Med* (2015) 373:1979. doi: 10.1056/NEJMc1510353
156. Morse MA, Overman MJ, Hartman L, Khoukaz T, Brutcher E, Lenz HJ, et al. Safety of Nivolumab Plus Low-Dose Ipilimumab in Previously Treated Microsatellite Instability-High/Mismatch Repair-Deficient Metastatic Colorectal Cancer. *Oncologist* (2019) 24:1453–61. doi: 10.1634/theoncologist.2019-0129
157. Eng C, Kim TW, Bendell J, Argiles G, Tebbutt NC, Di Bartolomeo M, et al. Atezolizumab With or Without Cobimetinib Versus Regorafenib in Previously Treated Metastatic Colorectal Cancer (IMblaze370): A Multicentre, Open-Label, Phase 3, Randomised, Controlled Trial. *Lancet Oncol* (2019) 20:849–61. doi: 10.1016/S1470-2045(19)30027-0
158. Tapia Rico G, Price TJ. Atezolizumab for the Treatment of Colorectal Cancer: The Latest Evidence and Clinical Potential. *Expert Opin Biol Ther* (2018) 18:449–57. doi: 10.1080/14712598.2018.1444024
159. Barroso-Sousa R, Krop IE, Trippa L, Tan-Wasielewski Z, Li T, Osmani W, et al. A Phase II Study of Pembrolizumab in Combination With Palliative Radiotherapy for Hormone Receptor-Positive Metastatic Breast Cancer. *Clin Breast Cancer* (2020) 20:238–45. doi: 10.1016/j.clbc.2020.01.012
160. Bourhis J, Stein A, Paul de Boer J, Van Den Eynde M, Gold KA, Stintzing S, et al. Avelumab and Cetuximab as a Therapeutic Combination: An Overview of Scientific Rationale and Current Clinical Trials in Cancer. *Cancer Treat Rev* (2021) 97:102172. doi: 10.1016/j.ctrv.2021.102172
161. Schmoll HJ, Arnold D, de Gramont A, Ducreux M, Grothey A, O'Dwyer PJ, et al. MODUL-A Multicenter Randomized Clinical Trial of Biomarker-Driven Maintenance Therapy Following First-Line Standard Induction Treatment of Metastatic Colorectal Cancer: An Adaptable Signal-Seeking Approach. *J Cancer Res Clin Oncol* (2018) 144:1197–204. doi: 10.1007/s00432-018-2632-6
162. Dolcetti R, De Re V, Canzonieri V. Immunotherapy for Gastric Cancer: Time for a Personalized Approach? *Int J Mol Sci* (2018) 19:1602. doi: 10.3390/ijms19061602
163. Shah MA, Kojima T, Hochhauser D, Enzinger P, Raimbourg J, Hollebecque A, et al. Efficacy and Safety of Pembrolizumab for Heavily Pretreated Patients With Advanced, Metastatic Adenocarcinoma or Squamous Cell Carcinoma of the Esophagus: The Phase 2 KEYNOTE-180 Study. *JAMA Oncol* (2019) 5:546–50. doi: 10.1001/jamaoncol.2018.5441
164. Kojima T, Shah MA, Muro K, Francois E, Adenis A, Hsu CH, et al. Randomized Phase III KEYNOTE-181 Study of Pembrolizumab Versus Chemotherapy in Advanced Esophageal Cancer. *J Clin Oncol* (2020) 38:4138–48. doi: 10.1200/JCO.20.01888
165. Ilson DH. Advances in the Treatment of Gastric Cancer. *Curr Opin Gastroenterol* (2018) 34:465–8. doi: 10.1097/MOG.0000000000000475
166. Janjigian YY, Bendell J, Calvo E, Kim JW, Ascierto PA, Sharma P, et al. CheckMate-032 Study: Efficacy and Safety of Nivolumab and Nivolumab Plus Ipilimumab in Patients With Metastatic Esophagogastric Cancer. *J Clin Oncol* (2018) 36:2836–44. doi: 10.1200/JCO.2017.76.6212
167. Ready N, Farago AF, de Braud F, Atmaca A, Hellmann MD, Schneider JG, et al. Third-Line Nivolumab Monotherapy in Recurrent SCLC: CheckMate 032. *J Thorac Oncol* (2019) 14:237–44. doi: 10.1016/j.jtho.2018.10.003
168. Kato K, Cho BC, Takahashi M, Okada M, Lin CY, Chin K, et al. Nivolumab Versus Chemotherapy in Patients With Advanced Oesophageal Squamous Cell Carcinoma Refractory or Intolerant to Previous Chemotherapy (ATTRACTION-3): A Multicentre, Randomised, Open-Label, Phase 3 Trial. *Lancet Oncol* (2019) 20:1506–17. doi: 10.1016/S1470-2045(19)30626-6
169. Lee JJ, Chu E. Recent Advances in the Clinical Development of Immune Checkpoint Blockade Therapy for Mismatch Repair Proficient (pMMR)/Non-MSI-H Metastatic Colorectal Cancer. *Clin Colorectal Cancer* (2018) 17:258–73. doi: 10.1016/j.clcc.2018.06.004
170. Derks S, Liao X, Chiaravalli AM, Xu X, Camargo MC, Solcia E, et al. Abundant PD-L1 Expression in Epstein-Barr Virus-Infected Gastric Cancers. *Oncotarget* (2016) 7:32925–32. doi: 10.18632/oncotarget.9076
171. Kim ST, Cristescu R, Bass AJ, Kim KM, Odegaard JI, Kim K, et al. Comprehensive Molecular Characterization of Clinical Responses to PD-1 Inhibition in Metastatic Gastric Cancer. *Nat Med* (2018) 24:1449–58. doi: 10.1038/s41591-018-0101-z

Conflict of Interest: The authors declare that the research was conducted in the absence of any commercial or financial relationships that could be construed as a potential conflict of interest.

Publisher's Note: All claims expressed in this article are solely those of the authors and do not necessarily represent those of their affiliated organizations, or those of the publisher, the editors and the reviewers. Any product that may be evaluated in this article, or claim that may be made by its manufacturer, is not guaranteed or endorsed by the publisher.

Copyright © 2021 Wang, Zuo, He and Li. This is an open-access article distributed under the terms of the Creative Commons Attribution License (CC BY). The use, distribution or reproduction in other forums is permitted, provided the original author(s) and the copyright owner(s) are credited and that the original publication in this journal is cited, in accordance with accepted academic practice. No use, distribution or reproduction is permitted which does not comply with these terms.

GLOSSARY

GEJ	gastric/esophagogastric junction
CRC	colorectal cancer
EC	esophageal cancer
GC	gastric cancer
ESCC	esophageal squamous cell carcinoma
SCC	esophageal adenocarcinoma
CRT	chemoradiotherapy
TNM	tumor node metastasis
CAR-T	chimeric antigen receptor-therapy
EGFR2	epidermal growth factor receptor 2
TAMs	tumor-associated macrophages
IFN	interferon
IL	interleukin
TCR	T cell receptor
BCR	B cell receptor
MHC	major histocompatibility complex
NK cell	natural killer cell
DCs	dendritic cells
CTLA-4	cytotoxic T-lymphocyte-associated protein 4
LAG-3	lymphocyte activation gene 3
ASCO	American Society of Clinical Oncology
TIM-3	T cell immunoglobulin 3
PD-1	programmed cell death 1
PD-L1	programmed cell death ligand 1
ACT	adoptive cell therapy
NKT cell	natural killer T cell
IDO	indoleamine 2,3-dioxygenase
MSI	microsatellite instability
MSS	microsatellite stability
dMMR	defective match repair
pMMR	proficient match repair
ORR	objective response rate
EBV	Epstein-Barr virus
APC	antigen-presenting cell
CMS 1-4	consensus molecular subtype 1-4
TGF-β	transforming growth factor β
TNF-α	tumor necrosis factor α
GM-CSF	granulocyte-macrophage colony stimulating factor
Mst1	macrophage stimulator 1
CCL2/ CCR2	C-C motif chemokine ligand 2/C-C motif chemokine ligand 2 receptor
CSF1R	colony stimulating factor-1 receptor
KIRs	killer-cell immunoglobulin-like receptors
NKG2A	CD94/NK group 2 member A
HLA	leukocyte antigen
TME	tumor microenvironment
TIME	tumor immune microenvironment
MDSCs	myeloid derived suppressor cells
CDR3	complementarity determining region 3
ADCP	antibody-dependent cellular phagocytosis
CEA	carcino-embryonic antigen
HER2	human epidermal growth factor receptor-2
GPC3	complement C3 protein
EpCAM	epithelial cell adhesion molecule
EGFR	epidermal growth factor receptor
VEGF	vascular endothelial growth factor
SIRPα	signal regulatory protein-α
PLR	platelet-lymphocyte ratio
TAP2	ATP binding cassette subfamily B member 3
ICI	immune checkpoint inhibitor therapy
ECM	extracellular matrix
TILs	tumor infiltrating lymphocytes
CAFs	cancer-associated fibroblasts
EGF	epidermal growth factor
Breg cells	regulatory B cells
Treg cells	regulatory T cells
RCC	renal cell carcinoma
CEA	carcinoembryonic antigen
ROS	reactive oxygen species
RNS	reactive nitrogen species
MMP9	matrix metalloproteinase 9
NETs	neutrophil extracellular traps
MSI-H	microsatellite instability-high
iNKT cells	invariant natural killer T cells
PFS	progression-free survival
OS	overall survival

frontiers in Immunology

SYSTEMATIC REVIEW
published: 16 August 2021
doi: 10.3389/fimmu.2021.731546

Comparison of Efficacy and Safety of Single and Double Immune Checkpoint Inhibitor-Based First-Line Treatments for Advanced Driver-Gene Wild-Type Non-Small Cell Lung Cancer: A Systematic Review and Network Meta-Analysis

Qian Xu[1†], Xue Zhang[1†], Miao Huang[1], Xin Dai[1,2], Jing Gao[1], Song Li[1], Lei Sheng[3], Kai Huang[1], Jian Wang[1] and Lian Liu[1]*

[1] Department of Medical Oncology, Qilu Hospital, Cheeloo College of Medicine, Shandong University, Jinan, China, [2] Department of Medical Oncology, Shandong Provincial Hospital of Traditional Chinese Medicine, Jinan, China, [3] Department of Thyroid Surgery, General Surgery, Qilu Hospital, Cheeloo College of Medicine, Shandong University, Jinan, China

OPEN ACCESS

Edited by:
Hubing Shi,
Sichuan University, China

Reviewed by:
Ming Yi,
Huazhong University of Science and Technology, China
Alessandro Rizzo,
Sant'Orsola-Malpighi Polyclinic, Italy

***Correspondence:**
Lian Liu
lianliu@sdu.edu.cn

[†]These authors have contributed equally to this work and share first authorship

Specialty section:
This article was submitted to Cancer Immunity and Immunotherapy, a section of the journal Frontiers in Immunology

Received: *27 June 2021*
Accepted: *27 July 2021*
Published: *16 August 2021*

Citation:
Xu Q, Zhang X, Huang M, Dai X, Gao J, Li S, Sheng L, Huang K, Wang J and Liu L (2021) Comparison of Efficacy and Safety of Single and Double Immune Checkpoint Inhibitor-Based First-Line Treatments for Advanced Driver-Gene Wild-Type Non-Small Cell Lung Cancer: A Systematic Review and Network Meta-Analysis. Front. Immunol. 12:731546. doi: 10.3389/fimmu.2021.731546

Background: Immune checkpoint inhibitors (ICIs) have improved survival for advanced wild-type non-small cell lung cancer (NSCLC) significantly, but few studies compared single ICI (SICI)-based treatments and double ICIs (DICI)-based treatments. We summarized the general efficacy of ICI-related treatments, compared the efficacy and safety of SICI-based [programmed death 1 (PD-1)/programmed death-ligand 1 (PD-L1) or cytotoxic T lymphocyte-associated antigen 4 (CTLA-4) inhibitors ± chemotherapy (CT)] and DICI-based (PD-1/PD-L1 inhibitors+CTLA-4 inhibitors ± chemotherapy) treatments *vs*. CT in the first-line treatment.

Methods: We included phase II/III randomized controlled trials (RCTs), including patients with histologically confirmed stage IIIB–IV driver-gene wild-type NSCLC who received first-line ICI-related therapy in at least one arm. PubMed, Embase, and Cochrane Library were searched from January 1, 2005, to December 31, 2020. This network meta-analysis was performed in a Bayesian framework using GEMTC and JAGS package in R.3.6.1. The research was registered with PROSPERO (CRD42020184534).

Results: Twenty RCTs were involved, including 13,032 patients and 17 treatment regimens. The results showed that ICI-based therapies could provide a pooled median overall survival (mOS) (POS) of 15.79 (95% CI: 14.85–16.73) months, and there were no significant differences in OS, progression-free survival (PFS), objective response rate (ORR), and grade 3 or higher adverse events (≥3AEs) between DICI-based treatments (POS: 14.81, 12.11–17.52 months) and SICI-based treatments (POS: 16.17, 14.59–17.74 months) in overall patients. However, DICI-based treatments had significantly prolonged the OS over SICI-based treatments in squamous and PD-L1 <1%

subgroups. The ranking of OS benefit by Bayesian surface under the cumulative ranking curve (SUCRA) spectrum showed that DICI+chemotherapy ranked first for overall population and subgroups including squamous, non-squamous, any level of PD-L1 expression, smoking, male, Eastern Cooperative Oncology Group performance status (ECOG PS) = 0/1, age < 65/≥65 while SICI+CT for low tumor mutation burden (TMB), non-smoking, and female subgroups, and DICI for high TMB subgroups.

Conclusions: In the first-line therapy for advanced wild-type NSCLC, both SICI- and DICI-based treatments could bring significant overall advantages over chemotherapy, with comparable outcomes of efficacy and ≥3AEs. DICI-based treatments were more effective than SICI-based treatments in squamous and PD-L1 <1% subgroups. For most populations, DICI+chemotherapy could be the best choice with a survival benefit, while SICI+chemotherapy has established its position actually.

Systematic Review Registration: [PROSPERO], identifier [CRD42020184534].

Keywords: non-small cell lung cancer, first-line, immune checkpoint inhibitors, single, double, network meta-analysis

INTRODUCTION

Lung cancer is the cancer with the highest mortality worldwide (1), among which non-small cell lung cancer (NSCLC) accounts for approximately 85% (2). Due to that advanced driver-gene wild-type NSCLC cannot benefit from targeted therapy (3), the third-generation platinum-containing chemotherapy (CT) was the standard first-line therapy in the past. Although pemetrexed or bevacizumab (BEV) maintenance therapy has brought survival benefits for non-squamous NSCLC, the 5-year overall survival (OS) rate of late-stage NSCLC is still limited (4). In recent years, with the development of immune checkpoint inhibitors (ICIs), including programmed death 1 (PD-1), programmed death-ligand 1 (PD-L1), and cytotoxic T lymphocyte-associated antigen 4 (CTLA-4) inhibitors (5), the first-line treatments for driver-gene negative advanced NSCLC have been enriched and optimized, significantly extending the survival of patients (6). As for single ICI (SICI), KEYNOTE 024 proved that pembrolizumab (PEM) significantly increased OS and progression-free survival (PFS) in advanced wild-type NSCLC patients with PD-L1 ≥50% (7, 8). In addition, IMpower 110 demonstrated atezolizumab (ATE) significantly prolonged OS in patients with Tumor cell/Immune cell (TC/IC) = 3 (9). Recently, EMPOWER-LUNG1 also demonstrated that cemiplimab (CEM) prolonged patients' OS and PFS in PD-L1 ≥50% significantly (10). For patients with a low expression of PD-L1, SICI plus CT (SICI+CT) showed better efficacy. KEYNOTE 021 (11, 12), KEYNOTE 189 (13, 14), KEYNOTE 407 (15, 16), CheckMate 227 part2 (17), CAMEL (18), ORIENT-11 (19), and ORIENT-12 (20) evaluated the efficacy of PD-1 inhibitors in combination with platinum-based CT and obtained significant benefits. However, great differences exist in the efficacy of anti-PD-L1 or CTLA-4 antibodies combined with CT in randomized controlled trials (RCTs) such as IMpower 130 (21), IMpower 131 (22), IMpower 132 (23, 24), Govindan (25), and Lynch (26). In addition to SICI-based treatments (including SICI and SICI+CT), dual ICIs (DICI)-based treatments have also been meaningfully explored. CheckMate 227 proved that nivolumab (NIV) combined with ipilimumab (IPI) improved OS and PFS in patients with advanced wild-type NSCLC (27). Furthermore, durvalumab (DUR) combined with tremelimumab (TRE) failed to indicate OS advantage over CT and is even inferior to CT in PFS in MYSTIC (28). CheckMate 9LA was the first study proving that DICI combined with CT (DICI+CT) significantly improved efficacy; NIV+IPI+CT gained longer OS and PFS over CT (29). While in CCTG BR.34, DUR+TRE+CT failed to obtain OS advantage in contrast to DICI (30).

Both SICI-based and DICI-based treatments have achieved certain success. However, no studies have been conducted to compare the two treatments directly. In theory, DICI-based treatments could target more immune checkpoints and should be more effective but may also produce more side effects. It has become a huge challenge perplexing clinicians whether DICI-based therapies are more effective and whether there exists the best treatment or beneficial populations among SICI, SICI+CT, DICI, and DICI+CT. To address such questions reasonably, we conducted an integrated analysis and network meta-analysis (NMA). Our study summarized the general effects of related treatments and compared the efficacy and safety among SICI, SICI+CT, DICI, DICI+CT, and CT in the first-line treatment of advanced wild-type NSCLC, which will provide valuable evidence for clinical decision-making.

MATERIALS AND METHODS

Literature Searching Strategies

This NMA was performed according to the PRISMA extension statement (**Supplementary Table 1**). We used strategies in **Supplementary Table 2** to search literature on first-line immunotherapy of advanced wild-type NSCLC in PubMed, Embase, and the Cochrane Central Register of Controlled

Trials (January 1, 2005–December 31, 2020). Abstracts of major international oncology conferences (American Society of Clinical Oncology, European Society of Medical Oncology, and World Conference on Lung Cancer) were also reviewed (2018–2020).

Inclusion Criteria

Published phase II/III RCTs reported in English that compared at least two first-line treatments, at least one arm containing ICIs, for histologically confirmed advanced (stage III–IV) driver-gene wild-type NSCLC patients who did not receive prior systemic therapies. The hazard ratio (HR) and 95% confidence interval (CI) of OS and PFS are available.

Exclusion Criteria

Trials involving targeted therapy for driver-gene mutation NSCLC patients or therapies other than ICIs or CT, such as surgery, radiotherapy, antiangiogenesis, immune cells, and cancer vaccines, or currently unavailable drugs such as the anti-TIGIT antibody tiragolumab. Trials that only reported outcomes of maintenance therapy were also excluded.

Data Extraction and Risk of Bias Assessment

We extracted study name, first author, publication year, number and characteristics of patients, OS, PFS, objective response rate (ORR), and the incidence of grade 3 or higher adverse events (≥3AEs) related to treatments. For the same study that reported outcomes of different follow-up times, we extracted the most recent data.

We assessed the bias risk of RCTs using the Cochrane Risk of Bias Tool, including seven items: random sequence generation, allocation concealment, blinding of participants and personnel, blinding of outcome assessment, incomplete outcome data, selective outcome reporting, and other sources of bias (31). RCTs can be evaluated as low, high, or ambiguous risk of bias. Data extraction and risk of bias assessment were conducted by two independent investigators (QX and XZ).

Data Analysis

To judge the median OS (mOS) of each treatment tentatively, we performed pairwise meta-analyses with the frequentist method for head-to-head trials. Heterogeneity between studies was assessed using the Q test and I^2 statistics. The random model was used when $I^2 \geq 50$ or $p < 0.05$, in which heterogeneity was considered statistically significant (32).

For survival variables (OS/PFS) and binary variables (ORR/≥3AEs), HR or odds ratio (OR) and corresponding 95% CIs were pooled according to the fixed or random model, which were compared using deviance information criteria (DIC) (33). We used the JAGS and GEMTC package in R.3.6.1 for Bayesian NMA using a Markov Chain Monte Carlo simulation technique. For each outcome, 150,000 sample iterations were generated with 100,000 burn-ins and a thinning interval of 1. To ensure the convergence of the model, visual inspection methods of trace plots and Brooks–Gelman–Rubin diagnostic were adopted (34). We used Stata 16.0 to generate network plots, indicating more directly the relationships between treatments. For network consistency, node splitting analysis was used to evaluate the differences between direct and indirect comparisons in the closed loop of treatments. Transitivity was evaluated using visual graphics for patient characteristics between treatment groups and control groups, respectively. To estimate the probability of each treatment being at each rank, we calculated the surface under the cumulative ranking curve (SUCRA). The higher SUCRA value represents that a treatment is to be ranked on the top more likely (35).

RESULTS

Study Characteristics of Network Meta-Analysis

According to the study screening process in **Figure 1**, 20 RCTs were eligible for our NMA, including 13,032 patients and 17 different treatments. They are SICI regimens, including PEM (7, 8, 36), CEM (10), NIV (37), ATE (9), and DUR (28); SICI+CT regimens, including PEM+CT (11–16), sintilimab (SIN)+CT (19, 20), ATE+CT (21–24), IPI+CT (25, 26), camrelizumab (CAM)+CT (18), and NIV+CT (17); DICI regimens, including DUR+TRE (28) and NIV+IPI (27, 38); DICI+CT regimens, including DUR+TRE+CT (28, 30) and NIV+IPI+CT (29); and CT as control group, including CT with maintenance with pemetrexed (Mpem) and platinum-based doublet CT. The baseline characteristics of the studies were shown in **Table 1**.

The assumption of transitivity was accepted because no variability of population baselines was identified in the treatment group and control group among studies except for KEYNOTE 021 (11, 12), which showed a significant deviation of male proportion (**Supplementary Figure 1**). The risk of bias assessment was summarized in **Supplementary Figure 2**. Model convergence was established in accordance with trace plots and Brooks–Gelman–Rubin diagnostic (**Supplementary Figure 3**).

Integrated Analysis of Median Overall Survival

We firstly performed an integrated analysis of mOS in eligible studies to get a pooled OS of current treatment strategies for advanced wild-type NSCLC. The pooled mOS (POS) of ICI-based treatments was 15.79 months (95% CI: 14.85–16.73). The POS of SICI-based treatments was 16.17 months (95% CI: 14.59–17.74), with 15.32 months (95% CI: 13.28–17.36) for SICI and 16.56 months (95% CI: 14.32–18.81) for SICI+CT. The POS of DICI-based treatments was 14.81 months (95% CI: 12.11–17.52), with 14.05 months (95% CI: 10.04–18.07) for DICI and 16.07 months (95% CI: 13.84–18.29) for DICI+CT (**Figure 2C**).

Network Meta-Analysis of Overall Survival, Progression-Free Survival, Objective Response Rate, Grade 3 or Higher Adverse Events in the Overall Population

We first compared the difference in efficacy between SICI/DICI-based treatments and CT (**Figure 2A**). Both SICI-based (HR = 0.78, 95% CI: 0.72–0.85) and DICI-based (HR = 0.74, 95% CI:

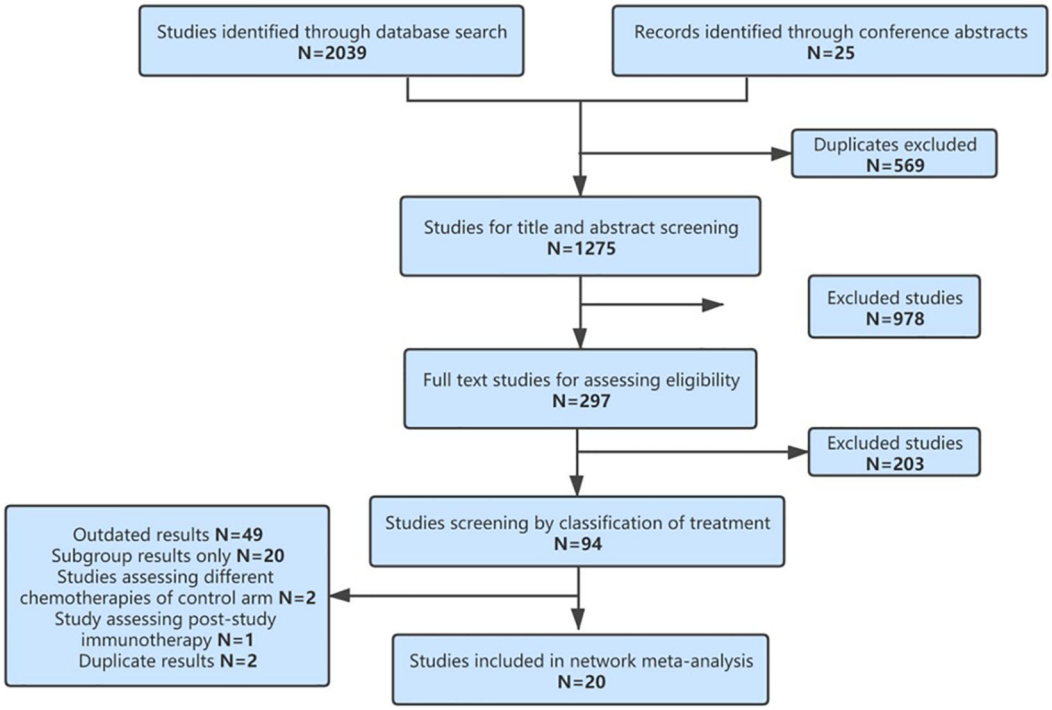

FIGURE 1 | Flowchart of study selection.

0.63–0.86) treatments showed significant benefits over CT in mOS, while only SICI-based treatments were superior to CT on median PFS (mPFS) (HR = 0.69, 95% CI: 0.60–0.78) and ORR (OR = 1.76, 95% CI: 1.43–2.18). There were no statistical differences in mOS, mPFS, ORR, and ≥3AEs between SICI-based and DICI-based treatments (**Figures 3A, B**).

We then compared the difference in efficacy among SICI, SICI+CT, DICI, DICI+CT, and CT (**Figure 2B**). For mOS, SICI (HR = 0.82, 95% CI: 0.73–0.93), DICI (HR = 0.77, 95% CI: 0.65–0.91), SICI+CT (HR = 0.76, 95% CI: 0.68–0.84), and DICI+CT (HR = 0.67, 95% CI: 0.52–0.86) showed better efficacy over that of CT, but there was no significant difference among the four treatments. For mPFS, SICI (HR = 0.82, 95% CI: 0.67–0.99), SICI +CT (HR = 0.63, 95% CI: 0.54–0.73), and DICI+CT (HR = 0.64, 95% CI: 0.44–0.94) showed significant advantages compared with CT; the efficacy of SICI (HR = 1.30, 95% CI: 1.02–1.65) and DICI (HR = 1.41, 95% CI: 1.06–1.88) was significantly lower than that of SICI+CT (**Figure 4A**).

For ORR, SICI+CT (OR = 2.07, 95% CI: 1.65–2.62) and DICI+CT (OR = 2.06, 95% CI: 1.10–3.86) showed superior efficacy over that of CT. In general, the ORRs of SICI (OR = 0.61, 95% CI: 0.42–0.89) and DICI (OR = 0.60, 95% CI: 0.38–0.94) were lower than that of SICI+CT (**Figure 4B**). In terms of ≥3AEs, those in SICI+CT and DICI+CT were markedly higher than those in SICI, DICI, and CT, while those in SICI and DICI were significantly lower than that in CT. In addition, the incidence of ≥3AEs was significantly lower in SICI compared with that in DICI (OR = 0.42, 95% CI: 0.35–0.51), while ≥3AEs in SICI+CT were significantly higher than that in DICI+CT (OR = 1.38, 95% CI: 1.02–1.86) (**Figure 4B**).

Network Meta-Analysis of Pathology Subgroup

In the squamous NSCLC subgroup, both SICI-based treatments and DICI-based treatments achieved significant OS advantages compared to CT only, while SICI-based treatments achieved significantly shorter mOS than that in DICI-based treatments (HR = 1.25, 95% CI: 1.01–1.54) (**Figure 3C** and **Supplementary Figure 4A**). SICI (HR = 0.73, 95% CI: 0.62–0.85), DICI (HR = 0.62, 95% CI: 0.49–0.78), SICI+CT (HR = 0.81, 95% CI: 0.73–0.89), and DICI+CT (HR = 0.64, 95% CI: 0.48–0.85) showed improved OS over that of CT. In the comparison of these four measures, the mOS of DICI was significantly longer than that of SICI+CT (HR = 0.77, 95% CI: 0.60–0.99) (**Figure 5A**). In terms of mPFS, SICI (HR = 0.57, 95% CI: 0.36–0.89) and SICI+CT (HR = 0.63, 95% CI: 0.45–0.82) showed significant benefits compared with that of CT (**Supplementary Figure 5A**). In non-squamous NSCLC, both SICI-based treatments and DICI-based treatments prolonged OS significantly compared with CT, with no difference between SICI-based and DICI-based treatments. SICI (HR = 0.80, 95% CI: 0.65–0.97), SICI+CT (HR = 0.74, 95% CI: 0.62–0.88), and DICI+CT (HR = 0.65, 95% CI: 0.46–0.92) showed significant OS advantages compared with CT, but DICI failed to prolong OS significantly *vs*. CT (HR = 0.79, 95% CI: 0.59–1.05) (**Figure 5A**); significant PFS benefits were achieved in SICI+CT (HR = 0.59,

TABLE 1 | Baseline characteristics of studies included in the network meta-analysis of patients with wild-type advanced non-small cell lung cancer.

Study name (year)	Phase	Population	Sample size	Median age	Male/Female	Intervention arm	Control arm
			SICI				
KEYNOTE 024 (2016/2019)	III	squ/non-squ PD-L1≥50%	154/151	65/66	187/118	PEM	CT
KEYNOTE 042 (2019)	III	squ/non-squ PD-L1≥1%	637/637	63/63	902/372	PEM	CT
IMpower 110 (2019)	III	squ/non-squ PD-L1≥1%	277/277	NG/NG	389/165	ATE	CT
MYSTIC (2020)	III	squ/non-squ	374/372	65/64	506/240	DUR	CT
CheckMate 026 (2017)	III	squ/non-squ PD-L1≥1%	271/270	63/65	332/209	NIV	CT
CheckMate 227 part1 (2019)	III	squ/non-squ PD-L1≥1%	396/397	64/64	532/261	NIV	CT
EMPOWER-LUNG1 (2020)	III	squ/non-squ	356/354	63/64	606/104	CEM	CT
			SICI+CT				
KEYNOTE 021G (2016/2019)	II	non-squ	60/63	63/63	48/75	PEM+CT	CT+Mpem
KEYNOTE 189 (2018/2020)	III	non-squ	410/206	65/64	363/253	PEM+CT	CT+Mpem
KEYNOTE 407 (2018/2020)	III	squ	278/281	65/65	455/104	PEM+CT	CT
IMpower 130 (2019)	III	non-squ	483/240	64/65	415/308	ATE+CT	CT
IMpower 132 (2018/2020)	III	non-squ	292/286	64/63	384/194	ATE+CT	CT+Mpem
IMpower 131 (2020)	III	squ	343/340	65/65	557/126	ATE+CT	CT
CAMEL (2019)	III	non-squ	205/207	59/61	295/117	CAM+CT	CT
ORIENT-12 (2020)	III	squ	179/178	64/62	327/50	SIN+CT	CT
ORIENT-11 (2020)	III	non-squ	266/131	61/61	303/94	SIN+CT	CT
CheckMate 227 part1 (2019)	III	squ/non-squ PD-L1<1%	177/186	64/64	255/108	NIV+CT	CT
CheckMate 227 part2 (2019)	III	squ/non-squ	377/378	63/64	528/227	NIV+CT	CT
Lynch (2012)	II	squ/non-squ	68/66	61/62	98/36	IPI+CT	CT
Govindan (2017)	III	squ	388/361	64/64	635/114	IPI+CT	CT
			DICI				
MYSTIC (2020)	III	squ/non-squ	372/372	66/64	516/228	DUR+TRE	CT
CheckMate 227 part1 (2019)	III	squ/non-squ PD-L1≥1%	396/397	64/64	515/278	NIV+IPI	CT
CheckMate 227 part1 (2019)	III	squ/non-squ PD-L1<1%	187/186	63/64	263/110	NIV+IPI	CT
			DICI+CT				
CheckMate 9LA (2020)	III	squ/non-squ	361/358	65/65	503/216	NIV+IPI+CT	CT
			Others				
CCTG BR.34 (2020)	III	squ/non-squ	151/150	65/63	162/139	DUR+TRE+CT	DUR+TRE

Data are expressed as intervention/control unless indicated otherwise.

Squ, squamous; Non-squ, non-squamous; NG, not given; PEM, pembrolizumab; CEM, cemiplimab; SIN, sintilimab; ATE, atezolizumab; NIV, nivolumab; DUR, durvalumab; TRE, tremelimumab; CAM, camrelizumab; IPI, ipilimumab; CT, chemotherapy; CT+Mpem, CT followed by maintenance with pemetrexed.

95% CI: 0.47–0.74) and DICI+CT (HR = 0.34, 95% CI: 0.13–0.84) (**Supplementary Figure 5A**).

Network Meta-Analysis of Programmed Death-Ligand 1 Expression Subgroup

In all PD-L1 expression subgroups, SICI-based and DICI-based treatments could prolong OS over CT (**Figures 3D, E**). In PD-L1 <1% subgroup, the OS of SICI-based treatments turned out to be significantly shorter than that in DICI-based treatments (HR = 1.23, 95% CI: 1.01–1.49) (**Figure 3D**). DICI (HR = 0.67, 95% CI: 0.55–0.81), SICI+CT (HR = 0.76, 95% CI: 0.68–0.85), and DICI+CT (HR = 0.62, 95% CI: 0.45–0.85) were obviously better than CT in mOS, while the efficacy of SICI was significantly worse than those of DICI (HR = 1.77, 95% CI: 1.22–2.58), SICI+CT (HR = 1.55, 95% CI: 1.11–2.17), and DICI+CT (HR = 1.90, 95% CI: 1.21–2.98) (**Figure 5B**). In terms of mPFS, DICI, SICI+CT, and DICI+CT also showed significant advantages over CT (**Supplementary Figure 5B**). In PD-L1 ≥1% subgroup, SICI (HR = 0.88, 95% CI: 0.81–0.95), DICI (HR = 0.88, 95% CI: 0.78–0.99), SICI+CT (HR = 0.72, 95% CI: 0.64–0.82), and DICI+CT (HR = 0.64, 95% CI: 0.50–0.82) all achieved obvious OS benefits compared with CT. In addition, both SICI+CT and DICI+CT were significantly better than SICI or DICI (**Figure 5B**). For mPFS, the advantages of DICI (HR = 0.82, 95% CI: 0.69–0.97), SICI+CT (HR = 0.53, 95% CI: 0.48–0.59), and DICI+CT (HR = 0.60, 95% CI: 0.40–0.91) over CT were maintained, while SICI could equally prolong OS compared with CT (HR = 1.00, 95% CI: 0.92–1.09). SICI+CT was superior to SICI and DICI, while DICI was significantly better than SICI (**Supplementary Figure 5B**).

In PD-L1 1%–49% subgroup, SICI+CT (HR = 0.77, 95% CI: 0.65–0.92) and DICI+CT (HR = 0.61, 95% CI: 0.44–0.84) had a significant OS advantage compared with CT. SICI (HR = 1.51, 95% CI: 1.06–2.15) and DICI (HR = 1.54, 95% CI: 1.05–2.26) had significantly worse mOS than that of DICI+CT. In addition, the effect of SICI+CT on mPFS was more prominent than those of SICI and CT (**Figure 5C** and **Supplementary Figure 5C**). In PD-L1 ≥50% subgroup, the OS benefits of SICI (HR = 0.71, 95% CI: 0.64–0.78), DICI (HR = 0.75, 95% CI: 0.62–0.90), SICI+CT (HR = 0.66, 95% CI: 0.54–0.81), and DICI+CT (HR = 0.58, 95% CI: 0.42–0.79) were conspicuous compared with that of CT, while all the differences disappeared within those four ICI-based therapies (**Figure 5C**). Besides, the mPFS of these four treatments was also significantly longer than that of CT, and the efficacy of SICI was significantly inferior to that of SICI+CT (HR = 1.74, 95% CI: 1.24–2.43) (**Supplementary Figure 5C**).

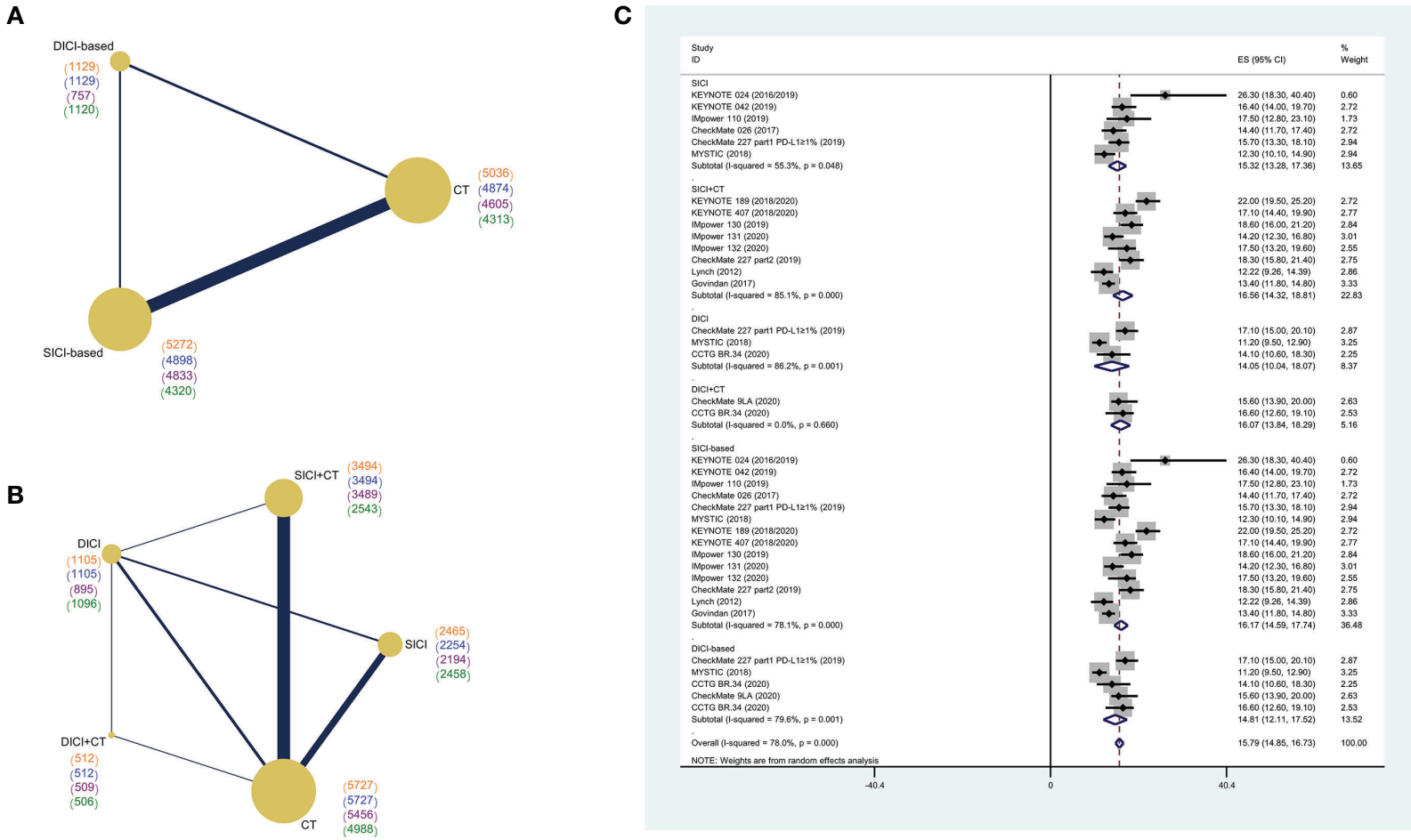

FIGURE 2 | Network diagram of comparisons on different outcomes of treatments and pooled estimates of median overall survival. **(A)** Network diagram of SICI or DICI-based treatments and CT. **(B)** Network diagram of SICI, DICI, SICI+CT, DICI+CT, and CT. Each circular node represents a type of treatment. The size of the nodes and the thickness of the lines are weighted according to the number of studies evaluating each treatment and direct comparison, respectively. The total number of patients receiving treatments was shown in brackets. Color "orange" for overall survival (OS), "blue" for progression-free survival (PFS), "purple" for objective response rate (ORR), "green" for adverse events of grade 3 or higher (≥3AEs). **(C)** Pooled median overall survival (POS) of treatments in the overall population. SICI-based, treatments including single immune checkpoint inhibitor; DICI-based, treatments including double immune checkpoint inhibitors; SICI, single immune checkpoint inhibitor; DICI, double immune checkpoint inhibitors; SICI+CT, single immune checkpoint inhibitor combined with chemotherapy; DICI+CT, double immune checkpoint inhibitors combined with chemotherapy; CT, chemotherapy.

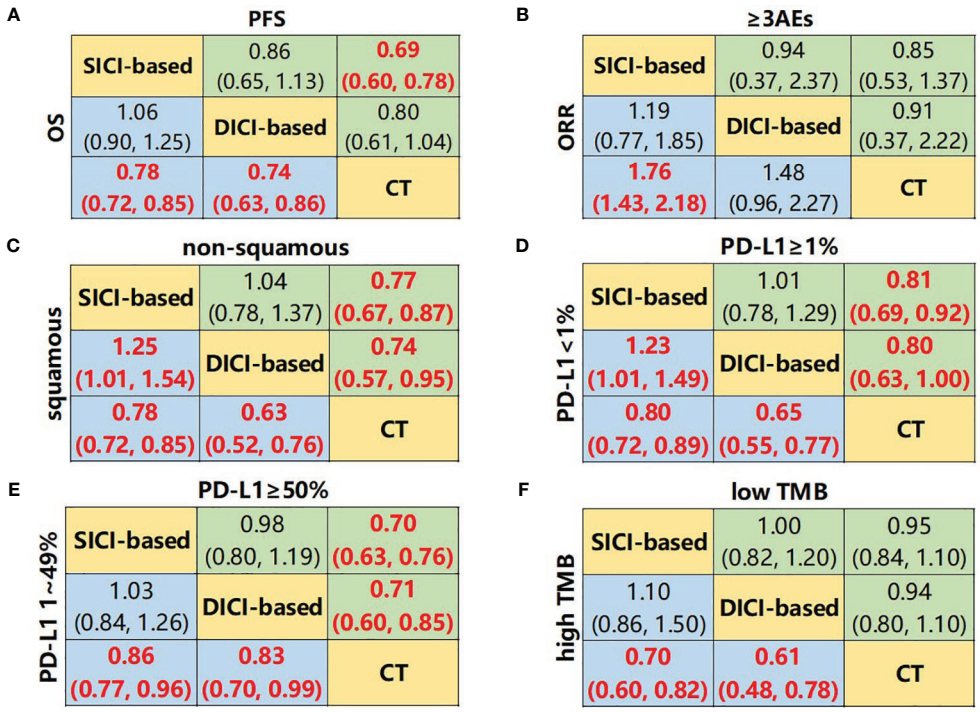

FIGURE 3 | Network meta-analysis composed of SICI- or DICI-based treatments and CT. **(A)** Pooled hazard ratio (HR) [95% CrIs (credible intervals)] for overall survival (OS) and progression-free survival (PFS) in the overall population. **(B)** Pooled odds ratio (OR) (95% CrIs) for objective response rate (ORR) and adverse events of grade 3 or higher (≥3AEs) in the overall population. **(C)** Pooled HR (95% CrIs) for OS of squamous and non-squamous subgroups. **(D)** Pooled HR (95% CrIs) for OS of PD-L1 <1% and PD-L1 ≥1% subgroups. **(E)** Pooled HR (95% CrIs) for OS of PD-L1 1%–49% and PD-L1 ≥50% subgroups. **(F)** Pooled HR (95% CrIs) for OS of high TMB and low TMB subgroups. Data in each cell are HR or OR (95% CrIs) for the comparison of upper row-defining treatment *vs*. lower row-defining treatment. HR less than 1 and OR more than 1 favor upper-row treatment. Significant results are highlighted in red and bold. SICI-based, treatments including single immune checkpoint inhibitor; DICI-based, treatment including double immune checkpoint inhibitors; CT, chemotherapy.

Network Meta-Analysis of Tumor Mutation Burden Subgroup

The superiority of SICI-based and DICI-based treatments over CT in OS and PFS was observed in the high TMB subgroup. However, there was no statistical difference between SICI and DICI. In the low TMB subgroup, there was also no statistical difference in mOS and mPFS between SICI-based or DICI-based treatments and CT (**Figure 3F** and **Supplementary Figure 4D**). In the high TMB populations, SICI, DICI, SICI+CT, and DICI+CT showed significant prolongation of both OS and PFS in contrast to those of CT (**Figure 5D** and **Supplementary Figure 5D**). In the low TMB populations, only SICI+CT showed a significant advantage over CT in mOS (HR = 0.75, 95% CI: 0.56–1.00) and mPFS (HR = 0.60, 95% CI: 0.46–0.77). In addition, the mPFS of SICI and DICI was statistically inferior to that of CT (**Figure 5D** and **Supplementary Figure 5D**).

Network Meta-Analysis of Smoking, Gender, Age, or Eastern Cooperative Oncology Group Subgroup

In smokers, all ICI-based measures significantly prolonged OS compared with CT, and SICI+CT was inferior to DICI+CT (HR = 1.28, 95% CI: 1.05–1.57) (**Supplementary Figure 6A**). In non-smokers, the four ICI-based strategies achieved equal outcomes on OS with CT (**Supplementary Figure 6B**). In males, they yielded superior OS than CT, while DICI is the same with DICI+CT (HR = 1.01, 95% CI: 0.82–1.26). DICI was significantly better than SICI; DICI and DICI+CT were also superior to SICI +CT (**Supplementary Figure 7A**).

DICI, SICI+CT, and DICI+CT all showed significant OS benefits compared with CT regardless of age (**Supplementary Figures 8A, B**). In patients <65 years old, the mOS of SICI+CT was significantly shorter than that of DICI+CT (HR = 1.29, 95% CI: 1.00–1.67) (**Supplementary Figure 8B**). In Eastern Cooperative Oncology Group performance status (ECOG PS) = 0 populations, DICI, SICI+CT, and DICI+CT obtained significantly longer mOS than CT, while DICI+CT dramatically reduced the risk of death by 52% (HR = 0.48, 95% CI: 0.32–0.72). When combined with CT, the efficacy of SICI+CT was significantly worse than that of DICI+CT (HR = 1.70, 95% CI: 1.10–2.63) (**Supplementary Figure 9A**). In the ECOG PS = 1 subgroup, SICI, DICI, SICI+CT, and DICI+CT all achieved significant OS benefits compared with CT, while there were no statistical differences among the four ICI-based measures (**Supplementary Figure 9B**).

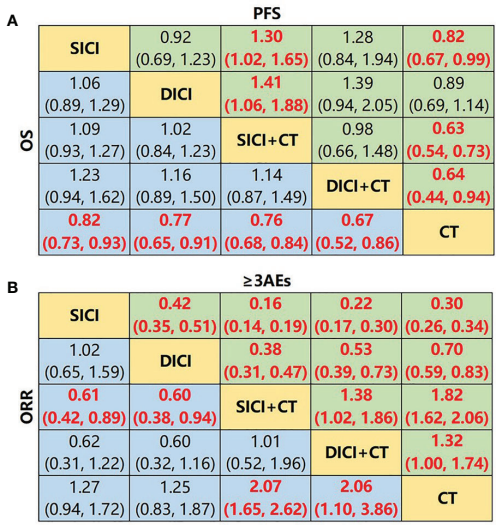

FIGURE 4 | Network meta-analysis of SICI, DICI, SICI+CT, DICI+CT, and CT. **(A)** Pooled hazard ratio (HR) [95% CrIs (credible intervals)] for overall survival (OS) and progression-free survival (PFS) in the overall population. **(B)** Pooled odds ratio (OR) (95% CrIs) for objective response rate (ORR) and adverse events of grade 3 or higher (≥3AEs) in the overall population. Data in each cell are HR or OR (95% CrIs) for the comparison of upper row-defining treatment *vs*. lower row-defining treatment. HR less than 1 and OR more than 1 favor upper-row treatment. Significant results are highlighted in red and bold. SICI, single immune checkpoint inhibitor; DICI, double immune checkpoint inhibitors; SICI+CT, single immune checkpoint inhibitor combined with chemotherapy; DICI+CT, double immune checkpoint inhibitors combined with chemotherapy; CT, chemotherapy.

Rank Probabilities

The Bayesian ranking curves of comparable treatments in different populations are shown in **Supplementary Figures S10A, B** (ranking profiles and corresponding SUCRA are shown in **Supplementary Figures 11A, B** and **Supplementary Figures 12A, B**). The result of Bayesian ranking is approximately consistent with NMA. Overall, DICI+CT was most likely to be ranked first for mOS; SICI+CT was ranked first for mPFS and ORR (**Supplementary Figure 10A**). In subgroup analysis, mOS of DICI+CT ranked first for squamous, non-squamous, any PD-L1 expression, smoking, males, ECOG PS = 0/1, age <65/≥65; SICI+CT for low TMB, non-smoking, and females; DICI for high TMB (**Supplementary Figures 11A, B**; **Supplementary Figures 12A, B**).

Inconsistency Assessment and Sensitivity Analyses

The fit of the consistency model in most comparisons was better than that of the inconsistency model, except for mOS (overall, non-squamous, females subgroups), mPFS (overall, squamous, non-squamous, PD-L1 ≥50% subgroups), and ORR, for which the random model was used (**Supplementary Table 3**). Inconsistency between direct and indirect comparisons using the node-splitting approach did not show significant differences in comparisons except for mOS and mPFS in the low TMB subgroup (**Supplementary Table 4**).

The populations of KEYNOTE 024, CheckMate 227, MYSTIC, IMpower 110, and EMPOWER-LUNG1 were all highly PD-L1 selected, which magnified the efficacy of SICI or DICI. Therefore, we conducted sensitivity analysis excluding

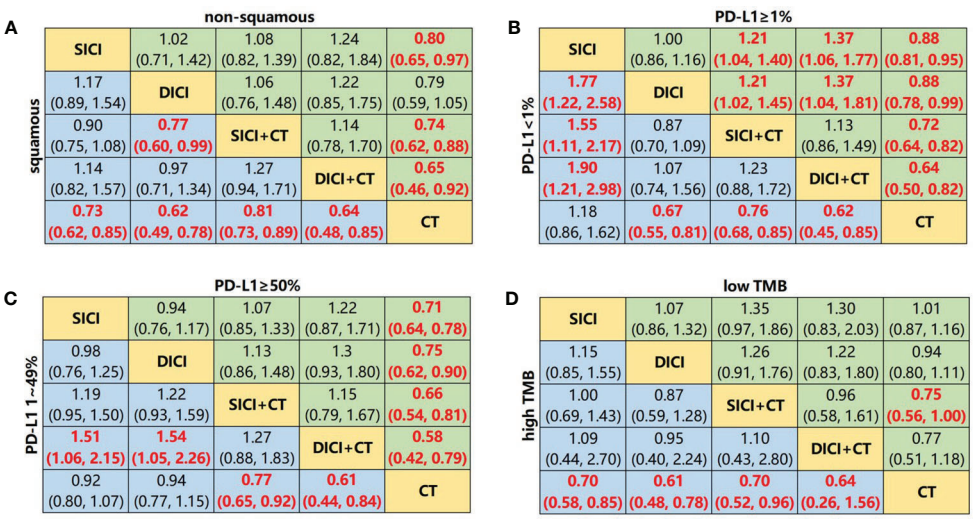

FIGURE 5 | Network meta-analysis for overall survival of subgroup analyses. **(A)** Pooled hazard ratio (HR) [95% CrIs (credible intervals)] for overall survival (OS) of squamous and non-squamous subgroups. **(B)** Pooled HR (95% CrIs) for OS of PD-L1 <1% and PD-L1 ≥1% subgroups. **(C)** Pooled HR (95% CrIs) for OS of PD-L1 1%–49% and PD-L1 ≥50% subgroups. **(D)** Pooled HR (95% CrIs) for OS of high TMB and low TMB subgroups. Data in each cell are HR (95% CrIs) for the comparison of upper row-defining treatment *vs*. lower row-defining treatment. HR less than 1 favors upper row-defining treatment. Significant results are highlighted in red and bold. SICI, single immune checkpoint inhibitor; DICI, double immune checkpoint inhibitors; SICI+CT, single immune checkpoint inhibitor combined with chemotherapy; DICI+CT, double immune checkpoint inhibitors combined with chemotherapy; CT, chemotherapy.

studies with highly selected populations in overall and squamous, non-squamous subgroups. Sensitivity analysis showed that the NMA results were relatively stable except for some small changes such as in mOS, SICI was significantly worse than SICI+CT (HR = 1.15, 95% CI: 1.04–1.28) and DICI+CT (HR = 1.29, 95% CI: 1.08–1.54); DICI was also inferior to DICI +CT (HR = 1.24, 95% CI: 1.04–1.47). In mPFS, both SICI (HR = 1.00, 95% CI: 0.82–1.23) and DICI (HR = 1.00, 95% CI: 0.78–1.28) were equally effective compared with CT, and the two treatments were inferior to ICI+CT (**Supplementary Figure 13A**). In the non-squamous subgroup, the significant OS advantage of SICI over CT disappeared, while SICI was significantly worse than CT on mPFS (**Supplementary Figures 13C, D**). In squamous NSCLC, DICI+CT replaced DICI to rank first on OS (**Supplementary Figure 14**).

Network Meta-Analysis of Specific Treatment Regimens

We compared the efficacy and safety of specific treatment regimens (**Supplementary Figure 15**). SICI-based regimens SIN+CT (HR = 0.59, 95% CI: 0.43–0.81), PEM+CT (HR = 0.67, 95% CI: 0.56–0.80), and CEM (HR = 0.68, 95% CI: 0.53–0.87) and DICI-based regimen NIV+IPI+CT (HR = 0.66, 95% CI: 0.55–0.80) significantly prolonged mOS compared with CT. For mPFS, SIN+CT, PEM+CT, CEM, and ATE+CT showed obvious advantages over CT ± Mpem. For ORR, PEM+CT and NIV+CT were superior to CT ± Mpem, while the advantages of SIN+CT over CT disappeared when compared with CT+Mpem. In terms of ≥3AEs, CT-free treatments showed markedly lower ≥3AEs than CT. Compared with CT, ≥3AEs in combination treatments were significantly higher except for DUR+TRE+CT (HR = 0.70, 95% CI: 0.33–1.51), PEM+CT (HR = 1.25, 95% CI: 0.92–1.70), and SIN+CT (HR = 1.19, 95% CI: 0.84–1.67) (**Supplementary Figures 16A, B**).

DISCUSSION

As mentioned above, to compare and evaluate the efficacy of SICI- and DICI-based therapies in advanced wild-type NSCLC, we performed an integrated analysis of survival outcomes and NMA among these first-line treatment strategies. Despite those negative primary endpoints of many ICI-related RCTs, we found that ICI-based therapies could provide a POS of nearly 16 months for overall patients with advanced NSCLC. Furthermore, both SICI-based therapies (POS: 16.17 months) and DICI-based therapies (POS: 14.81 months) had significant OS benefits compared with CT, without significant difference in mOS, mPFS, ORR, and ≥3AEs between the two ICI-based strategies. DICI-based therapies were significantly superior to SICI-based therapies in squamous and PD-L1 <1% subgroups on mOS. DICI was more effective than SICI in PD-L1 <1% and male subgroups. In subgroups such as smoking, male, age <65, ECOG PS = 0, DICI+CT obtained significantly longer OS than SICI+CT. Bayesian ranking spectrum showed that DICI+CT had the best OS advantage in the overall population and squamous, non-squamous, any PD-L1 level, smoking, male, ECOG PS = 0/1, <65/≥65 subgroups; SICI+CT ranked first in subgroups of low TMB, non-smoking, and female subgroups, while DICI ranked first in high TMB subgroups.

In our NMA, the overall efficacy of SICI-based and DICI-based therapies was consistent possibly due to the limited number of RCTs on DICI-based therapies with different conclusions. Notably, DICI-based therapies were significantly superior to SICI-based therapies in low immunogenicity subgroups (squamous or PD-L1 <1%), suggesting that dual-target interventions can improve the immune response by transforming the "cold" tumors to "hot" tumors and thereby lead to better efficacy. Interestingly, in populations with potentially high immune responses (smoking, male, <65, ECOG PS = 0), DICI+CT also brought more OS benefits than SICI+CT. In terms of specific treatment regimens, NIV+IPI, with or without CT, all obtained positive survival results and got Food and Drug Administration (FDA) approval, while DUR+TRE ± CT failed to replicate the success of NIV+IPI ± CT. So how to match the anti-PD-1/L1 and anti-CTLA-4 correctly is the key to get the most considerable benefit of DICI. Interestingly, when comparing anti-CTLA-4 plus anti-PD-1 therapy with anti-PD-1 monotherapy, we found that the OS of NIV+IPI was significantly higher than that of NIV monotherapy or DUR monotherapy, which is consistent with the finding of the previous study (39). However, the OS benefit of NIV+IPI *vs*. that of PEM monotherapy is comparable, manifesting that PEM may amplify the efficacy of SICI.

Obviously, further explorations are needed. The key to applying DICI-based treatments reasonably focuses on how to reduce the side effects of anti-CTLA-4 and maximize the efficacy and synergy of ICIs combined with CT. Although the current exploration of DICI-based regimens is still insufficient, with the increasing number of related studies and the effective control of drug dose and toxicities, such strategy possesses great potential to improve the survival of patients with advanced NSCLC to a large extent. For example, some novel anti-PD-L1 antibodies, such as M7824 (40) and YM101 (41), exhibited broader ranges of antitumor spectrum compared to the SICI recently. These biologicals simultaneously blocked transforming growth factor (TGF)-β and PD-L1 pathways, or targeted some new immune checkpoints other than PD-1/L1 or CTLA-4, thus having potential to overcome resistance to SICIs or the present DICI treatment in future clinical practices.

We found that SICI-based therapies also obtained satisfactory results. Due to a large number of such studies and participants involved, the integrated results and NMA comparison were more reliable and robust. Based on the current comparative results, SICI-based therapies, especially SICI+CT, were the first-line treatment regimen with definite efficacy and tolerable side effects. In terms of specific treatment regimens, SIN+CT and PEM+CT ranked in the top on OS, with equal ≥3AEs to that of CT alone. Therefore, SICI+CT is currently the most practical treatment for the unscreened population. How to optimize the period and duration of medication to achieve the unity of efficacy improvement and side effect reduction remains a key problem to be resolved.

Our study also has several limitations. First, some studies were classified as moderate or high risk of bias because of inadequate randomization, allocation concealment, and blinding. Second, although all the studies in our analysis included patients with advanced wild-type NSCLC, some studies included a few patients with driver-gene mutated NSCLC. Thirdly, mOS data in some studies were immature and were extracted or calculated from interim analysis or the latest meeting abstracts. Fourth, it is not possible to compare all treatment strategies in each subgroup due to the limited availability of outcomes. For example, the comparison of mPFS in the PD-L1 1%–49% subgroup lacked data on DICI-based therapies. Fifth, the prediction of SUCRA for treatment strategy ranking is not absolute; when SUCRA prediction contradicts NMA results, the HR estimation of NMA should be given priority. Finally, due to the limited number of RCTs and participants involved in DICI-based therapies, the reliability and robustness of related NMA results and conclusions need to be further verified.

CONCLUSIONS

In the first-line therapy for advanced wild-type NSCLC, both SICI-based and DICI-based treatments could bring significant overall advantages *vs*. CT, with comparable outcomes for mOS and ≥3AEs. DICI-based treatments were more effective than SICI-based treatments in squamous and PD-L1 <1% subgroups, while DICI in combination with CT could be the best first-line choice for most populations. We need more research to further evaluate the efficacy and safety of DICI-based treatments. At the same time, SICI-based therapies have established their position in the current first-line treatment. In addition, NMA and ranking possibilities of specific regimens could provide strong evidence for clinical selection of individualized treatment regimens to maximize survival benefits for related patients.

DATA AVAILABILITY STATEMENT

The raw data supporting the conclusions of this article will be made available by the authors, without undue reservation.

AUTHOR CONTRIBUTIONS

LL is the corresponding author. QX and XZ are joint first authors. LL contributed to the study concept and design. QX and XZ took part in the initial literature search and assessed the eligibilities of feasible studies. QX and XZ interpreted the findings and wrote the first draft of the manuscript. QX, XZ, MH, XD, JG, LS, SL, KH, and JW prepared the figures and tables. LL revised and edited the manuscript. All authors approved the final version of the manuscript. LL is the guarantor of this study and accepts full responsibility for the work, had access to the data, and controlled the decision to publish. The corresponding authors attest that all listed authors meet authorship criteria and that no other person meeting the criteria has been omitted. All authors contributed to the article and approved the submitted version.

FUNDING

This work was supported by the National Natural Science Foundation of China (81172487 to LL and 81500092 to SL), Natural Science Foundation of Shandong Province (ZR2017MH005 to LL), and Foundation of Shandong University Clinical Research Center (2020SDUCRCC011).

SUPPLEMENTARY MATERIAL

The Supplementary Material for this article can be found online at: https://www.frontiersin.org/articles/10.3389/fimmu.2021.731546/full#supplementary-material

REFERENCES

1. Bray F, Ferlay J, Soerjomataram I, Siegel RL, Torre LA, Jemal A. Global Cancer Statistics 2018: GLOBOCAN Estimates of Incidence and Mortality Worldwide for 36 Cancers in 185 Countries. *CA Cancer J Clin* (2018) 68:394–424. doi: 10.3322/caac.21492
2. Herbst RS, Morgensztern D, Boshoff C. The Biology and Management of non-Small Cell Lung Cancer. *Nature* (2018) 553:446–54. doi: 10.1038/nature25183
3. Lamberti G, Andrini E, Sisi M, Rizzo A, Parisi C, Di Federico A, et al. Beyond EGFR, ALK and ROS1: Current Evidence and Future Perspectives on Newly Targetable Oncogenic Drivers in Lung Adenocarcinoma. *Crit Rev Oncol Hematol* (2020) 156:103119. doi: 10.1016/j.critrevonc.2020.103119
4. Goldstraw P, Chansky K, Crowley J, Rami-Porta R, Asamura H, Eberhardt WE, et al. The IASLC Lung Cancer Staging Project: Proposals for Revision of the TNM Stage Groupings in the Forthcoming (Eighth) Edition of the TNM Classification for Lung Cancer. *J Thorac Oncol* (2016) 11:39–51. doi: 10.1016/j.jtho.2015.09.009
5. Iwai Y, Ishida M, Tanaka Y, Okazaki T, Honjo T, Minato N. Involvement of PD-L1 on Tumor Cells in the Escape From Host Immune System and Tumor Immunotherapy by PD-L1 Blockade. *Proc Natl Acad Sci U S A* (2002) 99:12293–7. doi: 10.1073/pnas.192461099
6. Nasser NJ, Gorenberg M, Agbarya A. First Line Immunotherapy for Non-Small Cell Lung Cancer. *Pharmaceut (Basel)* (2020) 13:373. doi: 10.3390/ph13110373
7. Reck M, Rodríguez-Abreu D, Robinson AG, Hui R, Csőszi T, Fülöp A, et al. Pembrolizumab *Versus* Chemotherapy for PD-L1-Positive Non-Small-Cell Lung Cancer. *N Engl J Med* (2016) 375:1823–33. doi: 10.1056/NEJMoa1606774
8. Reck M, Rodríguez-Abreu D, Robinson AG, Hui R, Csőszi T, Fülöp A, et al. Updated Analysis of KEYNOTE-024: Pembrolizumab *Versus* Platinum-Based Chemotherapy for Advanced Non-Small-Cell Lung Cancer With PD-L1 Tumor Proportion Score of 50% or Greater. *J Clin Oncol* (2019) 37:537–46. doi: 10.1200/JCO.18.00149
9. Herbst RS, Giaccone G, de Marinis F, Reinmuth N, Vergnenegre A, Barrios CH, et al. Atezolizumab for First-Line Treatment of PD-L1-Selected Patients with NSCLC. *N Engl J Med* (2020) 383:1328–39. doi: 10.1056/NEJMoa1917346
10. Sezer A, Kilickap S, Gümüş M, Bondarenko I, Özgüroğlu M, Gogishvili M, et al. LBA52 EMPOWER-Lung 1: Phase III First-Line (1L) Cemiplimab Monotherapy *vs* Platinum-Doublet Chemotherapy (Chemo) in Advanced Non-Small Cell Lung Cancer (NSCLC) With Programmed Cell Death-Ligand 1 (PD-L1) ≥50%. *Ann Oncol Annals Oncol* (2020) 31:S1182. doi: 10.1016/j.annonc.2020.08.2285
11. Langer CJ, Gadgeel SM, Borghaei H, Papadimitrakopoulou VA, Patnaik A, Powell SF, et al. Carboplatin and Pemetrexed With or Without Pembrolizumab for Advanced, non-Squamous non-Small-Cell Lung Cancer:

A Randomised, Phase 2 Cohort of the Open-Label KEYNOTE-021 Study. *Lancet Oncol* (2016) 17:1497–508. doi: 10.1016/S1470-2045(16)30498-3
12. Borghaei H, Langer CJ, Gadgeel S, Papadimitrakopoulou VA, Patnaik A, Powell SF, et al. 24-Month Overall Survival From KEYNOTE-021 Cohort G: Pemetrexed and Carboplatin With or Without Pembrolizumab as First-Line Therapy For Advanced Nonsquamous Non-Small Cell Lung Cancer. *J Thorac Oncol* (2019) 14:124–9. doi: 10.1016/j.jtho.2018.08.004
13. Gandhi L, Rodríguez-Abreu D, Gadgeel S, Esteban E, Felip E, De Angelis F, et al. Pembrolizumab Plus Chemotherapy in Metastatic Non-Small-Cell Lung Cancer. *N Engl J Med* (2018) 378:2078–92. doi: 10.1056/NEJMoa1801005
14. Gadgeel S, Rodríguez-Abreu D, Speranza G, Esteban E, Felip E, Dómine M, et al. Updated Analysis From KEYNOTE-189: Pembrolizumab or Placebo Plus Pemetrexed and Platinum for Previously Untreated Metastatic Nonsquamous Non-Small-Cell Lung Cancer. *J Clin Oncol* (2020) 38:1505–17. doi: 10.1200/JCO.19.03136
15. Paz-Ares L, Luft A, Vicente D, Tafreshi A, Gümüş M, Mazières J, et al. Pembrolizumab Plus Chemotherapy for Squamous Non-Small-Cell Lung Cancer. *N Engl J Med* (2018) 379:2040–51. doi: 10.1056/NEJMoa1810865
16. Paz-Ares L, Vicente D, Tafreshi A, Robinson A, Soto Parra H, Mazières J, et al. A Randomized, Placebo-Controlled Trial of Pembrolizumab Plus Chemotherapy in Patients With Metastatic Squamous NSCLC: Protocol-Specified Final Analysis of KEYNOTE-407. *J Thorac Oncol* (2020) 15:1657–69. doi: 10.1016/j.jtho.2020.06.015
17. Paz-Ares TEC L, Yu ea X. Nivolumab (NIVO) 1 Platinum-Doublet Chemotherapy (Chemo) *vs* Chemo as First-Line (1L) Treatment (Tx) for Advanced non-Small Cell Lung Cancer (aNSCLC): CheckMate 227 - Part 2 Final Analysis. *Ann Oncol* (2019) 30:xi67. doi: 10.1093/annonc/mdz453
18. Zhou GC C, Huang ea Y. A Randomized Phase 3 Study of Camrelizumab Plus Chemotherapy as 1st Line Therapy for Advanced/Metastatic Non-Squamous Non-Small Cell Lung Cancer. *J Thorac Oncol* (2019) 14:305–14. doi: 10.1016/S2213-2600(20)30365-9
19. Yang Y, Wang Z, Fang J, Yu Q, Han B, Cang S, et al. Efficacy and Safety of Sintilimab Plus Pemetrexed and Platinum as First-Line Treatment for Locally Advanced or Metastatic Nonsquamous NSCLC: A Randomized, Double-Blind, Phase 3 Study (Oncology Program by InnovENT Anti-PD-1-11). *J Thorac Oncol* (2020) 15:1636–46. doi: 10.1016/j.jtho.2020.07.014
20. Zhou C, Wu L, Fan Y, Wang Z, Liu L, Chen G, et al. LBA56 ORIENT-12: Sintilimab Plus Gemcitabine and Platinum (GP) as First-Line (1L) Treatment for Locally Advanced or Metastatic Squamous Non-Small-Cell Lung Cancer (sqNSCLC). *Ann Oncol* (2020) 31:S1186. doi: 10.1016/j.annonc.2020.08.2289
21. West H, McCleod M, Hussein M, Morabito A, Rittmeyer A, Conter HJ, et al. Atezolizumab in Combination With Carboplatin Plus Nab-Paclitaxel Chemotherapy Compared With Chemotherapy Alone as First-Line Treatment for Metastatic Non-Squamous Non-Small-Cell Lung Cancer (IMpower130): A Multicentre, Randomised, Open-Label, Phase 3 Trial. *Lancet Oncol* (2019) 20:924–37. doi: 10.1016/S1470-2045(19)30167-6
22. Jotte R, Cappuzzo F, Vynnychenko I, Stroyakovskiy D, Rodríguez-Abreu D, Hussein M, et al. Atezolizumab in Combination With Carboplatin and Nab-Paclitaxel in Advanced Squamous NSCLC (IMpower131): Results From a Randomized Phase III Trial. *J Thorac Oncol* (2020) 15:1351–60. doi: 10.1016/j.jtho.2020.03.028
23. Papadimitrakopoulou V CM, Bordoni R. IMpower132: PFS and Safety Results With 1L Atezolizumab + Carboplatin/Cisplatin + Pemetrexed in Stage IV Non-Squamous NSCLC. *J Thorac Oncol* (2018) 13:S332. doi: 10.1016/j.jtho.2018.08.262
24. Nishio M, Barlesi F, Ball S, Bordoni R, Cobo M, Dubray-Longeras P, et al. 375o Final Efficacy Results From IMpower132: First-Line Atezolizumab + Chemotherapy in Patients With Stage IV Non-Squamous NSCLC. *Ann Oncol* (2020) 31:S1386. doi: 10.1016/j.annonc.2020.10.369
25. Govindan R, Szczesna A, Ahn MJ, Schneider CP, Gonzalez Mella PF, Barlesi F, et al. Phase III Trial of Ipilimumab Combined With Paclitaxel and Carboplatin in Advanced Squamous Non-Small-Cell Lung Cancer. *J Clin Oncol* (2017) 35:3449–57. doi: 10.1200/JCO.2016.71.7629
26. Lynch TJ, Bondarenko I, Luft A, Serwatowski P, Barlesi F, Chacko R, et al. Ipilimumab in Combination With Paclitaxel and Carboplatin as First-Line Treatment in Stage IIIB/IV non-Small-Cell Lung Cancer: Results From a Randomized, Double-Blind, Multicenter Phase II Study. *J Clin Oncol* (2012) 30:2046–54. doi: 10.1200/JCO.2011.38.4032
27. Hellmann MD, Paz-Ares L, Bernabe Caro R, Zurawski B, Kim SW, Carcereny Costa E, et al. Nivolumab Plus Ipilimumab in Advanced Non-Small-Cell Lung Cancer. *N Engl J Med* (2019) 381:2020–31. doi: 10.1056/NEJMoa1910231
28. Rizvi NA, Cho BC, Reinmuth N, Lee KH, Luft A, Ahn MJ, et al. Durvalumab With or Without Tremelimumab *vs* Standard Chemotherapy in First-Line Treatment of Metastatic Non-Small Cell Lung Cancer: The MYSTIC Phase 3 Randomized Clinical Trial. *JAMA Oncol* (2020) 6:661–74. doi: 10.1001/jamaoncol.2020.0237
29. Reck M, Manuel Cobo Dols MS, Bogdan Zurawski JM, Eduardo Richardet JB, Enriqueta Felip OJ, Aurella Alexandru HS, et al. Nivolumab + Ipilimumab + 2 Cycles of Platinum Doublet Chemotherapy *vs* 4 Cycles Chemo as First-Line Treatment Forstage IV non Small Cell Lung Cancer :CheckMate 9la. *J Clin Oncol* (2020) 38:suppl 9501-9501. doi: 10.1200/JCO.2020.38.15_suppl.9501
30. Natasha B, Leighl SAL, Glenwood D, Goss BGMH, Martin R, Stockler MST, et al. CCTG BR.34: A Randomized Trial of Durvalumab and Tremelimumab +/- Platinum-Based Chemotherapy in Patients With Metastatic (Stage IV) Squamous or Nonsquamous Non-Small Cell Lung Cancer (NSCLC). *J Clin Oncol* (2020) 38:9502. doi: 10.1200/JCO.2020.38.15_suppl.9502
31. Nasser M. Cochrane Handbook for Systematic Reviews of Interventions. *Am J Public Health* (2020) 110:753–4. doi: 10.2105/AJPH.2020.305609
32. Higgins JP, Thompson SG, Deeks JJ, Altman DG. Measuring Inconsistency in Meta-Analyses. *BMJ* (2003) 327:557–60. doi: 10.1136/bmj.327.7414.557
33. Dias S, Welton NJ, Caldwell DM, Ades AE. Checking Consistency in Mixed Treatment Comparison Meta-Analysis. *Stat Med* (2010) 29:932–44. doi: 10.1002/sim.3767
34. Brooks S. General Methods for Monitoring Convergence of Iterative Simulations. *J Comput Graphical Stat* (1998) 7:434–55. doi: 10.1080/10618600.1998.10474787
35. Salanti G, Ades AE, Ioannidis JP. Graphical Methods and Numerical Summaries for Presenting Results From Multiple-Treatment Meta-Analysis: An Overview and Tutorial. *J Clin Epidemiol* (2011) 64:163–71. doi: 10.1016/j.jclinepi.2010.03.016
36. Mok T, Wu YL, Kudaba I, Kowalski DM, Cho BC, Turna HZ, et al. Pembrolizumab *Versus* Chemotherapy for Previously Untreated, PD-L1-Expressing, Locally Advanced or Metastatic Non-Small-Cell Lung Cancer (KEYNOTE-042): A Randomised, Open-Label, Controlled, Phase 3 Trial. *Lancet* (2019) 393:1819–30. doi: 10.1016/S0140-6736(18)32409-7
37. Carbone DP, Reck M, Paz-Ares L, Creelan B, Horn L, Steins M, et al. First-Line Nivolumab in Stage IV or Recurrent Non-Small-Cell Lung Cancer. *N Engl J Med* (2017) 376:2415–26. doi: 10.1056/NEJMoa1613493
38. Hellmann MD, Ciuleanu TE, Pluzanski A, Lee JS, Otterson GA, Audigier-Valette C, et al. Nivolumab Plus Ipilimumab in Lung Cancer With a High Tumor Mutational Burden. *N Engl J Med* (2018) 378:2093–104. doi: 10.1056/NEJMoa1801946
39. Wu K, Yi M, Qin S, Chu Q, Zheng X, Wu K. The Efficacy and Safety of Combination of PD-1 and CTLA-4 Inhibitors: A Meta-Analysis. *Exp Hematol Oncol* (2019) 8:26. doi: 10.1186/s40164-019-0150-0
40. Lan Y, Zhang D, Xu C, Hance KW, Marelli B, Qi J, et al. Enhanced Preclinical Antitumor Activity of M7824, a Bifunctional Fusion Protein Simultaneously Targeting PD-L1 and TGF-β. *Sci Transl Med* (2018) 10:eaan5488. doi: 10.1126/scitranslmed.aan5488
41. Yi M, Zhang J, Li A, Niu M, Yan Y, Jiao Y, et al. The Construction, Expression, and Enhanced Anti-Tumor Activity of YM101: A Bispecific Antibody Simultaneously Targeting TGF-β and PD-L1. *J Hematol Oncol* (2021) 14:27. doi: 10.1186/s13045-021-01045-x

Conflict of Interest: The authors declare that the research was conducted in the absence of any commercial or financial relationships that could be construed as a potential conflict of interest.

Publisher's Note: All claims expressed in this article are solely those of the authors and do not necessarily represent those of their affiliated organizations, or those of the publisher, the editors and the reviewers. Any product that may be evaluated in this article, or claim that may be made by its manufacturer, is not guaranteed or endorsed by the publisher.

Copyright © 2021 Xu, Zhang, Huang, Dai, Gao, Li, Sheng, Huang, Wang and Liu. This is an open-access article distributed under the terms of the Creative Commons Attribution License (CC BY). The use, distribution or reproduction in other forums is permitted, provided the original author(s) and the copyright owner(s) are credited and that the original publication in this journal is cited, in accordance with accepted academic practice. No use, distribution or reproduction is permitted which does not comply with these terms.

frontiers in Immunology

ORIGINAL RESEARCH
published: 26 August 2021
doi: 10.3389/fimmu.2021.724464

Predictive Value of Metabolic Parameters Derived From ^{18}F-FDG PET/CT for Microsatellite Instability in Patients With Colorectal Carcinoma

Hao Liu[1,2†], Zheng Ye[1†], Ting Yang[1†], Hongjun Xie[2], Ting Duan[1], Mou Li[1], Min Wu[1] and Bin Song[1*]*

[1] Department of Radiology, West China Hospital, Sichuan University, Chengdu, China, [2] Department of Nuclear Medicine, Sichuan Academy of Medical Sciences, Sichuan Provincial People's Hospital, Chengdu, China

OPEN ACCESS

Edited by:
Udo S. Gaipl, University Hospital Erlangen, Germany

Reviewed by:
Junqiang Lei, First Hospital of Lanzhou University, China
Peng Zhou, Sichuan Cancer Hospital, China

***Correspondence:**
Min Wu
wuminscu@scu.edu.cn
Bin Song
songlab_radiology@163.com

†These authors have contributed equally to this work and share first authorship

Specialty section:
This article was submitted to Cancer Immunity and Immunotherapy, a section of the journal Frontiers in Immunology

Received: *16 June 2021*
Accepted: *02 August 2021*
Published: *26 August 2021*

Citation:
Liu H, Ye Z, Yang T, Xie H, Duan T, Li M, Wu M and Song B (2021) Predictive Value of Metabolic Parameters Derived From ^{18}F-FDG PET/CT for Microsatellite Instability in Patients With Colorectal Carcinoma. Front. Immunol. 12:724464. doi: 10.3389/fimmu.2021.724464

Background: Microsatellite instability (MSI) is one of the important factors that determine the effectiveness of immunotherapy in colorectal cancer (CRC) and serves as a prognostic biomarker for its clinical outcomes.

Purpose: To investigate whether the metabolic parameters derived from ^{18}F-fluorodeoxyglucose (^{18}F-FDG) positron emission tomography/computed tomography (PET/CT) can predict MSI status in patients with CRC.

Materials and Methods: A retrospective analysis was performed on CRC patients who underwent ^{18}F-FDG PET/CT examination before surgery between January 2015 and April 2021. The metabolic ^{18}F-FDG PET/CT parameters of the primary CRC lesion were calculated and recorded with different thresholds, including the maximum, peak, and mean standardized uptake value (SUV_{max}, SUV_{peak}, and SUV_{mean}), as well as the metabolic tumor volume (MTV) and the total lesion glycolysis (TLG). The status of MSI was determined by immunohistochemical assessment. The difference of quantitative parameters between MSI and microsatellite stability (MSS) groups was assessed, and the receiver operating characteristic (ROC) analyses with area under ROC curves (AUC) was used to evaluate the predictive performance of metabolic parameters.

Results: A total of 44 patients (24 men and 20 women; mean ± standard deviation age: 71.1 ± 14.2 years) were included. There were 14 patients in the MSI group while there were 30 in the MSS group. $MTV_{30\%}$, $MTV_{40\%}$, $MTV_{50\%}$, and $MTV_{60\%}$, as well as $TLG_{50\%}$ and $TLG_{60\%}$ showed significant difference between two groups (all p-values <0.05), among which $MTV_{50\%}$ demonstrated the highest performance in the prediction of MSI, with an AUC of 0.805 [95% confidence interval (CI): 0.657–0.909], a sensitivity of 92.9% (95% CI: 0.661–0.998), and a specificity of 66.7% (95% CI: 0.472–0.827). Patients' age and $MTV_{50\%}$ were significant predictive indicators of MSI in multivariate logistic regression.

Conclusion: The metabolic parameters derived from ^{18}F-FDG PET/CT were able to preoperatively predict the MSI status in CRC, with $MTV_{50\%}$ demonstrating the highest predictive performance. PET/CT imaging could serve as a noninvasive tool in the guidance of immunotherapy and individualized treatment in CRC patients.

Keywords: PET/CT, metabolism, colorectal carcinoma, microsatellite instability, immunotherapy

INTRODUCTION

Colorectal cancer (CRC) is the third most common cancer and one of the major causes of cancer-associated mortality worldwide (1). Multiple treatments for primary and metastatic CRC have emerged, which includes curative surgery, radiotherapy, neoadjuvant chemotherapy, and immunotherapy (2). Immunotherapy is a treatment option that utilizes the body's own immune system to attack cancer cells (3). Blocking immune checkpoints is currently one of the most promising approaches to activate therapeutic anti-tumor immunity and has shown encouraging results in CRC therapy (4).

However, the strong heterogeneity of CRC often leads to different prognosis and clinical outcome in patients who received similar treatment (5). As previously reported, chromosomal and genetic alterations that occur during the pathogenesis of CRC may be one of the contributing factors of heterogeneity (6). Microsatellites are short tandem repeat DNA sequences of one to three base pairs distributed throughout the human genome. Owing to their repeated structure, microsatellites are particularly prone to replication errors that are normally repaired by the mismatch repair (MMR) system. Microsatellite instability (MSI), caused by the absence of one or more MMR genes, has been considered as a reliable biomarker in the prediction of treatment response and prognosis in patients with CRC. Passardi et al. found that CRC with MSI selectively displayed highly upregulated expression of multiple immune checkpoints, including programmed death-1 (PD-1) and programmed death-ligand 1 (PD-L1) (7). In other words, CRC with MSI seem to be particularly responsive to immunotherapy, such as anti-PD-1 or anti-PD-L1 drugs. Moreover, MSI was identified as an important indicator in the selection of chemotherapy drugs of CRC (8). Recent studies showed that CRC with MSI was resistant to 5-fluorouracil (5-FU) chemotherapy and did not benefit from it (9). Typically speaking, MSI status is assessed with pathological specimen after surgery or biopsy, which is invasive and subject to sampling error (10). Therefore, a noninvasive method is urgently needed to preoperatively evaluate the MSI status and better facilitate the immunotherapy of CRC patients.

Medical imaging can capture information about the heterogeneity of the entire tumor noninvasively and could well predict tumor subtypes and the sensitivity of immunotherapy (11, 12). Moreover, imaging biomarkers were reported to be one of the effective indicators for predicting MSI expression in CRC (13–15). Wu et al. found that the quantitative imaging features derived from dual-energy computed tomography (DECT) showed good predictive performance for MSI status in CRC patients (13). In addition, radiomics-based artificial intelligence (AI), such as MRI-based deep learning models, also demonstrated optimal diagnostic capability for discriminating MSI from microsatellite stability (MSS) (14). However, the abovementioned studies either failed to reflect tumor metabolism or entailed complicated procedure, which was unavailable in clinical practice yet. Positron emission tomography/computed tomography (PET/CT) is a molecular imaging technique that can reflect tumor microenvironment and metabolic information with clinical radiotracer, such as ^{18}F-fluorodeoxyglucose (^{18}F-FDG) (16). A recent study showed that glucose metabolic response could predict anti-PD-1 therapeutic response in lung cancer (17). However, the role of metabolic parameters in CRC and MSI predictions remained unknown. Therefore, the purpose of this study was to investigate whether metabolic parameters derived from ^{18}F-FDG PET/CT can predict MSI status in patients with CRC.

MATERIALS AND METHODS

Patients

This retrospective study was approved by the Institutional Review Board of our institution, and the written informed consent was waived. We screened the medical records of patients who underwent preoperative ^{18}F-FDG PET/CT followed by curative operations for CRC at our institution between January 2015 and April 2021. Detailed inclusion criteria were as follows: patients with (a) primary colorectal lesions diagnosed as colorectal adenocarcinoma by pathology; (b) complete preoperative whole body ^{18}F-FDG PET/CT images before surgery within 3 months; (c) adequate immunohistochemical staining for the assessment of MMR protein expression.

We initially included 92 patients, and patients (a) who received neoadjuvant chemoradiotherapy (CRT) before ^{18}F-FDG PET/CT examination (n = 10); (b) without complete surgical pathology records (n = 27) or immunohistochemical assessment (n = 2); and (c) diagnosed as other pathological types (n = 9) were excluded (**Figure 1**).

PET/CT Acquisition Protocol

All patients were asked to fast at least 8 h before the examination. In patients with diabetes, antihyperglycemic drugs were requested to stop for 12 h before the exam. The blood glucose of patients was tested before the injection of ^{18}F-FDG, and the blood glucose level was required to be lower than 8 mmol/L. Patients were intravenously administered 5.5 MBq/kg ^{18}F-FDG and received PET/CT examination after1 h rest.

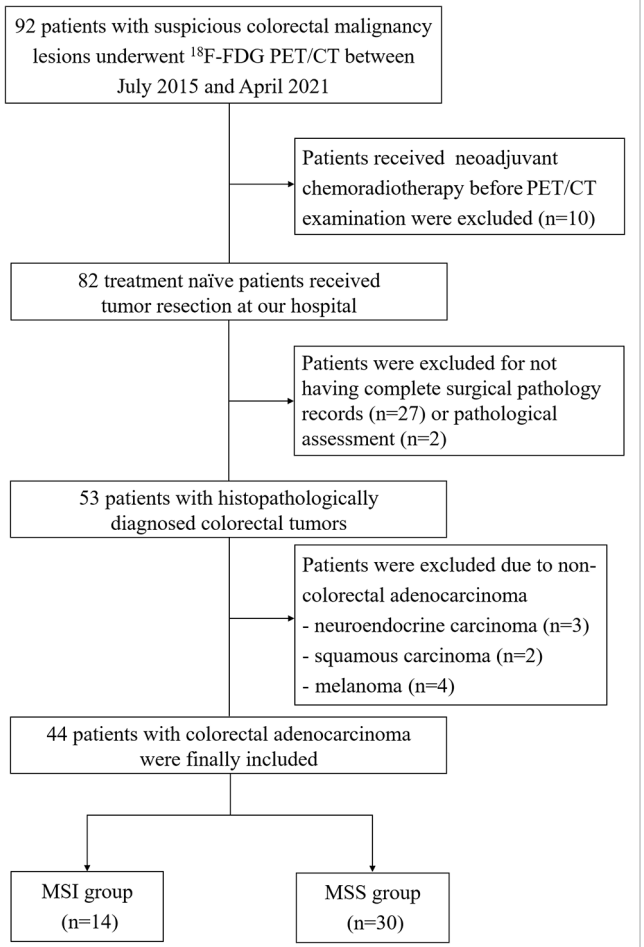

FIGURE 1 | The flowchart of patient inclusion and exclusion.

PET/CT examination was performed with a hybrid scanner (Biograph Duo or Biograph mCTFlow64-4R, Siemens Healthcare Solutions Knoxville, TN). A non-contrast CT scan was firstly performed for localization and attenuation correction, with a slice thickness of 5 mm, a tube voltage of 120 kV, and tube current depending on the patient's weight. Afterwards, PET images were acquired from the base of the skull to the proximal thigh for 3 min per bed position in a three-dimensional mode (Biograph Duo), or continuous table motion acquisitions (Biograph mCT Flow 64-4R). PET images were then reconstructed with an ordered method of ultra HD-PET, which included time of flight (TOF) and resolution recovery (TrueX) information.

Image Analysis

All PET/CT images were analyzed by using Syngo TrueD VE40E workstation (Siemens Medical Solutions). The primary lesions were identified and analyzed by two experienced independent nuclear physicians who were blinded to any clinical and pathological information. Malignant lesions typically showed higher ^{18}F-FDG concentration than that of the surrounding normal tissue. One of the physicians reviewed and analyzed all cases after a 2-week washout period.

The characteristic of suspicious colorectal lesions was diagnosed according to the location, shape, size, radioactivity distribution, and standardized uptake value (SUV) of the lesions. The semi-automatic quantitative measurements started with a manually placed elliptical working frame, which was drawn large enough to include the primary lesion, and manual adjustment was performed to exclude adjacent lymph nodes, metastatic lesions, and high physiologic uptake organs (**Figure 2**). The SUV_{max} and SUV_{peak} would be automatically calculated and generated after the placement of the working frame. Afterwards, a three-dimensional volume of interest (VOI) would be automatically outlined with chosen threshold within the working frame. According to previous studies, two common methods were selected to set the threshold. The first one was using the fixed threshold, also known as fixed absolute threshold; the thresholds of 2.5, 3.0, 4.0, and 5.0 were applied (18, 19). The second approach was using the percent threshold, also known as fixed percentage threshold, setting the threshold between 30% and 60% with an increment of 10% of the SUV_{max} (20, 21). With different thresholds, metabolic tumor volume (MTV), and SUV_{mean} could be identified inside the segmented VOI. Additionally, total lesion glycolysis (TLG) was calculated by MTV multiplying SUV_{mean} (TLG = MTV × SUV_{mean}), with representative images shown in **Figures 3**, **4**.

Immunohistochemical Evaluation

All patients underwent surgical resection within 3 months of PET/CT examination. The conventional HE and immunohistochemical staining of resected specimens were evaluated by a senior pathologist in a blind fashion. Specifically, the general pathological types, differentiation grade, TNM stages, and the expression of MMR proteins (MLH1, PMS2, MSH2, and MSH6) were assessed.

Proficient mismatch repair (pMMR) was identified when all of the four proteins were intact and expected to be microsatellite stable (MSS). On the contrary, those with the loss of one or more abovementioned MMR proteins were referred to as defective mismatch repair (dMMR) and characterized as MSI.

Statistical Analysis

The continuous variables were first checked for normality. The normally distributed data were expressed as the mean ± standard deviation (SD) and the difference was analyzed by Student's *t* test, while the data were expressed as medians and interquartile ranges and tested by Mann–Whitney *U*-test if not normally distributed. The categorical variables were shown as the number of cases and percentages, and compared by chi-squared test (or Fisher's exact test).

All quantitative PET/CT parameters were tested for inter-observer agreement and intra-observer agreement by interclass correlation coefficient (ICC) analysis, and ICC value greater than 0.90 was regarded as excellent agreement; between 0.75 and 0.90 as good agreement; between 0.5 and 0.75 as moderate agreement; and less than 0.50 as poor agreement. Receiver operating characteristic (ROC) analysis and the area under the ROC

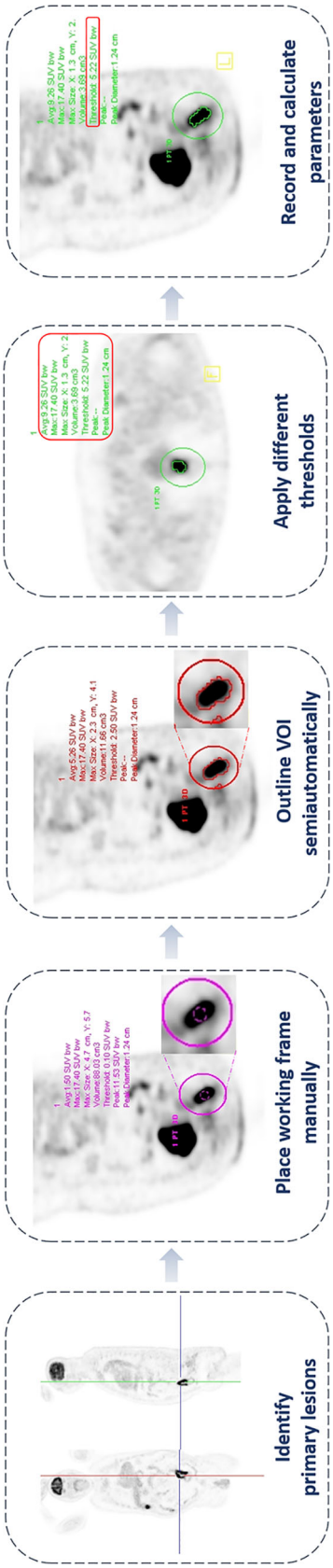

FIGURE 2 | The workflow of ^{18}F-FDG PET/CT metabolic parameter measurements.

curve (AUC) were used to compare the predictive capabilities of quantitative PET/CT parameters between MSI and MSS group, and the sensitivity, specificity, optimal cutoff value, and 95% confidence interval (CI) were also calculated for each parameter. The comparison of different AUCs was conducted by the method described by DeLong et al. (22). Significant clinicopathological factors and the metabolic parameters with highest AUCs were entered into the multivariate logistic regression analysis.

All statistical analysis was performed by using SPSS software (version 22.0 IBM Corp, Armonk, NY) and MedCalc software (version 15.8). Two-sided *p*-values less than 0.05 were considered statistically significant.

RESULTS

Patient Characteristics

A total of 44 patients were finally enrolled in this study (24 males, 20 females, age range 28–90 years, median age 73 years), with 14 patients in the MSI group and 30 patients in the MSS group. In the current cohort, patients in the MSI group were older and their tumors appeared more often in the colon than the MSS group. There was no difference in TNM stage, pathological general types, differentiation grade, and tumor size between two groups. Detailed patient information and clinicopathological characteristics are listed in **Table 1**.

Inter-Observer and Intra-Observer Agreement of PET/CT Parameters

The excellent inter-observer and intra-observer agreement was found in SUV_{max} and SUV_{peak} with ICC values ranging from 0.999 to1.000. Other quantitative parameters also showed excellent inter-observer and intra-observer agreement with ICC values ranging from 0.958 to 0.999.

Difference of PET/CT Parameters in MSI and MSS Groups

The detailed SUV_{max}, SUV_{peak}, SUV_{mean}, MTV, and TLG in MSI and MSS groups are demonstrated in **Tables 2**, **3**. Specifically, MTVs were larger in CRC patients with MSI, with $MTV_{30\%}$, $MTV_{40\%}$, $MTV_{50\%}$, and $MTV_{60\%}$ showing significant difference (all *p*-values <0.05). Moreover, $TLG_{50\%}$ and $TLG_{60\%}$ were significantly larger in the MSI group than in the MSS group (all *p*-values <0.05). No significant difference was found in SUV_{max}, SUV_{peak}, and SUV_{mean} between two groups.

Predictive Performance of PET/CT and Clinical Parameters for MSI

For PET/CT parameters, $MTV_{50\%}$ demonstrated the highest predictive performance among the metabolic parameters, although not in a significant statistical way (all *p*-values >0.050), with an AUC of 0.805 (95% CI: 0.657–0.909), a sensitivity of 92.9% (95% CI: 0.661–0.998), and a specificity of 66.7% (95% CI: 0.472–0.827), respectively. The detailed predictive performance of PET/CT parameters and its ROC curves is illustrated in **Table 4** and **Figure 5**. For clinical parameters, the AUCs of age and tumor

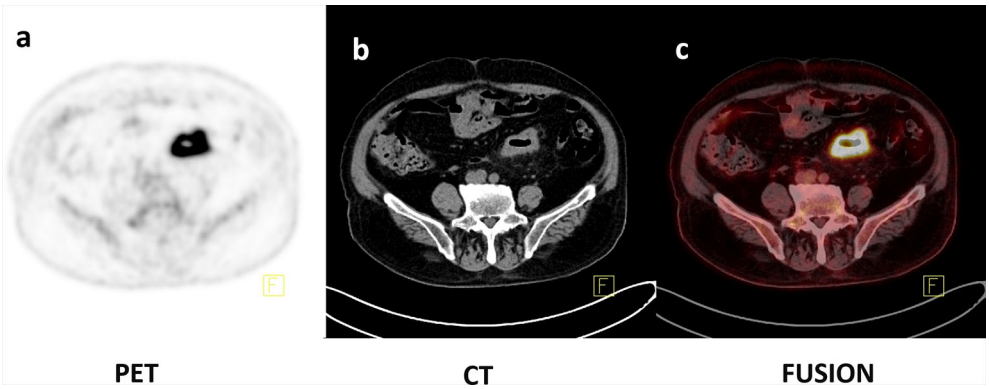

FIGURE 3 | Axial PET, CT, and fusion images of an 86-year-old female with histopathologically proven CRC with MSI **(A–C)**. ^{18}F-FDG PET/CT images showed that intense uptake in the sigmoid colon (SUV_{max} = 22.59, SUV_{peak} = 15.91, $SUV_{mean50\%}$ = 14.22, $MTV_{50\%}$ = 13.23 ml, $TLG_{50\%}$ = 188.13).

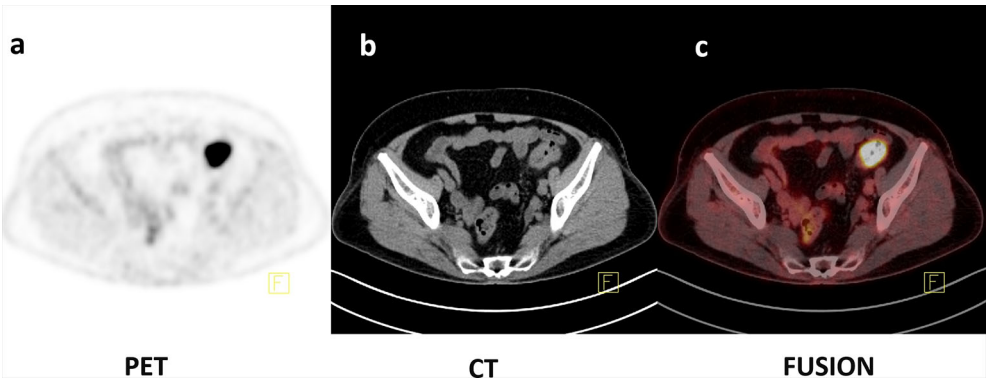

FIGURE 4 | Axial PET, CT, and fusion images of a 77-year-old female with histopathologically proven CRC with MSS **(A–C)**. ^{18}F-FDG PET/CT images showed that intense uptake in the sigmoid colon (SUV_{max} = 22.58, SUV_{peak} = 15.13, $SUV_{mean50\%}$ = 14.64, $MTV_{50\%}$ = 5.63 ml, $TLG_{50\%}$ = 82.4).

location were 0.843 (95% CI: 0.702–0.935) and 0.681 (95% CI: 0.523–0.813), respectively. No significant difference was found between AUCs of clinical and metabolic parameters (all $p > 0.050$). In multivariate logistic regression, age, tumor location, and metabolic parameters were entered. To avoid multicollinearity, we only selected one significant metabolic parameter in each category for assessment, which were $MTV_{50\%}$ and $TLG_{60\%}$. The odds ratio and p-value of age, tumor location, $MTV_{50\%}$, and $TLG_{60\%}$ were 0.819 ($p = 0.005$), 20.460 ($p = 0.059$), 0.831 ($p = 0.039$), and 1.008 ($p = 0.276$), respectively, which suggested age and $MTV_{50\%}$ as the independent predictive indicators for MSI.

DISCUSSION

The current study revealed that age, tumor location, and certain metabolic parameters with specific thresholds had a significant difference between the MSI and MSS groups in patients with CRC. MTV and TLG with higher percentage thresholds showed good predictive ability in identifying MSI, especially the$MTV_{50\%}$.

With the advancement of image analysis technology, MTV and TLG, which are volumetric indexes derived from ^{18}F-FDG PET, have been proposed for risk stratification of cancer patients (23). TLG is calculated by multiplying MTV by the SUV_{mean} of all voxels in the MTV, and represents both the degree of ^{18}F-FDG uptake and the size of the tumor. In other words, MTV is affected by tumor size and the distribution of the SUV, and TLG is affected by the whole metabolic and volumetric burden of the tumor (24–26). In fact, MTV and TLG were considered to be more reliable markers reflecting tumor burden and aggressiveness, as these indexes provide tumor burden information and additional information that takes into account intra-tumoral biologic variation. In the current study, we found that MTV and TLG were significantly different between MSI and MSS groups, which was in agreement with the previous findings (27). Jiang et al. (27) retrospectively analyzed the pretreatment parameters of PET and reported the highest diagnostic performance of $MTV_{3.0}$ and $TLG_{3.0}$ in predicting

TABLE 1 | Clinicopathological characteristics of included patients.

Characteristics	Overall (*n* = 44)	MSI (*n* = 14)	MSS (*n* = 30)	*p*-value
Sex				
Male	24	6	18	0.342
Female	20	8	12	
Age (years)[a]	71.1 ± 14.2	81.4 ± 8.5	66.3 ± 13.8	0.001
Tumor size (cm)[b]	5 (3.6, 6)	5.25 (4.63,7.25)	4.5 (3.15,5.5)	0.351
Tumor location				
Colon	30	13	17	0.019
Rectum	14	1	13	
Pathological general types				
Mass type	10	2	8	0.462
Ulcer type	34	12	22	
Differentiation grade				
Well or Moderate	29	7	22	0.177
Poor or	15	7	8	
Mucinous				
AJCC-TNM stage				
I–II	16	7	9	0.313
III–IV	28	7	21	
T stage				
T1–2	5	1	4	1.000
T3–4	38	12	26	
N stage				
Negative	20	9	11	0.112
Positive	24	5	19	
M stage				
Negative	29	11	18	0.314
Positive	15	3	12	

[a]*Data are presented in mean ± standard deviation (SD).*
[b]*data are presented in median (25th, 75th percentiles).*
MSI, microsatellite instability; MSS, microsatellite stability; AJCC, American Joint Committee on Cancer.

PD-L1 expression level in CRC. On the contrary, SUV_{max}, SUV_{peak}, and SUV_{mean} did not show a significant difference between MSI and MSS groups in the current study. SUV_{max} and SUV_{peak} only represent certain parts of the tumor and reflect the maximum extent of glucose metabolism within tumor cells (28), while SUV_{mean} was the average of tumor glucose uptake value. Therefore, SUV itself provides limited information on tumor lesion, and heterogeneity might not be accurately shown by the SUV values.

The present study found that patients' age and $MTV_{50\%}$ were significant predictive indicators of MSI, which was in agreement with a previous study (29) showing that CRC patients with MSI tended to be older. Similarly, Taieb et al. found that older age was associated with shorter survival after CRC recurrence (30). In addition, the predictive value of MTV with a higher percentage threshold tended to show better performance although not in a statistical way, which may due to the small sample size of the MSI group. Recent studies also confirmed that the different thresholds of MTV would affect the diagnostic performance. Bang's study (21) found that MTV calculated using various thresholds was significantly associated with the 3-year disease-free survival (DFS) rate of locally advanced rectal cancer, and MTV calculated using a higher threshold (40%–70% SUV_{max}) tended to be more strongly associated with 3-year DFS. In another study, various thresholds of metabolic parameters from FDG PET/CT were obtained and analyzed, and they found that $TLG_{40\%}$ can predict the treatment outcome of regorafenib in metastatic CRC (25). Moreover, we found that MTV with the percentage thresholds, rather than the fixed thresholds, showed better predictive performances of MSI

TABLE 2 | SUV measurements of CRC patients.

	SUV_{max}	SUV_{peak}	SUV_{mean} with fixed threshold method				SUV_{mean} with percent threshold method			
			2.5	3.0	4.0	5.0	30%	40%	50%	60%
MSI	19.34 ± 8.67	14.80 ± 6.01	6.94 ± 1.90	7.61 ± 2.12	8.61 ± 2.27	9.35 ± 2.38	9.83 ± 4.0	11.08 ± 4.35	12.34 ± 4.90	13.72 ± 5.61
MSS	21.43 ± 10.14	16.03 ± 8.35	6.97 ± 2.02	7.55 ± 2.15	8.62 ± 2.31	9.54 ± 2.45	10.77 ± 5.09	12.34 ± 5.84	13.94 ± 6.63	15.56 ± 7.46
***p*-value**	0.509	0.821	0.965	0.929	0.986	0.806	0.549	0.476	0.427	0.417

MSI, microsatellite instability; MSS, microsatellite stability.

TABLE 3 | MTV and TLG measurements of CRC patients.

	MTV with fixed threshold method				MTV with percent threshold method			
	2.5	3.0	4.0	5.0	30%	40%	50%	60%
MSI	72.0 (41.93,80.8)	62.97 (33.29,70.65)	50.92 (24.13,57.83)	41.60 (18.52,49.96)	38.24 (23.27,48.34)	27.38 (14.65,33.86)	17.40 (10.19,24.12)	10.16 (6.46,16.78)
MSS	40.21 (23.14,78.87)	34.12 (19.54,70.73)	25.83 (14.73,59.71)	20.37 (11.64,43.42)	17.90 (12.0,36.89)	11.79 (8.59,22.87)	7.49 (4.94,13.51)	4.45 (2.76,7.93)
***p*-value**	0.087	0.101	0.182	0.158	0.005	0.002	0.001	0.002
	TLG with fixed threshold method				**TLG with percent threshold method**			
	2.5	3.0	4.0	5.0	30%	40%	50%	60%
MSI	475.16 (209.33,632.36)	450.89 (209.33,632.36)	409.11 (178.06,582.65)	367.12 (156.62,546.46)	371.17 (185.63,474.80)	283.05 (137.02,413.55)	178.77 (106.44,335.98)	110.23 (69.57,228.48)
MSS	256.12 (136.95,600.94)	238.44 (129.04,578.47)	211.22 (114.0,528.22)	186.83 (100.83,476.36)	167.66 (105.18,167.66)	124.57 (86.95,316.87)	83.31 (68.57,223.38)	54.92 (43.47,105.0)
***p*-value**	0.208	0.226	0.208	0.208	0.091	0.07	0.028	0.022

MSI, microsatellite instability; MSS, microsatellite stability; MTV, metabolic tumor volume; TLG, total lesion glycolysis.

TABLE 4 | Predictive performance of metabolic parameters.

Parameters	AUC (95% CI)	Optimal cutoff value	Sensitivity (95% CI)	Specificity (95% CI)
MTV $_{30\%}$	0.764 (0.612,0.879)	19.27	0.857 (57.2–98.2)	0.600 (40.6–77.3)
MTV $_{40\%}$	0.795 (0.647,0.902)	13.25	0.929 (66.1–99.8)	0.600 (40.6–77.3)
MTV $_{50\%}$	0.805 (0.657,0.909)	8.89	0.929 (66.1–99.8)	0.667 (47.2–82.7)
MTV $_{60\%}$	0.795 (0.647,0.902)	5.62	0.929 (66.1–99.8)	0.667 (47.2–82.7)
TLG $_{50\%}$	0.707 (0.549,0.865)	97.02	0.857 (57.2–98.2)	0.600 (40.6–77.3)
TLG $_{60\%}$	0.717 (0.561,0.842)	74.11	0.786 (49.2–95.3)	0.600 (40.6–77.3)

AUC, area under the ROC curve; CI, confidence interval; MTV, metabolic tumor volume; TLG, total lesion glycolysis.

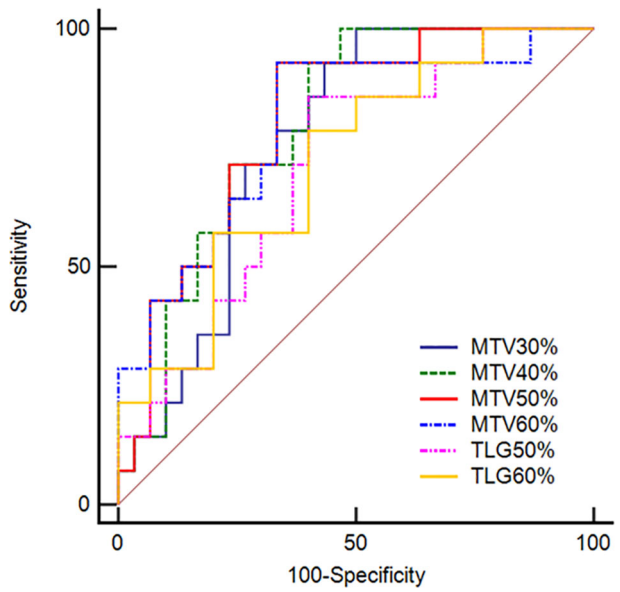

FIGURE 5 | Receiver operating characteristic curves of $MTV_{30\%}$, $MTV_{40\%}$, $MTV_{50\%}$, and $MTV_{60\%}$ as well as $TLG_{50\%}$ and $TLG_{60\%}$ derived from PET/CT images for predicting MSI in CRC patients. The AUCs for predicting MSI from MSS were 0.764, 0.795, 0.805, and 0.795 for $MTV_{30\%}$, $MTV_{40\%}$, $MTV_{50\%}$, and $MTV_{60\%}$, respectively. In addition, the AUCs were 0.707 and 0.717 for $TLG_{50\%}$ and $TLG_{60\%}$.

status in patients with CRC. Previous studies also demonstrated percentage thresholds method as a better way of measurements, as it was an easily evaluated semiquantitative measurement of tumor textural heterogeneity and could minimize individual variations (19, 21). In addition, Henriksson et al. found the association between FDG uptake and the intra-tumoral heterogeneity in nude mice (31). On the other hand, Smedt et al. reported significant higher levels of cytotoxic T cells in the tumor and peritumoral region of MSI compared with MSS tumors (32). Therefore, MTV calculated using a higher threshold might be a representative marker for tumor clinicopathological characteristics in patients with CRC.

We acknowledged several limitations in our study. First, there may be selection bias due to the retrospective nature of this study. Second, the sample size was limited in this study, and further validation is required by including a large cohort. Finally, our results were obtained from a single institution, and further multicenter investigations are needed to validate the utility of these metabolic parameters for predicting MSI in patients with CRC.

In conclusion, the metabolic parameters derived from ^{18}F-FDG PET/CT were able to preoperatively predict the MSI status in CRC, with $MTV_{50\%}$ demonstrating the highest predictive performance. Using these parameters, the noninvasive evaluation of MSI can be achieved, and thus better guiding immunotherapy in CRC patients.

DATA AVAILABILITY STATEMENT

The raw data supporting the conclusions of this article will be made available by the authors, without undue reservation.

ETHICS STATEMENT

The studies involving human participants were reviewed and approved by West China Hospital, Sichuan University. Written informed consent for participation was not required for this study in accordance with the national legislation, and the institutional requirements.

AUTHOR CONTRIBUTIONS

HL, TY, and BS contributed to conception and design of the study. HL and HX organized the image database and performed quantitative measurements. ZY, TD and ML performed the statistical analysis. HL and TY wrote the first draft of the manuscript. ZY, MW and BS revised the manuscript. All authors contributed to manuscript revision and read and approved the submitted version.

REFERENCES

1. Bray F, Ferlay J, Soerjomataram I, Siegel RL, Torre LA, Jemal A. Global Cancer Statistics 2018: GLOBOCAN Estims of Incidence and Mortality Worldwide for 36 Cancers in 185 Countries. *CA: Cancer J Clin* (2018) 68 (6):394–424. doi: 10.3322/caac.21492
2. Kuipers EJ, Grady WM, Lieberman D, Seufferlein T, Sung JJ, Boelens PG, et al. Colorectal Cancer. *Nat Rev Dis Primers* (2015) 1:15065. doi: 10.1038/nrdp.2015.65

3. Lichtenstern CR, Ngu RK, Shalapour S, Karin M. Immunotherapy, Inflammationand Colorectal Cancer. *Cells* (2020) 9(3):618. doi: 10.3390/cells9030618
4. Pardoll DM. The Blockade of Immune Checkpoints in Cancer Immunotherapy. *Nat Rev Cancer* (2012) 12(4):252–64. doi: 10.1038/nrc3239
5. Brudvik KW, Røsok B, Naresh U, Yaqub S, Fretland ÅA, Labori KJ, et al. Survival After Resection of Colorectal Liver Metastases in Octogenarians and Sexagenarians Compared to Their Respective Age-Matched National Population. *Hepatobiliary Surg Nutr* (2018) 7(4):234–41. doi: 10.21037/hbsn.2017.09.03
6. Grady WM, Carethers JM. Genomic and Epigenetic Instability in Colorectal Cancer Pathogenesis. *Gastroenterology* (2008) 135(4):1079–99. doi: 10.1053/j.gastro.2008.07.076
7. Passardi A, Canale M, Valgiusti M, Ulivi P. Immune Checkpoints as a Target for Colorectal Cancer Treatment. *Int J Mol Sci* (2017) 18(6):1324. doi: 10.3390/ijms18061324
8. Sargent DJ, Marsoni S, Monges G, Thibodeau SN, Labianca R, Hamilton SR, et al. Defective Mismatch Repair as a Predictivemarker for Lack of Efficacy of Fluorouracil-Based Adjuvant Therapy in Coloncancer. *J Clin Oncol* (2010) 28 (20):3219–26. doi: 10.1200/JCO.2009.27.1825
9. Romiti A, Rulli E, Pilozzi E, Gerardi C, Roberto M, Legramandi L, et al. Exploring the Prognostic Role Ofmicrosatellite Instability in Patients With Stage II Colorectal Cancer: ASystematic Review and Meta-Analysis. *Clin Colorectal Cancer* (2017) 16(2):e55–9. doi: 10.1016/j.clcc.2016.08.007
10. Shia J. Immunohistochemistry Versus Microsatellite Instability Testing Forscreening Colorectal Cancer Patients at Risk for Hereditary Nonpolyposiscolorectal Cancer Syndrome. Part I. The Utility of Immunohistochemistry. *J Mol Diagn* (2008) 10 (4):293–300. doi: 10.2353/jmoldx.2008.080031
11. Sun R, Limkin EJ, Vakalopoulou M, Dercle L, Champiat S, Han SR, et al. A Radiomics Approach Toassess Tumour-Infiltrating CD8 Cells and Response to Anti-PD-1 or Anti-PD-L1immunotherapy: An Imaging Biomarker, Retrospective Multicohort Study. *Lancet Oncol* (2018) 19(9):1180–91. doi: 10.1016/S1470-2045(18)30413-3
12. Punt CJ, Koopman M, Vermeulen L. From Tumour Heterogeneity to Advances in Precision Treatment of Colorectal Cancer. *Nat Rev Clin Oncol* (2017) 14(4):235–46. doi: 10.1038/nrclinonc.2016.171
13. Wu J, Lv Y, Wang N, Zhao Y, Zhang P, Liu Y, et al. The Value of Single-Source Dual-Energy CT Imaging for Discriminating Microsatellite Instability From Microsatellite Stability Human Colorectal Cancer. *Eur Radiol* (2019) 29 (7):3782–90. doi: 10.1007/s00330-019-06144-5
14. Zhang W, Yin H, Huang Z, Zhao J, Zheng H, He D, et al. Development and Validation of MRI-Based Deep Learning Models for Prediction of Microsatellite Instability in Rectal Cancer. *Cancer Med* (2021) 10:4164–73. doi: 10.1002/cam4.3957
15. Meacham CE, Morrison SJ. Tumour Heterogeneity and Cancer Cell Plasticity. *Nature* (2013) 501(7467):328–37. doi: 10.1038/nature12624
16. Wu M, Zhang Y, Zhang Y, Liu Y, Wu M, Ye Z. Imaging-Based Biomarkers for Predicting and Evaluating Cancer Immunotherapy Response. *Radiol Imaging Cancer* (2019) 1(2):e190031. doi: 10.1148/rycan.2019190031
17. Kaira K, Higuchi T, Naruse I, Arisaka Y, Tokue A, Altan B, et al. Metabolic Activity by 18F-FDG-PET/CT Is Predictive of Early Response After Nivolumab in Previously Treated NSCLC. *Eur J Nucl Med Mol Imaging* (2018) 45(1):56–66. doi: 10.1007/s00259-017-3806-1
18. Im HJ, Bradshaw T, Solaiyappan M, Cho SY. Current Methods to Define MetabolicTumor Volume in Positron Emission Tomography: Which One Is Better? *Nucl Med Mol Imaging* (2018) 52(1):5–15. doi: 10.1007/s13139-017-0493-6
19. Suzuki Y, Okabayashi K, Hasegawa H, Tsuruta M, Shigeta K, Murakami K, et al. Metabolic Tumor Volume and Total Lesion Glycolysis in PET/CT Correlate With the Pathological Findings of Colorectal Cancer and Allow Its Accurate Staging. *Clin Nucl Med* (2016) 41(10):761–5. doi: 10.1097/RLU.0000000000001332
20. Mapelli P, Bergamini A, Fallanca F, Rancoita PMV, Cioffi R, Incerti E, et al. Prognosticrole of FDG PET-Derived Parameters in Preoperative Staging of Endometrialcancer. *Rev Esp Med Nucl Imagen Mol (Engl Ed)* (2019) 38(1):3–9. doi: 10.1016/j.remn.2018.06.007. English,Spanish.
21. Bang JI, Ha S, Kang SB, Lee KW, Lee HS, Kim JS, et al. Prediction of Neoadjuvant Radiation Chemotherapy Response and Survival Using Pretreatment [(18)F]FDG PET/CT Scans in Locally Advanced Rectal Cancer. *Eur J Nucl Med Mol Imaging* (2016) 43(3):422–31. doi: 10.1007/s00259-015-3180-9
22. DeLong ER, DeLong DM, Clarke-Pearson DL. Comparing the Areas Under Two Ormore Correlated Receiver Operating Characteristic Curves: A Nonparametricapproach. *Biometrics* (1988) 44(3):837–45. doi: 10.2307/2531595
23. Romesser PB, Qureshi MM, Shah BA, Chatburn LT, Jalisi S, Devaiah AK. Superior Prognostic Utility of Gross and Metabolic Tumor Volume Compared to Standardized Uptake Value Using PET/CT in Head and Neck Squamous Cell Carcinoma Patients Treated With Intensity-Modulated Radiotherapy. *Ann Nucl Med* (2012) 26(7):527–34. doi: 10.1007/s12149-012-0604-5
24. Moon SH, Hyun SH, Choi JY. Prognostic Significance of Volume-Based PET Parameters in Cancer Patients. *Korean J Radiol* (2013) 14(1):1–12. doi: 10.3348/kjr.2013.14.1.1
25. Lim Y, Bang JI, Han SW, Paeng JC, Lee KH, Kim JH, et al. Total Lesion Glycolysis (TLG) as an Imaging Biomarker in Metastatic Colorectal Cancer Patients Treated With Regorafenib. *Eur J Nucl Med Mol Imaging* (2017) 44 (5):757–64. doi: 10.1007/s00259-016-3577-0
26. Rahim MK, Kim SE, So H, Kim HJ, Cheon GJ, Lee ES, et al. Recent Trends in PET Image Interpretations Using Volumetric and Texture-Based Quantification Methods in Nuclear Oncology. *Nucl Med Mol Imaging* (2014) 48(1):1–15. doi: 10.1007/s13139-013-0260-2
27. Jiang H, Zhang R, Jiang H, Zhang M, Guo W, Zhang J, et al. Retrospective Analysis of the Prognostic Value of PD-L1 Expression and 18F-FDG PET/CT Metabolic Parameters in Colorectal Cancer. *J Cancer* (2020) 11(10):2864–73. doi: 10.7150/jca.38689
28. Im HJ, Pak K, Cheon GJ, Kang KW, Kim SJ, Kim IJ, et al. Prognostic Value of Volumetric Parameters of (18)F-FDG PET in Non-Small-Cell Lung Cancer: A Meta-Analysis. *Eur J Nucl Med Mol Imaging* (2015) 42(2):241–51. doi: 10.1007/s00259-014-2903-7
29. Fujiyoshi K, Yamaguchi T, Kakuta M, Takahashi A, Arai Y, Yamada M, et al. Predictive Model for High-Frequency Microsatelliteinstability in Colorectal Cancer Patients Over 50 Years of Age. *Cancer Med* (2017) 6(6):1255–63. doi: 10.1002/cam4.1088
30. Taieb J, Shi Q, Pederson L, Alberts S, Wolmark N, Van Cutsem E, et al. Prognosis of Microsatellite Instability and/or Mismatch Repairdeficiency Stage III Colon Cancer Patients After Disease Recurrence Following adjuvant Treatment: Results of an ACCENT Pooled Analysis of Seven Studies. *Ann Oncol* (2019) 30(9):1466–71. doi: 10.1093/annonc/mdz208
31. Henriksson E, Kjellen E, Wahlberg P, Ohlsson T, Wennerberg J, Brun E. 2-Deoxy-2-[18F] Fluoro-D-Glucose Uptake and Correlation to Intratumoral Heterogeneity. *Anticancer Res* (2007) 27(4B):2155–9.
32. De Smedt L, Lemahieu J, Palmans S, Govaere O, Tousseyn T, Van Cutsem E, et al. Microsatellite Instable vs Stable Colon Carcinomas: Analysis of Tumour Heterogeneity, Inflammation and Angiogenesis. *Br J Cancer* (2015) 113 (3):500–9. doi: 10.1038/bjc.2015.213

Conflict of Interest: The authors declare that the research was conducted in the absence of any commercial or financial relationships that could be construed as a potential conflict of interest.

Publisher's Note: All claims expressed in this article are solely those of the authors and do not necessarily represent those of their affiliated organizations, or those of the publisher, the editors and the reviewers. Any product that may be evaluated in this article, or claim that may be made by its manufacturer, is not guaranteed or endorsed by the publisher.

Copyright © 2021 Liu, Ye, Yang, Xie, Duan, Li, Wu and Song. This is an open-access article distributed under the terms of the Creative Commons Attribution License (CC BY). The use, distribution or reproduction in other forums is permitted, provided the original author(s) and the copyright owner(s) are credited and that the original publication in this journal is cited, in accordance with accepted academic practice. No use, distribution or reproduction is permitted which does not comply with these terms.

frontiers in Immunology

CASE REPORT
published: 14 September 2021
doi: 10.3389/fimmu.2021.731774

Case Report: A Rare Case of Pembrolizumab-Induced Bullous Pemphigoid

Xiaoyan Zhang[1]*, *Dongjiang Sui*[1], *Dong Wang*[1], *Lina Zhang*[1] and *Ruiyan Wang*[2]

[1] Department of Pulmonary and Critical Care Medicine, Air Force Medical Center, Beijing, China, [2] Department of Dermatology, Air Force Medical Center, Beijing, China

The programmed cell death protein 1 inhibitor pembrolizumab, an immune checkpoint inhibitor, has subsequently been approved for the treatment of a wide variety of malignant tumors. Compared with conventional chemotherapy, immunotherapy is associated with a unique set of immune reactions, known collectively as immune-related adverse events. Although often mild, dermatologic toxicity can occasionally be high grade and potentially life-threatening. Here we describe a rare case of bullous pemphigoid (BP) associated with pembrolizumab. A 79-year-old male patient presented with scattered erythema, papules, blisters, and pruritus after pembrolizumab treatment. Then, the rash gradually aggravated and spread to the whole body. The extensive edematous erythema, blisters, bullae, and blood blisters were loose and easy to rupture, forming an erosive surface and with pruritus and obvious pain. The hemidesmosomal protein BP180 (type XVII collagen) was detectable in the serum, and the histological examination diagnosis was bullous pemphigoid. After 10 days of glucocorticoid (methylprednisolone, iv, 80 mg/day) treatment, new blister formation ceased. We need to increase the awareness on and facilitate the earlier identification of the cutaneous adverse effects of BP with immunotherapy so that treat can begin early in order to limit the duration and severity of toxicity.

Keywords: bullous pemphigoid, pembrolizumab, programmed cell death protein 1, immunotherapy, glucocorticoid

OPEN ACCESS

Edited by:
Hubing Shi,
Sichuan University, China

Reviewed by:
Alessandro Pileri,
Università di Bologna, Italy
Dario Didona,
University Hospital Giessen and Marburg, Germany
Ana Maria Abreu-Velez,
Georgia Dermatopathology Associates, United States

***Correspondence:**
Xiaoyan Zhang
zhangxyrespirology@163.com

Specialty section:
This article was submitted to Cancer Immunity and Immunotherapy, a section of the journal Frontiers in Immunology

Received: *28 June 2021*
Accepted: *23 August 2021*
Published: *14 September 2021*

Citation:
Zhang X, Sui D, Wang D, Zhang L and Wang R (2021) Case Report: A Rare Case of Pembrolizumab-Induced Bullous Pemphigoid. Front. Immunol. 12:731774. doi: 10.3389/fimmu.2021.731774

INTRODUCTION

Pembrolizumab is a humanized monoclonal antibody IgG4 programmed cell death protein 1 (PD-1) antagonist. As a new drug of immune checkpoint inhibitor, pembrolizumab has shown great promising prospects in clinical antitumor immunotherapy and has rapidly become the first-line therapy for a variety of advanced malignancies. It has been recommended in antitumor guidelines of many countries and opened a new era of tumor immunotherapy (1). While immune checkpoint inhibitors can enhance the immune system and cause cells to attack tumor cells, they can also cause cells to attack normal cells in the body, causing a series of inflammatory diseases mimicking autoimmune diseases, some of which may be serious. These major adverse effects are termed "immune-related adverse events" (irAEs) and present with organ-specific tissue inflammation (2–4). Here we report a case of bullous pemphigoid (BP) associated with pembrolizumab, emerging with a

potentially serious dermatologic toxicity, and we will use this case to highlight the diagnosis and management of cutaneous irAEs associated with checkpoint inhibitors.

CASE REPORT

In May 2019, a 79-year-old male patient underwent resection of the left kidney and ureter for invasive high-grade papillary urothelial carcinoma. The tumor size was 1.2 × 1 × 0.2 cm, and the tumor TNM scale was T1N0M1. In January 2020, multiple round nodules of different sizes can be seen in both lungs by CT and PET-CT, with a smooth boundary. The largest one is located in the left lower lung, about 2.2 × 1.8 cm. From February to September 2020, he had received 10 cycles of pembrolizumab therapy (100 mg, iv, q21d) because of lung metastatic carcinoma. From April 2020, erythema and pimples accompanied by pruritus appeared successively on the trunks and limbs of the patient. After symptomatic treatment, the rash subsided and appeared repeatedly. From November 2020, the rash aggravated gradually; macroscopically, the lesions appeared as strained blisters filled with serous fluid and blood on erythematous skin, spreading throughout the body. The blood bullae were big, loose, and easy to break, forming the erosive surface (**Figures 1A, B**), and accompanied by itchy and obvious pain. According to the descriptions of select cutaneous immune-related adverse events as defined by the CTCAE, version 5.0 (Common Terminology Criteria for Adverse Events), given the blisters of the patient covering >30% of body surface area which limit his self-care/activities of daily living, his disease grade was classified as grade 3.

Histopathological findings showed epidermal hyperplasia and edema, subepidermal blister formation, numerous eosinophils in the blister, and obvious eosinophil infiltration around the superficial dermis vessels (**Figures 2A, B**). Immunofluorescence was positive for IgG (**Figure 3**) and C3 (**Figure 4**). The hemidesmosomal protein BP180 (type XVII collagen) was detectable in the serum, with 137.32 U/ml titer by enzyme-linked immunosorbent assay (ELISA) method. BP230 detection was normal. Taken together, the clinical presentation and laboratory findings were consistent with the diagnosis of BP. According to Naranjo's adverse drug reaction assessment with a score of 8 (**Table 1**), BP probably caused by pembrolizumab was considered.

Our differential diagnosis included paraneoplastic pemphigus (PNP). Direct immunofluorescence did not show a deposition of immunoglobulins at the cell surface of keratinocytes. By employing PET-CT, multiple hypermetabolic metastases in the lungs were detected on January 10, 2020, while the PET-CT image taken on November 19, 2020 showed that the original lesions were not clearly displayed. This suggested that immunotherapy was effective in the early stage, and the tumor achieved clinical complete remission (CR) after the treatment. No typical malignant hypermetabolic lesions were found in the rest of the body, so PNP can be excluded. BP can be caused by some drugs, including furosemide and anti-DPP4 inhibitors. This patient was not prescribed with these drugs.

FIGURE 1 | **(A, B)** Skin lesions on admission.

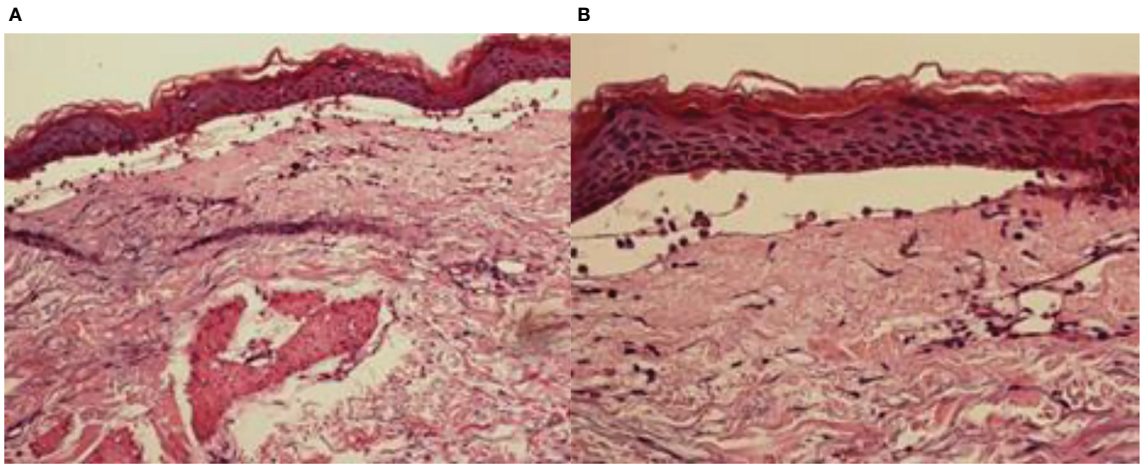

FIGURE 2 | Skin pathology: **(A)** H&E, ×200; **(B)** H&E, ×400.

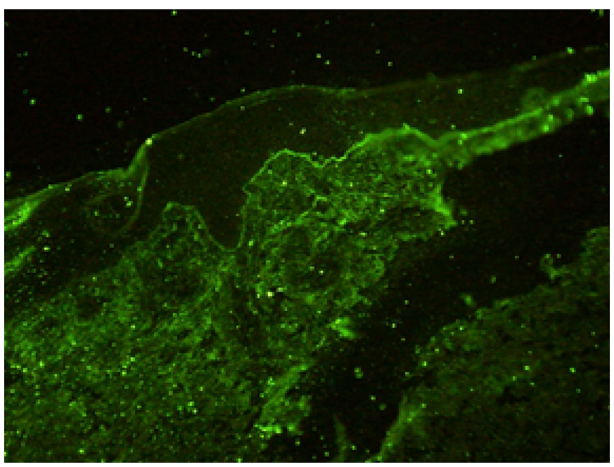

FIGURE 3 | IgG immunoglobulin deposits along the dermo-epidermal junction.

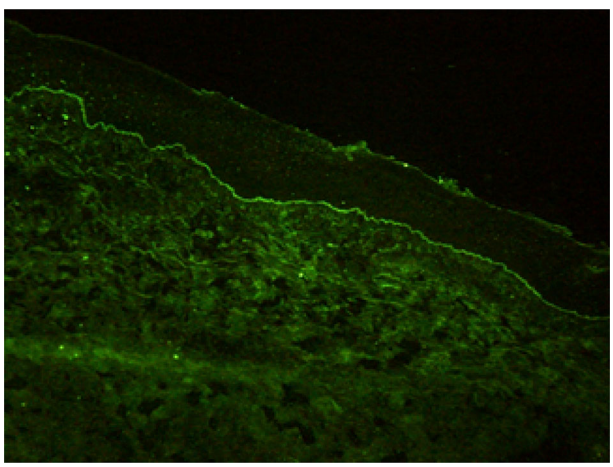

FIGURE 4 | C3 deposits along the dermo-epidermal junction.

After 3 days of glucocorticoid treatment (methylprednisolone, iv, 80 mg/day, 1.25 mg/kg/day), the cutaneous lesions improved. In some parts, the blister fluid was absorbed and the skin surface shrunk, the erosive surface began to scab and heal, and the color of erythema became pale. After 10 days, all the blisters disappeared, and new bullae formation ceased. All the superficial erosions were scabby and most of the scabs fell off, leaving dark red pigmentation spots (**Figures 5A, B**). After 2 weeks of glucocorticoid treatment, the methylprednisolone dose was changed to oral administration and gradually tapered. At 1 month later, BP180 detection was normal with 8.49 U/ml titer.

In February 2021, when methylprednisolone has been used as treatment for 4 months and was reduced to 24 mg/day, several blood blisters fused together with a size of about 20 × 7cm, which appeared in the skin of the left hip joint of the patient. BP180 was redetected, suggesting BP recurrence. The dose of methylprednisolone was increased to 44 mg for treatment. The blood blisters were broken and formed a big ulcer with yellow green pyoderma, and regular debridement and treatment with topical ointment, such as human epidermal growth factor gel, halometasone cream, and silver ion dressing, were continued for several months. So far (in July 2021), the skin lesions were not healed (**Figure 6**), the dose of methylprednisolone was reduced to 25 mg/day, and the monitored BP180 was in the normal range. In March 2021, the patient began to have a cough and low fever, and the lung CT showed invasive pulmonary fungal infection; he received antifungal treatment. During the antifungal treatment, for three times the lung CT showed that there was no lung carcinoma, and the carcinoma was still in CR.

DISCUSSION

As a new anti-tumor drug, pembrolizumab is an IgG4 antibody which antagonizes the PD-1 receptor. It has been approved for

TABLE 1 | Naranjo's assessment scale in the evaluation of adverse drug reaction (ADR).

Related issues	Results	Score
1. Is there any previous conclusive report on this ADR?	No	0
2. Does the ADR occur after the use of suspicious drugs?	Yes	2
3. Does the ADR get remission after drug withdrawal or anti-drug application?	Yes	1
4. Is the ADR repeated after the use of the suspected drug again?	Yes	1
5. Is there any other reason that can cause the ADR alone?	No	2
6. Does the ADR recur after placebo?	Unknown	0
7. Does the drug reach a toxic concentration in the blood or other body fluids?	Unknown	0
8. Does the ADR aggravate with the increase of dose or alleviate with the decrease of dose?	Yes	1
9. Has the patient ever been exposed to the same or similar drugs and had similar reactions?	No	0
10. Is there any objective evidence to confirm the reaction?	No	1
Total score		*r*

Naranjo's score: ≥ 9 points, definite; 5 – 8 points, probable, 1 – 4 points, possible; ≤ 0 points, doubtful.

FIGURE 5 | **(A, B)** Skin lesions on the 8th day after glucocorticoid treatment.

the treatment of a wide variety of malignant tumors, including melanoma, non-small cell lung cancer, head and neck squamous cell carcinoma, classical Hodgkin's lymphoma, urothelial carcinoma, gastric cancer, and cervical cancer. However, immune checkpoint inhibitors may abnormally enhance the normal immune response and cause T cells to attack the tumor cells in the body, causing a series of toxic reactions similar to autoimmune diseases (5, 6). Although the immune-related toxicity of pembrolizumab events are rare, serious adverse events, such as BP, can occur if it involves multiple systems and has a wide range of influence. It has been reported that the rash caused by the PD-1 inhibitor is often seen as pruritus or atypical macular papules in the early stage, and mucosal involvement is rare (7–9). The incidence of high-grade cutaneous toxicity with PD-1 inhibitors is low (approximately 1–2%) (10). Direct immunofluorescence showed the linear deposition of IgG and C3 at the dermo-epidermal junction. ELISA is the most commonly used antibody to detect the dermal component BP 180 (11), and in our case, BP 180 antibody was detected. The immune checkpoint inhibitors may determine the depletion of regulatory T cells (TREGs) that, in turn, leads to the proliferation of antigen-specific B cells and can facilitate the humoral response at the germinal center lever of lymphatic follicles. All these caused the production of the BP180 antibody

FIGURE 6 | Bullous pemphigoid reappearance after steroid tapering and continuous therapy for 5 months; skin of left hip joint.

(12). Sometimes the antibody to BP230 can be detected. Although this is the same pathomechanism believed to cause conventional BP, it is still unclear how anti-PD-1/PD-L1 immunotherapy facilitates this reaction (9).

Differently from other BP induced by traditional drugs, BP related to anti- PD-1/PDL1 may continue for several months after drug withdrawal. The incubation period of BP induced by PD-1 inhibitors is longer. Bullous lesions usually appear within the first 20–32 weeks of treatment; the mean time is 39 weeks, with some cases taking even more than 80 weeks. This may be related to the sustained immune activation (12, 13). BP is of high-grade dermatologic toxicity and potentially life-threatening if not be treated early. The delayed effect of the PD-1 inhibitor induced BP and may be the lasting effect of the drug itself, or the pathomechanism of the PD-1 inhibitor induced BP, which involves the key node in the pathogenesis of BP. Once triggered, it will form a positive feedback cycle and can no longer stop by itself. In our case, the onset of BP induced by PD-1 inhibitors is about 28 weeks.

Pembrolizumab has changed the treatment of malignant tumor, but more and more patients have immune-related adverse events. BP is of high-grade cutaneous toxicity to patients and potentially life-threatening. Although the continued use of anti-PD-1 drugs may aggravate BP, discontinuation does not lead to complete remission. These patients may still need intermittent or continuous treatment of BP. According to the severity of BP, glucocorticoid can be used locally or systematically. The systemic application of glucocorticoids can improve the prognosis of pemphigoid and reduce the mortality to 25–45%. After combining with other adjuvant therapy, the mortality was less than 10%. The cause of death of pemphigoid is very complex. Most scholars believed that respiratory tract infection and hormone adverse effects are the main cause. Some people think that the prognosis of pemphigoid is related to systemic failure and coronary heart disease. A few patients died of complications of long-term systemic use of high-dose corticosteroids and immunosuppressants, and infection was the most common cause of death (3).

CONCLUSION

With the use of pembrolizumab, clinicians should have increased awareness and facilitate the earlier identification of this rare but potentially serious cutaneous irAEs. Because cutaneous irAEs may occur late and even occur after pembrolizumab therapy has been completed, clinicians should keep in mind and evaluate carefully the new cutaneous adverse effects. Early treatment of BP is important to limit the duration and severity of toxicity. It is important to prevent and/or reduce interruptions in potentially life-saving cancer therapy.

DATA AVAILABILITY STATEMENT

The original contributions presented in the study are included in the article/supplementary material. Further inquiries can be directed to the corresponding author.

ETHICS STATEMENT

Written informed consent was obtained from the individual(s) for the publication of any potentially identifiable images or data included in this article.

AUTHOR CONTRIBUTIONS

XZ and DS contributed to data collection, data analysis, data interpretation, and manuscript preparation. DW and LZ contributed to data analysis and data interpretation. RW contributed to data collection. XZ contributed to data review and interpretation. All authors contributed to the article and approved the submitted version.

ACKNOWLEDGMENTS

We would like to give sincere thanks to the patient and his family for understanding and supporting the publication of the case.

REFERENCES

1. Yoest JM. Clinical Features, Predictive Correlates, and Pathophysiology of Immune-Related Adverse Events in Immune Checkpoint Inhibitor Treatments in Cancer: A Short Review. *Immunotarg Ther* (2017) 6:73–82. doi: 10.2147/ITT.S126227
2. Okane GM, Labbe C, Doherty MK, Young K, Albaba H, Leighl NB, et al. Monitoring and Management of Immune-Related Adverse Events Associated With Programmed Cell Death Protein-1 Axis Inhibitors in Lung Cancer. *Oncologist* (2017) 22(1):70–80. doi: 10.1634/theoncologist.2016-0164
3. De Velasco G, Je Y, Bosse D, Awad MM, Ott PA, Moreira RB, et al. Comprehensive Meta-Analysis of Key Immune-Related Adverse Events From CTLA-4 and PD-1/PDL1 Inhibitors in Cancer Patients. *Cancer Immunol Res* (2017) 5(4):312–8. doi: 10.1158/2326-6066.CIR-16-0237
4. Chen TW, Razak AR, Bedard PL, Siu LL, Hansen AR. A Systematic Review of Immune-Related Adverse Event Reporting in Clinical Trials of Immune Checkpoint Inhibitors. *Ann Oncol* (2015) 26(9):1824–9. doi: 10.1093/annonc/mdv182
5. Kennedy LB. A Review of Cancer Immunotherapy Toxicity. *CA Cancer J Clin* (2020) 70(2):86–104. doi: 10.3322/caac.21596
6. Champlat S, Lambotte O, Barreau E, Belkhir R, Berdelou A, Carbonnel F, et al. Management of Immune Checkpoint Blockade Dysimmune Toxicities: A Collaborative Position Paper. *Ann Oncol* (2016) 27(4):559–74. doi: 10.1093/annonc/mdv623
7. Honigman AD, Lai F, Elakis J, Prall O, Goh M, McCormack C, et al. Pembrolizumab-Induced Sarcoid Granulomatous Panniculitis and Bullous Pemphigoid in a Single Patient. *Clin Case Rep* (2019) 7(4):773–5. doi: 10.1002/ccr3.2090
8. Morris LM, Lewis HA, Cornelius LA, Chen DY, Rosman IS. Neutrophil-Predominant Bullous Pemphigoid Induced by Checkpoint Inhibitors: A Case Series. *J Cutan Pathol* (2020) 47(8):742–6. doi: 10.1111/cup.13687
9. Naidoo J, Schindler K, Querfeld C, Busam K, Cunningham J, Page DB, et al. Autoimmune Bullous Skin Disorders With Immune Checkpoint Inhibitors Targeting PD-1 and PD-L1. *Cancer Immunol Res* (2016) 4(5):383–9. doi: 10.1158/2326-6066.CIR-15-0123
10. Belum VR, Benhuri B, Postow MA, Hellmann MD, Lesokhin AM, Segal NH, et al. Characterisation and Management of Dermatologic Adverse Events to Agents Targeting the PD-1 Receptor. *Eur J Cancer* (2016) 60:12–25. doi: 10.1016/j.ejca.2016.02.010
11. Sadik CD, Langan EA, Gratz V, Zillikens D, Terheyden P. Checkpoint Inhibition may Trigger the Rare Variant of Anti-LAD-1 IgG-Positive, Anti-BP180 NC16A IgG-Negative Bullous Pemphigoid. *Front Immunol* (2019) 10:1934. doi: 10.3389/fimmu.2019.01934
12. Cosimati A, Rossi L, Didona D, Forcella C, Didona B. Bullous Pemphigoid in Elderly Woman Affected by Non-Small Cell Lung Cancer Treated With Pembrolizumab: A Case Report and Review of Literature. *J Oncol Pharm Pract* (2021) 27(3):727–33. doi: 10.1177/1078155220946370
13. Lopez AT, Khanna T, Antonov N, Audrey-Bayan C, Geskin L. A Review of Bullous Pemphigoid Associated With PD-1 and PD-L1 Inhibitors. *Int J Dermatol* (2018) 57(6):664–9. doi: 10.1111/ijd.13984

Conflict of Interest: The authors declare that the research was conducted in the absence of any commercial or financial relationships that could be construed as a potential conflict of interest.

Publisher's Note: All claims expressed in this article are solely those of the authors and do not necessarily represent those of their affiliated organizations, or those of the publisher, the editors and the reviewers. Any product that may be evaluated in this article, or claim that may be made by its manufacturer, is not guaranteed or endorsed by the publisher.

Copyright © 2021 Zhang, Sui, Wang, Zhang and Wang. This is an open-access article distributed under the terms of the Creative Commons Attribution License (CC BY). The use, distribution or reproduction in other forums is permitted, provided the original author(s) and the copyright owner(s) are credited and that the original publication in this journal is cited, in accordance with accepted academic practice. No use, distribution or reproduction is permitted which does not comply with these terms.

frontiers in Oncology

ORIGINAL RESEARCH
published: 15 September 2021
doi: 10.3389/fonc.2021.695006

Tumor-Infiltrating PD-1^{hi}CD8^{+}-T-Cell Signature as an Effective Biomarker for Immune Checkpoint Inhibitor Therapy Response Across Multiple Cancers

Zhenyu Yang[1,2†], *Yulan Deng*[1,2†], *Jiahan Cheng*[1,2], *Shiyou Wei*[1,2], *Hao Luo*[1,2] *and Lunxu Liu*[1,2*]

[1] Institute of Thoracic Oncology and Department of Thoracic Surgery, West China Hospital, Sichuan University, Chengdu, China, [2] Western China Collaborative Innovation Center for Early Diagnosis and Multidisciplinary Therapy of Lung Cancer, Sichuan University, Chengdu, China

OPEN ACCESS

Edited by:
Benjamin Frey,
University Hospital Erlangen, Germany

Reviewed by:
Stina Linnea Wickström,
Karolinska Institutet (KI), Sweden
Keywan Mortezaee,
Kurdistan University of Medical Sciences, Iran

***Correspondence:**
Lunxu Liu
lunxu_liu@aliyun.com

†These authors have contributed equally to this work

Specialty section:
This article was submitted to Cancer Immunity and Immunotherapy, a section of the journal Frontiers in Oncology

Received: 14 April 2021
Accepted: 25 August 2021
Published: 15 September 2021

Citation:
Yang Z, Deng Y, Cheng J, Wei S, Luo H and Liu L (2021) Tumor-Infiltrating PD-1^{hi}CD8^{+}-T-Cell Signature as an Effective Biomarker for Immune Checkpoint Inhibitor Therapy Response Across Multiple Cancers. Front. Oncol. 11:695006. doi: 10.3389/fonc.2021.695006

Background: Stratification of patients who could benefit from immune checkpoint inhibitor (ICI) therapy is of much importance. PD-1^{hi}CD8^{+} T cells represent a newly identified and effective biomarker for ICI therapy response biomarker in lung cancer. Accurately quantifying these T cells using commonly available RNA sequencing (RNA-seq) data may extend their applications to more cancer types.

Method: We built a transcriptome signature of PD-1^{hi}CD8^{+} T cells from bulk RNA-seq and single-cell RNA-seq (scRNA-seq) data of tumor-infiltrating immune cells. The signature was validated by flow cytometry and in independent datasets. The clinical applications of the signature were explored in non-small-cell lung cancer, melanoma, gastric cancer, urothelial cancer, and a mouse model of breast cancer samples treated with ICI, and systematically evaluated across 21 cancer types in The Cancer Genome Atlas (TCGA). Its associations with other biomarkers were also determined.

Results: Signature scores could be used to identify the PD-1^{hi}CD8^{+} T subset and were correlated with the fraction of PD-1^{hi}CD8^{+} T cells in tumor tissue (Pearson correlation, R=0.76, p=0.0004). Furthermore, in the scRNA-seq dataset, we confirmed the capability of PD-1^{hi}CD8^{+} T cells to secrete CXCL13, as well as their interactions with other immune cells. In 581 clinical samples and 204 mouse models treated with ICIs, high signature scores were associated with increased survival, and the signature achieved area under the receiver operating characteristic curve scores of 0.755 (ranging from 0.61 to 0.91) in predicting therapy response. In TCGA pan-cancer datasets, our signature scores were consistently correlated with therapy response (R=0.78, p<0.0001) and partially explained the diverse response rates among different cancer types. Finally, our signature generally outperformed other mRNA-based predictors and showed improved predictive performance when used in combination with tumor mutational burden (TMB).

The signature score is available in the R package "PD1highCD8Tscore" (https://github.com/Liulab/PD1highCD8Tscore).

Conclusion: Through estimating the fraction of the PD-1^{hi}CD8^{+} T cell, our signature could predict response to ICI therapy across multiple cancers and could serve as a complementary biomarker to TMB.

Keywords: immune checkpoint inhibitor, cancer, PD-1^{hi}CD8^{+} T cell, biomarker, CXCL13

INTRODUCTION

Genomic alterations in malignant tumors distinguish them from normal cells and produce persistent antigenic stimulation, thereby suppressing T cell functions (1–3). Immune checkpoint inhibitors (ICIs) successfully reinvigorate T cell functions and have led to impressive progress in the treatment of non-small-cell lung cancer (NSCLC), melanoma, and urothelial cancer, especially in the advanced stages (4–6). However, only a limited proportion of patients receiving ICI therapy have superior clinical outcomes across various cancer types. To solve this problem, several biomarkers have been identified in recent years, including tumor mutational burden (TMB), tumor-neoantigen burden, programmed cell death protein 1 (PD-1) or programmed cell death ligand 1 (PD-L1) expression level, interferon-gamma (IFNγ) signature, and CD8^{+} T cell infiltration (7–11). Although these factors are related to the effectiveness of ICIs, their predictive power is not sufficient (9, 12), nor do they fully explain the mechanism of resistance to ICIs. There is thus an urgent need for new biomarkers that can be used to identify patients sensitive to ICI therapy

PD-1^{hi}CD8^{+} T cells represent a distinct population of CD8^{+} T cells, which are upregulated in T-cell-exhaustion and cell proliferation process (13). A recent retrospective analysis used immunohistochemistry (IHC) assays to estimate the fraction of PD-1^{hi}CD8^{+} T cells in the tumor microenvironment (TME) and demonstrated that this was positively associated with treatment response and patient survival in cases of NSCLC treated with PD-1 blockade (13). This finding raised the question of whether the predictive value of PD-1^{hi}CD8^{+} T cells could be extrapolated to other cancer types. Commonly available datasets such as RNA sequencing (RNA-seq) datasets could help to settle this issue. Therefore, we built a transcriptional signature for PD-1^{hi}CD8^{+} T cells, validated its ability to quantify such cells in the TME, and further explored its predictive performance with respect to ICI therapy outcomes across multiple cancer types.

Abbreviations: AUC, area under the receiver operation characteristic curve; BLCA, bladder urothelial carcinoma; CAM, cell adhesion molecules; CCLE, The Cancer Cell Line Encyclopedia; CR, complete response; CRMA, Anti-CTLA4 resistance MAGE genes; COAD_MSI, colon adenocarcinoma with microsatellite instability phenotype; DCB, durable clinical benefit; DEG, differential expressed gene; FDA, Food and Drug Administration; GO, gene ontology; GSVA, gene set variation analysis; HCC, hepatocellular carcinoma; ICI, immune checkpoint inhibitor; IHC, immunohistochemistry; IPS, immunophenoscore; KEGG, Kyoto Encyclopedia of Genes and Genomes; LUAD, lung adenocarcinoma; LUSC, lung squamous cell carcinoma; MSigDB, Molecular Signatures Database; NSCLC, non-small cell lung cancer; NDB, nondurable benefit; ORR, objective response rate; OS, overall survival; OV, ovarian serous cystadenocarcinoma; PFS, progression-free survival; PR, partial response; scRNA-seq, single-cell RNA-seq; SD, stable disease; SKCM, skin cutaneous melanoma; TCGA, The Cancer Genome Atlas; TIL, tumor infiltrating lymphocytes; TMB, tumor mutational burden.

MATERIALS AND METHODS

Data Collection

We identified ICI-treated patients with available RNA-seq data from the Gene Expression Omnibus (GEO, https://www.ncbi.nlm.nih.gov/geo/) and Sequence Read Archive (SRA, https://www.ncbi.nlm.nih.gov/sra/) databases. Data from The Cancer Genome Atlas (TCGA, http://cancergenome.nih.gov/;legacy archive, version 2016_01_28) were downloaded from FIREBROWSE (http://firebrowse.org/). All the deposited datasets are summarized in **Table 1**.

Identification of Differentially Expressed Genes

The RNA-seq data were aligned to the human genome (GRCH38/hg38) using the STAR (24) version 2.5.4b 2-pass mapping strategy. Transcript assembly and gene level quantification were performed using StringTie version v1.3.4d (25). DEGs were identified using DESeq2 (30) (version 1.26.0). Genes were considered to be DEGs based on adjusted p value (p.adj) < 0.05 and |log2 [fold change (FC)]| >1.

Construction of Gene Signature for PD-1^{hi}CD8^{+} T Cells

The workflow followed to build the signature building is described in **Figure 1** (left). First, we combined CD8^{+}-T-cell-specific genes from Schmiedel et al. (39) with PD-1^{hi}CD8^{+}-T-cell-specific genes from NSCLC tumor-infiltrating lymphocytes (TILs) (13). In the latter case, PD-1^{hi}CD8^{+}-T-cell-specific genes were defined as genes that were significantly upregulated in PD-1^{hi}CD8^{+} T cells compared with other CD8^{+} T cells. Second, we excluded genes that were highly expressed in solid tumors using expression data from The Cancer Cell Line Encyclopedia (CCLE, https://portals.broadinstitute.org/ccle). Genes were retained if their median expression (log transcripts per million [TPM]) in cancer cells was below 3.1. Third, to determine the optimal threshold for filtering low expression genes in PD-1^{hi}CD8^{+} T cells, we scanned a range of cutoffs to select top genes as input for unsupervised hierarchical clustering (from 20% to 80%, with 20% increments). We found that the top 60% genes were sufficient to distinguish PD-1^{hi}CD8^{+} T cells from

TABLE 1 | Key resource table.

Resource	Source	Identifier
Deposited Data		
Solid tumor samples	CCLE	https://portals.broadinstitute.org/
Immune cell from healthy individuals	DICE	https://dice-database.org/
Pan-cancer tumor samples (21 types)	TCGA	http://firebrowse.org/
Sorted PD-1$^{hi/low/neg}$CD8^{+} T cells from NSCLC	Thommen et al. (13)	SRA: SRP108393
Sorted PD-1$^{hi/low/neg}$CD8^{+} T cells from HCC, flow cytometry, and RNA-seq results	Kim et al. (14)	GEO: GSE111389
Sorted PD-1$^{hi/low/neg}$CD8^{+} T cells from breast cancer	Guo et al. (15)	SRA: SRP189910
Anti-PD-1/anti-PD-1 combined with anti-CTLA4 treated melanoma (Gide)	Gide et al. (16)	ENA: ERP105482
Anti-PD-1 treated melanoma (Riaz)	Riaz et al. (17)	SRA: SRP094781
Anti-PD-1 treated gastric cancer	Kim et al. (18)	ENA: ERP107734
Anti-PD-L1 treated urothelial cancer	Mariathasan et al. (5)	http://research-pub.gene.com/IMvigor210CoreBiologies/
Anti-PD-1/PD-L1 treated NSCLC (Jung)	Jung et al. (19)	GEO: GSE135222
Anti-PD-1 treated NSCLC (Cho)	Cho et al. (20)	GEO: GSE126044
ScRNA-seq of immune cells in melanoma TME	Sade-Feldman et al. (21)	GEO: GSE120575
ScRNA-seq of T cells in NSCLC TME	Guo et al. (22)	GEO: GSE99254
Anti-PD1/anti-CTLA4 combination therapy treated mouse model of breast cancer	Hollern et al. (23)	GEO: GSE124821
Human genome (GRCH38/hg38)	Genome Reference Consortium	http://www.ncbi.nlm.nih.gov/projects/genome/assembly/grc/human
Software and Algorithms		
STAR version 2.5.4b	Dobin et al. (24)	https://github.com/alexdobin/STAR
Stringtie, version v1.3.4d	Pertea et al. (25)	https://ccb.jhu.edu/software/stringtie/
Metascape	Zhou et al. (26)	https://metascape.org/
CellPhoneDB	Efremova et al. (27)	https://github.com/Teichlab/cellphonedb
MSigDB	–	http://www.gsea-msigdb.org/gsea/msigdb
CIBERSORT	Newman et al. (28)	https://cibersort.stanford.edu/
quanTIseq	Finotello et al. (29)	https://github.com/icbi-lab/quanTIseq
R packages/scripts		
Codes used for scoring	This paper	https://github.com/Liulab/PD1highCD8Tscore
DESeq2 (1.26.0)	Love et al. (30)	https://bioconductor.org/packages/release/bioc/html/DESeq2.html
limma (3.41.16)	Ritchie et al. (31)	https://bioconductor.org/packages/release/bioc/html/limma.html
singscore (1.10.0)	Foroutan et al. (32)	https://www.bioconductor.org/packages/release/bioc/html/singscore.html
Seurat (3.1.0)	Butler et al. (33)	https://satijalab.org/seurat/
edgeR (3.27.13)	Robinson et al. (34)	https://bioconductor.org/packages/release/bioc/html/edgeR.html
fgsea (1.12.0)	Sergushichev (35)	http://bioconductor.org/packages/release/bioc/html/fgsea.html
pROC (1.15.3)	Robin et al. (36)	https://cran.r-project.org/web/packages/pROC/index.html
survival (3.1-12)	–	https://cran.r-project.org/web/packages/survival/index.html
survminer (0.4.8)	–	https://cran.r-project.org/web/packages/survminer/index.html
biomaRt (2.42.0)	Durinck et al. (37)	https://bioconductor.org/packages/release/bioc/html/biomaRt.html
immunophenoscore	Charoentong et al. (38)	https://tcia.at/tools/toolsMain

other CD8^{+} T cells and kept them as the initial gene set. The signature scores were calculated by singscore (32), where the background gene set was selected as genes with mean TPM>1 in TCGA samples (21 cancer types). When calculating the signature score of the initial gene set in a single-cell RNA-seq(scRNA-seq) dataset (GSE120575) (21), we found that a cluster of CD8^{+} T cells resembled PD-1^{hi}CD8^{+} T cells from NSCLC TILs (13). Therefore, we kept the cluster marker genes from the initial signature genes and got a reduced final signature. The discrimination abilities of the initial and final gene signature scores were compared using the area under the receiver operation characteristic curve (AUC). Finally, we supplied an easy-to-use R package "PD1highCD8Tscore" to calculate our signature score.

Signature Validation

To explore whether the signature genes were specific to PD-1^{hi}CD8^{+} T cells, we compared the expression levels of signature genes between PD-1^{hi}CD8^{+} T cells and other immune cells in an external dataset (39) after normalization by 15 house-keeping genes (RPL38, UBA52, RPL4, RPS29, SLC25A3, CLTC, RPL37, PSMA1, RPL8, PPP2CA, TXNL1, MMADHC, PSMC1, RPL13A, and MRFAP1) (40). Two previous studies also sorted and sequenced PD-1$^{hi/low/neg}$CD8^{+} T cells among hepatocellular carcinoma (HCC) and breast cancer TILs with a similar gating and sorting strategy (14, 15). To estimate whether our signature characterized similar cell populations in NSCLC, breast cancer, and HCC, we performed principal component analysis (PCA) and calculated the correlations between all cells after removing the batch effect using

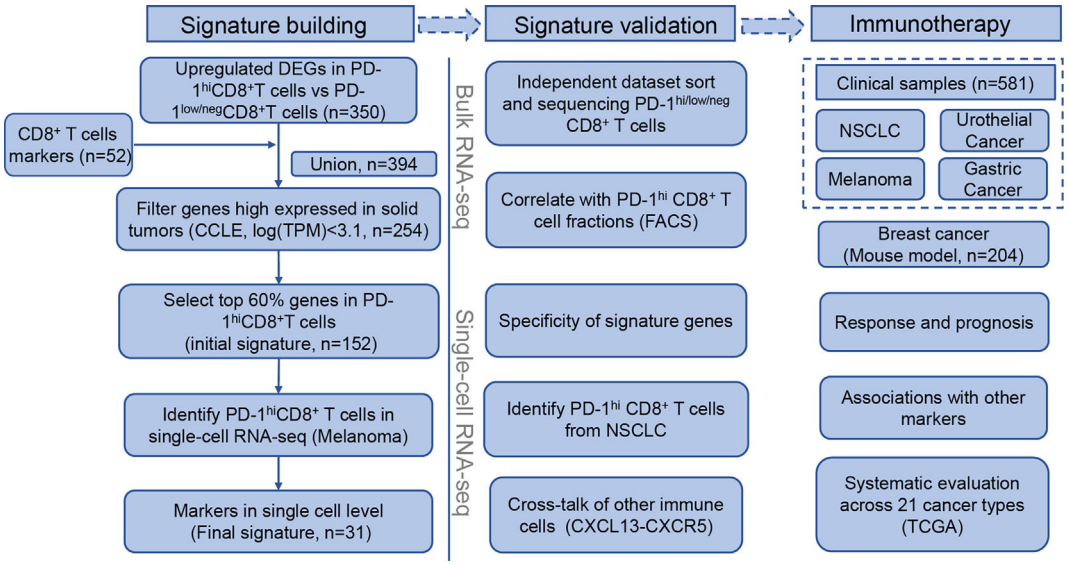

FIGURE 1 | Flowchart of PD-1^{hi}CD8^{+} T cells signature building, validation, and clinical implications in immune checkpoint inhibitor therapy.

the "limma" package (31). Scores were calculated and compared in each bulk RNA-seq dataset. Moreover, we calculated the scores in 17 HCC tumor samples and analyzed the correlation between scores and the absolute fraction of PD-1^{hi}CD8^{+} T cells. The absolute fraction of PD-1^{hi} CD8^{+} T cells was defined as the product of the relative fraction of PD-1^{hi} CD8^{+} T cells in CD8^{+} T cells and the fraction of CD8^{+} T cells in tumor samples. The former fraction was based on the flow cytometry results of Kim et al. (data were obtained by personal communications). The latter fraction was estimated by QuanTIseq (29).

We downloaded TPM data and/or count data and cell labels from two scRNA-seq (21, 22) datasets for immune cells. Cells with 1,000–5,000 detected genes and expressing <5% mitochondrial genes were retained. Standard procedures for variable gene selection, dimensionality reduction, and clustering were performed using Seurat version 3 (33), and the top 3,000 variable genes were selected. Signature scores were calculated based on TPM data. The cluster with the highest signature score was labeled the PD-1^{hi}CD8^{+} T cell, and other clusters were labeled according to the original paper. Clustering results were visualized using uniform manifold approximation and projection. Differential expression test was performed using the "FindMarkers" function with Wilcoxon rank-sum test in genes expressed in at least 25% of cells using the default threshold (|logFC|>0.25). Gene ontology (GO) enrichment analyses were performed using Metascape (26) with p<0.01 and enrichment score >1.5. Cell–cell communication analysis was conducted using CellPhoneDB (27).

Signature Scores in ICI-Treated Patients and Mouse Models

We scored all ICI-treated samples (5, 16–20) and compared the differences between responders (durable clinical benefit, DCB) and nonresponders (nondurable benefit, NDB) by Wilcoxon rank-sum test. DCB was defined as complete response (CR), partial response (PR), or stable disease (SD) for more than 6 months. NDB was defined as progressive disease (PD) or SD for less than 6 months. In two studies (17, 18), no detailed information was available on DCB/NDB; therefore, we compared the CR/PR group with the PD group as a surrogate. In a mouse model of ICI-treated breast cancer (23), we used the "biomaRt" package (37) to convert genes from mouse to human and compared the scores between ICI-resistant and ICI-sensitive samples. The predictive value of the signature score in response for ICI therapy was evaluated by calculating AUC values (36). Patients with survival data available were divided into high and low score groups according to the Yuden index. Overall survival (OS) and progression-free survival (PFS) were estimated by Kaplan-Meier curves, and the log-rank test was used to compare Kaplan-Meier survival curves. A multivariable Cox proportional hazard model was built to correct the effects of potential confounding factors.

TCGA Data Processing

Reported objective response rates (ORRs) across 21 cancer types were obtained from Lee and Ruppin (9). We scored 6,764 samples from TCGA in the corresponding cancer types. We investigated the correlation of the proportion of high signature score samples in each cancer type with the response rate. DEGs between the samples with the top 33% and bottom 33% signature scores were detected by edgeR (34). The definition of DEGs was the same as that in Section 2.2. Kyoto Encyclopedia of Genes and Genomes (KEGG) gene sets from the Molecular Signatures Database (MSigDB, http://www.gsea-msigdb.org/gsea/msigdb) were scored for DEGs using gene set variation analysis

(GSVA), where p<0.05 and |normalized enrichment score (NES)| >1 were considered to indicate significance.

Other ICI Therapy Biomarkers

We compared our signature with other predictive biomarkers for ICI. PD-L1 is an IHC biomarker approved by the Food and Drug Administration (FDA) (41). PD-L1 gene expression was used here as an IHC surrogate. PD-1 gene expression is also a predictor of ICI therapy response (7). IFNγ was found to be a response biomarker by Ayers et al. (10). The mean expression of six genes (IFNG, STAT1, IDO1, CXCL10, CXCL9, and HLA-DRA) in this pathway was used to estimate their performance (10). The score for Anti-CTLA4 resistance MAGE genes (CRMA) was calculated as the average of MAGEA3, MAGEA2, MAGEA2B, MAGEA12, and MAGEA6 (42). Immunophenoscore (IPS) was calculated using a script supplied by The Cancer Immunome Atlas (https://tcia.at/) (38). Tertiary lymphoid structure (TLS) signature genes were obtained from Cabrita et al. (43). CD8^{+} T cell proportions were estimated by CIBERSORT (28) (CD8^{+} T CIBERSROT). TMB was available for two cohorts. For **Figures 6A, B**, a logistic regression of TMB and signature score was used to assess the combined predictive value for ICI. In the survival analysis of **Figures 6C–F**, patients were divided into four groups, TMB^{high}Score^{high}, TMB^{low}Score^{high}, TMB^{high}Score^{low}, and TMB^{low}Score^{low}, according to their TMB and signature score. The cutoff was determined by the best Yuden index. Similarly, the effect of combination of PDL1 and our score was also analyzed.

Statistical Analysis

All the software packages and algorithms are summarized in **Table 1**. R version 3.5.1 was used for statistical analysis and visualization. The AUC was used to evaluate the predictive value of the signature score to ICI therapy. A two-sided Wilcoxon rank-sum test was used for between-group comparisons, and p-value<0.05 was regarded as statistically significant.

RESULTS

Building the PD-1^{hi}CD8^{+}-T-Cell-Derived Signature

The flowchart of the process of building the PD-1^{hi}CD8^{+}-T-cell signature is depicted in **Figure 1** (left). We first combined CD8^{+}-T-cells-specific genes and DEGs in PD-1^{hi}CD8^{+} T cells (**Supplementary Figure 1**), resulting in 394 genes. To identify immune-specific genes, the sequencing data of solid cancer from CCLE were downloaded, and 150 genes highly expressed (logTPM>3.1) in cancer cells were filtered. We selected the top 60% expressed genes in PD-1^{hi}CD8^{+} T cells as an initial signature (152 genes), which were sufficient for clustering PD-1^{hi}CD8^{+} T cells apart from PD-1$^{low/neg}$CD8^{+} T (**Supplementary Figures 2**, **3A, B**). In a scRNA-seq dataset, we found a cluster of cells with a high initial signature score that exhibited a similar phenotype to that of PD-1^{hi}CD8^{+} T cells (upregulated genes enriched in T cell exhaustion and cell proliferation/growth) (**Supplementary Figures 4A, B**). The common genes between the initial signature and marker genes of this cluster were considered as the final signature (31 genes, **Table S1**). The discrimination ability of the final signature was the same as that of the initial signature (AUC=1) (**Supplementary Figures 3A, B**). The signature included seven cell-cycle-associated genes (BARD1, CENPE, RAD51, SMC2, GINS2, CLSPN, and CCNF) and seven T-cell-exhaustion-associated genes (CTLA4, PDCD1, TOX, SIRPG, HAVCR2, TIGIT, and IGFLR1) (44, 45).

Validation of PD-1^{hi}CD8^{+}-T-Cell-Derived Signature

The PD-1^{hi}CD8^{+}-T-cell signature was validated in both bulk RNA-seq and scRNA-seq data (**Figure 1**, middle). In the bulk RNA-seq data (13, 39), we found that the signature score could discriminate PD-1^{hi}CD8^{+} T cells from other immune cells collected from healthy individuals (p<0.0001), and the signature genes were relatively specific (**Figures 2A, B**). In two independent studies (14, 15), PD-1$^{hi/low/neg}$CD8^{+} T cells were also sorted and sequenced from HCC and breast cancer TILs by flow cytometry. The PCA and correlation results showed that the sorted PD-1^{hi}CD8^{+} T cells had similar transcriptional features and were tissue-agnostic among lung, liver, and breast tissues (**Supplementary Figures 3C, D**). The PD-1^{hi}CD8^{+} T cells had the highest signature score compared with other CD8^{+} T cells and were accurately identified by our score (AUC=1) (**Figure 2C** and **Supplementary Figures 3A, B, E**). The signature score was correlated with the fraction of PD-1^{hi}CD8^{+} T cells in HCC tumor samples (Pearson correlation, R=0.76, p=0.0004, **Figure 2D**). Patients with high fractions of PD-1^{hi}CD8^{+} T cells had higher scores than other patients (p=0.0009, **Supplementary Figure 3F**). In scRNA-seq data of melanoma TILs (21), the PD-1^{hi}CD8^{+} T cells were identified by our score (**Figure 2E** and **Supplementary Figure 4A**), and most of the signature genes had higher expression values in this subset than other immune cells in the TME. (**Figure 2F**). Similar results were found in another scRNA-seq data of NSCLC TILs (**Supplementary Figure 4C**) (22). We identified a high-scoring subcluster of exhausted CD8^{+} T cells, with highly expressed genes enriched in cell proliferation/growth (**Supplementary Figure 4B**). GSVA analyses also confirmed that the cell cycle pathway was more activated in PD-1^{hi}CD8^{+} T cells compared with other exhausted CD8^{+} T cell subsets with PD-1 expression (melanoma: NES=2.07, p.adj=0.0059; NSCLC: NES=1.98, p.adj=0.0130). Increased glycolysis (melanoma: p<0.0001; NSCLC: p<0.0001) and secretion of CXCL13 were found in (melanoma: logFC=1.22, p.adj<0.0001; NSCLC: logFC=0.85, p.adj<0.0001) PD-1^{hi}CD8^{+} T cell, consistent with a previous report (**Supplementary Figure 5**) (13). The cell–cell interaction analysis using CellPhoneDB found that PD-1^{hi}CD8^{+} T cells interacted with B cells (mean= 5.424, p<0.0001), regulatory T cell (mean= 3.801, p<0.0001), and cytotoxicity T cells (mean= 3.683, p<0.0001) through the CXCL13-CXCR5 axis (**Figure 2G**).

Effectiveness of Signature Score in Predicting Response to ICI Therapy

To evaluate the effectiveness of our signature score in predicting response to ICI therapy, we obtained 581 RNA-seq samples from

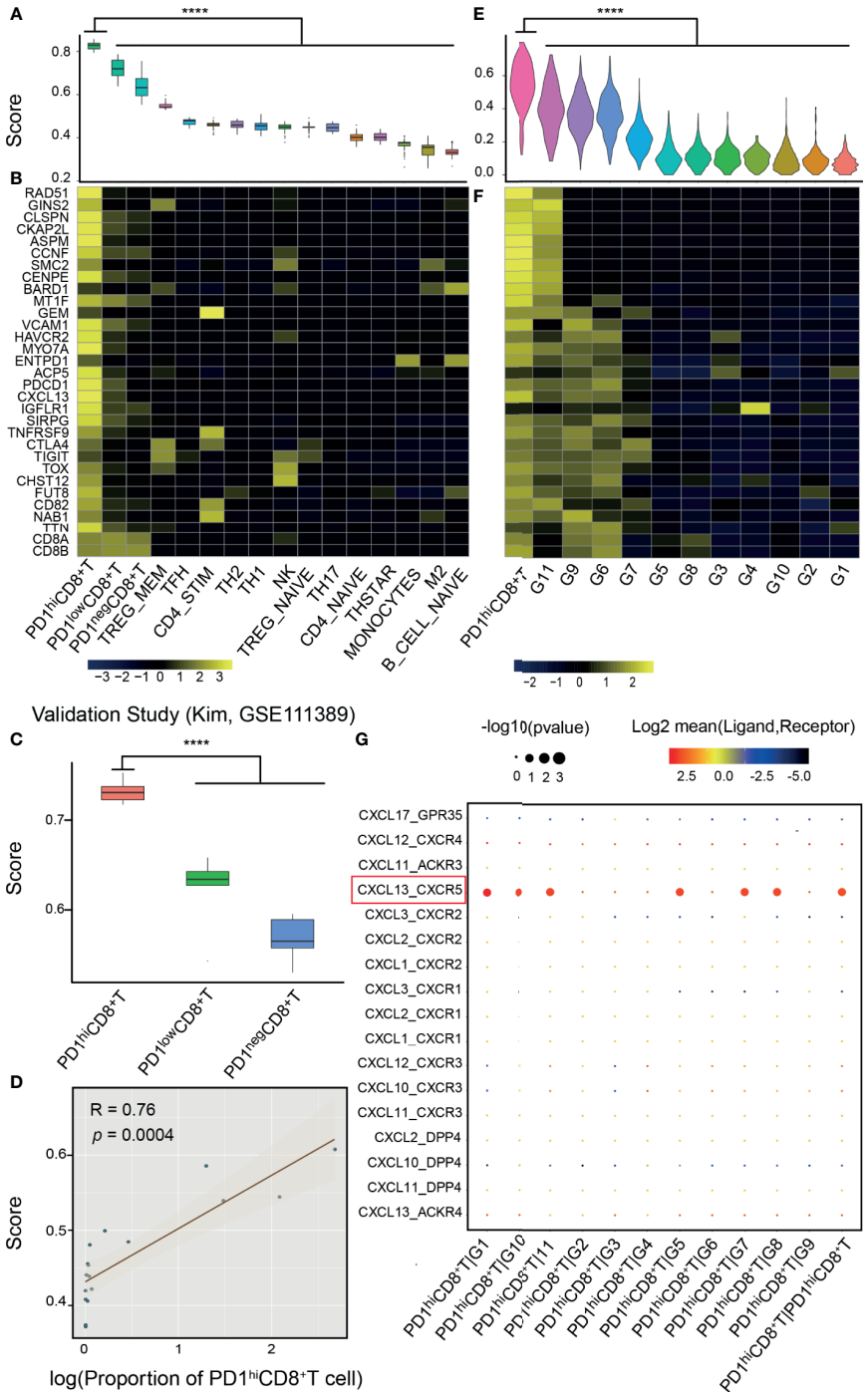

FIGURE 2 | Validation of the signature score from bulk and single-cell RNA-seq data. **(A)** Bulk RNA-seq data of PD-1^{hi}CD8^{+} T cells and other immune cells from the database of immune cell expression project were integrated after normalization by house-keeping genes. PD-1^{hi}CD8^{+} T cells had the highest score than other immune cells (****: p<0.0001). **(B)** Signature genes were specific to PD-1^{hi}CD8^{+} T cells. **(C)** The signature score can discriminate PD-1$^{hi/low/neg}$CD8^{+} T cells in another study (18), where these cells were sorted and sequenced from hepatocellular carcinoma (HCC). **(D)** The proportion of PD-1^{hi}CD8^{+} T cells in HCC tumor samples was correlated with the signature score (Pearson correlation, R=0.76, p=0.0004). **(E)** In single-cell RNA-seq of melanoma tumor infiltrating immune cells, PD-1^{hi}CD8^{+} T cells had the highest score (****: p<0.0001), and the signature genes were highly expressed in this cluster **(F)**. **(G)** The ligand–receptor interactions between PD1^{hi}CD8^{+}T cells and other immune cells. PD1^{hi}CD8^{+}T cells secreted CXCL13 chemokine and interacted with the chemokine receptor CXCR5 expressing on B cells, cytotoxicity lymphocytes, memory T cells, and regulatory T cells. G1, B cells; G2, plasma cells; G3, monocytes/macrophages; G4, dendritic cells; G5, lymphocytes; G6, exhausted CD8^{+} T cells; G7, regulatory T cells; G8, cytotoxicity lymphocytes; G9, exhausted/heat-shock CD8^{+} T cells; G10, memory T cells; G11, exhausted/cell cycle (CD4^{+} T cell).

eight cohorts (six studies) across four cancer types, NSCLC, melanoma, gastric cancer, and urothelial cancer (**Figure 1**, right). These studies are summarized in **Supplementary Table 2**. Interestingly, the signature scores were significantly higher in responders than in nonresponders, except in one cohort where the difference was nearly significant (p=0.096) (**Figures 3A–H**). In another 204 ICI-treated breast cancer mouse models, the sensitive groups had higher scores than resistant groups at all the 4 timepoints of sample collection (pretreatment, p<0.0001;3 days after ICI p=0.0002;7 days after ICI p=0.0001; end of study p<0.0001; **Supplementary Figure 6**). Next, we calculated AUCs to evaluate the predictive value of PD-1^{hi}CD8^{+} T cells for ICI therapy response. The median AUC across the eight cohorts was 0.755 (range: 0.61 to 0.91) (**Figure 3I**). In two studies involving both pretreatment and on-treatment datasets, the AUCs in the on-treatment groups were higher than those in the pretreatment group from the same study. Moreover, the signature score (continuous variable, **Table S3**) was positively associated with OS and PFS. We divided each cohort into high- and low-score groups and found that high-score patients had better survival with respect to either OS or PFS (**Figure 4**). Furthermore, to explore whether the signature score was an independent prognostic factor, we built a multivariable Cox proportional hazard model including age, sex, and treatment regimens if available. A high PD-1^{hi}CD8^{+} T cell score was found to be independently associated with a 76–94% reduction in the risk of disease progression and a 28–92% reduction in the risk for all mortality (**Table 2**). Similarly, the hazard ratios (HRs) in the

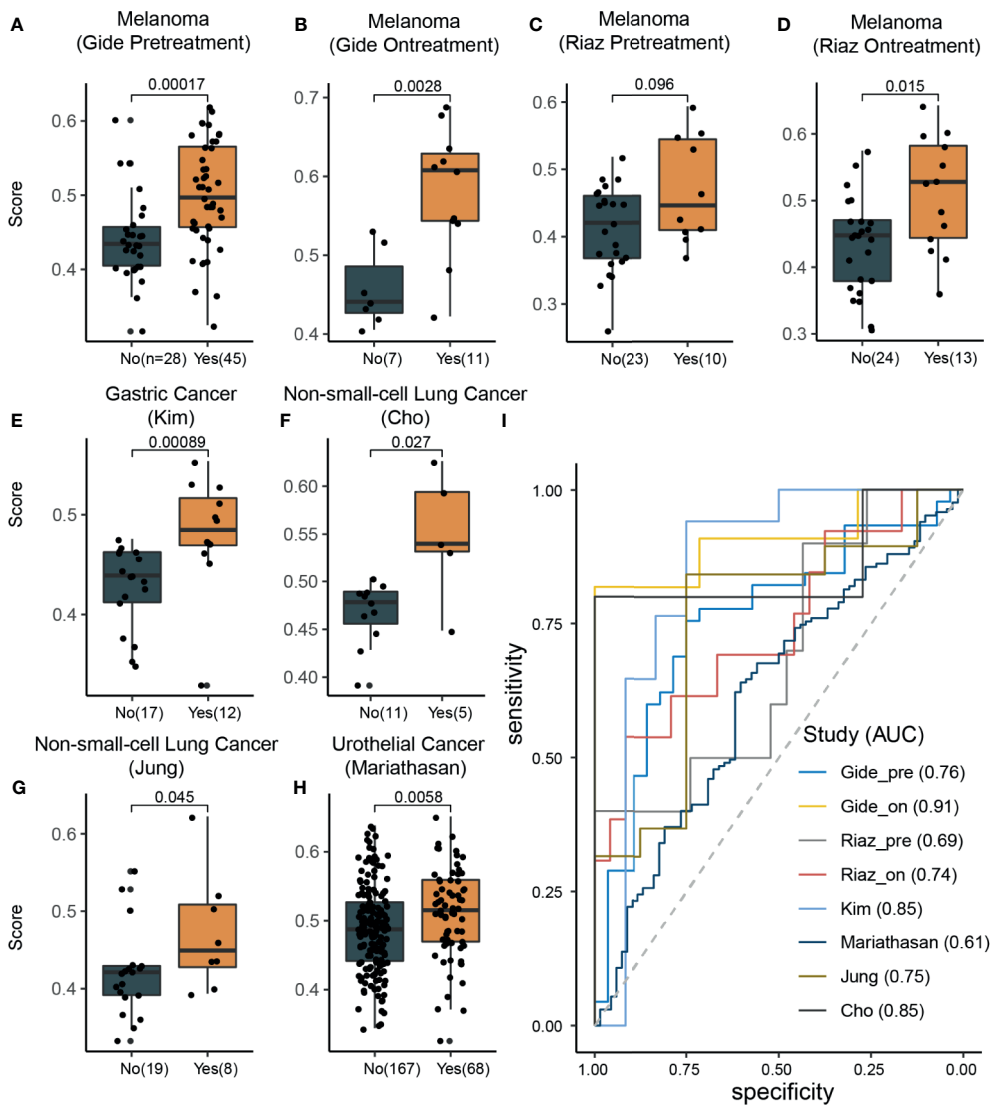

FIGURE 3 | The signature scores were associated with response rates across different cancer types. **(A–H)** In all datasets, the response group samples had significant (Wilcoxon rank-sum test) higher signature scores than nonresponse group samples (marginally significant in the Riaz pretreatment dataset; **C**). **(I)** Receiver operating characteristic curve analysis for response prediction in all datasets.

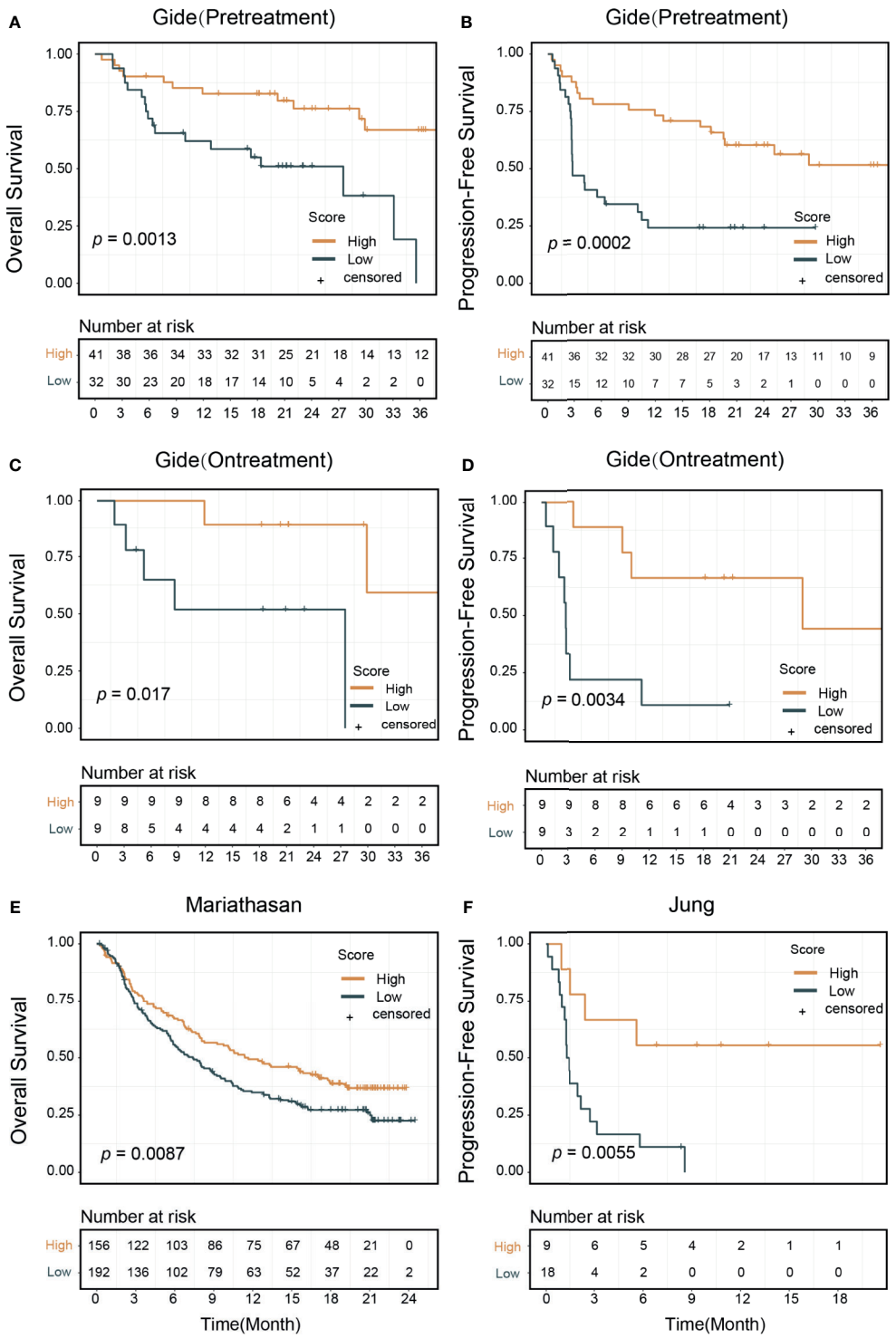

FIGURE 4 | Signature score and patients survival outcomes. Patients treated with immune checkpoint inhibitors were divided into high and low signature score groups. Kaplan–Meier curves showed that high score group patients had better survival outcomes: **(A)** In the pretreatment Gide dataset, p=0.013 (log-rank test) in overall survival, **(B)** p=0.0002 in progression-free survival. **(C)** In the on-treatment Gide dataset, p=0.017 for overall survival, **(D)** p=0.0034 in progression-free survival. **(E)** In the Mariathasan dataset, p=0.0087 for overall survival. **(F)** In the Jung dataset, p=0.0055 for progression-free survival.

on-treatment cohort (OS, HR=0.08, p=0.034; PFS, HR=0.06, p=0.003) were smaller than those in the pretreatment group (OS, HR=0.29, p=0.002; PFS, HR=0.29, p<0.001). Taken together, these results showed that our signature score could predict ICI therapy response and survival outcomes.

Predictive Value of the Signature Score in Pan-Cancer Analysis

We calculated the signature scores of 6,764 samples across 21 cancer types from TCGA and collected ORR data for anti-PD-1/PD-L1 therapy from Lee and Ruppin (9). The distribution of signature scores was higher in immune-hot tumors, including colon adenocarcinoma with microsatellite instability phenotype (COAD_MSI), lung squamous cell carcinoma (LUSC), lung adenocarcinoma (LUAD), head and neck squamous cell carcinoma, skin cutaneous melanoma (SKCM), and bladder urothelial carcinoma (BLCA) which were more sensitive to ICI therapy (**Figure 5**) (46, 47). In prostate adenocarcinoma, ovarian serous cystadenocarcinoma (OV) and glioblastoma multiforme tumors, which are known to be immune-cold tumors, the signature scores were lower (46, 47). Moreover, in the Mariathasan dataset, the immune-inflamed phenotype had higher scores than the immune-desert and immune-excluded phenotypes (**Supplementary Figure 7A**). Generally, the breast cancer samples showed low immune infiltration but had scores at the median level. This phenomenon could be attributed to the heterogeneity of tumor subtypes; triple-negative breast cancer had higher scores than other subtypes (p<0.0001, **Supplementary Figure 7B**). The fraction of high-score (80th-percentile) samples was correlated with ORR (Pearson correlation, R=0.78, p<0.0001). To explore the differences between high-score (top 33%) and low-score (bottom 33%) samples, DEGs were identified and their KEGG pathway enrichment was analyzed (**Supplementary Figure 8**). T cell receptor signaling pathway, cytokine–cytokine receptor interaction, and chemokine signaling pathway were activated in samples with high signature score across most cancer types (85%, [17/20], 100% [20/20], and 85%[17/20], respectively). The cell adhesion molecule (CAM) pathway, an important mediator of immune cell migration (48), was also upregulated in high-score samples (85%[17/20]). These results demonstrated that cancers with high signature scores had increased cell cross-talk and immune cell infiltration, reflecting an immune-hot phenotype. We also found that glycolysis and fatty acid metabolism were upregulated only in some ICI-therapy-sensitive cancer types. The interaction of PD-1 with the PD-L1 axis can upregulate aerobic glycolysis and induce fatty acid oxidation in T cells, leading to immunosuppression (49). Consequently, these cancer types were sensitive to anti-PD-1/PD-L1 therapy.

Comparison With Other ICI Biomarkers

We compared the predictive performance of our signature score with those of other widely used transcriptome biomarkers, including IFN-γ, PD-L1, PD-1, CRMA, TLS, IPS, and CD8^{+} T CIBERSORT. Our score was positively associated with all of

TABLE 2 | Multivariable Cox proportional model of signature score and other clinical factors.

Gide et al. pretreatment	HR	2.50%CI	97.50%CI	P
	Progression-free survival (n = 73)			
Score (n, %)				
Low (32, 43.8%)	Ref			
High (41, 56.5%)	0.29	0.15	0.56	<0.001
Age (mean ± sd: 61.6 ± 13.8)	0.99	0.97	1.02	0.559
Gender (n, %)				
Female (26, 35.6%)	Ref			
Male (47, 64.4)	1.44	0.74	2.8	0.286
Regimen (n, %)				
Monotherapy (41, 56.2%)	Ref			
Combined-therapy (32, 44.8)	0.43	0.22	0.85	0.015
Gide et al. on-treatment	Progression-free survival (n=18)			
Score (n, %)				
Low (32, 43.8%)				
High (41, 56.5%)	0.06	0.01	0.38	0.003
Age (mean ± sd: 60.3 ± 15.1)	0.97	0.92	1.02	0.295
Gender (n, %)				
Female (5, 27.8%)	Ref			
Male (13, 71.2%)	0.14	0.02	0.87	0.035
Regimen (n, %)				
Monotherapy (9, 50.0%)	Ref			
Combined-therapy (9, 50.0%)	1.38	0.37	5.17	0.63
Gide et al. pretreatment	Overall survival (n=73)			
Score (n, %)				
Low (32, 43.8%)				
High (41, 56.5%)	0.29	0.13	0.64	0.002
Age (mean ± sd: 61.6 ± 13.8)	1.00	0.97	1.03	0.938
Gender(n, %)				
Female (26, 35.6%)	Ref			
Male (47, 64.4)	1.60	0.67	3.83	0.294
Regimen(n, %)				
Monotherapy (41, 56.2%)	Ref			
Combined-therapy (32, 44.8)	0.25	0.09	0.7	0.008
Gide et al. on-treatment	Overall survival (n=18)			
Score(n, %)				
Low (32, 43.8%)	Ref			
High (41, 56.5%)	0.08	0.01	0.83	0.034
Age (mean ± sd: 60.3 ± 15.1)	1.00	0.97	1.03	0.938
Gender(n, %)				
Female (5, 27.8%)	Ref			
Male (13, 71.2%)	1.60	0.67	3.83	0.294
Regimen(n, %)				
Monotherapy (9, 50.0%)	Ref			
Combined-therapy (9, 50.0%)	0.25	0.09	0.70	0.008
Mariathasan et al.	Overall survival (n=348)			
Score (n, %)				
Low (192, 55.2%)	Ref			
High (156, 44.8%)	0.72	0.56	0.94	0.016
Gender (n, %)				
Female (76, 21.8%)	Ref			
Male (272, 78.2%)	0.81	0.60	1.10	0.183
Baseline ECOG (mean ± sd: 0.67 ± 0.57)	1.96	1.53	2.51	0
Smoking History (n, %)				
Current (35, 10.1%)	Ref			
Never (116, 33.3%)	1.18	0.75	1.87	0.472
Previous (197, 56.1%)	1.13	0.73	1.75	0.589
Received Platinum (n, %)				
No (76, 21.8%)	Ref			
Yes (272, 78.2%)	1.80	1.26	2.58	0.001
Jung et al.	Progression-free survival (n=27)			
Score (n, %)				

(Continued)

TABLE 2 | Continued

Gide et al. pretreatment	HR	2.50%CI	97.50%CI	P
	Progression-free survival (n = 73)			
Low (18, 66.7%)				
High (9, 33.3%)	0.23	0.08	0.71	0.011
Age (mean ± sd: 62.1 ± 9.0)	0.80	0.18	3.52	0.765
Gender (n, %)				
Female (5, 18.5%)	Ref			
Male (22, 81.5%)	0.94	0.31	2.87	0.92

these markers except CRMA (**Supplementary Figure 9A**). The net reclassification index showed that our score could better classify responders to ICI therapy except in two Riaz cohorts (**Supplementary Figure 9B**). A possible explanation was that in the Riaz cohorts, some of the patients had received ipilimumab therapy before PD-1 treatment, which may have influenced their immune status. The AUCs of the signature score, IFN-γ, and PD-L1 were higher than those of the other biomarkers (**Supplementary Figure 9C**). PD-L1 mRNA expression was correlated with our score (**Supplementary Figures 9A**, **10A–H**). In many cases (n=452), PD-L1 and our score stratified patients consistently (**Supplementary Table 4**). In the Mariathasan cohort, where there were 75 discordant samples between PD-L1 and our signature score, the combination of PD-L1 and our score resulted in slightly improved predictive value (AUC from 0.61 to 0.63). It is noteworthy that the OS rate was significantly higher for PD-L1^{high}Score^{high} samples than for other samples (log-rank, p=0.0025) (**Supplementary Figures 10I–K**). TMB has been reported as a genomic predictor of ICI therapy response in multiple cancer types (9). In two cohorts where TMB data were available, we found no significant association between TMB and our score (**Supplementary Figure 9A**). The combination of our signature and TMB was of higher predictive value than either our signature or TMB alone (**Figures 6A, B**). Next, we divided the patients into four groups by our signature score and TMB. The 1-year OS rates were 70.0% (95% CI: 59.0-83.0%) for the TMB^{high}Score^{high} group, 39.7% (95% CI: 29.0–54.3%) for the TMB^{high}Score^{low} group, 42.4% (95% CI: 31.8–56.7%) for the TMB^{low}Score^{high} group, and 30.1% (95% CI: 21.7–41.7%) for the TMB^{low}Score^{low} group (Mariathasan cohort, **Figure 6C**). The 1-year PFS rates were 60% (95% CI: 29–100%) for the TMB^{high}Score^{high} group and 50.0% (95% CI: 18.8–100%) for the TMB^{low}Score^{high}, in the other two groups; all patients progressed in less than 1 year (Jung cohort, **Figure 6D**). Patients in the TMB^{high}Score^{high} group showed better survival outcomes compared with other groups (log-rank p<0.001 for OS, p=0.045 for PFS, **Figures 6E, F**). In the Mariathasan cohort, patients in the TMB^{high}Score^{high} group showed increased OS compared with patients in the TMB^{high}Score^{low} group (log-rank p=0.008; HR=0.51, 95%CI: 0.30-0.84, p=0.008), suggesting that the signature score could act as a complementary biomarker to TMB.

DISCUSSION

The introduction of ICI therapy represents a milestone in cancer therapy. However, the low response rates to this type of therapy

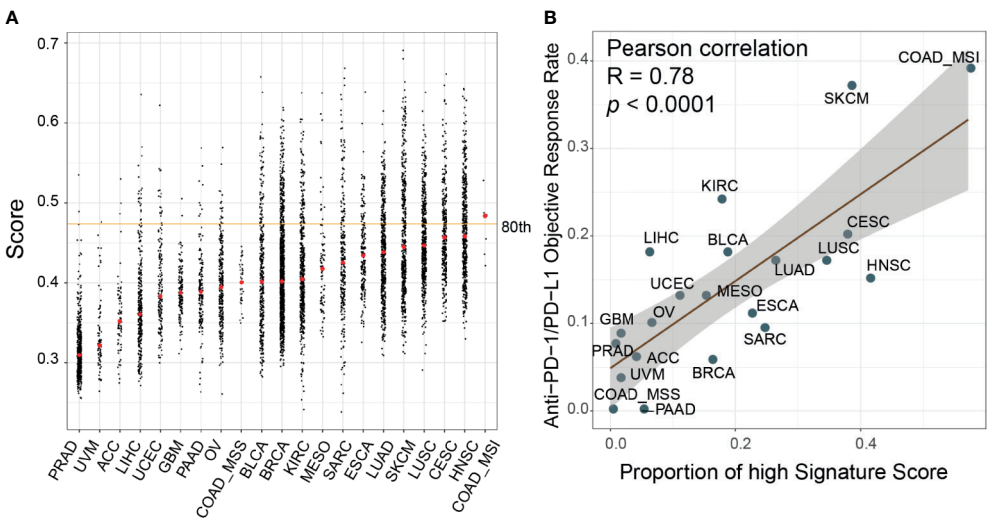

FIGURE 5 | Evaluation of the correlates of immune-check point inhibitors to signature scores across cancer types. **(A)** Distribution of the signature scores across 21 cancer types in The Cancer Genome Atlas (TCGA) dataset. The red dot within each cancer type denoted the median score; the orange line represented the 80th percentile score across all samples. **(B)** The proportion of high signature score (>80th percentile) samples was correlated with the reported objective response rates in a published paper (Pearson correlation, R=0.78, p<0.0001). ACC, adrenocortical carcinoma; BLCA, bladder urothelial carcinoma; BRCA, breast invasive carcinoma; CESC, cervical squamous cell carcinoma and endocervical adenocarcinoma; COAD, colon adenocarcinoma; ESCA, esophageal carcinoma; GBM, glioblastoma multiforme; HNSC, head and neck squamous cell carcinoma; KIRC, kidney renal clear cell carcinoma; LIHC, liver hepatocellular carcinoma; LUAD, lung adenocarcinoma; LUSC, lung squamous cell carcinoma; MESO, mesothelioma; OV, ovarian serous cystadenocarcinoma; PAAD, pancreatic adenocarcinoma; PRAD, prostate adenocarcinoma; SARC, sarcoma; SKCM, skin cutaneous melanoma; UCEC, uterine corpus endometrial carcinoma; UVM, uveal melanoma.

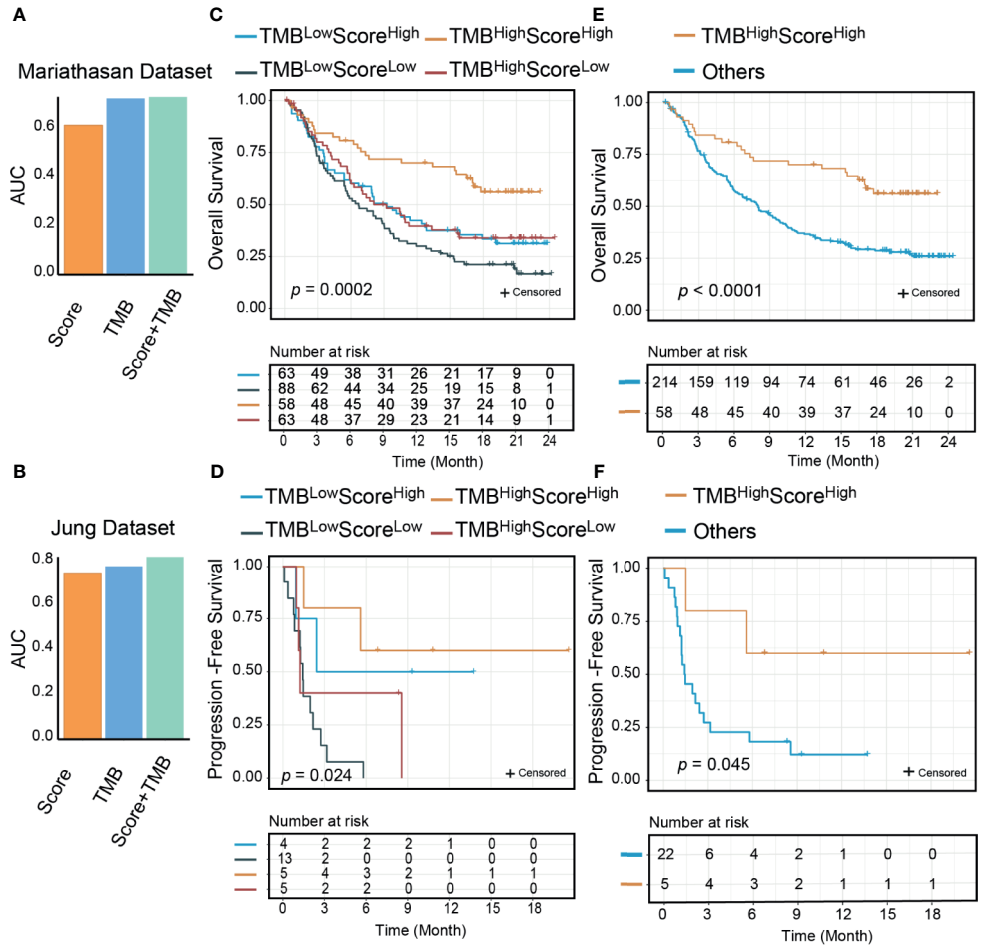

FIGURE 6 | The signature score could improve the predictive and prognostic value of tumor mutational burden (TMB). The area under the receiver operating characteristic curve (AUC) of the combination of the signature score and TMB was higher than TMB and the signature score (**A**: Mariathasan dataset; **B**: Jung dataset); Significant differences exist between the four groups (TMB^{high}Score^{high}, TMB^{low}Score^{high}, TMB^{high}Score^{low}, and TMB^{low}Score^{low}) in either overall survivals (**C**: Mariathasan dataset, p=0.0002) or progression-free survivals (**D**: Jung dataset, p=0.024) than other groups. TMB^{high}Score^{high} group patients had better overall survival (**E**: Mariathasan dataset, p<0.0001) and progression-free survival (**F**: Jung dataset, p=0.045) than other three groups.

will increase the economic burden on cancer patients. Treatment with anti-PD-1 agents requires about $6,000 per infusion, which is a much higher cost than transcriptome tests. Therefore, developing biomarkers for predicting ICI therapy response is an urgent and cost-effective field. In this study, we built a transcriptional signature of PD-1^{hi}CD8^{+} T cells. The signature score could discriminate this population from other immune cells in both bulk and single-cell-level datasets across different cancer types. Based on flow cytometry and RNA-seq results from an independent study, we validated the ability of our signature to quantify the fraction of PD-1^{hi}CD8^{+} T cells in tumor samples. Furthermore, we found that in NSCLC, melanoma, gastric cancer, urothelial cancer, and a mouse model of breast cancer, samples with high signature scores showed more benefit from ICI therapy. The predictive value of the signature score was better than those of other transcriptional markers. Combination of the signature score with TMB would improve its predictive value. In 21 TCGA cancer types, the signature score was correlated with ICI therapy response, revealing the intrinsic connection of the immunological activity of the TME described by the signature of each cancer tissue. Our study also offers an easy-to-use R package to evaluate PD-1^{hi}CD8^{+} T cell infiltration in more tumor samples.

Many studies have revealed that CD8^{+} TILs are heterogenous, and that different types of CD8^{+} TILs showed different response to ICIs (1, 21, 44). Our results also demonstrated the limited predictive value of CD8^{+} TILs. Persistent antigen exposure from tumor cells or antigen-presenting cells can cause CD8^{+} T cell exhaustion, inducing sustained expression of PD-1 in CD8^{+} TILs (1). Even within this dysfunctional compartment, CD8^{+} T cells have distinct roles in tumor immunity. Thommen et al. found that in NSCLC, the presence of PD-1^{hi}CD8^{+} T cells strongly predicted response to ICI therapy and was correlated with increased OS (13). In these cells, immune-checkpoint genes

(PD-1, CTLA4, TIGIT, HAVCR2/TIM-3, and TNFRSF9) (8) and transcription factor TOX, a central regulator of distinct exhausted T cell transformation (45), were highly expressed. PD-1^{hi}CD8^{+} T cells were distinct from other PD-1 positive CD8^{+} T cells, as the cell cycle and glycolysis process were upregulated in these cells. This phenotype was similar to that of the PD-1^{+}TIM-3^{+} T_{RM} cell identified by Clarke et al. (50), which was shown to be a favorable ICI therapy marker in NSCLC (50). Although it was not clear to what extent PD-1^{hi}CD8^{+} T cells overlapped with PD-1^{+}TIM-3^{+} T_{RM} cells, the predictive values of PD-1^{hi}CD8^{+} T cells were confirmed across 5 cancer types in nearly 600 clinical samples and 204 mouse models. Generally, we found that PD-1^{hi}CD8^{+} T cell scores of on-treatment samples were better than those of pretreatment samples because of the better reflection of immune status after therapy (51). Two studies have reported that the relative fraction of PD-1^{hi}CD8^{+} T cells in CD8^{+} cells, rather than the absolute fraction in total tumor tissue as estimated by our signature score, was negatively associated with ICI therapy outcomes (21, 52). In predicting ICI therapy response, the relative fraction of PD-1^{hi}CD8^{+} T cells might be largely influenced by the complex functions of other intratumor CD8^{+} T cells with negative or low PD-1 expression (21, 53).

Our results indicated that the PD-1^{hi}CD8^{+} T cell score was associated with the immune phenotype. Immune-hot tumors (COAD_MSI, SKCM, BLCA, LUSC, and LUAD) had higher signature scores and were sensitive to ICI therapy. Our score was predictive of the ORR to anti-PD-1/PD-L1 therapy across 21 cancer types in 6,764 TCGA samples (Pearson correlation, R=0.78, p<0.0001). In support of these results, we found that important pathways in antitumor activity were consistently upregulated in high-score samples, including cytokine–cytokine receptor interaction, chemokine signaling pathway, and T cell receptor signaling pathway (54). The CAM pathway was also activated in the high-score group, which was correlated with T cell infiltration in tumors (48). Moreover, in the Mariathasan dataset, immune-inflamed tumors had higher signature scores than immune-excluded or immune-desert samples. However, not all scores for these tumors were correlated with their phenotype. This discordance could be related to the spatial location of PD-1^{hi}CD8^{+} T cells and the impact of other immune cells, whereas our study mainly focused on the transcriptional features of PD-1^{hi}CD8^{+} T cells. Heterogeneity of tumor subtypes could also weaken the associations between our score and immune phenotypes. For example, breast cancer is generally considered as low immune-reactive cancer, but triple-negative breast cancer has been reported to be a high-immune-infiltration subtype (55). Our results consistently showed that this subtype had higher scores than other subtypes. Similarly, the COAD_MSI subtype was of immune-hot phenotype, unlike other COAD subtypes (56). On the other hand, glycolysis and fatty acid metabolism were only upregulated in some of the ICI-sensitive cancer samples with high scores. In PD-1 signaling, tumor cells can block antitumor immunity through this two metabolic pathways (49). These results partially explain why these cancer types are sensitive to anti-PD-1/PD-L1 therapy. Recent findings showed that targeting these metabolic interventions in combination with ICI could offer opportunities to improve therapy response; several clinical trials of such treatment are ongoing (57).

The main function of PD-1^{hi}CD8^{+} T cells is the secretion of CXCL13. In a previous study, CXCL13 was found to be mainly expressed by CD4^{+} follicular helper T cells, recruiting B cells and inducing TLS formation in the nonlymphoid tissue (58). In scRNA-seq data, as well as identifying a cluster of CD4^{+} T cells with high CXCL13 expression, we confirmed the secretion of CXCL13 from PD-1^{hi}CD8^{+} T cells and their interaction with B cells and regulatory T cells through the CXCL13-CXCR5 axis. These results indicated that PD-1^{hi}CD8^{+} T cells might recruit and organize immune cells through secretion of CXCL13, modulating the TME to an immune-hot phenotype. The positive association between the TLS score and the PD-1^{hi}CD8^{+} T cell score also supports this. The importance of CXCL13 in ICI therapy has been confirmed *in vivo*. Anti-PD-1 therapy failed in a CXCL13-null mouse model of BLCA, whereas the wild-type model showed a good response (59), and the treatment with a combination of CXCL13 and anti-PD-1 successfully retarded tumor growth in another mouse model of OV (60). Although the differences in CXCL13 secretion between CD4^{+} T cells and PD-1^{hi}CD8^{+} T cells remain elusive, these results indicate that CXCL13 is a potential therapeutic target that could be targeted in combination with ICI therapy.

Increasing evidence shows that response to ICI therapy is influenced by both immune cells and tumor-associated factors. PD-L1 positivity of tumor cells has been shown to be a good indicator of response to ICI therapy. In recent years, it has been recognized that high PD-L1 expression in dendritic cells, regulatory T cells, and macrophages can attenuate T cell activation and promote T cell exhaustion (61). The expression of PD-1 or PD-L1 in the TME is important for ICI therapy. In our study, patients in the PD-L1^{high}Score^{high} group benefited more from ICI therapy than other patients (**Supplementary Figure 10K**). TMB-high tumors had high levels of neoantigens, which make them more immunogenic and trigger a TIL response (11, 12). TMB has been approved by the FDA as a genomic biomarker in some cancer types (41, 62). However, TMB has some limitations as a biomarker, and it has been suggested that a combination of TMB with other predictors may show superior performance (12). Whereas TMB is reflective of tumor properties, our signature score for the PD-1^{hi}CD8^{+} T cell characterizes the tumor environment. In our analysis, TMB and the signature score both showed a good predictive value for ICI but were independent of each other. Therefore, it was intuitive to explore their potential combined effects. When samples were divided into four subtypes based on TMB and the signature score, the patients in the TMB^{high}Score^{high} group not only were highly immunogenic (characterized by a high TMB) but also showed an immune hot phenotype (characterized by a high signature score). These patients would be expected to be more sensitive to ICI therapy, and indeed they exhibited the best clinical outcomes in two independent datasets. These results warrant further confirmation and extension.

One of the potential limitations of our study was that our analysis was an integrated, retrospective study. Second, although the multivariable Cox proportional hazard model showed that the PD-1^{hi}CD8^{+} T cell score was an independent prognostic

indicator, some clinical prognostic factors, including the number of metastatic sites, first-line therapy information, and details of ICI therapy regimens, were not available. In the Riaz cohort, the difference between responders and nonresponders was not as obvious as those in other cohorts. Some patients receiving ipilimumab therapy before PD-1 treatment might be an additional confounder that would weaken the statistical power of our analysis (63, 64). Third, our study did not explore the mechanisms underlying the different effects of the PD-1^{hi}CD8^{+} T cell score in different cohorts or the variation in cutoff values for high-score samples in different cohorts. One possible mechanism may involve the complicated PD-L1 status in tumor cells or immune cells, like dendritic cells and macrophages. However, the gene expression of PD-L1 is a mixture of those cell types in RNA-seq; other methods including cytometry by time of flight and codetection by indexing may help explore this in the future.

CONCLUSIONS

In summary, we built a 31-gene signature to represent the fraction of PD-1^{hi}CD8^{+} T cells from bulk RNA-seq data and demonstrated promising potential of the PD-1^{hi}CD8^{+} T cell as a pan-cancer biomarker in patients receiving ICI therapy. The combination of the signature score with TMB could further increase its predictive value. The secretion of CXCL13 is a potential mechanism of how PD-1^{hi}CD8^{+} T cells modulate the TME and why high-scoring patients tend to have favorable outcomes of ICI therapy.

DATA AVAILABILITY STATEMENT

The original contributions presented in the study are included in the article/**Supplementary Material**. Further inquiries can be directed to the corresponding author.

AUTHOR CONTRIBUTIONS

Study concept and design: ZY, YD, and LL. Acquisition, analysis, or interpretation of data: ZY, YD, JC, SW, and HL. Drafting of the manuscript: all authors. Critical revision of the manuscript for important intellectual content: all authors. Study supervision: LL and YD. All authors contributed to the article and approved the submitted version.

FUNDING

This study was funded by the National Natural Science Foundation of China (NSFC 81672311 to LL and NSFC 31801119 to YD).

ACKNOWLEDGMENTS

We thank Prof. Hyung-Don Kim and Su-Hyung Park from Korea Advanced Institute of Science and Technology for kindly sharing bulk HCC tissue RNA-seq data as well as the percentage of PD-1^{hi}CD8^{+} TILs assessed by flow cytometry. We thank Prof. Shensi Shen from the Institute of Thoracic Oncology and Department of Thoracic Surgery, West China Hospital, Sichuan University for advice in revision.

SUPPLEMENTARY MATERIAL

The Supplementary Material for this article can be found online at: https://www.frontiersin.org/articles/10.3389/fonc.2021.695006/full#supplementary-material

REFERENCES

1. Thommen DS, Schumacher TN. T Cell Dysfunction in Cancer. *Cancer Cell* (2018) 33(4):547–62. doi: 10.1016/j.ccell.2018.03.012
2. O'Donnell JS, Teng MWL, Smyth MJ. Cancer Immunoediting and Resistance to T Cell-Based Immunotherapy. *Nat Rev Clin Oncol* (2019) 16(3):151–67. doi: 10.1038/s41571-018-0142-8
3. Mortezaee K. Immune Escape: A Critical Hallmark in Solid Tumors. *Life Sci* (2020) 258:118110. doi: 10.1016/j.lfs.2020.118110
4. Doroshow DB, Sanmamed MF, Hastings K, Politi K, Rimm DL, Chen L, et al. Immunotherapy in non-Small Cell Lung Cancer: Facts and Hopes. *Clin Cancer Res* (2019) 25(15):4592–602. doi: 10.1158/1078-0432.Ccr-18-1538
5. Mariathasan S, Turley SJ, Nickles D, Castiglioni A, Yuen K, Wang Y, et al. Tgfβ Attenuates Tumour Response to PD-L1 Blockade by Contributing to Exclusion of T Cells. *Nature* (2018) 554(7693):544–8. doi: 10.1038/nature25501
6. Beaver JA, Hazarika M, Mulkey F, Mushti S, Chen H, He K, et al. Patients With Melanoma Treated With an Anti-PD-1 Antibody Beyond RECIST Progression: A US Food and Drug Administration Pooled Analysis. *Lancet Oncol* (2018) 19(2):229–39. doi: 10.1016/s1470-2045(17)30846-x
7. Paré L, Pascual T, Seguí E, Teixidó C, Gonzalez-Cao M, Galván P, et al. Association Between PD1 mRNA and Response to Anti-PD1 Monotherapy Across Multiple Cancer Types. *Ann Oncol* (2018) 29(10):2121–8. doi: 10.1093/annonc/mdy335
8. Hu FF, Liu CJ, Liu LL, Zhang Q, Guo AY. Expression Profile of Immune Checkpoint Genes and Their Roles in Predicting Immunotherapy Response. *Brief Bioinform* (2020) 22(3):bbaa176. doi: 10.1093/bib/bbaa176
9. Lee JS, Ruppin E. Multiomics Prediction of Response Rates to Therapies to Inhibit Programmed Cell Death 1 and Programmed Cell Death 1 Ligand 1. *JAMA Oncol* (2019) 5(11):1614–8. doi: 10.1001/jamaoncol.2019.2311
10. Ayers M, Lunceford J, Nebozhyn M, Murphy E, Loboda A, Kaufman DR, et al. IFN-Γ-Related mRNA Profile Predicts Clinical Response to PD-1 Blockade. *J Clin Invest* (2017) 127(8):2930–40. doi: 10.1172/jci91190
11. Sha D, Jin Z, Budczies J, Kluck K, Stenzinger A, Sinicrope FA. Tumor Mutational Burden as a Predictive Biomarker in Solid Tumors. *Cancer Discovery* (2020) 10(12):1808–25. doi: 10.1158/2159-8290.Cd-20-0522
12. Jardim D, Goodman A, de Melo Gagliato D, Kurzrock R. The Challenges of Tumor Mutational Burden as an Immunotherapy Biomarker. *Cancer Cell* (2020) 39(2):154–73. doi: 10.1016/j.ccell.2020.10.001
13. Thommen DS, Koelzer VH, Herzig P, Roller A, Trefny M, Dimeloe S, et al. A Transcriptionally and Functionally Distinct PD-1 CD8 T Cell Pool With Predictive Potential in Non-Small-Cell Lung Cancer Treated With PD-1 Blockade. *Nat Med* (2018) 24(7):994–1004. doi: 10.1038/s41591-018-0057-z

14. Kim HD, Song GW, Park S, Jung MK, Kim MH, Kang HJ, et al. Association Between Expression Level of PD1 by Tumor-Infiltrating CD8(+) T Cells and Features of Hepatocellular Carcinoma. *Gastroenterology* (2018a) 155(6):1936–50.e17. doi: 10.1053/j.gastro.2018.08.030
15. Guo L, Cao C, Goswami S, Huang X, Ma L, Guo Y, et al. Tumoral PD-1hicd8+ T Cells are Partially Exhausted and Predict Favorable Outcome in Triple-Negative Breast Cancer. *Clin Sci (Lond)* (2020) 134(7):711–26. doi: 10.1042/cs20191261
16. Gide TN, Quek C, Menzies AM, Tasker AT, Shang P, Holst J, et al. Distinct Immune Cell Populations Define Response to Anti-PD-1 Monotherapy and Anti-PD-1/Anti-CTLA-4 Combined Therapy. *Cancer Cell* (2019) 35(2):238–55.e6. doi: 10.1016/j.ccell.2019.01.003
17. Riaz N, Havel JJ, Makarov V, Desrichard A, Urba WJ, Sims JS, et al. Tumor and Microenvironment Evolution During Immunotherapy With Nivolumab. *Cell* (2017) 171(4):934–49.e16. doi: 10.1016/j.cell.2017.09.028
18. Kim ST, Cristescu R, Bass AJ, Kim KM, Odegaard JI, Kim K, et al. Comprehensive Molecular Characterization of Clinical Responses to PD-1 Inhibition in Metastatic Gastric Cancer. *Nat Med* (2018b) 24(9):1449–58. doi: 10.1038/s41591-018-0101-z
19. Jung H, Kim HS, Kim JY, Sun JM, Ahn JS, Ahn MJ, et al. DNA Methylation Loss Promotes Immune Evasion of Tumours With High Mutation and Copy Number Load. *Nat Commun* (2019) 10(1):4278. doi: 10.1038/s41467-019-12159-9
20. Cho JW, Hong MH, Ha SJ, Kim YJ, Cho BC, Lee I, et al. Genome-Wide Identification of Differentially Methylated Promoters and Enhancers Associated With Response to Anti-PD-1 Therapy in Non-Small Cell Lung Cancer. *Exp Mol Med* (2020) 52(9):1550–63. doi: 10.1038/s12276-020-00493-8
21. Sade-Feldman M, Yizhak K, Bjorgaard SL, Ray JP, de Boer CG, Jenkins RW, et al. Defining T Cell States Associated With Response to Checkpoint Immunotherapy in Melanoma. *Cell* (2018) 175(4):998–1013.e20. doi: 10.1016/j.cell.2018.10.038
22. Guo X, Zhang Y, Zheng L, Zheng C, Song J, Zhang Q, et al. Global Characterization of T Cells in Non-Small-Cell Lung Cancer by Single-Cell Sequencing. *Nat Med* (2018) 24(7):978–85. doi: 10.1038/s41591-018-0045-3
23. Hollern D, Xu N, Thennavan A, Glodowski C, Garcia-Recio S, Mott K, et al. B Cells and T Follicular Helper Cells Mediate Response to Checkpoint Inhibitors in High Mutation Burden Mouse Models of Breast Cancer. *Cell* (2019) 179(5):1191–206.e21. doi: 10.1016/j.cell.2019.10.028
24. Dobin A, Davis CA, Schlesinger F, Drenkow J, Zaleski C, Jha S, et al. STAR: Ultrafast Universal RNA-Seq Aligner. *Bioinformatics* (2013) 29(1):15–21. doi: 10.1093/bioinformatics/bts635
25. Pertea M, Kim D, Pertea G, Leek J, Salzberg S. Transcript-Level Expression Analysis of RNA-Seq Experiments With HISAT, Stringtie and Ballgown. *Nat Protoc* (2016) 11: (9):1650–67. doi: 10.1038/nprot.2016.095
26. Zhou Y, Zhou B, Pache L, Chang M, Khodabakhshi AH, Tanaseichuk O, et al. Metascape Provides a Biologist-Oriented Resource for the Analysis of Systems-Level Datasets. *Nat Commun* (2019) 10(1):1523. doi: 10.1038/s41467-019-09234-6
27. Efremova M, Vento-Tormo M, Teichmann SA, Vento-Tormo R. Cellphonedb: Inferring Cell-Cell Communication From Combined Expression of Multi-Subunit Ligand-Receptor Complexes. *Nat Protoc* (2020) 15(4):1484–506. doi: 10.1038/s41596-020-0292-x
28. Newman AM, Liu CL, Green MR, Gentles AJ, Feng W, Xu Y, et al. Robust Enumeration of Cell Subsets From Tissue Expression Profiles. *Nat Methods* (2015) 12(5):453–7. doi: 10.1038/nmeth.3337
29. Finotello F, Mayer C, Plattner C, Laschober G, Rieder D, Hackl H, et al. Molecular and Pharmacological Modulators of the Tumor Immune Contexture Revealed by Deconvolution of RNA-Seq Data. *Genome Med* (2019) 11(1):34. doi: 10.1186/s13073-019-0638-6
30. Love MI, Huber W, Anders S. Moderated Estimation of Fold Change and Dispersion for RNA-Seq Data With Deseq2. *Genome Biol* (2014) 15(12):550. doi: 10.1186/s13059-014-0550-8
31. Ritchie M, Phipson B, Wu D, Hu Y, Law C, Shi W, et al. Limma Powers Differential Expression Analyses for RNA-Sequencing and Microarray Studies. *Nucleic Acids Res* (2015) 43(7):e47. doi: 10.1093/nar/gkv007
32. Foroutan M, Bhuva DD, Lyu R, Horan K, Cursons J, Davis MJ. Single Sample Scoring of Molecular Phenotypes. *BMC Bioinf* (2018) 19(1):404. doi: 10.1186/s12859-018-2435-4
33. Butler A, Hoffman P, Smibert P, Papalexi E, Satija R. Integrating Single-Cell Transcriptomic Data Across Different Conditions, Technologies, and Species. *Nat Biotechnol* (2018) 36(5):411–20. doi: 10.1038/nbt.4096
34. Robinson M, McCarthy D, Smyth GJB. Edger: A Bioconductor Package for Differential Expression Analysis of Digital Gene Expression Data. *Bioinformatics* (2010) 26(1):139–40. doi: 10.1093/bioinformatics/btp616
35. Sergushichev A. An Algorithm for Fast Preranked Gene Set Enrichment Analysis Using Statistic Calculation. *bioRxiv*. doi: 10.1101/060012
36. Robin X, Turck N, Hainard A, Tiberti N, Lisacek F, Sanchez J, et al. Proc: An Open-Source Package for R and s+ to Analyze and Compare ROC Curves. *BMC Bioinformatics* (2011) 12:77. doi: 10.1186/1471-2105-12-77
37. Durinck S, Spellman P, Birney E, Huber W. Mapping Identifiers for the Integration of Genomic Datasets With the R/Bioconductor Package Biomart. *Nat Protoc* (2009) 4(8):1184–91. doi: 10.1038/nprot.2009.97
38. Charoentong P, Finotello F, Angelova M, Mayer C, Efremova M, Rieder D, et al. Pan-Cancer Immunogenomic Analyses Reveal Genotype-Immunophenotype Relationships and Predictors of Response to Checkpoint Blockade. *Cell Rep* (2017) 18(1):248–62. doi: 10.1016/j.celrep.2016.12.019
39. Schmiedel BJ, Singh D, Madrigal A, Valdovino-Gonzalez AG, White BM, Zapardiel-Gonzalo J, et al. Impact of Genetic Polymorphisms on Human Immune Cell Gene Expression. *Cell* (2018) 175(6):1701–15.e16. doi: 10.1016/j.cell.2018.10.022
40. Sommariva S, Tarricone R, Lazzeri M, Ricciardi W, Montorsi F. Prognostic Value of the Cell Cycle Progression Score in Patients With Prostate Cancer: A Systematic Review and Meta-Analysis. *Eur Urol* (2016) 69(1):107–15. doi: 10.1016/j.eururo.2014.11.038
41. Vaddepally RK, Kharel P, Pandey R, Garje R, Chandra AB. Review of Indications of FDA-Approved Immune Checkpoint Inhibitors Per NCCN Guidelines With the Level of Evidence. *Cancers (Basel)* (2020) 12(3):738. doi: 10.3390/cancers12030738
42. Shukla SA, Bachireddy P, Schilling B, Galonska C, Zhan Q, Bango C, et al. Cancer-Germline Antigen Expression Discriminates Clinical Outcome to CTLA-4 Blockade. *Cell* (2018) 173(3):624–33.e8. doi: 10.1016/j.cell.2018.03.026
43. Cabrita R, Lauss M, Sanna A, Donia M, Skaarup Larsen M, Mitra S, et al. Tertiary Lymphoid Structures Improve Immunotherapy and Survival in Melanoma. *Nature* (2020) 577(7791):561–5. doi: 10.1038/s41586-019-1914-8
44. Wherry E, Kurachi M. Molecular and Cellular Insights Into T Cell Exhaustion. *Nat Rev Immunol* (2015) 15(8):486–99. doi: 10.1038/nri3862
45. Khan O, Giles JR, McDonald S, Manne S, Ngiow SF, Patel KP, et al. TOX Transcriptionally and Epigenetically Programs CD8(+) T Cell Exhaustion. *Nature* (2019) 571(7764):211–8. doi: 10.1038/s41586-019-1325-x
46. Duan Q, Zhang H, Zheng J, Zhang L. Turning Cold Into Hot: Firing Up the Tumor Microenvironment. *Trends Cancer* (2020) 6(7):605–18. doi: 10.1016/j.trecan.2020.02.022
47. Kather J, Suarez-Carmona M, Charoentong P, Weis C, Hirsch D, Bankhead P, et al. Topography of Cancer-Associated Immune Cells in Human Solid Tumors. *Elife* (2018) 7:e36967. doi: 10.7554/eLife.36967
48. Harjunpää H, Llort Asens M, Guenther C, Fagerholm SC. Cell Adhesion Molecules and Their Roles and Regulation in the Immune and Tumor Microenvironment. *Front Immunol* (2019) 10:1078. doi: 10.3389/fimmu.2019.01078
49. Li X, Wenes M, Romero P, Huang S, Fendt S, Ho P. Navigating Metabolic Pathways to Enhance Antitumour Immunity and Immunotherapy. *Nat Rev Clin Oncol* (2019) 16(7):425–41. doi: 10.1038/s41571-019-0203-7
50. Clarke J, Panwar B, Madrigal A, Singh D, Gujar R, Wood O, et al. Single-Cell Transcriptomic Analysis of Tissue-Resident Memory T Cells in Human Lung Cancer. *J Exp Med* (2019) 216(9):2128–49. doi: 10.1084/jem.20190249
51. Huang AC, Orlowski RJ, Xu X, Mick R, George SM, Yan PK, et al. A Single Dose of Neoadjuvant PD-1 Blockade Predicts Clinical Outcomes in Resectable Melanoma. *Nat Med* (2019) 25(3):454–61. doi: 10.1038/s41591-019-0357-y
52. Lepletier A, Madore J, O'Donnell JS, Johnston RL, Li XY, McDonald E, et al. Tumor CD155 Expression is Associated With Resistance to Anti-PD1 Immunotherapy in Metastatic Melanoma. *Clin Cancer Res* (2020) 26(14):3671–81. doi: 10.1158/1078-0432.Ccr-19-3925
53. van der Leun A, Thommen D, Schumacher T. CD8 T Cell States in Human Cancer: Insights From Single-Cell Analysis. *J Nat Rev Cancer* (2020) 20(4):218–32. doi: 10.1038/s41568-019-0235-4

54. Berraondo P, Sanmamed M, Ochoa M, Etxeberria I, Aznar M, Pérez-Gracia J, et al. Cytokines in Clinical Cancer Immunotherapy. *Br J Cancer* (2019) 120 (1):6–15. doi: 10.1038/s41416-018-0328-y
55. Stanton S, Adams S, Disis M. Variation in the Incidence and Magnitude of Tumor-Infiltrating Lymphocytes in Breast Cancer Subtypes: A Systematic Review. *JAMA Oncol* (2016) 2(10):1354–60. doi: 10.1001/jamaoncol.2016.1061
56. Zhang P, Liu M, Cui Y, Zheng P, Liu Y. Microsatellite Instability Status Differentially Associates With Intratumoral Immune Microenvironment in Human Cancers. *Brief Bioinform* (2021) 22(3):bbaa180. doi: 10.1093/bib/bbaa180
57. Cerezo M, Rocchi S. Cancer Cell Metabolic Reprogramming: A Keystone for the Response to Immunotherapy. *Cell Death Dis* (2020) 11(11):964. doi: 10.1038/s41419-020-03175-5
58. Gu-Trantien C, Migliori E, Buisseret L, de Wind A, Brohée S, Garaud S, et al. CXCL13-Producing TFH Cells Link Immune Suppression and Adaptive Memory in Human Breast Cancer. *JCI Insight* (2017) 2(11):e91487. doi: 10.1172/jci.insight.91487
59. Goswami S, Chen Y, Anandhan S, Szabo P, Basu S, Blando J, et al. ARID1A Mutation Plus CXCL13 Expression Act as Combinatorial Biomarkers to Predict Responses to Immune Checkpoint Therapy in Mucc. *Sci Trans Med* (2020) 12(548):eabc4220. doi: 10.1126/scitranslmed.abc4220
60. Yang M, Lu J, Zhang G, Wang Y, He M, Xu Q, et al. CXCL13 Shapes Immunoactive Tumor Microenvironment and Enhances the Efficacy of PD-1 Checkpoint Blockade in High-Grade Serous Ovarian Cancer. *J Immunother Cancer* (2021) 9(1):e001136. doi: 10.1136/jitc-2020-001136
61. Majidpoor J, Mortezaee K. The Efficacy of PD-1/PD-L1 Blockade in Cold Cancers and Future Perspectives. *Clin Immunol* (2021) 226:108707. doi: 10.1016/j.clim.2021.108707
62. Cohen EEW, Bell RB, Bifulco CB, Burtness B, Gillison ML, Harrington KJ, et al. The Society for Immunotherapy of Cancer Consensus Statement on Immunotherapy for the Treatment of Squamous Cell Carcinoma of the Head and Neck (HNSCC). *J Immunother Cancer* (2019) 7(1):184. doi: 10.1186/s40425-019-0662-5
63. Egen J, Ouyang W, Wu LJI. Human Anti-Tumor Immunity: Insights From Immunotherapy Clinical Trials. *Immunity* (2020) 52(1):36–54. doi: 10.1016/j.immuni.2019.12.010
64. Friedlander P, Wood K, Wassmann K, Christenfeld A, Bhardwaj N, Oh W. A Whole-Blood RNA Transcript-Based Gene Signature Is Associated With the Development of CTLA-4 Blockade-Related Diarrhea in Patients With Advanced Melanoma Treated With the Checkpoint Inhibitor Tremelimumab. *J Immunother Cancer* (2018) 6: (1):90. doi: 10.1186/s40425-018-0408-9

Conflict of Interest: The authors declare that the research was conducted in the absence of any commercial or financial relationships that could be construed as a potential conflict of interest.

Publisher's Note: All claims expressed in this article are solely those of the authors and do not necessarily represent those of their affiliated organizations, or those of the publisher, the editors and the reviewers. Any product that may be evaluated in this article, or claim that may be made by its manufacturer, is not guaranteed or endorsed by the publisher.

Copyright © 2021 Yang, Deng, Cheng, Wei, Luo and Liu. This is an open-access article distributed under the terms of the Creative Commons Attribution License (CC BY). The use, distribution or reproduction in other forums is permitted, provided the original author(s) and the copyright owner(s) are credited and that the original publication in this journal is cited, in accordance with accepted academic practice. No use, distribution or reproduction is permitted which does not comply with these terms.

frontiers in Oncology

SYSTEMATIC REVIEW
published: 23 September 2021
doi: 10.3389/fonc.2021.691002

The Prediction Potential of the Pretreatment Lung Immune Prognostic Index for the Therapeutic Outcomes of Immune Checkpoint Inhibitors in Patients With Solid Cancer: A Systematic Review and Meta-Analysis

Hui Liu[1], *Xiao-Li Yang*[2], *Xiao-Yun Yang*[3], *Zhao-Ru Dong*[1], *Zhi-Qiang Chen*[1], *Jian-Guo Hong*[1] *and Tao Li*[1,4]*

[1] Department of General Surgery, Qilu Hospital, Shandong University, Jinan, China, [2] Department of Nephrology, Jinan Central Hospital, Shandong University, Jinan, China, [3] Department of Gastroenterology, Qilu Hospital, Shandong University, Jinan, China, [4] Department of Hepatobiliary Surgery, The Second Hospital of Shandong University, Jinan, China

OPEN ACCESS

Edited by:
Xuelei Ma,
Sichuan University, China

Reviewed by:
Tibor Bakacs,
Alfred Renyi Institute of Mathematics, Hungary
Jelena Stojsic,
University of Belgrade, Serbia

***Correspondence:**
Tao Li
litao7706@163.com

Specialty section:
This article was submitted to Cancer Immunity and Immunotherapy, a section of the journal Frontiers in Oncology

Received: 05 April 2021
Accepted: 30 August 2021
Published: 23 September 2021

Citation:
Liu H, Yang X-L, Yang X-Y, Dong Z-R, Chen Z-Q, Hong J-G and Li T (2021) The Prediction Potential of the Pretreatment Lung Immune Prognostic Index for the Therapeutic Outcomes of Immune Checkpoint Inhibitors in Patients With Solid Cancer: A Systematic Review and Meta-Analysis. Front. Oncol. 11:691002. doi: 10.3389/fonc.2021.691002

Background: The lung immune prognostic index (LIPI) is recently developed to predict immune checkpoint inhibitors (ICIs) treatment outcomes for non-small cell lung cancer. However, its predictive value for other types of cancer remained unclear. This meta-analysis aimed to evaluate the association between pretreatment LIPI score and therapeutic outcomes in cancer patients treated with ICIs.

Methods: We searched PubMed, Cochrane Library literature databases and EMBASE for abstracts and full-text articles published from the inception of the database until 16th, Nov 2020. Meta-analyses were performed separately for progression-free survival (PFS) and overall survival (OS) by using the random-effects model.

Results: A total of 12 studies involving 4883 patients receiving ICIs treatment were identified for the primary analysis. The pooled results implied that compared with good LIPI score groups, patients with poor or intermediate LIPI score were significantly associated with worse OS (HR=3.33, 95%CI 2.64-4.21, $P < 0.001$, $I^2 = 64.2\%$; HR=1.71, 95%CI 1.43-2.04, $P < 0.001$, $I^2 = 43.6\%$, respectively) and PFS (HR=2.73,95%CI 2.00-3.73, $P < 0.001$, $I^2 = 78.2\%$; HR=1.43, 95%CI 1.28-1.61, $P < 0.001$, $I^2 = 16.3\%$, respectively). Also, for 1873 patients receiving chemotherapy, a poor LIPI score was significantly associated with worse OS (HR=2.30, 95%CI 1.73-3.07, $P < 0.001$; $I^2 = 56.2\%$) and PFS (HR=1.92,95%CI 1.69-2.17; $P < 0.001$; $I^2 = 0.0\%$) compared with good LIPI score groups.

Conclusions: A good LIPI score was significantly correlated with improved OS and PFS in cancer patients receiving ICIs or chemotherapy, regardless of the types of cancer.

Keywords: lung immune prognostic index, immune checkpoint inhibitors, solid cancer, chemotherapy, meta-analysis

INTRODUCTION

Immune checkpoint inhibitors (ICIs) mainly include antibodies against cytotoxic T lymphocyte-associated protein 4 (CTLA-4), programmed cell death 1 (PD-1), and its major ligand (PD-L1) (1). ICIs have marked efficacy in the treatment of patients with solid cancers (2–4), still the majority of patients show intrinsic resistance to ICIs treatment owing to the tumor microenvironment (TME) and an impaired T cell tumor interaction mediated by immune escape mechanisms of tumor and immune cells (5). Therefore, resistance to ICIs treatment restricts patients with advanced cancer to achieve durable responses.

There are no candidate biomarkers for predicting response or resistance to immunotherapy in solid cancers, including hepatocellular carcinoma (6). Biomarkers that can predict whether patients have long-term favorable respond to ICIs therapy are eagerly awaited. At present, several biomarkers have been recognized to be associated with clinical outcomes for ICIs treatment. PD-L1, PD-1, neutrophil-lymphocyte ratio (NLR), tumor-infiltrating lymphocyte (TIL), microsatellite instability (MSI), gene expression profiling (GEP), and tumor mutational burden (TMB) can improve the predictive accuracy for ICIs outcomes in solid cancers (7–10).

The lung immune prognostic index (LIPI) was developed on the basis of derived neutrophils/(leukocytes minus neutrophils) ratio (dNLR) greater than three and lactate dehydrogenase (LDH) greater than upper limit of normal (ULN), characterizing three groups (good LIPI score group, 0 factor; intermediate LIPI score group,1 factor; poor LIPI score group, 2 factors) (11). Current evidence proved that the LIPI score could be used to identify cancer patients who benefit from ICIs treatment in multiple cancers (11, 12). Meanwhile, contradictory results have also been published (13, 14).

Herein, we performed a systematic review and meta-analysis, to investigate the significance of the LIPI score as a predictive tool in solid cancer patients receiving ICIs treatment based on 12 published studies.

METHODS

This meta-analysis was performed by the Preferred Reporting Items for Systematic reviews and Meta-Analyses (PRISMA) guidelines (15), with inclusion criteria being set out according to the PICOS model.

Search Methods and Study Selection Criteria

Two authors (HL, XLY) independently searched relevant studies from the PubMed, EMBASE, and Cochrane Library literature databases from the inception of the database until 16th, Nov 2020. Those studies were restricted to the English language. The following search retrieval keywords for the literature were employed, including neoplasms, cancer, lung immune prognostic index, LIPI, PD-1, PD-L1, CTLA-4, nivolumab, atezolizumab, avelumab, durvalumab, ipilimumab, tremelimumab, pembrolizumab, ICIs, immune checkpoint inhibitor. The detailed search strategy is presented in **Supplementary Retrieval Methods**.

Two investigators (HL and XYY) independently screened the literature, and discrepancies were reviewed by another investigator on the team (TL) and resolved by consensus. The main criteria used for the eligibility study were as follows: (1) the studies in which patients were histologically diagnosed with cancer and treated with ICIs or chemotherapy. (2) the studies where the association between LIPI and therapeutic outcomes such as progression-free survival (PFS), overall survival (OS) were evaluated. (3) the studies where the related data could be collected directly or calculated indirectly. (4) the studies provided sufficient information to assess hazard ratio (HR) with 95% confidence interval (95%CI). (5) the studies that were published in English. For re-published research, only the latest literature and relevant data can be collected, or the research with the largest sample size can be selected.

Data Extraction and Quality Assessment

Two researchers (HL and XLY) independently performed the following data from each study: (1) first author, publication year, country, sample size, immune checkpoint inhibitors, study design, follow-up time. (2) the outcome measures (OS, PFS) and HR with 95% CI extracted from original studies. When both univariate analysis and multivariate analysis are available, we give priority to the results in multivariate analysis. If the information we needed was unreported or unable to be calculated indirectly, or not available after contacting the corresponding authors, the study will be used for systematic review or discarded.

The quality of studies will be evaluated by the Newcastle-Ottawa Scale (NOS) criteria (16). Studies with a score greater than seven were considered as high-quality literature, studies with a score of five to seven were considered as medium-quality literature, studies with a score less than five were considered as poor-quality literature.

Statistical Analysis

Data analyses were performed through Stata 12.0 statistical software (Stata Corp LP, College Station, TX), $P < 0.05$ was considered statistically significant. OS and PFS were used to evaluate the correlation between LIPI score and clinical data of cancer patients receiving ICIs or chemotherapy. HR with 95%CI was used for the pooled analyses of OS and PFS.

We compared the good LIPI score groups with the poor LIPI score, and intermediate LIPI score groups. Intermediate/poor (intermediate + poor) LIPI score groups were also compared with good LIPI score groups due to the combination of intermediate and poor LIPI score groups. Subgroup analyses were performed by cancer type, sample size, study region. At the same time, we also evaluated the association between different LIPI score and cancer patients receiving chemotherapy. Meta-analysis was used to pool the estimates, using the random-effects model.

Statistical heterogeneity was evaluated by using the Cochran Q and the inconsistency index (I^2) statistic tests. $P > 0.05$ and $I^2 <$

Abbreviations: LIPI, lung immune prognostic index; ICIs, immune checkpoint inhibitors; PFS, progression-free survival; OS, overall survival; CTLA-4, cytotoxic T lymphocyte-associated protein 4; PD-1, programmed cell death 1; TME, tumor microenvironment; NLR, neutrophil-lymphocyte ratio; TIL, tumor-infiltrating lymphocyte; MSI, microsatellite instability; GEP, gene expression profiling; TMB, tumor mutational burden; LDH, lactate dehydrogenase; ULN, upper limit of normal; NSCLC, non-small cell lung cancer; SCCHN, squamous cell carcinoma of the head and neck; irAEs, immune-related adverse events.

50% indicated a lack of heterogeneity among all studies. We chose the random effect model in this meta-analysis due to the inherent clinical heterogeneity among studies included in this meta-analysis (17). Funnel plots, Egger's regression asymmetry test, and Begg's rank correlation test were used to examine the potential publication bias (18).

RESULTS

Retrieval Result and Study Characteristics

A flow chart of the literature search process is summarized in **Figure 1**. In total, 76 records were initially identified. Then, 45 studies were retained after the removal of duplicates. After screening for titles and abstracts, 6 records were excluded (not relevant, review, not ICIs or chemotherapy). After reviewing the remaining 39 articles *via* the full-text view, 27 full-text articles were excluded due to lack of intended outcomes (OS, PFS), HR with 95% CI or repeatedly published studies. Finally, 12 studies published between 2018 and 2020 were included in this analysis (11–14, 19–26).

The detailed characteristics of all eligible studies are presented in **Table 1**. One of twelve studies was prospectively designed; the rest of the literature was retrospectively designed. In total, our meta-analysis included 4883 cancer patients receiving ICIs treatment. The sample size was ranging from 70 to 1489 per study. Eight studies were conducted in Europe; two were conducted in China; one was from Australia; one was conducted in Canada; a conference abstract was not reported. Among these studies, seven studies included patients with non-small cell lung cancer (NSCLC), one for hepatocellular carcinoma and one with squamous cell carcinoma of the head and neck (SCCHN); the rest four studies for other types or multiple cancers. All patients enrolled were treated with ICIs or chemotherapy. The quality assessment results of the all 12 studies ranged from 5 to 7, as shown in **Table 1**. Four studies scored 7 points, seven studies scored 6 points, and one study scored 5 points.

Association Between LIPI Score and OS or PFS of Cancer Patients Receiving ICIs Treatment

OS data was available in 8 studies involving 4443 patients receiving ICIs treatment. Compared with good LIPI score groups, poor LIPI score groups were significantly associated with worse OS (HR=3.33, 95%CI =2.64-4.21; P< 0.001), with a significant level of heterogeneity (I^2 = 64.2%, P=0.003) among the studies (**Figure 2**). Intermediate LIPI score predicted poor OS compared with good LIPI score groups (HR=1.717, 95%CI 1.43-2.04; P< 0.001) (**Figure 2**) with a moderate level of heterogeneity (I^2 = 43.6%, P=0.088). The sensitivity analysis

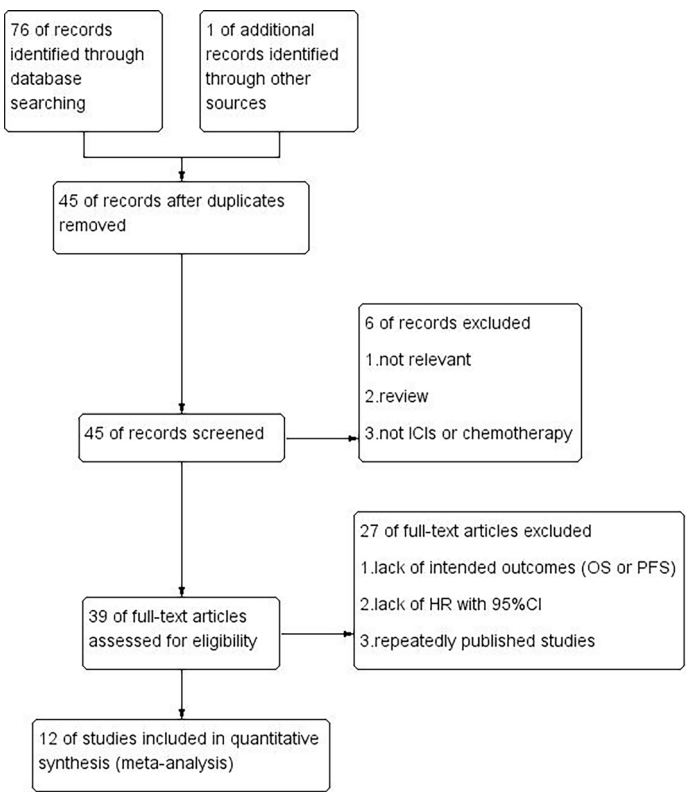

FIGURE 1 | Flow diagram of study selection.

TABLE 1 | The characteristics of included studies.

Author	Study period	Data collection	Country	Cancer type	ICIs	Sample size	Outcome	Median follow-up (months)	NOS
Wang	2016-2019	retrospective	China	NSCLC	NR	216	PFS,OS	NR	6
Sorich	NR	retrospective	Australia	NSCLC	Atezo	1489	PFS,OS, ORR	15.1 (14.7-15.4)	7
Mielgo	2015-2019	retrospective	Spain	NSCLC	Pembro	223	PFS,OS,DCR	NR	6
Meyers	2010-2019	retrospective	Canada	Multiple	Nivo, Pembro, Ipi/ Nivo	578	PFS,OS, ORR	23.5 (1.8-89.0)	7
Mazzaschi	2015-2019	prospective	Italy	NSCLC	Nivo,Pembro,Atezo	109	PFS,OS	17.3	7
Kazandjian	2013-2017	retrospective	Europe	mNSCLC	Atezo, Nivo, Pembro	1368	PFS,OS	NR	6
Herrera	2014-2019	retrospective	Europe	SCCHN	ICIs	190	PFS,OS, ORR	13.2	6
Ferreira	2015-2019	retrospective	Portugal	lung cancer	Pembro,Nivo	120	OS	13	6
Chen	2015-2019	retrospective	China	aHCC	Nivo,Pembro	108	PFS,OS	NR	6
Al Darazi	2015-2018	retrospective	France	Multiple	ICIs	259	OS	15 (11.6-17.5)	7
Santa	2015-2019	prospective	NR	Multiple	ICIs	70	PFS,OS, ORR	NR	6
Ruiz-Bañobre	2015-2017	retrospective	Spain	NSCLC	Nivo	153	PFS,OS,DCR	NR	5

NSCLC, Non-small Cell Lung Cancer; Atezo, atezolizumab; Nivo, nivolumab; Pembro, pembrolizuma; Ipi, Ipilimumab; ORR, objective response rate; DCR, disease control rate; NR, not reported; ICIs, immune checkpoint inhibitors; SCCHN, head and neck squamous cell carcinoma.

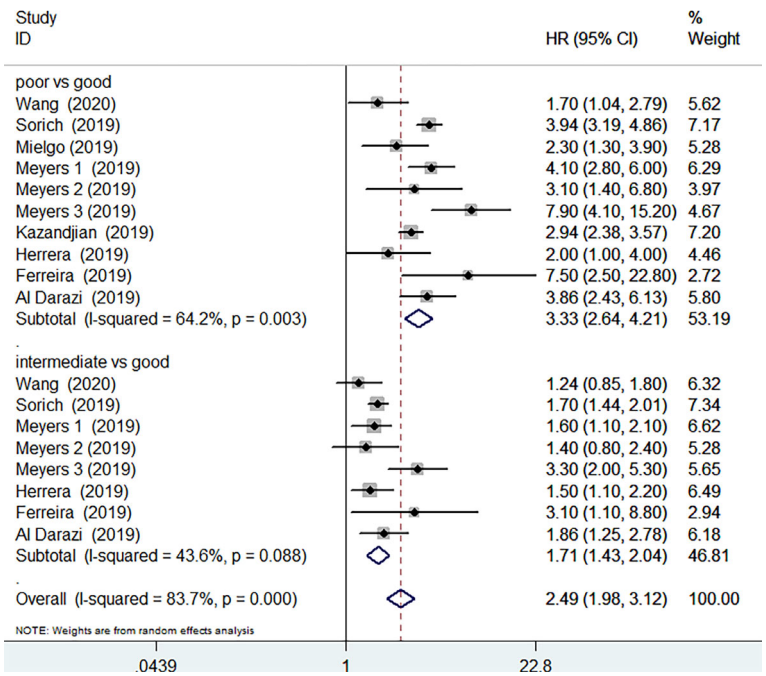

FIGURE 2 | Meta-analysis of OS in cancer patients after ICIs treatment (poor LIPI score groups *vs.* good LIPI score groups, intermediate LIPI score groups *vs.* good LIPI score groups).

showed that the pooled OS results (**Supplementary Figures 1** and **2**) were not significantly changed by any single study.

PFS data was available in 4 studies involving 3669 patients. The pooled results implied that poor LIPI score groups had a significantly higher risk of poor PFS compared with good LIPI score groups (HR =2.73, 95%CI 2.00-3.73, P < 0.001). The heterogeneity test showed significant heterogeneity existed among these studies (I^2 = 78.2%, P< 0.001) (**Figure 3**). The pooled results revealed that intermediate LIPI score indicated poor PFS compared with good LIPI score groups (HR=1.43, 95%CI 1.28-1.61, P< 0.001) with a moderate level of heterogeneity (I^2 = 16.3%, P=0.309) (**Figure 3**).

4 studies, covering 440 patients receiving ICIs treatment, were analyzed separately due to the combination of intermediate and

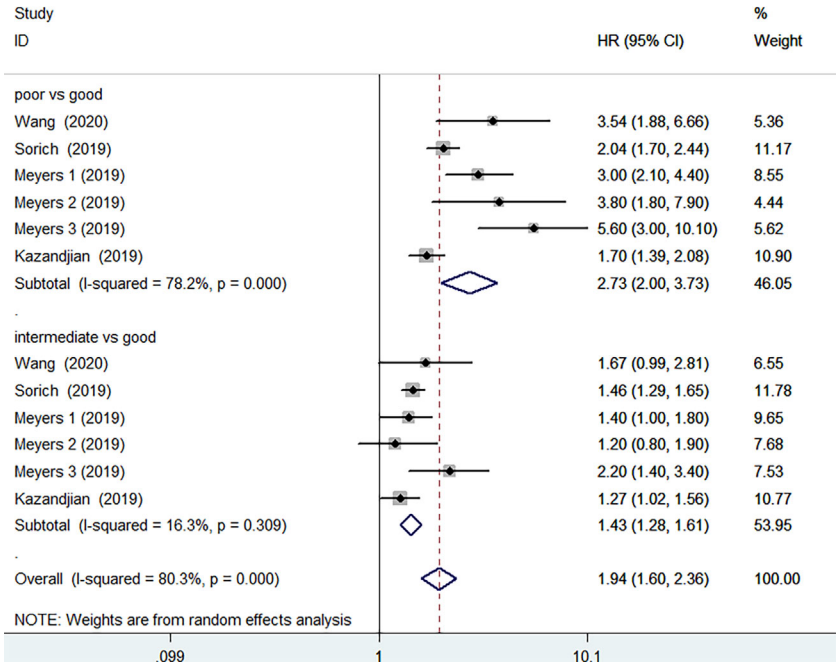

FIGURE 3 | Meta-analysis of PFS in cancer patients after ICIs treatment (poor LIPI score groups *vs.* good LIPI score groups, intermediate LIPI score groups *vs.* good LIPI score groups).

poor LIPI score groups (intermediate/poor LIPI score groups). Significantly worse OS was also found in intermediate/poor LIPI score groups than good LIPI score groups (HR=2.77, 95%CI 2.11-3.63, P < 0.001), without any heterogeneity (I^2 = 0.0%, P=0.396) (**Figure 4**). PFS data was available in 3 studies involving 370 patients receiving ICIs. Intermediate/poor LIPI score groups had inferior PFS (HR=2.13, 95%CI 1.55-2.93; P<0.001) compared with good LIPI score group. The heterogeneity test showed moderate heterogeneity existed among these studies (I^2 = 41.7%, P=0.18) (**Supplementary Figure 3**). The sensitivity analysis also showed that no individual research influenced the pooled effects on PFS (**Supplementary Figures 4** and **5**).

Association Between LIPI Score and OS or PFS of Cancer Patients Receiving Chemotherapy

3 of the 12 studies involving 1873 patients receiving chemotherapy provided OS and PFS data. According to the random-effects model, compared with the group with good LIPI score, the group with poor LIPI score was significantly correlated with the group with inferior OS (HR=2.30, 95%CI 1.73-3.07, P < 0.001) (**Figure 5**) and PFS(HR=1.92, 95%CI 1.69-2.17; P < 0.001) (**Figure 6**). The heterogeneity test showed that heterogeneity existed among these studies in OS (I^2 = 56.2%, P=0.077), but not PFS (I^2 = 0.0%, P=0.592). Intermediate LIPI score was also a significant association with worse OS (HR=1.54, 95%CI 1.27-1.86, P < 0.001) (**Figure 5**) and PFS (HR=1.45, 95%CI 1.29-1.64; P < 0.001) (**Figure 6**) compared with good LIPI score groups. Neither of them is heterogeneous (I^2 = 0.0%, P=0.646; I^2 = 0.0%, P=0.639). However, the LIPI score may not predict therapeutic outcomes in cancer patients receiving chemo-immunotherapy (26). The sensitivity analysis also showed that no individual study influenced the pooled effects on OS and PFS (**Supplementary Figures 6** and **7**).

Association Between Subgroup Analyses and OS or PFS

Subgroup analyses for OS and PFS were further performed to assess the interaction of LIPI score with cancer type, sample size, and study region and the results are shown in **Table 2**. When stratifying by cancer type, compared with the good LIPI score groups, poor LIPI score was significantly associated with worse OS and PFS in patients with NSCLC (OS: HR=3.011, 95%CI 2.303-3.936; P<0.001) (PFS: HR=3.011, 95%CI 2.303-3.936; P<0.001) and multiple/other (OS: HR=4.107, 95%CI 2.525-60681; P<0.001) (PFS: HR=4.791, 95%CI 2.997-7.659; P<0.001) (**Table 2**). The conclusion was the same when stratifying by sample size and study region. There was significant heterogeneity in the sample size less than 200 (I^2 = 82.8%, P=0.001), NSCLC (I^2 = 70.8%, P =0.003) and other study region (I^2 = 89.4%, P=0.002).

Publication Bias

The funnel plot indicated no significant publication bias in all the pooled analyses (**Supplementary Figures 8** and **9**). Funnel plot

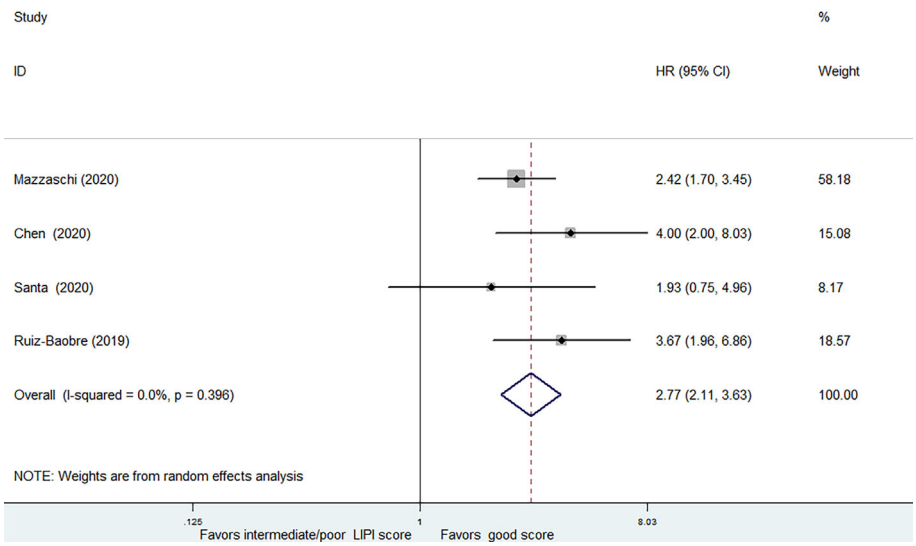

FIGURE 4 | Meta-analysis of OS in cancer patients after ICIs treatment (intermediate + poor LIPI score groups *vs.* good LIPI score groups).

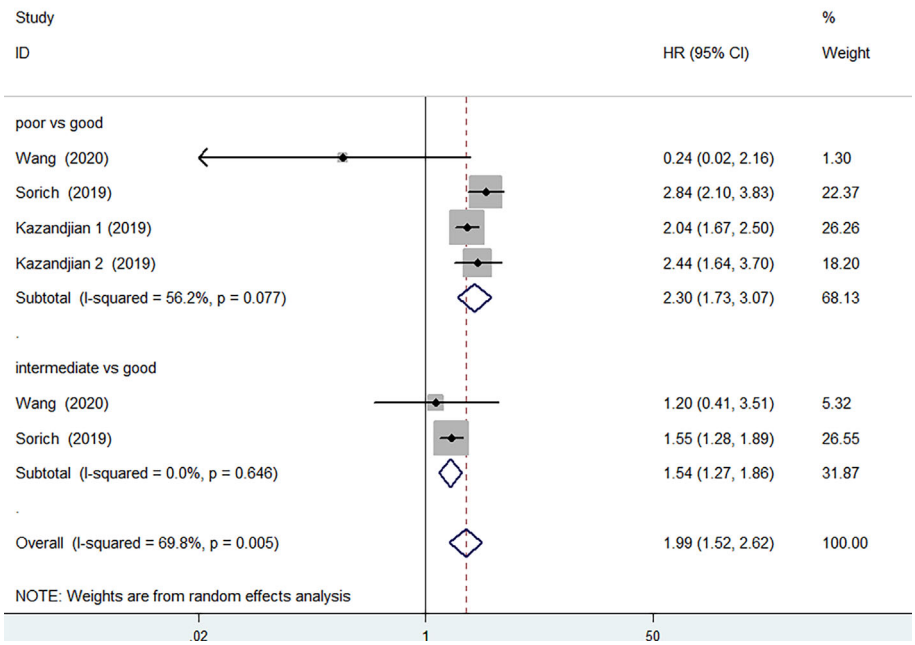

FIGURE 5 | Meta-analysis of OS in cancer patients after chemotherapy (poor LIPI score groups *vs.* good LIPI score groups, intermediate LIPI score groups *vs.* good LIPI score groups).

asymmetry was further assessed by the method of Egger's and Begg's linear regression test ($P < 0.05$ was considered a significant publication bias) (18). The Begg's and Egger's test also revealed no evidence of publication bias for OS (Begg's test: P = 0.534, Egger's test: P = 0.536) and PFS (Begg's test: P = 0.707, Egger's test P = 0.021) (**Supplementary Figures 10** and **11**). We did not conduct a publication bias analysis for those with too few studies.

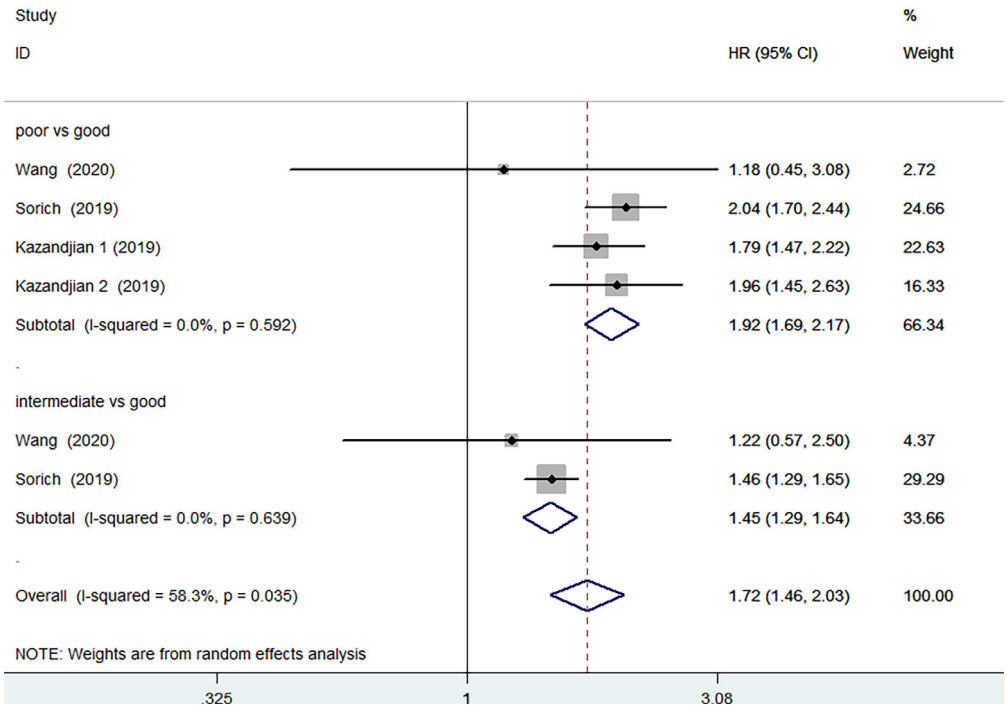

FIGURE 6 | Meta-analysis of PFS in cancer patients after chemotherapy (poor LIPI score groups *vs.* good LIPI score groups, intermediate LIPI score groups *vs.* good LIPI score groups).

TABLE 2 | Subgroup analyses of the associations between LIPI score and outcomes (poor *vs.* good).

	Subgroup	Number of studies	Pooled results		Heterogeneity test		Publication Bias test	
			HR (95CI %)	P	I2	P	P (Begg's)	P (Egger's)
Overall survival	All studies	10	3.332 (2.639-4.208)	<0.001	64.2	0.003	0.859	0.939
Cancer type	NSCLC	5	3.011 (2.303-3.936)	<0.001	70.8	0.008	0.462	0.376
	Multiple/other	5	4.107 (2.525-60681)	<0.001	58.5	0.047	1	0.75
Sample size	<200	4	3.571 (1.547-8.244)	0.003	82.8	0.001	0.734	0.388
	>200	6	3.416 (2.892-4.036)	<0.001	29.2	0.216	0.858	0.939
Study region	Canada	3	4.659 (2.896-7.496)	<0.001	48.9	0.141	1	0.874
	Europe	5	3.001 (2.301-3.914)	<0.001	33.6	0.198	1	0.747
	Others	2	2.669 (1.174-6.069)	0.019	89.4	0.002	1	0.219
Progression-free survival	All studies	6	2.733 (2.000-3.733)	<0.001	78.2	<0.001	0.707	0.021
Cancer type	NSCLC	4	2.242 (1.717-2.929)	<0.001	70.9	0.016	0.734	0.182
	Multiple/other	2	4.791 (2.997-7.659)	<0.001	0.0	0.427	1	
Sample size	<200	2	4.492 (2.867-7.039)	<0.001	4.9	0.305	1	
	>200	4	2.232 (1.704-2.922)	<0.001	70.3	0.018	0.737	0.198
Study region	Canada	3	3.760 (2.562-5.520)	<0.001	33.1	0.224	1	0.481
	Others	2	2.464 (1.476-4.114)	<0.001	62.9	0.1		

LIPI, lung immune prognostic index; NSCLC, non-small cell lung cancer; HR, hazard ratio.

DISCUSSION

The LIPI score is developed based on LDH and dNLR, which are simple and easy to calculate (11). In this meta-analysis, we have evaluated the association of LIPI score with the prognosis of cancer patients receiving ICIs or chemotherapy. Compared with good LIPI score groups, the pooled results show that regardless of whether the patients received ICIs or chemotherapy, the OS and PFS of the poor or intermediate LIPI score group were significantly reduced. Although some studies have shown that the LIPI score cannot be used to identify cancer patients who have benefited from chemotherapy, these data are not available (11).

Inflammation plays a key role in tumor progression, affecting the survival of cancer patients (27). The inflammatory status of various

cancers can be measured by dNLR. As an essential component of the inflammatory response, neutrophils not only target tumor cells, but also indirectly act on the tumor microenvironment to promote tumor development (28). Lymphocyte infiltration in the tumor is also associated with a better response to immunotherapy and prognosis in solid tumor patients (29). LDH and dNLR are independent risk factors for mortality among patients, and are correlated with poor outcomes in several solid cancer types according to the current evidence (30, 31).

Immunotherapy has demonstrated great clinical success in certain cancers, but so far, immunotherapy has only achieved success in a limited number of cancers (32). Specifically, Callahan, M.K., et al. have demonstrated that the majority of such patients can now be successfully treated with concurrent ipilimumab and nivolumab therapy (33). However, the deleterious effects of immune-related adverse events (irAEs) might outweigh the benefit from the addition of ipilimumab (34). Until now, there is still no biomarker for some cancers to predict the response or resistance to immunotherapy (6). Robust biomarkers are needed to predict patient responsiveness to immunotherapy and for their stratification (35). Our meta-analysis provides new evidence supporting that LIPI scores are used as prognostic indicators for cancer patients receiving ICIs or chemotherapy. In addition, LIPI score may also has prognostic value for doublet immunotherapy such as ipilimumab and nivolumab, as one included study has revealed the potential application of the LIPI scores in such circumstances (12). However, more studies are warranted to fully exploit its predictive value.

Our findings suggest that the LIPI scores may be a promising predictive biomarker for the therapeutic outcomes of ICIs or chemotherapy in solid cancer patients. The pooled results for subgroup analyses, which involved types of cancer, sample size, and study regions, indicated that there is significant heterogeneity in the sample size less than 200, and other study regions (including Australia and China). Previously, the LIPI score may be an independent and complemented indicator for improved survival in cancer patients receiving immunotherapy or chemotherapy, because there was no significant correlation among PD-L1, TMB, and LIPI score (36).

Although our analysis provided a comprehensive summary of current literature, our present study still had some limitations that need to be considered. First of all, the major limitation lies in the fact that most of the included studies were retrospective, leading to some unavoidable bias sources. Secondly, only studies published in English were included, which may lead to publication bias. Cancer type is also a limitation; thus, we performed a subgroup analysis to further explain the correlation between LIPI score and the clinicopathologic features of patients receiving ICIs or chemotherapy. Although there is significant heterogeneity when the sample size is less than 200, this does not affect our results. Further high-quality prospective study is warranted.

CONCLUSIONS

In summary, a good LIPI score was significantly correlated with improved OS and PFS in cancer patients receiving ICIs or chemotherapy, regardless of the different types of cancer. Our analysis supported that the LIPI score is a reliable predictive tool that can be used to identify cancer patients who benefit from ICIs or chemotherapy, and to guide decisions in the era of personalized cancer treatments.

DATA AVAILABILITY STATEMENT

The original contributions presented in the study are included in the article/**Supplementary Material**. Further inquiries can be directed to the corresponding author.

AUTHOR CONTRIBUTIONS

HL and TL designed the study. HL, X-LY, and Z-RD performed the systematic search. HL, X-LY, X-YY, Z-RD, and Z-QC selected eligible articles and conducted the quality assessment. HL and X-LY analyzed, interpreted the data, and drafted the manuscript. TL revised the manuscript. All authors contributed to the article and approved the submitted version.

FUNDING

This work was supported by the grants from the Taishan Scholars Program for Young Expert of Shandong Province (Grant No. tsqn20161064), National Natural Science Foundation of China (Grant No. 82073200 & 81874178), and founds for Independent Cultivation of Innovative Team from Universities in Jinan (Grant No. 2020GXRC023).

SUPPLEMENTARY MATERIAL

The Supplementary Material for this article can be found online at: https://www.frontiersin.org/articles/10.3389/fonc.2021.691002/full#supplementary-material

REFERENCES

1. Jia L, Gao Y, He Y, Hooper JD, Yang P. HBV Induced Hepatocellular Carcinoma and Related Potential Immunotherapy. *Pharmacol Res* (2020) 159:104992. doi: 10.1016/j.phrs.2020.104992
2. Brahmer JR, Drake CG, Wollner I, Powderly JD, Picus J, Sharfman WH, et al. Phase I Study of Single-Agent Anti-Programmed Death-1 (MDX-1106) in Refractory Solid Tumors: Safety, Clinical Activity, Pharmacodynamics, and Immunologic Correlates. *J Clin Oncol Off J Am Soc Clin Oncol* (2010) 28 (19):3167–75. doi: 10.1200/jco.2009.26.7609
3. Topalian SL, Hodi FS, Brahmer JR, Gettinger SN, Smith DC, McDermott DF, et al. Safety, Activity, and Immune Correlates of Anti-PD-1 Antibody in Cancer. *New Engl J Med* (2012) 366(26):2443–54. doi: 10.1056/NEJMoa1200690
4. Wang D, Hao H, Li X, Wang Z. The Effect of Intestinal Flora on Immune Checkpoint Inhibitors in Tumor Treatment: A Narrative Review. *Ann Trans Med* (2020) 8(17):1097. doi: 10.21037/atm-20-4535

5. Seliger B. The Role of the Lymphocyte Functional Crosstalk and Regulation in the Context of Checkpoint Inhibitor Treatment-Review. *Front Immunol* (2019) 10:2043. doi: 10.3389/fimmu.2019.02043
6. Pinter M, Scheiner B, Peck-Radosavljevic M. Immunotherapy for Advanced Hepatocellular Carcinoma: A Focus on Special Subgroups. *Gut* (2020) 70 (1):204–14. doi: 10.1136/gutjnl-2020-321702
7. Sha D, Jin Z, Budczies J, Stenzinger A, Sinicrope FA. Tumor Mutational Burden as a Predictive Biomarker in Solid Tumors. *Cancer Discovery* (2020). doi: 10.1158/2159-8290.cd-20-0522
8. Huang Y, Shen A. The Prediction Potential of Neutrophil-to-Lymphocyte Ratio for the Therapeutic Outcomes of Programmed Death Receptor-1/Programmed Death Ligand 1 Inhibitors in non-Small Cell Lung Cancer Patients: A Meta-Analysis. *Medicine* (2020) 99(34):e21718. doi: 10.1097/md.0000000000021718
9. Chen H, Wang D, Zhong Q, Tao Y, Zhou Y, Shi Y. Pretreatment Body Mass Index and Clinical Outcomes in Cancer Patients Following Immune Checkpoint Inhibitors: A Systematic Review and Meta-Analysis. *Cancer Immunol Immunother CII* (2020). doi: 10.1007/s00262-020-02680-y
10. Lu S, Stein JE, Rimm DL, Wang DW, Bell JM, Johnson DB, et al. Comparison of Biomarker Modalities for Predicting Response to PD-1/PD-L1 Checkpoint Blockade: A Systematic Review and Meta-Analysis. *JAMA Oncol* (2019) 5 (8):1195–204. doi: 10.1001/jamaoncol.2019.1549
11. Mezquita L, Auclin E, Ferrara R, Charrier M, Remon J, Planchard D, et al. Association of the Lung Immune Prognostic Index With Immune Checkpoint Inhibitor Outcomes in Patients With Advanced Non-Small Cell Lung Cancer. *JAMA Oncol* (2018) 4(3):351–7. doi: 10.1001/jamaoncol.2017.4771
12. Meyers DE, Stukalin I, Vallerand IA, Lewinson RT, Suo A, Dean M, et al. The Lung Immune Prognostic Index Discriminates Survival Outcomes in Patients With Solid Tumors Treated With Immune Checkpoint Inhibitors. *Cancers* (2019) 11(11). doi: 10.3390/cancers11111713
13. Mielgo Rubio X, Gomez Rueda A, Antoñanzas M, Falagan S, Núñez JA, Sánchez Peña AM, et al. Applicability of Lung Immune Prognostic Index (LIPI) to Predict Efficacy of First-Line Pembrolizumab in Advanced Non-Small Cell Lung Cancer (NSCLC). *Ann Oncol* (2019) 30:v619–20. doi: 10.1093/annonc/mdz260.031
14. Herrera Gomez RG, Mezquita L, Auclin E, Heraudet L, Plana M, Salas S, et al. The Head and Neck Lung Immune Prognostic Index (HN-LIPI): A Prognostic Score for Immune Checkpoint Inhibitors (ICI) in Recurrent or Metastatic Squamous Cell Carcinoma of the Head and Neck (R/M SCCHN) Patients. *Ann Oncol* (2019) 30:v469–70. doi: 10.1093/annonc/mdz252.051
15. Liberati A, Altman DG, Tetzlaff J, Mulrow C, Gøtzsche PC, Ioannidis JP, et al. The PRISMA Statement for Reporting Systematic Reviews and Meta-Analyses of Studies That Evaluate Healthcare Interventions: Explanation and Elaboration. *BMJ (Clin Res Ed)* (2009) 339:b2700. doi: 10.1136/bmj.b2700
16. Stang A. Critical Evaluation of the Newcastle-Ottawa Scale for the Assessment of the Quality of Nonrandomized Studies in Meta-Analyses. *Eur J Epidemiol* (2010) 25(9):603–5. doi: 10.1007/s10654-010-9491-z
17. DerSimonian R, Laird N. Meta-Analysis in Clinical Trials. *Controlled Clin Trials* (1986) 7(3):177–88. doi: 10.1016/0197-2456(86)90046-2
18. Egger M, Davey Smith G, Schneider M, Minder C. Bias in Meta-Analysis Detected by a Simple, Graphical Test. *BMJ (Clin Res Ed)* (1997) 315 (7109):629–34. doi: 10.1136/bmj.315.7109.629
19. Al Darazi G, Martin E, Delord JP, Korakis I, Betrian S, Poublanc M, et al. Improving Patient Selection for Immuno-Oncology Phase I Trials: An External Validation of Five Prognostic Scores at Claudius Regaud Institute of Toulouse, Oncopôle (IUCT-O). *Ann Oncol* (2019) 30:v186. doi: 10.1093/annonc/mdz244.055
20. Chen S, Huang Z, Jia W, Tao H, Zhang S, Ma J, et al. Association of the Pretreatment Lung Immune Prognostic Index With Survival Outcomes in Advanced Hepatocellular Carcinoma Patients Treated With PD-1 Inhibitors. *J Hepatocell Carcinoma* (2020) 7:289–99. doi: 10.2147/jhc.s277453
21. Ferreira S, Esteves S, Almodovar MTAS. Prognostic Biomarkers in Lung Cancer Patients Treated With Immunotherapy. *Ann Oncol* (2019) 30:xi6. doi: 10.1093/annonc/mdz447.019
22. Kazandjian D, Gong Y, Keegan P, Pazdur R, Blumenthal GM. Prognostic Value of the Lung Immune Prognostic Index for Patients Treated for Metastatic Non-Small Cell Lung Cancer. *JAMA Oncol* (2019) 5(10):1481–5. doi: 10.1001/jamaoncol.2019.1747
23. Mazzaschi G, Minari R, Zecca A, Cavazzoni A, Ferri V, Mori C, et al. Soluble PD-L1 and Circulating CD8+PD-1+ and NK Cells Enclose a Prognostic and Predictive Immune Effector Score in Immunotherapy Treated NSCLC Patients. *Lung Cancer* (2020) 148:1–11. doi: 10.1016/j.lungcan.2020.07.028
24. Santa Gadea OS, Hernando-Calvo A, Berché R, Matos I, Gardeazabal I, Pedrazzoli ABA, et al. Limited Efficacy of Immunotherapy Combination Regimens in Patients With Unselected "Cold" Tumours Enrolled in Early Clinical Trials. *Ann Oncol* (2020) 31:S489. doi: 10.1016/j.annonc.2020.08.686
25. Sorich MJ, Rowland A, Karapetis CS, Hopkins AM. Evaluation of the Lung Immune Prognostic Index for Prediction of Survival and Response in Patients Treated With Atezolizumab for NSCLC: Pooled Analysis of Clinical Trials. *J Thorac Oncol Off Publ Int Assoc Study Lung Cancer* (2019) 14(8):1440–6. doi: 10.1016/j.jtho.2019.04.006
26. Wang W, Huang Z, Yu Z, Zhuang W, Zheng W, Cai Z, et al. Prognostic Value of the Lung Immune Prognostic Index May Differ in Patients Treated With Immune Checkpoint Inhibitor Monotherapy or Combined With Chemotherapy for Non-Small Cell Lung Cancer. *Front Oncol* (2020) 10:572853. doi: 10.3389/fonc.2020.572853
27. Li Y, Zhang Z, Hu Y, Yan X, Song Q, Wang G, et al. Pretreatment Neutrophil-To-Lymphocyte Ratio (NLR) May Predict the Outcomes of Advanced Non-Small-Cell Lung Cancer (NSCLC) Patients Treated With Immune Checkpoint Inhibitors (ICIs). *Front Oncol* (2020) 10:654. doi: 10.3389/fonc.2020.00654
28. Templeton AJ, McNamara MG, Šeruga B, Vera-Badillo FE, Aneja P, Ocaña A, et al. Prognostic Role of Neutrophil-to-Lymphocyte Ratio in Solid Tumors: A Systematic Review and Meta-Analysis. *J Natl Cancer Institute* (2014) 106(6): dju124. doi: 10.1093/jnci/dju124
29. Gooden MJ, de Bock GH, Leffers N, Daemen T, Nijman HW. The Prognostic Influence of Tumour-Infiltrating Lymphocytes in Cancer: A Systematic Review With Meta-Analysis. *Br J Cancer* (2011) 105(1):93–103. doi: 10.1038/bjc.2011.189
30. Takada K, Takamori S, Matsubara T, Haratake N, Akamine T, Kinoshita F, et al. Clinical Significance of Preoperative Inflammatory Markers in non-Small Cell Lung Cancer Patients: A Multicenter Retrospective Study. *PloS One* (2020) 15(11):e0241580. doi: 10.1371/journal.pone.0241580
31. Liu C, Li L, Song K, Zhan ZY, Yao Y, Gong H, et al. A Nomogram for Predicting Mortality in Patients With COVID-19 and Solid Tumors: A Multicenter Retrospective Cohort Study. *J Immunother Cancer* (2020) 8(2). doi: 10.1136/jitc-2020-001314
32. Stephen ZR, Zhang M. Recent Progress in the Synergistic Combination of Nanoparticle-Mediated Hyperthermia and Immunotherapy for Treatment of Cancer. *Advanced Healthcare Mater* (2020) 7(1):341. doi: 10.1002/adhm.202001415
33. Callahan MK, Kluger H, Postow MA, Segal NH, Lesokhin A, Atkins MB, et al. Nivolumab Plus Ipilimumab in Patients With Advanced Melanoma: Updated Survival, Response, and Safety Data in a Phase I Dose-Escalation Study. *J Clin Oncol Off J Am Soc Clin Oncol* (2018) 36(4):391–8. doi: 10.1200/jco.2017.72.2850
34. Xing P, Zhang F, Wang G, Xu Y, Li C, Wang S, et al. Incidence Rates of Immune-Related Adverse Events and Their Correlation With Response in Advanced Solid Tumours Treated With NIVO or NIVO+IPI: A Systematic Review and Meta-Analysis. *J Immunother Cancer* (2019) 7(1):341. doi: 10.1186/s40425-019-0779-6
35. Pilla L, Alberti A, Di Mauro P, Gemelli M, Cogliati V, Cazzaniga ME, et al. Molecular and Immune Biomarkers for Cutaneous Melanoma: Current Status and Future Prospects. *Cancers* (2020) 12(11). doi: 10.3390/cancers12113456
36. Yuan P, Li Y, Jiang L, Liu Y, Liu W, Ying J. The Correlation Among PD-L1 Expression, TMB and Lung Immune Prognostic Index in Chinese Patients With Advanced Lung Adenocarcinoma. *J Thorac Oncol* (2018) 13(10):S708–9. doi: 10.1016/j.jtho.2018.08.1169

Conflict of Interest: The authors declare that the research was conducted in the absence of any commercial or financial relationships that could be construed as a potential conflict of interest.

Publisher's Note: All claims expressed in this article are solely those of the authors and do not necessarily represent those of their affiliated organizations, or those of the publisher, the editors and the reviewers. Any product that may be evaluated in this article, or claim that may be made by its manufacturer, is not guaranteed or endorsed by the publisher.

Copyright © 2021 Liu, Yang, Yang, Dong, Chen, Hong and Li. This is an open-access article distributed under the terms of the Creative Commons Attribution License (CC BY). The use, distribution or reproduction in other forums is permitted, provided the original author(s) and the copyright owner(s) are credited and that the original publication in this journal is cited, in accordance with accepted academic practice. No use, distribution or reproduction is permitted which does not comply with these terms.

frontiers in Immunology

ORIGINAL RESEARCH
published: 27 September 2021
doi: 10.3389/fimmu.2021.722807

Integrated Profiling Identifies *PLOD3* as a Potential Prognostic and Immunotherapy Relevant Biomarker in Colorectal Cancer

Junhong Shi[1], *Meiyu Bao*[2], *Weifeng Wang*[2], *Xuan Wu*[1], *Yueying Li*[1], *Changdong Zhao*[3*] and *Weiwei Liu*[1,4*]

[1] Department of Laboratory Medicine and Central Laboratory, Shanghai Tenth People's Hospital, Tongji University School of Medicine, Shanghai, China, [2] Department of Central Laboratory, Shanghai Tenth People's Hospital, Tongji University, Shanghai, China, [3] Department of Gastroenterology, Second People's Hospital of Lianyungang City, Lianyungang, China, [4] Department of Laboratory Medicine, Shanghai Skin Disease Hospital, Tongji University School of Medicine, Shanghai, China

OPEN ACCESS

Edited by:
Hubing Shi,
Sichuan University, China

Reviewed by:
Si-Cong Ma,
Southern Medical University, China
Yuyan Zhu,
The First Affiliated Hospital of China Medical University, China
Yanjie Zhao,
Qingdao University, China

***Correspondence:**
Changdong Zhao
lygzcdzcd@163.com
Weiwei Liu
huashanvivian@126.com

Specialty section:
This article was submitted to Cancer Immunity and Immunotherapy, a section of the journal Frontiers in Immunology

Received: 09 June 2021
Accepted: 08 September 2021
Published: 27 September 2021

Citation:
Shi J, Bao M, Wang W, Wu X, Li Y, Zhao C and Liu W (2021) Integrated Profiling Identifies PLOD3 as a Potential Prognostic and Immunotherapy Relevant Biomarker in Colorectal Cancer. Front. Immunol. 12:722807. doi: 10.3389/fimmu.2021.722807

Procollagen-Lysine,2-Oxoglutarate 5-Dioxygenase 3 (*PLOD3*) is related to a variety of human diseases. However, its function in Colorectal cancer (CRC) remains uncertain. *PLOD3* expression was analyzed using The Cancer Genome Atlas (TCGA) pan-cancer data. DAVID was used for enrichment analysis of *PLOD3*-related genes. The correlation between *PLOD3* expression and immune cell infiltration was evaluated. Four expression profile datasets (GSE17536, GSE39582, GSE74602, and GSE113513) from Gene Expression Omnibus, and two proteomic datasets were used as validation cohorts for assessing the diagnostic and prognostic value of *PLOD3* in CRC. What's more, we performed immunohistochemistry (IHC) staining for PLOD3 in 160 paired CRC specimens and corresponding adjacent non-tumor tissues. *PLOD3* was highly expressed in many tumors including CRC. *PLOD3* was upregulated in advanced stage CRCs, and high *PLOD3* expression was associated with poor survival. High *PLOD3* expression was associated with low levels of B cells, $CD4^+$ T cells, M1 macrophages, $CD8^+$ T cells, and multiple immunerelated characteristics. In addition, the high *PLOD3* expression group had a higher TIDE score and a lower tumor mutation burden and microsatellite instability, indicating that patients with high *PLOD3* expression may be resistant to immunotherapy. Additional datasets and IHC analysis were used to validate the diagnostic and prognostic value of *PLOD3* at the mRNA and protein levels in CRC. Patients with non-response to immunotherapy showed increased *PLOD3* expression in an immunotherapy treated dataset. *PLOD3* is a potential biomarker for CRC diagnosis and prognosis prediction. CRCs with high *PLOD3* expression may be resistant to immune checkpoint therapy.

Keywords: Colorectal cancer, *PLOD3*, biomarker, prognosis, immune therapy

INTRODUCTION

Colorectal cancer (CRC) is one of the most common malignant tumors of the digestive system, and its morbidity and mortality rates are high worldwide (1). Despite effective cancer screening measures and modern medicine, CRC remains the leading cause of cancer-related mortality worldwide (2). According to the "Cancer Statistics in China", the incidence and mortality of CRC have increased in China (3). Therefore, it is important to identify novel diagnostic and prognostic biomarkers and to explore potential relevant targets for the treatment of CRC.

Recently, growing evidence has reported that the elevated deposition of collagen and its cross-linking can worsen tumor progression by promoting cancer cell proliferation, migration, and invasion (4, 5). Collagen deposition and cross-linking are dependent on the hydroxylation of lysine residues, which is mainly catalyzed by procollagen-lysine, 2-oxoglutarate 5-dioxygenase (PLOD). *PLOD3*, a member of PLOD family (6), is a multifunctional enzyme with lysyl hydroxylase, collagen galactosyltransferase, and glucosyltransferase activities (7). Collagens constitute a highly specialized family of extracellular matrix (ECM) proteins that maintain tissue architecture and regulate cellular responses (8, 9). *PLOD3* is localized on chromosome 7q22.1, and its activity is critical for the biosynthesis of type IV and VI collagens (10). *PLOD3* overexpression is correlated with high circulating protein levels in some patients (11) and increasing evidence suggested that PLOD3 is associated with tumorigenesis in various cancer types. *PLOD3* is a novel diagnostic marker for early-stage hepatocellular carcinoma (12), human glioma prognosis (13) and ovarian cancer (14). In addition, PLOD3 interacts with STAT3 immunosuppressive signals, which promotes lung cancer metastasis *via* dysregulated RAS-MAP kinase pathway (15). These results suggested an underlying association between PLOD3 and tumor tumorigenesis as well as antitumor immunity. Several pancancer studies (16–18) published in the last year reminded us to explore the molecular features of *PLOD3* using the high-throughput sequencing data. The aim of this study was to uncover the functional role, as well as the diagnostic and prognostic value of *PLOD3* in CRC.

METHODS

Patients and Samples

A total of 160 paired paraffin-embedded CRC specimens and corresponding adjacent non-tumor tissues were collected to design a tissue array chip from the Shanghai Tenth People's Hospital, Tongji University School of Medicine. The study was approved by the Research Ethics Committee of Shanghai Tenth People's Hospital and carried out in accordance with the ethical standards formulated in the Helsinki Declaration. The related ethical approval code is 2020-KN155-01. Tissue microarray was constructed by 1.5-mm cores.

Immunohistochemistry

Immunohistochemistry (IHC) for PLOD3 was carried out on CRC tissue microarray slides. The slides were first incubated at 60°C for 4 h, deparaffinized in xylene, and then rehydrated in alcohol. After heating in citrate buffer for 23 min, we used 0.3% of hydrogen peroxide (H_2O_2) to block endogenous peroxidase activity. Slides were blocked with 3% bovine serum albumin for 30 min and incubated in the anti-PLOD3 antibody (diluted 1:200; ab128698; Abcam) overnight at 4°C. The next day, after 3 washes with PBS, slides were incubated with secondary antibody for 1 h, then we used the 3,3-diaminobenzidine (DAB) kit for visualization, and hematoxylin was used to stain nuclei. After the experiments, the slides were observed by microscope. All stainings were scored based on the staining intensity and extensity of positive cells, the intensity (0=genitive, 1=weak, 2=moderate, and 3=strong) and extensity (0 = 5% or less of cells stained positive; 1 = 5%-25%; 2 = 26% to 50%; 3 = 51% to 75%; and 4 = 75% or more) of tumor staining were evaluated. The positive cell density of each core was counted by two independent investigators blind to clinical outcome and knowledge of the clinicopathological data. The final IHC score was calculated by multiplying the strongest intensity score and the total extensity score (maximum value of 12).

Data Acquisition and Preprocessing

The Cancer Genome Atlas (TCGA) colon adenocarcinoma (COAD) and rectum adenocarcinoma (READ) data, including gene expression quantified by fragments per kilobase million and clinical information of 51 normal tissues and 638 tumor tissues, were obtained from the UCSC Xena project (http://xena.ucsc.edu/). Four independent validation cohorts (GSE17536, GSE39582, GSE74602, and GSE113513) were obtained from the Gene Expression Omnibus (GEO; https://www.ncbi.nlm.nih.gov/geo). Gene level mutations (Mutect2) of the COAD and READ cohorts were acquired from TCGA data portal (https://portal.gdc.cancer.gov/).

TIMER Database Analysis

The TIMER (12) database was used to analyze differences in *PLOD3* expression between tumors and normal controls from TCGA data set.

Comprehensive Tumor Immune Analysis

The pan-cancer immune cell infiltration scores for TCGA were obtained from a previously published study (19). The results were based on CIBERSORT (20) and were used for further analysis. TCGA CRC cancer samples were divided into two groups according to median *PLOD3* expression (high *versus* low), and immune cell infiltration was compared between groups. Tumor Immune Dysfunction and Exclusion (TIDE) algorithm (21) was used to estimate a tide score and the predicted response to immune checkpoint blockade. Immunescore and Stromalscore were calculated *via* "estimate" (22) package.

Biological Functions of *PLOD3* in CRC

The top 1000 genes showing the highest correlation with *PLOD3* were extracted from the LinkedOmics database (http://www.linkedomics.org) (23). Function annotations were performed to identify potentially involved biological processes and signaling pathways using DAVID (24) 6.8 (https://david.ncifcrf.gov/).

Mutation Analysis

Tumor mutation analysis was performed using the "maftools" package (25). High and low *PLOD3* expression oncoplots were generated *via* "oncoplot" function, and tumor mutation burden (TMB) was calculated using the "maftools" package. Differentially mutated genes between *PLOD3*-high and low groups were evaluated *via* Fisher's exact test.

Validation of the Diagnostic, Prognostic and Therapeutic Value of *PLOD3*

Four independent validation cohorts (GSE17536 (26), GSE39582 (27), GSE74602, and GSE113513) were obtained from the GEO database and used as validation cohorts to determine the diagnostic and prognostic value of *PLOD3*. GSE17536 (177 patients) and GSE39582 (585 patients) with relevant survival information were applied for *PLOD3*'s prognostic value validation; GSE74602 (30 pairs) and GSE113513 (14 pairs) including the CRC tissues and matched adjacent tissues were employed for validating the expression difference of *PLOD3* between tumor and normal tissues. In this analysis, patients were divided into low- and high-*PLOD3* groups according to an optimal *PLOD3* cutoff, which was generated using the association between *PLOD3* and survival data with the survminer package. GSE91061 (28) including 105 immunotherapy-treated samples was used for the validation of *PLOD3*'s therapeutic value. After immunotherapy treatment, samples were classified into the following categories according to the patient's response: complete response (CR), partial response (PR), stable disease (SD) and progressive disease (PD). Among them, CR and PR are recognized as patients who respond to immunotherapy. SD and PD are recognized as patients who do not respond to immunotherapy. Moreover, the protein levels of PLOD3 in colorectal tumors and normal tissues were assessed using a proteomic dataset (29). Another proteomic dataset (30) was used to validate the prognostic value of PLOD3 according to protein expression levels.

Statistical Analysis

Differences in variables between groups were tested using the Wilcoxon test or chi-squared test, as appropriate. Kaplan-Meier curves were drawn to estimate the overall survival distribution. The log-rank test was used to analyze the statistical difference in survival curves between two groups. Kruskal-Wallis tests were used for comparing *PLOD3*'s expression difference among more than two comparison groups and Wilcoxon test was used for comparison between two groups. The ROC curve was plotted *via* "pROC" package. All figures and statistical analyses were performed using R software (version 4.0.2; http://www.R-project.org). A value of $p < 0.05$ was considered statistically significant. All statistical tests were two-sided.

RESULTS

Pan-Cancer *PLOD3* Expression Analysis

Analysis of *PLOD3* using the TIMER2 database showed that *PLOD3* expression was higher in 19 TCGA tumors than in the corresponding normal tissues, including bladder urothelial carcinoma, breast invasive carcinoma, cholangiocarcinoma, COAD, esophageal carcinoma, Glioblastoma multiforme, head and neck squamous cell carcinoma, Kidney Chromophobe, kidney renal clear cell carcinoma, kidney renal papillary cell carcinoma, Liver hepatocellular carcinoma, lung adenocarcinoma, lung squamous cell carcinoma, Pheochromocytoma and Paraganglioma, Prostate adenocarcinoma, READ, Skin Cutaneous Melanoma, Stomach adenocarcinoma, and Uterine Corpus Endometrial Carcinoma (**Figure 1A**). Particularly, higher *PLOD3* expression was observed in TCGA COAD and READ cohorts, separately and collectively, compared with the adjacent normal tissues (**Figures 1B, C**), suggesting that *PLOD3* plays a role in the pathogenesis of CRC.

Correlations Between *PLOD3* Expression and Clinical Parameters in CRC Patients

The role of *PLOD3* in CRC remains unclear. Investigating the correlation between *PLOD3* expression and clinical features may clarify the function of *PLOD3* in the progression of CRC. In this study, we examined the relationship between *PLOD3* expression and the clinical parameters of CRC using TCGA cohort. The results showed that *PLOD3* expression differed significantly according to tumor N stage, M stage, clinical stage, and microsatellite instability (MSI) status. Increased N, M, and clinical stages were associated with increased *PLOD3* expression (all $p < 0.05$), suggesting that *PLOD3* may be a poor prognostic factor (**Figures 2A–C**). The microsatellite stable (MSS) group also showed higher *PLOD3* expression (**Figure 2D**). Survival analysis using *PLOD3* median expression as the cut-off value showed that CRCs with higher expression of *PLOD3* had a worse prognosis than those with lower expression (log rank $p < 0.01$) (**Figure 2E**).

Gene Function Annotation and Pathway Analysis

After determining the prognostic value of *PLOD3* in CRC, we next explored the biological functions associated with *PLOD3*. GO and KEGG enrichment analyses were performed, and the top GO terms and signaling pathways are shown in **Figures 3A, B**. *PLOD3* gene expression was associated with many biological processes, such as vesicle-mediated transport, ephrin receptor signaling pathway, and autophagy. *PLOD3* was also associated with Notch signaling, neurotrophin signaling, and glycosaminoglycan biosynthesis.

Differences in Genomic Mutation Profiles and TMB Between Different *PLOD3* Groups

To examine the relationship between *PLOD3* and mutation profiles in CRC, tumor mutations were compared between *PLOD3* high and low groups. We chose the top 20 mutation genes in the whole CRC cohort and compared the mutation frequency difference between *PLOD3* high (**Figure 4A**) and low (**Figure 4B**) groups using the Fisher's test. Furthermore, we visualized these mutation genes in a forest (**Figure 4C**). *TP53*, *APC*, and *KRAS*, were significantly mutated in the *PLOD3*-high

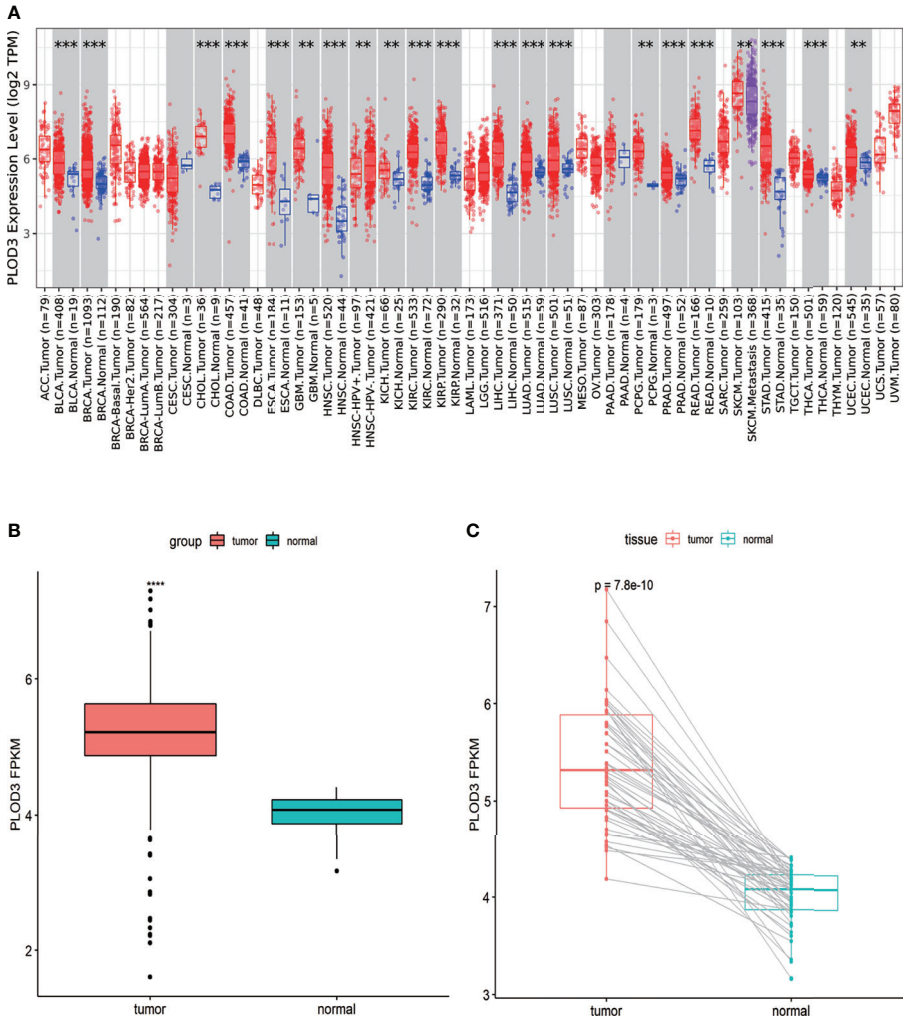

FIGURE 1 | Pan-cancer *PLOD3* expression analysis. **(A)** *PLOD3* expression in tumor and normal tissues from pan-cancer data of The Cancer Genome Atlas (TCGA). **(B)** *PLOD3* expression in tumor and normal tissues from CRC obtained from TCGA. **(C)** *PLOD3* expression in paired CRC tumor and normal tissues from TCGA. Data are expressed as the mean ± SD. $^{**}p < 0.01$, $^{***}p < 0.001$, $^{****}p < 0.0001$.

group, whereas *PIK3CA*, *FAT4*, and *OBSCN* were specifically mutated in the low-expression group. In addition, a significant ($p < 0.001$) negative correlation was observed between *PLOD3* and TMB (**Figure 4D**).

PLOD3 and the Immune Microenvironment in CRC

Next, we analyzed the immune cell infiltration difference between *PLOD3* high and low groups. The infiltration scores of B cell plasma, T cell CD8+, T cell CD4 memory resting, T cell CD4 memory activated, T cell follicular helper, T cell gamma delta, and macrophage M1 were higher in the *PLOD3*-low cohort than in the *PLOD3*-high cohort (**Figure 5A**). *PLOD3* was significantly negatively correlated with StromalScore (**Figure 5B**) and immuneScore (**Figure 5C**). In addition, *PLOD3* was significantly negatively correlated with multiple immune checkpoints (**Figure 5D**) and many other immune related genes, such as antigen-presentation, chemokines, interferons, and T cell inflamed genes (**Figure 5E**). What's more, a significantly higher TIDE score was observed in *PLOD3*-high group (**Figure 5F**). In an immunotherapy-treated cohort, patients showed non-response to immunotherapy presented with higher *PLOD3* expression (**Figure 5G**). Given that higher *PLOD3* expression was associated with lower immunescore, infiltration of multiple immune cells and many immune-related genes, TMB, and MSI score, consistent with the higher TIDE score, we speculated that CRC patients with high *PLOD3* expression may be resistant to immunotherapy, which was justified in an immunotherapy-treated cohort.

Validation of the Diagnostic and Prognostic Value of *PLOD3*

Two GEO datasets (GSE74602 and GSE113513) were used to validate the diagnostic value of *PLOD3* using paired tumor and

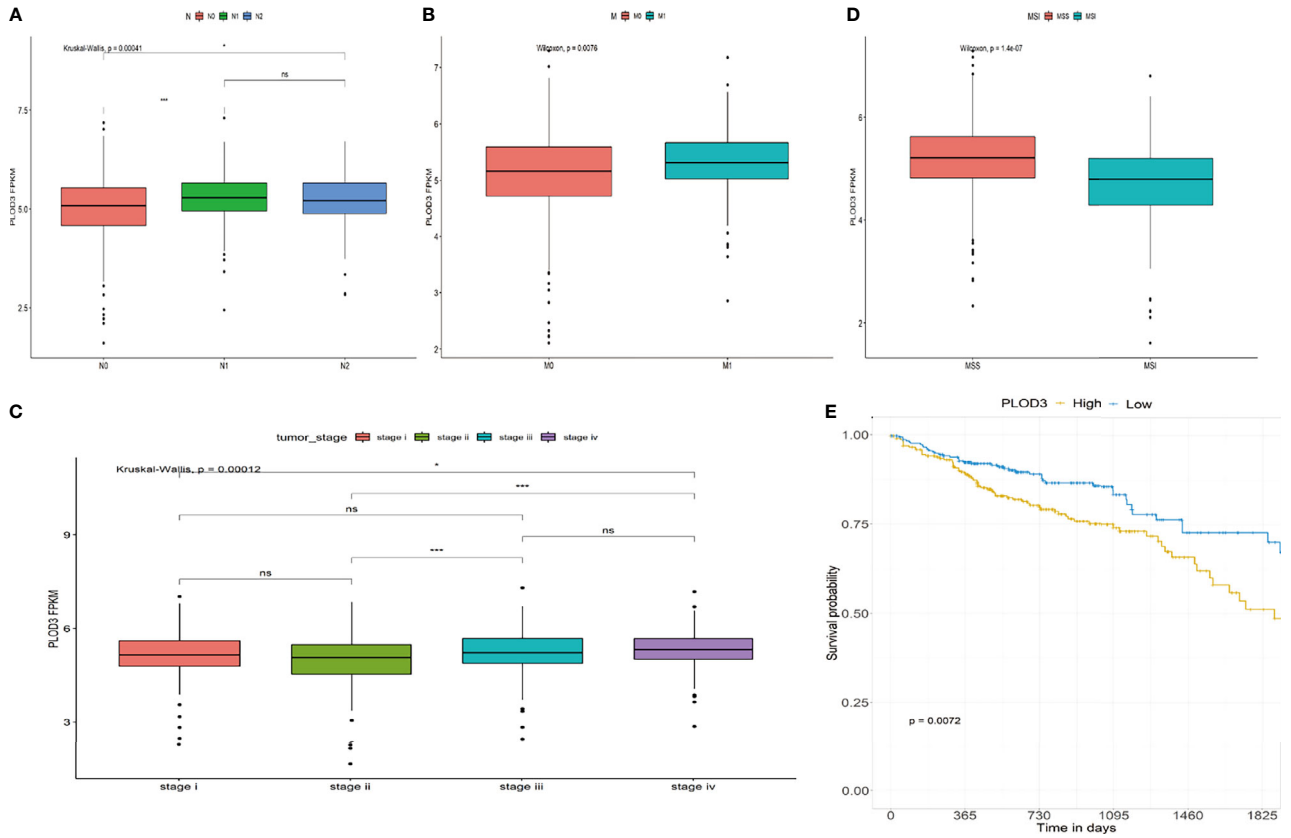

FIGURE 2 | Association of *PLOD3* expression with clinicopathological characteristics, including **(A)** CRC N stage, **(B)** CRC M stage, **(C)** CRC pathologic stage, **(D)** MSI and MSS, and **(E)** overall survival (OS). *$p < 0.05$, ***$p < 0.001$, ns, No Significance.

normal samples. *PLOD3* expression was significantly higher in tumor than in normal samples (**Figures 6A, B**). PLOD3 protein expression was higher in CRC than normal tissues (**Figure 6C**). **Figure 6D** showed PLOD3 protein presented with good diagnostic value between CRC and normal tissues. To further confirm the diagnostic value of PLOD3 in CRC patients, the expression of PLOD3 were analyzed by TMA-based IHC. we compared 160 CRC tumor tissues with paired adjacent normal tissues in a microarray, the representative IHC images of positive PLOD3 expression in tumor tissue and negative PLOD3 expression in normal tissue were shown (**Figure 6E**). Grossly, PLOD3 was overexpressed in tumor parts comparing to normal specimens (**Figure 6F**, p-value = 4.2e-14).

GSE17536 and GSE39582 were used to validate the prognostic value of *PLOD3*. In the GSE17536 dataset, patients with higher *PLOD3* expression had a worse disease-free survival (**Figure 6G**). In GSE39582, patients with higher *PLOD3* had a worse progression-free survival (**Figure 6H**). The proteomic dataset generated by Li et al. (30) was used to validate the prognostic value of PLOD3 protein expression, and the results revealed that patients with higher PLOD3 protein expression had a worse overall survival and progression-free survival (**Figures 6I, J**). Taken together, the results indicate that *PLOD3* is a promising biomarker for the diagnosis, prognosis, and treatment of CRC.

DISCUSSION

PLOD3, a collagen biosynthesis-related protein, was reported to contributes to carcinogenesis of HCC (12), glioma (13), ovarian cancer (14, 31), and lung cancer (15). However, the function of *PLOD3* in CRC remains to be elucidated. In the current study, we found that *PLOD3* was expressed at high levels in CRC tissues, and patients with higher *PLOD3* expression had worse survival. These results were validated at the mRNA and protein levels using additional datasets. CRCs with higher *PLOD3* expression showed a lower TMB, a higher TIDE score, and patients with MSS tended to have higher *PLOD3* expression, suggesting that these patients could present with immunotherapy resistance. An immunotherapy-treated cohort was enrolled to validate *PLOD3*'s predictive role for immunotherapy response.

PLODs are mainly regulated at the transcriptional level. For instance, hypoxia-induced factor-1 activates *PLOD1* in breast

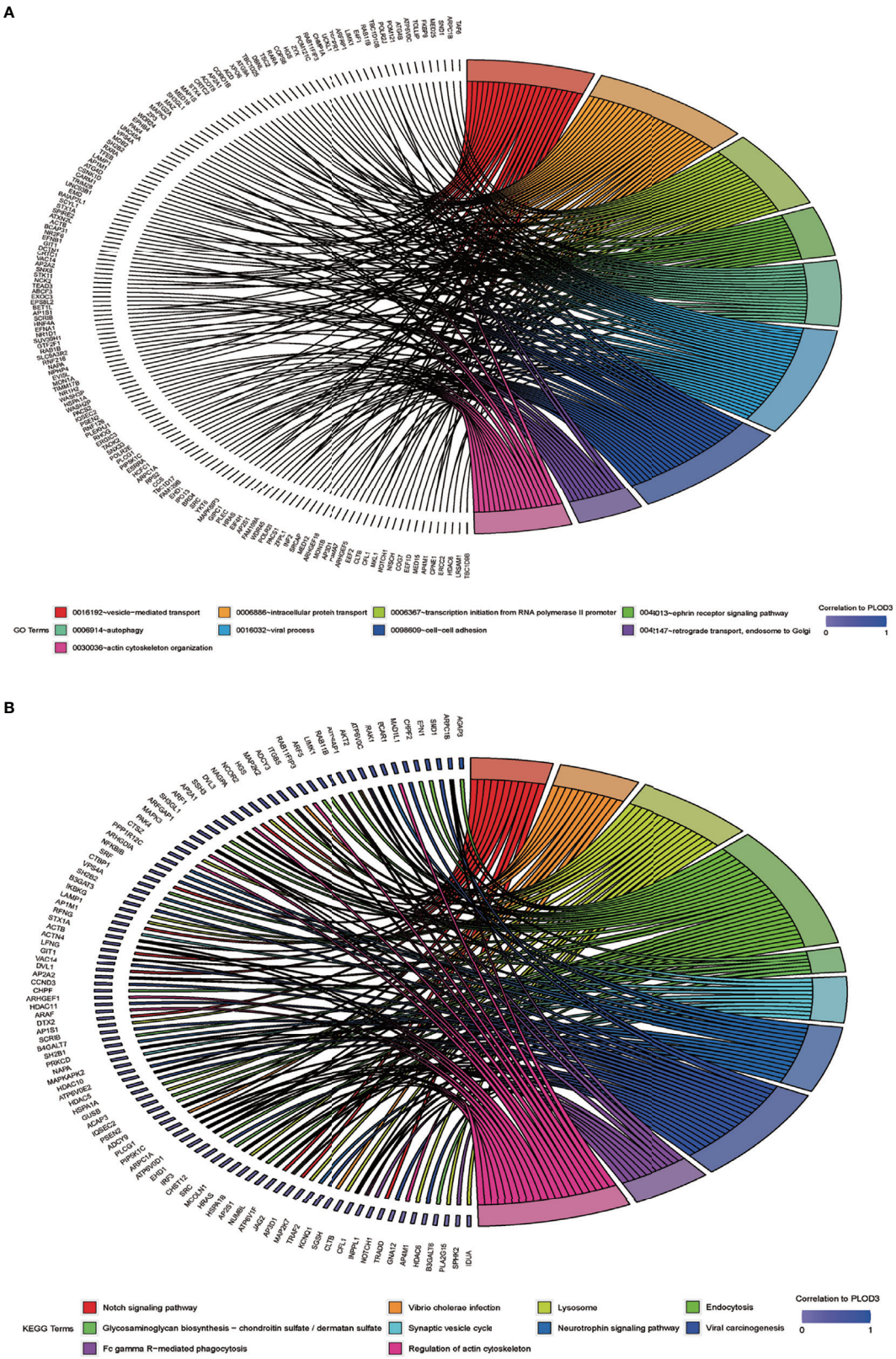

FIGURE 3 | **(A)** GO BP pathway analysis of PLOD3 related genes in CRC. **(B)** KEGG pathway analysis of PLOD3 related genes in CRC.

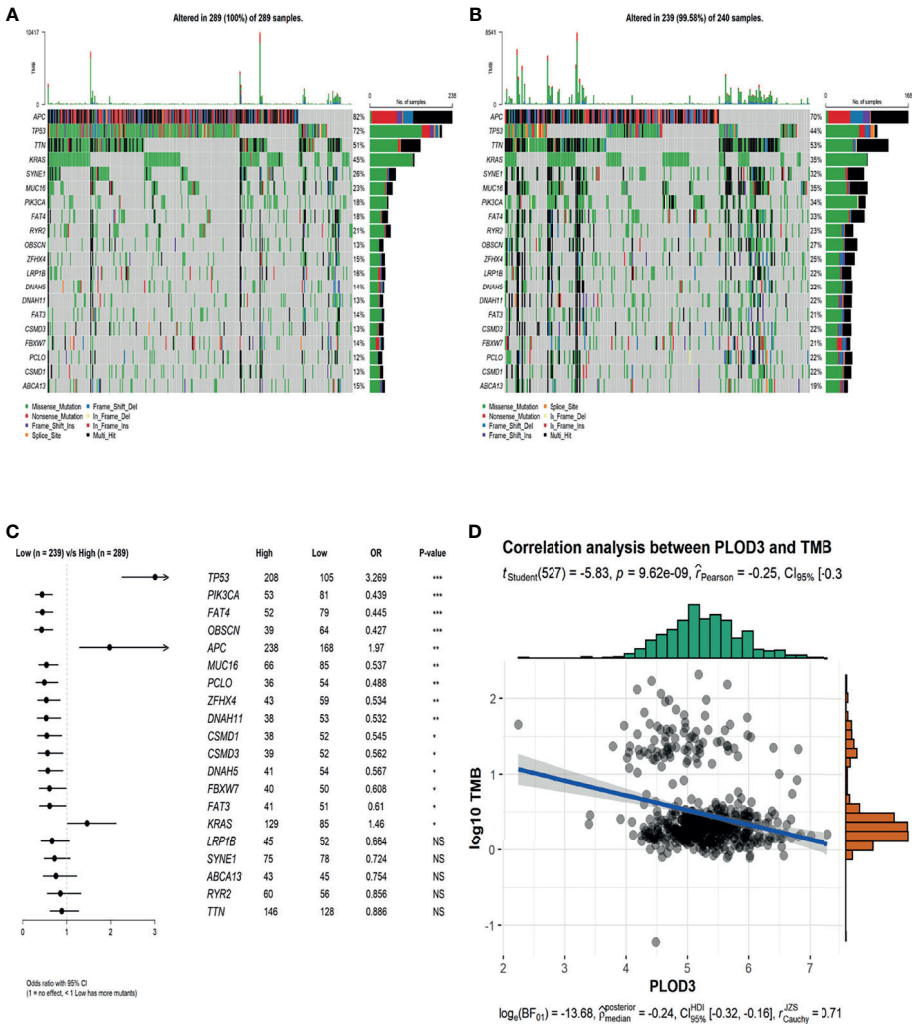

FIGURE 4 | Genomic mutation profiles and TMB characteristics of *PLOD3*-high and *PLOD3*-low groups. **(A)** Distribution of top 20 frequently mutated genes in *PLOD3*-high TCGA-CRC subgroups. The upper bar plot shows the TMB for each patient, and the left bar plot indicates the gene mutation frequency in different risk groups. **(B)** Distribution of top 20 frequently mutated genes in *PLOD3*-low TCGA-CRC subgroups. The upper bar plot shows the TMB for each patient, and the left bar plot indicates the gene mutation frequency in different risk groups. **(C)** Differentially mutated genes between *PLOD3*-high and low groups. The p values were calculated by Fisher's exact test. $^{*}p < 0.05$; $^{**}p < 0.01$; $^{***}p < 0.001$, NS, No Significance. **(D)** Correlation analysis of TMB and *PLOD3* in TCGA-CRC cohort.

cancer, and to a great extent, activates *PLOD2* in cancer development (32). *PLOD1* was found to be directly regulated by miR-140-5p and abnormally expressed *PLOD1* induced cancer aggressiveness in bladder cancer (33). Unlike *PLOD1* and *PLOD2*, the regulation of *PLOD3* in CRC is poorly understood. Data mining using TCGA datasets showed that *PLOD3* was overexpressed in 19 types of tumor tissues compared with normal tissues, indicating that *PLOD3* may serve as a novel biomarker in cancer. Increased *PLOD3* expression in CRC tumor tissues at the mRNA and protein levels indicated the potential diagnostic value of *PLOD3*. The prognostic value of *PLOD3* was validated in other datasets, confirming its prognostic potential.

In the present study, patients with advanced stage CRC showed higher *PLOD3* expression, indicating that *PLOD3* may be associated with metastasis. *PLODs* are implicated in metastasis because of their role in regulating collagen biosynthesis (34, 35). Collagens provide the scaffold for ECM assembly and are considered "highways" for cancer cell migration (36). *MicroRNA-663a* targets the 3′ untranslated region of *PLOD3* and decreases its expression, resulting in decreased accumulation of extracellular collagen (37). GO and KEGG enrichment analysis of *PLOD3*-related genes identified many associated pathways, such as the Notch signaling, neurotrophin signaling, and glycosaminoglycan biosynthesis pathways. Neurotrophin expression is associated with poor prognosis in cutaneous melanoma. The Notch signaling pathway is activated in CRC and other cancer types (38, 39) and could be related to poor-prognosis subtypes and metastasis in CRC (40), which may explain the association of *PLOD3* with

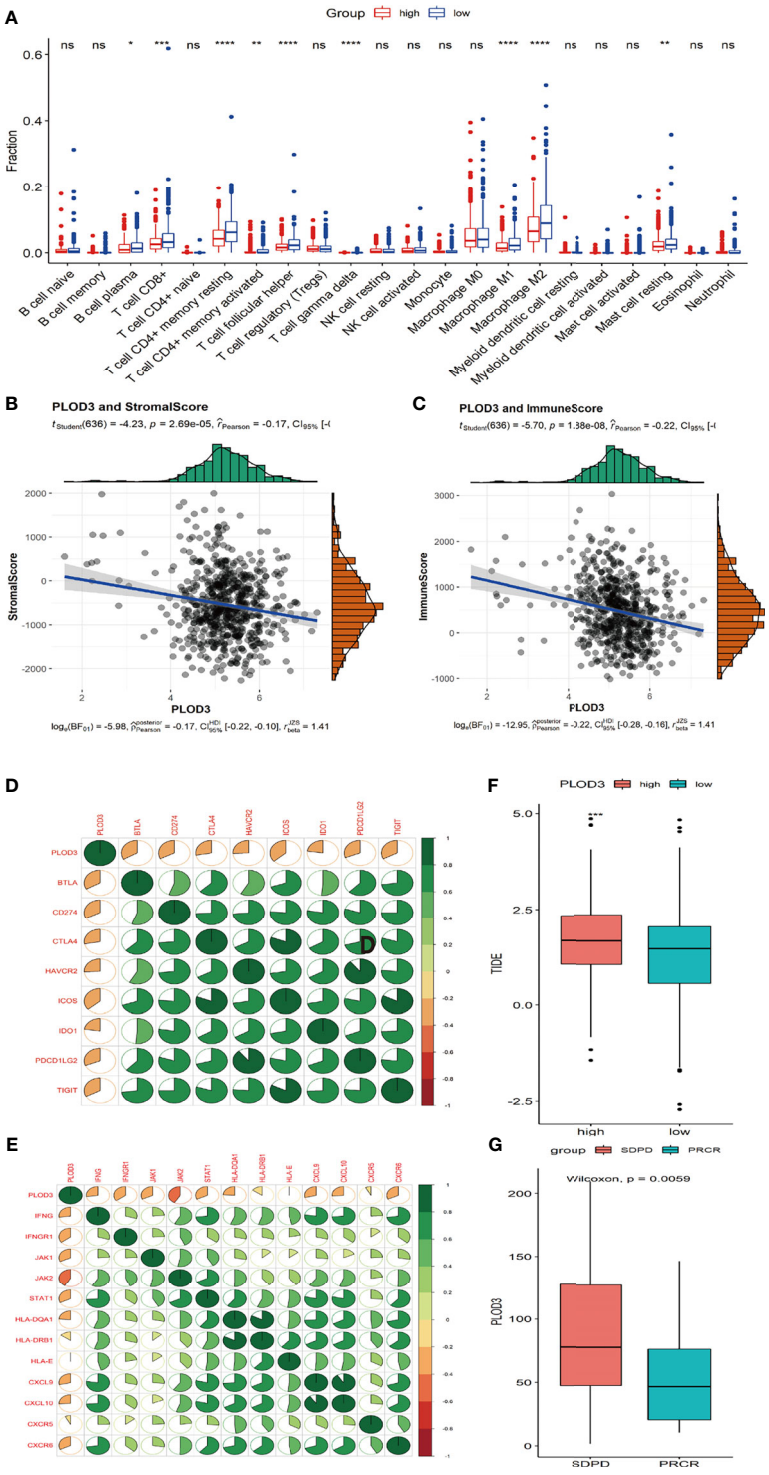

FIGURE 5 | Correlation analysis of immune cell infiltration and *PLOD3* in CRC. **(A)** Immune cell infiltration levels in high and low *PLOD3* expression groups from TCGA-CRC cohort. **(B)** Correlation analysis of StromalScore and *PLOD3* in TCGA-CRC cohort; **(C)** Correlation analysis of ImmueScore and *PLOD3* in TCGA-CRC cohort. **(D)** Correlation between *PLOD3* and immune checkpoint levels; green represents positive correlation, red represents negative correlation; color intensity is positively related with the strength of the correlation. **(E)** Correlation between PLOD3 and immune related genes; green represents positive correlation, red represents negative correlation; color intensity is positively related with the strength of the correlation. **(F)** Boxplot shows the TIDE score for high and low PLOD3 expression groups. Data are expressed as the mean ± SD. * $p < 0.05$, ** $p < 0.01$, ***$p < 0.001$, **** $p < 0.0001$. ns, not significant. **(G)** Boxplot shows the PLOD3 expression for immunotherapy response (CR and PR) and non-response groups (SD and PD). CR, complete response; PR, partial response; SD, stable disease; PD, progressive disease.

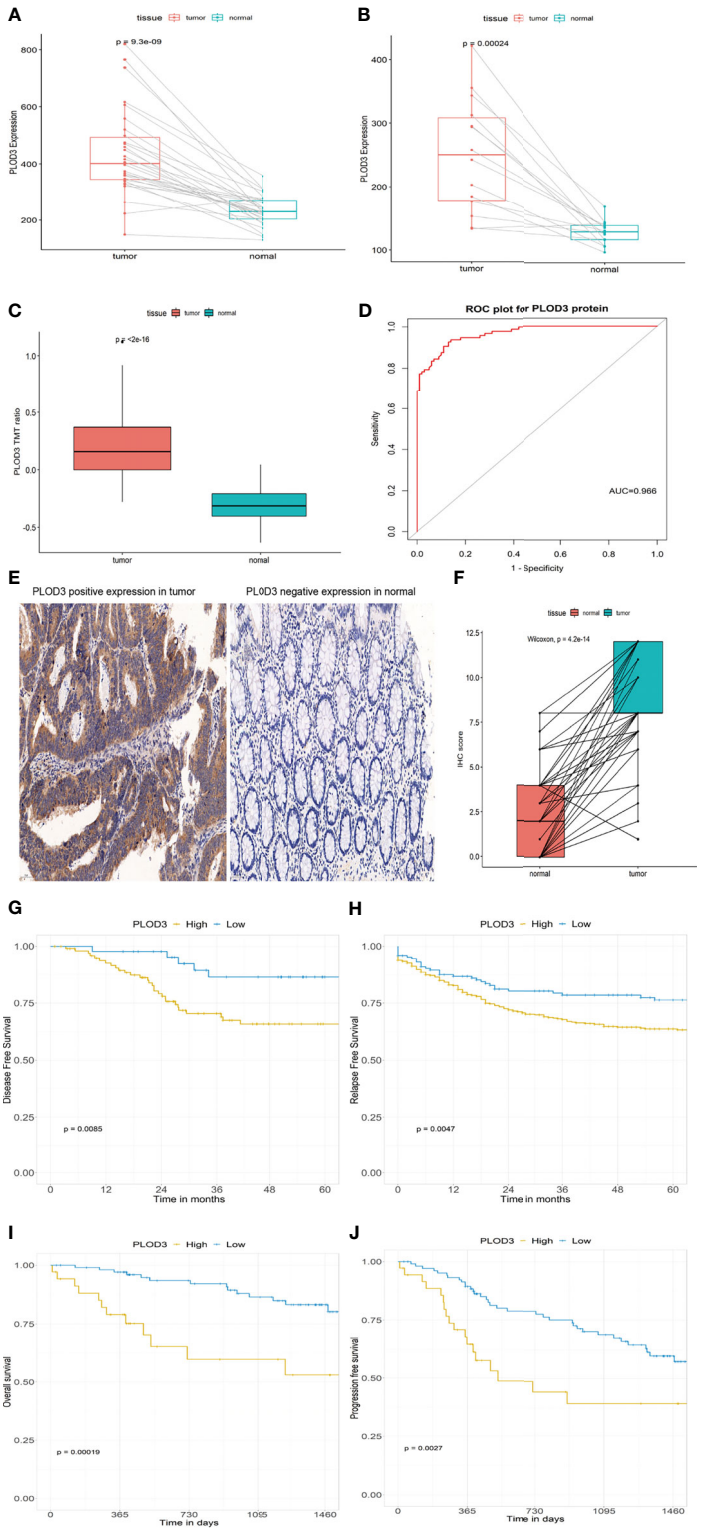

FIGURE 6 | *PLOD3* expression in CRC and normal tissues from the GSE74602 **(A)** and GSE113513 **(B)** cohorts; *PLOD3* protein expression difference in CRC and normal tissues and TMT ratio means the protein abundance by TMT-based quantitation **(C)** and ROC curve of *PLOD3* protein for discriminating tumor and normal tissues in proteome dataset **(D)**; **(E)** Representative microphotographs of PLOD3 immunohistochemical staining in CRC tissue and adjacent normal tissue by IHC. Scale bar = 50 μm. **(F)** IHC scores in CRC tissues and adjacent tissues. Prognostic value of *PLOD3* in the GSE17536 **(G)** and GSE39582 **(H)** cohorts; Prognostic value of *PLOD3* in the proteome dataset **(I, J)**.

poor prognosis. Some studies revealed the worse prognostic value of *TP53 (*41) and *KRAS* for CRCs (42). Higher mutation frequency of *TP53* and *KRAS* were observed in high-*PLOD3* group, which may account for the worse survival for this group. In contrast, *FAT4* was highly mutated in the *PLOD3*-low group and Zhuang et al. has demonstrated the better prognostic value of *FAT4* in CRC (43).

Immune cells play a role in the regulation of tumor cell behavior (44, 45), and accumulating evidence supports their significance in predicting outcomes and therapeutic efficacy in many cancer types (45, 46). In the present study, the infiltration levels of CD8-positive T cells and M1 macrophages were significantly lower in the *PLOD3*-high CRC group. *OBSCN (*47) was significantly associated favorable prognosis, immune-hot subtype and potentially better immunotherapeutic efficacy, which was consistent with more immune infiltration in *PLOD3*-low group. Moreover, negative correlations were observed between *PLOD3* expression and multiple immune related genes (48, 49), suggesting that *PLOD3* plays a negative role in regulating tumor immunology. Several indicators for immunotherapy response have been identified in CRC, such as TMB (50, 51) and MSI (52, 53) status. Remarkably, the expression of the *PLOD3* was negatively correlated with immuneScore and a previous study (54) in CRC indicated that CRC patients with a lower immuneScore had a poor overall survival. CRCs with higher *PLOD3* showed a lower ImmuneScore, TMB, a higher TIDE score, and patients with MSS tended to have higher *PLOD3* expression, suggesting the potential for immunotherapy resistance in CRC patients, which was validated in an immunotherapy treated cohort.

The fecal occult blood test methods are more easily accepted by patients, currently but they often suffered various interfering factors with some causes of false-negative, false-positive results, and low sensitivity rates for detecting colon polyps (55). Therefore, early, non-invasive, specific, and sensitive biomarkers are still required for screening strategies in colorectal cancer. We firstly reported the diagnostic and prognostic value of *PLOD3* in CRC and validated our finding in other transcriptome and proteome datasets. Given *PLOD3*'s good discriminating ability and its prognostic value, *PLOD3* was a promising biomarker for CRC.

Finally, we discovered, for the first time, the effect of *PLOD3* on CRC. We performed a comprehensive analysis to evaluate the functional role of *PLOD3* in CRC. The results suggest that *PLOD3* is a promising biomarker for the diagnosis and prognosis of CRC. In addition, the study evaluated the performance of *PLOD3* as a potential indicator for immunotherapy in CRC patients. These findings can facilitate the personalized treatment of CRC patients. However, the study had several limitations: The PLOD3's predictive role for immunotherapy was not validated in an immunotherapy-treated CRC cohort and further investigations are needed in the future.

In summary, *PLOD3* was identified as a promising biomarker for the diagnosis and prognosis prediction of CRC, and it could be valuable for the design of individualized treatment strategies for CRC patients.

DATA AVAILABILITY STATEMENT

The datasets analyzed during this study are available in the TCGA database (https://portal.gdc.cancer.gov) (TCGA-COAD and TCGA-READ), GEO database (https://www.ncbi.nlm.nih.gov/geo) (GSE17536, GSE39582, GSE74602, and GSE113513).

AUTHOR CONTRIBUTIONS

JS did bioinformatic analysis and wrote the manuscript. JS, XW, and YL collected the data. JS, MB, WW, CZ, and WL designed the research, organized the calculations. All authors contributed to the article and approved the submitted version.

FUNDING

This study was supported by grant from the Outstanding academic leaders plan of Shanghai (Grant No. 2018BR07) and "Qinglan Inheritance Project" Fund Project of the Second People's Hospital of Lianyungang City.

ACKNOWLEDGMENTS

The authors would like to acknowledge Mr. Sun Liangdong for his valuable help on this manuscript.

REFERENCES

1. Qaderi SM, Swartjes H, Custers J, Wilt J. Health Care Provider and Patient Preparedness for Alternative Colorectal Cancer Follow-Up; a Review. *Eur J Surg Oncol* (2020) 46(10 Pt A):1779–88. doi: 10.1016/j.ejso.2020.06.017
2. Arnold M, Sierra MS, Laversanne M, Soerjomataram I, Jemal A, Bray F. Global Patterns and Trends in Colorectal Cancer Incidence and Mortality. *Gut* (2017) 66(4):683–91. doi: 10.1136/gutjnl-2015-310912
3. Feng RM, Zong YN, Cao SM, Xu RH. Current Cancer Situation in China: Good or Bad News From The2018 Global Cancer Statistics? *Cancer Commun* (2019) 39(1):22. doi: 10.1186/s40880-019-0368-6
4. Jover E, Silvente A, Marin F, Martínez-González J, Orriols M, Martinez CM, et al. Inhibition of Enzymes Involved in Collagen Cross-Linking Reduces Vascular Smooth Muscle Cell Calcification. *FASEB J* (2018) 32:4459–69. doi: 10.1096/fj.201700653R
5. Xiong G, Lei D, Zhu J, Rychahou PG, Ren X. Prolyl-4-Hydroxylase α Subunit 2 Promotes Breast Cancer Progression and Metastasis by Regulating Collagen Deposition. *BMC Cancer* (2014) 14:1. doi: 10.1186/1471-2407-14-1
6. Salo AM, Sipil L, Sormunen R, Ruotsalainen H, Vainio S, Myllyl R. The Lysyl Hydroxylase Isoforms are Widely Expressed During Mouse Embryogenesis, But Obtain Tissue- and Cell-Specific Patterns in the Adult. *Matrix Biol* (2006) 25(8):475–83. doi: 10.1016/j.matbio.2006.08.260

7. Heikkinen J, Risteli M, Wang C, Latvala J, Rossi M, Valtavaara M, et al. Lysyl Hydroxylase 3 Is a Multifunctional Protein Possessing Collagen Glucosyltransferase Activity. *J Biol Chem* (2000) 275(46):36158–63. doi: 10.1074/jbc.M006203200
8. Reichenberger E, Olsen BR. Collagens as Organizers of Extracellular Matrix During Morphogenesis. *Semin Cell Dev Biol* (1996) 7(5):631–8. doi: 10.1006/scdb.1996.0077
9. Shrivastava A, Radziejewski C, Campbell E, Kovac L, Mcglynn M, Ryan TE, et al. An Orphan Receptor Tyrosine Kinase Family Whose Members Serve as Nonintegrin Collagen Receptors. *Mol Cell* (1997) 1(1):25–34. doi: 10.1016/S1097-2765(00)80004-0
10. Rautavuoma K, Takaluoma K, Sormunen R, Myllyharju J, Kivirikko KI, Soininen R. Premature Aggregation of Type IV Collagen and Early Lethality in Lysyl Hydroxylase 3 Null Mice. *Proc Natl Acad Sci USA* (2004) 101(39):14120–5. doi: 10.1073/pnas.0404966101
11. Salo AM, Wang C, Sipil L, Sormunen R, Vapola M, Kervinen P, et al. Lysyl Hydroxylase 3 (LH3) Modifies Proteins in the Extracellular Space, a Novel Mechanism for Matrix Remodeling. *J Cell Physiol* (2010) 207(3):644. doi: 10.1002/jcp.20596
12. Shen Q, Eun J, Lee K, Kim H, Yang H, Kim S, et al. Barrier to Autointegration Factor 1, Procollagen-Lysine, 2-Oxoglutarate 5-Dioxygenase 3, and Splicing Factor 3b Subunit 4 as Early-Stage Cancer Decision Markers and Drivers of Hepatocellular Carcinoma. *Hepatology (Baltimore Md)* (2018) 67(4):1360–77. doi: 10.1002/hep.29606
13. Tsai CK, Huang LC, Tsai WC, Huang SM, Hueng DY. Overexpression of PLOD3 Promotes Tumor Progression and Poor Prognosis in Gliomas. *Oncotarget* (2018) 9(21):15705–20. doi: 10.18632/oncotarget.24594
14. Guo T, Li B, Kang Y, Gu C, Xu C. COLGALT2 Is Overexpressed in Ovarian Cancer and Interacts With PLOD3. *Clin Trans Med* (2021) 11(3). doi: 10.1002/ctm2.370
15. Baek JH, Yun HS, Kwon GT, Kim JY, Lee CW, Song JY, et al. PLOD3 Promotes Lung Metastasis *via* Regulation of STAT3. *Cell Death Dis* (2018) 9 (12):1138. doi: 10.1038/s41419-018-1186-5.
16. Ju Q, Li X, Zhang H, Yan S, Li Y, Zhao Y. NFE2L2 Is a Potential Prognostic Biomarker and Is Correlated With Immune Infiltration in Brain Lower Grade Glioma: A Pan-Cancer Analysis. *Oxid Med Cell Longev* (2020) 2020:3580719. doi: 10.1155/2020/3580719
17. Ju Q, Li XM, Zhang H, Zhao YJ. BRCA1-Associated Protein Is a Potential Prognostic Biomarker and Is Correlated With Immune Infiltration in Liver Hepatocellular Carcinoma: A Pan-Cancer Analysis. *Front Mol Biosci* (2020) 7:573619. doi: 10.3389/fmolb.2020.573619
18. Consortium ITP-CAoWG. Pan-Cancer Analysis of Whole Genomes. *Nature* (2020) 578(7793):82–93. doi: 10.1038/s41586-020-1969-6
19. Li T, Fu J, Zeng Z, David C, Li J, Chen Q, et al. TIMER2.0 for Analysis of Tumor-Infiltrating Immune Cells. *Nucleic Acids Res* (2020) W1):W1. doi: 10.1093/nar/gkaa407
20. Newman AM, Liu CL, Green MR, Gentles AJ, Feng W, Xu Y, et al. Robust Enumeration of Cell Subsets From Tissue Expression Profiles. *Nat Methods* (2015) 12(5):453–7. doi: 10.1038/nmeth.3337
21. Jiang P, Gu S, Deng P, Fu J, Sahu A, Hu X, et al. Signatures of T Cell Dysfunction and Exclusion Predict Cancer Immunotherapy Response. *Nat Med* (2015) 24:1550–8. doi: 10.1158/2326-6074.CRICIMTEATIAACR18-B077
22. Yoshihara K, Shahmoradgoli M, Martínez E, Vegesna R, Kim H, Torres-Garcia W, et al. Inferring Tumour Purity and Stromal and Immune Cell Admixture From Expression Data. *Nat Commun* (2013) 4. doi: 10.1038/ncomms3612
23. Vasaikar SV, Peter S, Wang J, Zhang B. LinkedOmics: Analyzing Multi-Omics Data Within and Across 32 Cancer Types. *Nucleic Acids Res* (2018) 46:D956–63. doi: 10.1093/nar/gkx1090
24. Dennis G JR., Sherman BT, Hosack DA, Yang J, Gao W, Lane HC, et al. DAVID: Database for Annotation, Visualization, and Integrated Discovery. *Genome Biol* (2003) 4(5):P3. doi: 10.1186/gb-2003-4-5-p3
25. Mayakonda A, Lin DC, Assenov Y, Plass C, Koeffler HP. Maftools: Efficient and Comprehensive Analysis of Somatic Variants in Cancer. *Genome Res* (2018) 28(11):1747–56. doi: 10.1101/gr.239244.118
26. Chen MS, Lo YH, Xi C, Williams C, Shroyer N. Growth Factor Independent 1 Is a Tumor Suppressor Gene in Colorectal Cancer. *Mol Cancer Res* (2019) 17:697–708. doi: 10.1158/1541-7786.MCR-18-0666
27. Marisa L, de Reyniès A, Duval A, Selves J, Gaub MP, Vescovo L, et al. Gene Expression Classification of Colon Cancer Into Molecular Subtypes: Characterization, Validation, and Prognostic Value. *PloS Med* (2013) 10(5): e1001453. doi: 10.1371/journal.pmed.1001453
28. Riaz N, Havel JJ, Makarov V, Desrichard A, Urba WJ, Sims JS, et al. Tumor and Microenvironment Evolution During Immunotherapy With Nivolumab. *Cell* (2017) 171(4):1035–49.e19. doi: 10.1016/j.cell.2017.09.028
29. Vasaikar S, Huang C, Wang X, Petyuk VA, Savage SR, Wen B, et al.Proteogenomic Analysis of Human Colon Cancer Reveals New Therapeutic Opportunities. *Cell* (2019) 177(4):1035–49.e19. doi: 10.1016/j.cell.2019.03.030.
30. Li C, Sun YD, Yu GY, Cui JR, Zeng R. Integrated Omics of Metastatic Colorectal Cancer. *Cancer Cell* (2020) 38(5). doi: 10.1016/j.ccell.2020.08.002
31. Lyu Y, Feng C. Collagen Synthesis and Gap Junctions: The Highway for Metastasis of Ovarian Cancer. *Lab Invest* (2021) 101(5):540–2. doi: 10.1038/s41374-021-00546-0
32. Gilkes D, Bajpai S, Wong C, Chaturvedi P, Hubbi M, Wirtz D, et al. Procollagen Lysyl Hydroxylase 2 Is Essential for Hypoxia-Induced Breast Cancer Metastasis. *Mol Cancer Res: MCR* (2013) 11(5):456–66. doi: 10.1158/1541-7786.MCR-12-0629
33. Yamada Y, Kato M, Arai T, Sanada H, Uchida A, Misono S, et al. Aberrantly Expressed PLOD1 Promotes Cancer Aggressiveness in Bladder Cancer: A Potential Prognostic Marker and Therapeutic Target. *Mol Oncol* (2019) 13 (9):1898–912. doi: 10.1002/1878-0261.12532
34. Salo A, Cox H, Farndon P, Moss C, Grindulis H, Risteli M, et al. A Connective Tissue Disorder Caused by Mutations of the Lysyl Hydroxylase 3 Gene. *Am J Hum Genet* (2008) 83(4):495–503. doi: 10.1016/j.ajhg.2008.09.004
35. Qi Y, Xu R. Roles of PLODs in Collagen Synthesis and Cancer Progression. *Front Cell Dev Biol* (2018) 6:66. doi: 10.3389/fcell.2018.00066
36. Gilkes DM, Chaturvedi P, Bajpai S, Wong CC, Wei H, Pitcairn S, et al. Collagen Prolyl Hydroxylases Are Essential for Breast Cancer Metastasis. *Cancer Res* (2013) 73(11). doi: 10.1158/0008-5472.CAN-12-3963
37. Baek J, Yun H, Kwon G, Lee J, Kim J, Jo Y, et al. PLOD3 Suppression Exerts an Anti-Tumor Effect on Human Lung Cancer Cells by Modulating the PKC-Delta Signaling Pathway. *Cell Death Dis* (2019) 10(3):156. doi: 10.1038/s41419-019-1405-8
38. Sancho R, Cremona CA, Behrens A. Stem Cell and Progenitor Fate in the Mammalian Intestine: Notch and Lateral Inhibition in Homeostasis and Disease. *EMBO Rep* (2015) 16(5):571–81. doi: 10.15252/embr.201540188
39. Schmidt EM, Lamprecht S, Blaj C, Schaaf C, Krebs S, Blum H, et al. Targeting Tumor Cell Plasticity by Combined Inhibition of NOTCH and MAPK Signaling in Colon Cancer. *J Exp Med* (2018), jem.20171455. doi: 10.1084/jem.20171455
40. Jackstadt R, Hooff S, Leach JD, Cortes-Lavaud X, Sansom OJ. Epithelial NOTCH Signaling Rewires the Tumor Microenvironment of Colorectal Cancer to Drive Poor-Prognosis Subtypes and Metastasis. *Cancer Cell* (2019) 36(3):319–36.e7. doi: 10.1016/j.ccell.2019.08.003
41. Li H, Zhang J, Tong J, Chan A, To KF. Targeting the Oncogenic P53 Mutants in Colorectal Cancer and Other Solid Tumors. *Int J Mol Sci* (2019) 20 (23):5999. doi: 10.3390/ijms20235999
42. Phipps AI, Buchanan DD, Makar KW, Win AK, Baron JA, Lindor NM, et al. KRAS-Mutation Status in Relation to Colorectal Cancer Survival: The Joint Impact of Correlated Tumour Markers. *Br J Cancer* (2013) 108:1757–64. doi: 10.1038/bjc.2013.118
43. Zhuang Y, Wang H, Jiang D, Li Y, Liu P. Multi Gene Mutation Signatures in Colorectal Cancer Patients: Predict for the Diagnosis, Pathological Classification, Staging and Prognosis. *BMC Cancer* 21(1):380. doi: 10.1186/s12885-021-08108-9
44. Sahin Ozkan H, Ugurlu MU, Yumuk PF, Kaya H. Prognostic Role of Immune Markers in Triple Negative Breast Carcinoma. *Pathol Oncol Res* (2020) 26 (6):2733–45. doi: 10.1007/s12253-020-00874-4
45. Li C, Jiang P, Wei S, Xu X, Wang J.Regulatory T Cells in Tumor Microenvironment: New Mechanisms, Potential Therapeutic Strategies and Future Prospects. *Mol Cancer* (2020) 19(1):116. doi: 10.1186/s12943-020-01234-1.
46. Erin N, Grahovac J, Brozovic A, Efferth T. Tumor Microenvironment and Epithelial Mesenchymal Transition as Targets to Overcome Tumor Multidrug

Resistance. *Drug Resist Update* (2020) 53:100715. doi: 10.1016/j.drup.2020.100715
47. Liu Z, Wang L, Guo C, Liu L, Jiao D, Sun Z, et al. TTN/OBSCN 'Double-Hit' Predicts Favourable Prognosis, 'Immune-Hot' Subtype and Potentially Better Immunotherapeutic Efficacy in Colorectal Cancer. *J Cell Mol Med* (2021) 25 (7):3239–51. doi: 10.1111/jcmm.16393
48. Cohen R, Colle R, Pudlarz T, Heran M, André T. Immune Checkpoint Inhibition in Metastatic Colorectal Cancer Harboring Microsatellite Instability or Mismatch Repair Deficiency. *Cancers* (2021) 13(5):1149. doi: 10.3390/cancers13051149
49. Cohen R, Rousseau B, Vidal J, Colle R, Diaz L, André T. Immune Checkpoint Inhibition in Colorectal Cancer: Microsatellite Instability and Beyond. *Targeted Oncol* (2020) 15(1):11–24. doi: 10.1007/s11523-019-00690-0
50. Chen E, Jonker D, Loree J, Kennecke H, Berry S, Couture F, et al. Effect of Combined Immune Checkpoint Inhibition *vs* Best Supportive Care Alone in Patients With Advanced Colorectal Cancer: The Canadian Cancer Trials Group Co. *26 Study JAMA Oncol* (2020) 6(6):831–8. doi: 10.1001/jamaoncol.2020.0910
51. Schrock AB, Ouyang C, Sandhu J, Sokol E, Jin D, Ross JS, et al. Tumor Mutational Burden is Predictive of Response to Immune Checkpoint Inhibitors in MSI-High Metastatic Colorectal Cancer. *Ann Oncol* (2019) 30:1096–103. doi: 10.1093/annonc/mdz134
52. Diaz L, Marabelle A, Kim TW, Geva R, Cutsem EV, André T, et al. 386pefficacy of Pembrolizumab in Phase 2 KEYNOTE-164 and KEYNOTE-158 Studies of Microsatellite Instability High Cancers. *Ann Oncol* (2017) 28 (suppl_5). doi: 10.1093/annonc/mdx367.020
53. Prasad V, Kaestner V, Mailankody S. Cancer Drugs Approved Based on Biomarkers and 614 Not Tumor Type-FDA Approval of Pembrolizumab for Mismatch Repair-Deficient Solid 615 Cancers. *JAMA Oncol* (2018) 4(2):157–8. doi: 10.1001/jamaoncol.2017.4182
54. Wu B, Tao L, Yang D, Li W, Xu H, He Q. Development of an Immune Infiltration-Related Eight-Gene Prognostic Signature in Colorectal Cancer Microenvironment. *BioMed Res Int* (2020) 2020:2719739. doi: 10.1155/2020/2719739
55. Navarro M, Nicolas A, Ferrandez A, Lanas A, Diseases S, Blesa U, et al. Colorectal Cancer Population Screening Programs Worldwide in 2016: An Update. *World J Gastroenterol* (2017) 23:3632–42. doi: 10.3748/wjg.v23.i20.3632

Conflict of Interest: The authors declare that the research was conducted in the absence of any commercial or financial relationships that could be construed as a potential conflict of interest.

Publisher's Note: All claims expressed in this article are solely those of the authors and do not necessarily represent those of their affiliated organizations, or those of the publisher, the editors and the reviewers. Any product that may be evaluated in this article, or claim that may be made by its manufacturer, is not guaranteed or endorsed by the publisher.

Copyright © 2021 Shi, Bao, Wang, Wu, Li, Zhao and Liu. This is an open-access article distributed under the terms of the Creative Commons Attribution License (CC BY). The use, distribution or reproduction in other forums is permitted, provided the original author(s) and the copyright owner(s) are credited and that the original publication in this journal is cited, in accordance with accepted academic practice. No use, distribution or reproduction is permitted which does not comply with these terms.

frontiers in Immunology

ORIGINAL RESEARCH
published: 29 September 2021
doi: 10.3389/fimmu.2021.737076

Sanguisorbae Radix Suppresses Colorectal Tumor Growth Through PD-1/PD-L1 Blockade and Synergistic Effect With Pembrolizumab in a Humanized PD-L1-Expressing Colorectal Cancer Mouse Model

Eun-Ji Lee, Ji Hye Kim, Tae In Kim, Yeon-Ji Kim, Malk Eun Pak, Chang Hyun Jeon, Yeo Jin Park, Wei Li, Young Soo Kim, Jang-Gi Choi and Hwan-Suck Chung**

Korean Medicine Application Center, Korea Institute of Oriental Medicine, Daegu, South Korea

OPEN ACCESS

Edited by:
Udo S. Gaipl, University Hospital Erlangen, Germany

Reviewed by:
Jon Zugazagoitia, Independent Researcher, Madrid, Spain
Xuefeng Wang, Soochow University, China

***Correspondence:**
Jang-Gi Choi
jang-gichoi@kiom.re.kr
Hwan-Suck Chung
hschung@kiom.re.kr

Specialty section:
This article was submitted to Cancer Immunity and Immunotherapy, a section of the journal Frontiers in Immunology

Received: *06 July 2021*
Accepted: *13 September 2021*
Published: *29 September 2021*

Citation:
Lee E-J, Kim JH, Kim TI, Kim Y-J, Pak ME, Jeon CH, Park YJ, Li W, Kim YS, Choi J-G and Chung H-S (2021) Sanguisorbae Radix Suppresses Colorectal Tumor Growth Through PD-1/PD-L1 Blockade and Synergistic Effect With Pembrolizumab in a Humanized PD-L1-Expressing Colorectal Cancer Mouse Model. Front. Immunol. 12:737076. doi: 10.3389/fimmu.2021.737076

Immune checkpoints such as programmed death-1 (PD-1) have been proven as antitumor targets by enhancing cytotoxic T cell activity. All immune checkpoint blockades are antibody therapeutics that have large size and high affinity, as well as known immune-related side effects and low responses. To overcome the limitation of antibody therapeutics, we have explored PD-1/PD-L1 (programmed death-ligand 1) blockades in traditional oriental medicine, which has a long history but has not yet studied PD-1/PD-L1 blockades. Sanguisorbae Radix extract (SRE) blocked PD-1 and PD-L1 binding in competitive ELISA. SRE effectively inhibited the PD-1/PD-L1 interaction, thereby improving T cell receptor (TCR) signaling and the NFAT-mediated luciferase activity of T cells. SRE treatment reduced tumor growth in the humanized PD-L1 MC38 cell allograft humanized PD-1 mouse model. Additionally, the combination of SRE and pembrolizumab (anti-PD-1 antibody) suppressed tumor growth and increased infiltrated cytotoxic T cells to a greater extent did either agent alone. This study showed that SRE alone has anticancer effects *via* PD-1/PD-L1 blockade and that the combination therapy of SRE and pembrolizumab has enhanced immuno-oncologic effects.

Keywords: PD-1, PD-L1, Sanguisorbae Radix, cancer immunology, humanized PD-1 mice, tumor-infiltrating CD8⁺ T cell

INTRODUCTION

Colorectal cancer (CRC) is the third most common cancer in terms of morbidity and mortality around the world (1). The treatment of advanced CRC has applied chemotherapy, including 5-fluorouracil, oxaliplatin, and irinotecan, and targeted therapy, including bevacizumab and cetuximab, but these agents have resistance, dose-limiting side effects, and are strongly toxic to

normal cells (2, 3). As an improvement over these agents, immunotherapy has been developed as an effective treatment, increasing the strength of the immune system against malignant tumors in patients with CRC along with microsatellite types or mismatch-repair deficiency (4). In immunotherapy, immune checkpoint inhibitors (ICIs) targeting PD-1 or PD-L1 in several human cancers have recently been demonstrated. To date, six ICIs have been approved by the FDA, including pembrolizumab, nivolumab, cemiplimab, atezolizumab, avelumab, and durvalumab (5). The programmed death-1/programmed death-ligand 1 (PD-1/PD-L1) signaling axis can be important to tumor survival and development (6). The PD-L1 transmembrane protein is known to express on the surface of CRC, and its binding with PD-1 leads to the escape of cancer cells from immune-mediated destruction, thereby enhancing cancer cell growth (7). PD-1 is a crucial immune checkpoint molecule and is mainly expressed on the tumor-infiltrating T lymphocytes (TILs), including $CD4^+$ T cells (helper T cells) and $CD8^+$ T cells (cytotoxic T lymphocytes, CTLs) (8). TILs activated by the blocking of the PD-1/PD-L1 interaction release antitumor cytokines containing interleukin-2 (IL-2) and interferon (IFN)-γ, which indirectly help the immune system fight cancer cells (6). In particular, CTLs can directly induce cancer cell death by releasing lytic granules, such as the perforin (PRF) protein, which punches holes in the cancer cell membrane (9). Immunomodulatory activity according to the blocking of the PD-1/PD-L1 interaction enhances the antitumor activity of CTLs in the tumor microenvironment.

Recently, anti-PD-1 medications, such as pembrolizumab and nivolumab, in combination with chemoradiotherapy or targeted therapy has been reported to effectively inhibit the PD-1/PD-L1 interaction in CRC (10). Although these clinical therapies have the advantage of increasing survival rate in patients with CRC, their strong toxicity causes several adverse effects, they have a long half-life, and are expensive to produce (3). Use of novel supplementary therapies, including those from natural sources, is therefore imperative. Compared to clinical drugs, these are rapidly absorbed in the human body, and doses can be easily adjusted, raising the expectation of cure by enhancing patients' long-term survival rate (11). Medicinal herbs containing abundant bioactive ingredients have been utilized as CRC therapeutics to overcome the toxicity and resistance of clinical anticancer drugs (12). Previous investigations regarding the targeting of PD-1/PD-L1 have focused on antibody drugs for CRC immunotherapy but not on known traditional medicinal plants. To discover the more effective CRC immunotherapeutics, we focused on natural products to find combinatorial ICIs with potent synergistic efficacies on the PD-1/PD-L1 interaction.

Sanguisorbae Radix (SR), the dried root of *Sanguisorba officinalis*, also known as great burnet, is a traditional herbal medicine used to treat diarrhea, chronic intestinal inflammation, duodenal ulcers, and internal hemorrhage (13). Recently, multiple studies have reported its diverse pharmacological actions, including antiallergic, anti-inflammatory, antiobesity, and anticancerous (14–17). Although several studies have shown that SR extract (SRE) suppresses both *in vivo* and *in vitro* CRC growth (18, 19), to our knowledge, no literature has reported the antitumor effects of SRE on targeting the PD-1/PD-L1 signaling axis.

Ongoing screening of PD-1/PD-L1 inhibitor from herbal medicine, we found that SRE is a potent inhibitor of PD-1/PD-L1 interaction by *in vitro* competitive ELISA and cell-based luciferase assay. Additionally, we established the antitumor effect of SRE in combination with anti-PD-1 antibodies using a humanized PD-L1 MC38 CRC cell-bearing humanized PD-1 knockin mouse model. That is distinguished studies for CRC immunotherapies targeting human PD-1/PD-L1 in the animal model. Based on this investigation, we proposed a novel combination strategy to improve the effectiveness of immunotherapy by using SRE in cancer patients.

MATERIALS AND METHODS

Preparation of Plant Materials

SR was supplied by the National Development Institute of Korean Medicine (NIKOM, Gyeongsan, Korea). The dried whole plant (2.0 kg) was extracted with 5 L of 70% ethanol for 1 hour, three times. The extract was percolated with filter paper (3 mm; Whatman PLC, Kent, UK), condensed using a rotary evaporator (Buchi, Swiss), and lyophilized using a freeze dryer (Eyela, Japan). The extract powder (285.41 g; yield 14.27%; abbreviated as SRE) was dissolved in 50% dimethyl sulfoxide for stock solution (100 mg/mL) and diluted with culture medium for *in vitro* assay.

PD-1/PD-L1 Competitive ELISA

PD-1/PD-L1 competitive ELISA (#72005, BPS Bioscience, San Diego, CA, USA) was performed as per the manufacturer's protocol. As a positive control, an anti-PD-1 neutralizing antibody (#71120) was purchased from BPS Bioscience. Briefly, recombinant hPD-L1 protein (#71104, BPS Bioscience) was coated on the plates (0.32 cm^2, #3917, Corning, New York, NY, USA) at 1 μg/mL with phosphate-buffered saline (PBS, pH 7.4) and incubated overnight at 4°C. The plates were washed with PBS containing 0.05% Tween 20 (PBS-T) and blocked with PBS-T containing 2% (w/v) bovine serum albumin for 1 hour at room temperature (RT). The biotinylated hPD-1 (#71109, BPS Bioscience) of 0.5 μg/mL was added to each well and incubated for 2 hours at RT. The horseradish peroxidase (HRP)-conjugated streptavidin (#554066, BD Biosciences, San Jose, CA, USA) of 0.2 μg/mL was added to each well and incubated for 1 hour at RT. The relative chemiluminescence was measured using a SpectraMax L microplate reader (Molecular Devices, San Jose, CA, USA).

Cell Culture

Recombinant Jurkat T cells expressing human PD-1 and NFAT reporter gene (#60535, hPD-1/NFAT Jurkat T cells) and recombinant CHO-K1 cells expressing human PD-L1 and T cell receptor (TCR) activator (#60536, hPD-L1/TCR CHO-K1 cells) were purchased from BPS Bioscience. The hPD-1/NFAT

Jurkat T cells were maintained in Roswell Park Memorial Institute (RPMI) 1640 medium supplemented with 10% (v/v) heat-inactivated fetal bovine serum (FBS) and antibiotics (100 U/mL penicillin and 100 μg/mL streptomycin). The hPD-L1/TCR CHO-K1 cells were maintained in Ham's F-12 medium supplemented with 10% (v/v) heat-inactivated FBS and antibiotics. These cells were cultured in a complete medium with Geneticin (1 mg/mL) and Hygromycin B (200 μg/mL) to maintain stable cells containing genetic constructs. MC38 cells expressing human PD-L1 (hPD-L1 MC38 cells), derived from C57BL/6 murine colorectal adenocarcinoma, were purchased from Shanghai Model Organisms Center, Inc. (Shanghai, China). The hPD-L1 MC38 cells were maintained in Dulbecco's Modified Eagle Medium supplemented with 10% (v/v) heat-inactivated FBS, antibiotics, and Hygromycin B (50 μg/mL). The cells were incubated in a humidified incubator at 37°C under a 5% CO_2 atmosphere before the experiments. These solutions for cell culture were purchased from Hyclone Laboratories, Inc. (GE Healthcare Life Sciences, Chicago, IL, USA).

Cell Counting Kit-8 Assay

The cytotoxic effect of SRE was examined using CCK (#CK04, Dojindo Molecular Technologies, Inc., Rockville, MD, USA) assay. Briefly, the cells (1×10^4 cells/0.32 cm^2) were cultured in the indicated concentrations (0–400 μg/mL) of SRE at 37°C. CCK solution (10 μL) was added into each well, and the culture plates were incubated for 2 hours at 37°C. The absorbance of the formazan products in the cell culture medium was measured using a SpectraMax i3 microplate reader (Molecular Devices, San Jose, CA, USA) at 450 nm.

PD-1/PD-L1 Blockade Bioassay

PD-1/PD-L1 blockade bioassay (#J4011, Promega, Madison, WI, USA) was performed following the manufacturer's protocol. Briefly, hPD-L1/TCR CHO-K1 cells (1×10^4 cells/0.32 cm^2) as target cells were cocultured with the hPD-1/NFAT Jurkat T cells (2×10^4 cells/0.32 cm^2) as effector cells and the indicated concentrations of SRE (0–50 μg/mL) or anti-PD-1(0–0.5 μg/mL) neutralizing antibody for 24 hours at 37°C. Bio-Glo™ Assay reagent was added into each well, and the chemiluminescence of culture plates was measured using a SpectraMax L microplate reader.

Humanized PD-1 Mice

Genetically modified C57BL/6J mice that express human full-length PD-1 protein (humanized PD-1 mice) were purchased from Shanghai Model Organisms Center (Shanghai, China). Mice were granted free access to a standard diet with drinking water before the experiment. All mice were housed under specific-pathogen-free facilities of the Korea Institute of Oriental Medicine (KIOM). All mice were housed in laboratory cage rack systems maintained at a constant temperature (22 ± 1°C) and humidity (50 ± 5%) under a 12-hour dark/light cycle. All experimental procedures followed the Guidelines for the Care and Use of Laboratory Animals of the National Institutes of Health of Korea and were approved by the Institutional Animal Care and Use Committee of KIOM (approval number KIOM-D-20-073).

Isolation and Culture of Murine Splenocytes and Tumor-Infiltrating $CD8^+$ T Cells

Splenocytes were isolated from the spleens of hPD-L1 MC38 cell-bearing hPD-1 knockin mice. The single-cell suspension of splenocytes was obtained by first filtering through a 100-μm and 40-μm cell strainer (SPL Life Sciences, Pocheon, Korea) and then adding ammonium-chloride-potassium lysing buffer (Lonza, Basel, Switzerland) to remove red blood cells. Tumor-infiltrating $CD8^+$ T cells were isolated from tumor tissues of hPD-L1 MC38 cell-bearing hPD-1 knockin mice. The single-cell suspension of hPD-L1 MC38 tumor tissues was obtained by digesting the tissues with collagenase (0.5 mg/mL collagenase IV) for 1 hour at 37°C and then filtering through 100-μm and 40-μm cell strainer. The hPD-L1 MC38 tumor-infiltrating $CD8^+$ T cells was purified by immunomagnetic negative selection (#19853, STEMCELL Technologies, Inc., Vancouver, Canada). The cells were cultured in RPMI 1640 medium supplemented with 10% (v/v) heat-inactivated FBS and antibiotics.

T Cell-Mediated Killing of Cancer Cells by Coculture System

Murine lymphocytes and tumor-infiltrating $CD8^+$ T cells (1×10^6 cells/9.5 cm^2) as effector cells were activated with Dynabeads T-Activator CD3/CD28 (Life Technologies, Carlsbad, CA, USA) for 72 hours at 37°C. Murine hPD-L1 MC38 cells were stained with CellTrace™ Far Red Cell Proliferation Kit (Thermo Fisher Scientific, Waltham, MA, USA). The hPD-L1 MC38 cells (5×10^4 cells/1.9 cm^2) as target cells were treated with IFN-γ (10 ng/mL) for triggering reactive expression of PD-L1 for 24 hours at 37°C. The hPD-L1 MC38 cells were cocultured with the activated $CD8^+$ T cells (2.5×10^5 cells/1.9 cm^2) at an effector cell-to-target cell ratio of 5:1 or with splenocytes (5×10^5 cells/1.9 cm^2) at an effector cell-to-target cell ratio of 10:1 and the indicated concentrations (0–50 μg/mL) of SRE for 72 hours at 37°C. After 72 hours, the plates were washed with PBS, the remaining attached live cancer cells were stained with crystal violet solution and measured using a SpectraMax i3 microplate reader at 540 nm. The cocultured hPD-L1 MC38 cells were observed using fluorescence microscopy (Olympus, Tokyo, Japan) and analyzed using a flow cytometer (Beckman Coulter, Inc., Brea, CA, USA).

LDH Cytotoxicity Assay

The lactate dehydrogenase (LDH) liberated from the target cells *via* effector cells was measured using LDH cytotoxicity assay (#ab65393, Abcam, Cambridge, UK). Briefly, the cell culture medium was mixed with WST Substrate Mix and incubated for 30 min at RT. The reaction was stopped by adding a stop solution, and the absorbance of the formazan products was measured using a SpectraMax i3 microplate reader at 450 nm.

IL-2 Measurement Assay

The amount of IL-2 released by activated T cells in the cell coculture supernatants was measured using a sandwich ELISA

(#555148, BD Biosciences) according to the manufacturer's protocol. Briefly, an anti-mouse IL-2 monoclonal antibody was coated on the plates (0.32 cm^2, #3590, Corning) with 0.1 M sodium carbonate (pH 9.5) and incubated overnight at 4°C. The plates were washed with PBS-T and blocked with PBS containing 10% (w/v) FBS for 1 hour at RT. The biotinylated IL-2 antibody and streptavidin-HRP were added to each well and incubated for 1 hour at RT. The relative absorbance was measured using a SpectraMax i3 microplate reader at 450 nm.

PRF1 Measurement Assay

The concentrations of PRF1 released by activated T cells in the cell coculture supernatants were quantified using a sandwich ELISA (NBP3-00452, Novus Biologicals, Centennial, CO, USA) according to the manufacturer's protocol. Briefly, the standard and samples were added to the coating plates and incubated for 90 min at 37°C. The biotinylated PRF1 and HRP-streptavidin were added to each well, then incubated for 1 hour at 37°C. The relative absorbance was measured using a SpectraMax i3 microplate reader at 450 nm.

Tumor Allograft and SRE Treatment

Human PD-L1 MC38 cells (3×10^5 cells/200 μL PBS) were injected into the dorsal subcutaneous skin of C57BL/6J humanized PD-1 knockin mice. Tumor growth was monitored and tumor size was measured using digital calipers (Hi-Tech Diamond, Westmont, IL, USA), and tumor volume was calculated according to the formula (length × $width^2$)/2. The tumor volumes reached 20 mm^3 (day 10), and mice were randomized into groups of six animals per group. The vehicle (PBS) group and SRE-treated groups were orally administered 100 mg/kg and 300 mg/kg of SRE in 100 μL PBS/20 g once daily using oral zonde for 17 days, respectively. The anti-PD-1 antibody-treated group was administered 2.5 mg/kg of pembrolizumab in 100 μL PBS/20 g *via* intraperitoneal injection on days 1, 4, 8, and 15. All mice were euthanized for analysis 18 days after treatment.

Blood Biochemistry

Blood sera were collected *via* cardiac puncture of humanized PD-1 mice treated with SRE and anti-PD-1 antibodies using blood-collection tubes (#365967, BD Biosciences). The levels of AST, ALT, blood urea nitrogen (BUN), and creatinine were analyzed using biochemical analyzer XL 200 (Erba Lachema s.r.o, Mannheim, Germany).

Immunohistochemistry

For immunohistochemical analysis, the tumor tissues were fixed with 10% formalin in PBS and embedded in paraffin. The paraffin sections were incubated with a primary antibody against the CD8 (#98941, Cell Signaling Technology, Danvers, MA, USA) and PRF (#31647, Cell Signaling Technology). The tissue slides were visualized *via* DAKO EnVision kit (#K5007, DAKO, Jena, Germany). The sections were counterstained with hematoxylin. Hematoxylin-eosin stain was performed for histopathological examination of tumor tissues. Images were observed using an Olympus BX53 microscope and XC10 microscopic digital camera (Tokyo, Japan).

Statistical Analysis

The data are presented as the mean ± standard deviation and were analyzed using GraphPad Prism (GraphPad Software, Inc., La Jolla, CA, USA). The difference of mean values was analyzed by one-way ANOVA, followed by Tukey's *post hoc* test, which was used for comparisons between multiple groups, as indicated. Differences with a p-value <0.05 were considered significant. All experiments except those in the animal studies were conducted on at least three independent occasions.

RESULTS

SRE Blockade of PD-1/PD-L1 Interaction

To investigate the effect of SRE on PD-1/PD-L1 blockade, we experimented with competitive PD-1/PD-L1 ELISA-binding assays. The results showed that SRE blocked the binding of PD-1 to PD-L1 in a dose-dependent manner (**Figure 1A**). In controls, anti-PD-1 antibodies also inhibited PD-1/PD-L1 interaction in a concentration-dependent manner (**Figure 1B**). The 50% inhibitory concentration (IC_{50}) values of SRE and anti-PD-1 antibodies were 50.10 ± 15.14 μg/mL and 1.49 ± 20.59 μg/mL, respectively.

SRE Blockade of PD-1/PD-L1 in Luciferase Assay

To elucidate the effect of SRE on TCR activation, we conducted coculture systems using human PD-1-expressing Jurkat T cells that expressed NFAT-derived luciferase reporter (hPD-1/NFAT Jurkat cells) and human PD-L1-expressing aAPC/CHO-K1 cells designed to activate cognate TCR (hPD-L1/TCR CHO-K1 cells). The cell culture model was established to evaluate the effect of PD-1/PD-L1 blockade (20). To examine the cytotoxic effects of SRE, hPD-1 effector cells and hPD-L1/TCR CHO-K1 cells were treated with the indicated concentration (0–50 μg/mL) of SRE for 24 hours. SRE had no cytotoxic effect on cells up to the concentration of 50 μg/mL (**Figures 2A, B**). The 50% cytotoxic concentration (CC_{50}) values of SRE on the hPD-1/NFAT Jurkat cells and hPD-L1/TCR CHO-K1 cells for 24 hours were 97.03 ± 11.51 μg/mL and 139.45 ± 11.49 μg/mL, respectively. The effect of SRE in coculture cell model systems using a PD-1/PD-L1 blockade bioassay was examined. The 50% effective concentration (EC_{50}) values of SRE and anti-PD-1 antibodies were 4.974 ± 0.04 μg/mL and 0.239 ± 0.08 μg/mL, respectively (**Figures 2C, D**). These findings suggest that SRE effectively inhibited the PD-1/PD-L1 interaction, thereby improving TCR signaling and NFAT-mediated luciferase activity of T cells.

Enhancement of T Cell-Mediated Killing of Cancer Cells by SRE Blockade of PD-1/PD-L1

We hypothesized that SRE induces antitumor responses to blockade PD-1/PD-L1, as T cell activation by medicinal herb extracts has previously been reported (20). To confirm the cytotoxicity of SRE against murine CRC hPD-L1 MC38 cells and hPD-L1 MC38 cell-bearing hPD-1 mice-isolated splenocytes,

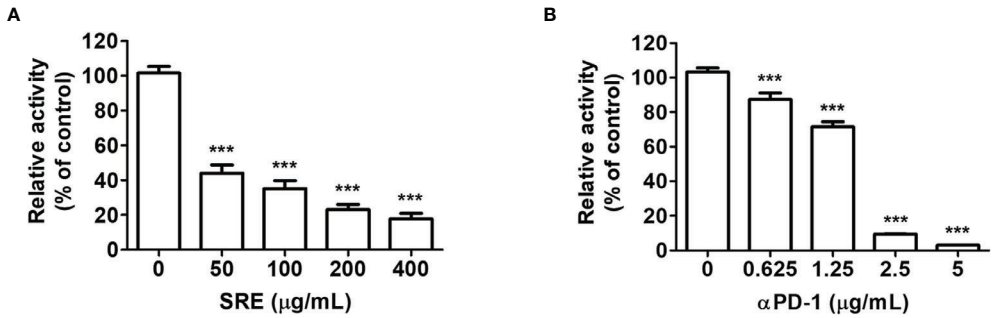

FIGURE 1 | Sanguisorbae Radix extract (SRE) blockade of programmed death-1/programmed death-1 ligand (PD-1/PD-L1) interaction using competitive ELISA. The competitive ELISA was performed using the PD-1/PD-L1 inhibitor screening assay kit. The indicated concentrations of SRE **(A)** and anti-PD-1 antibodies (αPD-1) **(B)** were treated on plates coated with PD-L1, then incubated with biotin-labeled PD-1. Data are presented as the mean ± SD. ***$p < 0.001$ compared to the control.

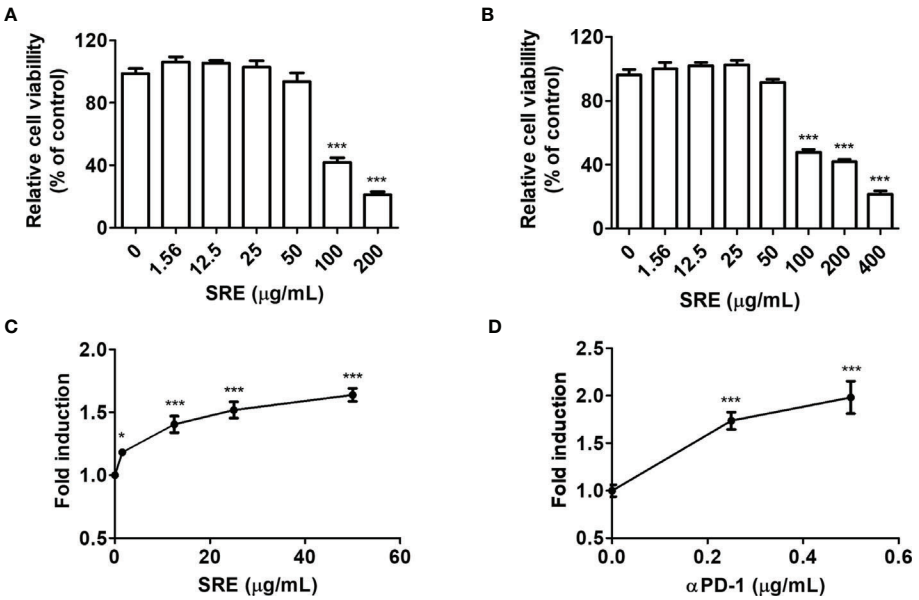

FIGURE 2 | SRE blockade of PD-1/PD-L1 interaction in coculture cell-based luciferase assay. **(A, B)** Cytotoxicity assay performed using Cell Counting Kit-8 (CCK) assay. The hPD-1/NFAT Jurkat T cells **(A)** and hPD-L1/TCR CHO-K1 cells **(B)** after treatment with SRE for 24 hours. **(C, D)** The PD-1/PD-L1 blockade bioassay was performed using the Bio-Glo™ luciferase assay system. After addition of hPD-1/NFAT Jurkat T cells and SRE **(C)** and anti-PD-1 antibodies (αPD-1) **(D)**, hPD-L1/TCR CHO-K1 cells were seeded for 20 hours. Data are presented as the mean ± SD. *$p < 0.05$ and ***$p < 0.001$ compared to the control.

cells were incubated with various concentrations of SRE for 72 hours. SRE had no cytotoxic effect on hPD-L1 MC38 cells up to the concentration of 50 μg/mL (**Figure 3A**). CC_{50} concentrations of SRE on these cells were 114.94 ± 14.09 μg/mL. SRE increased splenocyte viability dose-dependently, suggesting that SRE can improve immune cell function (**Figure 3B**).

To elucidate whether T cells mediate SRE's antitumor effect, coculture systems were conducted; hPD-1 splenocytes were used as effector cells, and hPD-L1 MC38 cancer cells known to express PD-L1 were used as target cells (21). At an effector cell-to-target cell ratio of 10:1, the cytotoxicity of hPD-L1 MC38 cells cocultured with hPD-1 splenocytes was gradually increased concentration-dependently (**Figures 3C, D**). CC_{50} concentrations of SRE on the hPD-L1 MC38 cells for 72 hours were 33.25 ± 7.20 μg/mL (**Figure 3C**). Moreover, released IL-2 increased dose-dependently, suggesting that T cells activated by SRE secrete IL-2 (**Figure 3E**). These results imply that SRE efficiently improved T cell immune function by blockading the PD-1/PD-L1 immune checkpoint pathway.

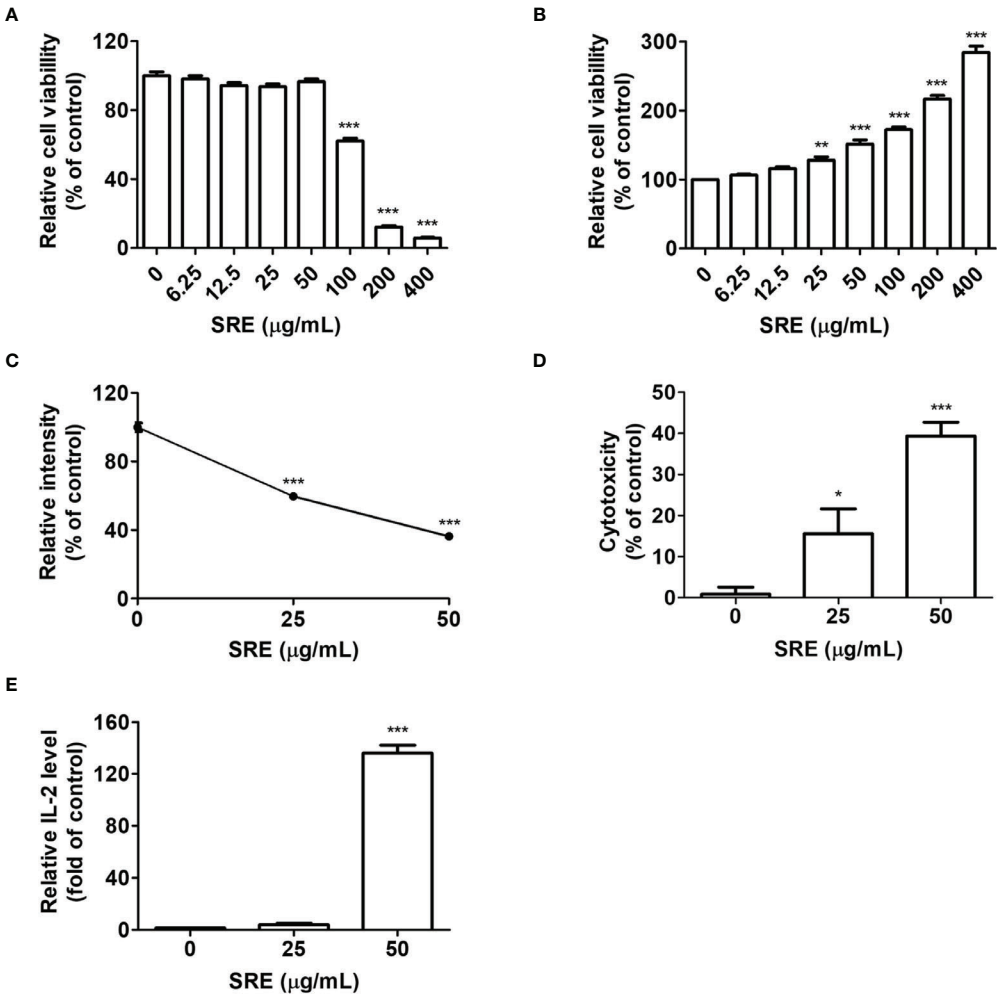

FIGURE 3 | SRE-induced activation of T cells and cytotoxic effect of T cell-mediated cancer cells. **(A, B)** The cell viability was performed using the CCK-8 assay. Splenocytes were isolated from hPD-L1 MC38 cell-bearing hPD-1 knockin mice. Murine CRC hPD-L1 MC38 cells **(A)** and hPD-1 mice splenocytes **(B)** were treated with SRE for 72 hours. **(C)** Cocultured hPD-L1 MC38 cell viability tested by crystal violet staining; **(D)** Lactate dehydrogenase (LDH) released by damaged cells, detected *via* LDH cytotoxicity assay; **(E)** Relative interleukin-2 (IL-2) level, determined using the mouse IL-2 ELISA set. Data are presented as the mean ± SD. $^{*}p < 0.05$, $^{**}p < 0.01$, and $^{***}p < 0.001$ compared to the control.

SRE Activation of hPD-1^{+} Tumor-Infiltrating CD8^{+} T Cells From hPD-L1 MC38 Tumor Tissues

We confirmed that SRE suppressed hPD-L1 MC38 tumor growth in both *in vitro* and *in vivo* models by activating hPD-1 T cells. The additional delineation of the anticancer effect of tumor-infiltrating CD8^{+} T cells based on T cell activation by SRE treatment in CRC can also be targeted by immunotherapy. To further examine the cytotoxic role of tumor-infiltrating CD8^{+} T cells by SRE treatment, coculture systems were conducted using hPD-L1 MC38 cell-bearing hPD-1 mice-isolated CD8^{+} T cells as effector cells and hPD-L1 MC38 cancer cells as target cells. At an effector cell-to-target cell ratio of 5:1, the cytotoxicity of hPD-L1 MC38 cells cocultured with hPD-1 CD8^{+} T cells was gradually increased concentration-dependently (**Figure 4A**). CC_{50} concentrations of SRE on the hPD-L1 MC38 cells for 72 hours were 42.14 ± 8.17 μg/mL. Additionally, proliferation of hPD-L1 MC38 cells (labeled with CellTrace^{TM} Far Red) was markedly reduced by SRE treatment (**Figures 4B, C**). Lactate dehydrogenase (LDH) release from the hPD-L1 MC38 cells, detected with use of LDH cytotoxicity assay, increased dose-dependently (**Figure 4D**). The released perforin 1 (PRF1) levels increased dose-dependently, suggesting that CD8^{+} T cells activated by SRE secrete PRF1 (**Figure 4E**). With the results of the effector cell-to-target cell coculture tests, this indicates that SRE efficiently enhanced tumor-infiltrating CD8^{+} T cell activation *via* blockade of PD-1/PD-L1 interaction in the CRC tumor microenvironment.

Antitumor Effect of SRE in hPD-L1 MC38 Tumor-Bearing Humanized PD-1 Mouse Model

We examined whether SRE could increase inhibition of tumor growth induced by activated T cells on the hPD-L1 MC38 cell-

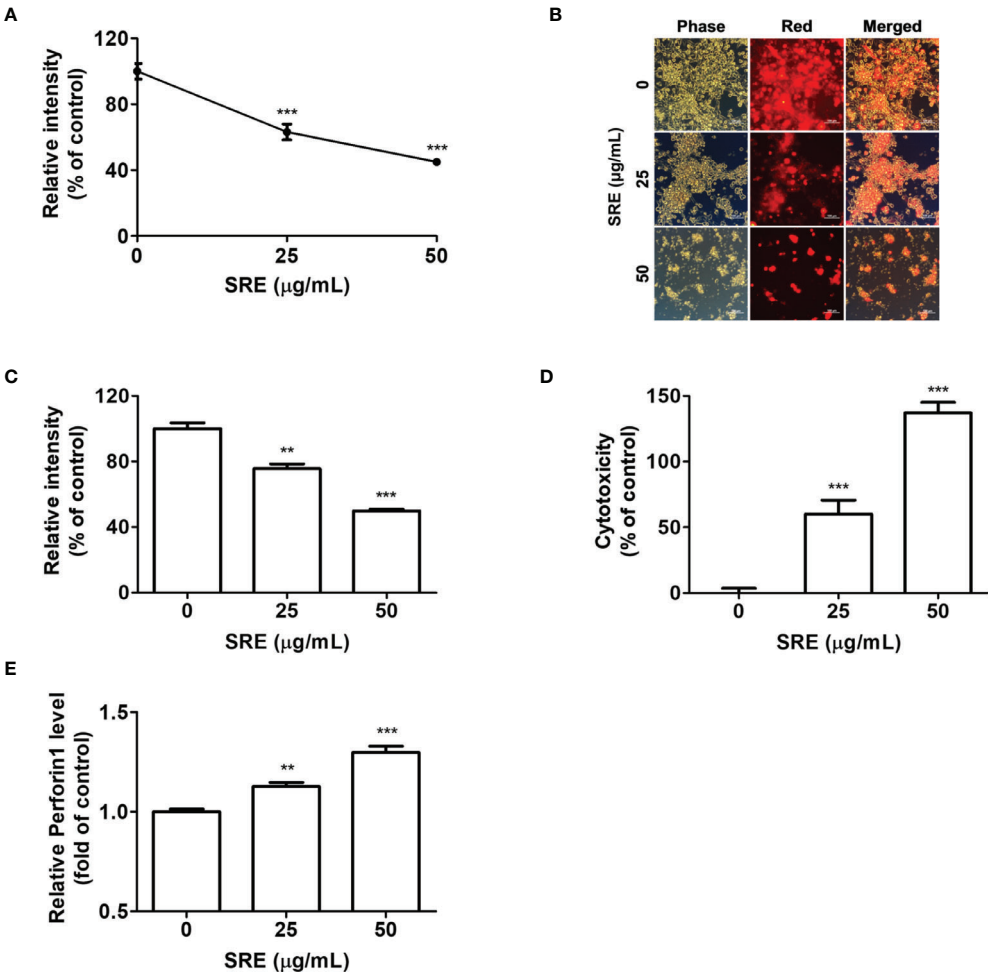

FIGURE 4 | SRE elevated the activation of hPD-1$^+$ CD8$^+$ T cells and the CD8$^+$ T cell-mediated killing effect on hPD-L1 MC38 cancer. **(A)** Cocultured hPD-L1 MC38 cell viability, tested by crystal violet staining. Cocultured hPD-L1 MC38 cells detected with fluorescence microscopy (× 200) **(B)** and determined by fluorescent-activated cell sorting analysis **(C)**. **(D)** LDH released from damaged cells; **(E)** Relative perforin 1 (PRF1) level, determined with use of the mouse PRF1 ELISA kit. Data are presented as the mean ± SD. $^{**}p < 0.01$ and $^{***}p < 0.001$ compared to the vehicle group.

bearing humanized PD-1 knockin mouse model. The hPD-L1 MC38 murine CRC cells were injected into the allograft mice model. After 10 days, tumor volumes reached 20 mm^3 and mice were randomized into groups of six animals per group to investigate the antitumor effect *in vivo*, of treatment with SRE and anti-PD-1 antibodies. SRE significantly inhibited hPD-L1 MC38 allograft tumor growth in a dose-dependent manner without affecting body weight, as observed by decreased tumor volume and weight (**Figures 5A–E**). Notably, the combination of SRE and anti-PD-1 antibodies synergistically suppressed tumor growth to a greater extent than did either agent alone. SRE and anti-PD-1 antibodies did not change aspartate aminotransferase (AST), alanine aminotransferase (ALT), BUN, or creatinine levels in mice serum (**Table 1**).

Immunohistochemistry staining showed that SRE and anti-PD-1 antibodies increased CD8 (a marker of CD8$^+$ T cells) and PRF1 granule exocytosis involved in cytotoxic T cell-mediated tumor cell death in the tumor tissues (**Figure 5F**). These investigations demonstrated that the combination of SRE and anti-PD-1 antibodies successfully suppressed tumor growth by improving CD8$^+$ T cell infiltration with antitumor immunity in the humanized PD-1 mouse model.

DISCUSSION

Research into antitumor immunity through immune checkpoint blockades with an anti-PD-1/PD-L1 interaction for the treatment of patients with CRC is notable (7). Some CRCs are characterized by advanced/metastatic solid malignancies, TIL enrichment, and upregulated PD-L1 expression within the tumor microenvironment (22). Pembrolizumab, as an anti-PD-1, has been approved for immunotherapy of CRC with microsatellite instability or mismatch-repair deficiency (23). However, clinical agents have a large molecular weight, which is slowly absorbed, and cause various side effects (3). To overcome the shortcomings of

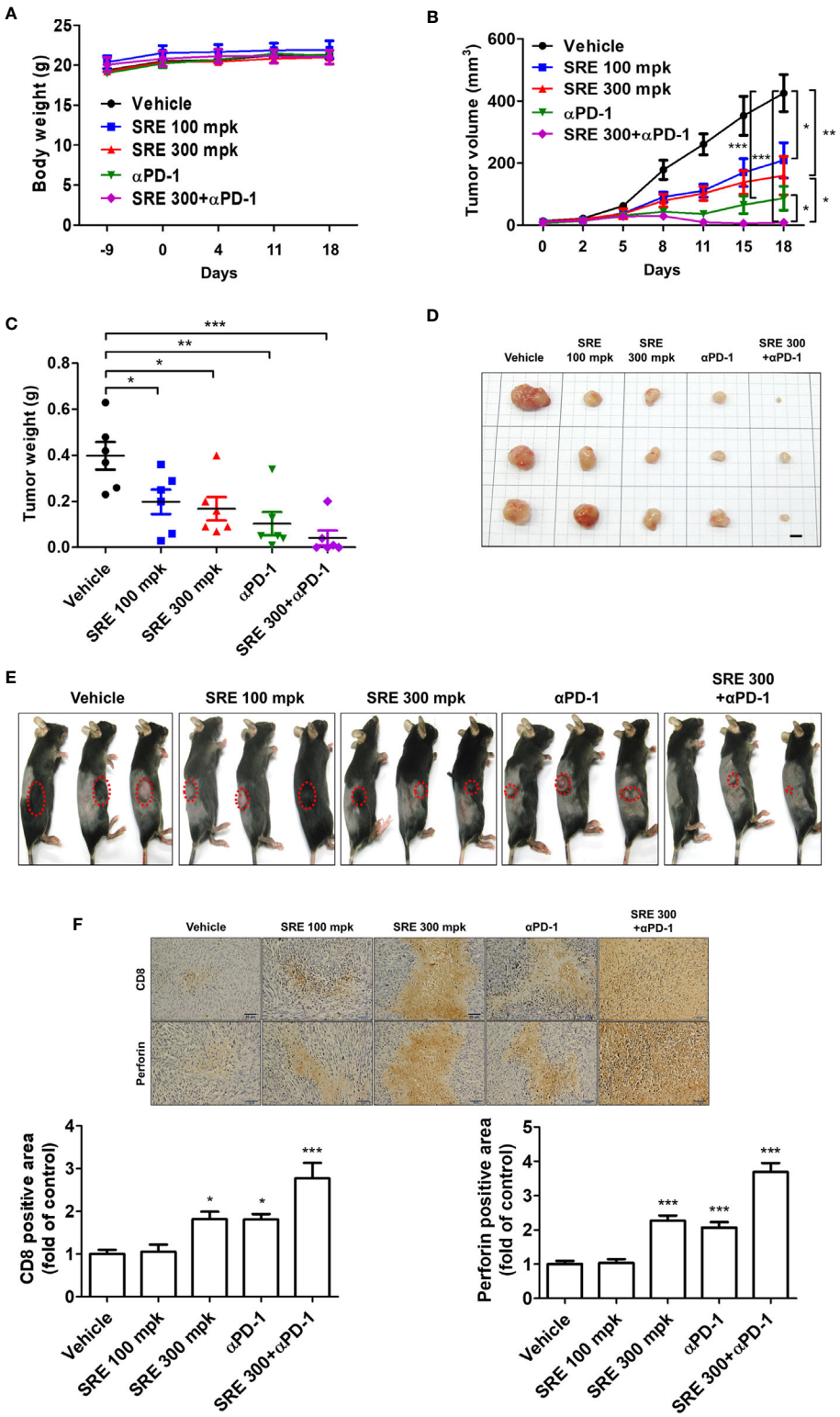

FIGURE 5 | Sanguisorbae Radix extract reduced tumor growth in the hPD-L1 MC38 cell allograft hPD-1 mouse model. **(A)** Body weight (grams); **(B)** Tumor volume after 18 days; **(C)** Tumor weight after 18 days; **(D)** Images of tumor tissues (bar indicates 5 mm); **(E)** hPD-L1 MC38 tumor-bearing mice 18 days after treatment; **(F)** Representative microscopic images (×400) of CD8 and PRF1-positive area of tumor tissues calculated using immunohistochemical analysis. Data are presented as mean ± standard deviation. $^{*}p < 0.05$, $^{**}p < 0.01$, and $^{***}p < 0.001$ compared with the vehicle group.

TABLE 1 | AST, ALT, BUN, and creatinine levels in SRE-treated mice serum.

	AST (IU/L)	ALT (IU/L)	BUN (mg/dL)	Creatinine (mg/dL)
Vehicle	97.66 ± 9.33	28.00 ± 9.03	32.33 ± 1.41	0.1
SRE 100 mpk	90.00 ± 30.54	19.33 ± 3.93	28.66 ± 2.50	0.1
SRE 300 mpk	74.00 ± 23.01	20.66 ± 4.67	35.66 ± 3.75	0.1
αPD-1	71.33 ± 16.47	23.33 ± 5.88	35.40 ± 5.60	0.1
SRE 300+αPD-1	82.00 ± 32.56	25.33 ± 8.71	30.53 ± 4.78	0.1

Values are presented as the mean ± SD of six mice. ALT, alanine aminotransferase; AST, aspartate aminotransferase; BUN, blood urea nitrogen.

clinical therapies in the CRC treatment, we tried to use an oriental medicinal herb, SRE, which has a low molecular weight.

Although several reports have shown SRE use in treatment of human CRC, breast cancer, and prostate cancer (18, 24, 25), SRE's anticancer activities *via* mediation of T cells had not been defined. This study demonstrated the experimental evidence on antitumor immunity by improving T cell activity with SRE. In the present study, we discovered the ability of SRE to enhance T cell functionality *via* PD-1/PD-L1 interaction blockade using PD-1/PD-L1 ELISA-binding assay and PD-1/PD-L1 blockade bioassay. Additionally, we found a difference, in that SRE activates tumor-infiltrating $CD8^+$ T cells and kills CRC cells in the tumor microenvironment. In particular, this study confirmed that $CD8^+$ T cells activated by SRE secrete PRF1 to kill CRC cells.

Nontoxic dose of SRE in splenocyte-tumor coculture systems, we tested the cytotoxicity of SRE in hPD-L1 MC38 cells and humanized PD-1 mice-isolated splenocytes (**Figure 3**). In line with a previous study (26), SRE over 100 μg/mL is cytotoxic to a liver cancer cell line; however, 50 μg/mL of SRE has a 40% cytotoxicity and extremely released IL-2 in splenocyte-tumor coculture systems. Interestingly, the more an SRE dose increases up to 400 μg/mL, the more proliferation of splenocytes increases and tumor proliferation decreases. There are reports of SRE inducing immunomodulatory effects including inflammatory responses and cytokine production (27, 28). Our findings suggest that SRE would not only have a cytotoxic effect on CRC cells but also promote T cell immunity and have anticancer effects *via* inhibition of PD-1/PD-L1 interaction in splenocyte-tumor coculture systems.

The humanized immune checkpoint mice are carefully designed as immuno-oncology mouse models for reliable *in vivo* evaluation and validation of checkpoint blockers drugs and their combination with other antitumor drugs (29). According to previous studies, although there are structural similarities between human and mouse PD-L1 proteins, there are significant differences in the druggability of these two proteins (30). In line with reported results, our study showed that small molecules, peptides, and some human anti-PD-L1 antibodies bound to human PD-L1, but not to mouse PD-L1. In addition, there were no effects observed in MC38 tumor-bearing immunocompetent mice treated with human anti-PD-L1 antibodies. Moreover, the MC38 used *in vivo* in this study is derived from tumors induced by carcinogen and established in C57BL/6 mice and represents a microsatellite-unstable CRC cell line (31). We have previously reported the PD-1/PD-L1-inhibiting abilities of medicinal herbs including *Salvia plebeia* alone and *Rubus coreanus* alone *in vivo* (20, 32). Here, we found that SRE in combination with anti-PD-1 antibodies *in vivo* is a potent PD-1/PD-L1 inhibitor. We assessed the synergistic effect of the combination of SRE and anti-PD-1 antibodies using humanized PD-1 knockin mice and humanized PD-L1 MC38 tumor cells and successfully established a CRC immunotherapy. As shown in **Figure 5**, the antitumor effect of SRE was higher in a dose of 300 mg/kg group than in a 100 mg/kg group; the effect of SRE in combination with anti-PD-1 antibodies was considerably greater than 300 mg/kg SRE alone or anti-PD-1 antibodies alone. In addition, combination of SRE and anti-PD-1 antibodies remarkably increased infiltration of $CD8^+$ T cells in tumor tissues more than either 300 mg/kg SRE alone or anti-PD-1 antibodies alone, as well as increasingly released PRF1 granules of tumor-infiltrating $CD8^+$ T cells *via* PD-1/PD-L1 blockade in the tumor microenvironment. The combination of SRE and anti-PD-1 antibodies is thus expected to be a workhorse for preclinical investigational studies in patients with CRC, supporting the validity of cancer immunotherapies.

Biochemical analysis also confirmed that the indicated dosages of SRE and anti-PD-1 antibodies have no significant toxic effect on the liver or kidneys in humanized PD-1 mice with humanized PD-L1 MC38 tumors (**Table 1**). In a Mongolian gerbil, daily oral administration of SRE at a dose of 400 mg/kg for 28 days, no gross histological changes were found (33). Moreover, the no changes were found in the relative weights of liver and kidney in the gerbil, or in AST and ALT in high-fat–diet-induced obese C57BL/6J mice after 8 weeks' treatment with 200 mg/kg/day SRE extracted with 50% ethanol (34). In the current study, 100 mg/kg/day of SRE in mice is equivalent to 480 mg/kg/day for a 60 kg human. *S. officinalis* is safe enough to be approved for use as a food ingredient, and the root of the plant, SR, is considered nontoxic.

This study provides evidence that SRE enhanced the potential antitumor immunologic response by regulating the PD-1/PD-L1 axis for the treatment of CRC. Additionally, it established that SRE in combination with anti-PD-1 antibodies has strong $CD8^+$ T cell-mediated antitumor activity in an hPD-L1 MC38 cell-bearing hPD-1 knockin mouse model. Recently, because ICIs alone have shown limited efficacy in patients with CRC, combinations of ICIs with other agents, such as anti-PD-L1 antibodies or chemotherapy, are being tested in patients with CRC in clinical studies (10); however, applied combination therapies have several adverse effects, including toxicity, resistance, and side effects (3). To improve upon the clinical combination therapies, we used a combination of clinical antibodies with SRE, with easy dose adjustment and fast absorption in a humanized mice model.

Among the ingredient compounds of SR, several phenolic compounds have been reported as antitumor agents (19). Several other chemical constituents, including tannin, triterpenoid, flavonoids, and triterpene glycoside, have been found in *S.*

officinalis roots (35–37). It is not clear which components are responsible for PD-1/PD-L1 blockade and the subsequent antitumor effect of CRC. Further studies are needed to elucidate, which molecules from SR inhibit the PD-1/PD-L1 interaction.

CONCLUSIONS

We demonstrated that SRE inhibits PD-1/PD-L1 interaction and suppresses growth of CRC cells by enhancing T cell functional activity. In addition, we established that SRE in combination with anti-PD-1 antibodies significantly reduces CRC tumor growth *via* tumor-infiltrating $CD8^+$ T cell activities in an hPD-L1 MC38 cell-bearing hPD-1 knockin mouse model. From these results, we suggest that SRE is a novel inhibitor of PD-1/PD-L1 interaction and, in combination with antibody drugs, may provide a new strategy for weakening CRC mortality as an antitumor immunity drug.

DATA AVAILABILITY STATEMENT

The original contributions presented in the study are included in the article/supplementary material. Further inquiries can be directed to the corresponding authors.

ETHICS STATEMENT

The animal study was conducted according to the guidelines of the Institutional Animal Care and Use Committee (IACUC) of the Korea Institute of Oriental Medicine (KIOM), and approved by the IACUC of the KIOM (approval number: KIOM-D-20-073).

AUTHOR CONTRIBUTIONS

E-JL, J-GC, and H-SC designed the study, conducted the experiments and wrote the manuscript. JK, TK, Y-JK, MP, CJ, YP, WL, and YK performed the experiments. H-SC supervised the research and wrote the manuscript. All authors contributed to the article and approved the submitted version.

FUNDING

This research was supported by the Korea Institute of Oriental Medicine (KIOM) Grant number KSN2021230 provided by the Ministry of Science and ICT, Republic of Korea.

REFERENCES

1. Siegel RL, Miller KD, Fuchs HE, Jemal A. Cancer Statistics, 2021. *CA Cancer J Clin* (2021) 71(1):7–33. doi: 10.3322/caac.21654
2. Calvo E, Cortés J, González-Cao M, Rodríguez J, Aramendía JM, Fernández-Hidalgo O, et al. Combined Irinotecan, Oxaliplatin and 5-Fluorouracil in Patients With Advanced Colorectal Cancer. A Feasibility Pilot Study. *Oncology* (2002) 63(3):254–65. doi: 10.1159/000065474
3. Golshani G, Zhang Y. Advances in Immunotherapy for Colorectal Cancer: A Review. *Therap Adv Gastroenterol* (2020) 13:1756284820917527. doi: 10.1177/1756284820917527
4. Tolba MF. Revolutionizing the Landscape of Colorectal Cancer Treatment: The Potential Role of Immune Checkpoint Inhibitors. *Int J Cancer* (2020) 147 (11):2996–3006. doi: 10.1002/ijc.33056
5. Vaddepally RK, Kharel P, Pandey R, Garje R, Chandra AB. Review of Indications of FDA-Approved Immune Checkpoint Inhibitors Per NCCN Guidelines With the Level of Evidence. *Cancers (Basel)* (2020) 12(3):738. doi: 10.3390/cancers12030738
6. Jiang X, Wang J, Deng X, Xiong F, Ge J, Xiang B, et al. Role of the Tumor Microenvironment in PD-L1/PD-1-Mediated Tumor Immune Escape. *Mol Cancer* (2019) 18(1):10. doi: 10.1186/s12943-018-0928-4
7. Yaghoubi N, Soltani A, Ghazvini K, Hassanian SM, Hashemy SI. PD-1/ PD-L1 Blockade as a Novel Treatment for Colorectal Cancer. *BioMed Pharmacother* (2019) 110:312–8. doi: 10.1016/j.biopha.2018.11.105
8. Pardoll DM. The Blockade of Immune Checkpoints in Cancer Immunotherapy. *Nat Rev Cancer* (2012) 12(4):252–64. doi: 10.1038/nrc3239
9. Martínez-Lostao L, Anel A, Pardo J. How Do Cytotoxic Lymphocytes Kill Cancer Cells? *Clin Cancer Res* (2015) 21(22):5047–56. doi: 10.1158/1078-0432.Ccr-15-0685
10. Lumish MA, Cercek A. Immunotherapy for the Treatment of Colorectal Cancer. *J Surg Oncol* (2021) 123(3):760–74. doi: 10.1002/jso.26357
11. Moody R, Wilson K, Jaworowski A, Plebanski M. Natural Compounds With Potential to Modulate Cancer Therapies and Self-Reactive Immune Cells. *Cancers (Basel)* (2020) 12(3):673. doi: 10.3390/cancers12030673
12. Aiello P, Sharghi M, Mansourkhani SM, Ardekan AP, Jouybari L, Daraei N, et al. Medicinal Plants in the Prevention and Treatment of Colon Cancer. *Oxid Med Cell Longev* (2019) 2019:2075614. doi: 10.1155/2019/2075614
13. Zhao Z, He X, Zhang Q, Wei X, Huang L, Fang JC, et al. Traditional Uses, Chemical Constituents and Biological Activities of Plants From the Genus Sanguisorba L. *Am J Chin Med* (2017) 45(2):199–224. doi: 10.1142/s0192415x17500136
14. Park KH, Koh D, Kim K, Park J, Lim Y. Antiallergic Activity of a Disaccharide Isolated From Sanguisorba Officinalis. *Phytother Res* (2004) 18(8):658–62. doi: 10.1002/ptr.1545
15. Seo CS, Jeong SJ, Yoo SR, Lee NR, Shin HK. Quantitative Analysis and *In Vitro* Anti-Inflammatory Effects of Gallic Acid, Ellagic Acid, and Quercetin From Radix Sanguisorbae. *Pharmacogn Mag* (2016) 12(46):104–8. doi: 10.4103/0973-1296.177908
16. Im SH, Wang Z, Lim SS, Lee OH, Kang IJ. Bioactivity-Guided Isolation and Identification of Anti-Adipogenic Compounds From Sanguisorba Officinalis. *Pharm Biol* (2017) 55(1):2057–64. doi: 10.1080/13880209.2017.1357736
17. Wu Z, Sun H, Li J, Ma C, Zhao S, Guo Z, et al. A Polysaccharide From Sanguisorbae Radix Induces Caspase-Dependent Apoptosis in Human Leukemia HL-60 Cells. *Int J Biol Macromol* (2014) 70:615–20. doi: 10.1016/j.ijbiomac.2014.06.062
18. Bai C, Sun Y, Pan X, Yang J, Li X, Wu A, et al. Antitumor Effects of Trimethylellagic Acid Isolated From Sanguisorba Officinalis L. @ on Colorectal Cancer *via* Angiogenesis Inhibition and Apoptosis Induction. *Front Pharmacol* (2019) 10:1646. doi: 10.3389/fphar.2019.01646
19. Liu MP, Liao M, Dai C, Chen JF, Yang CJ, Liu M, et al. Sanguisorba Officinalis L Synergistically Enhanced 5-Fluorouracil Cytotoxicity in Colorectal Cancer Cells by Promoting a Reactive Oxygen Species-Mediated, Mitochondria-Caspase-Dependent Apoptotic Pathway. *Sci Rep* (2016) 6:34245. doi: 10.1038/srep34245
20. Choi JG, Kim YS, Kim JH, Kim TI, Li W, Oh TW, et al. Anticancer Effect of Salvia Plebeia and Its Active Compound by Improving T-Cell Activity *via* Blockade of PD-1/PD-L1 Interaction in Humanized PD-1 Mouse Model. *Front Immunol* (2020) 11:598556. doi: 10.3389/fimmu.2020.598556
21. Shi G, Yang Q, Zhang Y, Jiang Q, Lin Y, Yang S, et al. Modulating the Tumor Microenvironment *via* Oncolytic Viruses and CSF-1r Inhibition Synergistically Enhances Anti-PD-1 Immunotherapy. *Mol Ther* (2019) 27 (1):244–60. doi: 10.1016/j.ymthe.2018.11.010
22. Rosenbaum MW, Bledsoe JR, Morales-Oyarvide V, Huynh TG, Mino-Kenudson M. PD-L1 Expression in Colorectal Cancer is Associated With Microsatellite Instability, BRAF Mutation, Medullary Morphology and

Cytotoxic Tumor-Infiltrating Lymphocytes. *Mod Pathol* (2016) 29(9):1104–12. doi: 10.1038/modpathol.2016.95
23. Yu G, Wu Y, Wang W, Xu J, Lv X, Cao X, et al. Low-Dose Decitabine Enhances the Effect of PD-1 Blockade in Colorectal Cancer With Microsatellite Stability by Re-Modulating the Tumor Microenvironment. *Cell Mol Immunol* (2019) 16(4):401–9. doi: 10.1038/s41423-018-0026-y
24. Wang N, Muhetaer G, Zhang X, Yang B, Wang C, Zhang Y, et al. Sanguisorba Officinalis L. Suppresses Triple-Negative Breast Cancer Metastasis by Inhibiting Late-Phase Autophagy *via* Hif-1α/Caveolin-1 Signaling. *Front Pharmacol* (2020) 11:591400. doi: 10.3389/fphar.2020.591400
25. Choi ES, Kim JS, Kwon KH, Kim HS, Cho NP, Cho SD. Methanol Extract of Sanguisorba Officinalis L. With Cytotoxic Activity Against PC3 Human Prostate Cancer Cells. *Mol Med Rep* (2012) 6(3):670–4. doi: 10.3892/mmr.2012.949
26. Jiang N, Li H, Sun Y, Zeng J, Yang F, Kantawong F, et al. Network Pharmacology and Pharmacological Evaluation Reveals the Mechanism of the Sanguisorba Officinalis in Suppressing Hepatocellular Carcinoma. *Front Pharmacol* (2021) 12:618522. doi: 10.3389/fphar.2021.618522
27. Chen X, Li B, Gao Y, Ji J, Wu Z, Chen S. Saponins From Sanguisorba Officinalis Improve Hematopoiesis by Promoting Survival Through FAK and Erk1/2 Activation and Modulating Cytokine Production in Bone Marrow. *Front Pharmacol* (2017) 8:130. doi: 10.3389/fphar.2017.00130
28. Lee YE, Kim S, Jung WJ, Lee HS, Kim MY. Immunomodulatory Effects of ZYM-201 on LPS-Stimulated B Cells. *Immune Netw* (2014) 14(5):260–4. doi: 10.4110/in.2014.14.5.260
29. Sanmamed MF, Chester C, Melero I, Kohrt H. Defining the Optimal Murine Models to Investigate Immune Checkpoint Blockers and Their Combination With Other Immunotherapies. *Ann Oncol* (2016) 27(7):1190–8. doi: 10.1093/annonc/mdw041
30. Magiera-Mularz K, Kocik J, Musielak B, Plewka J, Sala D, Machula M, et al. Human and Mouse PD-L1: Similar Molecular Structure, But Different Druggability Profiles. *iScience* (2021) 24(1):101960. doi: 10.1016/j.isci.2020.101960
31. Efremova M, Rieder D, Klepsch V, Charoentong P, Finotello F, Hackl H, et al. Targeting Immune Checkpoints Potentiates Immunoediting and Changes the Dynamics of Tumor Evolution. *Nat Commun* (2018) 9(1):32. doi: 10.1038/s41467-017-02424-0
32. Kim JH, Kim YS, Kim TI, Li W, Mun JG, Jeon HD, et al. Unripe Black Raspberry (Rubus Coreanus Miquel) Extract and Its Constitute, Ellagic Acid Induces T Cell Activation and Antitumor Immunity by Blocking PD-1/PD-L1 Interaction. *Foods* (2020) 9(11):1590. doi: 10.3390/foods9111590
33. Lee H-A, Hong S, Oh H-G, Park S-H, Kim Y-C, Park H, et al. Antibacterial Activity of Sanguisorba Officinalis Against Helicobacter Pylori. *Lab Anim Res* (2010) 26(3):257–63. doi: 10.5625/lar.2010.26.3.257
34. Jung DW, Lee OH, Kang IJ. Sanguisorba Officinalis L. Extracts Exert Antiobesity Effects in 3T3-L1 Adipocytes and C57BL/6J Mice Fed High-Fat Diets. *J Med Food* (2016) 19(8):768–79. doi: 10.1089/jmf.2016.3704
35. Mimaki Y, Fukushima M, Yokosuka A, Sashida Y, Furuya S, Sakagami H. Triterpene Glycosides From the Roots of Sanguisorba Officinalis. *Phytochemistry* (2001) 57(5):773–9. doi: 10.1016/s0031-9422(01)00083-8
36. Zhang S, Liu X, Zhang ZL, He L, Wang Z, Wang GS. Isolation and Identification of the Phenolic Compounds From the Roots of Sanguisorba Officinalis L. And Their Antioxidant Activities. *Molecules* (2012) 17 (12):13917–22. doi: 10.3390/molecules171213917
37. Hu J, Song Y, Li H, Yang B, Mao X, Zhao Y, et al. Cytotoxic Triterpene Glycosides From the Roots of Sanguisorba Officinalis. *Arch Pharm Res* (2015) 38(6):984–90. doi: 10.1007/s12272-014-0477-3

Conflict of Interest: The authors declare that the research was conducted in the absence of any commercial or financial relationships that could be construed as a potential conflict of interest.

Publisher's Note: All claims expressed in this article are solely those of the authors and do not necessarily represent those of their affiliated organizations, or those of the publisher, the editors and the reviewers. Any product that may be evaluated in this article, or claim that may be made by its manufacturer, is not guaranteed or endorsed by the publisher.

Copyright © 2021 Lee, Kim, Kim, Kim, Pak, Jeon, Park, Li, Kim, Choi and Chung. This is an open-access article distributed under the terms of the Creative Commons Attribution License (CC BY). The use, distribution or reproduction in other forums is permitted, provided the original author(s) and the copyright owner(s) are credited and that the original publication in this journal is cited, in accordance with accepted academic practice. No use, distribution or reproduction is permitted which does not comply with these terms.

frontiers in Immunology

SYSTEMATIC REVIEW
published: 29 September 2021
doi: 10.3389/fimmu.2021.751407

Tumor Mutational Burden Predicting the Efficacy of Immune Checkpoint Inhibitors in Colorectal Cancer: A Systematic Review and Meta-Analysis

Yan Li[1†], Yiqi Ma[1†], Zijun Wu[1], Fanxin Zeng[2,3], Bin Song[1], Yanrong Zhang[3], Jinxing Li[4], Su Lui[1] and Min Wu[1]*

[1] Huaxi MR Research Center (HMRRC), Department of Radiology, Functional and Molecular Imaging Key Laboratory of Sichuan Province, West China Hospital, Sichuan University, Chengdu, China, [2] Department of Clinic Medical Center, Dazhou Central Hospital, Dazhou, China, [3] Department of Radiology, School of Medicine, Stanford University, Stanford, CA, United States, [4] Department of Biomedical Engineering, Institute for Quantitative Health Science and Engineering (IQ), Michigan State University, East Lansing, MI, United States

OPEN ACCESS

Edited by:
Benjamin Frey,
University Hospital Erlangen, Germany

Reviewed by:
Shaocheng Zhu,
Henan Provincial People's Hospital, China
David Tougeron,
CHU Poitiers, France

***Correspondence:**
Min Wu
wuminscu@scu.edu.cn

[†]These authors have contributed equally to this work

Specialty section:
This article was submitted to Cancer Immunity and Immunotherapy, a section of the journal Frontiers in Immunology

Received: 01 August 2021
Accepted: 10 September 2021
Published: 29 September 2021

Citation:
Li Y, Ma Y, Wu Z, Zeng F, Song B, Zhang Y, Li J, Lui S and Wu M (2021) Tumor Mutational Burden Predicting the Efficacy of Immune Checkpoint Inhibitors in Colorectal Cancer: A Systematic Review and Meta-Analysis. Front. Immunol. 12:751407. doi: 10.3389/fimmu.2021.751407

Objectives: For colorectal cancer patients, traditional biomarker deficient mismatch repair/microsatellite instability (dMMR/MSI) is an accurate predictor of immune checkpoint inhibitors (ICIs). Recent years, researchers considered tumor mutation burden (TMB) as another predictive biomarker which means the number of nonsynonymous mutations in cancer cells. Several studies have proven that TMB can evaluate the efficacy of ICI therapy in diverse types of cancer, especially in non-small cell lung cancer and melanoma. However, studies on the association between TMB and the response to ICI therapy in colorectal cancer alone are still lacking. In this study, we aim to verify the effect of TMB as a biomarker in predicting the efficacy of ICIs in colorectal cancer.

Methods: We searched the PubMed and Ovid MEDLINE databases up to May 1, 2021 and screened studies for eligibility. Thirteen studies published from 2015 to 2021 with 5062 patients were included finally. We extracted and calculated hazard ratios (HRs) and odds ratios (ORs) of overall survival (OS) and objective response rates (ORRs) and their 95% confidence intervals (95% CIs). Pooled HR and OR were evaluated to compare OS and ORR between TMB-high and TMB-low groups in colorectal cancer patients. Meanwhile, we assessed heterogeneity with the I^2 statistic and p-values and performed publication bias assessments, sensitivity analyses, and subgroup analyses to search the cause of heterogeneity.

Results: The TMB-high patient group had a longer OS than the TMB-low patient group (HR = 0.68, 95% CI: 0.51, 0.92, p = 0.013) among colorectal cancer patients receiving ICIs. In addition, the TMB-high patient group was superior in terms of ORR (OR = 19.25, 95% CI: 10.06, 36.82, p < 0.001) compared to the TMB-low patient group.

Conclusions: In conclusion, this meta-analysis revealed that TMB can be used as a potential predictive biomarker of colorectal cancer patients receiving ICI therapy. Nevertheless, this finding is not stable enough. Therefore, many more randomized controlled trials are needed to prove that TMB is reliable enough to be used clinically to predict the efficacy of immunotherapy in colorectal cancer. And the most relevant biomarker remains to be determined when TMB high overlaps with other biomarkers like MSI and TILs.

Keywords: tumor mutation burden, immune checkpoint inhibitors, overall survival, objective response rate, colorectal cancer

INTRODUCTION

Colorectal cancer (CRC) is a common intestinal malignancy. On the basis of the Global Cancer Epidemiological Statistics (GLOBOCAN2020) released by World Health Organization, it is estimated that in 2020, the number of new cases and deaths of colorectal cancer ranked second and third among all malignant tumors, respectively (1). With the approval of the first immune checkpoint inhibitor (ICI) (nivolumab) for colorectal cancer by the Food and Drug Administration (FDA) based on the data from the CHECKMATE142 trial in 2017, patients with stage IV colorectal cancer (deficient mismatch repair) can be treated with ICIs even if the tumor progresses after standard chemotherapy (2). A number of studies have shown that the status of deficient mismatch repair (dMMR)/microsatellite instability (MSI) can be used as a biomarker to identify patients who may benefit from immunotherapy (3–5). However, only 5% of patients with mCRC are dMMR/MSI-High and some of them do not respond to immunotherapy, which has limited clinical benefits. Meanwhile, there are still a small number of CRC patients with MSS who may benefit from ICI treatment (6). Therefore, it is necessary to look for more effective biomarkers to expand the CRC population responding to immunotherapy.

In addition to the status of dMMR/MSI, scientists have identified several biomarkers, including programmed cell death ligand 1 (PD-L1) expression, tumor infiltrating lymphocytes (TILs), POLE mutation and tumor mutation load (TMB) (7–10). TMB means the number of nonsynonymous mutations in cancer cells, which can be evaluated by next-generation sequencing (NGS) or whole-exome sequencing (WES). The higher the TMB is, the greater the type and number of neoantigens are produced by tumor cells, and the more likely it is to be recognized by the immune system. When ICIs activate their own antitumor immune response, the probability that these tumor cells will be killed is greater (11). One research combining 45 clinical studies and data from 103078 cancer patients found that TMB-high is an adverse prognostic factor for patients receiving non-immunotherapy, and a favorable factor for survival and efficacy for patients receiving immunotherapy, regardless of cancer type and TMB detection method (12). At present, the role of TMB as a predictor of immunotherapy has been confirmed in several specific types of cancer, such as non-small cell lung cancer (NSCLC) and melanoma (13–18), and preliminary studies have been carried out in patients with mCRC. Schrock AB et al. collected the response data of 22 MSI-HCRC patients treated with PD-1/L1 inhibitors and measured TMB by NGS. They found that the strongest correlation existed between TMB and objective response rate (ORR) and progression-free survival (PFS) by univariate analysis and multivariate analysis (19).

The study of TMB as a predictive biomarker has made great progress in NSCLC and melanoma (20, 21), but research on TMB in colorectal cancer has not yet been refined. The existing evidence is not sufficient to determine whether TMB can be used as a predictive biomarker of the immunotherapy in colorectal cancer. In view of the fact that the overall efficiency of immunotherapy in the field of colorectal cancer is not high, it is more urgent to select the dominant population. Here, we conducted this systematic review and meta-analysis to assess the predictive value of TMB on the effect of ICI treatment in patients with colorectal cancer based on the latest clinical evidence.

METHODS

This meta-analysis conformed to the Preferred Reporting Items for Systematic Reviews and Meta-Analyses (PRISMA) guidelines (22).

Search Strategy, Study Selection, and Inclusion Criteria

We searched Ovid MEDLINE and PubMed databases up to May 1, 2021 with the following search terms: (mutational burden OR mutation burden OR mutational load OR mutation load OR TMB) AND (nivolumab OR pembrolizumab OR atezolizumab OR avelumab OR durvalumab OR ipilimumab OR tremelimumab OR immunotherapy OR PD-1 OR PD-L1 OR CTLA-4 OR immune checkpoint OR checkpoint blockade OR immune checkpoint inhibitors OR ICI OR ICIs OR immune checkpoint blockers OR ICB OR ICBs) AND (colon cancer OR colorectal cancer OR colorectal carcinoma OR colon carcinoma).

Studies were independently screened and reviewed by two investigators (Li and Ma), and differences were resolved through discussion and consensus. After removing duplicate reports, we first assessed the titles and abstracts of studies for eligibility following the present inclusion criteria: (1) studies had to assess

the effect of TMB in predicting the outcomes of ICIs, such as anti-PD-1, anti-PD-L1, anti-CTLA-4, their combination, or other ICIs, in colorectal cancer. (2) Studies ought to provide the TMB-related hazard ratio (HR) and its 95% confidence interval (95% CI) of overall survival (OS) or odds ratio (OR) and its 95% CI of ORR. If above conditions were not met, studies had to give Kaplan–Meier curves or original OS or ORR data to generate calculable metrics. (3) Animal studies, reviews, comments, case reports, editorials, and conference abstracts were excluded, and studies were written in English. Studies deemed eligible were enrolled after full-text view.

Data Extraction and Quality Assessment

We extracted the following data from the eligible studies: author, publication year, number of patients, type of ICI therapy, recruitment area of patients, proportion of dMMR/MSI, sample source, sequencing method of TMB, TMB cutoff value, TMB median value and its range, survival outcomes and HRs/ORs, and 95% CIs.

The types of eligible studies included randomized controlled trials (RCTs) and cohort studies. The quality assessment of cohort studies was performed *via* the Newcastle-Ottawa Scale (NOS) with scores of 0-9. Studies scores as 8-9 were recognized as high-quality studies, 5-7 indicated intermediate-quality studies and lower than 5 indicated low-quality studies and high risk of bias (23). Specifically, as we only included patients treated with durvalumab and tremelimumab in the RCT study, it was estimated by NOS as well (24).

Statistical Analysis

We compared the OS and ORR between high and low TMB patient groups through HR and OR to verify the effect of TMB in predicting the efficiency of ICIs in colorectal cancer patients. For studies that provided Kaplan–Meier curves without HR of OS, we used Engauge Digitizer to extract survival data and the program files provided by Tierney et al. to calculate HRs and corresponding 95% CIs (25). For studies with original data, a Cox proportional hazards regression model was applied to calculate the OR of the ORR and corresponding 95% CIs by IBM SPSS Statistics 20.0. The summary HR or OR and 95% CI and *p*-values were estimated *via* STATA 15.0 (Stata Corporation, College Station, TX, USA). Heterogeneity was also evaluated by the I^2 statistic and *p*-value using STATA. High heterogeneity meta-analysis was conducted under a random-effects model, and low heterogeneity meta-analysis was performed under a fixed-effects model. Values of 25% < I^2 < 50%, 50% < I^2 <75% and I^2 < 75% suggested low heterogeneity, intermediate heterogeneity and significant heterogeneity, respectively (26). When heterogeneity was large, publication bias assessments, sensitivity analyses, and subgroup analyses were conducted to investigate the cause of the heterogeneity. Funnel plots and Egger's test were conducted as publication bias assessments methods to estimate whether adequate eligible studies were included in our study (27). Egger's test was used to quantify the funnel plots, and $p > 0.05$ represented the absence of publication bias. Sensitivity analyses were used to estimate the impact of each study on the stability of the results. Subgroup analyses included subgroup by the number of patients, subgroup by recruitment area of patients, subgroup by TMB sequencing method and subgroup by TMB cutoff.

RESULTS

Search Results, Study Characteristics and Quality Assessment

Based on our search strategy, a total of 255 studies were retrieved from the Ovid MEDLINE and PubMed databases after removing 58 duplicate studies. Animal studies, reviews, comments, case reports and non-English language studies were excluded through title and abstract screening. After removing studies not related to the topic, studies that were not clinical trials or cohort studies and studies without adequate survival data and sample size by full-text review, 13 studies published from 2015 to 2021 were finally included (**Figure 1**) (9, 19, 24, 28–37).

Study characteristics are shown in **Table 1**. A total of 5062 patient samples ranging from 15 to 2083 from each study were included in this meta-analysis. Among them, 8 studies were from Western countries, and 5 studies were from multiple areas. This analysis was composed of 1 RCT (24), 1 cohort study (28) and 11 retrospective cohort studies (9, 19, 29–37). Regarding the types of ICI therapy, 1 study used anti-PD-1(pembrolizumab) monotherapy, 1 study used anti-PD-L1 monotherapy, 3 studies adopted anti-PD-1/L1 therapy, and the remaining 8 studies used anti-CTLA-4 or anti-PD-1/L1 as monotherapy or in combination. Only 6 studies mentioned the proportion of dMMR/MSI mCRC. In these studies, WES and NGS were adopted to detect blood or tumor tissue samples. All but one of the studies adopted tumor tissue samples. A special study used blood samples for circulating cell-free DNA (cfDNA) (24). Different studies defined diverse TMB cutoffs. The survival data for 10 studies were expressed as OS, and 3 were expressed as ORR. According to the NOS, 9 studies that obtained a score of 7 were regarded as intermediate-quality, and 4 studies with scores of 8-9 were assessed as high-quality.

Main Results and Assessment of Heterogeneity

Under a random-effects model, the summary HR of OS between the high and low TMB patient groups and the corresponding 95% CI were calculated based on 10 studies including 3849 patients (9, 24, 28–33, 36, 37). The results suggested that the OS of TMB-high patient group was longer than that of the TMB-low patient group (HR = 0.68, 95% CI: 0.51, 0.92, $p = 0.013$; **Figure 2**). The heterogeneity was significant in the comparison of OS in the TMB-high and TMB-low patient groups ($I^2 = 82.7\%$, $p < 0.001$). Similarly, we assessed the summary OR of ORR in 3 studies with 1213 patients under a fixed-effects model (19, 34, 35). The TMB-high patient group was superior in terms of ORR (OR = 19.25, 95% CI: 10.06, 36.82, $p < 0.001$; **Figure 3**), and the heterogeneity was low ($I^2 = 22.8\%$, $p = 0.274$).

Publication Bias, Sensitivity Analyses and Subgroup Analyses

To analyze the cause of high heterogeneity in the comparison of OS in TMB-high and low patient groups, we conducted

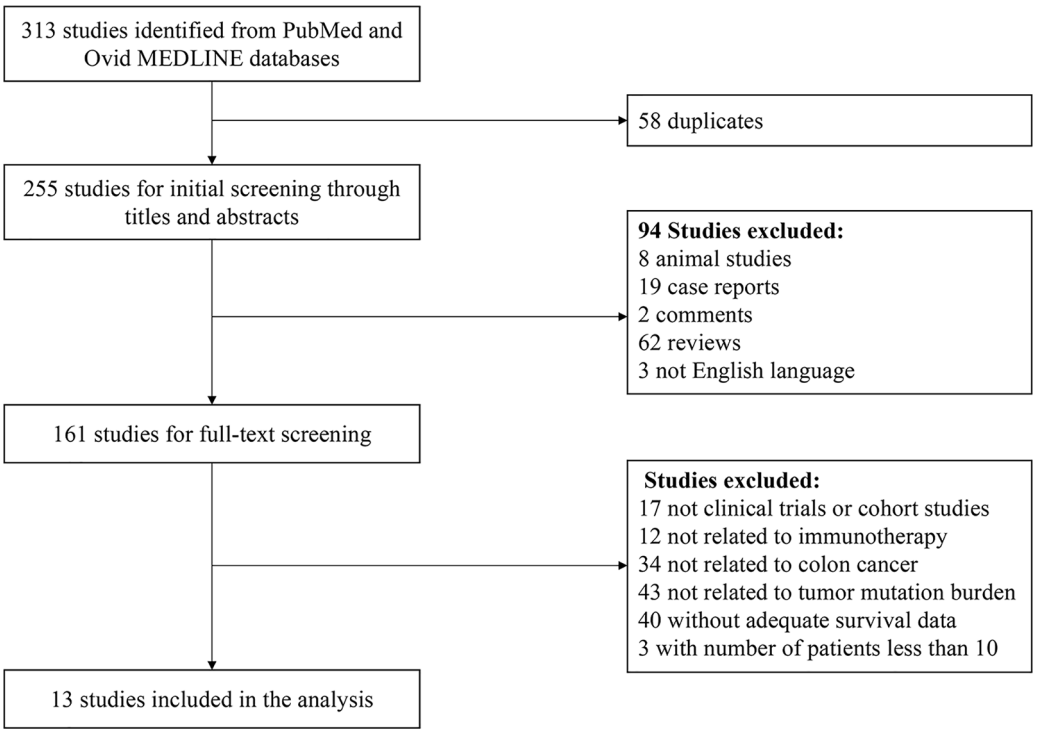

FIGURE 1 | The PRISMA flowchart.

publication bias, sensitivity analyses and subgroup analyses. The funnel plot is shown in **Figure 4**. Egger's test (p = 0.053) quantitatively indicated that no publication bias existed. Sensitivity analyses suggested that after removing the study reported by Zaidi et al. (36), the combined 95% CI of the remaining 9 studies exceeded 1 [95% CI: 0.61, 1.03], indicating that TMB had no effect on OS, which was inconsistent with the results mentioned before, i.e., this study had a significant impact on the results. Therefore, this study was considered to have poor stability. After removal of this study, the I^2 decreased to 71.1%.

Subgroup analyses were performed on 4 aspects: number of patients, recruitment area of patients, sequencing method and TMB cutoff (**Table 2**). In the number of patients ≥ 100 subgroup, the OS of TMB-high patient group was greater than the TMB-low patient group (HR = 0.70, 95% CI: 0.50, 0.98, p = 0.041), but the heterogeneity was significant (I^2 = 84.8%, p < 0.001). In terms of the number of patients < 100 subgroup, the TMB-high and low patient groups had no statistically significant difference (HR = 0.65, 95% CI: 0.42, 1.00, p = 0.051) with low heterogeneity (I^2 = 10.3%, p = 0.291). In addition, no heterogeneity was noted between the two subgroups (p = 0.783). For the recruitment area of patients subgroup analysis, in the Western countries subgroup, the TMB-high patient group also showed superior OS (HR = 0.55, 95% CI: 0.31, 0.95, p = 0.034), while no significant difference was found in the multiple areas subgroup (HR = 0.76, 95% CI: 0.45, 1.27, p = 0.294). The heterogeneity of each subgroup was high (I^2 = 79.0%, p = 0.001) in the Western countries subgroup; and I^2 = 82.7%, p < 0.001 in the multiple areas subgroup). Similarly, no heterogeneity existed between them (p = 0.400). The sequencing method subgroup analysis only included studies using NGS for the detection of TMB and excluded the study (28) using WES. In the NGS (MSK-IMPACT) subgroup, the OS of the TMB-high patient group was greater than that of the TMB-low patient group (HR = 0.34, 95% CI: 0.21, 0.56, p < 0.001) and no heterogeneity was found in this subgroup (I^2 = 0.0%, p = 0.675). The NGS (non-MSK-IMPACT) subgroup included the NGS (GuardantOMNI) and NGS (AmpliSeq panel) methods and had a lower OS in the TMB-high patient group (HR = 0.52, 95% CI: 0.25, 1.07, p = 0.076) than in the NGS (MSK-IMPACT) subgroup, although the difference was not statistically significant in the NGS (non-MSK-IMPACT) subgroup. The heterogeneity was high in the NGS (non-MSK-IMPACT) subgroup (I^2 = 80.7%, p = 0.023) and no heterogeneity was found between the two subgroups (p = 0.362). Furthermore, we conducted subgroup analysis according to TMB cutoff. In the TMB cutoff < 28 muts/Mb subgroup, a better OS was observed in the TMB-high patient group (HR = 0.34, 95% CI: 0.24, 0.48, p < 0.001). Besides, this subgroup showed a better response to ICIs in CRC patients with higher TMB than the TMB cutoff ≥ 28 muts/Mb subgroup (HR = 0.63, 95% CI: 0.42, 0.96, p = 0.029). No heterogeneity was observed in both the TMB cutoff < 28 muts/Mb subgroup (I^2 = 0.0%, p = 0.596) and the TMB cutoff ≥ 28 muts/Mb subgroup (I^2 = 0.0%, p = 0.434) and the heterogeneity was significant between the two subgroups (p = 0.021).

TABLE 1 | Characters of included studies in the meta-analysis.

Reference	Number of Patients (High/Low TMB)	Area	Type of ICIs	dMMR/ MSI	Sample Source	Sequencing Method	TMB Cutoff	Median TMB (Range)	Outcome	Score of NOS
Chen et al. 2020 (1, 24)	115(21/94)	Western	Anti-CTLA-4 and anti-PD-L1	0	Blood	NGS (GuardantOMNI)	28muts/Mb	15.3muts/Mb (0.96-85.4)	OS	7
Le et al. 2015 (1, 28)	15(NA)	Multiple areas	Anti-PD-1	60.0%	Tumor	WES	NA	771muts (5-4025)	OS	7
Lee et al. 2020 (1, 29)	63(NA)	western	Immune checkpoint inhibitors	NA	Tumor	NGS (MSK-IMPACT)	13.17muts/Mb	7.9muts/Mb (NA)	OS	7
Li et al. 2020 (1, 30)	403(NA)	Multiple areas	Immune checkpoint inhibitors	NA	Tumor	NA	NA	NA	OS	7
Lin et al. 2020 (1, 31)	109 (39/70)	western	Immune checkpoint inhibitors	NA	Tumor	NGS (MSK-IMPACT)	11muts/Mb	NA	OS	7
Peng et al. 2021 (1, 32)	398(NA)	western	Immune checkpoint inhibitors	NA	Tumor	NA	NA	9.95muts/Mb (0.05-188.32)	OS	7
Samstein et al. 2019 (1, 9)	110(22/88)	western	Immune checkpoint inhibitors	NA	Tumor	NGS (MSK-IMPACT)	52.2muts/Mb	7.90muts/Mb (0-203.64)	OS	8
Schrock et al. 2019 (1, 19)	22(13/9)	western	Anti-PD-1/L1	100%	Tumor	NGS	37-41muts/Mb	47.5muts/Mb (13-91)	ORR	7
Song et al. 2020 (1, 33)	109(87/22)	Multiple areas	Anti-PD-1/L1	NA	Tumor	NGS (MSK-IMPACT)	52.66muts/Mb	NA	OS	9
Valero et al. 2021 (1, 34)	50(43/7)	western	Anti-PD-1/L1	NA	Tumor	NGS (MSK-IMPACT)	10muts/Mb	NA	ORR	9
Yarchoan et al. 2019 (1, 35)	1141 (89/1052)	western	Anti-PD-1/L1	4.7%	Tumor	NGS (FoundationOne)	10muts/Mb	TMB-H:48.285 TMB-L:3.48	ORR	7
Zaidi et al. 2020 (1, 36)	2083(392/1691)	Multiple areas	Immune checkpoint inhibitors	14.7%	Tumor	NGS (AmpliSeq panel)	17muts/Mb	NA	OS	7
Zhou et al. 2021 (1, 37)	396(198/198)	Multiple areas	Immune checkpoint inhibitors	21%	Tumor	NA	96muts	96muts	OS	9

TMB, tumor mutational burden; ICIs, immune checkpoint inhibitors; CTLA-4, cytotoxic T lymphocyte-associated antigen 4; PD-L1, programmed death-ligand 1; PD-1, programmed cell death protein 1; dMMR, deficient mismatch repair; microsatellite instability, MSI; NGS, next-generation sequencing; WES, whole-exome sequencing; muts/Mb, mutations per megabase; muts mutations; OS, overall survival; ORR, objective response rate/overall response rate; NOS, Newcastle-Ottawa Scale; NA, not available.

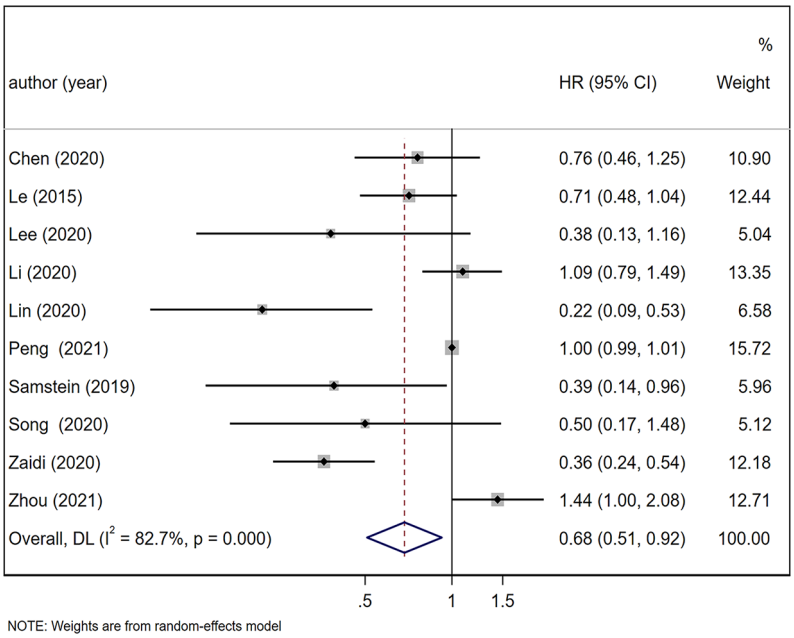

FIGURE 2 | Forest plot of meta-analysis results of the association between overall survival and TMB. TMB, tumor mutation burden; HR, hazard ratio; CI, confidence interval.

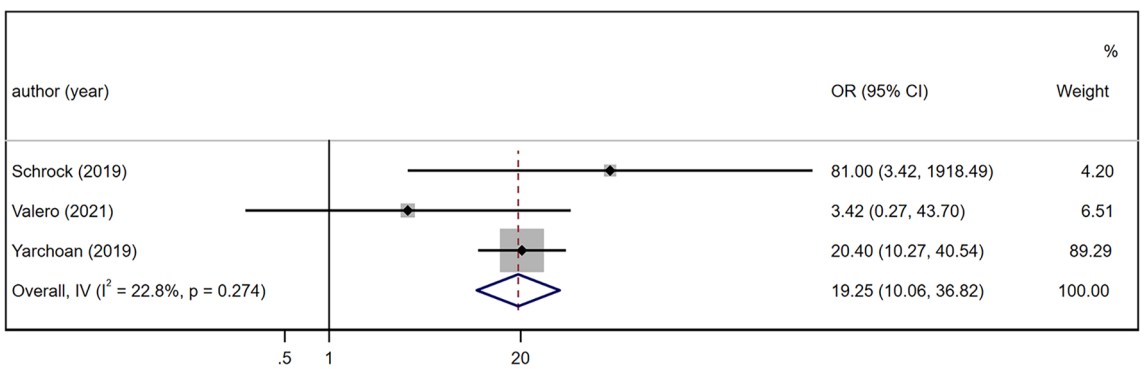

FIGURE 3 | Forest plot of meta-analysis results of the association between objective response rate and TMB. TMB, tumor mutation burden; OR, odds ratio; CI, confidence interval.

DISCUSSION

The results of our study confirmed that both the OS and ORR of the TMB-high patient group were better than those of the TMB-low patient group. That is, high TMB could indicate a better response to ICI treatment. In this study, for patients with high TMB, the risk of death was reduced by 32% and the ORR was 19.25 times higher than that of patients with low TMB. However, as shown in the results of heterogeneity analyses, heterogeneity was significant in the comparison of OS in the TMB-high and low patient groups. Based on results of publication bias analysis, no publication bias existed. The sensitivity analyses indicated that the study reported by Zaidi et al. had influence on the stability of the results (36). The heterogeneity was significantly reduced after this study was removed. The NOS quality assessment revealed that most articles were of medium quality for this meta-analysis including the study researched by Zaidi et al. (36). To further investigate the cause of high heterogeneity, we chose four aspects to conduct subgroup analyses. First, we performed subgroup analysis based on the number of patients as different sample size, especially small sample size, may cause bias in the results. The predictive value of TMB may vary among patient populations so we conducted another subgroup analysis according to the recruitment areas of patients. Obviously, TMB

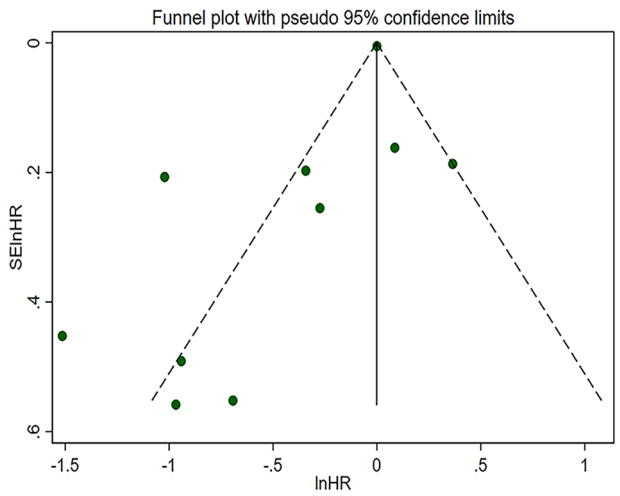

FIGURE 4 | Funnel plot with pseudo 95% confidence limits of pooled overall survival. HR, hazard ratio.

value of the same individual could be different depending on the sequencing method which was one of the causes of difference of predictive effect of TMB on the efficiency of ICIs. Moreover, TMB cutoffs differed among studies. To determine a relatively appropriate cutoff range, we performed the last subgroup analysis on the basis of TMB cutoff. As the results, it seemed that differences in the number of patients, recruitment areas of patients and sequencing method were not responsible for high heterogeneity while different TMB cutoffs may be one of the explanations of the high heterogeneity. When we excluded studies without information on sequencing methods, heterogeneity decreased significantly (I^2 = 50.5%, p = 0.059), and heterogeneity was further reduced after removal of the study reported by Zaidi et al. (I^2 = 37.8%, p = 0.154) (36). The lack of included RCTs may also be related to high heterogeneity.

TMB refers to the number of nonsynonymous mutations in somatic cells in a specific genomic region, which can indirectly reflect the ability and degree of tumors to produce neoantigens. A large number of studies have shown that TMB can predict the efficacy of immunotherapy for many kinds of tumors (9, 11, 38). The detection of TMB is affected by many factors, such as the sample quality, sample source, detection methods, and analysis methods. The conditions of TMB detection should be fully understood before clinical application. Early studies on TMB used the method of WES, which covered approximately 22000 genes in the coding region, accounting for 1% of the whole genome. Studies have found that TMB measured by WES is related to the clinical benefits of immunotherapy for a variety of tumors (28, 39). However, the clinical application of WES is limited because of its high cost, long detection time, complex data analysis and the need for fresh samples (40). With the development of NGS, the whole genome can be sequenced quickly with the ultrahigh throughput, scalability and speed of NGS, and some studies have described that there is a significant correlation between the TMB detected by WES and the targeted panel (38, 41, 42). Unfortunately, only one study using WES to detect TMB was included in our study, so it was impossible to compare the effects of these two sequencing methods on the results. At present, a number of targeted sequencing panels have been approved by the FDA, and four panels which we included were used in the study, including MSK-IMPAKT, FoundationOne, GuardantOMNI and a custom AmpliSeq panel (24, 35, 43). These panels differ in some key parameters, but the most basic requirement of TMB detection is using NGS large panels (or WES), and the recommended sequencing depth is also different. The minimum targeted sequencing depth recommended in some studies should be ≥ 200 or ≥ 500, but in principle, the coverage of targeted sequencing should not be < 1.0 Mb, so as to ensure the accuracy of reporting TMB and to provide sufficient information (44, 45). In view of the sample size, we report the difference in the immunotherapy effect of TMB detected by the NGS-based MSK-IMPAKT panel and non-MSK-IMPAKT panel. Subgroup analysis showed that compared with the non-MSK-IMPAKT panel, the detection of TMB by the MSK-IMPAKT panel was significantly associated with OS benefits in CRC patients with TMB-H, and there was no heterogeneity in the NGS-based MSK-IMPAKT subgroup. The high heterogeneity in the non-MSK-IMPAKT group is a normal phenomenon, which may be due to the inclusion of two different targeting sequencing panels (GuardantOMNI and the custom

TABLE 2 | Subgroup analysis of overall survival between TMB-high and TMB-low group.

Subgroup	Number of Study	HR [95% CI]	*p*-Value	I^2	Heterogeneity between subgroups
Number of patients					
patients ≥ 100	8	0.70 [0.50,0.98]	0.041	84.8%	*p* = 0.783
patients < 100	2	0.65 [0.42, 1.00]	0.051	10.3%	
Recruitment area of patients					
Western	5	0.55 [0.31, 0.95]	0.034	79.0%	*p* = 0.400
Multiple areas	5	0.76 [0.45, 1.27]	0.294	86.3%	
Sequencing method					
NGS (MSK-IMPACT)	4	0.34 [0.21, 0.56]	<0.001	0.0%	*p* =0.362
NGS (non-MSK-IMPACT)	2	0.52 [0.25, 1.07]	0.076	80.7%	
TMB cutoff					
TMB cutoff ≥ 28 muts/Mb	3	0.63 [0.42, 0.96]	0.029	0.0%	*p* =0.021
TMB cutoff < 28 muts/Mb	3	0.34 [0.24, 0.48]	<0.001	0.0%	

NGS, next-generation sequencing; TMB, tumor mutational burden; muts/Mb, mutations per megabase; HR, hazard ratio; CI, confidence interval.

AmpliSeq), and the predictive effect of TMB measured by these two panels is not as good as that of the MSK-IMPAKT group, either alone or in combination. This result may be due to the inadequate studies we included, but it also illustrates the potential advantages of MSK-IMPAKT panels. More researches will be needed in the future to explore the possible impact of TMB detection by different sequencing panels on the results.

Another factor affecting TMB detection is the source of samples. Tissue TMB (tTMB) detection is most common in clinical practice. In 2019, Samstein et al. conducted targeted NGS (MSK-IMPACT) of tumor tissues from 1662 patients with 10 advanced cancers treated with ICIs, including CRC. The results revealed that higher tTMB was responsible for better OS, and in most patients, the higher the tTMB was, the better the response to ICI treatment. This study provides strong evidence for the applicability of tTMB detection to more types of cancers (9). When tissue cannot be obtained clinically or the amount of tissue is not sufficient for TMB detection, the efficacy of immunotherapy can be predicted by evaluating blood TMB (bTMB). We included a RCT that analyzed the bTMB of patients with advanced refractory colorectal cancer who received combined ICIs and found that MSS patients with bTMB ≥ 28 mut/Mb had the greatest OS benefit (24). Although we did not perform a subgroup analysis of the sample sources due to the limitation of sample size in this meta-analysis, studies have confirmed that there is a significant correlation between bTMB and tTMB in NSCLC (13). At present, the correlation between the two still lacks of strong evidence in the clinical application of CRC, but it provides a possibility for patients with difficulties in obtaining tissue samples to predict the efficacy of immunotherapy and dynamically monitor treatment changes by evaluating bTMB.

One of the key problems of TMB is to determine the predictive cutoff point for immunotherapy. At present, there is no accurate standard for determining the critical value of TMB in solid tumors (including colorectal cancer). The TMB level was significantly different in various cancer types, with a difference of more than 1,000 times, and it was also highly heterogeneous in different patients with the same cancer type; for example, in malignant melanoma and lung cancer, the level of TMB of different patients varies from 0.1 to 100 mut/Mb (46). In 2020, the FDA approved anti-PD-1 therapy for any type of solid tumor with TMB ≥ 10 mut/Mb based on Keynote158 trial data (47). Although studies have confirmed that patients with TMB ≥ 10 mut/Mb have generally higher response rates to ICI treatment in many tumors (34), the predictive value of the TMB universal threshold is limited due to differences among various tumors, and it should be recommended to use the same threshold screening strategy with various tumors. A study published in 2019 by Memorial Sloan-Kettering Cancer Center on the prediction of TMB in the efficacy of tumor immunotherapy set the highest 20% TMB level in each histology as the cutoff value. The study found that in all patients, higher TMB was associated with better OS (HR 0.52; $p=1.6\times10^{-6}$), which is by far the largest cohort of patients receiving ICI treatment and may be a strategy for TMB threshold screening in multiple cancers (9). In our study, the difference of TMB cutoff point was still large, which may be due to the different detection methods, calculation methods and tumor heterogeneity (48–50). For example, Schrock et al. applied log-rank statistics to determine the optimal cut-point of TMB-H (19), Samstein et al. considered the top 20% of TMB in CRC patients as TMB-H group (9), while Valero et al. used the general threshold of TMB ≥ 10 approved by FDA (34), i.e. Because of the different TMB threshold screening strategies included in this study, it may be another reason for the heterogeneity of the results. In addition, in our study, the results of the subgroup analysis based on the TMB cutoff revealed that when the TMB cutoff < 28 muts/Mb, patients with higher TMB could have a better response to ICI therapy. Nevertheless, the optimal TMB cutoff point for CRC still needs to be determined through a large number of prospective clinical trials.

In theory, the more genetic mutations in cancer patients, the more neoantigens the cancer cells produce, and the more likely they are to be recognized by immune cells. There is a positive correlation between TMB and neoantigens, which is an important factor indicating that TMB can be used as a biomarker of ICIs. In addition to TMB, several other biomarkers also play an important role in predicting the prognosis of colorectal cancer and the efficacy of ICI. It is reported that these biomarkers overlap in varying degrees in CRC (51). Although the expression of PD-L1 is considered to be a biomarker for predicting ICI therapy in many cancers (such as lung cancer), current studies have shown that the expression of PD-L1 has no predictive value in CRC patients treated with ICI, and the prognostic value of its overexpression varies with the status of MSI (2, 28, 52). TILs and immunoscore also showed a good performance on prognosis and predictive value (8, 53). Immunoscore analysis of CRC patients showed better prognostic value than MSI, and patients with high immunoscore had a significantly lower risk of recurrence (54). At present, the researches on the predictive value of POLE mutation in ICI therapy are limited. Wang et al. analyzed the frequency of POLE/POLD1 gene mutation and its relationship with TMB and immunotherapy. The results showed that in the group of solid tumors treated with ICI, the total survival was better in patients with POLE or POLD1 mutation than that of non-carriers, and the TMB of patients with POLE or POLD1 gene mutation in a variety of tumors was significantly higher compared with that of non-carriers (including colorectal cancer). Among them, a small number of patients with POLE or POLD1 gene mutations were complicated with MSI-H, and the survival benefits were still significant even after removing these patients (55). In addition, in an analysis of the human cancer genome of 100,000 patients, it was found that the vast majority of MSI patients were TMB-high. The cooccurrence of these two phenotypes is highly dependent on the type of cancer. MSI-H and TMB-high always occur at the same time in gastrointestinal tumors, while TMB-high is quite common in melanoma, squamous cell carcinoma and lung cancer, but MSI-H is very rare (38). Fabrizio et al. also confirmed this view in CRC patients and found that nearly 3% of CRC patients with MSS were TMB-high (6). This finding may expand the CRC population that can benefit from ICI therapy.

The relationship between the above predictors highlights the importance of finding a biomarker or a combination of biomarkers that are most relevant to the prediction of curative effect. The combination of TMB and MSI status may help to screen out CRC patients with pMMR/MSS who can benefit from ICI therapy, and eliminate patients with dMMR/MSI who may not benefit from ICI treatment. Patients with high expression of PD-L1 and TMB at the same time have better results with immunotherapy, and they are independent predictors (42). When POLE mutation and dMMR/MSI occurred at the same time, PFS and OS were significantly prolonged after ICI therapy (56). In the future, it is necessary to explore the most relevant biomarker or the best combination of biomarkers to predict the efficacy of immunotherapy in large-scale RCTs.

According to the expert opinions on immunotherapy for patients with CRC, immunotherapy or combination therapy are not recommended for pMMR/MSS CRC patients outside the trial conditions, while some combination therapies have shown potential activity in phase I/II studies for mCRC patients with pMMR/MSS (57, 58). Chen et al. also found that CRC patients of MSS with TMB-high who received combined immunotherapy had the greatest OS benefits (24). A phase II study is also under way to evaluate the efficacy of ICI in pMMR/MSS mCRC patients with high immunoscore (59). The above results need to be further verified by randomized III phase studies to determine the best immunotherapy strategy for pMMR/MSS mCRC patients.

This study is the first meta-analysis on the effect of TMB in the efficacy of ICI therapy in patients with colorectal cancer, which is of reference value for future studies on the association between TMB and immunotherapy and the clinical application of TMB in colorectal cancer patients. However, there are still some shortcomings in this study. Generally, TMB is still a controversial biomarker in clinical practice. There are still many problems in the standardization of TMB detection. More prospective studies are needed to verify how to select the TMB detection platform and targeted sequencing panel, how to determine a threshold screening strategy that can be applied to all kinds of tumors, whether there is a correlation between tTMB and bTMB in the field of colorectal cancer, and the independent predictive value of TMB in the Chinese population. On the other hand, studies on TMB as a predictive biomarker in immunotherapy of colorectal cancer are still insufficient. The interaction between TMB and other predictive biomarkers and the optimal prediction combination need to be verified by large scale randomized trials. Researches on TMB mainly focused on melanoma and NSCLC due to the higher tumor mutation load compared with colorectal cancer (38). This is considered to be the most prominent reason for the efficacy of ICI treatment in these cancers.

CONCLUSIONS

Our meta-analysis demonstrated that CRC patients with high TMB can benefit from the ICI therapy, indicating that tumor mutation load can be used as another potential predictive biomarker for immunotherapy in CRC. However, this finding is not stable enough according to the results of sensitivity analysis. Hence, a large number of RCTs will be needed in the future to prove that TMB is a reliable biomarker for predicting the efficacy of immunotherapy for colorectal cancer. And the most relevant biomarker remains to be determined when TMB high overlaps with other biomarkers like MSI and TILs.

DATA AVAILABILITY STATEMENT

The original contributions presented in the study are included in the article. Further inquiries can be directed to the corresponding author.

AUTHOR CONTRIBUTIONS

YL and YM designed the study. YL, YM, ZW, FZ, and JL collected the data. YM, ZW, and YZ performed the statistical analysis. YL and YM wrote the first draft of the manuscript with support from other authors. BS, SL, and MW contributed to manuscript revision. All authors contributed to the article and approved the submitted version.

FUNDING

This work was supported by the Natural Science Foundation of China (Grant 81501462); the Chengdu International Science and Technology Cooperation Funding (Grant 2019-GH02-00074-HZ); the 1·3·5 Project for Disciplines of Excellence-Clinical Research Incubation Project, West China Hospital, Sichuan University; and the Functional and Molecular Imaging Key Laboratory of Sichuan Province (Grant 2012JO0011).

REFERENCES

1. Sung H, Ferlay J, Siegel RL, Laversanne M, Soerjomataram I, Jemal A, et al. Global Cancer Statistics 2020: Globocan Estimates of Incidence and Mortality Worldwide for 36 Cancers in 185 Countries. *CA Cancer J Clin* (2021) 71:209–49. doi: 10.3322/caac.21660
2. Overman MJ, McDermott R, Leach JL, Lonardi S, Lenz HJ, Morse MA, et al. Nivolumab in Patients With Metastatic DNA Mismatch Repair-Deficient or Microsatellite Instability-High Colorectal Cancer (Checkmate 142): An Open-Label, Multicentre, Phase 2 Study. *Lancet Oncol* (2017) 18:1182–91. doi: 10.1016/S1470-2045(17)30422-9
3. Dudley JC, Lin MT, Le DT, Eshleman JR. Microsatellite Instability as a Biomarker for Pd-1 Blockade. *Clin Cancer Res* (2016) 22:813–20. doi: 10.1158/1078-0432.CCR-15-1678
4. Le DT, Durham JN, Smith KN, Wang H, Bartlett BR, Aulakh LK, et al. Mismatch Repair Deficiency Predicts Response of Solid Tumors to Pd-1 Blockade. *Science* (2017) 357:409–13. doi: 10.1126/science.aan6733
5. Overman MJ, Kopetz S, McDermott RS, Leach J, Lonardi S, Lenz H-J, et al. Nivolumab +/- Ipilimumab in Treatment (Tx) of Patients (Pts) With Metastatic Colorectal Cancer (MCRC) With and Without High Microsatellite Instability (Msi-H): Checkmate-142 Interim Results. *J Clin Oncol* (2016) 34:3501. doi: 10.1200/JCO.2016.34.15_suppl.3501

6. Fabrizio DA, George TJJr., Dunne RF, Frampton G, Sun J, Gowen K, et al. Beyond Microsatellite Testing: Assessment of Tumor Mutational Burden Identifies Subsets of Colorectal Cancer Who may Respond to Immune Checkpoint Inhibition. *J Gastrointest Oncol* (2018) 9:610–7. doi: 10.21037/jgo.2018.05.06
7. Havel JJ, Chowell D, Chan TA. The Evolving Landscape of Biomarkers for Checkpoint Inhibitor Immunotherapy. *Nat Rev Cancer* (2019) 19:133–50. doi: 10.1038/s41568-019-0116-x
8. Kong JC, Guerra GR, Pham T, Mitchell C, Lynch AC, Warrier SK, et al. Prognostic Impact of Tumor-Infiltrating Lymphocytes in Primary and Metastatic Colorectal Cancer: A Systematic Review and Meta-Analysis. *Dis Colon Rectum* (2019) 62:498–508. doi: 10.1097/DCR.0000000000001332
9. Samstein RM, Lee CH, Shoushtari AN, Hellmann MD, Shen R, Janjigian YY, et al. Tumor Mutational Load Predicts Survival After Immunotherapy Across Multiple Cancer Types. *Nat Genet* (2019) 51:202–6. doi: 10.1038/s41588-018-0312-8
10. Domingo E, Freeman-Mills L, Rayner E, Glaire M, Briggs S, Vermeulen L, et al. Somatic Pole Proofreading Domain Mutation, Immune Response, and Prognosis in Colorectal Cancer: A Retrospective, Pooled Biomarker Study. *Lancet Gastroenterol Hepatol* (2016) 1:207–16. doi: 10.1016/S2468-1253(16)30014-0
11. Klempner SJ, Fabrizio D, Bane S, Reinhart M, Peoples T, Ali SM, et al. Tumor Mutational Burden as a Predictive Biomarker for Response to Immune Checkpoint Inhibitors: A Review of Current Evidence. *Oncologist* (2020) 25:e147–59. doi: 10.1634/theoncologist.2019-0244
12. Cao D, Xu H, Xu X, Guo T, Ge W. High Tumor Mutation Burden Predicts Better Efficacy of Immunotherapy: A Pooled Analysis of 103078 Cancer Patients. *Oncoimmunology* (2019) 8:e1629258. doi: 10.1080/2162402X.2019.1629258
13. Gandara DR, Paul SM, Kowanetz M, Schleifman E, Zou W, Li Y, et al. Blood-Based Tumor Mutational Burden as a Predictor of Clinical Benefit in Non-Small-Cell Lung Cancer Patients Treated With Atezolizumab. *Nat Med* (2018) 24:1441–8. doi: 10.1038/s41591-018-0134-3
14. Hellmann MD, Ciuleanu TE, Pluzanski A, Lee JS, Otterson GA, Audigier-Valette C, et al. Nivolumab Plus Ipilimumab in Lung Cancer With a High Tumor Mutational Burden. *N Engl J Med* (2018) 378:2093–104. doi: 10.1056/NEJMoa1801946
15. Hamid O, Molinero L, Bolen CR, Sosman JA, Muñoz-Couselo E, Kluger HM, et al. Safety, Clinical Activity, and Biological Correlates of Response in Patients With Metastatic Melanoma: Results From a Phase I Trial of Atezolizumab. *Clin Cancer Res* (2019) 25:6061–72. doi: 10.1158/1078-0432.CCR-18-3488
16. Cristescu R, Mogg R, Ayers M, Albright A, Murphy E, Yearley J, et al. Pan-Tumor Genomic Biomarkers for Pd-1 Checkpoint Blockade-Based Immunotherapy. *Science* (2018) 362:6411. doi: 10.1126/science.aar3593
17. Yusko E, Vignali M, Wilson RK, Mardis ER, Hodi FS, Horak C, et al. Association of Tumor Microenvironment T-Cell Repertoire and Mutational Load With Clinical Outcome After Sequential Checkpoint Blockade in Melanoma. *Cancer Immunol Res* (2019) 7:458–65. doi: 10.1158/2326-6066.CIR-18-0226
18. Wang Z, Duan J, Cai S, Han M, Dong H, Zhao J, et al. Assessment of Blood Tumor Mutational Burden as a Potential Biomarker for Immunotherapy in Patients With Non-Small Cell Lung Cancer With Use of a Next-Generation Sequencing Cancer Gene Panel. *JAMA Oncol* (2019) 5:696–702. doi: 10.1001/jamaoncol.2018.7098
19. Schrock AB, Ouyang C, Sandhu J, Sokol E, Jin D, Ross JS, et al. Tumor Mutational Burden Is Predictive of Response to Immune Checkpoint Inhibitors in Msi-High Metastatic Colorectal Cancer. *Ann Oncol* (2019) 30:1096–103. doi: 10.1093/annonc/mdz134
20. Kim JY, Kronbichler A, Eisenhut M, Hong SH, van der Vliet HJ, Kang J, et al. Tumor Mutational Burden and Efficacy of Immune Checkpoint Inhibitors: A Systematic Review and Meta-Analysis. *Cancers (Basel)* (2019) 11:1798. doi: 10.3390/cancers11111798
21. Sholl LM, Hirsch FR, Hwang D, Botling J, Lopez-Rios F, Bubendorf L, et al. The Promises and Challenges of Tumor Mutation Burden as an Immunotherapy Biomarker: A Perspective From the International Association for the Study of Lung Cancer Pathology Committee. *J Thorac Oncol* (2020) 15:1409–24. doi: 10.1016/j.jtho.2020.05.019
22. Moher D, Liberati A, Tetzlaff J, Altman DG, Group P. Preferred Reporting Items for Systematic Reviews and Meta-Analyses: The Prisma Statement. *PloS Med* (2009) 6:e1000097. doi: 10.1371/journal.pmed.1000097
23. Stang A. Critical Evaluation of the Newcastle-Ottawa Scale for the Assessment of the Quality of Nonrandomized Studies in Meta-Analyses. *Eur J Epidemiol* (2010) 25:603–5. doi: 10.1007/s10654-010-9491-z
24. Chen EX, Jonker DJ, Loree JM, Kennecke HF, Berry SR, Couture F, et al. Effect of Combined Immune Checkpoint Inhibition *vs* Best Supportive Care Alone in Patients With Advanced Colorectal Cancer: The Canadian Cancer Trials Group Co.26 Study. *JAMA Oncol* (2020) 6:831–8. doi: 10.1001/jamaoncol.2020.0910
25. Tierney JF, Stewart LA, Ghersi D, Burdett S, Sydes MR. Practical Methods for Incorporating Summary Time-to-Event Data Into Meta-Analysis. *Trials* (2007) 8:16. doi: 10.1186/1745-6215-8-16
26. Higgins JP, Thompson SG, Deeks JJ, Altman DG. Measuring Inconsistency in Meta-Analyses. *BMJ* (2003) 327:557–60. doi: 10.1136/bmj.327.7414.557
27. Egger M, Davey Smith G, Schneider M, Minder C. Bias in Meta-Analysis Detected by a Simple, Graphical Test. *BMJ* (1997) 315:629–34. doi: 10.1136/bmj.315.7109.629
28. Le DT, Uram JN, Wang H, Bartlett BR, Kemberling H, Eyring AD, et al. Pd-1 Blockade in Tumors With Mismatch-Repair Deficiency. *N Engl J Med* (2015) 372:2509–20. doi: 10.1056/NEJMoa1500596
29. Lee M, Samstein RM, Valero C, Chan TA, Morris LGT. Tumor Mutational Burden as a Predictive Biomarker for Checkpoint Inhibitor Immunotherapy. *Hum Vaccin Immunother* (2020) 16:112–5. doi: 10.1080/21645515.2019.1631136
30. Li M, Wang H, Li W, Peng Y, Xu F, Shang J, et al. Identification and Validation of an Immune Prognostic Signature in Colorectal Cancer. *Int Immunopharmacol* (2020) 88:106868. doi: 10.1016/j.intimp.2020.106868
31. Lin A, Zhang H, Hu X, Chen X, Wu G, Luo P, et al. Age, Sex, and Specific Gene Mutations Affect the Effects of Immune Checkpoint Inhibitors in Colorectal Cancer. *Pharmacol Res* (2020) 159:105028. doi: 10.1016/j.phrs.2020.105028
32. Peng L, Li Y, Gu H, Xiang L, Xiong Y, Wang R, et al. Mucin 4 Mutation Is Associated With Tumor Mutation Burden and Promotes Antitumor Immunity in Colon Cancer Patients. *Aging (Albany NY)* (2021) 13:9043–55. doi: 10.18632/aging.202756
33. Song Y, Huang J, Liang D, Hu Y, Mao B, Li Q, et al. DNA Damage Repair Gene Mutations Are Indicative of a Favorable Prognosis in Colorectal Cancer Treated With Immune Checkpoint Inhibitors. *Front Oncol* (2020) 10:549777. doi: 10.3389/fonc.2020.549777
34. Valero C, Lee M, Hoen D, Zehir A, Berger MF, Seshan VE, et al. Response Rates to Anti-Pd-1 Immunotherapy in Microsatellite-Stable Solid Tumors With 10 or More Mutations Per Megabase. *JAMA Oncol* (2021) 7:739–43. doi: 10.1001/jamaoncol.2020.7684
35. Yarchoan M, Albacker LA, Hopkins AC, Montesion M, Murugesan K, Vithayathil TT, et al. Pd-L1 Expression and Tumor Mutational Burden Are Independent Biomarkers in Most Cancers. *JCI Insight* (2019) 4:e126908. doi: 10.1172/jci.insight.126908
36. Zaidi SH, Harrison TA, Phipps AI, Steinfelder R, Trinh QM, Qu C, et al. Landscape of Somatic Single Nucleotide Variants and Indels in Colorectal Cancer and Impact on Survival. *Nat Commun* (2020) 11:3644. doi: 10.1038/s41467-020-17386-z
37. Zhou Z, Xie X, Wang X, Zhang X, Li W, Sun T, et al. Correlations Between Tumor Mutation Burden and Immunocyte Infiltration and Their Prognostic Value in Colon Cancer. *Front Genet* (2021) 12:623424. doi: 10.3389/fgene.2021.623424
38. Chalmers ZR, Connelly CF, Fabrizio D, Gay L, Ali SM, Ennis R, et al. Analysis of 100,000 Human Cancer Genomes Reveals the Landscape of Tumor Mutational Burden. *Genome Med* (2017) 9:34. doi: 10.1186/s13073-017-0424-2
39. Van Allen EM, Miao D, Schilling B, Shukla SA, Blank C, Zimmer L, et al. Genomic Correlates of Response to Ctla-4 Blockade in Metastatic Melanoma. *Science* (2015) 350:207–11. doi: 10.1126/science.aad0095
40. Campesato LF, Barroso-Sousa R, Jimenez L, Correa BR, Sabbaga J, Hoff PM, et al. Comprehensive Cancer-Gene Panels can be Used to Estimate Mutational Load and Predict Clinical Benefit to Pd-1 Blockade in Clinical Practice. *Oncotarget* (2015) 6:34221–7. doi: 10.18632/oncotarget.5950

41. Johnson DB, Frampton GM, Rioth MJ, Yusko E, Xu Y, Guo X, et al. Targeted Next Generation Sequencing Identifies Markers of Response to Pd-1 Blockade. *Cancer Immunol Res* (2016) 4:959–67. doi: 10.1158/2326-6066.CIR-16-0143
42. Rizvi H, Sanchez-Vega F, La K, Chatila W, Jonsson P, Halpenny D, et al. Molecular Determinants of Response to Anti-Programmed Cell Death (Pd)-1 and Anti-Programmed Death-Ligand 1 (Pd-L1) Blockade in Patients With Non-Small-Cell Lung Cancer Profiled With Targeted Next-Generation Sequencing. *J Clin Oncol* (2018) 36:633–41. doi: 10.1200/JCO.2017.75.3384
43. Zehir A, Benayed R, Shah RH, Syed A, Middha S, Kim HR, et al. Mutational Landscape of Metastatic Cancer Revealed From Prospective Clinical Sequencing of 10,000 Patients. *Nat Med* (2017) 23:703–13. doi: 10.1038/nm.4333
44. Büttner R, Longshore JW, López-Ríos F, Merkelbach-Bruse S, Normanno N, Rouleau E, et al. Implementing Tmb Measurement in Clinical Practice: Considerations on Assay Requirements. *ESMO Open* (2019) 4:e000442. doi: 10.1136/esmoopen-2018-000442
45. Cheng DT, Mitchell TN, Zehir A, Shah RH, Benayed R, Syed A, et al. Memorial Sloan Kettering-Integrated Mutation Profiling of Actionable Cancer Targets (Msk-Impact): A Hybridization Capture-Based Next-Generation Sequencing Clinical Assay for Solid Tumor Molecular Oncology. *J Mol Diagn* (2015) 17:251–64. doi: 10.1016/j.jmoldx.2014.12.006
46. Lawrence MS, Stojanov P, Polak P, Kryukov GV, Cibulskis K, Sivachenko A, et al. Mutational Heterogeneity in Cancer and the Search for New Cancer-Associated Genes. *Nature* (2013) 499:214–8. doi: 10.1038/nature12213
47. Marabelle A, Fakih M, Lopez J, Shah M, Shapira-Frommer R, Nakagawa K, et al. Association of Tumour Mutational Burden With Outcomes in Patients With Advanced Solid Tumours Treated With Pembrolizumab: Prospective Biomarker Analysis of the Multicohort, Open-Label, Phase 2 Keynote-158 Study. *Lancet Oncol* (2020) 21:1353–65. doi: 10.1016/S1470-2045(20)30445-9
48. Chan TA, Yarchoan M, Jaffee E, Swanton C, Quezada SA, Stenzinger A, et al. Development of Tumor Mutation Burden as an Immunotherapy Biomarker: Utility for the Oncology Clinic. *Ann Oncol* (2019) 30:44–56. doi: 10.1093/annonc/mdy495
49. Wu HX, Wang ZX, Zhao Q, Wang F, Xu RH. Designing Gene Panels for Tumor Mutational Burden Estimation: The Need to Shift From 'Correlation' to 'Accuracy'. *J Immunother Cancer* (2019) 7:206. doi: 10.1186/s40425-019-0681-2
50. Merino DM, McShane LM, Fabrizio D, Funari V, Chen SJ, White JR, et al. Establishing Guidelines to Harmonize Tumor Mutational Burden (Tmb): *In Silico* Assessment of Variation in Tmb Quantification Across Diagnostic Platforms: Phase I of the Friends of Cancer Research Tmb Harmonization Project. *J Immunother Cancer* (2020) 8:e000147. doi: 10.1136/jitc-2019-000147
51. Bae JM, Yoo SY, Kim JH, Kang GH. Immune Landscape and Biomarkers for Immuno-Oncology in Colorectal Cancers. *J Pathol Transl Med* (2020) 54:351–60. doi: 10.4132/jptm.2020.05.15
52. Lee LH, Cavalcanti MS, Segal NH, Hechtman JF, Weiser MR, Smith JJ, et al. Patterns and Prognostic Relevance of Pd-1 and Pd-L1 Expression in Colorectal Carcinoma. *Mod Pathol* (2016) 29:1433–42. doi: 10.1038/modpathol.2016.139
53. Pagès F, Mlecnik B, Marliot F, Bindea G, Ou FS, Bifulco C, et al. International Validation of the Consensus Immunoscore for the Classification of Colon Cancer: A Prognostic and Accuracy Study. *Lancet* (2018) 391:2128–39. doi: 10.1016/S0140-6736(18)30789-X
54. Mlecnik B, Bindea G, Angell HK, Maby P, Angelova M, Tougeron D, et al. Integrative Analyses of Colorectal Cancer Show Immunoscore Is a Stronger Predictor of Patient Survival Than Microsatellite Instability. *Immunity* (2016) 44:698–711. doi: 10.1016/j.immuni.2016.02.025
55. Wang F, Zhao Q, Wang YN, Jin Y, He MM, Liu ZX, et al. Evaluation of Pole and Pold1 Mutations as Biomarkers for Immunotherapy Outcomes Across Multiple Cancer Types. *JAMA Oncol* (2019) 5:1504–6. doi: 10.1001/jamaoncol.2019.2963
56. Garmezy B, Gheeya JS, Thein KZ, Pilie PG, Wang WL, Ahnert JR, et al. Correlation of Pathogenic Pole Mutations With Clinical Benefit to Immune Checkpoint Inhibitor Therapy. *J Clin Oncol* (2020) 38:2. doi: 10.1200/JCO.2020.38.15_suppl.3008
57. Fukuoka S, Hara H, Takahashi N, Kojima T, Kawazoe A, Asayama M, et al. Regorafenib Plus Nivolumab in Patients With Advanced Gastric or Colorectal Cancer: An Open-Label, Dose-Escalation, and Dose-Expansion Phase Ib Trial (Regonivo, Epoc1603). *J Clin Oncol* (2020) 38:2053–61. doi: 10.1200/JCO.19.03296
58. Ghiringhelli F, Chibaudel B, Taieb J, Bennouna J, Martin-Babau J, Fonck M, et al. Durvalumab and Tremelimumab in Combination With Folfox in Patients With Ras-Mutated, Microsatellite-Stable, Previously Untreated Metastatic Colorectal Cancer (MCRC): Results of the First Intermediate Analysis of the Phase Ib/Ii Medetreme Trial. *J Clin Oncol* (2020) 38:3006–6. doi: 10.1200/JCO.2020.38.15_suppl.3006
59. Gallois C, Emile JF, Kim S, Monterymard C, Gilabert M, Bez J, et al. Pembrolizumab With Capox Bevacizumab in Patients With Microsatellite Stable Metastatic Colorectal Cancer and a High Immune Infiltrate: The Ffcd 1703-Pochi Trial. *Dig Liver Dis* (2021) S1590-8659:80324–8. doi: 10.1016/j.dld.2021.06.009

Conflict of Interest: The authors declare that the research was conducted in the absence of any commercial or financial relationships that could be construed as a potential conflict of interest.

Publisher's Note: All claims expressed in this article are solely those of the authors and do not necessarily represent those of their affiliated organizations, or those of the publisher, the editors and the reviewers. Any product that may be evaluated in this article, or claim that may be made by its manufacturer, is not guaranteed or endorsed by the publisher.

Copyright © 2021 Li, Ma, Wu, Zeng, Song, Zhang, Li, Lui and Wu. This is an open-access article distributed under the terms of the Creative Commons Attribution License (CC BY). The use, distribution or reproduction in other forums is permitted, provided the original author(s) and the copyright owner(s) are credited and that the original publication in this journal is cited, in accordance with accepted academic practice. No use, distribution or reproduction is permitted which does not comply with these terms.

frontiers in Immunology

CASE REPORT
published: 29 September 2021
doi: 10.3389/fimmu.2021.749204

Case Report: Immune and Genomic Characteristics Associated With Hyperprogression in a Patient With Metastatic Deficient Mismatch Repair Gastrointestinal Cancer Treated With Anti-PD-1 Antibody

Wenyue Zhou[1†], Yuwen Zhou[1†], Cheng Yi[1†], Xinyao Shu[1], Guixia Wei[1], Xiaorong Chen[1], Xudong Shen[2] and Meng Qiu[1]*

[1] Department of Oncology, West China Hospital, Sichuan University, Chengdu, China, [2] The Medical Department, 3D Medicines Inc., Shanghai, China

OPEN ACCESS

Edited by:
Benjamin Frey,
University Hospital Erlangen, Germany

Reviewed by:
Zhang Xiaotian,
Peking University Cancer Hospital, China
Abdolreza Sotoodeh Jahromi,
Jahrom University of Medical Sciences, Iran

***Correspondence:**
Meng Qiu
qiumeng33@hotmail.com

[†]These authors share first authorship

Specialty section:
This article was submitted to Cancer Immunity and Immunotherapy, a section of the journal Frontiers in Immunology

Received: 29 July 2021
Accepted: 10 September 2021
Published: 29 September 2021

Citation:
Zhou W, Zhou Y, Yi C, Shu X, Wei G, Chen X, Shen X and Qiu M (2021) Case Report: Immune and Genomic Characteristics Associated With Hyperprogression in a Patient With Metastatic Deficient Mismatch Repair Gastrointestinal Cancer Treated With Anti-PD-1 Antibody. Front. Immunol. 12:749204. doi: 10.3389/fimmu.2021.749204

Microsatellite instability-high/deficient mismatch repair (MSI-H/dMMR) status of tumors is a distinct predictive biomarker of immune checkpoint inhibitors (ICIs) for colorectal and non-colorectal cancer populations. The overall response rate (ORR) varies from approximately 40% to 60%, indicating that nearly half of MSI-H tumors do not respond to ICIs. The mechanism of response heterogeneity in MSI-H/dMMR cancers is unclear. Some patients who have been treated with ICIs have developed a novel pattern of progression called hyperprogression, which is defined as unexpected accelerated tumor growth. No case of MSI-H/dMMR immunotherapy-associated hyperprogression has been reported in the literature. Here, we present the case of a patient with dMMR gastrointestinal cancer who suffered hyperprogressive disease (HPD) after treatment with nivolumab. We explored the potential mechanisms of HPD by clinical, immune, and genomic characteristics. Extremely high levels of serum LDH, low TMB and TILs, and the disruption of TGFβ signaling, may be related to hyperprogression.

Keywords: MSI-H/dMMR, immune checkpoint inhibitors, hyperprogression, gastrointestinal cancer, case report

1 INTRODUCTION

About 2–4% of diagnosed cancer patients are subtyped as "microsatellite instability-high (MSI-H)" or "deficient in mismatch repair (dMMR)" (1) Tumors with these genetic characteristics generally have exceptionally high tumor mutation burden and enriched infiltration of immune cells. These tumors are also known as "hot tumor" (2). Several vital clinical trials have confirmed that the microsatellite instability-high/deficient mismatch repair (MSI-H/dMMR) status is a distinct predictive biomarker of ICIs for colorectal (3) and non-colorectal (1, 4, 5) cancer populations. The overall response rate (ORRs) varies from approximately 40% to 60% (1, 3, 6, 7). Based on the

different responses to immunotherapy, this phenomenon attracts significant interest in the heterogeneity and relevant mechanisms of MSI-H/dMMR cancer.

In contrast to chemotherapy and other types of anti-tumor therapy, immunotherapy-induced progression patterns are distinctive, including pseudoprogression and hyperprogression disease (HPD) (8). Pseudoprogression is defined as an initial increase in the tumor burden followed by a later or dissociated response (9). On the other hand, HPD manifests as rapid tumor growth combined with poor overall survival. The acknowledged mechanisms and valuable predictors of HPD remain largely unclear. There is evidence that some gene variations and clinical characteristics may be involved in the mechanism of HPD in different types of cancer. In non-small cell lung cancer and melanoma, patients who harbor MDM2/MDM4 amplification and EGFR alterations are reported to be more likely to develop hyperprogression (10–12). In contrast, those harboring the TP53 mutation without co-existence of STK11 or EGFR mutation have a high CD8 T cell density and, thus, a high response to ICIs (10). Approximately 1–6% of gastrointestinal cancer patients exhibit hyperprogression (HPD) (13). With respect to HPD in MSI-H/dMMR cancers, these phenomena and the mechanisms have not been reported.

Here, we present the first case of a patient with dMMR gastrointestinal cancer with primary resistance to immunotherapy, who experienced HPD after two doses of nivolumab. Nivolumab is a programmed death receptor-1 (PD-1)-blocking antibody and is approved for different types of cancer. Rapid hyperprogression was not observed. Pre-immunotherapy circulating tumor DNA (ctDNA) analysis using 150-gene panel next-generation sequencing, immunohistochemistry, multiplex fluorescence immunohistochemistry (mIHC), and blood inflammatory indexes were used to examine the immune microenvironment as well as the patient's genomic and clinical features. We also explored possible mechanisms of HPD. Furthermore, we identified the underlying mechanism and demonstrated the importance of personalized treatment for clinical practice.

2 CASE DESCRIPTION

2.1 Case Presentation

A 47-year-old male patient presented with constant abdominal pain for 4 months and was sent to the hospital for physical examination in October 2017. Computed tomography (CT) revealed multiple masses in the pancreatic body and both the lungs, with enlarged abdominal and supraclavicular lymph nodes, suggesting a heavy tumor load. The patient underwent supraclavicular lymph node dissection. Immunohistochemistry results suggested poorly differentiated metastatic adenocarcinoma. Based on CT imaging, the doctor-in-charge diagnosed that the tumor originated from the pancreas. Gemcitabine plus paclitaxel (Abraxane) chemotherapy was used as first-line treatment. Two months later, follow-up CT revealed tumor progression in both the lungs (**Figure 1A**). Positron-emission tomography–CT revealed increased intake of ^{18}F-fluorodeoxyglucose in the intestinal mesentery, cervicothoracic, abdominal lymph nodes, and both the lungs, indicating significant tumor load once again (**Figure 1D**). One enlarged abnormal cervical lymph node was punctured for examination because the patient refused dissection biopsy and immunohistochemistry was used to analyze the possible site of origin, tumor expression of MMR protein, and gene variation. Immunohistochemistry (IHC) of the second biopsy indicated that the tumor most likely originated from the gastrointestinal duct (IHC showed CDX2 positivity as shown in **Figure 1B**, microscopic magnification ×100). A 5–10% loss of MLH1 and PMS2 protein expression and PD-L1 expression was also observed (**Figures 1C, D**, microscopic magnification ×100), suggesting a dMMR status in this patient. With a performance status (PS) score of 1, nivolumab (200 mg every 2 weeks) was used as second-line treatment. Unfortunately, 1.5 month after the commencement of nivolumab (one dose of nivolumab), the patient experienced rapid deterioration in lung function, including obvious dyspnea and lethargy, and his performance status score deteriorated to 3. A follow-up chest CT scan confirmed rapid metastatic progression in the lungs and lymph nodes (**Figure 1A**). Moreover, laboratory tests revealed significant high serum lactate dehydrogenase (1360 IU/L, ranging from to 110-220 IU/L). Two days later, the patient died of respiratory failure.

2.2 Diagnostic Assessments

2.2.1 Blood Test and Biopsy

Serum lactate dehydrogenase and other blood tests were obtained the day before each treatment. The dissected lymph supraclavicular lymph node, and punctured cervical lymph node tissues were obtained under ultrasound and CT guidance, respectively.

2.2.2 Diagnosis of HPD

Currently, the most accepted definition of HPD is based on the study by Baptiste et al. (9) which detailed the following criteria: time to failure <2 months and TGK_{exp}: TGK_{ref} >2. Tumor growth kinetics (TGK) are estimated to quantitatively assess the progression of the patient. According to Baptiste's definition, our patient's TGK_{exp} and TGK_{ref} were 2.1 and 0.7.8, respectively, and the ratio (TGK_{exp}: TGK_{ref}) was 2.18. This value was calculated with reference to a single lesion, but the CT scan revealed a large number of newly developed lesions (**Figure 1A**). The tumor growth curve as shown in **Figure 1E** also indicated explosive tumor progression. The time to failure of the patient was 1.5 months. The ratio of TGK_{exp} and TGK_{ref} was 2.18. As such, he met the definition of immunotherapy hyperprogression.

2.2.3 Gene Analysis

A 150-gene panel next generation sequencing (NGS) of circulating tumor DNA analysis (3D Medicines Co., Shanghai) before administration of nivolumab revealed six gene mutations with high frequency, including MLH1 p.N287Kfs (56.32%), TCF7L2 p.K462Sfs (36.85%), TP53 p.H179Y (41.4%), ACVR2A p.K437Rfs (69.51%), TGFBR2 p.K128Sfs (66.46%), and TSC1 p.T635Rfs (5.41%). Tumor NGS was detected *via* the punctured tissues. Three mutation genes were inspected (**Figure 2D**), including MLH1 p.N287Kfs (34.3%), TP53 p.H179Y (38.4%), and TSC1 p.T635Rfs (1.7%). Tumor

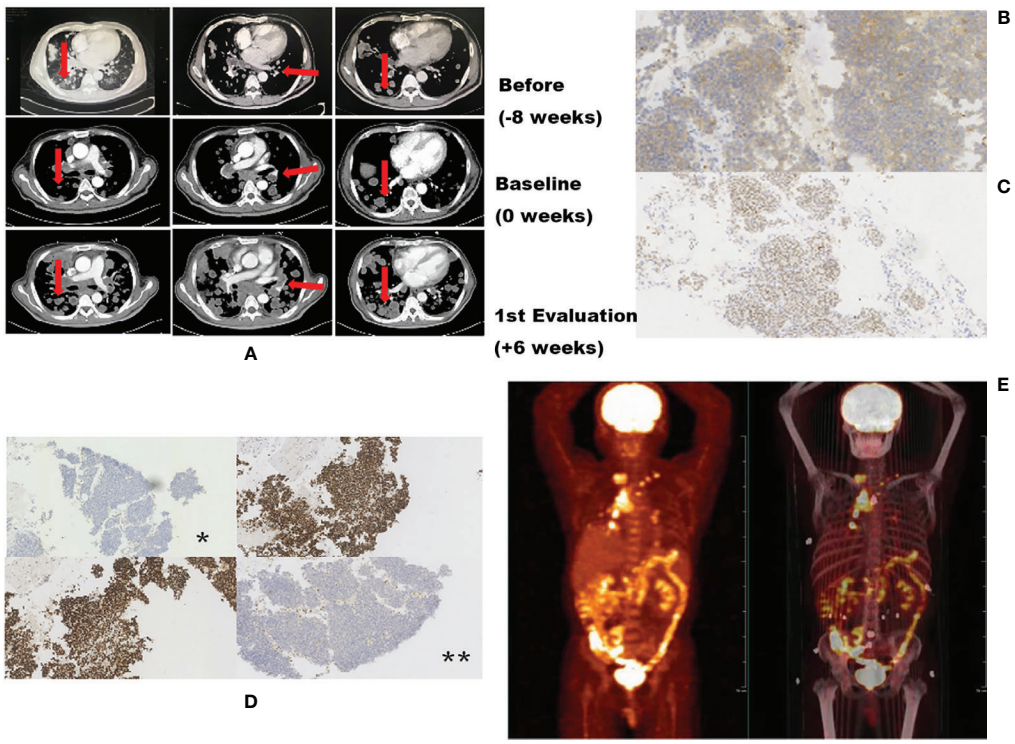

FIGURE 1 | Radiologic images before and after nivolumab showing distinct TGR differences. **(A)** Representative computed tomography scans of the patient's lung before, at baseline, and during treatment. **(B)** Second immunohistochemistry (IHC) showing CDX2 positivity, indicating that the possible original tumor site may be the gastrointestinal duct. **(C)** Second IHC indicating a PD-L1 expression rate of 5–10%. **(D)** Second IHC showing loss of MMR protein expression; *loss of MLH1 protein expression; **loss of expression of PMS2 protein. **(E)** Positron emission tomography/computed tomography (PET-CT) scan suggesting extensive tumor burden.

mutation burden (TMB) was also calculated. With a TMB of 7.26 Muts/Mb, the tumor was categorized as low TMB.

2.2.4 Analysis of the Tumor Immune Microenvironment

To further explore the possible refractory mechanism of HPD in this patient, the lymph node tissue tumor microenvironment (TME) of the patient was examined and PD-L1 protein expression was detected in the formalin-fixed, paraffin-embedded (FFPE) punctured tumor tissues using the Dako PD-L1 IHC 22C3 pharmDx assay. The expression levels of CD8+, CD68+, CD56+ cells, pan cytokeratin, and HLA-DR were assessed and calculated using multiplex fluorescence immunohistochemistry (mIHC). Quantitative analysis of the tumor microenvironment showed that the degree of CD8+, CD68+, and CD56+ cells in the tumor stroma, and tumor region, were 0.59% and 1.28%, respectively, along with 0.15%, 0.30%, and 0.63% and 0.49%, respectively (**Figure 2C**).

3 DISCUSSION

This is the first reported case of HPD in MSI-H/dMMR gastrointestinal cancer, with no HPD-related gene mutation found in our patient. This is also the first report to demonstrate characteristics such as performance status, laboratory tests, TMB, TME, and tumor immune infiltrations (TILs) factors, and some gene alterations, to explain the case better.

Some clinical parameters are reliable predictive prognostic factors for patients with ICI-treated cancer. Studies have shown that high levels of serum lactate dehydrogenase (LDH), tumor burden, and poor performance status are independent baseline factors associated with hyperprogression (14, 15). According to the authors, LDH levels are strongly correlated with prognosis. The prognosis of patients within the normal range is within 16.1 months, but decreases to 2.3 months for those with LDH levels 2.5 times above the upper limit. The authors also demonstrated that low tumor burden and good performance status are also characteristics of favorable OS. As described, the patient had poor performance status, high LDH level, and a rather high tumor burden. The unfortunate outcome was consistent with previous conclusions.

In this case, the patient went through HPD although his TMB was 7.26 Muts/Mb (150-gene panel). TMB is stratified into two subtypes: low and high TMB. High TMB is usually defined as above the median burden based on whole exome sequencing (WES) or different gene panels (16). Optimal TMB cut-offs vary among different studies. However, levels lower than 10 Muts/Mb are generally categorized as low (1, 11, 17). TMB is a reliable efficacy factor for immunotherapy (11, 18–21). Studies have

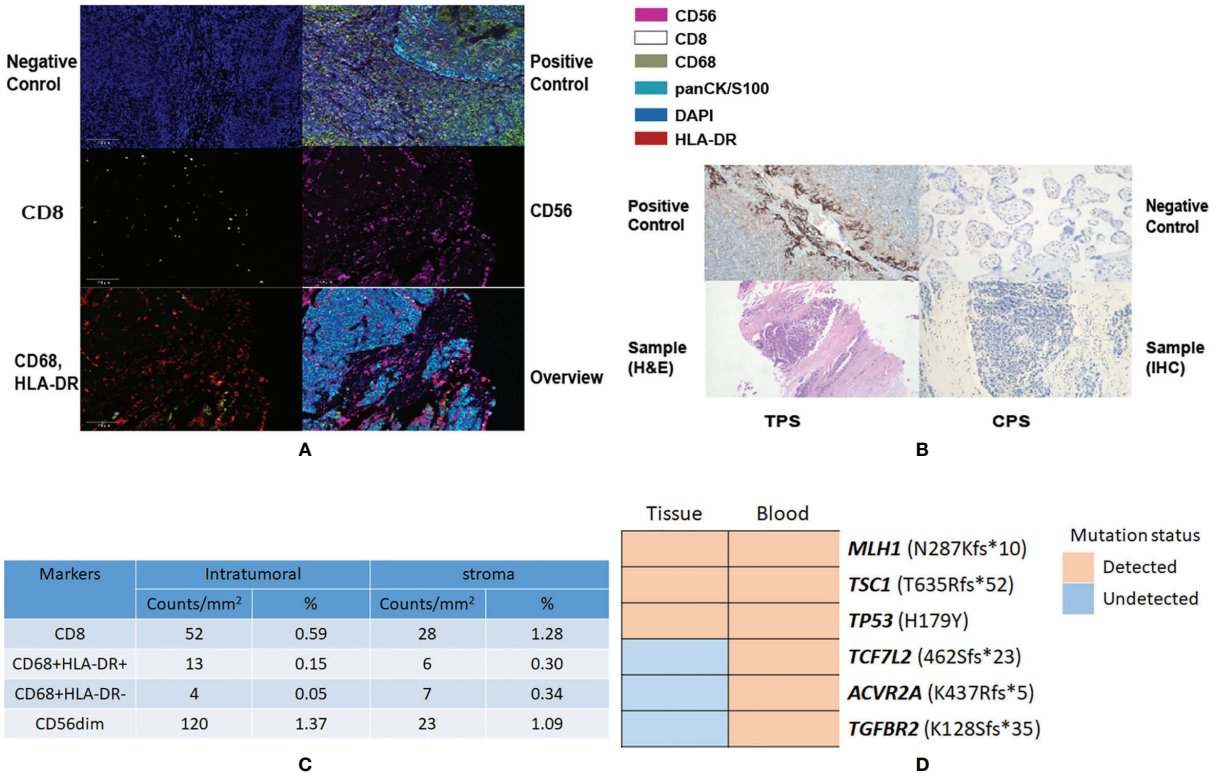

Markers	Intratumoral		stroma	
	Counts/mm²	%	Counts/mm²	%
CD8	52	0.59	28	1.28
CD68+HLA-DR+	13	0.15	6	0.30
CD68+HLA-DR-	4	0.05	7	0.34
CD56dim	120	1.37	23	1.09

C

FIGURE 2 | Results showing tumor microenvironment and genomic mutation copies alteration in autopsy specimens. **(A)** Representative images of PanCK (pan cytokeratin), CD56, CD8, CD68, and HLA-DR as shown by mIHC. Nuclei (blue) and counterstained by DAPI. Original magnification ×200. **(B)** Tumor proportion score (TPS) and combined positive score (CPS). **(C)** Quantification results of TIL percentages by mIHC in the tumor stroma and margin. **(D)** Alteration of the genomic mutation copies before and after immunotherapy.

demonstrated that those with low TMB, as seen in this case, showed less favorable survival rate (11, 17, 18, 20–24). MSI-H/dMMR tumors are identified with high clonality of non-synonymous mutations (also high TMB), leading to the presence of robust altered proteins, known as neoantigens (25). Neoantigens are thought to be relevant to tumor control, as they can be targeted by the immune system, leading to a series of cytolytic activities of the immune cells (1, 3, 25–27). With ORRs varies from 31.7% to 40% (3, 28, 29), nivolumab was approved for the treatment of melanoma, pancreatic, colorectal cancer, gastric cancer and so on. The intolerance and toxicities are mostly immune-mediated, along with infusion-related reactions and embryo-fatal adverse events. In this case, it is not hard to speculate that the low TMB reflected a minimal neoantigen, and was thus refractory to nivolumab. Hence, it is reasonable to assume that the heterogeneity of dMMR is partially responsible for the low levels of TMB and hyperprogression.

Heterogeneity of MSI-H/dMMR TILs was also observed by Harry H. Yoon et al. (30) TILs have been considered as positive prognostic predictive factors in tumor patients since the early 1900s. It is widely acknowledged that CD8+ TIL percentage is the most important predictive factor in immunotherapy (31). Compared with the MSS/pMMR status, CD3+ and CD8+ TILs are significantly more abundant in MSI-H/dMMR patients (30). In this case, as shown in **Figures 2A, C**, CD8+ lymphocytes, CD68+ macrophages, and CD56+ NK cell infiltration percentages were rather low. The PD-L1 assay (**Figure 2A**, original magnification ×200) also revealed extremely low lymphocytes. According to Yoon et al., lower TILs in dMMR are associated with younger, non-smoking, and low histological grade patients. The tumor proportion score (TPS) and combined positive score (CPS) were also examined (**Figure 2B**, original magnification ×200). The patient's TPS and CPS were 0% and 0%, respectively (Dako 22C3 pharmDx, Santa Barbara, CA).

TME is classified into four types based on T cell infiltration and the presence of PD-L1 (32), and TME type III was categorized in this case. While T cell infiltration was observed in the patient, it appears that some unknown mechanisms prevented the effector T cells from functioning normally. A recent study also described that abnormal function of effector T cells may be a hindrance to their proliferation, execution, and maturation in immunotherapy-resistant TME type III patients (33). In addition, TILs in the tumor context have been proven to be a major positive prognostic predictive factor (34). Hence, low TIL percentages in patients cannot be neglected when attempting to elucidate the mechanism. Finally, although not yet listed as a

negative factor of immunotherapy, some studies have indicated that TGFβ signaling could restrict T cells movement in TM. This then leads to a lack of response to anti-PD therapy and hyperprogression (35, 36).

Recent studies of TGFβ signaling may elucidate the possible mechanisms of hyperprogression. TGFβ is a bifunctional regulator that plays an important role in tumor initiation and progression, and deletions in the TGFBR2 gene loci can lead to TGFβ signaling disruption. Studies have confirmed that TGFβ-derived epithelial-mesenchymal transition (EMT) can increase mesenchymal cells and lead to tissue fibrosis (34, 37). The pivotal role of TGFβ in tumor microenvironment (TME) fibrogenesis suggests that TGFβ signaling may restrict T cell movement and counteract anti-tumor immunity (35). TGFβ also plays a vital role in immunotherapy. By limiting the infiltration of inflammatory/immune cells, it could suppress CD8+ T cells and NK cell-mediated anti-tumor response (38). TGFβ inhibits T cell proliferation at the transcriptional level and represses their cytotoxic activity, resulting in tumor progression, and in some cases, hyperprogression. Xiong et al. found regulated TGFβ in the consistent sequencing of two patients with HPD (36). Unfortunately, our patient did not exhibit such a tendency (**Figure 2D**), but the small sample size in the study by Xiong et al. limited its credibility. Although TGFβ has not yet been confirmed as a negative regulator in immunotherapy, it is a new mechanism that merits further exploration. Apart from TGFβ, deregulated WNT signaling could also increase resistance to TILs, as long as there is activation of epithelial-to-mesenchymal transition (EMT), and both methods could limit the infiltration of TILs, especially CD8+ lymph cells (39). In conclusion, TGFβ activation and WNT deregulation may explain the reason for nivolumab resistance and hyperprogression in this case.

Thus, HPD is a comprehensive-cause phenomenon. Studies have suggested that poor clinical characteristics, such as low TMB, heterogeneity of MSI-H/dMMR status, low levels of TILs, TGFBR2 alteration, and TME type III patients could develop mechanism-unknown immune resistance. In this case, they may also lead to HPD.

DATA AVAILABILITY STATEMENT

The original contributions presented in the study are publicly available. This data can be found here: https://www.ncbi.nlm.nih.gov/sra/PRJNA756873.

ETHICS STATEMENT

This study was approved by the institutional review board of the West China Medical College of Sichuan University (ethical approval letter 20211077). The patient provided informed consent for his treatments, the collection and study of his blood and tissue samples. All procedures were conducted according to the Declaration of Helsinki. Written informed consent was obtained from the participant for the publication of this case report.

AUTHOR CONTRIBUTIONS

MQ conceived the idea of the article. WZ mainly takes charge of writing and figure-making. YZ and CY plays a guiding role in article revision, polish, genetic analysis, and ethical review. All authors contributed to the revision and discussion. All authors contributed to the article and approved the submitted version.

ACKNOWLEDGMENTS

We would like to thank the patient and his family for their understanding and 3D Medicine Company for their help with the study.

REFERENCES

1. Marabelle A, Le DT, Ascierto PA, Di Giacomo AM, Jesus-Acosta A D, Delord J-P, et al. Efficacy of Pembrolizumab in Patients With Noncolorectal High Microsatellite Instability or Mismatch Repair-Deficient Cancer, Results From the Phase II KEYNOTE-158 Study. *J Clin Oncol* (2019) 37:1–10. doi: 10.1200/JCO.19.02105
2. Galon J, Bruni D. Approaches to Treat Immune Hot, Altered and Cold Tumours With Combination Immunotherapies. *Nat Rev Drug Discov* (2019) 18(3):197–218. doi: 10.1038/s41573-018-0007-y
3. Overman MJ, McDermott R, Leach JL, Lonardi S, Lenz H-J, Morse MA, et al. Nivolumab in Patients With Metastatic DNA Mismatch Repair-Deficient or Microsatellite Instability-High Colorectal Cancer (CheckMate 142): An Open-Label, Multicentre, Phase 2 Study. *Lancet Oncol* (2017) 18(9):1182–91. doi: 10.1016/S1470-2045(17)30422-9
4. Smith KN, Le DT, Durham JN. Mismatch-Repair Deficiency Predicts Response of Solid Tumors to PD-1 Blockade. *Science* (2017) 357:409–13. doi: 10.1126/science.aan6733
5. Le DT, Uram JN, Wang H, Bartlett BR, Kemberling H, Eyring AD, et al. PD-1 Blockade in Tumors With Mismatch-Repair Deficiency. *N Engl J Med* (2015) 372(26):2509–20. doi: 10.1056/NEJMoa1500596
6. Muro K, Chung HC, Shankaran V, Geva R, Catenacci D, Gupta S, et al. Pembrolizumab for Patients With PD-L1-Positive Advanced Gastric Cancer (KEYNOTE-012): A Multicentre, Open-Label, Phase 1b Trial. *Lancet Oncol* (2016) 17(6):717–26. doi: 10.1016/S1470-2045(16)00175-3
7. Le DT, Kim TW, Cutsem EV, Geva R, Jäger D, Hara H, et al. Phase II Open-Label Study of Pembrolizumab in Treatment-Refractory, Microsatellite Instability-High/Mismatch Repair-Deficient Metastatic Colorectal Cancer: KEYNOTE-164. *J Clin Oncol* (2019) 38:11–9. doi: 10.1200/JCO.19.02107
8. Fuentes-Antras J, Provencio M, Diaz-Rubio E. Hyperprogression as a Distinct Outcome After Immunotherapy. *Cancer Treat Rev* (2018) 70:16–21. doi: 10.1016/j.ctrv.2018.07.006
9. Kas B, Talbot H, Ferrara R, Richard C, Lamarque JP, Pitre-Champagnat S, et al. Clarification of Definitions of Hyperprogressive Disease During Immunotherapy for Non-Small Cell Lung Cancer. *JAMA Oncol* (2020) 6 (7):1039–46. doi: 10.1001/jamaoncol.2020.1634
10. Biton J, Mansuet-Lupo A, Pecuchet N, Alifano M, Ouakrim H, Arrondeau J, et al. TP53, STK11, and EGFR Mutations Predict Tumor Immune Profile and the Response to Anti-PD-1 in Lung Adenocarcinoma. *Clin Cancer Res* (2018) 24(22):5710–23. doi: 10.1158/1078-0432.CCR-18-0163
11. Samstein RM, Lee CH, Shoushtari AN, Hellmann MD, Shen R, Janjigian YY, et al. Tumor Mutational Load Predicts Survival After Immunotherapy Across Multiple Cancer Types. *Nat Genet* (2019) 51(2):202–6. doi: 10.1038/s41588-018-0312-8
12. Gatalica Z, Xiu J, Swensen J, Vranic S. Comprehensive Analysis of Cancers of Unknown Primary for the Biomarkers of Response to Immune Checkpoint

Blockade Therapy. *Eur J Cancer* (2018) 94:179–86. doi: 10.1016/j.ejca.2018.02.021
13. Champiat S, Dercle L, Ammari S, Massard C, Hollebecque A, Postel-Vinay S, et al. Hyperprogressive Disease Is a New Pattern of Progression in Cancer Patients Treated by Anti-PD-1/PD-L1. *Clin Cancer Res* (2017) 23(8):1920–8. doi: 10.1158/1078-0432.CCR-16-1741
14. Weide B, Martens A, Hassel JC, Berking C, Postow MA, Bisschop K, et al. Baseline Biomarkers for Outcome of Melanoma Patients Treated With Pembrolizumab. *Clin Cancer Res* (2016) 22(22):5487–96. doi: 10.1158/1078-0432.CCR-16-0127
15. Kim JY, Lee KH, Kang J, Borcoman E, Saada-Bouzid E, Kronbichler A, et al. Hyperprogressive Disease During Anti-PD-1 (PDCD1)/PD-L1 (CD274) Therapy: A Systematic Review and Meta-Analysis. *Cancers (Basel)* (2019) 11(11):1699. doi: 10.3390/cancers11111699
16. Rizvi NA, Hellmann MD, Snyder A, Kvistborg P, Makarov V, Havel JJ, et al. Mutational Landscape Determines Sensitivity to PD-1 Blockade in Non–Small Cell Lung Cancer. *Science* (2016) 348(6230):124–8. doi: 10.1126/science.aaa1348
17. Chida K, Kawazoe A, Kawazu M, Suzuki T, Nakamura Y, Nakatsura T, et al. A Low Tumor Mutational Burden and PTEN Mutations are Predictors of a Negative Response to PD-1 Blockade in MSI-H/dMMR Gastrointestinal Tumors. *Clin Cancer Res* (2021) 27:3714–24. doi: 10.1158/1078-0432.CCR-21-0401
18. Leslie M. High TMB Predicts Immunotherapy Benefit. *Cancer Discov* (2018) 8(6):668. doi: 10.1158/2159-8290.CD-NB2018-048
19. Saâda-Bouzid E, Defaucheux C, Karabajakian A, Coloma VP, Servois V, Paoletti X, et al. Hyperprogression During Anti-PD-1/PD-L1 Therapy in Patients With Recurrent and/or Metastatic Head and Neck Squamous Cell Carcinoma. *Ann Oncol* (2017) 28(7):1605–1611. doi: 10.1093/annonc/mdx178
20. Cristescu R, Mogg R, Ayers M, Albright A, Murphy E, Yearley J, et al. Pan-Tumor Genomic Biomarkers for PD-1 Checkpoint Blockade-Based Immunotherapy. *Science* (2018) 362(6411):eaar3593. doi: 10.1126/science.aar3593
21. Jones S, Anagnostou V, Lytle K, Parpart-Li S, Nesselbush M, Riley DR, et al. Personalized Genomic Analyses for Cancer Mutation Discovery and Interpretation. *Cancer* (2015) 7(283):283ra53. doi: 10.1126/scitranslmed.aaa7161
22. Liu L, Bai X, Wang J, Tang XR, Wu DH, Du SS, et al. Combination of TMB and CNA Stratifies Prognostic and Predictive Responses to Immunotherapy Across Metastatic Cancer. *Clin Cancer Res* (2019) 25(24):7413–23. doi: 10.1158/1078-0432.CCR-19-0558
23. Petrelli F, Ghidini M, Ghidini A, Tomasello G. Outcomes Following Immune Checkpoint Inhibitor Treatment of Patients With Microsatellite Instability-High Cancers: A Systematic Review and Meta-Analysis. *JAMA Oncol* (2020) 6(7):1068–71. doi: 10.1001/jamaoncol.2020.1046
24. Lu S, Stein JE, Rimm DL, Wang DW, Bell JM, Johnson DB, et al. Comparison of Biomarker Modalities for Predicting Response to PD-1/PD-L1 Checkpoint Blockade: A Systematic Review and Meta-Analysis. *JAMA Oncol* (2019) 5(8):1195–204. doi: 10.1001/jamaoncol.2019.1549
25. Baretti M, Le DT. DNA Mismatch Repair in Cancer. *Pharmacol Ther* (2018) 189:45–62. doi: 10.1016/j.pharmthera.2018.04.004
26. Yang W, Lee KW, Srivastava RM, Kuo F, Krishna C, Chowell D, et al. Immunogenic Neoantigens Derived From Gene Fusions Stimulate T Cell Responses. *Nat Med* (2019) 25(5):767–75. doi: 10.1038/s41591-019-0434-2
27. Schumacher TN, Schreiber RD. Neoantigens in Cancer Immunotherapy. *Science* (2015) 348(6230):69–74. doi: 10.1126/science.aaa4971
28. Weber JS, D'Angelo SP, Minor D, Hodi FS, Gutzmer R, Neyns B, et al. Nivolumab Versus Chemotherapy in Patients With Advanced Melanoma Who Progressed After Anti-CTLA-4 Treatment (CheckMate 037): A Randomised, Controlled, Open-Label, Phase 3 Trial. *Lancet Oncol* (2015) 16(4):375–84. doi: 10.1016/S1470-2045(15)70076-8
29. Robert C, Long GV, Brady B, Dutriaux C, Maio M, Mortier L, et al. Nivolumab in Previously Untreated Melanoma Without BRAF Mutation. *N Engl J Med* (2015) 372(4):320–30. doi: 10.1056/NEJMoa1412082
30. Yoon HH, Shi Q, Heying EN, Muranyi A, Bredno J, Ough F, et al. Intertumoral Heterogeneity of CD3(+) and CD8(+) T-Cell Densities in the Microenvironment of DNA Mismatch-Repair-Deficient Colon Cancers: Implications for Prognosis. *Clin Cancer Res* (2019) 25(1):125–33. doi: 10.1158/1078-0432.CCR-18-1984
31. Chiou SH, Sheu BC, Chang WC, Huang SC, Hong-Nerng H. Current Concepts of Tumor-Infiltrating Lymphocytes in Human Malignancies. *J Reprod Immunol* (2005) 67(1-2):35–50. doi: 10.1016/j.jri.2005.06.002
32. Taube JM, Anders RA, Young GD, Xu H, Sharma R, McMiller TL, et al. Colocalization of Inflammatory Response With B7-H1 Expression in Human Melanocytic Lesions Supports an Adaptive Resistance Mechanism of Immune Escape. *Sci Trans Med* (2012) 4(127):127ra37. doi: 10.1126/scitranslmed.3003689
33. Kim TK, Herbst RS, Chen L. Defining and Understanding Adaptive Resistance in Cancer Immunotherapy. *Trends Immunol* (2018) 39(8):624–31. doi: 10.1016/j.it.2018.05.001
34. Bremnes RM, Busund L-T, Kilvær TL, Andersen S, Richardsen E, Paulsen EE, et al. The Role of Tumor-Infiltrating Lymphocytes in Development, Progression, and Prognosis of Non–Small Cell Lung Cancer. *J Thorac Oncol* (2016) 11(6):789–800. doi: 10.1016/j.jtho.2016.01.015
35. Mariathasan S, Turley SJ, Nickles D, Castiglioni A, Yuen K, Wang Y, et al. TGFbeta Attenuates Tumour Response to PD-L1 Blockade by Contributing to Exclusion of T Cells. *Nature* (2018) 554(7693):544–8. doi: 10.1038/nature25501
36. Xiong D, Wang Y, Singavi AK, Mackinnon AC, George B, You M. Immunogenomic Landscape Contributes to Hyperprogressive Disease After Anti-PD-1 Immunotherapy for Cancer. *iScience* (2018) 9:258–77. doi: 10.1016/j.isci.2018.10.021
37. Morikawa M, Derynck R, Miyazono K. TGF-Beta and the TGF-Beta Family: Context-Dependent Roles in Cell and Tissue Physiology. *Cold Spring Harb Perspect Biol* (2016) 8(5):a021873. doi: 10.1101/cshperspect.a021873
38. Yang L, Pang Y, Moses HL. TGF-Beta and Immune Cells: An Important Regulatory Axis in the Tumor Microenvironment and Progression. *Trends Immunol* (2010) 31(6):220–7. doi: 10.1016/j.it.2010.04.002
39. Galluzzi L, Spranger S, Fuchs E, Lopez-Soto A. WNT Signaling in Cancer Immunosurveillance. *Trends Cell Biol* (2019) 29(1):44–65. doi: 10.1016/j.tcb.2018.08.005

Conflict of Interest: XDS is employed by 3D Medicines Inc.

The remaining authors declare that the research was conducted in the absence of any commercial or financial relationships that could be construed as a potential conflict of interest.

Publisher's Note: All claims expressed in this article are solely those of the authors and do not necessarily represent those of their affiliated organizations, or those of the publisher, the editors and the reviewers. Any product that may be evaluated in this article, or claim that may be made by its manufacturer, is not guaranteed or endorsed by the publisher.

Copyright © 2021 Zhou, Zhou, Yi, Shu, Wei, Chen, Shen and Qiu. This is an open-access article distributed under the terms of the Creative Commons Attribution License (CC BY). The use, distribution or reproduction in other forums is permitted, provided the original author(s) and the copyright owner(s) are credited and that the original publication in this journal is cited, in accordance with accepted academic practice. No use, distribution or reproduction is permitted which does not comply with these terms.

frontiers in Immunology

ORIGINAL RESEARCH
published: 10 November 2021
doi: 10.3389/fimmu.2021.697298

Immune Checkpoint Inhibitors With or Without Bone-Targeted Therapy in NSCLC Patients With Bone Metastases and Prognostic Significance of Neutrophil-to-Lymphocyte Ratio

Alberto Bongiovanni[1], Flavia Foca[2], Jessica Menis[3,4,5], Stefania Luigia Stucci[6], Fabrizio Artioli[7], Valentina Guadalupi[8], Maria Rosachiara Forcignanò[9], Manuela Fantini[10], Federica Recine[11], Laura Mercatali[1], Chiara Spadazzi[1], Marco Angelo Burgio[12], Valentina Fausti[1], Anna Miserocchi[2] and Toni Ibrahim[1]*

[1] Osteoncology and Rare Tumors Center (CDO-TR), IRCCS Istituto Romagnolo per lo Studio dei Tumori (IRST) "Dino Amadori", Meldola, Italy, [2] Unit of Biostatistics and Clinical Trials, IRCCS Istituto Romagnolo per lo Studio dei Tumori (IRST) "Dino Amadori", Meldola, Italy, [3] Department of Surgery, Oncology and Gastroenterology, University of Padova, Padova, Italy, [4] Medical Oncology Department, Istituto Oncologico Veneto IRCCS, Padova, Italy, [5] Medical Oncology, Department of Medicine, University of Verona, Azienda Ospedaliera Universitaria Integrata (AOUI) di Verona, Verona, Italy, [6] Medical Oncology Unit, Policlinico Hospital of Bari Department of Biomedical Sciences and Human Oncology University of Bari "A. Moro", Bari, Italy, [7] Division of Medical Oncology, Ramazzini Hospital, Carpi, Italy, [8] IRCCS National Cancer Institute (INT), Milan, Italy, [9] UOC di Oncologia Medica Ospedale Sacro cuore di Gesù, Gallipoli, Italy, [10] Oncology Unit, Infermi Hospital, Rimini, Italy, [11] San Camillo De Lellis Hospital, ASL Rieti, Rieti, Italy, [12] Department of Medical Oncology, IRCCS Istituto Romagnolo per lo Studio dei Tumori (IRST) "Dino Amadori", Meldola, Italy*

OPEN ACCESS

Edited by:
Hubing Shi,
Sichuan University, China

Reviewed by:
Francesca Colonese,
San Gerardo Hospital, Italy
Daniele Santini,
Campus Bio-Medico University, Italy

***Correspondence:**
Alberto Bongiovanni
alberto.bongiovanni@irst.emr.it

Specialty section:
This article was submitted to Cancer Immunity and Immunotherapy, a section of the journal Frontiers in Immunology

Received: *19 April 2021*
Accepted: *08 October 2021*
Published: *10 November 2021*

Citation:
Bongiovanni A, Foca F, Menis J, Stucci SL, Artioli F, Guadalupi V, Forcignanò MR, Fantini M, Recine F, Mercatali L, Spadazzi C, Burgio MA, Fausti V, Miserocchi A and Ibrahim T (2021) Immune Checkpoint Inhibitors With or Without Bone-Targeted Therapy in NSCLC Patients With Bone Metastases and Prognostic Significance of Neutrophil-to-Lymphocyte Ratio. Front. Immunol. 12:697298. doi: 10.3389/fimmu.2021.697298

Introduction: Bone metastases (BMs) are a negative prognostic factor in patients with non-small cell lung cancer (NSCLC). Although immune-checkpoint inhibitors (ICIs) have dramatically changed the therapeutic landscape of NSCLC, little information is available on BMs from NSCLC treated with ICIs alone or in association with bone-targeted therapy (BTT) such as zoledronate or denosumab.

Methods: From 2014 to 2020, 111 of the 142 patients with BMs secondary to NSCLC extrapolated from the prospective multicenter Italian BM Database were eligible for analysis. Information on blood count, comorbidities, and toxicity was retrospectively collected. The neutrophil-to-lymphocyte ratio (NLR) pre- and post-treatment was calculated. Survival was analyzed using the Kaplan–Meier method, with statistical significance of survival differences assessed using the log-rank test.

Results: Median age was 66 (range, 42–84) years. Performance status (PS) Eastern Cooperative Oncology Group (ECOG) was 0–1 in 79/111 patients. The majority of patients (89.2%) had adenocarcinoma histology. At a median follow-up of 47.4 months, median progression-free (mPFS) and overall survival (mOS) was 4.9 (95%CI, 2.8–10.0) and 11.9 (95%CI, 8.2–14.4) months, respectively. Forty-six (43.4%) patients with BM NSCLC underwent first- or further-line therapy with ICIs: 28 (60.8%) received nivolumab, 9 (19.6%)

pembrolizumab, and 9 (19.6%) atezolizumab. Of the 46 patients treated with ICIs, 30 (65.2%) underwent BTT: 24 (80.0%) with zoledronate and 6 (20.0%) with denosumab. The ICI-alone group had an mOS of 15.8 months [95%CI, 8.2–not evaluable (NE)] *vs*. 21.8 months (95%CI, 14.5–not evaluable) for the ICI plus BTT group and 7.5 (95%CI, 6.1–10.9) months for the group receiving other treatments ($p < 0.001$). NLR ≤5 had a positive impact on OS.

Conclusion: BTT appears to have a synergistic effect when used in combination with ICIs, improving patient survival.

Keywords: immune checkpoint inhibitors, NSCLC, bone metastases, zoledronate, denosumab, lung cancer

INTRODUCTION

Lung cancer remains, independently of gender, one of the leading causes of cancer death worldwide (1). Despite the therapeutic breakthrough following the development of molecular-targeted therapies and immune checkpoint inhibitors (ICIs), the prognosis of patients with metastatic disease, albeit highly variable, remains poor (2). Previous studies and routine clinical practice have confirmed that ICIs show good tolerance and clinical efficacy in patients with advanced or recurrent non-small cell lung cancer (NSCLC) in both first- and further-line settings (3–9). Nevertheless, the effect on specific subgroups warrants further investigation.

The bone is one of the most common sites of metastasis in NSCLC, with 30–66% of patients developing bone metastases (BMs) during the course of their disease (10). BMs usually appear as mainly lytic, mainly osteoblastic, or mixed lesions and are excluded from Response Evaluation Criteria in Solid Tumors (RECIST) because they are difficult to measure (11). For this reason, in 2004, Hamaoka et al. developed the MD Anderson response classification criteria (MDA criteria), which are specific for the assessment of BMs (12, 13).

Recently, a negative effect of BMs was seen in large populations of NSCLC patients treated with nivolumab, independently of the presence of brain or liver metastases or of poor Performance Status (PS) (14, 15). One explanation for this may be related to the immunosuppressive status of the tumor microenvironment (TME), which, in some patients, cannot be effectively reversed after ICI therapy (16).

In a preclinical breast cancer mouse model, a combination of anti-PD-1 antibody plus zoledronic acid induced a better antitumor response than untreated controls or single-agent treatment, without significant toxicity (17). The RANKL/RANK signaling pathway also appears to modulate the immune microenvironment and enhance the efficacy of anti-CTLA-4 and anti-PD-1 monoclonal antibodies against solid tumors. This positive synergistic effect has also been suggested in real-world studies on patients with metastatic melanoma and NSCLC (18, 19).

In addition to PD-L1 expression, tumor mutational burden, and mismatch repair deficiency or microsatellite instability, several other potential biomarkers have been investigated or are currently under evaluation (20). Despite the large-scale use of immunotherapy in early and advanced NSCLC, there are still no validated or reliable predictive biomarkers of response or resistance to immunological agents (2).

Although some authors have reported a predictive and prognostic role of the neutrophil-to-lymphocyte ratio (NLR) in patients with advanced NSCLC undergoing different systemic treatments, its role in NCSLC patients with BMs has yet to be clarified (21–26).

Given the above premises, we decided to investigate the efficacy and safety of ICIs in NSCLC patients with BMs treated with zoledronate or denosumab, usually referred to as bone-targeted therapy (BTT). We also explored the relationship between bone response and tumor control in patients treated with ICIs and evaluated the potential predictive and prognostic role of NLR in this population.

MATERIAL AND METHODS

Study Design, Patients, and Treatment

The present analysis was performed on information extrapolated from our Bone Metastasis Database (BMDB) and from retrospectively collected data. The Italian BMDB was a prospective, observational multicenter project designed to collect data on BMs from solid tumors. Details on the project and its main inclusion and exclusion criteria have been described elsewhere (27).

Briefly, we extrapolated data on patients aged ≥18 years, with a histological or cytological diagnosis of NSCLC, treated for advanced disease, and with Eastern Cooperative Oncology Group (ECOG) Performance Status (PS). Patients included in the analysis had received at least one dose of ICIs as first- or further-line treatment. Blood count, comorbidities, presence of brain metastases, and safety information were retrospectively collected. NLR was calculated by dividing neutrophils and lymphocytes measured in peripheral blood. We recorded the NLR before ICI +/– BTT treatment and at response. This study was conducted in accordance with the International Conference of Harmonization Guidelines for Clinical Practice and the principles laid down in the 1964 Declaration of Helsinki. The protocol was approved by the Institutional Review Board of each participating center. All patients provided written informed consent.

Outcome Measures

Tumor response was assessed using RECIST criteria version 1.1 (28). Investigator-assessed progression-free survival (PFS) and

overall survival (OS) were evaluated. OS was calculated for all patients as the time between the fist diagnosis of BM and the date of death or date of last follow-up visit. PFS was calculated for the subgroup of patients undergoing ICI +/– BTT as the time from the start of treatment until the first documented evidence of progressive disease (PD) or death, whichever occurred first. Patients were monitored for adverse events (AEs) using the National Cancer Institute Common Terminology Criteria for Adverse Events v4.0. MDA criteria were used to evaluate bone response (12, 29). A multidisciplinary group dedicated to bone evaluation was involved to better clarify the bone response (30).

Statistical Analysis

Objective response rate (ORR), PFS, OS, and safety were assessed. Reverse Kaplan–Meier method was used to estimate median follow-up. Efficacy and safety analyses were conducted on all patients who received at least one ICI dose. The chi-square test was used to evaluate the association between patient characteristics and ORR. PFS and OS were estimated using the Kaplan–Meier method, and 95% confidence intervals (95%CIs) were reported. Differences between survival curves were evaluated with the log-rank test. The Wilcoxon signed-rank test was used to compare pre- and post-treatment NLR values.

RESULTS

Patient Characteristics

From January 2014 to December 2020, 142 patients with BMs were selected from the lung cancer cohort of our BMDB, and 111 (78.2%) were eligible for analysis. Median age was 66 years (range, 42–84). Forty-six (43.4%) of the 111 patients had been treated with an ICI, 28 (60.8%) with nivolumab, 9 (19.6%) with pembrolizumab, and 9 (19.6%) with atezolizumab (**Figure 1**). Thirty-five patients only had one comorbidity (cardiovascular), while 44 patients had more than one comorbidity (**Table 1** and **Supplementary Table S1**).

Twenty (18.0%) patients only had BMs. Of those with both BMs and visceral metastases (n = 91, 81.9%), 18 (22.0%) also had brain lesions. The majority of patients had mainly osteolytic BMs (n = 77, 77.0%), 6 (6.0%) had mainly osteoblastic BMs, and 17 (17.0%) had mixed BMs. This information was not available for 11 patients. Fifty-four (48.7%) patients had multiple (>6) bone metastases, 33 (29.7%) had two to six BMs, and 24 (21.6%) had only one BM. Only five patients (11.6%) received bone radiotherapy (**Supplementary Table S2**).

We also recorded information on the molecular profile of tumors. Epidermal growth factor receptor (EGFR) mutation was

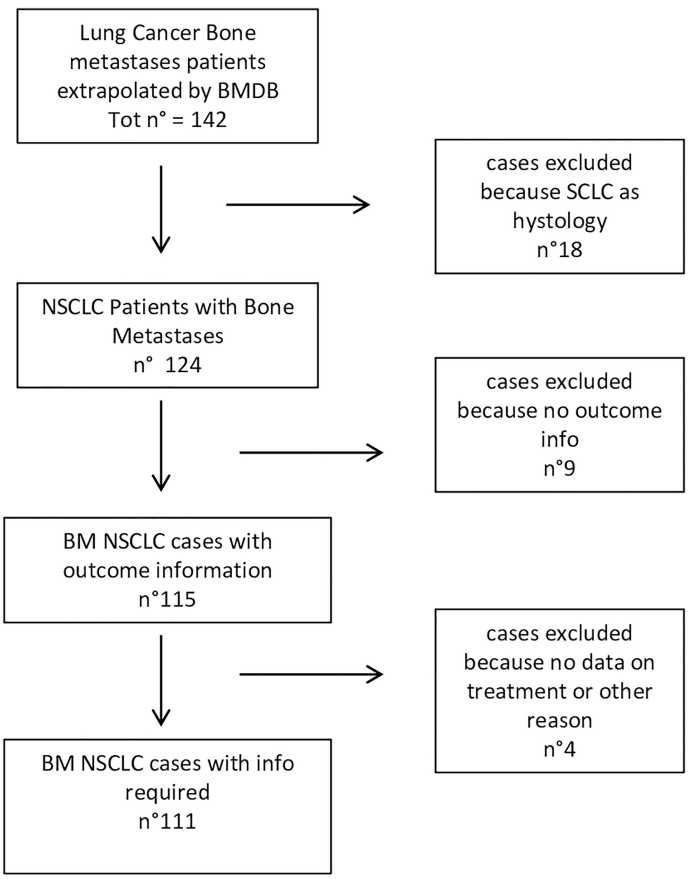

FIGURE 1 | Flow chart of patient selection.

TABLE 1 | Demographics and clinical characteristics of NSCLC patients (n = 111).

	Patients (n = 111)
Median age, years, at diagnosis of first bone metastasis (range)	**66 (42–84)**
	No. (%)
Age (years) at diagnosis of primary bone metastasis	
≤65	47 (42.3)
>65	64 (57.7)
Gender	
Male	70 (63.1)
Female	41 (36.9)
ECOG PS at diagnosis of first bone metastasis	
0	26 (30.6)
1	53 (62.4)
≥2	6 (7.0)
Unknown	26
Histology	
Adenocarcinoma	99 (89.2)
Squamous carcinoma	9 (8.1)
Large-cell carcinoma	1 (0.9)
Adenosquamous carcinoma	1 (0.9)
Undifferentiated	1 (0.9)
Grading (G)	
1	2 (4.1)
2	13 (26.5)
3	32 (65.3)
4	2 (4.1)
Unknown	62
Presence of visceral metastasis	
Yes	91 (82.0)
No	20 (18.0)
Presence of brain metastasis	
Yes	18 (22.0)
No	64 (78.0)
Unknown	29
Presence of comorbidity	
Cardiovascular	35 (42.2)
Cardiovascular + other*	10 (12.0)
Other§	5 (6.0)
None	33 (39.8)
Unknown	28

**Cardiovascular + other: 4 cardiovascular + diabetes; 1 cardiovascular + diabetes + renal impairment + other; 1 cardcardiovascular + diabetes + other; 2 cardiovascular + renal impairment; 2 cardiovascular + other.*
§Other: 2 diabetes, 1 renal impairment; 1 other, 1 diabetes + renal impairment.

present in 12 (12.5%) cases and wild type in 84 (87.5%). c-Ros oncogene 1 (ROS1) was rearranged in 3 (5.9%) patients and wild type in 48 (94.1%). Anaplastic lymphoma kinase (ALK) translocation was detected in 4 (5.6%) of the 67 patients in which it was evaluated. Ten (28.6%) of the 35 patients analyzed for KRAS (Kirsten rat sarcoma viral oncogene homolog) showed a mutation (**Table 2**).

Patient Outcome

At a median follow-up of 41.4 months, the median OS (mOS) of the entire population was 11.9 months (95%CI, 8.2–14.4). Of the 46 patient treated with ICIs, 30 (65.2%) underwent BTT, 24 (80.0%) with zoledronate, and 6 (20.0%) with denosumab. In all patients treated with ICI +/– BTT, the median PFS (mPFS) and mOS were 4.9 (95% CI, 2.8–10.0) and 19.2 (95%CI, 13.6–36.8) months, respectively.

TABLE 2 | Biological characteristics of NSCLC patients (n = 111).

	No. (%)
EGFR	
Mutated	12 (12.5)
Wild type	84 (87.5)
Not evaluated	12
Unknown	3
ALK	
Translocated	4 (5.6)
Wild type	67 (94.4)
Not evaluated	26
Unknown	14
ROS1	
Rearranged	3 (5.9)
Wild type	48 (94.1)
Not evaluated	30
Unknown	30
KRAS	
Mutated	10 (28.6)
Wild type	25 (71.4)
Not evaluated	48
Unknown	28
PDL1 (1)	
<50%	29 (76.3)
≥50%	9 (23.7)
Unknown	73
PDL1 (2)	
<1%	14 (36.8)
≥1%	24 (63.2)
Unknown	73

EGFR, epidermal growth factor receptor; ALK, anaplastic lymphoma kinase; ROS1, c-ros oncogene 1; KRAS, Kirsten rat sarcoma viral oncogene homolog; PDL1, programmed death-ligand 1.

No differences were seen according to the RECIST 1.1 criteria response in the two groups (**Supplementary Table S2**).

With regard to bone response evaluated using MD Anderson criteria, 10 (43.5%) patients obtained a partial response (PR) following ICIs plus BTT, while only 2 (16.7%) obtained the same response when treated with ICIs alone. In the latter group, stable disease (SD) as a response was more frequent than in the combination group ($p = 0.042$) (**Supplementary Table S3**).

Patients treated with ICIs plus BTT had an mOS of 21.8 months (95%CI, 14.5–NE) and a 24-month OS rate of 45.7% (95%CI, 26.5–62.9); those undergoing ICIs alone showed an mOS of 15.8 months (95%CI, 8.2–NE) and a 24-month OS of 30.8% (95%CI, 9.9–54.8); and the group receiving other treatments had an mOS of 7.5 months (95%CI, 6.1–10.9) and a 24-month OS of 12.2% (95%CI, 5.4–21.9). This difference was statistically significant ($p < 0.001$) (**Figure 2**).

There was no difference in PFS between patients treated or not with BTT, although those receiving denosumab (n = 6) had a better mPFS (15.9 months; 95%CI, 5.1–not estimable) than patients treated with ICIs alone or with zoledronate ($p = 0.068$).

Prognostic and Predictive Factors Evaluation

There were no differences in PFS and OS in relation to the number of BMs, type of BM, presence of visceral metastases, and age (**Figure 3**). ECOG PS had an impact on OS but not on PFS

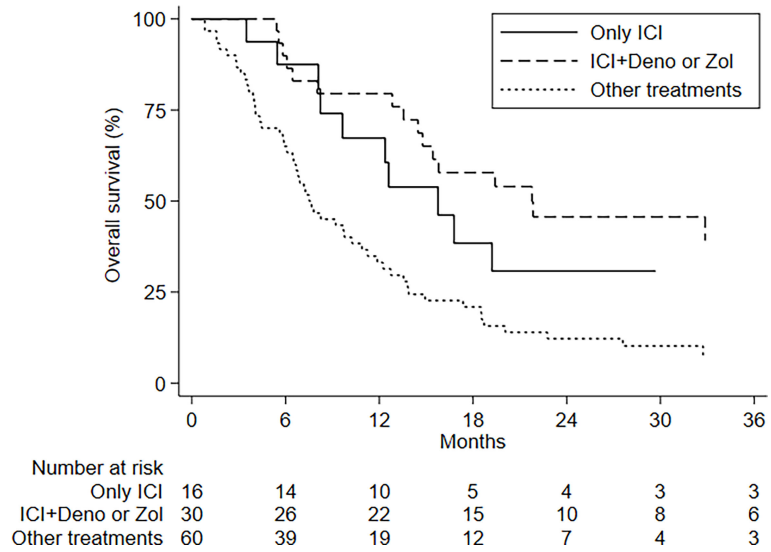

FIGURE 2 | OS by treatment.

(**Supplementary Table S5**). No differences in PFS and OS were seen in relation to PDL1 status and tumor molecular profile, with the exception of KRAS mutations; patients with KRAS-mutated disease had an mOS of 8 months (95%CI, 4.3–8.2–NE) compared to 38.8 months (95%CI, 13.9–NE) for those with KRAS wild-type tumors (**Figure 4** and **Tables 3**, **4**).

The mean NLR value in patients treated with ICI +/– BTT was 4.08 [standard deviation (SD), 1.83]. A statistically significant difference in OS was observed according to the basal value of NLR (**Figure 5A**). In particular, patients treated with ICIs alone or ICIs + BTT and with an NLR ≤5 had a better mOS (21.8 months; 95%CI, 15.4–NE) than those with an NLR >5 (14.5 months; 95%CI, 5.6–32.9). This difference was significant ($p = 0.042$) (**Supplementary Table S6**). There was also a positive trend for PFS, with an mPFS of 9.3 months (95%CI, 3.3–25.4) in the former group and 2.0 months (95%CI, 1.7–13.2) in the latter group (**Figure 5B**) ($p = 0.086$). However, patients who obtained PR or SD on ICIs +/– BTT showed a decrease in NLR with respect to NLR at best response [basal NLR value, 3.52 (SD, 1.56) *vs.* best response, 2.78 (SD, 1.64)] ($p = 0.030$) (**Supplementary**

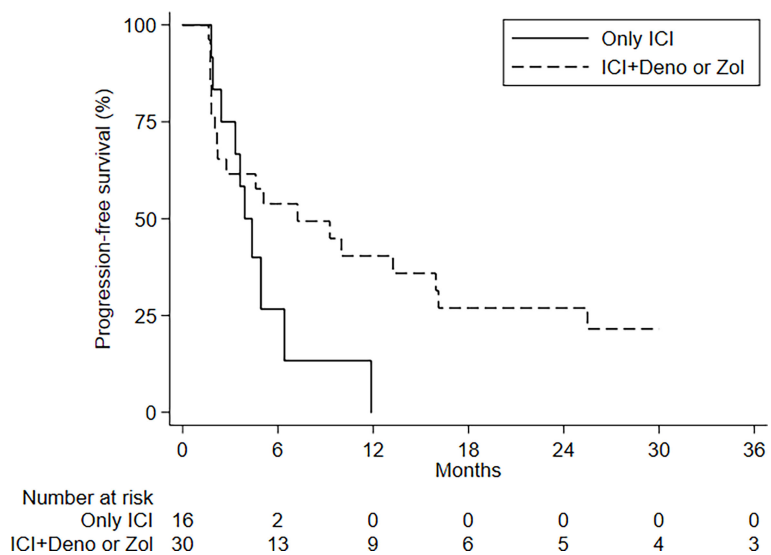

FIGURE 3 | PFS by treatment.

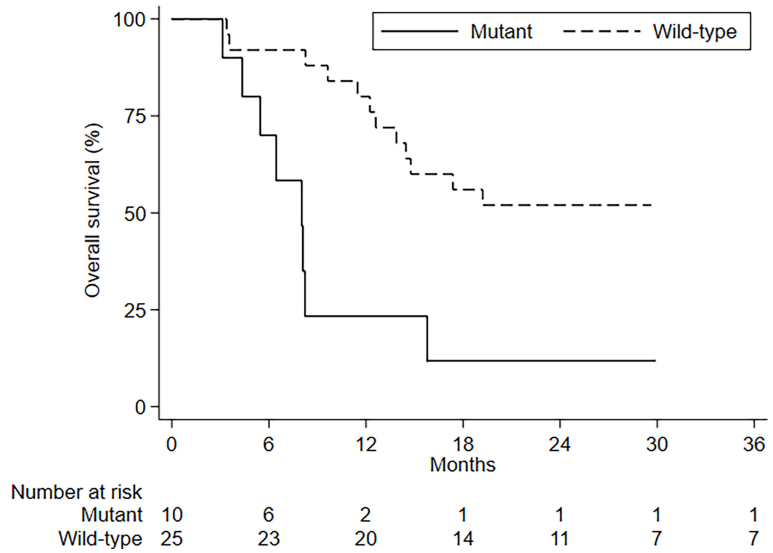

FIGURE 4 | OS by KRAS status.

Figure S1). Conversely, NLR increased in patients progressing after ICIs +/– BTT [mean basal NLR value, 3.65 (SD, 1.42) *vs.* 5.18 at progression (SD, 2.79)] ($p = 0.027$).

Safety

Patients treated with ICIs had mild and reversible toxicities (**Table 5**). In the combination group, six cases of grade (G)1 hypocalcemia, three cases of G1 renal toxicity, and one case of osteonecrosis of the jaw were reported. One case of G2 renal creatinine increase was recorded in the ICI-alone group. There were few cases of G3 toxicities (arthralgia, increased amylase and lipase, and dermatitis) related to ICI therapy, all of which were successfully resolved. The safety profile was consistent with literature data.

DISCUSSION

ICIs have dramatically changed the treatment of patients with NSCLC (2). However their immune-mediated antitumor activity is dependent on several complex mechanisms, also involving the microenvironment. In BMs, the microenvironment is represented by a particular landscape characterized by reciprocal interactions between cancer cells, local stromal cells, immune cells, and several other factors such as osteoclasts (members of the mononuclear-macrophage family) and cytokines (31).

The results from two large phase III studies, CheckMate 227 and CheckMate 057, not only suggested that bone involvement may be a negative prognostic factor in patients with metastatic NSCLC, but also that the presence of BMs could be predictive of a poor response to ICIs (32, 33). However, none of the randomized trials on immunotherapy, including CheckMate 227, stratified patients on the basis of the site of metastasis, thus precluding any definitive conclusions from being drawn (34).

In our study, the poor outcome of NSCLC patients with bone metastases was confirmed in patients treated or not with ICIs, the latter showing an mOS of 7.8 months.

This interest in defining the role of immunotherapy on the basis of the site of metastasis and, in particular, the bone (10–12) prompted us to explore this area using data extrapolated from the Italian BMDB. A strong point in our favor is that the characteristics, outcome, and safety data of the patients who received ICIs are consistent with literature data (35), thanks to the multicenter nature of our BMDB, the largest of its kind in Italy.

A recent study stressed the concept of the negative modulation of the immune response by BMs in NSCLC (15). However, data on the concomitant use of BTTs were not collected. The hypothesis of the potential immunomodulatory effect of BTTs such as denosumab and zoledronate has been gaining ground worldwide over the past two decades.

There is evidence from preclinical research into prostate cancer and breast cancer mouse models of the immunomodulatory effect of zoledronate and of its enhancement of the antitumor efficacy of the PD-1 blockade (17). Nitrogen-containing bisphosphonates (N-BPs) such as zoledronate inhibit farnesyl pyrophosphate synthesis in the mevalonate pathway, leading to increased levels of isopentenyl pyrophosphate in tumor cells, which renders them targets of Vγ9Vδ2 T cells, and thus contributing to innate immunity (36).

Although denosumab added to chemotherapy did not modify OS with respect to CT alone in the phase III SPLENDOUR trial, we observed that both zoledronate and denosumab improved ICI efficacy with respect to ICI alone, with a sustained OS and an increased bone response rate evaluated by MD Anderson criteria.

TABLE 3 | Univariable analysis of overall survival.

	No. patients	No. events	Median OS (95%CI)	12-month OS (95%CI)	24-month OS (95%CI)	*p*-valuelog-rank test
Overall no. patients	111	88	11.9 (8.2–14.4)	49.7 (40.0–58.7)	24.0 (16.3–32.6)	–
Age, years, at first diagnosis of BM						
<65	47	36	13.9 (8.0–18.6)	56.4 (40.8–69.3)	29.1 (16.7–42.8)	0.235
≥65	64	52	10.3 (6.9–13.6)	45.0 (32.5–56.7)	20.4 (11.2–31.6)	
Gender						
Male	70	54	12.4 (8.0–15.4)	50.9 (38.5–61.9)	21.6 (12.6–32.2)	0.842
Female	41	34	11.9 (5.8–15.8)	47.7 (31.7–62.1)	28.4 (15.2–43.1)	
ECOG at first diagnosis of BM						
0	26	14	32.9 (12.8–NE)	76.9 (55.7–88.9)	57.2 (36.1–73.6)	0.002
1	53	42	12.6 (7.2–15.4)	53.6 (39.1–66.0)	20.6 (10.4–33.1)	
≥2	6	6	5.6 (3.9–NE)	16.7 (0.7–51.7)	0	
Treatment						
ICI alone	16	11	15.8 (8.2–NE)	63.0 (38.3–84.9)	30.8 (9.9–54.8)	<0.001
ICI+Deno/Zol	30	17	21.8 (14.5–NE)	79.5 (59.9–90.2)	45.7 (26.5–62.9)	
No ICI	60	55	7.5 (6.1–10.9)	33.1 (21.5–45.1)	12.2 (5.4–21.9)	
Visceral metastasis						
No	20	16	14.9 (5.8–27.6)	53.6 (29.6–72.6)	37.5 (16.9–58.2)	0.413
Yes	91	72	11.9 (8.2–13.8)	48.9 (38.1–58.7)	20.9 (13.0–30.2)	
No. BMs						
1	24	19	15.4 (7.5–19.4)	59.9 (36.9–76.8)	23.0 (8.4–41.8)	0.761
2–6	33	26	9.8 (6.5–13.8)	48.5 (30.8–64.0)	25.9 (12.4–41.7)	
>6	54	43	10.9 (6.7–15.8)	46.1 (32.4–58.7)	23.1 (12.5–35.6)	
Type of bone lesion						
Osteoblastic	6	6	14.9 (1.6–NE)	66.7 (19.5–90.4)	–	0.386
Lytic	77	57	11.5 (8.2–15.8)	49.6 (37.8–60.3)	29.6 (19.6–40.3)	
Mixed	17	15	9.8 (5.4–15.4)	47.1 (22.9–67.9)	17.7 (4.3–38.3)	
EGFR status						
Mutated	12	10	12.2 (5.6–NE)	58.3 (27.0–80.1)	25.0 (6.0–50.5)	0.937
Wild type	84	65	12.6 (8.0–14.9)	50.3 (39.0–60.5)	25.4 (16.3–35.4)	
ALK status						
Translocated	4	2	–	–	–	–
Wild type	67	52	12.7 (8.2–14.9)	54.3 (41.5–65.4)	26.5 (16.3–37.9)	
ROS1 status						
Rearranged	3	2	–	–	–	
Wild type	48	32	13.9 (11.5–22.8)	63.6 (48.1–75.6)	35.8 (22.1–49.8)	
KRAS status						
Mutant	10	8	8.0 (3.1–15.8)	23.3 (3.6–52.9)	11.7 (0.6–40.1)	0.005
Wild type	25	15	36.8 (13.9–NE)	80.0 (58.4–91.2)	52.0 (31.3–69.2)	
PDL1 (1)						
<50%	29	19	15.7 (12.6–48.6)	78.8 (58.7–89.8)	37.7 (19.9–55.4)	0.995
≥50%	9	4	13.9 (5.4–NE)	63.5 (23.8–86.6)	47.6 (12.3–76.9)	
PDL1 (2)						
<1%	14	8	15.8 (13.6–NE)	100.0	42.8 (17.7–66.0)	0.275
≥1%	24	15	12.8 (8.2–NE)	59.4 (36.3–76.5)	38.2 (17.7–58.5)	
Mutational status (1)						
EGFR mutated	12	10	12.2 (5.6–NE)	58.3 (27.0–80.0)	25.0 (6.0–50.5)	0.114
ALK translocated	4	2	–			
KRAS mutated	10	8	8.0 (4.3–15.8)	23.3 (3.6–52.9)	11.7 (0.6–40.0)	
ROS1 rearranged	3	2	–			
EGFR, ALK, KRAS and ROS1 wild type	14	10	14.7 (9.6–NE)	71.4 (40.6–88.2)	42.9 (17.7–66.0)	
Mutational status (2)						
EGFR mutated or ALK translocated or ROS1 rearranged	19	14	17.4 (9.7–48.6)	73.7 (47.9–88.1)	36.8 (16.5–57.5)	0.778
None	36	24	14.5 (9.6–27.2)	62.5 (44.2–76.3)	37.3 (21.1–53.4)	

PFS, progression-free survival; 95%CI, 95% confidence interval; ECOG PS, Eastern Cooperative Oncology Group Performance Status; BM, bone metastasis; ICI, immune checkpoint inhibitor; Deno, denosumab; Zol, zoledronate; NE, not estimable; EGFR, epidermal growth factor receptor; ALK, anaplastic lymphoma kinase; ROS1, c-ros oncogene 1; KRAS, Kirsten rat sarcoma viral oncogene homolog; PDL1, programmed death-ligand 1.

Conversely, consistent with data from clinical trials on ICIs, PFS in our patients was not improved (19, 37).

Another point to be explored is that bone response seems to be correlated to medical therapy due to the low rate of patients treated with radiotherapy.

Bearing in mind the caveat of the limited number of patients involved in our study, we nonetheless observed that denosumab worked rapidly, whereas zoledronate exerted its action after at least 6 months, which fits in with the known slow effect of this drug on bone homeostasis (38). These data strongly suggest that

TABLE 4 | Univariable analysis of progression-free survival.

	No. patients	No. events	Median PFS (95%CI)	6-month PFS (95%CI)	12-month PFS (95%CI)	*p*-valuelog-rank test
Overall no. patients	46	30	4.9 (2.8–10.0)	47.4 (29.9–61.4)	29.9 (15.5–45.6)	–
Age, years, at first diagnosis of BM						
<65	18	11	6.4 (2.0–11.9)	57.1 (28.4–77.9)	11.4 (0.7–39.0)	0.698
≥65	28	19	4.6 (2.2–15.9)	40.6 (21.1–59.3)	36.1 (17.6–55.0)	
Gender						
Male	35	23	4.9 (2.2–10.0)	47.3 (28.3–64.2)	25.8 (10.9–34.7)	0.451
Female	11	7	5.1 (2.0–38.1)	44.4 (13.6–71.9)	44.4 (13.6–71.9)	
ECOG PS at first diagnosis of BM						
0	15	9	7.2 (2.1–NE)	54.5 (22.9–77.9)	21.8 (3.5–50.1)	0.955
1	29	21	4.9 (1.9–13.3)	43.5 (24.5–61.1)	33.8 (16.3–52.3)	
≥2	2	0	–	–	–	
Treatment						
Only ICIs	16	10	3.9 (1.9–6.4)	26.7 (5.1–55.6)	–	0.068
ICI+Deno	6	4	15.9 (5.1–NE)	83.3 (27.3–97.5)	66.7 (19.5–90.4)	
ICI+Zol	24	16	2.7 (1.8–13.3)	45.0 (23.1–65.7)	32.1 (12.8–53.4)	
Presence of visceral metastasis						
No	7	2	–	–	–	–
Yes	39	28	4.6 (2.2–9.3)	43.6 (26.7–59.3)	29.1 (14.4–45.5)	
No. BMs						
1	11	8	4.3 (1.7–16.1)	50.0 (18.4–75.3)	25.0 (4.1–54.9)	0.343
2–6	15	8	4.9 (2.4–NE)	45.5 (16.7–70.7)	36.4 (11.2–62.7)	
>6	20	14	5.1 (2.2–13.3)	45.4 (20.9–67.2)	27.2 (7.4–52.1)	
Type of bone lesion						
Osteoblastic	1	0	–	–	–	–
Lytic	38	24	6.4 (3.6–11.9)	51.9 (33.3–67.7)	31.9 (15.8–49.4)	
Mixed	6	5	1.8 (1.7–NE)	20.0 (0.8–58.2)	20.0 (0.8–58.2)	
Unknown	1	1	–	–	–	
EGFR status						
Mutant	1	0	–	–	–	–
Wild–type	38	24	5.1 (2.2–11.9)	47.8 (29.5–64.0)	31.9 (15.8–49.2)	
ALK status						
Translocated	0	–	–	–	–	–
Wild type	35	22	4.9 (2.4–9.3)	44.7 (26.5–62.2)	29.8 (13.1–48.6)	
ROS1 status						
Rearranged	1	–	–	–	–	–
Wild–type	30	20	5.1 (2.7–13.3)	48.1 (27.7–65.9)	32.1 (14.1–51.7)	
KRAS status						
Mutant	8	3	4.9 (1.7–NE)	44.4 (6.6–78.5)	44.4 (6.6–78.5)	0.565
Wild-type	13	11	7.2 (2.4–11.9)	61.5 (30.8–81.8)	20.5 (33.3–47.8)	
PDL1 (1)						
<50%	23	15	4.4 (2.2–7.2)	37.1 (16.3–58.2)	14.9 (2.6–36.8)	0.810
≥50%	7	6	5.1 (1.7–NE)	42.8 (9.8–73.4)	42.8 (9.8–73.4)	
PDL1 (2)						
<1%	12	8	4.6 (1.6–9.3)	50.0 (18.4–75.3)	12.5 (0.7–41.8)	0.941
≥1%	18	13	4.3 (2.2–13.3)	30.9 (10.5–54.3)	30.9 (10.5–54.3)	

PFS, progression-free survival; 95%CI, 95% confidence interval; ECOG PS, Eastern Cooperative Oncology Group Performance Status; BM, bone metastasis; ICI, immune checkpoint inhibitor; Deno, denosumab; Zol, zoledronate; NE, not estimable; EGFR, epidermal growth factor receptor; ALK, anaplastic lymphoma kinase; ROS1, c-ros oncogene 1; KRAS, Kirsten rat sarcoma viral oncogene homolog; PDL1, programmed death-ligand 1.

targeting the microenvironment to improve the efficacy of immunotherapy is a strategy worth considering. Another important indication comes from the NLR evaluated in our population. In patients with BMs from NSCLC receiving ICIs, an NLR cutoff ≤5 showed prognostic significance. Furthermore, this value changed in conjunction with a change in sensitivity to therapy, increasing in the event of disease progression or decreasing when response occurred (35).

Our study has a number of limitations, mainly that of limited sample size and the retrospective nature of the analysis (of note, the BMDA was prospectively built). Moreover, PD-L1 expression was not available for all patients. Despite these weaknesses, our data support the hypothesis that BTTs increase the activity of ICIs and reverse the negative impact of BMs on patient outcome. Larger prospective datasets or prospective randomized clinical trials are needed to provide more solid evidence of BTT potential.

There are still several open questions to be answered in the area of NSCLC, in particular how to overcome primary and acquired resistance to immunotherapy. This is often related to the status of the host's immune homeostasis and involves myeloid-derived suppressor cells (MDSCs), tumor-associated macrophages, and T-regulatory cells, all of which play immune-suppressive roles. The use of zoledronate or

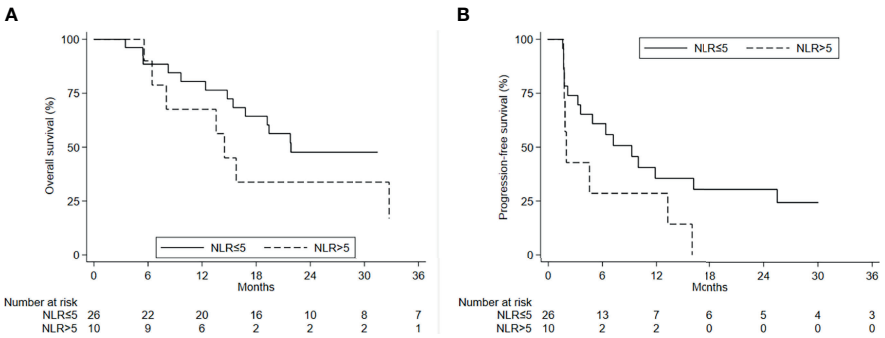

FIGURE 5 | **(A)** OS and **(B)** PFS by NLR values.

TABLE 5 | Toxicities recorded in both ICI and ICI+BTT treatments.

Toxicity	Grade			Total No. (%)
	1No. (%)	2No. (%)	3No. (%)	
Arthralgia	1 (2.2)	0 (0.0)	1 (2.2)	2 (4.3)
Asthenia	2 (4.3)	0 (0.0)	1 (2.2)	3 (6.5)
Dermatitis	0 (0.0)	0 (0.0)	1 (2.2)	1 (2.2)
Diarrhea	2 (4.3)	1 (2.2)	0 (0.0)	3 (6.5)
Dypnea	0 (0.0)	1 (2.2)	0 (0.0)	1 (2.2)
Infection	0 (0.0)	1 (2.2)	0 (0.0)	1 (2.2)
Creatinine increase	5 (10.9)	1 (2.2)	0 (0.0)	6 (13.0)
Hyperamylasemia	1 (2.2)	0 (0.0)	1 (2.2)	2 (4.3)
Hypertransaminasemia	2 (4.3)	0 (0.0)	1 (2.2)	3 (6.5)
Hypophosphatemia	0 (0.0)	1 (2.2)	0 (0.0)	1 (2.2)
Hypothyroidism	1 (2.2)	0 (0.0)	0 (0.0)	1 (2.2)
Neuropathy	0 (0.0)	1 (2.2)	0 (0.0)	1 (2.2)
Neutropenia	0 (0.0)	1 (2.2)	0 (0.0)	1 (2.2)
Pneumonitis	0 (0.0)	2 (4.3)	0 (0.0)	2 (4.3)
Skin rash	1 (2.2)	1 (2.2)	0 (0.0)	2 (4.3)
Lipase increase	1 (2.2)	0 (0.0)	1 (2.2)	2 (4.3)
Sepsis	0 (0.0)	0 (0.0)	1 (2.2)	1 (2.2)
Skin toxicity	0 (0.0)	0 (0.0)	1 (2.2)	1 (2.2)

denosumab in combination with ICIs could represent a potentially useful strategy to modulate the microenvironment and, consequently, the immune response.

CONCLUSIONS

Our data suggest that BTT could potentially increase the efficacy of immunotherapy in NSCLC patients with BMs. Prospective trials are warranted to further investigate this finding.

DATA AVAILABILITY STATEMENT

The raw data supporting the conclusions of this article will be made available by the authors, without undue reservation.

ETHICS STATEMENT

This study was reviewed and approved by the IRCCS IRST Ethics Committee (number of approval 1783/2014 of 20/03/2014). The patients/participants provided their written informed consent to participate in this study.

AUTHOR CONTRIBUTIONS

AB and TI conceived the idea for and designed the study. AB, JM, SS, FA, FR, VG, MRF, MB, and MF enrolled patients. FF performed the statistical analyses. VF, LM, and CS carried out the literature review. AB drafted the manuscript. All authors critically reviewed the manuscript, providing important feedback, and all read and approved the final version for submission.

SUPPLEMENTARY MATERIAL

The Supplementary Material for this article can be found online at: https://www.frontiersin.org/articles/10.3389/fimmu.2021.697298/full#supplementary-material

Supplementary Figure 1 | Differences between pre-treatment NLR values and NLR values **(A)** at disease progression (*p*-value from Wilcoxon signed-rank test: 0.027) and **(B)** at response (*p*-value from Wilcoxon signed-rank test: 0.030).

REFERENCES

1. Malvezzi M, Bertuccio P, Rosso T, Rota M, Levi F, La Vecchia C, et al. European Cancer Mortality Predictions for the Year 2015: Does Lung Cancer Have the Highest Death Rate in EU Women? *Ann Oncol* (2015) 26(4):779–86. doi: 10.1093/annonc/mdv001
2. Zappa C, Mousa SA. Non-Small Cell Lung Cancer: Current Treatment and Future Advances. *Transl Lung Cancer Res* (2016) 5(3):288–300. doi: 10.21037/tlcr.2016.06.07
3. Reck M, Rodríguez-Abreu D, Robinson AG, Hui R, Csőszi T, Fülöp A, et al. Pembrolizumab *Versus* Chemotherapy for PD-L1-Positive Non-Small-Cell Lung Cancer. *N Engl J Med* (2016) 375(19):1823–33. doi: 10.1056/NEJMoa1606774
4. Gandhi L, Rodríguez-Abreu D, Gadgeel S, Esteban E, Felip E, De Angelis F, et al. Pembrolizumab Plus Chemotherapy in Metastatic Non-Small-Cell Lung Cancer. *N Engl J Med* (2018) 378(22):2078–92. doi: 10.1056/NEJMoa1801005
5. Socinski MA, Jotte RM, Cappuzzo F, Orlandi F, Stroyakovskiy D, Nogami N, et al. Atezolizumab for First-Line Treatment of Metastatic Nonsquamous

NSCLC. *N Engl J Med* (2018) 378(24):2288–301. doi: 10.1056/NEJMoa1716948
6. Herbst RS, Baas P, Kim DW, Felip E, Pérez-Gracia JL, Han JY, et al. Pembrolizumab *Versus* Docetaxel for Previously Treated, PD-L1-Positive, Advanced Non-Small-Cell Lung Cancer (KEYNOTE-010): A Randomised Controlled Trial. *Lancet* (2016) 387(10027):1540–50. doi: 10.1016/S0140-6736(15)01281-7
7. Rittmeyer A, Barlesi F, Waterkamp D, Park K, Ciardiello F, von Pawel J, et al. Atezolizumab *Versus* Docetaxel in Patients With Previously Treated Non-Small-Cell Lung Cancer (OAK): A Phase 3, Open-Label, Multicentre Randomised Controlled Trial. *Lancet* (2017) 389(10066):255–65. doi: 10.1016/S0140-6736(16)32517-X
8. Borghaei H, Paz-Ares L, Horn L, Spigel DR, Steins M, Ready NE, et al. Nivolumab *Versus* Docetaxel in Advanced Nonsquamous Non-Small-Cell Lung Cancer. *N Engl J Med* (2015) 373(17):1627–39. doi: 10.1056/NEJMoa1507643
9. Brahmer J, Reckamp KL, Baas P, Crinò L, Eberhardt WE, Poddubskaya E, et al. Nivolumab *Versus* Docetaxel in Advanced Squamous-Cell non-Small-Cell Lung Cancer. *N Engl J Med* (2015) 373(2):123–35. doi: 10.1056/NEJMoa1504627
10. Kuchuk M, Addison CL, Clemons M, Kuchuk I, Wheatley-Price P. Incidence and Consequences of Bone Metastases in Lung Cancer Patients. *J Bone Oncol* (2013) 2(1):22–9. doi: 10.1016/j.jbo.2012.12.004
11. Santini D, Barni S, Intagliata S, Falcone A, Ferraù F, Galetta D, et al. Natural History of Non-Small-Cell Lung Cancer With Bone Metastases. *Sci Rep* (2015) 5:18670. doi: 10.1038/srep18670
12. Hamaoka T, Costelloe CM, Madewell JE, Liu P, Berry DA, Islam R, et al. Tumour Response Interpretation With New Tumour Response Criteria *vs* the World Health Organisation Criteria in Patients With Bone-Only Metastatic Breast Cancer. *Br J Cancer* (2010) 102(4):651–7. doi: 10.1038/sj.bjc.6605546
13. Costelloe CM, Chuang HH, Madewell JE, Ueno NT. Cancer Response Criteria and Bone Metastases: RECIST 1.1, MDA and PERCIST. *J Cancer* (2010) 1:80–92. doi: 10.7150/jca.1.80
14. da Silva LM, da Silva GT, Bergmann A, Costa GJ, Zamboni MM, Santos Thuler LC. Impact of Different Patterns of Metastasis in Non-Small-Cell Lung Cancer Patients. *Future Oncol* (2021) 17(7):775–82. doi: 10.2217/fon-2020-0587
15. Landi L, D'Incà F, Gelibter A, Chiari R, Grossi F, Delmonte A, et al. Bone Metastases and Immunotherapy in Patients With Advanced Non-Small-Cell Lung Cancer. *J Immunother Cancer* (2019) 7(1):316. doi: 10.1186/s40425-019-0793-8
16. Sterling JA, Edwards JR, Martin TJ, Mundy GR. Advances in the Biology of Bone Metastasis: How the Skeleton Affects Tumor Behavior. *Bone* (2011) 48 (1):6–15. doi: 10.1016/j.bone.2010.07.015
17. Li Y, Du Y, Sun T, Xue H, Jin Z, Tian J. PD-1 Blockade in Combination With Zoledronic Acid to Enhance the Antitumor Efficacy in the Breast Cancer Mouse Model. *BMC Cancer* (2018) 18(1):669. doi: 10.1186/s12885-018-4412-8
18. Simatou A, Sarantis P, Koustas E, Papavassiliou AG, Karamouzis MV. The Role of the RANKL/RANK Axis in the Prevention and Treatment of Breast Cancer With Immune Checkpoint Inhibitors and Anti-RANKL. *Int J Mol Sci* (2020) 21(20):7570. doi: 10.3390/ijms21207570
19. Liede A, Hernandez RK, Wade SW, Bo R, Nussbaum NC, Ahern E, et al. An Observational Study of Concomitant Immunotherapies and Denosumab in Patients With Advanced Melanoma or Lung Cancer. *Oncoimmunology* (2018) 7(12):e1480301. doi: 10.1080/2162402X.2018.1480301
20. Havel JJ, Chowell D, Chan TA. The Evolving Landscape of Biomarkers for Checkpoint Inhibitor Immunotherapy. *Nat Rev Cancer* (2019) 19(3):133–50. doi: 10.1038/s41568-019-0116-x
21. Ishihara M, Ochiai R, Haruyama T, Sakamoto T, Tanzawa S, Honda T, et al. Pretreatment Neutrophil-to-Lymphocyte Ratio Predicts Treatment Efficacy and Prognosis of Cytotoxic Anticancer Drugs, Molecular Targeted Drugs, and Immune Checkpoint Inhibitors in Patients With Advanced non-Small Cell Lung Cancer. *Transl Lung Cancer Res* (2021) 10(1):221–32. doi: 10.21037/tlcr-20-777
22. Ksienski D, Wai ES, Alex D, Croteau NS, Freeman AT, Chan A, et al. Prognostic Significance of the Neutrophil-to-Lymphocyte Ratio and Platelet-to-Lymphocyte Ratio for Advanced Non-Small Cell Lung Cancer Patients With High PD-L1 Tumor Expression Receiving Pembrolizumab. *Transl Lung Cancer Res* (2021) 10(1):355–67. doi: 10.21037/tlcr-20-541
23. Bongiovanni A, Foca F, Fantini M, Forcignanò MR, Artioli F, Berardi R, et al. First Prospective Data on Breast Cancer Patients From the Multicentre Italian Bone Metastasis Database. *Sci Rep* (2021) 11(1):4329. doi: 10.1038/s41598-021-83749-1
24. Petrova MP, Eneva MI, Arabadjiev JI, Conev NV, Dimitrova EG, Koynov KD, et al. Neutrophil to Lymphocyte Ratio as a Potential Predictive Marker for Treatment With Pembrolizumab as a Second Line Treatment in Patients With Non-Small Cell Lung Cancer. *Biosci Trends* (2020) 14(1):48–55. doi: 10.5582/bst.2019.01279
25. Giustini N, Bazhenova L. Recognizing Prognostic and Predictive Biomarkers in the Treatment of Non-Small Cell Lung Cancer (NSCLC) With Immune Checkpoint Inhibitors (Icis). *Lung Cancer (Auckl)* (2021) 12:21–34. doi: 10.2147/LCTT.S235102
26. Fukui T, Okuma Y, Nakahara Y, Otani S, Igawa S, Katagiri M, et al. Activity of Nivolumab and Utility of Neutrophil-to-Lymphocyte Ratio as a Predictive Biomarker for Advanced Non-Small-Cell Lung Cancer: A Prospective Observational Study. *Clin Lung Cancer* (2019) 20(3):208–14.e2. doi: 10.1016/j.cllc.2018.04.021
27. Eisenhauer EA, Therasse P, Bogaerts J, Schwartz LH, Sargent D, Ford R, et al. New Response Evaluation Criteria in Solid Tumours: Revised RECIST Guideline (Version 1.1). *Eur J Cancer* (2009) 45(2):228–47. doi: 10.1016/j.ejca.2008.10.026
28. U.S. Department of Health and Human Services. *Common Terminology Criteria for Adverse Events (CTCAE) Version 4.0 Published: May 28, 2009 (V4.03: June 14, 2010)*. Available at: https://www.eortc.be/services/doc/ctc/ctcae_4.03_2010-06-14_quickreference_5x7.pdf.
29. Ibrahim T, Mercatali L, Amadori D. Bone and Cancer: The Osteoncology. *Clin Cases Miner Bone Metab* (2013) 10(2):121–3.
30. Bongiovanni A, Recine F, Fausti V, Foca F, Casadei R, Falasconi MC, et al. Ten-Year Experience of the Multidisciplinary Osteoncology Center. *Support Care Cancer* (2019) 27(9):3395–402. doi: 10.1007/s00520-019-4635-5
31. Hellmann MD, Ciuleanu TE, Pluzanski A, Lee JS, Otterson GA, Audigier-Valette C, et al. Nivolumab Plus Ipilimumab in Lung Cancer With a High Tumor Mutational Burden. *N Engl J Med* (2018) 378(22):2093–104. doi: 10.1056/NEJMoa1801946
32. Peters S, Cappuzzo F, Horn L, Paz-Ares L, Borghaei H, Barlesi F, et al. OA03.05 Analysis of Early Survival in Patients With Advanced non-Squamous NSCLC Treated With Nivolumab *vs* Docetaxel in Checkmate 057. *J Thor Oncol* (2017) 12(1):S253. doi: 10.1016/j.jtho.2016.11.241
33. Yang K, Li J, Bai C, Sun Z, Zhao L. Efficacy of Immune Checkpoint Inhibitors in Non-Small-Cell Lung Cancer Patients With Different Metastatic Sites: A Systematic Review and Meta-Analysis. *Front Oncol* (2020) 10:2020.01098. doi: 10.3389/fonc.2020.01098
34. Hsu ML, Naidoo J. Principles of Immunotherapy in Non-Small Cell Lung Cancer. *Thorac Surg Clin* (2020) 30(2):187–98. doi: 10.1016/j.thorsurg.2020.01.009
35. Silva-Santos B, Serre K, Norell H. γδ T Cells in Cancer. *Nat Rev Immunol* (2015) 15(11):683–91. doi: 10.1038/nri3904
36. Peters S, Danson S, Hasan B, Dafni U, Reinmuth N, Majem M, et al. A Randomized Open-Label Phase III Trial Evaluating the Addition of Denosumab to Standard First-Line Treatment in Advanced NSCLC: The European Thoracic Oncology Platform (ETOP) and European Organisation for Research and Treatment of Cancer (EORTC) SPLENDOUR Trial. *J Thorac Oncol* (2020) 15(10):1647–56. doi: 10.1016/j.jtho.2020.06.011
37. Daubiné F, Le Gall C, Gasser J, Green J. Antitumor Effects of Clinical Dosing Regimens of Bisphosphonates in Experimental Breast Cancer Bone Metastasis. *J Natl Cancer Inst* (2007) 99(4):322–30. doi: 10.1093/jnci/djk054
38. Dalle Carbonare L, Zanatta M, Gasparetto A, Valenti MT, Clézardin P. Safety and Tolerability of Zoledronic Acid and Other Bisphosphonates in Osteoporosis Management. *Drug Healthc Patient Saf* (2010) 2:121–37. doi: 10.2147/DHPS.S6285

Conflict of Interest: The authors declare that the research was conducted in the absence of any commercial or financial relationships that could be construed as a potential conflict of interest.

Publisher's Note: All claims expressed in this article are solely those of the authors and do not necessarily represent those of their affiliated organizations, or those of

the publisher, the editors and the reviewers. Any product that may be evaluated in this article, or claim that may be made by its manufacturer, is not guaranteed or endorsed by the publisher.

Copyright © 2021 Bongiovanni, Foca, Menis, Stucci, Artioli, Guadalupi, Forcignanò, Fantini, Recine, Mercatali, Spadazzi, Burgio, Fausti, Miserocchi and Ibrahim. This is an open-access article distributed under the terms of the Creative Commons Attribution License (CC BY). The use, distribution or reproduction in other forums is permitted, provided the original author(s) and the copyright owner(s) are credited and that the original publication in this journal is cited, in accordance with accepted academic practice. No use, distribution or reproduction is permitted which does not comply with these terms.

frontiers in Oncology

CASE REPORT
published: 19 November 2021
doi: 10.3389/fonc.2021.767957

Durable Complete Response to Pembrolizumab in Esophageal Squamous Cell Carcinoma With Divergent Microsatellite Status: A Case Report

Tian Zeng[1†], Lei Zhang[2†], Can Chen[1], Xiang Zhao[1], Xiaoqing Liu[1], Fengwei Ran[1], Tingting Yong[1], Ying Yang[2], Henghui Zhang[3,4,5] and Yanling Zhang[1]*

[1] Department of Oncology, Southwest Hospital, Third Military Medical University (Army Medical University), Chongqing, China, [2] Genecast Biotechnology Co., Ltd., Wuxi, China, [3] Beijing Shijitan Hospital, Capital Medical University, Beijing, China, [4] Ninth School of Clinical Medicine, Peking University, Beijing, China, [5] School of Oncology, Capital Medical University, Beijing, China

OPEN ACCESS

Edited by:
Hubing Shi,
Sichuan University, China

Reviewed by:
Dantong Sun,
Chinese Academy of Medical Sciences and Peking Union Medical College, China
Vladimir Roudko,
Mount Sinai Hospital, United States

***Correspondence:**
Yanling Zhang
zhangyanl11@sina.com

[†]These authors have contributed equally to this work

Specialty section:
This article was submitted to Cancer Immunity and Immunotherapy, a section of the journal Frontiers in Oncology

Received: 31 August 2021
Accepted: 25 October 2021
Published: 19 November 2021

Citation:
Zeng T, Zhang L, Chen C, Zhao X, Liu X, Ran F, Yong T, Yang Y, Zhang H and Zhang Y (2021) Durable Complete Response to Pembrolizumab in Esophageal Squamous Cell Carcinoma With Divergent Microsatellite Status: A Case Report. Front. Oncol. 11:767957. doi: 10.3389/fonc.2021.767957

Microsatellite instability-high (MSI-H) is widely believed to be a biomarker for immune checkpoint inhibitors (ICIs) such as pembrolizumab in solid tumors. However, due to the low prevalence of MSI-H in most cancers, it tends to be insufficient to identify whether patients should receive ICIs according to this biomarker alone. Here, we report a Chinese esophageal squamous cell carcinoma (ESCC) patient with unusual divergent MSI status between the primary lesion (MSS) and metastatic lesion (MSI-H) which developed after platinum-based therapy and radiotherapy. Both his primary and metastatic tumors responded well to pembrolizumab-containing therapies or pembrolizumab monotherapy and maintained a complete response for over 24 months. Whole-exome sequencing and multiplex immunohistochemistry were used to examine his tissue specimens. Notably, there were multiple high-frequency mutations of DDR (DNA damage repair) genes shared in the primary lesion and metastatic lesion, especially in the latter. Besides, we observed considerable degrees of infiltrating $CD3^+/CD8^+$ lymphocytes in both of his primary tumor and metastatic tumor without obvious difference, suggesting that the conversion of microsatellite status had little effect on the infiltration of lymphocytes. Collectively, given the predictive role of DDR alterations for ICIs in other malignancies, the alterations of DDR genes might also be promising biomarkers in ESCC individuals receiving ICIs.

Keywords: esophageal squamous cell carcinoma, microsatellite instability, pembrolizumab, complete response, DNA damage repair

HIGHLIGHTS

Mutations of DDR (DNA damage repair) genes may be biomarkers for checkpoint blockade immunotherapy in esophageal squamous cell carcinoma (ESCC).

INTRODUCTION

Prior studies (1, 2) demonstrated improved responses to immune checkpoint blockade (ICB) in multiple solid tumors with mismatch-repair deficiency (dMMR) or microsatellite instability-high (MSI-H). Hence, pembrolizumab monotherapy has been approved by the FDA for dMMR or MSI-H patients with solid tumors, irrespective of the tissue of origin since 2017. However, the prevalence of MSI-H/dMMR is rather low in esophageal and esophagogastric junction carcinoma (2), implying that this biomarker alone may be insufficient to identify appropriate patients with esophageal cancer who could receive immune checkpoint inhibitors (ICIs). Herein, we encountered a Chinese esophageal squamous cell carcinoma (ESCC) patient who had unusual divergent MSI status between the primary lesion (MSS) and metastatic lesion (MSI-H). Surprisingly, he exhibited durable complete response (>24 months) to pembrolizumab in the setting of neck metastasis which developed after receiving platinum-based therapy and radiotherapy. To explore what accounted for this patient outcome, whole-exome sequencing (WES) and multiplex immunohistochemistry (mIHC) were used to characterize his genomic features and immune phenotypes in the tumor microenvironment.

CASE PRESENTATION

In February 2018, a 73-year-old Chinese man presented with a rough mass in his esophageal mucosa and surface hyperemia under gastroscopy. A biopsy sample of pathological diagnosis showed ESCC (**Figure 1A**). A computed tomography (CT) scan revealed obvious contrast-enhanced imaging of the upper esophagus with a thickening wall and narrowing lumen but without visible enlargement of the mediastinal lymph nodes (**Figure 1B**), and he was diagnosed with a T2N0M0, upper esophageal carcinoma. His biopsy tumor specimens were sent for next-generation sequencing (NGS) targeting 543 cancer-related genes as well as a PD-L1 (programmed death-ligand 1) assay at a CAP (College of American Pathologists)-certified laboratory (Genecast Biotechnology Co., Ltd.). Unfortunately, no actionable alterations with strong evidence for targeted therapy were identified in his primary lesion, where the expression level of PD-L1 (SP142 staining) was 5% (CPS close to 6) and microsatellite stability (MSS) was present (**Figures 1C**, **2A**). Owing to the upper location of his tumor, this patient was unable to receive surgery. Given the fact that he had radioactive esophagitis and tracheitis (grade 3) during radiotherapy, we adjusted the originally planned therapeutic regimen, and sequential chemotherapy plus radiotherapy rather than concomitant definitive chemoradiation was used for him. Specifically, he received 3 cycles of paclitaxel liposome plus nedaplatin for 2 months followed by radical intensity-modulated radiotherapy (IMRT) (66 Gy at 2.2 Gy/session to the esophageal tumor) for 1 month until early July 2018 (**Figure 1B**). Nevertheless, the CT scan showed multiple enlarged lymph nodes of the right-side neck with suspected metastasis on June 25, 2018 (**Figure 1B**), which was verified by pathological diagnosis of a puncture biopsy of the right cervical mass (**Figure 1A**). Next, his punctured samples of the metastatic tumor were sent to the same laboratory as before for another NGS test and PD-L1 assay. Surprisingly, MSI-H along with dMMR (**Figures 2A, B**) was observed in his metastatic tumor with the soaring percentage (TPS 70%, CPS 75) of PD-L1 (**Figure 1C**). According to these results, the patient was given adjusted treatments with pembrolizumab (100 mg, recommended dose 2 mg/kg at that time in China) combined with chemotherapy (docetaxel plus tegafur) or local IMRT (66 Gy at 2.2 Gy/session to the metastatic tumor) or single pembrolizumab treatment from July 2018 to March 2019 and exhibited sustained clinical response, regardless of primary or metastatic lesions (**Figure 1B**). Given the good response after adding pembrolizumab, this patient did not continue to undergo chemotherapy or radiotherapy but just maintained pembrolizumab (100 mg) monotherapy until June 2019 and achieved a complete response (CR) of both primary and metastatic tumors (**Figure 1B**). Subsequently, he stopped the above therapies in June 2019 and remained CR until the recent radiological evaluation in April 2021 (**Figure 1B**).

METHODS

WES and variant analysis of the carcinoma tissue specimens of the patient along with a peripheral blood sample were performed at a CAP-certified laboratory (Genecast Biotechnology Co., Ltd.). The tumor cellular contents of both primary and metastatic biopsies were >80%. DNA libraries were captured by a Roche NimbleGen SepCap EZ MedExome kit and sequenced on a NovaSeq 6000 system (Illumina) with a deduped depth of 200× in tissues. Somatic SNV calling was performed using GATK (v4.0.7.0, Mutect2) (3) and the alterations were annotated by Oncotator (4) and ANNOVAR (5). For neoantigen prediction, *HLA*-I (*A*, *B*, and *C*) genotyping based on WES data of genomic DNA of peripheral blood cells was performed using the HLA-HD algorithm (6). Novel 9–11 amino-acid peptides from somatic non-synonymous mutations detected in tumor tissues were determined, and binding affinities of mutant or wild-type peptides to *HLA*-I alleles were calculated *via* netMHC-4.0 (7). The novel peptides with predicted binding affinities <500 or 50 nm and the affinity ratio of wild-type peptides to mutant peptides >1.5 were defined as neoantigens or strong neoantigens (8), respectively. For the examination of the tumor immune microenvironment by mIHC, immunostaining, imaging, and quantitative analyses of multiple molecules in formalin-fixed paraffin-embedded (FFPE) tumor slides were performed as previously described (9, 10). Primary antibodies used in this work were listed as follows (clone name, catalog number, dilution ratio): CK5/6 (OTI1C7, ZM-0313, 1:100), CD3 (LN10, ZM-0417, 1:100), and CD8 (SP16, ZA0508, 1:100). All of them were purchased from ZSGB-BIO, Beijing, China. The stained slides were scanned by PerkinElmer Vectra (Vectra 3.0.5; PerkinElmer, MA, USA) and quantitative results were achieved by inForm Advanced Image Analysis software (inForm 2.3.0; PerkinElmer, MA, USA). For each

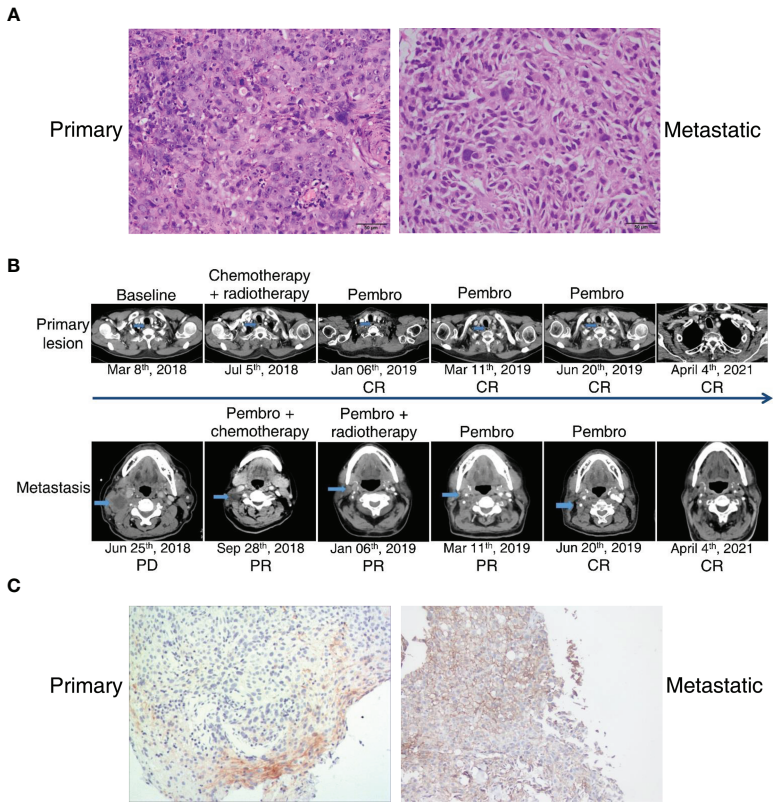

FIGURE 1 | Pathological results, radiological images, and PD-L1 assay of an esophageal squamous carcinoma patient with divergent MSI status between primary and metastatic lesions. **(A)** Histology of his primary and metastatic tumors. Magnification, ×200. **(B)** Representative CT images associated with his clinical outcomes during the whole treatment. Outcomes were valuated according to RECIST 1.1 criteria. **(C)** IHC staining with anti-PD-L1 antibody (SP142). Magnification, ×100.

slide, more than 15 fields were included to count the number, percentage, and density of positive cells in all nucleated cells under ×200 magnification. Mean percentages of certain cell subsets were calculated for further analysis.

RESULTS AND DISCUSSION

The discrepancy of microsatellite status detected by the MSI analysis system (Promega) between the primary and metastatic tumors of the patient was observed by targeted multigene panel sequencing as well. Based on calculation by the MSI-sensor software with WES data, the MSI scores of the primary and metastatic tumors were 2.22 and 21.11, respectively. According to the cutoff value (>10) for judging MS instability, the MS status of the primary tumor was judged as MSS, while the MS status of the metastatic tumor was judged as MSI-H. Besides, the TMB (tumor mutation burden) value was higher in the metastatic (18.25/Mb) than in the primary tumor (9.69/Mb) and it is consistent with their divergent MS status. Microsatellite instability is universally believed as the consequence of deficiency of four major MMR proteins encoded by *MLH1*, *MSH2*, *MSH6*, and *PMS2* (11), whereas there were not any detrimental alterations of these four genes identified in the above two NGS tests. To further examine the potential causes for this divergent MSI status, we performed WES of the tissue samples of the patient. As expected, WES results also displayed that MSI-H and MSS were present in metastatic and primary tumors, respectively. Notably, this individual had a lot of somatic alterations in well-documented DDR (DNA damage repair) genes (12) whose mutation frequencies were generally much higher in the metastatic than in the primary lesion, and three mutated DDR genes (*RAD51C*, *RECQL4*, *RMI1*) were only present in the former but absent in the latter (**Table 1**). All the variants were screened in public databases (ClinVar, OncoKB, COSMIC, CIViC), and almost all of them had uncertain significance except *TP53* p.R282W which was classified as pathogenic mutation. In view of the crucial role of DDR genes including MMR-related genes in maintaining genome integrity (12), we could speculate that chemotherapy as well as radiotherapy before immunotherapy might fuel the generation of high-frequency DDR alterations, further aggravating genome instability in the metastatic tumor relative to the primary tumor. Accordingly, microsatellite status was reshaped from MSS to MSI-H, though the detailed mechanisms remain to be studied.

Despite the lasting clinical response of this individual since adding pembrolizumab, can it be fully attributed to MSI-H status in metastasis? If so, it appeared to be unable to account for why the

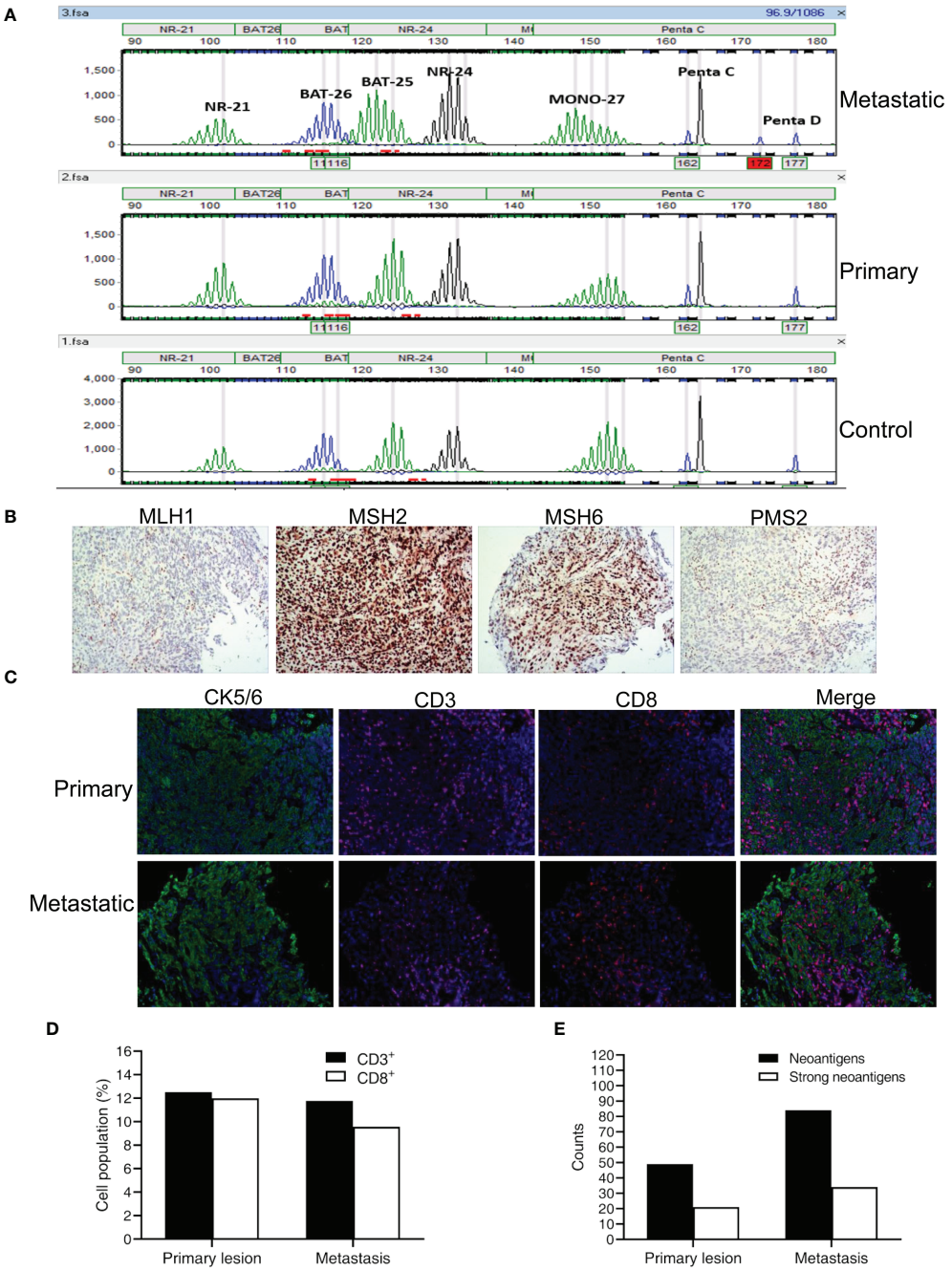

FIGURE 2 | MSI status, MMR results, and immune phenotypes together with neoantigens in primary and metastatic lesions of this patient. **(A)** Detection results of five microsatellite sites by the MSI analysis system (Promega). **(B)** MMR results of MLH1, MSH2, MSH6, and PMS2 in metastasis. **(C)** Representative images of CK5/6 (cytokeratin 5/6), CD3, and CD8 shown by mIHC in primary and metastatic lesions. Nuclei (blue) were counterstained by DAPI. Magnification, ×200. **(D)** Quantification results of mIHC from 15 random vision fields. **(E)** The number of predicted neoantigens in primary and metastatic tumors.

primary tumor with MSS of this patient likewise responded well. Theoretically, in addition to PD-L1, tumor-infiltrating lymphocytes (TILs) are also indispensable to successful ICB-based therapies (13). Indeed, as shown by mIHC images, there were considerable degrees of infiltrating $CD3^+/CD8^+$ lymphocytes in both the primary lesion and metastatic lesion (**Figure 2C**). Besides, quantitative results revealed that the percentages of $CD3^+/CD8^+$ TILs were even slightly higher in the former than in the latter (**Figure 2D**). In other words, the conversion of microsatellite status seemed to have little effect on the profiles of TILs. Therefore, it is reasonable to infer that MSI-H is not mainly responsible for such responsiveness to immunotherapy alone or combined with chemotherapy or

TABLE 1 | Alterations of DDR (DNA damage repair) genes in primary and metastatic lesions.

Alterations of DDR genes	Primary lesion (Fre, %)	Metastasis lesion (Fre, %)	DDR pathway	Core DDR pathway
***ERCC2* p.R666W**	10.88	28.1	NER	NER
***FANCM* p.Q740L**	7.62	28.28	FA, HR	FA
***RIF1* p.R2202C**	13.48	30.06	NHEJ, other	
***TP53* p.R282W**	28.09	77.59	Other	
***TTK* p.R854Gfs*39**	11.11	25.49	Other	
***PRKDC* p.M2429I**	5.39	21.8	NHEJ	NHEJ
***PRKDC* p.M2428I**	5.63	22.83	NHEJ	NHEJ
***PRKDC* p.L934Ffs*46**	10.87	22.88	NHEJ	NHEJ
***PRKDC* p.D2431Tfs*10**		20.14	NHEJ	NHEJ
***RAD51C* p.L265P**		6.31	FA, HR	
***RECQL4* c.1132-1G>T**		5.75	HR	
***RMI1* p.N377Mfs*6**		7	FA, HR	

Fre, frequency; NER, nucleotide excision repair; FA, Fanconi anemia; HR, homology-dependent recombination; NHEJ, non-homologous end joining.

radiotherapy, at least not the sole determinant. Furthermore, after discontinuation of all prior therapies since June 2019, this patient still achieved complete remission lasting over 24 months and survival of 40 months until now. This exceptional outcome was obviously better than that (median overall survival of 2.3 years) observed in ESCC patients with definitive chemoradiotherapy (14), indicating the potential of ICIs in improving the survival of ESCC patients. In the context of MSS primary tumor and MSI-H metastasis, complete response to pembrolizumab could be due to antigen spreading that was reported to be responsible for T-cell responses after initial activation (15). However, whether it is applicable to this patient outcome remains to be further studied. On the other hand, we believed that such good outcomes may be more likely because of a series of shared clonal neoantigens between primary and metastatic sites. Given their similar immune microenvironment is appropriate for immunotherapy, it is hypothesized that if this patient received pembrolizumab from the beginning without visible metastasis, his primary tumor may also have responded well. Although chemotherapy and radiotherapy were in favor of facilitating the release of neoantigens triggering immune response to some extent, pre-existing adaptive resistance mediated by the PD-1/PD-L1 pathway in the primary tumor was also enhanced in metastasis with the PD-L1 expression soaring from 5% to 70%. Thereafter, the anti-PD-1 inhibitor pembrolizumab relieved the restrained activity of CD8 T cells and brought about a durable survival benefit for this patient. In brief, favorable infiltration of T cells potentially associated with certain shared clonal mutations rather than just MS status played a crucial role in these satisfactory immunotherapy outcomes.

It is worth mentioning that alterations of DDR genes are viewed as promising biomarkers for the clinical benefit from ICIs in certain malignancies including lung cancer and urothelial cancer (16, 17), while the predictive value of DDR alterations for ICB treatments in esophageal carcinoma is rarely reported to date. Additionally, we noticed the higher number of predicted neoantigens based on WES data in the metastatic lesion over the primary lesion of the patient (**Figure 2E**), corresponding to the change of MSI status. Notwithstanding, more neoantigens *in silico* has not yet given rise to more TILs in the metastatic tumor compared with the primary tumor. It should be noted that there was a marked rising level of PD-L1 in the metastatic tumor before immunotherapy. In consideration of the favorable infiltration of $CD3^+/CD8^+$ T cells in the tumor microenvironment of the patient, it is plausible that chemotherapy and/or radiotherapy together with DDR alterations not only contributed to keeping the immune phenotype active to some extent but also intensified pre-existing adaptive resistance mediated by the PD-1/PD-L1 pathway (13). Such enhanced expression of PD-L1 was likely associated with the resistance of the metastatic lesion to chemotherapy followed by radiotherapy in the setting of partial response of the primary tumor. Under this circumstance, PD-1 blocking by pembrolizumab subsequently brought about desirable remission of both primary and metastatic lesions. In summary, the alterations of DDR genes may be valuable biomarkers in ESCC patients receiving ICIs Although pembrolizumab has been approved by the FDA for advanced or metastatic ESCC patients with PD-L1 (CPS ≥ 10), it seemed to be incapable of fully explaining the outstanding survival benefit of this individual. Whether anti-PD-1/PD-L1 inhibitors combined with chemotherapy or radiotherapy can achieve better clinical outcomes in those PD-L1-positive ESCC patients harboring DDR alterations deserves more research.

DATA AVAILABILITY STATEMENT

The WES data presented in this study can be found in online repository. The name of the repository and accession number can be found below: Genome Sequence Archive in National Genomics Data Center and accession number HRA001554 that are publicly accessible at https://bigd.big.ac.cn/gsa-human/browse/HRA001554. Other related data were shown in manuscript or can be obtained from the corresponding author upon reasonable request.

ETHICS STATEMENT

Ethical review and approval was not required for the study on human participants in accordance with the local legislation and institutional requirements. The patients/participants provided their written informed consent to participate in this study. Written informed consent was obtained from the individual(s)

for the publication of any potentially identifiable images or data included in this article.

AUTHOR CONTRIBUTIONS

Conception and design: TZ, LZ, and YZ. Data interpretation: LZ, YY, and TZ. Bioinformatic analysis: YY. Writing and editing of the manuscript: LZ, TZ, HZ, and YZ. TZ, CC, XZ, XL, FR, and TY identified and treated the patient and collected and presented related clinical data. All authors contributed to the article and approved the submitted version.

FUNDING

This study was supported by a grant from the National Key Sci-Tech Special Project of China (No. 2018ZX10302207).

REFERENCES

1. Le DT, Uram JN, Wang H, Bartlett BR, Kemberling H, Eyring AD, et al. PD-1 Blockade in Tumors With Mismatch-Repair Deficiency. *N Engl J Med* (2015) 372:2509–20. doi: 10.1056/NEJMoa1500596
2. Le DT, Durham JN, Smith KN, Wang H, Bartlett BR, Aulakh LK, et al. Mismatch Repair Deficiency Predicts Response of Solid Tumors to PD-1 Blockade. *Science* (2017) 357:409–13. doi: 10.1126/science.aan6733
3. Cibulskis K, Lawrence MS, Carter SL, Sivachenko A, Jaffe D, Sougnez C, et al. Sensitive Detection of Somatic Point Mutations in Impure and Heterogeneous Cancer Samples. *Nat Biotechnol* (2013) 31:213–9. doi: 10.1038/nbt.2514
4. Ramos AH, Lichtenstein L, Gupta M, Lawrence MS, Pugh TJ, Saksena G, et al. Oncotator: Cancer Variant Annotation Tool. *Hum Mutat* (2015) 36:E2423–9. doi: 10.1002/humu.22771
5. Wang K, Li M, Hakonarson H. ANNOVAR: Functional Annotation of Genetic Variants From High-Throughput Sequencing Data. *Nucleic Acids Res* (2010) 38:e164. doi: 10.1093/nar/gkq603
6. Kawaguchi S, Higasa K, Shimizu M, Yamada R, Matsuda F. HLA-HD: An Accurate HLA Typing Algorithm for Next-Generation Sequencing Data. *Hum Mutat* (2017) 38:788–97. doi: 10.1002/humu.23230
7. Andreatta M, Nielsen M. Gapped Sequence Alignment Using Artificial Neural Networks: Application to the MHC Class I System. *Bioinformatics* (2016) 32:511–7. doi: 10.1093/bioinformatics/btv639
8. Rosenthal R, Larose Cadieux E, Salgado R, Al Bakir M, Moore DA, Hiley CT, et al. Neoantigen-Directed Immune Escape in Lung Cancer Evolution. *Nature* (2019) 567:479–85. doi: 10.1038/s41586-019-1032-7
9. Gorris MAJ, Halilovic A, Rabold K, van Duffelen A, Wickramasinghe IN, Verweij D, et al. Eight-Color Multiplex Immunohistochemistry for Simultaneous Detection of Multiple Immune Checkpoint Molecules Within the Tumor Microenvironment. *J Immunol* (2018) 200:347–54. doi: 10.4049/jimmunol.1701262
10. Pang X, Qian J, Jin H, Zhang L, Lin L, Wang Y, et al. Durable Benefit From Immunotherapy and Accompanied Lupus Erythematosus in Pancreatic Adenocarcinoma With DNA Repair Deficiency. *J Immunother Cancer* (2020) 8:e000463. doi: 10.1136/jitc-2019-000463
11. Li K, Luo H, Huang L, Luo H, Zhu X. Microsatellite Instability: A Review of What the Oncologist Should Know. *Cancer Cell Int* (2020) 20:16. doi: 10.1186/s12935-019-1091-8
12. Knijnenburg TA, Wang L, Zimmermann MT, Chambwe N, Gao GF, Cherniack AD, et al. Genomic and Molecular Landscape of DNA Damage Repair Deficiency Across The Cancer Genome Atlas. *Cell Rep* (2018) 23:239–54. doi: 10.1016/j.celrep.2018.03.076
13. Sanmamed MF, Chen L. A Paradigm Shift in Cancer Immunotherapy: From Enhancement to Normalization. *Cell* (2018) 175:313–26. doi: 10.1016/j.cell.2018.09.035
14. Barbetta A, Hsu M, Tan KS, Stefanova D, Herman K, Adusumilli PS, et al. Definitive Chemoradiotherapy *Versus* Neoadjuvant Chemoradiotherapy Followed by Surgery for Stage II to III Esophageal Squamous Cell Carcinoma. *J Thorac Cardiovasc Surg* (2018) 155:2710–21. doi: 10.1016/j.jtcvs.2018.01.086
15. Hunder NN, Wallen H, Cao J, Hendricks DW, Reilly JZ, Rodmyre R, et al. Treatment of Metastatic Melanoma With Autologous CD4+ T Cells Against NY-ESO-1. *N Engl J Med* (2008) 358:2698–703. doi: 10.1056/NEJMoa0800251
16. *ASCO Abstract 9077* (2019). Available at: https://meetinglibrary.asco.org/record/174379/abstract.
17. Yuen Teo M, Seier K, Ostrovnaya I, Regazzi AM, Kania BE, Moran MM, et al. Alterations in DNA Damage Response and Repair Genes as Potential Marker of Clinical Benefit From PD-1/PD-L1 Blockade in Advanced Urothelial Cancers. *J Clin Oncol* (2018) 36:1685–94. doi: 10.1200/JCO.2017.75.7740

Conflict of Interest: The authors LZ and YY were employed by the company Genecast Biotechnology Co., Ltd.

The remaining authors declare that the research was conducted in the absence of any commercial or financial relationships that could be construed as a potential conflict of interest.

Publisher's Note: All claims expressed in this article are solely those of the authors and do not necessarily represent those of their affiliated organizations, or those of the publisher, the editors and the reviewers. Any product that may be evaluated in this article, or claim that may be made by its manufacturer, is not guaranteed or endorsed by the publisher.

Copyright © 2021 Zeng, Zhang, Chen, Zhao, Liu, Ran, Yong, Yang, Zhang and Zhang. This is an open-access article distributed under the terms of the Creative Commons Attribution License (CC BY). The use, distribution or reproduction in other forums is permitted, provided the original author(s) and the copyright owner(s) are credited and that the original publication in this journal is cited, in accordance with accepted academic practice. No use, distribution or reproduction is permitted which does not comply with these terms.

frontiers in Immunology

SYSTEMATIC REVIEW
published: 03 December 2021
doi: 10.3389/fimmu.2021.760737

A Network Comparison on Safety Profiling of Immune Checkpoint Inhibitors in Advanced Lung Cancer

Yi-Dan Yan[1†], Jiu-Jie Cui[2†], Jie Fu[1], Ying-Jie Su[1], Xiao-Yu Chen[3], Zhi-Chun Gu[1*] and Hou-Wen Lin[1]*

[1] Department of Pharmacy, Ren Ji Hospital, Shanghai Jiao Tong University School of Medicine, Shanghai, China, [2] Department of Oncology, Ren Ji Hospital, Shanghai Jiao Tong University School of Medicine, Shanghai, China, [3] Department of Pharmacy, The People's Hospital of Guangxi Zhuang Autonomous Region (Guangxi Academy of Medical Sciences), Nanning, China

OPEN ACCESS

Edited by:
Xuelei Ma,
Sichuan University, China

Reviewed by:
Cleo Goyvaerts,
Vrije University Brussel, Belgium
Pierpaolo Correale,
Azienda Ospedaliera 'Bianchi-Melacrino-Morelli', Italy
Huijuan Mao,
Nanjing Medical University, China

***Correspondence:**
Zhi-Chun Gu
guzhichun213@163.com
Xiao-Yu Chen
1534746296@qq.com

[†]These authors have contributed equally to this work and share first authorship

Specialty section:
This article was submitted to Cancer Immunity and Immunotherapy, a section of the journal Frontiers in Immunology

Received: *18 August 2021*
Accepted: *16 November 2021*
Published: *03 December 2021*

Citation:
Yan Y-D, Cui J-J, Fu J, Su Y-J, Chen X-Y, Gu Z-C and Lin H-W (2021) A Network Comparison on Safety Profiling of Immune Checkpoint Inhibitors in Advanced Lung Cancer. Front. Immunol. 12:760737. doi: 10.3389/fimmu.2021.760737

Background: Immune checkpoint inhibitors (ICIs) have become one of the standard treatment options for advanced lung cancer. However, adverse events (AEs), particularly immune–related AEs (irAEs), caused by these drugs have aroused public attention. The current network meta-analysis (NMA) aimed to compare the risk of AEs across different ICI–based regimens in patients with advanced lung cancer.

Methods: We systematically searched the PubMed, EMBASE, and Cochrane Library databases (from inception to 19 April 2021) for relevant randomized controlled trials (RCTs) that compared two or more treatments, with at least one ICI administered to patients with advanced lung cancer. The primary outcomes were treatment–related AEs and irAEs, including grade 1–5 and grade 3–5. The secondary outcomes were grade 1–5 and grade 3–5 irAEs in specific organs. Both pairwise and network meta-analyses were conducted for chemotherapy, ICI monotherapy, ICI monotherapy + chemotherapy, dual ICIs therapy, and dual ICIs + chemotherapy for all safety outcomes. Node–splitting analyses were performed to test inconsistencies in network. Sensitivity analyses were adopted by restricting phase III RCTs and studies that enrolled patients with non–small cell lung cancer.

Results: Overall, 38 RCTs involving 22,178 patients with advanced lung cancer were enrolled. Both pooled incidence and NMA indicated that treatments containing chemotherapy increased the risk of treatment–related AEs when compared with ICI-based regimens without chemotherapy. As for grade 1–5 irAEs, dual ICIs + chemotherapy was associated with the highest risk of irAEs (probability in ranking first: 50.5%), followed by dual-ICI therapy (probability in ranking second: 47.2%), ICI monotherapy (probability in ranking third: 80.0%), ICI monotherapy + chemotherapy (probability in ranking fourth: 98.0%), and finally chemotherapy (probability in ranking fifth: 100.0%). In grade 3–5 irAEs, subtle differences were observed; when ranked from least safe to safest, the trend was dual ICIs therapy (60.4%), dual ICIs + chemotherapy (42.5%), ICI monotherapy (76.3%), ICI monotherapy + chemotherapy (95.0%), and chemotherapy (100.0%). Furthermore, detailed comparisons between ICI–based options provided irAE profiles based on specific organ/system and severity.

Conclusions: In consideration of overall immune–related safety profiles, ICI monotherapy + chemotherapy might be a better choice among ICI–based treatments for advanced lung cancer. The safety profiles of ICI–based treatments are various by specific irAEs and their severity.

Systematic Review Registration: https://www.crd.york.ac.uk/prospero, identifier CRD42021268650

Keywords: immune checkpoint inhibitors, safety, lung cancer, adverse events, network comparison

INTRODUCTION

Lung cancer remains the leading cause of global cancer mortality, with approximately 1.8 million deaths annually (18% of the total cancer deaths) (1). Over the past decades, platinum–based chemotherapy has become the cornerstone for managing advanced lung cancer; however, its use is of concern due to inevitable resistance and intolerable adverse events (AEs) in these fragile patients (2, 3). Recently, immunotherapy has revolutionised treatment approaches for advanced lung cancer by making longer survival times a reality (4). Unlike traditional therapy (chemotherapy and targeted therapy), immune checkpoint Inhibitor (ICI) therapies use monoclonal antibodies to inhibit the expression of proteins [cytotoxic T lymphocyte associated antigen (CTLA4), programmed death-1 receptor (PD-1), and its ligand (PD-L1)], thereby boosting T–cell activation against cancer (5). To date, a series of ICIs [pembrolizumab, nivolumab, ipilimumab, atezolizumab, and durvalumab registered by the U.S. Food and Drug Administration (FDA); camrelizumab, sintilimab, and tislelizumab approved by the National Medical Products Administration (NMPA)] have been successfully introduced for use in patients with advanced lung cancer. Recently, ICI monotherapy with or without chemotherapy, dual ICIs combination, even dual ICIs combined with chemotherapy have been clinically applied as standard first–line treatment options for advanced lung cancer.

With a dramatic increase in the availability of ICI drugs and their superior efficacy, a substantial proportion of patients with lung cancer are administered these agents. Nonetheless, concerns regarding unique treatment–specific toxicities owing to their pharmacological mechanisms, namely immune–related AEs (irAEs), associated with ICI regimens are growing (6). IrAEs are unintended effects following the activation of the immune system by ICI–mediation and can occur in any organ or system, including the gastrointestinal tract, lungs, endocrine, skin, heart, renal, liver, and muscles (7). In published randomised controlled trials (RCTs), patients administered ICIs experienced fewer AEs than those undergoing chemotherapy, while the incidence of any irAEs seemed to be distinctly higher in the ICI group (8). Without timely identification and proper management, irAEs can become severe complications, resulting in treatment discontinuation or failure, and even death (9, 10).

Previous meta-analyses have examined the risks of irAEs associated with ICI therapy; however, most of them mainly involved patients with all types of cancers (11–13). In addition, these studies did not explicitly examine the risk of individual irAEs across different ICI regimens, which may vary according to cancer type. Recently, one network meta-analysis (NMA) (14) and six traditional meta-analyses (14–19) addressed this issue in patients with lung cancer. However, they focused on one or two specific irAEs; therefore, the entire toxicity spectrum in these patients is yet to be described. Since, to the best our knowledge, head–to–head comparisons among ICI regimens are lacking in current literature, an indirect analysis could be performed to obtain comparative results and rank all possible treatments (20). In the present study, we conducted an NMA using up-to-date data from ICI–treated patients with advanced lung cancer to compare the risk of developing AEs during or following various treatment strategies.

METHODS

Literature Search

This NMA was conducted according to the priori established protocol (PROSPERO: CRD42021268650; https://www.crd.york.ac.uk/prospero/#searchadvanced), and reported in accordance with the PRISMA (Preferred Reporting Items for Systematic Reviews and Meta-analyses) guidelines (21) and its extension statement for NMA (**Table S1**). The PubMed, EMBASE, and Cochrane Library databases were systematically searched from inception to 19 April 2021 with language restricted to English. The search terms and their combinations used in the search strategies are shown in **Table S2**. We also identified potential studies listed as references in the retrieved articles and searched unpublished data from the ClinicalTrials.gov website.

Study Selection

The eligibility criteria for published studies were as follows: head-to-head phase II and III RCTs comparing two or more treatments, including at least one ICI drug in patients with advanced lung cancer. Studies published only in the form of conference abstracts, posters, and presentations of ongoing RCTs were excluded. If several studies were derived from the same trial, the study that reported comprehensive safety data was involved. Two authors (Y.Y. and J.C.) independently screened all titles and abstracts, and further assessed potentially eligible full text based on the aforementioned criteria.

Study Outcomes and Data Extraction

The primary outcomes of this study were overall safety outcomes, viz. treatment–related adverse events and immune-

related adverse events as defined in each study (**Table S3**), including grade 1–5 and grade 3–5, respectively. The secondary outcomes were grade 1–5 and grade 3–5 irAEs in specific organ systems, including the gastrointestinal system (colitis and diarrhea), pulmonary system (pneumonitis), endocrine system (hyperthyroidism, hypothyroidism, thyroiditis, hypophysitis, and diabetes), skin (pruritus, rash, and severe skin reaction), and others (myocarditis, nephritis, hepatitis, myositis, and hypersensitivity/infusion reaction). Grading of AEs was reported according to the Common Terminology Criteria for Adverse Events (CTCAE), as reported in each study. Two authors (Y.Y. and J.C.) used a pre-designed form to extract the following data: study characteristics (study ID and publication year, NCT number, cancer type, study design, arms, treatment regimens, number of patients, follow–up time, and version of CTCAE), demographics and clinical characteristics (age, sex, PS score, brain/CNS metastasis, liver metastasis, bone metastasis, current/former smoker, prior surgery, and prior radiotherapy), and data on the aforementioned outcomes. The above information was extracted from the main text and **Supplementary Materials**, and only accessible data were analysed.

Quality Assessment

The methodological quality of the included trials was assessed using the Cochrane Collaboration Risk of Bias Tool (22). Low, moderate, or high risk of bias was assigned to each citation within the following five aspects: random sequence generation, allocation concealment, masking, assessment of outcomes, and selective reporting. Disagreements during study selection, data extraction, and quality assessment processes were resolved by consensus following a consultation with the corresponding investigator (Z.G.).

Statistical Analyses

To illustrate the direct and indirect comparisons among the treatments, a plot of the network geometry was generated. A pairwise meta-analysis of head-to-head comparisons was conducted to make direct estimates. Results were reported as relative risks (RRs) with 95% confidence intervals (95% CIs) using a random–effect model. Statistical heterogeneity was assessed using the I^2-test, with a value > 50% representing considerable heterogeneity (23). A sensitivity analysis was performed to assess the robustness of the results by sequentially eliminating each study from the pool (24, 25). Furthermore, meta-regression analyses were performed to explore the influence of potential factors on patient outcomes (26). When a single analysis involved > 10 studies, publication bias was evaluated using funnel plots, as well as Egger's and Begg's tests (27). For outcomes with potential publication bias, the trim and fill method were used to estimate the number of missing studies and to provide an estimated intervention effect to perform adjustment for publication bias. In the network comparison among treatment regimens, chemotherapy was used as the reference comparator. Random effects and consistency models were used to calculate RRs and their 95% CIs; these models are thought to be the most conservative approach to dealing with between–study heterogeneity. Cumulative probabilities were used to provide a hierarchy of the treatments. According to the cumulative probabilities, treatment regimens were ranked from the worst (i.e., associated with the highest risk of AEs) to the best (i.e., associated with the lowest risk of AEs) (28). Transitivity was appraised in consistency and coherence: first, interaction analyses were used to assess the comparability between the consistency and inconsistency models; second, node–splitting analyses were performed to test coherence in the network. To further ensure the robustness of the findings, sensitivity analyses were adopted by restricting the following factors: phase III RCTs and studies that enrolled patients with non–small cell lung cancer (NSCLC). The incidences of grade 1–5 and grade 3–5 AEs were also pooled using meta-analysis (29). All data were analysed by using STATA version13.0 (Statacorp, College Station, Texas, United States), with p values < 0.05 indicating a statistically significant difference.

RESULTS

Study Selection and Characteristics

Our initial search yielded 1,725 records from databases and 914 records from the ClinicalTrials.gov platform; 2,535 records were excluded following screening of titles and abstracts. The remaining 104 full–text articles were reviewed, and 66 articles were excluded for reasons depicted in **Figure 1** and **Table S4**. Given that only one trial (IMpower150) involved groups of ICI + targeted + chemotherapy and ICI + targeted therapy, which had no head-to-head comparison with other five treatments, it was excluded in

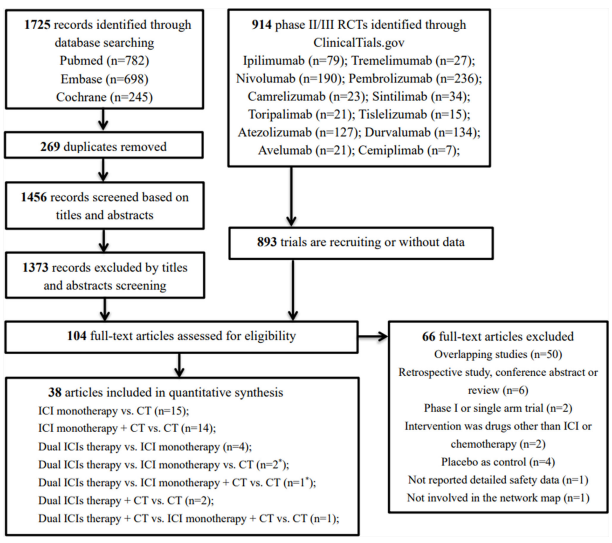

FIGURE 1 | Flow diagram for the selection of eligible studies. ICI, immune checkpoint inhibitor; CT, chemotherapy; n, number; *, one study involved two groups, dual ICIs therapy *vs.* ICI monotherapy *vs.* CT (group A) and dual ICIs therapy *vs.* ICI monotherapy + CT *vs.* CT (group B).

our network map. Finally, 38 studies (30–67) met the inclusion criteria, and their characteristics are listed in **Table 1**. Of these 38 studies, 30 were phase III trials, six were phase II trials, one was a phase I/II trial, and one was a phase II/III trial. As for the indication, 28 RCTs involved patients with NSCLC, and the remaining nine RCTs included patients with small cell lung cancer (SCLC). The sample sizes ranged from 73–1,739 participants, and the median follow–up time varied from 6.6–30.2 months across trials. As shown in the network map (**Figure 2**), a total of 22,178 patients with advanced lung cancer were included in five treatment regimens (8,768, 6,057, 4,917, 1,807, and 629 patients received chemotherapy, ICI monotherapy, ICI monotherapy + chemotherapy, dual ICIs therapy, and dual ICIs + chemotherapy, respectively). Detailed patient demographics and clinical characteristics are summarised in **Table S5**. The median age of patients was ranged from 50.1–66 years, and the proportion of males was 68.9%. Most of the patients were current or former smokers (84.4%), with a PS score of 0–1 (98.8%). Overall, 16.7% of the patients were reported to have metastasis (brain, liver, or bone) at baseline, while 3.4% and 4.8% of them were previously reported to have undergone surgery and radiotherapy, respectively.

Risk-of-Bias Assessment

The included RCTs satisfied three tool items, viz. random sequence generation, incomplete outcome data, and selective reporting. Twenty–seven open–label trials did not meet the item of allocation concealment or blinding of participants and personnel, resulting in a high risk of bias in the study assessment. Overall, 27 studies exhibited a high risk of bias, and 11 studies were considered to have a low risk of bias. The details of the quality assessment are presented in **Table S6**.

Pairwise Meta-Analysis Based on Head-to-Head Comparisons

Direct comparisons were conducted to assess safety profiles among five treatments options (**Table S7**). Compared with conventional chemotherapy, three treatment regimens (ICI monotherapy, dual ICIs, and dual ICIs + chemotherapy) had a similar risk for grade 1–5 AEs, except for ICI monotherapy + chemotherapy (RR: 1.03, 95% CI: 1.01–1.04). Meanwhile, dual ICIs therapy appeared to have a higher risk for grade 1–5 AEs than ICI monotherapy (RR: 1.17, 95% CI: 1.04–1.31). Regarding grade 3–5 AEs, chemotherapy showed a noticeably higher risk compared with ICI monotherapy (RR: 0.33, 95% CI: 0.27–0.40 for ICI monotherapy *vs.* chemotherapy), while there was a reduced risk when compared with dual ICIs + chemotherapy (RR: 0.33, 95% CI: 0.27–0.40 for dual ICIs + chemotherapy *vs.* chemotherapy). Other results were consistent with those observed in grade 1–5 AEs.

In terms of irAEs, the use of ICI monotherapy (RR: 4.06, 95% CI: 2.75–5.98 for grade 1–5; RR: 5.75, 95% CI: 3.50–9.43 for grade 3–5) or ICI monotherapy + chemotherapy (RR: 2.02, 95% CI: 1.63–2.52 for grade 1–5; RR: 2.93, 95% CI: 1.98–4.34 for grade 3–5) was associated with a significantly higher risk of developing these manifestations than chemotherapy. Dual ICIs therapy had a similar risk of grade 1–5 irAEs (RR: 1.48, 95% CI: 0.77–2.84) but a superior risk of grade 3–5 irAEs (RR: 2.12, 95% CI: 1.29–3.48) compared with ICI monotherapy. Detailed data in specific irAEs are listed in **Table S7**. Briefly, results from organ–specific irAEs, including colitis, pneumonitis, hyper/hypothyroidism, hepatitis, and rash, were comparable with those observed in overall irAEs. Regarding heterogeneity of pairwise meta-analysis comparisons, relatively high heterogeneity was found in primary outcomes (I^2: 38.2%–95.0%), except for two pairs (dual ICIs + chemotherapy *vs.* chemotherapy for grade 3–5 AEs and ICI monotherapy *vs.* chemotherapy for grade 3–5 irAEs). Overall, the general heterogeneity in individual irAEs was low to moderate.

Sensitivity analyses were conducted by sequentially removing each study. Following this, the pooled results were in line with the set primacy safety outcomes (**Table S8**). In addition, meta-regression analysis failed to detect any potential confounding factors affecting the primacy outcomes (**Table S9**). A visual inspection of the funnel plots and Begg's test showed relative symmetry, except for grade 3–5 AE in comparison of ICI monotherapy *vs.* chemotherapy (P = 0.018) (**Figure S1** and **Table S10**). However, P values of Egger's test in several outcomes were < 0.05, suggesting that publication bias existed in this study (**Table S10**). The trim and fill method were adopted to mitigate publication bias, and the outcomes were consistent with our primary results (P for interaction > 0.05) (**Table S10**).

Network Meta-Analysis for Overall Safety

The pooled incidence for five treatments showed the following rankings: ICI monotherapy + chemotherapy had the highest incidence of AEs (93.21% for grade 1–5, 58.48% for grade 3–5), followed by dual ICIs + chemotherapy (92.02%, 54.23%), chemotherapy (88.35%, 49.75%), dual ICIs therapy (76.47%, 31.38%), ICI monotherapy (65.99%, 15.22%) (**Figure 3A** and **Table S11**). Established NMA based on the consistency model indicated that ICI monotherapy had the lowest risk of causing grade 1–5 AEs compared with chemotherapy (RR: 3.7, 95% CI: 3.05–4.48 for chemotherapy *vs.* ICI monotherapy), ICI monotherapy + chemotherapy (RR: 0.19, 95% CI: 0.14–0.26), dual ICIs therapy (RR: 0.55, 95% CI: 0.41–0.74), as well as dual ICIs + chemotherapy (RR: 0.18, 95% CI: 0.10–0.33) (**Figure 3A**). Then was dual ICIs therapy (RR: 2.03, 95% CI: 1.46–2.81 for chemotherapy *vs.* dual ICIs; RR: 2.89, 95% CI: 1.94–4.29 for ICI monotherapy + chemotherapy *vs.* dual ICIs; RR: 0.33, 95% CI: 0.18–0.63 for dual ICIs *vs.* dual ICIs + chemotherapy). ICI monotherapy + chemotherapy showed a higher risk of causing grade 1–5 AEs than chemotherapy (RR: 0.70, 95% CI: 0.55–0.90 for chemotherapy *vs.* ICI + chemotherapy), while no significant difference was seen when compared with that of the ICIs + chemotherapy group (RR: 0.96, 95% CI: 0.54–1.70). Similar results were observed in grade 3–5 AEs. The ranking probabilities based on the five treatment groups are also depicted in **Figure 3A**. The rankings of grade 3–5 AEs were in line with those of grade 1–5 AEs, ranging from least safe to safest

TABLE 1 | Baseline characteristics of 38 studies.

Study, year	NCT number	Cancer type	Phase	Line of treatment	Arms	Treatment	Numbers	Median follow-up time (months)	CTCAE version
CA184-041, 2012	NCT00527735	NSCLC	II	1	1	Ipi 10mg/kg q3w+PC	138	NR	3.0
					2	PC	66	NR	
CA184-041, 2013	NCT00527735	SCLC	II	1	1	Ipi 10mg/kg q3w+PC	85	NR	3.0
					2	PC	45	NR	
CheckMate 057,2015	NCT01673867	Nonsquamous NSCLC	III	2	1	Niv 3mg/kg q2w	292	Min 13.2	4.0
					2	Docetaxel	290	Min 13.2	
CheckMate 017, 2015	NCT01642004	Squamous NSCLC	III	2	1	Niv 3mg/kg q2w	135	Min 11.0	4.0
					2	Docetaxel	137	Min 11.0	
CheckMate 032, 2016	NCT01928394	SCLC	I/II	≥2	1	Niv 3mg/kg q2w	98	6.6	4.0
					2	Niv 1mg/kg+Ipi 3mg/kg q3w	61	10.6	
					3	Niv 3mg/kg+Ipi 1mg/kg q3w	54	12.0	
POPLAR, 2016	NCT01903993	NSCLC	II	≥2	1	Ate 1200mg q3w	144	14.8	4.0
					2	Docetaxel	143	15.7	
KEYNOTE-010, 2016	NCT01905657	NSCLC	II/III	≥2	1	Pem 2mg/kg q3w	344	13.1	4.0
					2	Pem 10mg/kg q3w	346	13.1	
					3	Docetaxel	343	13.1	
KEYNOTE-021, 2016	NCT02039674	Nonsquamous NSCLC	II	1	1	Pem200mg q3w+AC	60	10.6	4.0
					2	AC	63	10.6	
CA184-156, 2016	NCT01450761	SCLC	III	1	1	Ipi 10mg/kg q3w+EP	478	10.5	3.0
					2	EP	476	10.2	
KEYNOTE 024, 2016	NCT02142738	NSCLC	III	1	1	Pem 200mg q3w	154	25.2	4.0
					2	P-based chemotherapy	151	25.2	
CheckMate 026, 2017	NCT02041533	NSCLC	III	1	1	Niv 3mg/kg q2w	271	13.5	4.0
					2	P-based chemotherapy	270	13.5	
Study 104, 2017	NCT01285609	Squamous NSCLC	III	1	1	Ipi 10 mg/kg q3w+PC	388	12.5	3.0
					2	PC	361	11.8	
OAK, 2017	NCT02008227	NSCLC	III	≥2	1	Ate 1200mg q3w	425	21	4.0
					2	Docetaxel	425	21	
JAVELIN Lung 200, 2018	NCT02395172	NSCLC	III	≥2	1	Ave 10 mg/kg q2w	396	18.9	4.0
					2	Docetaxel	396	17.8	
KEYNOTE-189, 2018	NCT02578680	Nonsquamous NSCLC	III	1	1	Pem 200mg q3w+AP	410	10.5	4.0
					2	AP	206	10.5	
IMpower133, 2018	NCT02763579	SCLC	III	1	1	Ate 1200mg q3w+EC	201	13.9	4.0
					2	EC	202	13.9	
KEYNOTE-407, 2018	NCT02775435	Squamous NSCLC	III	1	1	Pem 200mg q3w+PC/nPC	278	7.8	4.03
					2	PC/nPC	281	7.8	
CheckMate 227, 2019	NCT02477826	NSCLC	III	1	GroupA-1	Niv 3mg/kg q2w+Ipi 1mg/kg q6w	396	Min 29.3	4.0
					GroupA-2	Niv 240mg q2w	396	Min 29.3	
					GroupA-3	P-based chemotherapy	397	Min 29.3	
					GroupB-1	Niv 3mg/kg q2w+Ipi 1mg/kg q6w	187	Min 29.3	
					GroupB-2	Niv 360mg +P-based chemotherapy q3w	177	Min 29.3	
					GroupB-3	P-based chemotherapy	186	Min 29.3	
KEYNOTE-042, 2019	NCT02220894	NSCLC	III	1	1	Pem 200mg q3w	637	12.8	4.0
					2	P-based chemotherapy	637	12.8	
IFCT-1603, 2019	NCT03059667	SCLC	II	2	1	Ate 1200mg q3w	49	13.7	4.0

(Continued)

TABLE 1 | Continued

Study, year	NCT number	Cancer type	Phase	Line of treatment	Arms	Treatment	Numbers	Median follow-up time (months)	CTCAE version
					2	EC or topotecan	24	13.7	
IMpower130, 2019	NCT02367781	Nonsquamous NSCLC	III	1	1	Ate 1200mg q3w+nPC	483	18.5	4.0
					2	nPC	240	19.2	
CheckMate 078, 2019	NCT02613507	NSCLC	III	2	1	Niv 3mg/kg q2w	338	10.4	4.0
					2	Docetaxel	166	8.8	
PROLUNG, 2020	NCT02574598	NSCLC	II	2	1	Pem 200mg q3w+Docetaxel	40	8.9	NR
					2	Docetaxel	38	7.9	
IMpower110, 2020	NCT02409342	NSCLC	III	1	1	Ate 1200mg q3w	277	13.4	4.0
					2	P-based chemotherapy	277	13.4	
IMpower131, 2020	NCT02367794	Squamous NSCLC	III	1	1	Ate 1200mg q3w+PC	338	NR	4.0
					2	Ate 1200mg q3w+nPC	343	26.8	
					3	nPC	340	24.8	
IMpower132, 2020	NCT02657434	Nonsquamous NSCLC	III	1	1	Ate 1200mg q3w+AP	292	28.4	4.0
					2	AP	286	28.4	
ARCTIC, 2020	NCT02352948	NSCLC	III	≥3	1	Dur 20mg/kg+Tre 1mg/kg q4w	174	9.1	NR
					2	Dur 10mg/kg q2w	117	9.1	
					3	Tre 10mg/kg q4w	60	9.1	
MYSTIC, 2020	NCT02453282	NSCLC	III	1	1	Dur 20mg/kg q4w	374	30.2	NR
					2	Dur 20mg/kg q4w+Tre 1mg/kg q4w	372	30.2	
					3	P-based chemotherapy	372	30.2	
KEYNOTE-604, 2020	NCT03066778	SCLC	III	1	1	Pem 200mg q3w+EP	228	21.6	4.0
					2	EP	225	21.6	
ORIENT-11, 2020	NCT03607539	Nonsquamous NSCLC	III	1	1	Sin 200mg q3w+AP	266	8.9	4.03
					2	AP	131	8.9	
CameL, 2020	NCT03134872	Nonsquamous NSCLC	III	1	1	Cam 200mg q3w+AC	205	19.3	4.03
					2	AC	207	19.3	
CASPIAN, 2021	NCT03043872	SCLC	III	1	1	Dur 1500mg q3w+Tre 75mg q3w +EP	268	25.1	4.03
					2	Dur 1500mg q3w+EP	268	25.1	
					3	EP	269	25.1	
CheckMate 451, 2021	NCT02538666	SCLC	III	2	1	Niv 1mg/kg+Ipi 3mg/kg q3w	279	8.4	4.0
					2	Niv 240mg q2w	280	9.9	
CheckMate 9LA, 2021	NCT03215706	NSCLC	III	1	1	Niv 360mg q3w+Ipi 1mg/kg q6w +P-based chemotherapy	361	9.7	4.0
					2	P-based chemotherapy	358	9.7	
CheckMate 331, 2021	NCT02481830	SCLC	III	2	1	Niv 240mg q2w	284	7.0	4.0
					2	Topotecan or amrubicin	285	7.6	
KEYNOTE-598, 2021	NCT03302234	NSCLC	III	1	1	Pem 200mg q3w+Ipi 1mg/kg q6w	284	20.6	4.0
					2	Pem 200mg q3w	284	20.6	
EMPOWER-Lung 1, 2021	NCT03088540	NSCLC	III	1	1	Cem 350mg q3w	356	13.1	4.03
					2	P-based chemotherapy	354	13.1	
RATIONALE 307, 2021	NCT03594747	Squamous NSCLC	III	1	1	Tis 200mg q3w+PC	120	8.6	5.0
					2	Tis 200mg q3w+nPC	119	8.6	
					3	PC	121	8.6	

CTCAE, Common Terminology Criteria for Adverse Events; NSCLC, non–small cell lung cancer; SCLC, small cell lung cancer; mg, milligram; kg, kilogram; q3w, receive agents every three weeks; Ipi, ipilimumab; PC, paclitaxel + carboplatin; Niv, nivolumab; Ate, atezolizumab; Pem, pembrolizumab; AC, pemetrexed + carboplatin; EP, etoposide + cisplatin; P-based chemotherapy, platinum–based chemotherapy; Ave, avelumab; AP, pemetrexed + platinum; EC, etoposide + carboplatin; nPC, nanoparticle albumin-bound paclitaxel + carboplatin; Dur, durvalumab; Tre, tremelimumab; Sin, sintilimab; Cem, cemiplimab; Tis, tislelizumab; Min, minimum; NR, not report.

as follows: ICIs + chemotherapy (probability: 56.2% for grade 1–5; 68.5% for grade 3–5), ICI monotherapy + chemotherapy (56.0%; 67.9%), chemotherapy (91.9%; 91.1%), dual ICIs therapy (100.0%; 98.9%), and ICI monotherapy (100.0%; 100.0%) (**Table 2** and, **Table S12**).

As for overall irAEs, the pooled incidences for chemotherapy, ICI monotherapy, ICI monotherapy + chemotherapy, dual ICIs, and dual ICIs + chemotherapy were 17.04%, 30.14%, 41.60%, 43.20%, and 36.09% for grade 1–5 irAEs, and 2.27%, 6.59%, 11.42%, 13.77%, and 13.53% for grade 3–5 irAEs, respectively.

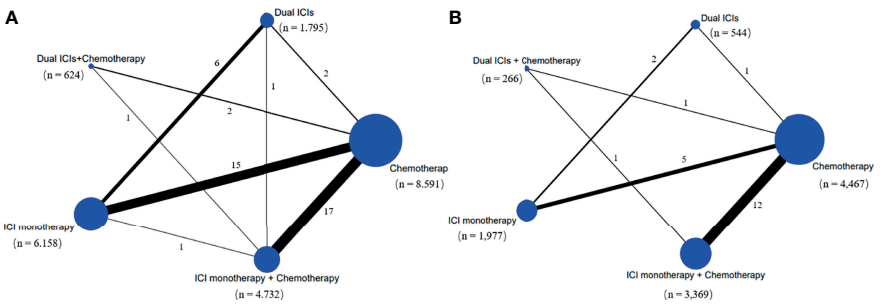

FIGURE 2 | Network map of comparisons based on five treatments in grade 1-5 adverse events **(A)** and grade 1-5 immune-related adverse events **(B)**. Each circular node represents a type of treatment. The node size is proportional to the total number of patients administering a treatment (in parentheses). Each line represents a type of head-to-head comparison. The width of lines is proportional to the total number of studies comparing the connected treatments. ICI, immune checkpoint inhibitor; n, number.

Based on NMA, the safety profiles (**Figure 3B**) of the five treatment choices indicated an extremely decreased risk of irAEs favoring chemotherapy over the other four treatment strategies for both grade 1–5 (RR: 0.18, 95% CI: 0.11–0.29 for chemotherapy *vs.* ICI monotherapy; RR: 0.35, 95% CI: 0.26–0.48 for chemotherapy *vs.* ICI monotherapy + chemotherapy; RR: 0.11, 95% CI: 0.05–0.22 for chemotherapy *vs.* dual ICI therapy; RR: 0.10, 95% CI: 0.04–0.27 for chemotherapy *vs.* dual ICIs + chemotherapy) and grade 3–5 events (RR: 6.65, 95% CI: 3.30–13.39 for ICI monotherapy *vs.* chemotherapy; RR: 3.27, 95% CI: 2.20–4.85 for ICI monotherapy + chemotherapy *vs.* chemotherapy; RR: 15.14, 95% CI: 5.82–39.40 for dual ICI therapy *vs.* chemotherapy; RR: 12.26, 95% CI: 3.89–38.64 for dual ICIs + chemotherapy *vs.* chemotherapy). Among ICI therapeutic schedules, ICI monotherapy + chemotherapy seemed safer than ICI monotherapy (RR: 1.93, 95% CI: 1.09–3.42 for ICI monotherapy *vs.* ICI monotherapy + chemotherapy in grade 1–5 irAEs; RR: 0.49, 95% CI: 0.22–1.10 in grade 3–5 irAEs), dual ICIs therapy (RR: 0.30, 95% CI: 0.13–0.68 in grade 1–5 irAEs; RR: 4.63, 95% CI: 1.64–13.04 for dual ICIs *vs.* ICI monotherapy + chemotherapy in grade 3–5 irAEs), and dual ICIs + chemotherapy (RR: 0.30, 95% CI: 0.12–0.74 in grade 1–5 irAEs; RR: 3.75, 95% CI: 1.25–11.28 for dual ICIs + chemotherapy *vs.* ICI monotherapy + chemotherapy in grade 3–5 irAEs), with one ICI being observed to be safer than two ICIs combination with regards to grade 3–5 irAEs (RR: 2.28, 95% CI: 1.06–4.48 for dual ICIs *vs.* ICI monotherapy). In aspect of safety ranking, dual ICIs + chemotherapy was associated with the worst ranking for grade 1–5 irAEs (probability: 50.5%), followed by dual ICIs (47.2%), ICI monotherapy (80.0%), ICI monotherapy + chemotherapy (98.0%), and finally chemotherapy (100.0%). The risk of experiencing grade 3–5 irAEs was ranked from high to low as follows: dual ICIs (60.4%), dual ICIs + chemotherapy (42.5%), ICI monotherapy (76.3%), ICI monotherapy + chemotherapy (95.0%), and chemotherapy (100.0%) (**Table 2**, **Table S12**).

The results pooled *via* the inconsistency model had a generally satisfactory fit compared with those calculated by the consistency model, except for minor comparisons based on

A Adverse events

n = 32 49.75% (45.52%, 53.99%)	n = 18 15.22% (12.91%, 17.53%)	n = 17 59.96% (54.52%, 65.39%)	n = 5 31.38% (20.32%, 42.44%)	n = 2 54.23% (43.56%, 64.90%)
Chemotherapy	**0.20** **(0.16, 0.26)**	**1.36** **(1.06, 1.74)**	**0.56** **(0.36, 0.89)**	1.60 (0.84, 3.04)
3.70 **(3.05, 4.48)**	ICI monotherapy	**6.80** **(4.81, 9.61)**	**2.82** **(1.83, 4.33)**	**7.99** **(4.01, 15.91)**
0.70 **(0.55, 0.90)**	**0.19** **(0.14, 0.26)**	ICI monotherapy+ Chemotherapy	**0.41** **(0.25, 0.69)**	1.18 (0.61, 2.28)
2.03 **(1.46, 2.81)**	**0.55** **(0.41, 0.74)**	**2.89** **(1.94, 4.29)**	Dual ICIs	**2.84** **(1.29, 6.22)**
0.67 (0.39, 1.17)	**0.18** **(0.10, 0.33)**	0.96 (0.54, 1.70)	**0.33** **(0.18, 0.63)**	Dual ICIs+ Chemotherapy
n = 32 88.35% (86.19%, 90.51%)	n = 19 65.99% (59.80%, 72.18%)	n = 17 93.21% (91.20%, 95.22%)	n = 6 76.47% (64.15%, 88.78%)	n = 2 92.02% (89.05%, 94.99%)

B Immune-related adverse events

n = 17 2.27% (1.44%, 3.09%)	n = 6 6.59% (4.52%, 8.67%)	n = 12 11.42% (7.77%, 15.06%)	n = 2 13.77% (9.09%, 18.46%)	n = 1 13.53%
Chemotherapy	**6.65** **(3.30, 13.39)**	**3.27** **(2.20, 4.85)**	**15.14** **(5.82, 39.40)**	**12.26** **(3.89, 38.64)**
0.18 **(0.11, 0.29)**	ICI monotherapy	0.49 (0.22, 1.10)	**2.28** **(1.06, 4.88)**	1.84 (0.48, 7.05)
0.35 **(0.26, 0.48)**	**1.93** **(1.09, 3.42)**	ICI monotherapy+ Chemotherapy	**4.63** **(1.64, 13.04)**	**3.75** **(1.25, 11.28)**
0.11 **(0.05, 0.22)**	0.58 (0.30, 1.13)	**0.30** **(0.13, 0.68)**	Dual ICIs	0.81 (0.18, 3.60)
0.10 **(0.04, 0.27)**	0.57 (0.20, 1.63)	**0.30** **(0.12, 0.74)**	0.99 (0.30, 3.30)	Dual ICIs+ Chemotherapy
n = 17 17.04% (11.80%, 22.28%)	n = 6 30.14% (19.79%, 40.48%)	n = 12 41.60% (31.06%, 52.14%)	n = 2 43.20% (13.72%, 72.67%)	n = 1 36.09%

FIGURE 3 | Safety profiles based on adverse events **(A)** and immune-related adverse events **(B)**. Pooled incidences and 95% confidence intervals of grade 1–5 events for each treatment are at bottom and that of grade 3–5 events are at top of the figure. Each cell of the safety profiles contains the pooled relative risks and 95% confidence intervals for grade 1–5 (light gray cell) and grade 3–5 (dark gray cell) events; significant results are in bold. The pooled relative risks and 95% confidence intervals indicate the results of the top treatment compared with the bottom treatment. ICI, immune checkpoint inhibitor; n, number.

TABLE 2 | Rankings based on overall AE and irAE.

	1st	2nd	3rd	4th	5th
Grade 1-5 AE	Dual ICIs + CT (56.2)	ICI monotherapy + CT (56.0)	Chemotherapy (91.9)	Dual ICIs (100.0)	ICI monotherapy (100.0)
Grade 3-5 AE	Dual ICIs + CT (68.5)	ICI monotherapy + CT (67.9)	Chemotherapy (91.1)	Dual ICIs (98.9)	ICI monotherapy (100.0)
Grade 1-5 irAE	Dual ICIs + CT (50.5)	Dual ICIs (47.2)	ICI monotherapy (80.0)	ICI monotherapy + CT (98.0)	Chemotherapy (100.0)
Grade 3-5 irAE	Dual ICIs (60.4)	Dual ICIs + CT (42.5)	ICI monotherapy (76.3)	ICI monotherapy + CT (95.0)	Chemotherapy (100.0)

The value in each parenthesis represents the probability of risk to rank (%). ICI, immune checkpoint inhibitor; CT, chemotherapy; AE, adverse event; irAE, immune-related adverse event.

chemotherapy (**Table S13**). Likewise, a less significant inconsistency was observed following the node–splitting analysis (**Table S14**).

Network Meta-Analysis for Specific IrAEs

NMAs and ranking probabilities for different treatment strategies in subgroups of irAEs are depicted in **Figures 4**, **5** and **Table 3**. Although the results for individual irAEs varied by organ system and severity, traditional chemotherapy presented the lowest risk in majority of irAEs.

For gastrointestinal irAEs (**Figures 4A, B**), ICI regimens were associated with higher risk of colitis than chemotherapy, with dual ICIs showing the highest risk (incidence: 3.66% for grade 1–5 and 2.53% for grade 3–5; ranking probability: 91.6% for grade 1–5 and 92.3% for grade 3–5). Nevertheless, a different trend was detected in the case of diarrhea. ICI regimens, especially ICI monotherapy, had a lower risk of causing diarrhea than treatment strategies that included chemotherapy.

For pulmonary irAEs, pneumonitis was significantly higher in patients receiving dual ICIs than in those receiving ICI monotherapy (RR: 0.43, 95% CI: 0.25–0.74 for ICI monotherapy *vs.* dual ICIs in grade 1–5; RR: 2.29, 95% CI: 1.23–4.28 in grade 3–5), or ICI monotherapy + chemotherapy (RR: 0.27, 95% CI: 0.12–0.59 for ICI monotherapy + chemotherapy *vs.* dual ICIs in grade 1–5; RR: 5.01, 95% CI: 1.83–13.67 in grade 3–5) (**Figure 4C**). The ranking order of ICIs regimens was as follows: dual ICIs (probability: 95.2% for grade 1–5; 88.5% for grade 3–5), ICI monotherapy (64.1%; 62.6%), dual ICIs + chemotherapy (31.9%; 35.4%), and ICI monotherapy + chemotherapy (58.6%; 67.9%).

For endocrine irAEs, patients administering dual ICIs with or without chemotherapy seemed to be associated with a high risk of hyperthyroidism, hypothyroidism, hypophysitis, thyroiditis, and diabetes. Owing to the low incidence of serious endocrine irAEs, no positive RRs were detected among the individual ICI strategies (**Figures 4D–G**).

For skin irAEs, the use of ICI monotherapy + chemotherapy, dual ICIs + chemotherapy, and dual ICIs presented the highest risk of pruritus, rash, and severe skin reaction, respectively (**Figures 5A–C**). For other irAEs, no significant difference was observed among the ICI regimens (**Figures 5D–H**).

Sensitivity Analysis in Network Meta-Analysis

Thirty phase III RCTs, and 29 studies that enrolled patients with NSCLC were separately included in the sensitivity analyses. The observed ranking orders were consistent with the original NMA, irrespective of the overall AEs and irAEs (**Table S15**).

DISCUSSION

Major Findings and Interpretation

The current NMA highlights the toxicity profile of ICI–based treatments among patients with advanced lung cancer based on 38 RCTs involving 22,178 patients. Our results indicated that the use of mono- or dual-ICI therapy may reduce the risk of treatment–related AEs at the expense of an increased risk of developing irAEs compared with chemotherapy. During therapy with ICI regimens, patients administering dual ICIs with chemotherapy may experience most AEs (either grade 1–5 or grade 3–5) and irAEs of any grade, and those receiving dual ICIs may have the highest risk of developing serious irAEs. There were differences observed in the toxicity spectra among the five treatment therapies. However, these results should be carefully interpreted because of the limited number of studies on groups receiving dual ICIs with and without chemotherapy.

Comparison With Previous Studies

Recently, developments in lung cancer patients with advanced stages of the disease have shown immunotherapy as a promising treatment option. However, the expanded use of ICIs has resulted in noticeable growth in adverse events, particularly irAEs (6, 68). With more treatment options with ICIs now approved for advanced lung cancer, a robust analysis is urgently required to compare the risk of safety profiles among all of the different treatment regimens.

To date, several systematic reviews and meta-analyses have been conducted to assess the safety profiles of ICIs in patients with cancer, yet few studies have focused on patients with lung cancer. The earliest meta-analysis, which pooled 22 RCTs for evaluating rare but severe irAEs resulting from the use of PD-1 and PD-L1 inhibitors in patients with NSCLC, indicated an increased all–grade pneumonitis risk from ICIs than chemotherapy (OR = 2.35, 95% CI, 1.32–4.20, P = 0.004) (15). However, this study had limited value because of the inclusion of minimal trials with a control group, which inevitably led to insufficient evidence for a conclusion; in addition, only ICI monotherapy was investigated. In 2020, an updated NMA of 25 RCTs was conducted for chemotherapy, ICI monotherapy, dual ICIs combination, and ICIs + chemotherapy, and reported a significantly reduced risk of immune–related pneumonitis in patients with lung cancer following ICIs + chemotherapy when compared with dual ICIs combination and ICI monotherapy (14). Furthermore, three other meta-analyses focused on gastrointestinal irAEs, including diarrhea and/or colitis, and consistently found that PD-1/PD-L1 inhibitors might lead to a higher risk of immune–mediated colitis but might result in a

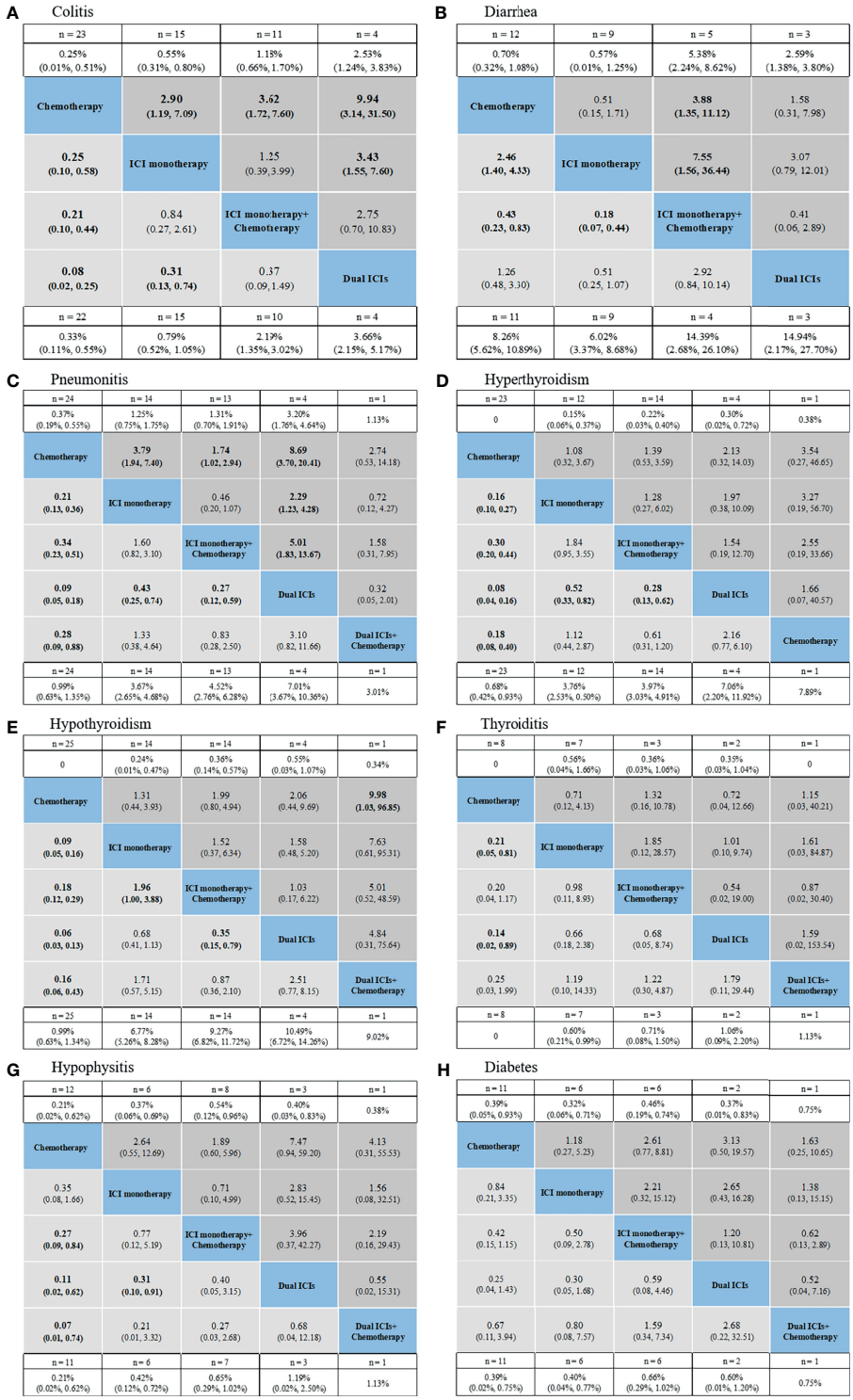

FIGURE 4 | Safety profiles based on specific organs: colitis **(A)**, diarrhea **(B)**, pneumonitis **(C)**, hyperthyroidism **(D)**, hypothyroidism **(E)**, thyroiditis **(F)**, hypophysitis **(G)**, diabetes **(H)**. Pooled incidences and 95% confidence intervals of grade 1–5 events for each treatment are at bottom and that of grade 3–5 events are at top of the figure. Each cell of the safety profiles contains the pooled relative risks and 95% confidence intervals for grade 1–5 (light gray cell) and grade 3–5 (dark gray cell) events; significant results are in bold. The pooled relative risks and 95% confidence intervals indicate the results of the top treatment compared with the bottom treatment. ICI, immune checkpoint inhibitor; n, number.

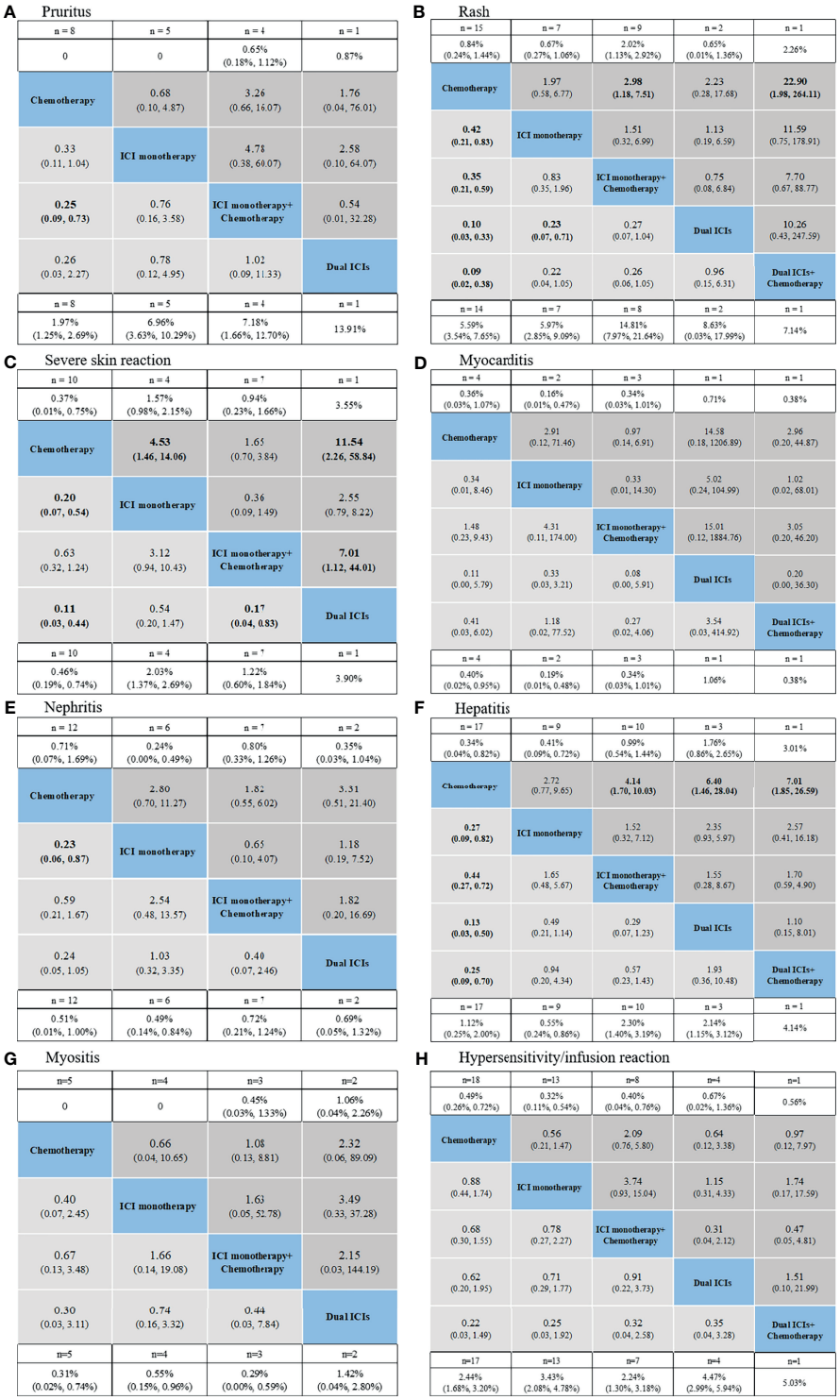

FIGURE 5 | Safety profiles based on specific organs: pruritus **(A)**, rash **(B)**, severe skin reaction **(C)**, myocarditis **(D)**, nephritis **(E)**, hepatitis **(F)**, myositis **(G)**, hypersensitivity/infusion reaction **(H)**. Pooled incidences and 95% confidence intervals of grade 1–5 events for each treatment are at bottom and that of grade 3–5 events are at top of the figure. Each cell of the safety profiles contains the pooled relative risks and 95% confidence intervals for grade 1–5 (light gray cell) and grade 3–5 (dark gray cell) events; significant results are in bold. The pooled relative risks and 95% confidence intervals indicate the results of the top treatment compared with the bottom treatment. ICI, immune checkpoint inhibitor; n, number.

TABLE 3 | Toxicity spectra and rankings based on each specific irAEs.

	1st	2nd	3rd	4th	5th
Gastrointestinal irAE					
sColitis G1-5	Dual ICIs (91.6)	ICI monotherapy + CT (54.0)	ICI monotherapy (61.8)	Chemotherapy (99.9)	–
Colitis G3-5	Dual ICIs (92.3)	ICI monotherapy + CT (57.2)	ICI monotherapy (63.7)	Chemotherapy (98.8)	–
Diarrhea G1-5	ICI monotherapy + CT (94.9)	Chemotherapy (68.1)	Dual ICIs (64.5)	ICI monotherapy (96.4)	–
Diarrhea G3-5	ICI monotherapy + CT (81.6)	Dual ICIs (52.4)	Chemotherapy (57.9)	ICI monotherapy (82.0)	–
Pulmonary irAE					
Pneumonitis G1-5	Dual ICIs (95.2)	ICI monotherapy (64.1)	Dual ICIs + CT (31.9)	ICI monotherapy + CT (58.6)	Chemotherapy (98.5)
Pneumonitis G3-5	Dual ICIs (88.5)	ICI monotherapy (62.6)	Dual ICIs + CT (35.4)	ICI monotherapy + CT (67.9)	Chemotherapy (87.1)
Endocrine irAE					
Hyperthyroidism G1-5	Dual ICIs (92.7)	ICI monotherapy (58.5)	Dual ICIs + CT (51.3)	ICI monotherapy + CT (89.2)	Chemotherapy (100.0)
Hyperthyroidism G3-5	Dual ICIs + CT (57.1)	Dual ICIs (32.2)	ICI monotherapy + CT (29.1)	ICI monotherapy (25.4)	Chemotherapy (31.8)
Hypothyroidism G1-5	Dual ICIs (88.0)	ICI monotherapy (76.6)	Dual ICIs + CT (45.3)	ICI monotherapy + CT (60.8)	Chemotherapy (100.0)
Hypothyroidism G3-5	Dual ICIs + CT (83.9)	Dual ICIs (38.4)	ICI monotherapy + CT (28.2)	ICI monotherapy (36.3)	Chemotherapy (57.6)
Thyroiditis G1-5	Dual ICIs (47.6)	ICI monotherapy (35.7)	ICI monotherapy + CT (32.0)	Dual ICIs + CT (30.3)	Chemotherapy (87.1)
Thyroiditis G3-5	Dual ICIs + CT (34.5)	ICI monotherapy + CT (27.7)	Chemotherapy (34.4)	ICI monotherapy (32.3)	Dual ICIs (31.6)
Hypophysitis G1-5	Dual ICIs + CT (58.6)	Dual ICIs (44.3)	ICI monotherapy + CT (40.5)	ICI monotherapy (47.6)	Chemotherapy (88.3)
Hypophysitis G3-5	Dual ICIs (57.5)	Dual ICIs + CT (24.0)	ICI monotherapy (33.8)	ICI monotherapy + CT (38.7)	Chemotherapy (66.0)
Diabetes G1-5	Dual ICIs (62.7)	ICI monotherapy + CT (43.7)	Dual ICIs + CT (24.0)	ICI monotherapy (27.4)	Chemotherapy (39.0)
Diabetes G3-5	Dual ICIs (49.3)	ICI monotherapy + CT (39.5)	Dual ICIs + CT (22.4)	ICI monotherapy (27.0)	Chemotherapy (38.3)
Skin irAE					
Pruritus G1-5	ICI monotherapy + CT (42.4)	Dual ICIs (23.9)	ICI monotherapy (38.8)	Chemotherapy (87.0)	–
Pruritus G3-5	ICI monotherapy + CT (57.6)	Dual ICIs (22.1)	Chemotherapy (38.0)	ICI monotherapy (46.2)	–
Rash G1-5	Dual ICIs + CT (51.8)	Dual ICIs (49.0)	ICI monotherapy + CT (62.5)	ICI monotherapy (64.6)	Chemotherapy (99.3)
Rash G3-5	Dual ICIs + CT (89.6)	ICI monotherapy + CT (49.5)	Dual ICIs (25.1)	ICI monotherapy (36.8)	Chemotherapy (70.0)
Severe skin reaction G1-5	Dual ICIs (88.4)	ICI monotherapy (86.2)	ICI monotherapy + CT (87.2)	Chemotherapy (91.1)	–
Severe skin reaction G3-5	Dual ICIs (93.4)	ICI monotherapy (87.0)	ICI monotherapy + CT (79.3)	Chemotherapy (87.5)	–
Other irAE					
Myocarditis G1-5	Dual ICIs (61.1)	ICI monotherapy (44.6)	Dual ICIs + CT (30.2)	Chemotherapy (40.2)	ICI monotherapy + CT (49.7)
Myocarditis G3-5	Dual ICIs (60.0)	ICI monotherapy (42.2)	Dual ICIs + CT (28.8)	Chemotherapy (37.7)	ICI monotherapy + CT (37.4)
Nephritis G1-5	ICI monotherapy + CT (42.4)	Dual ICIs (23.9)	ICI monotherapy (38.8)	Chemotherapy (87.0)	–
Nephritis G3-5	ICI monotherapy + CT (57.6)	Dual ICIs (22.1)	Chemotherapy (38.0)	ICI monotherapy (46.2)	–
Hepatitis G1-5	Dual ICIs (75.6)	ICI monotherapy (44.7)	Dual ICIs + CT (38.1)	ICI monotherapy + CT (69.6)	Chemotherapy (98.5)
Hepatitis G3-5	Dual ICIs + CT (49.8)	Dual ICIs (25.8)	ICI monotherapy + CT (38.2)	ICI monotherapy (60.0)	Chemotherapy (93.6)
Myositis G1-5	Dual ICIs (52.8)	ICI monotherapy (48.7)	ICI monotherapy + CT (34.7)	Chemotherapy (53.4)	–
Myositis G3-5	Dual ICIs (55.2)	ICI monotherapy + CT (25.0)	Chemotherapy (35.7)	ICI monotherapy (44.4)	–
Hypersensitivity/infusion reaction G1-5	Dual ICIs + CT (77.3)	Dual ICIs (39.6)	ICI monotherapy + CT (25.3)	ICI monotherapy (34.0)	Chemotherapy (45.1)
Hypersensitivity/infusion reaction G3-5	ICI monotherapy + CT (64.7)	Chemotherapy (33.8)	Dual ICIs + CT (16.7)	Dual ICIs (27.3)	ICI monotherapy (36.5)

The value in each parenthesis represents the probability of risk to rank (%). ICI, immune checkpoint inhibitor; CT, chemotherapy; irAE, immune-related adverse event; G, grade.

reduction in diarrhea when compared with chemotherapy (16–18). Notably, the above–mentioned studies focused on one specific irAE, making it difficult to unveil the panorama of toxicity from ICIs. Recently, Berti et al. compared overall and organ–specific irAEs between immunotherapy and immune–chemotherapy in lung cancer based on 16 phase III clinical trials and found that immunotherapy alone showed a significantly lower risk of irAEs than immunochemotherapy (69). The study investigators excluded phase II RCTs and ignored the discrepancy between ICI monotherapy and dual ICI combination therapy. Given these limitations, the current NMA comprehensively estimated the overall and organ–specific toxicity spectrum among all up to date ICI regimens by pooling all currently available phase II and III clinical trials involving patients with NSCLC and SCLC.

Safety Profile of ICI Regimens in Patients With Lung Cancer

It is well known that the incidence of overall adverse events during ICI monotherapy is lower than that for conventional chemotherapy, while exposure to immunotherapy increases the risk of irAEs, as seen in the present study. Interestingly, further analyses of ICI–based regimens found that ICI monotherapy + chemotherapy decreased the risk of grade 1–5 and grade 3–5 irAEs compared with ICI monotherapy and dual ICIs therapy. This trend was also observed in pneumonitis and myocarditis (grade1–5 and grade 3–5), as well as grade 1–5 hyperthyroidism, hypothyroidism, thyroiditis, severe skin reaction, hepatitis, myositis based on ranking. Consistent with our study, Chen et al. reported that the use of an ICI with chemotherapy led to less pneumonitis than use of ICI monotherapy or dual ICIs combination (14). One possible reason for the decreased risk in irAEs when chemotherapy is added to ICI regimens may be due to the fact that conventional chemotherapy consists of cytotoxic agents that are believed to cause chemotherapy–induced immunosuppression, augmenting stress on the entire immune system and resulting in a reduced immune function (70, 71). Another contributing factor might be the use of corticosteroids. In chemotherapy regimens containing cytotoxic agents such as platinum, pemetrexed and taxanes, which are the standard treatments for lung cancer, corticosteroids are commonly prescribed as binding pre-treatment for antiemetic and antiallergy purposes. The baseline or early use of corticosteroids at the time of initiating ICI therapy could blunt a proliferative burst of CD8-positive T cells, which are otherwise needed for the ICI therapeutic response, thus affecting the efficacy and toxicity (72, 73). In addition, corticosteroids are recommended immunosuppressive agents for various mild-to-severe irAEs such as pneumonitis, colitis, hepatitis, thyroiditis, rash, etc. (74). Accordingly, the risk of experiencing irAEs may be underestimated in circumstances with corticosteroids.

Some studies have pointed out that the incidence of irAEs in patients on a combination of two ICIs was higher than that observed with ICI monotherapy. In the present study, we did not observe any statistical differences between these two groups in terms of overall grade 1–5 irAEs, let alone for rare irAEs, such as thyroiditis, diabetes, myocarditis, nephritis, hepatitis, and myositis. Even between dual ICIs + chemotherapy and ICI monotherapy (both grade 1–5 and grade 3–5 irAEs), significant difference was not detected. However, this trend can be seen from the ranking either in grade 1–5 irAEs or grade 3–5 irAEs. Given the fact that a limited number of studies directly compared dual ICIs (with or without chemotherapy) with ICIs monotherapy, these results should be interpreted with caution. Therefore, more high–quality RCTs are needed to investigate the incidence of irAEs among different ICI–based regimens.

Clinical Implication

Our results provide possible safety speculations for clinical decision–making to tailor the best immunotherapy strategy for each patient with lung cancer. For instance, administration of an individual ICI or dual ICIs plus chemotherapy was reported to have a significantly lower risk of pneumonitis (grade 1–5 and grade 3–5) than ICI monotherapy and dual ICIs therapy and could perhaps be preferred in selected cases of lung fibrosis or severe chronic obstructive pulmonary disease. In addition, ICI monotherapy was associated with the lowest risk for both diarrhea and colitis among ICI regimens and could perhaps be preferred in selected patients in whom gastrointestinal irAEs could be a concern. Of course, these results should be proven in prospective registries or cohorts to better understand the safety of novel ICI–based options in this subset of patients.

Study Strengths and Limitations

The major strength of this study was to depict a full view of the safety profile of ICIs at different levels (risk of overall AEs of any grade and grade 3–5, any irAEs and severe irAEs by individual organs/system). Second, owing to the different toxicity spectrum based on cancer types, the study focused on a specific population of patients (i.e., with lung cancer). Third, except for combination of ICIs and targeted agents, we included all available ICI–based regimens to aid clinicians to tailor the ICI strategy for individual patient with lung cancer.

However, several limitations of this study need to be acknowledged. First, the included RCTs used different terms to describe irAEs. In clinical settings, AEs or irAEs are usually recognised and reported depending on the evaluation of the physician and are diagnosed based on their experience. Therefore, the identification of irAEs might not be completely accurate and might lead to bias in the assessment. In addition, few studies reported irAEs during the entire ICI monotherapy maintenance as separate outcome, making it difficult to investigate irAEs during this period. Second, the included studies showed heterogeneity in terms of subtype of cancer, pharmacological strategy, follow–up time, and other factors. As we focused on outlining the entire safety profile of ICI agents, subgroup analyses based on patients' histology, specified ICIs and kind of chemotherapy were not performed. However, we performed sensitivity analyses and meta-regression in pairwise meta-analysis, as well as sensitivity analyses in NMA, to control

for these possible confounders. Third, inconsistent results between direct and indirect comparisons were observed. Unlike direct comparison, network meta-analysis included both direct evidence and indirect effects from the other studies. Because of above-mentioned heterogeneity among RCTs, integrated results possibly underestimated or overestimated the actual results. Fourth, we did not obtain access to comorbidity data, which might be high–risk factors for certain irAEs. Lastly, we did not have the resources to review non-English publications. However, we enrolled studies identified following a comprehensive search of broad databases and are thus confident that this study covered the majority of trials in these special patients. Given aforementioned limitations, further studies are needed to confirm our findings.

CONCLUSIONS

In summary, this network meta-analysis contributes to clarifying the frequency and characteristics of adverse events during ICI treatment in patients with advanced lung cancer. We found that ICI monotherapy + chemotherapy had the best immune–related safety profile, followed by ICI monotherapy, dual ICIs therapy, dual ICIs + chemotherapy for grade 1–5 irAEs, and ICI monotherapy, dual ICIs + chemotherapy, dual ICIs therapy for grade 3–5 irAEs. The safety ranking of ICI-based choices is modulated by specific irAEs and severity.

DATA AVAILABILITY STATEMENT

The original contributions presented in the study are included in the article/**Supplementary Material**. Further inquiries can be directed to the corresponding authors.

AUTHOR CONTRIBUTIONS

Z-CG, X-YC, and H-WL are the guarantors of the entire manuscript. Z-CG and Y-DY contributed to the study conception and design, critical revision of the manuscript for important intellectual content, and final approval of the version to be published. J-JC, JF, and Y-JS contributed to the data acquisition, analysis, and interpretation. All authors contributed to the article and approved the submitted version.

FUNDING

This study was supported by the Ren Ji Boost Project of National Natural Science Foundation of China (RJTJ-JX-001), the Research Funds of Shanghai Health and Family Planning Commission (20184Y0022), Clinical Pharmacy Innovation Research Institute of Shanghai Jiao Tong University School of Medicine (CXYJY2019ZD001), and Shanghai "Rising Stars of Medical Talent" Youth Development Program – Youth Medical Talents – Clinical Pharmacist Program [SHWJRS (2019) 072].

ACKNOWLEDGMENTS

We sincerely thank Pedzisai M for language editing about our manuscript.

SUPPLEMENTARY MATERIAL

The Supplementary Material for this article can be found online at: https://www.frontiersin.org/articles/10.3389/fimmu.2021.760737/full#supplementary-material

REFERENCES

1. Sung H, Ferlay J, Siegel RL, Laversanne M, Soerjomataram I, Jemal A, et al. Global Cancer Statistics 2020: GLOBOCAN Estimates of Incidence and Mortality Worldwide for 36 Cancers in 185 Countries. *CA Cancer J Clin* (2021) 71(3):209–49. doi: 10.3322/caac.21660
2. Arbour KC, Riely GJ. Systemic Therapy for Locally Advanced and Metastatic Non-Small Cell Lung Cancer: A Review. *Jama* (2019) 322(8):764–74. doi: 10.1001/jama.2019.11058
3. Noronha V, Sekhar A, Patil VM, Menon N, Joshi A, Kapoor A, et al. Systemic Therapy for Limited Stage Small Cell Lung Carcinoma. *J Thorac Dis* (2020) 12 (10):6275–90. doi: 10.21037/jtd-2019-sclc-11
4. Mielgo-Rubio X, Uribelarrea EA, Cortés LQ, Moyano MS. Immunotherapy in Non-Small Cell Lung Cancer: Update and New Insights. *J Clin Transl Res* (2021) 7(1):1–21. doi: 10.18053/jctres.07.202101.001
5. Zhang H, Dai Z, Wu W, Wang Z, Zhang N, Zhang L, et al. Regulatory Mechanisms of Immune Checkpoints PD-L1 and CTLA-4 in Cancer. *J Exp Clin Cancer Res* (2021) 40(1):184. doi: 10.1186/s13046-021-01987-7
6. Lee DJ, Lee HJ Jr, Farmer JR, Reynolds KL. Mechanisms Driving Immune-Related Adverse Events in Cancer Patients Treated With Immune Checkpoint Inhibitors. *Curr Cardiol Rep* (2021) 23(8):98. doi: 10.1007/s11886-021-01530-2
7. Brahmer JR, Abu-Sbeih H, Ascierto PA, Brufsky J, Cappelli LC, Cortazar FB, et al. Society for Immunotherapy of Cancer (SITC) Clinical Practice Guideline on Immune Checkpoint Inhibitor-Related Adverse Events. *J Immunother Cancer* (2021) 9(6):e002435. doi: 10.1136/jitc-2021-002435
8. Gangadhar TC, Vonderheide RH. Mitigating the Toxic Effects of Anticancer Immunotherapy. *Nat Rev Clin Oncol* (2014) 11(2):91–9. doi: 10.1038/nrclinonc.2013.245
9. Puzanov I, Diab A, Abdallah K, Bingham CO 3rd, Brogdon C, Dadu R, et al. Managing Toxicities Associated With Immune Checkpoint Inhibitors: Consensus Recommendations From the Society for Immunotherapy of Cancer (SITC) Toxicity Management Working Group. *J Immunother Cancer* (2017) 5(1):95. doi: 10.1186/s40425-017-0300-z
10. Durrechou Q, Domblides C, Sionneau B, Lefort F, Quivy A, Ravaud A, et al. Management of Immune Checkpoint Inhibitor Toxicities. *Cancer Manag Res* (2020) 12:9139–58. doi: 10.2147/cmar.S218756
11. De Velasco G, Je Y, Bossé D, Awad MM, Ott PA, Moreira RB, et al. Comprehensive Meta-Analysis of Key Immune-Related Adverse Events From CTLA-4 and PD-1/PD-L1 Inhibitors in Cancer Patients. *Cancer Immunol Res* (2017) 5(4):312–8. doi: 10.1158/2326-6066.Cir-16-0237
12. Wang Y, Zhou S, Yang F, Qi X, Wang X, Guan X, et al. Treatment-Related Adverse Events of PD-1 and PD-L1 Inhibitors in Clinical Trials: A Systematic Review and Meta-Analysis. *JAMA Oncol* (2019) 5(7):1008–19. doi: 10.1001/jamaoncol.2019.0393
13. Wang Y, Kong D, Wang C, Chen J, Li J, Liu Z, et al. A Systematic Review and Meta-Analysis of Immune-Related Adverse Events of Anti-PD-1 Drugs in

Randomized Controlled Trials. *Technol Cancer Res Treat* (2020) 19:1533033820967454. doi: 10.1177/1533033820967454
14. Chen X, Zhang Z, Hou X, Zhang Y, Zhou T, Liu J, et al. Immune-Related Pneumonitis Associated With Immune Checkpoint Inhibitors in Lung Cancer: A Network Meta-Analysis. *J Immunother Cancer* (2020) 8(2): e001170. doi: 10.1136/jitc-2020-001170
15. Hu YB, Zhang Q, Li HJ, Michot JM, Liu HB, Zhan P, et al. Evaluation of Rare But Severe Immune Related Adverse Effects in PD-1 and PD-L1 Inhibitors in Non-Small Cell Lung Cancer: A Meta-Analysis. *Transl Lung Cancer Res* (2017) 6(Suppl 1):S8–s20. doi: 10.21037/tlcr.2017.12.10
16. Lin LL, Lin GF, Luo Q, Chen XQ. The Incidence and Relative Risk of PD-1/PD-L1 Inhibitors-Related Colitis in Non-Small Cell Lung Cancer: A Meta-Analysis of Randomized Controlled Trials. *Int Immunopharmacol* (2019) 77:105975. doi: 10.1016/j.intimp.2019.105975
17. Zhang C, Zhang S, Xu D, Liu R, Zhu Q, Zhao Y, et al. Incidence Risk of PD-1/PD-L1 Related Diarrhea in Non-Small Cell Lung Cancer (NSCLC) Patients: A Systematic Review and Meta-Analysis. *Cancer Manag Res* (2019) 11:3957–69. doi: 10.2147/cmar.S202756
18. Bishay K, Tandon P, Bourassa-Blanchette S, Laurie SA, McCurdy JD. The Risk of Diarrhea and Colitis in Patients With Lung Cancer Treated With Immune Checkpoint Inhibitors: A Systematic Review and Meta-Analysis. *Curr Oncol* (2020) 27(5):e486–94. doi: 10.3747/co.27.6251
19. Garrett N, da Costa ACC, Damiani G, Vasques CI. Patients With Lung Cancer Undergoing Immune Checkpoint Inhibitors: A Meta-Analysis of Dermatological Toxicities. *Crit Rev Oncol Hematol* (2020) 152:102983. doi: 10.1016/j.critrevonc.2020.102983
20. Yan YD, Ding Z, Pan MM, Xia Q, Cui JJ, Wang LW, et al. Net Clinical Benefit of Direct Oral Anticoagulants in Patients With Cancer and Venous Thromboembolism: A Systematic Review and Trade-Off Analysis. *Front Cardiovasc Med* (2020) 7:586020. doi: 10.3389/fcvm.2020.586020
21. Page MJ, Moher D, Bossuyt PM, Boutron I, Hoffmann TC, Mulrow CD, et al. PRISMA 2020 Explanation and Elaboration: Updated Guidance and Exemplars for Reporting Systematic Reviews. *BMJ* (2021) 372:n160. doi: 10.1136/bmj.n160
22. Higgins JP, Altman DG, Gøtzsche PC, Jüni P, Moher D, Oxman AD, et al. The Cochrane Collaboration's Tool for Assessing Risk of Bias in Randomised Trials. *BMJ* (2011) 343:d5928. doi: 10.1136/bmj.d5928
23. Higgins JP, Thompson SG. Quantifying Heterogeneity in a Meta-Analysis. *Stat Med* (2002) 21(11):1539–58. doi: 10.1002/sim.1186
24. Yan YD, Zhang C, Shen L, Su YJ, Liu XY, Wang LW, et al. Net Clinical Benefit of Non-Vitamin K Antagonist Oral Anticoagulants for Venous Thromboembolism Prophylaxis in Patients With Cancer: A Systematic Review and Trade-Off Analysis From 9 Randomized Controlled Trials. *Front Pharmacol* (2018) 9:575. doi: 10.3389/fphar.2018.00575
25. Gu ZC, Wei AH, Zhang C, Wang XH, Zhang L, Shen L, et al. Risk of Major Gastrointestinal Bleeding With New *vs.* Conventional Oral Anticoagulants: A Systematic Review and Meta-Analysis. *Clin Gastroenterol Hepatol* (2020) 18 (4):792–9.e761. doi: 10.1016/j.cgh.2019.05.056
26. Qian J, Yan YD, Yang SY, Zhang C, Li WY, Gu ZC. Benefits and Harms of Low-Dose Rivaroxaban in Asian Patients With Atrial Fibrillation: A Systematic Review and Meta-Analysis of Real-World Studies. *Front Pharmacol* (2021) 12:642907. doi: 10.3389/fphar.2021.642907
27. Egger M, Davey Smith G, Schneider M, Minder C. Bias in Meta-Analysis Detected by a Simple, Graphical Test. *Bmj* (1997) 315(7109):629–34. doi: 10.1136/bmj.315.7109.629
28. Zhang P, Wei S, Zhai K, Huang J, Cheng X, Tao Z, et al. Efficacy of Left Ventricular Unloading Strategies During Venoarterial Extracorporeal Membrane Oxygenation in Patients With Cardiogenic Shock: A Protocol for a Systematic Review and Bayesian Network Meta-Analysis. *BMJ Open* (2021) 11(10):e047046. doi: 10.1136/bmjopen-2020-047046
29. Zhao Z, Ma CL, Gu ZC, Dong Y, Lv Y, Zhong MK. Incidence and Risk of Infection Associated With Fingolimod in Patients With Multiple Sclerosis: A Systematic Review and Meta-Analysis of 8,448 Patients From 12 Randomized Controlled Trials. *Front Immunol* (2021) 12:611711. doi: 10.3389/fimmu.2021.611711
30. Lynch TJ, Bondarenko I, Luft A, Serwatowski P, Barlesi F, Chacko R, et al. Ipilimumab in Combination With Paclitaxel and Carboplatin as First-Line Treatment in Stage IIIB/IV Non-Small-Cell Lung Cancer: Results From a Randomized, Double-Blind, Multicenter Phase II Study. *J Clin Oncol* (2012) 30(17):2046–54. doi: 10.1200/jco.2011.38.4032
31. Reck M, Bondarenko I, Luft A, Serwatowski P, Barlesi F, Chacko R, et al. Ipilimumab in Combination With Paclitaxel and Carboplatin as First-Line Therapy in Extensive-Disease-Small-Cell Lung Cancer: Results From a Randomized, Double-Blind, Multicenter Phase 2 Trial. *Ann Oncol* (2013) 24 (1):75–83. doi: 10.1093/annonc/mds213
32. Borghaei H, Paz-Ares L, Horn L, Spigel DR, Steins M, Ready NE, et al. Nivolumab *Versus* Docetaxel in Advanced Nonsquamous Non-Small-Cell Lung Cancer. *N Engl J Med* (2015) 373(17):1627–39. doi: 10.1056/NEJMoa1507643
33. Brahmer J, Reckamp KL, Baas P, Crinò L, Eberhardt WE, Poddubskaya E, et al. Nivolumab *Versus* Docetaxel in Advanced Squamous-Cell Non-Small-Cell Lung Cancer. *N Engl J Med* (2015) 373(2):123–35. doi: 10.1056/NEJMoa1504627
34. Antonia SJ, López-Martin JA, Bendell J, Ott PA, Taylor M, Eder JP, et al. Nivolumab Alone and Nivolumab Plus Ipilimumab in Recurrent Small-Cell Lung Cancer (CheckMate 032): A Multicentre, Open-Label, Phase 1/2 Trial. *Lancet Oncol* (2016) 17(7):883–95. doi: 10.1016/s1470-2045(16)30098-5
35. Fehrenbacher L, Spira A, Ballinger M, Kowanetz M, Vansteenkiste J, Mazieres J, et al. Atezolizumab *Versus* Docetaxel for Patients With Previously Treated Non-Small-Cell Lung Cancer (POPLAR): A Multicentre, Open-Label, Phase 2 Randomised Controlled Trial. *Lancet* (2016) 387(10030):1837–46. doi: 10.1016/s0140-6736(16)00587-0
36. Herbst RS, Baas P, Kim DW, Felip E, Pérez-Gracia JL, Han JY, et al. Pembrolizumab *Versus* Docetaxel for Previously Treated, PD-L1-Positive, Advanced Non-Small-Cell Lung Cancer (KEYNOTE-010): A Randomised Controlled Trial. *Lancet* (2016) 387(10027):1540–50. doi: 10.1016/s0140-6736(15)01281-7
37. Langer CJ, Gadgeel SM, Borghaei H, Papadimitrakopoulou VA, Patnaik A, Powell SF, et al. Carboplatin and Pemetrexed With or Without Pembrolizumab for Advanced, Non-Squamous Non-Small-Cell Lung Cancer: A Randomised, Phase 2 Cohort of the Open-Label KEYNOTE-021 Study. *Lancet Oncol* (2016) 17(11):1497–508. doi: 10.1016/s1470-2045(16)30498-3
38. Reck M, Luft A, Szczesna A, Havel L, Kim SW, Akerley W, et al. Phase III Randomized Trial of Ipilimumab Plus Etoposide and Platinum *Versus* Placebo Plus Etoposide and Platinum in Extensive-Stage Small-Cell Lung Cancer. *J Clin Oncol* (2016) 34(31):3740–8. doi: 10.1200/jco.2016.67.6601
39. Reck M, Rodríguez-Abreu D, Robinson AG, Hui R, Csőszi T, Fülöp A, et al. Pembrolizumab *Versus* Chemotherapy for PD-L1-Positive Non-Small-Cell Lung Cancer. *N Engl J Med* (2016) 375(19):1823–33. doi: 10.1056/NEJMoa1606774
40. Carbone DP, Reck M, Paz-Ares L, Creelan B, Horn L, Steins M, et al. First-Line Nivolumab in Stage IV or Recurrent Non-Small-Cell Lung Cancer. *N Engl J Med* (2017) 376(25):2415–26. doi: 10.1056/NEJMoa1613493
41. Govindan R, Szczesna A, Ahn MJ, Schneider CP, Gonzalez Mella PF, Barlesi F, et al. Phase III Trial of Ipilimumab Combined With Paclitaxel and Carboplatin in Advanced Squamous Non-Small-Cell Lung Cancer. *J Clin Oncol* (2017) 35(30):3449–57. doi: 10.1200/jco.2016.71.7629
42. Rittmeyer A, Barlesi F, Waterkamp D, Park K, Ciardiello F, von Pawel J, et al. Atezolizumab *Versus* Docetaxel in Patients With Previously Treated Non-Small-Cell Lung Cancer (OAK): A Phase 3, Open-Label, Multicentre Randomised Controlled Trial. *Lancet* (2017) 389(10066):255–65. doi: 10.1016/s0140-6736(16)32517-x
43. Barlesi F, Vansteenkiste J, Spigel D, Ishii H, Garassino M, de Marinis F, et al. Avelumab *Versus* Docetaxel in Patients With Platinum-Treated Advanced Non-Small-Cell Lung Cancer (JAVELIN Lung 200): An Open-Label, Randomised, Phase 3 Study. *Lancet Oncol* (2018) 19(11):1468–79. doi: 10.1016/s1470-2045(18)30673-9
44. Gandhi L, Rodríguez-Abreu D, Gadgeel S, Esteban E, Felip E, De Angelis F, et al. Pembrolizumab Plus Chemotherapy in Metastatic Non-Small-Cell Lung Cancer. *N Engl J Med* (2018) 378(22):2078–92. doi: 10.1056/NEJMoa1801005
45. Horn L, Mansfield AS, Szczęsna A, Havel L, Krzakowski M, Hochmair MJ, et al. First-Line Atezolizumab Plus Chemotherapy in Extensive-Stage Small-Cell Lung Cancer. *N Engl J Med* (2018) 379(23):2220–9. doi: 10.1056/NEJMoa1809064
46. Paz-Ares L, Luft A, Vicente D, Tafreshi A, Gümüş M, Mazières J, et al. Pembrolizumab Plus Chemotherapy for Squamous Non-Small-Cell Lung Cancer. *N Engl J Med* (2018) 379(21):2040–51. doi: 10.1056/NEJMoa1810865

47. Hellmann MD, Paz-Ares L, Bernabe Caro R, Zurawski B, Kim SW, Carcereny Costa E, et al. Nivolumab Plus Ipilimumab in Advanced Non-Small-Cell Lung Cancer. *N Engl J Med* (2019) 381(21):2020–31. doi: 10.1056/NEJMoa1910231
48. Mok TSK, Wu YL, Kudaba I, Kowalski DM, Cho BC, Turna HZ, et al. Pembrolizumab *Versus* Chemotherapy for Previously Untreated, PD-L1-Expressing, Locally Advanced or Metastatic Non-Small-Cell Lung Cancer (KEYNOTE-042): A Randomised, Open-Label, Controlled, Phase 3 Trial. *Lancet* (2019) 393(10183):1819–30. doi: 10.1016/s0140-6736(18)32409-7
49. Pujol JL, Greillier L, Audigier-Valette C, Moro-Sibilot D, Uwer L, Hureaux J, et al. A Randomized Non-Comparative Phase II Study of Anti-Programmed Cell Death-Ligand 1 Atezolizumab or Chemotherapy as Second-Line Therapy in Patients With Small Cell Lung Cancer: Results From the IFCT-1603 Trial. *J Thorac Oncol* (2019) 14(5):903–13. doi: 10.1016/j.jtho.2019.01.008
50. West H, McCleod M, Hussein M, Morabito A, Rittmeyer A, Conter HJ, et al. Atezolizumab in Combination With Carboplatin Plus Nab-Paclitaxel Chemotherapy Compared With Chemotherapy Alone as First-Line Treatment for Metastatic Non-Squamous Non-Small-Cell Lung Cancer (IMpower130): A Multicentre, Randomised, Open-Label, Phase 3 Trial. *Lancet Oncol* (2019) 20(7):924–37. doi: 10.1016/s1470-2045(19)30167-6
51. Wu YL, Lu S, Cheng Y, Zhou C, Wang J, Mok T, et al. Nivolumab *Versus* Docetaxel in a Predominantly Chinese Patient Population With Previously Treated Advanced NSCLC: CheckMate 078 Randomized Phase III Clinical Trial. *J Thorac Oncol* (2019) 14(5):867–75. doi: 10.1016/j.jtho.2019.01.006
52. Arrieta O, Barrón F, Ramírez-Tirado LA, Zatarain-Barrón ZL, Cardona AF, Díaz-García D, et al. Efficacy and Safety of Pembrolizumab Plus Docetaxel *vs.* Docetaxel Alone in Patients With Previously Treated Advanced Non-Small Cell Lung Cancer: The PROLUNG Phase 2 Randomized Clinical Trial. *JAMA Oncol* (2020) 6(6):856–64. doi: 10.1001/jamaoncol.2020.0409
53. Herbst RS, Giaccone G, de Marinis F, Reinmuth N, Vergnenegre A, Barrios CH, et al. Atezolizumab for First-Line Treatment of PD-L1-Selected Patients With NSCLC. *N Engl J Med* (2020) 383(14):1328–39. doi: 10.1056/NEJMoa1917346
54. Jotte R, Cappuzzo F, Vynnychenko I, Stroyakovskiy D, Rodriguez-Abreu D, Hussein M, et al. Atezolizumab in Combination With Carboplatin and Nab-Paclitaxel in Advanced Squamous Non-Small-Cell Lung Cancer (IMpower131): Results From a Randomized Phase III Trial. *J Thorac Oncol* (2020) 15(8):1351–60. doi: 10.1016/j.jtho.2020.03.028
55. Nishio M, Barlesi F, West H, Ball S, Bordoni R, Cobo M, et al. Atezolizumab Plus Chemotherapy for First-Line Treatment of Non-Squamous Non-Small Cell Lung Cancer: Results From the Randomized Phase III IMpower132 Trial. *J Thorac Oncol* (2021) 16(4):653–64. doi: 10.1016/j.jtho.2020.11.025
56. Planchard D, Reinmuth N, Orlov S, Fischer JR, Sugawara S, Mandziuk S, et al. ARCTIC: Durvalumab With or Without Tremelimumab as Third-Line or Later Treatment of Metastatic Non-Small-Cell Lung Cancer. *Ann Oncol* (2020) 31(5):609–18. doi: 10.1016/j.annonc.2020.02.006
57. Rizvi NA, Cho BC, Reinmuth N, Lee KH, Luft A, Ahn MJ, et al. Durvalumab With or Without Tremelimumab *vs.* Standard Chemotherapy in First-Line Treatment of Metastatic Non-Small Cell Lung Cancer: The MYSTIC Phase 3 Randomized Clinical Trial. *JAMA Oncol* (2020) 6(5):661–74. doi: 10.1001/jamaoncol.2020.0237
58. Rudin CM, Awad MM, Navarro A, Gottfried M, Peters S, Csőszi T, et al. Pembrolizumab or Placebo Plus Etoposide and Platinum as First-Line Therapy for Extensive-Stage Small-Cell Lung Cancer: Randomized, Double-Blind, Phase III KEYNOTE-604 Study. *J Clin Oncol* (2020) 38(21):2369–79. doi: 10.1200/JCO.20.00793
59. Yang Y, Wang Z, Fang J, Yu Q, Han B, Cang S, et al. Efficacy and Safety of Sintilimab Plus Pemetrexed and Platinum as First-Line Treatment for Locally Advanced or Metastatic Nonsquamous NSCLC: A Randomized, Double-Blind, Phase 3 Study (Oncology Program by InnovENT Anti-PD-1-11). *J Thorac Oncol* (2020) 15(10):1636–46. doi: 10.1016/j.jtho.2020.07.014
60. Zhou C, Chen G, Huang Y, Zhou J, Lin L, Feng J, et al. Camrelizumab Plus Carboplatin and Pemetrexed *Versus* Chemotherapy Alone in Chemotherapy-Naive Patients With Advanced Non-Squamous Non-Small-Cell Lung Cancer (CameL): A Randomised, Open-Label, Multicentre, Phase 3 Trial. *Lancet Respir Med* (2020) 9(3):305–14. doi: 10.1080/15384047.2020.182926510.1016/s2213-2600(20)30365-9
61. Boyer M, Şendur MAN, Rodríguez-Abreu D, Park K, Lee DH, Çiçin I, et al. Pembrolizumab Plus Ipilimumab or Placebo for Metastatic Non-Small-Cell Lung Cancer With PD-L1 Tumor Proportion Score ≥ 50%: Randomized, Double-Blind Phase III KEYNOTE-598 Study. *J Clin Oncol* (2021) 39(21):2327–38. doi: 10.1200/jco.20.03579
62. Goldman JW, Dvorkin M, Chen Y, Reinmuth N, Hotta K, Trukhin D, et al. Durvalumab, With or Without Tremelimumab, Plus Platinum-Etoposide *Versus* Platinum-Etoposide Alone in First-Line Treatment of Extensive-Stage Small-Cell Lung Cancer (CASPIAN): Updated Results From a Randomised, Controlled, Open-Label, Phase 3 Trial. *Lancet Oncol* (2021) 22(1):51–65. doi: 10.1016/s1470-2045(20)30539-8
63. Owonikoko TK, Park K, Govindan R, Ready N, Reck M, Peters S, et al. Nivolumab and Ipilimumab as Maintenance Therapy in Extensive-Disease Small-Cell Lung Cancer: CheckMate 451. *J Clin Oncol* (2021) 39(12):1349–59. doi: 10.1200/jco.20.02212
64. Paz-Ares L, Ciuleanu TE, Cobo M, Schenker M, Zurawski B, Menezes J, et al. First-Line Nivolumab Plus Ipilimumab Combined With Two Cycles of Chemotherapy in Patients With Non-Small-Cell Lung Cancer (CheckMate 9LA): An International, Randomised, Open-Label, Phase 3 Trial. *Lancet Oncol* (2021) 22(2):198–211. doi: 10.1016/s1470-2045(20)30641-0
65. Sezer A, Kilickap S, Gümüş M, Bondarenko I, Özgüroğlu M, Gogishvili M, et al. Cemiplimab Monotherapy for First-Line Treatment of Advanced Non-Small-Cell Lung Cancer With PD-L1 of at Least 50%: A Multicentre, Open-Label, Global, Phase 3, Randomised, Controlled Trial. *Lancet* (2021) 397(10274):592–604. doi: 10.1016/s0140-6736(21)00228-2
66. Spigel DR, Vicente D, Ciuleanu TE, Gettinger S, Peters S, Horn L, et al. Second-Line Nivolumab in Relapsed Small-Cell Lung Cancer: CheckMate 331. *Ann Oncol* (2021) 32(5):631–41. doi: 10.1016/j.annonc.2021.01.071
67. Wang J, Lu S, Yu X, Hu Y, Sun Y, Wang Z, et al. Tislelizumab Plus Chemotherapy *vs.* Chemotherapy Alone as First-Line Treatment for Advanced Squamous Non-Small-Cell Lung Cancer: A Phase 3 Randomized Clinical Trial. *JAMA Oncol* (2021) 7(5):709–17. doi: 10.1001/jamaoncol.2021.0366
68. Fu Y, Zheng Y, Wang PP, Ding ZY. Toxicities of Immunotherapy for Small Cell Lung Cancer. *Front Oncol* (2021) 11:603658. doi: 10.3389/fonc.2021.603658
69. Berti A, Bortolotti R, Dipasquale M, Kinspergher S, Prokop L, Grandi G, et al. Meta-Analysis of Immune-Related Adverse Events in Phase 3 Clinical Trials Assessing Immune Checkpoint Inhibitors for Lung Cancer. *Crit Rev Oncol Hematol* (2021) 162:103351. doi: 10.1016/j.critrevonc.2021.103351
70. Steele TA. Chemotherapy-Induced Immunosuppression and Reconstitution of Immune Function. *Leuk Res* (2002) 26(4):411–4. doi: 10.1016/s0145-2126(01)00138-2
71. Krisl JC, Doan VP. Chemotherapy and Transplantation: The Role of Immunosuppression in Malignancy and a Review of Antineoplastic Agents in Solid Organ Transplant Recipients. *Am J Transplant* (2017) 17(8):1974–91. doi: 10.1111/ajt.14238
72. Oppong E, Cato AC. Effects of Glucocorticoids in the Immune System. *Adv Exp Med Biol* (2015) 872:217–33. doi: 10.1007/978-1-4939-2895-8_9
73. Cruellas M, Yubero A, Zapata M, Galvez EM, Gascon M, Isla D, et al. How Could Antibiotics, Probiotics and Corticoids Modify Microbiota and Its Influence in Cancer Immune Checkpoints Inhibitors: A Review. *Infect Immun* (2021) 89(9):e0066520. doi: 10.1128/IAI.00665-20
74. Neelapu SS, Adkins S, Ansell SM, Brody J, Cairo MS, Friedberg JW, et al. Society for Immunotherapy of Cancer (SITC) Clinical Practice Guideline on Immunotherapy for the Treatment of Lymphoma. *J Immunother Cancer* (2020) 8(2):e001235. doi: 10.1136/jitc-2020-001235
75. National Comprehensive Cancer Network Clinical Practice Guidelines in Oncology. Version 5. (2021). Available at: https://www.nccn.org/guidelines/guidelines-with-evidence-blocks.

Conflict of Interest: The authors declare that the research was conducted in the absence of any commercial or financial relationships that could be construed as a potential conflict of interest.

Publisher's Note: All claims expressed in this article are solely those of the authors and do not necessarily represent those of their affiliated organizations, or those of the publisher, the editors and the reviewers. Any product that may be evaluated in

this article, or claim that may be made by its manufacturer, is not guaranteed or endorsed by the publisher.

Copyright © 2021 Yan, Cui, Fu, Su, Chen, Gu and Lin. This is an open-access article distributed under the terms of the Creative Commons Attribution License (CC BY). The use, distribution or reproduction in other forums is permitted, provided the original author(s) and the copyright owner(s) are credited and that the original publication in this journal is cited, in accordance with accepted academic practice. No use, distribution or reproduction is permitted which does not comply with these terms.

frontiers in Immunology

ORIGINAL RESEARCH
published: 07 December 2021
doi: 10.3389/fimmu.2021.781221

The Effects of Differentially-Expressed Homeobox Family Genes on the Prognosis and HOXC6 on Immune Microenvironment Orchestration in Colorectal Cancer

Lina Qi[1,2,3†], *Chenyang Ye*[1,2,3†], *Ding Zhang*[1,2,3†], *Rui Bai*[1,2,3], *Shu Zheng*[2,3*], *Wangxiong Hu*[2,3*] *and Ying Yuan*[1,2,3*]

[1] Department of Medical Oncology, Key Laboratory of Cancer Prevention and Intervention, Ministry of Education, The Second Affiliated Hospital, Zhejiang University School of Medicine, Hangzhou, China, [2] Cancer Institute, Key Laboratory of Cancer Prevention and Intervention, Ministry of Education, The Second Affiliated Hospital, Zhejiang University School of Medicine, Hangzhou, China, [3] Cancer Center, Zhejiang University, Hangzhou, China

OPEN ACCESS

Edited by:
Hubing Shi,
Sichuan University, China

Reviewed by:
Doriana Fruci,
Bambino Gesù Children Hospital (IRCCS), Italy
Fucun Xie,
Peking Union Medical College Hospital (CAMS), China
Jinhui Liu,
Nanjing Medical University, China

***Correspondence:**
Ying Yuan
yuanying1999@zju.edu.cn
Wangxiong Hu
wxhu@zju.edu.cn
Shu Zheng
zhengshu@zju.edu.cn

†These authors have contributed equally to this work

Specialty section:
This article was submitted to Cancer Immunity and Immunotherapy, a section of the journal Frontiers in Immunology

Received: 22 September 2021
Accepted: 22 November 2021
Published: 07 December 2021

Citation:
Qi L, Ye C, Zhang D, Bai R, Zheng S, Hu W and Yuan Y (2021) The Effects of Differentially-Expressed Homeobox Family Genes on the Prognosis and HOXC6 on Immune Microenvironment Orchestration in Colorectal Cancer. Front. Immunol. 12:781221. doi: 10.3389/fimmu.2021.781221

Background: The homeobox (HOX) gene family encodes highly conserved transcription factors, that play important roles in the morphogenesis and embryonic development of vertebrates. Mammals have four similar HOX gene clusters, HOXA, HOXB, HOXC, and HOXD, which are located on chromosomes 7, 17,12 and 2 and consist of 38 genes. Some of these genes were found to be significantly related to a variety of tumors; however, it remains unknown whether abnormal expression of the HOX gene family affects prognosis and the tumor microenvironment (TME) reshaping in colorectal cancer (CRC). Therefore, we conducted this systematic exploration to provide additional information for the above questions.

Methods: RNA sequencing data from The Cancer Genome Atlas (TCGA) and mRNA expression data from Gene Expression Omnibus (GEO) combined with online tumor analysis databases (UALCAN, TIMER, PrognoScan) were utilized to explore the relationship among abnormal expression of HOX family genes, prognosis and the tumor immune microenvironment in CRC.

Results: 1. Differential expression and prognosis analysis: 24 genes were significantly differentially expressed in CRC compared to adjacent normal tissues, and seven upregulated genes were significantly associated with poor survival. Among these seven genes, univariate and multivariate Cox regression analysis revealed that only high expression of HOXC6 significantly contributed to poor prognosis; 2. The influence of overexpressed HOXC6 on the pathway and TME: High HOXC6 expression was significantly related to the cytokine pathway and expression of T cell attraction chemokines, the infiltration ratio of immune cells, expression of immune checkpoint

markers, tumor mutation burden (TMB) scores and microsatellite instability-high (MSI-H) scores; 3. Stratified analysis based on stages: In stage IV, HOXC6 overexpression had no significant impact on TMB, MSI-H, infiltration ratio of immune cells and response prediction of immune checkpoint blockers (ICBs), which contributed to significantly poor overall survival (OS).

Conclusion: Seven differentially expressed HOX family genes had significantly worse prognoses. Among them, overexpressed HOXC6 contributed the most to poor OS. High expression of HOXC6 was significantly associated with high immunogenicity in nonmetastatic CRC. Further research on HOXC6 is therefore worthwhile to provide potential alternatives in CRC immunotherapy.

Keywords: colorectal cancer, homeobox gene family, prognosis, HOXC6, tumor microenvironment

INTRODUCTION

As one of the most common digestive system malignant tumors, the incidence and mortality of CRC ranks third among various solid cancers worldwide (1). The main cause of death is metastasis. According to statistics, 20% of patients are diagnosed with advanced stage cancer and 25-30% of patients with stage I/II cancer suffer relapse within 5 years after a curative operation (2). In addition to traditional therapies, a variety of new methods, such as immunotherapy and targeted therapy have shown breakthrough effects. In 2015, Le and his colleagues found that pembrolizumab can bring exciting clinical benefits to dMMR/MSI-H metastatic CRC (mCRC), but its objective response rate (ORR) remained only 40% (3). Except for dMMR/MSI-H, new predictive biomarkers of immunotherapy efficacy in colorectal cancer are on the way, such as elevated TMB, POLE/POLD1 mutations, and ARID1A mutation (4–6). However, these current biomarkers are far from meeting the needs of patient screening who may benefit from immunotherapy. Further studies on the tumor microenvironment may provide clues for revealing the cause of tumor immune escape and developing new immunotherapy targets.

The HOX gene family encodes highly conserved transcription factors, that play important roles in the morphogenesis and embryonic development of vertebrates. Mammals have four similar homeobox gene clusters (HOXA, HOXB, HOXC, and HOXD), which consist of 38 genes and are located on chromosomes 7, 17,12 and 2. Many studies have revealed that diverse HOX genes can either inhibit or promote the development of tumors on the basis of their abnormal expression in certain organs: HOXB family in breast cancer (7), HOXA13 in gastric cancers (8), HOXB5 in leukemia (9) and hepatocellular carcinoma (10). In CRC, very few studies have focused on HOX genes. HOXA13, HOXD13 and HOXC6 were reported to promote cancer progression in CRC (11–13), and HOXB13 was reported to suppress tumors in CRC (14).

However, systematic studies on HOX gene family in CRC remain unclear. Therefore, we conducted this systematic analysis to explore whether the 38 HOX family genes were differentially expressed in CRC. Moreover, we further evaluated their prognostic values and TME orchestration abilities.

MATERIAL AND METHODS

Data Downloaded From TCGA

All level3 CRC RNA-Seq data and corresponding clinical information were obtained from TCGA dataset, in which the method of acquisition and application complied with the guidelines and policies. mRNA-seq data were analyzed in TPM format converted from counts.

Differential Expression Analysis of HOX Family Genes Between CRC and Normal Colon Tissues

UALCAN (www.ualcan.path.uab.edu), an online TCGA analysis database, was used for differential expression analysis of HOX family genes in CRC samples.),

GEO database: Expression microarray datasets GSE21815 and GSE37182 were used for differential expression analysis between CRC and normal colon tissues. 9 normal colon tissues and 132 CRC tissues were enrolled in GSE21815 (Platform: GPL6480, Agilent-014850 Whole Human Genome Microarray 4x44K G4112F). 88 normal colon tissues and 84 CRC tissues were enrolled in GSE37182 (Platform: GPL6947, Illumina HumanHT-12 V3.0 expression beadchip).

Prognostic Analysis of Differentially-Expressed Genes

TCGA database: For Kaplan-Meier curves, p-values and hazard ratio (HR) with 95% confidence interval (CI) were generated by log-rank tests and univariate Cox proportional hazards regression. The KM survival analysis with log-rank test were also used to compare the survival difference between above two groups. The whole cohort was divided into two or three groups equally according to HOXC6 expression values. Univariate and multivariate cox regression analysis was performed to identify the prognostic values of genes expression.

GEO database: GSE17536 and GSE12945 were used to validate the survival difference between top 25% HOXC6 high expression and top 25% HOXC6 low expression groups. KM plotter was drawn by GraphPad Prism 8.0.

Volcano Plots, GO, KEGG and GSEA Analysis

Limma package (version: 3.40.2) of R software was used to study the differential expression of mRNAs. The adjusted P-value was analyzed to correct for false positive results in TCGA or GTEx. "Adjusted P < 0.05 and Log (Fold Change) >1 or Log (Fold Change) < -1" were defined as the thresholds for the screening of differential expression of mRNAs between top 25% HOXC6 high expression and top 25% HOXC6 low expression groups.

Gene Ontology (GO) is a widely-used tool for annotating genes with functions, especially molecular function (MF), biological pathways (BP), and cellular components (CC). Kyoto Encyclopedia of Genes and Genomes (KEGG) Enrichment Analysis is a practical resource for analytical study of gene functions and associated high-level genome functional information. To better understand the carcinogenesis of mRNA, ClusterProfiler package (version: 3.18.0) in R was employed to analyze the GO function of potential targets and enrich the KEGG pathway.

Hallmark gene sets from the molecular signatures database (MSigDB) were used to determine whether any signatures were enriched in specific groups by gene set enrichment analysis (GSEA). Significantly enriched hallmarks were chosen according to a *P*-value < 0.05.

Effect of HOXC6 Expression on the Characteristics of Tumor Immune Microenvironment

TIMER (Tumor IMmune Estimation Resource, https://cistrome.shinyapps.io/timer), a web server for comprehensive analysis of tumor-infiltrating immune cells, was used to analyze the correlation of HOXC6 expression and chemokine expression, immune cell infiltration ratio, immune checkpoint marker expression. TIMER2.0 was used to analyze the immune cell infiltration ratio calculated by 5 different algorithms.

TCGA database: Immunedeconv, an R package including CIBERSORT algorithm was utilized to make reliable immune infiltration estimations. PDL1, CTLA4, TIM3, LAG3, PD1, PDL2 and TIGIT were selected as immune-checkpoint-relevant transcripts. CCL2, CCL3, CCL4, CCL5, CXCL9, CXCL10 and CXCL11 were selected as T cell attractive chemokines (15). The expression values of these 14 genes were extracted. Spearman's correlation analysis was used to analyze the correlation between HOXC6 expression and TMB/MSI scores (16). The whole cohort was divided into two groups equally according to HOXC6 expression values.

SNP analysis: Somatic variants in CRC was analyzed by Maftools, which is an efficient and comprehensive tool for analysis of somatic variants in cancer (17). The whole cohort was divided into two groups equally according to HOXC6 expression values. However, data was missing from several samples which resulted in unequal number in HOXC6 high (N=232) and low (N=167) groups.

Interaction Between CD8+ T and RKO Cells

Cell culture: The RKO cell line was purchased from ATCC and cultured with RPMI 1640 medium (Gibco) containing 10% fetal bovine serum (FBS, BI Industry). The cells were incubated at 37°C with 5% CO2.

Stable gene overexpression was constructed by lentiviral transfection system: HOXC6-overexpressed and negative control lentivirus were purchased from GeneChem (Shanghai, China). For infection, 10^5 cells were plated into 6-well plates and cocultured with 2.5 x 10^6 transducing-units (TU) virus in the presence of 1X HitransG (GeneChem, Shanghai, China) and standard medium. Twelve to 15 hours later, the medium was replaced with fresh complete culture medium. After 72h of transfection, 2mg/ml puromycin was added to the culture medium for RKO selection. Quantitative reverse transcription-polymerase chain reaction (qRT-PCR) were utilized to confirm HOXC6 overexpression.

CD8+ T induction from Peripheral Blood Mononuclear Cells (PBMC): PBMCs were isolated from a healthy donor's peripheral blood using Ficoll (GE Healthcare) following a standard protocol. PBMCs were cultured with RPMI 1640 medium (Gibco) containing 10% fetal bovine serum (FBS, BI Industry) inactivated by 56°C water bath, PHA (1 ug/ml), and IL-2 (10 ng/ml) for 3 days. Then the culture medium was replaced by RPMI 1640 medium (Gibco) containing 10% fetal bovine serum (FBS, BI Industry) inactivated by 56°C water bath, OKT3 (50 ng/ml), and IL-2 (10 ng/ml) for every 2 days. The cells were incubated at 37°C with 5% CO2. After 1 week inducement, cells were harvested for coculture experiment and induction identification was measured by flow cytometry and qRT- PCR.

Noncontact coculture of CD8+ T cells and RKO tumor cells: CD8+ T cells and RKO cells coculture were conducted with the noncontact coculture Transwell system (Corning, USA). Inserts containing 1.0×10^7 CD8+ T cells were transferred to 6-well plates previously seeded with RKO cells (2.5×10^5 cells per well) and cocultured in 1.5% FBS-containing medium for 72h. After coculture, CD8+ T and RKO cells were harvested for RNA extraction.

RNA extraction and qRT- PCR: Total RNA was extracted from RKO and CD8+ T cells using Trizol following a standard protocol. The Takara PrimeScript TM RT Master Mix Kit (Takara, RR036Q) was used for reverse transcription. The iTaq Universal SYBR Green Supermix (BioRad) and Applied Biosystems 7500 Fast Real-Time PCR System were applied for qRT- PCR. GAPDH was used as the loading control. Experiments were carried out in triplicate. The results were calculated as follows: $\Delta CT=CT_{\text{Experimental/NC}}-CT_{GAPDH}$, $\Delta\Delta CT=\Delta CT_{\text{Experimental/NC}}-\Delta CT_{NC}$, $\text{foldchange}=2^{-\Delta\Delta CT}$. The primers used for qRT-PCR are detailed in **Table S3**.

Coexpression Analysis

The dataset used comprised HOXC6, MLH1, PMS2, MSH2 and MSH6 mRNA-seq data from TCGA tumors. Multi-gene correlation map is displayed by the R software package pheatmap. Spearman's correlation analysis was used to describe the correlation between quantitative variables without a normal distribution. $P < 0.05$ was considered statistically significant.

HOXC6 Expression and MLH1 Mutation Analysis

For CRC patients in TCGA database, tumor gene mutation MAF data (TCGA) was downloaded from genomic data Commons (GDC) data portal (https://portal.gdc.cancer.gov) (18).

Prediction of ICB Efficacy Based on TIDE Algorithm

Potential ICB response was predicted with TIDE algorithm using raw counts of RNA-sequencing data (level 3) and corresponding clinical information of 407 nonmetastatic and 88 mCRC patients from TCGA (19). The whole cohort was divided into two groups equally according to HOXC6 expression values.

Statistical Analysis

Known batch effects were corrected using the ComBat function in the Bioconductor sva package (20). All the above analysis methods and R package were implemented by R foundation for statistical computing (2020) version 4.0.3 and software packages ggplot2 and pheatmap. P <0.05 was considered statistically significant. In addition, main R software packages used in this research were detailed in supplementary methods.

RESULTS

Differential Expression and Prognosis Analysis Of 38 HOX Family Genes in Colorectal Cancer

First, we performed differential expression analysis of 38 genes in the HOX gene family, and the results showed that compared with normal colon tissues, there were 15 genes whose expression was significantly upregulated (HOXA3, HOXA9, HOXA10, HOXA11, HOXB3, HOXB4, HOXB5, HOXB6, HOXB7, HOXB9, HOXC5, HOXC6, HOXC9, HOXC10, HOXC11) (**Figures 1A, D, E** and **S1**) and nine genes whose expression was significantly downregulated in tumor tissues (HOXA5, HOXA6, HOXA13, HOXC4, HOXD1, HOXD3, HOXD4, HOXD8, HOXD9) (**Figures 1C, I–K**, and **S2**). Second, we conducted a prognostic analysis of these 24 genes with significant differential expression, and the results showed that the differential expression of seven genes contributed significantly to survival (**Figures 1B, F–H, L–N**). In the analysis of these seven genes, the 4 genes HOXC4, HOXD4, HOXD8, and HOXD9 were significantly expressed at low levels in CRC, but the low expression group had a significantly better prognosis. The remaining three genes, HOXB4, HOXC6, and HOXC9 were significantly overexpressed in CRC, and the high expression groups had a significantly worse prognosis.

Therefore, we performed Cox univariate and multivariate prognostic analyses on the expression levels of four significantly downregulated genes (HOXC4, HOXD4, HOXD8, HOXD9) and three significantly upregulated genes (HOXB4, HOXC6, HOXC9). Univariate analysis identified that the high expression of HOXC4, HOXD4 and HOXD9 was associated with a significantly worse prognosis (**Figure 2A**). However, high expression of these four genes did not contribute to prognosis in the multivariate analysis (**Figure 2B**). For the three significantly upregulated genes, univariate analysis revealed that these three genes were associated with a significantly worse prognosis (**Figure 2C**). In the multivariate analysis, only high expression of HOXC6 had a significant contribution to the prognosis [**Figure 2D**, P= 0.046, HR= 1.316 (1.0048-1.723)]. Detailed clinical information and expression data of these three genes of CRC patients from TCGA database are listed in **Table S1**.

Four independent GSE datasets were used to confirm the conclusion that HOXC6 was significantly upregulated in CRC compared to normal colon tissues and that high expression of HOXC6 contributed significantly to poor survival. The GSE21815 and GSE37182 datasets showed that the expression of HOXC6 was significantly higher in CRC than in normal colon tissues (**Figures 2E, F**), which was consistent with previous results reported by other scientists (21). The GSE17536 and GSE12945 datasets showed that compared with the HOXC6 low expression group, the HOXC6 high expression group had significantly worse OS (**Figures 2G, H**).

The Influence of Overexpressed HOXC6 on Pathways

Through the above analysis, we found that HOXC6 was significantly overexpressed in CRC and that high expression was associated with a significantly worse prognosis. However, the changes of pathways caused by HOXC6 overexpression remain unknown. Therefore, we explored the changes in pathways. First, we analyzed the differentially expressed genes (DEGs) between the HOXC6 high and low expression groups and found that there were 347 upregulated and 132 downregulated genes in the HOXC6 high expression group compared with the HOXC6 low expression group (**Figure 3A**). To further explore the changes in pathways and biological functions caused by these DEGs, we further performed GSEA, KEGG, and GO analysis. GSEA found that HOXC6 overexpression was significantly related to chemokine signaling and cytokine receptor interactions (**Figure 3B** and **Table S2**). In KEGG analysis, we found that these upregulated genes were significantly enriched in inflammation-related pathways, such as cytokine and cytokine receptors, LPS, and IBD (**Figure 3C**). In GO analysis, these upregulated genes were mainly enriched in immune pathways, such as in response to IFN-γ, response to chemokines, and neutrophil migration (**Figure 3D**). We also performed KEGG and GO analyses on these downregulated genes, and the results are shown in **Figures 3E, F**.

In summary, overexpression of HOXC6 is likely to be associated with remodeling of the tumor immune microenvironment in CRC.

Correlation Between HOXC6 Overexpression and TME Characteristics

The above analysis indicated that HOXC6 overexpression was likely related to orchestration of the TME. In the TME, the proportion of immune cell infiltration and functional status are significantly related to the prognosis of tumor patients and the efficacy of immune checkpoint inhibitors. Therefore, we further analyzed the correlation between HOXC6 overexpression and tumor immune microenvironment characteristics, including chemokine expression level, immune cell infiltration ratio, immune checkpoint expression level, TMB score, and MSI-H status.

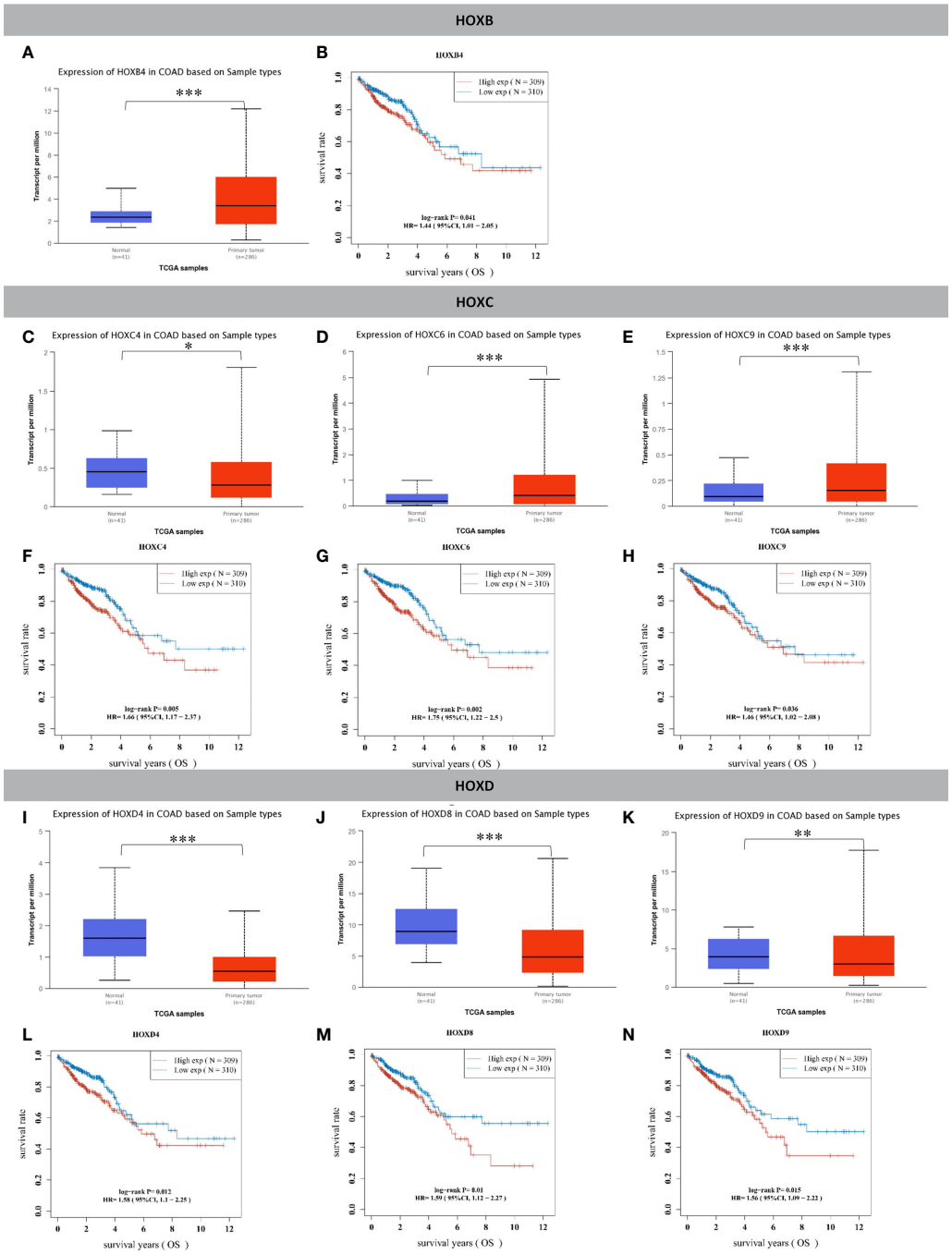

FIGURE 1 | HOX family genes were significantly differentially expressed in tumor tissues compared to normal colon tissues and had significant prognostic value. **(A)** HOXB4 was significantly upregulated in colon cancer compared to normal tissues. **(B)** The HOXB4 high expression group had significantly worse OS than the low expression group in CRC. **(C)** HOXC4 was significantly downregulated in colon cancer compared to normal tissues. **(D)** HOXC6 was significantly upregulated in colon cancer compared to normal tissues. **(E)** HOXC9 was significantly upregulated in colon cancer compared to normal tissues. **(F)** The HOXC4 high expression group had significantly worse OS than the low expression group in CRC. **(G)** The HOXC6 high expression group had significantly worse OS than the low expression group in CRC. **(H)** The HOXC9 high expression group had significantly worse OS than the low expression group in CRC. **(I)** HOXD4 was significantly downregulated in colon cancer compared to normal tissues. **(J)** HOXD8 was significantly downregulated in colon cancer compared to normal tissues. **(K)** HOXD9 was significantly downregulated in colon cancer compared to normal tissues. **(L)** The HOXD4 high expression group had significantly worse OS than the low expression group in CRC. **(M)** The HOXD8 high expression group had significantly worse OS than the low expression group in CRC. **(N)** The HOXD9 high expression group had significantly worse OS than the low expression group in CRC. $^{*}P < 0.05$, $^{**}P < 0.01$, $^{***}P < 0.001$.

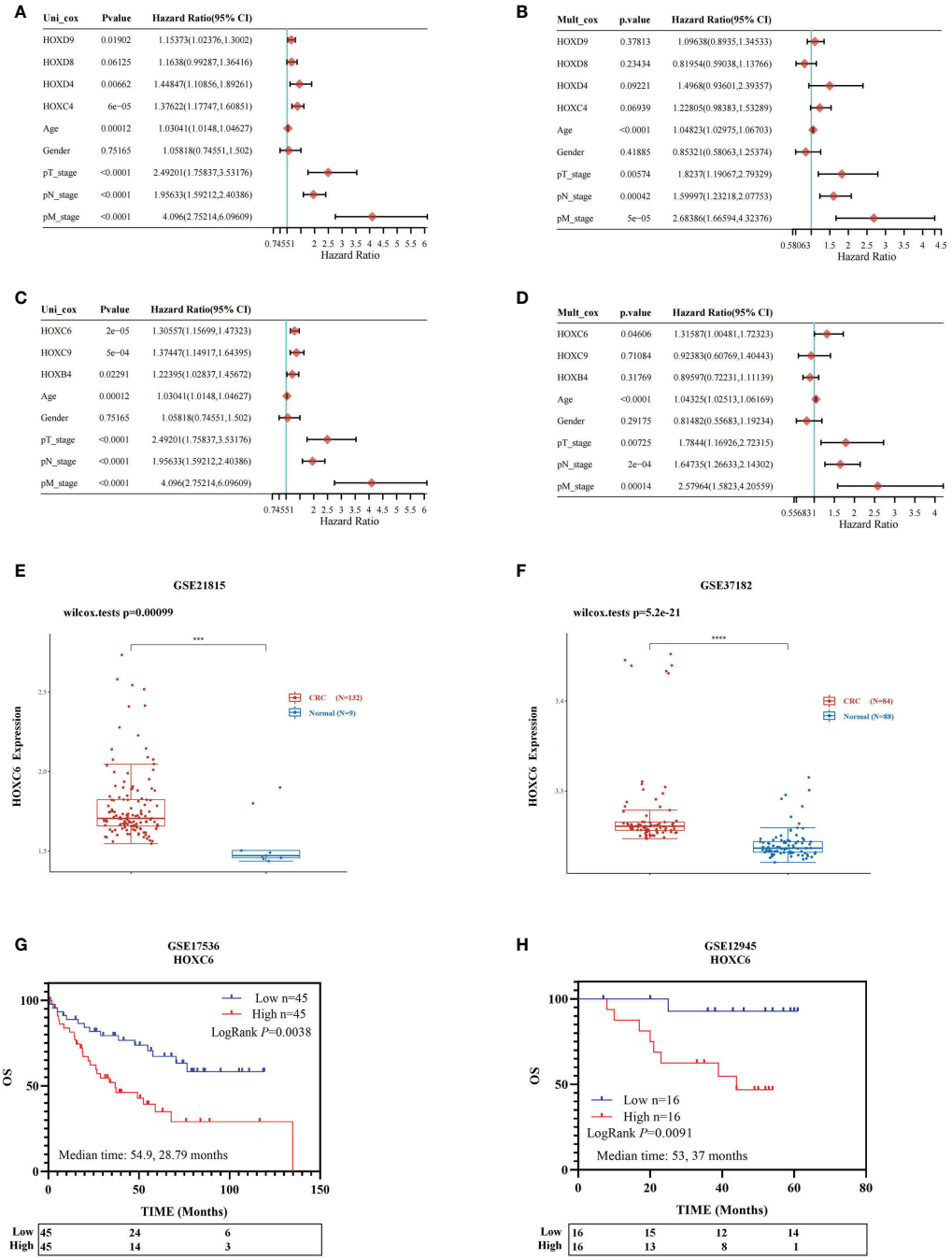

FIGURE 2 | Prognostic analysis of three significantly differentially expressed genes and identification of HOXC6 upregulation and prognostic value. Univariable and multivariable Cox regression analysis for the significantly downregulated genes **(A, B)**. **(A)** Univariable Cox regression analysis revealed that upregulation of HOXC4, HOXD4 and HOXD9 contributed to poor OS. **(B)** Multivariable Cox regression analysis revealed no significant results for HOXC4, HOXD4, HOXD8 and HOXD9. Univariable and multivariable Cox regression analysis for the significantly upregulated genes **(C, D)**. **(C)** Univariable Cox regression analysis revealed that upregulation of HOXB4, HOXC6, and HOXC9 contributed to poor OS. **(D)** Multivariable Cox regression analysis revealed that upregulation of HOXC6 contributed most to poor OS among HOXB4 and HOXC9. **(E)** The GSE21815 dataset confirmed that HOXC6 was significantly upregulated in CRC compared to normal colon tissue. **(F)** The GSE37182 dataset confirmed that HOXC6 was significantly upregulated in CRC compared to normal colon tissue. **(G)**. GSE17536 dataset confirmed that upregulation of HOXC6 was significantly associated with poor OS (P=0.0038, median follow-up time for high and low expression groups: 54.9 and 28.79 months). **(H)** The GSE12945 dataset confirmed that upregulation of HOXC6 was significantly associated with poor OS (P=0.0091, median follow-up time for high and low expression groups: 53 and 37 months). ***$P < 0.001$.

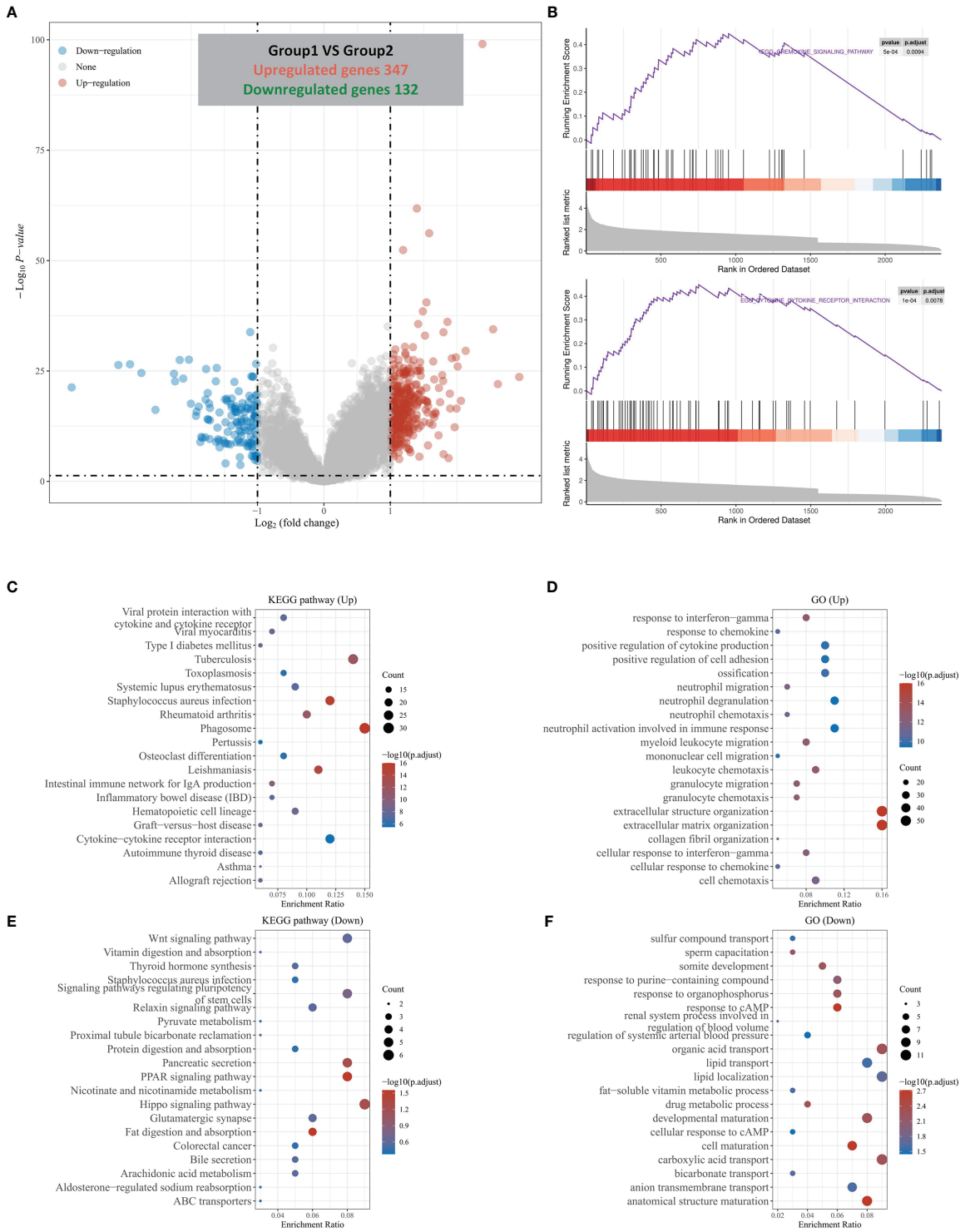

FIGURE 3 | DEGs divided by HOXC6 expression and GSEA, KEGG, and GO analysis of these DEGs. **(A)** A total of 347 upregulated genes and 132 downregulated genes were identified in the HOXC6 high-expression group compared to the low-expression group. **(B)** GSEA revealed that the cytokine interaction pathway and chemokine signaling pathway were significantly enriched in DEGs by HOXC6 upregulation. **(C)** KEGG pathway analysis for 347 upregulated DEGs. **(D)** GO analysis for 347 upregulated DEGs. **(E)** KEGG pathway analysis for 132 downregulated DEGs. **(F)** GO analysis for 132 downregulated DEGs.

First, we used the TIMER database to analyze the correlation between the expression of HOXC6 and the expression of T cell attractive chemokines (CCL2, CCL3, CCL4, CCL5, CXCL9, CXCL10, CXCL11) (**Figure 4A**), the infiltration ratio of the main immune infiltrating cell population (B cells, CD4+T, CD8+T, macrophage, neutrophil, dendritic cell) (**Figure 4B**), and the expression levels of major immune checkpoint molecules (PDL1, CTLA4, TIM3, PD1, PDL2, TIGIT) (**Figure 4C**). The results showed that the expression of HOXC6 was significantly positively correlated with these tumor immune microenvironment characteristics (**Figures 4A–C**). To verify the above results, we performed *in vitro* coculture experiments to identify the effect of HOXC6- upregulated colon cancers on CD8+ T cells. RKO, a commonly used CRC cell line, was selected in this experiment. CD8+ T cells *in vitro* induction was performed following the protocol detailed in **Figure 4D**. Then noncontact coculture of CD8+ T cells and RKO NC/RKO HOXC6-overexpressing (HOXC6-OE) cells was performed. Overexpression of HOXC6 in RKO cells led to significant upregulation of T cell attraction chemokines (CCL2, CCL5 and CXCL11) (**Figure 4E**) and immune checkpoint moleculars (PD-L1 and PD-L2) in RKO (**Figure 4F**). Moreover, overexpression of HOXC6 in RKO cells also caused significant upregulation of TIM3 and downregulation of IFN- γ in CD8+ T cells at the mRNA level (**Figure 4G**). This means, CRC cells with high HOXC6 expression attract more CD8+ T cells by upregulating T cell attraction chemokines, however the tumor killing function of CD8+ T cells might be exhausted by downregulation of IFN- γ.

Moreover, we used the TCGA mRNA expression data and verified that the expression of immune cell attraction chemokines and immune checkpoints was significantly higher in the HOXC6 high expression group than in the low expression group (**Figures 5A, B**). To verify the proportion of immune cell infiltration, we used the TIMER2.0 database, which uses a variety of algorithms to calculate the proportion of six types immune cells. The results showed that the four algorithms all indicated that the infiltration ratio of CD8+ T cells was significantly positively correlated with high HOXC6 expression (**Figure 5C**). Studies have shown that patients with high TMB have more abundant neoantigens and higher immunogenicity in CRC (22). Accordingly, we conducted a correlation analysis on the expression of HOXC6 and TMB score, and the results showed a significant positive correlation (**Figure 5D**, $P< 0.001$, R= 0.38). What's more, we further analyzed the tumor mutation signature between HOXC6 high and low groups and the result showed that the C> T mutation was the main type in both groups (**Figures S3A, B**). However, different from HOXC6 low expression group, proportion of T> G mutation was higher than T>A, and the Ti (Transition) mutation type was higher in HOXC6 high-expression group (**Figures S3A, B**). Percentage of mutations of specific genes, such as BRAF, RNF43, and PIK3C2B were significantly higher in HOXC6 high expression group (**Figure S3C**).

In the immunotherapy of CRC, National Comprehensive Cancer Network (NCCN) and Chinese Society of Clinical Oncology (CSCO) guidelines have recommended pembrolizumab as the first-line treatment for dMMR/MSI-H mCRC patients (23). dMMR/MSI-H is an important predictor biomarker of PD1 inhibitor efficacy, so we analyzed the correlation between HOXC6 expression and dMMR/MSI-H status. First, we found that the expression of HOXC6 was significantly positively correlated with the MSI-H score (**Figure 6A**, $P< 0.001$, R= 0.37). MSI-H patients are basically dMMR, which is caused by the loss of function of the four main mismatch repair genes, of which the loss of MLH1 expression is the most common situation. Therefore, we analyzed the expression correlation of HOXC6 and four mismatch repair genes, and found that the expression of HOXC6 and MLH1 had a significant negative correlation (**Figure 6B**, $P< 0.001$, R= -0.41). In sporadic dMMR CRC, the loss of MLH1 expression caused by MLH1 promoter methylation is the main cause. However, in Lynch syndrome, the loss of MLH1 expression is caused by MLH1 mutation (24). We found that compared with the HOXC6 low expression group, the expression of MLH1 was significantly lower in the HOXC6 high expression group (**Figure 6C**, $P< 0.001$). Moreover, the number of patients with MLH1 mutations was also significantly higher in the HOXC6 high expression group (**Figure 6D**, $P= 0.0078$). Moreover, we performed *in vitro* cell line experiments and found that MLH1- knockdown caused significant upregulation of HOXC6 in microsatellite stable (MSS) CRC cell lines (HT29 and Sw620) (25). In summary, the high expression of HOXC6 had a significant correlation with dMMR/MSI-H status in CRC.

Stratified Analysis Based on Stages

Furthermore, we analyzed the differential expression of HOXC6 and its prognostic value in different stages. First, we used TCGA expression data to analyze the expression of HOXC6 in stages I-IV, and the results showed that there was no significant difference in the expression of HOXC6 in different stages (**Figure 7A**). Second, in stages I, II, and III, patients were divided into three groups according to the expression level of HOXC6, followed by prognostic analysis, and the results showed that the expression level of HOXC6 had no significant prognostic impact (**Figure 7B**, $P= 0.11$). However, in stage IV, the HOXC6 high expression group had a significantly worse prognosis (**Figure 7C**, $P= 0.012$).

In stage IV patients, we analyzed the correlation between HOXC6 and TMB and MSI-H score and found that there was no significant correlation between HOXC6 and TMB and MSI-H score (**Figures 7D, E**). The expression of immune checkpoint related genes was significantly higher in HOXC6 high expression group than in the low (**Figure 7F**). In stage IV patients, compared with the HOXC6 low expression group, only CD4+ T cells, neutrophil and DC cell infiltration ratios were significantly higher in the HOXC6 high expression group (**Figure 7G**). For CD4+ T cells in several subgroups, we used CIBERSORT to evaluate the proportion of CD4+ T cells between the HOXC6 high and low groups and found that T cell follicular helper had significantly higher infiltration in the HOXC6 high expression group (**Figure 7H**, $P<0.05$). These results show that, compared with stage IV patients, the expression of HOXC6 had a greater impact on the tumor immune microenvironment in nonmetastatic CRC patients.

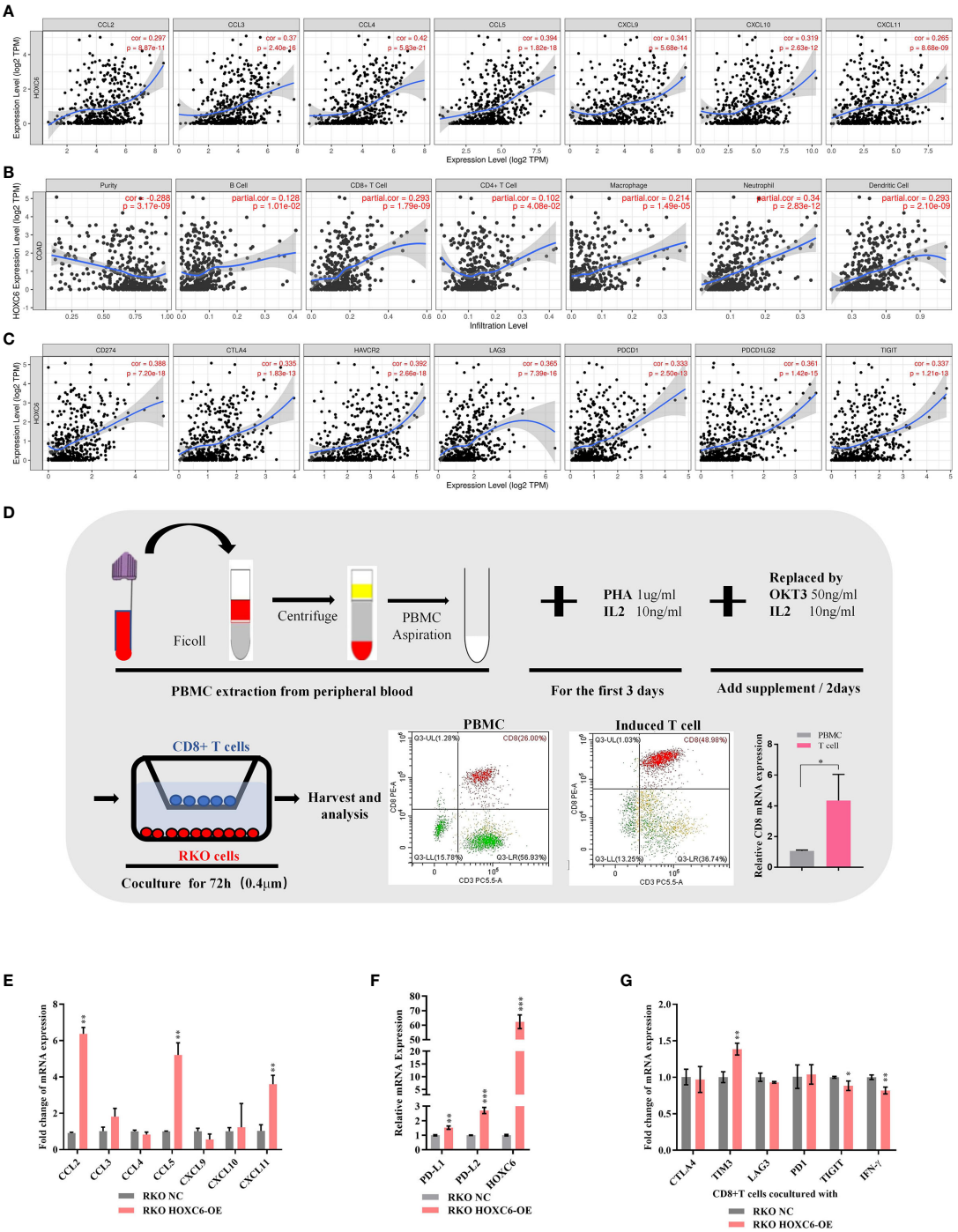

FIGURE 4 | The effect of upregulated HOXC6 on the tumor immune microenvironment in CRC. **(A)** Expression of HOXC6 had a significantly positive correlation with the expression of T cell attractive chemokines in the TIMER database. **(B)** Expression of HOXC6 had a significantly positive correlation with the infiltration ratio of various immune cells in the TIMER database. **(C)** Expression of HOXC6 had a significantly positive correlation with various immune checkpoint molecules in the TIMER database. **(D)** *In vitro* induction of CD8+ T cells from PBMCs isolated from peripheral blood and identification using flow cytometry and qRT- PCR. **(E)** The expression of CCL2, CCL5, and CXCL11 was significantly upregulated in the RKO HOXC6-OE group compared to RKO NC group (both groups were cocultured with CD8+ T cells). **(F)** The expression of PD-L1 and PD-L2 was significantly upregulated in the RKO HOXC6-OE group compared to RKO NC group (both groups were cocultured with CD8+ T cells). **(G)** Expression of TIM3 was significantly upregulated and IFN-γ was significantly downregulated in CD8+ T cells cocultured with RKO HOXC6-OE group compared to RKO NC group. $^{*}P < 0.05$, $^{**}P < 0.01$, $^{***}P < 0.001$.

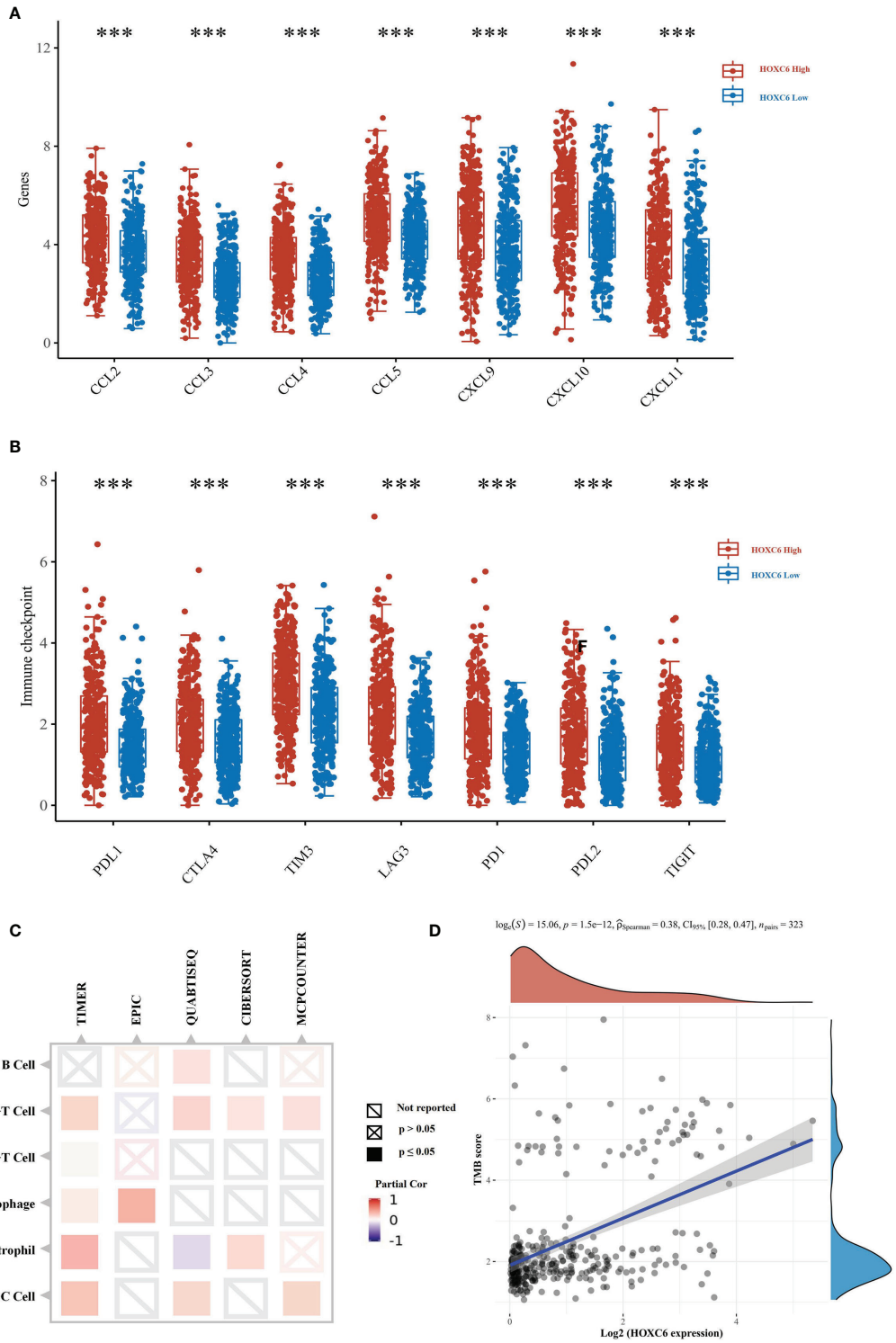

FIGURE 5 | TCGA verification of the effect of upregulated HOXC6 on the tumor immune microenvironment in CRC. **(A)** The expression of T cell attractive chemokines was significantly upregulated in the HOXC6 high-expression group compared to the low-expression group. **(B)** The expression of immune checkpoint molecules was significantly upregulated in the HOXC6 high-expression group compared to the low-expression group. **(C)** Expression of HOXC6 had a significantly positive correlation with the infiltration ratio of various immune cells using different algorithms. **(D)** Expression of HOXC6 had a significantly positive correlation with TMB score (P<0.001, R=0.36). ***P < 0.001.

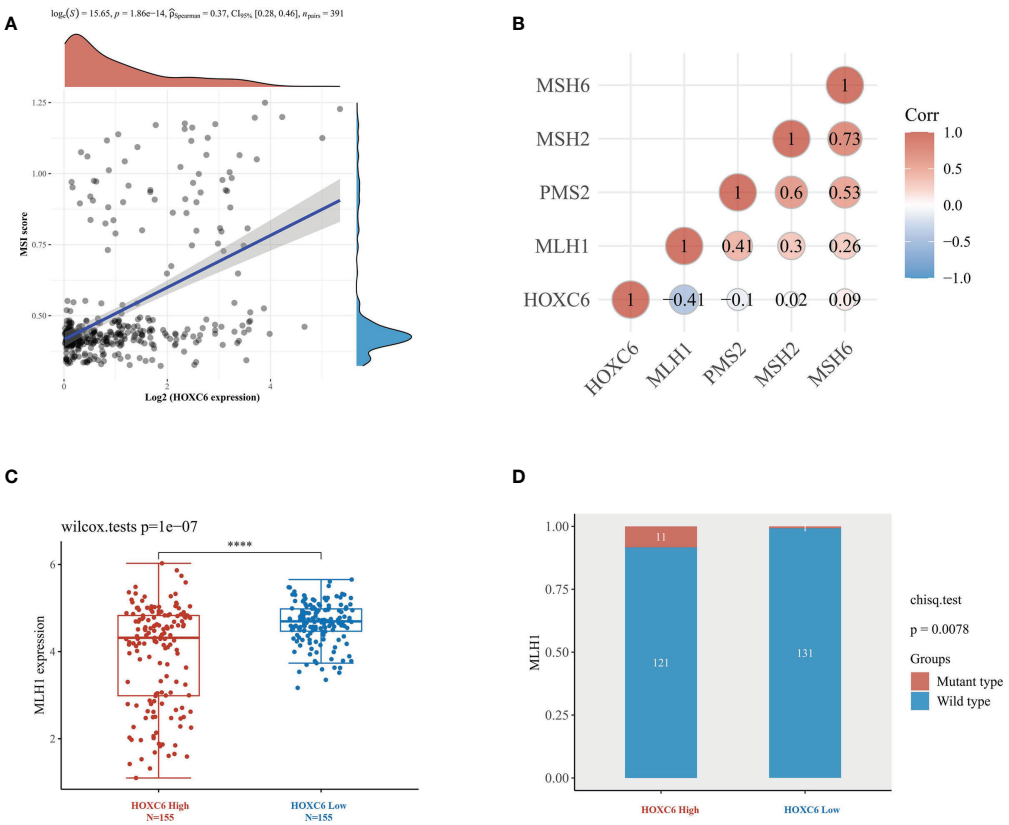

FIGURE 6 | High expression of HOXC6 was significantly correlated with high MSI-H score and dMMR status in CRC. **(A)** The expression of HOXC6 had a significantly positive correlation with MSI score (*P*<0.001, R=0.36). **(B)** The expression of HOXC6 had a significantly negative correlation with the expression of MLH1 (*P*<0.001, R=-0.41). **(C)** The expression of MLH1 was significantly downregulated in the HOXC6 high-expression group compared to the low-expression group (*P*<0.001). **(D)** The number of patients with MLH1 mutations was significantly higher in the HOXC6 high-expression group than in the low-expression group (*P*=0.0078). ****P <0.0001.

To evaluate the predictive value of HOXC6 expression on ICB response, the Tumor Immune Dysfunction and Exclusion (TIDE) algorithm was used in this analysis. TIDE uses a set of gene expression markers to evaluate two different tumor immune escape mechanisms, including the dysfunction of tumor-infiltrating cytotoxic T lymphocytes (CTLs) and the exclusion of CTLs by immunosuppressive factors. In nonmetastatic CRC patients, the HOXC6 high expression group had a significantly worse ICB response rate than the low expression group (**Figure 7I**, *P*<0.001). However, in mCRC patients, there was no significant difference between the HOXC6 high and low expression groups (**Figure 7J**).

The above results indicated that there was no significant difference in the prognosis of HOXC6 overexpression in patients with stage I- III disease. This may be caused by a higher proportion of infiltration of killer cells such as CD8+ T cells and a higher immunogenicity due to high HOXC6 expression. In stage IV patients, the overexpression of HOXC6 had a significantly worse prognosis, which may be related to a higher proportion of CD4+ T cell infiltration that promoted tumors, no difference in the infiltrated ratio of CD8+ T cells that killed tumors and a lower immunogenicity.

For response prediction of ICBs, the expression level of HOXC6 did not predict immunotherapy efficacy in mCRC patients. However, the results suggested that high expression of HOXC6 may be used as a potential biomarker for predicting immunotherapy efficacy, which may be used in nonmetastatic CRC treatment in the future. In other words, when immunotherapy is applied to stage II and III patients as adjuvant therapy such as ATOMIC (NCT 02912559) and POLEM trial (NCT 02912559), patients with high expression of HOXC6 may have worse immunotherapy efficacy.

DISCUSSION

In this study, we identified seven differentially expressed genes with prognostic significance in CRC compared to normal colon tissues. HOXC6, which had the greatest impact on the prognosis among these DEGs, was identified through cox univariate and multivariate prognostic analysis. Furthermore, high expression of HOXC6 was found to be significantly related to the tumor inflammatory microenvironment. Specifically, the expression of HOXC6 was significantly positively correlated with the

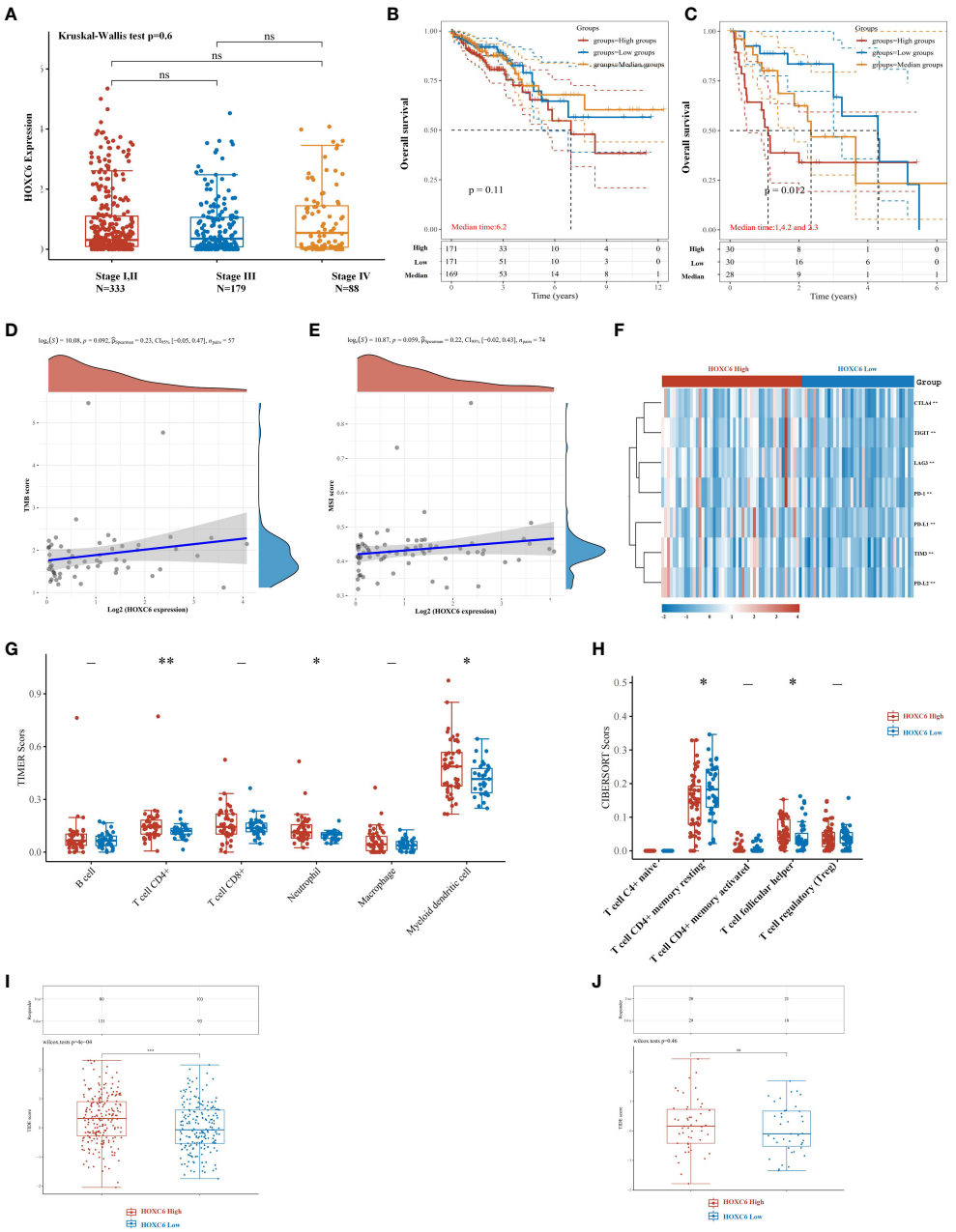

FIGURE 7 | High expression of HOXC6 significantly contributed to poor survival in stage IV with weakened immune microenvironment characteristics in CRC. **(A)** There was no significant difference in the expression of HOXC6 among stage I&II, stage III, and stage IV. **(B)** In stages I, II and III, high expression of HOXC6 had no significant contribution to poor survival (P=0.11) (The whole cohort was divided into three groups equally according to the HOXC6 expression values. The median follow-up time for these three groups was 6.2 years). **(C)** In stage IV, high expression of HOXC6 contributed significantly to poor survival (P=0.012) (The whole cohort was divided into three groups equally according to the HOXC6 expression values. The median follow-up times for the high, medium and low expression groups were 1, 4.2, and 2.3 years, respectively). **(D)** Expression of HOXC6 had no significant correlation with TMB score (P=0.092). **(E)** Expression of HOXC6 had no significant correlation with MSI score (P=0.059). **(F)** Immune checkpoints related gene expression heat map, where different colors represent the expression trend. **(G)** Expression of HOXC6 had a significantly positive correlation with the infiltration ratio of CD4+ T cell, neutrophils and myeloid dendritic cells. **(H)** Expression of HOXC6 had significantly positive correlation with the infiltration ratio of T cell follicular helper (P<0.05). **(I)** The predicted immune response scores were significantly higher in the HOXC6-high expression group than in the HOXC6-low expression group which indicates worse predicted ICB efficacy in the HOXC6-high expression group (P<0.001). **(J)** The predicted immune response scores revealed no significance between the HOXC6-high expression group and HOXC6-low expression group.
*P < 0.05, **P < 0.01, ns, no significance.

infiltration ratio of immune cells, immune checkpoint marker expression, TMB and MSI score. Finally, in the stratified analysis according to clinical stages, we found that there was no significant difference in the expression of HOXC6 in different stages. In terms of prognosis analysis, the differential expression of HOXC6 in nonmetastatic CRC had no significant prognostic value, but in metastatic CRC, the high expression of HOXC6 was significantly correlated with worse prognosis. These results indicate that it is very worthwhile to explore the mechanism of TME orchestration caused by HOXC6 upregulation, which is expected to provide a candidate biomarker for CRC adjuvant immunotherapy cohort screening.

Although the prognostic value of HOX family genes has already been explored in bladder cancer (26) and laryngeal squamous cell cancer (27), this was the first systemic prognostic study in CRC. More importantly, it was found for the first time that in CRC, the high expression of HOXC6 was significantly related to the remodeling of the TME, including chemokine expression level, immune cell infiltration ratio, immune checkpoint expression level, TMB score, and MSI-H status. In CRC, HOXA13, HOXD13 and HOXC6 were reported to promote cancer progression, and HOXB13 was reported to suppress tumors. To the best of our knowledge, in CRC, only two studies have reported that high expression of HOXC6 could promote tumor metastasis by activating the classical WNT pathway and promote proliferation through the TGF-β/smad pathways (13, 25). In addition, HOXB13 was reported to inhibit the proliferation of right-sided colon cancer through the DNMT3B-HOXB13-C-myc regulatory axis (14).

In this study, high expression of HOXC6 was significantly positively correlated with the infiltration ratio of macrophages and neutrophils and the upregulation of immune checkpoint markers. Tumor associated macrophages (TAM) can be divided into M1 and M2 types, of which M2 has a tumor-promoting effect (28, 29). Monoclonal antibody drugs targeted three famous "don't eat me" pathways on M2 macrophages to suppress the tumor promotion function of M2 macrophages (30–32). This strategy may serve as antitumor therapy in HOXC6 high-expression patients through more solid fundamental and animal experiments in the future. As the tumor progresses, locally infiltrated M1 macrophages gradually transform to M2 macrophages (33). Locally infiltrated neutrophils can also be divided into N1 and N2 types. Among them, the N2 type promotes tumors and NETs released after neutrophils apoptosis capture tumor cells and lead to their colonization and metastasis (34). The above various unfavorable factors cause the immunosuppressive microenvironment to promote tumor development and ultimately lead to tumor progression and poor prognosis.

Moreover, high expression of HOXC6 was also significantly positively correlated with the CD8+ T cell infiltration ratio, MSI-H score, TMB and dendritic cell infiltration ratio in our study. Although the increased infiltration of CD8+ T cells has the effect of killing tumor cells and is associated with a better prognosis, unfortunately tumors can induce the depletion or exhaustion of locally infiltrated CD8+ T cells by increasing the ICI on their surface, which leads to irreversible functional loss (35). High tumor load also has a reversible inhibitory effect on circulating CD8+ T cells, and immune function in the circulation can be reversed when the tumor load is reduced (36). Studies have found that MSI-H status can be used as an indicator of better prognosis in early-stage CRC, but in advanced patients, MSI-H had no survival benefit over MSS (37). The use of TMB as a predictive biomarker for immunotherapy is still controversial, and further research is needed (38). Locally infiltrated dendritic cells play an important role in the activation of CD8+ T cells *via* antigen presentation (39). High CD8+ T cells infiltration, MSI-H status, high TMB, and more dendritic cell infiltration were all favorable factors for antitumor ability. Inconsistent with this conclusion, the HOXC6 high expression group with these favorable prognostic factors did not have better survival in nonmetastatic CRC patients. High infiltration of M2 macrophages (40), elevated immune checkpoint markers (41) and high infiltration of CD4+ Tregs (42) resulted in CD8+ T functional loss. In summary, the combined results of various factors in the HOXC6 high expression groups did not result in a poor prognosis in nonmetastatic CRC.

For CD4+ T cells, the overexpression of HOXC6 may cause a higher proportion of CD4+ T cell infiltration, especially higher T cell follicular helper infiltration which was associated with favorable prognosis in mCRC patients (43). However, it has been reported that a high proportion of CD4+ T cell infiltration suggests a better prognosis in patients with CRC (44, 45). Tregs differentiated from naive CD4+ T cells could suppress the function of CD8+T cells (42). Moreover, CD8 + T cells stimulating capacity of CD4+ T cell follicular helper with increasing PD-1 expression in mCRC patients was inhibited by PD-1/PD-L1 pathway (43). These results combined with intratumoral metastasis promoting mechanisms induced by HOXC6 high expression (25) finally led to poor prognosis in mCRC patients.

There are some limitations in this study. Animal experiments should be performed to confirm our conclusion. More basic studies are needed to explain the lack of correlation between HOXC6 and TMB in mCRC. Further experiments are needed to confirm that the expression of HOXC6 may predict the efficacy of immunotherapy in nonmetastatic CRC. In addition, this is a preliminary study with practical limitation at this moment. Expression of HOXC6 should be quantified as absolute value further for clinical practice, such as the TPS, and IPS scores of PD-1 using IHC.

This study revealed that HOXC6 may serve as a potential biomarker for predicting the efficacy of immunotherapy in nonmetastatic CRC, which also provides clues for subsequent mechanistic studies.

DATA AVAILABILITY STATEMENT

The datasets presented in this study can be found in online repositories. The names of the repository/repositories and accession number(s) can be found in the article/**Supplementary Material**.

ETHICS STATEMENT

Ethical review and approval was not required for the study on human participants in accordance with the local legislation and institutional requirements. Written informed consent for participation was not required for this study in accordance with the national legislation and the institutional requirements.

AUTHOR CONTRIBUTIONS

LQ, WH, SZ, and YY designed the study. LQ performed TCGA analysis. CY and DZ performed GEO analysis. WH performed statistical analysis. LQ, CY, and DZ wrote the manuscript. RB reviewed and polished the manuscript. All authors contributed to the article and approved the submitted version.

FUNDING

This work was supported by National Natural Science Foundation of China (grant number: 81802883), Fundamental Research Funds for the Central Universities (grant number: 2018FZA7012) to WH, Zhejiang Basic Public Welfare Research Project (LGF18H160040) to RB, and National Natural Science Foundation of China (grant number: 82103102) to CY.

SUPPLEMENTARY MATERIAL

The Supplementary Material for this article can be found online at: https://www.frontiersin.org/articles/10.3389/fimmu.2021.781221/full#supplementary-material

Supplementary Figure 1 | Significantly upregulated HOX family genes in CRC tissues compared to normal colon tissues, however the upregulation had no effect on OS based on TCGA samples in UALCAN database.

Supplementary Figure 2 | Significantly downregulated HOX family genes in CRC tissues compared to normal colon tissues, however the downregulation had no effect on OS based on TCGA samples in UALCAN database.

Supplementary Figure 3 | (A) Mutation type analysis in HOXC6 high-expression group. **(B)** Mutation type analysis in HOXC6 low-expression group. **(C)** Top 10 significantly mutated genes in HOXC6 high-expression group compared to HOXC6 low-expression group ($P<0.01$). Ti: Transition; Tv: Transversion.

REFERENCES

1. Siegel RL, Miller KD, Fuchs HE, Jemal A. Cancer Statistics, 2021. *CA Cancer J Clin* (2021) 71(1):7–33. doi: 10.3322/caac.21654
2. Loree JM, Kopetz S. Recent Developments in the Treatment of Metastatic Colorectal Cancer. *Ther Adv Med Oncol* (2017) 9(8):551–64. doi: 10.1177/1758834017714997
3. Le DT, Uram JN, Wang H, Bartlett BR, Kemberling H, Eyring AD, et al. PD-1 Blockade in Tumors With Mismatch-Repair Deficiency. *N Engl J Med* (2015) 372(26):2509–20. doi: 10.1056/NEJMoa1500596
4. Samstein RM, Lee CH, Shoushtari AN, Hellmann MD, Shen R, Janjigian YY, et al. Tumor Mutational Load Predicts Survival After Immunotherapy Across Multiple Cancer Types. *Nat Genet* (2019) 51(2):202–6. doi: 10.1038/s41588-018-0312-8
5. Wang F, Zhao Q, Wang YN, Jin Y, He MM, Liu ZX, et al. Evaluation of POLE and POLD1 Mutations as Biomarkers for Immunotherapy Outcomes Across Multiple Cancer Types. *JAMA Oncol* (2019) 5(10):1504–6. doi: 10.1001/jamaoncol.2019.2963
6. Okamura R, Kato S, Lee S, Jimenez RE, Sicklick JK, Kurzrock R. ARID1A Alterations Function as a Biomarker for Longer Progression-Free Survival After Anti-PD-1/PD-L1 Immunotherapy. *J Immunother Cancer* (2020) 8(1):e000438. doi: 10.1136/jitc-2019-000438
7. de Bessa Garcia SA, Araújo M, Pereira T, Mouta J, Freitas R. HOX Genes Function in Breast Cancer Development. *Biochim Biophys Acta Rev Cancer* (2020) 1873(2):188358. doi: 10.1016/j.bbcan.2020.188358
8. Chen Z, Qin Z, Li L, Wo Q, Chen X. HOXA13, Negatively Regulated by miR-139-5p, Decreases the Sensitivity of Gastric Cancer to 5-Fluorouracil Possibly by Targeting Abcc4. *Front Oncol* (2021) 11:645979. doi: 10.3389/fonc.2021.645979
9. Chen M, Qu Y, Yue P, Yan X. The Prognostic Value and Function of HOXB5 in Acute Myeloid Leukemia. *Front Genet* (2021) 12:678368. doi: 10.3389/fgene.2021.678368
10. He Q, Huang W, Liu D, Zhang T, Wang Y, Ji X, et al. Homeobox B5 Promotes Metastasis and Poor Prognosis in Hepatocellular Carcinoma, *via* FGFR4 and CXCL1 Upregulation. *Theranostics* (2021) 11(12):5759–77. doi: 10.7150/thno.57659
11. Yin J, Guo Y. HOXD13 Promotes the Malignant Progression of Colon Cancer by Upregulating PTPRN2. *Cancer Med* (2021) 10(16):5524–33. doi: 10.1002/cam4.4078
12. Qiao C, Huang W, Chen J, Feng W, Zhang T, Wang Y, et al. IGF1-Mediated HOXA13 Overexpression Promotes Colorectal Cancer Metastasis Through Upregulating ACLY and IGF1R. *Cell Death Dis* (2021) 12(6):564. doi: 10.1038/s41419-021-03833-2
13. Ji M, Feng Q, He G, Yang L, Tang W, Lao X, et al. Silencing Homeobox C6 Inhibits Colorectal Cancer Cell Proliferation. *Oncotarget* (2016) 7(20):29216–27. doi: 10.18632/oncotarget.8703
14. Xie B, Bai B, Xu Y, Liu Y, Lv Y, Gao X, et al. Tumor-Suppressive Function and Mechanism of HOXB13 in Right-Sided Colon Cancer. *Signal Transduct Target Ther* (2019) 4:51. doi: 10.1038/s41392-019-0086-1
15. Maimela NR, Liu S, Zhang Y. Fates of CD8+ T Cells in Tumor Microenvironment. *Comput Struct Biotechnol J* (2019) 17:1–13. doi: 10.1016/j.csbj.2018.11.004
16. Bonneville R, Krook MA, Kautto EA, Miya J, Wing MR, Chen HZ, et al. Landscape of Microsatellite Instability Across 39 Cancer Types. *JCO Precis Oncol* (2017) 2017:PO.17.00073. doi: 10.1200/PO.17.00073
17. Mayakonda A, Lin DC, Assenov Y, Plass C, Koeffler HP. Maftools: Efficient and Comprehensive Analysis of Somatic Variants in Cancer. *Genome Res* (2018) 28(11):1747–56. doi: 10.1101/gr.239244.118
18. Hu W, Wang G, Chen Y, Yarmus LB, Liu B, Wan Y. Coupled Immune Stratification and Identification of Therapeutic Candidates in Patients With Lung Adenocarcinoma. *Aging (Albany NY)* (2020) 12(16):16514–38. doi: 10.18632/aging.103775
19. Jiang P, Gu S, Pan D, Fu J, Sahu A, Hu X, et al. Signatures of T Cell Dysfunction and Exclusion Predict Cancer Immunotherapy Response. *Nat Med* (2018) 24(10):1550–8. doi: 10.1038/s41591-018-0136-1
20. Johnson WE, Li C, Rabinovic A. Adjusting Batch Effects in Microarray Expression Data Using Empirical Bayes Methods. *Biostatistics* (2007) 8(1):118–27. doi: 10.1093/biostatistics/kxj037
21. Yuan Y, Chen J, Wang J, Xu M, Zhang Y, Sun P, et al. Development and Clinical Validation of a Novel 4-Gene Prognostic Signature Predicting Survival in Colorectal Cancer. *Front Oncol* (2020) 10:595. doi: 10.3389/fonc.2020.00595
22. Lizardo DY, Kuang C, Hao S, Yu J, Huang Y, Zhang L. Immunotherapy Efficacy on Mismatch Repair-Deficient Colorectal Cancer: From Bench to Bedside. *Biochim Biophys Acta Rev Cancer* (2020) 1874(2):188447. doi: 10.1016/j.bbcan.2020.188447
23. Casak SJ, Marcus L, Fashoyin-Aje L, Mushti SL, Cheng J, Shen YL, et al. FDA Approval Summary: Pembrolizumab for the First-Line Treatment of Patients With MSI-H/dMMR Advanced Unresectable or Metastatic Colorectal

Carcinoma. *Clin Cancer Res* (2021) 27(17):4680–4. doi: 10.1158/1078-0432.CCR-21-0557
24. Abidi A, Gorris MAJ, Brennan E, Jongmans MCJ, Weijers DD, Kuiper RP, et al. Challenges of Neoantigen Targeting in Lynch Syndrome and Constitutional Mismatch Repair Deficiency Syndrome. *Cancers (Basel)* (2021) 13(10):2345. doi: 10.3390/cancers13102345
25. Qi L, Chen J, Zhou B, Xu K, Wang K, Fang Z, et al. HomeoboxC6 Promotes Metastasis by Orchestrating the DKK1/Wnt/β-Catenin Axis in Right-Sided Colon Cancer. *Cell Death Dis* (2021) 12(4):337. doi: 10.1038/s41419-021-03630-x
26. Dong B, Liang J, Li D, Song W, Song J, Zhu M, et al. Identification of a Prognostic Signature Associated With the Homeobox Gene Family for Bladder Cancer. *Front Mol Biosci* (2021) 8:688298. doi: 10.3389/fmolb.2021.688298
27. Li J, Ye M, Zhou C. Expression Profile and Prognostic Values of HOXA Family Members in Laryngeal Squamous Cell Cancer. *Front Oncol* (2020) 10:368. doi: 10.3389/fonc.2020.00368
28. Wei C, Yang C, Wang S, Shi D, Zhang C, Lin X, et al. Crosstalk Between Cancer Cells and Tumor Associated Macrophages Is Required for Mesenchymal Circulating Tumor Cell-Mediated Colorectal Cancer Metastasis. *Mol Cancer* (2019) 18(1):64. doi: 10.1186/s12943-019-0976-4
29. Lin Y, Xu J, Lan H. Tumor-Associated Macrophages in Tumor Metastasis: Biological Roles and Clinical Therapeutic Applications. *J Hematol Oncol* (2019) 12(1):76. doi: 10.1186/s13045-019-0760-3
30. Jaiswal S, Jamieson CH, Pang WW, Park CY, Chao MP, Majeti R, et al. CD47 Is Upregulated on Circulating Hematopoietic Stem Cells and Leukemia Cells to Avoid Phagocytosis. *Cell* (2009) 138(2):271–85. doi: 10.1016/j.cell.2009.05.046
31. Barkal AA, Weiskopf K, Kao KS, Gordon SR, Rosental B, Yiu YY, et al. Engagement of MHC Class I by the Inhibitory Receptor LILRB1 Suppresses Macrophages and Is a Target of Cancer Immunotherapy. *Nat Immunol* (2018) 19(1):76–84. doi: 10.1038/s41590-017-0004-z
32. Barkal AA, Brewer RE, Markovic M, Kowarsky M, Barkal SA, Zaro BW, et al. CD24 Signalling Through Macrophage Siglec-10 Is a Target for Cancer Immunotherapy. *Nature* (2019) 572(7769):392–6. doi: 10.1038/s41586-019-1456-0
33. Herwig MC, Bergstrom C, Wells JR, Höller T, Grossniklaus HE. M2/M1 Ratio of Tumor Associated Macrophages and PPAR-Gamma Expression in Uveal Melanomas With Class 1 and Class 2 Molecular Profiles. *Exp Eye Res* (2013) 107:52–8. doi: 10.1016/j.exer.2012.11.012
34. Shao BZ, Yao Y, Li JP, Chai NL, Linghu EQ. The Role of Neutrophil Extracellular Traps in Cancer. *Front Oncol* (2021) 11:714357. doi: 10.3389/fonc.2021.714357
35. Dolina JS, Van Braeckel-Budimir N, Thomas GD, Salek-Ardakani S. CD8(+) T Cell Exhaustion in Cancer. *Front Immunol* (2021) 12:715234. doi: 10.3389/fimmu.2021.715234
36. Hiam-Galvez KJ, Allen BM, Spitzer MH. Systemic Immunity in Cancer. *Nat Rev Cancer* (2021) 1–15. doi: 10.1038/s41568-021-00347-z
37. Fujiyoshi K, Yamamoto G, Takenoya T, Takahashi A, Arai Y, Yamada M, et al. Metastatic Pattern of Stage IV Colorectal Cancer With High-Frequency Microsatellite Instability as a Prognostic Factor. *Anticancer Res* (2017) 37(1):239–47. doi: 10.21873/anticanres.11313
38. Chen EX, Jonker DJ, Loree JM, Kennecke HF, Berry SR, Couture F, et al. Effect of Combined Immune Checkpoint Inhibition vs Best Supportive Care Alone in Patients With Advanced Colorectal Cancer: The Canadian Cancer Trials Group CO.26 Study. *JAMA Oncol* (2020) 6(6):831–8. doi: 10.1001/jamaoncol.2020.0910
39. Wculek SK, Cueto FJ, Mujal AM, Melero I, Krummel MF, Sancho D. Dendritic Cells in Cancer Immunology and Immunotherapy. *Nat Rev Immunol* (2020) 20(1):7–24. doi: 10.1038/s41577-019-0210-z
40. Limagne E, Thibaudin M, Nuttin L, Spill A, Derangère V, Fumet JD, et al. Trifluridine/Tipiracil Plus Oxaliplatin Improves PD-1 Blockade in Colorectal Cancer by Inducing Immunogenic Cell Death and Depleting Macrophages. *Cancer Immunol Res* (2019) 7(12):1958–69. doi: 10.1158/2326-6066.CIR-19-0228
41. Blank CU, Haining WN, Held W. Defining 'T Cell Exhaustion'. *Nat Rev Immunol* (2019) 19(11):665–74. doi: 10.1038/s41577-019-0221-9
42. Takeuchi Y, Nishikawa H. Roles of Regulatory T Cells in Cancer Immunity. *Int Immunol* (2016) 28(8):401–9. doi: 10.1093/intimm/dxw025
43. Shi W, Dong L, Sun Q, Ding H, Meng J, Dai G, et al. Follicular Helper T Cells Promote the Effector Functions of CD8(+) T Cells *via* the Provision of IL-21, Which Is Downregulated Due to PD-1/PD-L1-Mediated Suppression in Colorectal Cancer. *Exp Cell Res* (2018) 372(1):35–42. doi: 10.1016/j.yexcr.2018.09.006
44. Kuwahara T, Hazama S, Suzuki N, Yoshida S, Tomochika S, Nakagami Y, et al. Intratumoural-Infiltrating CD4 + and Foxp3 + T Cells as Strong Positive Predictive Markers for the Prognosis of Resectable Colorectal Cancer. *Br J Cancer* (2019) 121(8):659–65. doi: 10.1038/s41416-019-0559-6
45. Ye L, Zhang T, Kang Z, Guo G, Sun Y, Lin K, et al. Tumor-Infiltrating Immune Cells Act as a Marker for Prognosis in Colorectal Cancer. *Front Immunol* (2019) 10:2368. doi: 10.3389/fimmu.2019.02368

Conflict of Interest: The authors declare that the research was conducted in the absence of any commercial or financial relationships that could be construed as a potential conflict of interest.

Publisher's Note: All claims expressed in this article are solely those of the authors and do not necessarily represent those of their affiliated organizations, or those of the publisher, the editors and the reviewers. Any product that may be evaluated in this article, or claim that may be made by its manufacturer, is not guaranteed or endorsed by the publisher.

Copyright © 2021 Qi, Ye, Zhang, Bai, Zheng, Hu and Yuan. This is an open-access article distributed under the terms of the Creative Commons Attribution License (CC BY). The use, distribution or reproduction in other forums is permitted, provided the original author(s) and the copyright owner(s) are credited and that the original publication in this journal is cited, in accordance with accepted academic practice. No use, distribution or reproduction is permitted which does not comply with these terms.

frontiers in Immunology

CASE REPORT
published: 15 December 2021
doi: 10.3389/fimmu.2021.799077

Case Report: Glucocorticoid Effect Observation in a Ureteral Urothelial Cancer Patient With ICI-Associated Myocarditis and Multiple Organ Injuries

*Xiajun Hu, Yumiao Wei and Xinxin Shuai**

Department of Cardiology, Union Hospital, Tongji Medical College, Huazhong University of Science and Technology, Wuhan, China

Immune checkpoint inhibitor (ICI)-associated immune-related adverse events (irAEs) are becoming important safety issues worthy of attention despite the exciting therapeutic prospects. The growing development of new ICIs also brings new cases of irAEs, raising more challenges to clinicians. Cardiac injury is rare but life-threatening among diverse organ injuries, and effective interventions are critical for patients. Here, we report a novel programmed cell death protein-1 (PD-1) inhibitor tislelizumab-associated severe myocarditis and myositis accompanied by liver and kidney damage in a ureteral urothelial cancer patient, who was firstly treated by cardiologists because of cardiac symptoms. Due to the lack of experience about ICI-associated irAEs, an initial low-dose (0.5 mg/kg/day) and short-term methylprednisolone therapy was used and found to be ineffective and risky to the patient; then, steroid therapy was modulated to a higher dose (1.5 mg/kg/day) with prolonged time course, and improvement of patient symptoms and laboratory markers were observed quickly and persistently. The patient did not show adverse events under this steroid dosage. This case reports a rare tislelizumab-related myocarditis and multiple organ injuries, which provides valuable experience to cardiologists like us. Early recognition of ICI-associated myocarditis and sufficient dosage and time course of glucocorticoid therapy are critical for severe cases. High-quality clinical evidence about the precise diagnosis and therapy in ICI-associated myocarditis and other organ injuries are necessary to guide our clinical works.

Keywords: immune checkpoint inhibitor, myocarditis, myositis, case report, tislelizumab, glucocorticoid therapy

OPEN ACCESS

Edited by:
Hubing Shi,
Sichuan University, China

Reviewed by:
Tibor Bakacs,
Alfred Renyi Institute of Mathematics, Hungary
Konstantinos Melissaropoulos,
Agios Andreas Hospital, Greece

***Correspondence:**
Xinxin Shuai
xinxinshuai@126.com

Specialty section:
This article was submitted to Cancer Immunity and Immunotherapy, a section of the journal Frontiers in Immunology

Received: *21 October 2021*
Accepted: *23 November 2021*
Published: *15 December 2021*

Citation:
Hu X, Wei Y and Shuai X (2021) Case Report: Glucocorticoid Effect Observation in a Ureteral Urothelial Cancer Patient With ICI-Associated Myocarditis and Multiple Organ Injuries. Front. Immunol. 12:799077. doi: 10.3389/fimmu.2021.799077

INTRODUCTION

Immune checkpoint inhibitors (ICIs) are one of the most promising therapies for cancer, but increasing numbers of reports about immune-related adverse events (irAEs) have indicated security issues worthy of attention during ICI therapy. IrAEs could cover multiple systems, incidence of cardiac injury is low according to the data from clinical trials, and single drug therapy induces less

than 1% of events (1). Clinical manifestation of cardiac toxicity could be myocarditis, pericarditis, arrhythmia, heart failure, and cardiac arrest (2). The risk of disease becomes extremely high once myocarditis occurs. A multicenter study showed 40% death in 131 patients suffering from ICI-related myocarditis (3). The balance of risks and benefits during ICI therapy is of great significance. In recent years, some new ICIs are developed, bringing new reports about irAEs. Here, we received a patient with anti-programmed cell death protein 1 (PD-1) monoclonal antibody tislelizumab-induced multiple organ irAEs including myocarditis, myositis, liver damage, and kidney damage. The patient was admitted to the coronary care unit (CCU) because of initial cardiac symptoms. We present the following case in accordance with the CARE reporting checklist.

CASE DESCRIPTION

A 66-year-old patient was admitted to the CCU because of persistent chest tightness for 3 days. He had been diagnosed as having ureteral urothelial cancer IV degree and had undergone several courses of radiotherapy and chemotherapy in the Oncology Department. Blood pressure, heart rate, and oxygen saturation of the patient were in the normal range. High sensitive Troponin I (Hs-TnI) was high up to 9,317 ng/L (normal <26.2 ng/L), creatine kinase-myocardial band (CK-MB) was elevated to 84.5 ng/ml (normal <6.6 ng/ml), and N-terminal pro B-type natriuretic peptide (NT-proBNP) level was 291 pg/ml (normal <125 pg/ml). Creatine kinase (CK) value was 4,700 U/L (normal <174 U/L). Aspartate aminotransferase (AST) and alanine aminotransferase (ALT) are greater than 3× the upper limit of normal (ULN). Creatinine level increased to 136 μmol/L (normal <114 μmol/L) with a downregulation of estimated glomerular filtration rate (eGFR) to 46.18 ml/(min/L); urine microprotein including albumin, transferrin, immunoglobulin G (IgG), and α1-microglobulin were detected, indicating acute kidney injury. $CD4^+$ T-cell, $CD8^+$ T-cell, B-cell, and natural killer cell populations were normal. Serology tests including coronavirus, hepatitis A, B, C virus, human immunodeficiency virus, cytomegalovirus, coxsackie virus, enterovirus, and Epstein–Barr virus were all negative. Positive auto-antibodies against β1 receptor, calcium channel, myosin heavy chain, and ribonucleoprotein indicated an autoimmune response. Coronary artery computer tomography showed slight atherosclerosis. Electrocardiogram (ECG) showed new-onset complete right bundle branch block (CRBBB), atrioventricular block, and intermittent junctional escape rhythm (**Figure 1A**). Cardiac structure and function evaluated by echocardiogram were still in the normal range. Cardiovascular magnetic resonance (CMR) imaging (**Figures 1B, C**) revealed slight multiple segmental myocardium edema and ventricular septum myocardium late gadolinium enhancement (LGE). We first diagnosed the patient as having acute myocarditis and myositis, and gave him a mild dosage of methylprednisolone (0.5 mg/kg/day) intravenously (IV). Symptoms and enzymology improvement were observed, and then methylprednisolone was stopped after 3 days of therapy. However, multiple organ injury-related laboratory indices rapidly rose again (**Figures 1D–H**). Despite chest distress, the patient progressively performed symptoms of cardiac and muscular damage like chest tightness, limb weakness, dorsal myasthenia, diplopia, and dysphagia. We realized that the patient was different from the normal patients we usually treat; autoimmune injuries were quite severe and hard to control in this patient. We further reviewed the patient's medical history and found that he accepted a single dose of tislelizumab 200 mg IV 20 days ago. An ICI-associated myocarditis and multiple organ injuries were clinically diagnosed. Due to the diverse clinical features and risk of ICI-associated myocarditis, we reference a series of guidelines (4–8) and gave a high dosage of methylprednisolone (1.5 mg/kg) therapy accompanied by intravenous immunoglobulin (IVIG) therapy for the first 4 days. Steroid therapy was prolonged to ensure effective inhibition of autoimmunity induced by tislelizumab. Time axis of diagnosis and therapy of the patient is shown in **Figure 2**. We observed a rapid and persistent improvement of hsTNI, CK-MB, CK, ALT, sCr, and urine microproteins, and gradual recovery of the patient. When hsTNI of the patient fell to 50 ng/L, he was transferred to another medical center for subsequent therapy. The patient accepted outpatient follow-up once after 1 year. Complete symptomatic remission was observed in this patient. No active myocardial or skeletal muscle damage existed according to the laboratory indexes (**Figure 3**). Echocardiogram showed normal cardiac structure and function, except for widening of ascending aorta, which is independent of ICI-associated cardiac injury. Meanwhile, CRBBB consistently existed.

DISCUSSION

Despite the tremendous efficacy of ICI therapy in cancer, irAEs owing to the growing use of ICIs are becoming major safety issues in cancer immunotherapy. The targets of ICIs, including cytotoxic T lymphocyte antigen 4 (CTLA-4), PD-1, and programmed cell death 1 ligand 1 (PD-L1), all have inhibitory effects on T-cell response, participating in the preservation of immune tolerance and prevention of autoimmunity in normal conditions (9). However, tumors can also evade the immune system by activating these immune checkpoints to develop a tolerable microenvironment to tumor cells. ICIs block the immune checkpoints and accelerate activated T cells to target and kill tumor cells, while the adverse effect of these immunomodulators is that immune tolerance to self-antigens could also be impaired and activated T cells begin to attack any organs of the body (9). The clinical spectrum of irAEs covers broad systems including skin, GI tract, lungs, and endocrine, adrenal, pituitary, musculoskeletal, renal, nervous, hematologic, cardiovascular, and ocular systems (8). The incidence of all adverse events has been estimated to range between 54% and 76% in a meta-analysis (10). The incidence can be increased when combination therapy is used, even reaching 97% (11). The incidence of fatal adverse events is estimated to be between 0.3% and 1.3% (12). Patients suffering from ICI-associated myocarditis have the highest fatality rate. ICI-associated myocarditis is also becoming a new recognized entity,

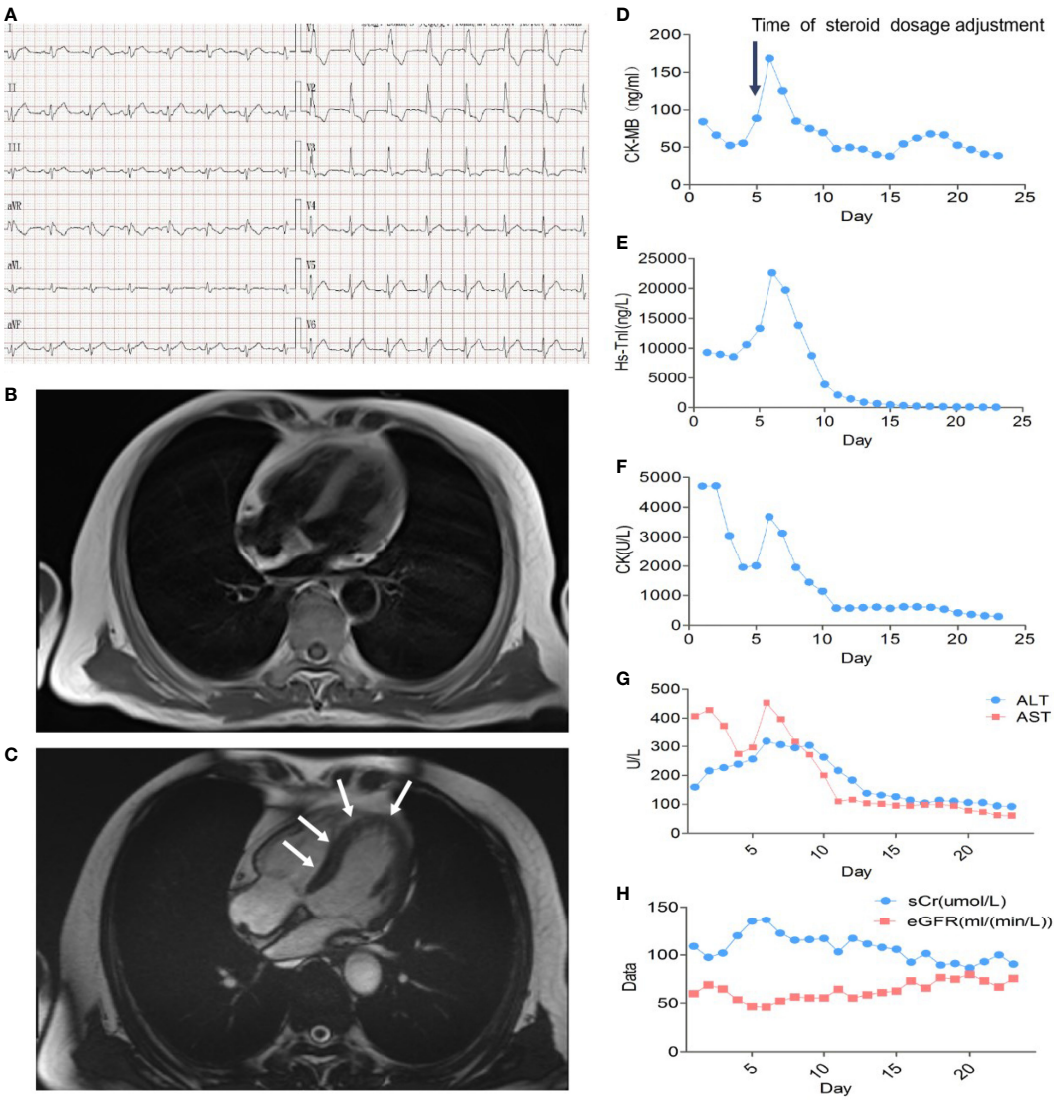

FIGURE 1 | Multiple organ injuries characterized by myocarditis and myositis. **(A)** Electrocardiogram at admission. **(B)** Normal and **(C)** contrast-enhanced imaging in CMR; the white arrow indicated ventricular myocardium LGE. **(D)** CK-MB, **(E)** Hs-TnI, **(F)** CK, **(G)** ALT and AST, and **(H)** sCr and eGFR variation curves during glucocorticoid therapy. The black arrow indicated the time we modulated the dosage of methylprednisolone from 0.5 mg/kg/day to 1.5 mg/kg/day.

drawing the attention of cardiologists. The risk of myocarditis is significantly higher than other organ injuries; myocarditis accompanied by myositis could be more life-threatening once the muscle injuries involve respiratory and swallowing-related muscles, so early recognition is very important; more aggressive therapies should be considered for those severe cases. Non-oncological clinicians should be vigilant to any suspected cases.

Our patient suffered from multiple organ irAEs due to tislelizumab therapy. Tislelizumab is a novel IgG4 monoclonal antibody with high affinity to PD-1 that was engineered to minimize binding to FcγR on macrophages in order to abrogate antibody-dependent cellular phagocytosis (13). Tislelizumab uniquely binds to the CC' loop of PD-1 with a slow-dissociated rate and completely blocks PD-1/PD-L1 interaction (14). As to ICI-related irAEs, pyrexia and infusion reaction are more specific during tislelizumab treatment (15). A summary about irAEs of tislelizumab in clinical trials is shown in **Figure 4**; myocarditis and myositis are not observed. Only one recent case reported multiple organ injuries following tislelizumab treatment in an advanced non-small cell lung cancer patient (21), while in this case, myocarditis is less severe, and there is not enough reference for us to follow. Our patient presented a rare tislelizumab-related myocarditis, accompanied by myositis and other organ injuries, which also intuitively showed the severity of ICI-associated irAEs to cardiologists like us.

Concerning the diagnosis and therapy, due to the absence of randomized controlled trials (RCTs) and observational studies,

Date	Symptoms	Stage	Glucocorticoid therapy	Other drugs
Sept 12-14	Chest tightness	Intermidiate-risk Myocarditis	Methylprednisolone 0.5mg/kg/day IV qd	GS+VitC Co-Q Salkubatroxartan Pantoprazole
Sept 15	Chest tightness Fatigue Weakness	ICI-related irAEs	None	GS+VitC Co-Q Salkubatroxartan Pantoprazole
Sept 16-30	Chest tightness Fatigue Weakness	Myocarditis G3-4 ⟹ G2 Myositis G4 ⟹ G2 Liver injury G2 ⟹ G1 Renal injury G1	Methylprednisolone 1.5mg/kg/day IV qd	IVIG 20g/day for 4 days Co-Q Salkubatroxartan Pantoprazole Vitamin D3 and calcium
Oct 1- (being transferred)	Fatigue	Myocarditis G2 Myositis G2	Recommend gradually tapering oral prednisone therapy	Co-Q Salkubatroxartan Pantoprazole Vitamin D3 and calcium

FIGURE 2 | The diagnosis and therapeutic process of the patient. GS, glucose solution; NS, normal saline; Co-Q, coenzyme Q; IVIG, intravenous immunoglobulin. Evaluation of the grade of irAEs is based on *NCCN guidelines insights: management of immunotherapy-related toxicities, version 1.2020* and *Society for Immunotherapy of Cancer (SITC) clinical practice guideline on immune checkpoint inhibitor-related adverse events.*.

there are still no standard diagnostic and therapeutic strategies. ICI medication history is critical. Clinical features of ICI-related myocarditis are similar to acute myocarditis (AM), which is based on symptoms with serum cardiac marker elevation and imageology changes in UCG and CMR. However, a cohort study indicated that LGE was less significant in ICI-associated myocarditis than non-ICI myocarditis (22), and the presence of LGE, LGE pattern, or elevated T2-weighted STIR were not associated with MACE. In our patient, UCG was normal and CMR only showed slight segmental LGE, which is why we underestimated the risk of the patient the first time. More reliable imaging diagnostic strategies are needed for ICI-associated myocarditis.

Corticosteroid therapy is recommended for myocarditis and other irAEs (Grades 2 to 5), but the safe and effective dosage is not precisely pointed out. High-dose glucocorticoids are recommended for severe cases. The ESC guidelines had no exact recommendation for acute active myocarditis due to autoimmunity. Guidelines and consensus of the European Society for Medical Oncology (ESMO) (4), the Society for Immunotherapy of Cancer (SITC) (6), and a recent Expert Consensus Document (7) all recommend prednisone 1–2 mg/kg for severe myocarditis, until the cardiac damage slows down. The National Comprehensive Cancer Network (NCCN) guideline (5) suggests a stronger pulse dosing 1 g/day methylprednisolone for 3–5 days for severe or life-threatening cases, and if cardiac function returns to baseline, the dosage tapers over 4–6 weeks. Meanwhile, recent preclinical trials highlight glucocorticoids' unexpected effects in cancer therapy like impairing the killing ability of tumor-infiltrating lymphocytes (23) and weakening the effect of ICI therapy (24). Broad adverse effects of glucocorticoid in multiple organs is another concern. Rheumatologists then recommended the concept of glucocorticoid sparing even in severe presentations. Tapering glucocorticoids to the lowest effective dose is recommended within weeks or as soon as improvement is achieved (23, 25). For unstable patients or patients with no improvement after high-dose glucocorticoids therapy, other immunosuppressive agents should be considered, like IVIG, antithymocyte globulin, infliximab, or mycophenolate (4–6, 8), but each with limited supporting data. IVIG can act as an immunomodulator on both innate and adaptive immunity, leading to decreased cardiac inflammation, which was proved to be protective in myocarditis (26). Multiple mechanisms including blocking Fc receptors to interrupt multiple immune cell functions, neutralizing antigens or complement components, and disrupting the apoptosis process may synergistically engage in the immune modulation effect of IVIG. In this case, due to the lack of experiences about ICI-associated myocarditis, we firstly gave a moderate-dose and short-term methylprednisolone therapy. The illness was not controlled and quickly progresses. Then, we tried a high-dose (1.5 mg/kg/day) and prolonged

A

Test Marker	Hs-TnI	CK-MB	CK	ALT	AST	sCr
Value	< 0.01ng/ml	< 2.5ng/ml	10.1U/L	20.6U/L	25.1U/L	120umol/L

B

Indexes of Echocardiogram	Value
Ascending Aorta	36mm
Left atrium	34mm
Left ventricle	47mm
Right atrium	32mm
Right ventricle	34mm
Interventricular septum	10mm
Ejection fraction	69%
E/A ratio	0.6

C

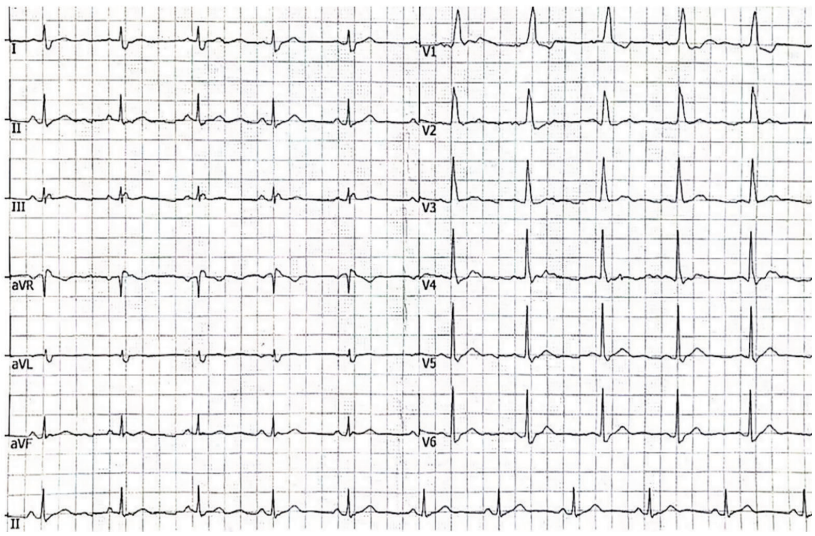

FIGURE 3 | Clinical data of the patient in 1-year follow-up. **(A)** Laboratory indexes involve myocardial zymogram as well as liver and kidney functions. **(B)** Cardiac structure and function evaluation in echocardiogram. **(C)** Electrocardiogram shows CRBBB.

Registration ID	Type of Cancer	Phase of trial	Sample size	Most common irAEs	Myocarditis	Reference
NCT03209973 (2020)	Relapsed/refractory Hodgkin lymphoma	Phase 2	70	Pyrexia (54.3%) Hypothyroidism (32.9%) Upper respiratory tract infection (≥G3，2.9%)	None	(16)
CTR20160872 (2020)	Advanced solid tumors	Phase 1/2	300	Anemia (23%) Increased aspartate aminotransferase (22%)	None	(17)
NCT04004221 /CTR20170071 (2020)	PD-L1-positive urothelial carcinoma	Phase 2	113	Anemia (27% ; ≥G3，7%) Pyrexia (19%) Hyponatremia (≥G3，5%)	None	(18)
NCT02407990 (2020)	Advanced solid tumors	Phase IA/IB	451	Fatigue (28%) Nausea (25%) Decreased appetite (20%) Anemia (≥G3，4.9%)	None	(19)
NCT04068519 (2020)	Advanced solid tumors	Phase IA/IB	70	Increased ALT (34.3%) and AST (31.4%)	None	(20)
NCT03419897 in progress	Unresectable hepatocellular carcinoma	Phase 2	228	-	-	-

FIGURE 4 | IrAEs of tislelizumab in clinical trials.

steroid treatment accompanied by short-term IVIG therapy; enzymology rapidly decreased and the symptoms of the patient improved in the following days.

CONCLUSION

This is a rare case of myocarditis and myositis associated with a novel PD-1 inhibitor tislelizumab, showing the diversity between ICI-associated myocarditis and common myocarditis. ICI-associated myocarditis and myositis is severe and even life-threatening to patients. Autoimmune damage is significant and persistent, so steroid therapy should be early, given in high doses, and prolonged. We tried a high dosage of steroids with short-term IVIG immunosuppressive therapy in this case, resulting in a positive outcome for the patient. The experience from one case is limited, and high-quality lines of evidence about the precise diagnosis and therapy of ICI-associated irAEs are necessary to guide our clinical works.

DATA AVAILABILITY STATEMENT

The original contributions presented in the study are included in the article/supplementary material. Further inquiries can be directed to the corresponding author.

ETHICS STATEMENT

Written informed consent was obtained from the individual(s) for the publication of any potentially identifiable images or data included in this article.

AUTHOR CONTRIBUTIONS

XH analyzed the patient data, designed the case report, and drafted the manuscript. YW collected the patient data. XS provided significant contributions to the analysis of the patient data and designed the case report. All authors contributed to the article and approved the submitted version.

FUNDING

This work was supported by the National Natural Science Foundation of China (Grant No. 31901004 and No. 81600317).

ACKNOWLEDGMENTS

We thank the patient for providing his information for this case report.

REFERENCES

1. Lyon AR, Yousaf N, Battisti N, Moslehi J, Larkin J. Immune Checkpoint Inhibitors and Cardiovascular Toxicity. *Lancet Oncol* (2018) 9:447–58. doi: 10.1016/S1470-2045(18)30457-1
2. Johnson DB, Balko JM, Compton ML, Chalkias S, Gorham J, Xu Y, et al. Fulminant Myocarditis With Combination Immune Checkpoint Blockade. *N Engl J Med* (2016) 375:1749–55. doi: 10.1056/NEJMoa1609214
3. Wang DY, Salem JE, Cohen JV, Chandra S, Johnson DB. Fatal Toxic Effects Associated With Immune Checkpoint Inhibitors: A Systematic Review and Meta-Analysis. *JAMA Oncol* (2018) 4:1721–8. doi: 10.1001/jamaoncol.2018.3923
4. Haanen JBAG, Carbonnel F, Robert C, Kerr KM, Peters S, Larkin J, et al. Management of Toxicities From Immunotherapy: ESMO Clinical Practice Guidelines for Diagnosis, Treatment and Follow-Up. *Ann Oncol* (2018) 29:iv264–266. doi: 10.1093/annonc/mdy162
5. Thompson JA, Schneider BJ, Brahmer J, Andrews S, Engh A. NCCN Guidelines Insights: Management of Immunotherapy-Related Toxicities, Version 1.2020. *J Natl Compr Cancer Network: JNCCN* (2020) 18:230–41. doi: 10.6004/jnccn.2020.0012
6. Puzanov I, Diab A, Abdallah K, Bingham CO, Brogdon C, Dadu R, et al. Managing Toxicities Associated With Immune Checkpoint Inhibitors: Consensus Recommendations From the Society for Immunotherapy of Cancer (SITC) Toxicity Management Working Group. *J Immunother Cancer* (2017) 5:95. doi: 10.1186/s40425-017-0300-z
7. Ammirati E, Frigerio M, Adler ED, Basso C, Birnie DH, Brambatti M, et al. Management of Acute Myocarditis and Chronic Inflammatory Cardiomyopathy. *Circulation: Heart Failure* (2020) 13:e007405. doi: 10.1161/CIRCHEARTFAILURE.120.007405
8. Brahmer JR, La cc hetti C, Schneider BJ, Atkins MB, Brassil KJ, Caterino JM, et al. Management of Immune-Related Adverse Events in Patients Treated With Immune Checkpoint Inhibitor Therapy: American Society of Clinical Oncology Clinical Practice Guideline. *J Clin Oncol* (2018) 36:1714–68. doi: 10.1200/JCO.2017.77.6385
9. June CH, Warshauer JT, Bluestone JA. Is Autoimmunity the Achilles' Heel of Cancer Immunotherapy? *Nat Med* (2017) 23:540–7. doi: 10.1038/nm.4321
10. Xu C, Chen YP, Du XJ, Liu JQ, Huang CL, Chen L, et al. Comparative Safety of Immune Checkpoint Inhibitors in Cancer: Systematic Review and Network Meta-Analysis. *BMJ* (2018) 363:k4226. doi: 10.1136/bmj.k4226
11. Tawbi HA, Forsyth PA, Alain A, Omid H, Stephen HF, Moschos SJ, et al. Combined Nivolumab and Ipilimumab in Melanoma Metastatic to the Brain. *New Engl J Med* (2018) 379:722–30. doi: 10.1056/NEJMoa1805453
12. Wang DY, Salem JE, Cohen JV, Chandra S, Johnson DB. Fatal Toxic Effects Associated With Immune Checkpoint Inhibitors: A Systematic Review and Meta-Analysis. *JAMA Oncol* (2018) 4:1721–8.
13. Zhang T, Song X, Xu L, Ma J, Zhang Y, Gong W, et al. The Binding of an Anti-PD-1 Antibody to FcgrI has a Profound Impact on its Biological Functions. *Cancer Immunol Immunother* (2018) 67:1079–90. doi: 10.1007/s00262-018-2160-x
14. Hong Y, Feng Y, Sun H, Zhang B, Wu H, Zhu Q, et al. Tislelizumab Uniquely Binds to the CC' Loop of PD-1 With Slow-Dissociated Rate and Complete PD-L1 Blockage. *FEBS Open Bio* (2021) 11:782–92. doi: 10.1002/2211-5463.13102
15. Li L, Li G, Rao B, Dong AH, Wu YZ. Landscape of Immune Checkpoint Inhibitor-Related Adverse Events in Chinese Population. *Sci REP-UK* (2020) 10:15567. doi: 10.1038/s41598-020-72649-5
16. Song Y, Gao Q, Zhang H, Fan L, Zhu J, Zou D, et al. Treatment of Relapsed or Refractory Classical Hodgkin Lymphoma With the Anti-PD-1, Tislelizumab: Results of a Phase 2, Single-Arm, Multicenter Study. *Leukemiahas a Profound Impact on Its Biological* (2020) 34:533–42. doi: 10.1038/s41375-019-0545-2
17. Shen L, Guo J, Zhang Q, Yuan Y, Bai Y, Liu T, et al. Tislelizumab in Chinese Patients With Advanced Solid Tumors: An Open-Label, Non-Comparative, Phase 1/2 Study. *J Immunother Cancer* (2020) 8:e000437. doi: 10.1136/jitc-2019-000437
18. Ye D, Liu J, Zhou A, Zou Q, Li H, Fu C, et al. Tislelizumab in Asian Patients With Previously Treated Locally Advanced or Metastatic Urothelial Carcinoma. *Cancer Sci* (2021) 112:305–13. doi: 10.1111/cas.14681

19. Desai J, Deva S, Lee JS, Lin C, Yen C, Chao Y. Phase IA/IB Study of Single-Agent Tislelizumab, an Investigational Anti-PD-1 Antibody, in Solid Tumors. *J Immunother Cancer* (2020) 8:e000453. doi: 10.1136/jitc-2019-000453
20. Shen L, Wu YL, Yuan Y, Bai Y, Zhang Q, Zhou Q. 552p Safety and Efficacy of Long-Term Exposure (LTE) to Tislelizumab in Chinese Patients With Advanced Solid Tumour. *Ann Onc* (2020) 31:S478–S47. doi: 10.1016/j.annonc.2020.08.666
21. Deng C, Yang M, Jiang H, Wang R, Yang Z, Sun H, et al. Immune-Related Multiple Organs Injuries Following ICIT reatment With Tislelizumabinan Advanced Non-Small Cell Lung Cancer Patient: A CaseReport. *Front. Oncol* (2021) 11:664809. doi: 10.3389/fonc.2021.664809
22. Lili Z, Magid A, Syed SM, Anju N, Malek ZOH, Franck T, et al. Cardiovascular Magnetic Resonance in Immune Checkpoint Inhibitor-Associated Myocarditis. *Eur Heart J* (2020) 41:1733–43. doi: 10.1093/eurheartj/ehaa051
23. Draghi A, Borch TH, Radic HD, Chamberlain CA, Gokuldass A, Svane IM, et al. Differential Effects of Corticosteroids and Anti-TNF on Tumor-Specific Immune Responses: Implications for the Management of irAEs. *Int J Cancer* (2019) 145:1408–13. doi: 10.1002/ijc.32080
24. Arbour KC, Mezquita L, Long N, Rizvi H, Auclin E, Ni A, et al. Impact of Baseline Steroids on Efficacy of Programmed Cell Death-1 and Programmed Death-Ligand 1 Blockade in Patients With Non-Small-Cell Lung Cancer. *Clin Oncol* (2018) 36:2872–8. doi: 10.1200/JCO.2018.79.0006
25. Cain DW, Cidlowski JA. Immune Regulation by Glucocorticoids. *Nat Rev Immunol* (2017) 17:233–47. doi: 10.1038/nri.2017.1
26. Mansourabadi AH, Afrakoti GMPL, Shabanian A, Shabanian R, Amirzargar A. Intravenous Immunoglobulin Therapy in Myocarditis. *Iran J Allergy Asthma Immunol Nat Rev Immunol* (2020) 19:323–36. doi: 10.18502/ijaai.v19i4.4109

Conflict of Interest: The authors declare that the research was conducted in the absence of any commercial or financial relationships that could be construed as a potential conflict of interest.

Publisher's Note: All claims expressed in this article are solely those of the authors and do not necessarily represent those of their affiliated organizations, or those of the publisher, the editors and the reviewers. Any product that may be evaluated in this article, or claim that may be made by its manufacturer, is not guaranteed or endorsed by the publisher.

Copyright © 2021 Hu, Wei and Shuai. This is an open-access article distributed under the terms of the Creative Commons Attribution License (CC BY). The use, distribution or reproduction in other forums is permitted, provided the original author(s) and the copyright owner(s) are credited and that the original publication in this journal is cited, in accordance with accepted academic practice. No use, distribution or reproduction is permitted which does not comply with these terms.

frontiers in Immunology

ORIGINAL RESEARCH
published: 15 December 2021
doi: 10.3389/fimmu.2021.784336

Check for updates

OPEN ACCESS

Edited by:
Hubing Shi,
Sichuan University, China

Reviewed by:
Jia Yang,
University of California, San Francisco, United States
André Filipe Oliveira,
Hospital do Divino Espírito Santo, Portugal
Mu-Yan Cai,
Sun Yat-sen University Cancer Center (SYSUCC), China

***Correspondence:**
Yuanhong Gao
gaoyh@sysucc.org.cn
Weiwei Xiao
xiaoww@sysucc.org.cn
Rong Zhang
zhangrong@sysucc.org.cn

†These authors have contributed equally to this work and share first authorship

‡These authors have contributed equally to this work and share senior authorship

Specialty section:
This article was submitted to Cancer Immunity and Immunotherapy, a section of the journal Frontiers in Immunology

Received: *27 September 2021*
Accepted: *15 November 2021*
Published: *15 December 2021*

Citation:
Zhou C, Jiang T, Xiao Y, Wang Q, Zeng Z, Cai P, Zhao Y, Zhao Z, Wu D, Lin H, Sun C, Zhang R, Xiao W and Gao Y (2021) Good Tumor Response to Chemoradioimmunotherapy in dMMR/MSI-H Advanced Colorectal Cancer: A Case Series. Front. Immunol. 12:784336. doi: 10.3389/fimmu.2021.784336

Good Tumor Response to Chemoradioimmunotherapy in dMMR/MSI-H Advanced Colorectal Cancer: A Case Series

Chengjing Zhou[1,2†], Ting Jiang[1†], Yajie Xiao[3†], Qiaoxuan Wang[1], Zhifan Zeng[1], Peiqiang Cai[4], Yongtian Zhao[3], Zhikun Zhao[3], Dongfang Wu[3], Hanqing Lin[3], Chao Sun[3], Rong Zhang[5‡], Weiwei Xiao[1*‡] and Yuanhong Gao[1*‡]*

[1] Department of Radiation Oncology, State Key Laboratory of Oncology in South China, Collaborative Innovation Center for Cancer Medicine, Sun Yat-sen University Cancer Center, Guangzhou, China, [2] School of Medicine, Southern University of Science and Technology, Shenzhen, China, [3] Department of Medicine, YuceBio Technology Co., Ltd., Shenzhen, China, [4] Department of Medical Imaging and Interventional Radiology, State Key Laboratory of Oncology in South China, Collaborative Innovation Center for Cancer Medicine, Sun Yat-sen University Cancer Center, Guangzhou, China, [5] Department of Endoscopy and Laser, State Key Laboratory of Oncology in South China, Collaborative Innovation Center for Cancer Medicine, Sun Yat-sen University Cancer Center, Guangzhou, China

Purpose: Immune checkpoint blockade has led to a significant improvement of patient survival in metastatic colorectal cancer (CRC) with DNA mismatch repair-deficiency (dMMR)/microsatellite instability-high (MSI-H). However, not all these patients are sensitive to monoimmunotherapy. We firstly presented a case series of advanced dMMR/MSI-H CRCs treating with PD-1 inhibitor-based chemoradioimmunotherapy (CRIT).

Methods and Materials: We assessed the short-term efficacy and safety of CRIT in advanced dMMR/MSI-H CRCs, and also did next-generation sequencing (NGS) assays.

Results: Our analysis included five advanced dMMR/MSI-H CRCs who have received toripalimab-based CRIT. Toripalimab was given 240mg every three weeks, and the radiation dose was 45-50 gray in 25 fractions. Chemotherapy regimens consisted of CAPOX in three patients, capecitabine in one patient, and mFOLFOX6 in one patient. Initially, two patients displayed complete response (CR), and three patients achieved partial response (PR) on imaging findings. Afterwards, one PR patient was confirmed pathological complete response after surgery, leading to three CR cases in total. Hematological toxicity was the most common adverse effect, and only two patients developed mild immune-related adverse effects besides. All the treatment-related adverse events were under control. Based on the NGS results, the median intratumor heterogeneity was 0.19 (range 0-0.957), which was less in CR patients than PR

patients (P = 0.019). Genetic mutations at DNA damage repair genes and the *JAK1* gene were also observed.

Conclusions: For advanced dMMR/MSI-H CRC, anti-PD-1 based CRIT is effective and safe. Further studies are required to better clarify the potential role and mechanism of CRIT as a viable therapeutic strategy in this population.

Keywords: chemotherapy, radiotherapy, immunotherapy, programmed cell death protein 1 inhibitor, colorectal cancer

INTRODUCTION

The latest cancer statistics showed that the incidence and mortality of colorectal cancer (CRC) ranked third among all cancer in men and women (1). By the year 2030, there will be more than 2.2 million new cases and 1.1 million deaths of CRC (2). In the past ten years, immunotherapy especially immune checkpoint blockade (ICB) therapy, has become a major therapeutic strategy for multiple types of solid cancers. ICB, including programmed cell death protein-1 (PD-1) inhibitors and anti-cytotoxic T lymphocyte antigen-4 (CTLA-4) antibodies, have significantly improved patients' survival in DNA mismatch repair-deficiency (dMMR)/microsatellite instability-high (MSI-H) metastatic colorectal cancer (mCRC) (3–8). As a result, the FDA has approved PD-1 inhibitors, pembrolizumab and nivolumab, as the second-line therapy for dMMR/MSI-H mCRC. Nivolumab ± ipilimumab or pembrolizumab alone were recommended for neoadjuvant treatments for resectable or unresectable synchronous liver and/or lung metastastic dMMR/MSI-H CRC by the NCCN guideline (9, 10), and for primary treatments for unresectable metachronous metastatic dMMR/MSI-H CRC who has received FOLFOX/CAPOX therapy within past 12 months (9, 10). However, there are still a large amount of dMMR/MSI-H CRCs who are resistant to ICB. To date, many ongoing clinical trials of combined ICB with chemotherapy, targeted therapy, or radiotherapy aim to improve the efficacy of ICB in these patients. For instance, chemoradiotherapy can upregulate PD-L1 expression in rectal cancer (11). PD-1 or PD-L1 antibodies did not only improve local control but also had a systemic efficacy in irradiated colon cancer mouse models (12). Besides, a preclinical study also showed that chemotherapy combined with ICB could enhance radiotherapy-induced abscopal effects (13). Therefore, it can be probably inferred that chemoradioimmunotherapy (CRIT) may improve the efficacy of ICB in dMMR/MSI-H CRC patients. Here, we firstly presented a retrospective case series of five advanced dMMR/MSI-H CRC patients who achieved good response to CRIT.

Abbreviations: CRC, colorectal cancer; dMMR, mismatch repair-deficiency; MSI-H, microsatellite instability-high; CRIT, chemoradioimmunotherapy; PD-1, programmed cell death protein-1; CR, complete response; PR, partial response; pCR, pathological complete response; ICB, immune checkpoint blockade; CTLA-4, cytotoxic T lymphocyte antigen-4; mCRC, metastatic colorectal cancer; FFPE, formalin-fixed paraffin-embedded; TMB, tumor mutational burden; TNB, tumor neoantigen burden; ITH, intratumor heterogeneity; COSMIC, the Catalogue of Somatic Mutations in Cancer; TRAE, treatment-related adverse events; DDR, DNA damage repair.

MATERIALS AND METHODS

Study Design

From March 2019 to December 2019, advanced dMMR/MSI-H CRC patients receiving CRIT were retrospectively analyzed in this study.

This study was conducted following the Declaration of Helsinki and received the full approval of the Sun Yat-sen University Cancer Center Institutional Review Board on Medical Ethics (B2020-141-01). All patients provided written informed consent before therapy.

Next-Generation Sequencing (NGS)

Five formalin-fixed paraffin-embedded (FFPE) specimens of all patients were obtained before CRIT. All specimens were primary tumors except abdominal metastasis of patient 2.

Genomic DNAs were isolated from FFPE specimens and blood using the GeneRead DNA FFPE Kit (Qiagen) and Qiagen DNA blood mini kit (Qiagen), respectively. Then, extracted DNAs were amplified, purified, and analyzed using an NGS panel (YuceOneTM Plus X, Yucebio, China).

Sequencing reads with > 10% N rate and/or > 10% bases with quality score < 20 were filtered using SOAPnuke (Version 1.5.6). The clean reads were mapped to the UCSC reference human genome (version hg19) using the Burrows Wheeler Alignment tool (BWA, Version 0.7.12). SAMtools (Version 1.3) was used for alignment data conversion, sorting, and indexing. The duplicates were marked by SAMBLASTER (Version 0.1.22) to reduce biases in downstream analyses. The single nucleotide variants were detected using VarScan (Version 2.4) with parameters –min-coverage-normal 20 –min-coverage-tumor 20 –min-reads23. The mutations were filtered using a customized Perl script to eliminate false positives and annotated by SnpEff (Version 4.3).

Tumor mutational burden (TMB) was calculated using non-silent somatic mutations, including coding base substitution and indels. TMB > 20 muts/Mb was defined as TMB-High (TMB-H). Microsatellite instability (MSI) scores were analyzed by MSIsensor (Version 0.2). MSI scores > 20 were defined as MSI-High (MSI-H). Tumor neoantigen burden (TNB) was measured as the number of mutations that could generate neoantigens per megabase. TNB > 4.5 neos/Mb was defined as TNB-High (TNB-H). The ratio of subclone mutations to all mutations was interpreted as intratumor heterogeneity (ITH).

Frameshift, nonsense, and splice site alterations were classified as deleterious. Missense mutations reported as

pathogenic by the Catalogue of Somatic Mutations in Cancer (COSMIC) (14) and/or ClinVar (15) databases, and/or with a SIFT score of <0.05 (16), were classified as deleterious.

Clinical Evaluation

Pretreatment tumors were staged according to the criteria of the American Joint Committee on Cancer 8th edition. Clinical response based imaging findings was assessed according to the RECIST 1.1 (17). For surgical specimens, no residual tumor cell was defined as pathological complete response (pCR). Follow-up data were collected from the follow-up platform of the hospital.

Statistical Analysis

Statistical analyses were performed using SPSS 26.0 statistical software (IBM, NY, USA). Comparisons between two groups were evaluated by Student t-test. $p < 0.05$ at two sides was considered statistically significant.

RESULTS

Patient Demographic and Clinical Characteristics

Overall, five dMMR/MSI-H CRC patients were identified and enrolled. The median age was 37 years old (range 27-64), and three (3/5) were male. Of all patients, primary tumors were located at right colon (n=3), left colon (n=1) and rectum (n=1). All patients were adenocarcinoma except one adenosquamous carcinoma. Two (2/5) patients had metastases: right kidney metastasis in patient 1, and liver and abdominal cavity metastases in patient 2. The other three patients had large tumors invaded adjacent organs and regions, including the gallbladder, duodenum, liver, and peritoneum of patient 3, peritoneum and abdominal wall of patient 4, and psoas major muscle and ureter of patient 5. Prior to this study, patient 4 had received three cycles of CAPOX, but no tumor regression. Besides, patient 5 had received surgery and adjuvant FOLFOX chemotherapy for the primary tumor but found the tumor regrowth a year later. The demographic, clinical, and therapeutic details of the patients were shown in **Table 1** and **Figure 1**.

Treatment Strategies

All patients received PD-1 inhibitor-Toripalimab 240 mg intravenously once every three weeks with a median number of 6 cycles (range 5-11 cycles) and a median treatment duration of 5.8 months (range 3.1-18.3 months). Each individualized chemotherapy regimen was decided according to patients' previous treatment and health conditions. Patient 3 received capecitabine as she was old and weak. The chemotherapy regime of patient 4 was switched to mFOLFOX6 because she was insensitive to CAPOX. Other patients all received CAPOX. All patients were also treated with intensity-modulated radiation therapy (IMRT) for the primary tumor at 45-50 gray in 25 fractions. After CRIT, patient 2 and patient 4 underwent radical surgery, whereas patient 5 underwent palliative surgery. The integral treatments for each patient were illustrated in **Table 1** and **Figure 1**.

TABLE 1 | Demographic features, clinical characteristics, and therapeutic regimens.

Items	Patient 1	Patient 2	Patient 3	Patient 4	Patient 5
Gender	Male	Male	Female	Female	Male
Age (years)	37	27	62	35	64
Tumor site	Rectum	Right colon	Right colon	Left colon	Right colon
Histology	Adenocarcinoma	Adenocarcinoma	Adenosquamous carcinoma	Adenocarcinoma	Adenocarcinoma
Stage	cT3N1M1a	cT3N+M1b	cT4bN2M0	cT4bN2aM0	rT4bN0M0
Metastatic site	Right kidney	Liver and abdominal cavity	None	None	None
Invaded adjacent organ	NA	NA	Gallbladder, duodenum, liver, and peritoneum	Peritoneum and abdominal wall	Psoas major muscle, and ureter
MSH2	+	+	+	–	+
MSH6	+	+	+	–	–
PMS2	–	–	–	+	+
MLH1	+	+	–	+	+
Previous chemotherapy	No	No	No	CAPOX	FOLFOX
Previous surgery	No	No	No	No	Radical surgery
Combined chemotherapy	CAPOX	CAPOX	Capecitabine	mFOLFOX6	CAPOX
Combined radiotherapy	50Gy/25F	50Gy/25F	45Gy/25F	48Gy/25F	50Gy/25F
Surgery after ICB	No	Radical surgery	No	Radical surgery	Palliative surgery
Total course of ICB	10	7	6	5	6
Course of ICB for best response	6	3	6	5	4
Imaging response	CR	PR	CR	PR	PR
Pathology response	NA	pCR	NA	TRG(2ypT4bN0M0)	NA

CR, complete response; ICB, immune checkpoint blockade; NA, not available; pCR, pathological complete response; PR, partial response; TRG, tumor regression response.

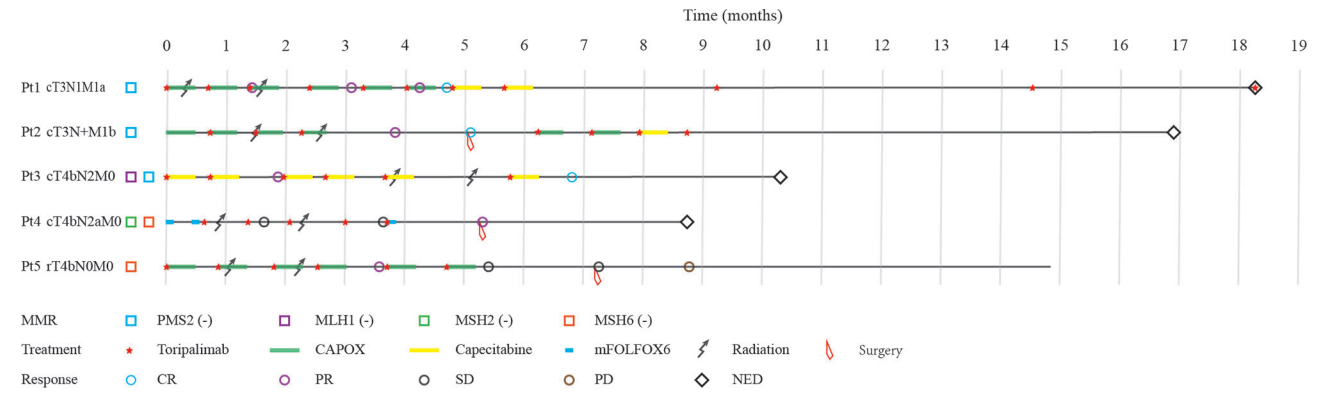

FIGURE 1 | Patient characteristics, treatments, and outcomes. CR, complete response; PD, progressive disease; PR, partial response; SD, stable disease.

Efficacy Results

After a median period of 4.4 months (range 3.1-6.8 weeks) from the first Toripalimab injection and 7.1 weeks (range 5.3-13.3 weeks) from the last IMRT, five patients all achieved objective responses, including two complete response (CR) and three partial responses (PR) according to RECIST 1.1. The two CR patients took a watch-and-wait strategy without surgery. Primary and metastases of patient 2 were confirmed pCR after surgery, resulting in three CR patients in total. Patient 4 underwent surgery and had a downstage tumor from T4bN2a to T4bN0, and the tumor regression grade was TRG2 based on NCCN guidelines. The primary tumor of patient 5 was smaller than the initial volume but found invaded the ureter, small intestine, and iliac blood vessels during surgery. As a result, patient 5 underwent palliative surgery for organ conservations. The images of all patients before and after CRIT were displayed in **Supplementary Figures 1–5**. With a median follow-up time of 14.8 months (range 8.1-18.3), only patient 5 had progressive disease at 8.8 months after the first Toripalimab injection. All the other cases had no clinical signs of disease progression or recurrence.

Treatment-Related Adverse Events (TRAEs)

Till September 2020, all TRAEs happened for all patients were shown **Table 2**. The most common adverse events were leukopenia and neutropenia. Most TRAEs in this study were at grade 1 or grade 2. Only one patient experienced grade 4 thrombocytopenia. One patient had grade 2 immune-related increased TSH, and therefore had levothyroxine therapy. All the adverse events were under control, and patients recovered during treatment.

Genetic Analyses

Based on NGS results shown in **Figures 2A–D**, the median value of TMB, MSI score, TNB and ITH were 60.48mut/Mb (range 32.31-77.18), 44.95 (range 27.45-69.06), 24.56 neos/Mb (range 5.98-40.09) and 0.116 (range 0-0.369), respectively. CR patients had a lower ITH than PR patients (p=0.019, **Figure 2D**). TMB, MSI scores, and TNB did not correlate with treatment response (**Supplementary Figures 6A–C**).

Additionally, 19 mutations in 12 DNA damage repair (DDR) genes were observed. Among them, most alternations were missense mutations (10/19, 52.6%), the remaining included

TABLE 2 | Treatment-related adverse events.

Adverse event	Grade 1 (n)	Grade 2 (n)	Grade 3 (n)	Grade 4 (n)
Any	4	5	3	1
Leukopenia	1	2	1	0
Neutropenia	3	0	1	0
Anemia	1	1	1	0
Thrombocytopenia	0	0	1	1
ALT elevation	0	2	0	0
AST elevation	3	0	0	0
Increased creatinine	1	0	0	0
Diarrhea	0	2	0	0
Nausea	0	1	0	0
Vomit	0	1	0	0
Rash	1	0	0	0
TSH increased	0	1	0	0
fT3 decreased	0	1	0	0
Infection	0	2	0	0

ALT, alanine aminotransferase; AST, aspartate aminotransferase; TSH, thyroid stimulating hormone; fT3, free triiodothyronine.

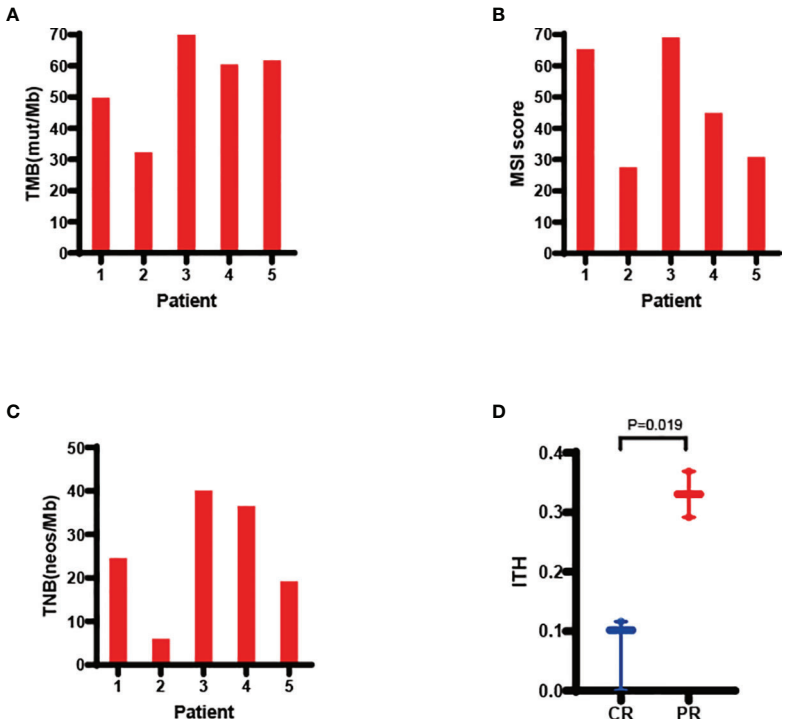

FIGURE 2 | Molecular analyses of TMB **(A)**, MSI score **(B)**, TNB **(C)**, and ITH **(D)**. ITH was lower in CR than PR patients. Values were presented as median and range. Comparisons between CR and PR patients was tested using two-sided t-test. CR, complete response; CRIT, chemoradioimmunotherapy; ITH, intratumor heterogeneity; MSI, microsatellite instability; PR, partial response; TMB, tumor mutational burden; TNB, tumor neoantigen burden.

frameshift mutations (6/19, 31.6%), splice site (2/19, 10.5%), and nonsense alterations (1/19, 5.3%). *ATM* (4/5, 80.0%) was the most commonly mutated DDR gene. All missense mutations were unique, of which only 7 were previously reported in COSMIC and/or ClinVar database and 5 of them were deleterious. In silico evaluation, another 2 potentially deleterious missense mutations were identified. The median number of deleterious DDR mutations patients harbored was 3 (range 1-6). All the DDR gene mutations were listed in **Supplementary Table 1**. Genes involved in the mismatch repair pathway (6/10, 60%) were the most common (**Supplementary Table 2**).

Furthermore, *JAK1* deleterious mutation was observed in patients 1 (K924fs) and 3 (T533M), and *JAK1* neutral mutation was found in patient 4 (R93H). The most frequently altered genes were *APC* (100%), *FAT1* (80%), *TRRAP* (80%), *KAT6B* (80%), *CIC* (80%) and *ATM* (80%) (**Supplementary Figure 7**).

DISCUSSION

In this study, we firstly reported a retrospective case series of advanced dMMR/MSI-H CRC patients treated with CRIT. After treatment, all five patients achieved beneficial responses of pCR (1/5, 20%), cCR (2/5, 40%), or PR (2/5, 40%), leading to a 100% overall response rate. The good efficacy suggested that this strategy might be a promising treatment for advanced dMMR/MSI-H CRC.

It has been well studied that locally advanced rectal cancer can benefit from neoadjuvant chemoradiotherapy. Our previous work found that locally advanced unresectable colon cancer responded well to neoadjuvant chemoradiotherapy, with a 26.3%-38.1% pCR rate (18, 19). Consequently, neoadjuvant chemoradiotherapy has been recommended for T4b patients with local invasion of the sigmoid colon by the Chinese Society of Clinical Oncology (20). However, whether dMMR/MSI-H CRC patients could benefit from preoperative chemoradiotherapy as well as microsatellite instability stale or low CRC was still a controversial clinical question (21, 22). In our present cohort, a 100% objective response rate and 60% CR rate were achieved, indicating that they could benefit from CRIT.

For patients whose primary tumor did not invade adjacent organs, immunotherapy alone or combined with chemotherapy could result in CR (23, 24). So, radiotherapy and chemotherapy may not be essential for these patients. But, the two T3 patients with metastases were treated with CRIT to maximize the abscopal effect, and they finally achieved CR. Similarly, a preclinical study also showed that the abscopal tumor has the best response to triple therapy of cisplatin, radiation, and PD-1 inhibitor (13), implying that CRIT is effective for mCRC.

Though all patients in our study were effective, two patients with T4b colon cancer did not achieve CR. One of them was still unresectable after CRIT, and his disease progressed 8.8 months after the Toripalimab initiation. In the NICHE study (23), only one patient with T4b tumor and three of seven patients with T4a

tumors did not achieve pCR. Also, some T4b tumors could not achieve CR after neoadjuvant PD-1 blockade in published case reports (24, 25). For dMMR/MSI-H CRC with large tumors invading multiple essential organs, the clinical response to single-agent immunotherapy or immunotherapy-based combination therapy is still unsatisfactory. Thus, it is necessary to explore optimized regimens of these therapeutic methods to achieve better clinical efficacy in these patients.

Up to now, DDR gene alterations, especially deleterious alternations, have been demonstrated to be associated with improved clinical outcomes in metastatic urothelial cancer (26), metastatic clear cell renal cell carcinoma (27), and non-small-cell lung cancer (28) treated with PD-(L)1 inhibitors. Likewise, a recent study also found that CRC patients with DDR mutations could obtain a better prognosis when using ICB (29). This was consistent with our patients that DDR genes alterations were frequent, which may contribute to their effective response to CRIT. Additionally, *ATM* was the most commonly mutated DDR gene in these CRC and patients with *ATM* mutations had a significantly better overall survival than those without when treated with ICB (30). In addition, *ATM* inhibitors potentiated anti-PD-1 therapy in the mouse model (30). It was also reported that *ATM* inhibition and radiation could enhance the efficacy of ICB by increasing tumoral immunogenicity (31). Therefore, *ATM* may be a potential biomarker of immunotherapy, and *ATM* inhibitors with ICB and radiation may be an efficacious therapeutic regimen. Interestingly, *ATM*, *ATR*, and *LIG3* genes co-mutation was only found in two PR patients. This might imply that the molecular contributions of multiple DDR gene co-mutation may differ from single DDR gene mutation. Further studies are needed to disclose the effects and mechanisms of how DDR mutations impact sensitivity to CRIT.

Additionally, driver mutations of the JAK-STAT pathway may contribute to tumor progression during immunotherapy (32, 33). In our study, both of the two patients with pathogenic *JAK1* mutation achieved CR, and the patient with neutral *JAK1* mutation achieved PR. Perhaps, chemoradiotherapy can dismiss the negative impact of *JAK1* mutations in some way.

There were some limitations to our study. Our study only enrolled five patients, and the follow-up period was short. Also, baseline characteristics and treatment strategies were not incoherent of all patients. Although we did genetic analysis, we could not illustrate the definite mechanism of CRIT. Consequently, our observations warrant further considerations and validations in a larger sample size. We are doing a phase II clinical study (NCT04301557) of Toripalimab combined with chemoradiotherapy for dMMR/MSI-H locally advanced CRC, which may provide more clinical evidence to clarify the role of CRIT for CRC.

In general, CRIT is effective and safe for advanced dMMR/MSI-H CRC. Further studies are required to investigate the potential role and mechanism of CRIT in this population.

DATA AVAILABILITY STATEMENT

The datasets presented in this study can be found in online repositories. The whole sequence data reported in this paper available in the Genome Warehouse in National Genomics Data Center, Beijing Institute of Genomics, Chinese Academy of Sciences, under accession number PRJCA007192 at https://ngdc.cncb.ac.cn/databases, upon reasonable request.

ETHICS STATEMENT

The studies involving human participants were reviewed and approved by Sun Yat-sen University Cancer Center Institutional Review Board on Medical Ethics. The patients/participants provided their written informed consent to participate in this study.

AUTHOR CONTRIBUTIONS

Conceptualization: CJZ, TJ, and WWX. Methodology: CJZ, WWX, and YJX. Data curation: CJZ, QXW, and PQC. Investigation: YTZ, ZKZ, DFW, and HQL. Resources: ZFZ, RZ, and YHG. Software: CJZ and WWX. Writing - Original draft: CJZ, WWX, and YJX. Editing: CS. Writing-Review and Editing: RZ and YHG. All authors contributed to the article and approved the submitted version.

FUNDING

This work was supported by the National Natural Science Foundation of China under Grant 81672987 and 82073329; and the Natural Science Foundation of Guangdong Province under Grant 2020A1515011286.

ACKNOWLEDGMENTS

We thank the medical staff and patients for their contribution to this study.

SUPPLEMENTARY MATERIAL

The Supplementary Material for this article can be found online at: https://www.frontiersin.org/articles/10.3389/fimmu.2021.784336/full#supplementary-material

REFERENCES

1. Siegel RL, Miller KD, Fuchs HE, Jemal A. Cancer Statistics, 2021. *CA Cancer J Clin* (2021) 71(1):7–33. doi: 10.3322/caac.21654
2. Arnold M, Sierra MS, Laversanne M, Soerjomataram I, Jemal A, Bray F. Global Patterns and Trends in Colorectal Cancer Incidence and Mortality. *Gut* (2017) 66(4):683–91. doi: 10.1136/gutjnl-2015-310912
3. Le DT, Uram JN, Wang H, Bartlett BR, Kemberling H, Eyring AD, et al. PD-1 Blockade in Tumors With Mismatch-Repair Deficiency. *N Engl J Med* (2015) 372(26):2509–20. doi: 10.1056/NEJMoa1500596
4. O'Neil BH, Wallmark JM, Lorente D, Elez E, Raimbourg J, Gomez-Roca C, et al. Safety and Antitumor Activity of the Anti-PD-1 Antibody Pembrolizumab in Patients With Advanced Colorectal Carcinoma. *PloS One* (2017) 12(12):e0189848. doi: 10.1371/journal.pone.0189848
5. Le DT, Durham JN, Smith KN, Wang H, Bartlett BR, Aulakh LK, et al. Mismatch Repair Deficiency Predicts Response of Solid Tumors to PD-1 Blockade. *Science* (2017) 357(6349):409–13. doi: 10.1126/science.aan6733
6. Overman MJ, McDermott R, Leach JL, Lonardi S, Lenz HJ, Morse MA, et al. Nivolumab in Patients With Metastatic DNA Mismatch Repair-Deficient or Microsatellite Instability-High Colorectal Cancer (CheckMate 142): An

Open-Label, Multicentre, Phase 2 Study. *Lancet Oncol* (2017) 18(9):1182–91. doi: 10.1016/s1470-2045(17)30422-9
7. Overman MJ, Lonardi S, Wong KYM, Lenz HJ, Gelsomino F, Aglietta M, et al. Durable Clinical Benefit With Nivolumab Plus Ipilimumab in DNA Mismatch Repair-Deficient/Microsatellite Instability-High Metastatic Colorectal Cancer. *J Clin Oncol* (2018) 36(8):773–9. doi: 10.1200/jco.2017.76.9901
8. Le DT, Kim TW, Van Cutsem E, Geva R, Jäger D, Hara H, et al. Phase II Open-Label Study of Pembrolizumab in Treatment-Refractory, Microsatellite Instability-High/Mismatch Repair-Deficient Metastatic Colorectal Cancer: KEYNOTE-164. *J Clin Oncol* (2020) 38(1):11–9. doi: 10.1200/jco.19.02107
9. National Comprehensive Cancer Network. (NCCN) Clinical Practice Guidelines in Oncology. *Rectal Cancer. Version 2.* (2021). Available at: https://www.nccn.org/patients/guidelines/cancers.aspx#rectal (Accessed 10 Sep 2021)
10. National Comprehensive Cancer Network. (NCCN) Clinical Practice Guidelines in Oncology. *Colon Cancer. Version 3.* (2021). Available at: https://www.nccn.org/patients/guidelines/cancers.aspx#colon (Accessed 10 Sep 2021)
11. Hecht M, Büttner-Herold M, Erlenbach-Wünsch K, Haderlein M, Croner R, Grützmann R, et al. PD-L1 Is Upregulated by Radiochemotherapy in Rectal Adenocarcinoma Patients and Associated With a Favourable Prognosis. *Eur J Cancer* (2016) 52–60. doi: 10.1016/j.ejca.2016.06.015
12. Dovedi SJ, Adlard AL, Lipowska-Bhalla G, McKenna C, Jones S, Cheadle EJ, et al. Acquired Resistance to Fractionated Radiotherapy Can Be Overcome by Concurrent PD-L1 Blockade. *Cancer Res* (2014) 74(19) 5458–68. doi: 10.1158/0008-5472.CAN-14-1258
13. Luo R, Firat E, Gaedicke S, Guffart E, Watanabe T, Niedermann G. Cisplatin Facilitates Radiation-Induced Abscopal Effects in Conjunction With PD-1 Checkpoint Blockade Through CXCR3/CXCL10-Mediated T-Cell Recruitment. *Clin Cancer Res* (2019) 25(23):7243–55. doi: 10.1158/1078-0432.Ccr-19-1344
14. Tate JG, Bamford S, Jubb HC, Sondka Z, Beare DM, Bindal N, et al. COSMIC: The Catalogue Of Somatic Mutations In Cancer. *Nucleic Acids Res* (2019) 47 (D1):D941–d7. doi: 10.1093/nar/gky1015
15. Landrum MJ, Lee JM, Benson M, Brown G, Chao C, Chitipiralla S, et al. ClinVar: Public Archive of Interpretations of Clinically Relevant Variants. *Nucleic Acids Res* (2016) 44(D1):D862–8. doi: 10.1093/nar/gkv1222
16. Kumar P, Henikoff S, Ng PC. Predicting the Effects of Coding Non-Synonymous Variants on Protein Function Using the SIFT Algorithm. *Nat Protoc* (2009) 4(7):1073–81. doi: 10.1038/nprot.2009.86
17. Eisenhauer EA, Therasse P, Bogaerts J, Schwartz LH, Sargent D, Ford R, et al. New Response Evaluation Criteria in Solid Tumours: Revised RECIST Guideline (Version 1.1). *Eur J Cancer* (2009) 45(2):228–47. doi: 10.1016/j.ejca.2008.10.026
18. Qiu B, Ding PR, Cai L, Xiao WW, Zeng ZF, Chen G, et al. Outcomes of Preoperative Chemoradiotherapy Followed by Surgery in Patients With Unresectable Locally Advanced Sigmoid Colon Cancer. *Chin J Cancer* (2016) 35(1):65. doi: 10.1186/s40880-016-0126-y
19. Chang H, Yu X, Xiao WW, Wang QX, Zhou WH, Zeng ZF, et al. Neoadjuvant Chemoradiotherapy Followed by Surgery in Patients With Unresectable Locally Advanced Colon Cancer: A Prospective Observational Study. *Oncol Targets Ther* (2018) 11:409–18. doi: 10.2147/ott.S150367
20. CSOCOC DATGFCCWG. Chinese Society of Clinical Oncology (CSCO) Diagnosis and Treatment Guidelines for Colorectal Cancer 2018 (English Version). *Chin J Cancer Res* (2019) 31(1):117–34. doi: 10.21147/j.issn.1000-9604.2019.01.07
21. Hasan S, Renz P, Wegner RE, Finley G, Raj M, Monga D, et al. Microsatellite Instability (MSI) as an Independent Predictor of Pathologic Complete Response (PCR) in Locally Advanced Rectal Cancer: A National Cancer Database (NCDB) Analysis. *Ann Surg* (2020) 271(4):716–23. doi: 10.1097/sla.0000000000003051
22. Cercek A, Dos Santos Fernandes G, Roxburgh CS, Ganesh K, Ng S, Sanchez-Vega F, et al. Mismatch Repair-Deficient Rectal Cancer and Resistance to Neoadjuvant Chemotherapy. *Clin Cancer Res* (2020) 26(13):3271–9. doi: 10.1158/1078-0432.Ccr-19-3728
23. Chalabi M, Fanchi LF, Dijkstra KK, Van den Berg JG, Aalbers AG, Sikorska K, et al. Neoadjuvant Immunotherapy Leads to Pathological Responses in MMR-Proficient and MMR-Deficient Early-Stage Colon Cancers. *Nat Med* (2020) 26 (4):566–76. doi: 10.1038/s41591-020-0805-8
24. Liu DX, Li DD, He W, Ke CF, Jiang W, Tang JH, et al. PD-1 Blockade in Neoadjuvant Setting of DNA Mismatch Repair-Deficient/Microsatellite Instability-High Colorectal Cancer. *Oncoimmunology* (2020) 9(1):1711650. doi: 10.1080/2162402x.2020.1711650
25. Zhang J, Cai J, Deng Y, Wang H. Complete Response in Patients With Locally Advanced Rectal Cancer After Neoadjuvant Treatment With Nivolumab. *Oncoimmunology* (2019) 8(12):e1663108. doi: 10.1080/2162402x.2019.1663108
26. Teo MY, Seier K, Ostrovnaya I, Regazzi AM, Kania BE, Moran MM, et al. Alterations in DNA Damage Response and Repair Genes as Potential Marker of Clinical Benefit From PD-1/PD-L1 Blockade in Advanced Urothelial Cancers. *J Clin Oncol* (2018) 36(17):1685–94. doi: 10.1200/jco.2017.75.7740
27. Ged Y, Chaim JL, DiNatale RG, Knezevic A, Kotecha RR, Carlo MI, et al. DNA Damage Repair Pathway Alterations in Metastatic Clear Cell Renal Cell Carcinoma and Implications on Systemic Therapy. *J Immunother Cancer* (2020) 8(1):e000230. doi: 10.1136/jitc-2019-000230
28. Ricciuti B, Recondo G, Spurr LF, Li YY, Lamberti G, Venkatraman D, et al. Impact of DNA Damage Response and Repair (DDR) Gene Mutations on Efficacy of PD-(L)1 Immune Checkpoint Inhibition in Non-Small Cell Lung Cancer. *Clin Cancer Res* (2020) 26(15):4135–42. doi: 10.1158/1078-0432.Ccr-19-3529
29. Zhang W, Zhang L, Jiang H, Li Y, Wang S, Wang Q. Mutations in DNA Damage Response Pathways as a Potential Biomarker for Immune Checkpoint Blockade Efficacy: Evidence From a Seven-Cancer Immunotherapy Cohort. *Aging* (2021) 13(21):24136–54. doi: 10.18632/aging.203670
30. Hu M, Zhou M, Bao X, Pan D, Jiao M, Liu X, et al. ATM Inhibition Enhances Cancer Immunotherapy by Promoting mtDNA Leakage and cGAS/STING Activation. *J Clin Invest* (2021) 131(3):e139333. doi: 10.1172/JCI139333
31. Zhang Q, Green MA-O, Lang X, Lazarus J, Parsels JD, Wei S, et al. Inhibition of ATM Increases Interferon Signaling and Sensitizes Pancreatic Cancer to Immune Checkpoint Blockade Therapy. *Cancer Res* (2019) 79(15):3940–51. doi: 10.1158/0008-5472.CAN-19-0761
32. Gao J, Shi LZ, Zhao H, Chen J, Xiong L, He Q, et al. Loss of IFN-γ Pathway Genes in Tumor Cells as a Mechanism of Resistance to Anti-CTLA-4 Therapy. *Cell* (2016) 167(2):397–404.e9. doi: 10.1016/j.cell.2016.08.069
33. Shin DS, Zaretsky JM, Escuin-Ordinas H, Garcia-Diaz A, Hu-Lieskovan S, Kalbasi A, et al. Primary Resistance to PD-1 Blockade Mediated by JAK1/2 Mutations. *Cancer Discov* (2017) 7(2):188–201. doi: 10.1158/2159-8290.Cd-16-1223

Conflict of Interest: Authors YJX, YTZ, ZKZ, DFW, HQL and CS are employed by YuceBio Technology Co., Ltd.

The remaining authors declare that the research was conducted in the absence of any commercial or financial relationships that could be construed as a potential conflict of interest.

The reviewer MYC declared a shared affiliation with several of the authors (CJZ, TJ, QXW, ZFZ, PQC, RZ, WWX and YHG) to the handling editor at time of review.

Publisher's Note: All claims expressed in this article are solely those of the authors and do not necessarily represent those of their affiliated organizations, or those of the publisher, the editors and the reviewers. Any product that may be evaluated in this article, or claim that may be made by its manufacturer, is not guaranteed or endorsed by the publisher.

Copyright © 2021 Zhou, Jiang, Xiao, Wang, Zeng, Cai, Zhao, Zhao, Wu, Lin, Sun, Zhang, Xiao and Gao. This is an open-access article distributed under the terms of the Creative Commons Attribution License (CC BY). The use, distribution or reproduction in other forums is permitted, provided the original author(s) and the copyright owner(s) are credited and that the original publication in this journal is cited, in accordance with accepted academic practice. No use, distribution or reproduction is permitted which does not comply with these terms.

frontiers in Immunology

CASE REPORT
published: 20 December 2021
doi: 10.3389/fimmu.2021.798276

Case Report: Clinical Management of a Patient With Metastatic Non-Small Cell Lung Cancer Newly Receiving Immune Checkpoint Inhibition During Symptomatic COVID-19

*Sibylle C. Mellinghoff[1,2,3,4], Kanika Vanshylla[5], Christine Dahlke[4,6,7], Marylyn M. Addo[4,6,7], Oliver A. Cornely[1,2,3,8], Florian Klein[3,5,9], Thorsten Persigehl[10], Jan Rybniker[1], Henning Gruell[5] and Paul J. Bröckelmann[1,11,12]**

[1] Faculty of Medicine and University Hospital of Cologne, Department I of Internal Medicine, Center for Integrated Oncology Aachen Bonn Cologne Düsseldorf (CIO ABCD), University of Cologne, Cologne, Germany, [2] Cologne Cluster of Excellence in Cellular Stress Responses in Aging-Associated Disease (CECAD), University of Cologne, Cologne, Germany, [3] German Centre for Infection Research (DZIF), Partner Site Bonn-Cologne, Cologne, Germany, [4] Department of Clinical Immunology of Infectious Diseases, Bernhard Nocht Institute for Tropical Medicine, Hamburg, Germany, [5] Institute of Virology, Faculty of Medicine and University Hospital Cologne, University of Cologne, Cologne, Germany, [6] Division of Infectious Diseases, First Department of Medicine, University Medical Center Hamburg-Eppendorf, Hamburg, Germany, [7] German Centre for Infection Research (DZIF), Partner Site Hamburg-Lübeck-Borstel-Riems, Hamburg, Germany, [8] Clinical Trials Centre Cologne (ZKS Köln), Cologne, Germany, [9] Center for Molecular Medicine Cologne (CMMC), University of Cologne, Cologne, Germany, [10] Institute for Diagnostic and Interventional Radiology, Faculty of Medicine and University Hospital Cologne, University of Cologne, Cologne, Germany, [11] Max-Planck Institute for the Biology of Ageing, Cologne, Germany, [12] Mildred-Scheel School of Oncology (MSSO) Aachen Bonn Cologne Düsseldorf, Cologne, Germany

OPEN ACCESS

Edited by:
Udo S. Gaipl,
University Hospital Erlangen, Germany

Reviewed by:
Javier Carbone,
Gregorio Marañón Hospital, Spain
Samita Andreansky,
University of Miami, United States

***Correspondence:**
Paul J. Bröckelmann
paul.broeckelmann@uk-koeln.de

Specialty section:
This article was submitted to Cancer Immunity and Immunotherapy, a section of the journal Frontiers in Immunology

Received: 19 October 2021
Accepted: 29 November 2021
Published: 20 December 2021

Citation:
Mellinghoff SC, Vanshylla K, Dahlke C, Addo MM, Cornely OA, Klein F, Persigehl T, Rybniker J, Gruell H and Bröckelmann PJ (2021) Case Report: Clinical Management of a Patient With Metastatic Non-Small Cell Lung Cancer Newly Receiving Immune Checkpoint Inhibition During Symptomatic COVID-19. Front. Immunol. 12:798276. doi: 10.3389/fimmu.2021.798276

Effects of initiation of programmed-death-protein 1 (PD1) blockade during active SARS-CoV-2 infection on antiviral immunity, COVID-19 course, and underlying malignancy are unclear. We report on the management of a male in his early 40s presenting with highly symptomatic metastatic lung cancer and active COVID-19 pneumonia. After treatment initiation with pembrolizumab, carboplatin, and pemetrexed, the respiratory situation initially worsened and high-dose corticosteroids were initiated due to suspected pneumonitis. After improvement and SARS-CoV-2 clearance, anti-cancer treatment was resumed without pembrolizumab. Immunological analyses with comparison to otherwise healthy SARS-CoV-2-infected ambulatory patients revealed a strong humoral immune response with higher levels of SARS-CoV-2-reactive IgG and neutralizing serum activity. Additionally, sustained increase of Tfh as well as activated $CD4^+$ and $CD8^+$ T cells was observed. Sequential CT scans showed regression of tumor lesions and marked improvement of the pulmonary situation, with no signs of pneumonitis after pembrolizumab re-challenge as maintenance. At the latest follow-up, the patient is ambulatory and in ongoing partial remission on pembrolizumab. In conclusion, anti-PD1 initiation during active COVID-19 pneumonia was feasible and cellular and humoral immune responses to SARS-CoV-2 appeared enhanced in our hospitalized patient.

However, distinguishing COVID-19-associated changes from anti-PD1-associated immune-related pneumonitis posed a considerable clinical, radiographic, and immunologic challenge.

Keywords: SARS-CoV-2, COVID-19, NSCLC, anti-PD1, immune checkpoint, immunotherapy, pneumonitis

INTRODUCTION

The coronavirus disease 2019 (COVID-19) pandemic caused by the Severe Acute Respiratory Syndrome Coronavirus-2 (SARS-CoV-2) has a major impact on global health. Cancer patients appear at increased risk for severe COVID-19, especially with cytostatic or B-cell-depleting treatment (1, 2). SARS-CoV-2 infection induces specific antibodies as well as $CD4^+$ and $CD8^+$ T cells (3). While underlying disease influences antibody kinetics, robust T-cell response is usually also observed with comorbidities (3). Initially, however, a significant T-cell reduction and functional exhaustion of the remaining T cells was observed (4), especially in cancer patients (5). Immune checkpoint inhibition (ICI) reversing T-cell exhaustion could therefore potentially be beneficial for COVID-19 patients. On the other hand, ICI may increase immune hyperactivation during COVID-19, thereby worsening outcomes (6, 7).

The effect of ICI initiation during acute SARS-CoV-2 infection, e.g., by programmed death protein 1 (PD1) blockade, on the course of COVID-19 and development of antiviral immunity remains largely unclear. We report the clinical course, management, and sequential immunological data after first initiation of anti-PD1-based anti-cancer treatment in a patient with newly diagnosed metastatic non-small cell lung cancer (NSCLC) during symptomatic COVID-19. By comparison to otherwise healthy SARS-CoV-2-infected controls (SARS-CoV-2 positive adult individuals with mild disease and without cancer disease), we provide novel insights into the interplay of anti-PD1 treatment with SARS-CoV-2 infection and immunity including potential immune-related adverse events (irAEs).

CLINICAL CASE DESCRIPTION

A male in his early 40s, who had not received vaccination against SARS-CoV-2, presented to a primary hospital due to progressive severe pain of the lower back and hip accompanied by weight loss. Diagnostics revealed widespread osteolytic lesions with unstable pathologic fractures of the spine and an extensive predominantly right-sided pulmonary tumor. Histopathology revealed NSCLC with relevant PD-Ligand 1 expression (TP-score 10%) but wild type for actionable genes, and staging showed cerebral, hepatic, osseous, peritoneal, pleural, and splenic metastases. During palliative radiotherapy to the spine, a routine nasopharyngeal swab revealed asymptomatic SARS-CoV-2 infection by polymerase chain reaction (PCR; day [D] 0) in the patient who had not received prior COVID-19 vaccination. Due to worsening general condition with Eastern Cooperative Oncology Group (ECOG) score 4, the patient transferred to our department (Timeline: **Table 1**).

A CT scan on D8 revealed progressive NSCLC and pulmonary infiltrations with mild ground glass opacities as well as mild consolidations attributable to early-stage COVID-19 pneumonia (**Figures 1A, B**). Laboratory examinations showed increased inflammatory markers (**Figure 1C**) and high naso-pharyngeal levels of SARS-CoV-2 RNA (qPCR Cycle threshold [Ct] 18, **Figure 1D**). Due to increase of cancer-related symptoms with immobilizing pain, treatment with pembrolizumab (200 mg Q3W), carboplatin (4 mg/AUC Q3W), and pemetrexed (375 mg/m^2 BSA) was initiated (D9). Prophylactic dexamethasone 4 mg (1-0-1) was administered peri-chemotherapy and continued at 4 mg/day due to meanwhile symptomatic COVID-19 thereafter.

Within days, the patient developed peripheral edema, pleural effusion, and ascites, judged as primarily pemetrexed-associated. Timely matching serum albumin and serum protein are depicted in **Figure 1C**. Despite adequate fluid management, respiratory symptoms worsened, requiring oxygen supplementation of up to 4 L/min for achieving stable oxygen saturation of >90%. Due to neutropenic fever (**Figure 1C**), empiric antibiotic treatment with piperacillin/tazobactam was initiated on D16; microbiological diagnostics were negative. A D20 CT scan showed progressive opacities consistent with worsening COVID-19 pneumonia but also treatment-related pneumonitis or—less likely—bacterial superinfection (**Figure 1A**) while the tumor manifestations were already regressive (**Figure 1B**). Repeated swabs showed decreasing nasopharyngeal SARS-CoV-2 RNA levels (**Figure 1D**). In light of persisting respiratory symptoms, dexamethasone 20 mg/day was administered (D20–25) for suspected pembrolizumab-associated pneumonitis. Symptoms and inflammatory markers improved subsequently, leading to termination of antibiotic treatment and corticosteroid tapering from D26 onwards, accompanied by regressive tumor and pulmonary opacities on D27 (**Figures 1A, B**).

After blood count recovery and improvement of the general condition, anti-cancer treatment was continued with carboplatin and paclitaxel-albumin (100 mg/m^2 Q1W) from D30 onwards. Except for prolonged leukopenia, treatment was well tolerated and accompanied by stereotactic radiation of the brain metastasis and palliative radiotherapy for spine and hip. D47 CT showed further regression of tumor lesions and marked improvement of the pulmonary situation with no sign of potential residual immune-related pneumonitis (**Figures 1A, B**). After initiating pembrolizumab maintenance on D81, the patient was discharged on D95 (ECOG 2). The most recent restaging 6 months after treatment start showed a partial response based on iRECIST with a reduced sum of target lesions from 125.4 to

TABLE 1 | Timeline of the episode of care.

Day 0 (D0)	First nasopharyngeal detection of SARS-CoV-2 by PCR
D0–D7	Progressive cancer-related immobilizing pain and B-symptoms, onset of symptomatic SARS-CoV-2 infection (ECOG 4), and transfer to our department
D8	CT scan reveals progressive metastatic NSCLC and COVID-19 pneumonia, nasopharyngeal swab with high SARS-CoV-2 viral load (qPCR Ct value 18)
D9	First administration of pembrolizumab, pemetrexed, and carboplatin
D10–D15	Peripheral edema, pleural effusion, and ascites judged pemetrexed-related, worsening of respiratory symptoms requiring oxygen supplementation
D16	Initiation of empiric antibiotic treatment with piperacillin/tazobactam due to neutropenic fever, consecutive microbiological diagnostics were negative
D20	CT scan shows changes consistent with worsening COVID-19 pneumonia while treatment-related immune-mediated pneumonitis cannot be ruled out
D20–D25	Empiric treatment with high-dose dexamethasone for suspected pembrolizumab-associated pneumonitis, steady improvement of respiratory symptoms
D27	CT scan shows regressive pulmonary opacities and tumor manifestations
D30	Continuation of anti-cancer treatment with carboplatin and paclitaxel-albumin at standard doses, with regular re-administration after blood count recovery. Concomitant palliative radiotherapy to hip and spine and stereotactic ablation of cerebral metastases.
D47	CT scan shows further regression of tumor lesions and marked improvement of the pulmonary situation, consistent with improved general status
D81	Completion of chemotherapy, initiation of pembrolizumab maintenance treatment
D95	Discharge in an improved overall condition, increasingly mobile with aids and partially capable of self-care (ECOG 2)
6 months	CT scan shows no sign of recurring pneumonitis during ongoing pembrolizumab treatment, and a partial response according to iRECIST is achieved

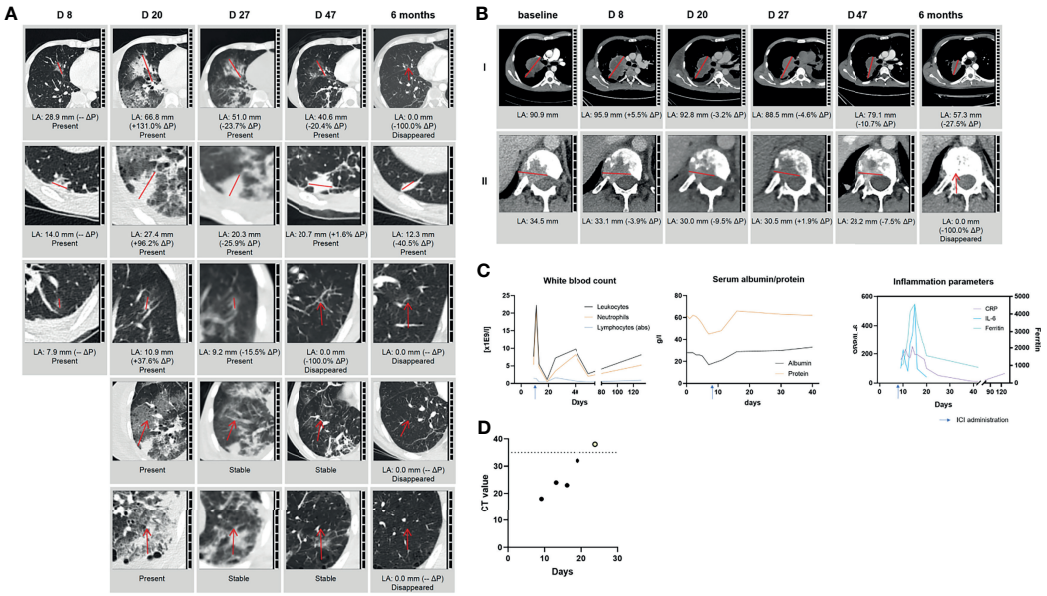

FIGURE 1 | Radiologic examinations and laboratory assessments after initiation of pembrolizumab-based treatment during active COVID-19. **(A)** Exemplary pulmonary infiltrations during SARS-CoV-2 disease course and treatment with pembrolizumab with ground glass infiltration (I+III), consolidation (II), and mixed ground glass and consolidation (IV+V); **(B)** change of the tumor target lesions (I) right upper lobe/hilus and (II) TH12 during SARS-CoV-2 disease course and treatment with pembrolizumab; **(C)** blood counts, inflammatory markers, and serum albumin/protein. **(D)** SARS-CoV-2 viral load reflected by Ct value of SARS-CoV-2 PCR from sequential nasopharyngeal swabs. LA, largest diameter; ΔP, change from previous assessment; DX, day in relation to first SARS-CoV-2 detection by PCR (=D0); CRP, C-reactive protein; IL-6, interleukin 6; LOD, level of detection.

57.3 mm (−54.3%, **Figure 1B**). Notably, there were no signs of active pneumonitis after re-exposure to anti-PD1 treatment. The patient continued ambulatory pembrolizumab maintenance and was increasingly capable of self-care.

IMMUNE TRAJECTORY

Cellular and humoral immune responses to SARS-CoV-2 were assessed prior to pembrolizumab infusion (D9) and sequentially thereafter (D11, D13, D19, D25, and D39) and compared to otherwise healthy SARS-CoV-2-infected individuals.

Serum antibodies targeting SARS-CoV-2 became detectable by D18 (**Figure 2A**). High levels of SARS-CoV-2-neutralizing activity were observed in serum as well as for purified serum IgG obtained on D25 and D39 (**Figure 2B**). The appearance of circulating antibodies coincided with decreasing SARS-CoV-2 RNA levels in nasopharyngeal swabs (**Figure 1D**). To further assess the magnitude of the humoral immune response observed on D25 after diagnosis, the findings were contrasted to results obtained within 20–30 days of PCR confirmation of infection from a cohort of overall healthy COVID-19 outpatients with mild disease (n = 6), which has been previously described in detail (8). Compared to those, the patient exhibited higher IgM

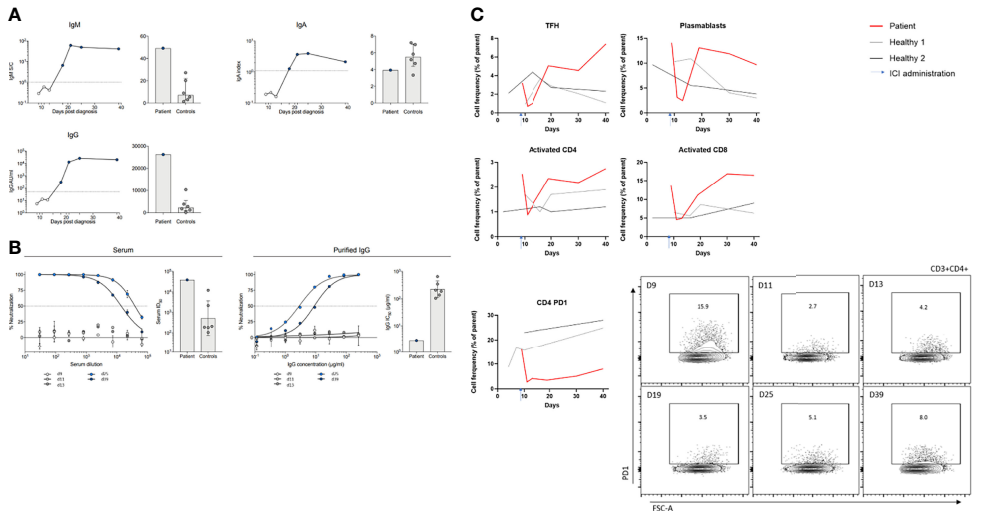

FIGURE 2 | Cellular and humoral immune trajectory during SARS-CoV-2 infection and immune checkpoint inhibition treatment. Cellular and humoral immune responses to SARS-CoV-2 infection were monitored on D9 prior to pembrolizumab infusion, and on D11, D13, D19, D25, and D39 and compared to controls (SARS-CoV-2-positive adult individuals with mild disease and without cancer disease). **(A)** Serum antibodies (IgM, IgA, and IgG) measured by ELISA (IgA, Euroimmun ELISA; IgM and IgG, Abbott Alinity CMIA) targeting SARS-CoV-2 became detectable by D18 post SARS-CoV-2 diagnosis. **(B)** SARS-CoV-2-neutralizing activity was measured, determined by a lentivirus-based pseudovirus neutralization assay as previously described (8) for serum and purified serum IgG from D25 on. Six patients with mild COVID-19 disease served as control for **(A, B)** [right panels; sample acquisition D20 to 30 after PCR confirmation of SARS-CoV-2 infection (8)]. **(C)** Lymphocyte subsets and their expression of activation/differentiation markers (Plasmablasts [$(CD20^{-}CD38^{high})$%$CD19^{+}$], T follicular helper cells [TFH; $PD1^{+}ICOS^{+}$], activation status of CD4 and CD8 T cells [$HLA\text{-}DR^{+}CD38^{+}$], and PD1 expression on $CD4^{+}$ T cells) were determined by flow cytometry. Two subjects with mild COVID-19 disease served as control (sample acquisition for the same period as the patient). Exemplarily, flow cytometry data are shown for $CD4^{+}$ $PD1^{+}$ T cells.

reactivity, 10-fold higher levels of IgG (**Figure 2A**), and 2-logs higher neutralizing serum/IgG activity (**Figure 2B**).

Lymphocyte subsets and their expression of activation/differentiation markers were determined by flow cytometry and compared to two otherwise healthy individuals infected with SARS-CoV-2 (n = 2, selected by the following criteria: SARS-CoV-2-positive adult individuals with mild disease and without cancer disease). Similar to antibody kinetics, a high proportion of plasmablasts [$(CD20^{-}CD38^{high})$%$CD19^{+}$] was observed at D18, sustained compared to controls. Of note, the patient had shown a high level of plasmablasts initially that rapidly decreased following ICI treatment. T follicular helper (Tfh) cells ($PD1^{+}ICOS^{+}$) showed similar dynamics and initially decreased after ICI initiation, deferredly increasing at D18 (**Figure 2C**). Administration of high-dose corticosteroids entailed stagnation of Tfh levels, but during tapering and thereafter, a further increase beyond the simultaneously measured control patients was found. Furthermore, activated $CD4^{+}$ and $CD8^{+}$ T cells ($HLA\text{-}DR^{+}CD38^{+}$) showed a similar pattern compared to plasmablasts and Tfh cells. In comparison to Tfh and activated CD4 T cells, $CD4^{+}$ T cells expressing PD1 decreased after ICI initiation and remained low. This pattern was not observed in controls.

DISCUSSION

We report the clinical and immune trajectory as well as our clinical management approach of a patient with active SARS-CoV-2 infection at the time of pembrolizumab-based treatment initiation for highly symptomatic newly diagnosed metastatic NSCLC. While the effects of SARS-CoV-2 infection in patients already receiving ICI are increasingly studied (9, 10), the effects of a first infusion of an anti-PD1 antibody during active symptomatic COVID-19 remain unknown. Furthermore, the complex case of newly diagnosed cancer patients with urgent need for treatment and concurrent SARS-CoV-2 infection is portrayed. In a situation of rapidly increasing COIVD-19 case numbers as of November 2021, this is highly topical and needs further investigation beyond this case report.

Before treatment initiation in our patient, the risk of potential negative effects of ICI-based anticancer treatment on the COVID-19 disease course was weighed, taking into account a potential benefit of such treatment by reversing T-cell exhaustion. While the patient's clinical situation initially worsened due to hypervolemia deemed pemetrexed-associated, the tumor manifestations were immediately responsive. Posing a considerable challenge, the patient developed worsening respiratory symptoms accompanied by heterogeneous pulmonary changes not clearly attributable to either COVID-19, bacterial superinfection, or immune-related pneumonitis. While the clinical improvement to corticosteroids hints at an irAE, morphologic features and the lack of pulmonary changes after pembrolizumab re-exposure question this etiology. Hypothetically, ICI-associated pneumonitis may have been aggravated during active SARS-CoV-2 infection due to antigen cross-reactivity and a local state of hyperinflammation.

Despite active cancer and exposure to chemotherapy, our patient showed an adequate humoral immune response with high levels of spike-specific antibodies and potent SARS-CoV-2 neutralizing activity. These values were higher than those seen in temporally matched convalescent individuals with a mild COVID-19 disease course that did not require hospitalization (8). Since mildly ill patients were shown to mount lower binding antibody responses compared to severely ill patients (3, 11), the different course of COVID-19 in our hospitalized patient and the control group has to be taken into account when discussing antibody kinetics. With regard to cellular immune response, we report higher levels of plasmablasts and activated as well as Tfh cells in our patient with ICI administration compared to controls, which is in line with a previous report from a SARS-CoV-2-infected individual under ICI treatment (10). Yet, an influence by the emerging pneumonitis to elevated adaptive immunity, especially with regard to CD4 and CD8 T cells, cannot be ruled out. Due to the lack of measurements in a control group consisting of NSCLC patients under ICI-based treatment without active COVID-19, it remains to be investigated in forthcoming studies to which extent the observed immunologic changes are influenced by initiation of anti-PD1 inhibition during active COVID-19. Immune response in SARS-CoV-2-infected immunocompromised patients has been shown to be frequently impaired, entailing severe COVID-19 courses as well as prolonged viral shedding (1). Correlating viral load, TFH, and plasmablast increase may therefore be additionally reflective of increased germinal center reaction due to antigen load (12). Taking into account the beforementioned circumstances and potential limitations, ICI treatment may possibly have contributed to the patient's robust humoral and cellular immune response to SARS-CoV-2 infection herein reported. A potentially superior immune response by suppression of the co-inhibitory molecule PD1 however requires substantial further investigation in this context. Besides these immunological observations, our case provides helpful details to inform clinicians managing patients with a first diagnosis of metastatic NSCLC requiring treatment initiation during SARS-CoV-2-related complications.

Due to scarce data, international expert panels strongly recommended to delay/discontinue antineoplastic treatment in SARS-CoV-2-positive tested patients whenever possible (1). On the other hand, uncontrolled malignancy was shown to be a risk factor for severe COVID-19. Initiation or administration of anti-cancer therapy may be highly urgent to preserve vital functions, achieve symptom control, and improve chances of durable remission. In light of the ongoing SARS-CoV-2 pandemic, oncologists must increasingly balance these multifaceted aspects to safely provide optimal antineoplastic care. The here reported case shows feasible and ultimately efficacious treatment initiation with chemo-immunotherapy in an NSCLC patient during acute SARS-CoV-2 infection. The complexity of this clinical course underlines the importance of interdisciplinary teams for treatment of such cases including, among others, oncologists, radiologists, and infectious disease specialists.

DATA AVAILABILITY STATEMENT

The raw data supporting the conclusions of this article will be made available by the authors upon request, without undue reservation.

ETHICS STATEMENT

The collection of human material involved in this study was reviewed and approved by the Institutional Review Board of the University of Cologne (No 13-091). The patients/participants provided their written informed consent to participate in this study.

AUTHOR CONTRIBUTIONS

PB and SM conceptualized the study, organized data and sample collection, analyzed cellular immune response, analyzed data, and wrote the first draft of the manuscript. KV and HG performed the assays on the humoral immune response and co-authored the manuscript. CD, MA, OC, FK, and JR supervised correlative studies and/or patient care and edited the manuscript. TP evaluated radiology images and edited the manuscript. All authors contributed to the article and approved the submitted version.

FUNDING

SM is supported by a DZIF clinical leave stipend and PB is supported by the Mildred Scheel School of Oncology (MSSO 202 Postgraduate Program, German Cancer Aid, Grant No. 70113307).

ACKNOWLEDGMENTS

We are grateful to our patient and everyone involved in his care. Peripheral blood samples were collected in the context of an institutional biobanking approved by the Institutional Review Board of the University of Cologne (No 13-091), and the patient has given his written informed consent. We specifically thank Lucia Nogova (MD), Rosanne Sprute (MD), Yannick D'Hargues (MD), Monika Friedrich (BTA), Maike Schlotz, and Johanna Worczinski who provided clinical care or supported with acquisition and/or processing of samples.

REFERENCES

1. Giesen N, Sprute R, Rüthrich M, Khodamoradi Y, Mellinghoff SC, Beutel G, et al. Evidence-Based Management of COVID-19 in Cancer Patients: Guideline by the Infectious Diseases Working Party (AGIHO) of the German Society for Haematology and Medical Oncology (DGHO). *Eur J Cancer (Oxford Engl 1990)* (2020) 140:86–104. doi: 10.1016/j.ejca.2020.09.009
2. Sullivan RJ, Johnson DB, Rini BI, Neilan TG, Lovly CM, Moslehi JJ, et al. COVID-19 and Immune Checkpoint Inhibitors: Initial Considerations. *J ImmunoTher Cancer* (2020) 8(1):e000933. doi: 10.1136/jitc-2020-000933

3. Koch T, Mellinghoff SC, Shamsrizi P, Addo MM, Dahlke C. Correlates of Vaccine-Induced Protection Against SARS-CoV-2. *Vaccines* (2021) 9(3):238. doi: 10.3390/vaccines9030238
4. Diao B, Wang C, Tan Y, Chen X, Liu Y, Ning L, et al. Reduction and Functional Exhaustion of T Cells in Patients With Coronavirus Disease 2019 (COVID-19). *Front Immunol* (2020) 11:827. doi: 10.3389/fimmu.2020.00827
5. Abdul-Jawad S, Baù L, Alaguthurai T, Del Molino Del Barrio I, Laing AG, Hayday TS, et al. Acute Immune Signatures and Their Legacies in Severe Acute Respiratory Syndrome Coronavirus-2 Infected Cancer Patients. *Cancer Cell* (2021) 39(2):257–75.e6. doi: 10.1016/j.ccell.2021.01.001
6. Indini A, Rijavec E, Ghidini M, Bareggi C, Cattaneo M, Galassi B, et al. Coronavirus Infection and Immune System: An Insight of COVID-19 in Cancer Patients. *Crit Rev Oncol Hematol* (2020) 153:103059–. doi: 10.1016/j.critrevonc.2020.103059
7. Moore JB, June CH. Cytokine Release Syndrome in Severe COVID-19. *Science* (2020) 368(6490):473–4. doi: 10.1126/science.abb8925
8. Vanshylla K, Di Cristanziano V, Kleipass F, Dewald F, Schommers P, Gieselmann L, et al. Kinetics and Correlates of the Neutralizing Antibody Response to SARS-CoV-2 Infection in Humans. *Cell Host Microbe* (2021) 29 (6):917–29.e4. doi: 10.1016/j.chom.2021.04.015
9. Luo J, Rizvi H, Egger JV, Preeshagul IR, Wolchok JD, Hellmann MD. Impact of PD-1 Blockade on Severity of COVID-19 in Patients With Lung Cancers. *Cancer Discovery* (2020) 10(8):1121–8. doi: 10.1158/2159-8290.CD-20-0596
10. Yatim N, Boussier J, Tetu P, Smith N, Bruel T, Charbit B, et al. Immune Checkpoint Inhibitors Increase T Cell Immunity During SARS-CoV-2 Infection. *Sci Adv* (2021) 7(34):eabg4081. doi: 10.1126/sciadv.abg4081
11. Wang Y, Zhang L, Sang L, Ye F, Ruan S, Zhong B, et al. Kinetics of Viral Load and Antibody Response in Relation to COVID-19 Severity. *J Clin Invest* (2020) 130(10):5235–44. doi: 10.1172/JCI138759
12. Masiá M, Telenti G, Fernández M, García JA, Agulló V, Padilla S, et al. SARS-CoV-2 Seroconversion and Viral Clearance in Patients Hospitalized With COVID-19: Viral Load Predicts Antibody Response. *Open Forum Infect Dis* (2021) 8(2):ofab005. doi: 10.1093/ofid/ofab005

Conflict of Interest: SM reports personal fees from Octapharma; outside the submitted work. OC reports grants and personal fees from Actelion, personal fees from Allecra Therapeutics, personal fees from Al-Jazeera Pharmaceuticals, grants and personal fees from Amplyx, grants and personal fees from Astellas, grants and personal fees from Basilea, personal fees from Biosys, grants and personal fees from Cidara, grants and personal fees from Da Volterra, personal fees from Entasis, grants and personal fees from F2G, grants and personal fees from Gilead, personal fees from Grupo Biotoscana, personal fees from IQVIA, grants from Janssen, personal fees from Matinas, grants from Medicines Company, grants and personal fees from MedPace, grants from Melinta Therapeutics, personal fees from Menarini, grants and personal fees from Merck/MSD, personal fees from Mylan, personal fees from Nabriva, personal fees from Noxxon, personal fees from Octapharma, personal fees from Paratek, grants and personal fees from Pfizer, personal fees from PSI, personal fees from Roche Diagnostics, grants and personal fees from Scynexis, personal fees from Shionogi, personal fees from Biocon, personal fees from CoRe Consulting, personal fees from Molecular Partners, from MSG-ERC, from Seres, other from Wiley (Blackwell); outside the submitted work. PB received research grants from BeiGene, Bristol Myers Squibb, Merck Sharpe & Dohme, and Takeda; and personal fees and non-financial support from Bristol-Myers Squibb, Celgene, and Takeda; outside the submitted work.

The remaining authors declare that the research was conducted in the absence of any commercial or financial relationships that could be construed as a potential conflict of interest.

Publisher's Note: All claims expressed in this article are solely those of the authors and do not necessarily represent those of their affiliated organizations, or those of the publisher, the editors and the reviewers. Any product that may be evaluated in this article, or claim that may be made by its manufacturer, is not guaranteed or endorsed by the publisher.

Copyright © 2021 Mellinghoff, Vanshylla, Dahlke, Addo, Cornely, Klein, Persigehl, Rybniker, Gruell and Bröckelmann. This is an open-access article distributed under the terms of the Creative Commons Attribution License (CC BY). The use, distribution or reproduction in other forums is permitted, provided the original author(s) and the copyright owner(s) are credited and that the original publication in this journal is cited, in accordance with accepted academic practice. No use, distribution or reproduction is permitted which does not comply with these terms.

frontiers in Immunology

REVIEW
published: 21 December 2021
doi: 10.3389/fimmu.2021.800879

Immune Checkpoint Inhibitor-Associated Colitis: From Mechanism to Management

Liansha Tang[1†], *Jialing Wang*[1†], *Nan Lin*[1†], *Yuwen Zhou*[1], *Wenbo He*[2], *Jiyan Liu*[1*] *and Xuelei Ma*[1*]

[1] Department of Biotherapy, Cancer Center, West China Hospital, Sichuan University, Chengdu, China, [2] Department of Neurosurgery, West China Hospital, Sichuan University, Chengdu, China

OPEN ACCESS

Edited by:
Hamid Reza Mirzaei,
Tehran University of Medical Sciences, Iran

Reviewed by:
Xuchen Zhang,
Yale University, United States
Alessandro Rizzo,
Sant'Orsola-Malpighi Polyclinic, Italy

***Correspondence:**
Jiyan Liu
liujiyan1972@163.com
Xuelei Ma
drmaxuelei@gmail.com

[†]These authors have contributed equally to this work

Specialty section:
This article was submitted to Cancer Immunity and Immunotherapy, a section of the journal Frontiers in Immunology

Received: 24 October 2021
Accepted: 29 November 2021
Published: 21 December 2021

Citation:
Tang L, Wang J, Lin N, Zhou Y, He W, Liu J and Ma X (2021) Immune Checkpoint Inhibitor-Associated Colitis: From Mechanism to Management. Front. Immunol. 12:800879. doi: 10.3389/fimmu.2021.800879

Immune checkpoint inhibitors (ICIs), as one of the innovative types of immunotherapies, including programmed cell death-1 (PD-1), programmed cell death-ligand 1 (PD-L1), and cytotoxic T lymphocyte antigen 4 (CTLA-4) inhibitors, have obtained unprecedented benefit in multiple malignancies. However, the immune response activation in the body organs could arise immune-related adverse events (irAEs). Checkpoint inhibitor colitis (CIC) is the most widely reported irAEs. However, some obscure problems, such as the mechanism concerning gut microbiota, the confusing differential diagnosis with inflammatory bowel disease (IBD), the optimal steroid schedule, the reintroduction of ICIs, and the controversial prognosis features, influence the deep understanding and precise diagnosis and management of CIC. Herein, we based on these problems and comprehensively summarized the relevant studies of CIC in patients with NSCLC, further discussing the future research direction of this specific pattern of irAEs.

Keywords: immune checkpoint inhibitor, colitis, diarrhoea, mechanism, diagnosis, management, prognosis

HIGHLIGHTS

- Gut microbiota, including *Faecalibacterium prausnitzii*, *Bacteroides fragilis*, and *Lactobacillus reuteri*, plays a critical role in the development of immune checkpoint-related colitis.
- Endoscopic biopsy is the gold standard of diagnosis, while endoscopic findings were not significantly associated with the severity of immune checkpoint-related colitis.
- Current management is based on symptomatic and steroid therapy. The utilization of biological agents according to the severity of immune checkpoint-related colitis grade is reasonable and recommended.
- Longer survival was found in patients who had a deteriorated or recurrent CIC instead of improved or resolved CIC. The influence of CIC outcome on overall survival requires to be explored further.

INTRODUCTION

Lung cancer is the leading cause of death among all cancers. In 2021, an estimated 131,880 deaths from lung cancer were recorded in the United States, with the death rate at 22% (1). As the most common type of lung cancer, non-small cell lung cancer (NSCLC) faces difficulties that over 50% of patients are diagnosed with advanced disease initially, for which the 5-year survival is nearly 5% (2). Moreover, the recommended standard treatment, chemotherapy and/or radiotherapy, offers generally modest efficacy for metastatic NSCLC patients. The 5-year survival varies from 6% to 30% when patients are treated with chemotherapy and/or radiotherapy (3, 4). Besides, target therapies, such as EGFR, ALK, and ROS1 tyrosine kinase inhibitors (TKIs), have contributed to unprecedented improvements for survival in NSCLC patients, with more moderate toxicity response than chemotherapy (5).

Recently, the emergence of immunotherapy fosters hopes for the treatment of multiple malignancies. Immune checkpoint inhibition, one of the innovative classes of immunotherapy, serves to restrain suppressive T-cell co-stimulatory signals, primarily cytotoxic $CD8^+$ T cells, by inhibiting programmed death protein-1 (PD-1), PD-ligand 1 (PD-L1), and cytotoxic T-lymphocyte associated protein-4 (CTLA-4) (6, 7). PD-1 inherently presents in T cells, B cells, tumor-infiltrating lymphocytes, monocytes, and dendritic cells (DCs). PD-L1 exists on the surface of both antigen-presenting cells (APCs) and tumor cells (8–10), resulting in self-tolerance promotion and autoimmunity attenuation after interacting with PD-1. Similarly, CTLA-4 is typically expressed on $CD4^+$/$CD8^+$ T cells, B-cell subsets, and thymocytes, which is associated with the suppression of T-cell activity (11). Immune checkpoint inhibitors (ICIs) have the ability of strengthening the immune attack and promoting tumor killing (12, 13), thus improving the survival of cancer patients.

To date, PD-1 inhibitors (nivolumab, pembrolizumab), PD-L1 inhibitors (atezolizumab, durvalumab), and CTLA-4 inhibitor (ipilimumab) have been approved by the U.S. Food and Drug Administration (FDA) and the European Medicines Agency (EMA) for the treatment of advanced NSCLC (14). The combination of nivolumab and ipilimumab contributed to prolonged overall survival (OS) and progression-free survival (PFS) in patients with NSCLC (15–17).

However, the eliminated immunoregulatory control could cause unrestrained immune response activation in body organs (18), like the gastrointestinal tract, liver, lung, heart, skin, and arthrosis, which leads to immune-related adverse events (irAEs) ultimately (19, 20). Among clinically reported irAEs, gastrointestinal toxicity is the most common irAEs that results in ICI discontinuation (21–23). Because of the similar symptoms with inflammatory bowel disease (IBD) and/or intestinal infection, the diagnosis of checkpoint inhibitor colitis (CIC) might be confused. As a result, precise diagnosis and optimized therapy are essential for recognizing this specific pattern of irAEs.

Prior studies have demonstrated the incidence, risk factors, diagnosis, and management of CIC (24–29). Nonetheless, they have variable concentrations and orientations, which are complementary but not deep and comprehensive. This review comprehensively summarized the relevant research studies and advanced progress of ICI-related colitis, especially the aspects less mentioned before, like the mechanism, evidence-based management schedules, rechallenge of ICIs, and prognosis of CIC. Besides, we provided a summary of cases and case series regarding CIC in NSCLC, aiming at identifying the clinicopathological and endoscopic features of these typical patients.

INCIDENCE AND ONSET

Nearly 20%–30% of patients would develop diarrhea after ICI therapy, while no more than 5% of patients have colitis (30). Patients treated with CTLA-4 inhibitors tend to experience three times higher CIC frequency than those with PD-1/PD-L1 inhibitors (19, 31, 32). It has been proposed that CTLA-4 blockade induces $CD4^+$ T-cell activation, resulting in a generalized immune response. In contrast, PD-1/PD-L1 blockades aim at late T-cell proliferation and, therefore, cause a more localized immune reaction (33). According to previous meta-analysis and systematic reviews (30, 33, 34), the overall incidence of diarrhea was 30.2%–35.4% for CTLA-4 inhibitors and 12.1%–13.7% for PD-1/PD-L1 inhibitors. The all-grade incidence of colitis was 5.7%–39.1% for CTLA-4 inhibitors and 0.7%–31.6% for PD-1/PD-L1 inhibitors. In lung cancer, the rates of all-grade and high-grade diarrhea were 9.1%–11.0% and 0.6%–1.1% for PD-1/PD-L1 inhibitors, respectively (34). All-grade and high-grade colitis caused by PD-1/PD-L1 inhibitors separately occurred at 0.4%–0.9% and 0.1%–0.6%. The combination of PD-1/PD-L1 inhibitors and CTLA inhibitors could reach 40.4% in all-grade diarrhea/colitis. We searched PubMed and Web of Science from 2017 to October 10, 2021, and included 32 occurrences of CIC in NSCLC patients. The search term we utilized were "non-small cell lung cancer*" AND "colitis*" AND "immunotherapy*" OR "immune checkpoint inhibitors*." All related case reports were included (**Table 1**). In our analysis, over 70% of patients were PD-1 inhibitor-related colitis, and patients treated with PD-1^+ CTLA inhibitors were prone to suffer grade 3 CIC (**Figure 1A**).

ICI-mediated colitis could appear at any time, such as during treatment initiation, the steroid tapering period, or after treatment termination (59). The overall onset of CIC spanned from 0 to 6.3 months (25, 53, 60–63). Prior research studies suggested that CIC onset might vary from different ICI types. Colitis induced by CTLA-4 inhibitors seemed to happen later than that caused by PD-1/PD-L1 inhibitors. The median time to the onset of ipilimumab-induced colitis was approximately 6 to 7 weeks, with an average after two to three infusions (64–68). The range of the median onset from the last injection to diarrhea was 0 to 2 months (67, 69). As for PD-1/PD-L1 inhibitors, symptomatic colitis was less predictable with the onset from nearly 1 week to 2 years (19, 70, 71). Besides, the onset of CIC seemed to be significantly earlier for patients who received

TABLE 1 | Published case reports and case series of immune checkpoint inhibitor-associated colitis.

Author	Year	Patient	Country	Cancer Type	Histologic Type	Genomic alterations (PD-1/PD-L1) (%)	Drug			Previous Therapy	CIC Grade	Time of Onset	Examination	Withdrew the Drug	Time to Withdraw the Drug	Treatment	Outcome		
							PD-1 Inhibitors	PD-L1 Inhibitors	CTLA-4 Inhibitors								CIC	CIC Course (weeks)	Other IrAEs
Kunogi et al. (35)	2021	62/M	Japan	NSCLC	AC	/	Pembrolizumab			Surgery; Chemotherapy	3	16 weeks	Colonoscopy	Yes	16 weeks	PSL; IFX; vedolizumab; TM	Deteriorated after PSL; IFX; vedolizumab; improved after TM	13	
Mourad and De Robles (36)	2021	62/M	Australia	NSCLC	Unknown	/	Pembrolizumab			Chemotherapy	2	9 weeks	CT	Yes	9 weeks	Symptomatic treatment; kept fasted	Improved (3 weeks)–recurrent (4 weeks)–deteriorated (8 weeks)	8	
Naito et al. (37)	2021	70/M	Japan	NSCLC	Unknown	/		Atezzolizumab		Chemotherapy; targeted therapy	3	5 weeks	CT/ endoscopy	Yes	5 weeks	PSL	Resolved	5	Rash
Omotehara et al. (38)	2021	61/F	Japan	NSCLC	AC	/	Pembrolizumab			Surgery	3	26 weeks	CT/ endoscopy	Yes	26 weeks	PSL	Improved	1	Thyroid toxicity
Hirabae et al. (39)	2020	60/M	Japan	NSCLC	AC	5%	Pembrolizumab			Chemotherapy	2	44 weeks	None	Yes	44 weeks	PSL	Resolved	4	
Grover et al. (40)	2020	54/F	USA	NSCLC	Unknown	/	Pembrolizumab			Unknown	2	7 weeks	CT	Yes	7 weeks	Steroid	Unknown	/	
Gallo et al. (41)	2020	57/F	Italy	NSCLC	AC	40%		Atezolizumab		Surgery; chemotherapy	3	2 weeks	Endoscopy	Yes	8 weeks	Probiotics; antidiarrheal drugs; antibiotics; MP	Improved (2 weeks), resolved (12 weeks), recurrence (17 weeks), maintained	52	
Yoshimura et al. (42)	2020	64/F	Japan	NSCLC	AC	100%	Pembrolizumab			Chemotherapy	3	1 week	CT; endoscopy	Yes	1 week	PSL; MP; IFX	Improved	/	
Yoshimura et al. (42)	2020	77/F	Japan	NSCLC	AC	Over 50%	Pembrolizumab			None	3	6 weeks	Endoscopy	Yes	6 weeks	Antidiarrheal drugs; PSL	Improved	0	
Yoshimura et al. (42)	2020	73/M	Japan	NSCLC	AC	Over 85%	Pembrolizumab			Unknown	2	8 weeks	Endoscopy	Yes	8 weeks	Antidiarrheal drugs; probiotics	Improved	/	
Babacan and Tanvetyanon (43)	2019	75/F	Turkey	NSCLC	NEC	/		Durvalumab	Tremelimumab	Chemotherapy	3	8 weeks	CT	Yes	8 weeks	Steroid; adalimumab; antibiotics	Improved (several days), deteriorated (2 months), resolved (a few weeks later)	12	
Babacan and Tanvetyanon (43)	2019	71/F	Turkey	NSCLC	AC	/	Nivolumab			Unknown	3	12 weeks	CT	Yes	68 weeks	Antidiarrheal drugs; antibiotics	Deteriorated (unknown)–improved (unknown)–resolved completely (after 68 weeks)	68	
Babacan and Tanvetyanon (43)	2019	72/M	Turkey	NSCLC	AC	/		Durvalumab		Target therapy	3	32 weeks	CT	Yes	32 weeks	Antibiotics; MP	Promptly improved–deteriorated (2 days)–resolved (1 week)	1 week	
Babacan and Tanvetyanon (43)	2019	69/M	Turkey	NSCLC	AC	/		Durvalumab	Tremelimumab	Chemotherapy	4	12 weeks	CT	Yes	20 weeks	Antibiotics; PS; IFX	Resolved (quickly)–recurrent (4 weeks)–resolved–recurrent (8 weeks)–resolved (16 weeks)	16	Hypophysitis
Babacan and Tanvetyanon (43)	2019	62/F	Turkey	NSCLC	AC	/	Nivolumab			Chemotherapy	2	56 weeks	CT	Yes	56 weeks	Antibiotics; PS	Resolved (4 weeks)–recurrent (taper)–improved (6 weeks)–recurrent (64 weeks)–resolved (88 weeks)	88	
Zhou et al. (44)	2019	56/F	USA	NSCLC	Unknown	/	Pembrolizumab			Chemotherapy	2	9 weeks	CT	Yes	9 weeks	Antibiotics; MP; PS	Improved (3 weeks)	3	
Deligiorgi et al. (45)	2019	72/M	Greece	NSCLC	SC	/	Nivolumab			Chemoradiotherapy	2	15 weeks	PET/CT; endoscopy	Yes	15 weeks	PSL	Resolved	6	Pneumonitis
Ni et al. (46)	2019	73/M	China	NSCLC	AC	/	Tislelizumab			Chemotherapy	3	26 weeks	CT; endoscopy	Yes	26 weeks	MP; antiviral drugs; antibiotics	Improved after MP (3 days); recurrent (4 weeks); resolved (8 weeks)	8	/
Alhatem et al. (47)	2019	78/M	USA	NSCLC	AC	/	Nivolumab			Surgery	2	48 weeks	Endoscopy	Yes	1 year	PS	Resolved	6	Gastritis
Ba'rbara; Cancela-Diez et al. (48)	2019	79/M	Spain	NSCLC	Unknown	/	Nivolumab			Chemoradiotherapy	4	21 weeks	Unknown	Yes	21 weeks	Probiotics; antidiarrheal drugs; MP	Improved (unknown time)–recurrent (8	10	Coronary toxicities

(Continued)

TABLE 1 | Continued

Author	Year	Patient	Country	Cancer Type	Histologic Type	Genomic alterations (PD-1/PD-L1) (%)	Drug			Previous Therapy	CIC Grade	Time of Onset	Examination	Withdrew the Drug	Time to Withdraw the Drug	Treatment	Outcome		
							PD-1 Inhibitors	PD-L1 Inhibitors	CTLA-4 Inhibitors								CIC	CIC Course (weeks)	Other IrAEs
																	weeks later)–deteriorated (10 weeks)		
Dhenin et al. (49)	2019	79/F	Belgium	NSCLC	AC	100%	Pembrolizumab			Surgery; chemotherapy	3	22 weeks	CT	Yes	22 weeks	MP	Resolved	1 day	Rash (grade 2), pericardial effusion, myasthenia gravis
Beck (50)	2019	62/F	USA	Lung cancer	AC	80	Pembrolizumab			None	3	8 weeks	CT/surgery	Yes	20 weeks	Surgery	Improved (1 week)–deteriorated (30 weeks)–improved (33 weeks)	33	/
Ibraheim et al. (51)	2019	78/F	UK	NSCLC	Unknown	/	Nivolumab		Ipilimumab	Unknown	2	12 weeks	X-ray/ endoscopy	Yes	12 weeks	BM	Resolved	5	Hepatitis; pneumonitis
Yasuda et al. (52)	2018	62/M	Japan	NSCLC	AC	/	Nivolumab			Chemotherapy	3	140 weeks	CT; endoscopy	Yes	140 weeks	Antibiotics; PSL	Resolved	3	
Yamauchi et al. (53)	2018	73/M	Japan	NSCLC	Unknown	/	Nivolumab			Unknown	3	15 weeks	Endoscopy	Yes	15 weeks	Probiotics; antidiarrheal drugs; mesalazine	Improved	/	
Yamauchi et al. (53)	2018	78/M	Japan	NSCLC	AC	/	Nivolumab			Unknown	2	7 weeks	Endoscopy	Yes	7 weeks	Probiotics; antidiarrheal drugs; MP	Improved	/	
Yamauchi et al. (53)	2018	49/M	Japan	NSCLC	AC	/	Nivolumab			Unknown	2	3 weeks	Endoscopy	Yes	3 weeks	Probiotics; MP	Improved	/	
Iyoda et al. (54)	2018	62/M	Japan	NSCLC	AC	/	Nivolumab			Chemotherapy	3	38.5 weeks	Endoscopy	Yes	38.5 weeks	DM; MP; IFX; cyclosporine	Improved to grade 1 (d10); deteriorated to grade 3 (d12); did not improve (d33); improved (d63); resolved (d74), recurrent (d88)	12.6	
Callens et al. (55)	2018	63/M	Belgium	NSCLC	AC	/	Nivolumab			Chemotherapy	2	64 weeks	CT; endoscopy	Yes	64 weeks	MP; IFX	Deteriorated	9	/
Santiago; Gonzalez-Vazquez et al. (56)	2017	43/M	Spain	NSCLC	AC	/		Atezolizumab		Chemotherapy	2	12 weeks	Endoscopy	Yes	12 weeks	Unknown	Unknown	/	
Takenaka et al. (57)	2017	45/F	Japan	NSCLC	AC	/	Nivolumab			Surgery; chemotherapy; targeted therapy	2	18 weeks	CT; endoscopy	Yes	18 weeks	PSL; IFX	Resolved (3 weeks)–recurrent (24 weeks)–resolved	26	
Kubo et al. (58)	2017	82/M	Japan	NSCLC	Unknown	/	Nivolumab			Chemotherapy	3	8 weeks	Endoscopy	Yes	14 weeks	Mesalazine	Improved	4	/

CIC, checkpoint inhibitor colitis; NSCLC, non-small cell lung cancer; AC, adenocarcinoma; NEC, neuroendocrine carcinoma; SC, squamous cell carcinoma; CT, computed tomography; PSL, prednisolone; IFX, infliximab; TM, tacrolimus; MP, methylprednisolone; PS, prednisone; BM, beclometasone; DM, dexamethasone.

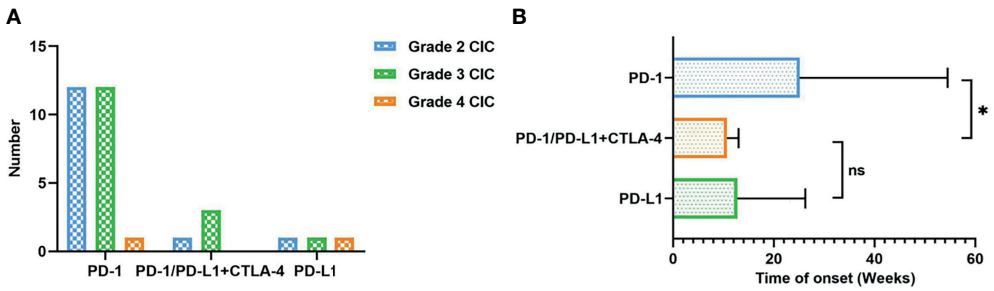

FIGURE 1 | **(A)** The number of CIC patients according to different ICI therapies and severity grade. **(B)** Time of onset (weeks) classified by different ICI therapies. CIC, checkpoint inhibitor colitis; ICIs, immune checkpoint inhibitors. *P < 0.05; ns, no significant.

combined ICIs (70). Our analysis also showed that CIC patients with PD-1/PD-L1 and CTLA-4 therapy had earlier onset than those with PD-1 inhibitors (10 vs. 25 weeks, $P < 0.05$) (**Figure 1B**). Moreover, it could also be affected by other therapies, including previous anticancer treatment, antibiotics, and non-steroidal anti-inflammatory drugs (NSAIDs) (72). The development of CIC was of great difficulty to be predicted before symptom onset (73). Lord et al. (74) suggested that the resolution time of CIC could exceed 130 days, over 10 times than the half-life period of ipilimumab. This implies the long-term influence of immunotherapy on the immune system instead of simply checkpoint blockade at the moment of treatment in the immune cascade. Therefore, we should keep continuous vigilance during the period of ICI utilization.

MECHANISM

The underlying mechanism of ICI-related colitis still remains obscure. However, extensive research studies have suggested that the proposed mechanisms included the hyperactivation of effector T cell (Teff cell), the infiltration of lymphocytes, and

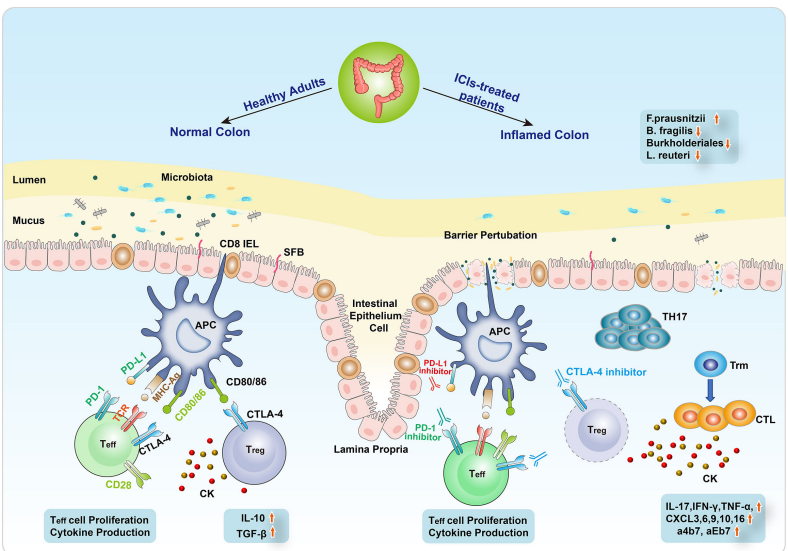

FIGURE 2 | The mechanism of ICI-related colitis. The normal intestinal epithelial barrier is a highly organized mucosal surface that prevents microbiota from entering into the lamina propria. The epithelium is composed of a single layer of intestinal epithelial cells (IECs) covered by a mucus layer. Segmented filamentous bacteria (SFB) seldom breach the barrier of mucus and contact with the IECs. Immune checkpoint inhibitors (ICIs) modulate the microbiota–intestinal barrier equilibrium by inducing IEC apoptosis, resulting in barrier perturbation. The alterations of intestinal flora include the decrease of *Bacteroides fragilis*, Burkholderiales, and *Lactobacillus reuteri* and the increase of *Faecalibacterium prausnitzii*. Barrier perturbation is further aggravated possibly due to pathogenic Th17 cells, leading to severe intestinal toxicity resembling an early sign of colitis. Besides, the differentiation from $CD8^+$ tissue-resident memory T (Trm) cells to cytotoxic T lymphocytes (CTLs) induced cytokines (IL-17, IFN-γ, TNF-α) to participate in the CIC emergence. In addition, CXCR3, 6, 9/10, 16, and a4b7/aEb7 receptors are also involved in the development of CIC.

the increase of circulating memory T cells, thus causing proinflammatory status and the emergence of autoimmune-type presentation (25, 75–77). Besides, the gut microbiome also plays a critical role in the regulation of intestinal mucosal homeostasis (**Figure 2**) (78, 79).

Mechanism of irAEs

To target and eliminate tumor cells, T cells need two stimulating signals to be activated (80–82). One is the direct antigen stimulation mediated by the T-cell receptor (TCR) and major histocompatibility complex (MHC) class II molecule on the APCs. The other depends on the co-stimulation between CD28 receptor on T cells and CD80/86 (B7) on APCs. T-cell activation results in its proliferation, cytokine production, and CTLA4 and PD1 expression (83). The role of CTLA-4, which is constitutively located on the surface of FOXP3 regulatory $CD4^+$ T cells, is to terminate this co-stimulation. As a co-inhibitory ligand, CTLA-4 harbors higher affinity than CD28, contributing to competitively bind CD80/86, thus blunting the immune response. In addition to the CTLA-4-mediated inhibitory interaction between T cells and APCs, immunosuppressive cytokines produced by regulatory T cells (Treg cells) include IL-10 and TGF-β and also inhibit T-cell activation and proliferation (84, 85). Conversely, PD-1 with PD-L1 does not restrain co-stimulation but suppresses the TCR downstream signaling, which results in the reduction of transcription factors and cytokines like TBET and GATA3, as well as the enhanced inhibitory effect of Treg cells (86, 87). Both CTLA and PD-1/PD-L1 inhibitors could strengthen the activation and proliferation of Teff cells, abrogate Treg cell function, induce inflammatory cytokines, probably boost humoral autoimmunity (88), and cause a range of autoimmunity-related adverse effects in multiple organs (**Figure 2**).

Mechanism of CIC

Several animal models with the absence of immune checkpoints have been utilized to simulate the immunological effects of CIC. Mice knocked out CTLA-4 presented diffuse immune cells infiltration in various organs and fatal colitis caused by increased T-cell activity (85, 89, 90). The PD-1 axis is of great importance in the development of innate lymphoid cells (ILCs), which have been regarded as critical effective cells at gastrointestinal mucosal surfaces (91–93). The severity of CIC was correlated to the growing mucosal number of group 3 ILCs (ILC3s) (94). Moreover, a high-level infiltration of $CD4^+$ T cells and $CD8^+$ T cells was reported in patients with severe colitis following immunotherapy, of which the former was more prevalent in those who underwent anti-CTLA-4 therapy and the latter usually occurred in anti-PD-1-induced colitis (95–97). Recently, a comprehensive single-cell analysis of CIC illustrated the differentiation from $CD8^+$ tissue-resident memory T (Trm) cells to cytotoxic T lymphocytes (CTLs) (97). It was hypothesized that the abundant $CD8^+$ Trm cells in the normal colon exerted a vital effect on CIC, and their activation prompted the subsequent assembly of $CD4^+$ and $CD8^+$ T cells. In addition, cytokines may participate in the emergence of CIC. The preclinical model of CIC has observed the rise of IL-17 (11, 98). The inducible gene and expression of IFN-γ and TNF-α, which induced cell death, showed a substantial increase in ICI-related colitis patients (97, 99). TNF-like cytokine 1A (TL1A) and its receptor DR3 were also upregulated in ICI-mediated colitis (100). Besides, CXCR3 and CXCR6 chemokine receptor (CXCR9/10 and CXCR16, respectively) genes presented high-level expression on colitis-related T-cell population, upregulating T-cell activity (101). Besides, three genes (*ITGB7*, *ITGA4*, and *ITGAE*), encoding a4b7 and aEb7 integrin receptors, were expressed in colitis-associated T-cell clusters. This might lead to lymphocyte retention in the intestinal mucosa (**Figure 2**) (102).

Gut Microbiome and CIC

Immunotherapy could modulate microbiota–gut barrier equilibrium by intraepithelial lymphocyte (IEL)-mediated apoptosis of intestinal epithelial cells (IECs), leading to barrier perturbation (103). The role of dysbiosis has been proposed to initiate irAEs, in which the product exposure derived by the microbiome could induce innate immune responses, probably activating self-reactive immune cells (104). Several species of gut bacteria have been indicated to potentiate Treg cell induction, which maintained intestinal tolerance (105). $CD4^+$ T helper cells induced by IL-17 (Th17), located in the lamina propria to focus specifically on intestinal-resident segmented filamentous bacteria (SFB), could deteriorate systemic autoimmune diseases under some circumstances (**Figure 2**) (106, 107).

Currently, accumulating evidence has demonstrated that gut microbiome features may be linked with the development of CIC and tumor response to ICI therapy (**Figure 2**) (77, 108–111). Chaput et al. (112) conducted a prospective study to evaluate the intestinal microbiome characteristics at baseline and the time of gastrointestinal toxicity in 26 patients who received ipilimumab. The results showed that ipilimumab could not influence the composition of the microbiome. Nonetheless, decreased microbiota diversity was found in ICI-related colitis, especially some genera like *Faecalibacterium prausnitzii* (*F. prausnitzii*) and *Bacteroides fragilis* (*B. fragilis*) in the Firmicutes phylum.

Enrichment of *F. prausnitzii* might be associated with the occurrence of colitis (112). As an obligate anaerobe, *F. prausnitzii* has the normal function of keeping colonic mucosa integrity (111). The increase of *F. prausnitzii* was linked to T-cell proliferation in the gut mucosa and facilitated the recruitment of Treg cells and a4b7 T cells. In addition, it could enhance CTL concentration in the tumor microenvironment, prolonging the OS and PFS (113). The strong and beneficial response would be presented in patients with the abundance of *F. prausnitzii* receiving anti-CTLA-4 and/or anti-PD-1 inhibitors, possibly with the cost of immunotherapy-induced colitis.

Fragilis increase is considered to be the protective factor of CIC (81, 108). It acts to play an anti-inflammatory role in the gastrointestinal tract (114). The CTLA-4 pathway was involved in the immunoregulatory process, in which *B. fragilis* produced polysaccharide A to upregulate the level of IL-10, thus alleviating inflammation (115). Moreover, the anti-CTLA-4 blockade has been verified to favor *B. fragilis* outgrowth in the colon (116). Although *B. fragilis* frequency keeps stable after anti-CTLA-4 therapy (81), the elevated number of *B. fragilis* could further decrease the size of tumor in patients treated with ipilimumab.

Besides, anti-CTLA-4 antibodies could also promote dysbiosis by reducing Burkholderiales and increasing Clostridiales bacteria presentation (103, 116, 117). The combination of *Burkholderia cepacia* (*B. cepacia*) and *B. fragilis* or the administration of *Bacteroides thetaiotaomicron* (*B. thetaiotaomicron*) allowed germ-free (GF) mice to decrease the gut toxicity and elicit anticancer immune response presented in normal microbiota mice (116, 118). This might be attributed to the accumulation and maturation of plasmacytoid DCs, which produced IL-12 subsequently to stimulate $ICOS^+$ Treg cells and thus promote antitumor immunity, induced by these bacteria in the gastrointestinal lamina propria. Furthermore, the response of anti-CTLA-4 inhibitors required microbiota-dependent T-cell activation. The therapeutic efficacy of the anti-CTLA-4 inhibitor could be restored by adoptively transferring *B. fragilis*-specific T cells into GF mice (117). Similar experiments conducted with PD-L1 inhibitors showed that *Bifidobacterium* species could mediate antitumor efficacy (119). This bacterium could attenuate bowel inflammation mediated by Treg cells without detriments to the antitumor response (120). Wang et al. (94) also established ICI-related colitis models to find the change of gut microbiota. The microbiota profiling showed that *Lactobacillus* presented lower abundance in the ICI-treated mice stool than in the control group. Similarly, a trinitrobenzene sulfonic acid (TNBS)-built mouse model showed that intestinal inflammation could be suppressed by specific *Lactobacillus reuteri* strains (121). In addition, *L. reuteri* could augment DC function to improve antitumor response after blocking PD-L1.

Therefore, the species and relative abundance of gut microbiota could influence the development of CIC. Some specific microbial species might orchestrate the inflammation initiation, while other subsets might help perpetuate CIC. More efforts should be dedicated to further learn the complex symbiosis between bacteria and ICI-induced colitis, with the ultimate aim to manipulate the microbiota for the balance of tumor response and irAEs.

RISK FACTORS

The current risk factors for CIC cover past medical history and tumor type, therapy management, and molecular markers. Specifically, these included medication history, preexisting autoimmune diseases, tumor type, combined ICI therapy, and inflammatory cell levels.

Past Medical History and Tumor Type

The utilization of NSAIDs has been regarded to increase the risk of CIC (77). Patients with CIC (31%) were more common to use NSAIDs than those without CIC (5%) (P = 0.003), which is similar with IBD, and there is a correlation between NSAIDs and increased IBD flare risk (122). Conversely, vitamin D use was found to reduce the risk for ICI-related colitis (123, 124). In addition, the risk of CIC of patients who had previous irAEs is controversial. Some studies suggested that patients who had irAEs with the first ICI initiation would experience a higher risk of irAEs following alternate ICI therapy (125, 126). However, other studies showed that patients did not develop recurrent severe diarrhea or CIC when they changed to subsequent PD-1/PD-L1 inhibitor therapy after ipilimumab (127, 128). Moreover, the occurrence of CIC might relate to malignancy types. Melanoma seemed to have a higher risk of CIC compared with renal carcinoma and NSCLC (33). However, the reason behind the discrepancy between the rates from these two cancer types remains obscure.

Autoimmune disorders, including IBD, were not always considered in ICI clinical trial criterion, since the disease might worsen by non-specific T-cell activation of ICIs. Nearly 27% of patients have underlying disease exacerbation after ICI therapy, which means increased or recurrent prior manifestations (129). Few studies demonstrated that patients with preexisting autoimmune diseases would experience a higher incidence of CIC (129, 130). The occurrence of CIC in underlying IBD patients who received ipilimumab was reported at 30%. Besides, Menzies et al. (126) reported that five cases with prior IBD history who received PD-1 blockade had great tolerance without disease flare. Therefore, PD-1 inhibitors are more recommended for IBD patients than ipilimumab. Currently, a prospective clinical protocol is recruiting IBD patients who have ICI indications (AIM-NIVO, NCT03816345). This would bring critical instruction for ICI therapy of IBD patients in evaluating risk and developing decision-making.

Therapy Management

The combination of ICI therapy is reported to present a higher occurrence of ICI-related colitis. A recent meta-analysis included 27 prospective studies reporting the risk of CIC in patients with lung cancer who received ICI therapy (31, 131). The results showed that the combination of anti-CTLA-4 and anti-PD-1 therapy had a higher risk of all grades of CIC than anti-PD-1 monotherapy (RR: 1.61, 95% CI: 1.14–2.29). The combined ICIs, such as ipilimumab and pembrolizumab/nivolumab (132) and durvalumab and tremelimumab (133, 134), obtained above 10% occurrence of colitis (79, 135). Moreover, the sequential administration of ipilimumab before nivolumab showed higher rates of grade 3 colitis than nivolumab before ipilimumab (16% vs. 10%) (136). No particular toxicities were found in the combination therapy (137). The same class of ICI therapy had a similar incidence of all grades of CIC. However, the combination of chemotherapy/radiotherapy and immunotherapy could not increase the incidence of colitis but could promote tumor response rates, PFS, and OS in NSCLC (138, 139).

Molecular Markers

Several potential molecular markers, such as increased IL-17, neutrophil, eosinophil, and WBC levels, have merged to predict the development of ICI-mediated colitis (31, 140–142). Decreased baseline granulocyte colony-stimulating factor (GCSF) level was found in CIC patients (143, 144). Moreover, the association between some cell surface markers and GI-irAEs was also investigated. Shahabi et al. (145) explored the gene expression profiling of whole blood in 162 patients who were treated with ipilimumab. They found that pretreatment elevated

the baseline levels of genes involved in cell cycle (*WDR1*, *FP36L2*, *PCGF1*, *BAT1*, *BANF1*, and *SPTAN1*), vesicle trafficking-correlated genes (*VAMP3*, *SNAP23*, and *PICALM*), and immune-related genes (*RAC2*, *IL-32*, *IL2RG*, *CD37*, *CD4*, and *CD3E*), and these were associated with developing GI-irAEs. After 3 weeks of treatment, the biomarker which distinguished GI-irAEs and non-GI-irAEs was CD177, a specific neutrophil surface biomarker that exerts effects in activating neutrophils and recruiting inflammatory cells. However, it could not be utilized alone to predict irAE occurrence because of large individual variability and its low sensitivity. Besides, CEA-associated cell adhesion molecule (CEACAM), as the essential adherent mediator in the migration of neutrophils, also showed a significant increase in the ICI-related GI toxicity group. Therefore, the changes in CEACAM and CD177 expression might become more sensitive markers than the absolute neutrophil level in the peripheral blood, and these activation steps happen in the early neutrophil recruitment.

MANIFESTATIONS

Clinical Manifestations

The majority of clinical trials discriminate diarrhea from colitis, although they overlap in the most practical cases. Diarrhea is evaluated by stool increase per day. Colitis is evaluated according to clinical symptoms (blood or mucus in stool, abdominal pain) or the diagnostic findings on the imaging and endoscopic observations (146). The grading of diarrhea/colitis was according to the Common Terminology Criteria for Adverse Events v5.0 (147).

Similar to IBD, diarrhea is the most common clinical symptom of CIC (**Figure 3A**). It is also characterized by abdominal pain, hematochezia, fever, vomiting, nausea, and loss of appetite (77). Intestinal perforation and weight loss are less common (148). In our analysis, almost all patients developed diarrhea, ranging from 4 to 30 times. Additionally, other common clinical manifestations also include abdominal pain (25%), loss of appetite (18.75%), and hematochezia (12.5%). Obstipation, tachycardia, and malnutrition were also reported in our patients with CIC.

Imaging Manifestations

CT and/or MRI is the major radiology examination for CIC. However, CT presents a relatively low negative predictive value, with 53%–85% sensitivity and 75%–78% specificity (22, 149, 150). Colonic mucosal hyperenhancement is the most common CT sign of CIC, followed by mesenteric vessel engorgement, bowel wall thickening, fluid-filled distended colon, pericolic fat stranding, and bowel wall edema (151). In our analysis, the most common features of CT in our analysis were bowel wall thickening (10/32) (**Figure 3B**). Universally, the patterns of CIC could be divided into pancolitis, segmental colitis associated with diverticulosis (SCAD) enterocolitis, and enteritis (152–154). It is reported that the different CT patterns of CIC are related to corresponding clinical features. For example, patients with diffuse colitis usually have watery diarrhea, while patients with SCAD pattern have mixed watery and bloody diarrhea and cramping pain (154). When severe colitis was complicated with bowel perforation and toxic megacolon, CT would be an effective tool for diagnosis (155). The sign of non-dependent extraluminal air close to the intestine might be conducive to bowel perforation. PET-CT was also applied in CIC patients with increased 2-deoxy-2-(18F) fluoro-D-glucose (FDG) uptake (50, 150). One of our cases showed colon inflammatory activity when PET/CT was performed (45).

Laboratory Features

The serological findings of patients with CIC are not specific. Some literature has reported that markers such as C-reactive

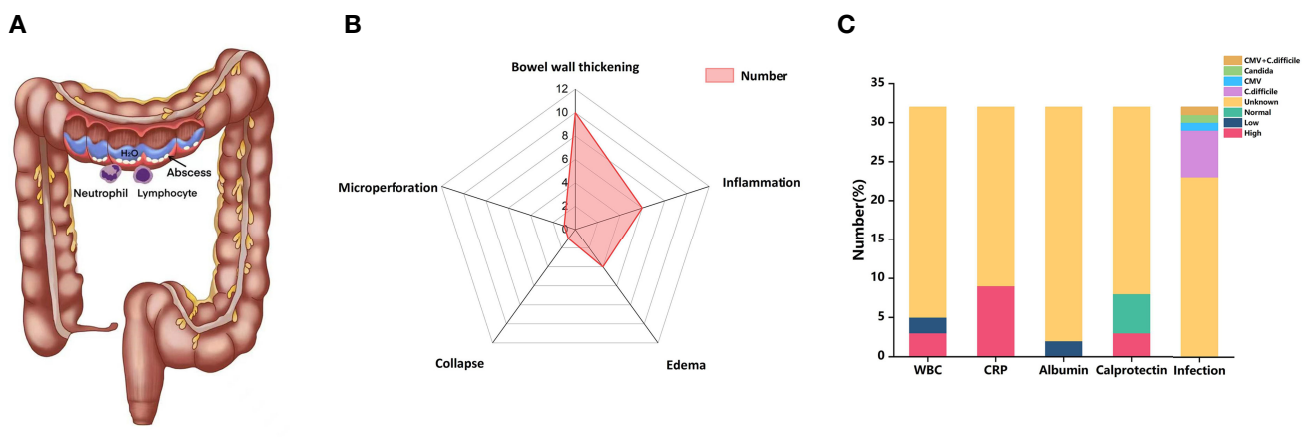

FIGURE 3 | **(A)** CIC physically presented more similarly with colitis than IBD, involving lymphocyte and neutrophil infiltration. **(B)** Radar chart of CT features of CIC. **(C)** Bar chart of laboratory features of CIC. CIC, checkpoint inhibitor colitis; ICIs, immune checkpoint inhibitors; WBC, while blood cells; CRP, C-reactive protein; CMV, cytomegalovirus; *C. difficile, Clostridium difficile*.

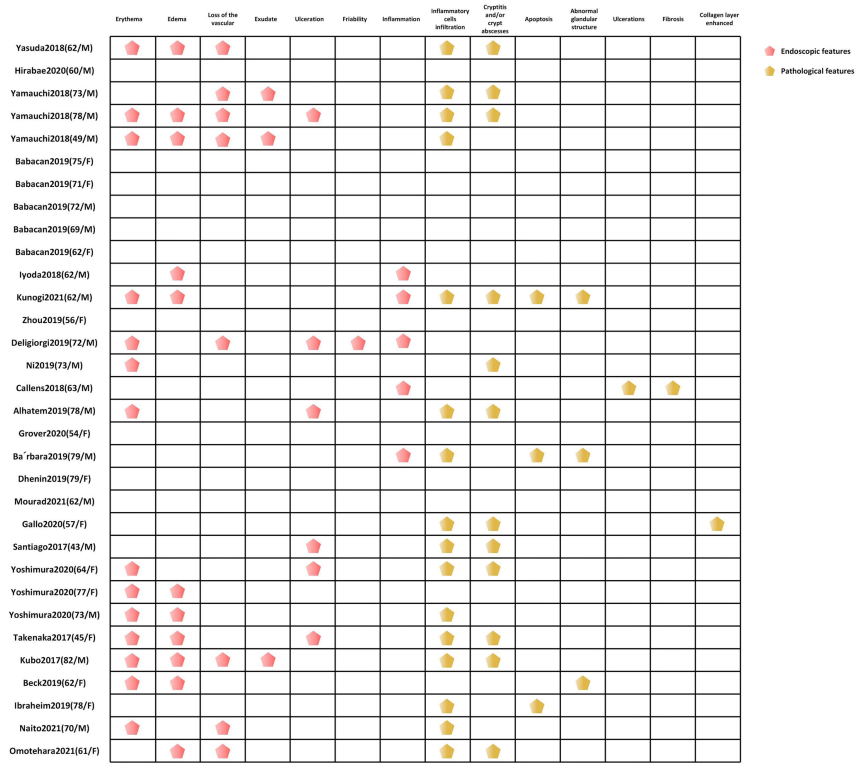

FIGURE 4 | The endoscopic and pathological features of CIC. CIC, checkpoint inhibitor colitis.

protein (CRP) or low serum albumin level counts increased in the serum of IMC patients, but this may be influenced by systemic inflammation. In a retrospective study by Abolhassani et al., 88 patients with advanced melanoma were diagnosed irAEs after receiving ICIs, and 42% of them had a high CRP level (156). In our analysis, 9 of 32 patients had an increased level of CRP, and two patients showed low albumin levels (**Figure 3C**). Other serum findings may also be related to CIC, such as increased IL-17 (157), eosinophil count (158), and neutrophil–lymphocyte ratio. Some patients with CIC may show anemia on serological findings because of chronic bleeding in the digestive tract (77). In our analysis, three patients showed a decreased level of WBC (**Figure 3C**). Besides, elevations were found in serum leucine-rich α2-glycoprotein (LRG) and creatinine (42). LRG was reported to distinguish different colitis forms like drug-related and *Cytomegalovirus* (CMV) colitis (42).

Fecal calprotectin is often elevated in the stool specimens of patients developing IMC, which is a predictor of disease activity and prognosis. We found two patients with CIC had elevated fecal calprotectin (**Figure 3C**). Zou et al. (159) retrospectively analyzed the fecal calprotectin of patients with CIC and found that it was increased at the onset of IMC while decreased after treatment. In terms of infectious pathogens, *Clostridium difficile* (*C. difficile*) was the most common pathogen. CMV and *Candida* were also reported in our included patients (**Figure 3C**).

Endoscopic Features

Early endoscopy examination is encouraged for diagnosis and prognostic assessment if CIC is suspected (22). Left-sided colitis (31%–43%) is the most commonly reported in CIC cases, followed with pancolitis (involvement of ≥3 segments) (23%–40%) and ileitis (11%–14%) (160, 161). Endoscopic inflammatory findings usually present with mucosal ulceration and non-ulcerative inflammation with similar incidence. Non-ulcerative inflammation is characterized by erythema, exudate, erosion, friability, loss of vascular pattern, and edematous or granular mucosa (58, 72, 79). Among these, erythema (14/32) and edema (11/32) were the most common endoscopic features in our CIC patients (**Figure 4**). Most inflammation changes are predominantly diffuse instead of patchy (73). However, half of the diarrhea patients were observed to have patchy distribution endoscopically (77), which resembles the presentation of IBD (162), especially ulcerative colitis (UC) (53, 58). Fewer individuals with CIC (35%) were found to have segmental performance, as what often appeared in Crohn's disease (77). There is no particular grading standard for the endoscopic manifestations in CIC. Nonetheless, the Mayo score, the van der Heide score for UC, or Simple Endoscopic Score (SES) for Crohn's disease could be utilized (61, 163, 164).

Several studies illustrated that clinical symptoms were not significantly associated with endoscopic manifestations (22, 165). We also conducted a correlation analysis between CIC grade and

TABLE 2 | Correlation of the grade of CIC with endoscopic features and histological features.

	Total (*N* = 32)	Grade 2 (*N* = 14)	Grades 3–4 (*N* = 18)	*P*-value
Endoscopic features				0.581
None	12 (37.50%)	6 (42.86%)	6 (33.33%)	
Inflammation	20 (62.50%)	8 (57.14%)	12 (66.67%)	
Histological features				0.821
None	13 (40.60%)	6 (42.86%)	7 (38.89%)	
Inflammation	19 (59.40%)	8 (57.14%)	11 (61.11%)	

Data were collected from studies in ***Table 1****.*
CIC, checkpoint inhibitor colitis.

endoscopic ($P = 0.581$)/histological features ($P = 0.821$), with no significant difference found (**Table 2**). However, the endoscopic findings, such as ulceration and pancolitis, are the indicative factors for steroid-refractory colitis (61). The findings in the endoscope could be categorized as low risk and high risk for steroid response. High-risk presentations were defined as either ulceration larger than 1 cm and/or deeper than 2 mm or extensive colitis from the proximity to the splenic flexure of the colon (166). High-risk patients need frequent utilization of biologics (vedolizumab or infliximab). Besides, they were significantly correlated with longer hospital stays, more disease recurrence, and more requirements for the repeat endoscopy (167). Furthermore, CIC patients who received colonoscopy within 1 week of onset would experience a significantly shorter period of symptoms and steroid therapy (166).

Pathological Features

The pathological features of CIC present from focal active colon injury with patchy crypt abscess to diffuse mucous inflammation (95). We found that inflammatory cell infiltration (50%), cryptitis, and/or crypt abscesses (33.3%) were the most frequently reported pathological features (**Figure 4**). These presentations might precede the onset of clinical symptoms. Coutzac et al. (95) included asymptomatic patients who received colonoscopy 1 to 2 weeks after treatment with ipilimumab and found that colon inflammation existed before the symptom development, although most of the symptoms of the patients occurred 3 weeks later. When they ultimately presented with symptomatic diarrhea or colitis, the histological observations exhibited more severe lamina propria infiltration. CIC pathological patterns could be summarized as follows: active colitis, chronic active colitis, microscopic (collagenous and lymphocytic) colitis, ischemic colitis, increased apoptosis, and non-specific inflammatory reactive changes (168–170). Patterns overlapping might exist in the microscopic presentation of CIC.

Active colitis is the most frequent pattern of histopathologic finding in ICI-mediated colitis. The typical manifestations of active colitis are lamina propria neutrophilic infiltrate, crypt abscesses, and neutrophilic cryptitis, with or without crypt dropout/atrophy (171, 172). The atrophic crypt epithelium is attenuated, which admixes apoptotic debris and inflammatory cell (173), resembling mycophenolate-caused colitis. Granulomas accompanied with crypt rupture have also been found (32, 174). Intraepithelial lymphocytes and increased apoptosis might or might not appear.

Microscopic colitis means lymphocytic and collagenous colitis (95), which has been found in 12% of CIC cases (66, 79, 175). Usually, lymphocytic colitis has the histological characteristics of a normal crypt structure, with increased lymphoplasmacytic inflammation in the lamina propria and intraepithelial lymphocyte infiltration, but no significant acute inflammatory presentation (176, 177). Collagenous colitis is an infrequent manifestation of CIC, which has increased intraepithelial lymphocytes and thickened subepithelial collagen (66). However, the atypical feature of microscopic colitis has also been reported, like crypt abscesses and neutrophilic cryptitis of active IBD (178). Gallo et al. (41) reported a patient with lung cancer who received atezolizumab presented collagenous colitis along with acute neutrophilic inflammation. Besides, Choi et al. (179) showed that patients with microscopic colitis induced by ICIs would have higher hospitalization rates and more aggressive course of disease and need more treatments like steroids and/or immunosuppressants than those without exposure to ICIs.

Chronic active colitis, one of the pathological patterns of IBD, has also been reported in ICI-mediated colon inflammation, particularly in patients with recurrent ICI therapy. This type is characterized by increased basal plasmacytosis and lymphoplasmacytic infiltration in the lamina propria, along with acute inflammation presentation of crypt abscess/cryptitis (172). The chronic manifestations, Paneth cell or pseudo-pyloric metaplasia and crypt structural distortion, constantly appear (63). The chronic feature could appear simultaneously with active colitis or develop gradually based on it. Yamauchi et al. (53) reported that three cases with colitis induced by nivolumab exhibited similar endoscopic and histopathologic features with ulcerative colitis at the initiation of diagnosis, and therapy for ulcerative colitis was applied successfully on these patients. Besides, one study (172) found that nearly half of patients who appeared with active colitis initially developed chronic features mentioned above. Therefore, ICI-related colitis has been considered as a specific IBD form (77). Approximately 60% of patients could have chronic inflammatory presence in the pathological section of ICI-induced colonic injury (22, 32, 180).

Increased crypt epithelial apoptosis always occurs in concurrence with other CIC patterns, including lymphocytic colitis, active colitis, and chronic active colitis. Isolated increased apoptosis with the absence of active and/or chronic inflammatory manifestation, imitating graft-versus-host disease, is less common (169). Ischemic colitis is also a rare pattern of

CIC, presenting with atrophic crypts, reactive epithelial changes, and fibrosis in the lamina propria (32). In addition, non-specific inflammatory reactive changes, including lymphoplasmacytic infiltrate increase in the lamina propria along with epithelial attenuation and reactive changes and depleted mucin, are also presented in the colon injury pattern.

DIAGNOSIS

New emerging abdominal symptoms after immunotherapy for NSCLC, especially acute diarrhea, need consideration of CIC (181). However, few patients only present with abdominal pain instead of diarrhea (50). Typically, the diagnosis of CIC is made by exclusion of infection, IBD, and tumor metastasis. Fecal etiology helps to rule out intestinal microbial infection. Endoscopy with biopsy, contributing to evaluate inflammatory severity, has been considered as the gold standard criteria for the diagnosis of ICI-related colitis. In addition, imaging examination like CT also assists in diagnosing serious complications such as toxic megacolon and intestinal perforation.

The most common differential diagnoses include infectious intestinal diseases and IBD. The infectious pathogens, such as CMV, *Salmonella*, *C. difficile*, and parasites, should be examined foremost for the diagnosis of CIC. It is worthy to notice that CIC could develop with bowel infection at the same time. One of our cases developed CIC that coexisted with CMV and *Salmonella* (46). Therefore, in addition to etiology detection, endoscopic biopsy is essential for accurate diagnosis. Moreover, tumor immunity could be triggered by blocking the pathways of PD-1/PD-L1/CTLA-4, while the immunity to infection could be inhibited. Therefore, several cases were infected with *C. difficile* after CIC (43). Under this condition, CIC would get worse, and it is necessary to add antibiotics in time. Besides, the pathogenesis and endoscopic manifestations of CIC resemble those of IBD (162, 166). However, there still exist differences in pathological appearance between CIC and IBD. Histologically, CIC is characterized with active colitis, such as neutrophilic infiltration, crypt microabscesses, and prominent crypt epithelial cell apoptosis, while IBD usually shows chronic inflammation signs, including basal lymphocytosis, crypt architectural irregularity, and Paneth cell metaplasia (173). In addition, compared with UC, CIC showed less basal plasmacytosis (14% vs. 92%), less crypt distortion (23% vs. 75%), and more apoptotic bodies ((17.6 ± 15.3 vs. 8.2 ± 4.2) (182). It is noteworthy that the clinical presentations could distinguish these different clinical entities when the histologic findings overlap, including the onset of symptoms soon after ICI initiation and other concurrent irAEs (25). Moreover, recent research illustrated distinct immunological features of colonoscopy from CIC and IBD patients, with predominantly $CD4^+$ T cells and Treg cells in the anti-CTLA-4-induced colitis and IBD patients, respectively (95).

In summary, the precise diagnosis of CIC requires multidisciplinary discussion and persistent monitoring, which also plays a critical role in grade assessment.

MANAGEMENT

At present, minimal prospective trials have been designed to evaluate the optimal therapeutic modality for CIC. Consequently, current management guidelines are on the strength of expert opinion and retrospective studies, recommending systemic corticosteroids as the first-line therapy uniformly (19, 71, 183). The treatment is ideally initiated not exceeding 5 days of symptom appearance (23). The specific management is mainly based on severity degree. Pretreatment examinations include infectious etiology (stool parasitism and calprotectin), blood testing (C-reactive protein, celiac disease serology, comprehensive metabolic panel, complete blood count, etc.), hepatitis serology, and tuberculosis testing, which are beneficial for monitoring treatment response and preparing for biologics if corticosteroids do not work (184).

Steroid

Systemic high-dose glucocorticoids are typically effective for CIC cases, equaled to prednisone of 1–2 mg/kg/day, obtaining nearly 90% efficacy (185).

Steroid Therapy Classified by Grade

For grade 1 diarrhea/colitis, supportive treatments, such as anti-motility agents (atropine/diphenoxylate, loperamide), adequate hydration, and dietary adjustments (low-fiber, bland diet), are recommended (186). Budesonide has been proposed to reduce symptoms in patients with ICI-mediated colitis (19). ICIs could continue to be utilized without delay or interruption in the management of colitis.

For grade 2 diarrhea/colitis, ruling out the infectious factors, systemic corticosteroids (prednisone/intravenous methyl-prednisolone of 1–2 mg/kg/day) should be initiated until symptom improves to grade 1 or less. After that, the taper of steroids is recommended for at least 4 to 6 weeks (186). Endoscopy and abdominal CT should be considered strongly. In terms of ICIs, anti-CTLA-4 agents should be discontinued permanently, while anti-PD-L1 agents could be continuously held. Besides, PD-L1 inhibitors also could be resumed as monotherapy when symptoms have improved/resolved, or prednisone is reduced to 10 mg/day or less (19, 183).

For grade 3 to 4 diarrhea/colitis, the discontinuation of ICIs should be immediate and permanent (19, 71, 183, 187). Patients are usually admitted to the hospital for urgent evaluation and continuous monitoring. Intravenous methylprednisolone of 1–2 mg/kg is the prompted initial therapy (24, 79). It is also necessary to keep electrolyte balance and implement aggressive fluid resuscitation for grade 3–4 CIC patients. The corticosteroid response for grade 2–4 toxicity should be assessed early after 2–3 days. Non-responders are recommended for escalation to a biological agent.

We also investigated the therapeutic features stratified by CIC grade (**Table 3**) and depicted the steroid duration and taper (**Figure 5**). We unified different steroid types to methylprednisolone (MP) equivalents and further classified them into high-dose, intermediate-dose, and low-dose groups, based on the initial administered dose. Since we observed that

TABLE 3 | The characteristics related to the management of CIC stratified by grade of CIC.

Grade of CIC Mean ± SD/*N* (%)	Total	Grade 2	Grades 3–4	*P*-value
N	32	14	18	
Steroid initial dose (mg/day)	63.00 ± 37.45	66.20 ± 36.17	61.00 ± 40.55	0.819
Steroid initial dose groups (mg/day)				0.071
Low dose <60	9 (69.23%)	2 (40.00%)	7 (87.50%)	
60 ≤ intermediate dose <300	4 (30.77%)	3 (60.00%)	1 (12.50%)	
Steroid initial dose (mg/kg/day)	1.37 ± 0.58	1.57 ± 0.57	1.23 ± 0.60	0.394
Steroid initial dose groups (mg/kg/day)				0.287
Low dose <1	5 (50.00%)	1 (25.00%)	4 (66.67%)	
1 ≤ intermediate dose <2	1 (10.00%)	1 (25.00%)	0 (0.00%)	
High dose ≥2	4 (40.00%)	2 (50.00%)	2 (33.33%)	
Steroid taper time (weeks)	5.64 ± 5.77	10.50 ± 9.47	3.70 ± 1.89	**0.041**
Antibiotics				**0.025**
No	23 (71.88%)	14 (87.50%)	7 (50.00%)	
Yes	9 (28.12%)	2 (12.50%)	7 (50.00%)	
Biological agents				0.36
No	25 (78.12%)	12 (85.71%)	13 (72.22%)	
Yes	7 (21.88%)	2 (14.29%)	5 (27.78%)	
OS				0.244
Alive	27 (84.38%)	13 (92.86%)	14 (77.78%)	
Dead	5 (15.62%)	1 (7.14%)	4 (22.22%)	
Survival weeks	75.26 ± 90.53	60.30 ± 71.06	86.77 ± 104.44	0.5
CIC course (weeks)	15.74 ± 22.22	17.11 ± 27.49	14.97 ± 19.62	0.823
CIC outcome				0.232
Resolved/improved	16 (53.33%)	8 (66.67%)	8 (44.44%)	
Deteriorated/recurrent	14 (46.67%)	4 (33.33%)	10 (55.56%)	
Tumor response				0.461
Complete response	1 (3.12%)	1 (6.25%)	0 (0.00%)	
Partial response	8 (25.00%)	3 (18.75%)	5 (35.71%)	
Tumor progressed	3 (9.38%)	2 (12.50%)	1 (7.14%)	
Stable	18 (56.25%)	10 (62.50%)	8 (57.14%)	
Recurrence times				0.834
0	24 (75.00%)	11 (78.57%)	13 (72.22%)	
1	6 (18.75%)	2 (14.29%)	4 (22.22%)	
2	2 (6.25%)	1 (7.14%)	1 (5.56%)	
Rechallenge times				0.49
0	28 (87.50%)	12 (85.71%)	16 (88.89%)	
1	3 (9.38%)	2 (14.29%)	1 (5.56%)	
2	1 (3.12%)	0 (0.00%)	1 (5.56%)	

Data were collected from studies in ***Table 1****.*
CIC, checkpoint inhibitor colitis; OS, overall survival.
Bold values: P < 0.05 which means significant differences between groups.

not all cases pointed out the weight of the patients, two distinct steroid dose specifications (mg/kg/day and mg/day) were established to describe the utilization of steroid. Our data showed that the median steroid initial dose was nearly 60 mg/day or 1 mg/kg/day (MP), with no significant difference found in grade 2 and 3–4 CIC patients (**Table 3**). In terms of dose group, low-dose steroid was more frequently used in grade 3–4 CIC patients, while high-dose steroid was more common in grade 2 CIC patients, although no significant discrepancy existed (**Table 3**). Extensive sample size studies with more specific steroid data are required to illustrate steroid use.

The Quantifying, Taper, and Maintenance of Steroid

Limited data underscore the quantifying of steroids in treating ICI-related diarrhea/colitis. A retrospective study (188) included 90 patients with ICI-induced gastroenterocolitis and divided them into three groups based on steroid dose: "limited or none," prednisone equivalents <7.5 mg/day on average for over 2 months; "moderate," prednisone equivalents >7.5 mg/day on average for over 2 months; and "high," prednisone equivalents ≥1 mg/kg/day for over 1 week (189, 190). They found that the high-dose steroid group had decreased PFS (HR = 2.54, 95% CI: 1.11–5.80, $P = 0.03$), while OS was not influenced by systemic steroid treatment for gastroenterocolitis mediated by ICIs, after the adjustment of covariates. Another study focused on the maintenance of steroid management (191). The results showed that grade 3 CIC has a median average steroid duration of 58 days. Overall grade steroid duration was 94 days, twice than grade 3 or 4 CIC steroid duration. This placed quite a few patients at risk of iatrogenic complications such as mood change and infection. Therefore, continuous supportive care during the utilization of steroid should be reinforced as well (192). The recommended taper time was 4 to 8 weeks (193, 194). The cases we included had a median steroid taper duration at nearly 5 weeks, with grade 2 and grade 3–4 CIC at about 10 and 5 weeks, respectively ($P = 0.041$) (**Table 3**). In 20 CIC patients with exact

TABLE 4 | Baseline characteristics of the NSCLC cases with CIC we included.

CIC outcome Mean ± SD/*N* (%)	Total	Improved/Resolved	Deteriorated/Recurrent	*P*-value
N	30	16	14	
Age	66.34 ± 10.23	69.50 ± 9.67	65.29 ± 8.65	0.222
Sex	30	16	14	0.765
Female	12 (40%)	6 (50%)	6 (50%)	
Male	18 (60%)	10 (55.56%)	8 (44.44%)	
Genomic alterations (%)	65.71 ± 35.41	68.00 ± 40.71	60.00 ± 28.28	0.434
Grade of CIC				0.20
Grade 2	14 (43.75%)	8 (50.00%)	4 (28.57%)	
Grade 3	16 (50.00%)	8 (50.00%)	8 (57.14%)	
Grade 4	2 (6.25%)	0 (0.00%)	2 (14.29%)	
Histologic type				0.36
AC	22 (68.75%)	10 (62.50%)	11 (78.57%)	
NEC	1 (3.12%)	0 (0.00%)	1 (7.14%)	
SC	1 (3.12%)	1 (6.25%)	0 (0.00%)	
Unknown	8 (25.00%)	5 (31.25%)	2 (14.29%)	
Dose of onset	10.47 ± 14.01	11.75 ± 17.83	10.07 ± 9.51	0.452
Time of onset	22.20 ± 26.81	23.06 ± 34.07	23.04 ± 18.62	0.261
Steroid initial dose (mg/day)	63.00 ± 37.45	57.22 ± 27.52	76.00 ± 57.13	0.428
Steroid initial dose groups (mg/day)				0.764
Low dose <60	9 (69.23%)	6 (66.67%)	3 (75.00%)	
60 ≤ intermediate dose <300	4 (30.77%)	3 (33.33%)	1 (25.00%)	
Steroid initial dose (mg/kg/day)	1.37 ± 0.58	1.41 ± 0.60	1.27 ± 0.64	0.736
Steroid initial dose groups (mg/kg/day)				0.7
Low dose <1	5 (50.00%)	3 (42.86%)	2 (66.67%)	
1 ≤ intermediate dose <2	1 (10.00%)	1 (14.29%)	0 (0.00%)	
High dose ≥2	4 (40.00%)	3 (42.86%)	1 (33.33%)	
Steroid taper time	5.64 ± 5.77	5.50 ± 5.21	5.75 ± 6.52	0.896
Antibiotics				**0.025**
No	23 (71.88%)	14 (87.50%)	7 (50.00%)	
Yes	9 (28.12%)	2 (12.50%)	7 (50.00%)	
Biological agents				**0.018**
No	25 (78.12%)	15 (93.75%)	8 (57.14%)	
Yes	7 (21.88%)	1 (6.25%)	6 (42.86%)	
OS				0.513
Alive	25 (83.33%)	14 (87.50%)	11 (78.57%)	
Dead	5 (16.67%)	2 (12.50%)	3 (21.43%)	
Survival weeks	75.26 ± 90.53	52.92 ± 89.69	114.56 ± 86.16	**0.015**
CIC course	15.74 ± 22.22	3.36 ± 2.06	25.47 ± 26.01	**<0.001**
Tumor response				0.587
Complete response	1 (3.12%)	1 (6.25%)	0 (0.00%)	
Partial response	8 (25.00%)	3 (18.75%)	5 (35.71%)	
Tumor progressed	3 (9.38%)	2 (12.50%)	1 (7.14%)	
Stable	18 (56.25%)	10 (62.50%)	8 (57.14%)	
Recurrence times				**<0.001**
0	24 (75.00%)	16 (100.00%)	6 (42.86%)	
1	6 (18.75%)	0 (0.00%)	6 (42.86%)	
2	2 (6.25%)	0 (0.00%)	2 (14.29%)	
Rechallenge times				**0.037**
0	26 (86.67%)	16 (100.00%)	10 (71.43%)	
1	3 (10.00%)	0 (0.00%)	3 (21.43%)	
2	1 (3.33%)	0 (0.00%)	1 (7.14%)	

*Data were collected from studies in **Table 1**.*

NSCLC, non-small cell lung cancer; CIC, checkpoint inhibitor colitis; AC, adenocarcinoma; NEC, neuroendocrine carcinoma; SC, squamous cell carcinoma.

Bold values: P < 0.05 which means significant differences between groups.

steroid data, 9 of them chose the steroid decrement after the improvement or resolution of CIC, and the duration of continuous steroid use varied from 3 days to 12 weeks (**Figure 5**).

Biological Agents

Approximately 30%–60% of ICI-reduced diarrhea/colitis patients appear recalcitrant to first-line glucocorticoid, showing no response to high-dose steroid within 72 h of onset or no complete response in 1 week (61). They should be considered for second-line immunosuppressants. Besides, patients who suffer relapses during the steroid decrement or after finishing the steroid course also require additional immunosuppression (28), with the recurrent incidence of 44% for CTLA-4 inhibitors and 34% for PD-1/PD-L1 inhibitors (195). Similarly, our analysis also suggested that patients

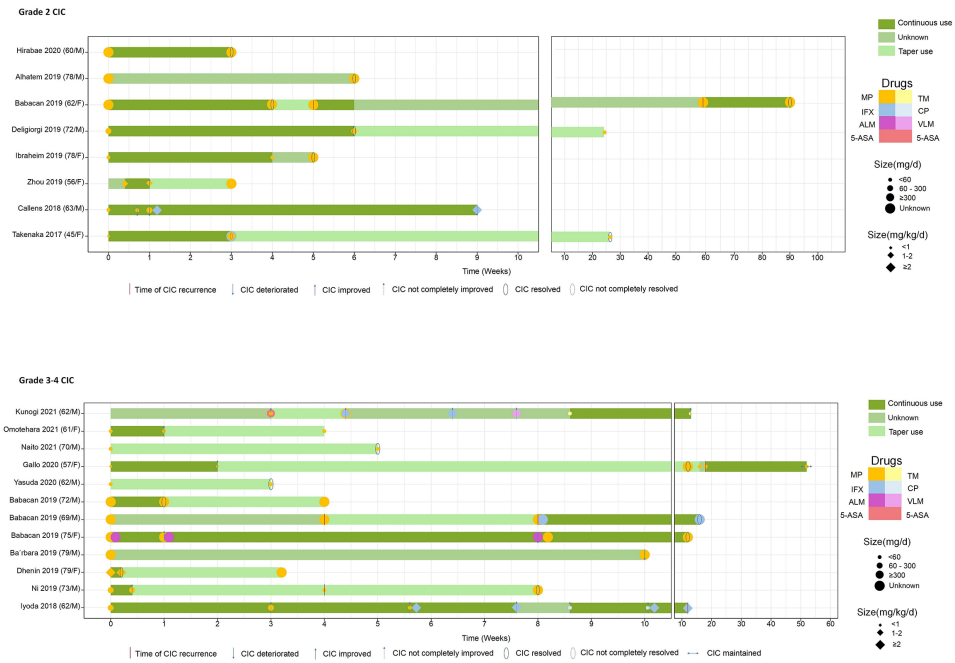

FIGURE 5 | The drugs that every case utilized and the definite continuous and taper time. All the steroid doses were converted to equivalent MP. MP, methylprednisolone; TM, tacrolimus; IFX, infliximab; CP, cyclosporine; ALM, adalimumab; VLM, vedolizumab; 5-ASA, 5-aminosalicylic acid.

were more likely to receive biological agents (42.86% vs. 6.25%, $P = 0.018$) if they suffered from a deteriorated or recurrent CIC outcome rather than an improved or resolved outcome (**Table 4**). Additionally, colon ulceration, pancolitis, and high van der Heide or Mayo score are identified as the predictive factors correlated to the utilization for secondary immunosuppression (22, 61, 167). In addition, the biopsy specimens of CIC patients who required infliximab showed higher CD68 scores and CD8/FoxP3 ratios than those who responded to steroid (196).

Current studies demonstrate that infliximab (IFX) and vedolizumab are the primary therapeutic approaches for steroid-refractory CIC patients (31, 71). Vedolizumab could be utilized in cases when infliximab is contraindicated or ineffective (186).

IFX, a TNF-α antagonist, has been verified to promote tumor immunity and relieve resistance to PD-1 inhibitors significantly (195, 197). Few prospective studies are conducted to illustrate the dose of IFX, while different guidelines showed almost universal recommendations that the initial dose is at 5 mg/kg (q2w) until symptoms improve (19, 71, 183, 198). Seventy-two percent of patients recover with one IFX dose, though the requirement for two or three doses is common (19, 77, 196, 197). However, IFX is reported to induce a rare type of hepatitis (199) and is limited in patients with hepatitis B virus or latent tuberculosis history (200, 201). Moreover, IFX utilization is notably correlated with lymphomas and skin cancer in young adults, while this correlation might be confounded by overall increased malignancy risk and previous thiopurine utilization (202). Golimumab, certolizumab, adalimumab, and etanercept could be alternatives to IFX if paradoxical adverse events occur in CIC patients (203).

Vedolizumab, an antagonist of α4β7 on $CD4^+$ T cells, prevents T cells from aggregating and homing into the inflammatory intestinal mucosa. The unique gut selective mechanism could avoid systemic immunosuppression without substantially changing antitumor response to chemotherapy (28). It is administered to treat steroid-refractory cases with 300 mg infusions at 0, 2, and 6 weeks or until laboratory or clinical improvement (204, 205). Bergqvist et al. (206) reported seven patients with steroid-refractory or steroid-dependent CIC who recovered by using vedolizumab. CIC with microscopic colitis on histopathology also has a response to vedolizumab (205). The potential risk of tumor progression in patients with lymph nodes metastasis might be minimized by vedolizumab since its gut selectivity (207). In addition, utilizing vedolizumab, which has the same potential as IFX, could not increase secondary tumor risk in vulnerable individuals.

Increasing research studies support the early introduction of biological agents in the therapy algorithm (60, 197, 208). Wang et al. (60) pointed out that a long period of steroid monotherapy could increase the infectious risk in contrast to a short period of steroid such as IFX, which suggests that the early utilization of steroid-sparing therapy might improve the prognosis. Abu-Sbeih et al. (208) recruited 179 CIC patients who received biologic therapy (IFX and vedolizumab) to explore their clinical outcomes. They found that over half of the patients significantly experienced lower hospitalization, shorter symptom duration, shorter steroid taper/taper attempt, and higher success rate of steroid taper. Decreased fecal calprotectin levels and the promoted histologic regression rate were found in patients

treated with over three infusions of biologics. Usually, the biologics withdrawal happens in the endoscopy finding of mucosal healing, if there is an attempt to resume ICI therapy. However, no prospective studies have emerged to verify the effectiveness of biologics as first-line therapy. ASCO guidelines stated that individualized therapeutic decisions should be recommended all along (79).

Besides, there are also other potential biologics for refractory ICI-related colitis (203). Anti-IL-1 blockade (anakinra), anti-IL-17 blockade (ixekizumab), anti-IL-23 and anti-IL-12 blockade (ustekinumab) (209), mycophenolate mofetil (MMF) (210, 211), and ciclosporin (54), aiming at blocking critical inflammatory components participating in the pathophysiological process of irAEs, are reported to exert considerable effects in treating severe CIC. Besides, Janus kinase (JAK) inhibitors (tofacitinib) have shown efficacy in CIC patients (212). More studies are warranted to evaluate the usefulness of these biologics in ICI-induced colitis.

Fecal Transplants

The intestinal microbiome has been hypothesized to play an essential role in the occurrence of CIC. Various gut microbiomes are correlated to induce or alleviate ICI-mediated colitis. Fecal transplantation, contributing to gut microbiome reconstitution and regulatory T cells relatively increasing within the colon mucosa, has been proposed as an optional therapeutic approach for patients with severe or refractory CIC. However, available guidance comes from limited case reports. Wang et al. (213) reported two cases with non-healing CIC who completely recovered after receiving fecal transplantation. Another case that was reported by Fasanello et al. had CIC healed successfully with fecal transplantation (214). Convincing prospective studies are required to verify these observations.

Surgery

Patients with CIC could deteriorate to colonic perforation, although with the estimated incidence of 1% to 1.5% (71). Emergency colectomy is recommended to be the most effective treatment. Specifically, subtotal colectomy is preferred since the colon lesions are extensive. Segmental colectomy is usually utilized in the remaining severe colonic inflammation in the postoperative period (77). We also included two NSCLC cases with colonic perforation after receiving ICI therapy (50). One recovered after surgery and rechallenge ICIs with ongoing partial regression (50), while the other ultimately succumbed to infectious complications (55). The predictive risk factors for colon perforation are limited. Smith et al. (215) found that CIC patients who received ipilimumab followed with high-dose IL-2 treatment were prone to present perforation than patients who received one of these therapies alone. Heightened vigilance and timely surgery to this severe complication can improve the clinical outcomes effectively.

PROGNOSIS

Several speculations arise from the association between CIC outcome and survival, whose evidence is rare and conflicting. Two retrospective studies reported that patients who developed ICI-related diarrhea/colitis had a superior OS than those without gastrointestinal toxicity (60, 216). In addition, two simultaneous or sequential irAEs may herald better clinical outcomes. Patients with both colitis and rash caused by immune therapy had a significantly better OS (28.6 vs. 19.9 months, $P = 0.018$) and PFS (16.1 vs. 3.2 months, $P = 0.001$), in contrast to patients with colitis but no rash (217). Obviously, irAEs indicated encouraging tumor response and clinical benefit in patients, which meant longer PFS and OS (216–219). Similarly, our analysis showed that CIC patients with deteriorated or recurrent outcomes had longer OS than those with improved or resolved outcomes (28.5 vs. 13 months, $P = 0.015$) (**Table 4**). Besides, the CIC course was shorter in CIC patients with resolution or improvement, compared with those with deterioration and recurrence (0.84 vs. 6.25 months, $P < 0.001$) (**Table 4**). Moreover, we found that over 60% of patients with grade 2 CIC experienced resolved or improved CIC outcomes, while nearly half of patients with grade 3–4 CIC experienced deteriorated or recurrent CIC outcome (**Table 3**). Generally, higher grade irAEs were reported to suffer inferior prognosis (220). However, several studies showed that no significant correlation was observed between CIC and survival (221, 222). Therefore, the correlation between irAEs and survival needs further verification, and the involved mechanisms are warranted to be clarified.

Predictors for CIC are still on exploration. Several serum markers like CRP, LDH, and fecal calcitonin and their association with CIC prognosis have been investigated. Justine et al. revealed that patients with elevated CRP level had a higher risk of irAE recurrence (223). LDH ≥618 IU/L was related to a poor prognosis in CIC patients (60). Conversely, the decrease of fecal calcitonin after treatment occurred more significantly in patients with CIC remission under endoscopy, which could be used as a non-invasive tool for monitoring and evaluating the response of CIC (159). Nevertheless, the value of fecal calcitonin was limited by its 54% specificity in predicting the endoscopic remission of CIC (166). Furthermore, CIC with immunosuppressive therapy might be associated with improved OS and PFS compared with CIC without immunosuppressive treatment (25, 60). Higher grade diarrhea could predict great prognosis (216). In addition, the application of antibiotics at any time was reported to decrease the incidence of CIC recrudescence, and patients in our analysis who experienced poor CIC prognosis ($P = 0.025$) or had higher CIC grade ($P = 0.025$) were more frequently utilized antibiotics (**Tables 3** and **4**). However, it could increase the frequency of hospitalization and intensive care unit hospitalization and exacerbate CIC severity (224).

RECHALLENGE AND RECURRENCE

A great number of meta-analyses and retrospective studies showed that the resumption after irAEs was potentially effective and relatively safe in selected individuals with careful monitoring (225–229). Universally, patients who improved to grade 1 or less diarrhea/colitis could resume ICI therapy. Any grade 4

irAEs, especially cardiac and neurologic toxicities, are not allowed to continue or reuse ICI (225). The patterns of ICI reintroduction included the same ICI utilized before, the same type of ICIs, and the switching of ICIs of distinct types. Kitagawa et al. (230) showed the safety and efficacy of rechallenging ICIs in patients with NSCLC reported in prior studies. They found that switching ICI class therapy obtained a superior outcome, with over 50% of patients experiencing stable or partial regression disease. Gobbini et al. (231) demonstrated that NSCLC patients discontinuing for irAEs had more prolonged survival than those discontinuing for disease progression. After ICI rechallenge, the recurrence rate of irAEs varied from 37% to 78% (227, 232–234). Among these recurrent irAEs, colitis showed significantly higher incidence than other irAEs (227). Nearly 20%–30% of patients would experience recurrent grade 3 CIC (195, 233). In our analysis, 12.5% (4/32) of patients (36, 43, 50, 54) were retreated with the same ICI therapy used before, one of which experienced the recurrence of grade 3 enterocolitis (54). All of these patients who were reintroduced to ICI therapy harbored deteriorated/recurrent CIC outcomes (P = 0.037) (**Table 4**). Furthermore, a multicenter retrospective study compared the clinical outcomes in ICI retreatment and discontinuation group patients (229). The results showed that retreatment patients had fewer steroid requirements and less hospitalizations (P = 0.007). Besides, the outcomes of recurrent irAEs were found to be more severe if patients were treated with immunosuppressants before, and thus, they need more intensive immunosuppressive treatment. A retrospective study (205) investigated a patient subset of reinitiation ICI therapy. They found that most of the patients need steroid, while a minority of them required IFX or vedolizumab, regardless of whether in the initial or recurrent episode. Our analysis showed that 25% (8/32) of patients (36, 41, 43, 46, 48, 54, 57) had recurrent ICI-mediated colitis without ICI retreatment, which received subsequent therapy involving probiotics, antidiarrheal drugs, antiviral drugs, steroid, and immunosuppressants. Four cases with CIC finally did not improve or deteriorate after the second treatment (36, 41, 48, 54). The risk factors associated with CIC recurrence included early irAE development, long duration of the initial CIC, initial application of immunosuppressants, pneumonitis, hepatitis, age over 65, advanced tumor stage, CTLA-4 inhibitors use (227), and less antibiotic therapy (205, 224). In addition, the factors—good performance status at ICI resumption, the duration and response of the initial ICI course, longer ICI-free interval, and high PD-L1 expression—were considered so far as correlated to clinical benefit from ICI retreatment (235, 236). Actually, with the increasing interest in immunotherapy reintroduction in recent years, we still need further *ad-hoc*-designed and prospective studies to assess the efficacy and safety of the diverse immunotherapy strategies.

SUMMARY

ICI-mediated colitis is the most common irAEs. The incidence varied with different types of ICIs, with combined ICI therapy obtaining the highest occurrence and severity. Gut microbiota plays a critical role in the development of CIC. Endoscopic biopsy is the gold standard of diagnosis, and the consideration combined with medication history is necessary. Current management is based on symptomatic and steroid therapy. The utilization of biological agents according to the severity of CIC grade is reasonable and recommended. The association between CIC and survival is obscure and requires to be explored further. Rechallenge of ICIs is on heated debate. On the condition of symptom control, the reintroduction of ICI is worthy of consideration, with persistent monitoring and evaluation certainly.

STRENGTHS AND LIMITATIONS

This review summarized the latest studies to demonstrate the comprehensive characteristics of ICI-related colitis, especially the mechanisms and treatment. We also collected the CIC cases with NSCLC as an example to analyze the differences between different CIC grades and outcomes. The association between endoscopic findings and the severity of ICIs-related colitis has been evaluated as well. We hoped that our comprehensive review could bring some inspiration in clinical practice. In addition, we explored the correlation between initial steroid dose and CIC outcome, but no significant results were found due to the small sample size and limited accurate data. Although we focused on the NSCLC cases with ICI-mediated colitis, the understanding of irAEs is regardless of cancer species. Moreover, we are conducting real-world studies in our center and we hope that large sample data could present more reliable results.

FUTURE DIRECTION

In the future, early prediction and detection and timely and effective treatment are the two main aspects we need to investigate continuously.

Most studies have focused on the predictive factors for survival outcomes or treatment response (237, 238), while comparatively limited research studies could find biomarkers characterizing irAEs (239, 240). Lim et al. established the CYTOX score covering 11 proinflammatory cytokines and validated its efficacy in predicting severe irAEs which need high-dose corticosteroid therapy (241). However, in view of the extensive organ specificity or systemic presentations in irAEs and the distinct potentially inflammatory mechanisms concerning the adverse events, it is still difficult to translate relevant results to clinical practice. Besides, specific biomarkers are warranted to be explored with a large number of verified preclinical models.

As for the treatment, the optimal steroid dose and continuous/taper time remain inconclusive. Besides, steroid utilization for treating irAEs has become a field with growing controversy. Quite a bit of evidence suggested that the antitumor efficacy of ICI could be weakened by the wide range of immunosuppressive function of steroid (242–244). However, a single-center study (245) recruited 372 patients according to the different indications (irAEs and

others) for steroid. They found that using systemic steroid for irAEs could not influence tumor response and OS, while for other indications (usually correlated to poor prognosis), it could. In addition, we also know little about the immune microenvironment effect by systemic corticosteroids administration. A few case reports implied a temporal correlation between steroid therapy, decreased cytokine expression, and irAE resolution (96). Notably, Tyan et al. (143) found that steroid could disrupt the specific harmonization pattern in irAE patients, which suggested the elimination of activated immune states and thus verified the worse outcome in patients without irAEs or in patients treated with steroid. More subgroup analysis is required to associate irAEs and steroid utilization with survival. Except for steroid treatment, current clinical trials, concerning the use of IFX and vedolizumab (NCT04407247) for CIC patients and tofacitinib (NCT04768504) for refractory CIC patients, are looking forward to presenting profound results. Clinical studies on fecal transplant involved in the gut microbiome have also been in the phase of recruiting participants (NCT03819296 and NCT04038619).

Numerous scientists have been persistently working to investigate the development of irAEs. We hope that one day in the future, irAEs could be specifically predicted and its risk could be assessed by simple and convenient detection biomarkers. The cooperation among multiple disciplines should be strengthened for the continuous monitoring of CIC. Novel treatment strategies are expected with a few side effects. Furthermore, we also need more research studies about the clinicopathological and biological characteristics of CIC to help us better understand this specific subset of irAEs.

STATISTICAL ANALYSIS

We analyzed the differences of CIC onset in different ICI therapy groups by Mann–Whitney *U* test. The descriptive analysis was conducted to describe the baseline features and the intergroup discrepancies in distinct CIC grade and CIC outcome groups. Fisher's exact or chi-square test and Kruskal–Wallis test were performed to analyze categorical and continuous variables, respectively. Categorical variables were expressed as counts and proportions. Continuous variables were delineated as means and standard deviations. We utilized the statistical software packages R and EmpowerStats (X&Y Solutions Inc., Boston, MA, USA) to perform all the statistical analyses. The statistical significance was presented as two-sided *P*-values less than 0.05.

AUTHOR CONTRIBUTIONS

LT and JW searched the literature and wrote the manuscript. NL and YZ helped collect the literature and participated in the discussion. LT and WH performed the statistical analysis. JL and XM examined and verified the study. All authors contributed to the article and approved the submitted version.

REFERENCES

1. Siegel RL, Miller KD, Fuchs HE, Jemal A. Cancer Statistics, 2021 (Vol 71, Pg 7, 2021). *CA Cancer J Clin* (2021) 71(4):359–9. doi: 10.3322/caac.21654
2. Cabezon-Gutierrez L, Custodio-Cabello S, Palka-Kotlowska M, Alonso-Viteri S, Khosravi-Shahi P. Biomarkers of Immune Checkpoint Inhibitors in Non-Small Cell Lung Cancer: Beyond PD-L1. *Clin Lung Cancer* (2021) 22 (5):381–9. doi: 10.1016/j.cllc.2021.03.006
3. Ettinger DS, Wood DE, Aggarwal C, Aisner DL, Akerley W, Bauman JR, et al. Non-Small Cell Lung Cancer, Version 1.2020 Featured Updates to the NCCN Guidelines. *J Natl Compr Cancer Netw* (2019) 17(12):1464–72. doi: doi: 10.6004/jnccn.2019.0059
4. Bei Y, Chen X, Raturi VP, Liu K, Ye S, Xu Q, et al. Treatment Patterns and Outcomes Change in Early-Stage Non-Small Cell Lung Cancer in Octogenarians and Older: A SEER Database Analysis. *Aging Clin Exp Res* (2021) 33(1):147–56. doi: 10.1007/s40520-020-01517-z
5. Lamberti G, Andrini E, Sisi M, Rizzo A, Parisi C, Di Federico A, et al. Beyond EGFR, ALK and ROS1: Current Evidence and Future Perspectives on Newly Targetable Oncogenic Drivers in Lung Adenocarcinoma. *Crit Rev Oncol Hematol* (2020) 156:103119. doi: 10.1016/j.critrevonc.2020.103119
6. Li X, Shao C, Shi Y, Han W. Lessons Learned From the Blockade of Immune Checkpoints in Cancer Immunotherapy. *J Hematol Oncol* (2018) 11:31. doi: 10.1186/s13045-018-0578-4
7. Li Y, Li F, Jiang F, Lv X, Zhang R, Lu A, et al. A Mini-Review for Cancer Immunotherapy: Molecular Understanding of PD-1/PD-L1 Pathway & Translational Blockade of Immune Checkpoints. *Int J Mol Sci* (2016) 17 (7):1151. doi: 10.3390/ijms17071151
8. Reddy HG, Schneider BJ, Tai AW. Immune Checkpoint Inhibitor-Associated Colitis and Hepatitis. *Clin Trans Gastroenterol* (2018) 9 (11):206. doi: 10.1038/s41424-018-0049-9
9. Lin X, Lu X, Luo G, Xiang H. Progress in PD-1/PD-L1 Pathway Inhibitors: From Biomacromolecules to Small Molecules. *Eur J Med Chem* (2020) 186:111876. doi: 10.1016/j.ejmech.2019.111876
10. Hayashi H, Nakagawa K. Combination Therapy With PD-1 or PD-L1 Inhibitors for Cancer. *Int J Clin Oncol* (2020) 25(5):818–30. doi: 10.1007/s10147-019-01548-1
11. Postow MA, Sidlow R, Hellmann MD. Immune-Related Adverse Events Associated With Immune Checkpoint Blockade. *N Engl J Med* (2018) 378 (2):158–68. doi: 10.1056/NEJMra1703481
12. Shannon VR. Pneumonitis Associated With Immune Checkpoint Inhibitors Among Patients With Non-Small Cell Lung Cancer. *Curr Opin Pulm Med* (2020) 26(4):326–40. doi: 10.1097/MCP.0000000000000689
13. Naidoo J, Nishino M, Patel SP, Shankar B, Rekhtman N, Illei P, et al. Immune-Related Pneumonitis After Chemoradiotherapy and Subsequent Immune Checkpoint Blockade in Unresectable Stage III Non-Small-Cell Lung Cancer. *Clin Lung Cancer* (2020) 21(5):E435–44. doi: 10.1016/j.cllc.2020.02.025
14. Remon J, Passiglia F, Ahn M-J, Barlesi F, Forde PM, Garon EB, et al. Immune Checkpoint Inhibitors in Thoracic Malignancies: Review of the Existing Evidence by an IASLC Expert Panel and Recommendations. *J Thorac Oncol* (2020) 15(6):914–47. doi: 10.1016/j.jtho.2020.03.006
15. Hellmann MD, Ciuleanu T-E, Pluzanski A, Lee JS, Otterson GA, Audigier-Valette C, et al. Nivolumab Plus Ipilimumab in Lung Cancer With a High Tumor Mutational Burden. *N Engl J Med* (2018) 378(22):2093–104. doi: 10.1056/NEJMoa1801946
16. Reck M, Borghaei H, O'Byrne KJ. Nivolumab Plus Ipilimumab in Non-Small-Cell Lung Cancer. *Future Oncol* (2019) 15(19):2287–302. doi: 10.2217/fon-2019-0031
17. Reck M, Ciuleanu T-E, Dols MC, Schenker M, Zurawski B, Menezes J, et al. Nivolumab (NIVO) Plus Ipilimumab (IPI)+2 Cycles of Platinum-Doublet Chemotherapy (Chemo) vs 4 Cycles Chemo as First-Line (1L) Treatment (Tx) for Stage IV/recurrent Non-Small Cell Lung Cancer (NSCLC): CheckMate 9la. *J Clin Oncol* (2020) 38(15):9501–9501. doi: 10.1200/JCO.2020.38.15_suppl.9501
18. Rizzo A, Brandi G. Biochemical Predictors of Response to Immune Checkpoint Inhibitors in Unresectable Hepatocellular Carcinoma. *Cancer Treat Res Commun* (2021) 27:100328. doi: 10.1016/j.ctarc.2021.100328

19. Puzanov I, Diab A, Abdallah K, Bingham COIII, Brogdon C, Dadu R, et al. Managing Toxicities Associated With Immune Checkpoint Inhibitors: Consensus Recommendations From the Society for Immunotherapy of Cancer (SITC) Toxicity Management Working Group. *J Immunother Cancer* (2017) 5:95. doi: 10.1186/s40425-017-0300-z
20. Haanen JBAG, Carbonnel F, Robert C, Kerr KM, Peters S, Larkin J, et al. Management of Toxicities From Immunotherapy: ESMO Clinical Practice Guidelines for Diagnosis, Treatment and Follow-Up (Vol 28, Pg 119, 2017). *Ann Oncol* (2018) 29:264–6. doi: 10.1093/annonc/mdy162
21. Abu-Sbeih H, Ali FS, Luo W, Raju G, Wang Y. The Importance of Endoscopic and Histological Evaluation in the Management of Immune Checkpoint Inhibitor-Induced Colitis. *Am J Gastroenterol* (2018) 113:S112–3. doi: 10.14309/00000434-201810001-00197
22. Wang Y, Abu-Sbeih H, Mao E, Ali N, Qiao W, Van Anh T, et al. Endoscopic and Histologic Features of Immune Checkpoint Inhibitor-Related Colitis. *Inflamm Bowel Dis* (2018) 24(8):1695–705. doi: 10.1093/ibd/izy104
23. Marin-Acevedo JA, Harris DM, Burton MC. Immunotherapy-Induced Colitis: An Emerging Problem for the Hospitalist. *J Hosp Med* (2018) 13 (6):413–8. doi: 10.12788/jhm.2925
24. Kroner PT, Mody K, Farraye FA. Immune Checkpoint Inhibitor-Related Luminal GI Adverse Events. *Gastrointest Endosc* (2019) 90(6):881–92. doi: 10.1016/j.gie.2019.09.009
25. Som A, Mandaliya R, Alsaadi D, Farshidpour M, Charabaty A, Malhotra N, et al. Immune Checkpoint Inhibitor-Induced Colitis: A Comprehensive Review. *World J Clin Cases* (2019) 7(4):405–18. doi: 10.12998/wjcc.v7.i4.405
26. Menon T, Afzali A. Immune-Mediated Colitis. *Curr Treat Options Gastroenterol* (2019) 17(4):506–23. doi: 10.1007/s11938-019-00263-0
27. Sehgal K, Khanna S. Gut Microbiome and Checkpoint Inhibitor Colitis. *Intest Res* (2020) 19(4):360–4. doi: 10.5217/ir.2020.00116
28. Dougan M, Wang Y, Rubio-Tapia A, Lim JK. AGA Clinical Practice Update on Diagnosis and Management of Immune Checkpoint Inhibitor Colitis and Hepatitis: Expert Review. *Gastroenterology* (2021) 160(4):1384–93. doi: 10.1053/j.gastro.2020.08.063
29. Portenkirchner C, Kienle P, Horisberger K. Checkpoint Inhibitor-Induced Colitis-A Clinical Overview of Incidence, Prognostic Implications and Extension of Current Treatment Options. *Pharmaceuticals* (2021) 14(4): e1344805. doi: 10.3390/ph14040367
30. Wang DY, Ye F, Zhao S, Johnson DB. Incidence of Immune Checkpoint Inhibitor-Related Colitis in Solid Tumor Patients: A Systematic Review and Meta-Analysis. *Oncoimmunology* (2017) 6(10). doi: 10.1080/2162402X.2017.1344805
31. Soularue E, Lepage P, Colombel JF, Coutzac C, Faleck D, Marthey L, et al. Enterocolitis Due to Immune Checkpoint Inhibitors: A Systematic Review. *Gut* (2018) 67(11):2056–67. doi: 10.1136/gutjnl-2018-316948
32. Gonzalez RS, Salaria SN, Bohannon CD, Huber AR, Feely MM, Shi C. PD-1 Inhibitor Gastroenterocolitis: Case Series and Appraisal of 'Immunomodulatory Gastroenterocolitis'. *Histopathology* (2017) 70 (4):558–67. doi: 10.1111/his.13118
33. Khoja L, Day D, Chen TW-W, Siu LL, Hansen AR. Tumour- and Class-Specific Patterns of Immune-Related Adverse Events of Immune Checkpoint Inhibitors: A Systematic Review. *Ann Oncol* (2017) 28(10):2377–85. doi: 10.1093/annonc/mdx286
34. Tandon P, Bourassa-Blanchette S, Bishay K, Parlow S, Laurie SA, McCurdy JD. The Risk of Diarrhea and Colitis in Patients With Advanced Melanoma Undergoing Immune Checkpoint Inhibitor Therapy: A Systematic Review and Meta-Analysis. *J Immunother* (2018) 41(3):101–8. doi: 10.1097/CJI.0000000000000213
35. Kunogi Y, Tominaga K, Abe K, Kanazawa M, Tanaka T, Watanabe S, et al. Refractory Immune Checkpoint Inhibitor-Induced Colitis Improved by Tacrolimus: A Case Report. *Healthcare* (2021) 9(4):418. doi: 10.3390/healthcare9040418
36. Mourad AP, De Robles MS. Chemoimmunotherapy-Related Enteritis Resulting in a Mechanical Small Bowel Obstruction - A Case Report. *Int J Surg Case Rep* (2021) 79:131–4. doi: 10.1016/j.ijscr.2020.12.096
37. Naito T, Nosaka T, Takahashi K, Ofuji K, Matsuda H, Ohtani M, et al. A Case of Immune Checkpoint Inhibitor-Related Colitis With a Distinctive Endoscopic Finding of Colonic Pseudolipomatosis. *Clin J Gastroenterol* (2021) 14(5):1431–6. doi: 10.1007/s12328-021-01459-7
38. Omotehara S, Nishida M, Yamanashi K, Sakurai K, Katsurada T, Komatsu Y, et al. A Case of Immune Checkpoint Inhibitor-Associated Gastroenteritis Detected by Ultrasonography. *J Clin Ultrasound* (2021) 49(6):605–9. doi: 10.1002/jcu.22975
39. Hirabae A, Ichihara E, Sunami R, Ota M, Iwamoto Y, Maeda Y, et al. Rapid Disease Progression of Advanced Non-Small Cell Lung Cancer Five Months After Cessation of Pembrolizumab. *Acta Med Okayama* (2020) 74(5):423–5. doi: 10.18926/AMO/60802
40. Grover S, Bond SA, Mansour MK, Friedman S. Management of Immunotherapy Colitis: Special Considerations in the COVID-19 Era. *Cancer* (2020) 126(21):4630–3. doi: 10.1002/cncr.33125
41. Gallo A, Talerico R, Novello L, Giustiniani MC, D'Argento E, Bria E, et al. Collagenous Colitis and Atezolizumab Therapy: An Atypical Case. *Clin J Gastroenterol* (2021) 14(1):165–9. doi: 10.1007/s12328-020-01276-4
42. Yoshimura K, Saku A, Karayama M, Inui N, Sugimura H, Suda T. Leucine-Rich α(2)-Glycoprotein as a Potential Biomarker for Immune-Related Colitis After Anti-PD-L1 Therapy: A Report of a Case Series. *Clin Lung Cancer* (2020) 21(6):e516–22. doi: 10.1016/j.cllc.2020.04.005
43. Babacan NA, Tanvetyanon T. Superimposed Clostridium Difficile Infection During Checkpoint Inhibitor Immunotherapy-Induced Colitis. *J Immunother* (2019) 42(9):350–3. doi: 10.1097/CJI.0000000000000270
44. Zhou C, Klionsky Y, Treasure ME, Bruno DS. Pembrolizumab-Induced Immune-Mediated Colitis in a Patient With Concurrent Clostridium Difficile Infection. *Case Rep Oncol* (2019) 12(1):164–70. doi: 10.1159/000497155
45. Deligiorgi MV, Panayiotidis MI, Trafalis DT. Parathyroid Hormone Related Protein (PTHrP)-Mediated Hypercalcemia in Malignancy Associated With Anti-PD-1 Immune Checkpoint Inhibitor Treatment and Related Inflammatory Reactions. *Int Immunopharmacol* (2019) 77:105942. doi: 10.1016/j.intimp.2019.105942
46. Ni J, Zhang X, Zhang L. Opportunistic Bowel Infection After Corticosteroid Dosage Tapering in a Stage IV Lung Cancer Patient With Tislelizumab-Related Colitis. *Thorac Cancer* (2020) 11(6):1699–702. doi: 10.1111/1759-7714.13401
47. Alhatem A, Patel K, Eriksen B, Bukhari S, Liu C. Nivolumab-Induced Concomitant Severe Upper and Lower Gastrointestinal Immune-Related Adverse Effects. *ACG Case Rep J* (2019) 6(11):e00249. doi: 10.14309/crj.0000000000000249
48. Cancela-Díez B, Gómez-De Rueda F, Antolinos Pérez MJ, Jiménez-Morales A, López-Hidalgo JL. Acute Coronary Syndrome and Recurrent Colitis as Immune-Related Adverse Events in a Lung Cancer Patient. *J Oncol Pharm Pract* (2020) 26(1):252–5. doi: 10.1177/1078155219865596
49. Dhenin A, Samartzi V, Lejeune S, Seront E. Cascade of Immunologic Adverse Events Related to Pembrolizumab Treatment. *BMJ Case Rep* (2019) 12(6):e229149. doi: 10.1136/bcr-2018-229149
50. Beck TN, Kudinov AE, Dulaimi E, Boumber Y. Case Report: Reinitiating Pembrolizumab Treatment After Small Bowel Perforation. *BMC Cancer* (2019) 19:379. doi: 10.1186/s12885-019-5577-5
51. Ibraheim H, Green M, Papa S, Powell N. Topical Beclometasone Dipropionate in the Management of Immune Checkpoint Inhibitor-Induced Microscopic Colitis. *BMJ Case Rep* (2019) 12(4):e226481. doi: 10.1136/bcr-2018-226481
52. Yasuda Y, Urata Y, Tohnai R, Ito S, Kawa Y, Kono Y, et al. Immune-Related Colitis Induced by the Long-Term Use of Nivolumab in a Patient With Non-Small Cell Lung Cancer. *Internal Med* (2018) 57(9):1269–72. doi: 10.2169/internalmedicine.9230-17
53. Yamauchi R, Araki T, Mitsuyama K, Tokito T, Ishii H, Yoshioka S, et al. The Characteristics of Nivolumab-Induced Colitis: An Evaluation of Three Cases and a Literature Review. *BMC Gastroenterol* (2018) 18(1):135. doi: 10.1186/s12876-018-0864-1
54. Iyoda T, Kurita N, Takada A, Watanabe H, Ando M. Resolution of Infliximab-Refractory Nivolumab-Induced Acute Severe Enterocolitis After Cyclosporine Treatment in a Patient With Non-Small Cell Lung Cancer. *Am J Case Rep* (2018) 19:360–4. doi: 10.12659/AJCR.908570
55. Callens R, Tamsin A, van Zandweghe L. Nivolumab-Induced Fulminant Immune-Related Colitis Despite Infliximab in a Patient With NSCLC. *J Thorac Oncol* (2019) 14(3):e49–50. doi: 10.1016/j.jtho.2018.11.014

56. Gonzalez-Vazquez S, de-la-Riva-Onandia S, Ignacio Echeveste J, Munoz-Navas M. Immune Mediated Colitis Caused by Lung Cancer Treatment With Atezolizumab. *Rev Esp Enferm Dig* (2017) 109(12):863–4. doi: 10.17235/reed.2017.5060/2017
57. Takenaka T, Yamazaki K, Miura N, Harada N, Takeo S. Osimertinib Reactivated Immune-Related Colitis After Treatment With Anti-PD1 Antibody for Non-Small Cell Lung Cancer. *Invest New Drugs* (2017) 35 (6):848–50. doi: 10.1007/s10637-017-0481-9
58. Kubo K, Kato M, Mabe K. Nivolumab-Associated Colitis Mimicking Ulcerative Colitis. *Clin Gastroenterol Hepatol* (2017) 15(9):XXXV–XXXVI. doi: 10.1016/j.cgh.2017.03.026
59. Durrechou Q, Domblides C, Sionneau B, Lefort F, Quivy A, Ravaud A, et al. Management of Immune Checkpoint Inhibitor Toxicities. *Cancer Manage Res* (2020) 12:9139–57. doi: 10.2147/CMAR.S218756
60. Wang Y, Abu-Sbeih H, Mao E, Ali N, Ali FS, Qiao W, et al. Immune-Checkpoint Inhibitor-Induced Diarrhea and Colitis in Patients With Advanced Malignancies: Retrospective Review at MD Anderson. *J Immunother Cancer* (2018) 6. doi: 10.1186/s40425-018-0346-6
61. Foppen MHG, Rozeman EA, van Wilpe S, Postma C, Snaebjornsson P, van Thienen JV, et al. Immune Checkpoint Inhibition-Related Colitis: Symptoms, Endoscopic Features, Histology and Response to Management. *ESMO Open* (2018) 3(1):e000278. doi: 10.1136/esmoopen-2017-000278
62. Hayashi Y, Hosoe N, Takabayashi K, Limpias Kamiya KJL, Tsugaru K, Shimozaki K, et al. Clinical, Endoscopic, and Pathological Characteristics of Immune Checkpoint Inhibitor-Induced Gastroenterocolitis. *Dig Dis Sci* (2021) 66(6):2129–34. doi: 10.1007/s10620-020-06441-w
63. Assarzadegan N, Montgomery E, Anders RA. Immune Checkpoint Inhibitor Colitis: The Flip Side of the Wonder Drugs. *Virchows Arch* (2018) 472 (1):125–33. doi: 10.1007/s00428-017-2267-z
64. Yanai S, Nakamura S, Matsumoto T. Nivolumab-Induced Colitis Treated by Infliximab. *Clin Gastroenterol Hepatol* (2017) 15(4):E80–1. doi: 10.1016/j.cgh.2016.09.017
65. Gondal B, Patel P, Gallan A, Hart J, Bissonnette M. Gastrointestinal Adverse Effects of Immunomodulation: Acute Colitis With Immune Check Point Inhibitor Nivolumab. *Inflamm Bowel Dis* (2016) 22:S12–3. doi: 10.1097/01.MIB.0000480057.88945.e3
66. Baroudjian B, Lourenco N, Pages C, Chami I, Maillet M, Bertheau P, et al. Anti-PD1-Induced Collagenous Colitis in a Melanoma Patient. *Melanoma Res* (2016) 26(3):308–11. doi: 10.1097/CMR.0000000000000252
67. Weber JS, Kaehler KC, Hauschild A. Management of Immune-Related Adverse Events and Kinetics of Response With Ipilimumab. *J Clin Oncol* (2012) 30(21):2691–7. doi: 10.1200/JCO.2012.41.6750
68. Hillock NT, Heard S, Kichenadasse G, Hill CL, Andrews J. Infliximab for Ipilimumab-Induced Colitis: A Series of 13 Patients. *Asia Pac J Clin Oncol* (2017) 13(5):E284–90. doi: 10.1111/ajco.12651
69. Boutros C, Tarhini A, Routier E, Lambotte O, Ladurie FL, Carbonnel F, et al. Safety Profiles of Anti-CTLA-4 and Anti-PD-1 Antibodies Alone and in Combination. *Nat Rev Clin Oncol* (2016) 13(8):473–86. doi: 10.1038/nrclinonc.2016.58
70. Wang DY, Mooradian MJ, Kim D, Shah NJ, Fenton SE, Conry RM, et al. Clinical Characterization of Colitis Arising From Anti-PD-1 Based Therapy. *Oncoimmunology* (2019) 8(1):e1524695. doi: 10.1080/2162402X.2018.1524695
71. Haanen JBAG, Carbonnel F, Robert C, Kerr KM, Peters S, Larkin J, et al. Management of Toxicities From Immunotherapy: ESMO Clinical Practice Guidelines for Diagnosis, Treatment and Follow-Up. *Ann Oncol* (2017) 28 (suppl_4):iv119–42. doi: 10.1093/annonc/mdx225
72. Nishida T, Iijima H, Adachi S. Immune Checkpoint Inhibitor-Induced Diarrhea/Colitis: Endoscopic and Pathologic Findings. *World J Gastrointest Pathophysiol* (2019) 10(2):17–28. doi: 10.4291/wjgp.v10.i2.17
73. Berman D, Parker SM, Siegel J, Chasalow SD, Weber J, Galbraith S, et al. Blockade of Cytotoxic T-Lymphocyte Antigen-4 by Ipilimumab Results in Dysregulation of Gastrointestinal Immunity in Patients With Advanced Melanoma. *Cancer Immun* (2010) 10:11–1.
74. Lord JD, Hackman RC, Moklebust A, Thompson JA, Higano CS, Chielens D, et al. Refractory Colitis Following Anti-CTLA4 Antibody Therapy: Analysis of Mucosal FOXP3(+) T Cells. *Dig Dis Sci* (2010) 55(5):1396–405. doi: 10.1007/s10620-009-0839-8
75. Liu Y-H, Zang X-Y, Wang J-C, Huang S-S, Xu J, Zhang P. Diagnosis and Management of Immune Related Adverse Events (irAEs) in Cancer Immunotherapy. *Biomed Pharmacother* (2019) 120:109437. doi: 10.1016/j.biopha.2019.109437
76. Barnes MJ, Griseri T, Johnson AMF, Young W, Powrie F, Izcue A. CTLA-4 Promotes Foxp3 Induction and Regulatory T Cell Accumulation in the Intestinal Lamina Propria. *Mucosal Immunol* (2013) 6(2):324–34. doi: 10.1038/mi.2012.75
77. Marthey L, Mateus C, Mussini C, Nachury M, Nancey S, Grange F, et al. Cancer Immunotherapy With Anti-CTLA-4 Monoclonal Antibodies Induces an Inflammatory Bowel Disease. *J Crohns Colitis* (2016) 10 (4):395–401. doi: 10.1093/ecco-jcc/jjv227
78. Siakavellas SI, Bamias G. Checkpoint Inhibitor Colitis: A New Model of Inflammatory Bowel Disease? *Curr Opin Gastroenterol* (2018) 34(6):377–83. doi: 10.1097/MOG.0000000000000482
79. Bellaguarda E, Hanauer S. Checkpoint Inhibitor-Induced Colitis. *Am J Gastroenterol* (2020) 115(2):202–10. doi: 10.14309/ajg.0000000000000497
80. Tadano H, Torigoe T. Immune-Related Adverse Events of Immune Checkpoint Inhibitors. *Nihon Rinsho Meneki Gakkai Kaishi* (2017) 40 (2):102–8. doi: 10.2177/jsci.40.102
81. Miller PL, Carson TL. Mechanisms and Microbial Influences on CTLA-4 and PD-1-Based Immunotherapy in the Treatment of Cancer: A Narrative Review. *Gut Pathog* (2020) 12(1):43. doi: 10.1186/s13099-020-00381-6
82. Sharpe AH, Abbas AK. Focus on Research: T-Cell Costimulation - Biology, Therapeutic Potential, and Challenges. *N Engl J Med* (2006) 355(10):973–5. doi: 10.1056/NEJMp068087
83. Nagorsen D, Scheibenbogen C, Marincola FM, Letsch A, Keilholz U. Natural T Cell Immunity Against Cancer. *Clin Cancer Res* (2003) 9(12):4296–303.
84. Qureshi OS, Zheng Y, Nakamura K, Attridge K, Manzotti C, Schmidt EM, et al. Trans-Endocytosis of CD80 and CD86: A Molecular Basis for the Cell-Extrinsic Function of CTLA-4. *Science* (2011) 332(6029):600–3. doi: 10.1126/science.1202947
85. Wing K, Onishi Y, Prieto-Martin P, Yamaguchi T, Miyara M, Fehervari Z, et al. CTLA-4 Control Over Foxp3(+) Regulatory T Cell Function. *Science* (2008) 322(5899):271–5. doi: 10.1126/science.1160062
86. Patsoukis N, Bardhan K, Chatterjee P, Sari D, Liu B, Bell LN, et al. PD-1 Alters T-Cell Metabolic Reprogramming by Inhibiting Glycolysis and Promoting Lipolysis and Fatty Acid Oxidation. *Nat Commun* (2015) 6:6692. doi: 10.1038/ncomms7692
87. Patsoukis N, Li L, Sari D, Petkova V, Boussiotis VA. PD-1 Increases PTEN Phosphatase Activity While Decreasing PTEN Protein Stability by Inhibiting Casein Kinase 2. *Mol Cell Biol* (2013) 33(16):3091–8. doi: 10.1128/MCB.00319-13
88. Ramos-Casals M, Brahmer JR, Callahan MK, Flores-Chavez A, Keegan N, Khamashta MA, et al. Immune-Related Adverse Events of Checkpoint Inhibitors. *Nat Rev Dis Primers* (2020) 6(1):31. doi: 10.1038/s41572-020-0160-6
89. Tivol EA, Borriello F, Schweitzer AN, Lynch WP, Bluestone JA, Sharpe AH. Loss of CTLA-4 Leads to Massive Lymphoproliferation and Fatal Multiorgan Tissue Destruction, Revealing a Critical Negative Regulatory Role of CTLA-4. *Immunity* (1995) 3(5):541–7. doi: 10.1016/1074-7613(95)90125-6
90. Klocke K, Sakaguchi S, Holmdahl R, Wing K. Induction of Autoimmune Disease by Deletion of CTLA-4 in Mice in Adulthood. *Proc Natl Acad Sci U S A* (2016) 113(17):E2383–92. doi: 10.1073/pnas.1603892113
91. Beck KE, Blansfield JA, Tran KQ, Feldman AL, Hughes MS, Royal RE, et al. Enterocolitis in Patients With Cancer After Antibody Blockade of Cytotoxic T-Lymphocyte-Associated Antigen 4. *J Clin Oncol* (2006) 24(15):2283–9. doi: 10.1200/JCO.2005.04.5716
92. Guthery SL, Heubi JE, Filipovich A. Enteral Metronidazole for the Prevention of Graft Versus Host Disease in Pediatric Marrow Transplant Recipients: Results of a Pilot Study. *Bone Marrow Transplant* (2004) 33 (12):1235–9. doi: 10.1038/sj.bmt.1704474
93. Kaehler KC, Piel S, Livingstone E, Schilling B, Hauschild A, Schadendorf D. Update on Immunologic Therapy With Anti-CTLA-4 Antibodies in Melanoma: Identification of Clinical and Biological Response Patterns, Immune-Related Adverse Events, and Their Management. *Semin Oncol* (2010) 37(5):485–98. doi: 10.1053/j.seminoncol.2010.09.003

94. Wang T, Zheng N, Luo Q, Jiang L, He B, Yuan X, et al. Probiotics Lactobacillus Reuteri Abrogates Immune Checkpoint Blockade-Associated Colitis by Inhibiting Group 3 Innate Lymphoid Cells. *Front Immunol* (2019) 10. doi: 10.3389/fimmu.2019.01235
95. Coutzac C, Adam J, Soularue E, Collins M, Racine A, Mussini C, et al. Colon Immune-Related Adverse Events: Anti-CTLA-4 and Anti-PD-1 Blockade Induce Distinct Immunopathological Entities. *J Crohns Colitis* (2017) 11 (10):1238–46. doi: 10.1093/ecco-jcc/jjx081
96. Yoshino K, Nakayama T, Ito A, Sato E, Kitano S. Severe Colitis After PD-1 Blockade With Nivolumab in Advanced Melanoma Patients: Potential Role of Th1-Dominant Immune Response in Immune-Related Adverse Events: Two Case Reports. *BMC Cancer* (2019) 19(1):1019. doi: 10.1186/s12885-019-6138-7
97. Luoma AM, Suo S, Williams HL, Sharova T, Sullivan K, Manos M, et al. Molecular Pathways of Colon Inflammation Induced by Cancer Immunotherapy. *Cell* (2020) 182(3):655–+. doi: 10.1016/j.cell.2020.06.001
98. Song M-Y, Hong C-P, Park SJ, Kim J-H, Yang B-G, Park Y, et al. Protective Effects of Fc-Fused PD-L1 on Two Different Animal Models of Colitis. *Gut* (2015) 64(2):260–71. doi: 10.1136/gutjnl-2014-307311
99. Badran YR, Cohen JV, Brastianos PK, Parikh AR, Hong TS, Dougan M. Concurrent Therapy With Immune Checkpoint Inhibitors and TNF Alpha Blockade in Patients With Gastrointestinal Immune-Related Adverse Events. *J Immunother Cancer* (2019) 7(1):226. doi: 10.1186/s40425-019-0711-0
100. Bamias G, Delladetsima I, Perdiki M, Siakavellas SI, Goukos D, Papatheodoridis GV, et al. Immunological Characteristics of Colitis Associated With Anti-CTLA-4 Antibody Therapy. *Cancer Invest* (2017) 35(7):443–55. doi: 10.1080/07357907.2017.1324032
101. Tokunaga R, Zhang W, Naseem M, Puccini A, Berger MD, Soni S, et al. CXCL9, CXCL10, CXCL11/CXCR3 Axis for Immune Activation - A Target for Novel Cancer Therapy. *Cancer Treat Rev* (2018) 63:40–7. doi: 10.1016/j.ctrv.2017.11.007
102. Neurath MF. Targeting Immune Cell Circuits and Trafficking in Inflammatory Bowel Disease. *Nat Immunol* (2019) 20(8):970–9. doi: 10.1038/s41590-019-0415-0
103. Pitt JM, Vetizou M, Waldschmitt N, Kroemer G, Chamaillard M, Boneca IG, et al. Fine-Tuning Cancer Immunotherapy: Optimizing the Gut Microbiome. *Cancer Res* (2016) 76(16):4602–7. doi: 10.1158/0008-5472.CAN-16-0448
104. Khan Z, Hammer C, Guardino E, Chandler GS, Albert ML. Mechanisms of Immune-Related Adverse Events Associated With Immune Checkpoint Blockade: Using Germline Genetics to Develop a Personalized Approach. *Genome Med* (2019) 11(1):39. doi: 10.1186/s13073-019-0652-8
105. Belkaid Y, Hand TW. Role of the Microbiota in Immunity and Inflammation. *Cell* (2014) 157(1):121–41. doi: 10.1016/j.cell.2014.03.011
106. Yang Y, Torchinsky MB, Gobert M, Xiong H, Xu M, Linehan JL, et al. Focused Specificity of Intestinal T(H)17 Cells Towards Commensal Bacterial Antigens. *Nature* (2014) 510(7503):152–+. doi: 10.1038/nature13279
107. Anderson R, Theron AJ, Rapoport BL. Immunopathogenesis of Immune Checkpoint Inhibitor-Related Adverse Events: Roles of the Intestinal Microbiome and Th17 Cells. *Front Immunol* (2019) 10. doi: 10.3389/fimmu.2019.02254
108. Dubin K, Callahan MK, Ren B, Khanin R, Viale A, Ling L, et al. Intestinal Microbiome Analyses Identify Melanoma Patients at Risk for Checkpoint-Blockade-Induced Colitis. *Nat Commun* (2016) 7:10391. doi: 10.1038/ncomms10391
109. Derosa L, Routy B, Kroemer G, Zitvogel L. The Intestinal Microbiota Determines the Clinical Efficacy of Immune Checkpoint Blockers Targeting PD-1/PD-L1. *Oncoimmunology* (2018) 7(6):e1434468. doi: 10.1080/2162402X.2018.1434468
110. Goubet A-G, Daillere R, Routy B, Derosa L, Roberti PM, Zitvogel L. The Impact of the Intestinal Microbiota in Therapeutic Responses Against Cancer. *C R Biol* (2018) 341(5):284–9. doi: 10.1016/j.crvi.2018.03.004
111. Routy B, Le Chatelier E, Derosa L, Duong CPM, Alou MT, Daillere R, et al. Gut Microbiome Influences Efficacy of PD-1-Based Immunotherapy Against Epithelial Tumors. *Science* (2018) 359(6371):91–+. doi: 10.1126/science.aan3706
112. Chaput N, Lepage P, Coutzac C, Soularue E, Le Roux K, Monot C, et al. Baseline Gut Microbiota Predicts Clinical Response and Colitis in Metastatic Melanoma Patients Treated With Ipilimumab. *Ann Oncol* (2019) 30 (12):2012–2. doi: 10.1093/annonc/mdz224
113. Gopalakrishnan V, Spencer CN, Nezi L, Reuben A, Andrews MC, Karpinets TV, et al. Gut Microbiome Modulates Response to Anti-PD-1 Immunotherapy in Melanoma Patients. *Science* (2018) 359(6371):97–103. doi: 10.1126/science.aan4236
114. Huang JY, Lee SM, Mazmanian SK. The Human Commensal Bacteroides Fragilis Binds Intestinal Mucin. *Anaerobe* (2011) 17(4):137–41. doi: 10.1016/j.anaerobe.2011.05.017
115. Mazmanian SK, Round JL, Kasper DL. A Microbial Symbiosis Factor Prevents Intestinal Inflammatory Disease. *Nature* (2008) 453(7195):620–5. doi: 10.1038/nature07008
116. Vetizou M, Pitt JM, Daillere R, Lepage P, Waldschmitt N, Flament C, et al. Anticancer Immunotherapy by CTLA-4 Blockade Relies on the Gut Microbiota. *Science* (2015) 350(6264):1079–+. doi: 10.1126/science.aad1329
117. Roy S, Trinchieri G. Microbiota: A Key Orchestrator of Cancer Therapy. *Nat Rev Cancer* (2017) 17(5):271–+. doi: 10.1038/nrc.2017.13
118. Dasgupta S, Erturk-Hasdemir D, Ochoa-Reparaz J, Reinecker H-C, Kasper DL. Plasmacytoid Dendritic Cells Mediate Anti-Inflammatory Responses to a Gut Commensal Molecule *via* Both Innate and Adaptive Mechanisms. *Cell Host Microbe* (2014) 15(4):413–23. doi: 10.1016/j.chom.2014.03.006
119. Sivan A, Corrales L, Hubert N, Williams JB, Aquino-Michaels K, Earley ZM, et al. Commensal Bifidobacterium Promotes Antitumor Immunity and Facilitates Anti-PD-L1 Efficacy. *Science* (2015) 350(6264):1084–9. doi: 10.1126/science.aac4255
120. Wang F, Yin Q, Chen L, Davis MM. Bifidobacterium can Mitigate Intestinal Immunopathology in the Context of CTLA-4 Blockade. *Proc Natl Acad Sci U S A* (2018) 115(1):157–61. doi: 10.1073/pnas.1712901115
121. Mu Q, Tavella VJ, Luo XM. Role of Lactobacillus Reuteri in Human Health and Diseases. *Front Microbiol* (2018) 9. doi: 10.3389/fmicb.2018.00757
122. Ananthakrishnan AN, Higuchi LM, Huang ES, Khalili H, Richter JM, Fuchs CS, et al. Aspirin, Nonsteroidal Anti-Inflammatory Drug Use, and Risk for Crohn Disease and Ulcerative Colitis: A Cohort Study. *Ann Internal Med* (2012) 156(5):350–9. doi: 10.7326/0003-4819-156-5-201203060-00007
123. Grover S, Dougan M, Tyan K, Giobbie-Hurder A, Blum SM, Ishizuka J, et al. Vitamin D Intake is Associated With Decreased Risk of Immune Checkpoint Inhibitor-Induced Colitis. *Cancer* (2020) 126(16):3758–67. doi: 10.1002/cncr.32966
124. Tyan K, Grover S, Dougan M, Sullivan RJ, Giobbie-Hurder A, Blum S, et al. Association of Vitamin D Intake With Decreased Risk of Immune Checkpoint Inhibitor-Induced Colitis. *J Clin Oncol* (2020) 38(5):S89. doi: 10.1200/JCO.2020.38.5_suppl.89
125. Bowyer S, Prithviraj P, Lorigan P, Larkin J, McArthur G, Atkinson V, et al. Efficacy and Toxicity of Treatment With the Anti-CTLA-4 Antibody Ipilimumab in Patients With Metastatic Melanoma After Prior Anti-PD-1 Therapy. *Br J Cancer* (2016) 114(10):1084–9. doi: 10.1038/bjc.2016.107
126. Menzies AM, Johnson DB, Ramanujam S, Atkinson VG, Wong ANM, Park JJ, et al. Anti-PD-1 Therapy in Patients With Advanced Melanoma and Preexisting Autoimmune Disorders or Major Toxicity With Ipilimumab. *Ann Oncol* (2017) 28(2):368–76. doi: 10.1093/annonc/mdw443
127. Wolchok JD, Neyns B, Linette G, Negrier S, Lutzky J, Thomas L, et al. Ipilimumab Monotherapy in Patients With Pretreated Advanced Melanoma: A Randomised, Double-Blind, Multicentre, Phase 2, Dose-Ranging Study. *Lancet Oncol* (2010) 11(2):155–64. doi: 10.1016/S1470-2045(09)70334-1
128. Kumar V, Chaudhary N, Garg M, Floudas CS, Soni P, Chandra AB. Current Diagnosis and Management of Immune Related Adverse Events (irAEs) Induced by Immune Checkpoint Inhibitor Therapy. *Front Pharmacol* (2017) 8. doi: 10.3389/fphar.2017.00049
129. Johnson DB, Sullivan RJ, Ott PA, Carlino MS, Khushalani NI, Ye F, et al. Ipilimumab Therapy in Patients With Advanced Melanoma and Preexisting Autoimmune Disorders. *JAMA Oncol* (2016) 2(2):234–40. doi: 10.1001/jamaoncol.2015.4368
130. Kaehler KC, Eigentler TK, Gesierich A, Heinzerling L, Loquai C, Meier F, et al. Ipilimumab in Metastatic Melanoma Patients With Pre-Existing Autoimmune Disorders. *Cancer Immunol Immunother* (2018) 67(5):825–34. doi: 10.1007/s00262-018-2134-z
131. Bishay K, Tandon P, Bourassa-Blanchette S, Laurie SA, McCurdy JD. The Risk of Diarrhea and Colitis in Patients With Lung Cancer Treated With

Immune Checkpoint Inhibitors: A Systematic Review and Meta-Analysis. *Curr Oncol (Toronto Ont)* (2020) 27(5):486–94. doi: 10.3747/co.27.6251

132. Paz-Ares L, Ciuleanu T-E, Cobo M, Schenker M, Zurawski B, Menezes J, et al. First-Line Nivolumab Plus Ipilimumab Combined With Two Cycles of Chemotherapy in Patients With Non-Small-Cell Lung Cancer (CheckMate 9LA): An International, Randomised, Open-Label, Phase 3 Trial. *Lancet Oncol* (2021) 22(2):198–211. doi: 10.1016/S1470-2045(20)30641-0
133. Hellmann MD, Paz-Ares L, Bernabe Caro R, Zurawski B, Kim SW, Carcereny Costa E, et al. Nivolumab Plus Ipilimumab in Advanced Non-Small-Cell Lung Cancer. *N Engl J Med* (2019) 381(21):2020–31. doi: 10.1056/NEJMoa1910231
134. Antonia S, Goldberg SB, Balmanoukian A, Chaft JE, Sanborn RE, Gupta A, et al. Safety and Antitumour Activity of Durvalumab Plus Tremelimumab in Non-Small-Cell Lung Cancer: A Multicentre, Phase 1b Study. *Lancet Oncol* (2016) 17(3):299–308. doi: 10.1016/S1470-2045(15)00544-6
135. Rocco D, Gravara LD, Gridelli C. The New Immunotherapy Combinations in the Treatment of Advanced Non-Small Cell Lung Cancer: Reality and Perspectives Open Access Plus. *Curr Clin Pharmacol* (2020) 15(1):11–9. doi: 10.2174/1574884714666190809124555
136. Weber JS, Gibney G, Sullivan RJ, Sosman JA, Slingluff CLJr., Lawrence DP, et al. Sequential Administration of Nivolumab and Ipilimumab With a Planned Switch in Patients With Advanced Melanoma (CheckMate 064): An Open-Label, Randomised, Phase 2 Trial. *Lancet Oncol* (2016) 17(7):943–55. doi: 10.1016/S1470-2045(16)30126-7
137. Sznol M, Ferrucci PF, Hogg D, Atkins MB, Wolter P, Guidoboni M, et al. Pooled Analysis Safety Profile of Nivolumab and Ipilimumab Combination Therapy in Patients With Advanced Melanoma. *J Clin Oncol* (2017) 35(34):3815–+. doi: 10.1200/JCO.2016.72.1167
138. Geng Y, Zhang Q, Feng S, Li C, Wang L, Zhao X, et al. Safety and Efficacy of Combination Therapy Using Programmed Cell Death Protein-1/Programmed Cell Death Ligand-1 Inhibitors and Radiotherapy in Patients With Non-Small-Cell Lung Cancer: A Systematic Review and Meta-Analysis. *Cancer Med* (2021) 10(4):1222–39. doi: 10.1002/cam4.3718
139. Wang M, Liang H, Wang W, Zhao S, Cai X, Zhao Y, et al. Immune-Related Adverse Events of a PD-(L)1 Inhibitor Plus Chemotherapy Versus a PD-(L)1 Inhibitor Alone in First-Line Treatment for Advanced Non-Small Cell Lung Cancer: A Meta-Analysis of Randomized Control Trials. *Cancer* (2021) 127(5):777–86. doi: 10.1002/cncr.33270
140. Fujisawa Y, Yoshino K, Otsuka A, Funakoshi T, Fujimura T, Yamamoto Y, et al. Fluctuations in Routine Blood Count Might Signal Severe Immune-Related Adverse Events in Melanoma Patients Treated With Nivolumab. *J Dermatol Sci* (2017) 88(2):225–31. doi: 10.1016/j.jdermsci.2017.07.007
141. Manson G, Norwood J, Marabelle A, Kohrt H, Houot R. Biomarkers Associated With Checkpoint Inhibitors. *Ann Oncol* (2016) 27(7):1199–206. doi: 10.1093/annonc/mdw181
142. Tarhini AA, Zahoor H, Lin Y, Malhotra U, Sander C, Butterfield LH, et al. Baseline Circulating IL-17 Predicts Toxicity While TGF-Beta 1 and IL-10 are Prognostic of Relapse in Ipilimumab Neoadjuvant Therapy of Melanoma. *J Immunother Cancer* (2015) 3:39. doi: 10.1186/s40425-015-0081-1
143. Tyan K, Baginska J, Brainard M, Giobbie-Hurder A, Severgnini M, Manos M, et al. Cytokine Changes During Immune-Related Adverse Events and Corticosteroid Treatment in Melanoma Patients Receiving Immune Checkpoint Inhibitors. *Cancer Immunol Immunother* (2021) 70(8):2209–21. doi: 10.1007/s00262-021-02855-1
144. Meshkibaf S, Martins AJ, Henry GT, Kim SO. Protective Role of G-CSF in Dextran Sulfate Sodium-Induced Acute Colitis Through Generating Gut-Homing Macrophages. *Cytokine* (2016) 78:69–78. doi: 10.1016/j.cyto.2015.11.025
145. Shahabi V, Berman D, Chasalow SD, Wang L, Tsuchihashi Z, Hu B, et al. Gene Expression Profiling of Whole Blood in Ipilimumab-Treated Patients for Identification of Potential Biomarkers of Immune-Related Gastrointestinal Adverse Events. *J Trans Med* (2013) 11:75. doi: 10.1186/1479-5876-11-75
146. Di Giacomo AM, Biagioli M, Maio M. The Emerging Toxicity Profiles of Anti-CTLA-4 Antibodies Across Clinical Indications. *Semin Oncol* (2010) 37(5):499–507. doi: 10.1053/j.seminoncol.2010.09.007
147. *NCI Common Terminology Criteria for Adverse Events (CTCAE) Data Files* . Available at: https://ctep.cancer.gov/protocolDevelopment/electronic_applications/ctc.htm#ctc_50.
148. Martins F, Sofiya L, Sykiotis GP, Lamine F, Maillard M, Fraga M, et al. Adverse Effects of Immune-Checkpoint Inhibitors: Epidemiology, Management and Surveillance. *Nat Rev Clin Oncol* (2019) 16(9):563–80. doi: 10.1038/s41571-019-0218-0
149. Garcia-Neuer M, Marmarelis ME, Jangi SR, Luke JJ, Ibrahim N, Davis M, et al. Diagnostic Comparison of CT Scans and Colonoscopy for Immune-Related Colitis in Ipilimumab-Treated Advanced Melanoma Patients. *Cancer Immunol Res* (2017) 5(4):286–91. doi: 10.1158/2326-6066.CIR-16-0302
150. Barina AR, Bashir MR, Howard BA, Hanks BA, Salama AK, Jaffe TA. Isolated Recto-Sigmoid Colitis: A New Imaging Pattern of Ipilimumab-Associated Colitis. *Abdom Radiol* (2016) 41(2):207–14. doi: 10.1007/s00261-015-0560-3
151. Gupta A, De Felice KM, Loftus EVJr., Khanna S. Systematic Review: Colitis Associated With Anti-CTLA-4 Therapy. *Aliment Pharmacol Ther* (2015) 42(4):406–17. doi: 10.1111/apt.13281
152. Mekki A, Dercle L, Lichtenstein P, Marabelle A, Michot J-M, Lambotte O, et al. Detection of Immune-Related Adverse Events by Medical Imaging in Patients Treated With Anti-Programmed Cell Death 1. *Eur J Cancer* (2018) 96:91–104. doi: 10.1016/j.ejca.2018.03.006
153. Tirumani SH, Ramaiya NH, Keraliya A, Bailey ND, Ott PA, Hodi FS, et al. Radiographic Profiling of Immune-Related Adverse Events in Advanced Melanoma Patients Treated With Ipilimumab. *Cancer Immunol Res* (2015) 3(10):1185–92. doi: 10.1158/2326-6066.CIR-15-0102
154. Kim KW, Ramaiya NH, Krajewski KM, Shinagare AB, Howard SA, Jagannathan JP, et al. Ipilimumab-Associated Colitis: CT Findings. *Am J Roentgenol* (2013) 200(5):W468–74. doi: 10.2214/AJR.12.9751
155. Mitchell KA, Kluger H, Sznol M, Hartman DJ. Ipilimumab-Induced Perforating Colitis. *J Clin Gastroenterol* (2013) 47(9):781–5. doi: 10.1097/MCG.0b013e31828f1d51
156. Abolhassani A-R, Schuler G, Kirchberger MC, Heinzerling L. C-Reactive Protein as an Early Marker of Immune-Related Adverse Events. *J Cancer Res Clin Oncol* (2019) 145(10):2625–31. doi: 10.1007/s00432-019-03002-1
157. Schindler K, Harmankaya K, Kuk D, Mangana J, Michielin O, Hoeller C, et al. Correlation of Absolute and Relative Eosinophil Counts With Immune-Related Adverse Events in Melanoma Patients Treated With Ipilimumab. *J Clin Oncol* (2014) 32(15):S9096. doi: 10.1200/jco.2014.32.15_suppl.9096
158. Nakamura Y, Tanaka R, Maruyama H, Ishitsuka Y, Okiyama N, Watanabe R, et al. Correlation Between Blood Cell Count and Outcome of Melanoma Patients Treated With Anti-PD-1 Antibodies. *Jpn J Clin Oncol* (2019) 49(5):431–7. doi: 10.1093/jjco/hyy201
159. Zou F, Wang X, Glitza IC, McQuade JL, Wang J, Zhang HC, et al. Fecal Calprotectin Concentration to Assess Endoscopic and Histologic Remission in Patients With Cancer With Immune-Mediated Diarrhea and Colitis. *J Immunother Cancer* (2021) 9(1):1. doi: 10.1136/jitc-2020-002058
160. Wright AP, Piper MS, Bishu S, Stidham RW. Systematic Review and Case Series: Flexible Sigmoidoscopy Identifies Most Cases of Checkpoint Inhibitor-Induced Colitis. *Aliment Pharmacol Ther* (2019) 49(12):1474–83. doi: 10.1111/apt.15263
161. Herlihy JD, Beasley S, Simmelink A, Maddukuri V, Amin A, Kamionek M, et al. Flexible Sigmoidoscopy Rather Than Colonoscopy Is Adequate for the Diagnosis of Ipilimumab-Associated Colitis. *South Med J* (2019) 112(3):154–8. doi: 10.14423/SMJ.0000000000000944
162. Dougan M. Checkpoint Blockade Toxicity and Immune Homeostasis in the Gastrointestinal Tract. *Front Immunol* (2017) 8. doi: 10.3389/fimmu.2017.01547
163. van der Heide H, van den Brandt-Gradel V, Tytgat GN, Endert E, Wiltink EH, Schipper ME, et al. Comparison of Beclomethasone Dipropionate and Prednisolone 21-Phosphate Enemas in the Treatment of Ulcerative Proctitis. *J Clin Gastroenterol* (1988) 10(2):169–72. doi: 10.1097/00004836-198804000-00013
164. Verschuren EC, van den Eertwegh AJ, Wonders J, Slangen RM, van Delft F, van Bodegraven A, et al. Clinical, Endoscopic, and Histologic Characteristics of Ipilimumab-Associated Colitis. *Clin Gastroenterol Hepatol* (2016) 14(6):836–42. doi: 10.1016/j.cgh.2015.12.028

165. Hughes MS, Molina GE, Chen ST, Zheng H, Deshpande V, Fadden R, et al. Budesonide Treatment for Microscopic Colitis From Immune Checkpoint Inhibitors. *J Immunother Cancer* (2019) 7(1):292. doi: 10.1186/s40425-019-0756-0
166. Abu-Sbeih H, Ali FS, Luo W, Qiao W, Raju GS, Wang Y. Importance of Endoscopic and Histological Evaluation in the Management of Immune Checkpoint Inhibitor-Induced Colitis. *J Immunother Cancer* (2018) 6(1):95. doi: 10.1186/s40425-018-0411-1
167. Jain A, Lipson EJ, Sharfman WH, Brant SR, Lazarev MG. Colonic Ulcerations may Predict Steroid-Refractory Course in Patients With Ipilimumab-Mediated Enterocolitis. *World J Gastroenterol* (2017) 23 (11):2023–8. doi: 10.3748/wjg.v23.i11.2023
168. Patil PA, Zhang X. Pathologic Manifestations of Gastrointestinal and Hepatobiliary Injury in Immune Checkpoint Inhibitor Therapy. *Arch Pathol Lab Med* (2021) 145(5):571–82. doi: 10.5858/arpa.2020-0070-RA
169. Zhang ML, Neyaz A, Patil D, Chen J, Dougan M, Deshpande V. Immune-Related Adverse Events in the Gastrointestinal Tract: Diagnostic Utility of Upper Gastrointestinal Biopsies. *Histopathology* (2020) 76(2):233–43. doi: 10.1111/his.13963
170. Shivaj UN, Jeffery L, Gui X, Smith SCL, Ahmad OF, Akbar A, et al. Immune Checkpoint Inhibitor-Associated Gastrointestinal and Hepatic Adverse Events and Their Management. *Ther Adv Gastroenterol* (2019) 12:1756284819884196. doi: 10.1177/1756284819884196
171. Karamchandani DM, Chetty R. Immune Checkpoint Inhibitor-Induced Gastrointestinal and Hepatic Injury: Pathologists' Perspective. *J Clin Pathol* (2018) 71(8):665–71. doi: 10.1136/jclinpath-2018-205143
172. Chen JH, Pezhouh MK, Lauwers GY, Masia R. Histopathologic Features of Colitis Due to Immunotherapy With Anti-PD-1 Antibodies. *Am J Surg Pathol* (2017) 41(5):643–54. doi: 10.1097/PAS.0000000000000829
173. Star KV, Ho VT, Wang HH, Odze RD. Histologic Features in Colon Biopsies Can Discriminate Mycophenolate From GVHD-Induced Colitis. *Am J Surg Pathol* (2013) 37(9):1319–28. doi: 10.1097/PAS.0b013e31829ab1ef
174. Sakellariou S, Zouki DN, Ziogas DC, Pouloudi D, Gogas H, Delladetsima I. Granulomatous Colitis in a Patient With Metastatic Melanoma Under Immunotherapy: A Case Report and Literature Review. *BMC Gastroenterol* (2021) 21(1):227. doi: 10.1186/s12876-021-01812-7
175. Bavi P, Butler M, Serra S, Chetty R. Immune Modulator-Induced Changes in the Gastrointestinal Tract. *Histopathology* (2017) 71(3):494–6. doi: 10.1111/his.13224
176. Garcia-Varona A, Odze RD, Makrauer F. Lymphocytic Colitis Secondary to Ipilimumab Treatment. *Inflamm Bowel Dis* (2013) 19(2):E15–6. doi: 10.1002/ibd.22846
177. St Romain PE, Salama AKS, Ferguson NL, Burbridge RA. Ipilimumab-Associated Lymphocytic Colitis: A Case Report. *Trans Gastrointest Cancer* (2016) 5(1):44–6. doi: 10.3978/j.issn.2224-4778
178. Ayata G, Ithamukkala S, Sapp H, Shaz BH, Brien TP, Wang HH, et al. Prevalence and Significance of Inflammatory Bowel Disease-Like Morphologic Features in Collagenous and Lymphocytic Colitis. *Am J Surg Pathol* (2002) 26(11):1414–23. doi: 10.1097/00000478-200211000-00003
179. Choi K, Abu-Sbeih H, Samdani R, Gonzalez GN, Raju GS, Richards DM, et al. Can Immune Checkpoint Inhibitors Induce Microscopic Colitis or a Brand New Entity? *Inflamm Bowel Dis* (2019) 25(2):385–93. doi: 10.1093/ibd/izy240
180. Du-Thanh A, Pallure V, Girard C, Dereure O, Guillot B. Clostridium Difficile Infection may Loom Behind Ipilimumab-Induced Auto-Immune Colitis. *Eur J Dermatol* (2015) 25(4):344–4. doi: 10.1684/ejd.2015.2561
181. Ledezma B, Binder S, Hamid O. Atypical Clinical Response Patterns to Ipilimumab: Four Case Studies of Advanced Melanoma. *Clin J Oncol Nurs* (2011) 15(4):393–403. doi: 10.1188/11.CJON.393-403
182. Adler BL, Pezhouh MK, Kim A, Luan L, Zhu Q, Gani F, et al. Histopathological and Immunophenotypic Features of Ipilimumab-Associated Colitis Compared to Ulcerative Colitis. *J Internal Med* (2018) 283(6):568–77. doi: 10.1111/joim.12744
183. Brahmer JR, Lacchetti C, Schneider BJ, Atkins MB, Brassil KJ, Caterino JM, et al. Management of Immune-Related Adverse Events in Patients Treated With Immune Checkpoint Inhibitor Therapy: American Society of Clinical Oncology Clinical Practice Guideline. *J Clin Oncol* (2018) 36(17):1714–+. doi: 10.1200/JCO.2017.77.6385
184. Friedman CF, Proverbs-Singh TA, Postow MA. Treatment of the Immune-Related Adverse Effects of Immune Checkpoint Inhibitors: A Review. *JAMA Oncol* (2016) 2(10):1346–53. doi: 10.1001/jamaoncol.2016.1051
185. Collins M, Michot JM, Danlos FX, Mussini C, Soularue E, Mateus C, et al. Inflammatory Gastrointestinal Diseases Associated With PD-1 Blockade Antibodies. *Ann Oncol* (2017) 28(11):2860–5. doi: 10.1093/annonc/mdx403
186. Thompson JA, Schneider BJ, Brahmer J, Andrews S, Armand P, Bhatia S, et al. Management of Immunotherapy-Related Toxicities. Version 1.2019. *J Natl Compr Cancer Netw* (2019) 17(3):255–88. doi: 10.6004/jnccn.2019.0013
187. Grover S, Rahma OE, Hashemi N, Lim RM. Gastrointestinal and Hepatic Toxicities of Checkpoint Inhibitors: Algorithms for Management. *Am Soc Clin Oncol Educ Book* (2018) 38:13–9. doi: 10.1200/EDBK_100013
188. Thompson LL, Katznelson E, Leet DE, Durbin SM, Yoon J, Reynolds KL, et al. Impact of Systemic Corticosteroids on Survival Outcomes in Immune Checkpoint Inhibitor-Induced Gastroenterocolitis. *Eur J Cancer (Oxford Engl 1990)* (2021) 142:143–6. doi: 10.1016/j.ejca.2020.09.022
189. Faje AT, Lawrence D, Flaherty K, Freedman C, Fadden R, Rubin K, et al. High-Dose Glucocorticoids for the Treatment of Ipilimumab-Induced Hypophysitis is Associated With Reduced Survival in Patients With Melanoma. *Cancer* (2018) 124(18):3706–14. doi: 10.1002/cncr.31629
190. Horvat TZ, Adel NG, Thu-Oanh D, Momtaz P, Postow MA, Callahan MK, et al. Immune-Related Adverse Events, Need for Systemic Immunosuppression, and Effects on Survival and Time to Treatment Failure in Patients With Melanoma Treated With Ipilimumab at Memorial Sloan Kettering Cancer Center. *J Clin Oncol* (2015) 33(28):3193–+. doi: 10.1200/JCO.2015.60.8448
191. Favara DM, Spain L, Au L, Clark J, Daniels E, Diem S, et al. Five-Year Review of Corticosteroid Duration and Complications in the Management of Immune Checkpoint Inhibitor-Related Diarrhoea and Colitis in Advanced Melanoma. *ESMO Open* (2020) 5(4):e000585. doi: 10.1136/esmoopen-2019-000585
192. Baden LR, Swaminathan S, Angarone M, Blouin G, Camins BC, Casper C, et al. Prevention and Treatment of Cancer-Related Infections, Version 2.2016. *J Natl Compr Cancer Netw* (2016) 14(7):882–913. doi: 10.6004/jnccn.2016.0093
193. Pernot S, Ramtohul T, Taieb J. Checkpoint Inhibitors and Gastrointestinal Immune-Related Adverse Events. *Curr Opin Oncol* (2016) 28(4):264–8. doi: 10.1097/CCO.0000000000000292
194. Kähler KC, Hassel JC, Heinzerling L, Loquai C, Mössner R, Ugurel S, et al. Management of Side Effects of Immune Checkpoint Blockade by Anti-CTLA-4 and Anti-PD-1 Antibodies in Metastatic Melanoma. *J Dtsch Dermatol Ges* (2016) 14(7):662–81. doi: 10.1111/ddg.13047
195. Abu-Sbeih H, Ali FS, Naqash AR, Owen DH, Patel S, Otterson GA, et al. Resumption of Immune Checkpoint Inhibitor Therapy After Immune-Mediated Colitis. *J Clin Oncol* (2019) 37(30):2738–45. doi: 10.1200/JCO.19.00320
196. Lo YC, Price C, Blenman K, Patil P, Zhang X, Robert ME. Checkpoint Inhibitor Colitis Shows Drug-Specific Differences in Immune Cell Reaction That Overlap With Inflammatory Bowel Disease and Predict Response to Colitis Therapy. *Am J Clin Pathol* (2021) 156(2):214–28. doi: 10.1093/ajcp/aqaa217
197. Johnson DH, Zobniw CM, Trinh VA, Ma J, Bassett RLJr., Abdel-Wahab N, et al. Infliximab Associated With Faster Symptom Resolution Compared With Corticosteroids Alone for the Management of Immune-Related Enterocolitis. *J Immunother Cancer* (2018) 6(1):103. doi: 10.1186/s40425-018-0412-0
198. Johnston RL, Lutzky J, Chodhry A, Barkin JS. Cytotoxic T-Lymphocyte-Associated Antigen 4 Antibody-Induced Colitis and its Management With Infliximab. *Dig Dis Sci* (2009) 54(11):2538–40. doi: 10.1007/s10620-008-0641-z
199. Zhang HC, Luo W, Wang Y. Acute Liver Injury in the Context of Immune Checkpoint Inhibitor-Related Colitis Treated With Infliximab. *J Immunother Cancer* (2019) 7(1):47. doi: 10.1186/s40425-019-0532-1
200. Robert C, Long GV, Brady B, Dutriaux C, Maio M, Mortier L, et al. Nivolumab in Previously Untreated Melanoma Without BRAF Mutation. *N Engl J Med* (2015) 372(4):320–30. doi: 10.1056/NEJMoa1412082
201. Rastogi P, Sultan M, Charabaty AJ, Atkins MB, Mattar MC. Ipilimumab Associated Colitis: An IpiColitis Case Series at MedStar Georgetown

University Hospital. *World J Gastroenterol* (2015) 21(14):4373–8. doi: 10.3748/wjg.v21.i14.4373
202. Cohn HM, Dave M, Loftus EVJr. Understanding the Cautions and Contraindications of Immunomodulator and Biologic Therapies for Use in Inflammatory Bowel Disease. *Inflamm Bowel Dis* (2017) 23(8):301–15. doi: 10.1097/MIB.0000000000001199
203. Martins F, Sykiotis GP, Maillard M, Fraga M, Ribi C, Kuntzer T, et al. New Therapeutic Perspectives to Manage Refractory Immune Checkpoint-Related Toxicities. *Lancet Oncol* (2019) 20(1):e54–64. doi: 10.1016/S1470-2045(18)30828-3
204. Onuki T, Morita E, Sakamoto N, Nagai Y, Sata M, Hagiwara K. Severe Upper Gastrointestinal Disorders in Pembrolizumab-Treated Non-Small Cell Lung Cancer Patient. *Respirol Case Rep* (2018) 6(6):e00334. doi: 10.1002/rcr2.334
205. Abu-Sbeih H, Ali FS, Alsaadi D, Jennings J, Luo W, Gong Z, et al. Outcomes of Vedolizumab Therapy in Patients With Immune Checkpoint Inhibitor-Induced Colitis: A Multi-Center Study. *J Immunother Cancer* (2018) 6(1):142. doi: 10.1186/s40425-018-0461-4
206. Bergqvist V, Hertervig E, Gedeon P, Kopljar M, Griph H, Kinhult S, et al. Vedolizumab Treatment for Immune Checkpoint Inhibitor-Induced Enterocolitis. *Cancer Immunol Immunother* (2017) 66(5):581–92. doi: 10.1007/s00262-017-1962-6
207. Hsieh AH, Ferman M, Brown MP, Andrews JM. Vedolizumab: A Novel Treatment for Ipilimumab-Induced Colitis. *BMJ Case Rep* (2016) 2016: bcr2016216641. doi: 10.1136/bcr-2016-216641
208. Abu-Sbeih H, Ali FS, Wang X, Mallepally N, Chen E, Altan M, et al. Early Introduction of Selective Immunosuppressive Therapy Associated With Favorable Clinical Outcomes in Patients With Immune Checkpoint Inhibitor-Induced Colitis. *J Immunother Cancer* (2019) 7(1):93. doi: 10.1186/s40425-019-0577-1
209. Thomas AS, Ma W, Wang Y. Ustekinumab for Refractory Colitis Associated With Immune Checkpoint Inhibitors. *N Engl J Med* (2021) 384(6):581–3. doi: 10.1056/NEJMc2031717
210. Mir R, Shaw HM, Nathan PD. Mycophenolate Mofetil Alongside High-Dose Corticosteroids: Optimizing the Management of Combination Immune Checkpoint Inhibitor-Induced Colitis. *Melanoma Res* (2019) 29(1):102–6. doi: 10.1097/CMR.0000000000000543
211. Alcantar D, Al-Jaashaami L, Giron F. A Case of Immune Checkpoint Inhibitor Refractory Colitis Treated With Mycophenolate and High-Dose Steroids. *Cureus* (2019) 11(12):e6392. doi: 10.7759/cureus.6392
212. Bishu S, Melia J, Sharfman W, Lao CD, Fecher LA, Higgins PDR. Efficacy and Outcome of Tofacitinib in Immune Checkpoint Inhibitor Colitis. *Gastroenterology* (2021) 160(3):932–4.e933. doi: 10.1053/j.gastro.2020.10.029
213. Wang Y, Wiesnoski DH, Helmink BA, Gopalakrishnan V, Choi K, DuPont HL, et al. Fecal Microbiota Transplantation for Refractory Immune Checkpoint Inhibitor-Associated Colitis. *Nat Med* (2018) 24(12):1804–8. doi: 10.1038/s41591-018-0238-9
214. Fasanello MK, Robillard KT, Boland PM, Bain AJ, Kanehira K. Use of Fecal Microbial Transplantation for Immune Checkpoint Inhibitor Colitis. *ACG Case Rep J* (2020) 7(4):e00360. doi: 10.14309/crj.0000000000000360
215. Smith FO, Goff SL, Klapper JA, Levy C, Allen T, Mavroukakis SA, et al. Risk of Bowel Perforation in Patients Receiving Interleukin-2 After Therapy With Anti-CTLA 4 Monoclonal Antibody. *J Immunother* (2007) 30(1):130–0. doi: 10.1097/01.cji.0000211334.06762.89
216. Abu-Sbeih H, Ali FS, Qiao W, Lu Y, Patel S, Diab A, et al. Immune Checkpoint Inhibitor-Induced Colitis as a Predictor of Survival in Metastatic Melanoma. *Cancer Immunol Immunother* (2019) 68(4):553–61. doi: 10.1007/s00262-019-02303-1
217. Molina GE, Allen IM, Hughes MS, Zubiri L, Lee H, Mooradian MJ, et al. Prognostic Implications of Co-Occurring Dermatologic and Gastrointestinal Toxicity From Immune Checkpoint Inhibition Therapy for Advanced Malignancies: A Retrospective Cohort Study. *J Am Acad Dermatol* (2020) 82(3):743–6. doi: 10.1016/j.jaad.2019.07.049
218. Ezponda Casajus A, Calvo Imirizaldu M, de Torres Tajes JP, Garcia-Baizan A, Castanon Alvarez E, Cano Rafart D, et al. Immune-Related Adverse Events as Predictors of Response in Cancer Patients Undergoing Immunotherapy. *Radiologia* (2020) 62(2):131–8. doi: 10.1016/j.rxeng.2019.10.006
219. Masuda K, Shoji H, Nagashima K, Yamamoto S, Ishikawa M, Imazeki H, et al. Correlation Between Immune-Related Adverse Events and Prognosis in Patients With Gastric Cancer Treated With Nivolumab. *BMC Cancer* (2019) 19(1):974. doi: 10.1186/s12885-019-6150-y
220. Pollack MH, Betof A, Dearden H, Rapazzo K, Valentine I, Brohl AS, et al. Safety of Resuming Anti-PD-1 in Patients With Immune-Related Adverse Events (irAEs) During Combined Anti-CTLA-4 and Anti-PD1 in Metastatic Melanoma. *Ann Oncol* (2018) 29(1):250–5. doi: 10.1093/annonc/mdx642
221. Freeman-Keller M, Kim Y, Cronin H, Richards A, Gibney G, Weber JS. Nivolumab in Resected and Unresectable Metastatic Melanoma: Characteristics of Immune-Related Adverse Events and Association With Outcomes. *Clin Cancer Res* (2016) 22(4):886–94. doi: 10.1158/1078-0432.CCR-15-1136
222. Weber JS, Hodi FS, Wolchok JD, Topalian SL, Schadendorf D, Larkin J, et al. Safety Profile of Nivolumab Monotherapy: A Pooled Analysis of Patients With Advanced Melanoma. *J Clin Oncol* (2017) 35(7):785–+. doi: 10.1200/JCO.2015.66.1389
223. Lauwyck J, Beckwee A, Santens A, Schwarze JK, Awada G, Vandersleyen V, et al. C-Reactive Protein as a Biomarker for Immune-Related Adverse Events in Melanoma Patients Treated With Immune Checkpoint Inhibitors in the Adjuvant Setting. *Melanoma Res* (2021) 31(4):371–7. doi: 10.1097/CMR.0000000000000748
224. Abu-Sbeih H, Herrera LN, Tang T, Altan M, Chaftari AP, Okhuysen PC, et al. Impact of Antibiotic Therapy on the Development and Response to Treatment of Immune Checkpoint Inhibitor-Mediated Diarrhea and Colitis. *J Immunother Cancer* (2019) 7(1):242. doi: 10.1186/s40425-019-0714-x
225. Simonaggio A, Michot JM, Voisin AL, Le Pavec J, Collins M, Lallart A, et al. Evaluation of Readministration of Immune Checkpoint Inhibitors After Immune-Related Adverse Events in Patients With Cancer. *JAMA Oncol* (2019) 5(9):1310–7. doi: 10.1001/jamaoncol.2019.1022
226. Haanen J, Ernstoff M, Wang Y, Menzies A, Puzanov I, Grivas P, et al. Rechallenge Patients With Immune Checkpoint Inhibitors Following Severe Immune-Related Adverse Events: Review of the Literature and Suggested Prophylactic Strategy. *J Immunother Cancer* (2020) 8(1):e000604. doi: 10.1136/jitc-2020-000604
227. Dolladille C, Ederhy S, Sassier M, Cautela J, Thuny F, Cohen AA, et al. Immune Checkpoint Inhibitor Rechallenge After Immune-Related Adverse Events in Patients With Cancer. *JAMA Oncol* (2020) 6(6):865–71. doi: 10.1001/jamaoncol.2020.0726
228. Park R, Lopes L, Saeed A. Outcomes Following Immunotherapy Re-Challenge After Immune-Related Adverse Event: Systematic Review and Meta-Analysis. *Immunotherapy* (2020) 12(16):1183–93. doi: 10.2217/imt-2020-0103
229. Abou Alaiwi S, Xie W, Nassar AH, Dudani S, Martini D, Bakouny Z, et al. Safety and Efficacy of Restarting Immune Checkpoint Inhibitors After Clinically Significant Immune-Related Adverse Events in Metastatic Renal Cell Carcinoma. *J Immunother Cancer* (2020) 8(1):e000144. doi: 10.1136/jitc-2019-000144
230. Kitagawa S, Hakozaki T, Kitadai R, Hosomi Y. Switching Administration of Anti-PD-1 and Anti-PD-L1 Antibodies as Immune Checkpoint Inhibitor Rechallenge in Individuals With Advanced Non-Small Cell Lung Cancer: Case Series and Literature Review. *Thorac Cancer* (2020) 11(7):1927–33. doi: 10.1111/1759-7714.13483
231. Gobbini E, Toffart AC, Perol M, Assie J-B, Duruisseaux M, Coupez D, et al. Immune Checkpoint Inhibitors Rechallenge Efficacy in Non-Small-Cell Lung Cancer Patients. *Clin Lung Cancer* (2020) 21(5):E497–510. doi: 10.1016/j.cllc.2020.04.013
232. Kartolo A, Holstead R, Khalid S, Emack J, Hopman W, Baetz T. Safety of Immunotherapy Rechallenge After Immune-Related Adverse Events in Patients With Advanced Cancer. *J Immunother* (2021) 44(1):41–8. doi: 10.1097/CJI.0000000000000337
233. Allouchery M, Lombard T, Martin M, Rouby F, Sassier M, Bertin C, et al. Safety of Immune Checkpoint Inhibitor Rechallenge After Discontinuation for Grade >= 2 Immune-Related Adverse Events in Patients With Cancer. *J Immunother Cancer* (2020) 8(2):1. doi: 10.1136/jitc-2020-001622

234. Santini FC, Rizvi H, Plodkowski AJ, Ni A, Lacouture ME, Gambarin-Gelwan M, et al. *Et Al*: Safety and Efficacy of Re-Treating With Immunotherapy After Immune-Related Adverse Events in Patients With NSCLC. *Cancer Immunol Res* (2018) 6(9):1093–9. doi: 10.1158/2326-6066.CIR-17-0755
235. Levra MG, Cotte F-E, Corre R, Calvet C, Gaudin A-F, Penrod JR, et al. Immunotherapy Rechallenge After Nivolumab Treatment in Advanced Non Small Cell Lung Cancer in the Real-World Setting: A National Data Base Analysis. *Lung Cancer (Amsterdam Netherlands)* (2020) 140:99–106. doi: 10.1016/j.lungcan.2019.12.017
236. Ito K, Oguri T, Takeda N, Fukumitsu K, Fukuda S, Kanemitsu Y, et al. A Case of Non-Small Cell Lung Cancer With Long-Term Response After Re-Challenge With Nivolumab. *Respir Med Case Rep* (2020) 29:100979. doi: 10.1016/j.rmcr.2019.100979
237. Kaehler KC, Hassel JC, Heinzerling L, Loquai C, Moessner R, Ugurel S, et al. Management of Side Effects of Immune Checkpoint Blockade by Anti-CTLA-4 and Anti-PD-1 Antibodies in Metastatic Melanoma. *J Dtsch Dermatol Ges* (2016) 14(7):662–81. doi: 10.1111/ddg.13047
238. Bridge JA, Lee JC, Daud A, Wells JW, Bluestone JA. Cytokines, Chemokines, and Other Biomarkers of Response for Checkpoint Inhibitor Therapy in Skin Cancer. *Front Med* (2018) 5. doi: 10.3389/fmed.2018.00351
239. Khan S, Khan SA, Luo X, Fattah FJ, Saltarski J, Gloria-McCutchen Y, et al. Immune Dysregulation in Cancer Patients Developing Immune-Related Adverse Events. *Br J Cancer* (2019) 120(1):63–8. doi: 10.1038/s41416-018-0155-1
240. Head L, Gorden N, Van Gulick R, Amato CM, Frazer-Abel A, Robinson W, et al. Biomarkers to Predict Immune-Related Adverse Events With Checkpoint Inhibitors. *J Clin Oncol* (2019) 37(8):S131. doi: 10.1200/JCO.2019.37.8_suppl.131
241. Lim SY, Lee JH, Gide TN, Menzies AM, Guminski A, Carlino MS, et al. Circulating Cytokines Predict Immune-Related Toxicity in Melanoma Patients Receiving Anti-PD-1-Based Immunotherapy. *Clin Cancer Res* (2019) 25(5):1557–63. doi: 10.1158/1078-0432.CCR-18-2795
242. Scott SC, Pennell NA. Early Use of Systemic Corticosteroids in Patients With Advanced NSCLC Treated With Nivolumab. *J Thorac Oncol* (2018) 13 (11):1771–5. doi: 10.1016/j.jtho.2018.06.004
243. Fuca G, Galli G, Poggi M, Lo Russo G, Proto C, Imbimbo M, et al. Modulation of Peripheral Blood Immune Cells by Early Use of Steroids and its Association With Clinical Outcomes in Patients With Metastatic Non-Small Cell Lung Cancer Treated With Immune Checkpoint Inhibitors. *ESMO Open* (2019) 4(1):e000457. doi: 10.1136/esmoopen-2018-000457
244. Jove M, Vilarino N, Nadal E. Impact of Baseline Steroids on Efficacy of Programmed Cell Death-1 (PD-1) and Programmed Death-Ligand 1 (PD-L1) Blockade in Patients With Advanced Non-Small Cell Lung Cancer. *Trans Lung Cancer Res* (2019) 8:S364–8. doi: 10.21037/tlcr.2019.06.06
245. Gaucher L, Adda L, Sejourne A, Joachim C, Chaby G, Poulet C, et al. Impact of the Corticosteroid Indication and Administration Route on Overall Survival and the Tumor Response After Immune Checkpoint Inhibitor Initiation. *Ther Adv Med Oncol* (2021) 13:1758835921996656. doi: 10.1177/1758835921996656

Conflict of Interest: The authors declare that the research was conducted in the absence of any commercial or financial relationships that could be construed as a potential conflict of interest.

Publisher's Note: All claims expressed in this article are solely those of the authors and do not necessarily represent those of their affiliated organizations, or those of the publisher, the editors and the reviewers. Any product that may be evaluated in this article, or claim that may be made by its manufacturer, is not guaranteed or endorsed by the publisher.

Copyright © 2021 Tang, Wang, Lin, Zhou, He, Liu and Ma. This is an open-access article distributed under the terms of the Creative Commons Attribution License (CC BY). The use, distribution or reproduction in other forums is permitted, provided the original author(s) and the copyright owner(s) are credited and that the original publication in this journal is cited, in accordance with accepted academic practice. No use, distribution or reproduction is permitted which does not comply with these terms.

frontiers in Immunology

ORIGINAL RESEARCH
published: 23 December 2021
doi: 10.3389/fimmu.2021.813331

A Combination of Biomarkers Predict Response to Immune Checkpoint Blockade Therapy in Non-Small Cell Lung Cancer

Zedong Jiang[1,2†], *Yao Zhou*[1,2†] *and Juan Huang*[1*]

[1] Department of Hematology, Sichuan Academy of Medical Sciences & Sichuan Provincial People's Hospital, University of Electronic Science and Technology of China, Chengdu, China, [2] College of Bioinformatics Science and Technology, Harbin Medical University, Harbin, China

Immune checkpoint blockade (ICB) therapy has provided clinical benefits for patients with advanced non-small-cell lung cancer (NSCLC), but the majority still do not respond. Although a few biomarkers of ICB treatment response have been developed, the predictive power of these biomarkers showed substantial variation across datasets. Therefore, predicting response to ICB therapy remains a challenge. Here, we provided a concise combinatorial strategy for predicting ICB therapy response and constructed the ICB treatment signature (ITS) in lung cancer. The prediction performance of ITS has been validated in an independent ICB treatment cohort of NSCLC, where patients with higher ITS score were significantly associated with longer progression-free survival and better response. And ITS score was more powerful than traditional biomarkers, such as TMB and PD-L1, in predicting the ICB treatment response in NSCLC. In addition, ITS scores still had predictive effects in other cancer data sets, showing strong scalability and robustness. Further research showed that a high ITS score represented comprehensive immune activation characteristics including activated immune cell infiltration, increased mutation load, and TCR diversity. In conclusion, our practice suggested that the combination of biomarkers will lead to a better prediction of ICB treatment prognosis, and the ITS score will provide NSCLC patients with better ICB treatment decisions.

Keywords: immune checkpoint blockade, immunotherapy, biomarker, biomarker combinations, non-small-cell lung cancer

OPEN ACCESS

Edited by:
Hubing Shi,
Sichuan University, China

Reviewed by:
Yaming Shan,
Jilin University, China
Qi Zhao,
University of Macau, China

****Correspondence:***
Juan Huang
huangjuanxy@med.uestc.edu.cn

†These authors have contributed equally to this work and share first authorship

Specialty section:
This article was submitted to Cancer Immunity and Immunotherapy, a section of the journal Frontiers in Immunology

Received: *11 November 2021*
Accepted: *07 December 2021*
Published: *23 December 2021*

Citation:
Jiang Z, Zhou Y and Huang J (2021) A Combination of Biomarkers Predict Response to Immune Checkpoint Blockade Therapy in Non-Small Cell Lung Cancer. Front. Immunol. 12:813331. doi: 10.3389/fimmu.2021.813331

INTRODUCTION

Lung cancer is the most common malignant tumor in the world (1). In the current clinical practice, immune checkpoint therapy (2, 3) and combination therapy strategy (4, 5) has achieved amazing therapeutic effects in the treatment of cancer and have changed the clinical management of cancer. However, despite the strong improvement of these antibodies in cancer treatment, it is important to note that most patients fail to respond to ICBs or even have to stop treatment because of immune-related adverse events (6). Therefore, predicting ICB response is a key challenge in guiding patients to select current checkpoint immunotherapy and providing indicators of early treatment response.

Several biomarkers for predicting responsiveness to ICB treatment were developed. PD-L1 expression was one of the most promising biomarkers, which higher level of expression contributed better benefit. Nevertheless, some studies reported that advanced NSCLC patients with lower PD-L1 expression still benefit from anti-PD1 therapy (6–8). Tumor mutation burden (TMB) emerged as a biomarker for ICB patient stratification, in which abundant non-synonymous mutations lead to an increased number of neoantigen, potentially increasing immune recognition and response (9). Higher TMB is associated with improved prognosis and increased response rate to ICB therapies in most studies (9–11). In addition, several immune escape mechanisms hindered the application of ICB therapy (12). Decreased T-cell infiltration has been reported to be associated with a poorer prognosis (13), and TGF-β signal limits the infiltration of T cells, forming a suppressed immune microenvironment (14, 15). These mechanisms were also used to develop ICB response biomarkers, such as TIDE (16) and PAN-fibroblast TGF-β response signature (17).

Due to the complexity of factors affecting immune checkpoint therapy, current biomarkers mainly involve a single ICB response mechanism, which is not good in predicting the prognosis of non-small cell lung cancer immune checkpoint therapy (18). Therefore, it is still a meaningful topic to explore the prognostic markers of ICB in non-small cell lung cancer.

Therefore, in this study, we focused on building a combinatorial biomarker for ICB treatment in lung cancer. Firstly, we evaluated genes related to ICB response biomarkers including cytotoxic T lymphocyte (CTL) level, TMB, and TGF-β signal. Then, an ICB treatment score (ITS) for lung cancer was established by integrating these genes. The relationship of the ITS with immune activity and mutations was also analyzed. Finally, we found that the ITS is a powerful prognostic biomarker and predicts the response to immune checkpoint inhibitors.

METHOD

Data Acquisition

Gene expression with the format of fragments per kilobase million (FPKM) and mutation data of TCGA-LUAD and TCGA-LUSC sample were obtained from UCSC Xena (http://xena.ucsc.edu). For the NSCLC ICB treatment cohort, we collected gene expression and the corresponding clinical response data of ICB pre-treatment patients from the Jung et al. (19) study. We also validated the prognosis efficiency of ITS score in three additional datasets including Gide et al. (20), Van Allen et al. (21), and Mariathasan et al. (17), involving two other cancer types. RNA-seq data of these ICB treatment cohorts were obtained through the supplementary materials of original publications.

Calculation of ICB Treatment Signature (ITS) Score

We used the average expression level of CD8A, CD8B, GZMA, GZMB, and PRF1 to characterize cytotoxic T lymphocyte (CTL) levels. The TGF-β signaling score was calculated based on signatures proposed by a previous study (22). By spearman's rank correlation test, we screened genes associated with CTL and TGF-β signaling with cor greater than 0.3 and FDR less than 0.01. According to TMB, patients were equally divided into three groups, high, middle, and low, and the differential genes between TMB-high and TMB-low group screened by Wilcoxon rank-sum test were considered to be TMB-related genes. Pathway enrichment analysis of genes was carried out with a hypergeometric test described previously (23). We selected genes associated with both high CTL level and high TMB and excluded immunosuppression-related genes as the ICB treatment signature (ITS). For each sample, the ITS score was calculated by ssGSEA (24) with default parameters in the "GSVA" R package. The interaction network analysis of ITS genes was performed by the Metascape online tool (25).

Robustness Evaluation of ITS

We assessed the robustness of the prognostic power of ITS using the following methods. Firstly, ITS scores calculated by GSVA (26), Zscore (27), and PLAGE (28) with default parameters were used to evaluate whether the prognostic efficacy of ITS depended on specific scoring methods. Then, we evaluated the prognostic efficacy of signatures derived from multiple combinations of genes related to CTL, TMB, and TGF-β to discuss the necessity of three factors. And we randomly selected genes from ITS 100 times in a fixed proportion, from 0.1 to 0.9, to discuss how much does the absence of some genes in ITS effects the predictive power.

Immune-Related and Genomic Features of Lung Cancer Sample

We calculated and collected expression signatures, CIBERSORT fractions, DNA damage scores, intratumor heterogeneity (ITH), TCR/BCR diversity, stromal fraction, and Leukocyte fraction for each lung cancer sample (22). Expression signatures include proliferation, macrophages regulation, overall lymphocyte infiltration, TGF-β response, IFN-g response, and wound healing. The composition ratio of 22 immune cells in the sample was inferred using the CIBERSORT algorithm (29). Some immune cell types were aggregated to a major class including total lymphocytes, total dendritic cells, total macrophage, and total mast cells. These proportions were multiplied by leukocyte fraction, estimated from a mixture model with specific methylation probes, to yield corresponding estimates in terms of overall fraction in samples. ABSOLUTE algorithm (30) was used to calculate tumor purity, aneuploidy scores, and ITH. The stromal fraction was defined as the total non-tumor cellular component, obtained by subtracting tumor purity from unity.

Screening Features Associated With ITS Scores

We used linear mixed-effects models to associate ITS score with TME features in lung cancers using the "lme4" R package. For each feature, we compared a model with the feature to a model without this feature using an ANOVA to determine whether the

ITS score was significantly associated with this feature in lung cancers. We adjusted patient age and sex and set cancer type as a random effect in every model. This allowed us to consider a different baseline value for the feature in LUAD and LUSC. The conditional R2 was reported which reflects the variance explained by the fixed and random factors. An FDR adjustment was applied to the p-values from the linear mixed-effect model. Features with FDR less than 0.01 were considered to be correlated with ITS score.

Statistics Analysis

All statistical analyses were performed with R statistical software version 3.5.2 (http://www.R-project.org). Wilcoxon rank-sum test was used to determine the significance of differences between the two groups. The correlation between the two continuous variables was evaluated by spearman's rank correlation test. The survival curves were calculated with Kaplan-Meier estimation, and the differences between survival curves were calculated by log-rank test. The hazard ratio, multivariate analysis adjusting for clinical parameters was determined through a Cox proportional hazards model. Survival analysis was carried out using the "survminer" and "survival" R packages.

RESULTS

Identification of Immune-Related Genes Used to Construct ICB Treatment Signature in Lung Cancer

To construct an integrated ICB response biomarker, we first evaluated genes and pathways associated with three mechanisms related to ICB response (CTL, TMB, and TGF-β signaling) in lung cancer samples (see Methods). We identified 756 and 1,100 genes associated with high CTL levels in lung adenocarcinoma (LUAD) and lung squamous carcinoma (LUSC), respectively, of which 608 genes were found in both cancers (**Figures 1A**, **S1A**). Pathway enrichment analysis showed that these genes converged to immune-related pathways, including innate immune system, adaptive immune system, and various cytokine pathways (**Table S1**, **Figure 1B**). The genes associated with TMB were significantly different between the two cancer types. A large number of genes in LUAD were associated with high levels of TMB compared to LUSC (**Figure S1B**). In LUAD, TMB-related genes were mainly enriched in RNA metabolism and regulatory pathways, while in LUSC, they were mainly enriched in the cell cycle pathway (**Table S1**, **Figure 1C**).

A large number of immunosuppressive-related genes were also identified in both cancer types (**Figures 1D**, **S1C**). These genes are associated with the abnormal glycosylation and extracellular matrix organization pathway (**Table S1**, **Figure 1E**). We found that the genes associated with high CTL infiltration and high TMB level still contained a certain number of immunosuppressive-related genes, which may have a poor contribution to the prognosis of immunotherapy, so we considered excluding these genes when constructing the biomarker. Finally, by combining three mechanisms related to ICB response, we selected genes associated with both high CTL level and high TMB and excluded immunosuppressive-related genes as the ICB treatment signature (ITS). In LUAD, ITS contained 91 genes (**Figure 1G**, **Table S2**), while in LUSC only one gene passed the screening criteria (**Figure 1F**), so we used ITS obtained from LUAD as a proxy for NSCLC. A close interaction network was formed between ITS genes, and we found three functional modules in the interaction network, which were respectively related to cell killing, interferon response, and transcription factor binding (**Figure S2**).

ITS Score Predicts the Prognosis of Lung Cancer Patients With ICB Treatment

Then, we used a cohort of NSCLC patients treated with ICB therapy to evaluate the prognosis efficacy of ITS. In this cohort, 85 genes in ITS had expression information. ITS score was estimated using single-sample gene set enrichment analysis (ssGSEA) with default parameters in each patient. Patients were divided into two groups based on median ITS scores. Patients with high ITS scores had significantly better progression-free survival ($p = 0.03$; **Figure 2A**) and higher objective response rates (53.8% *VS* 7.1%, $p = 0.01$; **Figure 2B**) than patients with low ITS scores. Meanwhile, the ITS score of responders was significantly higher than that of non-responders ($p = 0.008$; **Figure 2C**). Multivariate Cox analysis showed that the ITS score was an independent prognostic factor after adjustment for age and sex (HR = 0.097, $p = 0.02$). Alternatively, other algorithms such as PLAGE, GSVA, and Zscore could also be employed to calculate the ITS score. Patients with higher ITS scores could have better survival to immunotherapy (**Figure S3**). While for the PLAGE scores, higher scores may not indicate higher activities as PLAGE calculates the first principal component as the gene-set score.

To discuss whether the combination of CTL, TMB, and TGF-β is necessary to the predictive effectiveness in prognosis or response to immunotherapy, we built various signatures based on multiple combinations of these factors. Using these three factors alone, the only score of CTL-related genes had predictive power (**Figure 2D**). And the best predictive performance was achieved only when these factors were considered simultaneously (**Figure 2D**). We further evaluated the immunotherapy prognostic ability of each gene in ITS, and only 8.2% (7/85) genes had the prognostic ability (**Figure S4A**). we randomly selected genes from ITS 100 times in a fixed proportion to investigate the robustness of prognostic ability of ITS. It can be seen from the results that when 80% of the genes in ITS are lost, it can still ensure satisfactory prognostic efficacy (**Figure S4B**). It can be seen that these genes make ITS maintain very good stability in the application process because when we apply ITS, we cannot guarantee that every gene in ITS has expression information.

We also compared the prognosis efficacy of ITS with traditional biomarkers such as PD1, PD-L1, Teff, and TMB. None of these individual markers showed satisfactory predictive power, and only the ITS score was an independent prognostic

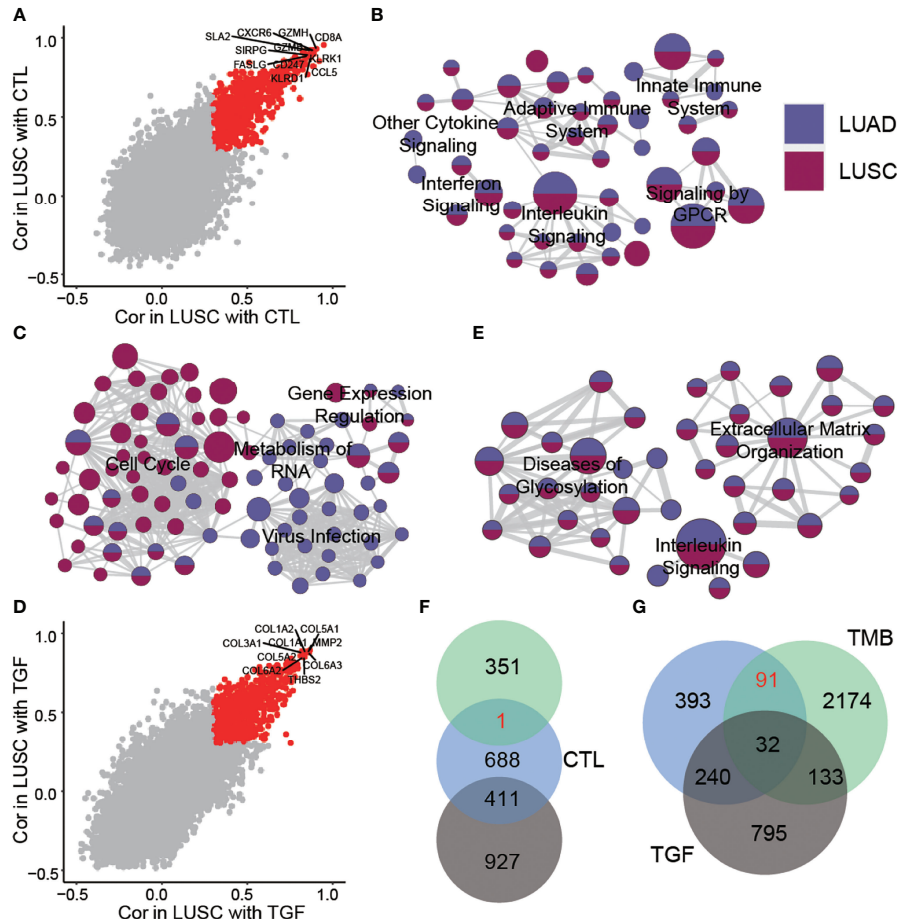

FIGURE 1 | Genes and pathways related to ICB treatment response biomarker. **(A)** Genes related to CTL in LUAD and LUSC. The red dots represent an association greater than 0.3 in two cancer types. **(B)** Pathways related to CTL in LUAD and LUSC. **(C)** Pathways related to TMB in LUAD and LUSC. **(D)** Genes related to TGF-β in LUAD and LUSC. The red dots represent an association greater than 0.3 in two cancer types. **(E)** Pathways related to TGF-β in LUAD and LUSC. **(F)** Relationship between genes related to CTL, TMB, and TGF-β in LUSC. **(G)** Relationship between genes related to CTL, TMB, and TGF-β in LUAD.

factor for ICB treatment (**Table S3**, **Figure 2D**). Typically, CTL ($p = 0.13$; **Figure S5A**) and TMB ($p = 0.36$; **Figure S5B**) did not show significant prognosis efficacy of ICB treatment. And, the AUC of ITS was higher than that of CTL and TMB in predicting the survival rate of patients at different periods, showing a better prognosis efficiency (**Figure 2E**). In terms of predicting the response to ICB treatment, ICB also had a higher AUC than other biomarkers (**Table S3**). Taken together, the ITS score was demonstrated as a promising biomarker for immunotherapy after immune checkpoint inhibitors.

ITS Score Represented Comprehensive Immune Characteristics

Further, we explored the biological explanation of the prognosis significance of the ITS score. The linear mixed-effect model was used to associate ITS score with TME and genomic features in lung cancers by adjusting for age and sex. LUAD samples were observed to have relatively high ITS scores than LUSC (**Figure S6A**). Therefore, cancer type was further incorporated as a random effect in the model, allowing us to consider a different baseline value for features in LUAD and LUSC.

Among the immune subtypes identified in previous studies (22), samples characterized by IFN-gamma dominance had the highest ITS scores, while lymphocyte-depleted samples possessed lower ITS scores (**Figure S6B**). Notably, C3 samples, which are predominantly immune-inflammatory and have the best prognosis, also had relatively low ITS scores, suggesting that some immune escape mechanism exists in these samples to influence the response to ICB treatment. We observed that proliferation rate ($R^2 = 0.269$, FDR = 1.17e-41) and four immune expression signatures, macrophages ($R^2 = 0.565$, FDR = 1.01e-80), lymphocyte infiltration ($R^2 = 0.615$, FDR = 2.76e-113), IFN-g response ($R^2 = 0.462$, FDR = 7.23e-61), and wound healing ($R^2 = 0.193$, FDR = 2.49e-27), were more active in sample with higher ITS score (**Table S4**, **Figures S7**, **3A**).

We found that higher stromal fraction ($R^2 = 0.287$, FDR = 9.06e-26) and leukocyte fraction ($R^2 = 0.355$, FDR = 5.03e-60) were associated with stronger ITS score (**Table S4**, **Figure S7**,

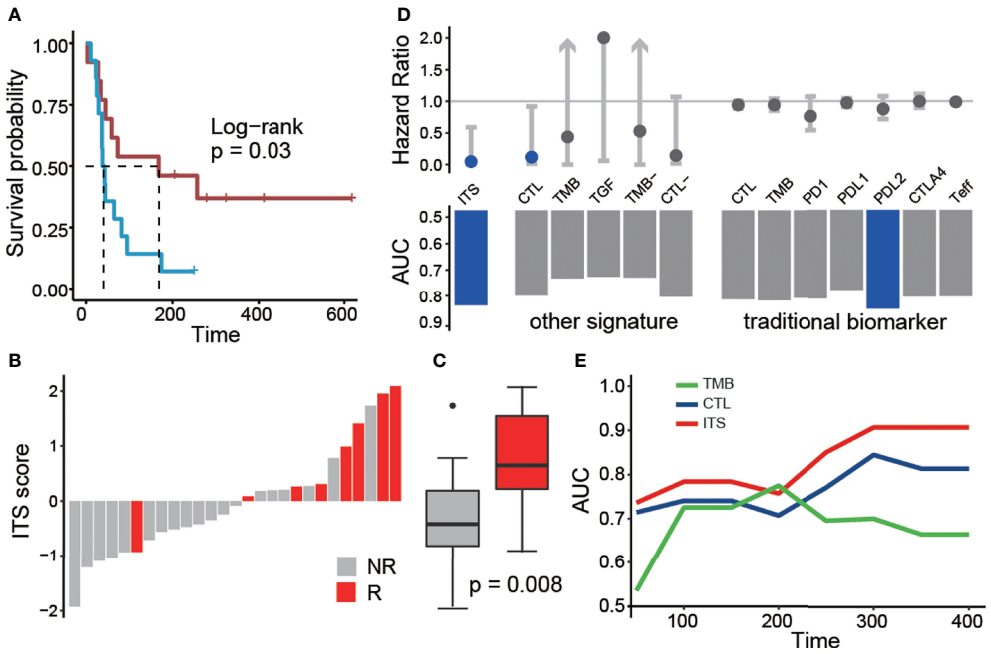

FIGURE 2 | Predictive efficacy of ITS scores in an ICB treatment dataset for NSCLC. **(A)** PFS difference between the two groups with high and low ITS scores. **(B)** Response to treatment between the two groups with ITS score. Red indicates the patient's response to treatment. **(C)** Differences in ITS scores between responders and non-responders. **(D)** Prognostic efficacy (top panel) and response prediction ability (bottom panel) of different signatures and biomarkers. **(E)** The area under the curve (AUC) was calculated for three prognostic models from 50 to 400 days. Blue: CTL; green: TMB; red: ITS.

Figure 3B). Of the 29 classes of tumor-infiltrating immune cells tested, infiltrating levels of 21 showed significant related with ITS score (FDR < 0.01; **Table S4**). Of these, ten were highly infiltrated and eleven less enriched in tumors with elevated ITS score (**Figures S7**, **3B**). The sample with higher ITS score had abundant adaptive immune cells, including CD8+ T cells (R^2 = 0.387, FDR = 7.01e-64), active Memory CD4 T cells (R^2 = 0.370, FDR = 4.96e-55), and Th2 cells (R^2 = 0.196, FDR = 4.27e-28). Low ITS score samples had more quiescent cells and activated innate immune cells, including resting mast cells (R^2 = 0.219, FDR = 5.82e-16) and activated dendritic cells (R^2 = 0.266, FDR = 2.10e-10), suggesting that patients in the low ITS group may have an insufficient adaptive immune response.

We also observed that samples with higher ITS score had increased tumor immunogenicity. For instance, elevated TCR richness (R^2 = 0.459, FDR = 4.87-71), BCR richness (R^2 = 0.199, FDR = 6.89e-19), TMB (R^2 = 0.205, FDR = 1.24e-11), and SNV neoantigens (R^2 = 0.199, FDR = 2.45e-10) were associated with high ITS score (**Figures S7**, **3C**). Considering the strong association of ITS score with mutational density, we next looked to determine whether these were selectively affected specific genes or chromosome regions. The mutation status of 69 genes was significantly correlated with the ITS score (FDR < 0.01; **Table S4**), of which 8 genes were related to immune or cancer genes (**Figure 3D**). Typically, mutations in the *EGFR* were associated with decreased ITS score (R^2 = 0.156, FDR = 0.004), consistent with previous descriptions that *EGFR* mutant tumors have generally a low response to immune checkpoint inhibitors (31). And we detected no specific copy number region associated with the ITS score (**Table S4**), indicating a general effect of association.

Overall, these results suggested that the ITS score may represent comprehensive immune characteristics to predict the outcome of ICB treatment.

Robustness of Prognosis Efficiency of ITS Score

To ensure the robustness of ITS scores for ICB treatment prognosis efficacy, it should be evaluated in more data sets. However, due to the lack of additional immunotherapy data for non-small cell lung cancer, we examined the prognostic efficacy of ITS scores for ICB treatment in other cancer types. In a melanoma cohort (20), immunotherapy-treated patients with higher ITS score demonstrated the longer OS (p = 0.002; **Figure 4A**) and PFS (p = 0.002; **Figure 4B**), and responders had significantly higher ITS scores than non-responders (p = 0.001; **Figure 4C**). In this dataset, some samples were also sequenced early during treatment (EDT), and we found that the ITS scores of almost all samples increased after treatment (**Figure 4D**), reflecting the dynamic changes of tumor immune microenvironment during ICB treatment. Similar findings were observed in another cohort of melanoma patients (21) (n = 42) treated with anti-CTLA-4 therapy. Patients with prolonged OS also noted in higher ITS score (p = 0.039; **Figure 4E**), and ITS score was significantly higher in responders and long-term survivors (p = 0.018; **Figure 4F**). In addition, ITS scores also

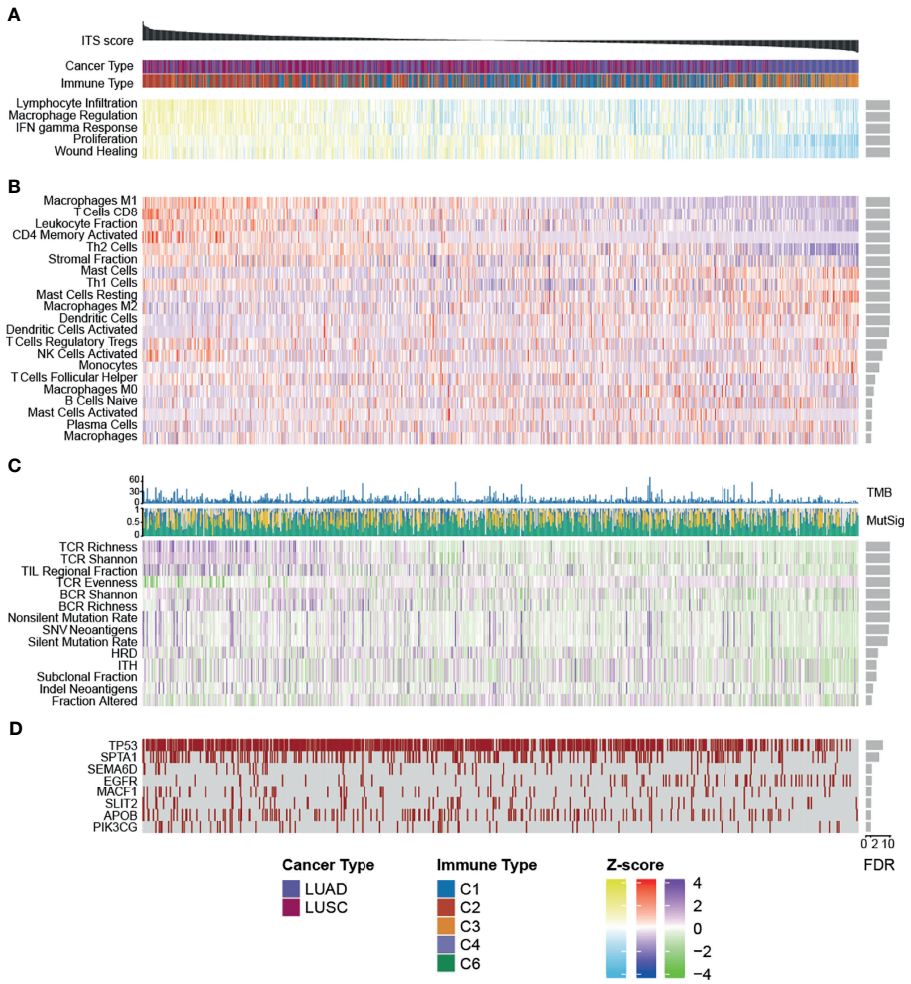

FIGURE 3 | Heatmap showing the relationship between **(A)** expression signatures, **(B)** TME features, **(C)** tumor immunogenicity, and **(D)** mutations and ITS score across TCGA lung samples. Samples are ordered by ITS score.

showed prognostic efficacy for ICB treatment in bladder cancer (17). Immunotherapy-treated patients with higher ITS score also displayed a superior prognosis compared with the other patients (p = 0.019; **Figure 4G**), and respondents were associated with higher ITS scores (p = 9.1e-5; **Figure 4H**). In summary, these results indicated the robust and practical prognosis efficacy of the ITS score. We also compared the prognosis and response prediction efficacy of ITS with traditional biomarkers in these three cohorts. ITS still showed satisfactory results (**Figure 4I**), although it was not trained in the corresponding cancer sample. This further confirms the prognostic potential of the combined strategies.

DISCUSSION

In this study, we analyzed genes and pathways associated with traditional biomarkers, including CTL level, TMB, and TGF-β signal, and designed a combined strategy to predict ICB treatment response and prognosis. We suggested that robust prognostic factors should include a comprehensive immune response mechanism and not be associated with immuno suppression. We applied this strategy to TCGA lung cancer samples and obtained an ICB treatment signature (ITS) with 91 genes. In independent ICB treatment cohorts, we demonstrated superior prediction performance of ITS scores over traditional biomarkers.

Drug resistance to targeted drugs including BRAF (32), MAPK (33), and MEK (34) signaling pathways in different cancer types affects patient treatment outcomes. Immunotherapy has been observed to show strong antitumor activity in advanced non-small-cell lung cancer. While the success of immunotherapy was exciting, it was important to note that only a subset of patients will benefit from ICB treatment. Therefore, predicting the treatment response of ICB was a challenge for researchers. At present, various predictive biomarkers have been constructed, but these markers have not achieved satisfactory prediction effects, and the prediction performance of these biomarkers has shown great

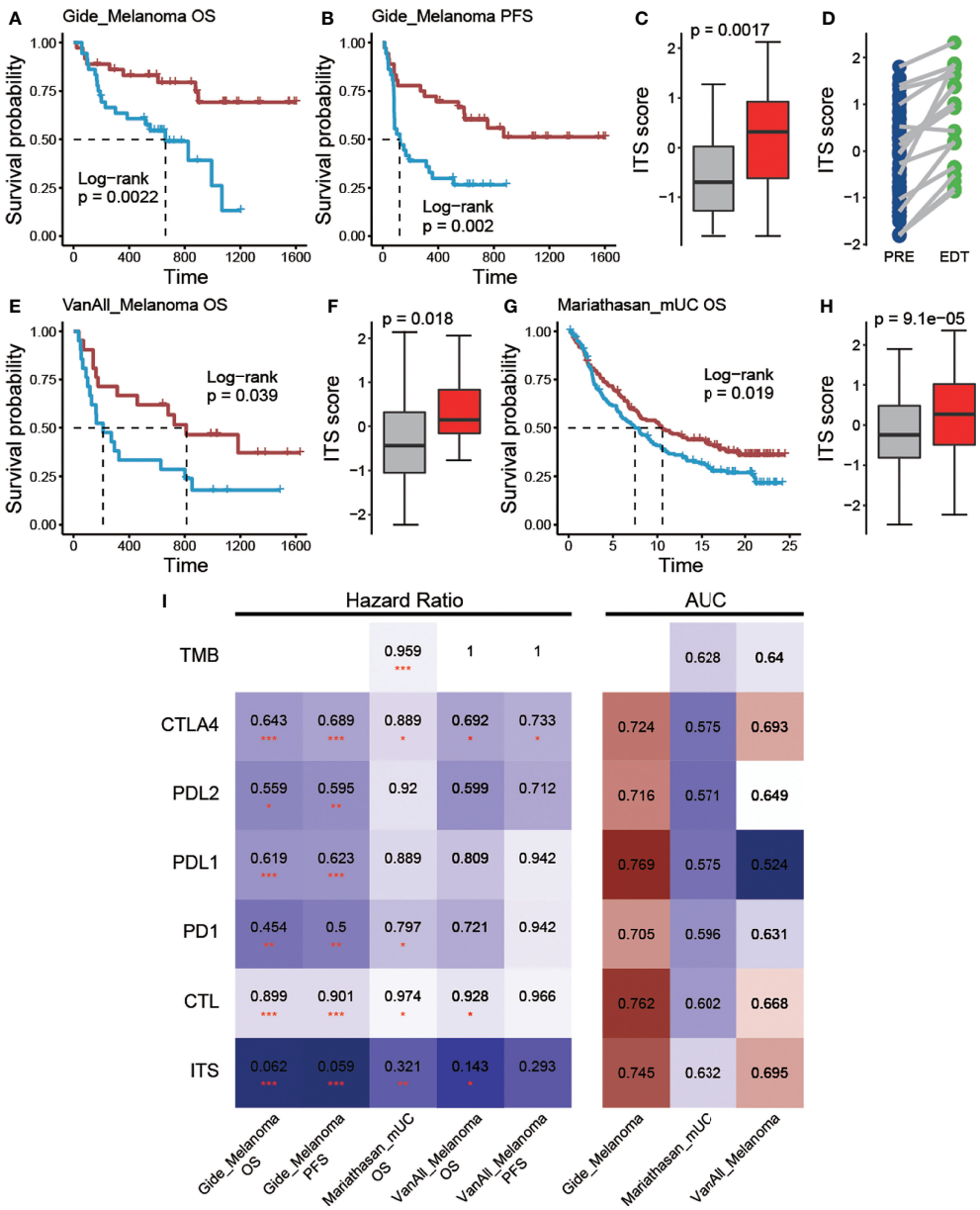

FIGURE 4 | Predictive efficacy of ITS scores in other ICB treatment cohorts. **(A)** OS and **(B)** PFS difference between the two groups with high and low ITS scores in the Gide cohort. **(C)** Differences in ITS scores between responders and non-responders in the Gide cohort. **(D)** ITS score changes after treatment. **(E)** OS difference between the two groups with high and low ITS scores in the VanAll cohort. **(F)** Differences in ITS scores between responders and non-responders in the VanAll cohort. **(G)** OS difference between the two groups with high and low ITS scores in the Mariathasan cohort. **(H)** Differences in ITS scores between responders and non-responders in the Mariathasan cohort. **(I)** Biomarkers are shown as rows and individual cohorts as columns. The heatmap indicates the hazard ratio derived from Cox regression (left panel) and AUC value derived from ROC curve (right panel), * denoted p <0.05, ** denoted p <0.01, *** denotes p < 0.001.

variability in different datasets (18). In NSCLC, PD-L1 expression was the most commonly used predictive biomarker in routine clinical practice. Some studies have shown that increased PD-L1 expression predicts longer progression-free survival and overall survival after ICB treatment (18). However, PD-L1 expression was not the best biomarker for some patients, because patients with low PD-L1 expression also showed a lasting response (35). Tumor mutation load (TMB) was the second most frequently studied biomarker, where higher TMB was associated with long-lasting clinical benefits and longer overall survival (9–11). Similarly, studies have shown that the tumor immune microenvironment can be used to predict the efficacy of immunotherapy in NSCLC patients. Clinical trials of ICB therapy in NSCLC patients have shown that higher effector T cell level is associated with greater clinical benefit (36). However, none of these markers achieved sufficient predictive power in the ICB dataset we analyzed. The

immune response depends on various elements (37), and the complexity of the immune therapy response mechanism led to the fact that prognostic markers designed based on a single mechanism can no longer meet the prediction needs.

Despite the agreement that they are associated with better ICB outcomes, our results suggested that pathways related to cytotoxic T lymphocytes (CTL) differ from pathways related to TMB. Genes related to CTL in LUAD and LUSC represent a broad range of immune response systems including the innate immune system, adaptive immune system, and cytokine pathways. In LUAD and LUSC, TMB-related genes were enriched in cell cycle and RNA metabolism and regulation pathways, respectively. This is consistent with the idea that they represent different immune response mechanisms. CTL plays a killing role in the tumor, and response to ICB treatment requires pre-existing immune microenvironment (38). Tumors with high TMB may be associated with the presence of a large number of neoantigens that can be recognized by CD8+ T cells (39). In addition, we found that the genes related to CTL and TMB contained a large number of genes related to immunosuppressive signature, suggesting that the use of these two types of biomarkers alone would ignore the immune escape mechanism, leading to the instability of prediction performance. We considered that the stable prognostic factors should include a comprehensive response mechanism and exclude the interference of immunosuppressive signals. Based on this idea, we constructed ITS scores in lung cancer to predict ICB treatment response.

ITS is a set of 91 genes identified in LUAD. We did not find a large number of genes associated with both CTL and TMB in LUSC, and one possible explanation is that differences in mutagenicity between the two cancer types lead to different patterns of genomic variation (40). Gene interactions in ITS are involved in cell killing, interferon response, and transcription factor binding. And ITS scores represented comprehensive immune activation characteristics including activated immune cell infiltration, increased mutation load, and TCR diversity. In the independent ICB treatment cohorts, ITS scores were more effective in predicting survival and response to treatment than the single biomarker. Multi-angle evaluation proves that ITS is stable in the application process. This suggests the need to combine multiple immune response mechanisms to predict ICB response.

However, more NSCLC ICB treatment datasets and prospective studies are needed to evaluate the clinical usefulness of ITS. Meanwhile, the ssGSEA method was used to calculate the ITS score in this study. It is not a robust sample classification method to classify samples only according to median ITS value, and more effective methods may be needed to explore the optimal cutoff value. In addition, the complex immune microenvironment of the samples also raises concerns. Gene expression at the bulk level does not take into account intra-tumor heterogeneity, which is an important factor affecting prognosis and treatment. These problems still need further research and exploration in the future.

In summary, this work demonstrated that the combination of biomarkers related to different response mechanisms contributed to better prediction performance of ICB treatment response, and provided a promising immune response biomarker in NSCLC, thus optimizing the treatment regimen of patients.

DATA AVAILABILITY STATEMENT

Publicly available datasets were analyzed in this study. TCGA data were downloaded from the UCSC Xena platform (https://xenabrowser.net/datapages/) under accession TCGA LUNG. RNA-seq data of NSCLC ICB treatment cohort were downloaded from the European Genome-phenome Archive under accession number EGAS00001003731. RNA-seq data of the Gide et al. study was available from ENA under accession number ERP105482. Other expression data and clinical information used in this study were obtained through the supplementary materials of original publications.

AUTHOR CONTRIBUTIONS

Conceptualization: ZJ and JH. Methodology: ZJ, YZ, and JH. Formal computational analysis: ZJ, YZ, and JH. Investigation: ZJ, YZ, and JH. Data visualization: ZJ, YZ, and JH. Original draft: ZJ, YZ, and JH. Writing—review and editing: ZJ, YZ, and JH. All authors contributed to the article and approved the submitted version.

ACKNOWLEDGMENTS

Thanks to the authors who provided us with data to support this study.

SUPPLEMENTARY MATERIAL

The Supplementary Material for this article can be found online at: https://www.frontiersin.org/articles/10.3389/fimmu.2021.813331/full#supplementary-material

REFERENCES

1. Siegel RL, Miller KD, Fuchs HE, Jemal A. Cancer Statistics, 2021. *CA Cancer J Clin* (2021) 71(1):7–33. doi: 10.3322/caac.21654
2. Antonia SJ, Villegas A, Daniel D, Vicente D, Murakami S, Hui R, et al. Overall Survival With Durvalumab After Chemoradiotherapy in Stage III NSCLC. *N Engl J Med* (2018) 379(24):2342–50. doi: 10.1056/NEJMoa1809697
3. Reck M, Rodriguez-Abreu D, Robinson AG, Hui R, Csoszi T, Fulop A, et al. Pembrolizumab Versus Chemotherapy for PD-L1-Positive Non-Small-Cell Lung Cancer. *N Engl J Med* (2016) 375(19):1823–33. doi: 10.1056/NEJMoa1606774
4. Liu X, Feng Y, Xu J, Shi Y, Yang J, Zhang R, et al. Combination of MAPK Inhibition With Photothermal Therapy Synergistically Augments the Anti-Tumor Efficacy of Immune Checkpoint Blockade. *J Cont Release* (2021) 332:194–209. doi: 10.1016/j.jconrel.2021.02.020

5. Liu X, Feng Y, Xu G, Chen Y, Luo Y, Song J, et al. MAPK-Targeted Drug Delivered by a pH-Sensitive MSNP Nanocarrier Synergizes With PD-1 Blockade in Melanoma Without T-Cell Suppression. *Adv Funct Mater* (2019) 29(12):1806916. doi: 10.1002/adfm.201806916
6. Walsh RJ, Soo RA. Resistance to Immune Checkpoint Inhibitors in Non-Small Cell Lung Cancer: Biomarkers and Therapeutic Strategies. *Ther Adv Med Oncol* (2020) 12:1758835920937902. doi: 10.1177/1758835920937902
7. Paz-Ares L, Luft A, Vicente D, Tafreshi A, Gumus M, Mazieres J, et al. Pembrolizumab Plus Chemotherapy for Squamous Non-Small-Cell Lung Cancer. *N Engl J Med* (2018) 379(21):2040–51. doi: 10.1056/NEJMoa1810865
8. Shen X, Zhao B. Efficacy of PD-1 or PD-L1 Inhibitors and PD-L1 Expression Status in Cancer: Meta-Analysis. *BMJ* (2018) 362:k3529. doi: 10.1136/bmj.k3529
9. Rizvi NA, Hellmann MD, Snyder A, Kvistborg P, Makarov V, Havel JJ, et al. Cancer Immunology. Mutational Landscape Determines Sensitivity to PD-1 Blockade in Non-Small Cell Lung Cancer. *Science* (2015) 348(6230):124–8. doi: 10.1126/science.aaa1348
10. Hellmann MD, Callahan MK, Awad MM, Calvo E, Ascierto PA, Atmaca A, et al. Tumor Mutational Burden and Efficacy of Nivolumab Monotherapy and in Combination With Ipilimumab in Small-Cell Lung Cancer. *Cancer Cell* (2018) 33(5):853–61.e4. doi: 10.1016/j.ccell.2018.04.001
11. Hellmann MD, Nathanson T, Rizvi H, Creelan BC, Sanchez-Vega F, Ahuja A, et al. Genomic Features of Response to Combination Immunotherapy in Patients With Advanced Non-Small-Cell Lung Cancer. *Cancer Cell* (2018) 33(5):843–52.e4. doi: 10.1016/j.ccell.2018.03.018
12. Beatty GL, Gladney WL. Immune Escape Mechanisms as a Guide for Cancer Immunotherapy. *Clin Cancer Res* (2015) 21(4):687–92. doi: 10.1158/1078-0432.CCR-14-1860
13. Schalper KA, Brown J, Carvajal-Hausdorf D, McLaughlin J, Velcheti V, Syrigos KN, et al. Objective Measurement and Clinical Significance of TILs in Non-Small Cell Lung Cancer. *J Natl Cancer Inst* (2015) 107(3):dju435. doi: 10.1093/jnci/dju435
14. Sharma P, Hu-Lieskovan S, Wargo JA, Ribas A. Primary, Adaptive, and Acquired Resistance to Cancer Immunotherapy. *Cell* (2017) 168(4):707–23. doi: 10.1016/j.cell.2017.01.017
15. Tauriello DVF, Palomo-Ponce S, Stork D, Berenguer-Llergo A, Badia-Ramentol J, Iglesias M, et al. TGFbeta Drives Immune Evasion in Genetically Reconstituted Colon Cancer Metastasis. *Nature* (2018) 554(7693):538–43. doi: 10.1038/nature25492
16. Jiang P, Gu S, Pan D, Fu J, Sahu A, Hu X, et al. Signatures of T Cell Dysfunction and Exclusion Predict Cancer Immunotherapy Response. *Nat Med* (2018) 24(10):1550–8. doi: 10.1038/s41591-018-0136-1
17. Mariathasan S, Turley SJ, Nickles D, Castiglioni A, Yuen K, Wang Y, et al. TGFbeta Attenuates Tumour Response to PD-L1 Blockade by Contributing to Exclusion of T Cells. *Nature* (2018) 554(7693):544–8. doi: 10.1038/nature25501
18. Sun S, Xu L, Zhang X, Pang L, Long Z, Deng C, et al. Systematic Assessment of Transcriptomic Biomarkers for Immune Checkpoint Blockade Response in Cancer Immunotherapy. *Cancers (Basel)* (2021) 13(7):1639. doi: 10.3390/cancers13071639
19. Jung H, Kim HS, Kim JY, Sun JM, Ahn JS, Ahn MJ, et al. DNA Methylation Loss Promotes Immune Evasion of Tumours With High Mutation and Copy Number Load. *Nat Commun* (2019) 10(1):4278. doi: 10.1038/s41467-019-12159-9
20. Gide TN, Quek C, Menzies AM, Tasker AT, Shang P, Holst J, et al. Distinct Immune Cell Populations Define Response to Anti-PD-1 Monotherapy and Anti-PD-1/Anti-CTLA-4 Combined Therapy. *Cancer Cell* (2019) 35(2):238–55.e6. doi: 10.1016/j.ccell.2019.01.003
21. Van Allen EM, Miao D, Schilling B, Shukla SA, Blank C, Zimmer L, et al. Genomic Correlates of Response to CTLA-4 Blockade in Metastatic Melanoma. *Science* (2015) 350(6257):207–11. doi: 10.1126/science.aad0095
22. Thorsson V, Gibbs DL, Brown SD, Wolf D, Bortone DS, Ou Yang TH, et al. The Immune Landscape of Cancer. *Immunity* (2018) 48(4):812–30 e14. doi: 10.1016/j.immuni.2018.03.023
23. Paczkowska M, Barenboim J, Sintupisut N, Fox NS, Zhu H, Abd-Rabbo D, et al. Integrative Pathway Enrichment Analysis of Multivariate Omics Data. *Nat Commun* (2020) 11(1):735. doi: 10.1038/s41467-019-13983-9
24. Barbie DA, Tamayo P, Boehm JS, Kim SY, Moody SE, Dunn IF, et al. Systematic RNA Interference Reveals That Oncogenic KRAS-Driven Cancers Require TBK1. *Nature* (2009) 462(7269):108–12. doi: 10.1038/nature08460
25. Zhou Y, Zhou B, Pache L, Chang M, Khodabakhshi AH, Tanaseichuk O, et al. Metascape Provides a Biologist-Oriented Resource for the Analysis of Systems-Level Datasets. *Nat Commun* (2019) 10(1):1523. doi: 10.1038/s41467-019-09234-6
26. Hänzelmann S, Castelo R, Guinney J. GSVA: Gene Set Variation Analysis for Microarray and RNA-Seq Data. *BMC Bioinf* (2013) 14:7. doi: 10.1186/1471-2105-14-7
27. Lee E, Chuang HY, Kim JW, Ideker T, Lee D. Inferring Pathway Activity Toward Precise Disease Classification. *PloS Comput Biol* (2008) 4(11):e1000217. doi: 10.1371/journal.pcbi.1000217
28. Tomfohr J, Lu J, Kepler TB. Pathway Level Analysis of Gene Expression Using Singular Value Decomposition. *BMC Bioinf* (2005) 6:225. doi: 10.1186/1471-2105-6-225
29. Newman AM, Liu CL, Green MR, Gentles AJ, Feng W, Xu Y, et al. Robust Enumeration of Cell Subsets From Tissue Expression Profiles. *Nat Methods* (2015) 12(5):453–7. doi: 10.1038/nmeth.3337
30. Carter SL, Cibulskis K, Helman E, McKenna A, Shen H, Zack T, et al. Absolute Quantification of Somatic DNA Alterations in Human Cancer. *Nat Biotechnol* (2012) 30(5):413–21. doi: 10.1038/nbt.2203
31. Hastings K, Yu HA, Wei W, Sanchez-Vega F, DeVeaux M, Choi J, et al. EGFR Mutation Subtypes and Response to Immune Checkpoint Blockade Treatment in Non-Small-Cell Lung Cancer. *Ann Oncol* (2019) 30(8):1311–20. doi: 10.1093/annonc/mdz141
32. Xu G, Luo Y, Wu W, Liu X, Yu X, Bao Y, et al. The Evolution of Acquired Resistance to BRAF(V600E) Kinase Inhibitor Is Sustained by IGF1-Driven Tumor Vascular Remodeling. *J Invest Dermatol* (2021). doi: 10.1016/j.jid.2021.07.162
33. Yu C, Zhang M, Song J, Zheng X, Xu G, Bao Y, et al. Integrin-Src-YAP1 Signaling Mediates the Melanoma Acquired Resistance to MAPK and PI3K/mTOR Dual Targeted Therapy. *Mol Biomed* (2020) 1(1):12. doi: 10.1186/s43556-020-00013-0
34. Yu C, Luo D, Yu J, Zhang M, Zheng X, Xu G, et al. Genome-Wide CRISPR-Cas9 Knockout Screening Identifies GRB7 as a Driver for MEK Inhibitor Resistance in KRAS Mutant Colon Cancer. *Oncogene* (2021). doi: 10.1038/s41388-021-02077-w
35. Rittmeyer A, Barlesi F, Waterkamp D, Park K, Ciardiello F, von Pawel J, et al. Atezolizumab Versus Docetaxel in Patients With Previously Treated Non-Small-Cell Lung Cancer (OAK): A Phase 3, Open-Label, Multicentre Randomised Controlled Trial. *Lancet* (2017) 389(10066):255–65. doi: 10.1016/S0140-6736(16)32517-X
36. Herbst RS, Giaccone G, de Marinis F, Reinmuth N, Vergnenegre A, Barrios CH, et al. Atezolizumab for First-Line Treatment of PD-L1-Selected Patients With NSCLC. *N Engl J Med* (2020) 383(14):1328–39. doi: 10.1056/NEJMoa1917346
37. Joyce JA, Fearon DT. T Cell Exclusion, Immune Privilege, and the Tumor Microenvironment. *Science* (2015) 348(6230):74–80. doi: 10.1126/science.aaa6204
38. Tumeh PC, Harview CL, Yearley JH, Shintaku IP, Taylor EJ, Robert L, et al. PD-1 Blockade Induces Responses by Inhibiting Adaptive Immune Resistance. *Nature* (2014) 515(7528):568–71. doi: 10.1038/nature13954
39. Schumacher TN, Scheper W, Kvistborg P. Cancer Neoantigens. *Annu Rev Immunol* (2019) 37:173–200. doi: 10.1146/annurev-immunol-042617-053402
40. Campbell JD, Alexandrov A, Kim J, Wala J, Berger AH, Pedamallu CS, et al. Distinct Patterns of Somatic Genome Alterations in Lung Adenocarcinomas and Squamous Cell Carcinomas. *Nat Genet* (2016) 48(6):607–16. doi: 10.1038/ng.3564

Conflict of Interest: The authors declare that the research was conducted in the absence of any commercial or financial relationships that could be construed as a potential conflict of interest.

Publisher's Note: All claims expressed in this article are solely those of the authors and do not necessarily represent those of their affiliated organizations, or those of the publisher, the editors and the reviewers. Any product that may be evaluated in this article, or claim that may be made by its manufacturer, is not guaranteed or endorsed by the publisher.

Copyright © 2021 Jiang, Zhou and Huang. This is an open-access article distributed under the terms of the Creative Commons Attribution License (CC BY). The use, distribution or reproduction in other forums is permitted, provided the original author(s) and the copyright owner(s) are credited and that the original publication in this journal is cited, in accordance with accepted academic practice. No use, distribution or reproduction is permitted which does not comply with these terms.

frontiers in Oncology

CASE REPORT
published: 03 January 2022
doi: 10.3389/fonc.2021.778185

Camrelizumab-Related Myocarditis and Myositis With Myasthenia Gravis: A Case Report and Literature Review

Jing Bai[1], Dan Li[1], Peidan Yang[1], Kunyan Xu[1], Yingnan Wang[2], Qian Li[3], Jiang Liu[1], Wenli Du[1], Fengbin Zhang[2] and Rui Feng[1*]*

[1] Department of Pharmacy, Fourth Hospital of Hebei Medical University, Shijiazhuang, China, [2] Department of Gastroenterology, Fourth Hospital of Hebei Medical University, Shijiazhuang, China, [3] Department of Thoracic Surgery, Fourth Hospital of Hebei Medical University, Shijiazhuang, China

Immune checkpoint inhibitors (ICIs) have substantially changed the treatment of a variety of malignant tumors. With the increasing of their usage, the unique immune-mediated toxicity profile of ICIs has become apparent. We report a case of esophageal squamous cell carcinoma in a patient who received anti-programmed cell death protein 1 (PD-1) (camrelizumab) therapy and the occurrence of sequential immune-related adverse events (irAEs). Although many irAEs have been reported, severe myositis caused by camrelizumab with simultaneous involvement of multiple organs, including the myocardium, respiratory muscles, and skeletal muscles, has rarely been described in literature. This 69-year-old male patient developed a grade 4 camrelizumab-induced adverse reaction according to the Common Terminology Criteria for Adverse Events (CTCAE) and was successfully treated with methylprednisolone and immunoglobulins. The early identification of irAEs, immediate discontinuation of immunotherapy, use of steroids and/or immunosuppressants, and adjuvant supportive treatment are critical to the clinical prognosis of patients. It should be aware that autoimmune complications can occur even when ICI treatment is ceased.

Keywords: camrelizumab, myocarditis, myositis, myasthenia gravis, immune-related adverse events

OPEN ACCESS

Edited by:
Xuelei Ma,
Sichuan University, China

Reviewed by:
Tapas Ranjan Behera,
Cleveland Clinic, United States
Zhe-Sheng Chen,
St. John's University, United States

****Correspondence:***
Fengbin Zhang
drfengbinZhang@163.com
Rui Feng
fengrui-125@163.com

Specialty section:
This article was submitted to Cancer Immunity and Immunotherapy, a section of the journal Frontiers in Oncology

Received: *16 September 2021*
Accepted: *29 November 2021*
Published: *03 January 2022*

Citation:
Bai J, Li D, Yang P, Xu K, Wang Y, Li Q, Liu J, Du W, Zhang F and Feng R (2022) Camrelizumab-Related Myocarditis and Myositis With Myasthenia Gravis: A Case Report and Literature Review. Front. Oncol. 11:778185. doi: 10.3389/fonc.2021.778185

INTRODUCTION

Malignant tumors have become a major public health problem worldwide (1). Surgery, chemotherapy, and radiotherapy are the main treatment methods used to fight cancers, but the mortality rate from tumors remains very high. Recently, immune checkpoint blockade therapy as immunotherapy has become a modality of cancer treatment. Immune checkpoint inhibitors (ICIs) that target and block the programmed cell death protein 1 pathway (PD-1/PD-L1) and cytotoxic T lymphocyte-associated antigen 4 (CTLA-4) have demonstrated treatment potential in a variety of malignant tumors (2). Since the FDA approved the first CTLA-4 inhibitor, ipilimumab, in 2011 and the first PD-1 inhibitor, pembrolizumab, for melanoma treatment in 2014, ICIs have been approved for the treatment of various other tumors and have shown considerable advantages and impressive results in the field of tumor immunotherapy.

PD-1 is a negative regulator of T cell activity; it can limit the activity of T cells at various stages of the immune response when it interacts with its two ligands, PD-L1 and PD-L, negatively regulates T cell activation, and plays a key role in tumor evasion of host immunity (3). PD-1 inhibitors can block this interaction, which normally leads to T cell activation. However, PD-1 inhibitors induce many immune-related adverse events (irAEs) while activating T cells (4). These irAEs can involve multiple systems and locations, including the gastrointestinal tract, endocrine glands, skin, and liver (5); furthermore, irAEs such as myocarditis, heart failure, rhabdomyolysis, myositis, and myasthenia gravis (MG) have high fatality rates, thus warranting high vigilance in clinical practice (6–9).

Camrelizumab is a PD-1 inhibitor developed by Jiangsu Hengrui Medicine Co. Ltd., China. It was conditionally approved in China in May 2019 for the treatment of relapsed or refractory classic type II Hodgkin's lymphoma in patients who had received at least second-line chemotherapy (10). Due to its good antitumor potential in a variety of malignant tumors, this drug has been approved for four indications in China to date: advanced esophageal cancer, advanced hepatocellular carcinoma, non-small cell lung cancer, and advanced esophageal squamous cell carcinoma. A number of clinical trials involving multiple indications for camrelizumab are ongoing (**Table 1**).

TABLE 1 | Key ongoing clinical trials of camrelizumab in cancers.

Trial Name	Indication	Phase	Status	NCT
Study of SHR-1210 in Combination with Chemotherapy in Advanced Esophageal Cancer	Advanced esophageal cancer	III	Recruiting	NCT03691090
A Trial of SHR-1210 (an Anti-PD-1 Inhibitor) in Combination with FOLFOX4 in Subjects with Advanced HCC Who Have Never Received Prior Systemic Treatment	Advanced hepatocellular carcinoma	III	Recruiting	NCT03605706
Phase III Study of Camrelizumab in Combination with Chemotherapy in Recurrent/Metastatic Nasopharyngeal Carcinoma	Nasopharyngeal carcinoma	III	Active, not recruiting	NCT03707509
A Study to Evaluate SHR-1210 in Subjects with Advanced HCC	Hepatocellular carcinoma (nonresectable)	II	Active, not recruiting	NCT02989922
PD-1 Antibody SHR-1210 in Patients with Relapsed or Refractory Classic Hodgkin's Lymphoma	Hodgkin lymphoma	II	Recruiting	NCT03155425
A Study to Evaluate SHR-1210 in Patients with Advanced or Metastatic NSCLC	Lung neoplasms, non-small cell lung carcinoma, respiratory tract neoplasms nec, bronchial neoplasm, bronchogenic carcinoma	II	Recruiting	NCT03085069
A Trial of SHR-1210 (an Anti-PD-1 Inhibitor) in Combination with Hypofraction Radiotherapy in Patients With NSCLC	Non-small cell lung cancer	II	Recruiting	NCT03557411
SHR-1210 in Recurrent/Metastatic Nasopharyngeal Carcinoma Who Have Received Previous at Least Two Lines of Chemotherapy	Nasopharyngeal carcinoma	II	Active, not recruiting	NCT03558191
A Study of SHR-1210 in Combination with Apatinib or Chemotherapy in Subjects with Advanced PLC or BTC	Advanced primary liver cancer, advanced biliary tract carcinoma	II	Recruiting	NCT03092895
A Study of SHR-1210 in Combination with Apatinib in Advanced Non-Small Cell Lung Cancer (NSCLC)	Non-small cell lung carcinoma	II	Recruiting	NCT03083041
Neoadjuvant Anti-PD-1 Antibody SHR-1210 and Radiation in Resectable Esophageal Squamous Cell Carcinoma	Esophageal neoplasms	II	Recruiting	NCT03200691
A Trial of SHR-1210 (an Anti-PD-1 Inhibitor) in Combination with Apatinib in Patients with Advanced HCC (RESCUE)	Hepatocellular carcinoma	II	Active, not recruiting	NCT03463876
Famitinib Plus Anti-PD1 Therapy for Advanced Urinary System Tumors, Advanced Gynecological Tumors	Renal cell carcinoma, urothelial carcinoma, cervical cancer, recurrent ovarian cancer, endometrial cancer	II	Recruiting	NCT03827837
SHR-1210 in Combination with GEMOX in Patients with Advanced BTC	Biliary tract cancer, cholangiocarcinoma	II	Recruiting	NCT03486678
A Study of SHR-1210 in Combination with Capecitabine + Oxaliplatin or Apatinib in Treatment of Advanced Gastric Cancer	Gastric cancer, gastroesophageal cancer	II	Active, not recruiting	NCT03472365
The Phase II Trial of SHR-1210 Combined with Preoperative Chemotherapy for Locally Advanced Esophageal Squamous Cell Carcinoma	Locally advanced esophageal squamous cell carcinoma	II	Recruiting	NCT03917966
Neoadjuvant Chemoradiation Plus PD-1 Antibody (SHR-1210) in Locally Advanced Proximal Stomach Adenocarcinoma	Gastric adenocarcinoma	II	Recruiting	NCT03631615
SHR-1210 Combined with Apatinib in the Treatment of ED-SCLC after Failure of First-Line Standard Therapy	Small cell lung cancer	II	Pending	NCT03417895
A Trial of SHR-1210 (an Anti-PD-1 Inhibitor) in Combination with Apatinib and Fluzoparib in Patients with TNBC	Triple negative breast cancer	I	Recruiting	NCT03945604
A Study to Evaluate the Safety and Efficacy of SHR-1210, Gemcitabine and Cisplatin by R/M NPC Subjects	Nasopharyngeal carcinoma	I	Active, not recruiting	NCT03121716

Data from nine clinical trials (n = 986) showed that most camrelizumab recipients experienced an adverse event, 24% of which were grade 3 or higher (10). Adverse events of any severity with an incidence of ≥ 10% included reactive cutaneous capillary endothelial proliferation (RCCEP), anemia, fever, hypothyroidism, fatigue, and proteinuria. RCCEP appears to be unique to patients treated with camrelizumab; moreover, studies have shown that RCCEP is generally a grade 1 or 2 adverse event, and the clinical efficacy of camrelizumab treatment is closely correlated with a survival benefit (11). For grade 3 or grade 4 treatment-related adverse events (TRAEs), common symptoms include elevated aspartate aminotransferase (AST) (12), a decreased neutrophil count (12), pulmonary infection (13), elevated blood bilirubin (12), a decreased platelet count (12), and elevated serum alkaline phosphatase (10). Here, we report a case of MG and myositis involving the myocardium and respiratory muscles induced by the treatment of advanced esophageal cancer with the PD-1 inhibitor camrelizumab. The conditions of the patient improved after treatment.

CASE PRESENTATION

A 69-year-old male was admitted to the hospital for examination due to hoarseness in January 2020. Gastroscopy showed an ulcerative neoplasia approximately 23 cm-31 cm from the incisors (**Figure 1A**), which resulted in luminal stenosis. Pathological diagnosis revealed poorly differentiated squamous cell carcinoma. Initial cervical-thoracic enhanced computed tomography (CT) showed middle and upper thoracic esophageal carcinoma, suspicious invasion of the fibrous membrane surface, and multiple swollen lymph nodes in the bilateral supraclavicular region, bilateral tracheoesophageal sulcus, and mediastinum (**Figure 1B**). The diagnosis was multiple lymph node metastases of esophageal squamous cell carcinoma. The patient had a history of diabetes for eight years. The patient had normal heart function and therefore received a normal TP regimen (paclitaxel injection 135 mg/m^2 d1, 3 w + cisplatin 75 mg/m^2 d1-d3, 3 w).

After two cycles of chemotherapy, reexamination of the enhanced cervical-thoracic CT image showed that the patient was not

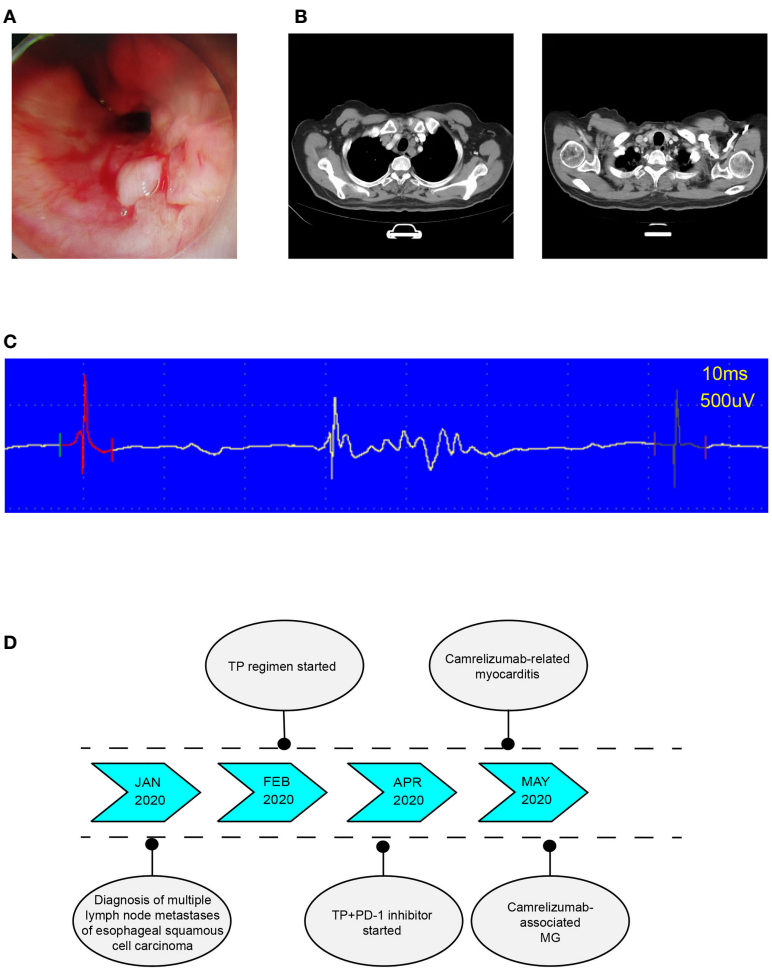

FIGURE 1 | **(A)** Endoscope images showing an ulcerative neoplasia. **(B)** In January 2020, posttreatment CT-scan showed middle and upper esophageal carcinoma with bilateral tracheoesophageal sulcus and right supraclavicular lymph node metastasis. **(C)** Typical electromyogram (EMG) of deltoid muscle showing the patient's myogenic damage. **(D)** Timeline of diagnosis, treatment, and immune-related adverse events.

responding to chemotherapy. On April 20, 2020, he started treatment with the TP regimen (paclitaxel injection 135 mg/m^2 d1, 3 w + cisplatin 75 mg/m^2 d1-d3, 3 w) for chemotherapy combined with a PD-1 monoclonal antibody and camrelizumab injections (200 mg/injection).

After the first injection of camrelizumab, the patient did not experience any discomfort and was discharged from the hospital. However, he developed left eyelid ptosis and limited movement of the left eyeball that was accompanied by weakness and soreness in both lower extremities 3 weeks after receiving the first dose of combination treatment. 2 days later, the patient presented with palpitations. Electrocardiogram (ECG) showed sinus tachycardia. Cardiac ultrasound and cardiac function tests revealed the following results: left ventricular ejection fraction 70%, right ventricular ejection fraction 77%, moderate left ventricular diastolic function reduction, and tachycardia. Myocardial enzymatic assays revealed the following results: creatine kinase (CK) 3503.1 U/L (normal value 50-310 U/L), creatine kinase isoenzyme (CK-MB) 178.7 U/L (normal value 0-25.0 U/L), lactate dehydrogenase (LDH) 622.6 U/L (normal value 120-250 U/L), α-hydroxybutyric acid 596.0 U/L (normal value 72-182 U/L) and myoglobin (Myo) 1248 μg/L (normal value 1.5-70 μg/L); cardiac troponin (cTnI) level was 0.35 ng/mL (normal value < 0.040 ng/mL) and rose to 0.63 ng/mL 6 hours later, and brain natriuretic peptide (BNP) is normal. Abnormal liver function was evidenced by the following results: alanine aminotransferase (ALT) 154.3 U/L (normal value 9-50 U/L) and AST 204.4 U/L (normal value 15-40 U/L). On electromyography, the examined muscles showed myogenic damage, and the left deltoid showed a spontaneous spot (active phase) manifestation (**Figure 1C**). Considering the clinical manifestations and laboratory test results, we considered camrelizumab injection-induced adverse myositis involving the myocardium and skeletal muscles accompanied by elevated transaminases, which is considered a grade 4 camrelizumab-induced adverse reaction according to the Common Terminology Criteria for Adverse Events (CTCAE) (The order of occurrence as shown in **Figure 1D**). The patient was immediately injected with methylprednisolone sodium succinate (120 mg daily days 1-5, with gradually decreasing doses); he complained of lower extremity weakness, but his soreness was significantly improved. On the sixth day, the methylprednisolone sodium succinate dose was reduced to 80 mg daily. The patient experienced rapid breathing and dyspnea. Blood gas analysis indicated type II respiratory failure. The patient was transferred to the intensive care unit (ICU), tracheal intubation was immediately performed, and the patient was connected to a ventilator to facilitate respiration. Cardiac troponin (cTnI) level rose to 0.89 ng/mL. Anti-acetylcholine receptor antibody (anti-AChR-Ab) was detected at 10.94 nmol/L. Camrelizumab-associated MG (CTCAE grade 4) was considered. The patient received oral pyridostigmine bromide (30 mg qid with gradually decreasing doses) to improve muscle weakness. Methylprednisolone sodium succinate was restarted at 120 mg with gradually decreasing doses. After five days, the patient's respiratory condition did not improve. Immunoglobulin injections were administered for one week.

The patient developed ventilator-associated pneumonia during hospitalization in the ICU. Sputum culture results showed *Klebsiella pneumoniae* and pan-drug-resistant *Acinetobacter baumannii*. After two weeks of anti-infective therapy with cefoperazone and sulbactam combined with tigecycline, the patient was weaned off the ventilator and was transferred to the general ward. Within two months, his dose of glucocorticoid therapy was gradually reduced and the levels of biomarkers of myocardial injury declined. His muscle strength gradually recovered, and he returned home to recuperate. During this period, he was treated with oral prednisone tablets (15 mg qd with gradually decreasing doses) and pyridostigmine bromide (30 mg tid).

At a follow-up examination two months later, cervical-thoracic enhanced CT showed a mass in the esophageal wall at the upper thoracic segment, with no obvious change compared to the previous examination, and enlarged lymph nodes on the right supraclavicular fossa and both sides of the tracheal sulcus, with no obvious change compared with the previous film. Cardiac magnetic resonance and ultrasound imaging results were all normal, and myocardial enzymes and liver and kidney functions were normal. Anti-AChR-Ab levels decreased slowly but did not reach a normal level.

DISCUSSION

Camrelizumab is a humanized high-affinity IgG4 monoclonal antibody against PD-1 (14). It binds to and blocks PD-1 for its binding to the ligand PD-L1 which is overexpressed on activated T lymphocytes, B cells, and natural killer (NK) cells in certain tumors, and PD-L2, which is primarily expressed on antigen-presenting cells. Camrelizumab prevents the activation of PD-1 and its downstream signaling pathways and restores immune function through the activation of cytotoxic T lymphocytes and cell-mediated immune responses directed against tumor cells or pathogens (15). Camrelizumab showed a high dose-dependent affinity for PD-1 (KD 3.31 nmol/L) when administered as a single 60-, 200-, or 400-mg intravenous treatment for patients with solid tumors (10). With a single 200-mg injection of camrelizumab, the peak receptor occupancy of circulating T lymphocytes was 85%, and receptor occupancy remained steadily high in patients who received repeated infusions (once every two weeks), with a receptor occupancy of 77% at the trough concentration after the first infusion of treatment cycle 5. The administration of a single 200-mg IV infusion of camrelizumab to patients with solid tumors (n = 12) produced a mean Cmax of 70.4 μg/mL after a median of 0.00347 days (time to the maximum concentration, tmax) and an area under the curve from zero to infinity (AUC∞) of 465 μg day/mL, and the mean half-life (t½) was 5.61 days (14). The elimination half-lives of PD-1 inhibitors are generally long, and they exhibit slow elimination. When serious adverse drug reactions occur, physicians must cease administration of the drug immediately to avoid drug accumulation and aggravate adverse reactions.

The incidence of immune-associated myocarditis is < 1% (16). ICI-induced myocarditis may be more common than previously thought because of its nonspecific clinical manifestations and the lack of methods for the routine detection of cardiac biomarkers (17). From 2009 to 2018, 613 fatal toxic events caused by ICIs were reported in VigiBase (WHO database). These included 333 deaths related to PD-1/PD-L1 inhibitors, including 27 deaths due to myocarditis (accounting for 8%) and 87 deaths related to the combination of CTLA-4 and PD-1/PD-L1 inhibitors, 22 of them were caused by myocarditis (accounting for 25%) (16). These fatal events indicate that the incidence and mortality of myocarditis significantly increases with combined CTLA-4 and PD-1/PD-L1 inhibitor therapy. The cardiac toxicity of ICIs was diagnosed based on the patients' drug history, clinical manifestations, cardiac biomarkers, electrocardiogram (ECG) results, endomyocardial biopsy, and imaging examinations. A single center study in China described 283 patients who received PD-1 or PD-L1 inhibitor monotherapy or combination therapy between January 1, 2018, and December 31, 2019: three of the patients had immune-related myositis (incidence: 1.06%), including two patients who received nivolumab monotherapy and one patient who received combination treatment with camrelizumab and gemcitabine, and both patients died (17). In another multicenter, randomized, nonblinded phase III clinical trial, one patient among 228 patients with metastatic esophageal squamous cell carcinoma who received camrelizumab treatment developed myocarditis and died (18). Because most cases of immune-related myocarditis occur at the early stage of ICI treatment and rapidly deteriorate, baseline examination and regular monitoring of myocardial markers and ECG are necessary for the early detection of myocarditis (17).

ICI-induced neuromuscular side effects are rare but often severe and include musculoskeletal pain, myositis, polymyalgia rheumatica, ocular myositis, and MG. Myositis occurs in 1% of patients treated with PD-1 inhibitors (according to the prescribing information for Opdivo®) (19); there was one fatality in a trial of pembrolizumab as an adjuvant treatment and a mortality rate less than 1% in patients treated with ipilimumab (according to the prescribing information for Yervoy®) (20). A Japanese study of 10,277 patients who received monotherapy with either nivolumab or ipilimumab reported 12 cases of MG among the patients treated with nivolumab but none among the patients treated with ipilimumab, indicating that the incidence of PD-1 inhibitor-induced MG was higher than the incidence of CTLA-4 inhibitor-induced MG (21). Nivolumab-induced myositis (22) and CTLA-4 inhibitor-induced ophthalmic myositis myopathy have been reported (23). These drugs have also been reported to induce severe MG-induced respiratory disorders when used alone or in combination (24).

The side-effect registry and institutional databases of 10 skin cancer centers were queried for reports of myositis and neuromuscular side effects induced by ICIs. Myositis (19/38) was the most frequently reported neuromuscular adverse event. Thirty-two percent of myositis patients had myocarditis (n = 6), 5% of myositis patients had MG, and two patients died from myositis, which is consistent with findings from a WHO registry: myocarditis was associated with myositis in 25% of cases and with MG in 11% of cases. A death case of MG with immune-related myositis involving the myocardium has been reported after camrelizumab treatment (25). Surprisingly, MG also occurred concomitantly in 11 (10%) of 101 patients with myocarditis (26). The specific mechanism underlying myositis associated with myocarditis and MG remains unknown. However, the mechanism might reflect a shared antigen profile and immune phenotype between cardiac and skeletal muscles (17).

In the case of grade 3–4 immune-related myocarditis/myositis (27), ICI treatment must be discontinued, and intravenous glucocorticoids should be started as soon as possible. The initial dosage of prednisone is 1–2 mg/kg daily (or an equal dose of methylprednisolone). If immune-related myocarditis/myositis is accompanied by severe damage (weakness, severely restricted activities, cardiac respiratory insufficiency, difficulty swallowing), plasma exchange and combined intravenous immunoglobulin therapy can also be considered. If symptoms do not improve within two to three days, immunosuppressants should be increased or changed. Recently, two cases of immunotherapy-related myocarditis were reported in the literature. After treatment with alemtuzumab and abatacept, the condition was controlled (6, 7). In this study, the patient received an intravenous injection of a large dose of glucocorticoids combined with gamma immunoglobulin as the main therapeutic drug, with improved results. Glucocorticoid maintenance treatment can take place for four to six weeks after symptoms improve to ≤ grade 1. Patients with myositis respond well to steroid therapy. Notably, doctors should be cautious of recurrent conditions during the dose reduction process of their patients. Shortness of breath and an increased heart rate occurred in this patient during the first dose reduction of methylprednisolone. Blood gas analysis showed that the patient had type II respiratory failure and respiratory acidosis. Progressive aggravation of myositis involving the respiratory muscles was considered. The severity of muscle weakness increased, and the dose of methylprednisolone was increased to and maintained at 120 mg. The dose was reduced after the patient's condition improved. The case revealed that patients usually can benefit from high dose of glucocorticoid and a slower course of dose reduction.

Supportive care is also very important. The patient was transferred to the ICU for ventilator-assisted ventilation when type II respiratory failure occurred, which led to ventilator-associated pneumonia. Therefore, weaning from the ventilator as early as possible is very important. When a lung infection occurs, the ability to treat the patient with the correct antibiotic will determine the hospitalization time and rehabilitation.

Treatment for MG usually involves symptomatic treatment and immunosuppressive therapy (28). Pyridostigmine bromide, an acetylcholinesterase inhibitor, should be considered as part of the initial treatment for most patients with MG. All MG patients who have received a sufficient amount of pyridostigmine bromide without achieving the treatment goal should receive

glucocorticoids or immunosuppressants. This patient was treated with a PD-1 inhibitor and had immune-related myositis involving the myocardium and respiratory muscles accompanied by MG. Therefore, pyridostigmine bromide served as a symptomatic immunotherapeutic treatment.

Lau (29) and Zhu (30) reported that patients with a history of MG showed muscle weakness after receiving pembrolizumab for the treatment of metastatic melanoma. In addition, some patients had high levels of anti-AChR-Ab before receiving nivolumab. After they received treatment, a myasthenic crisis was reported (31). Therefore, for patients with a history of MG, the use of ICIs might activate the T cell autoimmune response and may induce MG.

For patients with a history of MG or other immune-related diseases, physicians should weigh the risk of serious immune-related adverse reactions caused by immune activation due to the use of ICIs. ICI-induced myositis is rare but serious and sometimes fatal. The immediate discontinuation of immunotherapy and timely administration of adequate steroids can reduce the risk of death. Pyridostigmine bromide can be used to treat immune-related polymyositis with MG caused by ICIs and can reduce sequelae. While we emphasize the importance of tumor killing with ICI therapy, we focus on being alert to autoimmune complications in patients who have received ICI therapy, even after the discontinuation of ICI treatment. Early identification and effective management of irAEs are very important.

DATA AVAILABILITY STATEMENT

The original contributions presented in the study are included in the article/supplementary material. Further inquiries can be directed to the corresponding authors.

ETHICS STATEMENT

Written informed consent was obtained from the individual(s) for the publication of any potentially identifiable images or data included in this article.

AUTHOR CONTRIBUTIONS

FZ: Conceptualization, project administration, funding acquisition, writing – review and editing. WD, RF: Writing – review and editing. JL, YW, QL: Supervision. JB: Writing – original draft, formal analysis. KX: Case tracking. PY: Literature review. DL: Data collection. All authors contributed to the article and approved the submitted version.

FUNDING

Support was provided by the Hebei Natural Science Foundation (No. H2019206614; Shijiazhuang, China).

REFERENCES

1. Siegel RL, Miller KD, Jemal A. Cancer Statistics, 2019. *CA Cancer J Clin* (2019) 69:7–34. doi: 10.3322/caac.21551
2. Postow MA, Callahan MK, Wolchok JD. Immune Checkpoint Blockade in Cancer Therapy. *J Clin Oncol* (2015) 33:1974–82. doi: 10.1200/JCO.2014.59.4358
3. Wang S, Luo LL, Lv M, Ma YF. Pd-1/Pd-Ll Signaling Pathway and Its Application in Tumor. *J Int Pharm Res* (2015) 42:143–5. doi: 10.13220/j.cnki.jipr.2015.02.003
4. Postow MA, Sidlow R, Hellmann MD. Immune-Related Adverse Events Associated With Immune Checkpoint Blockade. *N Engl J Med* (2018) 378:158–68. doi: 10.1056/NEJMra1703481
5. Wang DY, Salem JE, Cohen JV, Chandra S, Menzer C, Ye F, et al. Fatal Toxic Effects Associated With Immune Checkpoint Inhibitors: A Systematic Review and Meta-Analysis. *JAMA Oncol* (2018) 4:1721–8. doi: 10.1001/jamaoncol.2018.3923
6. Salem JE, Allenbach Y, Vozy A, Brechot N, Johnson DB, Moslehi JJ, et al. Abatacept for Severe Immune Checkpoint Inhibitor-Associated Myocarditis. *N Engl J Med* (2019) 380:2377–9. doi: 10.1056/NEJMc1901677
7. Esfahani K, Buhlaiga N, Thébault P, Lapointe R, Johnson NA, Miller WJ. Alemtuzumab for Immune-Related Myocarditis Due to Pd-1 Therapy. *N Engl J Med* (2019) 380:2375–6. doi: 10.1056/NEJMc1903064
8. Moslehi JJ, Salem JE, Sosman JA, Lebrun-Vignes B, Johnson DB. Increased Reporting of Fatal Immune Checkpoint Inhibitor-Associated Myocarditis. *Lancet* (2018) 391:933. doi: 10.1016/S0140-6736(18)30533-6
9. March KL, Samarin MJ, Sodhi A, Owens RE. Pembrolizumab-Induced Myasthenia Gravis: A Fatal Case Report. *J Oncol Pharm Pract* (2018) 24:146–9. doi: 10.1177/1078155216687389
10. Markham A, Keam SJ. Camrelizumab: First Global Approval. *Drugs* (2019) 79:1355–61. doi: 10.1007/s40265-019-01167-0
11. Chen X, Ma L, Wang X, Mo H, Wu D, Lan B, et al. Reactive Capillary Hemangiomas: A Novel Dermatologic Toxicity Following Anti-Pd-1 Treatment With Shr-1210. *Cancer Biol Med* (2019) 16:173–81. doi: 10.20892/j.issn.2095-3941.2018.0172
12. Fang W, Yang Y, Ma Y, Hong S, Lin L, He X, et al. Camrelizumab (Shr-1210) Alone or in Combination With Gemcitabine Plus Cisplatin for Nasopharyngeal Carcinoma: Results From Two Single-Arm, Phase 1 Trials. *Lancet Oncol* (2018) 19:1338–50. doi: 10.1016/S1470-2045(18)30495-9
13. Huang J, Xu B, Mo H, Zhang W, Chen X, Wu D, et al. Safety, Activity, and Biomarkers of Shr-1210, an Anti-Pd-1 Antibody, for Patients With Advanced Esophageal Carcinoma. *Clin Cancer Res* (2018) 24:1296–304. doi: 10.1158/1078-0432.CCR-17-2439
14. Mo H, Huang J, Xu J, Chen X, Wu D, Qu D, et al. Safety, Anti-Tumour Activity, and Pharmacokinetics of Fixed-Dose Shr-1210, an Anti-Pd-1 Antibody in Advanced Solid Tumours: A Dose-Escalation, Phase 1 Study. *Br J Cancer* (2018) 119:538–45. doi: 10.1038/s41416-018-0100-3
15. Alsaab HO, Sau S, Alzhrani R, Tatiparti K, Bhise K, Kashaw SK, et al. Pd-1 and Pd-L1 Checkpoint Signaling Inhibition for Cancer Immunotherapy: Mechanism, Combinations, and Clinical Outcome. *Front Pharmacol* (2017) 8:561. doi: 10.3389/fphar.2017.00561
16. Johnson DB, Balko JM, Compton ML, Chalkias S, Gorham J, Xu Y, et al. Fulminant Myocarditis With Combination Immune Checkpoint Blockade. *N Engl J Med* (2016) 375:1749–55. doi: 10.1056/NEJMoa1609214
17. Wang F, Sun X, Qin S, Hua H, Liu X, Yang L, et al. A Retrospective Study of Immune Checkpoint Inhibitor-Associated Myocarditis in a Single Center in China. *Chin Clin Oncol* (2020) 9:16. doi: 10.21037/cco.2020.03.08
18. Huang J, Xu J, Chen Y, Zhuang W, Zhang Y, Chen Z, et al. Camrelizumab Versus Investigator's Choice of Chemotherapy as Second-Line Therapy for Advanced or Metastatic Oesophageal Squamous Cell Carcinoma (Escort): A Multicentre, Randomised, Open-Label, Phase 3 Study. *Lancet Oncol* (2020) 21:832–42. doi: 10.1016/S1470-2045(20)30110-8
19. Eggermont AM, Blank CU, Mandala M, Long GV, Atkinson V, Dalle S, et al. Adjuvant Pembrolizumab Versus Placebo in Resected Stage Iii Melanoma. *New Engl J Med* (2018) 378:1789–801. doi: 10.1056/NEJMoa1802357

20. Tan R, Toh CK, Takano A. Continued Response to One Dose of Nivolumab Complicated by Myasthenic Crisis and Myositis. *J Thorac Oncol* (2017) 12: e90–1. doi: 10.1016/j.jtho.2017.02.024
21. Suzuki S, Ishikawa N, Konoeda F, Seki N, Fukushima S, Takahashi K, et al. Nivolumab-Related Myasthenia Gravis With Myositis and Myocarditis in Japan. *Neurology* (2017) 89:1127–34. doi: 10.1212/WNL.0000000000004359
22. Goldstein BL, Gedmintas L, Todd DJ. Drug-Associated Polymyalgia Rheumatica/Giant Cell Arteritis Occurring in Two Patients After Treatment With Ipilimumab, an Antagonist of Ctla-4. *Arthritis Rheumatol* (2014) 66:768–9. doi: 10.1002/art.38282
23. Pushkarevskaya A, Neuberger U, Dimitrakopoulou-Strauss A, Enk A, Hassel JC. Severe Ocular Myositis After Ipilimumab Treatment for Melanoma: A Report of 2 Cases. *J Immunother* (2017) 40:282–5. doi: 10.1097/CJI.0000000000000178
24. John S, Antonia SJ, Rose TA, Seifert RP, Centeno BA, Wagner AS, et al. Progressive Hypoventilation Due to Mixed Cd8(+) and Cd4(+) Lymphocytic Polymyositis Following Tremelimumab - Durvalumab Treatment. *J Immunother Cancer* (2017) 5:54. doi: 10.1186/s40425-017-0258-x
25. Chen Y, Jia Y, Liu Q, Shen Y, Zhu H, Dong X, et al. Myocarditis Related to Immune Checkpoint Inhibitors Treatment: Two Case Reports and Literature Review. *Ann Palliat Med* (2021) 10:8512–7. doi: 10.21037/apm-20-2620
26. Moreira A, Loquai C, Pföhler C, Kähler KC, Knauss S, Heppt MV, et al. Myositis and Neuromuscular Side-Effects Induced by Immune Checkpoint Inhibitors. *Eur J Cancer* (2019) 106:12–23. doi: 10.1016/j.ejca.2018.09.033
27. Brahmer JR, Lacchetti C, Schneider BJ, Atkins MB, Brassil KJ, Caterino JM, et al. Management of Immune-Related Adverse Events in Patients Treated With Immune Checkpoint Inhibitor Therapy: American Society of Clinical Oncology Clinical Practice Guideline. *J Clin Oncol* (2018) 36:1714–68. doi: 10.1200/JCO.2017.77.6385
28. Sanders DB, Wolfe GI, Benatar M, Evoli A, Gilhus NE, Illa I, et al. Intenational Consensus Guidance for Management of Myasthenia Gravis: Executive Summary. *Neurology* (2016) 87:419–25. doi: 10.1212/WNL.0000000000002790
29. Lau KH, Kumar A, Yang IH, Nowak RJ. Exacerbation of Myasthenia Gravis in a Patient With Melanoma Treated With Pembrolizumab. *Muscle Nerve* (2016) 54:157–61. doi: 10.1002/mus.25141
30. Zhu J, Li Y. Myasthenia Gravis Exacerbation Associated With Pembrolizumab. *Muscle Nerve* (2016) 54:506–7. doi: 10.1002/mus.25055
31. Shirai T, Sano T, Kamijo F, Saito N, Miyake T, Kodaira M, et al. Acetylcholine Receptor Binding Antibody-Associated Myasthenia Gravis and Rhabdomyolysis Induced by Nivolumab in a Patient With Melanoma. *Jpn J Clin Oncol* (2016) 46:86–8. doi: 10.1093/jjco/hyv158

Conflict of Interest: The authors declare that the research was conducted in the absence of any commercial or financial relationships that could be construed as a potential conflict of interest.

Publisher's Note: All claims expressed in this article are solely those of the authors and do not necessarily represent those of their affiliated organizations, or those of the publisher, the editors and the reviewers. Any product that may be evaluated in this article, or claim that may be made by its manufacturer, is not guaranteed or endorsed by the publisher.

Copyright © 2022 Bai, Li, Yang, Xu, Wang, Li, Liu, Du, Zhang and Feng. This is an open-access article distributed under the terms of the Creative Commons Attribution License (CC BY). The use, distribution or reproduction in other forums is permitted, provided the original author(s) and the copyright owner(s) are credited and that the original publication in this journal is cited, in accordance with accepted academic practice. No use, distribution or reproduction is permitted which does not comply with these terms.

frontiers in Immunology

MINI REVIEW
published: 06 January 2022
doi: 10.3389/fimmu.2021.802049

The Role of m6A Epigenetic Modification in the Treatment of Colorectal Cancer Immune Checkpoint Inhibitors

Huan Tong[1,2†], *He Wei*[3,4†], *Alhaji Osman Smith*[2] *and Juan Huang*[1*]

[1] Department of Hematology, Sichuan Academy of Medical Sciences & Sichuan Provincial People's Hospital,University of Electronic Science and Technology of China, Chengdu, China, [2] Blood Diseases Institute, Xuzhou Medical University, Xuzhou, China & Department of Hematology, The Affiliated Hospital of Xuzhou Medical University, Xuzhou, China & Key Laboratory of Bone Marrow Stem Cell, Xuzhou, China, [3] Department of Gastroenterology, The Second Affiliated Hospital of Chengdu Medical College, Nuclear Industry 416 Hospital, Chengdu, China, [4] School of Bioscience and Technology, Chengdu Medical College, Chengdu, China

OPEN ACCESS

Edited by:
Hubing Shi,
Sichuan University, China

Reviewed by:
Lizeng Gao,
Institute of Biophysics (CAS), China
Liu Yang,
China Medical University, China

***Correspondence:**
Juan Huang
huangjuanxy@med.uestc.edu.cn

[†]*These authors share first authorship*

Specialty section:
This article was submitted to Cancer Immunity and Immunotherapy, a section of the journal Frontiers in Immunology

Received: *26 October 2021*
Accepted: *22 December 2021*
Published: *06 January 2022*

Citation:
Tong H, Wei H, Smith AO and Huang J (2022) The Role of m6A Epigenetic Modification in the Treatment of Colorectal Cancer Immune Checkpoint Inhibitors. Front. Immunol. 12:802049. doi: 10.3389/fimmu.2021.802049

Tumor immunotherapy, one of the efficient therapies in cancers, has been called to the scientific community's increasing attention lately. Among them, immune checkpoint inhibitors, providing entirely new modalities to treat cancer by leveraging the patient's immune system. They are first-line treatments for varieties of advanced malignancy, such as melanoma, gastrointestinal tumor, esophageal cancer. Although immune checkpoint inhibitors (ICIs) treatment has been successful in different cancers, drug resistance and relapses are common, such as in colorectal cancer. Therefore, it is necessary to improve the efficacy of immune checkpoint therapy for cancer patients who do not respond or lowly response to current treatments. N6-methyladenosine (m6A), as a critical regulator of transcript expression, is the most frequently internal modification of mRNA in the human body. Recently, it has been proposed that m6A epigenetic modification is a potential driver of tumor drug resistance. In this report, we will briefly outline the relevant mechanisms, general treatment status of immune checkpoint inhibitors in colorectal cancer, how m6A epigenetic modifications regulate the response of ICIs in CRC and provide new strategies for overcoming the resistance of ICIs in CRC.

Keywords: colorectal cancer, ICB, resistance, m6A epigenetics, overcome resistance

INTRODUCTION

The 2018 Global Cancer Statistics estimates the incidence and mortality of 36 cancers in 185 countries around the world. It is reported that the incidence of colorectal cancer is 6.1%, and the mortality rate is 9.2%. The incidence and mortality rate of colorectal cancer is second only to breast cancer in women. In contrast, the incidence and mortality of colorectal cancer in men are second only to lung cancer and prostate cancer (1). In short, the incidence and mortality of colorectal cancer are currently at a high position, which should be paid great attention to and urgently needed effective measures to reduce. In the previous low-incidence areas, the incidence of colorectal cancer showed an upward trend (2).

Recently, it has been suggested that the patterns and trends of the incidence and mortality of colorectal cancer are connected to human beings' current living standards and lifestyles (3). While China's economic situation is now changing from developing countries to developed countries, Chinese average living standards get remarkably improved. Simultaneously, China is currently also in the stage of cancer transformation, the cancer spectrum is changing toward developed countries, and the cancer burden of colorectal cancer is increasing rapidly (4). Therefore, it is essential to prevent the onset of colorectal cancer and cure colorectal cancer patients, then to improve people's quality of life.

The current management strategies for colorectal cancer mainly include surgery, chemotherapy, radiotherapy, and immunotherapy (5, 6). Among them, cancer immunotherapy, containing active immunotherapy, passive immunotherapy, and immune checkpoint inhibitors, is gradually becoming the mainstream of modern cancer treatment (7), which has become a new research direction for cancer treatment and has received extensive attention (8, 9).

Recently, tumor immunotherapy, especially in immune checkpoint blockade treatment, has achieved remarkable success in the treatment of colorectal cancer. In particular, immune checkpoint inhibitors have been used in mismatch repair defects and high microsatellite instability (dMMR – MSI-H) metastasis, which have been shown to be effective in patients with colorectal cancer and have been approved by the FDA, such as pembrolizumab, nivolumab. Compared with most other treatments for malignant metastatic cancer, immune checkpoint blockade achieved long-term and durable remission in some patients, highlighting the excellent prospects of immune checkpoint blockade in treating colorectal cancer (10–14).

However, with the significant improvement of people's living standards, the quantity of patients with colorectal cancer has continued to hoist, increasing treatment difficulties are found nowadays. It is currently believed that only a tiny proportion of patients with colorectal cancer respond to immune checkpoint inhibitors treatment. While most proficient in mismatch repair (pMMR) and microsatellite stabilization (MSS) or low levels tumors with microsatellite instability (MSI-L) (called pMMR-MSI-L tumors) are ineffective. In these tumors, low tumor mutation burden and lack of immune cell infiltration are thought to be mechanisms of immune resistance (15, 16).

Because most pMMR and MSS or MSI-L patients with colorectal cancer is ineffective in ICIs, we wonder that, whether there exist some deeply resistant mechanisms in these patients. It has been proposed that epigenetic modification is a potential driver of tumor drug resistance (17). Since epigenetic inheritance is reversible in nature, the strategy of reversing epigenetic abnormalities is considered to be helpful in treating cancer and reversing drug resistance in cancer therapy (18–20).

In this report, we will briefly outline the relevant mechanisms of tumor immunity, the possible mechanism of tumor ICIs in treating tumors, the current status of colorectal cancer immune checkpoint inhibitors, and a potential method of m6A epigenetic modifications to regulate colorectal cancer ICIs response.

IMMUNOLOGICAL MECHANISMS FOR CANCER

In human immune system is divided into three categories: the immune defense, immune surveillance, and immune stability, in which tumorigenesis is closely related to the immune surveillance function in the body. Specifically, when the body discovers some cells become cancerous, the immune system will develop an innate immune response and an adaptive immune response targeting to tumor cells or antigens. These immune effector mechanisms influence and regulate each other to achieve the removal of tumor cells within the body (21–25).

In this process, cancer cells secrete some cytokines, which will stimulate the maturation of immature antigen-presenting cells, such as dendritic cells. Mature antigen-presenting cells then present relevant antigens to CD4+ or CD8+ T cells to make them respond, such as secreting some cytokines, which can further act on cytotoxic lymphocytes, Natural killer Cells, macrophages, and enhance the killing of cancer cells, as shown in **Figure 1A**.

However, even due the body has a series of intelligent immune surveillance, immune clearance of tumor cells, tumor cells escape the body's immune response and weaken the immune system, that result in tumor immune escape mechanism (21, 25).

Regarding the tumor immune escape mechanism, the current standard views are as follows: a. The immunogenicity of tumor cells is weakened or missing, b. Tumor antigen modulation, that is, due to the body's immune response to tumor antigens, tumor cell surface antigens are reduced, weakened, or disappear, thus leaving the immune system unrecognizable, allowing the tumor cells to escape the host immune attack, c. tumor cell surface antigens are covered or blocked, d. tumor antigens induce immune tolerance, e. tumor cells would resist apoptosis and induce immune cell apoptosis through Fas/FasL, PD-1/PD-L1 pathways, tumor cells induce immune suppression (21, 25, 26) as displayed in **Figure 1B**.

TUMOR IMMUNE CHECKPOINT INHIBITORS

Given that the body's immune system plays a vital role in the development and progression of tumors, tumor immunotherapy utilizing the body's own immune system to fight against tumor cells is booming. Immunotherapy is expected to become a new development following surgery, chemotherapy, radiotherapy, and targeted tumor therapy as a generation of tumor treatment methods (5, 6). The goal of tumor immunotherapy is to release the negative regulatory mechanism in the body and then enhance the immune response of cancer immunity (27). A typical example is to block PD-1/PD-L1 or CTLA-4.

Both PD-1 and CTLA-4 are checkpoints that co-inhibit signaling, which controls T-cell activities, such as activation, proliferation. Immune checkpoint inhibitors, such as PD-1/PD-L1 inhibitors and CTLA-4 inhibitors, is a way to remove tumor cells from the inhibitory effect of tumor cells on the immune

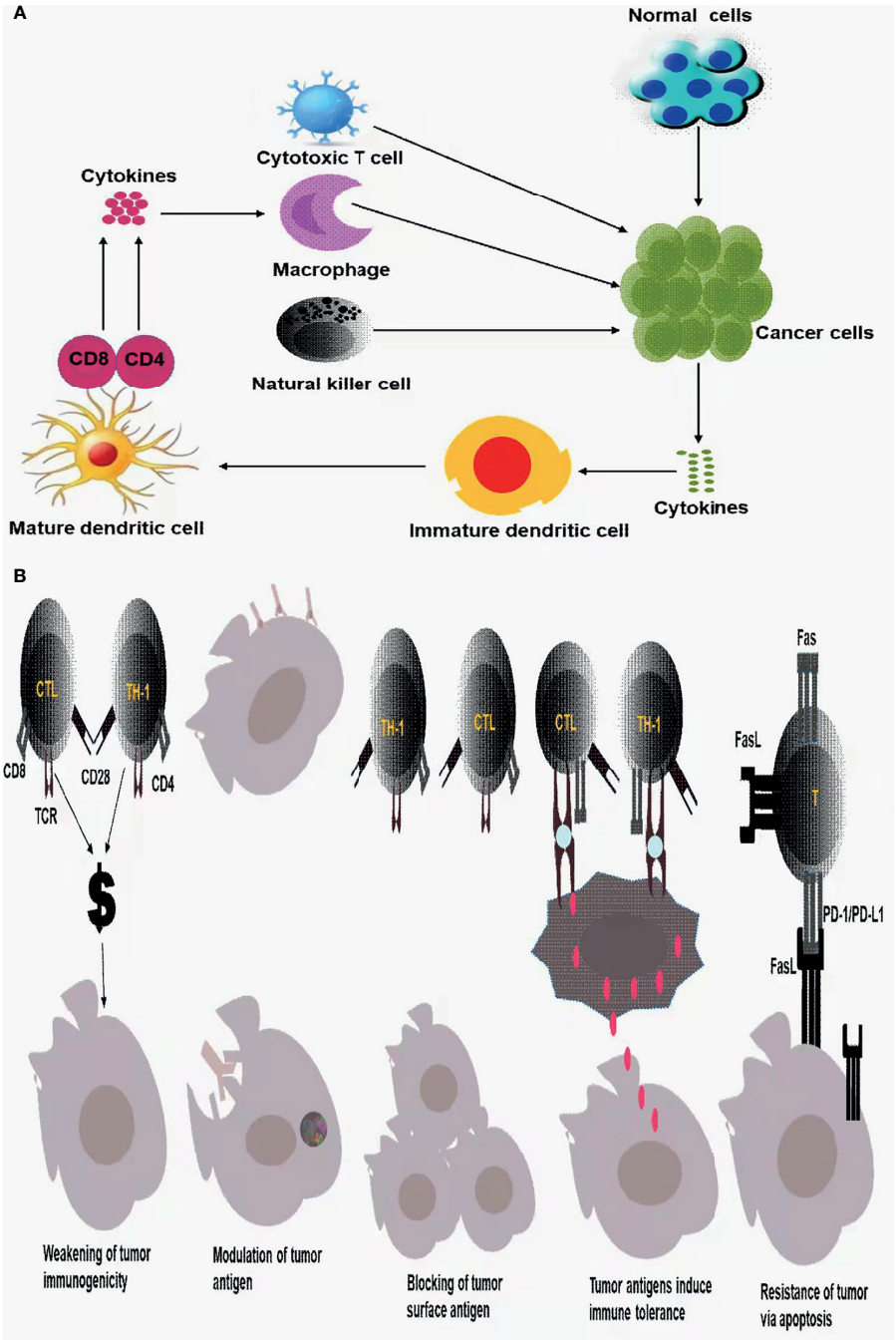

FIGURE 1 | **(A)** Innate immune response and adaptive immune response to tumor cells; **(B)** tumor immune escape mechanism.

system, release immune responses, and eliminate tumor cells, which are the excellent content of immunotherapy for colorectal cancer. On the surface of natural killer cells, dendritic cells, B cells,T cells, macrophages, MDSCs, et al. there exists substantial receptors—PD-1(PDCD1/CD279) (28–30). However, PD-1 is usually not expressed in inactivated T cells. PD-1 are not highly expressed until T cells are activated. The ligand—PD-L1/PD-L2, is a transmembrane protein that can bind to PD-1 and then negatively regulate T cell function, specifically, T cells' activation, proliferation, and survival (31). In tumor microenvironment, tumor cells and tumor-associated APCs highly express PD-L1, while tumor-infiltrating lymphocytes are gradually rich in PD-1 expression under long-term stimulation of tumor antigens. The combination of PD-L1 and PD-1 can

induce T cell apoptosis, disability, and depletion (**Figure 2**), thereby inhibiting the activation, proliferation, and anti-tumor function of tumor antigen-specific CD8+ T cells and achieving tumor immune escape (32–39). Noticeably, the use of PD-1/PD-L1 inhibitors would block the PD-1 signaling pathway, restore the body's tumor immunity to normal, and eliminate tumor cells in the body.

CTLA-4(CD152), is a transmembrane protein, whose receptors are B7-1(CD80) and B7-2(CD86). CTLA-4 and CD28 share the same receptor, but each of them in the body plays a completely different role. Triggering CD28 will strongly up-regulate T cells function, enhancing T cell activation and cytokine production, while triggering CTLA-4 wouldn't not only produce the same effect, but may also down-regulate CD28-mediated effects. Generally speaking, CD28 is expressed on resting and activated T cells while CTLA-4 is only expressed on activated T cells. Furthermore, CTLA-4 has a stronger affinity for B7 molecules than CD28 (40). After the TCR-CD3 complex is formed, CTLA-4 will rapidly up-regulate and bind with its high affinity to the co-activated receptors CD80 and CD86 expressed on antigen-presenting cells, thus negatively regulates the activation and function of T cells (41–47). In the tumor microenvironment, the expression of CTLA-4 in tumor infiltrating regulatory T cells (Treg) is increased (38, 48–50),

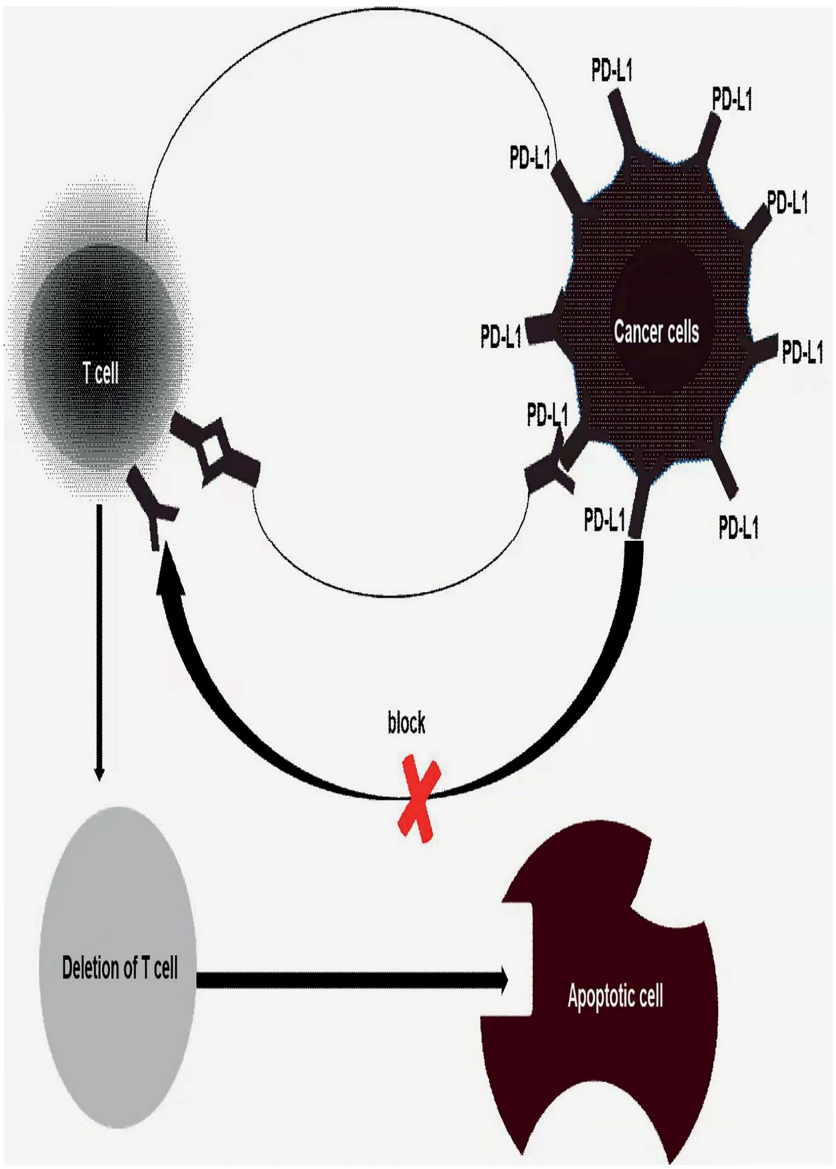

FIGURE 2 | Once tumor's PD-L1 binds to T cells's PD-1 induced depletion, disability and apoptosis of T cells, achieves tumor immune escape. Thus, block the binding of PD1/PD-L1 would be an effective treatment for human cancer or inhibiting tumor proliferation and metastasis.

thereby inhibiting the activation of tumor antigen-specific T cells, proliferation and anti-tumor function, realize tumor escape. Unlike PD-1/PD-L1 inhibitors, the using of CTLA-4 inhibitors would like to relieve the inhibitory effect of regulatory T cells (Treg) in the tumor microenvironment, enhancing the body's tumor immunity to eliminate tumor cells in the body.

Inhibition of PD1/PD-L1 and/or CTLA, beyond all doubt, would become an effective therapy to treat human cancers including colorectal cancer or to inhibit tumor proliferation and metastasis.

ICIS TREATMENT FOR COLORECTAL CANCER

Starting from this mechanism of tumor immune escape, inhibit the binding of tumor PD-L1 and T cell surface PD-1, block negative regulatory signals, restore the normal immune response of T cells to tumor cells to realize the role of removing tumor cells. Based on this mechanism, a large number of colorectal cancer patients have now been treated with ICIs. Fortunately, in treating colorectal cancer patients with PD-1, PD-L1, and CTLA-4 inhibitors, patients with high microsatellite stability (MSI-H) and mismatch repair defects showed fine efficacy (10–14, 51, 52). Recent researches demonstrated that Cytotoxic T cells, memory T cells, Th1 cells, N.K. Cells, TFH cells, B cells, activated and mature D.C., M1 macrophages, $FOXP3^{low}CD45RA-$ Treg cells, high PD-L1 expression on the exterior of immune cells were confirmed to be strongly associated with a favorable prognosis of CRC (53–59), while CRC patients with massive infiltration of $FOXP3^{hi-}$ Treg cells, Th17 cells, M2 macrophages, MDSCs, LAMP3 DC and neutrophils have generally a poor prognosis (60–63). Therefore, by raising the level of cells associated with good prognosis of colorectal cancer or lowering the level of cells associated with poor prognosis of colorectal cancer, it may improve the efficacy of colorectal cancer patients. Besides, one of the evaluation indicators over ICIs treatment response is the quantification of circulating tumor DNA (ctDNA). As a practical predictive approach, this indicator can be used in early monitoring to assess the tumor response of patients receiving anti-PD-1 therapy (64). Furthermore, it has shown that MSI, tumor mutation burden(TMB), and MMR played a critical role in the ICB response of colorectal cancer. Generally speaking, CRC patients with MSI-H, high TMB, and dMMR are considered to have a positive reaction to ICIs treatment. Thus CRC patients can get a considerably brilliant prognosis (65–67).

In 2010, Julie R Brahmer, et al. first reported anti-PD-1 in 39 patients with different advanced maglicies, in which one CRC receiving durable complete remission, while other cancers, like melanoma, renal cell cancer did not meet the PR criteria but had significant tumor lesion regression (68). With the in-depth study of anti-immune checkpoint treatment of cancer subsequent studies showed significant activity of PD-1 blockers in multiple cancers, leading to clinical approval for the treatment of multiple tumors, such as gastric cancer (69), colorectal cancer (70), liver cancer (71), and pancreatic cancer (72–74). However, despite of abundant success in treating CRC, there still exists resistance to ICIs in colorectal cancer. The results of current clinical studies are quite explorable, which encourage us to further explore the underlying mechanism of non-response or low-response to ICIs for CRC patients.

Thus, varieties of researches including basic and clinical are done over enhancing CRC efficiency. Researchers made a conclusion that CRC patients with MSI-H, high TMB and dMMR are demonstrated to get a nice response to ICIs treatment and own a considerably brilliant prognosis (65–67, 75–77). Following, FDA approved pebrolizumab used for the treatment of refractory, metastatic solid tumors with mismatch repair defects, high microsatellite instability, and applied nivolumab approval for the treatment of colorectal cancer with a mismatch repair defect and high microsatellite instability.

However, although this colorectal cancer type with very good response to ICIs treatment, there may still exist some resistance and patients still have poor response to ICIs treatment. Romain Cohen, et al. analyzed 38 colorectal cancer patients diagnosed with MSI or dMMR and treated with ICIs and found five had ICB resistance, immediately after they reassessed the status of MSI or dMMR and found that three mCRC patients are characterized with MSS or pMMR (78) showing that MSI-H or dMMR mCRC is misdiagnosed into MSS or pMMR as MSI-H or dMMR status. Therefore, it appears crucial to make a correct diagnosis and to determine MSS and MMR status by immunohistochemistry or PCR before ICIs treatment. Besides, Carino Gurjao, et al. reported that a patient with MSI-H and extremely high neoantigen load found continued disease progression despite with ICIs treatment. Then they tested the intrinsic resistance of CRC by testing the genomic, transcriptomes, immunohistochemistry of patient tumors and related immune microenvironment. They found that the possible reasons for intrinsic resistance to MSI-CRC were biallelic deletion of B2M (associated with antigen presentation) and increasing infiltration of NK cells and M2 macrophage (79). Therefore, attempting to improve B2M biallelic deletion status and reducing NK cell and M2 macrophage infiltration are possible effective pathways to improve intrinsic resistance to MSI-CRC. Next, CRC patients with MSI-H or dMMR with BRAF mutations also have relatively poor prognosis (80–82), therefore, such patients should be specific analysis, and utilize different therapeutic targets or combination therapy may be needed to improve efficacy.

Unfortunately, CRC patients with MSI-H or dMMR who respond well to ICIs efficacy account for only 10–15% of the entire CRC patient population, and approximately 85–90% of CRC patients belongs to the MSS or pMMR type. The current general view is that mCRC tumor cells accompanied by pMMR or MSS features have reduced immunogenicity to CD8 + T cells, reduced tumor cell mutation load, reduced HLA class molecule expression, and missing B2M protein are the possible reasons for their poor or even no response to ICIs treatment. There is no doubt that it's urgent to improve the efficacy of CRC patients

with MSS or pMMR to significantly improve the quality of life of CRC patients.

It is widely accepted that pMMR or MSS mCRC tumor cells have reduced immunogenicity, lower mutational load, low expression of HLA class molecules, and loss of 2-heterococytoprotein may be the main reason of (83) for its low or non-response to ICIs treatment. An increasing quantity of researchers have invested basic and clinical research to improve ICIs treatment response in pMMR or MSS mCRC patients, in order to improve progression-free survival and improve their quality of life in CRC patients. They found that ICIs combined with Fruquitinib or Regorafenib (an antiangiogenic drug, the former combination works better than the latter and could significantly improve the progression-free survival of mCRC patients) (84), LDH-A inhibitors (85), MEK inhibitors (86, 87), celecoxib (an inhibitor of the cyclooxidase COX2) (88), TGF-β inhibitors (89), CXCR4 inhibitors (90) combined treatment of pMMR or MSS mCRC, could significantly improve the treatment response of such patients to ICB in response, which provides a vision of a promising cure for CRC, however, drugs partly produce some toxic side effects such as colitis and duodenal ulcer, one of the pathogenic factors in colorectal cancer. Therefore, there is an urgent need to explore an effective treatment of CRC patients, including MSI-H or dMMR characteristics and pMMR or MSS characteristics, to improve progression-free survival and improve their quality of life in CRC patients.

m6A EPIGENETIC MODIFICATION

Current studies have shown that epigenetic defects played a crucial role in all malignant tumors with genetic defects (18, 19, 91, 92). Cancer is a disease caused by the continuous accumulation of genetic and epigenetic alteration. Generally, epigenetic alteration often precedes cancer and then induce gene mutations which lead to cancer (93). Almost all human cancer types contain epigenetic alterations. Because epigenetic modifications are reversible in nature (18–20), epigenetics has become an attractive target for cancer therapy. Recent studies have found that, in addition to being related to cancer progression, epigenetic modification is also a potential driver of drug resistance (17).

N6-methyladenosine (m6A) modification is the most common epigenetic methylation modification in RNA, such as mRNAs, ncRNAs, approximately 80% of all RNA methylation modification *in vivo* (94), which influences RNA function, for example, it has an great effect on RNA splicing, export, stability and translation. m6A modification is a reversible and dynamic in RNA epigenetic process. It is adjusted by m6A regulators, the main regulators containing "writer" (methyltransferase), "reader" (signal converter), combined with "eraser" (demethylation basease) (95).

Specifically, the writers, whose function is adding methylation into RNA to make the RNA methylated, up to date, are composed of METTL3, METTL14, WTAP, RBM15, RBM15B, ZC3H13 and KIAA1429 (96, 97). The readers, identifying methylation sites, are contained with YTHDC1, YTHDC2, YTHDF1, YTHDF2, YTHDF3, HNRNPC,IMP2 and HNRNPA2B1 (98–101). The erasers, whose role is deleting the methylation of RNA, mainly consist of FTO and ALKBH5 (102, 103) as revealed in **Figure 3**.

m6A MODIFICATION, ICIs IN CRC

At present, anti-immune checkpoint treatment of CRC is the thoroughly studied type of immunotherapy and has left some treating troubles so far (17). Researches lately have displayed that, in addition to being related to cancer progression, m6A epigenetic modification is also a potential driver of drug resistance (104). There are several main mechanisms that lead to anti-cancer drug resistance: changes in drug metabolism, deregulation of drug transport, mutations or changes in target protein expression, the above-mentioned mechanisms are the main reasons for the decrease in the efficacy of anti-cancer drugs (105–109).

Among several new methods to achieve the goal of drug sensitive, the regulation of m6A RNA modification has been demonstrated to be an overwhelming strategy for the drug resistance of various types of cancer cells. M6A regulates RNA's different-stage function, such as RNA splicing, degradation and translation to take part in a variety of biological processes including cell proliferation, metabolism and metastasis, and the caused anti-tumor resistance (109).

Immune checkpoint inhibitors have been utilized to colorectal cancer therapy and provides a promising clinical advantage; however, it usually shows that CRC patients make a low response or resistance (110). To improve the efficacy of ICB, it is urgently needed to identify the underlying mechanism for the low-response or resistance of ICIs in CRC. Recent studies have shown that m6A modifications are highly related with the low-response or resistance of ICIs in CRC, one possible reason that m6A tightly connected with microenvironment of tumor and immune cells in CRC.

The m6A modification pathway is often misregulated in cancer (111). Bo Zhang, et al. revealed that m6A modification is necessary in TME (112–115). The high m6A score, characterized by decreased mutation burden and immune activation, is related to reduced neoantigen load and poor response to ICIs (115). Patients with higher m6A-related risks have lower expression of immune checkpoint molecules, indicating that ICIs treatment may be less efficient for this subgroup. Therefore, m6A risk characteristics could be used as immunotherapy predictors for STAD prognosis in a clinical setting, and the underlying mechanism of the relationship between immune checkpoint molecules and m6A methylation needs to be further studied (115). In the same way as gastric cancer, does this apply to the colorectal tumors belonging to the digestive tract tumor? This will provide new ideas for clinically predicting the ICIs response of patients with colorectal cancer and further strengthening ICIs therapeutic response in colorectal cancer.

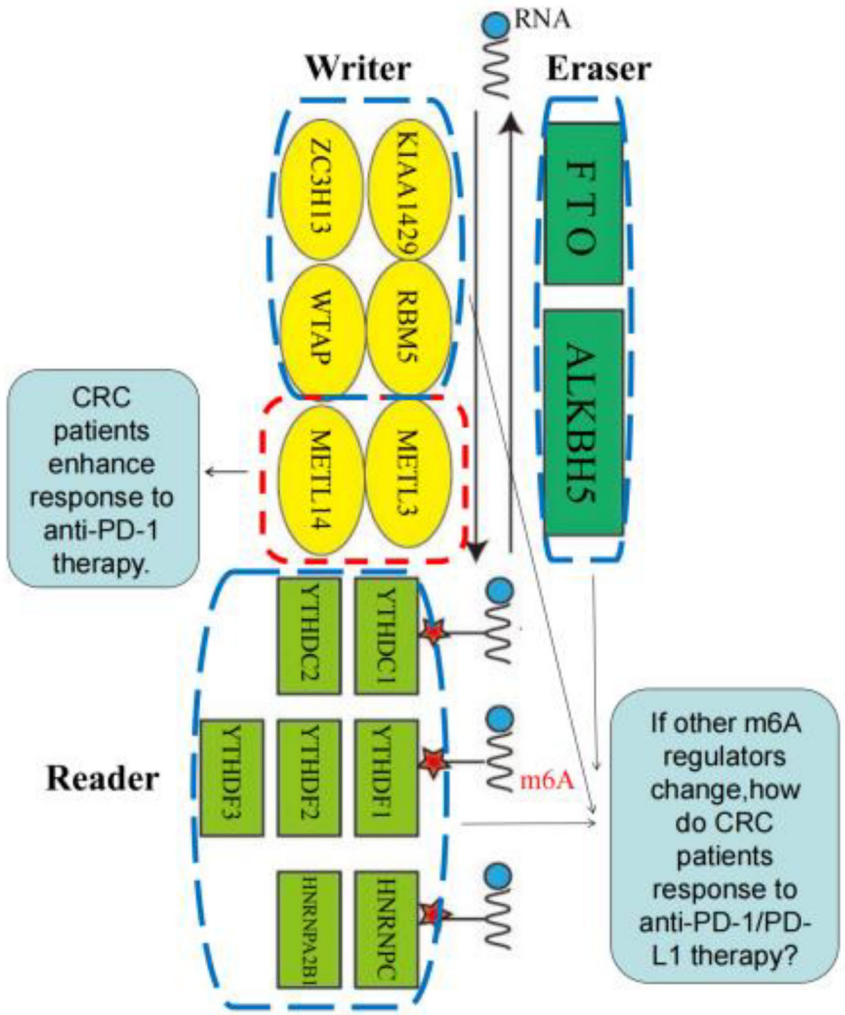

FIGURE 3 | m6A regulators, including "writer" (methyltransferase), "reader" (signal converter) and "eraser" (demethylation basease).

m6A Writers, ICIs in CRC

M6A modification regulated by METTL3 may promotes D.C. activation and maturation, Specific knockout Mettl3 in D.C. causes impaired phenotypic and functional maturation of D.C. and decreases their capacities of stimulating T cell responses (112). Specific depletion of Mettl3 in tumor-associated macrophages(TAM) resulted in CD8+ T cells dysfunction and tumor growth (113). With the reducing of m6A regulated by Mettl14, expression of the tumor suppressor KLF4 will be substantially increased and will further promote the migration of CRC cells and invasion (114). Interestingly some reseachers believed that m6A writers, such as Mettl3, WTAP, is positively associated with CRC cells invasion, migration, progression, and tumor stem cells with stemness and drug resistance (116–119).

Chen Xiaoxiang, et al. explored the function of m6A modification in CRC, illustrated the mechanism of m6A modification involved in the biological process of CRC, and confirmed that METTL14 is related to the progression of CRC *in vivo* and *in vitro* (112–114, 116–120). Lingling Wang et al. found that the deletion of methyltransferases Mettl3 and Mettl14 inhibited N6 methyladenosine (m6A) mRNA modification, enhanced pMMR-MSI-L colorectal cancer and melanoma patients' response to anti-PD-1 therapy, and significantly slowed down tumor grows and prolongs the patient's survival. In addition, the deficiency of MettL3 or Mettl14 in tumors results in enhancing cytotoxic tumor-infiltrating CD8+ T cells, and increasing the secretion of IFN-c, Cxcl9 and Cxcl10 in TME *in vivo*, which proves that the immune system and tumor microenvironment have metastasized in tumor m6A mRNA. Changes will occur after the enzyme is removed. In patients with colorectal cancer and melanoma undergoing immunotherapy, changes in the transcriptome profile of methyltransferase-deficient tumors in tumor cells indicate that the activation of

IFN-c signaling is the key to resensitization, while external transcriptome analysis shows that IFN -c-Stat1-Irf1 axis transcript lacking m6A modification contributes to the stabilization of m6A reader Ythdf2-mediated transcripts, thereby explaining the up-regulation of IFN-c signaling and changes in the tumor microenvironment (121), this discovery will further promote the understanding and in-depth study of m6A methyltransferase in the anti-PD-1/PD-L1 treatment of colorectal cancer.

However, whether and how m6A modifications writers alteration influence the efficiency of ICIs in colorectal cancer, still remains further research.

m6A Erasers, ICIs in CRC

Zeyan Zhang, et al. studied m6A erasers and found that reducing FTO expression, inhibiting MZF1 expression, and thus c-Myc expression and hindered CRC cell proliferation and progression (122). Contrary to the conclusion, Danyun Ruan, et al. and Sebastien Relier, et al. suggested that inhibiting FTO expression would promote CRC metastasis, poor prognosis and high recurrence in CRC patients (101, 123).

The study by Seungwon Yang, et al. found that under the action of the demethylase FTO, m6A will promote the growth of melanoma and reduce its response to anti-PD-1 blocking immunotherapy. When FTO is knocked out, it can increase m6A methylation in key tumorigenic melanoma cells (including PD-1, CXCR4 and SOX10), resulting in increased RNA attenuation through m6A reader YTHDF2, and then cause that melanoma cells are sensitive to interferon-γ (IFN-γ) and make melanoma sensitive to anti-PD-1 treatment. It is generally believed that inhibiting the combination of FTO and anti-PD-1 blockade may attenuate the resistance of melanoma to immunotherapy and improve the treatment response (124). However, they did not conduct research on colorectal cancer like Lingling Wang et al., but this will open a new way of thinking about ICIs resistance in colorectal cancer patients.

Then the study by Na Lia, et al. found that the knockout of the m6A demethylase ALKBH5 would make tumors susceptible to cancer immunotherapy. Specifically, ALKBH5 regulates the expression level and lactic acid content of Mct4/Slc16a3 in the TME and the constitution of tumor infiltrating Tregs and myeloid-derived suppressor cells. The research results show that m6A demethylase in tumor cells contributes to the effect of immunotherapy, and ALKBH5 is identified as a potential therapeutic target to improve the efficacy of immunotherapy for melanoma, colorectal cancer and other potential cancers (125).

However, whether and how m6A modifications erasers variations influence the efficiency of ICIs in colorectal cancer, still remains further research.

m6A Readers, ICIs in CRC

Numerous studies on m6A Reader have confirmed four genes (YTHDF1, IGF2BP1, IGF2BP1, IGFBP3, EIF3B) is a potential biomarker of CRC. It was found to downregulate YTHDF1 or IMP2, can further regulate the GLS1-glutamine metabolic axis, improve the stability of the m6A-modified GSK3β mRNA, inhibition of Wnt/-catenin/cyclin D1 expression, inhibition of CRC cell proliferation, colony formation, and increase the apoptosis levels in CRC cells, To sensitized cisplatin-resistant CRC cells (126–128).

Kazuo Tsuchiya, et al. used immunohistochemistry to detect the protein expression levels of m6A readers, such as YTHDF1 and YTHDF2 in 603 cases of non-small cell lung cancer tissues and evaluated four subgroups as TILs in tumor nests and surrounding stroma (PD-1, CD8, Foxp3 and CD45RO), and to study the differential expression of PD-L1 in lung cancer cells lacking YTHDF1 and YTHDF2. They found that YTHDF1 and YTHDF2 lowerly expressed in advanced tumors than that of early tumors, and the expression of YTHDF1 and YTHDF2 were also advised to be independent favorable prognostic factors for recurrence-free survival. In tumors with high expression of YTHDF1 and YTHDF2, the TIL density of almost all four lymphocyte subgroups in the stroma was significantly increased. *In vitro*, YTHDF1 and YTHDF2 knockout in cells up-regulated the expression of tumor PD-L1 and changed a variety of immune-related genes. It shows that the high expression of YTHDF1 and YTHDF2 is related to the good prognosis of NSCLC patients, the increase in the number of TIL and the down-regulation of PD-L1. YTHDF1 and YTHDF2 may be new prognostic and drug targets related to lung cancer tumor immune microenvironment (129). However, whether the up-regulation of YTHDF1 and YTHDF2 is effective for patients with colorectal cancer needs further research.

However, whether and how m6A modifications readers changes influence the efficiency of ICIs in colorectal cancer, still remains further research.

The possible reasons for such interestingly different and even opposite conclusions for different researchers in the same study subject maybe depended on m6A modified different RNA sites, different patterns in different immune cells, or different types of CRC, for example, MSS/pMMR or MSI-H/dMMR and whether accompanied by BRAF mutations.

However, due to methodological limitations, these studies are limited to one or two RNA modification "writers", "erasers" or "readers", but the antitumor effects of RNA modifications are characterized by highly complicated interactions of many regulators. Thus, a comprehensive and full understanding of how the regulatory networks of multiple RNA modification, there is no doubt that, will absolutely help us to have a better understanding of immunomodulatory and development of immunotherapy strategies in low-response or resistance of ICIs in CRC patients.

CONCLUSIONS AND PROSPECTS

The success of tumor immunotherapy, especially the success of ICIs treatment, has brought encouraging hope and confidence for better treatment and possible cure of colorectal cancer patients. However, because about 85-90% of colorectal cancer patients have the characteristics of pMMR or MSI-L in clinical practice, whose typical feature is that the tumor with a lower mutation burden has a poor curative effect, usually showing resistance to ICIs treatment. So this will force us to further

explore the cure of colorectal cancer and the mechanism of PD-1/PD-L1 resistance.

In this review, we summarized the mechanism of immune escape in the process of general cancer and the current status of immune checkpoint blockade treatment of colorectal cancer. At the same time, we also deeply explored and guess the role of m6A in mechanism of resistance in colorectal cancer anti-PD-1/PD-L1 therapy.

For the brief mechanism of m6A to relieve the resistance of colorectal cancer patients to anti-PD-1/PD-L1 therapy, we summarize the existing research and speculate the following findings. The m6A modification regulated by the m6A regulator includes the "writer" (methyltransferase_METTL3, METL14), "reader" (signal converter_YTHDC1, YTHDC2) and "eraser" (demethylase_FTO, ALKBH5) (67). Inhibition of "writers" (methyltransferase_Mettl3, Mettl14) can inhibit m6A modification, enhance the response of pMMR-MSI-L colorectal cancer patients to anti-PD-1 treatment, and significantly slow down tumor growth and prolong patient survival; activation the high expression of "readers" (signal converters_YTHDF1 and YTHDF2) may be related to the good prognosis of patients with colorectal cancer, the increase in the number of TIL, and the down-regulation of PD-L1, and may become a novel related to the immune microenvironment of colorectal cancer. The prognosis and drug targets of the drug; inhibiting the "eraser" (demethylase_FTO, ALKBH5) may increase the sensitivity of colorectal cancer patients to immune checkpoint therapy and reduce resistance after the anti-PD-1/PD-L1 therapy.

At present, in colorectal cancer ICIs treatment resistance research, only Lingling Wang et al. from the m6A "author" (methyltransferase_Mettl3, Mettl14) point of view, found that the deletion of methyltransferase Mettl3 and Mettl14 inhibits N6 methyladenosine (m6A) mRNA modification, enhances the response of pMMR-MSI-L colorectal cancer and melanoma patients to anti-PD-1 treatment, and significantly slows tumor growth and prolongs patient survival. And whether m6A "reader" (signal converter_YTHDF1, YTHDF2), "eraser" (demethylase_FTO, ALKBH5), etc. or how to convert can increase the sensitivity of colorectal cancer patients to immune checkpoint therapy and reduce the resistance of colorectal cancer patients to anti-PD-1/PD-L1 therapy still needs further research.

AUTHOR CONTRIBUTIONS

HT, HW, and AS made significant contribution on writing this review. JH designed the topic and checked the manuscript. All authors contributed to the article and approved the submitted version.

REFERENCES

1. Bray F, Ferlay J, Soerjomataram I, Siegel RL, Torre LA, Jemal A. Global Cancer Statistics 2018: GLOBOCAN Estimates of Incidence and Mortality Worldwide for 36 Cancers in 185 Countries. *CA Cancer J Clin* (2018) 68 (6):394–424. doi: 10.3322/caac.21492
2. Arnold M, Abnet CC, Neale RE, Vignat J, Giovannucci EL, McGlynn KA, et al. Global Burden of 5 Major Types of Gastrointestinal Cancer. *Gastroenterology* (2020) 159(1):335–349.e15. doi: 10.1053/j.gastro.2020.02.068
3. Arnold M, Sierra MS, Laversanne M, Soerjomataram I, Jemal A, Bray F. Global Patterns and Trends in Colorectal Cancer Incidence and Mortality. *Gut* (2017) 66(4):683–91. doi: 10.1136/gutjnl-2015-310912
4. Feng RM, Zong YN, Cao SM, Xu RH. Current Cancer Situation in China: Good or Bad News From the 2018 Global Cancer Statistics? *Cancer Commun (Lond)* (2019) 39(1):22. doi: 10.1186/s40880-019-0368-6
5. Mármol I, Sánchez-de-Diego C, Pradilla Dieste A, Cerrada E, Rodriguez Yoldi MJ. Colorectal Carcinoma: A General Overview and Future Perspectives in Colorectal Cancer. *Int J Mol Sci* (2017) 18(1):197. doi: 10.3390/ijms18010197
6. Tang Y, Zhang T, Zhou X, Zhao Y, Xu H, Liu Y, et al. The Preoperative Prognostic Value of the Radiomics Nomogram Based on CT Combined With Machine Learning in Patients With Intrahepatic Cholangiocarcinoma. *World J Surg Oncol* (2021) 19(1):45. doi: 10.1186/s12957-021-02162-0
7. Li B, Cui Y, Nambiar DK, Sunwoo JB, Li R. The Immune Subtypes and Landscape of Squamous Cell Carcinoma. *Clin Cancer Res* (2019) 25 (12):3528–37. doi: 10.1158/1078-0432.CCR-18-4085
8. Finck A, Gill SI, June CH. Cancer Immunotherapy Comes of Age and Looks for Maturity. *Nat Commun* (2020) 11(1):3325. doi: 10.1038/s41467-020-17140-5
9. Liu Z, Ravindranathan R, Kalinski P, Guo ZS, Bartlett DL. Rational Combination of Oncolytic Vaccinia Virus and PD-L1 Blockade Works Synergistically to Enhance Therapeutic Efficacy. *Nat Commun* (2017) 8:14754. doi: 10.1038/ncomms14754
10. Schreiber RD, Old LJ, Smyth MJ. Cancer Immunoediting: Integrating Immunity's Roles in Cancer Suppression and Promotion. *Science* (2011) 331(6024):1565–70. doi: 10.1126/science.1203486
11. Wang S, He Z, Wang X, Li H, Liu XS. Antigen Presentation and Tumor Immunogenicity in Cancer Immunotherapy Response Prediction. *Elife* (2019) 8:e49020. doi: 10.7554/eLife.49020
12. Schmid D, Park CG, Hartl CA, Subedi N, Cartwright AN, Puerto RB, et al. T Cell-Targeting Nanoparticles Focus Delivery of Immunotherapy to Improve Antitumor Immunity. *Nat Commun* (2017) 8(1):1747. doi: 10.1038/s41467-017-01830-8
13. Ciardiello D, Vitiello PP, Cardone C, Martini G, Troiani T, Martinelli E, et al. Immunotherapy of Colorectal Cancer: Challenges for Therapeutic Efficacy. *Cancer Treat Rev* (2019) 76:22–32. doi: 10.1016/j.ctrv.2019.04.003
14. Ganesh K, Stadler ZK, Cercek A, Mendelsohn RB, Shia J, Segal NH, et al. Immunotherapy in Colorectal Cancer: Rationale, Challenges and Potential. *Nat Rev Gastroenterol Hepatol* (2019) 16(6):361–75. doi: 10.1038/s41575-019-0126-x
15. Galon J, Costes A, Sanchez-Cabo F, Kirilovsky A, Mlecnik B, Lagorce- Pagès C, et al. Type, Density, and Location of Immune Cells Within Human Colorectal Tumors Predict Clinical Outcome. *Science* (2006) 313 (5795):1960–4. doi: 10.1126/science.1129139
16. Le DT, Durham JN, Smith KN, Wang H, Bartlett BR, Aulakh LK, et al. Mismatch Repair Deficiency Predicts Response of Solid Tumors to PD-1 Blockade. *Science* (2017) 357(6349):409–13. doi: 10.1126/science.aan6733
17. Adelaiye-Ogala R, Budka J, Damayanti NP, Arrington J, Ferris M, Hsu CC, et al. EZH2 Modifies Sunitinib Resistance in Renal Cell Carcinoma by Kinome Reprogramming. *Cancer Res* (2017) 77(23):6651–66. doi: 10.1158/0008-5472.CAN-17-0899
18. Tomar T, de Jong S, Alkema NG, Hoekman RL, Meersma GJ, Klip HG, et al. Genome-Wide Methylation Profiling of Ovarian Cancer Patient-Derived Xenografts Treated With the Demethylating Agent Decitabine Identifies Novel Epigenetically Regulated Genes and Pathways. *Genome Med* (2016) 8 (1):107. doi: 10.1186/s13073-016-0361-5
19. Vijayaraghavalu S, Dermawan JK, Cheriyath V, Labhasetwar V. Highly Synergistic Effect of Sequential Treatment With Epigenetic and Anticancer Drugs to Overcome Drug Resistance in Breast Cancer Cells Is Mediated *via* Activation of P21 Gene Expression Leading to G2/M Cycle Arrest. *Mol Pharm* (2013) 10(1):337–52. doi: 10.1021/mp3004622

20. Ahn DH, Javle M, Ahn CW, Jain A, Mikhail S, Noonan AM, et al. Next-Generation Sequencing Survey of Biliary Tract Cancer Reveals the Association Between Tumor Somatic Variants and Chemotherapy Resistance. *Cancer* (2016) 122(23):3657–66. doi: 10.1002/cncr.30247
21. Mohme M, Riethdorf S, Pantel K. Circulating and Disseminated Tumour Cells - Mechanisms of Immune Surveillance and Escape. *Nat Rev Clin Oncol* (2017) 14(3):155–67. doi: 10.1038/nrclinonc.2016.144
22. Ricklin D, Hajishengallis G, Yang K, Lambris JD. Complement: A Key System for Immune Surveillance and Homeostasis. *Nat Immunol* (2010) 11 (9):785–97. doi: 10.1038/ni.1923
23. Swann JB, Smyth MJ. Immune Surveillance of Tumors. *J Clin Invest* (2007) 117(5):1137–46. doi: 10.1172/JCI31405
24. Gajewski TF, Schreiber H, Fu YX. Innate and Adaptive Immune Cells in the Tumor Microenvironment. *Nat Immunol* (2013) 14(10):1014–22. doi: 10.1038/ni.2703
25. Kim R, Emi M, Tanabe K. Cancer Immunoediting From Immune Surveillance to Immune Escape. *Immunology* (2007) 121(1):1–14. doi: 10.1111/j.1365-2567.2007.02587.x
26. Jiang X, Wang J, Deng X, Xiong F, Ge J, Xiang B, et al. Role of the Tumor Microenvironment in PD-L1/PD-1-Mediated Tumor Immune Escape. *Mol Cancer* (2019) 18(1):10. doi: 10.1186/s12943-018-0928-4
27. Liu Y, Zheng P. Preserving the CTLA-4 Checkpoint for Safer and More Effective Cancer Immunotherapy. *Trends Pharmacol Sci* (2020) 41(1):4–12. doi: 10.1016/j.tips.2019.11.003
28. Schwartz RH. T Cell Anergy. *Annu Rev Immunol* (2003) 21:305–34. doi: 10.1146/annurev.immunol.21.120601.141110
29. Pardoll DM. The Blockade of Immune Checkpoints in Cancer Immunotherapy. *Nat Rev Cancer* (2012) 12(4):252–64. doi: 10.1038/nrc3239
30. Finger LR, Pu J, Wasserman R, Vibhakar R, Louie E, Hardy RR, et al. The Human PD-1 Gene: Complete cDNA, Genomic Organization, and Developmentally Regulated Expression in B Cell Progenitors. *Gene* (1997) 197(1-2):177–87. doi: 10.1016/s0378-1119(97)00260-6
31. Shi L, Chen S, Yang L, Li Y. The Role of PD-1 and PD-L1 in T-Cell Immune Suppression in Patients With Hematological Malignancies. *J Hematol Oncol* (2013) 6(1):74. doi: 10.1186/1756-8722-6-74
32. Thibult ML, Mamessier E, Gertner-Dardenne J, Pastor S, Just-Landi S, Xerri L, et al. PD-1 is a Novel Regulator of Human B-Cell Activation. *Int Immunol* (2013) 25(2):129–37. doi: 10.1093/intimm/dxs098
33. Topalian SL, Drake CG, Pardoll DM. Targeting the PD-1/B7-H1(PD-L1) Pathway to Activate Anti-Tumor Immunity. *Curr Opin Immunol* (2012) 24 (2):207–12. doi: 10.1016/j.coi.2011.12.009
34. Luo Y, Yang J, Yu J, Liu X, Yu C, Hu J, et al. Long Non-Coding RNAs: Emerging Roles in the Immunosuppressive Tumor Microenvironment. *Front Oncol* (2020) 10:48. doi: 10.3389/fonc.2020.00048
35. Ghebeh H, Mohammed S, Al-Omair A, Qattan A, Lehe C, Al-Qudaihi G, et al. The B7-H1 (PD-L1) T Lymphocyte-Inhibitory Molecule is Expressed in Breast Cancer Patients With Infiltrating Ductal Carcinoma: Correlation With Important High-Risk Prognostic Factors. *Neoplasia* (2006) 8(3):190–8. doi: 10.1593/neo.05733
36. Wong RM, Scotland RR, Lau RL, Wang C, Korman AJ, Kast WM, et al. Programmed Death-1 Blockade Enhances Expansion and Functional Capacity of Human Melanoma Antigen-Specific CTLs. *Int Immunol* (2007) 19(10):1223–34. doi: 10.1093/intimm/dxm091
37. Ni Y, Zhou X, Yang J, Shi H, Li H, Zhao X, et al. The Role of Tumor-Stroma Interactions in Drug Resistance Within Tumor Microenvironment. *Front Cell Dev Biol* (2021) 9:637675. doi: 10.3389/fcell.2021.637675
38. Ahmadzadeh M, Johnson LA, Heemskerk B, Wunderlich JR, Dudley ME, White DE, et al. Tumor Antigen-Specific CD8 T Cells Infiltrating the Tumor Express High Levels of PD-1 and are Functionally Impaired. *Blood* (2009) 114(8):1537–44. doi: 10.1182/blood-2008-12-195792
39. Fourcade J, Sun Z, Benallaoua M, Guillaume P, Luescher IF, Sander C, et al. Upregulation of Tim-3 and PD-1 Expression is Associated With Tumor Antigen-Specific CD8+ T Cell Dysfunction in Melanoma Patients. *J Exp Med* (2010) 207(10):2175–86. doi: 10.1084/jem.20100637
40. Boussiotis VA. Molecular and Biochemical Aspects of the PD-1 Checkpoint Pathway. *N Engl J Med* (2016) 375(18):1767–78. doi: 10.1056/NEJMra1514296
41. Gordon SR, Maute RL, Dulken BW, Hutter G, George BM, McCracken MN, et al. PD-1 Expression by Tumour-Associated Macrophages Inhibits Phagocytosis and Tumour Immunity. *Nature* (2017) 545(7655):495–9. doi: 10.1038/nature22396
42. Linsley PS, Bradshaw J, Greene J, Peach R, Bennett KL, Mittler RS. Intracellular Trafficking of CTLA-4 and Focal Localization Towards Sites of TCR Engagement. *Immunity* (1996) 4(6):535–43. doi: 10.1016/s1074-7613(00)80480-x
43. Walunas TL, Lenschow DJ, Bakker CY, Linsley PS, Freeman GJ, Green JM, et al. CTLA-4 can Function as a Negative Regulator of T Cell Activation. *Immunity* (1994) 1(5):405–13. doi: 10.1016/1074-7613(94)90071-x
44. Fallarino F, Fields PE, Gajewski TF. B7-1 Engagement of Cytotoxic T Lymphocyte Antigen 4 Inhibits T Cell Activation in the Absence of CD28. *J Exp Med* (1998) 188(1):205–10. doi: 10.1084/jem.188.1.205
45. Krummel MF, Allison JP. CD28 and CTLA-4 Have Opposing Effects on the Response of T Cells to Stimulation. *J Exp Med* (1995) 182(2):459–65. doi: 10.1084/jem.182.2.459
46. Masteller EL, Chuang E, Mullen AC, Reiner SL, Thompson CB. Structural Analysis of CTLA-4 Function In Vivo. *J Immunol (Baltimore Md 1950)* (2000) 164,10:5319–27. doi: 10.4049/jimmunol.164.10.5319
47. Peggs KS, Quezada SA, Chambers CA, Korman AJ, Allison JP. Blockade of CTLA-4 on Both Effector and Regulatory T Cell Compartments Contributes to the Antitumor Activity of Anti-CTLA-4 Antibodies. *J Exp Med* (2009) 206 (8):1717–25. doi: 10.1084/jem.20082492
48. van der Merwe PA, Bodian DL, Daenke S, Linsley P, Davis SJ. CD80 (B7-1) Binds Both CD28 and CTLA-4 With a Low Affinity and Very Fast Kinetics. *J Exp Med* (1997) 185(3):393–403. doi: 10.1084/jem.185.3.393
49. Qureshi OS, Kaur S, Hou TZ, Jeffery LE, Poulter NS, Briggs Z, et al. Constitutive Clathrin-Mediated Endocytosis of CTLA-4 Persists During T Cell Activation. *J Biol Chem* (2012) 287(12):9429–40. doi: 10.1074/jbc.M111.304329
50. Walker LS, Sansom DM. The Emerging Role of CTLA4 as a Cell-Extrinsic Regulator of T Cell Responses. *Nat Rev Immunol* (2011) 11(12):852–63. doi: 10.1038/nri3108
51. André T, Shiu KK, Kim TW, Jensen BV, Jensen LH, Punt C, et al. KEYNOTE-177 Investigators. Pembrolizumab in Microsatellite-Instability-High Advanced Colorectal Cancer. *N Engl J Med* (2020) 383(23):2207–18. doi: 10.1056/NEJMoa2017699
52. Le DT, Uram JN, Wang H, Bartlett BR, Kemberling H, Eyring AD, et al. PD-1 Blockade in Tumors With Mismatch-Repair Deficiency. *N Engl J Med* (2015) 372(26):2509–20. doi: 10.1056/NEJMoa1500596
53. Kim HR, Ha SJ, Hong MH, Heo SJ, Koh YW, Choi EC, et al. PD-L1 Expression on Immune Cells, But Not on Tumor Cells, is a Favorable Prognostic Factor for Head and Neck Cancer Patients. *Sci Rep* (2016) 6:36956. doi: 10.1038/srep36956
54. Bruni D, Angell HK, Galon J. The Immune Contexture and Immunoscore in Cancer Prognosis and Therapeutic Efficacy. *Nat Rev Cancer* (2020) 20 (11):662–80. doi: 10.1038/s41568-020-0285-7
55. Tosolini M, Kirilovsky A, Mlecnik B, Fredriksen T, Mauger S, Bindea G, et al. Clinical Impact of Different Classes of Infiltrating T Cytotoxic and Helper Cells (Th1, Th2, Treg, Th17) in Patients With Colorectal Cancer. *Cancer Res* (2011) 71(4):1263–71. doi: 10.1158/0008-5472.CAN-10-2907
56. Coca S, Perez-Piqueras J, Martinez D, Colmenarejo A, Saez MA, Vallejo C, et al. The Prognostic Significance of Intratumoral Natural Killer Cells in Patients With Colorectal Carcinoma. *Cancer* (1997) 79(12):2320–8. doi: 10.1002/(sici)1097-0142(19970615)79:12<2320::aid-cncr5>3.0.co;2-p
57. Melero I, Rouzaut A, Motz GT, Coukos G. T-Cell and NK-Cell Infiltration Into Solid Tumors: A Key Limiting Factor for Efficacious Cancer Immunotherapy. *Cancer Discov* (2014) 4(5):522–6. doi: 10.1158/2159-8290.CD-13-0985
58. Kinouchi M, Miura K, Mizoi T, Ishida K, Fujibuchi W, Sasaki H, et al. Infiltration of CD40-Positive Tumor-Associated Macrophages Indicates a Favorable Prognosis in Colorectal Cancer Patients. *Hepatogastroenterology* (2013) 60(121):83–8. doi: 10.5754/hge12372
59. Malietzis G, Lee GH, Jenkins JT, Bernardo D, Moorghen M, Knight SC, et al. Prognostic Value of the Tumour-Infiltrating Dendritic Cells in Colorectal Cancer: A Systematic Review. *Cell Commun Adhes* (2015) 22(1):9–14. doi: 10.3109/15419061.2015.1036859

60. Saito T, Nishikawa H, Wada H, Nagano Y, Sugiyama D, Atarashi K, et al. Two FOXP3(+)CD4(+) T Cell Subpopulations Distinctly Control the Prognosis of Colorectal Cancers. *Nat Med* (2016) 22(6):679–84. doi: 10.1038/nm.4086
61. Aras S, Zaidi MR. TAMeless Traitors: Macrophages in Cancer Progression and Metastasis. *Br J Cancer* (2017) 117(11):1583–91. doi: 10.1038/bjc.2017.356
62. Mosser DM, Edwards JP. Exploring the Full Spectrum of Macrophage Activation. *Nat Rev Immunol* (2008) 8(12):958–69. doi: 10.1038/nri2448
63. Sandel MH, Dadabayev AR, Menon AG, Morreau H, Melief CJ, Offringa R, et al. Prognostic Value of Tumor-Infiltrating Dendritic Cells in Colorectal Cancer: Role of Maturation Status and Intratumoral Localization. *Clin Cancer Res* (2005) 11(7):2576–82. doi: 10.1158/1078-0432.CCR-04-1448
64. Cabel L, Riva F, Servois V, Livartowski A, Daniel C, Rampanou A, et al. Circulating Tumor DNA Changes for Early Monitoring of Anti-PD1 Immunotherapy: A Proof-of-Concept Study. *Ann Oncol* (2017) 28 (8):1996–2001. doi: 10.1093/annonc/mdx212
65. Eso Y, Shimizu T, Takeda H, Takai A, Marusawa H. Microsatellite Instability and Immune Checkpoint Inhibitors: Toward Precision Medicine Against Gastrointestinal and Hepatobiliary Cancers. *J Gastroenterol* (2020) 55(1):15–26. doi: 10.1007/s00535-019-01620-7
66. Liu X, Feng Y, Xu J, Shi Y, Yang J, Zhang R, et al. Combination of MAPK Inhibition With Photothermal Therapy Synergistically Augments the Anti-Tumor Efficacy of Immune Checkpoint Blockade. *J Control Release* (2021) 332:194–209. doi: 10.1016/j.jconrel.2021.02.020
67. Xu G, Luo Y, Wu W, Liu X, Yu X, Bao Y, et al. The Evolution of Acquired Resistance to BRAFV600E Kinase Inhibitor Is Sustained by IGF1-Driven Tumor Vascular Remodeling. *J Invest Dermatol* (2021) S0022-202X (21):01669–9. doi: 10.1016/j.jid.2021.07.162
68. Brahmer JR, Drake CG, Wollner I, Powderly JD, Picus J, Sharfman WH, et al. Phase I Study of Single-Agent Anti-Programmed Death-1 (MDX-1106) in Refractory Solid Tumors: Safety, Clinical Activity, Pharmacodynamics, and Immunologic Correlates. *J Clin Oncol* (2010) 28(19):3167–75. doi: 10.1200/JCO.2009.26.7609
69. Fuchs CS, Doi T, Jang RW, Muro K, Satoh T, Machado M, et al. Safety and Efficacy of Pembrolizumab Monotherapy in Patients With Previously Treated Advanced Gastric and Gastroesophageal Junction Cancer: Phase 2 Clinical KEYNOTE-059 Trial. *JAMA Oncol* (2018) 4(5):e180013. doi: 10.1001/jamaoncol.2018.0013
70. Francis DM, Manspeaker MP, Schudel A, Sestito LF, O'Melia MJ, Kissick HT, et al. Blockade of Immune Checkpoints in Lymph Nodes Through Locoregional Delivery Augments Cancer Immunotherapy. *Sci Transl Med* (2020) 12(563):eaay3575. doi: 10.1126/scitranslmed.aay3575
71. El-Khoueiry AB, Sangro B, Yau T, Crocenzi TS, Kudo M, Hsu C, et al. Nivolumab in Patients With Advanced Hepatocellular Carcinoma (CheckMate 040): An Open-Label, non-Comparative, Phase 1/2 Dose Escalation and Expansion Trial. *Lancet* (2017) 389(10088):2492–502. doi: 10.1016/S0140-6736(17)31046-2
72. Diaz Beveridge R, Alcolea V, Aparicio J, Segura Á, García J, Corbellas M, et al. Management of Advanced Pancreatic Cancer With Gemcitabine Plus Erlotinib: Efficacy and Safety Results in Clinical Practice. *JOP* (2014) 15 (1):19–24. doi: 10.6092/1590-8577/1570
73. Cardin DB, Goff L, Li CI, Shyr Y, Winkler C, DeVore R, et al. Phase II Trial of Sorafenib and Erlotinib in Advanced Pancreatic Cancer. *Cancer Med* (2014) 3(3):572–9. doi: 10.1002/cam4.208
74. Llosa NJ, Cruise M, Tam A, Wicks EC, Hechenbleikner EM, Taube JM, et al. The Vigorous Immune Microenvironment of Microsatellite Instable Colon Cancer is Balanced by Multiple Counter-Inhibitory Checkpoints. *Cancer Discov* (2015) 5(1):43–51. doi: 10.1158/2159-8290.CD-14-0863
75. Biasci D, Smoragiewicz M, Connell CM, Wang Z, Gao Y, Thaventhiran JED, et al. CXCR4 Inhibition in Human Pancreatic and Colorectal Cancers Induces an Integrated Immune Response. *Proc Natl Acad Sci U S A* (2020) 117(46):28960–70. doi: 10.1073/pnas.2013644117
76. Overman MJ, McDermott R, Leach JL, Lonardi S, Lenz HJ, Morse MA, et al. Nivolumab in Patients With Metastatic DNA Mismatch Repair-Deficient or Microsatellite Instability-High Colorectal Cancer (CheckMate 142): An Open-Label, Multicentre, Phase 2 Study. *Lancet Oncol* (2017) 18(9):1182–91. doi: 10.1016/S1470-2045(17)30422-9
77. Han X, Yang J, Luo J, Chen P, Zhang Z, Alu A, et al. Application of CT-Based Radiomics in Discriminating Pancreatic Cystadenomas From Pancreatic Neuroendocrine Tumors Using Machine Learning Methods. *Front Oncol* (2021) 11:606677. doi: 10.3389/fonc.2021.606677
78. Cohen R, Hain E, Buhard O, Guilloux A, Bardier A, Kaci R, et al. Association of Primary Resistance to Immune Checkpoint Inhibitors in Metastatic Colorectal Cancer With Misdiagnosis of Microsatellite Instability or Mismatch Repair Deficiency Status. *JAMA Oncol* (2019) 5(4):551–5. doi: 10.1001/jamaoncol.2018.4942
79. Gurjao C, Liu D, Hofree M, AlDubayan SH, Wakiro I, Su MJ, et al. Intrinsic Resistance to Immune Checkpoint Blockade in a Mismatch Repair-Deficient Colorectal Cancer. *Cancer Immunol Res* (2019) 7(8):1230–6. doi: 10.1158/2326-6066.CIR-18-0683
80. Venderbosch S, Nagtegaal ID, Maughan TS, Smith CG, Cheadle JP, Fisher D, et al. Mismatch Repair Status and BRAF Mutation Status in Metastatic Colorectal Cancer Patients: A Pooled Analysis of the CAIRO, CAIRO2, COIN, and FOCUS Studies. *Clin Cancer Res* (2014) 20(20):5322–30. doi: 10.1158/1078-0432.CCR-14-0332
81. Yu C, Luo D, Yu J, Zhang M, Zheng X, Xu G, et al. Genome-Wide CRISPR-Cas9 Knockout Screening Identifies GRB7 as a Driver for MEK Inhibitor Resistance in KRAS Mutant Colon Cancer. *Oncogene* (2021). doi: 10.1038/s41388-021-02077-w
82. Cheng Y, Han X, Mo F, Zeng H, Zhao Y, Wang H, et al. Apigenin Inhibits the Growth of Colorectal Cancer Through Down-Regulation of E2F1/3 by miRNA-215-5p. *Phytomedicine* (2021) 89:153603. doi: 10.1016/j.phymed.2021.153603
83. Lee JJ, Chu E. Recent Advances in the Clinical Development of Immune Checkpoint Blockade Therapy for Mismatch Repair Proficient (pMMR)/non-MSI-H Metastatic Colorectal Cancer. *Clin Colorectal Cancer* (2018) 17 (4):258–73. doi: 10.1016/j.clcc.2018.06.004
84. Sun L, Huang S, Li D, Mao Y, Wang Y, Wu J. Efficacy and Safety of Fruquintinib Plus PD-1 Inhibitors Versus Regorafenib Plus PD-1 Inhibitors in Refractory Microsatellite Stable Metastatic Colorectal Cancer. *Front Oncol* (2021) 11:754881. doi: 10.3389/fonc.2021.754881
85. Zhang Y, Li J, Wang B, Chen T, Chen Y, Ma W. LDH-A Negatively Regulates dMMR in Colorectal Cancer. *Cancer Sci* (2021) 112(8):3050–63. doi: 10.1111/cas.15020
86. Loi S, Dushyanthen S, Beavis PA, Salgado R, Denkert C, Savas P, et al. RAS/MAPK Activation Is Associated With Reduced Tumor-Infiltrating Lymphocytes in Triple-Negative Breast Cancer: Therapeutic Cooperation Between MEK and PD-1/PD-L1 Immune Checkpoint Inhibitors. *Clin Cancer Res* (2016) 22(6):1499–509. doi: 10.1158/1078-0432.CCR-15-1125
87. Yu C, Zhang M, Song J, Zheng X, Xu G, Bao Y, et al. Integrin-Src-YAP1 Signaling Mediates the Melanoma Acquired Resistance to MAPK and PI3K/mTOR Dual Targeted Therapy. *Mol Biomed* (2020) 1(1):12. doi: 10.1186/s43556-020-00013-0
88. Liu X, Feng Y, Xu G, Chen Y, Luo Y, Song J, et al. MAPK-Targeted Drug Delivered by a pH-Sensitive MSNP Nanocarrier Synergizes With PD-1 Blockade in Melanoma Without T-Cell Suppression. *Adv Funct Mater* (2019) 1806916. doi: 10.1002/adfm.201806916
89. Chalabi M, Fanchi LF, Dijkstra KK, Van den Berg JG, Aalbers AG, Sikorska K, et al. Neoadjuvant Immunotherapy Leads to Pathological Responses in MMR-Proficient and MMR-Deficient Early-Stage Colon Cancers. *Nat Med* (2020) 26(4):566–76. doi: 10.1038/s41591-020-0805-8
90. Tauriello DVF, Palomo-Ponce S, Stork D, Berenguer-Llergo A, Badia-Ramentol J, Iglesias M, et al. Tgfβ Drives Immune Evasion in Genetically Reconstituted Colon Cancer Metastasis. *Nature* (2018) 554(7693):538–43. doi: 10.1038/nature25492
91. Yoo CB, Jones PA. Epigenetic Therapy of Cancer: Past, Present and Future. *Nat Rev Drug Discovery* (2006) 5(1):37–50. doi: 10.1038/nrd1930
92. Pan Y, Liu G, Zhou F, Su B, Li Y. DNA Methylation Profiles in Cancer Diagnosis and Therapeutics. *Clin Exp Med* (2018) 18(1):1–14. doi: 10.1007/s10238-017-0467-0
93. Xie VK, Li Z, Yan Y, Jia Z, Zuo X, Ju Z, et al. DNA-Methyltransferase 1 Induces Dedifferentiation of Pancreatic Cancer Cells Through Silencing of Krüppel-Like Factor 4 Expression. *Clin Cancer Res* (2017) 23(18):5585–97. doi: 10.1158/1078-0432.CCR-17-0387

94. Jian D, Wang Y, Jian L, Tang H, Rao L, Chen K, et al. METTL14 Aggravates Endothelial Inflammation and Atherosclerosis by Increasing FOXO1 N6-Methyladeosine Modifications. *Theranostics* (2020) 10(20):8939–56. doi: 10.7150/thno.45178
95. Tu Z, Wu L, Wang P, Hu Q, Tao C, Li K, et al. N6-Methylandenosine-Related lncRNAs Are Potential Biomarkers for Predicting the Overall Survival of Lower-Grade Glioma Patients. *Front Cell Dev Biol* (2020) 8:642. doi: 10.3389/fcell.2020.00642
96. Cao G, Li HB, Yin Z, Flavell RA. Recent Advances in Dynamic M6a RNA Modification. *Open Biol* (2016) 6(4):160003. doi: 10.1098/rsob.160003
97. Schöller E, Weichmann F, Treiber T, Ringle S, Treiber N, Flatley A, et al. Interactions, Localization, and Phosphorylation of the M6a Generating METTL3-METTL14-WTAP Complex. *RNA* (2018) 24(4):499–512. doi: 10.1261/rna.064063.117
98. Li A, Chen YS, Ping XL, Yang X, Xiao W, Yang Y, et al. Cytoplasmic M6a Reader YTHDF3 Promotes mRNA Translation. *Cell Res* (2017) 27(3):444–7. doi: 10.1038/cr.2017.10
99. Alarcón CR, Goodarzi H, Lee H, Liu X, Tavazoie S, Tavazoie SF. HNRNPA2B1 Is a Mediator of M(6)A-Dependent Nuclear RNA Processing Events. *Cell* (2015) 162(6):1299–308. doi: 10.1016/j.cell.2015.08.011
100. Wu R, Yao Y, Jiang Q, Cai M, Liu Q, Wang Y, et al. Epigallocatechin Gallate Targets FTO and Inhibits Adipogenesis in an mRNA M6a-YTHDF2-Dependent Manner. *Int J Obes (Lond)* (2018) 42(7):1378–88. doi: 10.1038/s41366-018-0082-5
101. Relier S, Ripoll J, Guillorit H, Amalric A, Achour C, Boissière F, et al. FTO-Mediated Cytoplasmic m6Am Demethylation Adjusts Stem-Like Properties in Colorectal Cancer Cell. *Nat Commun* (2021) 12(1):1716. doi: 10.1038/s41467-021-21758-4
102. Tang C, Klukovich R, Peng H, Wang Z, Yu T, Zhang Y, et al. ALKBH5-Dependent M6a Demethylation Controls Splicing and Stability of Long 3'-UTR mRNAs in Male Germ Cells. *Proc Natl Acad Sci U S A* (2018) 115(2):E325–33. doi: 10.1073/pnas.1717794115
103. Riley RS, June CH, Langer R, Mitchell MJ. Delivery Technologies for Cancer Immunotherapy. *Nat Rev Drug Discov* (2019) 18(3):175–96. doi: 10.1038/s41573-018-0006-z
104. Bivona TG, Doebele RC. A Framework for Understanding and Targeting Residual Disease in Oncogene-Driven Solid Cancers. *Nat Med* (2016) 22(5):472–8. doi: 10.1038/nm.4091
105. Chen Z, Shi T, Zhang L, Zhu P, Deng M, Huang C, et al. Mammalian Drug Efflux Transporters of the ATP Binding Cassette (ABC) Family in Multidrug Resistance: A Review of the Past Decade. *Cancer Lett* (2016) 370(1):153–64. doi: 10.1016/j.canlet.2015.10.010
106. Joyce H, McCann A, Clynes M, Larkin A. Influence of Multidrug Resistance and Drug Transport Proteins on Chemotherapy Drug Metabolism. *Expert Opin Drug Metab Toxicol* (2015) 11(5):795–809. doi: 10.1517/17425255.2015.1028356
107. Wang Y, Fang Z, Hong M, Yang D, Xie W. Long-Noncoding RNAs (lncRNAs) in Drug Metabolism and Disposition, Implications in Cancer Chemo-Resistance. *Acta Pharm Sin B* (2020) 10(1):105–12. doi: 10.1016/j.apsb.2019.09.011
108. Zhitomirsky B, Assaraf YG. Lysosomes as Mediators of Drug Resistance in Cancer. *Drug Resist Updat* (2016) 24:23–33. doi: 10.1016/j.drup.2015.11.004
109. Li B, Jiang J, Assaraf YG, Xiao H, Chen ZS, Huang C. Surmounting Cancer Drug Resistance: New Insights From the Perspective of N6-Methyladenosine RNA Modification. *Drug Resist Updat* (2020) 53:100720. doi: 10.1016/j.drup.2020.100720
110. Chen H, Yao J, Bao R, Dong Y, Zhang T, Du Y, et al. Cross-Talk of Four Types of RNA Modification Writers Defines Tumor Microenvironment and Pharmacogenomic Landscape in Colorectal Cancer. *Mol Cancer* (2021) 20(1):29. doi: 10.1186/s12943-021-01322-w
111. Yang F, Jin H, Que B, Chao Y, Zhang H, Ying X, et al. Dynamic M6a mRNA Methylation Reveals the Role of METTL3-M6a-CDCP1 Signaling Axis in Chemical Carcinogenesis. *Oncogene* (2019) 38(24):4755–72. doi: 10.1038/s41388-019-0755-0
112. Wang H, Hu X, Huang M, Liu J, Gu Y, Ma L, et al. Mettl3-Mediated mRNA M6a Methylation Promotes Dendritic Cell Activation. *Nat Commun* (2019) 10(1):1898. doi: 10.1038/s41467-019-09903-6
113. Dong L, Chen C, Zhang Y, Guo P, Wang Z, Li J, et al. The Loss of RNA N6-Adenosine Methyltransferase Mettl14 in Tumor-Associated Macrophages Promotes CD8+ T Cell Dysfunction and Tumor Growth. *Cancer Cell* (2021) 39(7):945–57.e10. doi: 10.1016/j.ccell.2021.04.016
114. Wang S, Gan M, Chen C, Zhang Y, Kong J, Zhang H, et al. Methyl CpG Binding Protein 2 Promotes Colorectal Cancer Metastasis by Regulating N6-Methyladenosine Methylation Through Methyltransferase-Like 14. *Cancer Sci* (2021) 112(8):3243–54. doi: 10.1111/cas.15011
115. Zhang B, Wu Q, Li B, Wang D, Wang L, Zhou YL. M6a Regulator-Mediated Methylation Modification Patterns and Tumor Microenvironment Infiltration Characterization in Gastric Cancer. *Mol Cancer* (2020) 19(1):53. doi: 10.1186/s12943-020-01170-0
116. Zheng Y, Wang Y, Liu Y, Xie L, Ge J, Yu G, et al. N6-Methyladenosine Modification of PTTG3P Contributes to Colorectal Cancer Proliferation *via* YAP1. *Front Oncol* (2021) 11:669731. doi: 10.3389/fonc.2021.669731
117. Liu X, Su K, Sun X, Jiang Y, Wang L, Hu C, et al. Sec62 Promotes Stemness and Chemoresistance of Human Colorectal Cancer Through Activating Wnt/β-Catenin Pathway. *J Exp Clin Cancer Res* (2021) 40(1):132. doi: 10.1186/s13046-021-01934-6
118. Chen C, Yuan W, Zhou Q, Shao B, Guo Y, Wang W, et al. N6-Methyladenosine-Induced Circ1662 Promotes Metastasis of Colorectal Cancer by Accelerating YAP1 Nuclear Localization. *Theranostics* (2021) 11(9):4298–315. doi: 10.7150/thno.51342
119. He RZ, Jiang J, Hu X, Lei M, Li J, Luo W, et al. Stabilization of UCA1 by N6-Methyladenosine RNA Methylation Modification Promotes Colorectal Cancer Progression. *Cancer Cell Int* (2021) 21(1):616. doi: 10.1186/s12935-021-02288-x
120. Chen X, Xu M, Xu X, Zeng K, Liu X, Sun L, et al. METTL14 Suppresses CRC Progression *via* Regulating N6-Methyladenosine-Dependent Primary miR-375 Processing. *Mol Ther* (2020) 28(2):599–612. doi: 10.1016/j.ymthe.2019.11.016
121. Wang L, Hui H, Agrawal K, Kang Y, Li N, Tang R, et al. M6 A RNA Methyltransferases METTL3/14 Regulate Immune Responses to Anti-PD-1 Therapy. *EMBO J* (2020) 39(20):e104514. doi: 10.15252/embj.2020104514
122. Zhang Z, Gao Q, Wang S. Kinase Gsk3β Functions as a Suppressor in Colorectal Carcinoma Through the FTO-Mediated MZF1/c-Myc Axis. *J Cell Mol Med* (2021) 25(5):2655–65. doi: 10.1111/jcmm.16291
123. Ruan DY, Li T, Wang YN, Meng Q, Li Y, Yu K, et al. FTO Downregulation Mediated by Hypoxia Facilitates Colorectal Cancer Metastasis. *Oncogene* (2021) 40(33):5168–81. doi: 10.1038/s41388-021-01916-0
124. Yang S, Wei J, Cui YH, Park G, Shah P, Deng Y, et al. M6a mRNA Demethylase FTO Regulates Melanoma Tumorigenicity and Response to Anti-PD-1 Blockade. *Nat Commun* (2019) 10(1):2782. doi: 10.1038/s41467-019-10669-0
125. Li N, Kang Y, Wang L, Huff S, Tang R, Hui H, et al. ALKBH5 Regulates Anti-PD-1 Therapy Response by Modulating Lactate and Suppressive Immune Cell Accumulation in Tumor Microenvironment. *Proc Natl Acad Sci U S A* (2020) 117(33):20159–70. doi: 10.1073/pnas.1918986117
126. Kuai D, Zhu S, Shi H, Yang R, Liu T, Liu H, et al. Aberrant Expression of M6a mRNA Methylation Regulators in Colorectal Adenoma and Adenocarcinoma. *Life Sci* (2021) 273:119258. doi: 10.1016/j.lfs.2021.119258
127. Chen P, Liu XQ, Lin X, Gao LY, Zhang S, Huang X. Targeting YTHDF1 Effectively Re-Sensitizes Cisplatin-Resistant Colon Cancer Cells by Modulating GLS-Mediated Glutamine Metabolism. *Mol Ther Oncolytics* (2021) 20:228–39. doi: 10.1016/j.omto.2021.01.001
128. Li H, Zhang N, Jiao X, Wang C, Sun W, He Y, et al. Downregulation of microRNA-6125 Promotes Colorectal Cancer Growth Through YTHDF2-Dependent Recognition of N6-Methyladenosine-Modified GSK3β. *Clin Transl Med* (2021) 11(10):e602. doi: 10.1002/ctm2.602
129. Tsuchiya K, Yoshimura K, Inoue Y, Iwashita Y, Yamada H, Kawase A, et al. YTHDF1 and YTHDF2 are Associated With Better Patient Survival and an Inflamed Tumor-Immune Microenvironment in non-Small-Cell Lung Cancer. *Oncoimmunology* (2021) 10(1):1962656. doi: 10.1080/2162402X.2021.1962656

Conflict of Interest: The authors declare that the research was conducted in the absence of any commercial or financial relationships that could be construed as a potential conflict of interest.

Publisher's Note: All claims expressed in this article are solely those of the authors and do not necessarily represent those of their affiliated organizations, or those of the publisher, the editors and the reviewers. Any product that may be evaluated in

this article, or claim that may be made by its manufacturer, is not guaranteed or endorsed by the publisher.

Copyright © 2022 Tong, Wei, Smith and Huang. This is an open-access article distributed under the terms of the Creative Commons Attribution License (CC BY). The use, distribution or reproduction in other forums is permitted, provided the original author(s) and the copyright owner(s) are credited and that the original publication in this journal is cited, in accordance with accepted academic practice. No use, distribution or reproduction is permitted which does not comply with these terms.

frontiers in Immunology

ORIGINAL RESEARCH
published: 06 January 2022
doi: 10.3389/fimmu.2021.800951

Co-Mutation of FAT3 and LRP1B in Lung Adenocarcinoma Defines a Unique Subset Correlated With the Efficacy of Immunotherapy

Mingyu Zhu[1,2,3,4,5†], *Lu Zhang*[4,5†], *Haiyan Cui*[4,5], *Qiang Zhao*[4,5], *Hao Wang*[1,2,3,6], *Baochao Zhai*[1,2,3,7], *Richeng Jiang*[1,2,3,4,5*] *and Zhansheng Jiang*[1,2,3,8*]

[1] *Tianjin Medical University Cancer Institute and Hospital, National Clinical Research Center for Cancer, Tianjin, China,* [2] *Key Laboratory of Cancer Prevention and Therapy, Tianjin, China,* [3] *Tianjin's Clinical Research Center for Cancer, Tianjin, China,* [4] *Cancer Precise Diagnosis Center, Tianjin Cancer Hospital Airport Hospital, Tianjin, China,* [5] *Center for Precision Cancer Medicine & Translational Research, Tianjin Medical University Cancer Institute and Hospital, Tianjin, China,* [6] *Department of Breast Oncology, Tianjin Cancer Hospital Airport Hospital, Tianjin, China,* [7] *Medical Affairs Office, Tianjin Cancer Hospital Airport Hospital, Tianjin, China,* [8] *Department of Integrative Oncology, Tianjin Medical University Cancer Institute and Hospital, Tianjin, China*

Immunotherapy based on immune checkpoint inhibitors (ICIs) have demonstrated remarkable survival benefits and gained regulatory approval in non-small cell lung cancer (NSCLC) patients without an actionable driver mutation, but currently there is no well-established standard for how to screen the most suitable population for ICIs treatment. Here, we conducted a comprehensive analysis of the somatic mutation landscape of lung adenocarcinoma (LUAD) samples. After the stepwise screening of high-frequency mutated genes, two genes with prominent significance, FAT3 and LRP1B, were finally screened out. Through further analysis, we discovered that the co-mutation of FAT3 and LRP1B was associated with an earlier age of onset and occurred more frequently in Black/African American. Furthermore, co-mutation defines a unique subgroup of lung adenocarcinoma that can increase tumor mutational burden (TMB), boost cytotoxicity and tumor immunogenicity, and facilitate lymphocyte infiltration. The results of gene set enrichment analysis (GSEA) indicated that co-mutation can influence tumorigenesis through a variety of mechanisms. More strikingly, the subset of LUAD with co-mutation of FAT3 and LRP1B exhibited significantly prolonged immunotherapy progression free survival (PFS). In summary, co-mutation of FAT3 and LRP1B is a promising useful biomarker for predicting the efficacy of immunotherapy, which can improve the clinical efficiency of practicing precision medicine in lung adenocarcinoma patients.

Keywords: FAT3, LRP1B, co-mutation, lung adenocarcinoma, immunotherapy

OPEN ACCESS

Edited by:
Hubing Shi,
Sichuan University, China

Reviewed by:
Song Xu,
Tianjin Medical University General Hospital, China
Hongqing Zhuang,
Peking University Third Hospital, China

***Correspondence:**
Richeng Jiang
jiangricheng@tjmuch.com
Zhansheng Jiang
zhjiang@tmu.edu.cn

†These authors have contributed equally to this work and share first authorship

Specialty section:
This article was submitted to Cancer Immunity and Immunotherapy, a section of the journal Frontiers in Immunology

Received: *24 October 2021*
Accepted: *17 December 2021*
Published: *06 January 2022*

Citation:
Zhu M, Zhang L, Cui H, Zhao Q, Wang H, Zhai B, Jiang R and Jiang Z (2022) Co-Mutation of FAT3 and LRP1B in Lung Adenocarcinoma Defines a Unique Subset Correlated With the Efficacy of Immunotherapy. Front. Immunol. 12:800951. doi: 10.3389/fimmu.2021.800951

INTRODUCTION

Lung cancer is currently the leading cause of cancer death and second most diagnosed cancer worldwide, with an incidence of 11.4% and a mortality far higher than any other cancer types (18.0%) (1). Approximately 1.8 million patients died of lung cancer and 2.2 million new lung cancer cases globally in 2020 (1). Despite great progress have been made in the treatment of lung cancer, the five-year survival rate for patients diagnosed between 2010 and 2014 was only 10% to 20% in most countries (2). The prevalence of lung cancer in China has been among the top for many years. In 2015, lung cancer was the most common malignancy and caused the most cancer-related deaths in China (3). Adenocarcinoma is the most common histologic subtype of lung cancer, belonging to NSCLC (4). In recent years, immunotherapy based on monoclonal antibodies targeting immune checkpoint programmed cell death-1 (PD-1) and programmed cell death-1 ligand (PD-L1) has achieved remarkable clinical success and shown unprecedented durable responses for NSCLC patients without an actionable driver mutation (5–8). The emergence of ICIs has become an exciting treatment option for these patients, and has dramatically changed the way they are treated (9). Unfortunately, only a minority of NSCLC patients can really benefit from ICIs treatment (10).

PD-L1 expression, microsatellite instability high (MSI-H)/mismatch repair deficiency (dMMR) and TMB have gained regulatory approval as predictive biomarkers for ICIs in the treatment of NSCLC (5, 8, 11–13). PD-L1 expression is the first biomarker developed to enrich the population who are sensitive to PD-1/PD-L1 targeted immunotherapy. The interpretation of PD-L1 immunohistochemistry (IHC) requires professional pathologists to undergo special training to ensure the accuracy of the results. Different ICIs need to be detected by diverse antibodies, and different antibodies require distinct IHC platforms and have various positivity interpretation standards (14). MSI-H occurs when MMR proteins are dysfunctional and unable to repair errors caused by DNA replication in the microsatellite (15). MSI-H/dMMR mainly exists in colorectal cancer, endometrial cancer and gastric cancer, and its incidence in LUAD is very low (16). TMB is generally determined by whole-exome sequencing or targeted gene panel sequencing with a coding sequence (CDS) greater than or equal to 1.0Mb, and has been used as an effective indicator of response in immunotherapy for many cancer types (17). In most cancers, PD-L1 expression and TMB are two independent biomarkers, and the level of PD-L1 expression has no connection with the level of TMB (18, 19). MSI-H can be understood as a subset of TMB-H. Patients with TMB-H are not necessarily MSI-H, but most patients with MSI-H are also TMB-H (20, 21), because in addition to errors in mismatch repair, defects in other DNA damage repair pathways can also lead to increased mutation rates (22). Tumor somatic mutations can generate non-self neoantigens that confer immunogenicity and induce anti-tumor immune response (23). Therefore, mutations not only contribute to tumorigenesis and progression, but also increase the chance of tumors being recognized by the host immune system and lead to tumor elimination in the meanwhile.

It is well established that simpler methods, such as single-gene or multi-gene co-mutation detection can be used as an alternative to predict TMB (22, 24, 25). LRP1B is a tumor suppressor gene, encoding low-density lipoprotein (LDL) family receptor (26), and its mutation frequency is among the top ten in LUAD (27). The correlation of LRP1B with TMB and immunotherapy efficacy has been confirmed in multiple cancers, including lung cancer, melanoma and other solid tumors (28, 29). FAT3 belongs to the FAT family genes encoding large proteins with extracellular Cadherin repeats, EGF-like domains, and Laminin G-like domains, and is involved in tumor suppression and planar cell polarity (PCP) (30). Similarly, FAT3 mutations have been linked to prognosis and elevated TMB level in NSCLC (31), esophageal cancer (ESCA) (32) and triple-negative breast cancer (TNBC) (33). Although FAT3 gene mutations are common in many cancers, including lung adenocarcinoma, there are few studies on the association between FAT3 gene and immunotherapy.

In this study, we comprehensively analyzed the gene sequencing data of lung adenocarcinoma samples, and screened out 18 genes with non-synonymous mutations frequencies greater than 20% in the coding region. Next, we further explored the correlation between these high-frequency mutated genes and TMB, mRNA expression levels of recombinant cluster of differentiation 8A (CD8A) and interferon gamma (IFNG), neoantigen and immunotherapy benefit, and finally acquired two significantly related genes, FAT3 and LRP1B. Considering the co-occurrence relationship between these two key genes, we conducted an in-depth analysis of LUAD samples with co-mutation of FAT3 and LRP1B, performed GSEA analysis and investigated the impact of co-mutation on immune infiltration. Overall, our results demonstrate that compared with FAT3 or LRP1B single-mutation samples, the LUAD subset with co-mutation of FAT3 and LRP1B exhibit more unique clinical profiles and is more closely associated with the efficacy of immunotherapy.

MATERIALS AND METHODS

Patient Selection

The study cohort consisted of 506 LUAD patients selected and retrieved from The Cancer Genome Atlas (TCGA, http://cancergenome.nih.gov), and the mutation and expression data from these populations were used for comprehensive integrated analysis. The cohort was obtained by screening samples with both somatic mutation and mRNA expression profiling. A total of 90 LUAD samples from Rizvi et al. (15 cases) (34) and Hellmann et al. (75 cases) (18) were used to explore the association of gene mutations with neoantigen and the efficacy of immunotherapy. In addition, 485 LUAD samples from Imielinksi et al. (183 cases) (35) and Chen et al. (302 cases) (36) were used to verify the relationship between mutation status

and TMB level. Gene mutations were defined as all mutations in CDS region except synonymous and intron mutations, including indels, missense mutations, nonsense mutations and splice mutations. Given the absence of patient identification information and the retrospective nature of the study, ethical approval and informed consent was waived.

Identification of Frequently Mutated Genes

Based on the original gene mutation results of 506 LUAD samples from TCGA, a TXT file annotated by hg19 reference genome was generated, including only three columns of sample ID, mutant gene and variant class. Among them, the variant class was composed of all mutations in CDS region except synonymous and intron mutations. The TXT file was visualized through the GenVisR package for somatic mutations, ranking mutated genes in the order of mutation frequency from high to low to obtain 18 genes with mutation frequency greater than 20% in the cohort.

Molecular Characteristics Analysis

The total number of non-synonymous somatic variants obtained from whole exome sequencing (WES) data, divided by the size of the exome, was used as the formula to calculate the TMB of LUAD samples. All single nucleotide variants (SNVs) and indels were included. The expression of CD8A and IFNG were evaluated through transcriptome data in RNASeqV2 RSEM format, $\log_2$(RSEM+1) transformed. The level of neoantigen had previously been measured in the immunotherapy cohort by published methods (18, 34). By assessing the correlation of these 18 genes with TMB, the expression levels of CD8A and IFNG, and neoantigen for stepwise screening, the two key genes, FAT3 and LRP1B, which had important implications in LUAD, were finally obtained.

Gene Set Enrichment Analysis

In order to explore the mechanism of the mutation status of target genes in the occurrence and development of LUAD tumors, we divided the TCGA cohort into two groups, FAT3 and LRP1B co-mutation and wild-type, and performed GSEA by RNA-seq data. Using GSEA software (version 4.1.0) (37), we analyzed which classic signaling pathways are affected by co-mutation of FAT3 and LRP1B. Enrichment score (ES) reflected the degree to which a gene set was overrepresented at top or bottom of the entire ranked list, and ES was normalized according to the size of gene set to yield normalized enrichment score (NES). Permutations for each analysis were set as 1000 times. Pathways with a normal p-value less than 0.05 were considered to be significantly enriched.

Co-Mutation and Tumor-Infiltrating Lymphocytes

Based on the deconvolution algorithm CIBERSORT (38), we used RNA-seq data to evaluate the relative abundance of 22 tumor-infiltrating immune cells in the TCGA LUAD dataset. We then divided the cohort into FAT3 and LRP1B co-mutation and wild-type groups according to the mutation status of target genes to discuss the effect of co-mutation on the degree of lymphocyte infiltration. The correlation between immune cells was visualized using corrplot package and Pearson correlation coefficient was calculated.

Statistical Analysis

Demographic, clinicopathological, and molecular characteristics were treated as either continuous (e.g., age, TMB, mRNA expression) or categorical (e.g., sex, stage, race) variables as appropriate. We used the nonparametric Mann-Whitney for all comparisons of continuous data, and categorical variables were compared using the Fisher exact test. For the analysis of the association of target gene mutations with the efficacy of ICIs treatment, survival curves were plotted using the Kaplan-Meier method and compared by the log-rank test. The PFS data were evaluated by Response Evaluation Criteria in Solid Tumors, version 1.1 (RECISTv1.1). PFS was defined as the time from the initiation of therapy to the date of disease progression or death from any cause. Statistical analyses were conducted using R (version 3.6.1), SPSS (version 25.0) and GraphPad Prism (version 8.0). All statistical tests were two-tailed, and p value under 0.05 was deemed significant.

RESULTS

Somatic Mutation Landscape in Lung Adenocarcinoma

Using 20% as the cut-off value of gene mutation frequency, we screened out 18 genes (TP53, TTN, MUC16, CSMD3, RYR2, LRP1B, ZFHX4, USH2A, KRAS, SPTA1, FLG, XIRP2, CSMD1, FAT3, PCDH15, ZNF536, NAV3 and COL11A1) based on the waterfall plot of 506 LUAD samples, of which TP53 had the highest mutation frequency (52.0%, 263 of 506) (**Figure 1**). All mutations in the CDS region that might alter the amino acid sequence were included, such as indels, missense mutations, nonsense mutations and splice mutations. Missense mutation was the most common type of variation.

The Association of Target Gene Mutations With TMB and the Expression Levels of CD8A and IFNG

TMB reflects the number of mutations contained in tumor cells, usually measured by the number of mutations per Mb in the CDS region of the genome, and has been used as an effective predictor of immunotherapy response in lung cancer (5, 8). LUAD patients with TP53, TTN, MUC16, CSMD3, RYR2, LRP1B, ZFHX4, USH2A, SPTA1, FLG, XIRP2, CSMD1, FAT3, PCDH15, ZNF536, NAV3 and COL11A1 mutations in the cohort exhibited a much higher TMB than wild-type patients (**Figure 2A**). The TMB of the dataset ranged from 0.00 to 53.29 mutations/Mb, with a median of 5.42 mutations/Mb. Further analysis indicated that regardless of the median TMB or 10 mutations/Mb as the threshold, the level of TMB had no significant correlation with the prognosis of LUAD (**Supplementary Figure 1**).

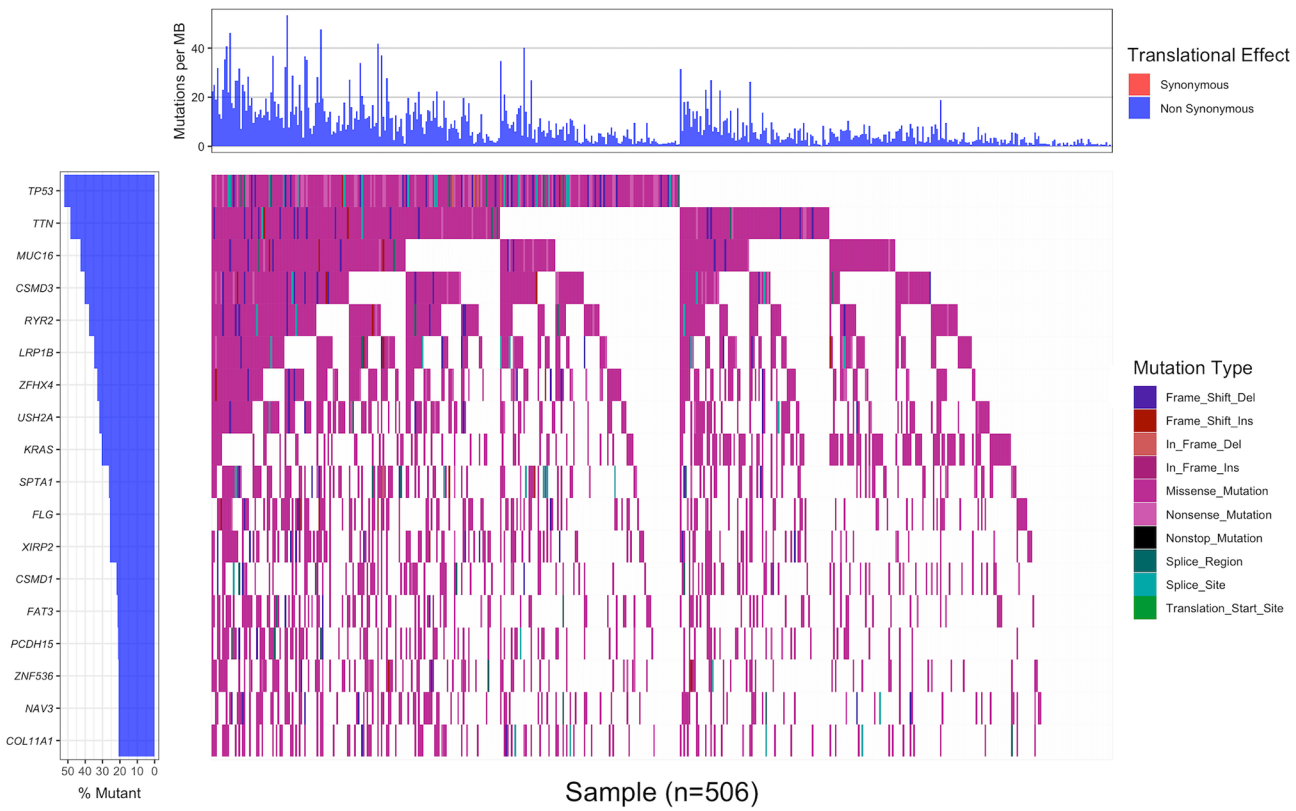

FIGURE 1 | The waterfall plot displaying the landscape of frequently mutated genes in 506 LUAD samples with non-synonymous mutation frequency in the coding region greater than 20%. Genes were arranged in descending order of mutation frequency (left panel), and different colors represented different mutation types (right panel). The upper panel indicated the number of non-synonymous mutations in the coding region per Mb of each sample.

Tumors possessing higher level of TMB may stimulate the immune system to produce more potent cytotoxicity. To discover whether these target genes that were significantly related to TMB had similar impact on the tumor microenvironment (TME), we further examined the cytotoxic T-cell markers of mutant LUADs. Compared with wild-type group, the expression of CD8A (**Figure 2B**) and IFNG (**Figure 2C**) were significantly upregulated in LUAD patients with TP53, LRP1B, USH2A, SPTA1 and FAT3 mutations. Collectively, LUAD subgroups with TP53, LRP1B, USH2A, SPTA1 and FAT3 mutations harbored higher TMB level and exhibited enhanced cytotoxicity.

Gene Mutations Are Relevant With Neoantigen Level and Immunotherapy Outcome

A large number of non-synonymous mutations are thought to cause the emergence of more neoantigens, which further enhances immunogenicity and makes tumors more sensitive to ICIs treatment (13). To investigate whether higher TMB can translate into favorable immunotherapy response, we conducted a more in-depth examination of subgroups with target gene mutations. Through a dataset containing 90 LUAD samples treated with ICIs, we found that TP53, LRP1B, USH2A, SPTA1 and FAT3-mutant LUADs all had higher neoantigen loads than wild-type (**Figure 3A**). More importantly, LUADs with LRP1B (22.1 months vs 6.5 months, HR=0.55, 95% CI=0.32-0.94, p=0.0495) and FAT3 (not reached vs 6.5 months, HR=0.38, 95% CI=0.22-0.68, p=0.012) mutations also had significantly prolonged immunotherapy PFS (**Figures 3B–F**). In general, these results suggested that LUAD samples with LRP1B and FAT3 mutations possessed increased immunogenicity and better immunotherapy outcomes.

Characteristics of Lung Adenocarcinoma Patients With FAT3 and LRP1B Mutations

Across 506 LUAD patients, the mutation frequencies of LRP1B and FAT3 genes were 21.34% (108 of 506) and 34.78% (176 of 506), respectively, and the frequency of co-mutation of FAT3 and LRP1B genes was 10.87% (55 of 506). Furthermore, co-occurrence and mutual exclusivity analysis of mutations confirmed that FAT3 and LRP1B mutations tended to occur simultaneously (Fisher's exact test, p<0.001). Consequently, we sought to divide the LUAD cohort into four groups: FAT3 and LRP1B co-mutation group ($FAT3^+/LRP1B^+$), FAT3 mutation only group ($FAT3^+$), LRP1B mutation only group ($LRP1B^+$), and FAT3 and LRP1B double wild-type group (WT), to analyze the

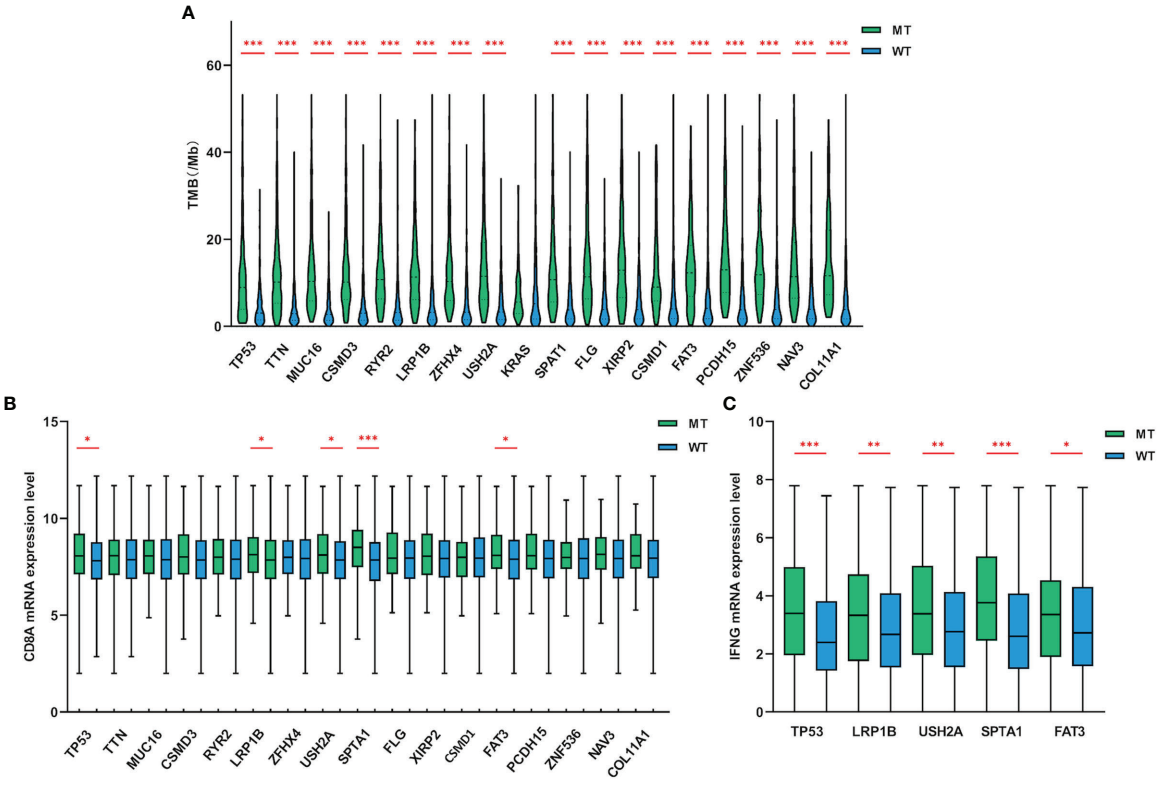

FIGURE 2 | Gene mutations were related to TMB and the expression levels of CD8A and IFNG. **(A)** Compared with wild-type groups, LUAD samples with TP53, TTN, MUC16, CSMD3, RYR2, LRP1B, ZFHX4, USH2A, SPTA1, FLG, XIRP2, CSMD1, FAT3, PCDH15, ZNF536, NAV3 and COL11A1 mutations had significantly higher TMB. **(B, C)** LUAD samples with TP53, LRP1B, USH2A, SPTA1 and FAT3 mutations had higher CD8A and IFNG mRNA expression levels (adding one pseudo-count and $\log_2$ transformation) than wild-type. WT=wild-type. p values indicate comparisons between mutant and wild-type LUADs by Mann-Whitney test. *p < 0.05, **p < 0.01, ***p < 0.001.

relationship between mutation status and demographic and clinicopathological characteristics of lung adenocarcinoma patients (**Table 1**). Compared with wild-type LUADs, patients in the FAT3$^+$/LRP1B$^+$ group were correlated with earlier cancer onset (median age 63.5 vs 67 years old, p=0.012), and the tumors were more commonly occurred in Black/African American (18.18% vs 8.30%, p=0.037). There were no significant differences between the FAT3$^+$/LRP1B$^+$ and WT groups in terms of sex, stage, grade and tumor status. Additionally, compared with the WT group, the FAT3$^+$ and LRP1B$^+$ groups had no striking differences in these characteristics.

The Subgroup of Lung Adenocarcinoma With Co-Mutation of FAT3 and LRP1B Exhibited Favorable Immunotherapy Efficacy

Considering the co-occurrence of FAT3 and LRP1B mutations, as well as the unique clinical characteristics of the co-mutation group, we attempted to check whether the molecular features of the FAT3$^+$/LRP1B$^+$ group were also worthy of attention. We found that LUADs in the FAT3$^+$/LRP1B$^+$ group had the highest level of TMB, even significantly higher than that of the FAT3$^+$ (**Figure 4A**, 16.5 vs 8.3, p<0.001) and LRP1B$^+$ (**Figure 4A**, 16.5 vs 9.0, p<0.001) groups. To evaluate the accuracy of using FAT3 and LRP1B co-mutation to predict TMB level in LUAD, 10 mutations/Mb was regarded as the cut-off value of TMB like most studies (5, 8). The positive rate of high TMB (>10 mutations/Mb) among the FAT3$^+$/LRP1B$^+$ group was 85.45% (47 of 55), while that of the remaining samples of LUAD cohort was 21.06% (95 of 451), p<0.001 (Fisher exact test). Besides, to determine the sensitivity and specificity of FAT3 and LRP1B co-mutation for predicting the level of TMB, receiver operating characteristic (ROC) curve was performed. The area under the ROC curve (AUC) of co-mutation group was 0.655, with a sensitivity of 33.1% and a specificity of 97.8% (**Figure 4B**, p<0.001). The AUC of the FAT3$^+$/LRP1B$^+$ group was higher than that of the FAT3$^+$, LRP1B$^+$ and WT groups, illustrating that the FAT3 and LRP1B co-mutation had superior predictive performance for TMB level. What's more, another dataset composed of 485 LUAD samples was used as the validation group, further supporting the view that the TMB level of the co-mutation group was higher than that of the FAT3 and LRP1B groups (**Figure 4C**). At the same time, although the previous result indicated that the population with FAT3 and LRP1B mutations had higher CD8A expression level than wild-type

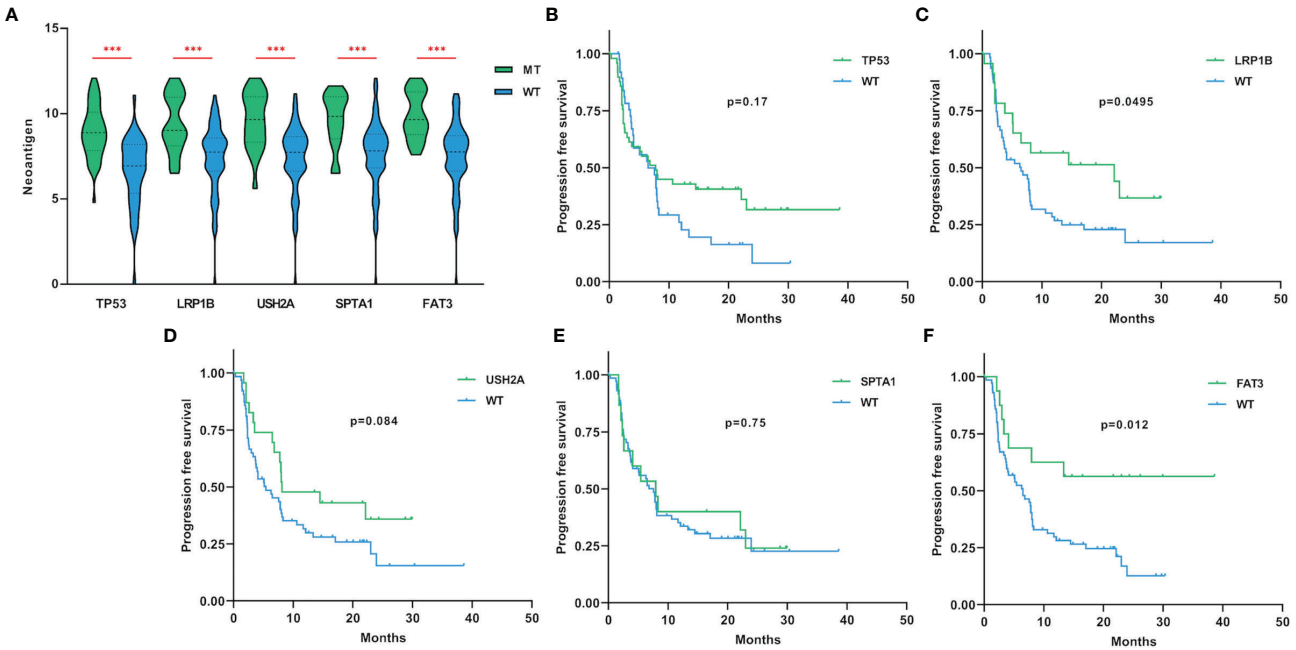

FIGURE 3 | The associations of gene mutations with neoantigen and immunotherapy PFS. **(A)** LUAD samples with TP53, LRP1B, USH2A, SPTA1 and FAT3 mutations had higher levels of neoantigen (adding one pseudo-count and $\log_2$ transformation). **(B–F)** Compared with non-mutated LUAD samples, LUADs with LRP1B and FAT3 mutations had significantly longer PFS for immunotherapy. WT=wild-type. Statistical comparisons between different groups were made by Mann-Whitney test **(A)**, and survival curves were plotted using the Kaplan-Meier method and compared by the log-rank test **(B–F)**. ***p < 0.001.

LUADs, a more detailed group comparison result proved that compared with the WT group, the CD8A expression level of the $FAT3^+/LRP1B^+$ group was significantly up-regulated, while not the same case in the $FAT3^+$ and $LRP1B^+$ groups (**Figure 4D**).

Similarly, through a population of 90 LUAD patients that received ICIs treatment, we discovered that the $FAT3^+/LRP1B^+$ group had strikingly higher neoantigen level than the $FAT3^+$ (**Figure 4E**, p<0.01) and $LRP1B^+$ (**Figure 4E**, p<0.001) groups. Even more importantly, LUAD patients with co-mutation of FAT3 and LRP1B had significantly better immunotherapy outcomes (**Figure 4F**, p=0.026). Moreover, when the entire cohort was divided into two groups, only the co-mutation group exhibited significantly prolonged PFS, while the immunotherapy response of the FAT3 and LRP1B single-mutation groups showed no advantage (**Supplementary Figure 2**). Taken together, these data suggest that the co-mutation of FAT3 and LRP1B defines a unique subset and may be a promising novel biomarker for screening candidates for ICIs therapy of lung adenocarcinoma.

Pathway Enrichment Analysis of FAT3 and LRP1B Co-Mutation

Gene set enrichment analysis was performed with the TCGA LUAD dataset to explore the effects of FAT3 and LRP1B co-mutation on the physiological processes and functions of the body. The analysis results of GSEA indicated that LUADs with FAT3 and LRP1B co-mutation were significantly enriched in Regulation of double strand break repair *via* homologous recombination, Basic amino acid transmembrane transporter activity, DNA replication, Regulation of spindle assembly, Histone methyltransferase complex and SWI/SNF superfamily type complex pathways (**Figure 5**), which revealed the potential mechanism of co-mutation in the occurrence and development of LUAD tumors, and also provided a direction for subsequent further research.

Co-Mutation of FAT3 and LRP1B Affects Lymphocyte Infiltration

The efficacy of ICIs treatment in cancer patients has been linked to the quality and magnitude of tumor-infiltrating lymphocytes (TILs) within the microenvironment (39). The infiltration degree of 22 immune cells in the LUAD was calculated using the CIBERSORT algorithm, and the proportion of immune cells in each sample in the cohort was displayed through stacked bars (**Figure 6A**). The results showed that compared with the wild-type samples, the TME of the LUADs with co-mutation of FAT3 and LRP1B contained more $CD8^+$ T cells, activated $CD4^+$ memory T cells and M1 macrophages, but fewer resting $CD4^+$ memory T cells, resting dendritic cells and activated dendritic cells (**Figure 6B**). Besides, Pearson correlation analysis of immune cell abundance revealed the feedback relationship between immune cells (**Figure 6C**). From the correlation matrix, the strongest positive correlation existed between $CD8^+$ T cells and activated $CD4^+$ memory T cells, while the negative correlation between activated NK cells and resting NK cells was the strongest.

TABLE 1 | Demographic and clinicopathological characteristics in the LUAD cohort according to FAT3 and LRP1B mutation status.

	$FAT3^+/LRP1B^+$	$FAT3^+$	$LRP1B^+$	WT	p value ($FAT3^+/LRP1B^+$ *vs* WT)	p value ($FAT3^+$ *vs* WT)	p value ($LRP1B^+$ *vs* WT)
Number	55 (10.87%)	53 (10.47%)	121 (23.91%)	277 (54.74%)			
Age	63.5 (41-87)	63 (39-81)	66 (38-87)	67 (40-88)	**0.012**†	0.065†	0.181†
Sex					0.239	0.368	0.51
Female	25 (45.45%)	25 (47.17%)	71 (58.68%)	151 (54.51%)			
Male	30 (54.55%)	28 (52.83%)	50 (41.32%)	126 (45.49%)			
Race					**0.037**	0.178	0.564
Asian	1 (1.82%)	0	2 (1.65%)	5 (1.81%)			
White	34 (61.82%)	36 (67.92%)	93 (76.86%)	217 (78.34%)			
Black/African American	10 (18.18%)	8 (15.09%)	11 (9.09%)	23 (8.30%)			
Other	0	0	1 (0.83%)	0			
Unknown	10 (18.18%)	9 (16.98%)	14 (11.57%)	32 (11.55%)			
Stage					0.54	0.7	0.221
I	27 (49.09%)	26 (49.06%)	69 (57.02%)	152 (54.87%)			
II	18 (32.73%)	15 (28.30%)	21 (17.36%)	66 (23.83%)			
III	6 (10.91%)	10 (18.87%)	26 (21.49%)	41 (14.80%)			
IV	3 (5.45%)	2 (3.77%)	5 (4.13%)	17 (6.14%)			
Unknown	1 (1.82%)	0	0	1 (0.36%)			
pT stage					0.595	0.942	0.671
T1	17 (30.91%)	18 (33.96%)	44 (36.36%)	88 (31.77%)			
T2	29 (52.73%)	29 (54.72%)	65 (53.72%)	149 (53.79%)			
T3	8 (14.55%)	5 (9.43%)	7 (5.79%)	25 (9.03%)			
T4	1 (1.82%)	1 (1.89%)	5 (4.13%)	12 (4.33%)			
Unknown	0	0	0	3 (1.08%)			
pN stage					0.958	0.58	0.165
N0	37 (67.27%)	31 (58.49%)	77 (63.64%)	179 (64.62%)			
N1	12 (21.82%)	12 (22.64%)	18 (14.88%)	54 (19.49%)			
N2	6 (10.91%)	9 (16.98%)	24 (19.83%)	34 (12.27%)			
N3	0	0	1 (0.83%)	1 (0.36%)			
Unknown	0	1 (1.89%)	1 (0.83%)	9 (3.25%)			
pM stage					1	0.746	0.802
M0	36 (65.45%)	37 (69.81%)	82 (67.77%)	183 (66.06%)			
M1	3 (5.45%)	2 (3.77%)	5 (4.13%)	15 (5.42%)			
Unknown	16 (29.09%)	14 (26.42%)	34 (28.10%)	79 (28.52%)			
Neoplasm Cancer Status					0.717	0.718	1
Tumor Free	36 (65.45%)	35 (66.04%)	69 (57.02%)	164 (59.21%)			
With Tumor	11 (20.00%)	11 (20.75%)	26 (21.49%)	61 (22.02%)			
Unknown	8 (14.55%)	7 (13.21%)	26 (21.49%)	52 (18.77%)			
New Neoplasm Event Post Initial Therapy Indicator					0.517	0.869	0.906
Yes	16 (29.09%)	17 (32.08%)	43 (35.54%)	95 (34.30%)			
No	31 (56.36%)	29 (54.72%)	64 (52.89%)	146 (52.71%)			
Unknown	8 (14.55%)	7 (13.21%)	14 (11.57%)	36 (13.00%)			

Data are n (%) or median (range). Bold values represent statistical differences. †Determined by Mann-Whitney test. Other statistical comparisons between groups were made by Fisher exact test.

DISCUSSION

Based on a TCGA dataset consisting of 506 samples, we conducted an integrated analysis of the somatic mutation landscape of lung adenocarcinoma. After stepwise screening, we obtained FAT3 and LRP1B, two key genes closely related to the immunogenicity, cytotoxicity and immunotherapy response of lung adenocarcinoma patients. Further analysis showed that there was a co-occurrence relationship between FAT3 and LRP1B mutations, so we took the LUAD subgroup with FAT3 and LRP1B co-mutation as a whole to conduct a more in-depth exploration. The results demonstrated that the frequency of co-mutation of FAT3 and LRP1B in LUAD patients was 10.87% (55 out of 506), which was associated with an earlier age of onset and occurred more frequently in Black/African American. Besides, LUAD patients with FAT3 and LRP1B co-mutation displayed substantially higher TMB, CD8A expression level and neoantigen. More importantly, the subset of LUAD with co-mutation of FAT3 and LRP1B exhibited significantly prolonged immunotherapy PFS, so we performed GSEA and immune infiltration analysis on this subset to explore the effect of co-mutation on the degree of lymphocyte infiltration and tumorigenesis in lung adenocarcinoma.

FAT3 mutations occurred in 21.34% (108 out of 506) of LUAD samples in the TCGA cohort, which is consistent with previous conclusions in TNBC and ESCA that FAT3 gene has higher mutation rate (32, 33). Similarly, LRP1B gene not only has a relatively high mutation frequency (34.78%, 176/506) in this study, but also frequently mutates in multiple tumors, such as melanoma, ESCA

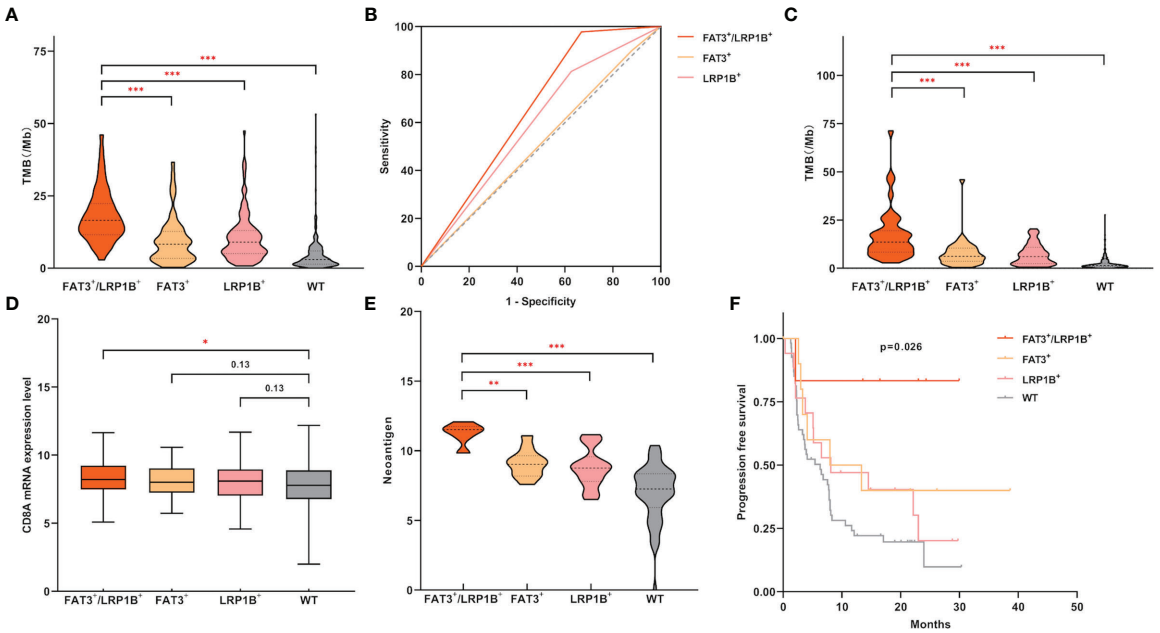

FIGURE 4 | LUAD samples with FAT3 and LRP1B co-mutation had significantly higher TMB levels and exhibited unique immune characteristics. **(A)** Compared with LUADs with only FAT3 or LRP1B mutations alone, the LUAD subgroup with co-mutation of FAT3 and LRP1B had significantly higher TMB level. **(B)** High specificity of FAT3 and LRP1B co-mutation status for predicting TMB-H (>10 mutations/Mb). The prediction performance of the FAT3$^+$/LRP1B$^+$ group for TMB-H exceeded that of the FAT3$^+$ and LRP1B$^+$ groups, with an AUC of 0.655, a 95% confidence interval of 0.596-0.713, and p<0.001. **(C)** The validation cohort of 485 LUAD samples confirmed the FAT3$^+$/LRP1B$^+$ group had the highest TMB level. **(D)** Compared with wild-type samples, LUADs in the FAT3$^+$/LRP1B$^+$ group had significantly higher CD8A mRNA expression level (adding one pseudo-count and $\log_2$ transformation). **(E)** The level of neoantigen (adding one pseudo-count and log2 transformation) in the FAT3$^+$/LRP1B$^+$ group was higher than that in the FAT3$^+$ and LRP1B$^+$ groups. **(F)** The immunotherapy PFS of the FAT3$^+$/LRP1B$^+$ group was significantly prolonged. Statistical comparisons between different groups were made by Mann-Whitney test **(A, C–E)**, and survival curves were plotted using the Kaplan-Meier method and compared by the log-rank test **(F)**. *p < 0.05, **p < 0.01, ***p < 0.001.

and colorectal cancer (CRC) (28). Previous studies have demonstrated that in a variety of solid tumors, samples with FAT3 (31–33) or LRP1B (28, 29) mutations may have elevated TMB. However, according to our data, we found that although the LUAD samples with a single mutation of FAT3 or LRP1B had higher levels of TMB than the wild-type group, the TMB level of LUADs with co-mutation of FAT3 and LRP1B was even significantly higher than that of the FAT3 and LRP1B single-mutation groups. The increased TMB level of the co-mutation group was also reflected in its elevated neoantigen level, which was higher than that in the FAT3$^+$ and LRP1B$^+$ groups. Higher neoantigen load represents enhanced immunogenicity, which can stimulate more potent cytotoxicity, and our research suggests that only the FAT3$^+$/LRP1B$^+$ group has significantly increased CD8A expression level, while the FAT3 or LRP1B single-mutation groups have no significant difference from the wild-type group. It is worth noting that although the subset with FAT3 or LRP1B mutations displayed superior immunotherapy PFS than the wild-type, the results of a more detailed study of the cohort based on the co-mutation status indicated that only LUAD patients with co-mutation of FAT3 and LRP1B receive ICIs treatment can achieve better efficacy. Taken together, our study proves that while a series of studies have confirmed the predictive role of FAT3 and LRP1B mutations in tumor immunotherapy, the results of genetic testing found that LUAD patients with FAT3 or LRP1B mutations may not necessarily benefit from immunotherapy, only the LUAD population with both FAT3 and LRP1B mutations can benefit from ICIs therapy.

GSEA results showed that multiple signaling pathways were enriched in the LUAD subset with co-mutation of FAT3 and LRP1B. Basic amino acid transmembrane transporter activity enables the transfer of basic amino acids from one side of a membrane to the other, thereby providing nutrients for human metabolism. Most of the remaining enriched pathways are related to cell cycle and transcriptional regulation, illustrating that co-mutation may affect the occurrence and development of tumors through these mechanisms. Strikingly, the DNA homologous recombination repair (HRR) pathway is also enriched in the FAT3$^+$/LRP1B$^+$ group. Homologous recombination deficiency (HRD) leads to the accumulation of a large amount of DNA with damage that cannot be repaired, thus increasing genomic instability, which may be one of the reasons for the higher TMB level of LUADs with co-mutation of FAT3 and LRP1B. Studies have shown that NSCLC patients with HRD have better response to ICIs treatment (40, 41), which further validates the viewpoints put forward in this study.

The immune system and tumor microenvironment play an important role in tumor growth and progression, and can contribute to the efficacy of immunotherapy (42). Immune cells

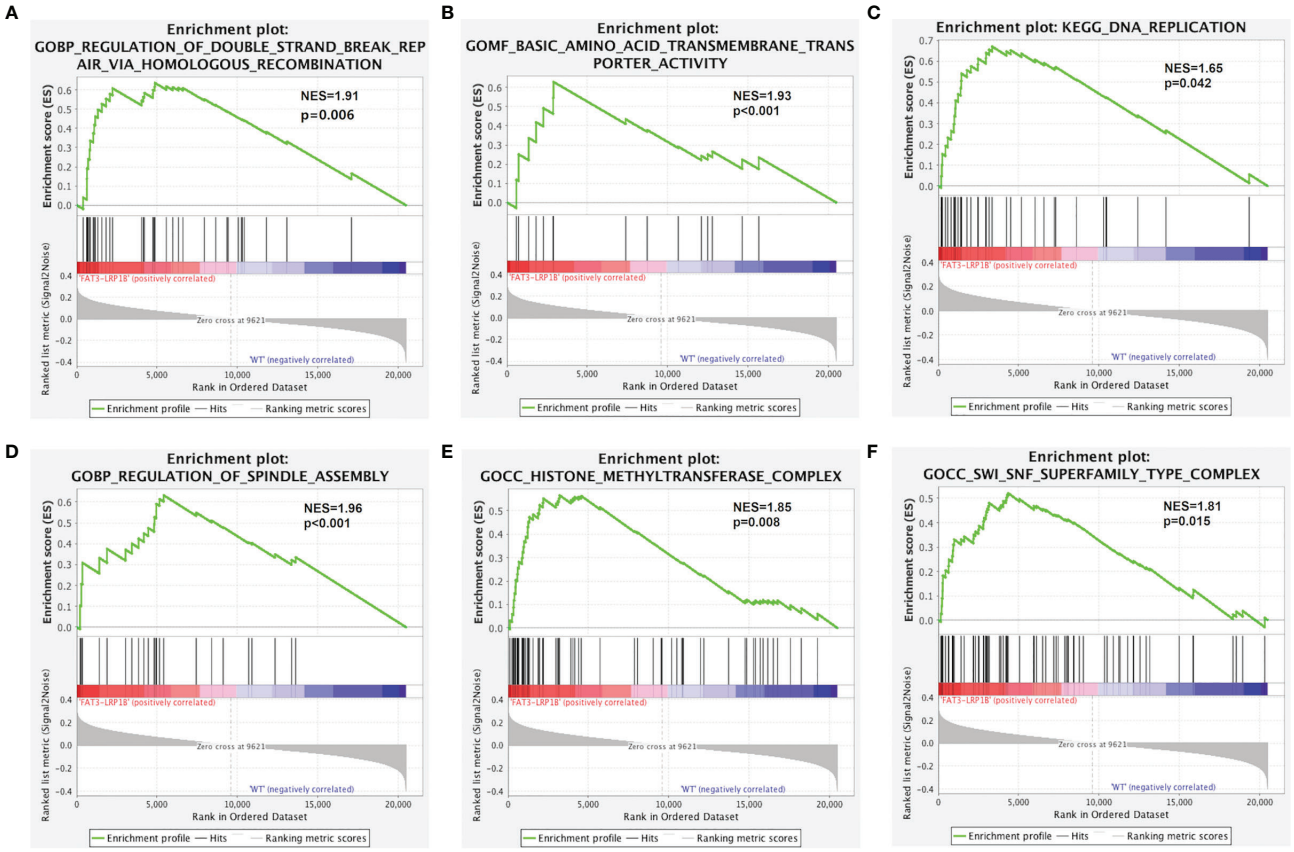

FIGURE 5 | Significantly enriched pathways associated with LUAD samples with co-mutations of FAT3 and LRP1B. GSEA analysis revealed that the FAT3$^+$/LRP1B$^+$ subgroup significantly enriched in **(A)** Regulation of double strand break repair *via* homologous recombination, **(B)** Basic amino acid transmembrane transporter activity, **(C)** DNA replication, **(D)** Regulation of spindle assembly, **(E)** Histone methyltransferase complex, **(F)** SWI/SNF superfamily type complex. NES, normalized enrichment score.

are an important component of the tumor microenvironment. We found that compared with wild-type samples, LUADs with co-mutation of FAT3 and LRP1B displayed a higher degree of infiltration of CD8$^+$ T cells, activated CD4$^+$ memory T cells and M1 macrophages. Cytotoxic CD8$^+$ T cells (CTLs) are the most powerful effectors in the anti-cancer immune response, because they can detect intracellular antigens presented by major histocompatibility complex (MHC), which constitute the backbone of cancer immunotherapy (43). CD4$^+$ T cells can help enhance the function of CTLs, enabling CTLs to overcome the barriers that typically hinder anti-cancer immunity (44). And M1 macrophages promote inflammatory response and play an active role in the elimination of pathogens and tumor cells (45). ICIs therapy can induce polarization of M1 macrophages, thus enhancing the antineoplastic effect (46, 47). The simultaneous prominence of the three types cells, CD8$^+$ T cells, activated CD4$^+$ memory T cells and M1 macrophages, implying that co-mutation of FAT3 and LRP1B can be used to predict the cytotoxic effect of lymphocytes against tumor cells and the beneficial response of immunotherapy in LUAD.

Our study also has some limitations. In view of the retrospective nature of this study that did not collect real-world samples, the conclusions obtained need to be verified by a large-sample prospective analysis. In addition, the cohort used for mutation and expression analysis is completely different from the population that has received immunotherapy, making our findings may need to be interpreted with caution. Nevertheless, we believe that the data of this paper has proved that in patients with lung adenocarcinoma, the co-mutation status of FAT3 and LRP1B deserves further attention and research. Considering that FAT3 and LRP1B genes lack hotspot mutations in lung adenocarcinoma, and these two genes may not even be included in the list of clinical routine gene testing (especially FAT3), we recommend that whole exon or even the whole gene level mutations of FAT3 and LRP1B should be comprehensively detected in clinical practice, which will provide more useful information for treatment options of lung adenocarcinoma.

In conclusion, through a comprehensive analysis of lung adenocarcinoma samples, the results of this study provide insights into the immunotherapeutic implications of co-occurrence of some common mutations in lung adenocarcinoma. We found that co-mutation of FAT3 and LRP1B has prominent significance, which can increase somatic mutational load, boost cytotoxicity and tumor immunogenicity, facilitate lymphocyte infiltration in the microenvironment, and significantly influence

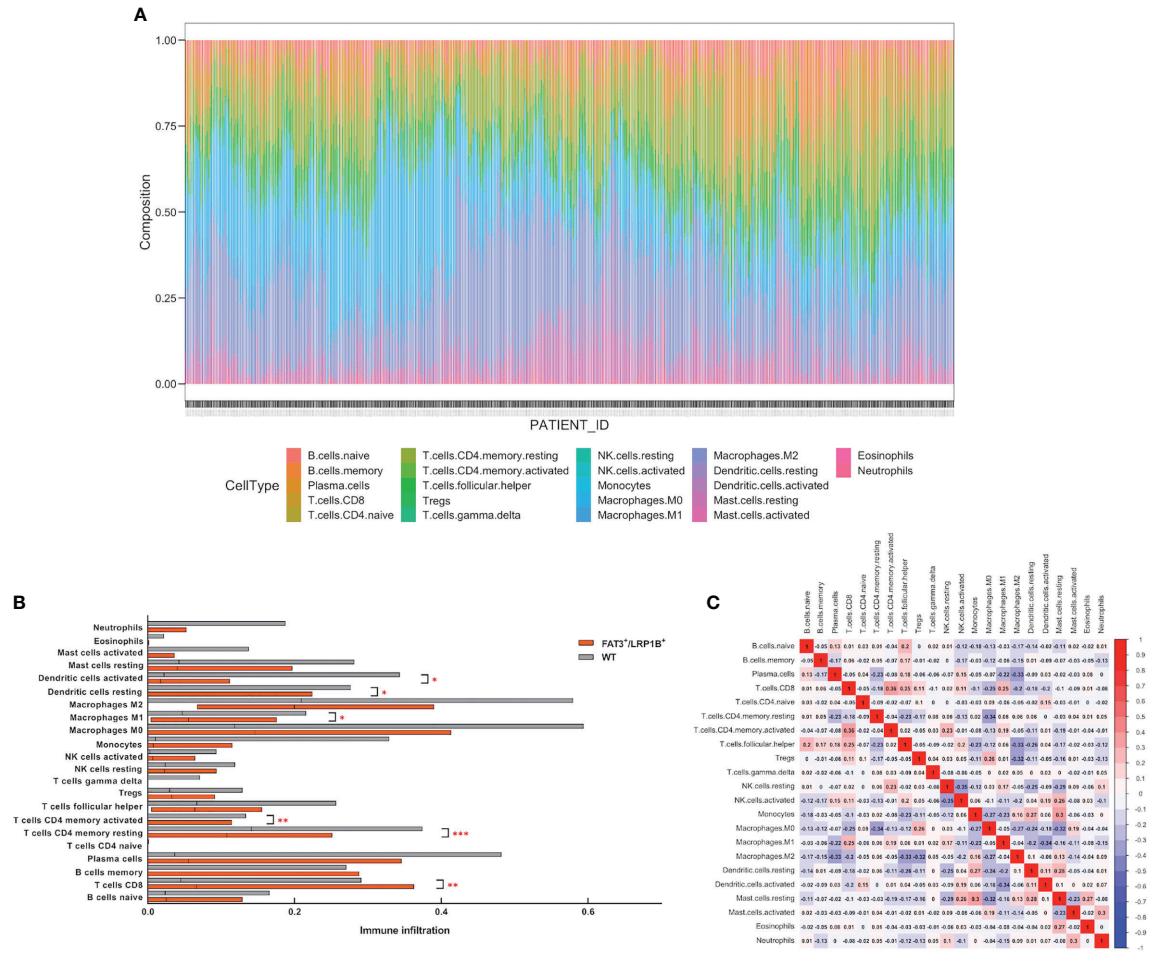

FIGURE 6 | Co-mutation of FAT3 and LRP1B can affect the degree of lymphocyte infiltration in LUAD. **(A)** The proportion of 22 immune cells in each sample in the LUAD dataset. **(B)** Differential tumor-infiltrating immune cells between FAT3$^+$/LRP1B$^+$ group and wild-type group. **(C)** Correlation analysis of immune cell abundance in tumor microenvironment. Red represents positive correlation, blue represents negative correlation. p values indicate comparisons between FAT3$^+$/LRP1B$^+$ and wild-type LUADs by Mann-Whitney test. *p < 0.05, **p < 0.01, ***p < 0.001.

the outcome of immunotherapy. This research provides evidence that co-mutation of FAT3 and LRP1B may be a very promising novel biomarker for screening candidates of ICIs therapy in lung adenocarcinoma and lays a preliminary foundation for subsequent further exploration.

DATA AVAILABILITY STATEMENT

Publicly available datasets were analyzed in this study. This data can be found here: The Cancer Genome Atlas (TCGA, http://cancergenome.nih.gov).

AUTHOR CONTRIBUTIONS

MZ, RJ, and ZJ conceived and designed the study. MZ and LZ performed the study. MZ, LZ, HC, QZ, HW, and BZ analyzed the result. MZ, LZ, RJ, and ZJ wrote the paper. All authors reviewed the manuscript and approved the submitted version.

FUNDING

This work was supported by grants from the National Natural Science Foundation of China (No. 81803914), Tianjin Cancer Hospital College-level Research Seed Fund (No. 1810) and Health Science and Technology Project of Tianjin City of China (No. RC20189).

SUPPLEMENTARY MATERIAL

The Supplementary Material for this article can be found online at: https://www.frontiersin.org/articles/10.3389/fimmu.2021.800951/full#supplementary-material

REFERENCES

1. Sung H, Ferlay J, Siegel RL, Laversanne M, Soerjomataram I, Jemal A, et al. Global Cancer Statistics 2020: GLOBOCAN Estimates of Incidence and Mortality Worldwide for 36 Cancers in 185 Countries. *CA Cancer J Clin* (2021) 71(3):209–49. doi: 10.3322/caac.21660
2. Allemani C, Matsuda T, Di Carlo V, Harewood R, Matz M, Niksic M, et al. Global Surveillance of Trends in Cancer Survival 2000-14 (CONCORD-3): Analysis of Individual Records for 37 513 025 Patients Diagnosed With One of 18 Cancers From 322 Population-Based Registries in 71 Countries. *Lancet* (2018) 391(10125):1023–75. doi: 10.1016/S0140-6736(17)33326-3
3. Zhang S, Sun K, Zheng R, Zeng H, Wang S, Chen R, et al. Cancer Incidence and Mortality in China, 2015. *J Natl Cancer Center* (2021) 1(1):2–11. doi: 10.1016/j.jncc.2020.12.001
4. Travis WD, Brambilla E, Noguchi M, Nicholson AG, Geisinger KR, Yatabe Y, et al. International Association for the Study of Lung Cancer/American Thoracic Society/European Respiratory Society International Multidisciplinary Classification of Lung Adenocarcinoma. *J Thorac Oncol* (2011) 6(2):244–85. doi: 10.1097/JTO.0b013e318206a221
5. Hellmann MD, Ciuleanu TE, Pluzanski A, Lee JS, Otterson GA, Audigier-Valette C, et al. Nivolumab Plus Ipilimumab in Lung Cancer With a High Tumor Mutational Burden. *N Engl J Med* (2018) 378(22):2093–104. doi: 10.1056/NEJMoa1801946
6. Spigel D, De Marinis F, Giaccone G, Reinmuth N, Vergnenegre A, Barrios C, et al. IMpower110: Interim Overall Survival (OS) Analysis of a Phase III Study of Atezolizumab (Atezo) vs Platinum-Based Chemotherapy (Chemo) as First-Line (1L) Treatment (Tx) in PD-L1–selected NSCLC. *Ann Oncol* (2019) 30: v915. doi: 10.1093/annonc/mdz293
7. Berton D, Banerjee SN, Curigliano G, Cresta S, Arkenau H-T, Abdeddaim C, et al. Antitumor Activity of Dostarlimab in Patients With Mismatch Repair-Deficient/Microsatellite Instability–High Tumors: A Combined Analysis of Two Cohorts in the GARNET Study. *J Clin Oncol* (2021) 39(15_suppl):2564–2564. doi: 10.1200/JCO.2021.39.15_suppl.2564
8. Marabelle A, Fakih M, Lopez J, Shah M, Shapira-Frommer R, Nakagawa K, et al. Association of Tumour Mutational Burden With Outcomes in Patients With Advanced Solid Tumours Treated With Pembrolizumab: Prospective Biomarker Analysis of the Multicohort, Open-Label, Phase 2 KEYNOTE-158 Study. *Lancet Oncol* (2020) 21(10):1353–65. doi: 10.1016/S1470-2045(20)30445-9
9. Bodor JN, Kasireddy V, Borghaei H. First-Line Therapies for Metastatic Lung Adenocarcinoma Without a Driver Mutation. *J Oncol Pract* (2018) 14(9):529–35. doi: 10.1200/JOP.18.00250
10. Mencoboni M, Ceppi M, Bruzzone M, Taveggia P, Cavo A, Scordamaglia F, et al. Effectiveness and Safety of Immune Checkpoint Inhibitors for Patients With Advanced Non Small-Cell Lung Cancer in Real-World: Review and Meta-Analysis. *Cancers (Basel)* (2021) 13(6):1388. doi: 10.3390/cancers13061388
11. Brahmer J, Rodriguez-Abreu D, Robinson A, Hui R, Csőszi T, Fülöp A, et al. LBA51 KEYNOTE-024 5-Year OS Update: First-Line (1L) Pembrolizumab (Pembro) vs Platinum-Based Chemotherapy (Chemo) in Patients (Pts) With Metastatic NSCLC and PD-L1 Tumour Proportion Score (TPS)≥ 50%. *Ann Oncol* (2020) 31:S1181–S2. doi: 10.1016/j.annonc.2020.08.2284
12. Le DT, Uram JN, Wang H, Bartlett BR, Kemberling H, Eyring AD, et al. PD-1 Blockade in Tumors With Mismatch-Repair Deficiency. *N Engl J Med* (2015) 372(26):2509–20. doi: 10.1056/NEJMoa1500596
13. Bodor JN, Boumber Y, Borghaei H. Biomarkers for Immune Checkpoint Inhibition in Non-Small Cell Lung Cancer (NSCLC). *Cancer* (2020) 126(2):260–70. doi: 10.1002/cncr.32468
14. Lantuejoul S, Sound-Tsao M, Cooper WA, Girard N, Hirsch FR, Roden AC, et al. PD-L1 Testing for Lung Cancer in 2019: Perspective From the IASLC Pathology Committee. *J Thorac Oncol* (2020) 15(4):499–519. doi: 10.1016/j.jtho.2019.12.107
15. Li K, Luo H, Huang L, Luo H, Zhu X. Microsatellite Instability: A Review of What the Oncologist Should Know. *Cancer Cell Int* (2020) 20(1):1–13. doi: 10.1186/s12935-019-1091-8
16. Takamochi K, Takahashi F, Suehara Y, Sato E, Kohsaka S, Hayashi T, et al. DNA Mismatch Repair Deficiency in Surgically Resected Lung Adenocarcinoma: Microsatellite Instability Analysis Using the Promega Panel. *Lung Cancer* (2017) 110:26–31. doi: 10.1016/j.lungcan.2017.05.016
17. Samstein RM, Lee CH, Shoushtari AN, Hellmann MD, Shen R, Janjigian YY, et al. Tumor Mutational Load Predicts Survival After Immunotherapy Across Multiple Cancer Types. *Nat Genet* (2019) 51(2):202–6. doi: 10.1038/s41588-018-0312-8
18. Hellmann MD, Nathanson T, Rizvi H, Creelan BC, Sanchez-Vega F, Ahuja A, et al. Genomic Features of Response to Combination Immunotherapy in Patients With Advanced Non-Small-Cell Lung Cancer. *Cancer Cell* (2018) 33(5):843–52.e4. doi: 10.1016/j.ccell.2018.03.018
19. Yarchoan M, Albacker LA, Hopkins AC, Montesion M, Murugesan K, Vithayathil TT, et al. PD-L1 Expression and Tumor Mutational Burden are Independent Biomarkers in Most Cancers. *JCI Insight* (2019) 4(6):e126908. doi: 10.1172/jci.insight.126908
20. Salem ME, Grothey A, Kim ES, Xiu J, Goldberg RM, Korn WM, et al. Impact of MLH1, PMS2, MSH2, and MSH6 Alterations on Tumor Mutation Burden (TMB) and PD-L1 Expression in 1,057 Microsatellite Instability-High (MSI-H) Tumors. *J Clin Oncol* (2018) 39(15_suppl):3572–3572. doi: 10.1200/JCO.2018.36.15_suppl.3572
21. Luchini C, Bibeau F, Ligtenberg MJL, Singh N, Nottegar A, Bosse T, et al. ESMO Recommendations on Microsatellite Instability Testing for Immunotherapy in Cancer, and Its Relationship With PD-1/PD-L1 Expression and Tumour Mutational Burden: A Systematic Review-Based Approach. *Ann Oncol* (2019) 30(8):1232–43. doi: 10.1093/annonc/mdz116
22. Chalmers ZR, Connelly CF, Fabrizio D, Gay L, Ali SM, Ennis R, et al. Analysis of 100,000 Human Cancer Genomes Reveals the Landscape of Tumor Mutational Burden. *Genome Med* (2017) 9(1):34. doi: 10.1186/s13073-017-0424-2
23. Yi M, Qin S, Zhao W, Yu S, Chu Q, Wu K. The Role of Neoantigen in Immune Checkpoint Blockade Therapy. *Exp Hematol Oncol* (2018) 7(1):28. doi: 10.1186/s40164-018-0120-y
24. Dong ZY, Zhong WZ, Zhang XC, Su J, Xie Z, Liu SY, et al. Potential Predictive Value of TP53 and KRAS Mutation Status for Response to PD-1 Blockade Immunotherapy in Lung Adenocarcinoma. *Clin Cancer Res* (2017) 23(12):3012–24. doi: 10.1158/1078-0432.CCR-16-2554
25. Song Z, Cheng G, Xu C, Wang W, Shao Y, Zhang Y. Clinicopathological Characteristics of POLE Mutation in Patients With Non-Small-Cell Lung Cancer. *Lung Cancer* (2018) 118:57–61. doi: 10.1016/j.lungcan.2018.02.004
26. Liu C-X, Li Y, Obermoeller-McCormick LM, Schwartz AL, Bu G. The Putative Tumor Suppressor LRP1B, a Novel Member of the Low Density Lipoprotein (LDL) Receptor Family, Exhibits Both Overlapping and Distinct Properties With the LDL Receptor-Related Protein. *J Biol Chem* (2001) 276(31):28889–96. doi: 10.1074/jbc.M102727200
27. Ding L, Getz G, Wheeler DA, Mardis ER, McLellan MD, Cibulskis K, et al. Somatic Mutations Affect Key Pathways in Lung Adenocarcinoma. *Nature* (2008) 455(7216):1069–75. doi: 10.1038/nature07423
28. Chen H, Chong W, Wu Q, Yao Y, Mao M, Wang X. Association of LRP1B Mutation With Tumor Mutation Burden and Outcomes in Melanoma and non-Small Cell Lung Cancer Patients Treated With Immune Check-Point Blockades. *Front Immunol* (2019) 10:1113. doi: 10.3389/fimmu.2019.01113
29. Brown LC, Tucker MD, Sedhom R, Schwartz EB, Zhu J, Kao C, et al. LRP1B Mutations are Associated With Favorable Outcomes to Immune Checkpoint Inhibitors Across Multiple Cancer Types. *J Immunother Cancer* (2021) 9(3):e001792. doi: 10.1136/jitc-2020-001792
30. Katoh M. Function and Cancer Genomics of FAT Family Genes (Review). *Int J Oncol* (2012) 41(6):1913–8. doi: 10.3892/ijo.2012.1669
31. Qiu Y, Liu L, Yang H, Chen H, Deng Q, Xiao D, et al. Integrating Histologic and Genomic Characteristics to Predict Tumor Mutation Burden of Early-Stage Non-Small-Cell Lung Cancer. *Front Oncol* (2020) 10:608989. doi: 10.3389/fonc.2020.608989
32. Guo Z, Yan X, Song C, Wang Q, Wang Y, Liu X-P, et al. FAT3 Mutation Is Associated With Tumor Mutation Burden and Poor Prognosis in Esophageal Cancer. *Front Oncol* (2021) 11:603660. doi: 10.3389/fonc.2021.603660
33. Gao C, Li H, Liu C, Xu X, Zhuang J, Zhou C, et al. Tumor Mutation Burden and Immune Invasion Characteristics in Triple Negative Breast Cancer: Genome High-Throughput Data Analysis. *Front Immunol* (2021) 12:650491. doi: 10.3389/fimmu.2021.650491
34. Rizvi NA, Hellmann MD, Snyder A, Kvistborg P, Makarov V, Havel JJ, et al. Cancer Immunology. Mutational Landscape Determines Sensitivity to PD-1

Blockade in non-Small Cell Lung Cancer. *Science* (2015) 348(6230):124–8. doi: 10.1126/science.aaa1348
35. Imielinski M, Berger AH, Hammerman PS, Hernandez B, Pugh TJ, Hodis E, et al. Mapping the Hallmarks of Lung Adenocarcinoma With Massively Parallel Sequencing. *Cell* (2012) 150(6):1107–20. doi: 10.1016/j.cell.2012.08.029
36. Chen J, Yang H, Teo ASM, Amer LB, Sherbaf FG, Tan CQ, et al. Genomic Landscape of Lung Adenocarcinoma in East Asians. *Nat Genet* (2020) 52 (2):177–86. doi: 10.1038/s41588-019-0569-6
37. Subramanian A, Tamayo P, Mootha VK, Mukherjee S, Ebert BL, Gillette MA, et al. Gene Set Enrichment Analysis: A Knowledge-Based Approach for Interpreting Genome-Wide Expression Profiles. *Proc Natl Acad Sci USA* (2005) 102(43):15545–50. doi: 10.1073/pnas.0506580102
38. Newman AM, Liu CL, Green MR, Gentles AJ, Feng W, Xu Y, et al. Robust Enumeration of Cell Subsets From Tissue Expression Profiles. *Nat Methods* (2015) 12(5):453–7. doi: 10.1038/nmeth.3337
39. Paijens ST, Vledder A, de Bruyn M, Nijman HW. Tumor-Infiltrating Lymphocytes in the Immunotherapy Era. *Cell Mol Immunol* (2021) 18 (4):842–59. doi: 10.1038/s41423-020-00565-9
40. van Wilpe S, Tolmeijer SH, Koornstra RHT, de Vries IJM, Gerritsen WR, Ligtenberg M, et al. Homologous Recombination Repair Deficiency and Implications for Tumor Immunogenicity. *Cancers (Basel)* (2021) 13(9):2249. doi: 10.3390/cancers13092249
41. Shim JH, Kim HS, Cha H, Kim S, Kim TM, Anagnostou V, et al. HLA-Corrected Tumor Mutation Burden and Homologous Recombination Deficiency for the Prediction of Response to PD-(L)1 Blockade in Advanced Non-Small-Cell Lung Cancer Patients. *Ann Oncol* (2020) 31 (7):902–11. doi: 10.1016/j.annonc.2020.04.004
42. Teng MW, Ngiow SF, Ribas A, Smyth MJ. Classifying Cancers Based on T-Cell Infiltration and PD-L1. *Cancer Res* (2015) 75(11):2139–45. doi: 10.1158/0008-5472.CAN-15-0255
43. Raskov H, Orhan A, Christensen JP, Gogenur I. Cytotoxic CD8(+) T Cells in Cancer and Cancer Immunotherapy. *Br J Cancer* (2021) 124(2):359–67. doi: 10.1038/s41416-020-01048-4
44. Borst J, Ahrends T, Babala N, Melief CJM, Kastenmuller W. CD4(+) T Cell Help in Cancer Immunology and Immunotherapy. *Nat Rev Immunol* (2018) 18(10):635–47. doi: 10.1038/s41577-018-0044-0
45. Duan Z, Luo Y. Targeting Macrophages in Cancer Immunotherapy. *Signal Transduct Target Ther* (2021) 6(1):127. doi: 10.1038/s41392-021-00506-6
46. Ma Q, Gu JT, Wang B, Feng J, Yang L, Kang XW, et al. PlGF Signaling and Macrophage Repolarization Contribute to the Anti-Neoplastic Effect of Metformin. *Eur J Pharmacol* (2019) 863:172696. doi: 10.1016/j.ejphar.2019.172696
47. Meng Y, Qu Y, Wu W, Chen L, Sun L, Tai G, et al. Galactan Isolated From Cantharellus Cibarius Modulates Antitumor Immune Response by Converting Tumor-Associated Macrophages Toward M1-Like Phenotype. *Carbohydr Polym* (2019) 226:115295. doi: 10.1016/j.carbpol.2019.115295

Conflict of Interest: The authors declare that the research was conducted in the absence of any commercial or financial relationships that could be construed as a potential conflict of interest.

The reviewer SX declared a shared affiliation with the authors to the handling editor at the time of review.

Publisher's Note: All claims expressed in this article are solely those of the authors and do not necessarily represent those of their affiliated organizations, or those of the publisher, the editors and the reviewers. Any product that may be evaluated in this article, or claim that may be made by its manufacturer, is not guaranteed or endorsed by the publisher.

Copyright © 2022 Zhu, Zhang, Cui, Zhao, Wang, Zhai, Jiang and Jiang. This is an open-access article distributed under the terms of the Creative Commons Attribution License (CC BY). The use, distribution or reproduction in other forums is permitted, provided the original author(s) and the copyright owner(s) are credited and that the original publication in this journal is cited, in accordance with accepted academic practice. No use, distribution or reproduction is permitted which does not comply with these terms.

frontiers in Immunology

REVIEW
published: 14 January 2022
doi: 10.3389/fimmu.2021.808964

Tumor-Infiltrating Lymphocytes in Colorectal Cancer: The Fundamental Indication and Application on Immunotherapy

Ziyi Bai[1,2], *Yao Zhou*[2], *Zifan Ye*[1], *Jialong Xiong*[1], *Hongying Lan*[1] *and Feng Wang*[1*]

[1] Key Laboratory of Molecular Medicine and Biotherapy, School of Life Science, Beijing Institute of Technology, Beijing, China, [2] College of Bioinformatics Science and Technology, Harbin Medical University, Harbin, China

The clinical success of immunotherapy has revolutionized the treatment of cancer patients, bringing renewed attention to tumor-infiltrating lymphocytes (TILs) of various cancer types. Immune checkpoint blockade is effective in patients with mismatched repair defects and high microsatellite instability (dMMR-MSI-H) in metastatic colorectal cancer (CRC), leading the FDA to accelerate the approval of two programmed cell death 1 (PD-1) blocking antibodies, pembrolizumab and nivolumab, for treatment of dMMR-MSI-H cancers. In contrast, patients with proficient mismatch repair and low levels of microsatellite stability or microsatellite instability (pMMR-MSI-L/MSS) typically have low tumor-infiltrating lymphocytes and have shown unsatisfied responses to the immune checkpoint inhibitor. Different TILs environments reflect different responses to immunotherapy, highlighting the complexity of the underlying tumor-immune interaction. Profiling of TILs fundamental Indication would shed light on the mechanisms of cancer-immune evasion, thus providing opportunities for the development of novel therapeutic strategies. In this review, we summarize phenotypic diversities of TILs and their connections with prognosis in CRC and provide insights into the subsets-specific nature of TILs with different MSI status. We also discuss current clinical immunotherapy approaches based on TILs as well as promising directions for future expansion, and highlight existing clinical data supporting its use.

Keywords: tumor-infiltrating lymphocytes, tertiary lymphoid structures, microsatellite instability, immunotherapy, colorectal cancer

OPEN ACCESS

Edited by:
Xuelei Ma,
Sichuan University, China

Reviewed by:
Qi Zhao,
University of Macau, China
Vincenzo Barnaba,
Sapienza University of Rome, Italy
Peng Xiao,
Shandong University, China

****Correspondence:***
Feng Wang
wfeng@bit.edu.cn

Specialty section:
This article was submitted to Cancer Immunity and Immunotherapy, a section of the journal Frontiers in Immunology

Received: *04 November 2021*
Accepted: *24 December 2021*
Published: *14 January 2022*

Citation:
Bai Z, Zhou Y, Ye Z, Xiong J, Lan H and Wang F (2022) Tumor-Infiltrating Lymphocytes in Colorectal Cancer: The Fundamental Indication and Application on Immunotherapy. Front. Immunol. 12:808964. doi: 10.3389/fimmu.2021.808964

INTRODUCTION

Colorectal cancer (CRC) is a clinically common malignant tumor of the digestive system. According to Global Cancer Statistics of 2020, there are approximately 1.9 million newly diagnosed CRC patients and 935,000 CRC-related deaths, accounting for 10% of cancer cases and 9.4% of cancer-related deaths worldwide (1). With deeper understanding of pathophysiology in colorectal cancer,

the optimization of screening and the application of various treatments have effectively improved the 5-year survival rate (2–5). However, nearly 40% of patients with CRC end up relapsing, with recurrent or advanced metastasis. As a result, extensive researches are now being conducted to overcome the barriers to relapse and resistance, and to explore more effective targets.

In the past decade immunotherapy has achieved impressive success in eradicating malignant cells by harnessing the inherent mechanisms of the host immune system, transforming the therapeutic landscape for a variety of solid and hematological malignancies (6, 7). Among cancer immunotherapy strategies, immune checkpoint blockade has shown significant benefits. It is the most thoroughly studied class of immunotherapy to date, increasing the overall survival (OS) rates of patients with advanced melanoma, non-small-cell lung cancer (NSCLC), urothelial cancer (8–10). Immune checkpoint therapy rejuvenates T cells and allows the adaptive immune system to block immune escape caused by cascade activation of tumor-specific immune checkpoints, such as those controlled by programmed cell death protein (PD-1), programmed death-ligand 1 (PD-L1) or cytotoxic T lymphocyte-associated protein 4 (CTLA-4) (11, 12). In the treatment of CRC, the PD-1 inhibitors pembrolizumab and nivolumab, which have been approved by the Food and Drug Administration (FDA), led a to durable response in patients with metastatic CRC that is mismatch-repair-deficient (dMMR) and microsatellite instability-high (MSI-H) (dMMR-MSI-H). Another inhibitor, ipilimumab, a fully-humanized monoclonal antibody that blocks CTLA-4, has also been approved by the FDA for combination with nivolumab in patients with dMMR-MSI-H CRC who have previously received chemotherapy.

According to The Cancer Genome Atlas Project's CRC study based on the array and sequencing technologies, CRC can be classified into two main types: (1) ~ 16% hypermutated (>12 mutations per 10^6 DNA bases) cancers with dMMR-MSI-H signature and (2) ~ 84% percent non-hypermutated (<8.24 mutations per 10^6 DNA bases) with mismatch-repair-proficient (pMMR) and have low levels of microsatellite instability (MSI-L) or microsatellite stable (MSS) (pMMR-MSI-L/MSS) signature (13). Patients with pMMR-MSI-L/MSS have a worse prognosis than dMMR-MSI-H (14), and show unsatisfied responses to immune checkpoint inhibitors (ICIs) (15). In general, pMMR-MSI-L/MSS have low TMB, are often poorly infiltrated by TILs. Accumulating evidence has shown that tumor mutation burden and tumor-infiltrating-lymphocytes (TILs) correlate with ICIs response (16–18). Therefore, it is important to understand the relationship between genetic heterogeneity and the molecular level of TILs in CRC. In this review, we discuss the accumulating evidence about the fundamental feature of TILs and their prognostic value in the tumor micro-environment of CRC. We also review the clinical development of immune checkpoint inhibition in CRC and discuss the emerging clinical therapies for targeting TILs. Collectively, this work clarifies some aspects of TILs subsets discrepancy, which provides a scientific basis for a better understanding of the excessive interactions between immune cells and different genetic types of CRC.

THE ROLE OF TILS IN ANTI-TUMOR IMMUNITY

It is an increasing variety of investigations that support the importance of tumor immune infiltration, including lymphocytes [T cells, B cells, and natural killer (NK) cells], macrophages, dendritic cells, and neutrophils, revealing a wide patient-patient diversity (19, 20). For a long time in the past, colorectal cancer was regarded as immunogenic and difficult to be treated by immunotherapy. However, advances in the molecular characterization of tumor-associated antigens defined by T cells and methods for detecting antigen-specific T cell responses have changed the scientific community's view of this issue. Tumors with microsatellite instability, including CRC, accumulate inserts and deletions in DNA repeat sequences. About two-thirds of MSI tumors are sporadic, and one-third are hereditary (Lynch syndrome). The high mutational load and frequent frameshift mutations in MSI tumors lead to the production of many neoantigens recognized by the immune system, which can trigger the lymphocytic infiltrates. Although a portion of TILs is composed of immunosuppressant cells, these cells are specifically recruited and/or directed by the tumor to maintain the immune-privileged microenvironment. In contrast, some TILs reflect attempts by the immune system to counter tumor responses (21, 22).

It is noteworthy that several studies have identified a broad association among TILs, different histological characteristics of cancer, disease-free survival (DFS), cancer-specific survival (CS) and OS (23–26). A meta-analysis of 43 trials describing 21,015 CRC patients showed that high generalized tumor inflammatory infiltrate was associated with good OS (hazard ratio (HR), 0.65; 95% confidence interval (95% CI, 0.54-0.77), CS (HR, 0.58; 95% CI, 0.46-0.73) and DFS (HR, 0.72; 95% CI, 0.60–0.88) (27). Similarly, Rozek et al. found that high TILs (HR = 0.76, 95% CI = 0.64 to 0.89, $p < 0.001$) was favorable prognostic factors for specific and OS in colorectal cancer through a multivariate analysis of 2,369 cases (28). However, the quantity and quality can significantly vary among CRC patients within CRC different MSI statue (29, 30). Next, we reviewed the association between TILs and survival in patients with CRC and the characteristics of major subsets of TILs in the literature with different MSI statue.

$CD8^+$ CYTOTOXIC T CELLS

$CD8^+$ cytotoxic T lymphocytes (CTLs), a key component of the adaptive immune system, play an important role in immune defense against intracellular pathogens such as viruses, bacteria and tumors, which were regarded as a major driver of anti-tumor immunity (31, 32). The cytotoxicity process is carried out by several substances produced by $CD8^+$ T cells, such as perforin, granzymes, granulysin, Fas ligand, and tumor necrosis factor α (TNF-α) (33, 34). $CD8^+$ CTLs mediates tumor rejection by recognizing tumor antigens and directly kill transformed cells. Effector $CD8^+$ T cells in the tumor microenvironment generate Interleukin-2 (IL-2), IL-12 and Interferon-γ (IFN-γ), which enhance $CD8^+$ CTLs, leading to targeted tumor cell killing (35, 36).

A recent study of most tumor-infiltrating immune cell subtypes revealed that $CD8^+$ T cells had the greatest impact on patient survival (37). The role of $CD8^+$ CTLs in prognosis was first analyzed in a large cohort of CRC more than 10 years ago (24, 32). Several studies have shown that elevated levels of CTLs in the tumor microenvironment are associated with antitumor effects and improved prognosis in various cancers (30, 38–40). Moreover, tumors from the patient cohorts categorized by a high or low density of immune infiltrate and presence or absence of metastases revealed that adequate immune infiltration with successful initiation and differentiation of $CD8^+$ T cells is vital for successful suppression of metastasis development (41).

Microsatellite instability is a good predictor of the prognosis of colorectal cancer, and there is a close relationship between microsatellite instability and the abundance of tumor-infiltrating T-cells (**Table 1**). It is noteworthy that a study of automatic image analysis on 768 colorectal cancers has identified the density of T cell subsets in neoplastic epithelial areas was positively correlated with MSI-H (39). In particular, several immunohistochemistry studies have revealed an especially high infiltration of intraepithelial activated $CD8^+$ T cells within microsatellite instability colorectal tumors (42–45). Dolcetti et al. using immunohistochemistry found that there were many cytotoxic infiltrating structures in tumor epithelial cells in MSI-H patients. Moreover, granase B expression showed that these cytotoxic effects were more active in MSI-H tumors (5.3 ± 4.5 vs 0.6 ± 1.3, $p < 0.001$) (46). Similarly, in another study evaluating the number of multiple immune cells in an *in situ* immune response of 490 patients with CRC, the total density of cytotoxic T cells was significantly higher in MSI samples than in MSS samples. Interestingly, due to the importance of accurate intratumoral localization of infiltrating immune cells, the study also measured the density within the tumor glands (intratumoral) or stroma. The group reported that MSI-H and MSS patients showed similar stromal $CD8^+$ T cell densities and there was a significant increase in the density of $CD8^+$ T cells within the tumor glands in MSI patients, in both the core and invasive margin of tumor (all $p < 0.05$) (47). The same conclusion was also found in the study of Smedt et al., which identified high numbers of intra-epithelial $CD8^+$ cells in MSI compared with MSS tumors (48, 49).

T HELPER CELLS

$CD4^+$ helper T lymphocytes are mediators of cellular immunity and play a key role in the activation of other immune cells, such as B cells and cytotoxic T cells, modulating immune responses. $CD4^+$ helper T cells further differentiate into subsets with broad functions characterized by cytokine secretion and effector

TABLE 1 | The association of tumor infiltrating lymphocytes with microsatellite stability status in colorectal cancer.

Author	Markers	Sample size (dMMR-MSI-H | pMMR-MSI-L/ MSS)	Disease stage	TILs feature
Liu et al. (42)	CD3, CD4, CD8, CD56	167/163	I-IV	dMMR group displayed higher CD8 cells ($p < 0.01$). $CD56^+$ cells $CD4^+$ cell than pMMR group (both $p < 0.05$).
Flahec et al. (43)	CD3, CD4, CD8, CD20, CD68, FOXP3	35/34	I-IV	dMMR tumors have more numerous intraepithelial ($CD3^+$, $CD8^+$, $FOXP3^+$) and stromal ($CD8^+$) lymphocytes
Michael-Robinson et al. (44)	CD3, CD8, CD20	32/70	Duke's stage A-D	TILs were most abundant in MSI-H colorectal cancers in which 23/32 (72%) scored as TILs positive. Only 5/40 (12.5%) MSS tumours and 9/30 (30%) MSI-L cancers were TILs positive ($p < 0.0001$).
Phillips et al. (45)	CD3, CD4, CD8	26/138	NA	MSI-H tumours showed significantly higher counts for $CD3^+$ and $CD8^+$ cells, but no differences were found in CD4 counts.
Dolcetti et al. (46)	CD3, CD4, CD8, CD56	18/37	Duke's A-D	MSI cases carried significantly higher numbers of cytotoxic lymphocytes infiltrating within neoplastic epithelial structures ($p < 0.001$)
Mlecnik et al. (47)	CD8, CD20, CD68, IL-17, NKp46, CD45RO	186/114	I-IV	A significant increase in cytotoxic T cell, B cell in tumors from MSI patients. MSI tumors had higher densities of Th1. The MSS patients showed a significantly increased Th17 infiltration in the core and invasive margin of tumor ($p < 0.05$)
Smedt et al. (48)	CD3, CD4, CD8, CD20, CD68	29/27	I-IV	An increased number of tumor-infiltrating cytotoxic T-lymphocytes ($CD8^+$) in MSI compared with MSS tumors for both the tumor and peritumoral area. Quantification showed high numbers of intra-epithelial $CD3^+$, $CD4^+$, $CD8^+$, $CD20^+$ and $CD68^+$ cells in MSI compared with MSS cancers (all $p <= 0.01$).
Nestarenkaite et al. (49)	CD8, CD20, CD68	39/48	I-IV	The $CD8^+$ densities within tumor-stroma interface zone (IZ) and the intratumoral densities were higher in MSI than in MSS tumors, whereas no differences in IZ and intratumoral $CD20^+$ cell densities were observed comparing MSI and MSS tumors
Gouvello et al. (50)	IL-17	10/11	I-IV	Higher tumoral expression of Foxp3, IL-17, IL1-beta, IL-6 and TGF-β was associated with the MSS phenotype, and the IL-17 T/TN (colon cancers/autologous normal colon mucosa) ratio was higher in MSS tissues than in MSI-H tissues.
Michel et al. (51)	CD3, CD8, FOXP3	37/33	I-IV and NA	The elevated number of $CD8^+$ lymphocytes found in MSI-H colorectal cancers is paralleled by an enhanced infiltration with $CD8^-$ $FOXP3^+$ cells

Th, T helper; Treg, regulatory T cell; dMMR-MSI-H, mismatch-repair-deficient and microsatellite instability-high; pMMR-MSI-L/MSS, mismatch-repair-proficient and microsatellite-stable or have low levels of microsatellite instability; TILs, tumor infiltrating lymphocytes.

function, including T helper 1 (Th1) cells, T helper 2 (Th2) cells, T helper 17 (Th17) cells, follicular helper T (Tfh) cells (reviewed in the later section) and regulatory T (T_{reg}) cells.

The main effector function of Th1 cells lie in cell-mediated immunity and inflammation, including the activation of other immune cells such as macrophages, B cells and $CD8^+$ CTLs lysis and other effector functions, which play an important role in clearing intracellular infection and assisting in killing tumor cells. Th1 cells and their derived cytokines (e.g., IFN-γ, TNF-α, etc.) are strongly associated with good clinical outcomes in almost all cancer types (21, 25, 41, 52). In contrast to the effects of Th1, analysis of the effect of other $CD4^+$ T cell subsets on clinical outcomes has yielded apparent contradictory results, remaining a matter of debate (**Table 2**). The prognostic effects of other T-helper cell populations (Th2, Th17, and T_{reg} cells) are also different across cancer types and stages. Th2 cells are usually associated with aggressive tumors, either by activating B cells or producing the immunosuppressive cytokine IL-10 (55, 56, 86). However, it is not a universal phenomenon. Multiple studies have shown that Th2 cells are associated with a good prognosis in Hodgkin's lymphoma (53) and breast cancer (54), but not in ovarian (55), gastric (57) and pancreatic cancer (56). There were also conflicting results regarding the role of Th17 cells, which are associated with poor prognosis [e.g., NSCLC (62) and hepatocellular carcinoma (63)] and improved survival [esophageal cancer (58), gastric cancer (59), ovarian cancer (60), cervical cancer (61)]. Th17 cells recruitment have been observed in a variety of malignancies in comparison with normal tissue. On the one hand, the potential of Th17 cells to transdifferentiate into a more immunosuppressive phenotype plays a role in tumor immune evasion. IL-17 (a cytokine produced by Th17 cells) cytokines are associated with increased vascular growth and thus increase tumor growth and metastasis in some models. On the other hand, Th17 cells recruit CTLs and dendritic cells to the tumor site to promote tumor clearance, similar to their ability to convert to a Th1 phenotype that secretes IFN-γ under specific environmental factors (87). The role of Th17 cells in cancer progression appears to be highly dependent on the specific tumor microenvironment. Harnessing this plasticity to control them and improve anti-tumor responses may be a useful strategy for developing cancer immunotherapies. T_{reg} cells can inhibit anti-autoimmune reactions, and there are different subsets (including thymic-derived T_{reg}, peripheral T_{reg}, etc.). Similarly, the role of regulatory T cells has been a matter of debate for the past decade. Curiel et al. first demonstrated a correlation of intratumoral T_{reg} cells and poor survival in ovarian cancer (70). However, subsequent studies have reported inconsistent results, with T_{reg} cells having no effect on survival of anal squamous cell carcinoma (67), glioma (68), and glioblastoma (69), while showing positive effects on nasopharyngeal cancer (64), head and neck cancer (65), and hematological malignancies (66).

A growing number of studies have investigated the characteristics and prognostic potential of T helper cells in CRC adaptive immune response (**Table 1**). A study conducted by Liu and his colleagues showed that the dMMR group displayed much less $CD56^+$ cell, $CD4^+$ cell and MHC class I expression (all $p < 0.05$) and higher CD8 expression ($p < 0.01$) than the pMMR group. Besides, in the dMMR group, low CD4 and CD56 expression were risk factors for low MHC class I expression in the univariate model (42). However, due to helper cells exhibiting a great diversity in phenotype, identification of the T helper cell subsets in tumors requires evaluation of some specific markers (including, but not limited to, mRNA and key cytokines) in addition to $CD4^+$. A study of 52 patients with CRC showed that IL-17 was co-stained with CD4 and CD68 by confocal microscopy analysis, which indicated IL-17 in colorectal cancer was expressed by macrophage and Th17. Compared to T_{reg} cells, other T-helper cell subsets generally do not express distinct surface markers. As a result, several studies have assessed T helper cell abundance through gene expression profiles. In 2013, Bindea et al. performed microarray expression experiments in tumors from 105 CRC patients showed that $CD8^+$ and Th1 were associated with a good prognosis (DFS, HR < 1) (88), confirming previous reports from the same group (24). In this report, Th17 cells were also found to negatively influence the patient outcome (DFS, HR > 1, $p < 0.05$). In a large study of 125 frozen colorectal tumor specimens, immune-related genes indicated that patients with high expression of the Th17 cluster had a poor prognosis, whereas patients with high expression of the Th1 cluster had prolonged disease-free survival. In contrast, their results did not support the

TABLE 2 | The association of different types of TILs with tumor prognosis.

The types of TILs	Reference	Prognosis	Tumor types
$CD8^+$ cell	(30, 37–40)	Good	Colorectal cancer etc.
Th1 cell	(21, 25, 41, 52)	Good	Colorectal cancer etc.
Th2 cell	(53, 54)	Good	Hodgkin lymphoma; Breast cancer
	(55–57)	Poor	Ovarian cancer; Pancreatic cancer; Gastric cancer
Th17 cell	(58–61)	Good	Esophageal squamous cell carcinoma; Gastric adenocarcinoma; Ovarian cancer; Squamous cervical cancer
	(62, 63)	Poor	Non-small cell lung cancer; Hepatocellular carcinoma
T_{reg} cell	(64–66)	Good	Nasopharyngeal carcinoma; Head and neck cancer; Urinary bladder cancer
	(67–69)	None	Anal squamous cell carcinoma; Glioma; Glioblastomas
	(70)	Poor	Ovarian carcinoma
NK cell	(71–76)	Good	Metastatic prostate cancer; Non-small cell lung cancer; Colorectal cancer; Mantle cell lymphoma
	(77, 78)	Poor	Infiltrating ductal carcinoma of breast; Digestive cancer
B cell	(79–83)	Good	Hepatocellular carcinoma with lymphocytic infiltration; Melanoma; Ovarian cancer; Non-small cell lung cancer; Stage IB cervical squamous cell carcinoma
	(84, 85)	Poor	Ovarian cancer; Breast cancer

primary role of Th2 cells in patient outcomes (52). Using single cell RNA-seq, Zhang et al. (89) found that among $CD4^+$ T cells, most tumor-infiltrating Treg cells showed clonal exclusivity, while certain Treg cell clones were associated with the development of several T helper cells clones by single T cell transcriptome analysis (89). Notably, two $IFNG^+$ Th1-like cell clusters were also found in this study, only $CXCL13^+$ $BHLHE40^+$ Th1-like cells were preferentially enriched in patients with microsatellite-instable tumors.

T_{reg} cell is characterized by high expression of CD25 and the transcription factor fork head box protein P3 (FOXP3) (64, 90). Using quantitative reverse transcription-PCR (qRT-PCR) quantified for the expression of 15 markers of the immune response, Cui et al. found that higher expression of FOXP3, IL-17, IL1-β, IL-6 and TGF-β were associated with the MSS phenotype (50). Moreover, a large study of 1,420 tumor samples found a significantly higher amount of $FOXP3^+$ tumor-infiltrating T_{reg} in pMMR CRC samples (38). This study also observed an association between a high frequency of tumor-infiltrating $FOXP3^+$ T_{reg} and improved survival in CRC patients, which is in accordance with the results reported by Gunnarsson et al. and Frey et al. (91, 92). In contrast, several studies have challenged the characterization of T_{reg} cells in CRC. In MSI-H CRC, Michel et al. found a significant increase in intraepithelial infiltration of $FOXP3^+$ cells and in the ratio of intraepithelial to stromal infiltration. Similarly, in another study, $CD45RO^+$ and $FOXP3^+$ cell densities were significantly correlated with MSI-H and the densities of $CD8^+$, $CD45RO^+$ and $FOXP3^+$ cells were significantly associated with patient survival in CRC (43). Given the diversity of T_{reg} populations observed in cancer, it is a great challenge of studying T helper cell subpopulations in the context of immunopathology.

NK CELLS

In recent years, the rapid and potent anti-tumor function of innate immunity, which even occurs at a very early stage of tumor progression, has attracted increasing attention. NK cells, as a subset of innate lymphoid cells, are able to control tumor growth as well as the initial stages of metastatic dissemination (93–95). Unlike other lymphocytes (including B cells, T cells, and natural killer T cells), NK cells do not express antigen-specific receptors such as B cell receptor/T cell receptor or CD3. Instead, NK cells possess cytotoxic abilities similar to $CD8^+$ T cells, acting in an antigen-independent manner in the adaptive immunity. In addition to cytotoxic effects, NK cells have been reported to produce a large number of cytokines similar to T cells, including IL-2 (96), IL-7 (97), IL-15 (98), and IFN-γ (99), to modulate adaptive immune responses and participate in other related pathways. Despite many similarities, compared with effector T cells, NK cells are more cytotoxic to tumors, possess lower immunogenicity and respond to target cells more quickly (100, 101). NK cells are highly heterogeneous, characterized by the abundance of surface receptors. According to surface CD56 expression, NK cells can be divided into 2 developmentally related, but functionally distinct, subsets: $CD56^{bright}$ and $CD56^{dim}$. $CD56^{dim}$ NK cells are comprise 80%–95% of peripheral blood NK cells, and are always also $CD16^+$, expressing high levels of KIR and LFA-1 and showing cell killing ability (102). However, $CD56^{bright}$ NK cells are traditionally considered ineffective antitumor responders that instead function primarily in immunomodulation, which mainly secrete cytokines such as IFN-γ, TNF-β, and granulote-macrophage colony-stimulating factor (GM-CSF) (103–105). Nevertheless, NK cells in various tissues (106–108), even in the same organ and tissue (109), have diverse features.

The specific role of NK cells, with the complexity of intrinsic signaling pathways, remains controversial in distinct cancer types (**Table 2**). Due to the complex and variable functional status, NK cells were shown to vary survival and therapeutic response in different types of cancer (71, 77, 78, 110–112). In CRC, NK cells have been consistently associated with increased survival in patients (72–76). It is noteworthy that CRC patients with dMMR-MSI-H and pMMR-MSI-L/MSS also seem to display different NK cell features (**Table 1**). The surface markers of NK cells vary greatly and it is difficult to accurately identify NK cell type by one or two simple molecules. However, in many studies, NK cells have been detected using CD56 as a phenotypic marker. Liu et al. assessed for the presence of NK cell infiltration in CRC tissues using the expression of CD56, and found that $CD56^+$ cells were reduced in the dMMR group ($p < 0.05$) through immunohistochemical (42). In apparent contrast with these observations, Mlecnik et al. quantified the number of cells by detecting NKp46 and found no significant difference in NK cells between MSI and MSS patients (47). The mechanism of NK cells is complex and variable, and its actual role in the tumor microenvironment remains to be further clarified.

B CELLS, TFH, AND TERTIARY LYMPHOID STRUCTURES

Tumor-Infiltrating B Lymphocytes

B cells, with a variety of immune functions, are recognized as the main effector cells of the humoral adaptive immune response. However, TIBs can be observed in various solid tumors, but their role in cancer remains controversial (**Table 2**). In HCC (79), melanoma (80), high-grade serous ovarian cancer (81), NSCLC (82) and stage IB cervical squamous cell carcinoma (83), increased B cell count is associated with improved clinical outcomes. However, in epithelial ovarian cancer (84) and breast cancer (85), B cell infiltration is correlated with poor prognosis. At present, studies on the prognostic potential of B cells are limited. It is worth noting that most of the current studies quantify TIBs by CD20. A recently reported systematic review of TIBs into CRC showed that patients whose tumors were highly infiltrated by $CD20^+$ B lymphocytes had a significantly improved DFS improvement DFS (HR = 0.45, 95% CI 0.28-0.73, $p = 0.001$). Moreover, the author also found that $CD20^+$ B lymphocytes were highly and positively associated with $CD8^+$ T lymphocytes ($p < 0.001$) (113). Interestingly, a report demonstrated that an increase in the number of TIBs was associated with improved clinical outcomes for CRC (88).

However, another report has given a complex interpretation of the roles of TIBs in CRC (49). It was observed that $CD8^+$ and $CD20^+$ immunogradient indicators, that reflect cell migration towards the tumor, were associated with improved patient survival, while the infiltrative tumor growth pattern was linked to worse patient outcomes. In addition, this study also found that high numbers of intra-epithelial $CD20^+$ cells were observed in MSI tumors compared with MSS tumors and MSS colorectal tumors were characterized by elevated levels of intratumoral $CD20^+$.

Tfh and TLSs

Tfh cells, a T helper cells subset, are essential for the maturation and activation of B cells, which are characterized by the expression of CXCR5, an inducible T-cell co-stimulator. B cells, Tfh and related pathways also maintain the structure and function of the tertiary lymphoid structure. The interactions among Tfh cells, B cells and follicular dendritic cells are the basis of the adaptive immune response, which results in B cells differentiating into memory B cells and long-term surviving plasma cells. In addition, B cells can infiltrate into tumors and affect tumor progression through CXCL13 secreted by Tfh and follicular dendritic cells (114, 115). B cells, Tfh and related pathways also maintain the structure and function of the TLS. The current consensus is that the Tfh cell and B cell axis within tumor-associated TLSs contribute to the formation of anti-tumor immune structures (116). TLSs are transient ectopic lymphoid organs that share several structural and functional features with secondary lymphoid organs (117), and consist of B cell follicle and T-cell-rich areas that are sites for the differentiation of T cells and B cells (118) (**Figure 1**). B cell follicle, composed of a core germinal centre containing mostly B cells, but also Tfh cells, follicular DCs and macrophages, surrounded by a ring of naive B cells; and a T-cell-rich area, composed of clusters of T cells and mature DCs (119).

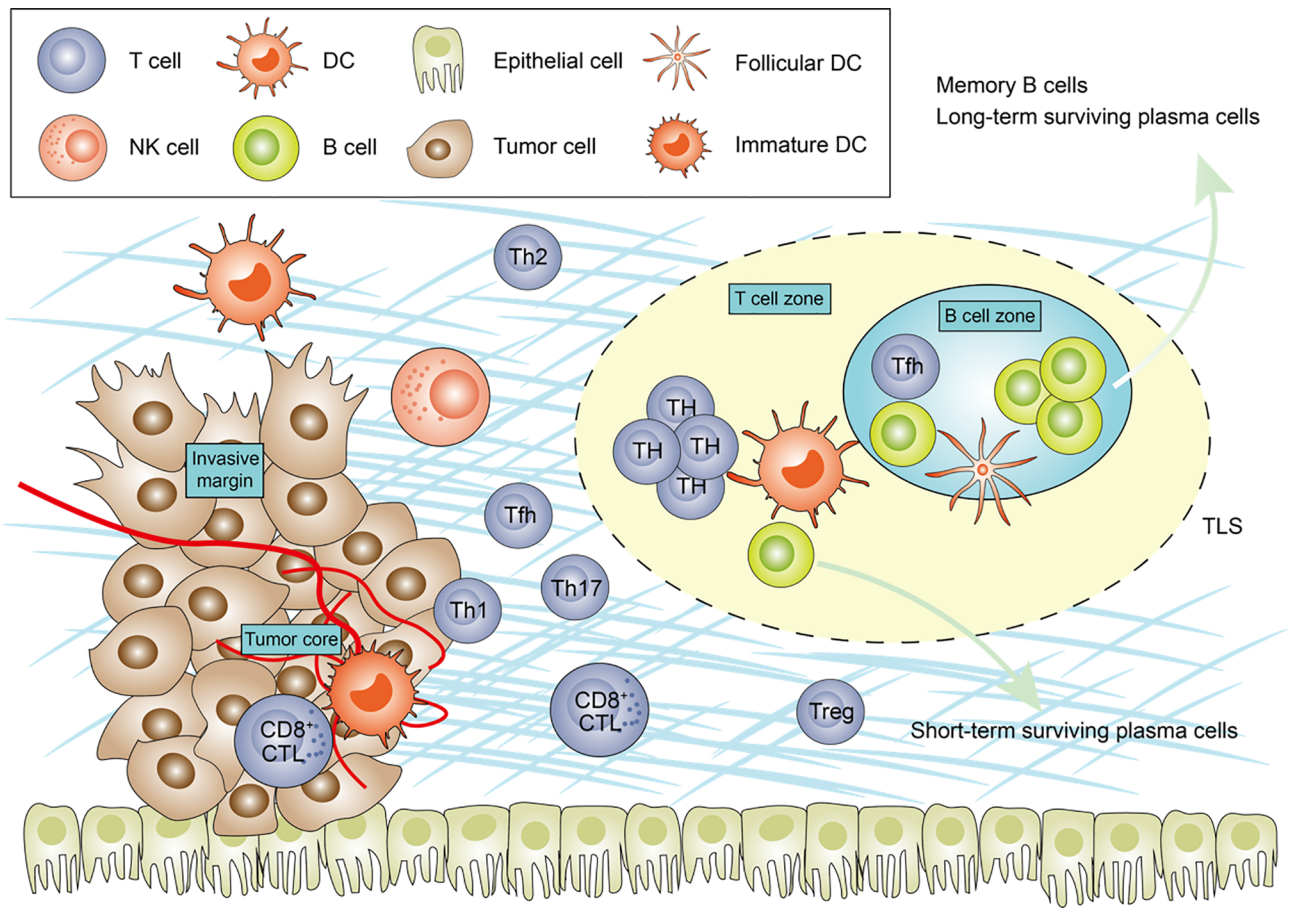

FIGURE 1 | The main tumor-infiltrating lymphocytes and tertiary lymphoid structures components in cancer. The schematic representation shows the features of the immune contexture, including tumor-infiltrating lymphocytes and tertiary lymphoid structures (TLSs). TLSs are usually located in the invasive margin or in the stroma rather than the tumor core. Tfh cells are the most important sources of CXCL13, induced TLSs formation. Th17 cells, B cells have been shown to be able to initiate of TLSs genesis in various pathological contexts. The synergistic effect of $CD8^+$ cytotoxic effector T cells and B cells, generated in TLS, enable to direct kill tumour cell. Central memory B cells generated in TLSs protect against metastasis. TH, T helper cell; Treg, regulatory T cell; Tfh, follicular helper T; CTL, cytotoxic T cells; DC, dendritic cell.

There is increasing evidence that TLS is an effective modulator of immune responses. TLSs are often [NSCLC (120), HER2$^+$ breast cancer (121), melanoma (122)], but not always [HCC (123)], associated with favourable clinical outcomes in most types of cancer. In local and metastatic CRCs, TLSs are associated with improved survival and may represent activation of an adaptive immune response to malignant cells (124, 125). In a cohort study involving a consecutive series of 351 patients with stage II and III colorectal cancer, the TLSs density and infiltration of patients with stage II are correlated and coordinated to predict better patient outcomes (126). In addition, the murine model showed an active role of TLSs in the recruitment of lymphocytes to tumor areas. Moreover, certain heterogeneities exist among TLSs from different cancer types, locations and stages. Posch et al. performed a comprehensive molecular, tissue, laboratory, and clinical analysis of 109 patients with stage II/III CRC (127). TLSs were found to be formed in most tumors and were more prevalent in CRC with MSI-H and/or BRAF mutations. In addition, the authors also found that TLSs maturation contained important prognostic information about the risk of disease recurrence. In a recent report examing the cellular composition and association with patients' prognosis in each TLSs, the authors reported that the densities of T helper cells and macrophages in TLSs were significantly higher in relapsed patients than in not-relapsed patients ($p = 0.043$ and $p = 0.0076$) (128). Multivariate analysis also showed that a high proportion of T helper cells was the most significant independent risk factor for disease recurrence. In contrast, there is little data available regarding Tfh cells supporting anti-tumor responses in CRC. A high expression of Tfh and B cell genes was found strongly associated with a good prognosis in CRC according to Bindea et al. (88). The authors also found that Tfh and intrinsic cell density increased with tumor progression. Obviously, there are clearly interesting complexities to Tfh-associated biology in the context of cancer, and the available data show that much more needs to be learned.

TILS AND IMMUNOTHERAPY

T-Cell-Based Immunotherapy

In CRC, T cell infiltration into the tumor has been associated with good outcomes, and prevention of its exhaustion and apoptosis in tumors is the goal of immunotherapy, especially immune checkpoint inhibitors. ICIs target negative costimulation receptors or their ligands of TCR signals, such as CTLA4, PD-1 and PD-L1, to prevent tumor cells attenuate T-cell activation (129).

ICIs have shown very limited clinical activity in early studies of CRC treatment (130, 131). In 2015, a phase II study investigated the efficacy of pembrolizumab, a humanized IgG4 antibody directed against surface-expressed PD-1, in three separate cohorts of 41 patients with MSI-H and MSS CRC tumors, and MSI-H tumors from other sites (non-CRC). Results showed that the immune-related objective response rate was 40% (4 had a partial response and 5 had the stable disease) with dMMR-MSI-H patients, whereas there was no objective response in patients with MSS CRC. The median progression-free survival (PFS) and OS were not yet reached in the dMMR-MSI-H cohort but were 2.2 months and 5.0 months, respectively, in the pMMR-MSI-L/MSS cohort (HR for disease progression 0.10 ($p < 0.001$); HR for death 0.22 ($p = 0.05$) (14). Similarly, another study of 53 patients treated with pembrolizumab showed the benefit of immune checkpoint blockade in dMMR-MSI-H tumors. The response rate was 50% (95% CI 31–69%), and the disease control rate was 89% (25/28) in the 28 patients with dMMR-MSI-H tumors. At 24 months, PFS was 61%, and OS was 66%. None of the 18 patients with pMMR-MSI-L/MSS CRC responded and the disease control rate was 16% (4/25) (132). On May 23, 2017, FDA approved pembrolizumab based on the data from 149 patients (84% for colorectal cancer) for the treatment of adult and pediatric patients with unresectable or metastatic, dMMR-MSI-H solid tumors, regardless of tumor site or histology (133) (**Figure 2**). In addition to pembrolizumab, nivolumab, another PD-1 inhibitor, was tested in 74 patients with dMMR-MSI-H metastatic colorectal cancer (134). At a median follow-up duration of 12 months, the objective response rate was 31% (23/74), and in 69% (51/74) patients who had disease control for 12 weeks or longer were observed. In July 2017, FDA expedited approval of nivolumab for the second-line treatment of patients with dMMR-MSI-H CRC.

Compared with patients with dMMR-MSI-H CRC, immunotherapy alone has not shown a clinical benefit in patients with pMMR-MSI-L/MSS CRC. As a result, alternative approaches to immune modulation studies are ongoing. Tumor immune microenvironment, as a critical obstacle to the development of immunotherapy, has been studied with medications that have immunomodulatory properties. Indomethacin 2,3-double oxygenase 1 (IDO1) is an intracellular enzyme that can cause tryptophan depletion, has been reported to play multiple roles in cancer, including inhibiting T and NK cells, producing active Treg and myeloid-derived suppressor cells and promoting tumor angiogenesis (135). Kitsou et al. found that IDO1 was significantly overexpressed in CRC and exhibited anticancer activity (136). In murine intestinal adenomas cell-specific Stat1 deletion models, loss of IDO1$^+$ Paneth cells had profound effects on the intratumoral immune cell composition. Moreover, the patient samples and TCGA expression data supported corresponding cells in human colorectal tumors, suggesting IDO1$^+$ Paneth cells as a target for immunotherapy (137). Epacadostat, an IDO1 inhibitor, was planned to combinate with pimuzumab and azacytidine in the MSS CRC study. However, this study has been terminated at an early stage. Overall, the molecular of IDO1 inhibitor shows promising anti-tumor potential.

With the knowledge in CRC biology improved, another immunomodulatory strategy, the combination of MEK and PD-L1 inhibition, was developed. In many preclinical studies, inhibition of MEK, a downstream effector of the RAS-MAPK pathway, was found to induce PD-L1 upregulation (138). Preclinical data reported in 2016 showed that 4 of 23 patients with CRC had a partial response, in which three patients had confirmed pMMR-MSI-L (139). In addition, many clinical trials are also studying the combination of MEK inhibitor with anti-PD1 antibody and other chemotherapeutic drugs.

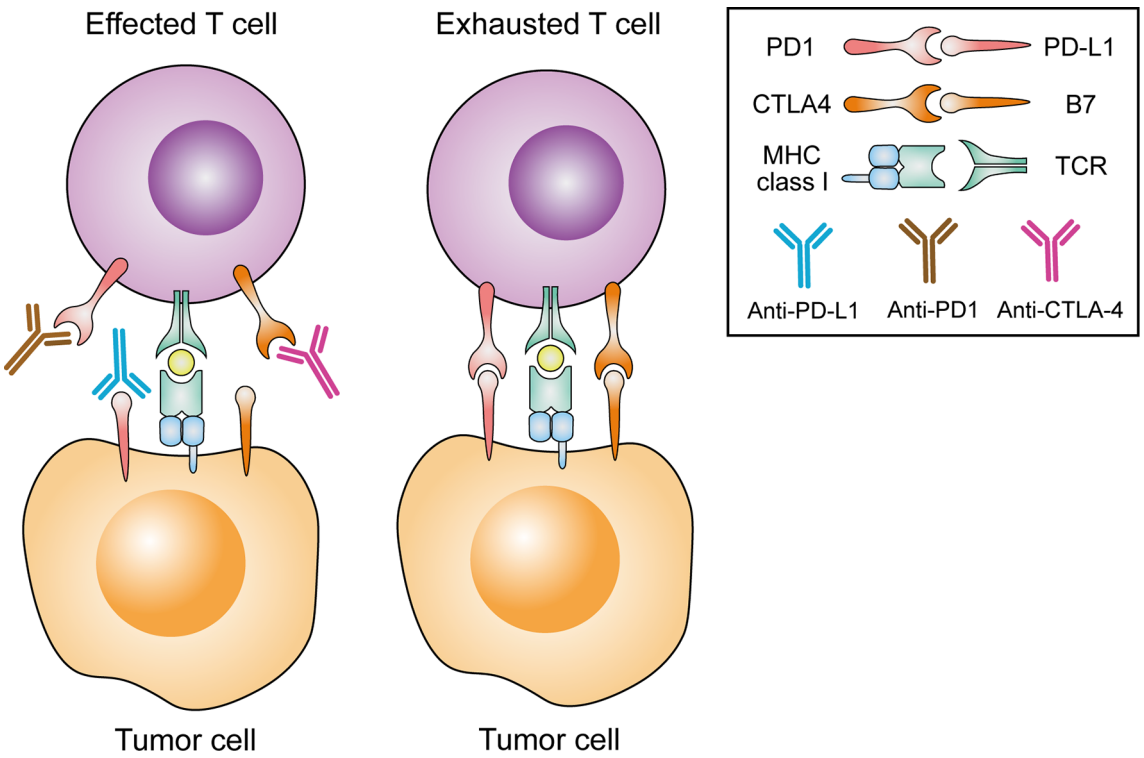

FIGURE 2 | Rationale for the current FDA-approved CRC immune checkpoint inhibitor strategies. TCR, T cell receptor; MHC, major histocompatibility complex; CTLA4, cytotoxic T lymphocyte antigen 4; PD1, programmed cell death 1; PD-L1, programmed cell death 1 ligand 1.

The Emergence of Natural Killer Cells as a Target in Cancer Immunotherapy

NK cells, as an important natural immune effector, are effector lymphocytes that control several types of tumors and microbial infections. In recent years, research on NK cell-related immunotherapy has been developing vigorously, and a number of NK cell-based therapeutic studies achieved favorable results. Recently, several studies have shown that cytokine supplementation can promote the development and cytotoxicity of NK cells. It has been revealed that direct contact with membrane-bound IL-15 on adjacent stromal cells could induce stronger cytotoxic effects in NK cells in the mice model (140). In a human multicenter phase I study, NKTR-214, a novel IL-2 pathway agonist, showed clinical activity including tumor shrinkage and durable disease stabilization in heavily pretreated patients (141). Moreover, in parallel with $CD8^+$ T cells, NK cells can also be suppressed by immune checkpoint molecules. NKG2D, an essential receptor for the activation of NK cells, has been reported to be upregulated by many ligands in tumor cells (142). Andrade et al. designed antibodies targeting the MICA α3 domain and found that these antibodies prevented human cancer cells from loss of cell surface MICA and MICB (NKG2D ligands). In addition, these antibodies inhibited tumor growth in multiple fully immunocompetent mouse models and reduced human melanoma metastases in a humanized mouse model (143). Monalizumab, a clinically used antibody targeting NKG2A, has been developed to promote NK cell function and has shown the potential to enhance the efficacy of anti-PD-1 therapy in MSS metastatic CRC (144). In addition, other antibodies designed specifically for NK cells, such as lirilumab, are also under clinical trials. Overall, a number of studies have elucidated the possible mechanisms of NK cells, paving the way for clinical research into NK cell-based cancer therapies, and lighting up hope for patients currently resistant to T cell-based immunotherapy.

B Cell-Based Cancer Immunotherapy

In addition to T and NK cells, the development of B cell-based immunotherapy strategies may be effective. By bulk and single-cell RNA sequencing, Helmink et al. observed significantly higher levels of B-cell-related gene (such as *MZB1*, *JCHAIN* and *IGLL5*) expression, increased BCR diversity, and clonal expansion in tumor samples from melanoma patients who responded to ICB treatment than patients who did not (145). Besides, a study of gene expression profiles of 608 different subtypes of soft tissue sarcomas found that B cells are the strongest prognostic factor even in the context of high or low $CD8^+$ T cells and cytotoxic contents (146). Considering the relationship between B cells and patient prognosis, enhancing anti-tumor B cell activity or may have an anti-tumor effect. It has been established that TIL B cells support antitumor immunity and promote immunotherapy responses by acting as APCs, producing high-affinity antibodies and secreting antitumor cytokines. Katoh et al. identified sulfated glycosaminoglycans as the main functional B cell antigen and its natural antibodies showed

robust growth-suppressive functions against a wide variety of human malignancies (147). Intra-tumoral injection of IL-12 was also shown to activate B cells, leading to good outcomes in HNSCC patients (148). Interestingly, Lu et al. found a subpopulation of B cells, $ICOSL^+$ B cells, in breast cancer patients who received neoadjuvant chemotherapy. Moreover, using B-cell specific deletion mice, $ICOSL^+$ B cells were found to enhance anti-tumor immunity by enhancing effects that modulate T cell proportions (149). Over the past decade, a population of suppressor B cells, regulatory B (B_{reg}) cells, have been shown to play a pivotal role in regulating immune responses involved in cancer. Schioppa et al. identified a population of splenic IL-10 producing B_{reg} cells implicated in the suppression of $CD8^+$ T cells, which promoted papilloma development and cancer growth in a mouse model of induced skin carcinogenesis (150). The presence of tumor-induced B_{reg} cells has also been reported. In a variety of tumor types, IL-21 induced Granzyme B-Expressing B_{reg} cells has been found to modulate cellular adaptive immune responses by promoting tumor avoidance mechanisms against anti-tumor immune attack (151). On the other hand, in PDAC mice models with KRAS-mutations, IL35-producing B cells have been reported to play a protumorigenic role, which could be inhibited by CD20 specific monoclonal antibody (152). In advanced CRC, Rituximab, a humanized monoclonal antibody targeting human CD20, apparently reduced the tumor burden (153). All of the above evidence points to the potential of B cell immunotherapy. In the future, new immunotherapy strategies should focus on activating TIL B cells, and how to exploit plasma B cells to promote lymphocyte infiltration and stimulate cytotoxic T cell activation to increase the antitumor immune response.

CONCLUSION

In recent years, significant achievements have been witnessed in the field of CRC immunotherapy. $CD8^+$ TILs are essential for an effective anti-tumor immune response. Monoclonal antibodies that block immune checkpoints to prevent T cell exhaustion and promote tumor destruction by cytotoxic $CD8^+$ T cells, have been shown to be effective in mCRC patients with dMMR-MSI-H. In 2017, pembrolizumab was approved by the FDA for the treatment of all dMMR-MSI-H metastatic solid tumors, becoming the first biomarker-based cancer treatment regimen. However, not all dMMR-MSI-H CRC cases respond to ICIs. Compared with dMMR-MSI-H, pMMR-MSI-L/MSS, which accounts for the majority of CRC with a lower mutation load, also shows an unsatisfactory response to ICIs. In tumors without active immune responses, active induction of immune responses by other immunotherapy methods may be required to achieve tumor control in the vast majority of patients with pMMR-MSI-L/MSS.

Increasing evidence supports the major role of infiltrating immune cells, especially TILs, in tumor control. In addition to $CD8^+$ T cells, other TILs also have shown the potential in immunotherapy. $CD4^+$ T cells play a key role in enhancing tumor control, both during effector T cell initiation and in the tumor microenvironment. Vaccines designed to induce a CD4 response have shown significant promise in improving clinical outcomes in subgroups of patients with melanoma and breast cancer (154). While several early trials have yielded promising data, further studies are needed to verify its safety and effectiveness. Moreover, a growing number of studies have the potential to improve our understanding of NK and B cells antitumor functions, promising positive research in related fields. With insights gained from trials based on NK and B cells, novel therapeutic strategies will likely help to guide clinicians towards a more personalized treatment for CRC patients.

In conclusion, tumor-infiltrating lymphocytes play a significant role in the tumor immune environment. As the regulatory role of TILs in CRC continues to be elucidated, we anticipate that personalized immunotherapy for CRC patients will be realized, and these advances will further drive the clinical success of immunotherapy.

AUTHOR CONTRIBUTIONS

FW and ZB conceptualized the study. FW oversaw the literature review was involved in all aspects of designing and writing the manuscript. ZB and YZ performed the literature review. ZB wrote the manuscript and designed the figures. JX and ZY provided input on the discussion of various sections. All authors contributed to the article and approved the submitted version.

FUNDING

This work was supported by the National Natural Science Foundation of China grants 31770827 and 21736002.

REFERENCES

1. Jemal A, Bray F, Center MM, Ferlay J, Ward E, Forman D. Global Cancer Statistics. *CA Cancer J Clin* (2011) 61(2):69–90. doi: 10.3322/caac.20107
2. Dekker E, Tanis PJ, Vleugels JLA, Kasi PM, Wallace MB. Colorectal Cancer. *Lancet* (2019) 394(10207):1467–80. doi: 10.1016/S0140-6736(19)32319-0
3. Guren MG. The Global Challenge of Colorectal Cancer. *Lancet Gastroenterol Hepatol* (2019) 4(12):894–5. doi: 10.1016/S2468-1253(19)30329-2
4. Schreuders EH, Ruco A, Rabeneck L, Schoen RE, Sung JJ, Young GP, et al. Colorectal Cancer Screening: A Global Overview of Existing Programmes. *Gut* (2015) 64(10):1637–49. doi: 10.1136/gutjnl-2014-309086
5. Kaminski MF, Robertson DJ, Senore C, Rex DK. Optimizing the Quality of Colorectal Cancer Screening Worldwide. *Gastroenterology* (2020) 158(2):404–17. doi: 10.1053/j.gastro.2019.11.026
6. Ahmed S, Rai KR. Interferon in the Treatment of Hairy-Cell Leukemia. *Best Pract Res Clin Haematol* (2003) 16(1):69–81. doi: 10.1016/S1521-6926(02)00084-1

7. Rosenberg SA. Il-2: The First Effective Immunotherapy for Human Cancer. *J Immunol* (2014) 192(12):5451–8. doi: 10.4049/jimmunol.1490019
8. Hodi FS, O'Day SJ, McDermott DF, Weber RW, Sosman JA, Haanen JB, et al. Improved Survival With Ipilimumab in Patients With Metastatic Melanoma. *N Engl J Med* (2010) 363(8):711–23. doi: 10.1056/NEJMoa1003466
9. Borghaei H, Paz-Ares L, Horn L, Spigel DR, Steins M, Ready NE, et al. Nivolumab Versus Docetaxel in Advanced Nonsquamous Non-Small-Cell Lung Cancer. *N Engl J Med* (2015) 373(17):1627–39. doi: 10.1056/NEJMoa1507643
10. Rosenberg JE, Hoffman-Censits J, Powles T, van der Heijden MS, Balar AV, Necchi A, et al. Atezolizumab in Patients With Locally Advanced and Metastatic Urothelial Carcinoma Who Have Progressed Following Treatment With Platinum-Based Chemotherapy: A Single-Arm, Multicentre, Phase 2 Trial. *Lancet* (2016) 387(10031):1909–20. doi: 10.1016/S0140-6736(16)00561-4
11. Iwai Y, Ishida M, Tanaka Y, Okazaki T, Honjo T, Minato N. Involvement of Pd-L1 on Tumor Cells in the Escape From Host Immune System and Tumor Immunotherapy by Pd-L1 Blockade. *Proc Natl Acad Sci USA* (2002) 99 (19):12293–7. doi: 10.1073/pnas.192461099
12. Leach DR, Krummel MF, Allison JP. Enhancement of Antitumor Immunity by Ctla-4 Blockade. *Science* (1996) 271(5256):1734–6. doi: 10.1126/science.271.5256.1734
13. Cancer Genome Atlas N. Comprehensive Molecular Characterization of Human Colon and Rectal Cancer. *Nature* (2012) 487(7407):330–7. doi: 10.1038/nature11252
14. Le DT, Uram JN, Wang H, Bartlett BR, Kemberling H, Eyring AD, et al. Pd-1 Blockade in Tumors With Mismatch-Repair Deficiency. *N Engl J Med* (2015) 372(26):2509–20. doi: 10.1056/NEJMoa1500596
15. Zaanan A, Shi Q, Taieb J, Alberts SR, Meyers JP, Smyrk TC, et al. Role of Deficient DNA Mismatch Repair Status in Patients With Stage Iii Colon Cancer Treated With Folfox Adjuvant Chemotherapy: A Pooled Analysis From 2 Randomized Clinical Trials. *JAMA Oncol* (2018) 4(3):379–83. doi: 10.1001/jamaoncol.2017.2899
16. Lavin Y, Kobayashi S, Leader A, Amir ED, Elefant N, Bigenwald C, et al. Innate Immune Landscape in Early Lung Adenocarcinoma by Paired Single-Cell Analyses. *Cell* (2017) 169(4):750–65.e717. doi: 10.1016/j.cell.2017.04.014
17. Sadanandam A, Lyssiotis CA, Homicsko K, Collisson EA, Gibb WJ, Wullschleger S, et al. A Colorectal Cancer Classification System That Associates Cellular Phenotype and Responses to Therapy. *Nat Med* (2013) 19(5):619–25. doi: 10.1038/nm.3175
18. Havel JJ, Chowell D, Chan TA. The Evolving Landscape of Biomarkers for Checkpoint Inhibitor Immunotherapy. *Nat Rev Cancer* (2019) 19(3):133–50. doi: 10.1038/s41568-019-0116-x
19. Senovilla L, Vacchelli E, Galon J, Adjemian S, Eggermont A, Fridman WH, et al. Trial Watch: Prognostic and Predictive Value of the Immune Infiltrate in Cancer. *Oncoimmunology* (2012) 1(8):1323–43. doi: 10.4161/onci.22009
20. Jochems C, Schlom J. Tumor-Infiltrating Immune Cells and Prognosis: The Potential Link Between Conventional Cancer Therapy and Immunity. *Exp Biol Med (Maywood)* (2011) 236(5):567–79. doi: 10.1258/ebm.2011.011007
21. Fridman WH, Pagès F, Sautès-Fridman C, Galon J. The Immune Contexture in Human Tumours: Impact on Clinical Outcome. *Nat Rev Cancer* (2012) 12 (4):298–306. doi: 10.1038/nrc3245
22. Fridman WH, Galon J, Pagès F, Tartour E, Sautès-Fridman C, Kroemer G. Prognostic and Predictive Impact of Intra- and Peritumoral Immune Infiltrates. *Cancer Res* (2011) 71(17):5601–5. doi: 10.1158/0008-5472.CAN-11-1316
23. Mlecnik B, Bindea G, Pagès F, Galon J. Tumor Immunosurveillance in Human Cancers. *Cancer Metastasis Rev* (2011) 30(1):5–12. doi: 10.1007/s10555-011-9270-7
24. Galon J, Costes A, Sanchez-Cabo F, Kirilovsky A, Mlecnik B, Lagorce-Pagès C, et al. Type, Density, and Location of Immune Cells Within Human Colorectal Tumors Predict Clinical Outcome. *Science* (2006) 313 (5795):1960–4. doi: 10.1126/science.1129139
25. Fridman WH, Zitvogel L, Sautès-Fridman C, Kroemer G. The Immune Contexture in Cancer Prognosis and Treatment. *Nat Rev Clin Oncol* (2017) 14(12):717–34. doi: 10.1038/nrclinonc.2017.101
26. Pagès F, Galon J, Dieu-Nosjean MC, Tartour E, Sautès-Fridman C, Fridman WH. Immune Infiltration in Human Tumors: A Prognostic Factor That Should Not Be Ignored. *Oncogene* (2010) 29(8):1093–102. doi: 10.1038/onc.2009.416
27. Idos GE, Kwok J, Bonthala N, Kysh L, Gruber SB, Qu C. The Prognostic Implications of Tumor Infiltrating Lymphocytes in Colorectal Cancer: A Systematic Review and Meta-Analysis. *Sci Rep* (2020) 10(1):3360. doi: 10.1038/s41598-020-60255-4
28. Rozek LS, Schmit SL, Greenson JK, Tomsho LP, Rennert HS, Rennert G, et al. Tumor-Infiltrating Lymphocytes, Crohn's-Like Lymphoid Reaction, and Survival From Colorectal Cancer. *J Natl Cancer Inst* (2016) 108(8): djw207. doi: 10.1093/jnci/djw027
29. Llosa NJ, Cruise M, Tam A, Wicks EC, Hechenbleikner EM, Taube JM, et al. The Vigorous Immune Microenvironment of Microsatellite Instable Colon Cancer Is Balanced by Multiple Counter-Inhibitory Checkpoints. *Cancer Discov* (2015) 5(1):43–51. doi: 10.1158/2159-8290.CD-14-0863
30. Dahlin AM, Henriksson ML, Van Guelpen B, Stenling R, Oberg A, Rutegård J, et al. Colorectal Cancer Prognosis Depends on T-Cell Infiltration and Molecular Characteristics of the Tumor. *Mod Pathol* (2011) 24(5):671–82. doi: 10.1038/modpathol.2010.234
31. Zhang N, Bevan MJ. Cd8(+) T Cells: Foot Soldiers of the Immune System. *Immunity* (2011) 35(2):161–8. doi: 10.1016/j.immuni.2011.07.010
32. Pagès F, Berger A, Camus M, Sanchez-Cabo F, Costes A, Molidor R, et al. Effector Memory T Cells, Early Metastasis, and Survival in Colorectal Cancer. *N Engl J Med* (2005) 353(25):2654–66. doi: 10.1056/NEJMoa051424
33. Russell JH, Ley TJ. Lymphocyte-Mediated Cytotoxicity. *Annu Rev Immunol* (2002) 20:323–70. doi: 10.1146/annurev.immunol.20.100201.131730
34. Golstein P, Griffiths GM. An Early History of T Cell-Mediated Cytotoxicity. *Nat Rev Immunol* (2018) 18(8):527–35. doi: 10.1038/s41577-018-0009-3
35. Alspach E, Lussier DM, Schreiber RD. Interferon γ and Its Important Roles in Promoting and Inhibiting Spontaneous and Therapeutic Cancer Immunity. *Cold Spring Harb Perspect Biol* (2019) 11(3):a028480. doi: 10.1101/cshperspect.a028480
36. Liu Y, Zhou N, Zhou L, Wang J, Zhou Y, Zhang T, et al. Il-2 Regulates Tumor-Reactive Cd8(+) T Cell Exhaustion by Activating the Aryl Hydrocarbon Receptor. *Nat Immunol* (2021) 22(3):358–69. doi: 10.1038/s41590-020-00850-9
37. Bruni D, Angell HK, Galon J. The Immune Contexture and Immunoscore in Cancer Prognosis and Therapeutic Efficacy. *Nat Rev Cancer* (2020) 20 (11):662–80. doi: 10.1038/s41568-020-0285-7
38. Salama P, Phillips M, Grieu F, Morris M, Zeps N, Joseph D, et al. Tumor-Infiltrating Foxp3+ T Regulatory Cells Show Strong Prognostic Significance in Colorectal Cancer. *J Clin Oncol* (2009) 27(2):186–92. doi: 10.1200/JCO.2008.18.7229
39. Nosho K, Baba Y, Tanaka N, Shima K, Hayashi M, Meyerhardt JA, et al. Tumour-Infiltrating T-Cell Subsets, Molecular Changes in Colorectal Cancer, and Prognosis: Cohort Study and Literature Review. *J Pathol* (2010) 222(4):350–66. doi: 10.1002/path.2774
40. Mlecnik B, Tosolini M, Kirilovsky A, Berger A, Bindea G, Meatchi T, et al. Histopathologic-Based Prognostic Factors of Colorectal Cancers Are Associated With the State of the Local Immune Reaction. *J Clin Oncol* (2011) 29(6):610–8. doi: 10.1200/JCO.2010.30.5425
41. Camus M, Tosolini M, Mlecnik B, Pagès F, Kirilovsky A, Berger A, et al. Coordination of Intratumoral Immune Reaction and Human Colorectal Cancer Recurrence. *Cancer Res* (2009) 69(6):2685–93. doi: 10.1158/0008-5472.CAN-08-2654
42. Liu SS, Yang YZ, Jiang C, Quan Q, Xie QK, Wang XP, et al. Comparison of Immunological Characteristics Between Paired Mismatch Repair-Proficient and -Deficient Colorectal Cancer Patients. *J Transl Med* (2018) 16(1):195. doi: 10.1186/s12967-018-1570-z
43. Le Flahec G, Badic B, Guibourg B, Doucet L, Bail JP, Marcorelles P, et al. Mismatch Repair-Deficient Colorectal Cancer: A Model of Immunogenic and Immune Cell-Rich Tumor Despite Nonsignificant Programmed Cell Death Ligand-1 Expression in Tumor Cells. *Hum Pathol* (2018) 72:135–43. doi: 10.1016/j.humpath.2017.09.019
44. Michael-Robinson JM, Biemer-Hüttmann A, Purdie DM, Walsh MD, Simms LA, Biden KG, et al. Tumour Infiltrating Lymphocytes and Apoptosis Are Independent Features in Colorectal Cancer Stratified

According to Microsatellite Instability Status. *Gut* (2001) 48(3):360–6. doi: 10.1136/gut.48.3.360
45. Phillips SM, Banerjea A, Feakins R, Li SR, Bustin SA, Dorudi S. Tumour-Infiltrating Lymphocytes in Colorectal Cancer With Microsatellite Instability Are Activated and Cytotoxic. *Br J Surg* (2004) 91(4):469–75. doi: 10.1002/bjs.4472
46. Dolcetti R, Viel A, Doglioni C, Russo A, Guidoboni M, Capozzi E, et al. High Prevalence of Activated Intraepithelial Cytotoxic T Lymphocytes and Increased Neoplastic Cell Apoptosis in Colorectal Carcinomas With Microsatellite Instability. *Am J Pathol* (1999) 154(6):1805–13. doi: 10.1016/S0002-9440(10)65436-3
47. Mlecnik B, Bindea G, Angell HK, Maby P, Angelova M, Tougeron D, et al. Integrative Analyses of Colorectal Cancer Show Immunoscore Is a Stronger Predictor of Patient Survival Than Microsatellite Instability. *Immunity* (2016) 44(3):698–711. doi: 10.1016/j.immuni.2016.02.025
48. De Smedt L, Lemahieu J, Palmans S, Govaere O, Tousseyn T, Van Cutsem E, et al. Microsatellite Instable Vs Stable Colon Carcinomas: Analysis of Tumour Heterogeneity, Inflammation and Angiogenesis. *Br J Cancer* (2015) 113(3):500–9. doi: 10.1038/bjc.2015.213
49. Nestarenkaite A, Fadhil W, Rasmusson A, Susanti S, Hadjimichael E, Laurinaviciene A, et al. Immuno-Interface Score to Predict Outcome in Colorectal Cancer Independent of Microsatellite Instability Status. *Cancers (Basel)* (2020) 12(10):2902. doi: 10.3390/cancers12102902
50. Le Gouvello S, Bastuji-Garin S, Aloulou N, Mansour H, Chaumette MT, Berrehar F, et al. High Prevalence of Foxp3 and Il17 in Mmr-Proficient Colorectal Carcinomas. *Gut* (2008) 57(6):772–9. doi: 10.1136/gut.2007.123794
51. Michel S, Benner A, Tariverdian M, Wentzensen N, Hoefler P, Pommerencke T, et al. High Density of Foxp3-Positive T Cells Infiltrating Colorectal Cancers With Microsatellite Instability. *Br J Cancer* (2008) 99 (11):1867–73. doi: 10.1038/sj.bjc.6604756
52. Tosolini M, Kirilovsky A, Mlecnik B, Fredriksen T, Mauger S, Bindea G, et al. Clinical Impact of Different Classes of Infiltrating T Cytotoxic and Helper Cells (Th1, Th2, Treg, Th17) in Patients With Colorectal Cancer. *Cancer Res* (2011) 71(4):1263–71. doi: 10.1158/0008-5472.CAN-10-2907
53. Schreck S, Friebel D, Buettner M, Distel L, Grabenbauer G, Young LS, et al. Prognostic Impact of Tumour-Infiltrating Th2 and Regulatory T Cells in Classical Hodgkin Lymphoma. *Hematol Oncol* (2009) 27(1):31–9. doi: 10.1002/hon.878
54. Yoon NK, Maresh EL, Shen D, Elshimali Y, Apple S, Horvath S, et al. Higher Levels of Gata3 Predict Better Survival in Women With Breast Cancer. *Hum Pathol* (2010) 41(12):1794–801. doi: 10.1016/j.humpath.2010.06.010
55. Kusuda T, Shigemasa K, Arihiro K, Fujii T, Nagai N, Ohama K. Relative Expression Levels of Th1 and Th2 Cytokine Mrna Are Independent Prognostic Factors in Patients With Ovarian Cancer. *Oncol Rep* (2005) 13 (6):1153–8. doi: 10.3892/or.13.6.1153
56. De Monte L, Reni M, Tassi E, Clavenna D, Papa I, Recalde H, et al. Intratumor T Helper Type 2 Cell Infiltrate Correlates With Cancer-Associated Fibroblast Thymic Stromal Lymphopoietin Production and Reduced Survival in Pancreatic Cancer. *J Exp Med* (2011) 208(3):469–78. doi: 10.1084/jem.20101876
57. Ubukata H, Motohashi G, Tabuchi T, Nagata H, Konishi S, Tabuchi T. Evaluations of Interferon-Γ/Interleukin-4 Ratio and Neutrophil/Lymphocyte Ratio as Prognostic Indicators in Gastric Cancer Patients. *J Surg Oncol* (2010) 102(7):742–7. doi: 10.1002/jso.21725
58. Lv L, Pan K, Li XD, She KL, Zhao JJ, Wang W, et al. The Accumulation and Prognosis Value of Tumor Infiltrating Il-17 Producing Cells in Esophageal Squamous Cell Carcinoma. *PloS One* (2011) 6(3):e18219. doi: 10.1371/journal.pone.0018219
59. Chen JG, Xia JC, Liang XT, Pan K, Wang W, Lv L, et al. Intratumoral Expression of Il-17 and Its Prognostic Role in Gastric Adenocarcinoma Patients. *Int J Biol Sci* (2011) 7(1):53–60. doi: 10.7150/ijbs.7.53
60. Kryczek I, Banerjee M, Cheng P, Vatan L, Szeliga W, Wei S, et al. Phenotype, Distribution, Generation, and Functional and Clinical Relevance of Th17 Cells in the Human Tumor Environments. *Blood* (2009) 114(6):1141–9. doi: 10.1182/blood-2009-03-208249
61. Punt S, Fleuren GJ, Kritikou E, Lubberts E, Trimbos JB, Jordanova ES, et al. Angels and Demons: Th17 Cells Represent a Beneficial Response, While Neutrophil Il-17 Is Associated With Poor Prognosis in Squamous Cervical Cancer. *Oncoimmunology* (2015) 4(1):e984539. doi: 10.4161/2162402X.2014.984539
62. Chen X, Wan J, Liu J, Xie W, Diao X, Xu J, et al. Increased Il-17-Producing Cells Correlate With Poor Survival and Lymphangiogenesis in Nsclc Patients. *Lung Cancer* (2010) 69(3):348–54. doi: 10.1016/j.lungcan.2009.11.013
63. Zhang JP, Yan J, Xu J, Pang XH, Chen MS, Li L, et al. Increased Intratumoral Il-17-Producing Cells Correlate With Poor Survival in Hepatocellular Carcinoma Patients. *J Hepatol* (2009) 50(5):980–9. doi: 10.1016/j.jhep.2008.12.033
64. Zhang YL, Li J, Mo HY, Qiu F, Zheng LM, Qian CN, et al. Different Subsets of Tumor Infiltrating Lymphocytes Correlate With Npc Progression in Different Ways. *Mol Cancer* (2010) 9:4. doi: 10.1186/1476-4598-9-4
65. Badoual C, Hans S, Rodriguez J, Peyrard S, Klein C, Agueznay Nel H, et al. Prognostic Value of Tumor-Infiltrating Cd4+ T-Cell Subpopulations in Head and Neck Cancers. *Clin Cancer Res* (2006) 12(2):465–72. doi: 10.1158/1078-0432.CCR-05-1886
66. Winerdal ME, Marits P, Winerdal M, Hasan M, Rosenblatt R, Tolf A, et al. Foxp3 and Survival in Urinary Bladder Cancer. *BJU Int* (2011) 108 (10):1672–8. doi: 10.1111/j.1464-410X.2010.10020.x
67. Grabenbauer GG, Lahmer G, Distel L, Niedobitek G. Tumor-Infiltrating Cytotoxic T Cells But Not Regulatory T Cells Predict Outcome in Anal Squamous Cell Carcinoma. *Clin Cancer Res* (2006) 12(11 Pt 1):3355–60. doi: 10.1158/1078-0432.CCR-05-2434
68. Heimberger AB, Abou-Ghazal M, Reina-Ortiz C, Yang DS, Sun W, Qiao W, et al. Incidence and Prognostic Impact of Foxp3+ Regulatory T Cells in Human Gliomas. *Clin Cancer Res* (2008) 14(16):5166–72. doi: 10.1158/1078-0432.CCR-08-0320
69. Jacobs JF, Idema AJ, Bol KF, Grotenhuis JA, de Vries IJ, Wesseling P, et al. Prognostic Significance and Mechanism of Treg Infiltration in Human Brain Tumors. *J Neuroimmunol* (2010) 225(1-2):195–9. doi: 10.1016/j.jneuroim.2010.05.020
70. Curiel TJ, Coukos G, Zou L, Alvarez X, Cheng P, Mottram P, et al. Specific Recruitment of Regulatory T Cells in Ovarian Carcinoma Fosters Immune Privilege and Predicts Reduced Survival. *Nat Med* (2004) 10(9):942–9. doi: 10.1038/nm1093
71. Pasero C, Gravis G, Granjeaud S, Guerin M, Thomassin-Piana J, Rocchi P, et al. Highly Effective Nk Cells Are Associated With Good Prognosis in Patients With Metastatic Prostate Cancer. *Oncotarget* (2015) 6(16):14360–73. doi: 10.18632/oncotarget.3965
72. Coca S, Perez-Piqueras J, Martinez D, Colmenarejo A, Saez MA, Vallejo C, et al. The Prognostic Significance of Intratumoral Natural Killer Cells in Patients With Colorectal Carcinoma. *Cancer* (1997) 79(12):2320–8. doi: 10.1002/(SICI)1097-0142(19970615)79:12<2320::AID-CNCR5>3.0.CO;2-P
73. Okada K, Sadahiro S, Chan LF, Ogimi T, Miyakita H, Saito G, et al. The Number of Natural Killer Cells in the Largest Diameter Lymph Nodes Is Associated With the Number of Retrieved Lymph Nodes and Lymph Node Size, and Is an Independent Prognostic Factor in Patients With Stage II Colon Cancer. *Oncology* (2018) 95(5):288–96. doi: 10.1159/000491019
74. Tang YP, Xie MZ, Li KZ, Li JL, Cai ZM, Hu BL. Prognostic Value of Peripheral Blood Natural Killer Cells in Colorectal Cancer. *BMC Gastroenterol* (2020) 20(1):31. doi: 10.1186/s12876-020-1177-8
75. Menon AG, Janssen-van Rhijn CM, Morreau H, Putter H, Tollenaar RA, van de Velde CJ, et al. Immune System and Prognosis in Colorectal Cancer: A Detailed Immunohistochemical Analysis. *Lab Invest* (2004) 84(4):493–501. doi: 10.1038/labinvest.3700055
76. Melero I, Rouzaut A, Motz GT, Coukos G. T-Cell and Nk-Cell Infiltration Into Solid Tumors: A Key Limiting Factor for Efficacious Cancer Immunotherapy. *Cancer Discov* (2014) 4(5):522–6. doi: 10.1158/2159-8290.CD-13-0985
77. Rathore AS, Goel MM, Makker A, Kumar S, Srivastava AN. Is the Tumor Infiltrating Natural Killer Cell (Nk-Tils) Count in Infiltrating Ductal Carcinoma of Breast Prognostically Significant? *Asian Pac J Cancer Prev* (2014) 15(8):3757–61. doi: 10.7314/APJCP.2014.15.8.3757
78. Liu Y, Cheng Y, Xu Y, Wang Z, Du X, Li C, et al. Increased Expression of Programmed Cell Death Protein 1 on Nk Cells Inhibits Nk-Cell-Mediated Anti-Tumor Function and Indicates Poor Prognosis in Digestive Cancers. *Oncogene* (2017) 36(44):6143–53. doi: 10.1038/onc.2017.209

79. Wada Y, Nakashima O, Kutami R, Yamamoto O, Kojiro M. Clinicopathological Study on Hepatocellular Carcinoma With Lymphocytic Infiltration. *Hepatology* (1998) 27(2):407–14. doi: 10.1002/hep.510270214
80. Ladányi A, Kiss J, Mohos A, Somlai B, Liszkay G, Gilde K, et al. Prognostic Impact of B-Cell Density in Cutaneous Melanoma. *Cancer Immunol Immunother* (2011) 60(12):1729–38. doi: 10.1007/s00262-011-1071-x
81. Nielsen JS, Sahota RA, Milne K, Kost SE, Nesslinger NJ, Watson PH, et al. Cd20+ Tumor-Infiltrating Lymphocytes Have an Atypical Cd27- Memory Phenotype and Together With Cd8+ T Cells Promote Favorable Prognosis in Ovarian Cancer. *Clin Cancer Res* (2012) 18(12):3281–92. doi: 10.1158/1078-0432.CCR-12-0234
82. Al-Shibli KI, Donnem T, Al-Saad S, Persson M, Bremnes RM, Busund LT. Prognostic Effect of Epithelial and Stromal Lymphocyte Infiltration in Non-Small Cell Lung Cancer. *Clin Cancer Res* (2008) 14(16):5220–7. doi: 10.1158/1078-0432.CCR-08-0133
83. Nedergaard BS, Ladekarl M, Nyengaard JR, Nielsen K. A Comparative Study of the Cellular Immune Response in Patients With Stage Ib Cervical Squamous Cell Carcinoma. Low Numbers of Several Immune Cell Subtypes Are Strongly Associated With Relapse of Disease Within 5 Years. *Gynecol Oncol* (2008) 108(1):106–11. doi: 10.1016/j.ygyno.2007.08.089
84. Yang C, Lee H, Pal S, Jove V, Deng J, Zhang W, et al. B Cells Promote Tumor Progression *Via* Stat3 Regulated-Angiogenesis. *PloS One* (2013) 8(5):e64159. doi: 10.1371/journal.pone.0064159
85. Shen M, Wang J, Ren X. New Insights Into Tumor-Infiltrating B Lymphocytes in Breast Cancer: Clinical Impacts and Regulatory Mechanisms. *Front Immunol* (2018) 9:470. doi: 10.3389/fimmu.2018.00470
86. Tassi E, Gavazzi F, Albarello L, Senyukov V, Longhi R, Dellabona P, et al. Carcinoembryonic Antigen-Specific But Not Antiviral Cd4+ T Cell Immunity Is Impaired in Pancreatic Carcinoma Patients. *J Immunol* (2008) 181(9):6595–603. doi: 10.4049/jimmunol.181.9.6595
87. Guéry L, Hugues S. Th17 Cell Plasticity and Functions in Cancer Immunity. *BioMed Res Int* (2015) 2015:314620. doi: 10.1155/2015/314620
88. Bindea G, Mlecnik B, Tosolini M, Kirilovsky A, Waldner M, Obenauf AC, et al. Spatiotemporal Dynamics of Intratumoral Immune Cells Reveal the Immune Landscape in Human Cancer. *Immunity* (2013) 39(4):782–95. doi: 10.1016/j.immuni.2013.10.003
89. Zhang L, Yu X, Zheng L, Zhang Y, Li Y, Fang Q, et al. Lineage Tracking Reveals Dynamic Relationships of T Cells in Colorectal Cancer. *Nature* (2018) 564(7735):268–72. doi: 10.1038/s41586-018-0694-x
90. Schmetterer KG, Neunkirchner A, Pickl WF. Naturally Occurring Regulatory T Cells: Markers, Mechanisms, and Manipulation. *FASEB J* (2012) 26(6):2253–76. doi: 10.1096/fj.11-193672
91. Frey DM, Droeser RA, Viehl CT, Zlobec I, Lugli A, Zingg U, et al. High Frequency of Tumor-Infiltrating Foxp3(+) Regulatory T Cells Predicts Improved Survival in Mismatch Repair-Proficient Colorectal Cancer Patients. *Int J Cancer* (2010) 126(11):2635–43. doi: 10.1002/ijc.24989
92. Gunnarsson U, Strigård K, Edin S, Gkekas I, Mustonen H, Kaprio T, et al. Association Between Local Immune Cell Infiltration, Mismatch Repair Status and Systemic Inflammatory Response in Colorectal Cancer. *J Transl Med* (2020) 18(1):178. doi: 10.1186/s12967-020-02336-6
93. Sun JC, Lanier LL. Nk Cell Development, Homeostasis and Function: Parallels With Cd8$^+$ T Cells. *Nat Rev Immunol* (2011) 11(10):645–57. doi: 10.1038/nri3044
94. Mandal A, Viswanathan C. Natural Killer Cells: In Health and Disease. *Hematol Oncol Stem Cell Ther* (2015) 8(2):47–55. doi: 10.1016/j.hemonc.2014.11.006
95. Vivier E, Raulet DH, Moretta A, Caligiuri MA, Zitvogel L, Lanier LL, et al. Innate or Adaptive Immunity? The Example of Natural Killer Cells. *Science* (2011) 331(6013):44–9. doi: 10.1126/science.1198687
96. Marrack P, Kappler J. Control of T Cell Viability. *Annu Rev Immunol* (2004) 22:765–87. doi: 10.1146/annurev.immunol.22.012703.104554
97. Cui G, Staron MM, Gray SM, Ho PC, Amezquita RA, Wu J, et al. Il-7-Induced Glycerol Transport and Tag Synthesis Promotes Memory Cd8+ T Cell Longevity. *Cell* (2015) 161(4):750–61. doi: 10.1016/j.cell.2015.03.021
98. Clénet ML, Gagnon F, Moratalla AC, Viel EC, Arbour N. Peripheral Human Cd4(+)Cd8(+) T Lymphocytes Exhibit a Memory Phenotype and Enhanced Responses to Il-2, Il-7 and Il-15. *Sci Rep* (2017) 7(1):11612. doi: 10.1038/s41598-017-11926-2
99. Luetke-Eversloh M, Cicek BB, Siracusa F, Thom JT, Hamann A, Frischbutter S, et al. Nk Cells Gain Higher Ifn-Γ Competence During Terminal Differentiation. *Eur J Immunol* (2014) 44(7):2074–84. doi: 10.1002/eji.201344072
100. Vivier E, Ugolini S, Blaise D, Chabannon C, Brossay L. Targeting Natural Killer Cells and Natural Killer T Cells in Cancer. *Nat Rev Immunol* (2012) 12(4):239–52. doi: 10.1038/nri3174
101. Sun JC, Beilke JN, Lanier LL. Adaptive Immune Features of Natural Killer Cells. *Nature* (2009) 457(7229):557–61. doi: 10.1038/nature07665
102. Cichocki F, Grzywacz B, Miller JS. Human Nk Cell Development: One Road or Many? *Front Immunol* (2019) 10:2078. doi: 10.3389/fimmu.2019.02078
103. Wagner JA, Rosario M, Romee R, Berrien-Elliott MM, Schneider SE, Leong JW, et al. Cd56bright Nk Cells Exhibit Potent Antitumor Responses Following Il-15 Priming. *J Clin Invest* (2017) 127(11):4042–58. doi: 10.1172/JCI90387
104. Cooper MA, Fehniger TA, Caligiuri MA. The Biology of Human Natural Killer-Cell Subsets. *Trends Immunol* (2001) 22(11):633–40. doi: 10.1016/S1471-4906(01)02060-9
105. Cooper MA, Fehniger TA, Turner SC, Chen KS, Ghaheri BA, Ghayur T, et al. Human Natural Killer Cells: A Unique Innate Immunoregulatory Role for the Cd56(Bright) Subset. *Blood* (2001) 97(10):3146–51. doi: 10.1182/blood.V97.10.3146
106. Marquardt N, Kekäläinen E, Chen P, Kvedaraite E, Wilson JN, Ivarsson MA, et al. Human Lung Natural Killer Cells Are Predominantly Comprised of Highly Differentiated Hypofunctional Cd69(-)Cd56(Dim) Cells. *J Allergy Clin Immunol* (2017) 139(4):1321–30.e1324. doi: 10.1016/j.jaci.2016.07.043
107. Marquardt N, Béziat V, Nyström S, Hengst J, Ivarsson MA, Kekäläinen E, et al. Cutting Edge: Identification and Characterization of Human Intrahepatic Cd49a+ Nk Cells. *J Immunol* (2015) 194(6):2467–71. doi: 10.4049/jimmunol.1402756
108. Boulenouar S, Michelet X, Duquette D, Alvarez D, Hogan AE, Dold C, et al. Adipose Type One Innate Lymphoid Cells Regulate Macrophage Homeostasis Through Targeted Cytotoxicity. *Immunity* (2017) 46(2):273–86. doi: 10.1016/j.immuni.2017.01.008
109. Simoni Y, Fehlings M, Kløverpris HN, McGovern N, Koo SL, Loh CY, et al. Human Innate Lymphoid Cell Subsets Possess Tissue-Type Based Heterogeneity in Phenotype and Frequency. *Immunity* (2017) 46(1):148–61. doi: 10.1016/j.immuni.2016.11.005
110. Picard E, Godet Y, Laheurte C, Dosset M, Galaine J, Beziaud L, et al. Circulating Nkp46(+) Natural Killer Cells Have a Potential Regulatory Property and Predict Distinct Survival in Non-Small Cell Lung Cancer. *Oncoimmunology* (2019) 8(2):e1527498. doi: 10.1080/2162402X.2018.1527498
111. Zhou XH, Zhang XY, Liang JH, Zhu HY, Wang L, Xia Y, et al. Low Absolute Nk Cell Counts in Peripheral Blood Are Associated With Inferior Survival in Patients With Mantle Cell Lymphoma. *Cancer biomark* (2019) 24(4):439–47. doi: 10.3233/CBM-182193
112. Fend L, Rusakiewicz S, Adam J, Bastien B, Caignard A, Messaoudene M, et al. Prognostic Impact of the Expression of Ncr1 and Ncr3 Nk Cell Receptors and Pd-L1 on Advanced Non-Small Cell Lung Cancer. *Oncoimmunology* (2017) 6(1):e1163456. doi: 10.1080/2162402X.2016.1163456
113. Edin S, Kaprio T, Hagström J, Larsson P, Mustonen H, Böckelman C, et al. The Prognostic Importance of Cd20(+) B Lymphocytes in Colorectal Cancer and the Relation to Other Immune Cell Subsets. *Sci Rep* (2019) 9(1):19997. doi: 10.1038/s41598-019-56441-8
114. Wang SS, Liu W, Ly D, Xu H, Qu L, Zhang L. Tumor-Infiltrating B Cells: Their Role and Application in Anti-Tumor Immunity in Lung Cancer. *Cell Mol Immunol* (2019) 16(1):6–18. doi: 10.1038/s41423-018-0027-x
115. Kobayashi S, Watanabe T, Suzuki R, Furu M, Ito H, Ito J, et al. Tgf-β Induces the Differentiation of Human Cxcl13-Producing Cd4(+) T Cells. *Eur J Immunol* (2016) 46(2):360–71. doi: 10.1002/eji.201546043
116. Galon J, Angell HK, Bedognetti D, Marincola FM. The Continuum of Cancer Immunosurveillance: Prognostic, Predictive, and Mechanistic Signatures. *Immunity* (2013) 39(1):11–26. doi: 10.1016/j.immuni.2013.07.008
117. Pitzalis C, Jones GW, Bombardieri M, Jones SA. Ectopic Lymphoid-Like Structures in Infection, Cancer and Autoimmunity. *Nat Rev Immunol* (2014) 14(7):447–62. doi: 10.1038/nri3700
118. Germain C, Gnjatic S, Tamzalit F, Knockaert S, Remark R, Goc J, et al. Presence of B Cells in Tertiary Lymphoid Structures Is Associated With a

Protective Immunity in Patients With Lung Cancer. *Am J Respir Crit Care Med* (2014) 189(7):832–44. doi: 10.1164/rccm.201309-1611OC
119. Kroeger DR, Milne K, Nelson BH. Tumor-Infiltrating Plasma Cells Are Associated With Tertiary Lymphoid Structures, Cytolytic T-Cell Responses, and Superior Prognosis in Ovarian Cancer. *Clin Cancer Res* (2016) 22 (12):3005–15. doi: 10.1158/1078-0432.CCR-15-2762
120. Dieu-Nosjean MC, Antoine M, Danel C, Heudes D, Wislez M, Poulot V, et al. Long-Term Survival for Patients With Non-Small-Cell Lung Cancer With Intratumoral Lymphoid Structures. *J Clin Oncol* (2008) 26(27):4410–7. doi: 10.1200/JCO.2007.15.0284
121. Liu X, Tsang JYS, Hlaing T, Hu J, Ni YB, Chan SK, et al. Distinct Tertiary Lymphoid Structure Associations and Their Prognostic Relevance in Her2 Positive and Negative Breast Cancers. *Oncologist* (2017) 22(11):1316–24. doi: 10.1634/theoncologist.2017-0029
122. Cabrita R, Lauss M, Sanna A, Donia M, Skaarup Larsen M, Mitra S, et al. Tertiary Lymphoid Structures Improve Immunotherapy and Survival in Melanoma. *Nature* (2020) 577(7791):561–5. doi: 10.1038/s41586-019-1914-8
123. Finkin S, Yuan D, Stein I, Taniguchi K, Weber A, Unger K, et al. Ectopic Lymphoid Structures Function as Microniches for Tumor Progenitor Cells in Hepatocellular Carcinoma. *Nat Immunol* (2015) 16(12):1235–44. doi: 10.1038/ni.3290
124. Ogino S, Nosho K, Irahara N, Meyerhardt JA, Baba Y, Shima K, et al. Lymphocytic Reaction to Colorectal Cancer Is Associated With Longer Survival, Independent of Lymph Node Count, Microsatellite Instability, and Cpg Island Methylator Phenotype. *Clin Cancer Res* (2009) 15 (20):6412–20. doi: 10.1158/1078-0432.CCR-09-1438
125. Meshcheryakova A, Tamandl D, Bajna E, Stift J, Mittlboeck M, Svoboda M, et al. B Cells and Ectopic Follicular Structures: Novel Players in Anti-Tumor Programming With Prognostic Power for Patients With Metastatic Colorectal Cancer. *PloS One* (2014) 9(6):e99008. doi: 10.1371/journal.pone.0099008
126. Di Caro G, Bergomas F, Grizzi F, Doni A, Bianchi P, Malesci A, et al. Occurrence of Tertiary Lymphoid Tissue Is Associated With T-Cell Infiltration and Predicts Better Prognosis in Early-Stage Colorectal Cancers. *Clin Cancer Res* (2014) 20(8):2147–58. doi: 10.1158/1078-0432.CCR-13-2590
127. Posch F, Silina K, Leibl S, Mündlein A, Moch H, Siebenhüner A, et al. Maturation of Tertiary Lymphoid Structures and Recurrence of Stage Ii and Iii Colorectal Cancer. *Oncoimmunology* (2018) 7(2):e1378844. doi: 10.1080/2162402X.2017.1378844
128. Yamaguchi K, Ito M, Ohmura H, Hanamura F, Nakano M, Tsuchihashi K, et al. Helper T Cell-Dominant Tertiary Lymphoid Structures Are Associated With Disease Relapse of Advanced Colorectal Cancer. *Oncoimmunology* (2020) 9(1):1724763. doi: 10.1080/2162402X.2020.1724763
129. Wei SC, Duffy CR, Allison JP. Fundamental Mechanisms of Immune Checkpoint Blockade Therapy. *Cancer Discov* (2018) 8(9):1069–86. doi: 10.1158/2159-8290.CD-18-0367
130. Chung KY, Gore I, Fong L, Venook A, Beck SB, Dorazio P, et al. Phase Ii Study of the Anti-Cytotoxic T-Lymphocyte-Associated Antigen 4 Monoclonal Antibody, Tremelimumab, in Patients With Refractory Metastatic Colorectal Cancer. *J Clin Oncol* (2010) 28(21):3485–90. doi: 10.1200/JCO.2010.28.3994
131. Brahmer JR, Tykodi SS, Chow LQ, Hwu WJ, Topalian SL, Hwu P, et al. Safety and Activity of Anti-Pd-L1 Antibody in Patients With Advanced Cancer. *N Engl J Med* (2012) 366(26):2455–65. doi: 10.1056/NEJMoa1200694
132. Le DT, Uram JN, Wang H, Bartlett B, Kemberling H, Eyring A, et al. Programmed Death-1 Blockade in Mismatch Repair Deficient Colorectal Cancer. *J Clin Oncol* (2016) 34(15_suppl):103–3. doi: 10.1200/JCO.2016.34.15_suppl.103
133. Lemery S, Keegan P, Pazdur R. First Fda Approval Agnostic of Cancer Site - When a Biomarker Defines the Indication. *N Engl J Med* (2017) 377 (15):1409–12. doi: 10.1056/NEJMp1709968
134. Overman MJ, McDermott R, Leach JL, Lonardi S, Lenz HJ, Morse MA, et al. Nivolumab in Patients With Metastatic DNA Mismatch Repair-Deficient or Microsatellite Instability-High Colorectal Cancer (Checkmate 142): An Open-Label, Multicentre, Phase 2 Study. *Lancet Oncol* (2017) 18(9):1182–91. doi: 10.1016/S1470-2045(17)30422-9
135. Prendergast GC, Smith C, Thomas S, Mandik-Nayak L, Laury-Kleintop L, Metz R, et al. Indoleamine 2,3-Dioxygenase Pathways of Pathogenic Inflammation and Immune Escape in Cancer. *Cancer Immunol Immunother* (2014) 63(7):721–35. doi: 10.1007/s00262-014-1549-4
136. Kitsou M, Ayiomamitis GD, Zaravinos A. High Expression of Immune Checkpoints Is Associated With the Til Load, Mutation Rate and Patient Survival in Colorectal Cancer. *Int J Oncol* (2020) 57(1):237–48. doi: 10.3892/ijo.2020.5062
137. Pflugler S, Svinka J, Scharf I, Crncec I, Filipits M, Charoentong P, et al. Ido1 (+) Paneth Cells Promote Immune Escape of Colorectal Cancer. *Commun Biol* (2020) 3(1):252. doi: 10.1038/s42003-020-0989-y
138. Lee MH, Yanagawa J, Tran L, Walser TC, Bisht B, Fung E, et al. Fra1 Contributes to Mek-Erk Pathway-Dependent Pd-L1 Upregulation by Kras Mutation in Premalignant Human Bronchial Epithelial Cells. *Am J Transl Res* (2020) 12(2):409–27.
139. Bendell JC, Kim TW, Goh BC, Wallin J, Oh DY, Han SW, et al. Clinical Activity and Safety of Cobimetinib (Cobi) and Atezolizumab in Colorectal Cancer (Crc). *Am Soc of Clin Oncol* (2016) 3502. doi: 10.1200/JCO.2016.34.15_suppl.3502
140. Kobayashi H, Dubois S, Sato N, Sabzevari H, Sakai Y, Waldmann TA, et al. Role of Trans-Cellular Il-15 Presentation in the Activation of Nk Cell-Mediated Killing, Which Leads to Enhanced Tumor Immunosurveillance. *Blood* (2005) 105(2):721–7. doi: 10.1182/blood-2003-12-4187
141. Bentebibel SE, Hurwitz ME, Bernatchez C, Haymaker C, Hudgens CW, Kluger HM, et al. A First-In-Human Study and Biomarker Analysis of Nktr-214, a Novel Il2rβγ-Biased Cytokine, in Patients With Advanced or Metastatic Solid Tumors. *Cancer Discov* (2019) 9(6):711–21. doi: 10.1158/2159-8290.CD-18-1495
142. Takaki R, Hayakawa Y, Nelson A, Sivakumar PV, Hughes S, Smyth MJ, et al. Il-21 Enhances Tumor Rejection Through a Nkg2d-Dependent Mechanism. *J Immunol* (2005) 175(4):2167–73. doi: 10.4049/jimmunol.175.4.2167
143. Ferrari de Andrade L, Tay RE, Pan D, Luoma AM, Ito Y, Badrinath S, et al. Antibody-Mediated Inhibition of Mica and Micb Shedding Promotes Nk Cell-Driven Tumor Immunity. *Science* (2018) 359(6383):1537–42. doi: 10.1126/science.aao0505
144. Segal NH, Naidoo J, Curigliano G, Patel S, Sahebjam S, Papadopoulos KP, et al. First-In-Human Dose Escalation of Monalizumab Plus Durvalumab, With Expansion in Patients With Metastatic Microsatellite-Stable Colorectal Cancer. *J Clin Oncol* (2018) 36(15_suppl):3540–0. doi: 10.1200/JCO.2018.36.15_suppl.3540
145. Helmink BA, Reddy SM, Gao J, Zhang S, Basar R, Thakur R, et al. B Cells and Tertiary Lymphoid Structures Promote Immunotherapy Response. *Nature* (2020) 577(7791):549–55. doi: 10.1038/s41586-019-1922-8
146. Petitprez F, de Reyniès A, Keung EZ, Chen TW, Sun CM, Calderaro J, et al. B Cells Are Associated With Survival and Immunotherapy Response in Sarcoma. *Nature* (2020) 577(7791):556–60. doi: 10.1038/s41586-019-1906-8
147. Katoh H, Komura D, Konishi H, Suzuki R, Yamamoto A, Kakiuchi M, et al. Immunogenetic Profiling for Gastric Cancers Identifies Sulfated Glycosaminoglycans as Major and Functional B Cell Antigens in Human Malignancies. *Cell Rep* (2017) 20(5):1073–87. doi: 10.1016/j.celrep.2017.07.016
148. van Herpen CM, van der Voort R, van der Laak JA, Klasen IS, de Graaf AO, van Kempen LC, et al. Intratumoral Rhil-12 Administration in Head and Neck Squamous Cell Carcinoma Patients Induces B Cell Activation. *Int J Cancer* (2008) 123(10):2354–61. doi: 10.1002/ijc.23756
149. Lu Y, Zhao Q, Liao JY, Song E, Xia Q, Pan J, et al. Complement Signals Determine Opposite Effects of B Cells in Chemotherapy-Induced Immunity. *Cell* (2020) 180(6):1081–97.e1024. doi: 10.1016/j.cell.2020.02.015
150. Schioppa T, Moore R, Thompson RG, Rosser EC, Kulbe H, Nedospasov S, et al. B Regulatory Cells and the Tumor-Promoting Actions of Tnf-α During Squamous Carcinogenesis. *Proc Natl Acad Sci USA* (2011) 108(26):10662–7. doi: 10.1073/pnas.1100994108
151. Lindner S, Dahlke K, Sontheimer K, Hagn M, Kaltenmeier C, Barth TF, et al. Interleukin 21-Induced Granzyme B-Expressing B Cells Infiltrate Tumors and Regulate T Cells. *Cancer Res* (2013) 73(8):2468–79. doi: 10.1158/0008-5472.CAN-12-3450
152. Lee KE, Spata M, Bayne LJ, Buza EL, Durham AC, Allman D, et al. Hif1a Deletion Reveals Pro-Neoplastic Function of B Cells in Pancreatic

Neoplasia. *Cancer Discov* (2016) 6(3):256–69. doi: 10.1158/2159-8290.CD-15-0822
153. Barbera-Guillem E, Nelson MB, Barr B, Nyhus JK, May KF Jr, Feng L, et al. B Lymphocyte Pathology in Human Colorectal Cancer. Experimental and Clinical Therapeutic Effects of Partial B Cell Depletion. *Cancer Immunol Immunother* (2000) 48(10):541–9. doi: 10.1007/pl00006672
154. Melssen M, Slingluff CLJr. Vaccines Targeting Helper T Cells for Cancer Immunotherapy. *Curr Opin Immunol* (2017) 47:85–92. doi: 10.1016/j.coi.2017.07.004

Conflict of Interest: The authors declare that the research was conducted in the absence of any commercial or financial relationships that could be construed as a potential conflict of interest.

Publisher's Note: All claims expressed in this article are solely those of the authors and do not necessarily represent those of their affiliated organizations, or those of the publisher, the editors and the reviewers. Any product that may be evaluated in this article, or claim that may be made by its manufacturer, is not guaranteed or endorsed by the publisher.

Copyright © 2022 Bai, Zhou, Ye, Xiong, Lan and Wang. This is an open-access article distributed under the terms of the Creative Commons Attribution License (CC BY). The use, distribution or reproduction in other forums is permitted, provided the original author(s) and the copyright owner(s) are credited and that the original publication in this journal is cited, in accordance with accepted academic practice. No use, distribution or reproduction is permitted which does not comply with these terms.

frontiers in Oncology

CASE REPORT
published: 28 February 2022
doi: 10.3389/fonc.2022.820408

Case Report: Opportunities and Challenges of Immunotherapy in Heavily-Treated EGFR-Mutant Advanced Squamous Cell Lung Carcinoma After Progression on EGFR-TKIs and Chemotherapy

Wei Jin[1], *Xin Wang*[2], *Jie Wang*[3*] *and Lin Lin*[3*]

[1] *Department of Chinese Medicine, National Cancer Center/National Clinical Research Center for Cancer/Cancer Hospital, Chinese Academy of Medical Sciences and Peking Union Medical College, Beijing, China,* [2] *Department of Pathology, National Cancer Center/National Clinical Research Center for Cancer/Cancer Hospital, Chinese Academy of Medical Sciences and Peking Union Medical College, Beijing, China,* [3] *Department of Medical Oncology, National Cancer Center/ National Clinical Research Center for Cancer/Cancer Hospital, Chinese Academy of Medical Sciences and Peking Union Medical College, Beijing, China*

OPEN ACCESS

Edited by:
Hubing Shi,
Sichuan University, China

Reviewed by:
Valerio Gristina,
University of Palermo, Italy
Yongfeng Yu,
Shanghai Jiaotong University, China

***Correspondence:**
Jie Wang
zlhuxi@163.com
Lin Lin
doctor.linlin@outlook.com

Specialty section:
This article was submitted to Cancer Immunity and Immunotherapy, a section of the journal Frontiers in Oncology

Received: *23 November 2021*
Accepted: *31 January 2022*
Published: *28 February 2022*

Citation:
Jin W, Wang X, Wang J and Lin L (2022) Case Report: Opportunities and Challenges of Immunotherapy in Heavily-Treated EGFR-Mutant Advanced Squamous Cell Lung Carcinoma After Progression on EGFR-TKIs and Chemotherapy. Front. Oncol. 12:820408. doi: 10.3389/fonc.2022.820408

Background: Epidermal growth factor receptor (EGFR) mutations have a low incidence in squamous cell lung cancer (SqCLC), and the clinical efficacy of EGFR tyrosine kinase inhibitors (TKIs) in *EGFR*-mutated SqCLC is far less than that in *EGFR*-mutated lung adenocarcinoma. The treatment strategy for patients with *EGFR*-mutated non-small cell lung cancer who are refractory to EGFR TKIs has become a current dilemma and challenge.

Case Presentation: A case of a 69-year-old male patient suffering from intermittent cough and hemoptysis was diagnosed with *EGFR*-mutated advanced SqCLC (stage cT2bN2M1). The patient was treated with camrelizumab alone after five courses of different systemic therapies and achieved a partial response, with an eminent progression-free survival of more than 24 months. Grade 1 to 2 reactive cutaneous capillary endothelial proliferation and mild pruritus were observed during the treatment. No other immune-related adverse events were observed.

Conclusion: Monotherapy of immune-checkpoint inhibitors may be considered as a later-line option for *EGFR*-mutated advanced SqCLC patients with PD-L1 expression.

Keywords: immunotherapy, camrelizumab, epidermal growth factor receptor (EGFR) mutations, advanced squamous cell lung carcinoma (SqCLC), case report

INTRODUCTION

Lung cancer is currently the malignant tumor with the highest morbidity and mortality around the world. Squamous cell lung carcinoma (SqCLC) is a common pathological type of lung cancer, accounting for about 25 to 30% in non-small cell lung cancer (NSCLC) (1, 2). Epidermal growth factor receptor (EGFR) mutation is one of the most common driver mutations in NSCLC but occur in only 3.3–4.6% of patients with SqCLC (3). Patients with *EGFR*-mutated advanced SqCLC benefit limitedly from EGFR tyrosine kinase inhibitors (TKIs). In 2013, Fang *et al.* reported that the

objective response rate (ORR) and median progression-free survival (mPFS) of first-generation EGFR-TKIs (gefitinib or erlotinib) in 15 advanced SqCLC patients with *EGFR* mutation was 26.7% and 3.9 months, respectively (4). Another pooled analysis from Japan demonstrated that the mPFS of gefitinib in 27 *EGFR*-mutated SqCLC patients was only 3.1 months, with an ORR of 30% (5). As the resistance to targeted therapy is inevitable and the mechanisms are complex, the treatment strategy after EGFR-TKI resistance has become a dilemma and challenge for patients with *EGFR*-mutated advanced NSCLC. With the advent of immunotherapy, a variety of immune-checkpoint inhibitors (ICIs) targeting programmed cell death protein 1/programmed cell death ligand 1 (PD-1/PD-L1) have been proven to benefit patients with advanced NSCLC (6–10). However, only about 20% of NSCLC patients could benefit from immunotherapy in second-line treatment (8). Due to the complex clinical features and gene mutations of SqCLC, which make its treatment challenging, whether patients with *EGFR*-mutated advanced NSCLC can benefit from immunotherapy has become a hot issue.

Here we describe a case of *EGFR*-mutated advanced SqCLC treated with PD-1 inhibitor monotherapy and which achieved an eminent PFS of 24.4 months in the sixth-line treatment and provide an assessment of the efficacy and safety of the treatment.

BACKGROUND

In June 2018, a 69-year-old male with a 15-year smoking history went to our hospital; he had been suffering from intermittent cough and hemoptysis for 3 months. An enhanced computed tomography (CT) scan of the chest revealed a proximal interlobular pleural mass in the left lung upper lobe, multiple nodules and masses in the left lung lower lobe, a mass-like opacity in the right lung upper lobe, and a right renal mass. SqCLC was confirmed by pathological examination and immunohistochemistry study of CT-guided biopsy specimens from the mass of the left upper lobe (**Figure 1A**). The patient's condition was staged as cT2bN2M1 (stage IV) according to the 8th Edition of the American Joint Committee on Cancer TNM Staging System (2017). The next-generation sequencing (NGS) analysis of the patient's peripheral blood sample with a panel (Repugene Technology, Hangzhou, China) including 18 somatic genes related to NSCLC and the efficacy of targeted drugs suggested *EGFR Exon 21 L858R*, *G719A*, and *S768I* mutations. Other driver gene mutations, such as *ALK*, *ROS1*, *ERBB2* (*HER2*), *BRAF*, *KRAS*, *TP53*, *PIK3CA*, *etc.*, were not detected.

In July 2018, with an Eastern Cooperative Oncology Group performance status score of 0, the patient received first-line treatment with icotinib (**Figure 2**), a first-generation EGFR-TKI, and achieved a partial response (PR). A CT scan in January 2019 revealed multiple nodules in the right lung and enlarged lesions in the left lung and right kidney, indicating a progressive disease (PD). The PFS for the first-line treatment was 6 months.

The second NGS analysis of the whole blood sample with a large panel (Genetron Health, Beijing, China), including 824 somatic genes, suggested *EGFR G719A* and *S768I* mutations and negative *EGFR* T790M mutation. On January 24, 2019, the pathological examination of an ultrasound-guided biopsy of the right renal mass revealed a poorly differentiated squamous cell carcinoma, which may be derived from tumor metastasis. On January 30, 2019, the second-line treatment consisting of

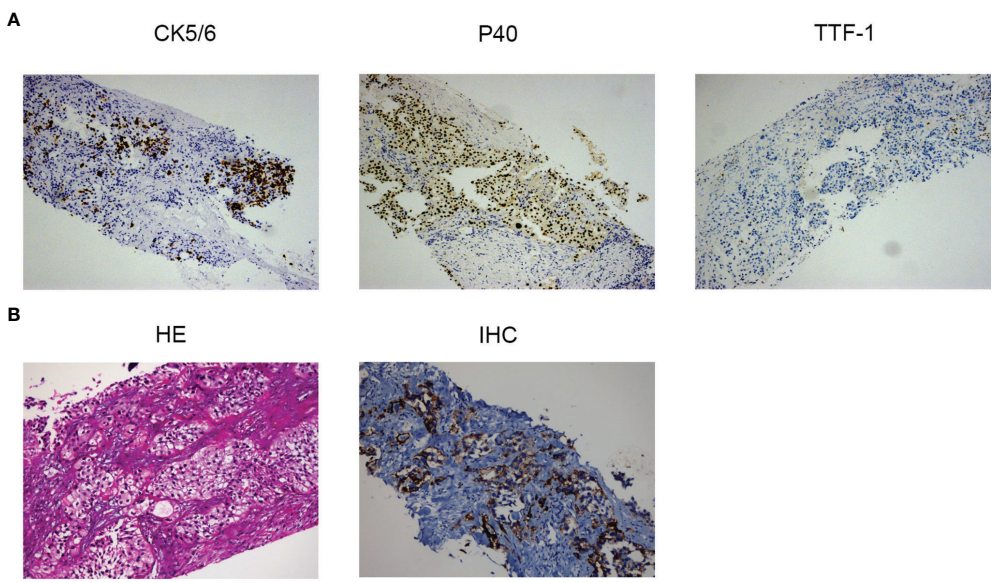

FIGURE 1 | **(A)** Histopathology of the left upper lobe mass at diagnosis: expression of cell keratin 5/6 and P40 thyroid transcription factor-1 by immunohistochemistry (original magnification, ×10). **(B)** Pathologic findings of the patient's right kidney metastasis before the sixth-line treatment with camrelizumab: hematoxylin and eosin staining of PD-L1 (original magnification, ×20) and immunohistochemistry of PD-L1 (original magnification, ×10).

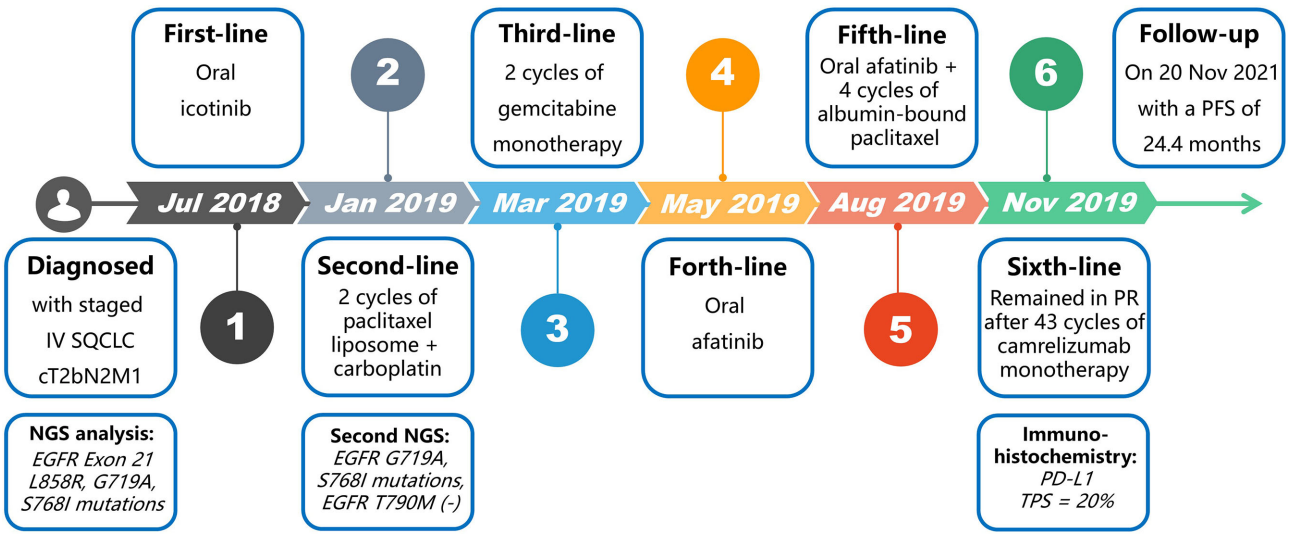

FIGURE 2 | Diagnosis and treatment procedure.

paclitaxel liposome in combination with carboplatin was administered. A re-examination after 2 cycles of treatment revealed enlarged primary and metastatic lesions, along with lymph node metastases presenting between the abdominal aorta and inferior vena cava, suggesting PD. The second-line therapy was continued for 1.2 months.

The third-line treatment with 2 cycles of gemcitabine monotherapy was started on March 17, 2019 and was continued for 2.2 months. Then, the disease progressed with bilateral frontal lobe metastases as revealed by magnetic resonance imaging.

The treatment was switched to oral afatinib, a second-generation *EGFR*-TKI, in May 2019 and lasted 2.8 months until the disease progressed with new liver metastases.

On August 26, 2019, the patient was given a systemic chemotherapy of afatinib combined with albumin-bound paclitaxel. Nevertheless, his disease progressed again after 4 cycles of this fifth-line treatment, as the re-examination suggested enlargement of the liver metastases and the right kidney metastasis (**Figure 3A**), with a PFS of 2.6 months.

Since an immunohistochemistry study of the right kidney metastasis showed a PD-L1 tumor proportion score (TPS) of 20% (22c3 antibody on the Dako Link-48 platform) (**Figure 1B**), single-agent camrelizumab (200 mg every 2 weeks) was started on November 19, 2019. The patient's cough was obviously relieved, and the re-examination indicated a stable disease after 3 cycles of camrelizumab. PR was achieved after 6 cycles and confirmed again by the response evaluation after 10 cycles. The patient remained in PR after 43 cycles (**Figure 3B**) and was about to receive the 50th cycle of monotherapy with camrelizumab as of the time of writing of this case report (November 20, 2021), with a PFS of 24.4 months.

After 6 cycles of camrelizumab, the patient presented with reactive cutaneous capillary endothelial proliferation (RCCEP), multiple bright red spots ("red-nevus-like"), with a spot on the skin surface of the neck measuring 1 to 2 mm in diameter (grade 1 RCCEP) (**Figure 4A**) and with a "pearl-like" nodule in the nasal cavity. After 8 cycles of camrelizumab, the nodule in the nasal cavity developed into a "tumor-like" nodule, >10 mm in diameter (**Figure 4B**), along with several "pearl-like" nodules on the occipital skin surface at 5 mm in diameter (**Figure 4C**). The nodule on the left occipital skin surface enlarged to a pedicled "tumor-like" nodule, >10 mm in diameter (**Figure 4D**), after 10 cycles of camrelizumab. Both "tumor-like" and "pearl-like" nodules on the surface of the nasal cavity and the occiput were treated with laser and underwent resection. After 35 cycles of camrelizumab, the patient developed pruritus all over the body and the extremities (grade 1 under the Common Terminology Criteria for Adverse Events). During the sixth-line treatment with camrelizumab, there was no ulceration, hemorrhage (grade 2 RCCEP), or other immune-related adverse events (irAEs) observed except for RCCEP.

DISCUSSION

EGFR mutation is an important molecular marker of NSCLC. *EGFR Exon 21 L858R* mutation, a classical activating mutation, is considered related to a better outcome in NSCLC patients, granting a complete blockade of the EGFR signaling pathway by EGFR-TKIs (11). The 6 months of PFS of the first-line treatment with icotinib and the *L858R* mutation that disappeared in the second NGS testing after icotinib treatment in our case demonstrated the *L858R* mutation as a positive predictor of clinical prognosis which responds well to first-generation EGFR-TKI. *G719A* mutation is one of the common *EGFR exon 18* mutations, which was reported as a predictor of augmented sensitivity to afatinib or neratinib (12). The *EGFR*

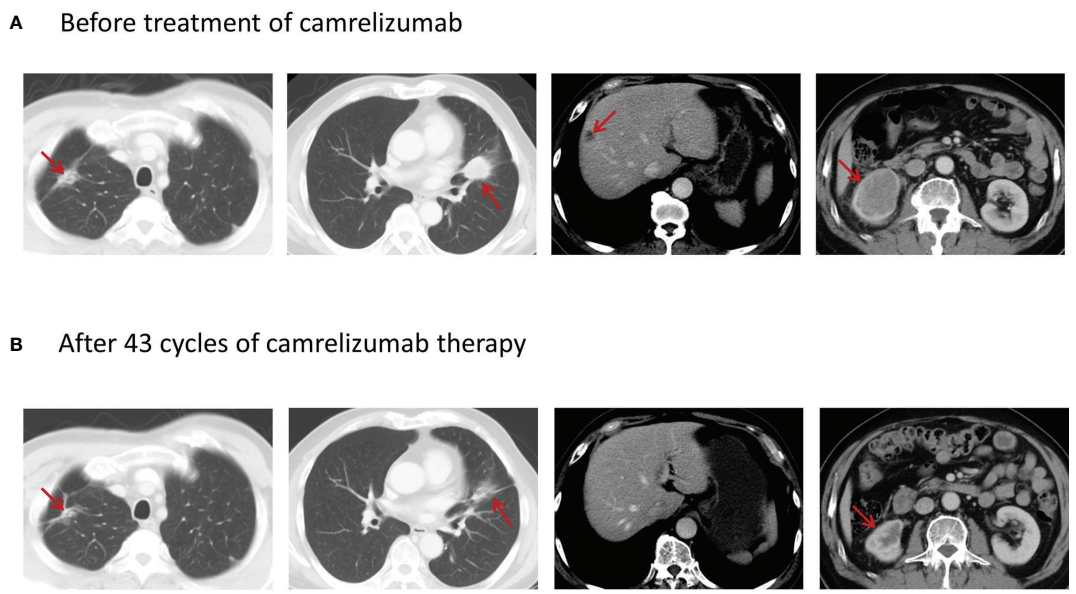

FIGURE 3 | **(A)** Enhanced CT scan before the treatment of camrelizumab showing a mass-like opacity in the upper lobe of the right lung with a maximum cross-sectional area of about 3.4 × 1.4 cm, a 3.3 × 2.8-cm tumor in the upper lobe of the left lung near the interlobar pleura, a low-density subcapsular nodule in the right lobe of the liver of about 1.5 × 1.4 cm in size, and a metastatic tumor in the lower right kidney with the size of about 5.9 × 4.3 cm. **(B)** Enhanced CT scan after 43 cycles of treatment with camrelizumab showing that the tumor in the upper lobe of the right lung was of 3.1 × 2.3 cm in maximum cross-sectional area, the tumor in the upper lobe of the left lung near the interlobar pleura decreased to the size of 1.7 × 0.8 cm, the subcapsular lesion in the right lobe of the liver was calcified, and the tumor in the lower right kidney decreased to the size of 2.6 × 1.9 cm.

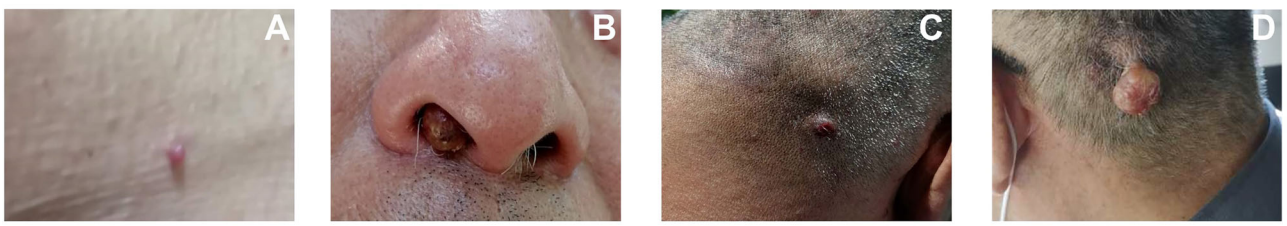

FIGURE 4 | Reactive cutaneous capillary endothelial proliferation. **(A)** "Red-nevus-like" nodule with a diameter of 1 to 2 mm on the skin surface of the neck. **(B)** "Tumor-like" nodule with a diameter of >10 mm in the nasal cavity. **(C)** "Pearl-like" nodule with a diameter of 5 mm on the occipital skin surface. **(D)** The nodule on the left occipital skin surface enlarged to a pedicled "tumor-like" nodule with a diameter of >10 mm.

exon 20 S768I mutation is a rare mutation at a frequency of between 0.6 and 1% of EGFR mutations in NSCLC (13) and often co-occurs with other *EGFR* point mutations to form complex mutations—for example, *S768I/G719X* (*G719X* including *G719S*, *G719A*, *G719C*, and *G719D* substitutions) or *S768I/L858R* complex mutations. FDA approved afatinib for NSCLC patients with *EGFR S768I* mutations based on 100% of ORR and 14.7 months of mPFS for eight patients with *S768I* mutant NSCLC in a *post-hoc* analysis (14). Furthermore, the *S768I/G719A* co-mutation was confirmed to be resistant to first-generation and highly sensitive to afatinib (15). Thus, in our case, we used afatinib for fourth-line treatment in the SqCLC patient with a *S768I/G719A* co-mutation. However, unfortunately, gene detections after progression in the later-line treatments were lacking due to realistic reasons, and whether the genetic mutation changed during the different treatments is unknown, so the mechanism of repeated resistance to EGFR-TKIs and chemotherapies is uncertain.

EGFR-TKI is a standard treatment option for *EGFR*-mutated NSCLC, but the treatment strategy after drug resistance to EGFR-TKIs has been a great challenge. There is an urgent need for immunotherapy to achieve the precise treatment of *EGFR*-mutated NSCLC patients, bringing new hope to *EGFR*-mutated NSCLC patients. However, patients with *EGFR* mutations were once considered to be "immune-privilege" populations. A subgroup analysis of most previous studies showed little benefit from mono-immunotherapy in *EGFR*/*ALK*-mutated patients. A phase II clinical trial (NCT02879994)

explored ICI monotherapy as the first-line treatment for *EGFR*-mutated NSCLC with 11 patients enrolled, but the recruitment was stopped due to lack of efficacy. Most clinical trials of first-line mono-immunotherapy excluded patients with *EGFR*-mutated NSCLC.

Regarding the second-line treatment with ICIs, the outcomes of the CHECKMATE-057 study (8) showed that the PFS and the overall survival (OS) were not significantly improved with nivolumab than with docetaxel among patients with *EGFR*-mutated advanced non-squamous NSCLC that had progressed after chemotherapy treatment. The KEYNOTE-010 study (pembrolizumab) (16) and the OAK study (atezolizumab) (10) showed similar results that revealed no OS benefit in *EGFR*-mutated subgroups. A retrospective study from Massachusetts General Hospital, which enrolled 28 patients with *EGFR+/ALK+* NSCLC, indicated a significantly lower ORR of immunotherapy in *EGFR+/ALK+* patients than that of *EGFR-/ALK-* patients (3.6 *vs.* 23.3%) (17). Other meta-analyses, including CHECKMATE-057, KEYNOTE-010, and POPLAR studies, showed that patients with *EGFR*-mutated advanced NSCLC cannot benefit from ICIs (18).

Although many studies have confirmed that *EGFR*-mutated advanced NSCLC is not sensitive to immunotherapy, two patients in the CA209-003 study had progressed after more than two lines of treatment, received nivolumab monotherapy, and survived for more than 5 years in the follow-up (19). In 2020, the ATLANTIC study (20), the largest prospective trial of anti-PD-1/PD-L1 treatments for patients with positive driver gene mutations so far, updated its results. In this trial, eligible patients were assigned into three groups based on the status of *EGFR/ALK* mutations and PD-L1 expression to evaluate the safety and efficacy of durvalumab for third-line or above treatment and found that the ORR (12.2 *vs.* 3.6%) and mOS (13.3 *vs.* 10.9 months) of patients with *EGFR+/ALK+* NSCLC with a PD-L1 TPS of ≥25% were higher than those with *EGFR-/ALK-* NSCLC with a PD-L1 TPS of ≥25%. These results denied the previous conclusion that *EGFR+/ALK+* patients are not fit for immunotherapy. For patients with *EGFR* mutations, PD-L1 may be used as a biomarker to predict the clinical efficacy of immunotherapy, which may provide another option of the third- or later-line treatment for *EGFR*-mutated NSCLC with PD-L1 overexpression. However, most of the patients included in the above-mentioned studies were *EGFR*-mutated lung adenocarcinoma case. In the *EGFR+/ALK+* group of the ATLANTIC study, only one of 111 patients was a case of SqCLC. There was no detailed report on this rare case.

Immunotherapy for EGFR-mutant patients is faced with opportunities and challenges. Combination immunotherapy is becoming a new exploration direction. Pre-clinical studies found that EGFR activation upregulated PD-L1 through p-ERK1/2/p-c-Jun and induced the apoptosis of T cells. Accordingly, EGFR-TKIs could alleviate the inhibition effect of PD-L1/PD-1 axis on T cells and increase the production of interferon-γ. Moreover, PD-L1 expression is significantly elevated in EGFR-TKI-resistant cell lines, whereas anti-PD-1 antibody could suppress the viability of EGFR-TKI-resistant NSCLC cells (21), which may explain the good response to camrelizumab after repeated drug resistance to EGFR-TKIs in our case. Considering the potential interaction of PD-L1/PD-1 inhibitors and EGFR-TKIs, a number of trials regarding the combination therapy of ICIs with EGFR-TKIs have been conducted, such as the cohort of nivolumab combined with erlotinib in CheckMate 012 study (22), the KEYNOTE-021 study of pembrolizumab in combination with erlotinib or gefitinib (23), the phase-I open-label, multicenter trial of durvalumab plus gefitinib (NCT02088112) (24), the TATTON study of durvalumab combined with osimertinib (25), and the phase Ib study of atezolizumab plus erlotinib (26). The results of these studies suggest that ICIs combined with EGFR-TKIs can achieve various degrees of ORR but will also cause intolerable toxicity at the same time. In particular, due to the high incidence of interstitial pneumonitis during the treatment of durvalumab plus osimertinib, the TATTON study and the phase III CAURAL study were terminated. In addition, the study of CTLA-4 inhibitors plus targeted therapy suspended the recruitment (27) due to dose-limiting toxicity. Currently, the development of immune-based combinations remains a crucial unmet need. To explore the optimal combination strategy of immune-based therapy, reducing its toxic side effects and revealing its efficacy mechanism in *EGFR*-mutated NSCLC patients will be among the challenges for future research in this field.

ICIs combined with chemotherapy and anti-angiogenic drugs is another combination treatment strategy. The IMpower150 study is a phase III clinical study of the first-line treatment of advanced non-squamous NSCLC (28), and the subgroup analysis showed a significant improvement in OS (median OS: 29.4 *vs.* 18.1 months, HR = 0.60; 95% CI: 0.31–1.14) of ICIs combined with chemotherapy and anti-angiogenic therapy (atezolizumab + bevacizumab + carboplatin + paclitaxel) compared with that of chemotherapy combined with anti-angiogenic therapy (bevacizumab + carboplatin + paclitaxel) among 124 *EGFR*-mutated non-squamous NSCLC patients who had a failed previous targeted therapy. The IMpower150 study is currently the only phase III clinical trial in which immune combination therapy brought a survival benefit to *EGFR*-mutated patients. This global multi-center study overturns the theory of immune privilege resulting from *EGFR* mutations and provides new opportunities for the later-line treatment after EGFR-TKI resistance.

Camrelizumab is an IgG4-humanized monoclonal antibody against PD-1, which can inhibit the binding of PD-L1 and PD-L2 to PD-1, and has a promising anti-tumor efficacy. The patient with *EGFR*-mutated SqCLC in this paper has received multiple courses of targeted therapy, chemotherapy, and the combination of chemotherapy with targeted therapy, but the disease has progressed rapidly. Based on the PD-L1 expression status of the metastasis in the right kidney, the patient received 49 cycles of mono-immunotherapy with camrelizumab and achieved PR. The patient is still receiving maintenance treatment with camrelizumab alone, with a PFS of more than 24 months. This case report provides further evidence that a small number of patients with *EGFR*-mutated advanced SqCLC can benefit from mono-immunotherapy. Thus, mono-immunotherapy still has the opportunity to play an important role in the later-line

treatment of *EGFR*-mutated advanced SqCLC, especially after multiple courses of different types of therapy, and PD-L1 may be used as a biomarker to predict the clinical efficacy of immunotherapy. The mechanism related to the prominent response to camrelizumab monotherapy and whether *S768I/G719A* mutation is one of the possible mechanisms need more inspection and exploration.

As with clinical trials, case reports regarding the treatment of ICIs for *EGFR*-mutated NSCLC are mostly cases of lung adenocarcinoma (29–31) or about a changed phenotype from lung adenocarcinoma to SqCLC (32). The patient in this case was first diagnosed with SqCLC and has a longer PFS (>24 *vs*. 16 months) during the treatment with camrelizumab compared with that of the patient with *EGFR*-mutated NSCLC in the CA209-003 trial who received durvalumab as a third-line treatment and had an OS of >5 years (19).

The patient developed grade 1 to 2 RCCEP during the treatment of camrelizumab, without other irAEs. RCCEP, a common, typical irAE of camrelizumab, mainly occurred on the skin surface of the head, neck, trunk, and extremities but rarely in other parts such as the oral mucosa, nasal mucosa, and eyelid conjunctiva and was never observed in visceral organs (33, 34). The mechanism of RCCEP is unclear and may be related to the imbalance between angiogenesis accelerants and inhibitors. Most RCCEPs are self-limited and have little impact on the quality of life. However, for patients with a high risk of bleeding, if the RCCEP is severely congested, fragile, located in the friction sites, or repeatedly bleeding, local resection may be a better choice. RCCEP may be used as a marker to predict the efficacy of camrelizumab. Studies have found that patients who develop RCCEP during the treatment with camrelizumab have an ORR of 28.9%, while patients without RCCEP do not respond to camrelizumab (33). In this report, the patient developed "red-nevus-like", "pearl-like", and "tumor-like" nodules, and both "pearl-like" and "tumor-like" nodules had been removed. Although the patient had grade 1 to 2 RCCEP, the immune response was obvious, consistent with the results previously reported in the literatures.

CONCLUDING REMARKS

At present, EGFR-TKIs are still the standard regimen for *EGFR*-mutated advanced NSCLC, but due to the complex drug resistance mechanism, mono-immunotherapy or a combination therapy of immunotherapy with other treatments needs to be optimized. The studies mentioned before have shown that the vast majority of patients with advanced NSCLC refractory to EGFR-TKIs had a poor curative effect to ICIs. However, in view of the fact that ICIs could exert anti-tumor effects through the patients' own immune system, there are still a small number of *EGFR*-mutated advanced NSCLC that can benefit from immunotherapy after drug resistance to EGFR-TKIs. Mono-immunotherapy could be considered as one of the later-line treatment options for patients with *EGFR*-mutated advanced SqCLC, especially for those without *EGFR* T790M mutation or with high PD-L1 expression. The national, multi-center, randomized, double-blind phase III TREASURE study, CHECKMATE-722 study, KEYNOTE-789 study, and ORIENT-31 study are ongoing to explore the efficacy of immunotherapy for patients with NSCLC after PD on EGFR-TKIs. More and more clinical and basic research concerns were expected in these patients to further screen the advantageous population of ICIs in the treatment of *EGFR*-mutated advanced SqCLC, to find predictive biomarkers of clinical efficacy, and to achieve a personalized precision treatment.

DATA AVAILABILITY STATEMENT

The original contributions presented in the study are included in the article/supplementary material. Further inquiries can be directed to the corresponding authors.

ETHICS STATEMENT

The studies involving human participants were reviewed and approved by the Ethics Committee of the National Cancer Center/National Clinical Research Center for Cancer/Cancer Hospital, Chinese Academy of Medical Sciences. The patients/participants provided their written informed consent to participate in this study. Written informed consent was obtained from the individual(s) for the publication of any potentially identifiable images or data included in this article.

AUTHOR CONTRIBUTIONS

All authors were involved in the clinical management of the presented case and participated in manuscript preparation. All authors contributed to the article and approved the submitted version.

ACKNOWLEDGMENTS

This case was from the National Cancer Center/National Clinical Research Center for Cancer/Cancer Hospital, Chinese Academy of Medical Sciences and Peking Union Medical College.

REFERENCES

1. Houston KA, Henley SJ, Li J, White MC, Richards TB. Patterns in Lung Cancer Incidence Rates and Trends by Histologic Type in the United States, 2004-2009. *Lung Cancer* (2014) 86(1):22–8. doi: 10.1016/j.lungcan.2014.08.001
2. Siegel R, Naishadham D, Jemal A. Cancer Statistics, 2013. *CA Cancer J Clin* (2013) 63(1):11–30. doi: 10.3322/caac.21166
3. Heist RS, Sequist LV, Engelman JA. Genetic Changes in Squamous Cell Lung Cancer: A Review. *J Thorac Oncol* (2012) 7(5):924–33. doi: 10.1097/JTO.0b013e31824cc334

4. Fang W, Zhang J, Liang W, Huang Y, Yan Y, Wu X, et al. Efficacy of Epidermal Growth Factor Receptor-Tyrosine Kinase Inhibitors for Chinese Patients With Squamous Cell Carcinoma of Lung Harboring EGFR Mutation. *J Thorac Dis* (2013) 5(5):585–92. doi: 10.3978/j.issn.2072-1439.2013.09.15
5. Shukuya T, Takahashi T, Kaira R, Ono A, Nakamura Y, Tsuya A, et al. Efficacy of Gefitinib for Non-Adenocarcinoma Non-Small-Cell Lung Cancer Patients Harboring Epidermal Growth Factor Receptor Mutations: A Pooled Analysis of Published Reports. *Cancer Sci* (2011) 102(5):1032–7. doi: 10.1111/j.1349-7006.2011.01887.x
6. Reck M, Rodríguez-Abreu D, Robinson AG, Hui R, Csőszi T, Fülöp A, et al. Pembrolizumab Versus Chemotherapy for PD-L1-Positive Non-Small-Cell Lung Cancer. *N Engl J Med* (2016) 375(19):1823–33. doi: 10.1056/NEJMoa1606774
7. Langer CJ, Gadgeel SM, Borghaei H, Papadimitrakopoulou VA, Patnaik A, Powell SF, et al. Carboplatin and Pemetrexed With or Without Pembrolizumab for Advanced, Non-Squamous Non-Small-Cell Lung Cancer: A Randomised, Phase 2 Cohort of the Open-Label KEYNOTE-021 Study. *Lancet Oncol* (2016) 17(11):1497–508. doi: 10.1016/S1470-2045(16)30498-3
8. Borghaei H, Paz-Ares L, Horn L, Spigel DR, Steins M, Ready NE, et al. Nivolumab Versus Docetaxel in Advanced Nonsquamous Non-Small-Cell Lung Cancer. *N Engl J Med* (2015) 373(17):1627–39. doi: 10.1056/NEJMoa1507643
9. Gandhi L, Rodríguez-Abreu D, Gadgeel S, Esteban E, Felip E, De Angelis F, et al. Pembrolizumab Plus Chemotherapy in Metastatic Non-Small-Cell Lung Cancer. *N Engl J Med* (2018) 378(22):2078–92. doi: 10.1056/NEJMoa1801005
10. Fehrenbacher L, von Pawel J, Park K, Rittmeyer A, Gandara DR, Ponce Aix S, et al. Updated Efficacy Analysis Including Secondary Population Results for OAK: A Randomized Phase III Study of Atezolizumab Versus Docetaxel in Patients With Previously Treated Advanced Non-Small Cell Lung Cancer. *J Thorac Oncol* (2018) 13(8):1156–70. doi: 10.1016/j.jtho.2018.04.039
11. Gristina V, La Mantia M, Galvano A, Cutaia S, Barraco N, Castiglia M, et al. Non-Small Cell Lung Cancer Harboring Concurrent EGFR Genomic Alterations: A Systematic Review and Critical Appraisal of the Double Dilemma. *J Mol Pathol* (2021) 2(2):173–96. doi: 10.3390/jmp2020016
12. Kobayashi Y, Togashi Y, Yatabe Y, Mizuuchi H, Jangchul P, Kondo C, et al. EGFR Exon 18 Mutations in Lung Cancer: Molecular Predictors of Augmented Sensitivity to Afatinib or Neratinib as Compared With First- or Third-Generation TKIs. *Clin Cancer Res* (2015) 21(23):5305–13. doi: 10.1158/1078-0432.CCR-15-1046
13. Leventakos K, Kipp BR, Rumilla KM, Winters JL, Yi ES, Mansfield AS. S768I Mutation in EGFR in Patients With Lung Cancer. *J Thorac Oncol* (2016) 11(10):1798–801. doi: 10.1016/j.jtho.2016.05.007
14. Yang JCH, Sequist LV, Geater SL, Tsai C-M, Mok TSK, Schuler M, et al. Clinical Activity of Afatinib in Patients With Advanced Non-Small-Cell Lung Cancer Harbouring Uncommon EGFR Mutations: A Combined Post-Hoc Analysis of LUX-Lung 2, LUX-Lung 3, and LUX-Lung 6. *Lancet Oncol* (2015) 16(7):830–8. doi: 10.1016/S1470-2045(15)00026-1
15. Gristina V, Malapelle U, Galvano A, Pisapia P, Pepe F, Rolfo C, et al. The Significance of Epidermal Growth Factor Receptor Uncommon Mutations in Non-Small Cell Lung Cancer: A Systematic Review and Critical Appraisal. *Cancer Treat Rev* (2020) 85:101994. doi: 10.1016/j.ctrv.2020.101994
16. Herbst RS, Baas P, Kim D-W, Felip E, Pérez-Gracia JL, Han J-Y, et al. Pembrolizumab Versus Docetaxel for Previously Treated, PD-L1-Positive, Advanced Non-Small-Cell Lung Cancer (KEYNOTE-010): A Randomised Controlled Trial. *Lancet* (2016) 387(10027):1540–50. doi: 10.1016/S0140-6736(15)01281-7
17. Gainor JF, Shaw AT, Sequist LV, Fu X, Azzoli CG, Piotrowska Z, et al. EGFR Mutations and ALK Rearrangements Are Associated With Low Response Rates to PD-1 Pathway Blockade in Non-Small Cell Lung Cancer: A Retrospective Analysis. *Clin Cancer Res* (2016) 22(18):4585–93. doi: 10.1158/1078-0432.CCR-15-3101
18. Lee CK, Man J, Lord S, Cooper W, Links M, Gebski V, et al. Clinical and Molecular Characteristics Associated With Survival Among Patients Treated With Checkpoint Inhibitors for Advanced Non-Small Cell Lung Carcinoma: A Systematic Review and Meta-Analysis. *JAMA Oncol* (2018) 4(2):210–6. doi: 10.1001/jamaoncol.2017.4427
19. Gettinger S, Horn L, Jackman D, Spigel D, Antonia S, Hellmann M, et al. Five-Year Follow-Up of Nivolumab in Previously Treated Advanced Non-Small-Cell Lung Cancer: Results From the CA209-003 Study. *J Clin Oncol* (2018) 36(17):1675–84. doi: 10.1200/JCO.2017.77.0412
20. Garassino MC, Cho B-C, Kim J-H, Mazières J, Vansteenkiste J, Lena H, et al. Durvalumab as Third-Line or Later Treatment for Advanced Non-Small-Cell Lung Cancer (ATLANTIC): An Open-Label, Single-Arm, Phase 2 Study. *Lancet Oncol* (2018) 19(4):521–36. doi: 10.1016/S1470-2045(18)30144-X
21. Chen N, Fang W, Zhan J, Hong S, Tang Y, Kang S, et al. Upregulation of PD-L1 by EGFR Activation Mediates the Immune Escape in EGFR-Driven NSCLC: Implication for Optional Immune Targeted Therapy for NSCLC Patients With EGFR Mutation. *J Thorac Oncol* (2015) 10(6):910–23. doi: 10.1097/JTO.0000000000000500
22. Gettinger S, Hellmann MD, Chow LQM, Borghaei H, Antonia S, Brahmer JR, et al. Nivolumab Plus Erlotinib in Patients With EGFR-Mutant Advanced NSCLC. *J Thorac Oncol* (2018) 13(9):1363–72. doi: 10.1016/j.jtho.2018.05.015
23. Yang JC-H, Gadgeel SM, Sequist LV, Wu C-L, Papadimitrakopoulou VA, Su W-C, et al. Pembrolizumab in Combination With Erlotinib or Gefitinib as First-Line Therapy for Advanced NSCLC With Sensitizing EGFR Mutation. *J Thorac Oncol* (2019) 14(3):553–9. doi: 10.1016/j.jtho.2018.11.028
24. Creelan BC, Yeh TC, Kim S-W, Nogami N, Kim D-W, Chow LQM, et al. A Phase 1 Study of Gefitinib Combined With Durvalumab in EGFR TKI-Naive Patients With EGFR Mutation-Positive Locally Advanced/Metastatic Non-Small-Cell Lung Cancer. *Br J Cancer* (2021) 124(2):383–90. doi: 10.1038/s41416-020-01099-7
25. Oxnard GR, Yang JCH, Yu H, Kim SW, Saka H, Horn L, et al. TATTON: A Multi-Arm, Phase Ib Trial of Osimertinib Combined With Selumetinib, Savolitinib, or Durvalumab in EGFR-Mutant Lung Cancer. *Ann Oncol* (2020) 31(4):507–16. doi: 10.1016/j.annonc.2020.01.013
26. Rudin C, Cervantes A, Dowlati A, Besse B, Ma B, Costa D, et al. MA15.02 Long-Term Safety and Clinical Activity Results From a Phase Ib Study of Erlotinib Plus Atezolizumab in Advanced NSCLC. *J Thorac Oncol* (2018) 13(10):S407. doi: 10.1016/j.jtho.2018.08.440
27. Morrissey KM, Yuraszeck TM, Li CC, Zhang Y, Kasichayanula S. Immunotherapy and Novel Combinations in Oncology: Current Landscape, Challenges, and Opportunities. *Clin Transl Sci* (2016) 9(2):89–104. doi: 10.1111/cts.12391
28. Socinski MA, Nishio M, Jotte RM, Cappuzzo F, Orlandi F, Stroyakovskiy D, et al. IMpower150 Final Overall Survival Analyses for Atezolizumab Plus Bevacizumab and Chemotherapy in First-Line Metastatic Nonsquamous NSCLC. *J Thorac Oncol* (2021) 16(11):1909–24. doi: 10.1016/j.jtho.2021.07.009
29. Hochmair MJ, Weinlinger C, Prosch H. Successful Immune Checkpoint Inhibition in an EGFR-Mutant Lung Cancer Patient Refractory to Epidermal Growth Factor Receptor Tyrosine Kinase Inhibitor Treatment. *Anticancer Drugs* (2020) 31(3):310–3. doi: 10.1097/CAD.0000000000000876
30. Watanabe H, Ohashi K, Nishii K, Seike K, Makimoto G, Hotta K, et al. A Long-Term Response to Nivolumab in a Case of PD-L1-Negative Lung Adenocarcinoma With an EGFR Mutation and Surrounding PD-L1-Positive Tumor-Associated Macrophages. *Intern Med* (2019) 58(20):3033–7. doi: 10.2169/internalmedicine.2875-19
31. Kunimasa K, Nakamura H, Sakai K, Kimura M, Inoue T, Tamiya M, et al. Heterogeneity of EGFR-Mutant Clones and PD-L1 Highly Expressing Clones Affects Treatment Efficacy of EGFR-TKI and PD-1 Inhibitor. *Ann Oncol* (2018) 29(10):2145–7. doi: 10.1093/annonc/mdy312
32. Roca E, Pozzari M, Vermi W, Tovazzi V, Baggi A, Amoroso V, et al. Outcome of EGFR-Mutated Adenocarcinoma NSCLC Patients With Changed Phenotype to Squamous Cell Carcinoma After Tyrosine Kinase Inhibitors: A Pooled Analysis With an Additional Case. *Lung Cancer* (2019) 127:12–8. doi: 10.1016/j.lungcan.2018.11.016
33. Chen X, Ma L, Wang X, Mo H, Wu D, Lan B, et al. Reactive Capillary Hemangiomas: A Novel Dermatologic Toxicity Following Anti-PD-1 Treatment With SHR-1210. *Cancer Biol Med* (2019) 16(1):173–81. doi: 10.20892/j.issn.2095-3941.2018.0172
34. Song Y, Wu J, Chen X, Lin T, Cao J, Liu Y, et al. A Single-Arm, Multicenter, Phase II Study of Camrelizumab in Relapsed or Refractory Classical Hodgkin Lymphoma. *Clin Cancer Res* (2019) 25(24):7363–9. doi: 10.1158/1078-0432.CCR-19-1680

Conflict of Interest: The authors declare that the research was conducted in the absence of any commercial or financial relationships that could be construed as a potential conflict of interest.

Publisher's Note: All claims expressed in this article are solely those of the authors and do not necessarily represent those of their affiliated organizations, or those of the publisher, the editors and the reviewers. Any product that may be evaluated in

this article, or claim that may be made by its manufacturer, is not guaranteed or endorsed by the publisher.

Copyright © 2022 Jin, Wang, Wang and Lin. This is an open-access article distributed under the terms of the Creative Commons Attribution License (CC BY). The use, distribution or reproduction in other forums is permitted, provided the original author(s) and the copyright owner(s) are credited and that the original publication in this journal is cited, in accordance with accepted academic practice. No use, distribution or reproduction is permitted which does not comply with these terms.

frontiers in Immunology

ORIGINAL RESEARCH
published: 01 March 2022
doi: 10.3389/fimmu.2022.836338

Safety and Feasibility of Esophagectomy Following Combined Immunotherapy and Chemotherapy for Locally Advanced Esophageal Squamous Cell Carcinoma: A Propensity Score Matching Analysis

Zhi-Nuan Hong[1,2,3,4†], *Lei Gao*[1,2,3,4†], *Kai Weng*[1,2,3,4†], *Zhixin Huang*[1,2,3,4], *Wu Han*[1,2,3,4] *and Mingqiang Kang*[1,2,3,4*]

[1] Department of Thoracic Surgery, Fujian Medical University Union Hospital, Fuzhou, China, [2] Key Laboratory of Cardio-Thoracic Surgery (Fujian Medical University), Fujian Province University, Fuzhou, China, [3] Key Laboratory of Ministry of Education for Gastrointestinal Cancer, Fujian Medical University, Fuzhou, China, [4] Fujian Key Laboratory of Tumor Microbiology, Fujian Medical University, Fuzhou, China

OPEN ACCESS

Edited by:
Hubing Shi,
Sichuan University, China

Reviewed by:
Chen-Yuan Lin,
China Medical University Hospital, Taiwan
Cheng Zhan,
Fudan University, China

***Correspondence:**
Mingqiang Kang
kangmingqiang0799@163.com

†These authors have contributed equally to this work and share first authorship

Specialty section:
This article was submitted to Cancer Immunity and Immunotherapy, a section of the journal Frontiers in Immunology

Received: 15 December 2021
Accepted: 31 January 2022
Published: 01 March 2022

Citation:
Hong Z-N, Gao L, Weng K, Huang Z, Han W and Kang M (2022) Safety and Feasibility of Esophagectomy Following Combined Immunotherapy and Chemotherapy for Locally Advanced Esophageal Squamous Cell Carcinoma: A Propensity Score Matching Analysis. Front. Immunol. 13:836338. doi: 10.3389/fimmu.2022.836338

Objectives: The combination of neoadjuvant chemotherapy and immunotherapy (nICT) is a novel treatment for locally advanced esophageal cancer. There is concern that nICT may increase operation difficulty, postoperative morbidity, and mortality. This study aimed to compare short-term outcomes among esophagectomy after neoadjuvant chemoradiotherapy (nCRT) and nICT and for locally advanced esophageal squamous cell carcinoma (ESCC).

Methods: A retrospective analysis of a prospectively maintained database was performed to identify patients (from January 2017 through July 2021) who underwent surgery for ESCC following neoadjuvant therapy. A 1:1 propensity score matching (PSM) with a caliper 0.05 was conducted to balance potential bias.

Results: A 1:1 PSM was conducted based on clinical stage, age, body mass index (BMI), and tumor location, and then 32 comparable pairs were matched. After PSM, age, gender, BMI, American Society of Anesthesiologists (ASA) status, smoking history, clinical stage, tumor location, lymphadenectomy field, pathological stage, anastomotic position, route of gastric conduit, procedure type, and operative approach were comparable between groups. Compared with the nICT group (median, 300 min), the operation time was significantly longer in the nCRT group (median, 376 min). However, both groups were comparable in intraoperative blood loss, thoracic drainage volume, intensive care unit (ICU) stay, postoperative hospital stays, and hospital cost. Further, 30-day mortality, 30-day readmission, ICU readmission, and major complications were similar in both groups. The nCRT group had an advantage in pathological response. The pathological complete response (pCR) was 18.8% (6/32) in the nICT group and 43.8% (14/32) in the

nCRT group (p = 0.03). The major pathological response (MPR) was 71.9% (23/32) in the nCRT group and 34.4% (11/32) in the nICT group (p = 0.03).

Conclusions: Based on our preliminary experience, esophagectomy appears to be safe and feasible following combined neoadjuvant immunotherapy with chemotherapy for locally advanced esophageal cancer.

Keywords: esophagectomy, neoadjuvant chemotherapy and immunotherapy, neoadjuvant chemoradiotherapy, esophageal squamous cell carcinoma, propensity score matching (PSM)

BACKGROUND

Esophageal cancer (EC) is one of the most common and challenging types of cancer with 572,000 new diagnosis cases and 500,000 deaths annually. More than 50% of EC occurred in East Asia, and 90% of those patients have esophageal squamous cell carcinoma (ESCC) (1, 2). Esophagectomy plays an important role in the treatment of locally advanced EC. However, esophagectomy alone is often associated with high recurrence and metastasis rates reaching up to 43.3%–50.0% (3).

Neoadjuvant chemotherapy (nCT) or neoadjuvant chemoradiotherapy (nCRT) plus surgery had been applied to improve long-term results. Kamarajah et al. reported that nCT or nCRT followed by surgery for esophageal adenocarcinoma were equal in 5-year survival rates, and nCRT followed by surgery had an advantage in 5-year survival rates for ESCC (4). Currently, nCRT plus esophagectomy is recommended as first-line therapy for locally advanced ESCC (5). However, based on the long-term result of NEOCRTEC5010 Randomized Clinical Trial, the 5-year cumulative incidence of locoregional recurrence, distant recurrence, and overall recurrence in the nCRT group were 15.3%, 24.3%, and 32.2%, respectively, in locally advanced ESCC, which were still not promising (6). Further, a meta-analysis showed that compared with the surgery alone group, nCRT followed by surgery had an increased risk of total postoperative mortality and treatment-related mortality in patients diagnosed with ESCC (7). Thus, it is necessary to explore the novel pattern of neoadjuvant therapy for ESCC.

Based on CheckMate 577 trails results, Kelly et al. reported that nivolumab adjuvant therapy could prolong 11.4 months of disease-free survival among patients with resected esophageal or gastroesophageal junction cancer who had received nCRT (8). Further, pembrolizumab (PD-1 antagonist) plus chemotherapy has been recommended as first-line therapy for advanced EC (9). Considering the antibodies against the immune inhibitory pathway of programmed death 1 (PD-1) protein or PD-1 ligand 1 (PD-L1) checkpoint inhibitors is a new mechanism for the treatment of ESCC. nCT and immunotherapy (nICT) plus surgery may bring long-term benefits to patients diagnosed with ESCC. Recently, single-arm studies have revealed that the application of nICT in patients with locally advanced ESCC is safe and effective (10, 11).

To explore a new pattern of therapy, preoperative safety and short-term outcomes are the first concern for surgeons. However, a handful of studies focused on the comparison of short-term results and pathological response between nICT and nCRT. This study compared short-term results between nICT and nCRT to evaluate the potential effect of nICT on preoperative outcomes especially surgery safety and pathology response.

METHODS

Patient Selection and Study Design

This is a retrospective review based on prospectively collected data conducted with consecutive patients who underwent esophagectomy followed nICT or nCRT for ESCC at Fujian Medical University Union Hospital from January 2017 to April 2021. This study was approved by the Ethics Committee of the Fujian Medical University Union Hospital, China (YF033-01). Inclusion criteria included aged between 18 and 75 years old; diagnosed with ESCC; receiving nICT or nCRT following esophagectomy; staged with cT1N1-3M0 or cT2-4aN0-3M0; and with normal hematologic, hepatic, and renal function. Exclusion criteria included patients with non-resectable tumors or metastases during exploratory surgery; patients receiving nCT or other targeted therapy; patients receiving salvage surgery; and patients with palliative surgery.

Neoadjuvant Treatment Protocols

Patients in the nICT group received 2–4 cycles of intravenous PD-1 inhibitor (sintilimab at a dose of 200 mg, pembrolizumab at a dose of 200 mg, toripalimab at a dose of 240 mg, and camrelizumab at a dose of 200 mg) every 3 weeks (day 1) and simultaneous chemotherapy consisted of platinum-based drugs and paclitaxel (TP regimen). The details of the regimen are as follows: cisplatin (60 mg/m^2) on day 1, albumin-bound paclitaxel (125 mg/m^2) on days 1 and 8, and sintilimab/pembrolizumab/camrelizumab (200 mg) on day 1 were administered intravenously during each cycle (of 21-day duration). Docetaxel (75 mg/m^2), cisplatin (60 mg/m^2), and toripalimab (240 mg) were administered intravenously during each cycle (of 21-day duration) on day 1. Corticosteroids, thyroid function [including T3, T4, and thyroid-stimulating hormone (TSH)], glucose, and myocardial enzyme were routinely examined before each cycle of nICT for early detection of immunotherapy-related adverse events. When grade 2 above immunotherapy-related events occurred, we stopped the application of nICT and prioritized the management of adverse reactions. For patients who successfully received two cycles of neoadjuvant therapy, we conducted another clinical evaluation, followed by a

multidisciplinary consultation to determine whether the patient should undergo surgery or continue treatment.

Patients in the nCRT group received chemotherapy (paclitaxel or 5-fluorouracil plus platinum) concurrent radiotherapy, which consisted of 40–56 Gy in daily fractions of 1.8 Gy five times a week. Radiation targets are mapped on CT using all diagnostic information by an experienced radiation oncologist.

Surgery Protocols

For patients suitable for radical esophagectomy after clinical evaluation, the surgery was performed within 4–8 weeks from the end of the last neoadjuvant treatment if there were no contraindications for surgery treatment. Patients received McKeown minimally invasive esophagectomy (MIE) with or without robot-assisted, including 2-field or 3-field lymphadenectomy and gastric reconstruction. We regularly conducted 2-field lymphadenectomy, and standard three-field lymphadenectomy was performed in patients with suspected swollen lymph nodes in the neck. During the operation, patients with severe adhesion or intraoperative bleeding were transferred to thoracotomy. All operations were conducted by experienced surgeons with more than 50 cases annually, which ensured the surgery quality.

Outcome Measures

Postoperative complications were coded by Clavien–Dindo classification, and Clavien–Dindo classification grade $\geqq 3$ was defined as major complications. The comprehensive complication index (CCI) applied as a tool to evaluate complications systematically was calculated at www.assessurgery.com (12). The primary end point was 30-day complications (including pneumonia, anastomotic leakage, pleural infusion, chylothorax, and cardiac events). Secondary end points included pathological response, operation time, postoperative thoracic drainage, thoracic drainage tube stay, 30-day readmission rate, and 30-day mortality. Interval to surgery was defined as the last measured from the end of last neoadjuvant treatment to the date of surgery, and operative time was measured from incision to wound closure. Intensive care unit (ICU) stay was defined from the day of into ICU to the day of leaving the ICU. Postoperative hospital stay was defined from the day of operation to the day of leaving Fujian Medical University Union Hospital.

The pathological TNM stage was staged according to the 8th edition of the American Joint Committee on Cancer/Union for International Cancer Control staging system. Major pathological reaction (MPR) was defined as less than 10% residual tumor cells, and pathological complete response (pCR) was defined as evidence of no residual tumor cells.

Statistical Analysis

Patients were classified into two groups based on neoadjuvant therapy patterns. Propensity score matching (PSM) was calculated based on a logistic regression model, with a caliper 0.05, matching ratio = 1:1 to balance potential bias. The minor mirror histogram of propensity scores is listed to show the matching details (13, 14). The continuous variables were expressed as median (quartile difference), and the categorical variables were expressed as numbers (percentage). χ^2 test was used for classification data, and Mann–Whitney U test was used for anomaly distribution data comparison. Statistical analysis was performed in R Version 4.0.4 (R Foundation for Statistical Computing, Vienna, Austria). Bilateral p-values <0.05 were considered significant.

RESULTS

Patient Selection and Baseline Characteristics

The patient selection chart and PSM details are shown in **Figure 1**. A total of 52 patients in the nICT group and 35

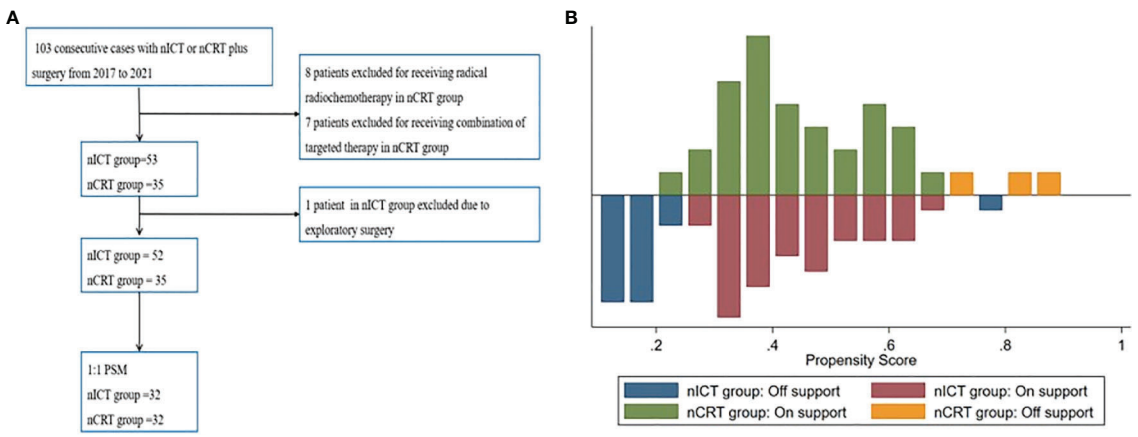

FIGURE 1 | **(A)** Patient selection flowchart. **(B)** Mirror histogram of propensity scores for patients. PSM, propensity score matching; nICT, neoadjuvant chemotherapy and immunotherapy; nCRT, neoadjuvant chemoradiotherapy.

patients in the nCRT group were included for further analysis. Then, to balance the potential bias, a 1:1 PSM was conducted based on clinical stage, age, body mass index (BMI), and tumor location. Finally, 32 comparable pairs were matched.

The baseline characteristics after PSM with 32 patients in each group are summarized in **Table 1**. After PSM, the clinical and demographic characteristics of the two groups were well balanced, including age, gender, BMI, American Society of Anesthesiologists (ASA) status, hypertension history, smoking history, tumor location, preoperative albumin, preoperative hemoglobin, forced expiratory volume in 1 s (FEV1), ejection fractions (EF), lymphadenectomy filed, clinical stage, histologic subtype, anastomotic position, route of gastric conduit, procedure type, clinical stage, and operative approach.

Comparisons of Short-Term Outcomes

All patients in both the nICT group and nCRT group successfully received MIE without conversion into thoracotomy, although lymph nodes moved number in the nICT group (median 39) was more than that in the nCRT group (median 32). However, compared with the nICT group (319.2 ± 80.2 min), the operation time was significantly longer in the nCRT group (378.8 ± 72.7 min). Both groups were comparable in intraoperative blood loss, thoracic drainage tube stays, thoracic drainage volume, postoperative hospital stay, and hospital cost. Further, 30-day mortality, 30-day readmission, and ICU readmission were also similar in both groups. Compared with the nICT group, the nCRT group had an advantage in pathological response. The pCR was 18.8% (6/32) in the nICT group and 43.8% (14/32) in the nCRT group (p = 0.03). The major pathological response (MPR) was 71.9% (23/32) in the nCRT group and 34.4% (11/32) in the nICT group (p = 0.03). Perioperative outcomes after PSM were summarized in **Table 2**.

The complications within 30-day after PSM are summarized in **Table 3**. The incidence of pneumonia, pleural effusion, palsy of recurrent laryngeal nerve, chylothorax, and postoperative blood transfusion were comparable in both groups. Major complications and CCI were comparable in both groups. Comparison details of 30-day major complications and CCI after PSM are listed in **Figure 2**.

TABLE 1 | Baseline characteristic before and after propensity score matching.

Characteristics	Before PSM			After PSM		
	nICT	nCRT	*p*	nICT	nCRT	*p*
Number	52	35		32	32	
Age	62 (56, 67)	59 (54, 65)	0.36	62 (55, 67)	60 (54, 65)	0.68
Male	39	29	0.38	21	27	0.08
BMI	22.0 (20.3, 22.7)	22.0 (20.5, 23.7)	0.76	22.0 (19.6, 22.8)	22.0 (20.7, 23.7)	0.46
ASA			0.16			0.72
≤2	47	28		27	28	
≥3	5	7		5	4	
Diabetes	5	0	0.07	3	0	0.07
Hypertension	10	3	0.17	7	2	0.07
Smoking history	30	21	0.83	15	21	0.13
FEV1	2.6 (1.9, 3.1)	2.6 (2.4, 3.0)	0.65	2.6 (1.9, 3.1)	2.6 (2.4, 3.0)	0.76
EF%	67.7 (64.1, 71.4)	66.3 (61.9, 69.4)	0.22	68.4 (64.1, 71.5)	66.3 (61.9, 69.4)	0.19
Preoperative Hb (g/L)	125 (112, 133)	126 (113, 135)	0.82	121 (105, 133)	127 (114, 133)	0.38
Preoperative albumin (g/l)	40.2 (37.7, 43.2)	40.8 (38.1, 43.9)	0.48	39.7 (36.6, 44.0)	41.2 (39.2, 43.9)	0.18
Tumor location			0.012			0.51
Upper third	3	4		2	1	
Middle third	30	28		29	28	
Lower third	19	3		1	3	
cTNM before neoadjuvant therapy			0.12			0.43
≤2	14	15		10	13	
≥3	38	20		12	19	
Lymphadenectomy			0.07			0.27
2-field	43	23		25	21	
3-field	9	12		7	11	
Anastomotic position			1.00			1.00
Cervical	52	32		32	32	
Thoracic	0	0		0	0	
Route of gastric conduit			0.66			0.23
Posterior mediastinal	46	32		27	30	
Restro-sternal	6	3		5	2	
Procedure type			0.93			1.00
Robot-assisted	10	7		6	6	
Video-assisted	42	28		26	26	

ASA, American Society of Anesthesiologists; BMI, body mass index; nICT, neoadjuvant chemotherapy and immunotherapy; nCRT, neoadjuvant chemoradiotherapy; Hb, hemoglobin, FEV1, forced expiratory volume in 1 s; EF, ejection fractions; PSM, propensity score matching.

TABLE 2 | Perioperative outcomes after propensity score matching.

Outcomes	nICT group	nCRT group	*p*
Operative time (min)	300 (270, 382)	376 (330, 413)	0.003
Converted to open surgery in thoracic procedure	0	0	NA
Intraoperative blood loss (ml)	100 (50, 100)	100 (100, 150)	0.33
Lymph nodes moved number	39 (33, 49)	32 (27, 36)	0.013
Thoracic drainage tube stays (days)	8 (7, 11)	8 (7, 10)	0.87
Thoracic drainage volume (ml)	1,235 (832, 1,625)	1,148 (550, 2,136)	0.75
ICU readmission (n)	1	0	0.31
30-day mortality (n)	0	1	0.31
30-day readmission (n)	2	4	0.39
postoperative hospital stays (days)	11 (8, 14)	9 (8, 11)	0.17
CCI	20.9 (12.2, 31.4)	22.6 (8.7, 28.9)	0.36
Hospital cost (10,000 RMB)	8.9 (8.0, 10.3)	8.2 (6.7, 10.2)	0.095
Pathological response			
pCR	6	14	0.03
pCR+MPR	11	23	0.03

ICU, intense care unit; CCI, comprehensive complication index; nICT, neoadjuvant chemotherapy and immunotherapy; nCRT, neoadjuvant chemoradiotherapy; pCR, pathological complete response; MPR, major pathological response; NA, not applicable.

TABLE 3 | Postoperative complications within 30-day after operation evaluated by Clavien–Dindo classification.

Complications	nICT Group	nCRT Group	*p*
Pneumonia			
≥Grade 2	13	9	0.29
≥Grade 3	9	7	0.33
Anastomotic leakage			
≥Grade 2	2	1	0.55
≥Grade 3	0	0	NA
Pleural effusion			
≥Grade 2	14	9	0.19
≥Grade 3	7	9	0.56
Palsy of recurrent laryngeal nerve			
≥Grade 1	0	0	NA
Cardiac events			
≥Grade 1	8	4	0.20
≥Grade 2	5	4	0.72
Chylothorax			
≥Grade 1	3	2	0.64
≥Grade 2	0	2	0.15
≥Grade 3	0	1	0.31
Postoperative blood transfusion			0.55
Grade 2	2	1	

nICT, neoadjuvant chemotherapy and immunotherapy; nCRT, neoadjuvant chemoradiotherapy; NA, not applicable.

Immune-Related Adverse Events

Immune dermatitis was relatively common, with an incidence of 6.25% (2/32). Only one patient underwent grade 3 pneumonitis on the 10th day after the operation. This patient was admitted into ICU and treated with 40 mg of methylprednisolone for 7 days. Then, the symptoms were relieved, and this patient recovered without intubation. The chest scan changes are summarized in **Figure 3**.

DISCUSSION

Compared with the nICT group (median, 300 min), the operation time was significantly longer in the nCRT group (median, 376 min). The 30-day complications measured by CCI and major complications were comparable between the nICT group and nCRT group after PSM. The 30-day mortality, 30-day readmission, and ICU readmission were similar in both groups. The nCRT group had an advantage in both pCR and MPR ($p < 0.03$).

The postoperative mortality and morbidity were comparable between the nICT group and the nCRT group. Additional neoadjuvant immunotherapy did not increase postoperative mortality and morbidity, and our finding was consistent with the previous report. Sihag et al. compared the major complications between patients receiving neoadjuvant immunotherapy and chemoradiotherapy and nCRT and found that additional neoadjuvant immunotherapy was not associated with a statistically significantly increased risk of developing major complications (including pulmonary complications, anastomotic

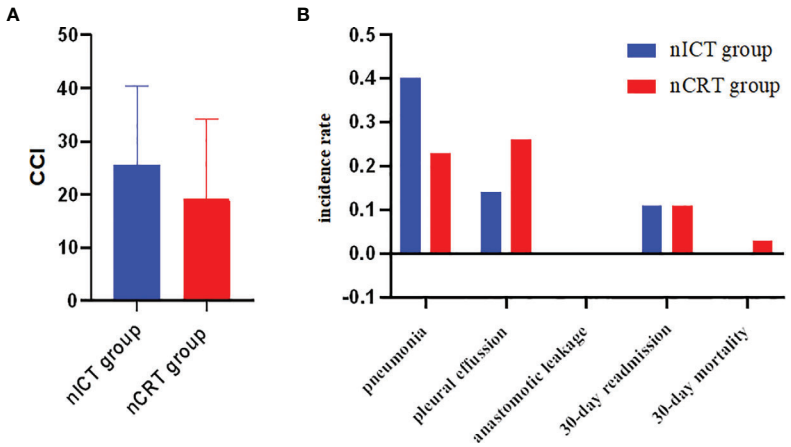

FIGURE 2 | **(A)** Comparisons of CCI between nICT group and nCRT group after PSM. **(B)** Comparisons of major complications between nICT group and nCRT group after PSM. CCI, comprehensive complication index; nICT, neoadjuvant chemotherapy and immunotherapy; nCRT, neoadjuvant chemoradiotherapy; PSM, propensity score matching.

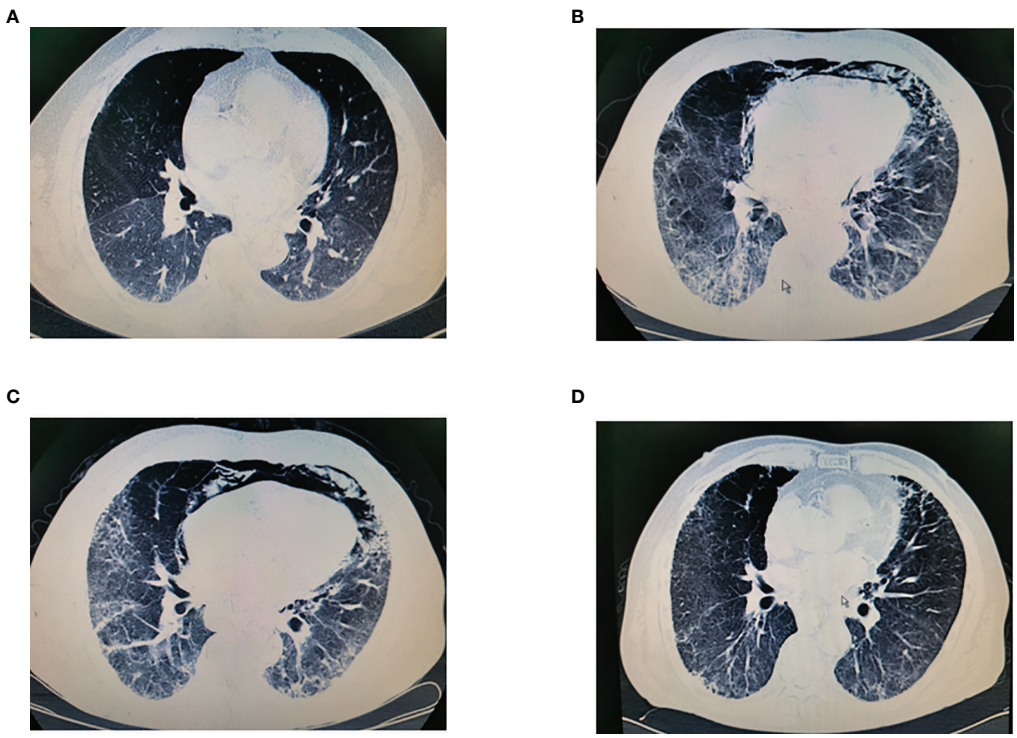

FIGURE 3 | **(A)** Chest CT scan before surgery. **(B)** Chest scan on 5th day after operation. **(C)** Chest scan after application of methylprednisolone for 7 days. **(D)** Chest scan in 3 months after discharge.

leakage, and other complications) (15). However, additional neoadjuvant immunotherapy brings additional immune-related AEs. In this study, one patient had grade 3 pneumonitis on the 7th day after the operation and finally recovered by administration of methylprednisolone treatment. A recent meta-analysis including 12,876 patients from 23 randomized control trials showed that the incidence of pneumonitis associated with PD-1 inhibitors was 5.17%, with an incidence of grade 3–5 pneumonitis of 4.14% (16). The time to onset pneumonitis had a really wide time window ranging from 9 days to 19.2 months (17). Pneumonia is one of the

most common complications after esophagectomy. However, due to the various radiological subtypes of pneumonia, sometimes distinguishing pneumonia from pneumonitis is really a challenge. Thus, it is necessary to be vigilant for the incidence of pneumonitis when patients' symptoms do not correspond to sputum, serum etiology, and inflammatory markers. Antibiotic treatment is recommended before pneumonitis is diagnosed.

Operation time is an indicator of surgical difficulty, and moved lymph number is an indicator of surgical quality in esophagectomy. Operation time in the nCRT group was longer than that in the nCRT group, and moved lymph nodes in nICT were more than that in the nCRT group (both above 15), although previous studies indicated that surgical resection of non-small cell lung cancer (NSCLC) following neoadjuvant immunotherapy increased surgical difficulty and challenge due to dense fibrosis, especially in mediastinal and hilar dissection (18, 19). Further, there was also a possibility of unexpected conversion into thoracotomy in patients following immunotherapy (20). For patients with NSCLC, there was a reduction of moved lymph nodes in the neoadjuvant immunotherapy group (21). However, there was still no similar report in esophagectomy following nICT. In this study, all patients in the nICT group received McKeown MIE without any transformation thoracotomy. We admitted that after the application of nICT, the primary tumor shrunk, and there was fibrous scarring in the esophageal mesentery, which led to difficulty in distinguishing the boundary between the tumor and surrounding organs or tissues. Clinical practice showed that after nICT, the fibrosis was not dense, and for experienced surgeons, MIE was still applicable. For patients receiving nCRT, the primary tumor site of esophageal cancer often exhibits necrosis, fibrosis, and organizational alterations (**Figure 4**). Further, in some cases, the normal tissue gap disappears and transforms into dense fibrosis. Adhesive fibrosis is more serious in patients with obvious tumor invasion before radiotherapy (22). Thus, resection in the nCRT group is more difficult and requires more time to separate the esophagus from surrounding tissues and organs. In summary, for resection following nICT or nCRT, the surgical procedures have high technical requirements for surgeons. Such procedures should be conducted by experienced surgeons. Based on the present evidence, it seems that compared with nCRT, esophagectomy following nICT had a lower operation difficulty.

The nCRT group had an advantage in pathological response. The pCR rate was 18.8% (6/32) in the nICT group and 43.8% (14/32) in the nCRT group ($p = 0.03$). pCR was proved to be associated with long-term survival. Kamarajah et al. analyzed the National Cancer Database (2006–2015) including 2,367 with ESCC (nCRT 2,155 and nCT 212) and found that for ESCC, nCRT followed by surgery had advantage in pCR rate (50.9% versus 30.4%; $p < 0.001$), margin-negative resections (92.8% versus 82.4%, $p < 0.001$), and a statistically significant overall survival benefit (hazard ratio (HR) 0.78, 0.62 to 0.97) (23). A recent meta-analysis including 4,529 patients (nCT 2,035 and nCRT 2,494) showed that compared with nCT, nCRT could provide a higher 3-year survival benefit, higher R0 resection, and

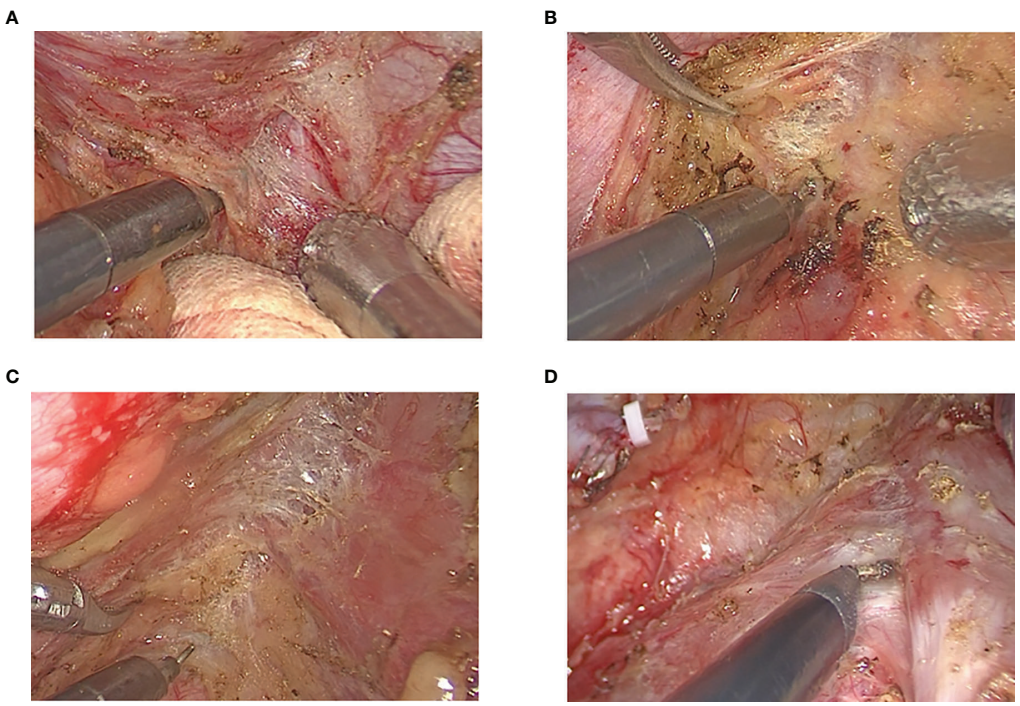

FIGURE 4 | **(A)** Fibrosis in esophageal mesentery near primary tumor. **(B)** Fibrosis in esophageal mesentery near pericardium. **(C)** Fibrosis in esophageal mesentery near thoracic aorta. **(D)** Fibrosis in esophageal mesentery near trachea.

pCR rates, but no increase in 5-year survival (24). Zhang et al. conducted a propensity score-matched study from the National Cancer Center to compare the long-term results between nCRT and nCT and found that significantly higher pCR rates in the nCRT group did not lead to a longer survival (25). Thus, considering the different mechanisms of immunotherapy, it is worth conducting a long-term follow-up to evaluate the effect of nICT. Whether nICT could challenge nCRT or nCT in the first-line treatment of locally advanced ESCC requires the evaluation of long-term results in a cohort with a sufficient sample size.

To our best knowledge, this is the first study that compares the short-term outcomes between nICT and nCRT. We tried to solve the potential selection and detection bias by strict patient selection and PSM. However, this study was still limited by its retrospective nature, and it was also only conducted in a single institution with a relatively limited case number. Due to the lack of patients' compliance and the quality control of radiotherapy, the application of nCRT was relatively limited, and nCT was a more popular pattern in China. Some patients received nCRT in other hospitals and then received surgery in our institution. Thus, the case number of the nCRT group in our institution was limited with potential bias. We used pCR to evaluate the antitumor effect of neoadjuvant therapy. Although pCR has been proved to be associated with long-term survival, long-term follow-up is necessary for further confirming the effect of nICT. To determine whether nICT could challenge the status of nCRT in the treatment of locally advanced ESCC and to establish a new treatment model based on immunotherapy, there is an urgent need for more phase III clinical trials and more convincing research results.

CONCLUSION

Compared with nCRT, esophagectomy following nICT had a lower operation difficulty, similar postoperative complications, and similar mortality. Esophagectomy following nICT is safe and feasible for locally advanced ESCC. Long-term follow-up is necessary to evaluate the effect of nICT.

DATA AVAILABILITY STATEMENT

The raw data supporting the conclusions of this article will be made available by the authors, without undue reservation.

ETHICS STATEMENT

The studies involving human participants were reviewed and approved by Fujian Medical University Union Hospital. The patients/participants provided their written informed consent to participate in this study.

AUTHOR CONTRIBUTIONS

Z-NH conceived the concept and coordinated the design. Z-NH drafted the manuscript with significant contributions from LG and KW. All authors listed have made a substantial, direct, and intellectual contribution to the work and approved it for publication.

FUNDING

This study was sponsored by the Key Laboratory of Cardio-Thoracic Surgery (Fujian Medical University), Fujian Province University.

ACKNOWLEDGMENTS

We deeply appreciate Toedit for its excellent language service.

REFERENCES

1. Chen W, Zheng R, Baade PD, Zhang S, Zeng H, Bray F, et al. Cancer Statistics in China, 2015. *CA Cancer J Clin* (2016) 66(2):115–32. doi: 10.3322/caac.21338
2. He F, Wang J, Liu L, Qin X, Wan Z, Li W, et al. Esophageal Cancer: Trends in Incidence and Mortality in China From 2005 to 2015. *Cancer Med* (2021) 10 (5):1839–47. doi: 10.1002/cam4.3647
3. Lagergren J, Smyth E, Cunningham D, Lagergren P. Oesophageal Cancer. *Lancet* (2017) 390(10110):2383–96. doi: 10.1016/S0140-6736(17)31462-9
4. Ajani JA, D'Amico TA, Bentrem DJ, Chao J, Corvera C, Das P, et al. Esophageal and Esophagogastric Junction Cancers, Version 2.2019, NCCN Clinical Practice Guidelines in Oncology. *J Natl Compr Canc Netw* (2019) 17 (7):855–83. doi: 10.6004/jnccn.2019.0033
5. van Hagen P, Hulshof MC, van Lanschot JJ, Steyerberg EW, van Berge Henegouwen MI, Wijnhoven BP, et al. Preoperative Chemoradiotherapy for Esophageal or Junctional Cancer. *N Engl J Med* (2012) 366(22):2074–84. doi: 10.1056/NEJMoa1112088
6. Yang H, Liu H, Chen Y, Zhu C, Fang W, Yu Z, et al. Neoadjuvant Chemoradiotherapy Followed by Surgery Versus Surgery Alone for Locally Advanced Squamous Cell Carcinoma of the Esophagus (NEOCRTEC5010): A Phase III Multicenter, Randomized, Open-Label Clinical Trial. *J Clin Oncol* (2018) 36(27):2796–803. doi: 10.1200/JCO.2018.79.1483
7. Ando N, Kato H, Igaki H, Shinoda M, Ozawa S, Shimizu H, et al. A Randomized Trial Comparing Postoperative Adjuvant Chemotherapy With Cisplatin and 5-Fluorouracil Versus Preoperative Chemotherapy for Localized Advanced Squamous Cell Carcinoma of the Thoracic Esophagus (JCOG9907). *Ann Surg Oncol* (2012) 19(1):68–74. doi: 10.1245/s10434-011-2049-9
8. Yarchoan M, Johnson BA3rd, Lutz ER, Laheru DA, Jaffee EM. Targeting Neoantigens to Augment Antitumour Immunity. *Nat Rev Cancer* (2017) 17 (9):569. doi: 10.1038/nrc.2017.74
9. Smyth EC, Gambardella V, Cervantes A, Fleitas T. Checkpoint Inhibitors for Gastroesophageal Cancers: Dissecting Heterogeneity to Better Understand Their Role in First-Line and Adjuvant Therapy. *Ann Oncol* (2021) 32(5):590–9. doi: 10.1016/j.annonc.2021.02.004
10. Shen D, Chen Q, Wu J, Li J, Tao K, Jiang Y. The Safety and Efficacy of Neoadjuvant PD-1 Inhibitor With Chemotherapy for Locally Advanced Esophageal Squamous Cell Carcinoma. *J Gastrointest Oncol* (2021) 12(1):1–10. doi: 10.21037/jgo-20-599
11. Yang G, Su X, Yang H, Luo G, Gao C, Zheng Y, et al. Neoadjuvant Programmed Death-1 Blockade Plus Chemotherapy in Locally Advanced

Esophageal Squamous Cell Carcinoma. *Ann Transl Med* (2021) 9(15):1254. doi: 10.21037/atm-21-3352
12. Slankamenac K, Graf R, Barkun J, Puhan MA, Clavien PA. The Comprehensive Complication Index: A Novel Continuous Scale to Measure Surgical Morbidity. *Ann Surg* (2013) 258(1):1–7. doi: 10.1097/SLA.0b013e318296c732
13. Zhan C, Yang X, Song X, Yan L. Radiotherapy vs Surgery for T1-2N0M0 Laryngeal Squamous Cell Carcinoma: A Population-Based and Propensity Score Matching Study. *Cancer Med* (2018) 7(7):2837–47. doi: 10.1002/cam4.1525
14. Yang X, Sun F, Chen L, Shi M, Shi Y, Lin Z, et al. Prognostic Value of Visceral Pleural Invasion in non-Small Cell Lung Cancer: A Propensity Score Matching Study Based on the SEER Registry. *J Surg Oncol* (2017) 116(3):398–406. doi: 10.1002/jso.24677
15. Sihag S, Ku GY, Tan KS, Nussenzweig S, Wu A, Janjigian YY, et al. Safety and Feasibility of Esophagectomy Following Combined Immunotherapy and Chemoradiotherapy for Esophageal Cancer. *J Thorac Cardiovasc Surg* (2021) 161(3):836–43.e1. doi: 10.1016/j.jtcvs.2020.11.106
16. Su Q, Zhu EC, Wu JB, Li T, Hou YL, Wang DY, et al. Risk of Pneumonitis and Pneumonia Associated With Immune Checkpoint Inhibitors for Solid Tumors: A Systematic Review and Meta-Analysis. *Front Immunol* (2019) 10:108. doi: 10.3389/fimmu.2019.00108
17. Naidoo J, Wang X, Woo KM, Iyriboz T, Halpenny D, Cunningham J, et al. Pneumonitis in Patients Treated With Anti-Programmed Death-1/Programmed Death Ligand 1 Therapy. *J Clin Oncol* (2017) 35(7):709–17. doi: 10.1200/JCO.2016.68.2005
18. Kitagawa S, Hakozaki T, Kitadai R, Hosomi Y. Switching Administration of Anti-PD-1 and Anti-PD-L1 Antibodies as Immune Checkpoint Inhibitor Rechallenge in Individuals With Advanced Non-Small Cell Lung Cancer: Case Series and Literature Review. *Thorac Cancer* (2020) 11(7):1927–33. doi: 10.1111/1759-7714.13483
19. Chaft JE, Hellmann MD, Velez MJ, Travis WD, Rusch VW. Initial Experience With Lung Cancer Resection After Treatment With T-Cell Checkpoint Inhibitors. *Ann Thorac Surg* (2017) 104(3):e217–8. doi: 10.1016/j.athoracsur.2017.03.038
20. Bott MJ, Cools-Lartigue J, Tan KS, Dycoco J, Bains MS, Downey RJ, et al. Safety and Feasibility of Lung Resection After Immunotherapy for Metastatic or Unresectable Tumors. *Ann Thorac Surg* (2018) 106(1):178–83. doi: 10.1016/j.athoracsur.2018.02.030
21. Zhang F, Qiu B, Ji Y, Guo W, Li N, Xue Q, et al. Comparison of Surgical Difficulty in Patients With Resectable Non-Small Cell Lung Cancer Under Different Neoadjuvant Treatment Modes: A Retrospective Cohort Study. *J Thorac Dis* (2021) 13(10):5604–16. doi: 10.21037/jtd-21-1007
22. Liu G, Han Y, Peng L, Wang K, Fan Y. Reliability and Safety of Minimally Invasive Esophagectomy After Neoadjuvant Chemoradiation: A Retrospective Study. *J Cardiothorac Surg* (2019) 14(1):97. doi: 10.1186/s13019-019-0920-0
23. Kamarajah SK, Phillips AW, Ferri L, Hofstetter WL, Markar SR. Neoadjuvant Chemoradiotherapy or Chemotherapy Alone for Oesophageal Cancer: Population-Based Cohort Study. *Br J Surg* (2021) 108(4):403–11. doi: 10.1093/bjs/znaa121
24. Han J, Wang Z, Liu C. Survival and Complications After Neoadjuvant Chemotherapy or Chemoradiotherapy for Esophageal Cancer: A Meta-Analysis. *Future Oncol* (2021) 17(17):2257–74. doi: 10.2217/fon-2021-0021
25. Zhang G, Zhang C, Sun N, Xue L, Yang Z, Fang L, et al. Neoadjuvant Chemoradiotherapy Versus Neoadjuvant Chemotherapy for the Treatment of Esophageal Squamous Cell Carcinoma: A Propensity Score-Matched Study From the National Cancer Center in China. *J Cancer Res Clin Oncol* (2021). doi: 10.1007/s00432-021-03659-7

Conflict of Interest: The authors declare that the research was conducted in the absence of any commercial or financial relationships that could be construed as a potential conflict of interest.

Publisher's Note: All claims expressed in this article are solely those of the authors and do not necessarily represent those of their affiliated organizations, or those of the publisher, the editors and the reviewers. Any product that may be evaluated in this article, or claim that may be made by its manufacturer, is not guaranteed or endorsed by the publisher.

Copyright © 2022 Hong, Gao, Weng, Huang, Han and Kang. This is an open-access article distributed under the terms of the Creative Commons Attribution License (CC BY). The use, distribution or reproduction in other forums is permitted, provided the original author(s) and the copyright owner(s) are credited and that the original publication in this journal is cited, in accordance with accepted academic practice. No use, distribution or reproduction is permitted which does not comply with these terms.

frontiers in Public Health

ORIGINAL RESEARCH
published: 02 March 2022
doi: 10.3389/fpubh.2022.790225

Cost-Effectiveness Analysis of Pembrolizumab in Patients With Advanced Esophageal Cancer Based on the KEYNOTE-181 Study

Mei Zhan[1,2], *Ting Xu*[1], *Hanrui Zheng*[1,2] *and Zhiyao He*[1]*

[1] Department of Pharmacy, State Key Laboratory of Biotherapy and Cancer Center, National Clinical Research Center for Geriatrics, West China Hospital, Sichuan University, Chengdu, China, [2] West China School of Pharmacy, Sichuan University, Chengdu, China

Background and Purpose: The KEYNOTE-181 study demonstrated that pembrolizumab for advanced or metastatic esophageal cancer in patients with programmed death ligand-1 (PD-L1) combined positive score (CPS) ≥ 10 had a survival advantage and better tolerability than chemotherapy. However, at the same time, pembrolizumab places an economic burden on patients. This study assessed the cost-effectiveness of pembrolizumab based on the KEYNOTE181 study.

Materials and Methods: A three-state Markov model [progression-free survival (PFS), progressive disease (PD), and death] based on data from the KEYNOTE-181 study was used to estimate the incremental cost-effectiveness ratio (ICER) of pembrolizumab versus chemotherapy for advanced or metastatic esophageal cancer. The model evaluates the outcomes from the Chinese society's perspective. Costs, quality-adjusted life-years (QALYs), and the ICER in terms of 2021 US$ per QALY gained, were calculated. one-way and probabilistic sensitivity analyses were performed to evaluate the model robustness.

Results: Compared with chemotherapy, pembrolizumab increased costs by $37,201.68, while gaining 0.23 QALYs, resulting in an ICER of $163,165.26 per QALY in patients with PD-L1 CPS ≥ 10. The ICER is $202,708.62 per QALY and $163,643.19 per QALY in the total population and patients with esophageal squamous cell carcinoma, respectively. The ICER was much higher than the commonly accepted willingness-to-pay threshold ($11,105.8 per QALY). One-way and sensitivity analyses showed that the costs of pembrolizumab and the utility of PD were the crucial factors in determining the ICER, and probabilistic sensitivity analyses demonstrated pembrolizumab is unlikely to be cost-effective at a willingness-to-pay threshold of $11,105.8 per QALY. The result was robust across sensitivity analyses.

Conclusion: Pembrolizumab is not a cost-effective treatment option for the second-line treatment of esophageal cancer from the perspective of Chinese society.

Keywords: cost-effectiveness, esophageal cancer, pembrolizumab, chemotherapy, PD-L1

OPEN ACCESS

Edited by:
Benjamin Frey,
University Hospital Erlangen, Germany

Reviewed by:
Valeria Internò,
University of Bari Aldo Moro, Italy
George Gourzoulidis,
Econcare, Greece

***Correspondence:**
Zhiyao He
heyaode@163.com;
zhiyaohe@scu.edu.cn

Specialty section:
This article was submitted to Health Economics, a section of the journal Frontiers in Public Health

Received: *06 October 2021*
Accepted: *28 January 2022*
Published: *02 March 2022*

Citation:
Zhan M, Xu T, Zheng H and He Z (2022) Cost-Effectiveness Analysis of Pembrolizumab in Patients With Advanced Esophageal Cancer Based on the KEYNOTE-181 Study. Front. Public Health 10:790225. doi: 10.3389/fpubh.2022.790225

INTRODUCTION

Esophageal cancer is a highly lethal malignancy, with 604,100 new cases and 544,076 deaths in 2020 (1). The incidence of esophageal cancer in Eastern Asia is higher when compared to the world (1, 2). China was a high-incidence area of esophageal cancer and accounted for about half of the global morbidity and mortality (3). The prognosis of esophageal cancer is improving but remains poor, with an overall 5-year survival rate of about 20% (4, 5). Approximately 39% of esophageal cancer with distant metastases at initial diagnosis and the 5-year relative survival for these esophageal cancers is about 5% (6). Although targeted drugs have demonstrated efficacy in many cancers, no targeted drugs are approved for esophageal squamous cell carcinoma. Until immune checkpoint inhibitors were approved for esophageal cancer, the treatment after first-line was limited. The goal of second-line treatment for metastatic esophageal cancer was to palliate symptoms. Unresectable, locally advanced, or metastatic esophageal cancer are not curable. Esophageal cancer contributed to a massive burden on public health care systems in China (7).

Esophageal squamous cell carcinoma is the predominant histology in China. The superiority of pembrolizumab over chemotherapy for second-line therapy in patients with metastatic esophageal squamous cell carcinoma, as well as with programmed death ligand-1 (PD-L1) combined positive score (CPS) $\geq$ 10 tumors, was shown in the KEYNOTE-181 study. Based on the KEYNOTE-181 study, National Medical Products Administration and the US Food and Drug Administration approved pembrolizumab for patients with locally advanced or metastatic esophageal squamous cell carcinoma that express PD-L1 (CPS $\geq$ 10) after one prior line in China and the USA. And the National Comprehensive Cancer Network (NCCN) recommended pembrolizumab for second-line therapy for esophageal squamous cell carcinoma with PD-L1 CPS $\geq$ 10 (8).

Although the KEYNOTE-181 study demonstrated a survival advantage and better tolerability for pembrolizumab, pembrolizumab is dramatically expensive for patients and insurance payers. As such, we sought to evaluate the cost-effectiveness of pembrolizumab for advanced esophageal cancer from the Chinese society perspective.

MATERIALS AND METHODS

Patients and Regimens

The clinical information was derived from the randomized phase III, open-label KEYNOTE-181 (9). The KEYNOTE-181 study recruited adult patients with histologically confirmed, advanced, or metastatic esophageal cancer. When they progressed after first-line chemotherapy. they were randomly assigned to receive pembrolizumab 200 mg every 3 weeks or investigator's choice of treatment with paclitaxel 80–100 mg/m^2 on days 1, 8, and 15 of each 28-day cycle, docetaxel 75 mg/m^2 every 3 weeks, or irinotecan 180 mg/m^2 every 2 weeks until disease progression or the development of unacceptable toxic effects. Overall survival (OS) and progression-free survival (PFS) were evaluated in patients with PD-L1 CPS $\geq$ 10, in patients with squamous cell carcinoma, and in the total population.

Markov Model

A Markov model was constructed using Treeage software (Treeage, Williamstown, MA, USA) to evaluate the cost and quality-adjusted life-years (QALYs) of pembrolizumab and chemotherapy. The Markov model had three health states: PFS, progressive disease (PD), and death. The initial state was assumed to be PFS, and the patients could stay in their assigned health state or progress to another health state based on the transition probabilities during each Markov cycle. The model structure is shown in **Figure 1**. The cycle length was 1-month based on the time span of disease duration and progression. The 5-year survival rate was about 5% for metastatic esophageal cancer (10). Therefore, we used a 5-year time horizon in the Markov model. We calculated the incremental cost-effectiveness ratio (ICER) of pembrolizumab compared with chemotherapy, and the results are described using costs per QALY. The ICER was calculated using the following formula: ICER = ($Cost_{[the\ pembrolizumab\ group]}$ - $Cost_{[the\ chemotherapy\ group]}$)/($QALY_{[the\ pembrolizumab\ group]}$ - $QALY_{[the\ chemotherapy\ group]}$). A 3% annual discount rate was used for costs and effectiveness according to the WHO guidelines (11).

Survival Estimates and Utilities

Clinical data on efficacy and safety were obtained from the KEYNOTE-181 study (**Table 1**). The probability of being in each state was obtained by digitizing the Kaplan-Meier curves of PFS and OS from the KEYNOTE-181 study. We used Microsoft Excel (version 2016) to reconstruct the OS and PFS survival curves. Monthly transition probabilities in the reconstructed model were calibrated to best fit the Kaplan-Meier curves of OS and PFS. The monthly transition probabilities were listed in **Table 2** and the calibration curves were shown in **Figure 2**. In the KEYNOTE-181 study, they used EORTC QLQ -C30 and QLQ-OES18, eEuroQol-5D (EQ-5D) questionnaires to assess Health-related quality of life. However, there is no information about the utility scores of the PFS and PD state in the KEYNOTE-181 study. Thus, health state utility scores were derived from previously published literature. The utility values of PFS state, PD state, and death were 0.75, 0.67, and 0, respectively (12).

Cost Estimates

The direct medical costs were estimated from the perspective of Chinese society. Total costs in our analysis included costs of the drugs, tests, management of grade 3–4 adverse reactions, and follow-up. Only grade 3 or higher AEs from the KEYNOTE-181 study were used to calculate the costs of AEs, grade 1-2 AEs were considered manageable within standard patient monitoring. The cost of drugs and tests was based on the 2021 fee standards of West China Hospital, Sichuan University. We assumed that patients in the current study with a 1.72 m^2 body surface area to calculate the dosage of chemotherapy agents (13–15). After the disease progressed, the data of patients who received subsequent treatment was insufficient from the KEYNOTE-181 study. Hence, the costs of subsequent-line therapy were derived from a previously published study (16). The details of the cost information are provided in **Table 3**. The WHO guidelines

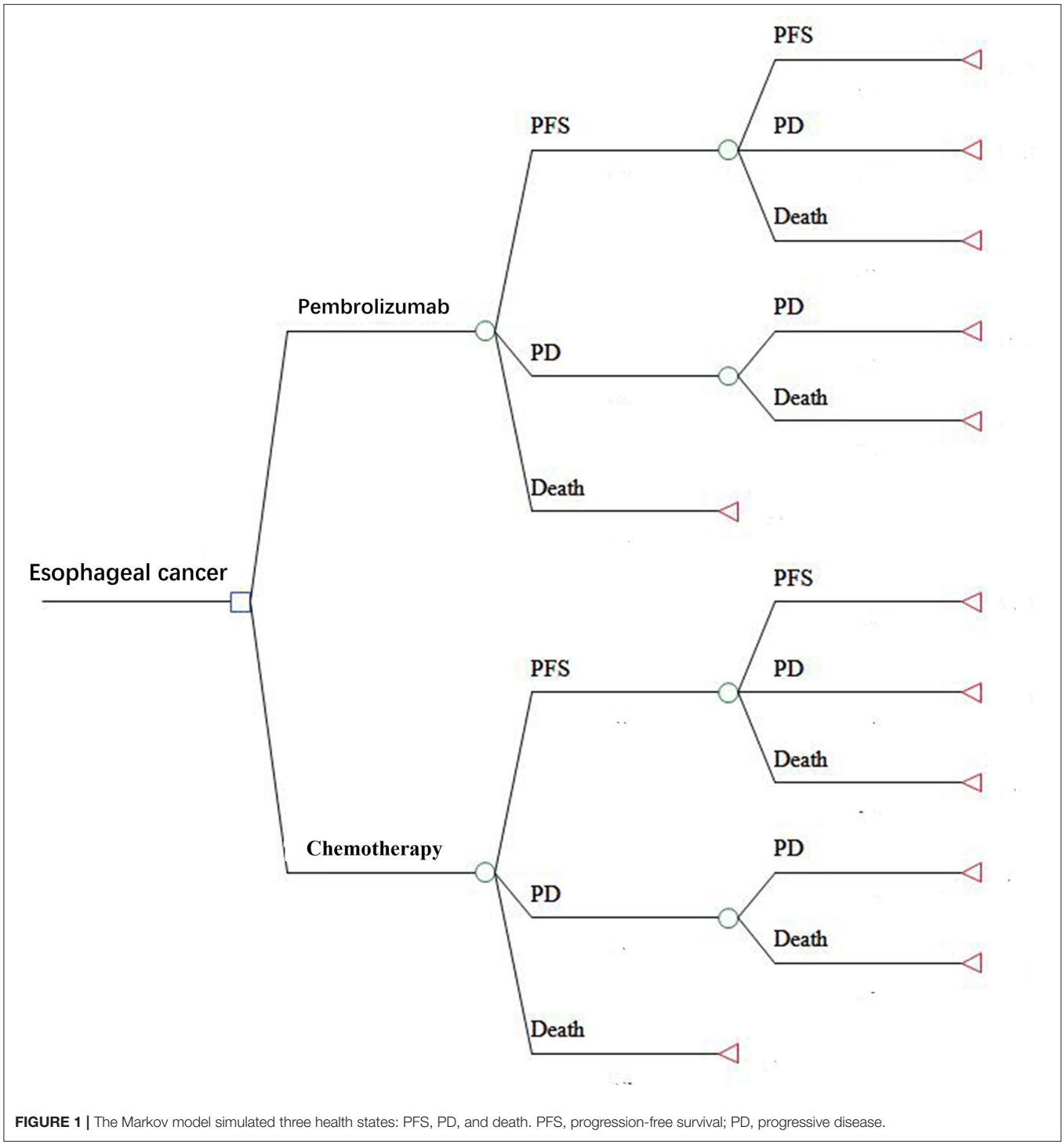

FIGURE 1 | The Markov model simulated three health states: PFS, PD, and death. PFS, progression-free survival; PD, progressive disease.

recommended 1–3 times the Gross Domestic Product per capita (GDP) as the threshold of willingness to pay (WTP) (17). As a result, $11,105.8/QALY was set according to the per capita GDP of China 2020 released by the National Bureau of Statistics. All costs were converted into US dollars, with an exchange rate of $1 = ¥6.4831 (August 11, 2021).

Sensitivity Analysis

One-way sensitivity analysis was performed by varying key parameters within ± 20% of its baseline value individually to examine the potential influence on the results. Probabilistic sensitivity analysis (PSA) was conducted with 10,000 Monte Carlo simulations. Gamma distribution was selected for the

TABLE 1 | Basic information and base-case costs.

Variables	Pembrolizumab	Chemotherapy
OS (months)		
Total population	7.1	7.1
Combined positive score ≥ 10	9.3	6.7
Squamous cell carcinoma	8.2	7.1
Probability of grade 3/4 AEs (%)		
Fatigue	0.64	0.34
Decreased appetite	0.64	1.01
Asthenia	1.27	1.01
Nausea	0.00	2.36
Diarrhea	0.64	3.04
Vomiting	0.32	2.03
Anemia	1.27	7.77
Alopecia	0.00	0.34
Neutrophil count decreased	0.32	9.80
Peripheral sensory neuropathy	0.00	0.34
WBC count decreased	0.00	10.14
Neutropenia	0.00	7.09
Cost per month($)		
Pembrolizumab	7370.14	0.00
Chemotheapy	0.00	2231.66
Tests	916.94	727.18
Grade ≥ 3 AEs	12.23	131.79
subsequent-line therapy	150.14	150.14

TABLE 2 | Transition probabilities in the Markov.

Total population	Pembrolizumab	Chemotherapy
pPFS-PFS	0.781	0.812
pPFS-PD	0.130	0.124
pPFS-Death	0.089	0.064
pPD-PD	0.900	0.806
pPD-Death	0.100	0.194
Squamous cell carcinoma		
pPFS-PFS	0.812	0.803
pPFS-PD	0.106	0.122
pPFS-Death	0.082	0.075
pPD-PD	0.911	0.832
pPD-Death	0.089	0.168
Combined positive score ≥ 10		
pPFS-PFS	0.849	0.792
pPFS-PD	0.091	0.135
pPFS-Death	0.060	0.073
pPD-PD	0.897	0.816
pPD-Death	0.103	0.184

cost parameters, beta distribution was selected for utility. The results of the PSA were represented by cost-acceptance curves. If the ICER was below the threshold of WTP, interventions were defined as cost-effective.

RESULTS

Base-Case Analysis

In the base-case analysis, for the whole population, the total costs of the pembrolizumab group were $34,272.16, and the total costs of the chemotherapy group were $15,217.55. The overall QALYs in the Pembrolizumab group were higher than that in the chemotherapy group (0.57 vs. 0.48 QALYs). The ICER of the pembrolizumab group compared with the chemotherapy group was $202,708.62 per QALY, which was almost 6 times higher than the WTP threshold for cost-effectiveness ($11,105.8 per QALY in China). Subgroup analysis showed that pembrolizumab gained the most QALY in the subgroup with PD-L1 CPS ≥ 10. Pembrolizumab cost $37,201.68 more than chemotherapy and provided additional.23 QALYs, leading to an ICER of $163,165.26 per QALY in patients with PD-L1 CPS ≥ 10. When pembrolizumab was administered in patients with squamous cell carcinoma, the ICERs were $163,643.19 /QALY, in comparison with chemotherapy. The ICERs were beyond the WTP thresholds in all subgroups, demonstrating that pembrolizumab was not a cost-effective strategy for patients with advanced or metastatic esophageal cancer from the Chinese perspective. The details are listed in **Table 4**.

Sensitivity Analyses

In one-way sensitivity analysis, for different subgroups, the most influential factor on the results was different. The price of pembrolizumab had the highest impact on the ICER for patients with PD-L1 CPS ≥ 10 or squamous cell carcinoma of the esophagus. For the total population, the utility of PD had the most influential factor in our model, but the price of pembrolizumab also had a great impact on the robustness of the cost-effectiveness analysis. The one-way sensitivity analyses revealed that the price of pembrolizumab and the utility of PD was the most sensitive model input. Other variables, such as the utility of PFS, the costs of chemotherapy and test had a moderate impact on the results, and the cost of AEs and subsequent-line therapy had a minimal impact on the outcome. Changing individual parameters did not change the results, pembrolizumab had no chance to be cost-effective at the current WTP threshold. More details of one-way sensitivity analyses were depicted in **Figure 3**. The results of probability sensitivity analyses for different subgroups are shown in **Figure 4**. With the increasing WTP value, the acceptable proportion of the chemotherapy group was decreased, whereas the pembrolizumab group was increased. However, pembrolizumab had no possibility of being a cost-effective treatment unless the threshold of cost-effectiveness analysis sharply increased to about $175,000 per QALY. And it seems that China's GDP cannot reach this level in the short term.

DISCUSSION

In this study, we found that pembrolizumab was not cost-effective for advanced or metastatic esophageal cancer compared

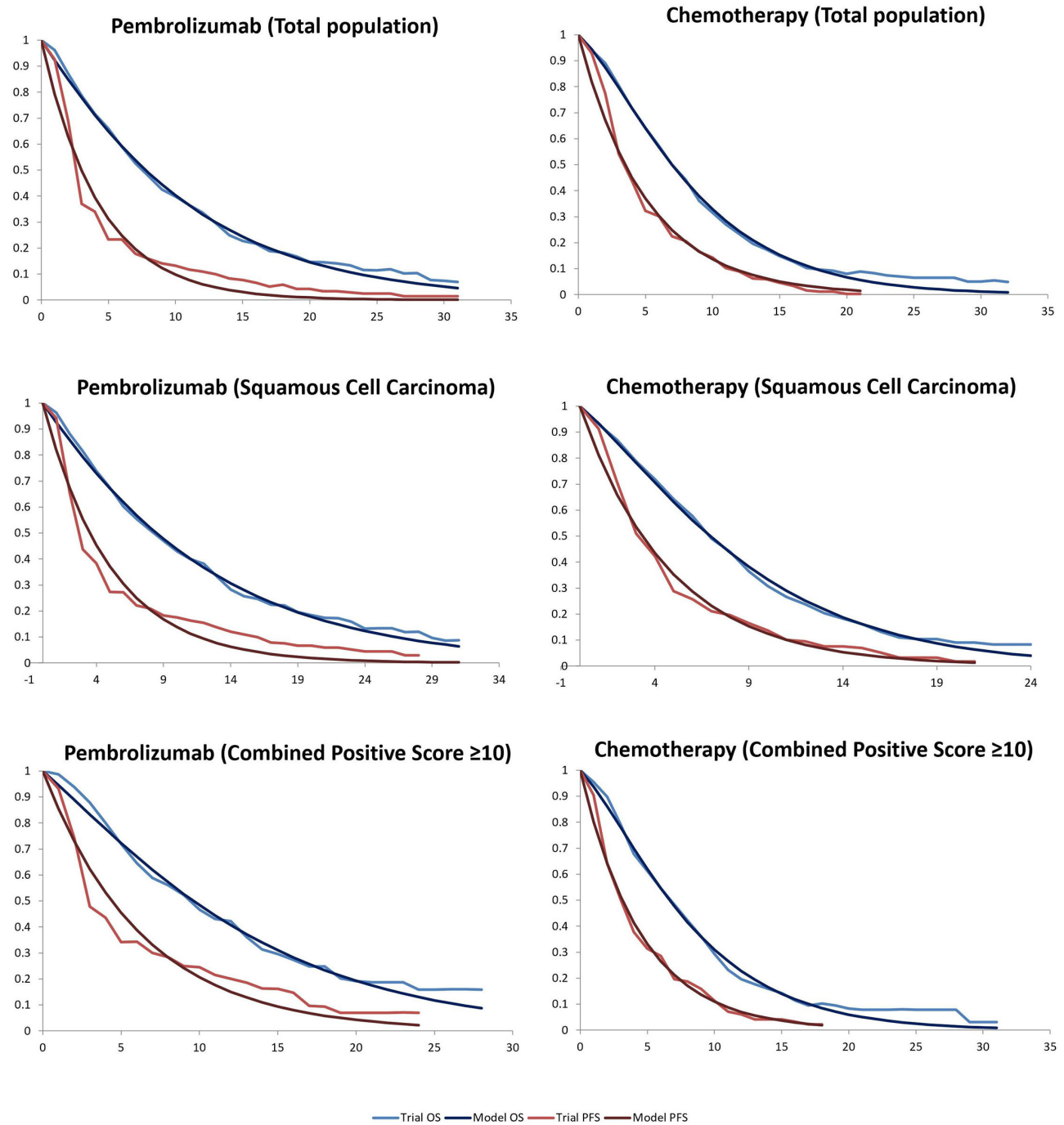

FIGURE 2 | Kaplan-Meier survival for the pembrolizumab and chemotherapy groups in the KEYNOTE181 and modeled curves. OS, overall survival; PFS, progression-free survival.

with chemotherapy. The price of pembrolizumab had the highest impact on the ICER when pembrolizumab was administered in patients with squamous cell carcinoma or PD-L1 CPS ≥ 10. Because of the assistance programs for esophageal cancer, patients with squamous cell carcinoma and PD-L1 CPS ≥ 10 can buy two cycles of pembrolizumab and obtain two cycles of pembrolizumab free. When we calculated the cost of pembrolizumab according to the donation plan, the ICER dropped to $65,122.91 per QALY and $53,955.88 per QALY in patients with PD-L1 CPS ≥ 10 and squamous cell carcinoma, respectively. Although pembrolizumab provided the greatest clinical benefit in QALYs for patients with PD-L1 CPS ≥ 10,

the cost of PFS state was less in the esophageal squamous cell carcinoma due to the shorter PFS compared with the PD-L1 CPS $\geq$ 10. The KEYNOTE181 study showed that the greatest survival benefit was observed in patients with squamous cell carcinoma and PD-L1 CPS $\geq$ 10. But the **Supplementary Appendix** of the KEYNOTE-181 study only provided the OS curve, not the PFS curve in patients with squamous cell carcinoma PD-L1 CPS $\geq$ 10 tumors, we cannot estimate the probability of being in each state based on the PFS and OS curves. We did not conduct the Markov model to assess the cost-effectiveness of pembrolizumab in patients with squamous cell carcinoma PD-L1 CPS $\geq$ 10 tumors.

PD-1 and PD-L1 inhibitors have become an effective treatment strategy for advanced esophageal cancer (18–21), and have been increasingly used after first-line therapies in advanced esophageal cancer (22). Pembrolizumab prolonged survival in patients with many solid cancers (23), but due to the high price of pembrolizumab, the economics of pembrolizumab is controversial (24). Factors including clinical effectiveness, safety, and drug price had an impact on the results of the pharmacoeconomic evaluation. Treatment options are limited for metastatic esophageal cancer, especially after first-line treatment. The survival benefit of Chemotherapy is modest and the side effects of chemotherapy reduce the quality of life. Immunotherapy using immune checkpoint inhibitors, such as nivolumab, pembrolizumab, and camrelizumab, has resulted in survival benefits and fewer side effects for patients with metastatic esophageal cancer. The study performed a Markov model to assess the cost-effectiveness of nivolumab vs. chemotherapy in the second-line treatment for advanced esophageal squamous cell carcinoma based on the ATTRACTION-3 trial. The results of the study showed that nivolumab was not a cost-effective treatment option compared with chemotherapy from the Chinese society perspective (25). Because of the sharp price reduction of camrelizumab, the pharmacoeconomic research results of camrelizumab as second-line therapy for advanced or metastatic esophageal squamous cell carcinoma were inconsistent (14, 15, 26), Yang et al. (14) showed camrelizumab was not cost-effective as second-line therapy for advanced or metastatic esophageal squamous cell carcinoma compared with chemotherapy in China. The cost of camrelizumab in Yang et al. was $2,802 per 200 mg. Both Lin et al. (26) and Cai et al. (15) showed camrelizumab was cost-effective compared with chemotherapy for advanced or metastatic esophageal squamous cell carcinoma (15, 26). The price of camrelizumab was only $452.87 per 200 mg and $432 per 200 mg in Lin et al. (26) and Cai et al. (15), respectively. Up to date,

TABLE 3 | Cost parameters input in the model.

Parameter	Value($)
Drug acquisition	
Pembrolizumab 100 mg	2763.80
Paclitaxel 30 mg	104.89
Docetaxel 20 mg	200.52
Irinotecan 100 mg	273.50
Laboratory tests and scans	
12-Lead Electrocardiogram	16.20
PT/INR and Aptt	6.79
Chemistry panel	23.29
Routine blood tests	2.31
Urinalysis	4.94
T3, FT4, and TSH	47.35
Echocardiography	37.79
Chest and abdomen CT	389.63
Other	377.44
Bed fee/day	6.32
SAE management cost per event	
Fatigue or Asthenia	214.43
Decreased appetite	105.57
Nausea or Vomiting	98.83
Anemia	328.90
Peripheral sensory neuropathy	17.49
WBC or Neutropenia count decreased	356.31

TABLE 4 | Results of the cost-effectiveness analysis.

Subgroups and strategies	Total population		Combined positive score ≥10		Squamous cell carcinoma	
	Pembrolizumab	Chemotherapy	Pembrolizumab	Chemotherapy	Pembrolizumab	Chemotherapy
Costs ($)						
PFS state($)	33412.67	14718.98	50050.34	13173.71	39525.06	13985.27
PD state($)	859.46	498.57	842.62	517.55	909.93	539.81
Total cost ($)	34272.16	15217.55	50892.96	13691.28	40434.99	14252.08
Incremental cost ($)	19054.61	/	37201.68	/	26182.91	/
Effectiveness(QALYs)						
PFS state (QALYs)	0.25	0.30	0.38	0.27	0.30	0.28
PD state (QALYs)	0.32	0.18	0.31	0.19	0.34	0.20
Total effectiveness (QALYs)	0.57	0.48	0.69	0.46	0.64	0.48
Incremental effectiveness (QALYs)	0.09	/	0.23	/	0.16	/
ICERs compared with PC alone ($/QALY)	202708.62		163165.26		163643.19	

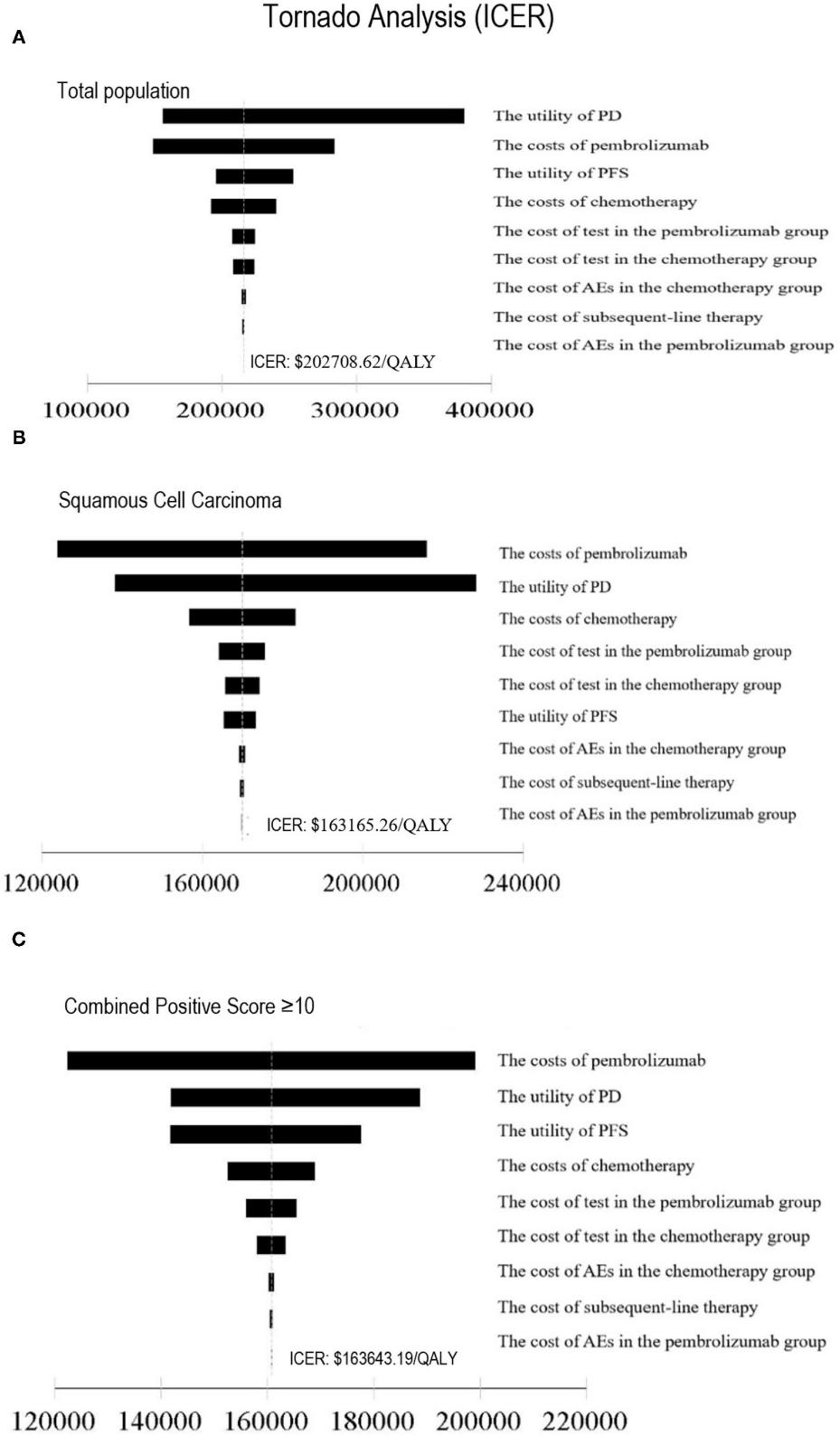

FIGURE 3 | Tornado diagram of one-way sensitivity analysis. This summarizes the results of one-way sensitivity analysis, listing influential parameters in descending order according to their effect on the ICER over the variation of each parameter value. ICER, Incremental Cost-Effectiveness Ratio; **(A)** Total population, **(B)** Squamous Cell Carcinoma, **(C)** Combined Positive Score ≥10, PFS, progression-free survival; PD, progressive disease; AE, adverse event.

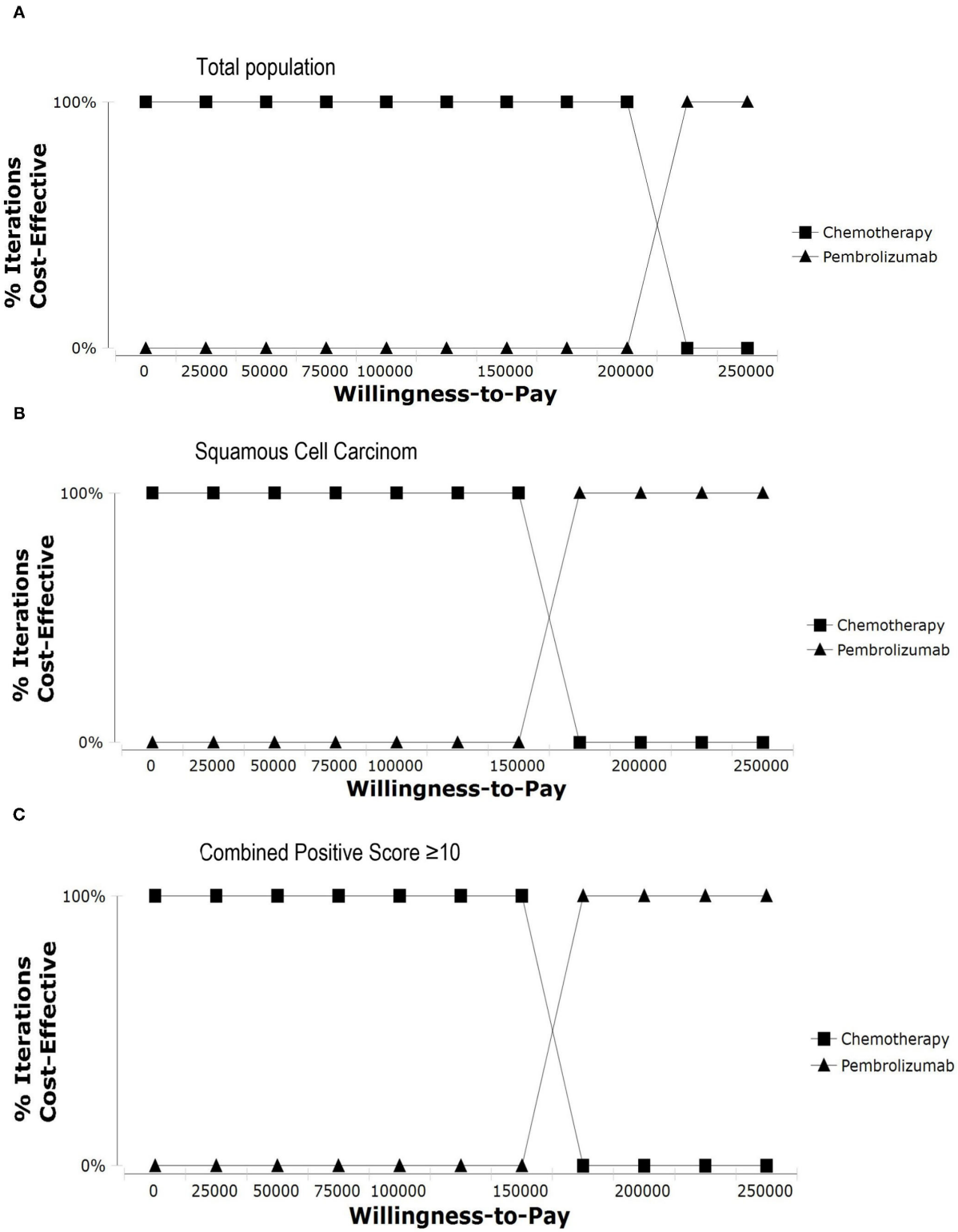

FIGURE 4 | Cost-effectiveness acceptability curves. Cost-effectiveness acceptability curves show the probability of each treatment strategy being cost-effective at different WTP thresholds. **(A)** Total population, **(B)** Squamous Cell Carcinoma, **(C)** Combined Positive Score ≥ 10.

there has been no cost-effectiveness analysis of pembrolizumab as second-line therapy for advanced esophageal cancer.

WTP is a critical parameter to determine whether the intervention is cost-effective. If the ICER was lower than the WTP, the intervention is considered to be favorably cost-effective. The WTP was set as 1–3 times GDP per capita according to the WHO guidelines that were widely referenced in the last decade (27). But some studies suggest that three times of GDP per capita as WTP is too high and the WTP threshold is below 1 × GDP per capita (28, 29). The National Institute of Health and Clinical Excellence (NICE) proposed that the cost-effectiveness threshold of life-extending treatments for patients with terminally ill patients could increase to £50,000/QALY (30, 31) The WTP threshold used in Greek cost-effectiveness studies showed that the median WTP threshold used in oncology studies [€51,000 (€50,000–57,000)] was higher than in non-oncology studies [€34,000 (€30,000–€35,000); p-value < 0.001] (32). There is no established standard in China for the WTP. According to the guidelines and literature, 1 × GDP per capita was set as WTP in our study. The research has certain limitations associated with model-based cost-effectiveness analyses. We primarily relied on the data from a phase III trial rather than real-world experience. Occasionally, real-world experience may deviate from that seen in trials. In addition, detailed data on the clinical and economic burden of treatment-related adverse events remain limited. First, the KEYNOTE181 study only reported the OS and PFS in patients with PD-L1 CPS $\geq$ 10 tumors, squamous cell carcinoma, and in all patients, respectively, but reported the adverse events in all patients. We hypothesized that the incidences of AEs were similar between different subgroups and estimated the cost of AEs according to the safety outcomes in the total population. Second, the cost data in the model were obtained from official or published prices, but the cost of drugs and tests varied across different regions in China. Third, nutrition support plays an important part in the management of esophageal cancer. As this part of the information was not mentioned in the KEYNOTE-048 trial, these costs were not considered. Besides, due to the lack of utility data in China, the utility values were obtained from Western countries. Imprecise estimates and assumptions were necessary and this uncertainty was evaluated using sensitivity analysis. The results of sensitivity analyses with a range of ± 20% of variation showed that the results were stable.

China has launched national reforms on centralizing drug procurement to contain drug costs. A series of Chinese domestic PD-1 inhibitors including camrelizumab, sintilimab, toripalimab, tislelizumab were included in medical insurance with a price reduction of more than 64%. With the development of the drug industry, more and more PD-1 inhibitors will emerge, which might provide an alternative for patients with esophageal squamous cell carcinoma in China and promote the price reduction of pembrolizumab. With the price adjustment of PD-1 inhibitors, the economy of these drugs will be improved.

DATA AVAILABILITY STATEMENT

The original contributions presented in the study are included in the article/**Supplementary Material**, further inquiries can be directed to the corresponding author.

ETHICS STATEMENT

Ethical review and approval was not required for the study on human participants in accordance with the local legislation and institutional requirements. Written informed consent for participation was not required for this study in accordance with the national legislation and the institutional requirements.

AUTHOR CONTRIBUTIONS

MZ participated in research design, data processing, and manuscript writing, TX and HZ in data processing. ZH participated in research design and manuscript revising. All authors contributed to the article and approved the submitted version.

FUNDING

This work was supported by the 1.3.5 project for disciplines of excellence-clinical research incubation project, West China Hospital, Sichuan University (2021HXFH064).

SUPPLEMENTARY MATERIAL

The Supplementary Material for this article can be found online at: https://www.frontiersin.org/articles/10.3389/fpubh.2022.790225/full#supplementary-material

REFERENCES

1. Sung H, Ferlay J, Siegel RL, Laversanne M, Soerjomataram I, Jemal A, et al. Global cancer statistics 2020: GLOBOCAN estimates of incidence and mortality worldwide for 36 cancers in 185 countries. *CA Cancer J Clin.* (2021) 71:209–49. doi: 10.3322/caac.21660
2. Uhlenhopp DJ, Then EO, Sunkara T, Gaduputi V. Epidemiology of esophageal cancer: update in global trends, etiology and risk factors. *Clin J Gastroenterol.* (2020) 13:1010–21. doi: 10.1007/s12328-020-01237-x
3. Chen W, Zheng R, Baade PD, Zhang S, Zeng H, Bray F, et al. Cancer statistics in China, 2015. *CA Cancer J Clin.* (2016) 66:115–32. doi: 10.3322/caac.21338
4. Lagergren J, Smyth E, Cunningham D, Lagergren P. Oesophageal cancer. *Lancet.* (2017) 390:2383–96. doi: 10.1016/S0140-6736(17)31462-9
5. Siegel RL, Miller KD, Fuchs HE, Jemal A. Cancer statistics, 2021. *CA Cancer J Clin.* (2021) 71:7–33. doi: 10.3322/caac.21654
6. Howlader N, Noone AM, Krapcho M, Miller D, Brest A, Yu M, et al. *SEER Cancer Statistics Review, 1975-2018: National Cancer Institute.* Available online at: https://seer.cancer.gov/csr/1975_2018/ (accessed October 09, 2021).
7. Yang S, Lin S, Li N, Deng Y, Wang M, Xiang D, et al. Burden, trends, and risk factors of esophageal cancer in China from 1990 to 2017: an up-to-date

overview and comparison with those in Japan and South Korea. *J Hematol Oncol.* (2020) 13:146. doi: 10.1186/s13045-020-00981-4
8. National Comprehensive Cancer Network. *Esophageal and Esophagogastric Junction Cancers,Version 4.2021*. (2021). Available online at: https://www.nccn.org/professionals/physician_gls/pdf/esophageal.pdf (accessed August 28, 2021).
9. Kojima T, Shah MA, Muro K, Francois E, Adenis A, Hsu CH, et al. Randomized phase III KEYNOTE-181 study of pembrolizumab versus chemotherapy in advanced esophageal cancer. *J Clin Oncol.* (2020) 38:4138–48. doi: 10.1200/JCO.20.01888
10. Noone AM, Cronin KA, Altekruse SF, Howlader N, Lewis DR, Petkov VI, et al. Cancer incidence and survival trends by subtype using data from the surveillance epidemiology and end results program, 1992-2013. *Cancer Epidemiol Biomarkers Prev.* (2017) 26:632–41. doi: 10.1158/1055-9965.EPI-16-0520
11. Murray CJ, Evans DB, Acharya A, Baltussen RM. Development of WHO guidelines on generalized cost-effectiveness analysis. *Health Econ.* (2000) 9:235–51. doi: 10.1002/(sici)1099-1050(200004)9:3<235::aid-hec502>3.0.co;2-o.
12. Marguet S, Adenis A, Delaine-Clisant S, Penel N, Bonastre J. Cost-utility analysis of continuation versus discontinuation of first-line chemotherapy in patients with metastatic squamous-cell esophageal cancer: economic evaluation alongside the E-DIS trial. *Value Health.* (2021) 24:676–82. doi: 10.1016/j.jval.2020.11.017
13. Wu B, Ye M, Chen H, Shen JF. Costs of trastuzumab in combination with chemotherapy for HER2-positive advanced gastric or gastroesophageal junction cancer: an economic evaluation in the Chinese context. *Clin Ther.* (2012) 34:468–79. doi: 10.1016/j.clinthera.2012.01.012
14. Yang F, Fu Y, Kumar A, Chen M, Si L, Rojanasarot S. Cost-effectiveness analysis of camrelizumab in the second-line treatment for advanced or metastatic esophageal squamous cell carcinoma in China. *Ann Transl Med.* (2021) 9:1226. doi: 10.21037/atm-21-1803
15. Cai H, Xu B, Li N, Zheng B, Zheng Z, Liu M. Cost-effectiveness analysis of camrelizumab versus chemotherapy as second-line treatment of advanced or metastatic esophageal squamous cell carcinoma. *Front Pharmacol.* (2021) 12:732912. doi: 10.3389/fphar.2021.732912
16. Casamayor M, Morlock R, Maeda H, Ajani J. Targeted literature review of the global burden of gastric cancer. *Ecancermedicalscience.* (2018) 12:883. doi: 10.3332/ecancer.2018.883
17. Bertram MY, Lauer JA, De Joncheere K, Edejer T, Hutubessy R, Kieny MP, et al. Cost-effectiveness thresholds: pros and cons. *Bull World Health Organ.* (2016) 94:925–30. doi: 10.2471/BLT.15.164418
18. Jin Z, Shen J, Wang C, Chen D, Zhang B, Zhang J, et al. Narrative review of pembrolizumab for the treatment of esophageal cancer: evidence and outlook. *Ann Transl Med.* (2021) 9:1189. doi: 10.21037/atm-21-2804
19. Kang YK, Boku N, Satoh T, Ryu MH, Chao Y, Kato K, et al. Nivolumab in patients with advanced gastric or gastro-oesophageal junction cancer refractory to, or intolerant of, at least two previous chemotherapy regimens (ONO-4538-12, ATTRACTION-2): a randomised, double-blind, placebo-controlled, phase 3 trial. *Lancet.* (2017) 390:2461–71. doi: 10.1016/S0140-6736(17)31827-5
20. Yang W, Chang L, Guo Q, Chen J, Yu W, Zhang W. Programmed cell death protein-1 inhibitors in the treatment of digestive system tumors in Chinese population: an observational study of effectiveness and safety. *Ann Palliat Med.* (2021) 10:9015–24. doi: 10.21037/apm-21-1827
21. Yamamoto S, Kato K. Immuno-oncology for esophageal cancer. *Future Oncol.* (2020) 16:2673–81. doi: 10.2217/fon-2020-0545
22. Allaire JC, Balk M, Azmi S, Handl HL, Yang K, Barnes G. Use of PD-1 and PD-L1 inhibitors after first-line therapy in esophageal cancer patients in the US. *Curr Med Res Opin.* (2021) 37:1403–7. doi: 10.1080/03007995.2021.1929134
23. Wang M, Ma X, Guo L, Xia F. Safety and efficacy profile of pembrolizumab in solid cancer: pooled reanalysis based on randomized controlled trials. *Drug Des Develop Ther.* (2017) 11:2851–60. doi: 10.2147/DDDT.S146286
24. da Veiga CRP, da Veiga CP, Drummond-Lage AP. Concern over cost of and access to cancer treatments: a meta-narrative review of nivolumab and pembrolizumab studies. *Crit Rev Oncol Hematol.* (2018) 129:133–45. doi: 10.1016/j.critrevonc.2018.07.002
25. Zhang PF, Xie D, Li Q. Cost-effectiveness analysis of nivolumab in the second-line treatment for advanced esophageal squamous cell carcinoma. *Future Oncol.* (2020) 16:1189–98. doi: 10.2217/fon-2019-0821
26. Lin YT, Chen Y, Liu TX, Kuang F, Huang P. Cost-effectiveness analysis of camrelizumab immunotherapy versus docetaxel or irinotecan chemotherapy as second-line therapy for advanced or metastatic esophageal squamous cell carcinoma. *Cancer Manag Res.* (2021) 13:8219–30. doi: 10.2147/CMAR.S335515
27. Leech AA, Kim DD, Cohen JT, Neumann PJ. Use and misuse of cost-effectiveness analysis thresholds in low- and middle-income countries: trends in cost-per-DALY Studies. *Value Health.* (2018) 21:759–61. doi: 10.1016/j.jval.2017.12.016
28. Woods B, Revill P, Sculpher M, Claxton K. Country-level cost-effectiveness thresholds: initial estimates and the need for further research. *Value Health.* (2016) 19:929–35. doi: 10.1016/j.jval.2016.02.017
29. Ochalek J, Wang H, Gu Y, Lomas J, Cutler H, Jin C. Informing a cost-effectiveness threshold for health technology assessment in china: a marginal productivity approach. *Pharmacoeconomics.* (2020) 38:1319–31. doi: 10.1007/s40273-020-00954-y
30. NICE. *PMG19 Addendum A—Final amendments to the NICE technology appraisal processes and methods guides to support the proposed new Cancer Drugs Fund arrangements*. London: NICE (2016).
31. Thokala P, Ochalek J, Leech AA, Tong T. Cost-effectiveness thresholds: the past, the present and the future. *Pharmacoeconomics.* (2018) 36:509–22. doi: 10.1007/s40273-017-0606-1
32. Tzanetakos C, Stefanou G, Gourzoulidis G. PNS61 does a standard willingness-to-pay threshold exist in Greece? *Value Health.* (2019) 22:S772–3. doi: 10.1016/j.jval.2019.09.1963

Conflict of Interest: The authors declare that the research was conducted in the absence of any commercial or financial relationships that could be construed as a potential conflict of interest.

Publisher's Note: All claims expressed in this article are solely those of the authors and do not necessarily represent those of their affiliated organizations, or those of the publisher, the editors and the reviewers. Any product that may be evaluated in this article, or claim that may be made by its manufacturer, is not guaranteed or endorsed by the publisher.

Copyright © 2022 Zhan, Xu, Zheng and He. This is an open-access article distributed under the terms of the Creative Commons Attribution License (CC BY). The use, distribution or reproduction in other forums is permitted, provided the original author(s) and the copyright owner(s) are credited and that the original publication in this journal is cited, in accordance with accepted academic practice. No use, distribution or reproduction is permitted which does not comply with these terms.

frontiers in Immunology

REVIEW
published: 17 March 2022
doi: 10.3389/fimmu.2022.795972

Neoadjuvant Immunotherapy for MSI-H/dMMR Locally Advanced Colorectal Cancer: New Strategies and Unveiled Opportunities

Xuan Zhang[1†], Tao Wu[1†], Xinyi Cai[1†], Jianhua Dong[1], Cuifeng Xia[1], Yongchun Zhou[2], Rong Ding[3], Renfang Yang[1], Jing Tan[4], Lijuan Zhang[5], Ya Zhang[4], Yuqin Wang[5], Chao Dong[6] and Yunfeng Li[1]*

[1] Department of Colorectal Surgery, Yunnan Cancer Hospital, The Third Affiliated Hospital of Kunming Medical University, Kunming, China, [2] Laboratory of Molecular Diagnosis Center, Yunnan Cancer Hospital, The Third Affiliated Hospital of Kunming Medical University, Kunming, China, [3] Department of Minimally Invasive Intervention, Yunnan Cancer Hospital, The Third Affiliated Hospital of Kunming Medical University, Kunming, China, [4] Department of Imaging, Yunnan Cancer Hospital, The Third Affiliated Hospital of Kunming Medical University, Kunming, China, [5] Department of Pathology, Yunnan Cancer Hospital, The Third Affiliated Hospital of Kunming Medical University, Kunming, China, [6] Department of Oncology, Yunnan Cancer Hospital, The Third Affiliated Hospital of Kunming Medical University, Kunming, China

OPEN ACCESS

Edited by:
Hubing Shi,
Sichuan University, China

Reviewed by:
Srijayaprakash Babu Uppada,
University of Alabama, United States
Mohamed Alshafredi,
University of Kentucky, United States

***Correspondence:**
Yunfeng Li
zhangxuan66@kmmu.edu.cn

[†]These authors share first authorship

Specialty section:
This article was submitted to Cancer Immunity and Immunotherapy, a section of the journal Frontiers in Immunology

Received: *15 October 2021*
Accepted: *22 February 2022*
Published: *17 March 2022*

Citation:
Zhang X, Wu T, Cai X, Dong J, Xia C, Zhou Y, Ding R, Yang R, Tan J, Zhang L, Zhang Y, Wang Y, Dong C and Li Y (2022) Neoadjuvant Immunotherapy for MSI-H/dMMR Locally Advanced Colorectal Cancer: New Strategies and Unveiled Opportunities. Front. Immunol. 13:795972. doi: 10.3389/fimmu.2022.795972

Patients with locally advanced colorectal cancer (LACRC) have a high risk of recurrence and metastasis, although neoadjuvant therapy may provide some benefit. However, patients with high microsatellite instability/deficient mismatch repair (MSI-H/dMMR) LACRC receive little benefit from neoadjuvant chemoradiotherapy (nCRT) or neoadjuvant chemotherapy (nCT). The 2015 KEYNOTE-016 trial identified MSI-H/dMMR as a biomarker indicative of immunotherapy efficacy, and pointed to the potential use of immune checkpoint inhibitors (ICIs). In 2017, the FDA approved two ICIs (pembrolizumab and nivolumab) for treatment of MSI-H/dMMR metastatic CRC (mCRC). In 2018, the CheckMate-142 trial demonstrated successful treatment of mCRC based on "double immunity" provided by nivolumab with ipilimumab, a regimen that may become a standard first-line treatment for MSI-H mCRC. In 2018, the FDA approved nivolumab alone or with ipilimumab for patients who progressed to MSI-H/dMMR mCRC after standard chemotherapy. The FDA then approved pembrolizumab alone as a first-line treatment for patients with MSI-H/dMMR CRC that was unresectable or metastatic. There is now interest in using these drugs in neoadjuvant immunotherapy (nIT) for patients with MSI-H/dMMR non-mCRC. In 2020, the NICHE trial marked the start of using nIT for CRC. This novel treatment of MSI-H/dMMR LACRC may change the approaches used for neoadjuvant therapy of other cancers. Our review of immunotherapy for CRC covers diagnosis and treatment, clinical prognostic characteristics, the mechanism of nIT, analysis of completed prospective and retrospective studies, and ongoing clinical trials, and the clinical practice of using nIT for MSI-H/dMMR LACRC. Our team also proposes a new organ-preservation strategy for patients with MSI-H/dMMR low LARC.

Keywords: locally advanced colorectal cancer, neoadjuvant therapy, immunotherapy, mismatch repair deficiency, microsatellite instability-high

INTRODUCTION

Global cancer statistics for 2020 indicated that colorectal cancer (CRC) is the most common malignant tumor of the digestive system, and that CRC ranked third in incidence rate and second in mortality rate among all cancers (1). The increases in industrialization and urbanization and in the number of elderly have contributed to the significantly increasing incidence rate and mortality rate of CRC during recent years. Most CRC patients are in the stage of local progression upon diagnosis, making effective treatment more difficult.

Locally advanced colorectal cancer (LACRC) is defined as CRC stage II (cT3–4, N0)/stage III (any cT, N+). During recent years, advancements in standardized surgery and subsequent improvements in neoadjuvant therapy have improved outcomes. The advantages of neoadjuvant therapy are that it can reduce tumor stage, improve the rate of R0 resection, decrease the rate of local recurrence, and enable some patients to achieve a clinical complete response (cCR) or even a pathological complete response (pCR) (2). However, distant metastases, surgical morbidities, and adverse effects (AEs) caused by neoadjuvant radiotherapy or chemotherapy remain significant problems.

With the advent of the era of precision medicine, researchers have begun to explore the effect of microsatellite status on the characteristics of tumors (3). However, high microsatellite instability/defective mismatch repair (MSI-H/dMMR) LACRC has low sensitivity to current neoadjuvant therapies. Fortunately, the emergence of neoadjuvant immunotherapy (nIT) brings new hope to these patients (4). It is necessary to examine the suitability of nIT for patients with MSI-H/dMMR locally advanced rectal cancer (LARC). Therefore, this review comprehensively summarizes the new strategies and opportunities that nIT may provide for these patients.

CURRENT DILEMMAS IN TREATMENT OF LOCALLY ADVANCED COLORECTAL CANCER

LACRC has a high risk of postoperative local recurrence and distant metastasis. The traditional mode of surgical resection cannot meet the needs of all of these patients, although neoadjuvant therapy can sometimes provide additional efficacy. What is the efficacy of neoadjuvant chemotherapy (nCT) for LACRC patients with MSI-H/dMMR? Subgroup analysis of data in the FOxTROT study, which was reported at the 2019 ASCO Annual Meeting, indicated that the effective rate of nCT for CRC in patients with MSI-H/dMMR was only 4.7% (5). Among all patients, 73.6% had tumor regression based on tumor pathological examination, but only 26.6% who had proficient mismatch repair/microsatellite stability (pMMR/MSS) had no tumor regression (5). A 2020 article in Clinical Cancer Research described the use of FOLFOX as a nCT regimen for rectal cancer in a trial conducted at the Memorial Sloan Kettering Cancer Center. The results indicated that tumor progression occurred in 29% of patients in the MSI-H/dMMR group, but in none of the patients in the pMMR group (6). These two studies thus illustrated that most CRC patients with MSI-H/dMMR do not benefit from the FOLFOX nCT regimen.

For patients with LARC, the National Comprehensive Cancer Network (NCCN) guidelines recommend "neoadjuvant chemoradiotherapy (nCRT) + total mesorectal excision + adjuvant chemotherapy", and this is generally recognized as a standard treatment scheme worldwide (7). Nevertheless, there are some different views regarding the efficacy of nCRT in these patients. First, although nCRT for rectal cancer reduces the local recurrence rate, it does not improve the long-term survival rate of patients. Second, nCRT for rectal cancer can lead to post-surgical complications, such as anastomotic leakage and poor healing of the perineal wound, as well as long-term toxicities, such as bladder dysfunction, loss of anal sphincter function, and sexual dysfunction. Finally, about 20% of LACRC patients are insensitive to nCRT, and if the tumor progresses after nCRT, these patients may miss the opportunity of radical operation. A retrospective study in the United States National Cancer Data Base indicated that the postoperative pCR rate of LACRC patients after nCRT was 8.9% in an MSS group and 5.9% in an MSI-H group ($P = 0.01$). These results suggested that LACRC patients with MSI-H were less sensitive to radiotherapy and chemotherapy (8).

Treatments for CRC have continued to improve. Molecular genotyping and determination of microsatellite status were significant contributions to the development of precision therapies (9). In recent years, immune checkpoint inhibitors

(ICIs), antibodies that target PD-1, PD-L1, or CTLA-4, have emerged as effective treatments for a variety of cancers (10). The benefits provided by these ICIs even surpass those provided by targeted therapy in some aspects, and ICIs may also provide an improved treatment for CRC (11). Thus, although CRC patients with MSI-H status may have poor prognoses, they also uniquely benefit from treatment with ICIs.

SIGNIFICANCE OF MSI-H/dMMR IN TUMORS

MSI refers to variation of MS sequence length or base composition due to insertion or deletion mutations during DNA replication, an alteration often caused by dMMR. The MS status of a tumor may be classified as stable (MSS), or as having low instability (MSI-L) or high instability (MSI-H) (12). MSI-H has a high incidence in solid tumors, such as endometrial cancer, CRC, and gastric cancer (13). dMMR can be due to a germline mutation of the MMR gene (Lynch syndrome), in which case there is a hereditary pattern of malignant tumors (14). However, dMMR more commonly occurs from sporadic mutations of the MMR gene, a condition usually accompanied by the CpG island methylation phenotype (CIMP). Notably, 50% of the sporadic cases also exhibit a BRAF-activating mutation (V600E). Thus, Lynch syndrome can be usually excluded in patients with CIMP and this BRAF mutation (15, 16). The clinical presentations of patients with dMMR and MSI-H are

indistinguishable, and their detection rates are consistently very high. Although these two aberrations are often not distinguished in the clinic, they are not identical (17). Most clinical studies demonstrated that patients with MSI-H/dMMR solid tumors received obvious benefits from ICIs (18–20). Moreover, a key factor determining the benefit of ICI therapy is the MSI-H status of the patient, not the specific kind of cancer (21).

In 2017, the United States FDA approved pembrolizumab (anti-PD-1 antibody) for the treatment of patients with advanced MSI-H/dMMR or metastatic solid tumors. These patients typically experience disease progression following standard treatment, and no other satisfactory alternative treatments are available. This is the first approved anti-tumor therapy that considered specific biomarkers rather than the type of tumor. Since then, MSI status has become an important consideration in clinical oncology. Because of the importance of MSI-H/dMMR status in predicting response to tumor immunotherapy, many guidelines recommend determination of the MSI status of patients with advanced solid tumors before administering immunotherapy (22).

UNIQUE PROGNOSTIC CHARACTERISTICS OF MSI-H/dMMR CRC

MSI-H/dMMR CRC is a unique type of CRC defined by biomarker status that is present in 12 to 15% of all CRC patients, and is more likely to occur in those with right-sided cancers (i.e., poorly differentiated and/or mucinous adenocarcinoma). Only 2% of patients with rectal cancer are MSI-H (18). There is also evidence that the MS status of CRC changes during cancer progression. In particular, patients with late-stage cancers are less likely to be MSI-H (23); patients with early-stage MSI-H/dMMR CRC have good prognoses, but this status is considered a poor prognostic factor in patients with metastatic CRC (mCRC) (24).

Patients with MSI-H/dMMR locally advanced colon cancer (LACC) have unique clinicopathological and molecular biological characteristics, and typically experience slow clinical progression. These patients are less likely to experience lymph node metastasis and distant metastasis. Patients with MSI-H/dMMR stage II CRC generally have good prognoses. Following surgery alone, these patients have a 5-year survival rate as high as 80%, and fluorouracil alone provides little additional benefit. Thus, the present consensus is that adjuvant chemotherapy is not needed for patients with low-risk stage II CRC after surgery. However, patients with MSI-H/dMMR stage III CRC who received postoperative adjuvant chemotherapy have better prognoses than MSS patients. Moreover, the efficacy of oxaliplatin adjuvant therapy appeared to be unaffected by MSI/MMR status (25, 26).

Patients with MSI-H/dMMR stage IV CRC account for about 4 to 5% of all CRC patients (18). A summary analysis of four clinical studies on first-line treatment for mCRC indicated that the median overall survival (OS) was 13.6 months for patients with dMMR and 16.8 months for patients with pMMR (HR = 1.35; 95% CI: 1.13~1.61; P = 0.001) (27). The prognosis of patients with MSI-H/dMMR mCRC is poor, especially in those with the BRAF V600E mutation (28).

A 2016 study revealed that the levels of cytotoxic cells, CD8+, Th1, Th2, follicular helper T cells, and T cell markers were significantly higher in patients with MSI-H/dMMR CRC than in those with MSS/pMMR CRC (24). Another 2019 study reported that patients with MSI-H/dMMR CRC had a higher tumor mutation burden (TMB), tumor neoantigen burden (TNB), and greater lymphocyte infiltration of tumor tissues. Notably, these patients also had increased expression of PD-L1 in the tumor microenvironment (TME), suggesting that ICIs have potential for treatment of these individuals (29).

CURRENT STATUS OF IMMUNOTHERAPY FOR MSI-H/dMMR CRC

The latest NCCN guidelines (v1.2021) for gastric cancer (30), colon cancer (31) and rectal cancer (32) revised the previous recommendations for detection of MSI/MMR status. These new guidelines recommend that all newly diagnosed patients should be tested for MSI using the polymerase chain reaction and for MMR using immunohistochemistry (IHC). The previous recommendations limited this testing to patients with suspected metastasis. The new guidelines therefore mean that ICIs are not only suitable for rescue treatment of patients with MSI-H/dMMR stage IV CRC, but also as nIT for patients with earlier stages of CRC.

For patients who have unresectable advanced or mCRC and are suitable for high-intensity chemotherapy, the v1.2021 NCCN guidelines recommend nivolumab ± ipilimumab (O ± Y) or pembrolizumab as a first-line treatment for patients with MSI-H/dMMR status (32, 31). These guidelines recommend pembrolizumab as the preferred treatment, indicating that immunotherapy now has priority over traditional chemotherapy ± targeted therapy.

In contrast to the 2020 NCCN guidelines for colon cancer, the newest guidelines added nivolumab ± ipilimumab or pembrolizumab (preferred) as adjuvant treatment for patients with MSI-H/dMMR CRC (31) — a new immune adjuvant treatment scheme for these patients. In addition, the newest guidelines recommend nivolumab ± ipilimumab or pembrolizumab (preferred) as an option for preoperative neoadjuvant therapy for resectable MSI-H/dMMR mCRC (31, 32). This is the first time the NCCN recommended an immunotherapy as a preoperative neoadjuvant therapy for CRC. However, the NCCN has not yet provided guidelines regarding the use of nIT for LACRC.

ANTI-TUMOR MECHANISM OF NIT

The most widely studied ICIs are antibodies that target CTLA-4, PD-1, and PD-L1, and several ICIs are approved for different types of cancers. PD-L1 binds to PD-1, and this immune

checkpoint pathway has a key role in inhibiting T cell-mediated antitumor immune response due to the interaction of PD-1 and CD80 on T cells in the TME. PD-1 and PD-L1 inhibitors inhibit the activity of this immune checkpoint, effectively "releasing the immune brake" in the TME by inducing T cell activation, reactivating the immune response of T cells on tumors, and increasing immune system function (33, 34). The aim of traditional nCT is to reduce tumor staging, whereas nIT aims to enhance the body's general immunity to tumor antigens. Patients with early- and middle-stage tumors have relatively sound immune systems, and their tumor burdens are generally not as severe. These patients express many new tumor antigens before operation, and this can increase the activity of anti-tumor immune T cells, followed by dispersal throughout the body and removal of micro-metastases. After a multi-line treatment, the physical and immune state of these patients has various degrees of dysfunction. Therefore, a better response could theoretically be achieved by earlier application of immunotherapy.

The basis of nIT is that it induces the expansion of T cells during the early stage of cancer and leads to less impairment of T cell function by targeting the elevated level of endogenous tumor antigens in the primary tumor. Thereafter, nIT can kill tumor cells, eliminate micro-metastases, promote preoperative down-staging, improve the rates of R0 resection and pathological remission, and reduce the rate of postoperative recurrence (35) (**Figure 1**).

Studies of animal models indicated that nIT produced more tumor-related CD8+ effector T cells in the peripheral blood and organs. The survival time of most mice with high levels of CD8+T cells was more than 100 days. Even after tumor clearance, the number of specific CD8+T cells remained stable. This suggests that nIT may induce the immune system to continue killing tumor cells, thus providing a long-term and robust response (36).

PROSPECTIVE CLINICAL TRIALS OF NIT FOR MSI-H/dMMR NON-MCRC

The discovery of MSI-H/dMMR as a potential biomarker for CRC immunotherapy greatly stimulated research in this area. There has been extensive investigation of the effect of anti-PD-1/anti-PD-L1 therapy on non-mCRC, and there are many encouraging preliminary results (37). Below, we summarize the recent clinical progress in the use of nIT for LACRC to illustrate the potential of nIT for these patients (**Table 1**).

NICHE Study: "Pioneering Research" of nIT

The single-arm NICHE study from the Netherlands was published in Nature Medicine during 2020 (38). This study examined 40 patients (21 patients with dMMR status and 19 with pMMR status) who had stage I~III colon cancer. The double immune neoadjuvant therapy consisted of nivolumab (anti-PD-1 antibody) combined with ipilimumab (anti-CTLA-4 antibody). Remarkably, all patients in the dMMR group survived without disease, with a median follow-up time of 8.1 months. These results indicated that the nivolumab + ipilimumab regimen was a suitable nIT for patients with dMMR non-mCRC, and suggested that immunotherapy could provide a lasting curative effect after the initial benefit. Moreover, the nIT was safe, feasible, and well tolerated (**Table 1**). Thus, it is likely that nIT would not adversely affect the outcome of the subsequent operation, in that there should be no unexpected or redundant post-surgical complications. The most likely reason for the significant reduction in toxicity was the use of a lower dose of ipilimumab and the shorter duration of the nIT. The NICHE study pioneered the use of nIT for CRC, and therefore provided hope to patients with MSI-H/dMMR LACRC.

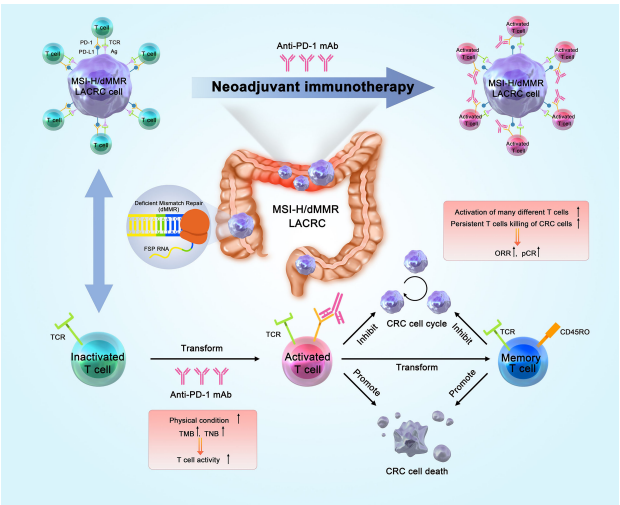

FIGURE 1 | Anti-tumor mechanism of nIT in patients with MSI-H/dMMR CRC. nIT, Neoadjuvant immunotherapy; MSI-H, Microsatellite instability-high; dMMR, Deficient mismatch repair; CRC, Colorectal cancer; TMB, Tumor mutation burden; TNB, Tumor neo-antigen; ORR, Objective response rate; pCR, Pathological complete response.

TABLE 1 | Prospective clinical trials of nIT for MSI-H/dMMR non-mCRC.

Study	Year	Country	Cases	Location	Stage	Neoadjuvant therapy strategy	Efficacy	AEs
NICHE (Phase II)	2020	Netherlands	dMMR: 20 pMMR: 15	Colon cancer	I-III	dMMR/pMMR: Ipilimumab (1mg/kg Day 1); Nivolumab (3mg/kg Day 1+15) → surgery pMMR: Ipilimumab (1mg/kg Day 1); Nivolumab (3mg/kg Day 1+15); Celecoxib (200mg daily) → surgery	pathologic response: dMMR vs pMMR = 100%(20/20) vs 27% (4/15); MPR: dMMR vs pMMR = 95%(19/20) vs 20%(3/15); pCR in dMMR = 60%(12/20)	Grade 3-4 immunotherapy related AEs =13%; Surgery related complications =10%
NICOLE (Phase II)	2021	/	Nivolumab group: 22 (MSI-H vs MSS=3 vs 19) Control group: 22 (MSI-H vs MSS=5 vs 17)	Colon cancer	II-III	Nivolumab group: nivolumab 2cycles→ surgery; control group: surgery	Nivolumab group: R0 resection rate = 100%; Down-staging rate = 70%	Nivolumab group: Delay or surgical complications = 0 ; Grade 3 diarrhea = 4.5%(1/22)
VOLTAGE-A (Phase II)	2020	Japan	MSS: 37 (A1 group) MSI-H: 5 (A2 group)	Rectal cancer	II-III	nCRT(50.4Gy+Cape)→Those who did not progress were enrolled→ 5 courses of nivolumab in the intermittent period→ Surgery→ Adjuvant chemotherapy with FOLFOX or XELOX	MSS: MPR=38%(14/37), pCR=30%(11/37); 1 case adapted W&W strategy after achieving cCR; MSI-H: pCR = 60%(3/5)	Grade 3 myasthenia, interstitial nephritis and grade 2 peripheral motor neuropathy occurred, but they could be relieved without affecting the subsequent surgery
NRG-GI002 (Phase II)	2021	America	Control group: 68 Pembrolizumab group: 69	Rectal cancer	II-III	FOLFOX * 4months→ nCRT (50.4Gy+Cape) +/-Pembrolizumab (200mg q3w*6cycles) → Surgery (8~12 weeks after radiotherapy)	control group vs pembrolizumab group: NAR score: 14.08 vs 11.53 (p=0.26); pCR: 29.4% vs 31.9%(p=0.75); cCR: 13.6% vs 13.9%(p=0.95); Sphincter preserving surgery: 71.0% vs 59.4%(p=0.15)	Grade 3-4 AEs in Pembrolizumab group: During nCRT vs after nIT = 48.2% vs 37.3%
NCT04231552 (Phase II)	2021	China	pMMR: 26 dMMR: 1	Rectal cancer	II-III	SCRT(5x5Gy) → One week later, Capox + Carrelizumab (200mg q3w*2cycles) → Surgery after 1 week	pCR: 48.1% [MSS vs MSI-H = 46%(12/26) vs100%(1/1)]; Down-staging rate: 70%; Anus preserving rate: 89%; R0 resection rate: 100%	Grade 1-2 reactive skin capillary hyperplasia occured; Grade 3 AEs occurred in 7 patients (26%); Surgery related complications =14.8%
AVANA (Phase II)	2021	Italy	96 (MSI-H:1; MSS:38; Unknown:57)	Rectal cancer	II-III	nCRT(50.4Gy+Cape) + Avelumab 10 mg/kg q2w → Surgery(8~12 weeks after radiotherapy)	MPR=61.5%(59/96); pCR=23%(22/96)	Grade 3 ~ 4 non-immune and immune related AEs: 8% and 4%, respectively

non-mCRC, Non-metastatic colorectal cancer; nIT, Neoadjuvant immunotherapy; nCRT, Neoadjuvant chemoradiotherapy; SCRT, Short-Course Radiotherapy; dMMR, Deficient mismatch repair; pMMR, Proficient mismatch repair; MSI-H, Microsatellite instability-high; MSS, Microsatellite stability; MPR, Major pathologic response; TRG, Tumor regression grade; pCR, Pathological complete response; cCR, Clinical complete response; W&W, Watch & wait; NAR, Neoadjuvant rectal score; AEs, Adverse effects.

NICOLE Study: "First Exploration" of Monoimmunotherapy

The NICOLE study (NCT04123925) is the first study to examine the effect of neoadjuvant nivolumab for treatment of early-stage colon cancer without selection for MMR status. This study enrolled 44 patients with cT3/T4 resectable colon cancer. The experimental cohort (86% with MSS) received 2 cycles of nivolumab, and then surgery, and the control cohort (77% with MSS) received surgery. The primary end points were the feasibility of preoperative nIT, the degree of pathological response, and molecular and immunophenotypic changes in the tumor and peripheral blood. The results showed that more than 70% of the patients in nivolumab group experienced significant tumor regression (**Table 1**). The nivolumab group also had significantly higher levels of CD8− and CD8+ non-inhibitory T cells.

VOLTAGE-A Study: "Innovative Exploration" of Sequential nIT With nCRT

The sort-term results of the exploratory VOLTAGE-A phase II study from Japan were published in the Journal of Clinical Oncology during 2020 (39). This study, which compared LACRC patients in an MSS group and an MSI-H group, examined the effect of an initial long-term nCRT, followed by nIT, surgical resection, and then adjuvant chemotherapy. Both groups achieved major pathologic response (MPR) (**Table 1**). As of January 2020, the median follow-up time was 22.5 months for the MSS group and 6.6 months for the MSI-H group. In the MSS group, 2 patients had local recurrence and 2 had distant metastases; however, no patients in the MSI-H group had recurrence.

The FOWARC study (40, 41) found that the pCR rate of mFOLFOX6 combined with preoperative radiotherapy was 28%.

However, this improvement of pCR was not accompanied by improvements in final survival. The pCR rate in the VOLTAGE study was 30%, however, whether this treatment can also provide a survival benefit likely depends on whether the nIT after nCRT was able to activate the immune system and remove small residual lesions. A long-term follow-up of patient survival is needed. Although the sample size of the VOLTAGE study was small, it was the first to compare the application of nIT combined with nCRT for patients who had MSI-H and MSS LACRC. Moreover, the results suggested a better combination biomarker for predicting the efficacy of nIT — PD-L1 positivity and a high ratio of CD8+/Treg cells. This combination biomarker has potential for use in subsequent studies.

NRG-GI002 Study: "Future Prospects" of TNT Combined With nIT

NRG-GI002 is an ongoing phase II clinical research platform that is examining the effect of total neoadjuvant therapy (TNT) for LARC (42). One experimental arm received pembrolizumab with TNT, and researchers evaluated the efficacy and safety of this regimen. The most recent data were presented orally at the 2021 ASCO-GI Annual Meeting (**Table 1**). The results indicated that a TNT consisting of the combination of pembrolizumab with nCRT was safe and led no unexpected short-term toxicities. Nevertheless, it failed to improve the neoadjuvant rectal (NAR) score. In contrast to the previous VOLTAGE-A study of sequential immunotherapy after radiotherapy, this study combined radiotherapy and chemotherapy with immunotherapy. It is not yet known whether this combined therapy will further enhance the sensitivity to radiotherapy or activate the immune response in combination with ICIs while releasing new antigens during radiotherapy. We look forward to seeing the upcoming reports of survival data.

NCT04231552 Study: "Perfect Combination" of Short-Course Radiotherapy, Chemotherapy, and nIT

Professor Zhang Tao reported a phase II study of delayed surgical treatment of LARC after short-range radiotherapy combined with CAPOX and camrelizumab (anti-PD-1 antibody) at the 2021 ASCO-GI Annual Meeting (43). The results showed that all patients exhibited a very high pCR rate regardless of MMR status (**Table 1**). This study was the first to put forward a new neoadjuvant treatment mode of short-range large-fractionated radiotherapy combined with chemotherapy and a PD-1 inhibitor for patients with LARC. This regimen greatly reduced the preoperative treatment time and cost and ensured a good quality-of-life, and therefore provides a foundation for the formulation of novel neoadjuvant treatment strategies for LARC. These results provide hope to patients with low or very low LARC to achieve organ retention and adopt a "Watch & Wait" (W&W) strategy in the future.

AVANA Study: "Continuous Exploration" of nCRT Combined With nIT

The AVANA study is a multicenter phase II study that is examining the efficacy of nCRT combined with avelumab (anti-PD-L1 antibody) for treatment of LARC (44). The results suggest that nCRT can induce the antigen release of low neoantigen burden tumors (such as mismatched CRC) and activate dendritic cells, leading to a CD8+ T lymphocyte-mediated anticancer immune response. nCRT combined with avelumab further increased the expression of PD-L1 in tumor cells, so the researchers strongly recommended using the combination of nCRT and ICIs. Among the 96 patients for whom a pathological response was evaluable, 22 (23%) achieved pCR and 59 (61.5%) achieved MRP (**Table 1**).

These six studies illustrate that MSI-H/dMMR LACRC is inseparable from anti-PD-(L)1 neoadjuvant therapy. The exploration of different and novel combinations and targets, such as chemoimmunotherapy, immunoradiotherapy, combinational checkpoint immunotherapy, and even chemoimmunoradiotherapy, can provide new directions for examining the most suitable population of CRC patients, and even patients with other cancers. In addition, we summarized the ongoing clinical trials of nIT for LACRC (**Table 2**).

RETROSPECTIVE STUDIES OF NIT FOR MSI-H/dMMR LACRC

In recent years, several retrospective studies performed in diverse countries have examined the effect of nIT for MSI-H/dMMR CRC (**Table 3**).

In September 2019, Chinese researchers first reported that two patients with MSI-H/dMMR LARC received nIT treatment with nivolumab (6 cycles). One patient with low rectal cancer adopted a W&W anus-preserving strategy after achieving cCR, and experienced no recurrence after 1 year of follow-up. The other patient received TME surgery and was confirmed as pCR (45). This study was the first to examine the efficacy of nIT as a treatment for MSI-H LARC. In April 2020, Belgian researchers reported that a patient with MSI-H/dMMR low LARC received nIT consisting of nivolumab + ipilimumab. After 3 cycles, TME surgery was performed and it was pathologically confirmed as pCR (46). In June 2020, Chinese researchers reported that two patients with MSI-H LACRC received nIT alone or in combination with targeted therapy. Both patients had confirmed pCR after the operation (47). In July 2020, researchers from the U.S. reported that three patients with MSI-H/dMMR LACRC received nIT: one with monoimmunotherapy, one with monoimmunotherapy combined chemotherapy, and one with double immunotherapy. Their outcomes were pCR, pCR, and W&W with cCR, respectively (48). In December 2020, a retrospective study examined eight patients with MSI-H locally advanced/recurrent metastatic CRC who received monoimmunization or double immunization. The remission rate was 100%. Among the four LACRC patients, one with cCR adopted a W&W approach, and two had confirmed pCR based on postoperative pathology (49).

NIT FOR MSI-H/dMMR LACRC AT OUR CENTER

Our center also conducted a trial to examine the efficacy and safety of neoadjuvant anti-PD-1 monoimmunotherapy for

TABLE 2 | Ongoing clinical trials of nIT for LACRC.

NCT number	Study Title	Phase of trial	Number of participants	Condition	Intervention	Primary outcome measures	Secondary outcome measures	Trial status
NCT04130854	INNATE: Immunotherapy During Neoadjuvant Therapy for Rectal Cancer, a Phase II Randomized Multi-center Trial of Neoadjuvant Therapy With and Without APX005M, an Anti-CD40 Agonist, APX005M, for Locally Advanced Rectal Adenocarcinoma	II	58	LARC	Experimental: APX005M(an anti-CD40 agonist)on day 3 of SCRT(5Gy x 5 days) and on day 3 of cycles 1-5 of mFOLFOX → the 6th cycle of only mFOLFOX → Surgery; Active Comparator: SCRT(5Gy x 5 days) + 6 cycle of mFOLFOX →Surgery	pCR rate	1. OS 2. DFS 3. Rate of resection 4. Safety and tolerability 5. Disease recurrence 6. Development of disease 7. Clinical imaging response 8. cCR rate	Recruiting
NCT04165772	A Phase II Study of Induction PD-1 Blockade in Subjects With Locally Advanced Mismatch Repair Deficient Rectal Adenocarcinoma	II	30	MSI-H/ dMMR LARC	9 cycles of TSR-042 (a PD-1 antibody, 500mg; q3w); participants who exhibit CR will proceed to W&W; participants who do not have a CR will received standard nCRT →Surgery	pCR rate; cCR rate	/	Recruiting
NCT04304209	PD-1 Antibody Sintilimab ± Chemoradiotherapy for Locally Advanced Rectal Cancer	II/III	25	LARC (cohort A: dMMR/ MSI-H; Cohort B: pMMR/ MSS MSI-L;)	Cohort A: 4 cycles of Sintilimab(a PD-1 antibody) → Surgery or W&W → 4 cycles of Sintilimab ± CapeOx according to pathologic response; Cohort B-arm 1: 4 cycles of Sintilimab, nCRT with CapeOx → Surgery or W&W, → 4 cycles of Cape0x; Cohort B-arm 2: 4 cycles of nCRT with CapeOx → Surgery or W&W → 4 cycles of CapeOx	pCR rate	1. Acute toxicities 2. TRG 3. R0 resection rate 4. Surgical complication 5. Local recurrence 6. Distant metastasis 7. 3-year DFS	Recruiting
NCT03985891	A Randomized, Prospective Clinical Trial of Safety and Efficacy of JS001 Combined With Chemotherapy in Patients With Locally Advanced Colon Cancer (Perioperative Treatment)	I/II	40	LACC	Experimental: JS001(a PD-1 antibody) in combination with FOLFOX for 6 cycles before and after operation. Active Comparator: FOLFOX for 6 cycles before and after operation.	pCR rate; cCR rate; ORR	1. DFS 2. OS	Recruiting
NCT03299660	Phase II Trial PD-L1/PD-1 Blockade Avelumab (MSB0010718C) With Chemoradiotherapy for Locally Advanced Resectable Rectal Cancer	II	45	LARC	nCRT with capecitabine for 6 weeks → 4 cycles of Avelumab(a PD-L1 antibody) → Surgery	pCR rate	1. Response as per structural imaging 2. Overall FDG PET response 3. Toxicity 4. Rate of downstaging	Recruiting
NCT04340401	A Phase II Study of Total Neoadjuvant Therapy Plus SHR1210 for High-risk Locally Advanced Rectal Cancer and Biomarker Screening Base on Neoantigen	II	25	LARC	3 cycles Capeox+SHR-1210(an anti-PD-1 inhibitor) → nCRT with capecitabine → 2 cycles CapeOx → Surgery	pCR rate	1. Toxicity of TNT+SHR-1210 2. Change of TCR repertoire 3. DFS 4. Surgical complication rate 5. Major AEs	Recruiting
NCT04230759	Radiochemotherapy +/- Durvalumab for Locally-	II	178	LASCC	Experimental: 5FU+Mitomycin C-based radiochemotherapy	DFS	1. Major AEs 2. cCR	Recruiting

(Continued)

TABLE 2 | Continued

NCT number	Study Title	Phase of trial	Number of participants	Condition	Intervention	Primary outcome measures	Secondary outcome measures	Trial status
	advanced Anal Carcinoma. A Multicenter, Randomized, Phase II Trial of the German Anal Cancer Study Group (RADIANCE)				+Durvalumab (a PD-L1 antibody); Active Comparator: 5FU+Mitomycin C -based Radiochemotherapy		3. OS 4. Colostomy-free survival 5. locoregional recurrence 6. Distant recurrence 7. Quality of life 8. questionnaires	
NCT04293419	Phase II Study of Durvalumab (MEDI4736) Plus Total Neoadjuvant Therapy (TNT) in Locally Advanced Rectal Cancer (The DUREC Trial)	II	58	LARC	6 cycles of mFOLFOX6 → nCRT with capecitabine → Surgery. Patients will receive durvalumab(a PD-L1 antibody,1500mg;q4w) during induction chemotherapy, nCRT and waiting period until surgery	pCR rate	1. Tumor downstaging 2. TRG 3. R0 resection rate 4. 3-year DFS 5. Toxicity profile 6. Surgical complications 7. NAR score	Recruiting
NCT03127007	A Phase Ib/II Study to Evaluate Safety and Efficacy of Atezolizumab Combined With Radio-chemotherapy in a Preoperative Setting for Patients With Localized Rectal Cancer (R-IMMUNE)	I/II	54	LARC	Experimental: nCRT with 5-FU, Atezolizumab (a PD-L1 antibody, 1200mg) is given on day 1 of week 3, 6, 9 and 12. Surgery is planned during week 15; Active Comparator: nCRT with 5-FU. Surgery is planned during week 15	Rate of AEs; pCR rate	/	Recruiting
NCT05202314	Camrelizumab Combined With Neoadjuvant Chemotherapy After Stent Placement for Left-Sided Obstructive Colonic Cancer (NACSOC-02)	II	20	Obstructive colonic cancer	Camrelizumab (a PD-1 antibody, 200mg) 2 cycles + mFOLFOX6 3 cycles or CapeOx 2 cycles → Surgery	pCR rate	1. 3-year OS 2. 3-year DFS	Recruiting

LARC, Locally advanced rectal cancer; LACC, Locally advanced colon cancer; LASCC, locally-advanced anal squamous cell carcinoma; nIT, Neoadjuvant immunotherapy; nCRT, Neoadjuvant chemoradiotherapy; SCRT, Short-Course Radiotherapy; TNT, Total Neoadjuvant Therapy; dMMR, Deficient mismatch repair; pMMR, Proficient mismatch repair; MSI-H, Microsatellite instability-high; MSI-L, Microsatellite instability-low; MSS, Microsatellite stability; ORR,Objective response rate; TRG, Tumor regression grade; CR, Complete response; pCR, Pathological complete response; cCR, Clinical complete response; W&W, Watch & wait; NAR, Neoadjuvant rectal score; AEs, Adverse effects; OS, Overall survival; DFS, Disease free survival; TCR, T Cell Receptor.

patients with MSI-H/dMMR LACRC. At present, 18 patients with MSI-H/dMMR LACRC (including ascending colon cancer, descending colon cancer, sigmoid colon cancer, and rectal cancer) have received nIT with Tislelizumab, and the tumors of all patients (100%) have achieved significant regression. Two patients with LARC and 5 patients with LACC underwent surgery, and all had confirmed pCR (**Figure 2**). Two patients with low LARC adopted a W&W approach after achieving cCR (**Figure 3**). The remaining patients will also undergo surgery. We look forward to reporting the final outcomes, including rates of tumor regression grade (TRG), MPR (TRG 0~1), and pCR (TRG 0).

NEW ORGAN PRESERVATION STRATEGY FOR MSI-H/dMMR LOW LARC

The W&W non-surgical organ preservation strategy was first reported by Harba-Gamal et al. in 2004 (50). This approach was applied to patients with rectal cancer who had cCR after nCRT. Instead of receiving traditional surgery, these patients entered a period of close follow-up and observation in an effort to preserve organ function without affecting tumor survival rate. There is increasing use of neoadjuvant therapy for rectal cancer, but it must be confirmed whether other patients who achieve cCR after neoadjuvant therapy are suitable for a W&W strategy. However, based on the results of previous studies and the known lasting benefits of immunotherapy that has been effective, patients with cCR after nIT for LARC seem especially well-suited for the W&W strategy.

The breakthrough efficacy of nIT for many patients with MSI-H/dMMR LACRC provides colorectal oncologists with great hope, especially for patients with MSI-H/dMMR low LARC. Patients with low rectal cancer face potential risks from surgery that include anal dysfunction, abnormal fecal control, and sexual dysfunction. The prospective and retrospective studies described above indicate that nIT was associated with less risk of sphincter dysfunction, sexual dysfunction, and bladder dysfunction than traditional nCT and nCRT. Furthermore, nIT can provide lasting benefits to the patient. By adopting a W&W strategy after a patient with MSI-H/dMMR low LARC achieves cCR due to nIT, surgery and its concomitant complications can be avoided, thus providing organ preservation

TABLE 3 | Retrospective studies of nIT for MSI-H/dMMR LACRC.

Published journal	Published date	Country	Cases	Gender	Age (years)	Personal or familial history of cancer	Lynch syndrome	Tumor location	Distance from anal verge (cm)	cTNM stage	MRF	EMVI	Type of pathology	MMR (IHC)	MSI (NGS)	RAS
OncoImmunology	2019.9	China	2	Male	27	Mother:rectal cancer and endometrial carcinoma; mother's brother:colon cancer	Yes	Rectum	6.4	cT4bN2M0, III	+	+	Adenocarcinoma	MSH2 (-), MSH6 (-)	MSI-H	Wild type
				Female	64	20 years ago: rectal cancer surgery; 9 years ago: endometrial carcinoma surgery	Yes	Rectum	1	cT4bN2M0, III	–	+	Adenocarcinoma	MSH2 (-), MSH6 (-)	MSI-H	KRAS Mutation (p.G12D)
EJC	2020.4	Belgium	1	Female	27	Father, paternal grandfather and paternal great-grandfather: colon cancer	Yes	Rectum	N/A	cT3N2 M0, III	+	–	Adenocarcinoma	MSH2 (-)	MSI-H	N/A
EJSO	2020.6	China	2	Male	60	N/A	N/A	Descending colon	N/A	cT4aN2M0, III	N/A	N/A	Adenocarcinoma	MSH6 (-)	MSI-H	Wild type
				Female	46	N/A	N/A	Rectosigmoid junctions	N/A	cT4aN2M0, III	N/A	N/A	Adenocarcinoma	MSH2 (-), MSH6 (-)	MSI-H	KRAS Mutation (p.G12D)
JNCCN	2020.7	America	3	Male	81	10 years ago: prostate cancer surgery	N/A	Mid -rectum; lower rectum	5;2	cT3N1M0, III; cT2N0 M0,I	+;–	–;–	Adenocarcinoma	MSH2 (-), MSH6 (-)	MSI-H	N/A
				Male	55	25 years ago: right-sided colon surgery	N/A	Lower rectum	3	cT3N1M0,III	+	–	Adenocarcinoma	PMS2 (-)	MSI-H	Wild type
				Female	38	N/A	Yes	Mid -rectum	N/A	cT3N2M0,III	+	–	Mucinous adenocarcinoma	MSH2 (-)	MSI-H	N/A
OncoImmunology	2020.12	China	4	Female	51	N/A	Yes	N/A	N/A	cT3N1M0,III	N/A	N/A	N/A	N/A	MSI-H	N/A
				Female	19	N/A	Yes	N/A	N/A	cT3N1M0,III	N/A	N/A	N/A	N/A	MSI-H	KRAS Mutation
				Female	49	N/A	Yes	N/A	N/A	cT3N1M0,III	N/A	N/A	N/A	N/A	MSI-H	KRAS Mutation
				Male	34	N/A	Yes	N/A	N/A	cT4bN2M0, III	N/A	N/A	N/A	N/A	MSI-H	Wild type

Published journal	Cases	BRAF	TMB	Previous treatment	Previous treatment response	nIT strategy	nIT response evaluation	AEs during nIT	Radical resection after nIT	ypTNM stage	Adjuvant therapy	Follow-up
OncoImmunology	2	Wild type	High	None	None	Nivolumab 3mg/kg,q2w; 6cycles	PR	Fatigue, grade 2	Yes	ypT0N0M0 (pCR)	None	NED (>1 year after operation)
		Wild type	High	FOLFOXIRI;4cycles	SD	Nivolumab 3mg/kg,q2w; 6cycles	CR	None	No	N/A	None	NED (1 year after nIT)

(Continued)

TABLE 3 | Continued

Published journal	Cases	BRAF	TMB	Previous treatment	Previous treatment response	nIT strategy	nIT response evaluation	AEs during nIT	Radical resection after nIT	ypTNM stage	Adjuvant therapy	Follow-up
EJC	1	N/A	N/A	None	None	Ipilimumab 1mg/kg + Nivolumab 3mg/kg,q2w; 2cycles; Nivolumab3mg/kg,1cycle	CR	None	Yes	ypT0N0M0 (pCR)	nivolumab 3mg/kg, q2w ,4 months	NED (6 months after operation)
EJSO	2	Wild type	N/A	None	None	Toripalimab 240mg +XELOX q3w;4cycles	PR	Nausea, grade 1	Yes	ypT0N0M0 (pCR)	None	NED
		Wild type	N/A	XELOX	None	Sintilimab200mg,q3w; 5cycles + bevacizumab 500mg,q3w;4cycles	PR	None	Yes	ypT0N0M0 (pCR)	None	NED
JNCCN	3	N/A	N/A	None	None	Pembrolizumab 200mg, q3w;11cycles	CR	Fatigue, grade 2	No	N/A	None	NED (17 months after nIT)
		Wild type	High	FOLFOX; 8cycles	SD	Nivolumab 3mg/kg + Ipilimumab 1mg/kg, q3w;7cycles	CR	Fatigue and rash,grade 1	No	N/A	None	NED (12 months after nIT)
		N/A	N/A	None	None	Pembrolizumab +FOLFOX;7cycles	PR	Rash, grade 1	Yes	ypT0N0M0 (pCR)	None	NED (10 months after nIT)
OncoImmunology	4	N/A	N/A	None	None	Pembrolizumab240mg +XELOX, q3w;2cycles	PR	N/A	Yes	ypT0N0M0 (pCR)	N/A	N/A
		Wild type	N/A	None	None	Pembrolizumab 200mg +Ipilimumab 50mg,q3w; 4cycles	CR	N/A	No	N/A	N/A	N/A
		Wild type	N/A	None	None	Nivolumab 140mg,q3w; 12cycles	PR	N/A	Yes	ypT0N0M0 (pCR)	N/A	N/A
		Wild type	N/A	None	None	Pembrolizumab 200mg,q3w;4cycles	PR	N/A	Yes	TRG 2 (PR)	N/A	N/A

LACRC, Locally advanced colorectal cancer; nIT, Neoadjuvant immunotherapy; nCRT, Neoadjuvant chemoradiotherapy; EJC, European Journal of Cancer; EJSO, European Journal of Surgical Oncology; JNCCN, Journal of the National Comprehensive Cancer Network; MRF, Mesorectal fascia; EMVI, Extramural vascular invasion; MMR, Mismatch repair gene; IHC, Immunohistochemistry; MSI, Microsatellite instability; NGS, Next generation sequencing; TMB, Tumor mutation burden; PR, Partial response; PD, Progressive disease; SD, Stable disease; pCR, Pathological complete response; cCR, Clinical complete response; NED, No Evidence of Disease; TRG, Tumor regression grade; AEs, Adverse effects; N/A, not available;+, Positive;–, Negative.

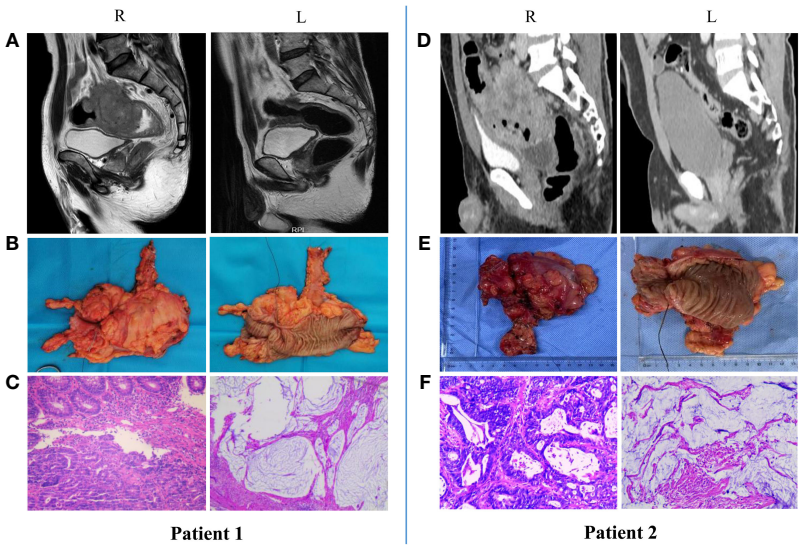

FIGURE 2 | Radiologic and pathological response to nIT with Tislelizumab, and surgical specimens in two patients with MSI-H/dMMR LACRC (pCR). **(A, D)** Imaging: Pretreatment (R) VS After 6 cycles of nIT (L); **(B, E)** Surgical specimens: After 6 cycles of nIT (R/L); **(C, F)** Pathology: Pretreatment (R) VS After 6 cycles of nIT (L).

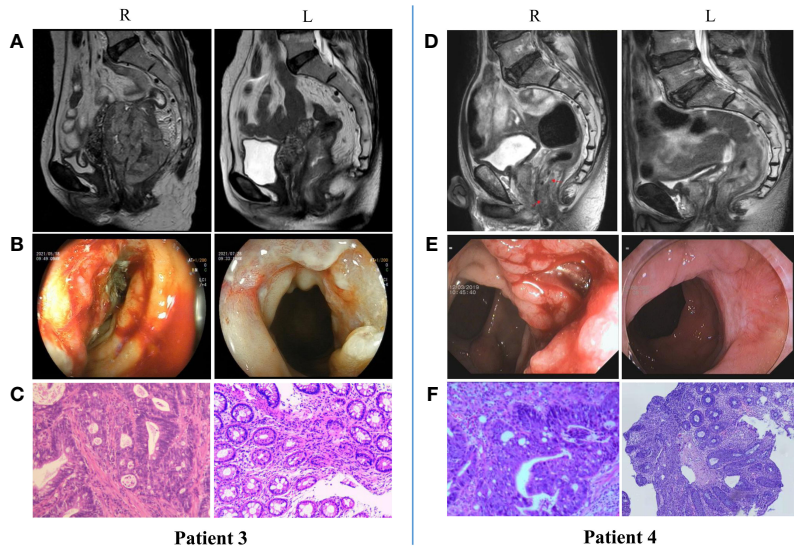

FIGURE 3 | Radiologic, colonoscopic and pathological response to nIT with Tislelizumab in two patients with MSI-H/dMMR LARC (cCR). **(A, D)** Imaging: Pretreatment (R) VS After 6 cycles of nIT (L); **(B, E)** Colonoscopy: Pretreatment (R) VS After 6 cycles of nIT with (L); **(C, F)** Pathology: Pretreatment tumor biospy (R) VS Re-biospy after 6 cycles of nIT (L).

and improving the long-term prognosis. It remains very important to develop additional biomarkers for complete remission as future developments of nIT continue.

CONCLUSIONS AND PERSPECTIVES

In summary, we suggest that careful selection of neoadjuvant therapy for patients with LACRC should be guided by risk degree classification and molecular typing. Thus, patients with MSI-H/dMMR LACRC typically have poor sensitivity to traditional nCRT and nCT. A nIT that uses a single ICI, or two ICIs, or an ICI combined with nCRT/nCT can be considered as a reasonable choice and promising strategy for these patients.

The use of molecular screening to identify patients most suitable for specific nITs will allow clinicians to formulate

more reasonable individualized layered diagnoses and treatment strategies for patients with LACRC. This approach may help prevent poor long-term prognosis caused by treatment deviation or deficiency, and may prevent the decline in quality-of-life caused by over-treatment. For patients with low MSI-H/dMMR LARC, a W&W strategy after achieving cCR following nIT could provide opportunities for organ preservation without adversely affecting prognostic survival. Further studies of nIT for LACRC should consider relevant biomarkers in combination with TMB, TNB, liquid biopsy assays, TME immune scores, and other methods to develop a predictive system or model that improves prognosis and clinical efficacy from multiple dimensions.

AUTHOR CONTRIBUTIONS

Drafting the work and/or revising it critically: XZ, TW, and XC.Final approval of the version to be published: XZ, and YL. All authors contributed to the article and approved the submitted version.

FUNDING

This study was supported by the National Natural Science Foundation of China (82060542 to CD), and the Yunnan Provincial Department of Education Science Research Fund Project (2022J0227 to XZ).

REFERENCES

1. Sung H, Ferlay J, Siegel RL, Laversanne M, Soerjomataram I, Jemal A, et al. Global Cancer Statistics 2020: GLOBOCAN Estimates of Incidence and Mortality Worldwide for 36 Cancers in 185 Countries. *CA Cancer J Clin* (2021) 71(3):209–49. doi: 10.3322/caac.21660
2. Sauer R, Liersch T, Merkel S, Fietkau R, Hohenberger W, Hess C, et al. Preoperative Versus Postoperative Chemoradiotherapy for Locally Advanced Rectal Cancer: Results of the German CAO/ARO/AIO-94 Randomized Phase III Trial After a Median Follow-Up of 11 Years. *J Clin Oncol* (2012) 30 (16):1926–33. doi: 10.1200/JCO.2011.40.1836
3. Lichtenstern CR, Ngu RK, Shalapour S, Karin M. Immunotherapy, Inflammation and Colorectal Cancer. *Cells* (2020) 9(3):618. doi: 10.3390/cells9030618
4. Tan E, Sahin IH. Defining the Current Role of Immune Checkpoint Inhibitors in the Treatment of Mismatch Repair-Deficient/Microsatellite Stability-High Colorectal Cancer and Shedding Light on Future Approaches. *Expert Rev Gastroenterol Hepatol* (2021) 15(7):735–42. doi: 10.1080/17474124.2021.1886077
5. Foxtrot Collaborative Group. Feasibility of Preoperative Chemotherapy for Locally Advanced, Operable Colon Cancer: The Pilot Phase of a Randomised Controlled Trial. *Lancet Oncol* (2012) 13(11):1152–60. doi: 10.1016/S1470-2045(12)70348-0
6. Cercek A, Dos Santos Fernandes G, Roxburgh CS, Ganesh K, Ng S, Sanchez-Vega F, et al. Mismatch Repair-Deficient Rectal Cancer and Resistance to Neoadjuvant Chemotherapy. *Clin Cancer Res* (2020) 26(13):3271–9. doi: 10.1158/1078-0432.CCR-19-3728
7. Benson AB, Venook AP, Al-Hawary MM, Cederquist L, Chen YJ, Ciombor KK, et al. Rectal Cancer, Version 2.2018, NCCN Clinical Practice Guidelines in Oncology. *J Natl Compr Canc Netw* (2018) 16(7):874–901. doi: 10.6004/jnccn.2010061
8. Al-Sukhni E, Attwood K, Mattson DM, Gabriel E, Nurkin SJ. Predictors of Pathologic Complete Response Following Neoadjuvant Chemoradiotherapy for Rectal Cancer. *Ann Surg Oncol* (2016) 23(4):1177–86. doi: 10.1245/s10434-015-5017-y
9. Malone ER, Oliva M, Sabatini PJB, Stockley TL, Siu LL. Molecular Profiling for Precision Cancer Therapies. *Genome Med* (2020) 12(1):8. doi: 10.1186/s13073-019-0703-1
10. Rotte A. Combination of CTLA-4 and PD-1 Blockers for Treatment of Cancer. *J Exp Clin Cancer Res* (2019) 38(1):255. doi: 10.1186/s13046-019-1259-z
11. Oliveira AF, Bretes L, Furtado I, Oliveira AF, Bretes L, Furtado I. Review of PD-1/PD-L1 Inhibitors in Metastatic dMMR/MSI-H Colorectal Cancer. *Front Oncol* (2019) 9:396. doi: 10.3389/fonc.2019.00396
12. Cohen R, Hain E, Buhard O, Guilloux A, Bardier A, Kaci R, et al. Association of Primary Resistance to Immune Checkpoint Inhibitors in Metastatic Colorectal Cancer With Misdiagnosis of Microsatellite Instability or Mismatch Repair Deficiency Status. *JAMA Oncol* (2019) 5(4):551–5. doi: 10.1001/jamaoncol.2018.4942
13. Hause RJ, Pritchard CC, Shendure J, Salipante SJ. Classification and Characterization of Microsatellite Instability Across 18 Cancer Types. *Nat Med* (2016) 22(11):1342–50. doi: 10.1038/nm.4191
14. Aaltonen LA, Salovaara R, Kristo P, Canzian F, Hemminki A, Peltomäki P, et al. Incidence of Hereditary Nonpolyposis Colorectal Cancer and the Feasibility of Molecular Screening for the Disease. *N Engl J Med* (1998) 338 (21):1481–7. doi: 10.1056/NEJM199805213382101
15. Herman JG, Umar A, Polyak K, Graff JR, Ahuja N, Issa JP, et al. Incidence and Functional Consequences of Hmlh1 Promoter Hypermethylation in Colorectal Carcinoma. *Proc Natl Acad Sci USA* (1998) 95(12):6870–5. doi: 10.1073/pnas.95.12.6870
16. Domingo E, Laiho P, Ollikainen M, Pinto M, Wang L, French AJ, et al. BRAF Screening as a Low-Cost Effective Strategy for Simplifying HNPCC Genetic Testing. *J Med Genet* (2004) 41(9):664–8. doi: 10.1136/jmg.2004.020651
17. Wu Y, Berends MJ, Mensink RG, Kempinga C, Sijmons RH, van Der Zee AG, et al. Association of Hereditary Nonpolyposis Colorectal Cancer-Related Tumors Displaying Low Microsatellite Instability With MSH6 Germline Mutations. *Am J Hum Genet* (1999) 65(5):1291–8. doi: 10.1086/302612
18. Overman MJ, McDermott R, Leach JL, Lonardi S, Lenz HJ, Morse MA, et al. Nivolumab in Patients With Metastatic DNA Mismatch Repair-Deficient or Microsatellite Instability-High Colorectal Cancer (CheckMate 142): An Open-Label, Multicentre, Phase 2 Study. *Lancet Oncol* (2017) 18(9):1182–91. doi: 10.1016/S1470-2045(17)30422-9
19. Le DT, Uram JN, Wang H, Bartlett BR, Kemberling H, Eyring AD, et al. PD-1 Blockade in Tumors With Mismatch-Repair Deficiency. *N Engl J Med* (2015) 372(26):2509–20. doi: 10.1056/NEJMoa1500596
20. Marabelle A, Le DT, Ascierto PA, Di Giacomo AM, De Jesus-Acosta A, Delord JP, et al. Efficacy of Pembrolizumab in Patients With Noncolorectal High Microsatellite Instability/Mismatch Repair-Deficient Cancer: Results From the Phase II KEYNOTE-158 Study. *J Clin Oncol* (2020) 38(1):1–10. doi: 10.1200/JCO.19.02105
21. Le DT, Durham JN, Smith KN, Wang H, Bartlett BR, Aulakh LK, et al. Mismatch Repair Deficiency Predicts Response of Solid Tumors to PD-1 Blockade. *Science* (2017) 357(6349):409–13. doi: 10.1126/science.aan6733
22. Van Cutsem E, Cervantes A, Adam R, Sobrero A, Van Krieken JH, Aderka D, et al. ESMO Consensus Guidelines for the Management of Patients With Metastatic Colorectal Cancer. *Ann Oncol* (2016) 27(8):1386–422. doi: 10.1093/annonc/mdw235
23. Li SKH, Martin A. Mismatch Repair and Colon Cancer: Mechanisms and Therapies Explored. *Trends Mol Med* (2016) 22(4):274–89. doi: 10.1016/j.molmed.2016.02.003
24. Gelsomino F, Barbolini M, Spallanzani A, Pugliese G, Cascinu S. The Evolving Role of Microsatellite Instability in Colorectal Cancer: A Review. *Cancer Treat Rev* (2016) 51:19–26. doi: 10.1016/j.ctrv.2016.10.005
25. Tougeron D, Mouillet G, Trouilloud I, Lecomte T, Coriat R, Aparicio T, et al. Efficacy of Adjuvant Chemotherapy in Colon Cancer With Microsatellite Instability: A Large Multicenter AGEO Study. *J Natl Cancer Inst* (2016) 108 (7). doi: 10.1093/jnci/djv438
26. Sargent DJ, Marsoni S, Monges G, Thibodeau SN, Labianca R, Hamilton SR, et al. Defective Mismatch Repair as a Predictive Marker for Lack of Efficacy of Fluorouracil-Based Adjuvant Therapy in Colon Cancer. *J Clin Oncol* (2010) 28(20):3219–26. doi: 10.1200/JCO.2009.27.1825

27. Venderbosch S, Nagtegaal ID, Maughan TS, Smith CG, Cheadle JP, Fisher D, et al. Mismatch Repair Status and BRAF Mutation Status in Metastatic Colorectal Cancer Patients: A Pooled Analysis of the CAIRO, CAIRO2, COIN, and FOCUS Studies. *Clin Cancer Res* (2014) 20(20):5322–30. doi: 10.1158/1078-0432.CCR-14-0332
28. Goldstein J, Tran B, Ensor J, Gibbs P, Wong HL, Wong SF, et al. Multicenter Retrospective Analysis of Metastatic Colorectal Cancer (CRC) With High-Level Microsatellite Instability (MSI-H). *Ann Oncol* (2014) 25(5):1032–8. doi: 10.1093/annonc/mdu100
29. Luchini C, Bibeau F, Ligtenberg MJL, Singh N, Nottegar A, Bosse T, et al. ESMO Recommendations on Microsatellite Instability Testing for Immunotherapy in Cancer, and Its Relationship With PD-1/PD-L1 Expression and Tumour Mutational Burden: A Systematic Review-Based Approach. *Ann Oncol* (2019) 30(8):1232–43. doi: 10.1093/annonc/mdz116
30. NCCN Clinical Practice Guideline in Oncology. Version 1.2021. Available at: Gastric Cancer.NCCN.org.
31. NCCN Clinical Practice Guideline in Oncology. Version 1.2021. Available at: Colon Cancer.NCCN.org.
32. NCCN Clinical Practice Guideline in Oncology. Version 1.2021. Available at: Rectal Cancer.NCCN.org.
33. Ganesh K, Stadler ZK, Cercek A, Mendelsohn RB, Shia J, Segal NH, et al. Immunotherapy in Colorectal Cancer: Rationale, Challenges and Potential. *Nat Rev Gastroenterol Hepatol* (2019) 16(6):361–75. doi: 10.1038/s41575-019-0126-x
34. Wu T, Wu X, Wang HY, Chen L. Immune Contexture Defined by Single Cell Technology for Prognosis Prediction and Immunotherapy Guidance in Cancer. *Cancer Commun (Lond)* (2019) 39(1):21. doi: 10.1186/s40880-019-0365-9
35. Topalian SL, Taube JM, Pardoll DM. Neoadjuvant Checkpoint Blockade for Cancer Immunotherapy. *Science* (2020) 367(6477):eaax0182. doi: 10.1126/science.aax0182
36. Liu J, Blake SJ, Yong MC, Harjunpää H, Ngiow SF, Takeda K, et al. Improved Efficacy of Neoadjuvant Compared to Adjuvant Immunotherapy to Eradicate Metastatic Disease. *Cancer Discov* (2016) 6(12):1382–99. doi: 10.1158/2159-8290.CD-16-0577
37. Wang F, Wang ZX, Chen G, Luo HY, Zhang DS, Qiu MZ, et al. Expert Opinions on Immunotherapy for Patients With Colorectal Cancer. *Cancer Commun (Lond)* (2020) 40(10):467–72. doi: 10.1002/cac2.12095
38. Chalabi M, Fanchi LF, Dijkstra KK, Van den Berg JG, Aalbers AG, Sikorska K, et al. Neoadjuvant Immunotherapy Leads to Pathological Responses in MMR-Proficient and MMR-Deficient Early-Stage Colon Cancers. *Nat Med* (2020) 26(4):566–76. doi: 10.1038/s41591-020-0805-8
39. Yuki S, Bando H, Tsukada Y, Inamori K, Komatsu Y, Homma S, et al. Short-Term Results of VOLTAGE-A: Nivolumab Monotherapy and Subsequent Radical Surgery Following Preoperative Chemoradiotherapy in Patients With Microsatellite Stable and Microsatellite Instability-High Locally Advanced Rectal Cancer. *J Clin Oncol* (2020) 38(15_suppl):4100. doi: 10.1200/JCO.2020.38.15_suppl.4100
40. Cheng YK, Qin QY, Huang XY, Lan P, Wang L, Gao X, et al. Effect of Interval Between Preoperative Radiotherapy and Surgery on Clinical Outcome and Radiation Proctitis in Rectal Cancer From FOWARC Trial. *Cancer Med* (2020) 9(3):912–9. doi: 10.1002/cam4.2755
41. Deng Y, Chi P, Lan P, Wang L, Chen W, Cui L, et al. Neoadjuvant Modified FOLFOX6 With or Without Radiation Versus Fluorouracil Plus Radiation for Locally Advanced Rectal Cancer: Final Results of the Chinese FOWARC Trial. *J Clin Oncol* (2019) 37(34):3223–33. doi: 10.1200/JCO.18.02309
42. Rahma OE, Yothers G, Hong TS, Russell MM, You YN, Parker W, et al. Use of Total Neoadjuvant Therapy for Locally Advanced Rectal Cancer: Initial Results From the Pembrolizumab Arm of a Phase 2 Randomized Clinical Trial. *JAMA Oncol* (2021) 7(8):1225–30. doi: 10.1001/jamaoncol.2021.1683
43. Lin Z, Cai M, Zhang P, Li G, Liu T, Li X, et al. Short-Course Radiotherapy and Subsequent CAPOX Plus Camrelizumab Followed by Delayed Surgery for Locally Advanced Rectal Cancer:Short-Term Results of a Phase II Trial. *J Clin Oncol* (2021) 39(3_suppl):63. doi: 10.1200/JCO.2021.39.3_suppl.63
44. Salvatore L, Bensi M, Corallo S, Bergamo F, Tortora G, et al. Phase II Study of Preoperative (PREOP) Chemoradiotherapy (CTRT) Plus Avelumab (AVE) in Patients (PTS) With Locally Advanced Rectal Cancer(LARC): The AVANA Study. *J Clin Oncol* (2021) 39(no. 15_suppl):3511. doi: 10.1200/JCO.2021.39.15_suppl.3511
45. Zhang J, Cai J, Deng Y, Wang H. Complete Response in Patients With Locally Advanced Rectal Cancer After Neoadjuvant Treatment With Nivolumab. *Oncoimmunology* (2019) 8(12):e1663108. doi: 10.1080/2162402X.2019.1663108
46. Mans L, Pezzullo M, D'Haene N, Van de Stadt J, Van Laethem JL. Pathological Complete Response After Neoadjuvant Immunotherapy for a Patient With Microsatellite Instability Locally Advanced Rectal Cancer: Should We Adapt Our Standard Management for These Patients? *Eur J Cancer* (2020) 135:75–7. doi: 10.1016/j.ejca.2020.04.046
47. Zhang Z, Cheng S, Gong J, Lu M, Zhou J, Zhang X, et al. Efficacy and Safety of Neoadjuvant Immunotherapy in Patients With Microsatellite Instability-High Gastrointestinal Malignancies: A Case Series. *Eur J Surg Oncol* (2020) 46(10 Pt B):e33–9. doi: 10.1016/j.ejso.2020.06.034
48. Demisse R, Damle N, Kim E, Gong J, Fakih M, Eng C, et al. Neoadjuvant Immunotherapy-Based Systemic Treatment in MMR-Deficient or MSI-High Rectal Cancer: Case Series. *J Natl Compr Canc Netw* (2020) 18(7):798–804. doi: 10.6004/jnccn.2020.7558
49. Liu DX, Li DD, He W, Ke CF, Jiang W, Tang JH, et al. PD-1 Blockade in Neoadjuvant Setting of DNA Mismatch Repair-Deficient/Microsatellite Instability-High Colorectal Cancer. *Oncoimmunology* (2020) 9(1):1711650. doi: 10.1080/2162402X.2020.1711650
50. Habr-Gama A, Perez RO, Nadalin W, Sabbaga J, Ribeiro U Jr, Silva e Sousa AH Jr, et al. Operative Versus Nonoperative Treatment for Stage 0 Distal Rectal Cancer Following Chemoradiation Therapy: Long-Term Results. *Ann Surg* (2004) 240(4):711–7. doi: 10.1097/01.sla.0000141194.27992.32

Conflict of Interest: The authors declare that the research was conducted in the absence of any commercial or financial relationships that could be construed as a potential conflict of interest.

Publisher's Note: All claims expressed in this article are solely those of the authors and do not necessarily represent those of their affiliated organizations, or those of the publisher, the editors and the reviewers. Any product that may be evaluated in this article, or claim that may be made by its manufacturer, is not guaranteed or endorsed by the publisher.

Copyright © 2022 Zhang, Wu, Cai, Dong, Xia, Zhou, Ding, Yang, Tan, Zhang, Zhang, Wang, Dong and Li. This is an open-access article distributed under the terms of the Creative Commons Attribution License (CC BY). The use, distribution or reproduction in other forums is permitted, provided the original author(s) and the copyright owner(s) are credited and that the original publication in this journal is cited, in accordance with accepted academic practice. No use, distribution or reproduction is permitted which does not comply with these terms.

frontiers in Immunology

ORIGINAL RESEARCH
published: 29 March 2022
doi: 10.3389/fimmu.2022.845217

A SIRPαFc Fusion Protein Conjugated With the Collagen-Binding Domain for Targeted Immunotherapy of Non-Small Cell Lung Cancer

Jiayang Liu[1,2†], Zhefeng Meng[1†], Tongyang Xu[1], Kudelaidi Kuerban[1,2], Songna Wang[1,2], Xuyao Zhang[1,2], Jiajun Fan[1,2], Dianwen Ju[1,2], Wenzhi Tian[3], Xuan Huang[1,2], Xiting Huang[1], Danjie Pan[1,2], Huaning Chen[1,2], Weili Zhao[4] and Li Ye[1,2]*

[1] Minhang Hospital & Department of Biological Medicines at School of Pharmacy, Fudan University, Shanghai, China, [2] Shanghai Engineering Research Center of Immunotherapeutics, School of Pharmacy, Fudan University, Shanghai, China, [3] ImmuneOnco Biopharma (Shanghai) Co., Ltd., Shanghai, China, [4] Department of Medicinal Chemistry, School of Pharmacy, Fudan University, Shanghai, China

OPEN ACCESS

Edited by:
Udo S. Gaipl,
University Hospital Erlangen, Germany

Reviewed by:
Raymond B. Birge,
Rutgers, The State University of New Jersey, United States
Johannes vom Berg,
University of Zurich, Switzerland

***Correspondence:**
Li Ye
yelil@fudan.edu.cn

[†]These authors have contributed equally to this work and share first authorship

Specialty section:
This article was submitted to Cancer Immunity and Immunotherapy, a section of the journal Frontiers in Immunology

Received: 29 December 2021
Accepted: 03 March 2022
Published: 29 March 2022

Citation:
Liu J, Meng Z, Xu T, Kuerban K, Wang S, Zhang X, Fan J, Ju D, Tian W, Huang X, Huang X, Pan D, Chen H, Zhao W and Ye L (2022) A SIRPαFc Fusion Protein Conjugated With the Collagen-Binding Domain for Targeted Immunotherapy of Non-Small Cell Lung Cancer. Front. Immunol. 13:845217. doi: 10.3389/fimmu.2022.845217

The SIRPαFc fusion protein can block the immunosuppressive CD47-SIRPα signal between macrophages and tumor cells as a decoy receptor and has demonstrated its immunotherapeutic efficacy in various tumors. However, its clinical application was limited because of the potential hematologic toxicity. The heptapeptide "TKKTLRT" is a collagen-binding domain (CBD) which can bind collagen specifically. Herein, we aim to improve the tumor targeting of SIRPαFc and therefore avoid its unnecessary exposure to normal cells through synthesizing a TKKTLRT–SIRPαFc conjugate. Experiments at molecular and cellular levels indicate that the TKKTLRT–SIRPαFc conjugate-derived collagen-binding affinity and the introduction of CBD did not impact the CD47-binding affinity as well as its phagocytosis-promoting effect on NSCLC cells. *In vivo* distribution experiments showed that CBD–SIRPαFc accumulated in tumor tissue more effectively compared to unmodified SIRPαFc, probably due to the exposed collagen in the tumor vascular endothelium and stroma resulting from the abnormal vessel structure. On an A549 NSCLC nude mouse xenograft model, CBD–SIRPαFc presented more stable and effective antitumor efficacy than SIRPαFc, along with significantly increased $CD11b^{+}F4/80^{+}$ macrophages especially MHC II^{+} M1 macrophages within tumors. All of these results revealed that CBD brought a tumor-targeting ability to the SIRPαFc fusion protein, which contributed to the enhanced antitumor immune response. Altogether, the CBD–SIRPαFc conjugate may have the potential to be an effective tumor immunotherapy with improved antitumor efficacy but less non-tumor-targeted side effect.

Keywords: SIRPαFc fusion protein, collagen, macrophage, conjugate, cancer immunotherapy

INTRODUCTION

The incidence and mortality of cancer have increased rapidly in recent years, of which solid tumors account for the majority (1). According to the data from the Global Cancer Observatory, lung cancer accounts for 23.8% of all cancer deaths (2), of which non-small cell lung cancer (NSCLC) accounts for 85% of the diagnoses (3). Studies on antitumor treatments have greatly developed, but an effective therapy is still important and urgent (4). Traditional surgery, chemotherapy, and radiotherapy are initially used to fight against cancer, but the poor survival and high recurrence still remain problems (5). Over the past decade, cancer immunotherapy has grown rapidly. However, cancer cells could always manage themselves to escape from immune surveillance *via* several mechanisms such as upregulation of ligands for immune checkpoints, secreting immunosuppressive cytokines (VEGF, TGF-b1, IL-10, etc.), and epigenetic silencing (4, 6).

T-cell immune checkpoint inhibitors are most common and successful agents used in cancer immunotherapy (6), which would activate the immune system through targeting cancer immune checkpoints such as PD-1/PD-L1, CTLA-4, and block immunosuppression signals (7). Many checkpoint inhibitors (CPIs) such as nivolumab, pembrolizumab, atezolizumab, and ipilimumab have proved their validity in the clinical treatment of NSCLC (8, 9), which mainly target the adaptive immune system and activate T-cell responses (10, 11). However, those CPIs generally only work in the part of patients. Recently, in order to further improve immunotherapy, many studies are focusing on another branch of immune system—innate immune system, which is also crucial to antitumor immunity (12, 13).

Macrophages, known as major immune cells in innate immunity, have also played an important role in cancer immunotherapy (5). The CD47-SIRPα axis is the most thoroughly studied signal pathway regulating phagocytosis by macrophages and other phagocytes, which could be an ideal target (14). CD47 binding to its natural ligand SIRPα (signal regulatory protein alpha) will deliver a "don't eat me" signal to phagocytes through activating the SHP-1 and SHP-2 signal pathway, inducing phagocytosis inhibition (15). Tumor cells could escape from the innate immunity by expressing high-level CD47 on its surface. Previous studies have shown that blocking the CD47-SIRPα signal could not only restart phagocytosis but also enhance tumor antigen presentation and activate specific antitumor immune response, reacting in both innate and adaptive immunity (16–18).

CD47 is widely expressed in solid tumors (19), promoting multiple agents targeting CD47 or SIRPα, such as anti-CD47 or anti-SIRPα antibodies and fusion proteins (20). SIRPαFc is a fusion protein combining the human SIRPα extracellular domain with the human IgG1 Fc fragment. It could not only effectively block immunosuppressive CD47-SIRPα signals but also induce Fcγ receptor reaction by its Fc fragment. While blocking endogenic CD47-SIRPα signals between tumor cells and phagocytes, SIRPαFc would promote antitumor innate immunity and tumor antigen presenting to activate adaptive immunity (14, 17). Through binding to the Fcγ receptor, SIRPαFc could also mediate antibody-dependent cell-mediated cytotoxicity (ADCC) and antibody-dependent cellular phagocytosis (ADCP) to suppress tumor (5, 20). In previous studies, we have confirmed its antitumor efficacy on non-small cell lung cancer and glioblastoma (21–23).

Erythrocytes and platelets also contain high-level CD47, which help to eliminate senescent cells and maintain the balance (24–27). Thus, agents targeting CD47 may bind to erythrocytes or platelets and the subsequent phagocytosis could induce hematologic toxicity such as hemolytic anemia and thrombocytopenia (28, 29). Although SIRPαFc binds less to CD47 on human erythrocytes than the anti-CD47 antibody, the SIRPαFc-related anemia, thrombocytopenia, and neutropenia still happened in clinically enrolled subjects, thus raising a safety concern (30). Therefore, reducing binding to normal cells including healthy erythrocytes is critical to anti-CD47 immunotherapies.

Collagen is the most common protein in mammals, which appears in almost all the tissues (31), especially the vascular endothelium and tumor stroma. In tumors, vessels were recognized as unhealed wound to be repaired (32), inducing an abnormal and incomplete structure in the vascular wall. Due to the fragmentary vessels, macromolecules in circulation derived from enhanced permeability would keep retention in tumor, which was summarized as EPR (enhanced permeability and retention) effect, while collagen was also exposed around tumor vessels more than in normal tissues (32, 33).

There is a plethora of studies using protein engineering to introduce the collagen-binding domain or protein-binding molecules, which introduces retention or homing of therapeutic proteins in tumors (34, 35) or in other diseases (36, 37). The collagen-binding domain (CBD) is a series of polypeptides which are able to bind collagen. They have a variety of sources such as von Willebrand factor (vWF), fibronectin, or collagenase, containing both natural and artificial sequences (38). "TKKTLRT" is the smallest CBD peptide designed based on the collagenase cleavage site in the collagen-type I α2 chain. This heptapeptide was found to have good tissue penetration and could continuously release a small size of antibody molecules or fusion proteins when binding to the exposed collagen in tumor tissues as conjugates such as CBD–scFv or CBD–Fab fusion protein (39, 40).

Here, we designed and synthesized a TKKTLRT-SIRPαFc conjugate. We propose that the conjugation would confer SIRPαFc collagen affinity. Due to the fragmentary vessels and exposed stroma collagen of solid tumor, our conjugate would specifically accumulate in tumor rather than normal tissues, which represents tumor targeting and leads to better antitumor efficacy by effective and sustainable immune activation and improved safety results from less non-tumor binding (35).

MATERIALS AND METHODS

Synthesis of the CBD–SIRPαFc Conjugate

The construction, expression, and purification of human SIRPαFc fusion protein was performed as previously described

(21). Polypeptide "TKKTLRTC" was synthesized by Yuan Peptide (Nanjing) with a purity above 95% detected by HPLC. SIRPαFc was incubated with 15 equivalents of 4-(N-maleimidomethyl)cyclohexane-1-carboxylic acid 3-sulfo-N-hydroxysuccinimide ester sodium salt (Sulfo-SMCC, Sigma-Aldrich, St. Louis, MO, USA) in pH 7.4 PBS for 40 min at room temperature. Dissociative Sulfo-SMCC was removed through 3 × 4 h dialysis in pH 7.4 PBS. The intermediate was then incubated with 10 equivalents of polypeptide "TKKTLRTC" for 1 h at room temperature in the absence of oxygen. A 3 × 4 h dialysis in pure water was performed to eliminate excess polypeptides and desalt. The reaction mixture was frozen at -80°C for 48 h. Freeze-drying was performed to derive CBD–SIRPαFc conjugate powder.

Identification of CBD–SIRPαFc

Sodium dodecyl sulfate polyacrylamide gel electrophoresis (SDS-PAGE) was first performed to examine whether there was impurity in CBD–SIRPαFc freeze-dried powder. The purified product was dissolved in PBS and then reduced by SDS-PAGE Loading Buffer (Beyotime, P0015, Shanghai, China) according to the manufacturer's instruction. SDS-PAGE was performed on 12% separating gel. Gel images were acquired with the ChemiDoc™ XRS+ System with Image Lab™ Software (Bio-Rad, Hercules, CA, USA).

Matrix-assisted laser desorption/ionization time-of-flight mass spectrometry (MALDI-TOF-MS) was then performed to determine the exact molecular weight and the ratio of the polypeptide conjugated to SIRPαFc. SIRPαFc and CBD–SIRPαFc were dissolved in pure water and diluted to 1 μg/μl. Proteins were ionized in the matrix of 3,5-dimethoxy-4-hydroxycinnamic acid (sinapic acid, SA), and MALDI-TOF-MS was performed. All spectrograms were collected and analyzed with analysis software Data Explorer™ Software.

Affinity of CBD–SIRPαFc to CD47 and Collagen

Binding between SIRPαFc/CBD–SIRPαFc and CD47 was detected with Biacore. Sensor S Sensor Chip CM5 (GE Healthcare, Chicago, IL, USA) was activated by EDC-NHS and then caught SIRPαFc/CBD–SIRPαFc proteins on its surface. Human CD47 solution was attenuated into six gradients and flew through the chip in order. A signal–time curve was recorded and analyzed with Biacore T200 (GE Healthcare).

ELISA was performed to measure the affinity between CBD–SIRPαFc and collagen type I. A 96-well ELISA plate was coated with 100 μg/ml collagen type I (Corning, Tewksbury, MA, USA) or 2% BSA at 4°C overnight, then blocked by 2% BSA in PBS-T for 2 h at 37°C. Wells were washed with PBS-T for 5 times and incubated with SIRPαFc or CBD–SIRPαFc in five concentration gradients at 37°C for 2 h. After being washed, wells were incubated with HRP-conjugated anti-human IgG1 Fc fragment antibody at 37°C for 2 h. After a final wash, wells were incubated with TMB substrate at 37°C for 30 min. Absorbance at 450 nm was measured, and an absorbance–concentration curve was drawn in GraphPad Prism 8 software. The K_D value was calculated through non-linear regression (assuming one-site specific binding).

Binding of CBD–SIRPαFc to Cancer Cells and Collagen

Flow cytometry was performed to detect the binding of SIRPαFc/CBD–SIRPαFc to cancer cells. 1×10^5 A549 cells were resuspended in PBS (control group), 10 μg/ml SIRPαFc, or CBD–SIRPαFc respectively and incubated at 37°C for 2 h. After being washed with PBS, cells were incubated with DyLight 680-labeled anti-human IgG Fc fragment antibody at 37°C for 1 h. After being washed, cells were resuspended in 200 μl PBS in 96-well plates and detected with Beckman CytoFlex S Flow Cytometer using the APC A700 channel. CytExpert Software was used to analyze the flow cytometry data.

We also performed modified ELISA to test whether CBD–SIRPαFc could bind tumor cells and collagen simultaneously. The 96-well ELISA plate was coated with 100 μg/ml collagen type I (Corning) at 4°C overnight, then blocked with 2% BSA in PBS-T for 2 h at 37°C. Wells were washed with PBS-T for 5 times and incubated with PBS (control group), 100 μg/ml SIRPαFc, or CBD–SIRPαFc at 37°C for 2 h. After washing, 5×10^4 CFDA SE-labeled A549 cells were inoculated and incubated at 37°C for 2 h. After being washed with PBS for 3 times, wells were observed and cells were counted under a laser confocal fluorescence microscope. One-way-ANOVA was performed to analyze the significance in GraphPad Prism 8 software.

Phagocytosis Test

A phagocytosis test was performed to detect whether CBD conjugation would influence the enhancement of phagocytosis induced by SIRPαFc. 1×10^5 macrophage Ana-1 cells were first inoculated in confocal dishes. After being incubated for 8 to 12 h till the cells had tightly adhered, they were cultivated in serum-free medium for 2 h. After inoculating 2×10^5 CFDA SE-labeled A549, NCI-H1975, or PC-9 cells, cells were respectively incubated in complete medium with no drugs (control group), 10 μg/ml SIRPαFc, or CBD–SIRPαFc in every group for 2 h. Dissociative tumor cells were washed away with PBS, then cells were observed and counted under the laser confocal fluorescence microscope. A phagocytic index (number of phagocytized cancer cells in every 100 ana-1 cells) was calculated to measure the phagocytosis.

Mice and Cell Lines

Male BALB/c nude mice aged 6 to 8 weeks were obtained from the Shanghai SLAC Laboratory. All procedures involving animals were conducted in accordance with the standards approved by the Animal Ethical Committee of School of Pharmacy at Fudan University. A549 cells, NCI-H1975 cells, PC-9 cells, and Ana-1 cells were kindly provided by Stem Cell Bank, Chinese Academy of Sciences, and cultured according to the instructions in RPMI 1640 medium (BI) containing 10% of fetal bovine serum (Gibco, Grand Island, NY, USA) at 37°C in an incubator with 5% CO_2.

Collagen and CBD–SIRPαFc Distribution *In Vivo*

A total of 1×10^7 A549 cells were resuspended in 200 μl PBS then inoculated subcutaneously at the right flank of male BALB/c nude mice aged 6 to 8 weeks. Tumors and paired normal tissues were harvested when reaching 200 mm^3 and fixed in 4% paraformaldehyde. After embedding in paraffin, tissues were cut into 5-μm-thick sections. Masson-trichrome staining and immunofluorescent staining were performed to label blood vessels and collagen in tumors and normal tissues. In immunofluorescent staining, DAPI (Servicebio, Wuhan, China, G1012) was used to label the cell nucleus. Goat anti-mouse CD31 antibody (Servicebio, GB13063) and Cy3-conjugated donkey anti-goat IgG (H+L) antibody (Servicebio, GB21404) were used to label CD31, which indicated vessels. Rabbit anti-mouse/human collagen I antibody (Servicebio, GB11022-3) and FITC-conjugated donkey anti-rabbit IgG (H+L) antibody (Servicebio, GB22403) were used to label collagen type I.

SIRPαFc and CBD–SIRPαFc were first labeled by FITC and then quantified. Mice bearing tumors reaching 200 mm^3 were injected with 10 mg/kg FITC-labeled SIRPαFc or CBD–SIRPαFc intraperitoneally. Mice were euthanized with CO_2 inhalation at 2 or 4 h later after the injection, respectively. Tumors, hearts, livers, spleens, lungs, and kidneys were harvested, and fluorescence signals at 2 h were acquired and measured with Living Image software and counted with GraphPad Prism 8 software. Immunofluorescent staining was performed on tumors and main organs at 4 h to label blood vessels and collagen in tumor tissues. Cell nucleus, CD31, and collagen type I were labeled respectively as described above. Immunofluorescent staining images were acquired with CaseViewer Software.

In Vivo Antitumor Efficacy

An A549 BALB/c nude mouse xenograft model was established as described above. When tumors reached 200 mm^3 at about 14 days later, mice were injected with 200 μl PBS, SIRPαFc (10 mg/kg), or CBD–SIRPαFc (10 mg/kg) intraperitoneally twice a week. Tumor volume and mouse weight were measured every time before administration. At the 29th day after the first dose, blood was derived from anesthetized mice. Then mice were euthanized with CO_2 inhalation and tumors, hearts, livers, spleens, lungs, and kidneys were harvested. Part of tumors and organs were fixed in 4% paraformaldehyde then embedded in paraffin for histology and immunology analysis. Tumor volume curves were analyzed with two-way ANOVA in GraphPad Prism 8 software.

Flow Cytometry

Fresh tumors and spleens were ground and filtered through a 70-μm cell strainer (Falcon, 352350) to prepare single-cell suspension. Antibodies against the following molecules were used according to the manufacturer's instructions: anti-mouse CD45 (violetFluor 450-labeled, clone: 30-F11, MULTI SCIENCES, Hangzhou, China), anti-human/mouse CD11b (PerCP-Cy5.5-labeled, clone: M1/70, MULTI SCIENCES), anti-mouse F4/80 (PE-Cy7-labeled, clone: BM8.1, MULTI SCIENCES), anti-mouse MHC II (PE-labeled, clone: M5/114.15.2, MULTI SCIENCES), and anti-mouse CD206 (MMR, APC-labeled, clone: C068C2, MULTI SCIENCES). Intracellular staining was performed using FIX & PERM Kit (MULTI SCIENCES) according to the manufacturer's instructions. Flow cytometry was performed with Beckman CytoFlex S Flow Cytometer. CytExpert Software was used to analyze the flow cytometry data.

Immunohistochemistry Staining Analysis

Tumors embedded in paraffin were cut into 5-μm-thick sections. Ki67 and F4/80 immunohistochemistry staining was respectively performed to study the proliferation and macrophage infiltration in tumor. Rabbit anti-mouse Ki67 antibody (Servicebio, GB111141) and rabbit anti-mouse F4/80 antibody (Servicebio, GB11027) were used for Ki67 staining and F4/80 staining as primary antibodies, respectively. HRP-conjugated goat anti-rabbit IgG (H+L) antibody (Servicebio, GB23303) was used in both staining as secondary antibody. Images were captured by Inverted Phase Contrast Fluorescence Microscope (Olympus, Tokyo, Japan). Proportions of the positive area were counted by ImageJ software and analyzed by one-way ANOVA in GraphPad Prism 8 software.

Histology Staining Analysis

Tumors embedded in paraffin were cut into 5-μm-thick sections. Hematoxylin–eosin (H-E) staining was performed to study the necrosis in tumors, which may result from SIRPαFc or CBD–SIRPαFc injection. Images were captured by Inverted Phase Contrast Fluorescence Microscope (Olympus). Focal necrosis in all samples was counted and analyzed by one-way ANOVA in GraphPad Prism 8 software.

Statistical Analysis

The data were analyzed by GraphPad Prism 8 (GraphPad Software Inc., La Jolla, CA, USA) as described above, and the results were presented as mean ± SD. p value < 0.05 was considered statistically significant.

RESULTS

CBD Conjugates to SIRPαFc Through Sulfo-SMCC

CBD polypeptide "TKKTLRT" was conjugated to human SIRPαFc fusion protein through a two-step reaction (**Figure 1A**). In the first step, SIRPαFc linked to the N-succinimide group in Sulfo-SMCC with its dissociative amidogen at room temperature. After dialysis for removing excess linkers, polypeptide "TKKTLRT" with a designed cysteine at the C-terminal was added to the maleimide group of Sulfo-SMCC in the intermediate with its sulfhydryl in the absence of oxygen at room temperature. MALDI-TOF-MS analysis indicated that the CBD conjugation was easier to be ionized than the unmodified protein since its mass-to-charge ratio remained only one-sixth (**Figures 1B, C**). The main peak (m-z ratio about 14,000) in the CBD–SIRPαFc spectrogram was divided into three sub-peaks with a difference of about one-sixth of the total weight of one molecule of Sulfo-SMCC (436 D) and one molecule of polypeptide "TKKTLRTC" (1,452 D; one-sixth

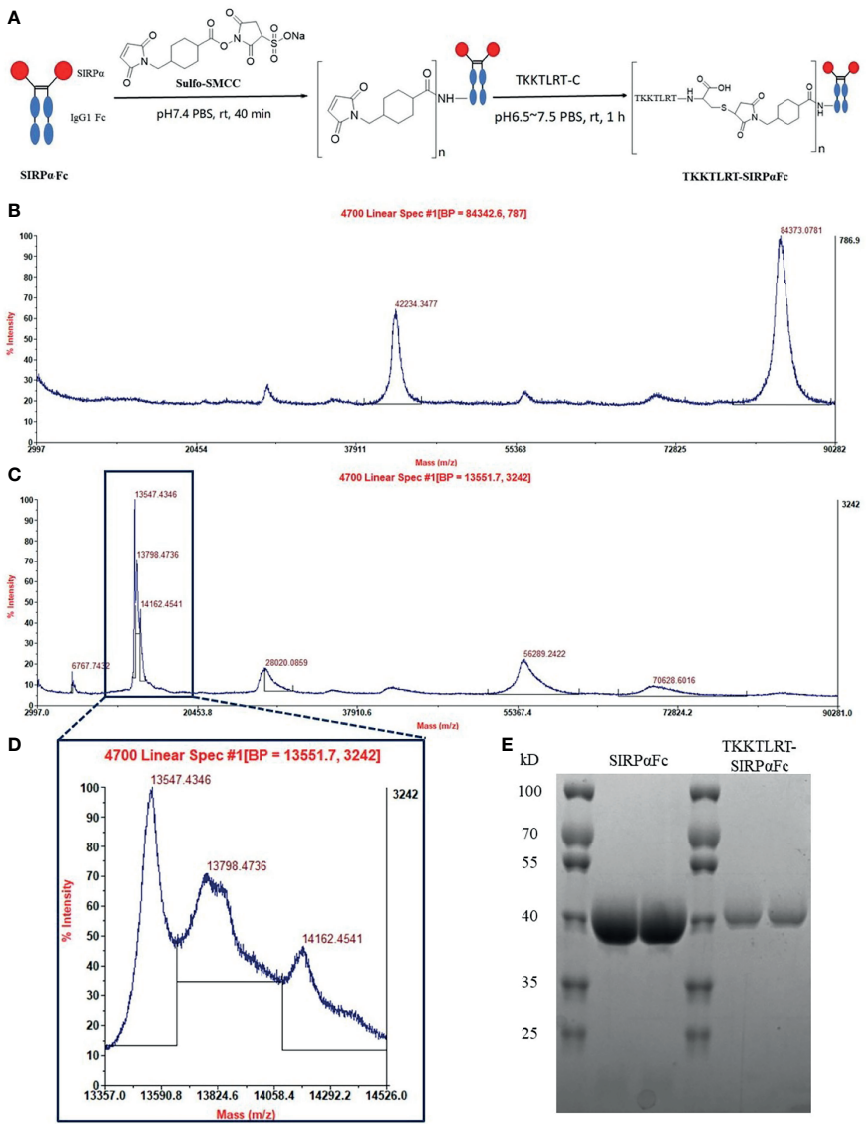

FIGURE 1 | CBD–SIRPαFc conjugate was synthesized and identified. **(A)** Polypeptide "TKKTLRT" conjugates to human SIRPαFc fusion protein with its designed cysteine terminal and a linker Sulfo-SMCC through a two-step reaction. **(B)** The exact molecular weight of SIRPαFc was detected in MALDI-TOF-MS. SIRPαFc weighted 84,373 D and tended to be ionized with two charges, which represented a half mass-to-charge ratio weighting about 42,234 D (data representative of 2 replicates). **(C)** CBD–SIRPαFc was ionized into multiple-charged ions with three (m-z ratio about 28,000), six (m-z ratio about 14,000), or twelve (m-z ratio about 7,000) charges, while some molecules may share charges and represented a non-integral mass-to-charge ratio such as two-thirds (about 56,000) and five-sixths (about 70,000) of the single charge ion (data representative of 2 replicates). **(D)** The main peak (m-z ratio about 14,000) in the CBD–SIRPαFc spectrogram was divided into three sub-peaks. There was a difference of about one-sixth of the total weight of one molecule of Sulfo-SMCC and one molecule of polypeptide "TKKTLRTC" (about 300 D) between each sub-peaks, indicating that one or two molecules of the CBD polypeptide had conjugated to one molecule of SIRPαFc. **(E)** Protein bands were shown in reductive SDS-PAGE (two replicates). SIRPαFc was just below 40 kD. CBD–SIRPαFc showed a simple band at 40 kD above the SIRPαFc band.

of the total weight was about 300 D) between adjacent sub-peaks, indicating that up to two CBD polypeptides were bound to one SIRPαFc protein (**Figure 1D**). SDS-PAGE analysis verified the completeness of CBD–SIRPαFc conjugation that no structural damage happened to SIRPαFc in the reaction, and CBD–SIRPαFc represented a little higher molecular weight than SIRPαFc (**Figure 1E**).

CBD–SIRPαFc Binds to CD47 and Collagen

After the conjugate was successfully synthesized, its impact on the target affinity of SIRPαFc was first characterized. The binding affinity of SIRPαFc and CBD–SIRPαFc to CD47 was detected by Biacore. SIRPαFc and CBD–SIRPαFc were first caught on the activated sensor chip, respectively, then the gradient concentration

of human CD47 flew to combine and dissociate (**Figures 2A, B**). CBD–SIRPαFc bound to CD47 with a similar dissociation constant value (K_D value) to the unmodified protein, which both represented high binding affinities ($K_D = 1.437 \times 10^{-9}$ M for CBD–SIRPαFc and $K_D = 3.298 \times 10^{-9}$ M for SIRPαFc) (**Figure 2C**).

It was reported that CBD peptide "TKKTLRTC" could bind to collagen cross species such as rat, mouse, and human (35, 39, 40). Due to the uncertain molecular weight of collagen and its strong non-specific adsorption to the sensor chip, we performed ELISA to detect the binding of CBD to collagen type I. Five concentrations of SIRPαFc and CBD–SIRPαFc were assayed for collagen binding, and the K_D value was calculated by non-linear curve fit (**Figure 2D**). The CBD polypeptide conjugated to SIRPαFc showed effective collagen binding ability to collagen type I (K_D = 180 nM) as previously reported (38), while unconjugated SIRPαFc had no detected binding signals (**Figure 2E**). Both SIRPαFc and CBD–SIRPαFc showed limited binding to BSA as comparison, claiming the specific binding between CBD and collagen type I (**Figures 2D, E**).

CBD–SIRPαFc Binds to Tumor Cells and Collagen

The abovementioned experiments confirmed the binding affinity of CBD–SIRPαFc to CD47 and collagen at a molecular level. In order to verify the binding at the cellular level, we performed flow cytometry to detect the CD47-binding activity of SIRPαFc and CBD–SIRPαFc on tumor cells. Our previous study proved that A549 NSCLC cells express a high level of CD47 (23). Fluorescence signals revealed that SIRPαFc and CBD–SIRPαFc significantly bound to A549 cells compared to the control group which only incubated with anti-human IgG Fc antibody (**Figures 2F, G**), and they bound to A549 cells with almost the same efficiency (**Figure 2H**).

Another ELISA was performed to detect SIRPαFc and CBD–SIRPαFc binding to tumor cells and collagen simultaneously. CBD–SIRPαFc first bound to collagen coated on the 96-well ELISA plate, then incubated with CFDA SE-labeled A549 cells and counted under the laser confocal fluorescence microscope (**Figure 3A**). Bindings in wells of each group were counted and analyzed. A549 cells in the CBD–SIRPαFc group were obviously bound and remained in the wells, while no binding was detected in the control group (incubated with no drugs) and very few bindings in the SIRPαFc group, which may be attributed to the adhesion-promoting function of collagen (**Figure 3B**).

All of these results clarified the dual specificity of the designed conjugate, and the introduction of CBD would not influence the affinity of SIRPαFc to its target on tumor cells.

CBD–SIRPαFc Promotes Phagocytosis *In Vitro*

The function of SIRPαFc in promoting phagocytosis was previously reported, but whether the CBD–SIRPαFc conjugate

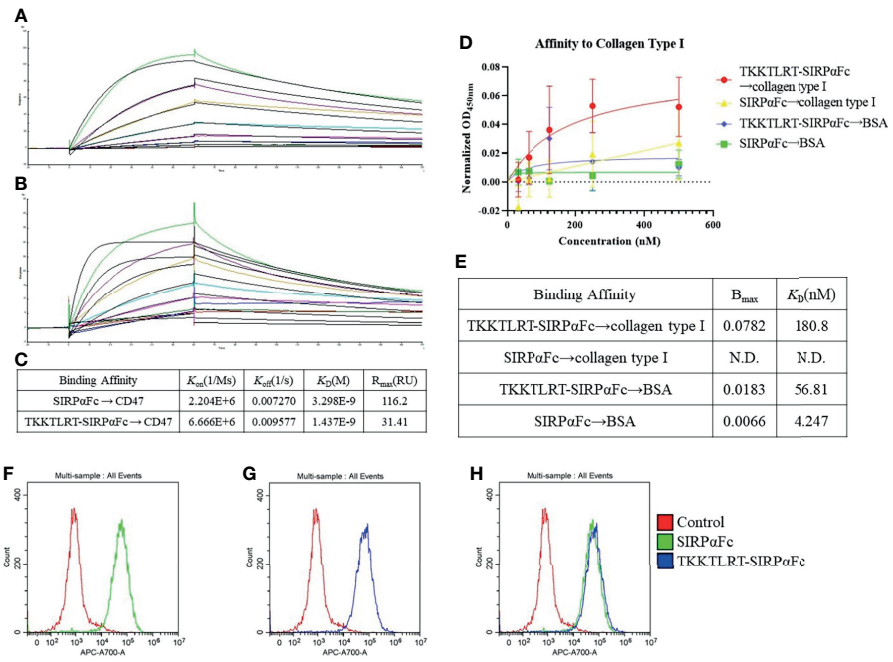

FIGURE 2 | CBD–SIRPαFc showed effective CD47 and collagen affinity at the molecular and cellular levels. Binding of CBD–SIRPαFc to CD47 and to collagen was detected respectively. **(A–C)** The affinity of SIRPαFc **(A)** and CBD–SIRPαFc **(B)** to human CD47 was examined, fitted, and analyzed with Biacore. CBD–SIRPαFc represented a similar CD47-binding affinity to unmodified SIRPαFc **(C)**. **(D, E)** A collagen affinity of CBD–SIRPαFc was detected with ELISA. The binding curve was fitted and analyzed through a non-linear curve fit (n = 5, mean ± SD) **(D)**. CBD–SIRPαFc showed a coincident collagen type I affinity as reported, while SIRPαFc did not represent a specific affinity to collagen type I **(E)**. Both SIRPαFc and CBD–SIRPαFc showed limited binding to BSA **(D, E)**. **(F–H)** Binding of SIRPαFc or CBD–SIRPαFc to tumor cells was detected with flow cytometry. Both SIRPαFc **(F)** and CBD–SIRPαFc **(G)** showed significant binding to A549 cells compared to the control group, while their signals were almost at the same level **(H)**.

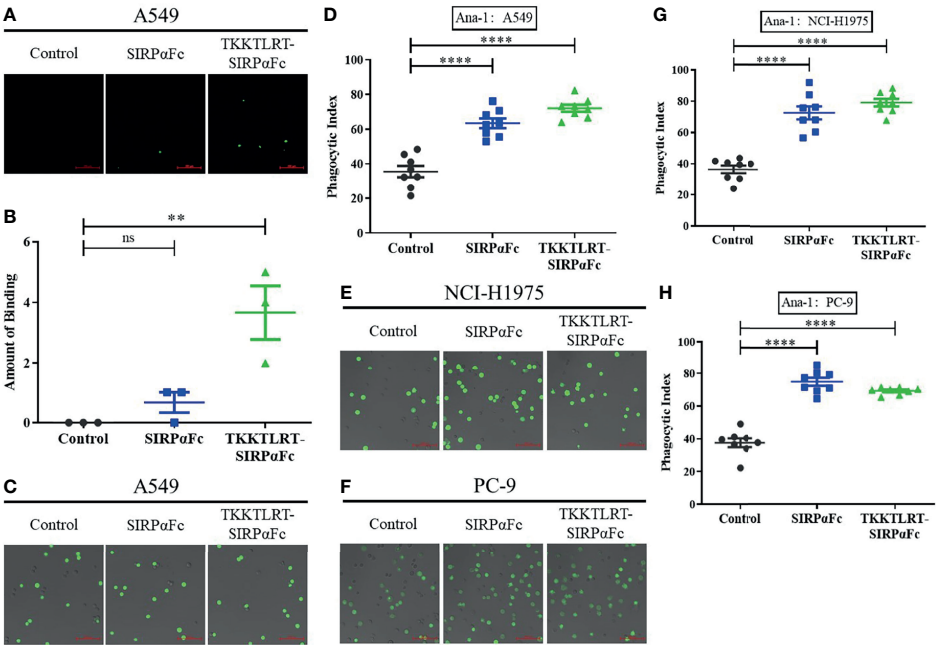

FIGURE 3 | CBD–SIRPαFc retained the coincident *in vitro* effect as SIRPαFc. **(A, B)** CBD conjugation made SIRPαFc derive the ability of binding collagen and tumor cells simultaneously. Significantly more CFDA SE-labeled A549 cells were binding to the CBD–SIRPαFc-incubated group in collagen-coated wells than to the SIRPαFc group (n = 3, mean ± SD ns, no significant, $^{**}p < 0.0021$). **(C–H)** Phagocytosis of Ana-1 macrophages to A549, NCI-H1975, and PC-9 was detected using the laser confocal fluorescence microscope while tumor cells were labeled with CFDA SE **(C, E, F)**. Macrophages that swallowed tumor cells or not were counted respectively, and the phagocytic index was calculated, in which SIRPαFc and CBD–SIRPαFc showed a similar promoting effect on phagocytosis (n = 8, mean ± SD, $^{****}p < 0.0001$) **(D, G, H)**.

retained this function still needs to be tested. The effect on macrophage-mediated phagocytosis was detected using the laser confocal fluorescence microscope. We chose three tumor cell lines to test the enhanced phagocytosis induced by CBD–SIRPαFc. After incubation with no drug (control group), SIRPαFc, or CBD–SIRPαFc for 2 h, CFDA SE-labeled A549 cells, NCI-H1975 cells, and PC-9 cells were significantly phagocytosed by Ana-1 macrophages (**Figures 3C, E, F**). The phagocytic index was calculated as described in *Materials and Methods*, in which the SIRPαFc-treated group increased from 35.49 to 63.44 in A549 cells, from 36.39 to 72.71 in NCI-H1975 cells, and from 37.57 to 74.84 in PC-9 cells when compared with the control group. Improved phagocytosis also appeared in the CBD–SIRPαFc group with average phagocytic index values of 72.07, 79.21, and 69.25 in A549, NCI-H1975, and PC-9 cells, respectively, which had no significant difference to the SIRPαFc group (**Figures 3D, G, H**). Therefore, CBD–SIRPαFc retained a similar ability in promoting phagocytosis as SIRPαFc.

CBD–SIRPαFc Accumulates in Tumor More Quickly Where Collagen Is Abundant

We hypothesized that CBD conjugation would help SIRPαFc to target tumor tissues based on the abundant collagen in tumor stroma. Therefore, we performed Masson-trichrome staining and immunofluorescent staining to determine the content and distribution of collagen in tumor. In both staining experiments, we could find collagen, stained blue in Masson-trichrome staining (**Figure 4A**) and pink in immunofluorescent staining (**Figure 4D**), respectively, which largely existed in tumor tissues compared to paired normal tissues. It is worth noting that in immunofluorescent staining, collagen tended to distribute around the vessels (indicated by CD31 red staining, **Figure 4D**). We then labeled SIRPαFc and CBD–SIRPαFc with FITC and injected it into mice bearing about 200 mm^3 A549 subcutaneous xenograft. Two hours after administration, CBD–SIRPαFc accumulated more in tumor than SIRPαFc (**Figures 4B, C**) did, as reflected by the stronger fluorescent signal observed in CBD–SIRPαFc-treated tumors. No such signal was detected in other main organs. In the immunofluorescent staining of tumor at 4 h after administration, it was noted that more CBD–SIRPαFc could be detected than SIRPαFc in tumor, which mainly distribute around vessels and collagen (**Figures 4E, F**).

CBD Conjugation to SIRPαFc Improves Antitumor Efficacy *In Vivo*

In order to examine the *in vivo* antitumor efficacy, we established an A549 subcutaneous xenograft model in nude mice. After administration for 4 weeks, both SIRPαFc and CBD–SIRPαFc exhibited obvious antitumor effects, while CBD–SIRPαFc performed better than SIRPαFc (**Figure 5A**). In a more thorough analysis, suppression on tumor growth varied more

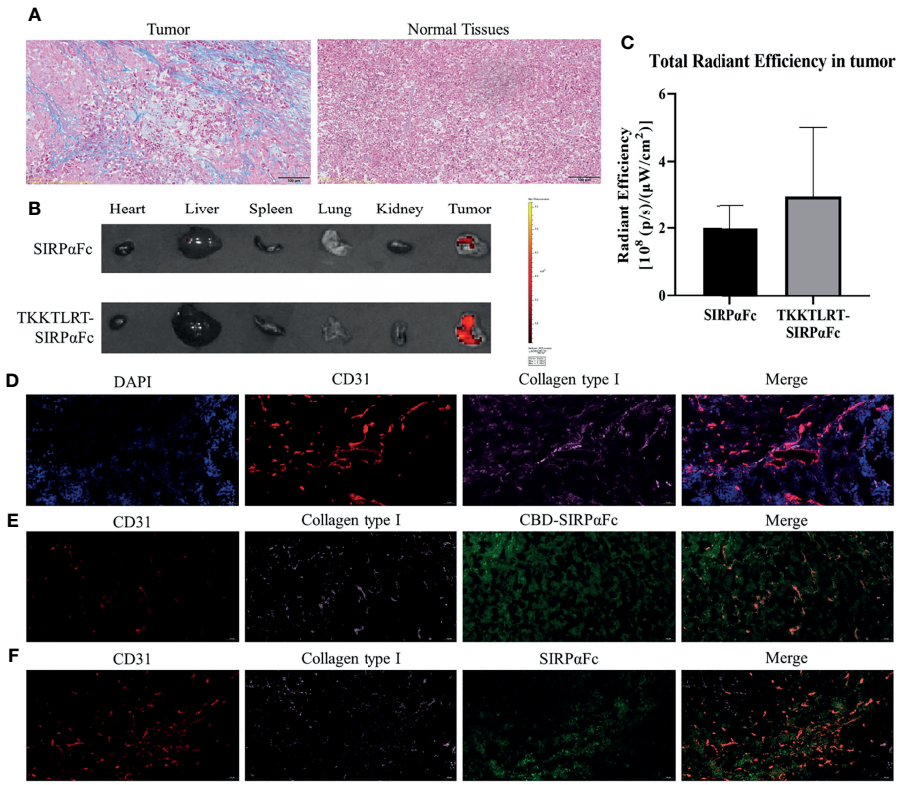

FIGURE 4 | Collagen was abundant in tumors where CBD–SIRPαFc would accumulate. **(A)** Masson-trichrome staining showed collagenous fiber (blue) and muscle fiber (red) in tumors and paired normal tissues. Collagen was largely distributed in tumors compared to normal tissues. **(B, C)** FITC-labeled SIRPαFc and CBD–SIRPαFc distributed in tumor, and main organs at 2 h after intraperitoneal injection were detected, when more CBD–SIRPαFc accumulated in tumor than SIRPαFc (n = 3) **(B)**. Total radiant efficiency in tumor was measured with Living Image software and counted with GraphPad Prism 8 software **(C)**. **(D)** Immunofluorescent staining showed cell nucleus (blue), blood vessels (indicated by CD31, red), and collagen type I (pink) in tumor. Collagen was abundant and tended to be around vessels. **(E, F)** Immunofluorescent staining on tumors at 4 h after injection showed FITC-labeled SIRPαFc **(E)** or CBD–SIRPαFc **(F)** in tumor. Blood vessels indicated by CD31 were stained red and collagen type I was stained pink, while SIRPαFc and CBD–SIRPαFc were green. More CBD–SIRPαFc accumulated in tumor than SIRPαFc and distributed mainly around collagen.

widely on each mouse in the SIRPαFc group as compared to the control group (**Figures 5B, C**), while most of the mice in CBD–SIRPαFc derived stable antitumor efficacy (**Figure 5D**). In Ki67 immunohistochemistry staining (**Figure 5E**) and H-E staining (**Figure 5F**), tumors proliferated a little faster in the control group than in the SIRPαFc and CBD–SIRPαFc group (**Figure 5E**), while more focal necrosis appeared in CBD–SIRPαFc and SIRPαFc than in the control group (**Figure 5F**).

CBD Conjugation to SIRPαFc Enhances Antitumor Immunity

To determine if the antitumor immunity happened in the *in vivo* study, we performed flow cytometry to investigate macrophage responses in tumors and spleens. Macrophages in tumors were determined by $CD45^+CD11b^+F4/80^+$ signals (**Figure 6A**), and percentages of $F4/80^+$ cells in $CD45^+$ cells were calculated and analyzed (**Figure 6B**). CBD–SIRPαFc treatment increased the higher frequency of $F4/80^+$ macrophages in total $CD45^+$ cells within tumor than SIRPαFc compared to the control group (**Figure 6B**). For further study, M1 and M2 macrophages were indicated by MHC II and CD206 respectively (**Figures 6C, E**). CBD–SIRPαFc significantly increased the frequency of MHC II^+ M1 macrophages in $CD45^+F4/80^+$ macrophages within the tumor (**Figure 6D**), but the frequency of $CD206^+$ M2 macrophages was maintained in all groups (**Figure 6F**). The increase of MHC II^+ M1 macrophages may indicate better tumor antigen presentation, leading to its effect on adaptive immunity.

Macrophages in spleen were also analyzed (**Figure 6G**). The frequency of $CD11b^+F4/80^+$ macrophages in total $CD45^+$ cells within spleen represented a similar but weaker trend as in the tumor (**Figure 6H**), which suggested that CBD–SIRPαFc mainly improved antitumor immunity within the tumor. Analogously, M1 macrophages in spleen indicated by MHC II (**Figure 6I**) increased in the CBD–SIRPαFc group (**Figure 6J**) while M2 macrophages indicated by CD206 (**Figure 6K**) still remained with no significant differences (**Figure 6L**).

We also performed F4/80 immunohistochemistry staining for tumors. The proportion of the $F4/80^+$ area was higher in the CBD–SIRPαFc group than in the SIRPαFc group and control group (**Figure 6M**), which revealed the same conclusion.

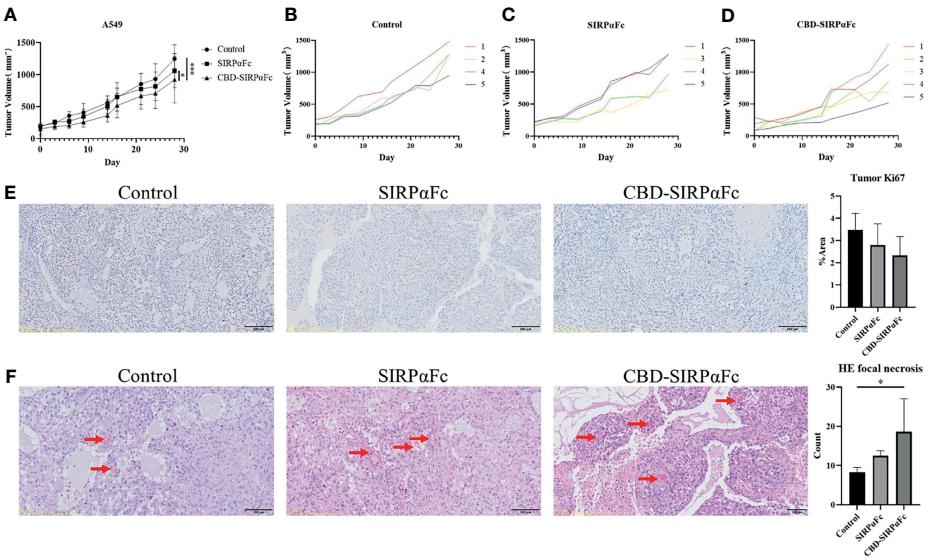

FIGURE 5 | CBD conjugation improved the antitumor efficacy of SIRPαFc *in vivo*. **(A–D)** A total of 1×10^7 A549 cells were resuspended in 200 μl PBS then inoculated subcutaneously at the right flank of each BALB/c nude mouse to establish the xenograft model. Mice were administrated intraperitoneally with PBS, 10 mg/kg SIRPαFc, or CBD–SIRPαFc for 28 days. Tumor volumes were measured and analyzed with two-way ANOVA in GraphPad Prism 8 software between groups (n = 5 for the CBD–SIRPαFc group and n = 4 for the control group and SIRPαFc group, mean ± SD, $^*p < 0.0332$, $^{***}p < 0.0002$) **(A)** or in a single group **(B–D)**. One mouse in the control group and one in the SIRPαFc group died before the terminal. **(E)** Ki67 immunohistochemistry staining was performed to study the proliferation in tumor. Tumors in the control group showed a more severe trend of proliferation than the SIRPαFc and CBD–SIRPαFc group. Proportions of the positive area were counted by ImageJ software and analyzed by one-way ANOVA in GraphPad Prism 8 software (n = 5 for the CBD–SIRPαFc group and n = 4 for the control group and SIRPαFc group, mean + SD). **(F)** Hematoxylin–eosin (H-E) staining was performed to study the necrosis in tumors. Focal necrosis indicated by red arrows were more and larger in the SIRPαFc and CBD–SIRPαFc group than in the control group. Focal necrosis in all samples was counted and analyzed by one-way ANOVA in GraphPad Prism 8 software (n = 5 for the CBD–SIRPαFc group and n = 4 for the control group and SIRPαFc group, mean + SD, $^*p < 0.0332$).

DISCUSSION

In recent years, multiple reagents targeting the CD47-SIRPα axis raised and showed a remarkable antitumor efficacy in multiple solid tumors, some of which were already at the phase I study, supporting the essential effect of regulating the CD47-SIRPα signal in cancer immunotherapy (28, 41, 42). Previously, we determined the antitumor efficacy of SIRPαFc fusion protein and found that SIRPαFc elicited potent macrophage-mediated antitumor efficacy in NSCLC *via* blocking endogenous CD47-SIRPα phagocytosis-suppressive signals and inducing antitumor phagocytosis (21). SIRPαFc also represented significant efficacy in refractory NSCLC with resistance caused by anti-angiogenic therapy (23). However, beyond the effective efficacy, adverse reactions induced by blocking CD47 in non-human primates still remained a potential problem (30). Although it is a common barrier in cancer immunotherapy, adverse reactions in anti-CD47 immunotherapy are still worth the attention because anemia or other side effects being induced by antibodies or fusion proteins' binding to erythrocytes or other hemocytes also means less antibodies accumulating in the tumor (43). Therefore, tumor targeting seems to be an idea killing two birds with one stone, which would improve SIRPαFc in both antitumor efficacy and less adverse reaction.

The collagen-binding domain brought an effective tumor-targeting strategy, which has already been examined in other antitumor antibodies and fusion proteins (35, 39, 40). Collagen is widely distributed in multiple organs and tissues but is especially abundant in the tumor (31, 33). The abnormal and fragmentary blood vessels in the tumor bring the critical chance for CBD to carrier macromolecules to the exposed tumor (32). Compared with some tumor-specific targets such as CD20 and Her2, the common but pivotal elements for tumor targeting of CBD in solid tumors support it to become a general tumor-targeting method crossing different types of tumors (38).

Through MALDI-TOF-MS, we determined the polypeptide–fusion protein ratio showing that one or two molecules of CBD polypeptides bound to one molecule of the SIRPαFc fusion protein. CBD–SIRPαFc retained the same affinity to CD47 as SIRPαFc, which was detected by Biacore, while it also derived collagen type I affinity due to the addition of CBD, which was confirmed by ELISA. In an *in vitro* study, CBD–SIRPαFc would promote phagocytosis of macrophages toward tumor cells, which was satisfactorily not influenced by CBD conjugation. Further, when injected intraperitoneally, CBD–SIRPαFc accumulated in the tumor more quickly compared to SIRPαFc, while almost no conjugate was detected in other main organs. On the A549 NSCLC nude mouse xenograft model, CBD–SIRPαFc represented better antitumor efficacy than SIRPαFc with significantly increased MHC II^+ M1 macrophages in tumor and spleen tissues, while M2 macrophages were maintained.

The notable increase of MHC II^+ M1 macrophages revealed a regulating function of CBD–SIRPαFc in macrophage polarization

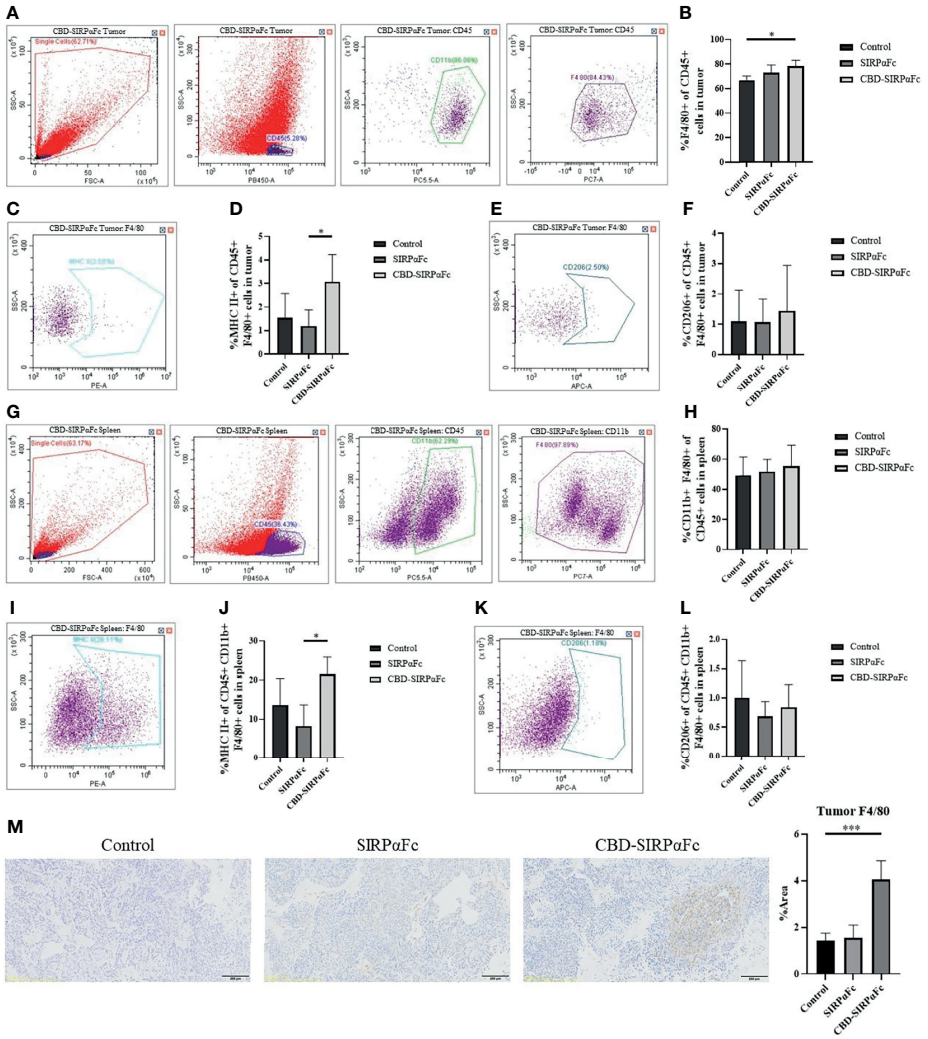

FIGURE 6 | CBD conjugation enhanced antitumor immunity. **(A–L)** Flow cytometry was performed to study the immune cell infiltration in tumors and spleens. **(A–F)** Macrophages in tumors were recognized by $CD45^+CD11b^+F4/80^+$ signals **(A)**. The percentage of $F4/80^+$ cells in total $CD45^+$ cells was analyzed, showing more macrophage infiltration in tumor in the CBD–SIRPαFc group than the SIRPαFc and control group **(B)**. M1 and M2 macrophages were also analyzed, in which MHC II^+ M1 macrophages **(C)** and $CD206^+$ M2 macrophages **(E)** were labeled. MHC II+ M1 macrophages were more in the CBD–SIRPαFc group **(D)**, supporting better tumor antigen presentation. M2 macrophages were maintained in all groups **(F)** (n = 5 for the CBD–SIRPαFc group and n = 4 for the control group and SIRPαFc group, mean + SD, *p < 0.3332). **(G–L)** Macrophages in spleen were also selected as described above **(G)**, and the percentage of $CD11b^+F4/80^+$ macrophages in total $CD45^+$ cells represented the same but weaker trend as in tumor **(H)**. MHC II^+ M1 macrophages and $CD206^+$ M2 macrophages in spleens were labeled as in tumors **(I, K)**. High frequency of MHC II^+ M1 macrophages appeared in the CBD–SIRPαFc group **(J)** while $CD206^+$ M2 macrophages still represented no significant differences **(L)** (n = 5 for the CBD–SIRPαFc group and n = 4 for the control group and SIRPαFc group, mean + SD, *p < 0.3332). **(M)** F4/80 immunohistochemistry staining was performed to help with studying the macrophage infiltration in tumors. $F4/80^+$ signals appeared with a higher frequency in tumors of the CBD–SIRPαFc group, which was coincident to the result of flow cytometry. Proportions of positive area were counted by ImageJ software and analyzed by one-way ANOVA in GraphPad Prism 8 software (n = 5 for CBD–SIRPαFc and n = 4 for the control group and SIRPαFc group, mean + SD, ***p < 0.0002).

and antigen presentation. M1 macrophages were regarded as proinflammatory phenotype, which could secrete inflammatory cytokines such as TNF-α and IL-1β (44). In antitumor immunity, M1 macrophages not only promote Th1 response to enhance inflammatory reaction but also improve antigen processing and presentation, as well as costimulatory activation of T cells through upregulating related genes (45). Actually, M1 macrophages combine innate immunity and adaptive immunity. Conversely, tumor-associated macrophages (TAM) suppress antitumor immunity through an anti-inflammatory reaction, which have a similar phenotype or consist of M2 macrophages in different theories (46). In a previous study, anti-CD47 was reported to promote M1 macrophage polarization (47). CBD–SIRPαFc increased the proportion of MHC II^+ M1 macrophages, supporting its function in promoting antigen presentation and following T-cell activation. CBD–SIRPαFc may elicit M1

macrophages through a lasting Fcγ receptor reaction (48), revealing the essential effect of CBD conjugation. Moreover, the proportion of macrophages increased less in spleens than in tumors, revealing that its immunity induction effect focused on tumors, which also suggested that its less non-tumor binding benefited from tumor targeting.

However, as we could see from the *in vivo* experiments, both SIRPαFc and CBD–SIRPαFc did not gain very significant antitumor efficacy in an A549 NSCLC nude mouse xenograft model, which was probably caused by the absence of T cells. As mentioned above, SIRPαFc and other CD47 blocking therapy perform their functions through both innate immunity and adaptive immunity; thus, the lack of T cells would diminish the antitumor efficacy of SIRPαFc to a certain extent (16, 18). Our present study reported a novel CBD–SIRPαFc conjugate, mainly focusing on the synthesis, identification, and affinity examination, with a preliminary *in vivo* efficacy trial. The detailed mechanism of immunological effects such as promoting antigen presentation and T-cell activation and potentially erythrocyte-sparing properties remained to be further investigated. Further *in vivo* antitumor efficacy study should be performed on the human immune system-reconstructed mouse model to involve the T-cell-activating effect of CBD–SIRPαFc. In addition, we are attempting to derive the CBD–SIRPαFc conjugate with a stable CBD–fusion protein ratio through optimizing reaction conditions, as well as designing integrated CBD–SIRPαFc fusion proteins with a stable combination and ratio in order to solve the potential doubts resulted from the multiple-conjugating ratio in the current conjugate.

In conclusion, we make an artificially designed CBD polypeptide "TKKTLRT" conjugate to the SIRPαFc fusion protein through a simple reaction for the first time. We observed that CBD–SIRPαFc gained collagen affinity while its original CD47 affinity and phagocytosis-promoting effect remained the same, which were examined at both molecular and cellular levels. For the *in vivo* study, CBD–SIRPαFc accumulated more and faster in tumor, which also brought an enhanced antitumor innate immunity and efficacy on nude mouse models. There are still mists in conjugate synthesis, but also the predictable effect on adaptive immunity remained to be explored, which is also the way ahead for our study. Taken together, the present study provides a potential strategy to improve the tumor targeting of the phagocytosis checkpoint inhibitor SIRPαFc fusion protein, therefore avoiding unnecessary exposure to normal cells.

DATA AVAILABILITY STATEMENT

The original contributions presented in the study are included in the article/supplementary material. Further inquiries can be directed to the corresponding author.

ETHICS STATEMENT

The animal study was reviewed and approved by the Animal Ethical Committee of School of Pharmacy at Fudan University.

AUTHOR CONTRIBUTIONS

LY, DJ, JL, and ZM contributed to the conception of the study. JL and ZM performed the experiments. TX and KK contributed to the cell experiments. TX and SW contributed to the animal experiments. WT, XZ, and JF contributed to the design and synthesis of SIRPαFc fusion protein. WZ contributed to the design and synthesis of TKKTLRT-SIRPαFc conjugate. JL, ZM, TX, and LY performed the data analysis and wrote the manuscript. XuH, XiH, DP, and HC helped perform the analysis with constructive discussions. All authors contributed to the article and approved the submitted version.

FUNDING

This work was supported by the Scientific and Innovative Action Plan of Shanghai (nos. 20S11901600 and 18431902800) and National Natural Science Foundation of China (No. 81572979).

REFERENCES

1. Bray F, Ferlay J, Soerjomataram I, Siegel RL, Torre LA, Jemal A. Global Cancer Statistics 2018: GLOBOCAN Estimates of Incidence and Mortality Worldwide for 36 Cancers in 185 Countries. *CA Cancer J Clin* (2018) 68 (6):394–424. doi: 10.3322/caac.21492
2. Xiong A, Wang J, Zhou C. Immunotherapy in the First-Line Treatment of NSCLC: Current Status and Future Directions in China. *Front Oncol* (2021) 11:757993. doi: 10.3389/fonc.2021.757993
3. Berghmans T, Cadranel J, Grigoriu B. Editorial: New Advances in Non-Small Cell Lung Cancer Management: Immune Modulation and Targeted Therapies. *Front Med (Lausanne)* (2021) 8:761078. doi: 10.3389/fmed.2021.761078
4. Oiseth SJ, Aziz MS. Cancer Immunotherapy: A Brief Review of the History, Possibilities, and Challenges Ahead. *J Cancer Metastasis Treat* (2017) 3:250–61. doi: 10.20517/2394-4722.2017.41
5. Feng M, Jiang W, Kim BYS, Zhang CC, Fu YX, Weissman IL. Phagocytosis Checkpoints as New Targets for Cancer Immunotherapy. *Nat Rev Cancer* (2019) 19(10):568–86. doi: 10.1038/s41568-019-0183-z
6. Ribas A, Wolchok JD. Cancer Immunotherapy Using Checkpoint Blockade. *Science* (2018) 359(6382):1350–5. doi: 10.1126/science.aar4060
7. Lei X, Lei Y, Li J-K, Du W-X, Li R-G, Yang J, et al. Immune Cells Within the Tumor Microenvironment: Biological Functions and Roles in Cancer Immunotherapy. *Cancer Lett* (2020) 470:126–33. doi: 10.1016/j.canlet.2019.11.009
8. Denault MH, Melosky B. Immunotherapy in the First-Line Setting in Wild-Type NSCLC. *Curr Oncol* (2021) 28(6):4457–70. doi: 10.3390/curroncol28060378
9. Miller M, Hanna N. Advances in Systemic Therapy for Non-Small Cell Lung Cancer. *Bmj* (2021) 375:n2363. doi: 10.1136/bmj.n2363
10. Haanen JB, Robert C. Immune Checkpoint Inhibitors. *Prog Tumor Res* (2015) 42:55–66. doi: 10.1159/000437178
11. Chen L, Han X. Anti-PD-1/PD-L1 Therapy of Human Cancer: Past, Present, and Future. *J Clin Invest* (2015) 125(9):3384–91. doi: 10.1172/jci80011

12. Tumeh PC, Harview CL, Yearley JH, Shintaku IP, Taylor EJ, Robert L, et al. PD-1 Blockade Induces Responses by Inhibiting Adaptive Immune Resistance. *Nature* (2014) 515(7528):568–71. doi: 10.1038/nature13954
13. Liu Z, Han C, Fu Y-X. Targeting Innate Sensing in the Tumor Microenvironment to Improve Immunotherapy. *Cell Mol Immunol* (2020) 17(1):13–26. doi: 10.1038/s41423-019-0341-y
14. Murata Y, Saito Y, Kotani T, Matozaki T. CD47-Signal Regulatory Protein Alpha Signaling System and Its Application to Cancer Immunotherapy. *Cancer Sci* (2018) 109(8):2349–57. doi: 10.1111/cas.13663
15. Weiskopf K. Cancer Immunotherapy Targeting the CD47/Sirpalpha Axis. *Eur J Cancer* (2017) 76:100–9. doi: 10.1016/j.ejca.2017.02.013
16. Liu X, Pu Y, Cron K, Deng L, Kline J, Frazier WA, et al. CD47 Blockade Triggers T Cell-Mediated Destruction of Immunogenic Tumors. *Nat Med* (2015) 21(10):1209–15. doi: 10.1038/nm.3931
17. Sockolosky JT, Dougan M, Ingram JR, Ho CC, Kauke MJ, Almo SC, et al. Durable Antitumor Responses to CD47 Blockade Require Adaptive Immune Stimulation. *Proc Natl Acad Sci USA* (2016) 113(19):E2646–54. doi: 10.1073/pnas.1604268113
18. McCracken MN, Cha AC, Weissman IL. Molecular Pathways: Activating T Cells After Cancer Cell Phagocytosis From Blockade of CD47 "Don't Eat Me" Signals. *Clin Cancer Res* (2015) 21(16):3597–601. doi: 10.1158/1078-0432.Ccr-14-2520
19. Willingham SB, Volkmer JP, Gentles AJ, Sahoo D, Dalerba P, Mitra SS, et al. The CD47-Signal Regulatory Protein Alpha (Sirpa) Interaction is a Therapeutic Target for Human Solid Tumors. *Proc Natl Acad Sci USA* (2012) 109(17):6662–7. doi: 10.1073/pnas.1121623109
20. Veillette A, Chen J. Sirpalpha-CD47 Immune Checkpoint Blockade in Anticancer Therapy. *Trends Immunol* (2018) 39(3):173–84. doi: 10.1016/j.it.2017.12.005
21. Zhang X, Fan J, Wang S, Li Y, Wang Y, Li S, et al. Targeting CD47 and Autophagy Elicited Enhanced Antitumor Effects in Non-Small Cell Lung Cancer. *Cancer Immunol Res* (2017) 5(5):363–75. doi: 10.1158/2326-6066.Cir-16-0398
22. Zhang X, Chen W, Fan J, Wang S, Xian Z, Luan J, et al. Disrupting CD47-Sirpα Axis Alone or Combined With Autophagy Depletion for the Therapy of Glioblastoma. *Carcinogenesis* (2018) 39(5):689–99. doi: 10.1093/carcin/bgy041
23. Zhang X, Wang Y, Fan J, Chen W, Luan J, Mei X, et al. Blocking CD47 Efficiently Potentiated Therapeutic Effects of Anti-Angiogenic Therapy in Non-Small Cell Lung Cancer. *J Immunother Cancer* (2019) 7(1):346. doi: 10.1186/s40425-019-0812-9
24. Burger P, de Korte D, van den Berg TK, van Bruggen R. CD47 in Erythrocyte Ageing and Clearance - The Dutch Point of View. *Transfus Med Hemother* (2012) 39(5):348–52. doi: 10.1159/000342231
25. Burger P, Hilarius-Stokman P, de Korte D, van den Berg TK, van Bruggen R. CD47 Functions as a Molecular Switch for Erythrocyte Phagocytosis. *Blood* (2012) 119(23):5512–21. doi: 10.1182/blood-2011-10-386805
26. Oldenborg PA, Zheleznyak A, Fang YF, Lagenaur CF, Gresham HD, Lindberg FP. Role of CD47 as a Marker of Self on Red Blood Cells. *Science* (2000) 288 (5473):2051–4. doi: 10.1126/science.288.5473.2051
27. Arias CF, Arias CF. How Do Red Blood Cells Know When to Die? *R Soc Open Sci* (2017) 4(4):160850. doi: 10.1098/rsos.160850
28. Sikic BI, Lakhani N, Patnaik A, Shah SA, Chandana SR, Rasco D, et al. First-in-Human, First-in-Class Phase I Trial of the Anti-CD47 Antibody Hu5F9-G4 in Patients With Advanced Cancers. *J Clin Oncol* (2019) 37(12):946–53. doi: 10.1200/JCO.18.02018
29. Li S, Zhang Z, Lai W-F, Cui L, Zhu X. How to Overcome the Side Effects of Tumor Immunotherapy. *Biomed Pharmacother* (2020) 130:110639. doi: 10.1016/j.biopha.2020.110639
30. Petrova PS, Viller NN, Wong M, Pang X, Lin GH, Dodge K, et al. Tti-621 (Sirpαfc): A CD47-Blocking Innate Immune Checkpoint Inhibitor With Broad Antitumor Activity and Minimal Erythrocyte Binding. *Clin Cancer Res* (2017) 23(4):1068–79. doi: 10.1158/1078-0432.Ccr-16-1700
31. Ricard-Blum S. The Collagen Family. *Cold Spring Harb Perspect Biol* (2011) 3 (1):a004978. doi: 10.1101/cshperspect.a004978
32. Nagy JA, Chang SH, Dvorak AM, Dvorak HF. Why are Tumour Blood Vessels Abnormal and Why Is It Important to Know? *Br J Cancer* (2009) 100(6):865–9. doi: 10.1038/sj.bjc.6604929
33. Zhou ZH, Ji CD, Xiao HL, Zhao HB, Cui YH, Bian XW. Reorganized Collagen in the Tumor Microenvironment of Gastric Cancer and Its Association With Prognosis. *J Cancer* (2017) 8(8):1466–76. doi: 10.7150/jca.18466
34. Momin N, Mehta NK, Bennett NR, Ma L, Palmeri JR, Chinn MM, et al. Anchoring of Intratumorally Administered Cytokines to Collagen Safely Potentiates Systemic Cancer Immunotherapy. *Sci Transl Med* (2019) 11 (498):eaaw2614. doi: 10.1126/scitranslmed.aaw2614
35. Ishihara J, Ishihara A, Sasaki K, Lee SS, Williford JM, Yasui M, et al. Targeted Antibody and Cytokine Cancer Immunotherapies Through Collagen Affinity. *Sci Transl Med* (2019) 11(487):eaau3259. doi: 10.1126/scitranslmed.aau3259
36. Hulme JT, D'Souza WN, McBride HJ, Yoon BP, Willee AM, Duguay A, et al. Novel Protein Therapeutic Joint Retention Strategy Based on Collagen-Binding Avimers. *J Orthop Res* (2018) 36(4):1238–47. doi: 10.1002/jor.23756
37. Han S, Wang B, Jin W, Xiao Z, Chen B, Xiao H, et al. The Collagen Scaffold With Collagen Binding BDNF Enhances Functional Recovery by Facilitating Peripheral Nerve Infiltrating and Ingrowth in Canine Complete Spinal Cord Transection. *Spinal Cord* (2014) 52(12):867–73. doi: 10.1038/sc.2014.173
38. Addi C, Murschel F, De Crescenzo G. Design and Use of Chimeric Proteins Containing a Collagen-Binding Domain for Wound Healing and Bone Regeneration. *Tissue Eng Part B Rev* (2017) 23(2):163–82. doi: 10.1089/ten.TEB.2016.0280
39. Liang H, Li X, Chen B, Wang B, Zhao Y, Zhuang Y, et al. A Collagen-Binding EGFR Single-Chain Fv Antibody Fragment for the Targeted Cancer Therapy. *J Control Release* (2015) 209:101–9. doi: 10.1016/j.jconrel.2015.04.029
40. Liang H, Li X, Wang B, Chen B, Zhao Y, Sun J, et al. A Collagen-Binding EGFR Antibody Fragment Targeting Tumors With a Collagen-Rich Extracellular Matrix. *Sci Rep* (2016) 6:18205. doi: 10.1038/srep18205
41. Querfeld C, Thompson JA, Taylor MH, DeSimone JA, Zain JM, Shustov AR, et al. Intralesional TTI-621, a Novel Biologic Targeting the Innate Immune Checkpoint CD47, in Patients With Relapsed or Refractory Mycosis Fungoides or Sézary Syndrome: A Multicentre, Phase 1 Study. *Lancet Haematol* (2021) 8(11):e808–17. doi: 10.1016/s2352-3026(21)00271-4
42. Liu J, Wang L, Zhao F, Tseng S, Narayanan C, Shura L, et al. Pre-Clinical Development of a Humanized Anti-CD47 Antibody With Anti-Cancer Therapeutic Potential. *PloS One* (2015) 10(9):e0137345. doi: 10.1371/journal.pone.0137345
43. Russ A, Hua AB, Montfort WR, Rahman B, Riaz IB, Khalid MU, et al. Blocking "Don't Eat Me" Signal of CD47-Sirpalpha in Hematological Malignancies, an in-Depth Review. *Blood Rev* (2018) 32(6):480–9. doi: 10.1016/j.blre.2018.04.005
44. van Dalen FJ, van Stevendaal M, Fennemann FL, Verdoes M, Ilina O. Molecular Repolarisation of Tumour-Associated Macrophages. *Molecules* (2018) 24(1):9. doi: 10.3390/molecules24010009
45. Anderson NR, Minutolo NG, Gill S, Klichinsky M. Macrophage-Based Approaches for Cancer Immunotherapy. *Cancer Res* (2021) 81(5):1201–8. doi: 10.1158/0008-5472.Can-20-2990
46. Yunna C, Mengru H, Lei W, Weidong C. Macrophage M1/M2 Polarization. *Eur J Pharmacol* (2020) 877:173090. doi: 10.1016/j.ejphar.2020.173090
47. Zhang M, Hutter G, Kahn SA, Azad TD, Gholamin S, Xu CY, et al. Anti-CD47 Treatment Stimulates Phagocytosis of Glioblastoma by M1 and M2 Polarized Macrophages and Promotes M1 Polarized Macrophages. *In Vivo PloS One* (2016) 11(4):e0153550. doi: 10.1371/journal.pone.0153550
48. Funes SC, Rios M, Escobar-Vera J, Kalergis AM. Implications of Macrophage Polarization in Autoimmunity. *Immunology* (2018) 154(2):186–95. doi: 10.1111/imm.12910

Conflict of Interest: Author WT is employed by ImmuneOnco Biopharma (Shanghai).

The remaining authors declare that the research was conducted in the absence of any commercial or financial relationships that could be construed as a potential conflict of interest.

Publisher's Note: All claims expressed in this article are solely those of the authors and do not necessarily represent those of their affiliated organizations, or those of the publisher, the editors and the reviewers. Any product that may be evaluated in this article, or claim that may be made by its manufacturer, is not guaranteed or endorsed by the publisher.

Copyright © 2022 Liu, Meng, Xu, Kuerban, Wang, Zhang, Fan, Ju, Tian, Huang, Huang, Pan, Chen, Zhao and Ye. This is an open-access article distributed under the terms of the Creative Commons Attribution License (CC BY). The use, distribution or reproduction in other forums is permitted, provided the original author(s) and the copyright owner(s) are credited and that the original publication in this journal is cited, in accordance with accepted academic practice. No use, distribution or reproduction is permitted which does not comply with these terms.

frontiers in Immunology

ORIGINAL RESEARCH
published: 31 March 2022
doi: 10.3389/fimmu.2022.843106

Visual Analysis of Colorectal Cancer Immunotherapy: A Bibliometric Analysis From 2012 to 2021

Long Ma, Jixiang Ma, Muzhou Teng and Yumin Li**

The Second Clinical Medical College of Lanzhou University, Department of General Surgery, Lanzhou University Second Hospital, Key Laboratory of Digestive System Tumors of Gansu Province, Lanzhou, China

An increasing number of studies have shown that immunotherapy serves a significant role in treating colorectal cancer (CRC) and has become a hotspot. However, few studies used the bibliometric method to analyze this field comprehensively. This study collected 1,899 records of CRC immunotherapy from 2012 to October 31, 2021, and used CiteSpace to analyze regions, institutions, journals, authors, and keywords to predict the latest trends in CRC immunotherapy research. The United States and China, contributing more than 60% of publications, were the main drivers in this field. Sun Yat-sen University was the most active institution, while the National Cancer Institute had the highest frequency of citations. Most publications were published in the *Journal for Immunotherapy of Cancer.* Adam E Snook was the most prolific writer, while Dung T. Le was the most commonly co-cited author. "T cell", "MMI" and "PD-1blocked" were the most widely studied aspects of CRC immunotherapy. "Immune checkpoint inhibitor", "combination therapy", "drug therapy" and "liver metastases" were current research hotspots. "Tumor microenvironment", "neutrophils", "tumor-associated macrophages", and "suppressor cell" have emerged as research hotspots in recent years. "Gut microbiota", "nanoparticle" and "tumor mutational burden" as recently emerged frontiers of research that should be closely monitored.

Keywords: colorectal cancer, immunotherapy, bibliometric, CiteSpace, immune checkpoint, gut microbiota

OPEN ACCESS

Edited by:
Benjamin Frey,
University Hospital Erlangen, Germany

Reviewed by:
Yong Yang,
China Pharmaceutical University, China
Qiutong Huang,
The University of Queensland, Australia

****Correspondence:***
Yumin Li
liym@lzu.edu.cn
Muzhou Teng
tengmz@lzu.edu.cn

Specialty section:
This article was submitted to Cancer Immunity and Immunotherapy, a section of the journal Frontiers in Immunology

Received: *24 December 2021*
Accepted: *09 March 2022*
Published: *31 March 2022*

Citation:
Ma L, Ma J, Teng M and Li Y (2022) Visual Analysis of Colorectal Cancer Immunotherapy: A Bibliometric Analysis From 2012 to 2021. Front. Immunol. 13:843106. doi: 10.3389/fimmu.2022.843106

INTRODUCTION

CRC is one of the most common cancers in the world. According to statistics, there have 1.9 million new cases of CRC in 2020, and it is expected to reach 2.5 million in 2035 (1). Although the availability of screening has improved the 5-year survival rate for CRC, approximately 30% of patients present with metastatic disease at diagnosis and approximately 50% of non-metastatic patients eventually progress to metastatic disease (2). Over the past decade, increased understanding of CRC pathogenesis has led to the recognising that almost all CRCs displayed activation of the RAS/RAF/MEK signaling cascade. Targeting EGFR, HER2, KRAS, NRAS, or BRAF, which were linked to their activation, has resulted in a reduction in the proportion of CRC patients. However, due to the highly mutagenic and adaptable nature of tumor cells, drug-resistant clones will arise in the vast majority of cases (3, 4).

Ioannides and Whiteside first introduced the tumor microenvironment (TME), which refers to the local biological environment during tumor development, providing a scaffold and barrier for tumor cell growth and generating immune-exempt areas to provide a 'breeding ground' for tumors. TME helps tumor cells evade immune surveillance by providing an environment for tumor growth and suppressing local immune responses (5, 6). A balance is established between the tumor and the adaptive immune system, shaping each other (7). Immunotherapy, which aims to use the immune system to fight tumors, has shown a promising future in treating CRC.

On May 23, 2017, the FDA approved Pembrolizumab for use in adult or pediatric patients with unresectable or metastatic, MSI-H/dMMR solid tumors, including colorectal cancer. On July 31 of the same year, the FDA approved Nivolumab to treat patients aged 12 years or older with MSI-H/dMMR colorectal cancer (2). on July 10, 2018, the FDA approved the combination of Ipilimumab and Nivolumab to treat patients aged 12 years or older with MSI-H/dMMR colorectal cancer. on June 29, 2020, the FDA again approved Pembrolizumab for intravenous infusion for the first-line treatment of patients with unresectable or metastatic MSI-H/dMMR colorectal cancer and does not require concomitant use with chemotherapy. Pembrolizumab and Nivolumab are PD-1 inhibitors, and Ipilimumab is a CTLA-4 inhibitor. T cells express PD-1 receptors that bind to their ligands PD-L1 and PD-L2, inhibiting T cell proliferation and cytokine production. PD-1 ligands are upregulated in some tumor cells, and signaling through this pathway can inhibit immune surveillance of tumors by activated T cells. PD-1 inhibitors are monoclonal antibodies that bind to the PD-1 receptor, blocking the interaction of PD-1 with PDL1 and PD-L2 and relieving PD-1 pathway-mediated suppression of immune responses, including antitumor immune responses. In a homologous mouse tumor model, blockade of PD-1 activity inhibited tumor growth (8, 9). Ipilimumab is an anti-CTLA-4 antibody. CTLA-4 is expressed on the surface of T cells. CTLA-4 exerts its inhibitory effect during the T cell activation phase: early in the immune response, CTLA-4 competes with CD28 to bind to B7 on antigen-presenting cells, and when CTLA-4 signaling is stronger, T cells are inhibited, while when CD28 signaling is stronger, T cells are activated and continue to replicate and produce greater killing capacity. Ipilimumab inhibits the competitive binding of CTLA-4 to CD28, thus allowing T cells to multiply and increasing the ability to kill tumors (10, 11).

Immune checkpoint inhibitors (ICIs), modulating the interaction of T cells, antigens-presenting cells (APCs) and tumor cells to help unleash suppressed immune responses, emerged as a very effective therapy for patients with mCRC that is mismatch-repair-deficient (dMMR) or microsatellite instability-high (MSI-H) (termed dMMR/MSI-H mCRC). Due to the efficacious, stable and durable responses, pembrolizumab and nivolumab (with or without Ipilimumab) were approved by US Food and Drug Administration (FDA) to treat these patients. However, mCRC is characterized by insufficient mutated tumor antigen (12), thus the main challenge is to provide the benefit of immunotherapy for the vast majority of mCRC patients that are mismatch-repair-proficient (pMMR) or microsatellite-stable (MSS) or low microsatellite instability (MSI-L) (termed pMMR/MSS/MSI-L mCRC) (13).

Bibliometric analysis adopts the number of citations as a proxy measure of research quality, which is a useful tool for assessing the trend of research efforts statistically and qualitatively. It provides an objective assessment of the contributions of academic groups and individual researchers through a comprehensive analysis of the authors, countries, journals, citations and publication dates of selected articles, thus providing a method for understanding trends in specific fields and ranking academic groups and individuals (14). In addition, keywords that appear more frequently in the included articles and hot words that have emerged in recent years were analyzed to provide supporting evidence for future trends (15).

There was currently no similar analysis in CRC. This paper utilized bibliometric analysis to describe the literature related to CRC immunotherapy over the last decade to understand its features and forecast future research trends and hotspots. Therefore, to better capture the current status and trends in CRC immunotherapy research, the purposes of this study were to reveal present study trends, explore into possible research hotspots and guide researchers in their future work by using bibliometric methods to visualize references.

MATERIALS AND METHOD

The Web of Science (WOS) core database from Clarivate Analytics was deemed the best for bibliometric analysis (16, 17), so we selected it to perform the search. The WOS core database was searched on November 1, 2021, for all articles related to CRC immunotherapy from 2012 to October 31, 2021, using the following search formula: TS=(Rectal Neoplasm* OR Rectal Tumor* OR Rectal Cancer* OR Rectum Neoplasm* OR Rectum Cancer* OR Cancer of the Rectum OR Cancer of Rectum OR Colorectal Neoplasm* OR Colorectal Tumor* OR Colorectal Cancer* OR Colorectal Carcinoma* OR Colonic Neoplasm* OR Colon Neoplasm* OR Cancer of Colon OR Colon Cancer* OR Cancer of the Colon OR Colonic Cancer*) AND TS=(Immunotherapy OR Immunotherapies OR immunotherapeutic). The literature inclusion criteria were as follows: (1) The manuscript was based on the theme of immunotherapy for CRC and the whole content was accessible; (2) Document types included Article and Review;(3) Written in English. The exclusion criteria were as follows:(1) The major themes were not related to immunotherapy for CRC or could not be evaluated. (2) Articles were meeting abstracts, news, briefings, etc. The complete text was evaluated by two reviewers separately against the inclusion and exclusion criteria. Any disagreements between the two reviewers (L M and JX M) were resolved by negotiation and the document was exported in plain text format (**Figure 1**).

The annual publication was analyzed and plotted using GraphPad prism v8.0.2. Furthermore, bibliometric methods were used to gather the research foundation, frontier knowledge, and trends. In this study, the acquired bases were imported into the

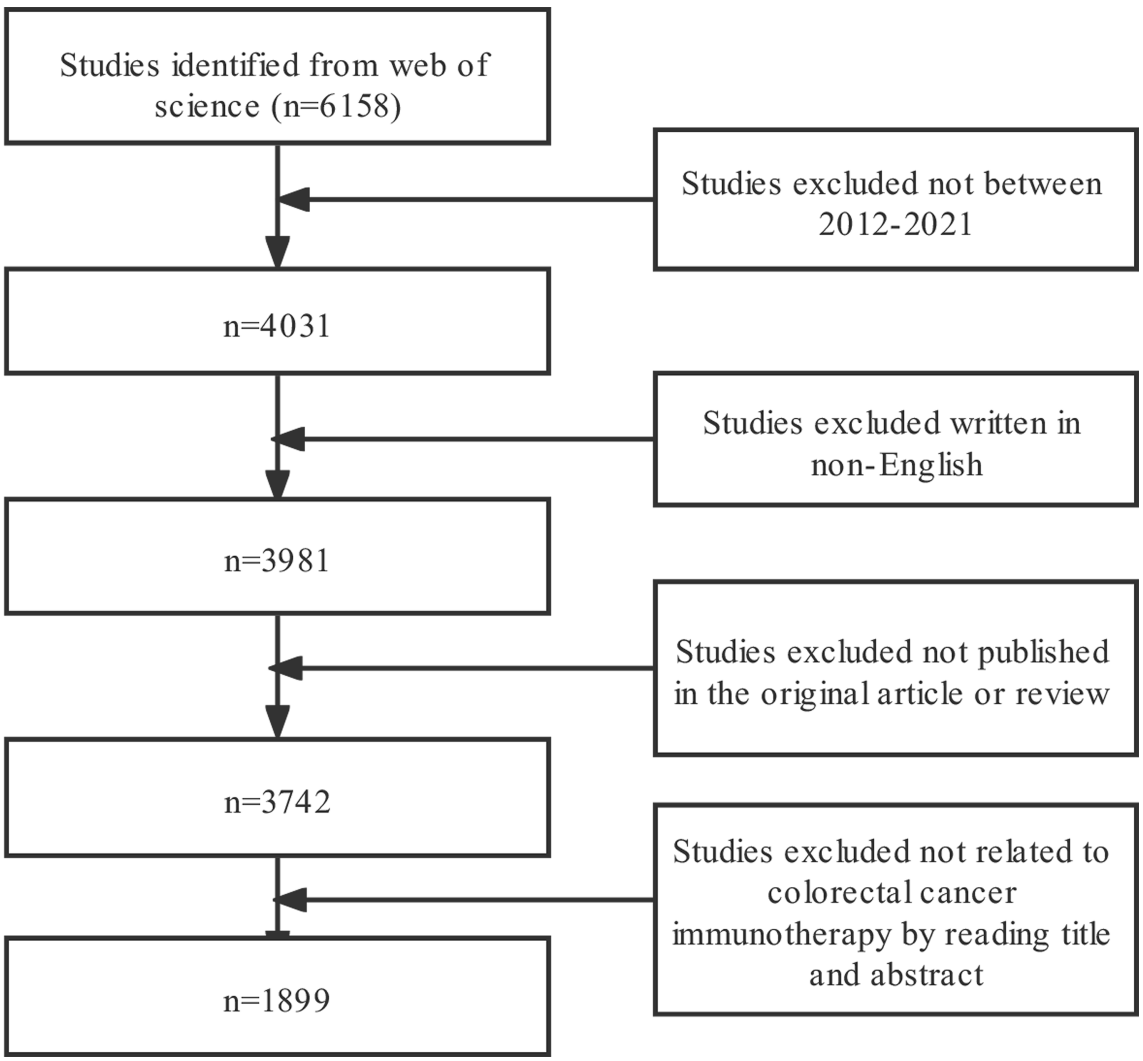

FIGURE 1 | Flowchart depicting the article selection process.

CiteSpace (5.6.R3) software (18), a literature Visibility App Tool created by Prof. Chaomei Chen for analyzing indicators such as country, journal, institution, author, reference. In addition, CiteSpace was also used to analyze outbreak keywords and visualize them to predict trends in the field. The centrality of a node is a graph-theoretical property that quantifies the importance of the node's position in a network. A commonly used metric is betweenness centrality (In this study, all centrality refers to betweenness centrality).Betweenness centrality is a concept introduced by the American sociologist Freeman (19),it measures the percentage of shortest paths in the network to which a given node belongs (20). Formula:

$$g(v) = \sum_{s \neq v \neq t} \frac{\sigma_{st}(v)}{\sigma_{st}}$$

$g(v)$ represents the centrality value of the vertex v. σ_{st} (v) represents the number of shortest paths passing through v between vertex s and vertex t. σ_{st} represents the number of all shortest paths from vertex s to vertex t. Burst detection is used to detect significant changes in the number of references at a given time. It is used to discover the decline or rise of a certain subject term or keyword. The algorithm invented by Kleinberg, J was used in cite space to predict the change of keywords at a certain stage and thus to predict the field's future development (21). The higher the burst strength indicates the higher the frequency of this keyword in the observed time period.

The CiteSpace parameters were set as follows: Time-slicing was chosen from 2012 to 2021, year per slice(1), and all options in the term source were selected, node types were selected one at a time, selection criteria (g-index, g2 ≤ k Si≤gci,k ∈ Z+,k = 25). Each node in the figure indicated an observation including country, institution, author, co-cited literature and keywords. If the publication is issued in cooperation with several countries, institutions and authors, then each country, institution and

author is taken into account, which is the basis for the network of institutional, national and author cooperation.

The node size represented the frequency of occurrence; the larger the node, the higher the frequency of occurrence. Connections between nodes represented collaborative, co-occurring or co-referential relationships. The different colors of nodes represented different years; the different colors of circles from inside to outside indicated the years from 2012 to 2021. The outermost purple ring indicated that the node has very high centeredness and was often regarded as a critical point in a specific domain (22). The impact factor (IF) and the 2020 edition of Journal Citation Reports (JCR) were both included in the analysis as crucial indications of the research's scientific worth (23).

RESULTS

A total of 1899 publications on CRC immunotherapy were published on the web of science from 2012 to October 31, 2021, including 1454 (76.57%) ARTICLES and 445 REVIEWS (23.43%). The literature covered 66 countries or regions and 367 institutions.

The annual number of publications for immunotherapy on CRC from 2012 to 2021 as shown in **Figure 2A**, and we divided it into three periods, slow growth period (2012-2015), acceleration period (2016-2017) and rapid growth period (2018-2021). The number of publications increased relatively slowly before 2016 and rapidly after 2016, with more than 150 publications per year and a second acceleration period in 2018. The number of publications on CRC immunotherapy in 2021 was the highest in the last decade, reaching 445 as of October 31, 2021, and the number of publications continued to rise by a large margin.

Countries and Institutions

The annual trend publications associated with immunotherapy for CRC by country from 2012 to 2021 were presented in **Figure 2B**. The United States of America (USA) was the most frequent publisher in this field with 601 publications (31.65 of 1899 publications), followed by China (31.17, with 592 publications), Germany (5.90, with 112 publications), Japan (5.90%, with 112 publications) and Italy (5.69%, with 108 publications) (**Table 1**). The top 5 countries with the highest centrality were: USA, UK, Spain, Canada and Germany (**Figure 3A**). The United States and China contributed 62.82% of the total publications, far more than any other country. China initially had trailed the US in the number of annual publications, but after 2018 its publications in this field have increased rapidly and surpassed the US in 2020, maintaining a high-speed growth rate in 2021. In addition, the annual increase of publications in China was the fastest since 2012, to be followed by the United States, while Japan and the Netherlands grew slowly.

Among the top 10 countries/regions regarding publications, the U.S. had 19,051 citations, far more than all other countries, while it had a high citation/publication ratio (31.65). Although China had many citations (9285), its citation/publication rate (15.68) was lower than other countries. It is to be noted that France had the highest citation/publication ratio (52.32) among the ten countries, despite the relatively low number of publications, which also indicated the high quality of its published papers.

The analysis of the international collaboration network (**Figure 3A**) showed that the United States, which had the highest volume of output, and China worked closely together. China mainly cooperated closely with Singapore and Greece, while the United States largely cooperated with England, France, South Korea, Italy and Spain. China already leads the world in publication output, but its centrality was 0.05, compared to 0.20 in the US.

The top ten activist institutions were listed in **Table 2**. Sun Yat-sen University published 41 papers with 431 citations, followed by the University of Texas M. D. Anderson Cancer Center (33 papers, 1,437 citations) and Fudan University (30 papers, 300 citations). The ten most prolific institutions were from China and the United States, excluding the German Cancer Research Center. Among the top ten productive institutions, the National Cancer Institute (NCI) had the highest citation/publication rate (53.7). Institutional cooperation analysis was produced to reveal the cooperation between institutions (**Figure 3B**).

Analysis of Journals and Co-Cited Journals

The top ten most prolific and co-cited journals were listed in **Tables 3**, **4**. *Journal for Immunotherapy of Cancer* (66 articles, 3.48%) published the most documents in this field, followed by *Oncoimmunology* (63 articles, 3.32%), *Cancer* (57 articles, 3.00%), *Frontiers in Immunology* (57 articles. 3.00%) and *Cancer Immunology Immunotherapy* (53 articles, 2.79%). Among the top ten most prolific journals, the *Journal for Immunotherapy of Cancer* had the highest IF of 13.751 and *Cancer Research* had the highest citation/publication rate (52.33). Of the top 10 journals, 80% were classified as Q1 (top 25% of IF distribution), remaining two journals were Q2 (between 25th and 50th quartiles) and Q4 (between 50th and 100th quartiles). The most frequently co-cited journal was the Journal of Clinical Oncology (4270 citations), followed most frequently by *Clinical Cancer Research* (3841 citations) and *Cancer Research* (3807 citations). Among the top 10 co-cited journals, *New England Journal of Medicine* was cited 3640 times with the highest IF of 91.253. Except for *Journal of Immunology*, the rest of the journals were in Q1.

The subject distribution of academic journals was depicted by a dual-map overlay of the journals (24) (**Figure 4**). The citing journal is on the left, and the cited journal is on the right, with the citation relationship indicated by the colored path. The mapping identifies 2 colored primary citation pathways, meaning that researches published to journals in the field of molecular/biology/genetics were primarily cited by researches published in molecular/biology/immunology and medical/medical/clinical journals.

Analysis of Authors and Co-Cited Authors

Of all authors who published literature related to colorectal cancer immunotherapy in the last decade, the 10 most productive authors were listed in **Table 5**. Adam E Snook (17

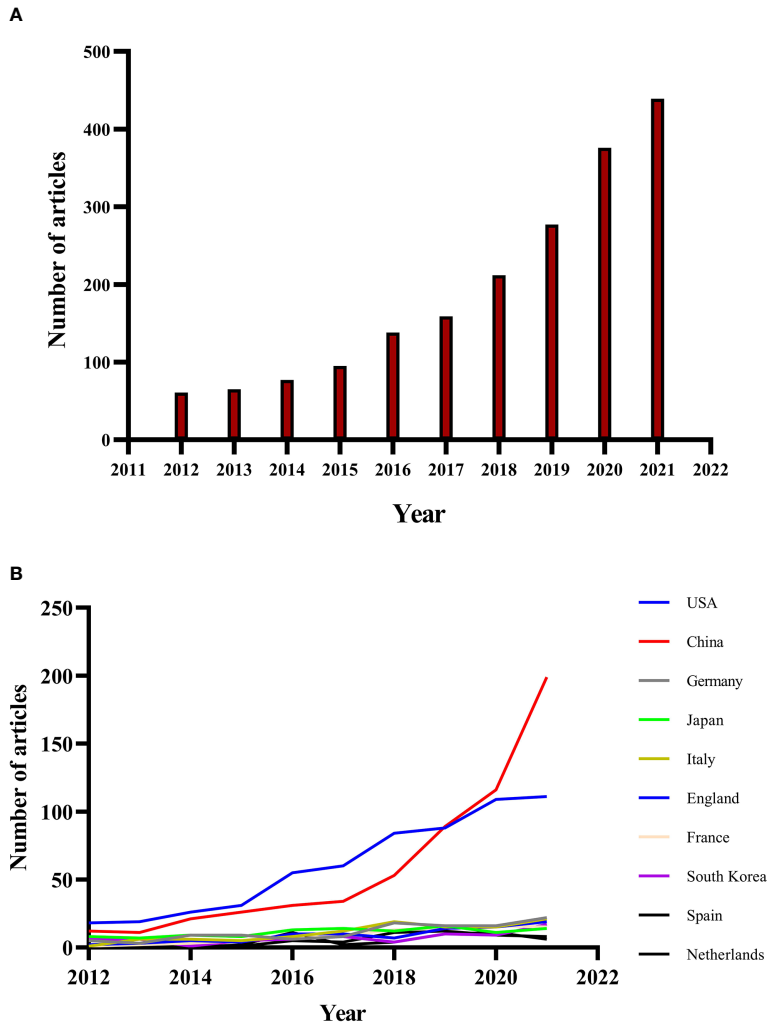

FIGURE 2 | **(A)** Annual publications of immunotherapy in colorectal cancer from 2012 to 2021. **(B)** The country's annual trend publications related to colorectal cancer immunotherapy from 2012 to 2021.

publications) has published the most papers, followed by Scott A Waldman (14 publications) and Michael A Morse (14 publications). Further analysis revealed that six of the top ten authors were from the United States, two were from China, and two were from Germany and France. The co-cited author network was visualized by **Figure 5A**. The most prominent nodes were linked to the most co-cited authors, which including Le DT (567Citation), Topalian SL (314Citation),

TABLE 1 | The top 10 productive countries/regions related to colorectal cancer immunotherapy.

Rank	Country/region	Article counts	Percentage (N/1899)	Citation	Citation per publication
1	United States	601	31.65	19051	31.70
2	China	592	31.17	9285	15.68
3	Germany	112	5.90	3478	31.05
4	Japan	112	5.90	2604	23.25
5	Italy	108	5.69	3671	33.99
6	England	89	4.69	3196	35.91
7	France	86	4.53	4500	52.32
8	South Korea	72	3.79	1168	16.22
9	Spain	56	2.95	1936	34.57
10	Netherlands	49	2.58	1737	33.45

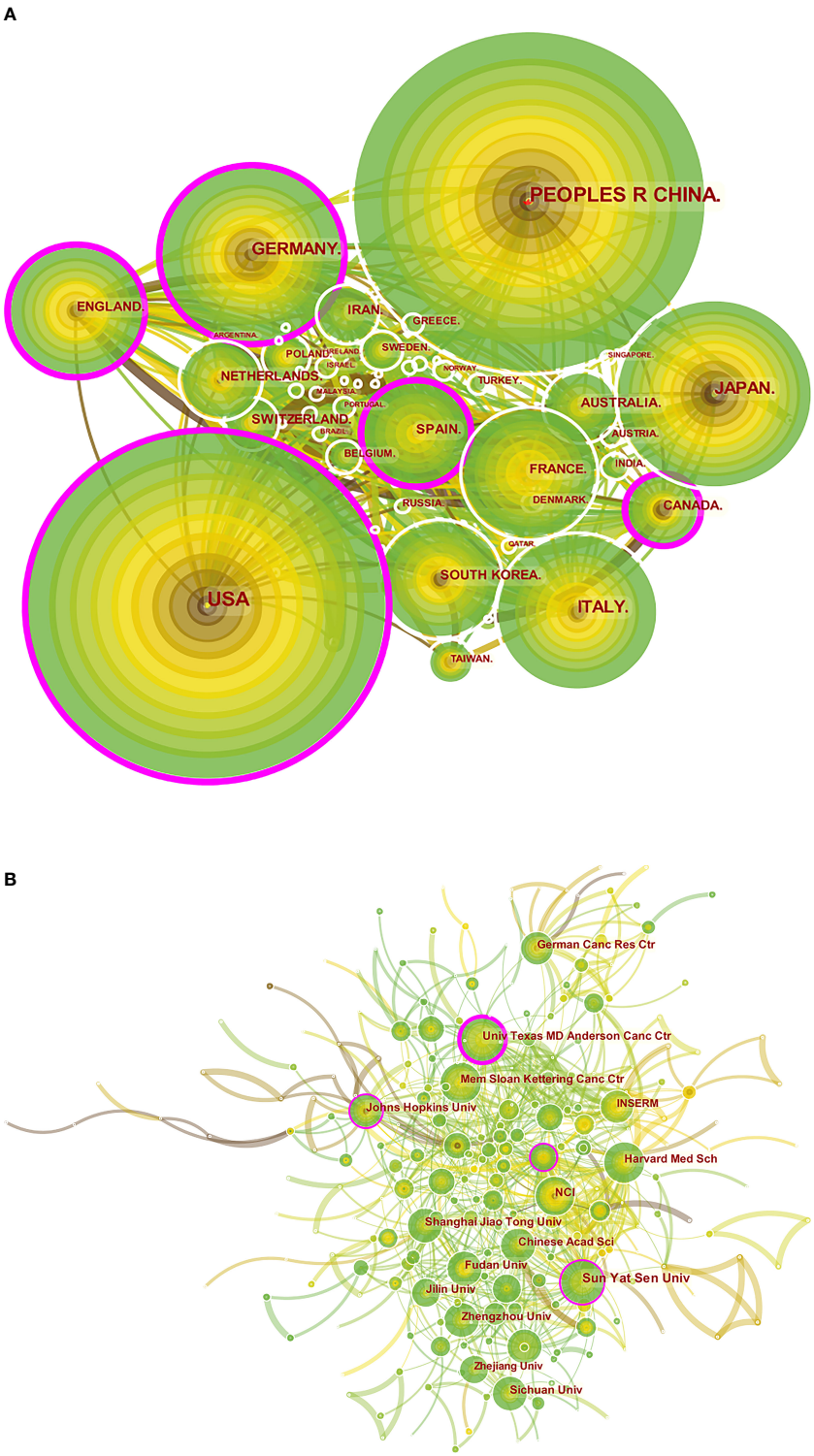

FIGURE 3 | A visual map for CiteSpace network of countries/regions and institutions associated with colorectal cancer immunotherapy. **(A)** Country/regional collaboration analysis; **(B)** Institutional collaboration analysis. The nodes represent countries/regions or institutions, and the lines connect them. Nodes represent countries/regions or institutions. The number of publications grows proportionally to the size of the nodes. The lines between the nodes represent the cooperation relationship, and the thickness of the connecting lines represents the strength of their cooperation, the closer the cooperation, the thicker the connecting lines. the nodes with the outermost purple circles have higher centrality. From 2012 to 2021, the color changes from brown to green.

TABLE 2 | Top 10 institutions published literature related to colorectal cancer immunotherapy from 2010 to 2021.

Rank	Institution	Country	Number of studies	Total citations	Average citation
1	Sun Yat-sen University	China	41	431	10.5
2	The University of Texas MD Anderson Cancer Center	USA	33	1437	43.5
3	Fudan University	China	30	424	14.1
4	Shanghai Jiao Tong University	China	30	300	10
5	National Cancer Institute (NCI)	USA	29	1556	53.7
6	Chinese Academy of Sciences	China	29	1113	38.4
7	Harvard Medical School	USA	27	1232	45.6
8	German Cancer Research Center	Germany	27	584	21.6
9	Johns Hopkins University	USA	26	392	15.1
10	Sichuan University	China	26	278	10.7

Galon J (313Citation), Overman MJ (301Citation), and Siegel RL (278Citation) (**Table 5**).

Analysis of Cited References

The co-cited literature network diagram was composed of 850 nodes and 4135 links, with a time slice set to 1 year and a period set to 2012-2021 (**Figure 5B**). According to the five most frequently co-cited articles (**Tables 6**, **7**), PD-1 Blockade in Tumors with Mismatch-Repair Deficiency (with 343 co-citations) published in the *New England Journal of Medicine* (IF=91.253) was the most cited article by Dung T. Le. In addition, 2 of the top 5 co-cited papers were written by Dung T. Le and published in different journals.

Moreover, we performed a temporal co-citation analysis and mapped the timeline view of co-cited references (**Figure 6**). We found that "CEA" (Cluster4) was a relatively early hotspot, "cytokine-induced killer cells" (Cluster3) was a mid-term (2008-2016) research hotspot, and "prognosis" (Cluster0) had the darkest color representing the most publications and was a consistent research hotspot for CRC immunotherapy. "Microsatellite instability" (Cluster1), "programmed cell death protein ligand1" (Cluster2), "hormone replacement" (Cluster5), "braf" (Cluster6) and "gut microbiota" (Cluster7) demonstrated that the issues of these clusters are the current new hotspots in the field.

Analysis of Keyword Co-Occurrence Clustering and Time Zone

Based on the number of citations and centrality analysis of keywords through CiteSpace (**Table 8**), we found that the most popular keywords were Expression, T cell, Dendritic Cell, cell, survival, activation, regulatory t cell, and chemotherapy after removing meaningless keywords (**Table 8**). We also built a network map to visualize keyword clusters (**Figure 7**), and we

TABLE 3 | The top 10 productive journals related to colorectal cancer immunotherapy.

Rank	Journal	Article counts	Percentage (N/1899)	Citation per article	IF	Quartile in category
1	Journal For Immunotherapy Of Cancer	66	3.48	14.12	13.751	Q1
2	Oncoimmunology	63	3.32	18.52	8.1	Q1
3	Cancer	57	3.00	8.00	6.86	Q1
4	Frontiers In Immunology	57	3.00	13.91	7.561	Q1
5	Cancer Immunology Immunotherapy	53	2.79	17.62	6.968	Q1
6	Frontiers In Oncology	34	1.79	5.26	6.244	Q2
7	Cancer Immunology Research	31	1.63	32.97	11.151	Q1
8	Clinical Cancer Research	27	1.42	66.11	12.531	Q1
9	Oncology Letters	23	1.21	9.39	2.967	Q4
10	Cancer Research	21	1.11	52.33	12.701	Q1

TABLE 4 | The top 10 co-cited journals associated with colorectal cancer immunotherapy.

Rank	Cited Journal	Citation	IF (2020)	Quartile in category
1	Journal of Clinical Oncology	4270	44.544	Q1
2	Clinical Cancer Research	3841	12.531	Q1
3	Cancer Research	3807	12.701	Q1
4	New England Journal of Medicine	3640	91.253	Q1
5	Nature	2792	49.962	Q1
6	Science	2761	47.728	Q1
7	Journal Of Immunology	2445	5.422	Q2
8	Proceedings of the National Academy of Sciences of the United States of America (PNAS)	1867	11.205	Q1
9	Cell	1655	41.584	Q1
10	Nature Medicine	1583	53.44	Q1

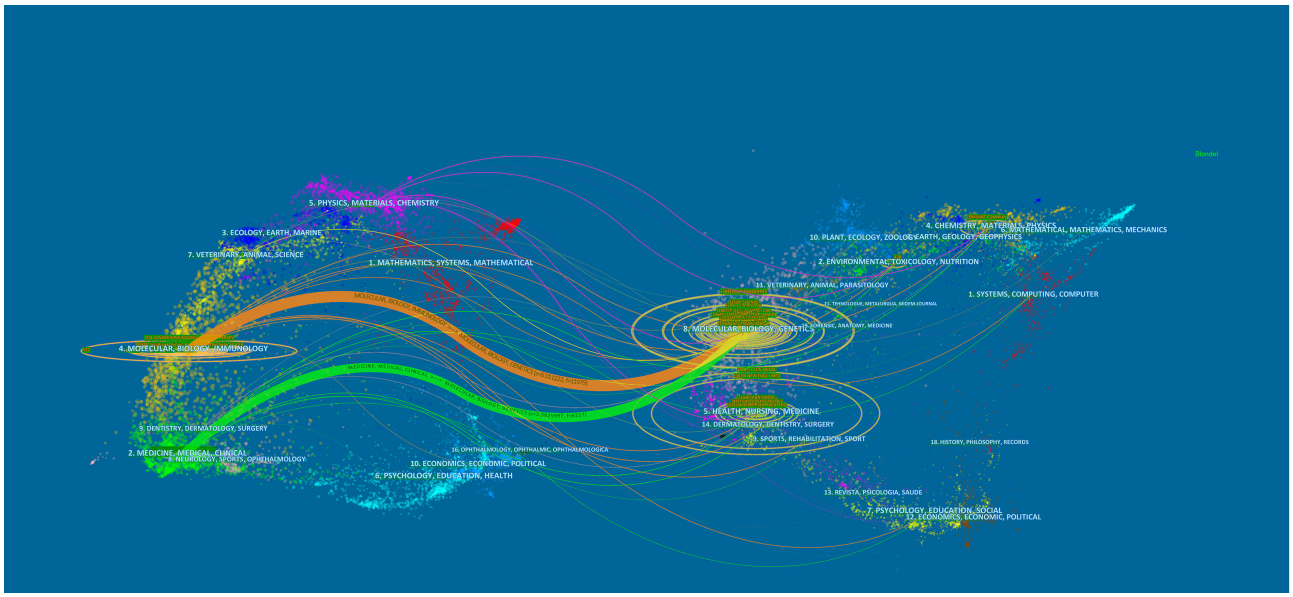

FIGURE 4 | The dual-map overlay of journals related to colorectal cancer immunotherapy. Notes: On the left were the citing journals, on the right were the cited journals, and the colored path represented the citation relationship.

found that "immune checkpoint inhibitor" (Cluster0), "microsatellite instability" (Cluster1), "suppressor" (Cluster4), "probiotics" (Cluster5), "nf kappa b" (Cluster6) and "cd55" (Cluster7) were the hot spots of research since 2012.

CiteSpace designed the keyword time zone view to show high-frequency keywords' evolution clearly. The keywords were situated in the years in which they first appeared together, and colors of the links represented the years when the two keywords first appeared together. High-frequency keywords (T > 80) were displayed in **Figure 8**, as threshold was a cumulative number, resulting in some of the most recent keywords not reaching 80 cumulatively. Therefore, the top five annual high-frequency keywords from 2013 to 2021 were added to complement the time zone view (**Figure 8**).

Keyword Burst Analysis

We use CiteSpace to detect emergent keywords to identify the frontiers of research in this field. Among the 103 keywords with high citation outbreaks, we focused on those with bursts starting in 2020 (**Figure 9**), including "immune checkpoint inhibitors" (burst intensity of 7.71), "gut microbiota" (burst intensity of 3. 92), "tumor microenvironment" (burst intensity of 3.49) "liver metastasis" (burst intensity of 3.35), "nanoparticles" (burst intensity of 3.31), "combination therapy" (burst intensity of 2.87).

DISCUSSION

In this study, we obtained 1899 publications on colorectal cancer immunotherapy from 2012 to 2021 by searching the web of science core database and manual screening. In terms of annual publications, publications increased rapidly after 2015. In terms of national and regional distribution, the United States has been the driving force behind the highest academic contribution to colorectal cancer immunotherapy in the last decade, as reflected by the number of publications, centrality, citation frequency and citation

TABLE 5 | Top 10 most prolific and co-cited authors in the field of colorectal cancer immunotherapy.

Rank	Author	Count	Location	Rank	Co-cited author	Citation
1	Adam E Snook	17	USA	1	Dung T. Le	567
2	Scott A Waldman	14	USA	2	Topalian SL	314
3	Michael A Morse	14	USA	3	Galon J	313
4	Jefferey Schlom	14	USA	4	Overman MJ	301
5	Kebin Liu	11	China	5	Siegel RL	278
6	Thierry Andre	10	France	6	Brahmer JR	223
7	Niels Halama	10	Germany	7	Pages F	221
8	Dung T Le	10	USA	8	Llosa NJ	198
9	Chunwan Lu	9	USA	9	Bray F	176
10	Yuquan Wei	9	China	10	Mlecnik B	169

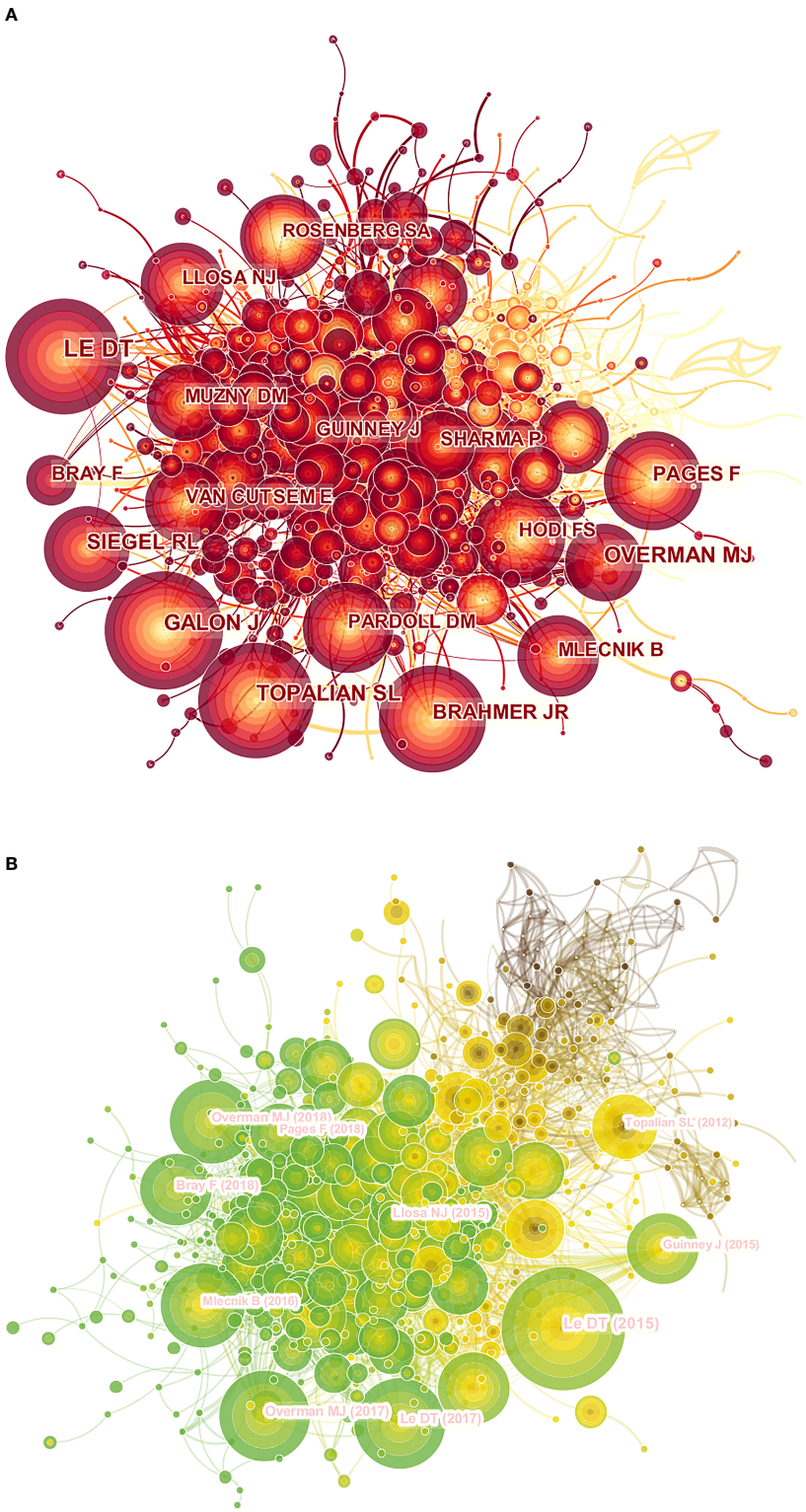

FIGURE 5 | A CiteSpace network visualization of co-cited authors and references regarding colorectal cancer immunotherapy. **(A)** Network visualization diagram of the co-cited authors of the Publications. **(B)** Network visualization diagram of cited references. Co-cited authors or cited references are indicated by the node. The co-citation relationship is indicated by the line connecting the nodes. The node area grows as the number of co-citations increases. The colors represent different years, in A, the color changes from yellow to red from 2012 to 2021, and in B, the color changes from brown to green from 2012 to 2021.

TABLE 6 | The top five co-cited references related to colorectal cancer immunotherapy.

Rank	Title	Journal IF (2020)	First author	Publication time	Total citations	Quartile in category
1	PD-1 Blockade in Tumors with Mismatch-Repair Deficiency	New England Journal of Medicine (IF=91.253)	Dung T. Le	May,2015	343	Q1
2	Nivolumab in patients with metastatic DNA mismatch repair-deficient or microsatellite instability-high colorectal cancer (Check Mate 142): an open-label, multicentre, phase 2 study	Lancet Oncology (IF=41.316)	Michael J. Overman	July,2017	225	Q1
3	Mismatch-repair deficiency predicts response of solid tumors to PD-1 blockade	Science (IF=47.728)	Dung T. Le	Jun,2017	197	Q1
4	Durable Clinical Benefit with Nivolumab Plus Ipilimumab in DNA Mismatch Repair-Deficient/Microsatellite Instability-High Metastatic Colorectal Cancer	Journal of clinical oncology (IF=44.544)	Michael J Overman	Jan,2018	174	Q1
5	Global cancer statistics 2018: GLOBOCAN estimates of incidence and mortality worldwide for 36 cancers in 185 countries	CA: A Cancer Journal for Clinicians (IF=508.702)	Freddie Bray	September,2018	173	Q1

publication ratio. China's annual publications proliferated after 2016, and since 2020 China has surpassed the United States. Although the average citation was relatively low, the higher total number of citations showed the high contribution of China to the development of the field. France, Spain, Italy and South Korea have lower publication numbers, but their publications have multiplied in recent years, related to the cooperation with the United States.

INSTITUTIONS AND INSTITUTIONAL COOPERATION

90% of the 10 most productive institutions were from China and the United States, indicating that China and the United States played significant roles in the academic development of the field. Interestingly, Sun Yat-sen University, the most productive institution globally, had the lowest average citation among the top ten institutions. The National Cancer Institute (NCI) had the highest total citations (1556) and average citations (53.7) among the top 10 institutions, indicating that NCI published higher quality articles in the field and played a crucial role in promoting the development of the field.

JOURNALS AND CITED JOURNALS

Among the ten most active journals, *Journal for Immunotherapy of Cancer* (66 articles), *Oncoimmunology* (63 articles), *Cancer* (57 articles), *Frontiers in Immunology* (57 articles) and *Cancer Immunology Immunotherapy* (53 articles) published more than 50 papers. The *Journal of Clinical Oncology* received the highest citations. Notably, both *Clinical Cancer Research* (66.11) and *Cancer Research* (52.33) had more than 50 citations per article and ranked 2nd and 3rd, respectively, among co-cited journals. thus, they are recognized as research resources for CRC immunotherapy.

Most of the top 10 productive journals were related to immunology and clinical, while most of the 10 highly co-cited journals were related to biology, which was consistent with the dual-map overlay analysis. The dual-map overlay represented the subject distribution of academic journals. **Figure 4** showed that

TABLE 7 | The top five centralities of co-cited references related to colorectal cancer immunotherapy.

Rank	Title	Journal IF (2020)	First author	Publication time	Centrality	Quartile in category
1	Nivolumab plus Ipilimumab in Advanced Melanoma	New England Journal Of Medicine (IF=91.253)	Jedd D. Wolchok	Jun,2013	0.19	Q1
2	Characterization of the immunophenotypes and antigenomes of colorectal cancers reveals distinct tumor escape mechanisms and novel targets for immunotherapy	Genome Biology (IF=13.583)	Mihaela Angelova	Mar,2015	0.11	Q
3	Improved survival with ipilimumab in patients with metastatic melanoma.	New England Journal Of Medicine (IF=91.253)	F Stephen Hodi	Aug,2010	0.11	Q1
4	Primary, Adaptive, and Acquired Resistance to Cancer Immunotherapy	Cell (IF=41.584)	Padmanee Sharma	Feb,2017	0.09	Q1
5	Durable Cancer Regression Off-treatment and Effective Re-induction Therapy with an Anti-PD-1 Antibody	Clinical cancer research (IF=12.531)	Evan J. Lipson	Jan,2013	0.09	Q1

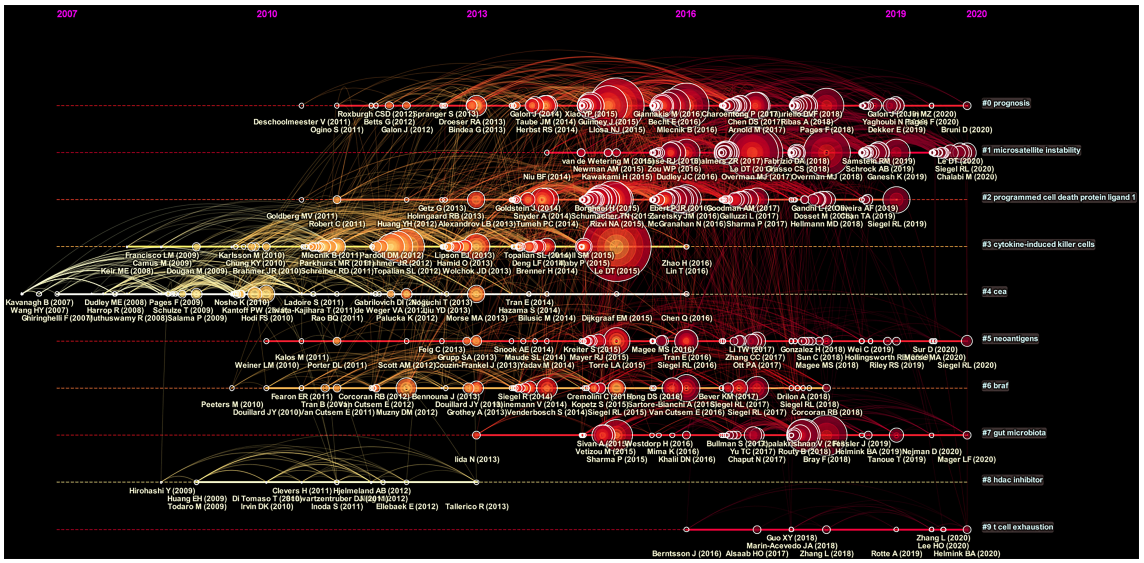

FIGURE 6 | A timeline view for co-cited references associated with colorectal cancer immunotherapy. The node's position on the horizontal axis represents the time when the reference first appeared, and the node's size is positively correlated with the number of citations of the reference. The lines between the nodes represent co-cited relationships. The redder the color means closer to 2021, and the more yellow the color means closer to 2012.The clusters with redder colors and larger nodes included more publications, demonstrating that the issue of this cluster was a hot topic in the field.

studies from molecular/biology/genetics co-cited journals were mainly cited by journals published in molecular/biology/immunology and medicine/medical/clinical, which implied that there were two broad main directions of research related to CRC immunotherapy, one direction was focused on basic. The other direction was focused on translational research from basic to clinical. Meanwhile, journals with high IF in the JCR division accounted for the vast majority of the top 10 journals (80%) and co-cited journals (90%) in the first quarter, indicating that these journals were interested in and played an essential role in research related to CRC immunotherapy.

AUTHORS AND CITED AUTHORS

Dung T. Le from Johns Hopkins University was ranked first among all co-cited authors, and his publications in the field of CRC immunotherapy were placed 8th among all authors, indicating his outstanding contribution to the development of the field. Two of his highly cited articles, "PD-1 Blockade in Tumors with Mismatch-Repair Deficiency" and "Mismatch-repair deficiency predicts response of solid tumors to PD-1 blockade", were published in *New England Journal of Medicine* (IF=91.253) and *Science* (IF=47.728), respectively. Researchers first evaluated the clinical activity of PD-1 inhibitors in patients for progressive CRC with/without mismatch repair (MMR) and found that microsatellite instable (MSI) CRC (MSI-CRC) were more sensitive to PD-1 blockade responses compared to microsatellite stable (MSS) tumors (25). The researchers then expanded the study to evaluate the effects of PD-1 inhibitors in 12 different types of advanced MMR tumors. They found that in mismatch repair deficient(dMMR) tumors, most mutant neoantigens made them sensitive to immune checkpoint blockade, regardless of the origin of the cancer tissue (26).

TABLE 8 | The top 10 most frequent and centralized keywords related to colorectal cancer immunotherapy.

Rank	Keyword	Counts	Rank	Keyword	Centrality
1	Expression	334	1	Progression	0.12
2	T cell	244	2	Pd 1 blockade	0.10
3	Microsatellite instability	216	3	Mechanism	0.10
4	Dendritic cell	184	4	Combination	0.10
5	Cell	152	5	Chemotherapy	0.09
6	Blockade	139	6	Monoclonal antibody	0.09
7	Survival	135	7	Expression	0.08
8	Activation	120	89	Regulatory t cell	0.08
9	Regulatory t cell	110	9	Receptor	0.08
10	Chemotherapy	109	10	Activation	0.07

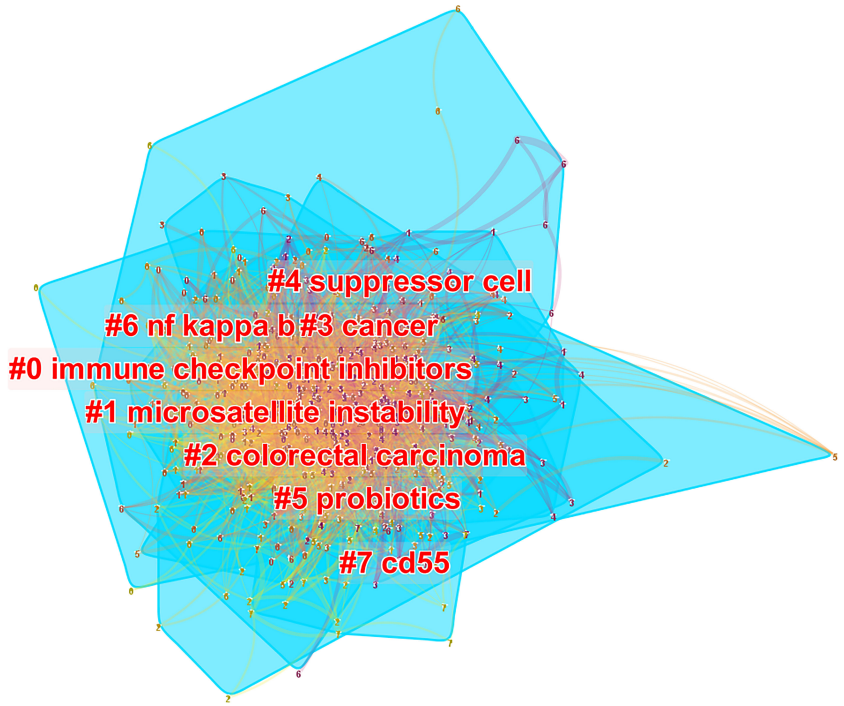

FIGURE 7 | The cluster of keywords related to colorectal cancer immunotherapy. The different colors represented different clusters. Each point represents a keyword, and the number on the node represents the cluster to which the keyword belongs. The lines between the points represent two keywords with co-occurrence relationship. The color of the line segment represents the year, from 2012 to 2021, the color changes from purple to yellow. The blue blocks represent the extent of each cluster in the network space.

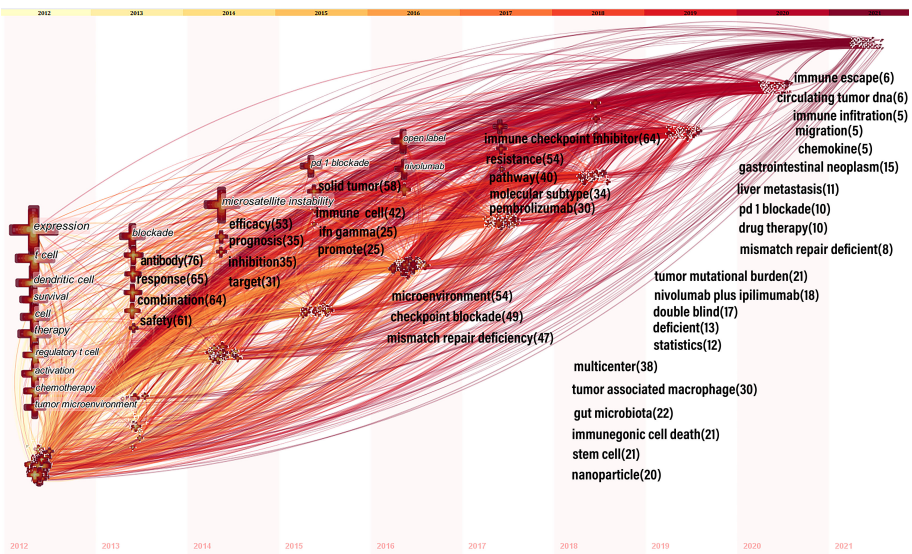

FIGURE 8 | Time zone view of keywords for colorectal cancer immunotherapy. In 2012-2016, keywords with co-occurrence rate ≥80 were shown; from 2013-2021, we manually added annual top5 keywords and their co-occurrence frequency. The position of the cross on the horizontal axis represents the year in which the keyword first appeared. The size of the cross reflects the frequency of co-occurrence, and the larger the cross represents the higher frequency of co-occurrence. The lines between the crosses represent the co-occurrence of two keywords. The lines are colored to indicate the different years. From 2012 to 2021, the color changes from yellow to red.

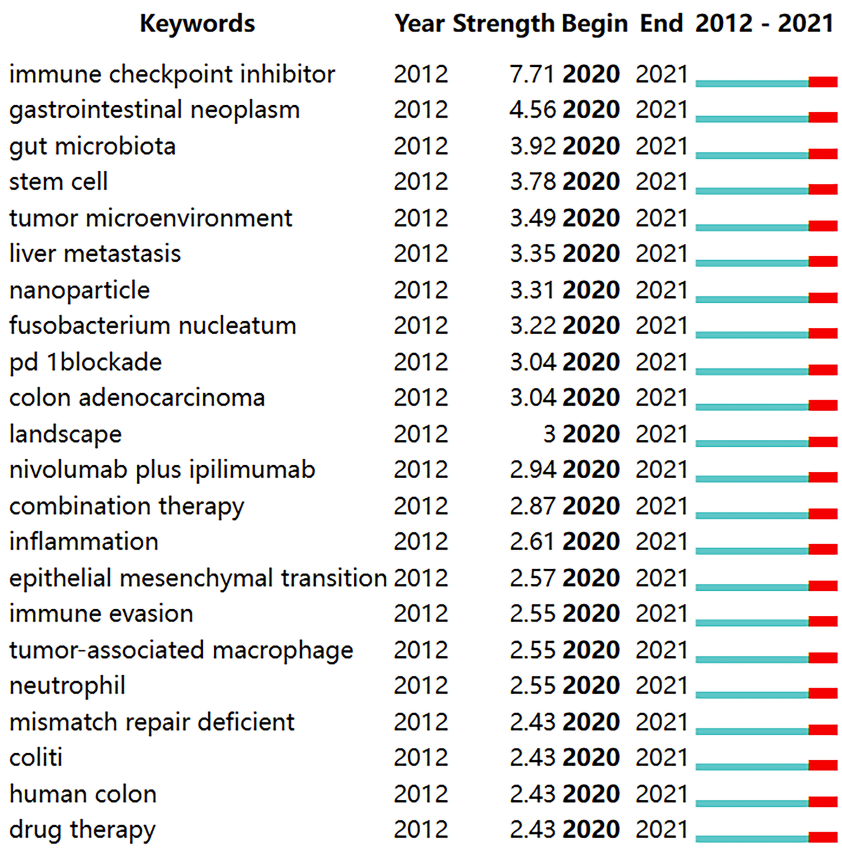

FIGURE 9 | Keywords with burst periods from 2020 onward among the top 103 burst keywords in articles related to colorectal cancer immunotherapy. A blue line indicates the timeline, and the intervals in which bursts were found are indicated by red sections on the blue timeline, indicating the start year, the end year, and the burst duration.

Therefore, these articles were considered reliable resources for future studies on mismatch repair and PD-1.

CO-CITED REFERENCES

We found that most 5 co-cited articles with the highest frequency and centrality were related to immune checkpoint inhibitors (ICIs) and MSI, which indicated the importance of ICIs and MSI in the field. Among the top five co-cited references, the article titled "Global cancer statistics 2018: GLOBOCAN estimates of incidence and mortality worldwide for 36 cancers in 185 countries" was focused on a global review of cancer prevalence and treatment measures (27). Based on the top 5 cited articles by centrality, there was 1 article analyzed the immunophenotypic and antigenic genomic characterization of CRC, revealing different targets of immune escape and tumor immunity (28). It is well known that immune escape, a process by which tumor cells escape killing by the immune system, was a critical factor affecting the effectiveness of tumor therapy. Therefore, this highly cited paper demonstrated that revealing the mechanism of immune escape may help to discover potential targets for immunotherapy of colon cancer. Another article with a high centrality revealed the mechanism of cancer immunotherapy resistance (29), which indicated that immunotherapy resistance had received much attention in CRC immunotherapy.

The timeline view of the co-cited literature showed that most of the studies were published after 2007. The prognosis (Cluster0) has the darkest color and the most published literature and has been a consistent focus of CRC immunotherapy. Microsatellite instability (Cluster1), programmed cell death protein ligand1 (Cluster2) have appeared in recent years and have larger nodes and warmer colors, indicating that the problems under these clusters were hot research topics in recent research years. Microsatellite instability (Cluster1), programmed cell death protein ligand1 (Cluster2) have emerged in recent years and have larger nodes and warmer colors, indicating that the problems under these clusters were hot spots of research in recent years, which was consistent with the above highly co-cited literature focusing on PD-1/PD-L1 and mismatch repair.In addition, in recent years, cytokine-induced killer cells (Cluster3) and t cell exhaustion (Cluster9) may be new research hotspots in CRC immunotherapy. It has been shown that gut microbes can promote colorectal carcinogenesis by stimulating specific immune responses (30). Gut microbiota (Cluster7) may be a research hotspot

in recent years to understand the mechanisms of colorectal carcinogenesis and identify relevant immunotherapeutic strategies. Moreover, hormone replacement (Cluster5) may be one of the hot spots in reducing the risk of colon cancer in MSI type of high-aged menopausal women.

KEYWORDS

In bibliometric analysis, keyword bursts can reflect research hotspots in academic fields (31), and time zone maps can show the evolution of new hotspots (32). Based on the change in the number of publications, we divided the evolution of keywords into three phases: slow growth period (2012-2014), acceleration period (2015-2017) and rapid development period (2018-2021). During the slow growth period (2012-2014) rising terms mainly covered: "expression", "t cell", "dendritic cell", "regulatory t cell", "tumor microenvironment", "blockade", "antibody", "microsatellite instability", "inhibitor", and "target", mainly associated with treatments and mechanisms. In the acceleration period (2015-2017), most new terms focus on clinical and mechanistic studies of ICIs, MSI, and drug resistance. These keywords include: "pd 1 blockade", "ifn gamma", "open label", "nivolumab", "microenvironment", "checkpoint blockade", "mismatch repair deficiency", "immune checkpoint inhibitor", "resistance", and "pembrolizumab". During the rapid development period (2018-2021), emerging topics included "tumor-associated macrophages", "gut microbiota", "immunogenic cell death", "stem cells", "nanoparticles", "tumor mutation burden", "liver metastasis", "drug therapy", "immune escape", and "circulating tumor dna". These themes inherited the characteristics of the accelerated phase and used novel technologies such as nanomaterials, and gave rise to many research directions such as gut microbes, stem cells, tumor-associated macrophages, and immune escape.

According to the citation count and keyword centrality analysis, which mainly included keywords related to immunotherapy mechanism of CRC included "Microsatellite instability", "T cell", "PD-1blockade". It was similar to Nicolas J. Llosa et al. (33), who reported that in dMMR or microsatellite instability-high (MSI-H) (dMMR/MSI-H) tumors. The major histocompatibility presented on the surface of the tumor cell complex (MHC) class I peptide complex induces the migration of CD8 tumor-infiltrating lymphocytes, helper T cells 1, CD4 T cells and macrophages into the tumor microenvironment to induce IFN-γ secretion for antitumor effects and to balance this active microenvironment, dMMR/MSI-H tumors selected for sustained upregulation of the T cell suppressor ligands PD-L1, CTLA-4, fostering immune escape.

Several studies have confirmed the significant anti-tumor effects of PD-1blockade in dMMR/MSI-H CRC immunotherapy (25, 34), further confirming that these keywords were the current hot topic of research in the field of CRC immunotherapy. A review of CRC immunotherapy by Ahui Fan et al. (35) also focused on the treatment of microsatellite unstable and microsatellite stable CRC, mainly surrounding various therapeutic approaches with ICIs. In addition, most CRC immunotherapies were associated with keywords such as PD-1blockade, MSI, and T cell (2), indicating that these aspects were the hot topics in recent years.

A comprehensive analysis of keyword emergence and timezone view can reveal the hot spots and future research trends in the field of CRC immunotherapy. The keywords that emerged since 2020 include "Immune checkpoint inhibitor", "pd-1blockade", "nivolumab plus ipilimumab", "combination therapy", and "drug therapy" with burst strength of:7.71, 3.04, 2.94 and 2.43, respectively. These keywords imply that research in these aspects has been prevalent in this field over the past year. Monotherapy of dMMR/MSI-H CRC showed a significant increase in the durable response rate of the drug with a manageable safety profile, but more than 50% of patients were ineffective to treatment (36). Therefore, discovering new strategies to overcome primary ICI resistance was essential to improve its antitumor effect. Combination with other ICIs such as the CTLA-4 inhibitor ipilimumab may enhance the durable clinical benefit of treating dMMR/MSI-H CRC (37). Recent studies have shown that PD-1 inhibitors combined with CTLA-4 prolong OS in advanced refractory CRC (38), which confirmed that combining multiple ICIs may be a hot topic for future research in this field. Unlike dMMR/MSI-H CRC, mismatch repair proficiency(pMMR) or microsatellite instability-low (MSI-L) (pMMR/MSI-L) tumors, which account for 95% of all metastatic colorectal cancer (mCRC) cases, had a lower mutational burden and poorer immune cell recruitment, resulting in a sub-optimal response to ICIs (13). Researchers found that nivolumab combined with ipilimumab observed pathologic responses in 27% of patients with early-stage pMMR tumors (39). Furthermore, since KRAS/NRSA/BRAF wild-type mCRC was associated with increased CTLA-4 and PD-L1 expression for EGFR monoclonal resistance, ICIs combined with EGFR monoclonal antibodies showed good safety and efficacy in the treatment of MSS mCRC (40). Anti-angiogenic drugs can enhance the anti-tumor activity of CD8 T cells by upregulating PD-L1 expression and reducing immunosuppressive cells such as TAM and Treg. Several studies have shown encouraging ICIs in combination with the anti-angiogenic agent regorafenib in pMMR-MSS (41). Radiation-induced cell injury may increase response to immunotherapy through *in vitro* effects. In a study by Aparna Raj Parikh et al. (42), CTLA-4 and PD-1 dual blockade combined with radiotherapy showed encouraging efficacy in treating patients with pMMR/MSI-L mCRC. In addition, several trials of ICIs in combination with bispecific antibody and MEK were in progress (NCT03428126, NCT03271047, NCT04137289). These studies suggested that combining other therapeutic modalities such as chemotherapy, antigenic combinations, MEK, bispecific antibody, and radiotherapy may increase the immunotherapy response. It was similar to the results reported by Wang et al. (35) and further confirmed that ICIs in combination with other therapeutic modalities were the most popular direction of research in this field. Keyword burst and clustering showed that "immune checkpoint inhibitors", "combination therapy", and "drug therapy" were hot topics in this field and promised to be studied more deeply in the future.

The liver was the most common location of distant metastases from mCRC and the central organ of immune tolerance (43, 44). In a preclinical model of liver metastasis from CRC, liver metastases gathered activated CD8 T cells from the body circulation and liver myeloid cells induced T cell apoptosis *via* the Fas-FasL signaling pathway, resulting in the systemic immune desert (45). The results of another study showed that liver metastasis induced tumor-specific immunosuppression in distant tumors by activating Tregs and regulating CD11b monocytes in a preclinical model of CRC (46). Fujiyoshi et al. found that MSS-mCRC patients were more likely to present with liver metastases than MSI-H mCRC patients (71.0% vs 26.7%, p=0.001) (47). Thus, liver metastases may be one of the reasons for the ineffectiveness of ICI therapy in patients with MSS mCRC, which was supported by a recent study by Want et al. (48). Therefore, an in-depth investigation into the mechanisms of drug resistance development in CRC liver metastasis models may focus on future research.

The tumor microenvironment was the internal environment for tumor cell growth and metastasis, mainly composed of endothelial cells, immune cells, and fibroblasts (49). There was accumulating evidence that many suppressor cells in the tumor microenvironment hindered tumor killing by immune cells and caused the immune escape of tumor cells. Tumor-associated macrophages (TAM) were innate immune cells, accounting for 50% of the human tumor cell mass, and were divided into tumor suppressor M1 and tumor promoter M2. It has been shown that M2 was strongly associated with epithelial-mesenchymal transition and chemoresistance in CRC (50). In addition, TAM suppressed T-cell responses and thus diminished the effectiveness of ICIs (51). Targeting TAM seemed to be a promising treatment modality. Neutrophil extracellular traps (NETs) were reticulated structures consisting of chromatin DNA, dispersed cytoplasm and granular proteins squeezed by activated neutrophils to capture and kill bacteria (52). Zhang et al. (53) reported that inhibition of NETs in a mouse model increased CD8+ T cell infiltration and toxicity, thereby overcoming PD-1 resistance. Comito et al. (54, 55) showed that tumor cells modified the microenvironment by reducing tumor-specific T cells and converting some killer T cells into regulatory T cells (Tregs),which expressed high levels of inhibitory receptors (e.g. PD-1), thus generating an immunosuppressive microenvironment hindering immune killing. In addition, suppressor cells in the tumor microenvironment, such as myeloid-derived suppressor cells and tumor-associated stromal cells, are also resistant to anti-tumor T-cell responses to sustain tumor immune tolerance (56, 57). Therefore, it is critical to explore the CRC tumor microenvironment and reshape the immune microenvironment to improve tumor-infiltrating T cells in CRC immunotherapy. Keyword clustering and bursting showed that topics such as "tumor microenvironment", "neutrophil", "tumor-associated macrophage", "suppressor cell", and "immune evasion" were considered as new research hotspots.

As technology advanced, many technologies drove the development of immunotherapy for CRC. Nanotechnology-based antioxidants and therapeutics were considered the next generation of cancer treatment tools (22). Duan et al. (58) synthesized OxPt/DHA nanoparticles, which significantly enhanced the efficacy of ICIs by increasing the uptake of DHA and OxPt precursors by CRC cells and enhancing the infiltration of CD8+ T cells within the tumor. In addition, Xu et al. (59) used converted nanoparticles containing the photosensitizer chlorine e6 and Toll-like-receptor-7 agonist combined with an immune checkpoint inhibitor that generated potent anti-tumor immunity in CRC cells and exhibited long-term immune memory capacity. The review by Oliveira et al. showed that nanomaterials have emerged as a new direction for CRC immunotherapy. With the development of sequencing technology, researchers have found that tumor mutational burden was an independent predictor of the treatment efficacy with ICIs. In clinical trials of CRC treated by PD-L1 combined with CTLA-4, higher TMB was associated with better OS (38). Therefore, researches related to nanomaterials and tumor mutation burden were expected to be further explored in the future.

An increasing number of studies have shown that gut microbes play essential roles in cancer development. Tanoue et (60) showed that anti-PD-1 treatment was significantly improved after inoculation of a consortium of 11 bacteria in a mouse model of MC38 colon adenocarcinoma. In addition, Marge et al. (61) used a Bifidobacterium pseudolongum combined with an ICIs treatment regimen in germ-free mice bearing colon cancer cells, which increased T-cell activation and reduced tumor volume in the animals. These studies showed a promising future of gut microbes in CRC immunotherapy. Recently, significant leaps have been made to study gut microbes in overcoming ICB acquired drug resistance. Baruch et al. (62) showed that FMT from CR donors combined with anti-PD-1 therapy-induced clinical responses in patients with anti- PD-1 refractory metastatic melanoma. Davar et al. (63) found that 40% of melanoma patients could overcome acquired resistance to anti-PD-1 therapy with FMT treatment. All of these data indicated the critical role of gut microbes in immunotherapy. Keyword bursts indicated that "gut microbiota" would be a new research hotspot in the field of CRC immunotherapy, and in the future, more and more attention would be focused on gut microbiota.

Taking our research and discussions together, we believe there are some aspects of clinical work that should be noted. Defective DNA mismatch repair (MMR) can be detected either by the lack of immunohistochemical staining of the MMR proteins MLH1, MSH2, MSH6 or PMS2 or by PCR-identified alterations in the lengths of microsatellites between a patient's tumour and a sample of normal tissue or blood. The use of immunotherapy for dMMR/MSI-H CRC may lead to better outcomes, and the combination of multiple immune checkpoint inhibitors may achieve satisfactory results compared to single agents. Patients should be observed for immune-related side effects during treatment, such as immune-related nephritis, immune-related endocrine disorders and toxicity. However, there are still some challenges in the clinical treatment of this population, such as the keyword "resistance" that appeared in **Figure 8** 2018, suggesting that some colorectal cancer patients in the clinic become resistant to immunotherapy drugs. There is still no good way to overcome

drug resistance and recover the effectiveness of immunotherapy. For patients with pMMR-MSI-L colorectal cancer, combination therapy with PD1 inhibitors and other immune checkpoint molecular modulators (e.g., CTLA4) may benefit a small subset of patients with pMMR-MSI-L tumors, but for most patients with this CRC subtype, an alternative approach to immunomodulation is necessary. For example, the combination of Bispecific antibody therapy, radiation therapy, anti-angiogenic drugs. Overall, finding ways to increase the immune cells infiltrating the tumor environment is critical to their immunotherapy for this category of patients. In addition, tumor mutational burden is an independent factor in predicting the efficacy of ICI treatment. In clinical trials of treating CRC with PD-L1 in combination with CTLA-4, higher TMB was associated with better OS, so stratification of patients by immune mutational load prior to treatment may help determine patient treatment efficacy and thus contribute to the selection of therapeutic agents.

LIMITATIONS

We should explain the limitations of the study. On the one hand, these data are collected from a single source, the web of science core, only, leading to the omission of articles from other sources. In addition, the manual removal of papers unrelated to the study by the investigator may lead to selection bias. Last, only English articles were entered in this study, which may lead to source bias.

CONCLUSION

To our knowledge, our study was the first comprehensive metrological and statistical analysis of CRC immunotherapy over the past 10 years. In this study, we found that the United States has contributed significantly to the advancement of the field by publishing the most significant number of articles in the field and keeping the quality of articles high. China's publications in this field snowballed after 2018, surpassing the U.S. since 2020, and maintaining a rapid growth trend that may be related to government financial support. The rapid growth of publications also indicated that CRC immunotherapy was becoming of increasing interest worldwide.

Our research showed a trend for cooperation between various countries and institutions. However, there was a still lack of intensive cooperation between different institutions/countries. Notably, the National Cancer Institute (NCI) and Sun Yat-sen University have made significant contributions to the progress of the field. Therefore, institutions can strengthen their cooperation with them to promote the future development of the field better.

Journal of Clinical Oncology and *Journal for Immunotherapy of Cancer* were the most cited and most published journals. In addition, the most prolific and co-cited authors were Adam E Snook and Dung T. Le, respectively. Thus, researchers can better grasp the research progress in this field through articles published in these journals or authors who will be potential collaborators in the field.

Our research indicated that nanomaterials might be the most advanced and popular technology in recent research. In addition, CRC immunotherapy is associated with microsatellite status. Research on immunotherapy for MSI-CRC has focused on PD-1blockade, T cell and combination with other ICIs. Research on immunotherapy for microsatellite stabilized CRC has focused on immune checkpoint inhibitors, combination therapy, and drug therapy. These aspects will remain significant research hotspots in the future. Colorectal cancer liver metastasis has received increasing attention from researchers due to its characteristics. In addition, research on the immune microenvironment has drawn attention to its vital role in immunotherapy, and improving the effectiveness of immunotherapy by modulating the immune microcircuit has become increasingly important in the treatment of CRC. We can predict that the research on tumor microenvironment will become more enthusiastic in the future. The role of gut microbes in CRC immunotherapy may soon become a research hotspot and should be closely monitored.

DATA AVAILABILITY STATEMENT

The datasets presented in this study can be found in online repositories. The names of the repository/repositories and accession number(s) can be found in the article/supplementary material.

AUTHOR CONTRIBUTIONS

LM: Writing- Original draft preparation, Investigation, table and figure preparation. JM: Investigation and table preparation. MT : Supervision. YL: Conceptualization, Methodology, Supervision. All authors contributed to the article and approved the submitted version.

FUNDING

This work was supported by National Natural Science Foundation of China (31770537) and Major Science and Technology Special Project of Gansu Province (20ZD7FA003).

REFERENCES

1. Sung H, Ferlay J, Siegel RL, Laversanne M, Soerjomataram I, Jemal A, et al. Global Cancer Statistics 2020: GLOBOCAN Estimates of Incidence and Mortality Worldwide for 36 Cancers in 185 Countries. *CA Cancer J Clin* (2021) 71(3):209–49. doi: 10.3322/caac.21660
2. Ganesh K, Stadler ZK, Cercek A, Mendelsohn RB, Shia J, Segal NH, et al. Immunotherapy in Colorectal Cancer: Rationale, Challenges and Potential. *Nat Rev Gastroenterol Hepatol* (2019) 16(6):361–75. doi: 10.1038/s41575-019-0126-x
3. Sveen A, Kopetz S, Lothe RA. Biomarker-Guided Therapy for Colorectal Cancer: Strength in Complexity. *Nat Rev Clin Oncol* (2020) 17(1):11–32. doi: 10.1038/s41571-019-0241-1

4. Giordano G, Remo A, Porras A, Pancione M. Immune Resistance and EGFR Antagonists in Colorectal Cancer. *Cancers (Basel).* (2019) 11(8):1089. doi: 10.3390/cancers11081089
5. Hinshaw DC, Shevde LA. The Tumor Microenvironment Innately Modulates Cancer Progression. *Cancer Res* (2019) 79(18):4557–66. doi: 10.1158/0008-5472.CAN-18-3962
6. Chmielik E. Pathology and Tumor Microenvironment: Past, Present, and Future. *Pathobiology* (2020) 87(2):55–7. doi: 10.1159/000507222
7. Zhang H, Chen J. Current Status and Future Directions of Cancer Immunotherapy. *J Cancer* (2018) 9(10):1773–81. doi: 10.7150/jca.24577
8. Liu J, Chen Z, Li Y, Zhao W, Wu J, Zhang Z. PD-1/PD-L1 Checkpoint Inhibitors in Tumor Immunotherapy. *Front Pharmacol* (2021) 12:731798. doi: 10.3389/fphar.2021.731798
9. Alsaab HO, Sau S, Alzhrani R, Tatiparti K, Bhise K, Kashaw SK, et al. PD-1 and PD-L1 Checkpoint Signaling Inhibition for Cancer Immunotherapy: Mechanism, Combinations, and Clinical Outcome. *Front Pharmacol* (2017) 8:561. doi: 10.3389/fphar.2017.00561
10. Zhang H, Dai Z, Wu W, Wang Z, Zhang N, Zhang L, et al. Regulatory Mechanisms of Immune Checkpoints PD-L1 and CTLA-4 in Cancer. *J Exp Clin Cancer Res* (2021) 40:184. doi: 10.1186/s13046-021-01987-7
11. Agarwal P, Le DT, Boland PM. Immunotherapy in Colorectal Cancer. *Adv Cancer Res* (2021) 151:137–96. doi: 10.1016/bs.acr.2021.03.002
12. Yang Y. Cancer Immunotherapy: Harnessing the Immune System to Battle Cancer. *J Clin Invest.* (2015) 125:3335–7. doi: 10.1172/JCI83871
13. Kim CW, Chon HJ, Kim C. Combination Immunotherapies to Overcome Intrinsic Resistance to Checkpoint Blockade in Microsatellite Stable Colorectal Cancer. *Cancers (Basel).* (2021) 13(19):4906. doi: 10.3390/cancers13194906
14. Ahn SK, Hwang JW. Global Trends in Immunotherapy Research on Breast Cancer Over the Past 10 Years. *J Oncol* (2020) 2020:4708394. doi: 10.1155/2020/4708394
15. Wang S, Wu K, Zhang Z, Xu Z, Wu J, Xu S. Mapping Theme Trends and Recognizing Research Hot Spots in the Use of Ultrasound in Orthopaedics: A Bibliometric Analysis of Global Research. *Am J Transl Res* (2021) 13(8):9892–911.
16. Ke L, Lu C, Shen R, Lu T, Ma B, Hua Y. Knowledge Mapping of Drug-Induced Liver Injury: A Scientometric Investigation (2010-2019). *Front Pharmacol* (2020) 11:842. doi: 10.3389/fphar.2020.00842
17. Aggarwal A, Lewison G, Idir S, Peters M, Aldige C, Boerckel W, et al. The State of Lung Cancer Research: A Global Analysis. *J Thorac Oncol* (2016) 11(7):1040–50. doi: 10.1016/j.jtho.2016.03.010
18. Chen C, Song M. Visualizing a Field of Research: A Methodology of Systematic Scientometric Reviews. *PloS One* (2019) 14(10):e0223994. doi: 10.1371/journal.pone.0223994
19. Brandes U. A Faster Algorithm for Betweeness Centrality. *J Math Sociol* (2001) 25:163–77. doi: 10.1080/0022250x.2001.9990249
20. Chen C. CiteSpace II: Detecting and Visualizing Emerging Trends and Transient Patterns in Scientific Literature. *J Am Soc Infor Sci Technol* (2006) 57:359–77. doi: 10.1002/asi.20317
21. Kleinberg J. Bursty and Hierarchical Structure in Streams *. *Data Min Knowl Discov* (2002) 7(4):91–101. doi: 10.1145/775060.775061
22. Chen H, Li R, Zhang F, Yao Q, Guo Y. A Scientometric Visualization Analysis for Natural Products on Cancer Research From 2008 to 2020. *Front Pharmacol* (2021) 12:650141. doi: 10.3389/fphar.2021.650141
23. Li T, Yang A, Liu G, Zou S, Chen Y, Ni B, et al. Status Quo and Research Trends of Craniopharyngioma Research: A 10-Year Bibliometric Analyses (From 2011 to 2020). *Front Oncol* (2021) 11:744308. doi: 10.3389/fonc.2021.744308
24. Zhang J, Song L, Xu L, Fan Y, Wang T, Tian W, et al. Knowledge Domain and Emerging Trends in Ferroptosis Research: A Bibliometric and Knowledge-Map Analysis. *Front Oncol* (2021) 11:686726. doi: 10.3389/fonc.2021.686726
25. Le DT, Uram JN, Wang H, Bartlett BR, Kemberling H, Eyring AD, et al. PD-1 Blockade in Tumors With Mismatch-Repair Deficiency. *N Engl J Med* (2015) 372(26):2509–20.
26. Le DT, Durham JN, Smith KN, Wang H, Bartlett BR, Aulakh LK, et al. Mismatch Repair Deficiency Predicts Response of Solid Tumors to PD-1 Blockade. *Science* (2017) 357(6349):409–13. doi: 10.1126/science.aan6733
27. Bray F, Ferlay J, Soerjomataram I, Siegel RL, Torre LA, Jemal A. Global Cancer Statistics 2018: GLOBOCAN Estimates of Incidence and Mortality Worldwide for 36 Cancers in 185 Countries. *CA Cancer J Clin* (2018) 68(6):394–424. doi: 10.3322/caac.21492
28. Angelova M, Charoentong P, Hackl H, Fischer ML, Snajder R, Krogsdam AM, et al. Characterization of the Immunophenotypes and Antigenomes of Colorectal Cancers Reveals Distinct Tumor Escape Mechanisms and Novel Targets for Immunotherapy. *Genome Biol* (2015) 16(1):64. doi: 10.1186/s13059-015-0620-6
29. Sharma P, Hu-Lieskovan S, Wargo JA, Ribas A. Primary, Adaptive, and Acquired Resistance to Cancer Immunotherapy. *Cell* (2017) 168(4):707–23. doi: 10.1016/j.cell.2017.01.017
30. Yang Y, Li L, Xu C, Wang Y, Wang Z, Chen M, et al. Cross-Talk Between the Gut Microbiota and Monocyte-Like Macrophages Mediates an Inflammatory Response to Promote Colitis-Associated Tumourigenesis. *Gut* (2020) 70(8):1495–506. doi: 10.1136/gutjnl-2020-320777
31. Xiao F, Li C, Sun J, Zhang L. Knowledge Domain and Emerging Trends in Organic Photovoltaic Technology: A Scientometric Review Based on CiteSpace Analysis. *Front Chem* (2017) 5:67. doi: 10.3389/fchem.2017.00067
32. Liu G, Jiang R, Jin Y. Sciatic Nerve Injury Repair: A Visualized Analysis of Research Fronts and Development Trends. *Neural Regener Res* (2014) 9(18):1716–22. doi: 10.4103/1673-5374.141810
33. Llosa NJ, Cruise M, Tam A, Wicks EC, Hechenbleikner EM, Taube JM, et al. The Vigorous Immune Microenvironment of Microsatellite Instable Colon Cancer is Balanced by Multiple Counter-Inhibitory Checkpoints. *Cancer Discovery* (2015) 5(1):43–51. doi: 10.1158/2159-8290.CD-14-0863
34. André T, Shiu KK, Kim TW, Jensen BV, Jensen LH, Punt C, et al. Pembrolizumab in Microsatellite-Instability-High Advanced Colorectal Cancer. *N Engl J Med* (2020) 383(23):2207–18. doi: 10.1056/NEJMoa2017699
35. Fan A, Wang B, Wang X, Nie Y, Fan D, Zhao X, et al. Immunotherapy in Colorectal Cancer: Current Achievements and Future Perspective. *Int J Biol Sci* (2021) 17(14):3837–49. doi: 10.7150/ijbs.64077
36. Rotte A. Combination of CTLA-4 and PD-1 Blockers for Treatment of Cancer. *J Exp Clin Cancer Res* (2019) 38(1):255. doi: 10.1186/s13046-019-1259-z
37. Overman MJ, Lonardi S, Wong K, Lenz HJ, Gelsomino F, Aglietta M, et al. Durable Clinical Benefit With Nivolumab Plus Ipilimumab in DNA Mismatch Repair-Deficient/Microsatellite Instability-High Metastatic Colorectal Cancer. *J Clin Oncol* (2018) 36(8):773–9. doi: 10.1200/JCO.2017.76.9901
38. Chen EX, Jonker DJ, Loree JM, Kennecke HF, Berry SR, Couture F, et al. Effect of Combined Immune Checkpoint Inhibition vs Best Supportive Care Alone in Patients With Advanced Colorectal Cancer: The Canadian Cancer Trials Group CO.26 Study. *JAMA Oncol* (2020) 6(6):831–8. doi: 10.1001/jamaoncol.2020.0910
39. Chalabi M, Fanchi LF, Dijkstra KK, Van den Berg JG, Aalbers AG, Sikorska K, et al. Neoadjuvant Immunotherapy Leads to Pathological Responses in MMR-Proficient and MMR-Deficient Early-Stage Colon Cancers. *Nat Med* (2020) 26(4):566–76. doi: 10.1038/s41591-020-0805-8
40. Lee MS, Loehrer PJ, Imanirad I, Cohen S, Ciombor KK, Moore DT, et al. Phase II Study of Ipilimumab, Nivolumab, and Panitumumab in Patients With KRAS/NRAS/BRAF Wild-Type (WT) Microsatellite Stable (MSS) Metastatic Colorectal Cancer (mCRC). *J Clin Oncol* (2021) 39(3):7. doi: 10.1200/JCO.2021.39.3_suppl.7
41. Fukuoka S, Hara H, Takahashi N, Kojima T, Kawazoe A, Asayama M, et al. Regorafenib Plus Nivolumab in Patients With Advanced Gastric or Colorectal Cancer: An Open-Label, Dose-Escalation, and Dose-Expansion Phase Ib Trial (REGONIVO, Epoc1603). *J Clin Oncol* (2020) 38(18):2053–61. doi: 10.1200/JCO.19.03296
42. Parikh AR, Clark JW, Wo J, Yeap BY, Allen JN, Blaszkowsky LS, et al. A Phase II Study of Ipilimumab and Nivolumab With Radiation in Microsatellite Stable (MSS) Metastatic Colorectal Adenocarcinoma (mCRC). *J Clin Oncol* (2019) 37(15):3514. doi: 10.1200/JCO.2019.37.15_suppl.3514
43. Kim CG, Kim C, Yoon SE, Kim KH, Choi SJ, Kang B, et al. Hyperprogressive Disease During PD-1 Blockade in Patients With Advanced Hepatocellular Carcinoma. *J Hepatol* (2021) 74(2):350–9. doi: 10.1016/j.jhep.2020.08.010
44. Hegde PS, Chen DS. Top 10 Challenges in Cancer Immunotherapy. *Immunity* (2020) 52(1):17–35. doi: 10.1016/j.immuni.2019.12.011
45. Yu J, Green MD, Li S, Sun Y, Journey SN, Choi JE, et al. Liver Metastasis Restrains Immunotherapy Efficacy *via* Macrophage-Mediated T Cell Elimination. *Nat Med* (2021) 27(1):152–64. doi: 10.1038/s41591-020-1131-x
46. Lee JC, Mehdizadeh S, Smith J, Young A, Mufazalov IA, Mowery CT, et al. Regulatory T Cell Control of Systemic Immunity and Immunotherapy Response in Liver Metastasis. *Sci Immunol* (2020) 5(52):eaba0759. doi: 10.1126/sciimmunol.aba0759

47. Fujiyoshi K, Yamamoto G, Takenoya T, Takahashi A, Arai Y, Yamada M, et al. Metastatic Pattern of Stage IV Colorectal Cancer With High-Frequency Microsatellite Instability as a Prognostic Factor. *Anticancer Res* (2017) 37 (1):239–47. doi: 10.21873/anticanres.11313
48. Wang C, Sandhu J, Ouyang C, Ye J, Lee PP, Fakih M. Clinical Response to Immunotherapy Targeting Programmed Cell Death Receptor 1/Programmed Cell Death Ligand 1 in Patients With Treatment-Resistant Microsatellite Stable Colorectal Cancer With and Without Liver Metastases. *JAMA Netw Open* (2021) 4(8):e2118416. doi: 10.1001/jamanetworkopen.2021.18416
49. Xia A, Zhang Y, Xu J, Yin T, Lu XJ. T Cell Dysfunction in Cancer Immunity and Immunotherapy. *Front Immunol* (2019) 10:1719. doi: 10.3389/fimmu.2019.01719
50. Zhang X, Chen Y, Hao L, Hou A, Chen X, Li Y, et al. Macrophages Induce Resistance to 5-Fluorouracil Chemotherapy in Colorectal Cancer Through the Release of Putrescine. *Cancer Lett* (2016) 381(2):305–13. doi: 10.1016/j.canlet.2016.08.004
51. Li X, Liu R, Su X, Pan Y, Han X, Shao C, et al. Harnessing Tumor-Associated Macrophages as Aids for Cancer Immunotherapy. *Mol Cancer* (2019) 18 (1):177. doi: 10.1186/s12943-019-1102-3
52. Ravindran M, Khan MA, Palaniyar N. Neutrophil Extracellular Trap Formation: Physiology, Pathology, and Pharmacology. *Biomolecules* (2019) 9(8):365. doi: 10.3390/biom9080365
53. Zhang H, Wang Y, Onuma A, He J, Wang H, Xia Y, et al. Neutrophils Extracellular Traps Inhibition Improves PD-1 Blockade Immunotherapy in Colorectal Cancer. *Cancers (Basel)* (2021) 13(21). doi: 10.3390/cancers13215333
54. Lim WC, Olding M, Healy E, Millar TM. Human Endothelial Cells Modulate CD4(+) T Cell Populations and Enhance Regulatory T Cell Suppressive Capacity. *Front Immunol* (2018) 9:565. doi: 10.3389/fimmu.2018.00565
55. Comito G, Iscaro A, Bacci M, Morandi A, Ippolito L, Parri M, et al. Lactate Modulates CD4(+) T-Cell Polarization and Induces an Immunosuppressive Environment, Which Sustains Prostate Carcinoma Progression *via* TLR8/miR21 Axis. *Oncogene* (2019) 38(19):3681–95. doi: 10.1038/s41388-019-0688-7
56. Yin K, Xia X, Rui K, Wang T, Wang S. Myeloid-Derived Suppressor Cells: A New and Pivotal Player in Colorectal Cancer Progression. *Front Oncol* (2020) 10:610104. doi: 10.3389/fonc.2020.610104
57. Jiang P, Gu S, Pan D, Fu J, Sahu A, Hu X, et al. Signatures of T Cell Dysfunction and Exclusion Predict Cancer Immunotherapy Response. *Nat Med* (2018) 24(10):1550–8. doi: 10.1038/s41591-018-0136-1
58. Duan X, Chan C, Han W, Guo N, Weichselbaum RR, Lin W. Immunostimulatory Nanomedicines Synergize With Checkpoint Blockade Immunotherapy to Eradicate Colorectal Tumors. *Nat Commun* (2019) 10 (1):1899. doi: 10.1038/s41467-019-09221-x
59. Xu J, Xu L, Wang C, Yang R, Zhuang Q, Han X, et al. Near-Infrared-Triggered Photodynamic Therapy With Multitasking Upconversion Nanoparticles in Combination With Checkpoint Blockade for Immunotherapy of Colorectal Cancer. *ACS Nano* (2017) 11(5):4463–74. doi: 10.1021/acsnano.7b00715
60. Tanoue T, Morita S, Plichta DR, Skelly AN, Suda W, Sugiura Y, et al. A Defined Commensal Consortium Elicits CD8 T Cells and Anti-Cancer Immunity. *Nature* (2019) 565(7741):600–5. doi: 10.1038/s41586-019-0878-z
61. Mager LF, Burkhard R, Pett N, Cooke N, Brown K, Ramay H, et al. Microbiome-Derived Inosine Modulates Response to Checkpoint Inhibitor Immunotherapy. *Science* (2020) 369(6510):1481–9. doi: 10.1126/science.abc3421
62. Baruch EN, Youngster I, Ben-Betzalel G, Ortenberg R, Lahat A, Katz L, et al. Fecal Microbiota Transplant Promotes Response in Immunotherapy-Refractory Melanoma Patients. *Science* (2021) 371(6529):602–9. doi: 10.1126/science.abb5920
63. Davar D, Dzutsev AK, McCulloch JA, Rodrigues RR, Chauvin JM, Morrison RM, et al. Fecal Microbiota Transplant Overcomes Resistance to Anti-PD-1 Therapy in Melanoma Patients. *Science* (2021) 371(6529):595–602. doi: 10.1126/science.abf3363

Conflict of Interest: The authors declare that the research was conducted in the absence of any commercial or financial relationships that could be construed as a potential conflict of interest.

Publisher's Note: All claims expressed in this article are solely those of the authors and do not necessarily represent those of their affiliated organizations, or those of the publisher, the editors and the reviewers. Any product that may be evaluated in this article, or claim that may be made by its manufacturer, is not guaranteed or endorsed by the publisher.

Copyright © 2022 Ma, Ma, Teng and Li. This is an open-access article distributed under the terms of the Creative Commons Attribution License (CC BY). The use, distribution or reproduction in other forums is permitted, provided the original author(s) and the copyright owner(s) are credited and that the original publication in this journal is cited, in accordance with accepted academic practice. No use, distribution or reproduction is permitted which does not comply with these terms.

frontiers | Frontiers in Oncology

CASE REPORT
published: 01 April 2022
doi: 10.3389/fonc.2022.801924

Nivolumab Combined With Ipilimumab Treatment Induced Hypophysitis and Immune-Mediated Liver Injury in Advanced Esophageal Squamous Cell Carcinoma: A Case Report

Yi Feng[1,2,3], *Chengyang Li*[4], *Yuan Ji*[5], *Ying Liu*[6], *Lu Gan*[1,2,3], *Yiyi Yu*[1,2,3] *and Tianshu Liu*[1,2,3*]

[1] Department of Medical Oncology, Zhongshan Hospital, Fudan University, Shanghai, China, [2] Center of Evidence-Based Medicine, Fudan University, Shanghai, China, [3] Cancer Center, Zhongshan Hospital, Fudan University, Shanghai, China, [4] Clinical Pharmacology, The Ohio State University, Columbus, OH, United States, [5] Department of Pathology, Zhongshan Hospital, Fudan University, Shanghai, China, [6] Department of Clinical Coordination, Hangzhou Simo Co., Ltd., Hangzhou, China

OPEN ACCESS

Edited by:
Hubing Shi,
Sichuan University, China

Reviewed by:
Alessandro Granito,
University of Bologna, Italy
Elisabetta Razzuoli,
Experimental Zooprophylactic Institute for Piedmont, Liguria and Valle d'Aosta (IZSTO), Italy

***Correspondence:**
Tianshu Liu
liu.tianshu@zs-hospital.sh.cn

Specialty section:
This article was submitted to Cancer Immunity and Immunotherapy, a section of the journal Frontiers in Oncology

Received: *26 October 2021*
Accepted: *09 March 2022*
Published: *01 April 2022*

Citation:
Feng Y, Li C, Ji Y, Liu Y, Gan L, Yu Y and Liu T (2022) Nivolumab Combined With Ipilimumab Treatment Induced Hypophysitis and Immune-Mediated Liver Injury in Advanced Esophageal Squamous Cell Carcinoma: A Case Report. Front. Oncol. 12:801924. doi: 10.3389/fonc.2022.801924

Immune checkpoint inhibitors (ICIs) have transformed the treatment in malignancies because of the impact on reactivating the immune cells to kill tumor cells. Because anti-CTLA-4 antibody and anti-PD-1 antibody (or anti-PD-L1 antibody) work in different ways, they have synergistic effects when used in combination in many cancers. However, it has been found that a strong immune response may lead to more serious and multi-system immune-related adverse events (irAE). We describe an advanced esophageal squamous cell carcinoma patient who received nivolumab combined with ipilimumab resulting in hypophysitis and immune-mediated liver injury. He was enrolled into a CheckMate 648 global, multicenter, randomized phase 3 Clinical Trial (CTR20171227) investigating the combined potency of nivolumab and ipilimumab in the treatment of patients with advanced esophageal squamous cell carcinoma and admitted to our center (site 0200). The patient developed hypophysitis and immune-related hepatitis rapidly after ICIs therapy, leading to the interruption of anti-tumor therapy. Then the patient developed Herpes zoster and recurrence of tuberculosis after treatment of irAEs with glucocorticoids. We report this case in the hope that doctors need to have sufficient knowledge and attention to the occurrence of irAE during the anti-immune combination therapy and actively intervene as soon as possible to obtain better anti-tumor effects and less harm to patients.

Keywords: immune checkpoint inhibitor, immune-related adverse events, hypophysitis, immune-mediated liver injury, steroid therapy

INTRODUCTION

Cytotoxic T lymphocyte associated antigen-4 (CTLA-4) and programmed death-1 (PD-1) pathways are commonly involved in suppressing antitumor immune responses (1). In the tumor microenvironment, the expression of immunosuppressive molecules such as CTLA-4, PD-1 and its ligand PD-L1 (programmed death ligand 1), is significantly increased, resulting in apoptosis or inactivation of cytotoxic T lymphocytes, which allows tumor cells to escape the immune surveillance and clearance (2). Immune checkpoint inhibitors (ICIs) become a major development in cancer treatment because of the impact on reactivating immune cells. Ipilimumab (anti-CTLA-4 antibody), nivolumab (anti-PD-1 antibody), pembrolizumab (anti-PD-1 antibody), atezolizumab (anti-PD-L1 antibody), devaluzumab (anti-PD-L1 antibody), etc., are the ICIs approved for clinical cancer treatment. They certainly have a strong potency in many tumors. However, they also destroy the homeostasis of immune system and increase the risk of immune-related adverse events (irAEs). irAEs can affect all tissues and organs with different severity, mainly in the intestines, skin, endocrine glands, liver, lungs, etc. (1, 3). Khoja et al. summarized the irAE caused by different ICI treatments from 48 trials (6,938 patients), namely, 26 CTLA-4, 17 PD-1, 2 PD-L1 trials, and 3 studies tested by both CTLA-4 and PD-1. They found that different ICIs have distinct irAE profiles. Anti-CTLA-4 treatment has more possibility to induce grade 3/4 irAE (3). Appropriate treatment for irAE, therefore, is very important to avoid subsequent adverse events. Here, we describe an advanced esophageal squamous cell carcinoma patient who received nivolumab combined with ipilimumab resulting in hypophysitis and immune-mediated liver injury. He was enrolled onto a CheckMate 648 global, multicenter, randomized phase 3 Clinical Trial (CTR20171227) investigating the combined potency of nivolumab and ipilimumab in the treatment of patients with advanced esophageal squamous cell carcinoma and admitted to our center (site 0200). The patient developed herpes zoster and recurrence of tuberculosis after treatment of irAEs with glucocorticoids. We report this case to discuss the identification and intervention in the early stages of irAEs caused by cancer immunotherapy. We hope it will be helpful in diagnosis and the subsequent treatment of irAEs.

CASE

Patient

A 55-year-old male patient was diagnosed with esophageal squamous cell carcinoma (cTxNxM1 stage IV lymph node) in March 2019. On 3 April 2019, he entered "an unresectable late-stage recurrent or metastatic esophageal squamous cell carcinoma that has not been treated before a randomized phase 3 study of nivolumab + ipilimumab or nivolumab combined with fluorouracil + cisplatin versus fluorouracil + cisplatin". The patient was randomly assigned to group A (nivolumab + ipilimumab regimen). The first cycle of treatment started from 16 April 2019 with nivolumab (3 mg/kg) 204 mg dl, 15, 30 and ipilimumab (1 mg/kg) 68 mg dl, q6w. The first-week treatment was successfully completed. Previously the patient denied the history of hypertension, diabetes, coronary heart disease, liver disease or autoimmune diseases. Hepatitis B and hepatitis C antibodies were negative before being enrolled in the study. Tuberculosis was diagnosed in 2004, and he was cured after 8 months of anti-tuberculosis. T-SPOT (T-SPOT.TB, one type of interferon-gamma-release assay) and chest CT (computed tomography) were all negative before enrollment in the study. Skin itching (neck, face, back) began on 22 April 2019, with swelling on the face, ears to the lower neck on 4 May 2019, accompanied by dry mouth. On 20 May 2019, swelling occurred on the scalp, following by aggravating and spreading to the entire face and neck, which has affected the daily life of the patient. There was no swelling of the lower limbs and decrease in urine output. Physical examination revealed a small number of scattered rashes on the neck, face and back, obvious swelling on the face without depression, and restricted neck movement (**Figure 1**).

Laboratory and Imaging Examinations

30 April 2019 Liver function indicators: ALT/AST 63/55 U/L, 10 May 2019 Normal thyroid function indicators: TSH, fT4, fT3, liver function indicators: ALT/AST/γ-GT 74/43/119U/L, 28 May 2019 Blood endocrine indicators: TSH: 0.080 Uiu/ml, fT4, fT3, ACTH: 2.8 pg/ml, Cortisol: 33.2 nmol/L, anti-SS-A antibody (+), 28 May 2019 tumor evaluation is based on the RECIST 1.1 (Response Evaluation Criteria in Solid Tumors 1.1) standard, and the evaluation effect is SD (stable disease). 31 May 2019 Enhanced MRI of the pituitary gland showed no abnormalities and mild sphenoid sinusitis (**Figure S1**). 4 June 2019 Liver function indicators are ALT/γ-GT 61/70 U/L, TT3 1.1 nM, TSH 0.120 uIU/ml, ACTH <1.5 pg/ml, cortisol: 19.5 nmol/L and FT3, TT4, FT4, Testosterone and growth hormone are in the

FIGURE 1 | Patient pictures. Left picture: Before treatment; Right picture: One month after treatment.

normal range. 18 June 2019 Liver function indicators are ALT/γ-GT 67/133 U/L, TT3 1.0 nM, TSH 0.220 uIU/ml and FT3, TT4, FT4 are all within the normal range. 9 July 2019 ALT/AST 212/100 U/L, 16 July 2019 ACTH: 2.0 pg/ml, cortisol: 10.0 nmol/L, thyroid function indicators: in the normal range. Antibodies to hepatitis A, hepatitis C, and hepatitis E were all negative. 23 July 2019 ALT/AST/γ-GT 170/63/163 U/L, 31 July 2019 liver puncture guided by B-ultrasound, pathology: (liver puncture) morphology features suggested immune-related hepatitis (**Figure 2** and **Table 1**).

DIAGNOSIS

Combined with the clinical manifestations, physical examination and laboratory examinations of the patient, he was clinically diagnosed as grade 2 hypophysitis on 28 May 2019 with head, face and neck swelling, lower cortisol and ACTH value than normal, which is considered as an irAE. Meanwhile, his clinical treatment was suspended. On 31 July 2019, it was proved to be a manifestation of immune-related hepatitis pathologically by liver puncture. Considering the too long toxic and side effects, the patient got out of this clinical trial.

FOLLOW-UP TREATMENT

He started oral prednisolone acetate 20 mg tid on 28 May 2019. Facial swelling was significantly alleviated after 3 days of oral administration, and then the dose of glucocorticoid was gradually reduced. From 6 July 2019, the dose of prednisolone acetate was reduced to 10 mg qd PO. On 9 July 2019, ALT/AST is

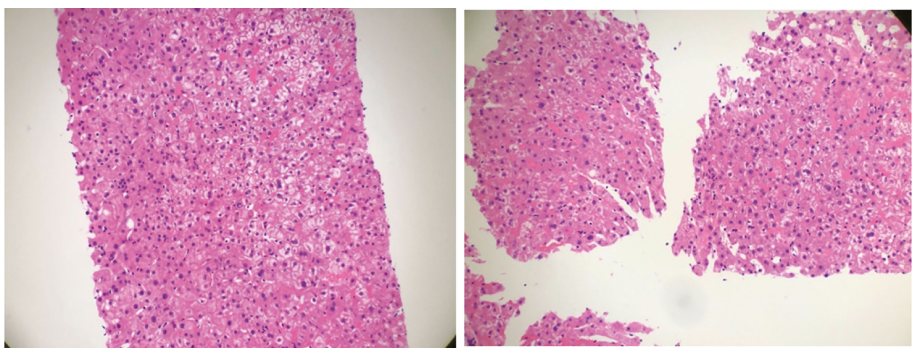

FIGURE 2 | Hematoxylin–eosin staining of liver biopsy. It showed that the structure of liver lobules was intact. Part of liver cells was turbid and swollen. Mild congestion and lymphocytes were seen in the liver sinusoids. Neutrophil aggregation was seen in small foci.

TABLE 1 | The hormone levels of this patient in various stages.

	TT3	TT4	FT3	FT4	TSH	ACTH	COR	PTH
11 April 2019	/	/	3.9	15.7	1.19	/	/	/
10 May 2019	1.7	94.5	4.6	15	1.14	/	/	/
28 May 2019	/	/	4.5	12.9	0.08	2.8	33.2	47
4 June 2019	1.1	117	3.6	21.5	0.12	<1.5	19.5	/
18 June 2019	1	72.2	3.1	14.2	0.22	/	/	/
9 July 2019	/	/	4.5	16.3	2.99	/	/	/
30 July 2019	0.7	73	2.4	16.1	0.19	<1.5	36.9	/
10 September 2019	1.3	117	3.7	18.8	1.02	/	/	/
Normal range	1.3-3.1nmol/L	66-181nmol/L	2.8-7.1pmol/L	12-22pmol/L	0.27-4.2uIU/L	7.2-63.3 pg/mL	133.0-537.0 nmol/L	15-65pg/mL

	LH	FSH	PRL	E2	PRG	TTE	GH
11 April 2019	/	/	/	/	/	/	/
10 May 2019	/	/	/	/	/	/	/
28 May 2019	/	/	/	/	/	/	/
4 June 2019	14.6	19.9	294	<18.4	<0.159	7.6	0.1
18 June 2019	/	/	/	/	/	/	/
9 July 2019	/	/	/	/	/	/	/
30 July 2019	/	/	/	/	/	/	/
10 September 2019	/	/	/	/	/	/	/
Normal range	1.7-8.6mIU/mL	1.5-12.4mIU/mL	131-647mIU/L	94.8-223pmol/L	<0.159nmol/L	9.9-27.8nmol/L	0-1ng/ml

212/100 U/L. On 16 July 2019, ACTH is 2.0 pg/ml and cortisol is 10.0 nmol/L. Thyroid function indicators are in normal range. Liver puncture on 31 July 2019 confirmed the manifestation of immune-related hepatitis pathologically (**Figure 2**).

THE TREATMENT OF COMPLICATIONS CAUSED BY LONG-TERM ORAL ADMINISTRATION OF GLUCOCORTICOIDS

The prednisolone acetate dose of the patient was reduced to 10 mg qd P-O on 30 August 2019. On 13 August 2019, he felt abdominal distension and the skin on the right lower abdomen showed a band-like tingling sensation accompanied by itching and also decreased appetite, constipation and fatigue. Physical examination: ECOG (Eastern Cooperative Oncology Group) score 1, abdominal swelling, percussion drum sounds, pinpoint papules in the right lower abdomen, slightly higher local skin temperature and the lower limbs without swollen. On 16 August 2019, the dermatologist diagnosed this illness as "herpes zoster". The patient was treated with antiviral, analgesic, and vitamin supplementation. At the same time, glucocorticoids were suspended. Liver function is under close follow-up. The herpes subsided a week later, but the pain persisted and was treated with analgesics. With follow-up CT on 30 September 2019, the tumor assessment is still SD. Chest CT showed that there were new nodules on the lateral edge of the right lung, possibly inflammatory (**Figure 3**). The blood T-SPOT was positive, and CT-guided puncture of the right lung nodule was performed on 8 October 8 2019. Postoperative pathology showed granulomatous lesions with coagulative necrosis. Acid-fast staining showed 2 positive bacteria, so mycobacteria could not be excluded. But the PCR test result was negative. Considering that the patient still has grade 2 immune liver damage (ALT/γ-GT 156/323 U/L, AST in normal range), amikacin 0.6 g qd vgtt + levofloxacin 0.4 g qd PO + ethamidine alcohol 0.75 g qd PO will be given from 11 October 2019.

We plotted the patient timeline to summary the entire treatment (**Figure 4**).

DISCUSSION

The binding of CTLA-4, PD-1 ligand and its receptor plays an important role in the suppression of the immune system. Ipilimumab is a monoclonal antibody that targets the CTLA-4 receptor and prevents its interaction with CD80/CD86 (4). Inhibition of CTLA-4 receptors has been proven to enhance the activation and proliferation of T cells, while also reducing the function of T-reg cells so that the immune system can better dominate the tumor (4). Otherwise, nivolumab is a monoclonal antibody directed at blocking the PD-1 receptor. The mechanism is to combine competitively with PD-1 ligands such as PD-L1 and PD-L2 to liberate the immune response suppressed by the PD-1 pathway (5). Nivolumab has been proven to enhance the anti-tumor effect of the immune system and reduce the tumor growth (5). Nivolumab combined with ipilimumab could cause stronger T cell activation and anti-tumor effects in certain cancer types than single therapy. However, the risk of adverse reactions of combination therapy is also greater than that of single-agent therapy (6).

Immune-related hepatitis and hypophysitis are two common adverse reactions caused by immune checkpoint inhibitors. The case discussed in this article was diagnosed by doing specific work-up to investigate the cause of liver injury including autoantibodies, serum gammaglobulin levels as same as these reporters described (7, 8). However, its occurrence is particularity due to the simultaneous onset of two immune-related adverse reactions and the recurrence of viral infection after hormone therapy. Similar cases have not been reported according to the results of the literature search. The 2019 National Cancer Comprehensive Network (NCCN) guidelines

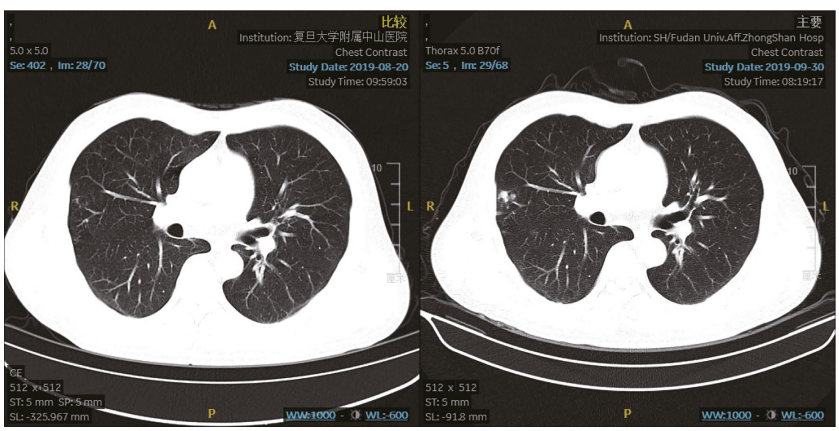

FIGURE 3 | Chest computed tomography scan. The chest computed tomography lung window (left picture 20 August 2019; right picture 30 September 2019) shows new nodules on the lateral edge of the right lung, which may suggest inflammatory.

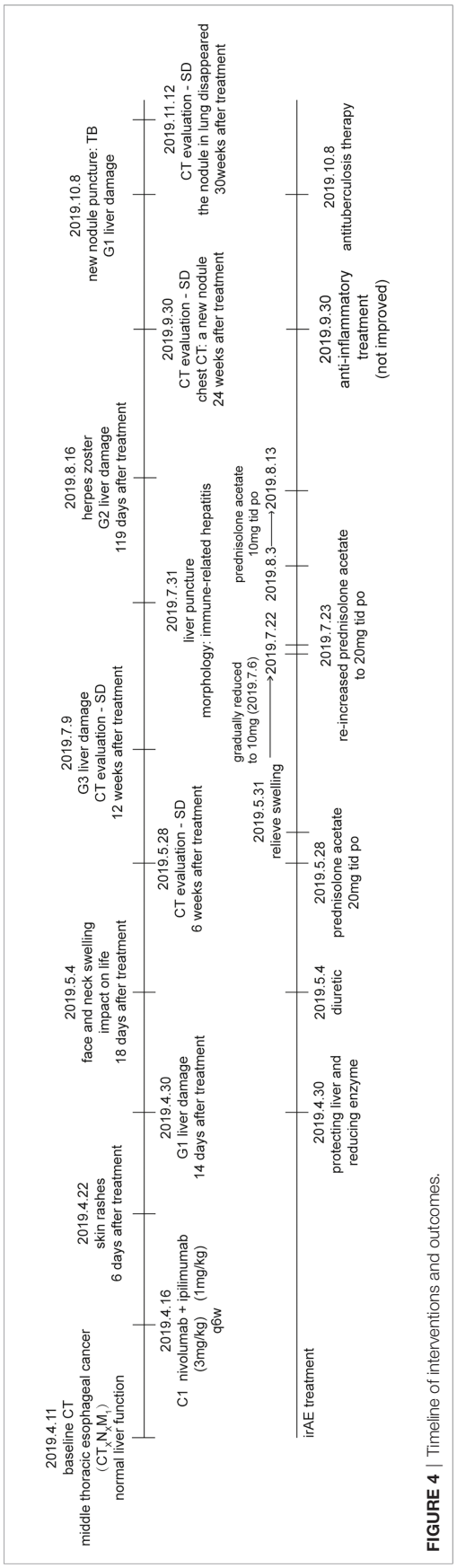

FIGURE 4 | Timeline of interventions and outcomes.

on immunotherapy-related toxicity management still proposed that glucocorticoids are the preference for the treatment of immune-related adverse reactions. In the treatment of pituitary inflammation caused by immune checkpoint inhibitors, if the patient has related symptoms, hormonal replacement therapy should be used. However, when neurological symptoms such as visual disturbances are present, high doses of glucocorticoids should be used and immunotherapy should be suspended until the acute symptoms of the patient are eliminated (1, 9). Also, another report described that the early treatment of high-dose glucocorticoid for irAE is associated with poorer prognosis in advanced melanoma (10). So, it is important to measure the state of disease and give the correct treatment strategy.

Correspondingly, in the treatment of hepatitis caused by immune checkpoint inhibitors, the NCCN guidelines also pointed out that glucocorticoids are the most common treatment option, but the specific dosage is not mentioned in the guidelines. A recent study showed that in the treatment of hepatitis caused by immune checkpoint inhibitors, customized therapy based on the own condition of the patient may be more effective than systemic treatment with glucocorticoids (10). When diagnosing hepatitis caused by immune checkpoint inhibitors, it is usually difficult to distinguish it from immune hepatitis based on the symptoms and signs of the patient, but histological and imaging results could help to do it (11, 12). A recent study summarized the histological characteristics of hepatitis caused by CTLA-4 inhibitors and PD-1 inhibitors. This information is helpful for doctors to find out the specific drugs that cause adverse reactions when immune checkpoint inhibitors combination, so that the treatment becomes more specific (13).

The results of the CheckMate 648 clinical study have been published in the New England Journal of Medicine since February 2022. Although the study was not designed to compare the efficacy between nivolumab plus ipilimumab and nivolumab plus chemotherapy, we could also find that the treatment with nivolumab plus ipilimumab provided better survival benefits for patients and the rate of adverse events did not increase significantly. In addition, treatment with nivolumab plus ipilimumab resulted in a longer median duration of response (11.8 months) than treatment with nivolumab plus chemotherapy (8.2 months) or chemotherapy alone (5.7 months). Nivolumab plus ipilimumab therapy may offer a new option for advanced esophageal squamous-cell carcinoma patients (14). Therefore, it is particularly important to carry out reasonable management and treatment for the possible side effects of immunotherapy combination.

In the case discussed in this article, the resurgence of tuberculosis and the onset of herpes zoster occurred three months after the patient received prednisolone treatment. Based on the past medical history of tuberculosis of the patient, the recurrence of tuberculosis after receiving long-term glucocorticoid therapy is expected. However, the patient has not previously reported any history of varicella infection or close contact with varicella-infected patients, so we did not expect the resurgence of herpes zoster virus during the treatment. This case emphasizes the importance of comprehensive collection of the past medical history upon admission of the patient. In addition,

multiple case reports mentioned that patients treated with PD-1 inhibitors are at risk of developing tuberculosis infection (15–17). Therefore, physicians should be vigilant about possible opportunistic infections when using immunotherapy, regardless of whether the patient has a history of previous infections.

Furthermore, it is important to study the mechanism of irAE. T cells, B cells and antigen presenting cells (APCs) are all enrolled in the occurrence of irAE (18). Otherwise, Tregs are also the important subgroup for the balance of immune function. The inhibition of Tregs may contribute to the irAE (18, 19). The discussion of the mechanism could help researchers find a new way to avoid the occurrence of irAE.

CONCLUSION

Combination therapy with CTLA-4 and PD-1 immune checkpoint inhibitors has a higher risk of adverse reactions than monotherapy. Patients who develop multiple adverse reactions to immunotherapy at the same time usually receive higher doses and longer courses of glucocorticoid therapy, which greatly increases the risk of complications such as the resurgence of the virus in this case. The current guidelines lack information on the adverse reactions of multiple immune treatment and complications caused by the treatment of their adverse reactions. This case emphasizes the importance of early diagnosis and intervention in patients with multiple immune-related adverse reactions. It opens a window for subsequent studies on immune-related adverse reactions and complications. Follow-up research is essential for the systematic management of multiple immune-related adverse reactions.

DATA AVAILABILITY STATEMENT

The raw data supporting the conclusions of this article will be made available by the authors, without undue reservation.

ETHICS STATEMENT

The studies involving human participants were reviewed and approved by the Ethics Committee of Zhongshan Hospital, Fudan University. The patients/participants provided their written informed consent to participate in this study. Written informed consent was obtained from the individual(s) for the publication of any potentially identifiable images or data included in this article.

AUTHOR CONTRIBUTIONS

YF participates in all aspects of the center's research as Sub-I and is familiar with the screening, treatment, efficacy, adverse reactions and outcomes of each selected patient. YF also wrote this manuscript. CL is a doctor of pharmacy. He gave professional opinions and analysis of possible causes in pharmacy on the multiple immune-related adverse reactions that occurred after the patient's dual-immune treatment. YJ is a pathologist in our hospital, specializing in pathological genetic diagnosis and pathological manifestations of adverse immune reactions, providing a very professional analysis for the patient's pathological diagnosis. YL is a CRC in our center, assisting my work and follows up the patient for a long time after drug withdrawal. Both doctors LG and YY gave me a lot of assistance during the diagnosis and treatment of the patient during the hospitalization after the occurrence of irAE. As the PI of the branch center, the corresponding author, TL gave me the most professional guidance and help during the entire research process and controlled the progress of the entire research project in our center. All authors listed have made a substantial, direct, and intellectual contribution to the work and approved it for publication.

SUPPLEMENTARY MATERIAL

The Supplementary Material for this article can be found online at: https://www.frontiersin.org/articles/10.3389/fonc.2022.801924/full#supplementary-material

REFERENCES

1. Thompson JA, Schneider BJ, Brahmer J, Andrews S, Armand P, Bhatia S, et al. Management of Immunotherapy-Related Toxicities, Version 1.2019. *J Natl Compr Canc Netw* (2019) 17(3):255–89. doi: 10.6004/jnccn.2019.0013
2. Darvin P, Toor SM, Sasidharan Nair V, Elkord E. Immune Checkpoint Inhibitors: Recent Progress and Potential Biomarkers. *Exp Mol Med* (2018) 50 (12):1–11. doi: 10.1038/s12276-018-0191-1
3. Khoja L, Day D, Wei-Wu Chen T, Siu LL, Hansen AR. Tumour- and Class-Specific Patterns of Immune-Related Adverse Events of Immune Checkpoint Inhibitors: A Systematic Review. *Ann Oncol* (2017) 28(10):2377–85. doi: 10.1093/annonc/mdx286
4. *YERVOY (Ipilimumab) Injection, for Intravenous Use Initial.* Available at: https://www.accessdata.fda.gov/drugsatfda_docs/label/2018/125377s096lbl.pdf.
5. *HIGHLIGHTS OF PRESCRIBING INFORMATION.* Available at: https://packageinserts.bms.com/pi/pi_opdivo.pdf.
6. Wang DY, Salem JE, Cohen JV, Chandra S, Menzer C, Ye F, et al. Fatal Toxic Effects Associated With Immune Checkpoint Inhibitors: A Systematic Review and Meta-Analysis. *JAMA Oncol* (2018) 4(12):1721–8. doi: 10.1001/jamaoncol.2018.3923
7. Granito A, Muratori P, Ferri S, Pappas G, Quarneti C, Lenzi M, et al. Diagnosis and Therapy of Autoimmune Hepatitis. *Mini Rev Med Chem* (2009) 9(7):847–60. doi: 10.2174/138955709788452676
8. Granito A, Muratori P, Quarneti C, Pappas G, Cicola R, Muratori L. Antinuclear Antibodies as Ancillary Markers in Primary Biliary Cirrhosis. *Expert Rev Mol Diagn* (2012) 12(1):65–74. doi: 10.1586/erm.11.82
9. Stelmachowska-Banaś M, Czajka-Oraniec I. Management of Endocrine Immune-Related Adverse Events of Immune Checkpoint Inhibitors: An Updated Review. *Endocr Connect* (2020) 9(10):R207–28. doi: 10.1530/EC-20-0342
10. De Martin E, Michot JM, Papouin B, Champiat S, Mateus C, Lambotte O, et al. Characterization of Liver Injury Induced by Cancer Immunotherapy Using Immune Checkpoint Inhibitors. *J Hepatol* (2018) 68(6):1181–90. doi: 10.1016/j.jhep.2018.01.033
11. Cramer P, Bresalier RS. Gastrointestinal and Hepatic Complications of Immune Checkpoint Inhibitors. *Curr Gastroenterol Rep* (2017) 19(1):3. doi: 10.1007/s11894-017-0540-6
12. Alessandrino F, Tirumani SH, Krajewski KM, Shinagare AB, Jagannathan JP, Ramaiya NH, et al. Imaging of Hepatic Toxicity of Systemic Therapy in a Tertiary Cancer Centre: Chemotherapy, Haematopoietic Stem Cell Transplantation,

Molecular Targeted Therapies, and Immune Checkpoint Inhibitors. *Clin Radiol* (2017) 72(7):521–33. doi: 10.1016/j.crad.2017.04.003
13. Bai X, Hu J, Betof Warner A, Quach HT, Cann CG, Zhang MZ, et al. Early Use of High-Dose Glucocorticoid for the Management of irAE Is Associated With Poorer Survival in Patients With Advanced Melanoma Treated With Anti-PD-1 Monotherapy. *Clin Cancer Res* (2021) 27(21):5993–6000. doi: 10.1158/1078-0432.CCR-21-1283
14. Doki Y, Ajani JA, Kato K, Xu J, Wyrwicz L, Motoyama S, et al. Nivolumab Combination Therapy in Advanced Esophageal Squamous-Cell Carcinoma. *N Engl J Med* (2022) 386(5):449–62. doi: 10.1056/NEJMoa2111380
15. Takata S, Koh G, Han Y, Yoshida H, Shiroyama T, Takada H, et al. Paradoxical Response in a Patient With non-Small Cell Lung Cancer Who Received Nivolumab Followed by Anti-Mycobacterium Tuberculosis Agents. *J Infect Chemother* (2019) 25(1):54–8. doi: 10.1016/j.jiac.2018.06.016
16. Tsai CC, Chen JH, Wang YC, Chang FY. Re-Activation of Pulmonary Tuberculosis During Anti-Programmed Death-1 (PD-1) Treatment. *QJM* (2019) 112(1):41–2. doi: 10.1093/qjmed/hcy243
17. Mourik BC, Leenen PJ, de Knegt GJ, Huizinga R, van der Eerden BC, Wang J, et al. Immunotherapy Added to Antibiotic Treatment Reduces Relapse of Disease in a Mouse Model of Tuberculosis. *Am J Respir Cell Mol Biol* (2017) 56 (2):233–41. doi: 10.1165/rcmb.2016-0185OC
18. Weinmann SC, Pisetsky DS. Mechanisms of Immune-Related Adverse Events During the Treatment of Cancer With Immune Checkpoint Inhibitors. *Rheumatol (Oxford)* (2019) 58(Suppl 7):vii59–67. doi: 10.1093/rheumatology/kez308
19. Granito A, Muratori L, Lalanne C, Quarneti C, Ferri S, Guidi M, et al. Hepatocellular Carcinoma in Viral and Autoimmune Liver Diseases: Role of CD4+ CD25+ Foxp3+ Regulatory T Cells in the Immune Microenvironment. *World J Gastroenterol* (2021) 27(22):2994–3009. doi: 10.3748/wjg.v27.i22.2994

Conflict of Interest: Author YL is employed by Hangzhou Simo Co., Ltd.

The remaining authors declare that the research was conducted in the absence of any commercial or financial relationships that could be construed as a potential conflict of interest.

Publisher's Note: All claims expressed in this article are solely those of the authors and do not necessarily represent those of their affiliated organizations, or those of the publisher, the editors and the reviewers. Any product that may be evaluated in this article, or claim that may be made by its manufacturer, is not guaranteed or endorsed by the publisher.

Copyright © 2022 Feng, Li, Ji, Liu, Gan, Yu and Liu. This is an open-access article distributed under the terms of the Creative Commons Attribution License (CC BY). The use, distribution or reproduction in other forums is permitted, provided the original author(s) and the copyright owner(s) are credited and that the original publication in this journal is cited, in accordance with accepted academic practice. No use, distribution or reproduction is permitted which does not comply with these terms.

frontiers | Frontiers in Immunology

ORIGINAL RESEARCH
published: 05 April 2022
doi: 10.3389/fimmu.2022.764643

What Is Long-Term Survival and Which First-Line Immunotherapy Brings Long-Term Survival for Advanced Wild-Type Non-Small Cell Lung Cancer: A Network Meta-Analysis Based on Integrated Analysis

*Xue Zhang†, Qian Xu†, Xuejun Yu†, Miao Huang, Song Li, Lei Sheng, Xin Dai, Kai Huang, Jian Wang and Lian Liu**

Department of Medical Oncology, Qilu Hospital, Cheeloo College of Medicine, Shandong University, Jinan, China

OPEN ACCESS

Edited by:
Hubing Shi,
Sichuan University, China

Reviewed by:
Xianding Wang,
Sichuan University, China
Jianxin Xue,
Sichuan University, China

***Correspondence:**
Lian Liu
lianliu@sdu.edu.cn

†These authors have contributed equally to this work and share first authorship

Specialty section:
This article was submitted to Cancer Immunity and Immunotherapy, a section of the journal Frontiers in Immunology

Received: *25 August 2021*
Accepted: *07 March 2022*
Published: *05 April 2022*

Citation:
Zhang X, Xu Q, Yu X, Huang M, Li S, Sheng L, Dai X, Huang K, Wang J and Liu L (2022) What Is Long-Term Survival and Which First-Line Immunotherapy Brings Long-Term Survival for Advanced Wild-Type Non-Small Cell Lung Cancer: A Network Meta-Analysis Based on Integrated Analysis. Front. Immunol. 13:764643. doi: 10.3389/fimmu.2022.764643

Background: Immune checkpoint inhibitors (ICIs) have significantly improved survival for advanced wild-type non-small cell lung cancer, but there is no direct comparison to confirm which first-line treatment may lead to the longest overall survival. What qualifies as long-term survival (LS) is even unclear.

Methods: By searching PubMed, Embase, and the Cochrane Central Register of Controlled Trials from January 2005 to December 2020, we included randomized controlled trials (RCTs) of first-line ICI-containing treatments to perform an integrated analysis (IA) to determine the criterion of LS and then screened regimens with LS for network meta-analysis (NMA). The main outcomes for NMA were median overall survival (mOS), 1-year survival rate (1ySR), and 2-year survival rate (2ySR); those for IA were the pooled mOS (POS), 1ySR (P1SR), and 2ySR (P2SR).

Results: By IA of 16 first-line ICIs from 20 RCTs, the POS was 16.20 (95% CI 14.79–17.60) months, with P1SR of 63% (95% CI 59–66%) and P2SR of 37% (33–41%). Thus, we defined LS as mOS ≥ POS (16.20 m) for regimens and screened for RCTs with outcomes meeting this criterion. Eleven ICI-based regimens can bring LS for the overall population, among which ICI with bevacizumab and chemotherapy achieved the longest POS of 19.50 m (16.90–22.10 m) and the highest P1SR (74%, 61%–87%) and P2SR (49%, 38%–61%). Pembrolizumab with chemotherapy ranked first in mOS and 1ySR, while atezolizumab plus bevacizumab and chemotherapy ranked first in 2ySR.

Conclusions: Through the IA of first-line treatment regimens, a POS of 16.20 m can be determined as the LS standard. Further considering 1ySR and 2ySR, atezolizumab combined with bevacizumab and chemotherapy or pembrolizumab plus chemotherapy

are likely to bring the longest LS in the overall population, while single ICI may be adequate for patients with a high PD-L1 expression. ICIs with bevacizumab and chemotherapy may be the best combination for LS for its further advantage over time.

Keywords: long-term survival, first-line, immunotherapy, non-small cell lung cancer, network meta-analysis, integrated analysis

INTRODUCTION

In recent years, the development and application of immune checkpoint inhibitors (ICIs), including programmed cell death protein 1 (PD-1) antibody, programmed death ligand 1 (PD-L1) antibody, and cytotoxic T-lymphocyte-associated protein 4 (CTLA-4) antibody, have provided significant survival benefits for patients with wild-type advanced NSCLC. In the successful randomized controlled trials (RCTs), such as KEYNOTE189 (1), KEYNOTE407 (2), IMpower110 (3), IMpower130 (4), IMpower132 (5), and CheckMate227 (6, 7), immuno-related therapy can prolong the mOS of advanced wild-type NSCLC to 17~22 months. The 5-year survival rate in the KEYNOTE024 study with PD-L1 ≥50% NSCLC increased to 31.9% in the PEM monotherapy group (8). The unprecedented long-term survivals of patients with immunotherapy are determined by the characteristics of the immune response process. Tumor cells recognized and killed by activated T lymphocytes will further release antigens to activate more T lymphocytes, thus forming a positive cycle of the self-activation process, during which immune memory cells are also generated (9). The positive feedback promotes the immune-active T cells to function for a long time, thus bringing a longer survival to these patients.

At present, it is widely accepted that immunotherapy can bring long-term survival to patients with advanced wild-type NSCLC. In fact, large differences existed in OS among different ICIs [11.2 (10) ~26.3 months (8)]. Therefore, we can hardly judge how long in general the first-line immuno-related treatment can bring to advanced NSCLC patients. Neither do we know whether there is a difference in efficacy among the treatments that have achieved significant OS benefits and are recommended by kinds of guidelines, or in other words, which regimen can lead to the longest survival. In fact, for immunotherapy, how to define long-term survival (LS) is an open question.

In order to answer these questions, we conducted an integrated analysis of the survival outcomes of RCTs on first-line immuno-related therapies. Pooled median OS (POS) was taken as the cutoff value for LS to screen the treatment regimens that can bring LS. Then, a network meta-analysis (NMA) based on the Bayesian model was performed to compare and rank these treatment regimens with LS according to mOS, 1-year survival rate (1ySR), 2-year survival rate (2ySR), and other efficacy and adverse effects (AEs) in the general population and special population. Our goal was to provide valuable information for clinicians looking for the best first-line treatment for patients with advanced driver gene-negative NSCLC.

MATERIALS AND METHODS

This NMA was performed in accordance with the PRISMA extension statement for NMA (**Supplementary Table 1**) (11). The research was registered with PROSPERO (CRD42020184534).

Data Sources and Searches

PubMed, Embase, the Cochrane Central Register of Controlled Trials, and ClinicalTrials.gov databases were searched to find relevant articles from January 2005 to December 2020. Abstracts on NSCLC from several important international conferences (American Society of Clinical Oncology, ESMO, and World Conference on Lung Cancer) from 2015 to 2020 were inspected to identify potentially relevant studies. For an outcome in the same trial, only the most recent data were kept. The detailed search strategy is shown in **Supplementary Table 2**.

Eligibility Criteria

We included published phase II/III RCTs reported in English. The mOS integrated analysis enrolled previously untreated patients with advanced (stage III/IV or recurrent) histologically confirmed wild-type NSCLC, treated with ICI-containing regimens, and the mOS or 1- or 2-year survival rate with a 95% confidence interval (CI) was available. According to the POS criteria, RCTs meeting the needs of LS were screened for NMA analysis. mOS of subgroups such as high PD-L1 expression or tumor mutation burden (TMB) that met the LS criteria was included in subgroup analysis. Large RCTs with chemotherapy (CT) combined with anti-angiogenesis therapy (AA) were included in the network as controls. Exclusion criteria included targeted therapy for advanced NSCLC with positive driver genes, trials including radiotherapy, cell therapy, vaccine, heat shock protein, and other non-ICI-related therapy.

Data Extraction and Risk-of-Bias Assessment

The bias risk of included trials was assessed using the Cochrane risk-of-bias tool, consisting of random sequence generation, allocation concealment, blinding of participants and personnel, blinding of outcome assessment, incomplete outcome data, selective outcome reporting, and other sources of bias (12) (**Supplementary Figure 1**). We extracted detailed clinical trial data (e.g., study ID, first author, year of publication, number of patients, patient characteristics), treatments, and outcomes into a spreadsheet. Data extraction and quality assessment were conducted independently by the two authors (ZX and XQ), and any differences were resolved through discussion and negotiation.

Data Synthesis and Analysis

First, the mOS of first-line immuno-related therapy in advanced wild-type NSCLC was analyzed using STATA 16.0 to determine LS criteria. We also pooled the 1ySR and 2ySR using STATA 16.0 (13). For PFS and OS in NMA, the hazard ratio (HR) and its 95% creditable intervals (CrIs) were calculated, while for binary variables, such as 1ySR and 2ySR, 1-year progression-free survival rate (1yPR), overall response rate (ORR), ≥3 AEs, odds ratio (OR) and 95% CrIs were calculated. For some indexes, some of the studies (5 (14–18) of 15 for the 1-year OS rate, 5 (3, 7, 14–16) of 13 for the 2-year OS rate, 6 (3, 14–17, 19) of 14 for the 1-year PFS rate) did not provide ORs for which we got them from the Kaplan–Meier curve and calculated them by STATA 16.0. All network evidence maps were obtained by STATA16.0 (20). The NMA was performed in a Bayesian framework using a Markov chain Monte Carlo simulation technique within the GEMTC package in the R-Statistics and the J.A.G.S. program. We used non-informative uniform and normal prior distributions to fit the model, with four different sets of initial values. For each outcome, 150,000 sample iterations were generated with 100,000 burn-ins and a thinning interval of 1 except for ORR and ≥3 AEs, for which we increased the thinning interval to 10 to minimize auto-correlation. The convergence of the model is evaluated by a diagnostic convergence graph and a trace density graph (21). Fixed- and random-effect models were considered and compared using deviance information criteria (DIC). If the DIC difference between the random model and the fixed model was less than 5, the fixed model was selected. A direct and indirect comparison of inconsistency analysis was verified by DIC and node analysis (22). Preferred probability ranking was obtained from the surface under the cumulative ranking curve (SUCRA). The line charts for the rankings were produced using GraphPad Prism 8.

RESULTS

Qualified Studies for Integrated Analysis

In the integrated analysis of the available mOS and survival rates of first-line immuno-related treatments in patients with advanced driver gene-negative NSCLC, a total of 20 qualified RCTs were included (**Figure 1**), involving 7,462 patients and 16 treatment regimens, including single ICIs such as pembrolizumab (PEM) (8, 18), atezolizumab (ATE) (3), nivolumab (NIV) (23), durvalumab (DUR) (10), and cemiplimab (CEM) (24); dual ICIs such as ipilimumab (IPI) combined with NIV (NIV+IPI) (6) and tremelimumab (TRE) combined with DUR (DUR+TRE) (10); ICIs combined with CT such as PEM+CT (1, 2, 19), ATE+CT (4, 5, 25, 26), NIV+CT (7), IPI+CT (27, 28), camrelizumab (CAM) combined with CT (CAM+CT) (17), NIV+IPI+CT (29), and DUR +TRE+CT (16); and ICIs combined with AA and CT, such as ATE combined with bevacizumab (BEV) and CT (ATE+BEV+CT) (26), and NIV+BEV+CT (30) (**Supplementary Table 3**).

Integrated Analysis

First, we integrated the available mOS of 13 first-line immuno-related treatments in wild-type patients (**Figure 2A**) and found that POS was 16.20 (95% CI 14.79~17.60) months. Therefore, we set mOS over 16.20 months as the standard for LS for immunotherapy. In the ITT population, there were 11 treatments that met the criteria for long-term survival (**Figure 3**), most of which were ICIs combined with CT and/or AA, including PEM+CT, NIV+CT, ATE+CT, CAM+CT, DUR+TRE+CT, ATE+BEV+CT, and NIV+BEV+CT, and single ICI (PEM, ATE) and dual ICIs (NIV+IPI, DUR+ TRE) (**Supplementary Table 4**). In subgroups with PD-L1 ≥50%, treatments leading to LS included single ICIs (CEM, PEM, ATE, DUR, NIV), ICIs combined with CT (PEM+CT, ATE+CT), and dual ICIs (NIV+IPI) or in combination of CT (NIV+IPI+CT) (**Supplementary Table 5**). Among the TMB-high subgroups, single ICIs (PEM, NIV, ATE, DUR) or immune combination regimens (PEM+CT, NIV+IPI, TRE+DUR, DUR+TRE+CT) can bring LS.

Among the various treatment strategies, ICIs+BEV+CT led to the longest POS (19.50, 16.90~22.10 months), followed by single ICIs+CT (16.82, 14.71~18.93 months) and dual ICIs+CT (16.07 months, 13.84~18.29). Single ICIs (15.41 months, 12.73~18.09) and dual ICIs (14.08 months, 10.00~18.15) had the shortest POS (**Figure 2A**). Comparing the different ICI targets, the anti-PD-1-containing regimens had a maximum POS of 18.00 (15.52~20.48) months, followed by the anti-PD-L1 regimens of 17.23 (15.17~19.30) months. Comparing different ICIs, the regimens containing PEM had the longest POS of 19.09 (15.69~22.48) months, while the IPI-containing regimens had the shortest POS of 13.10 (11.80~14.39) months (**Supplementary Table 6**).

In the integrated analysis of 1ySR, a total of 20 RCTs were included, involving 16 regimens, including single ICIs [PEM (8, 18), ATE (3), CEM (24), NIV (23), DUR (10)], dual ICIs [NIV+IPI (6), DUR+TRE (10)], ICIs+CT [PEM+CT (1, 2, 19), ATE+CT (4, 5, 25, 26), NIV+CT (7), CAM+CT (17), IPI+CT (27, 28), NIV+IPI+CT (29), DUR+TRE+CT (16)], and ICIs+BEV+CT [NIV+BEV+CT (30), ATE+BEV+CT (26)]. The P1SR was 0.63 (0.59~0.66). Among them, the P1SR of single ICIs, dual ICIs, single ICIs+CT, dual ICIs+CT, and ICIs+BEV+CT were 0.60 (0.54~0.67), 0.55 (0.45~0.65), 0.64 (0.60~0.68), 0.62 (0.58~0.66), and 0.74 (0.67~0.87), respectively (**Figure 2B**). In the integrated analysis of 19 RCTs with LS (1–8, 10, 16, 18, 19, 23–30), we found the P2SR to be 0.37 (0.33~0.41). ICIs+BEV+CT brought the highest P2SR (0.49, 0.38~0.61), and single ICIs, dual ICIs, single ICIs+CT, and dual ICIs+CT got 0.38 (0.30~0.46), 0.35 (0.25~0.45), 0.36 (0.30~0.42), and 0.33 (0.17~0.49), respectively (**Figure 2C**).

In terms of pathological types, non-squamous cell lung carcinoma had a POS of 19.32 (18.12~20.51) months in first-line ICIs regimens, longer than that of 15.13 (13.39~16.88) months in squamous cell lung carcinoma patients. The P1SR and P2SR were 0.69 (0.64~0.73) and 0.44 (0.37~0.50) in the non-squamous group, and 0.60 (0.55~0.66) and 0.33 (0.27~0.38) in the squamous subgroup, respectively (**Supplementary Figures 2A, B**).

In the population with PD-L1 ≥50%, the P1SR and P2SR induced by the first-line immunotherapy were 0.67 (0.65~0.69)

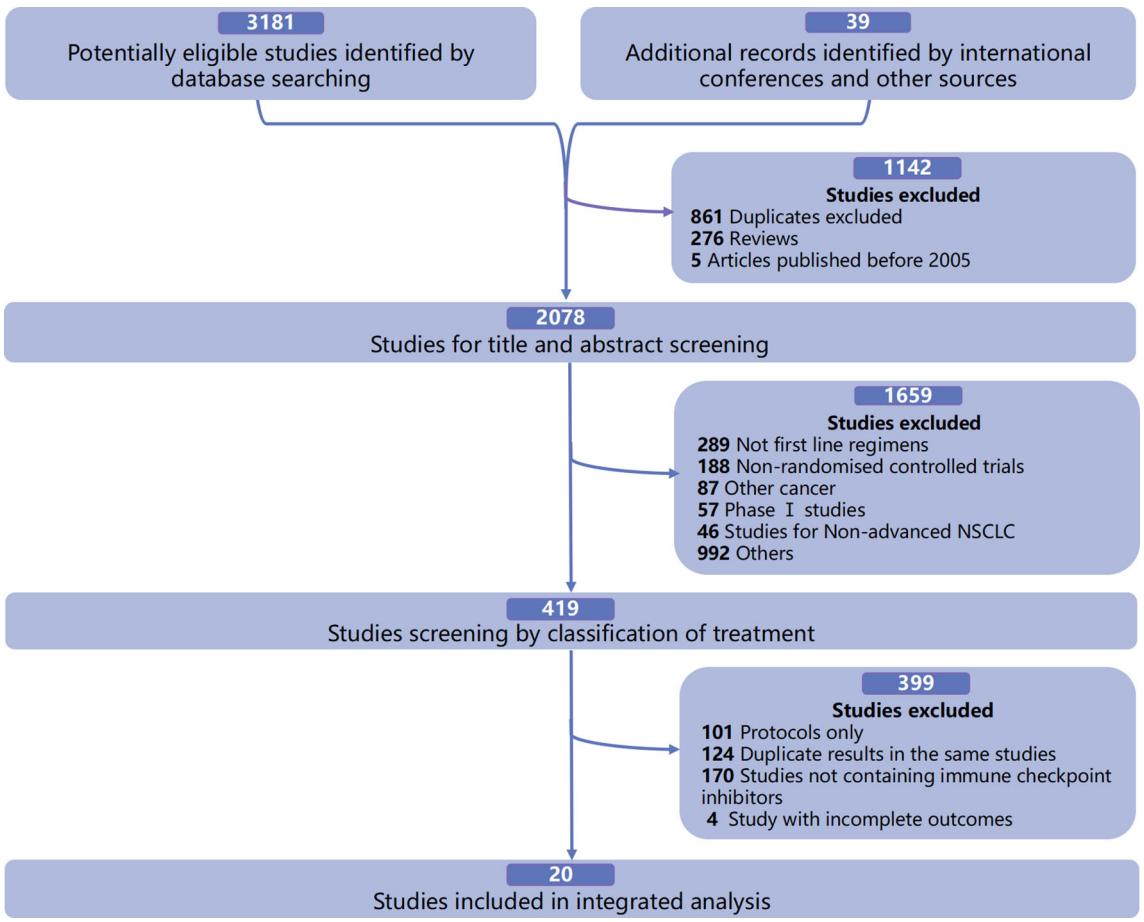

FIGURE 1 | Study selection.

and 0.46 (0.44~0.48), respectively (**Supplementary Figure 2C**). When comparing regimens, similar to the ITT population, the combination of single ICIs with AA and CT seemed to bring the highest P1SR (0.75,0.65~0.85) and P2SR (0.56, 0.45~0.67). The P2SR was similar between the single ICIs (0.47, 0.44~0.50) and the dual ICIs (0.48, 0.41~0.55). Moreover, the addition of CT to single ICIs or dual ICIs failed to improve the P2SR over ICIs alone (**Supplementary Table 6**).

NMA for the ITT Population

An assessment of the risk bias in the included studies is shown in **Supplementary Figure S2**. It should be noted that some treatment options that only met the LS criteria in the corresponding subgroup were included in the subgroup analysis. For example, NIV+IPI+CT of CheckMate 9LA was only included in the subgroup analysis for PD-L1 ≥50% (29), while BEV+CT and CT alone were included as controls in NMA (14, 15).

Among the treatments that resulted in an LS of 16.20 months or more for the all-comer population (**Figure 3**), PEM+CT (relative to CT: 0.62, 0.54~0.72) ranked first in mOS, followed by ATE+BEV+CT (0.71, 0.56~0.90), and the third is the NIV+IPI (0.73, 0.64~0.84) (**Figures 4A**, **5**, and **Supplementary Figure 3**). Almost all immuno-related therapies significantly prolonged OS compared with CT, and the OS of PEM+CT was prolonged significantly compared to NIV+CT (0.77, 0.61~0.97) and ATE+CT (0.79, 0.65~0.96) (**Figure 6A**). In terms of median progression-free survival (mPFS), the top three rankings of SUCRA cumulative probability were NIV+BEV+CT, ATE+BEV+CT, and PEM+CT(**Figure 5** and **Supplementary Figure 3**). Both ATE+BEV+CT and NIV+BEV+CT regimens were significantly superior to any other regimens in mPFS, and all regimens yielded greater benefits than CT alone. However, there was no significant difference between ATE+BEV+CT and NIV+BEV+CT in both OS and PFS (**Figure 6A**).

In terms of 1ySR, PEM+CT ranked first, followed by NIV+CT and ATE+BEV+CT according to SUCRA cumulative probability (**Figures 4B**, **5**, and **Supplementary Figure 3**). The 1ySR of PEM +CT was improved significantly compared to ATE+CT (OR 1.57, 1.15~2.15) and NIV+IPI (1.53, 1.10~2.12). Except for ATE, CAM+CT, and NIV+BEV+CT, almost all immuno-related treatments have significantly improved 1ySR compared to CT

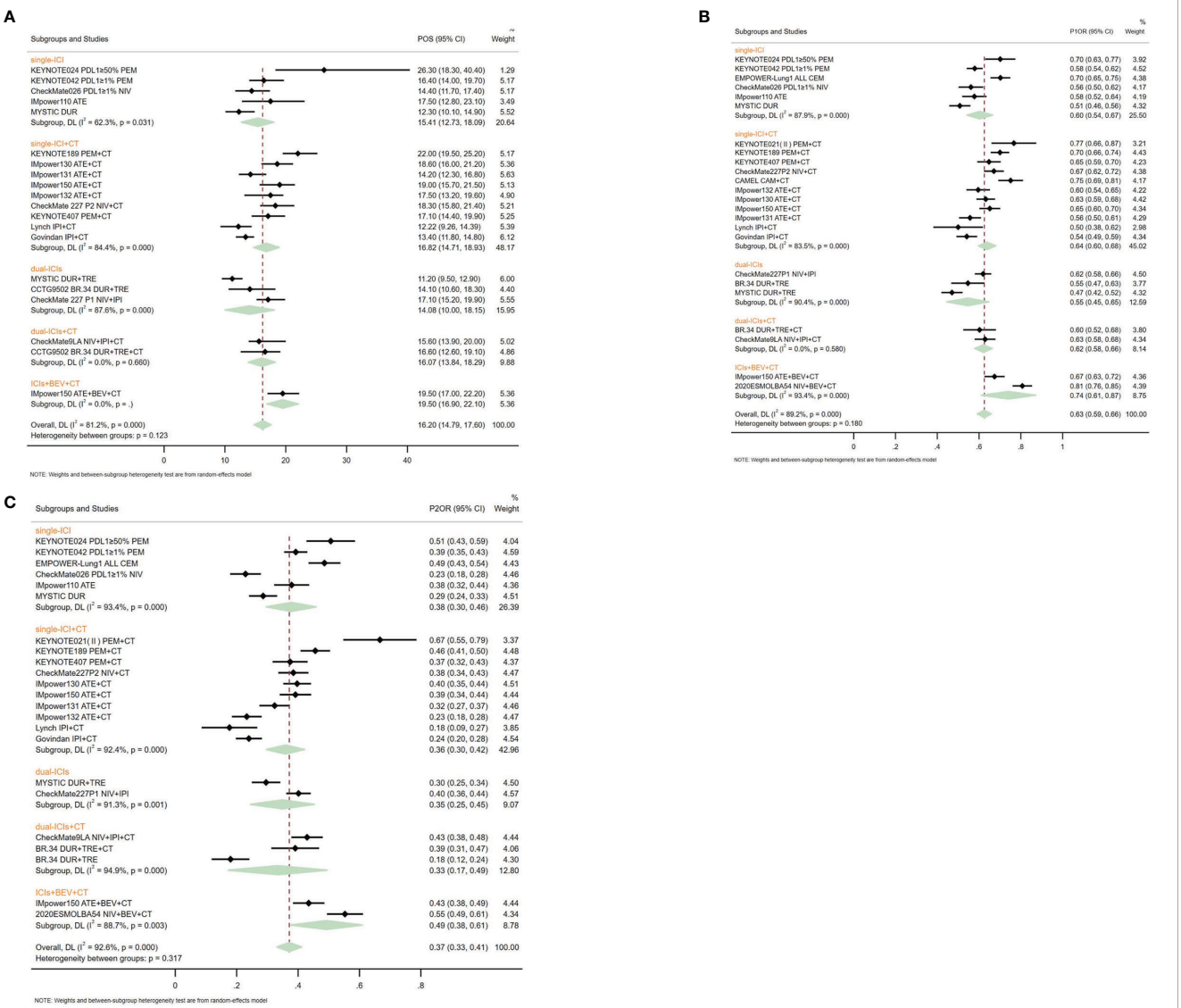

FIGURE 2 | Pooled survival outcomes from integrated analysis of median overall survival **(A)**, 1-year survival rate **(B)**, and 2-year survival rate **(C)** of different therapy strategies containing immune checkpoint inhibitors in patients with advanced wild-type non-small cell lung cancer.

alone (**Figure 6B**). For 1yPR, PEM+CT, ATE+CT, ATE+BEV+CT, NIV+BEV+CT, and BEV+CT were significantly higher than that of CT (**Supplementary Figure 4**).

In terms of 2ySR, the top three cumulative probabilities of SUCRA were ATE+BEV+CT (versus CT: 1.80, 1.29~2.52), PEM+CT (1.79, 1.41~2.27), and PEM (1.67, 1.32~2.11). Moreover, 2ySR of NIV+IPI (1.55, 1.22~1.98) and ATE+CT (1.46, 1.17~1.81) also increased significantly in contrast to CT (**Figures 5**, **6B** and **Supplementary Figure 3**). It is worth noting that the 2ySR (1.45, 1.08~1.95) of ATE+BEV+CT was significantly higher compared with BEV+CT, although the 1ySR (1.29, 0.96~1.75) of ATE+BEV+CT was improved without significance (**Figure 6B**).

In terms of ORR, all regimens demonstrated significant benefits compared to CT. Of these, ATE+BEV+CT, NIV+BEV+CT, and PEM+CT ranked top three according to SUCRA (**Figure 5** and **Supplementary Figure 3**). ATE showed the lowest rates of ≥3 AEs among all regimens, and ≥3 AEs in ATE+BEV+CT were higher than those in any other treatments except CAM+CT and NIV+BEV+CT (**Figure 6C**).

NMA for Subgroups

Different from the LS treatments in the ITT population, dual ICIs combined with CT (NIV+IPI+CT) were also included in the subgroup with PD-L1 ≥50%, in addition to single ICIs and ICIs combined with CT (PEM+CT, ATE+CT; **Supplementary**

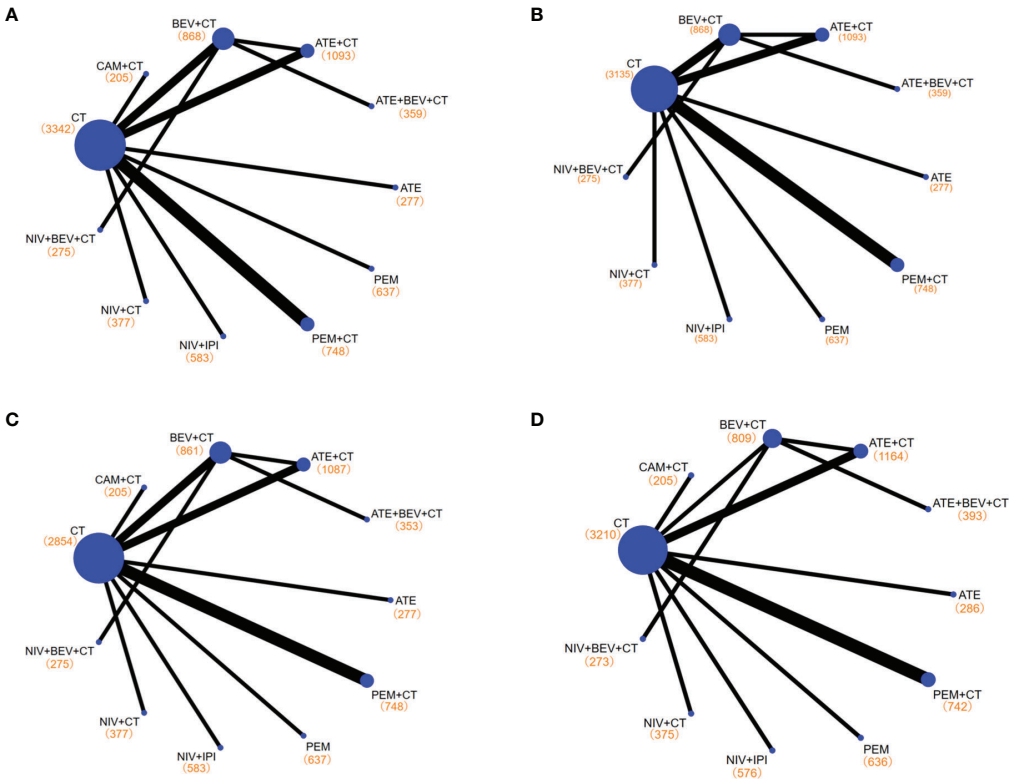

FIGURE 3 | Network diagrams of comparisons on different outcomes of treatments with long-term survival time in patients with advanced wild-type non-small cell lung cancer. **(A)** Comparisons on overall survival (OS) and progression-free survival (PFS) and 1-year survival rate and 1-year PFS rate. **(B)** Comparisons on 2-year survival rate. **(C)** Comparisons on objective response rate (ORR). **(D)** Comparisons on adverse events of grade 3 or higher (≥3 AEs). Each circular node represents a type of treatment. Each line represents a type of head-to-head comparison. The size of the nodes and the thickness of the lines are weighted according to the number of studies evaluating each treatment and direct comparison, respectively. The total number of patients receiving a treatment is shown in brackets. PEM, pembrolizumab; ATE, atezolizumab; NIV, nivolumab; CAM, camrelizumab; BEV, bevacizumab; CEM, cemiplimab; CT, chemotherapy.

Figures 5A–C). All ICI-related regimens except DUR significantly improved OS compared to CT alone but showed no significant difference between them (**Supplementary Figure 6A**). In terms of SUCRA ranking and line chart ranking of mOS, CEM, PEM+CT, and ATE ranked top three (**Supplementary Figures 3**, **7**). In terms of 1ySR, almost all ICI-related treatments were significantly better than CT, the best of which was PEM+CT (versus CT: HR 2.95, 1.62~5.44), followed by CEM (2.25, 1.59~3.21) and NIV+IPI+CT (2.23, 1.21~4.18). For 2ySR, CEM (relative to CT: OR 2.75, 1.94~3.93), ATE (2.54, 1.40~4.71), and PEM (1.96, 1.49~2.57) ranked top three, and almost all ICI-related measures were significantly improved compared to CT (**Supplementary Figures 3** and **6B**).

In patients with high bTMB or tTMB (**Supplementary Figures 5D, E**), the treatment options that led to LS were PEM, NIV+IPI, PEM+CT, DUR+TRE, and DUR+TRE+CT. PEM (0.62, 0.48~0.80), NIV+IPI (0.68, 0.51~0.91), and PEM+CT (0.70, 0.52~0.96) ranked the top three in SUCRA cumulative probability rankings and line chart (**Supplementary Figures 3** and **6D**).

In the non-squamous subgroup, the regimens meeting the LS criteria included ICIs+CT (PEM+CT, ATE+CT, CAM+CT), dual ICIs (NIV+IPI), and ICIs combined with AA and CT (ATE+BEV+CT; **Supplementary Figures 5F, G**). For mOS, the SUCRA value of PEM+CT ranked the first, whose mOS was significantly improved compared to ATE+CT (0.71, 0.56~0.89), NIV+IPI (0.71, 0.55~0.91), and NIV+CT (0.65, 0.49~0.87), but without significant difference with ATE+BEV+CT (0.79, 0.58~1.08). ATE+BEV+CT and NIV+BEV+CT were superior to any other regimens in PFS, but no significant difference was found in OS and PFS between the two regimens (**Supplementary Figures 3** and **6E**).

Due to the limited data available of the non-highly selected population in the squamous subgroup, only PEM+CT and NIV+CT from KEYNOTE 407 (2) and CheckMate227-Part2 (7) studies were included. Both NIV+CT and PEM+CT significantly improved OS and PFS compared to CT in patients with squamous cell carcinoma (**Supplementary Figure 6F**).

Consistency and Inconsistency Assessment

The density and trace diagram prove that our NMA results are stable and reliable (**Supplementary Figure 8**). According to DIC analysis, after choosing a random or fixed model, the difference between the DIC of the consistency and inconsistency models is within 5, and the consistency model is selected (**Supplementary**

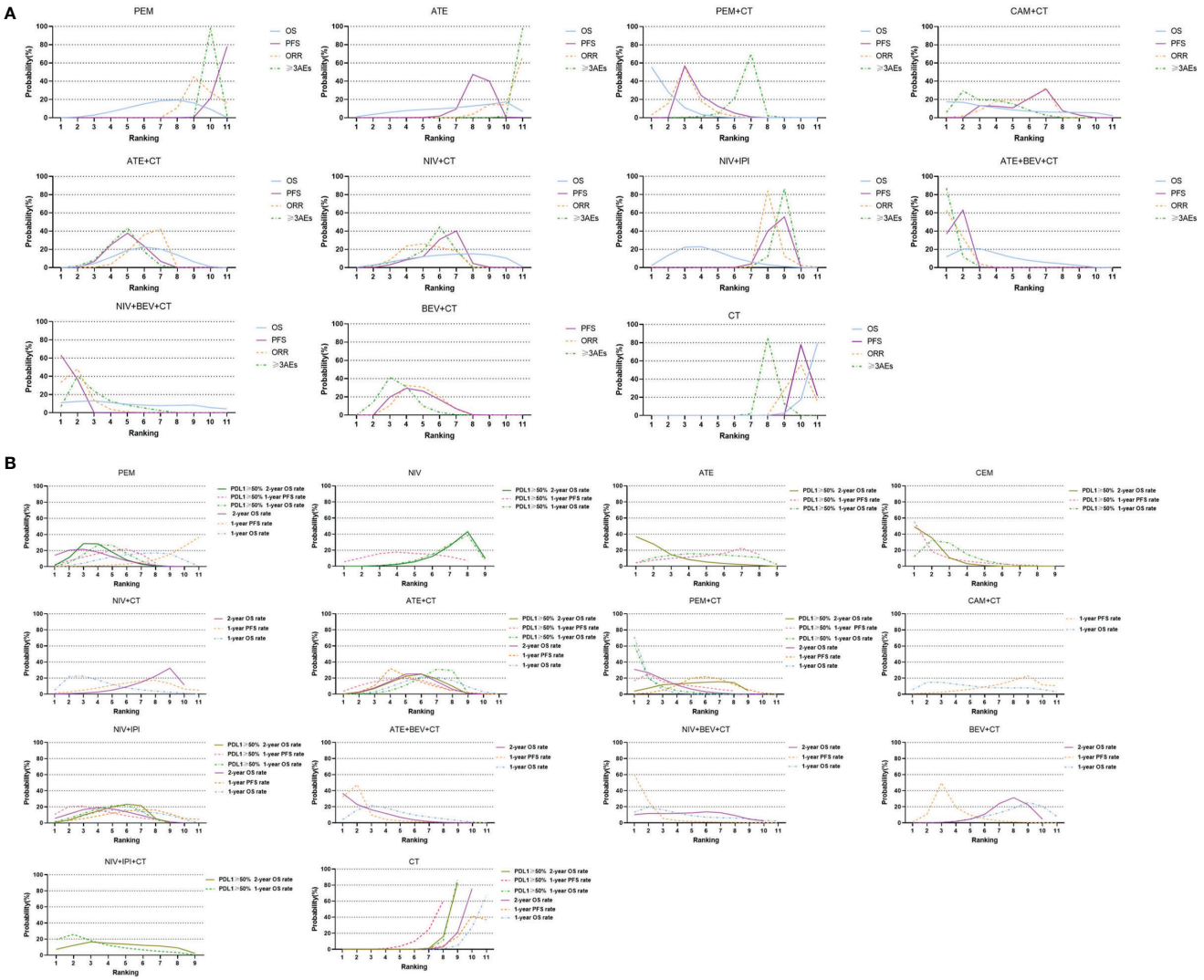

FIGURE 4 | Bayesian ranking profiles of comparable treatments with long-term survival on efficacy and safety for patients with advanced NSCLC. **(A)** Profiles indicate the probability of each comparable treatment being ranked from first to last on overall survival (OS), progression-free survival (PFS), objective response rate (ORR), and grade 3 or higher adverse events (≥3 AEs). **(B)** Profiles indicate the probability of each comparable treatment being ranked from first to last on 1-year survival rate and 1-year PFS rate and 2-year survival rate in the overall population, and 1-year survival rate and 1-year PFS rate and 2-year survival rate in patients with high PD-L1 subgroups. PEM, pembrolizumab; ATE, atezolizumab; NIV, nivolumab; DUR, durvalumab; TRE, tremelimumab; IPI, ipilimumab; CAM, camrelizumab; CEM, cemiplimab; BEV, bevacizumab; CT, chemotherapy.

Table 7). Combining the direct comparison results of traditional frequency methods (**Supplementary Figure 9**) and the direct comparison between Bayesian models with NMA results (**Supplementary Figure 10**) and node analysis (**Supplementary Table 8**), there was no statistical difference between the direct and indirect comparisons in terms of the mOS and 1ySR and 2ySR.

Sensitivity Analysis

In the integrated analysis, we excluded Lynch (28), Govindan (27), and MYSTIC (10) studies with the largest deviation in survival time to perform the sensitivity analysis. In the sensitivity analysis, the mOS of first-line immuno-related treatments was 17.32 (16.16, 18.47) months, and the 1ySR and 2ySR were 0.65 (0.62, 0.68) and 0.40 (0.35, 0.44), respectively (**Supplementary Table 6**). Furthermore, in order to ensure the reliability and robustness of the results, we conducted one sensitivity analysis by excluding phase II studies [KEYNOTE021 (19), Niho (15)] for NMA, and the treatments that ranked the best in the overall results remained unchanged (**Supplementary Figures 11, 12**). The equations should be inserted in editable format from the equation editor.

DISCUSSION

As mentioned above, the integrated analysis showed that POS for advanced NSCLC with immuno-related therapy was 16.20

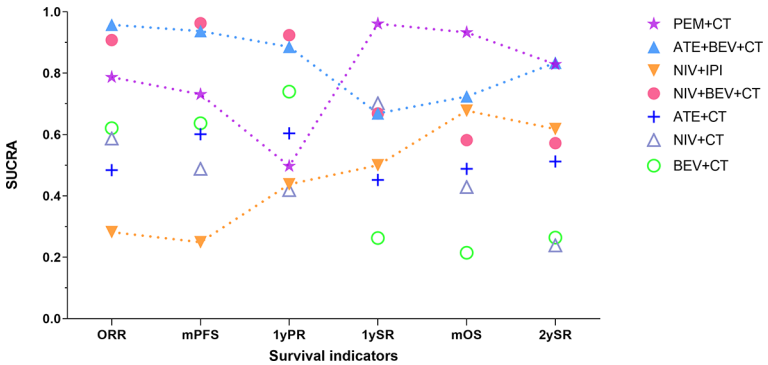

FIGURE 5 | Changing tendency in efficacy ranking of main immuno-related therapies for advanced wild-type NSCLC as time goes on. The vertical axis represents the SUCRA value of ranking probability, and the horizontal axis represents survival indicators arranged in chronological order. PEM, pembrolizumab; ATE, atezolizumab; NIV, nivolumab; IPI, ipilimumab; BEV, bevacizumab; CT, chemotherapy; ORR, objective response rate; mPFS, median progression-free survival time; 1yPR, 1-year PFS rate, mOS, median overall survival time; 1ySR, 1-year survival rate; 2ySR, 2-year survival rate.

months, with P1SR and P2SR of 63% and 37%. With 16.20 months as the standard of LS, the combination of ICIs and CT was more effective than either single or dual ICIs, and the addition of AA to ICI+CT resulted in the longest OS benefit and higher 1ySR and 2ySR. Considering the slow onset but longer duration of efficacy of immunotherapy, we are more inclined to regard the survival rate rather than median survival as the standard for evaluating the ICI-containing treatments, to reflect the efficacy character of immunotherapy more accurately. According to our pooled results, the POS was about 16~17 months, which was less than 1.5 years, while the P2SR was close to 40%, consistent with the recently published trend of the 5-year survival rate of 23.2% for first-line pembrolizumab treatment in advanced NSCLC (31). In this research, we focused on the 1ySR and 2ySR by integrated analysis, NMA, and ranking probability of various first-line ICI-containing treatments, to provide strong evidence for comprehensive comparison and assessment of the ability of each treatment to bring LS for advanced NSCLC in a relative longer observation time.

Immunotherapy combined with CT plays an important role in achieving LS in ITT patients with advanced wild-type NSCLC compared to either single or dual ICIs. The combination of ICIs and CT was superior to CT or ICIs alone (32), while there was no difference in mOS or survival rates between single ICI or dual ICIs without CT. The addition of CT helps not only overcome the shortcoming of the slow onset and the possible early ICI-related hyper-progression to improve the short-term response rate but also produce *in situ* vaccines to promote tumor antigen presentation to increase the efficacy of immunotherapy. Once activated, the immune response works continuously, making up for the short-effect duration of CT. Therefore, the synergism of immunotherapy and CT makes their combination the most reliable treatment strategy for LS of patients.

Among the top regimens, PEM+CT ranked the 1st, 1st, and 2nd in 1ySR, mOS, and 2ySR in the ITT population, respectively, while the corresponding rankings of ATE+BEV+CT were 4th, 2nd, and 1st. Notably, the pooled outcome of the ICIs+CT+AA strategy based on ATE+BEV+CT and NIV+BEV+CT has resulted in a P1SR of 74%, POS 19.5 months, and P2SR 49%, much better than other strategies. Therefore, adding AA on the basis of immuno-CT can not only yield a higher short-term effective rate and PFS but also translate them into a longer-term survival benefit. When considering the longest survival indicator 2ySR, the combination of ICIs+CT+AA was the strongest. As shown in **Figure 5**, if we arranged the SUCRA ranking values of efficacy indicators in a chronological order, only the immuno-AA-CT mode, instead of immuno-CT, dual immunotherapy, or AA-CT, showed a continuously rising tendency in the time span from 1 to 2 years of survival. The tendency may continue beyond 2 years. Consistently, another triplet similar to IMpower 150, NIV+BEV+CT failed to improve mOS and 1ySR compared to BEV+CT but significantly surpassed BEV+CT in 2ySR. It may be related to the synergistic role of ICIs and AA to target and transform the tumor microenvironment from immunosuppression into immune response, which takes a long time and functions for a long time. Obviously, further research is needed to determine which combination of immuno-AA-CT will lead to optimal survival. At the same time, we should pay full attention to the monitoring and handling of the side effects of the triplet therapy.

Another hot topic in clinical discussions is whether to apply single-ICI or ICI-combination therapy for patients with high PD-L1 expression. We found that among the regimens that resulted in LS in NSCLC with PD-L1 ≥50%, PEM+CT ranked first in 1ySR, while CEM monotherapy ranked first in mOS and 2ySR. Although immunotherapy shows a lasting and significant survival benefit over CT in the highly selected population, it is worth noting that dual ICIs or ICIs+CT failed to bring further benefits than single ICIs in terms of mOS, 1ySR, and 2ySR. Furthermore, the addition of CT to NIV+IPI also did not yield further benefits according to the survival indicators mOS, 1ySR, and 2ySR. It seems that the dominant position of PD-L1 inhibitors in patients with a high PD-L1 expression is unbreakable, possibly leaving limited space for CTLA-4

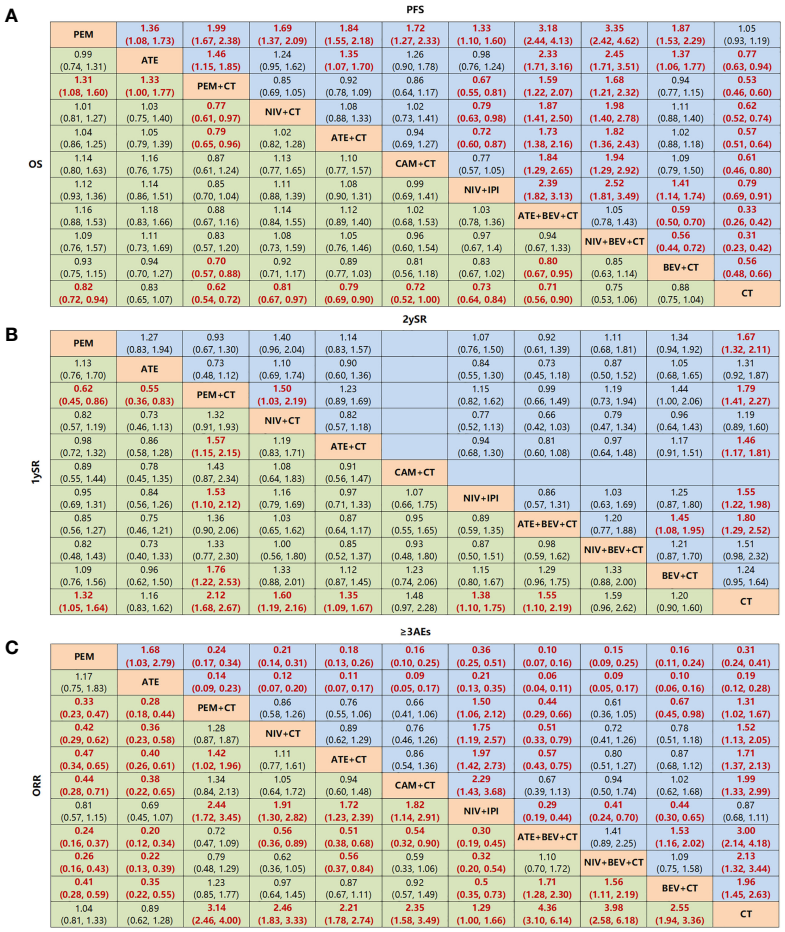

FIGURE 6 | Network meta-analysis of specific immuno-related regimens with long-term survival in overall population. **(A)** Pooled HR (95% CrIs) for overall survival (OS) and progression-free survival (PFS) in comparisons of all treatment strategies. **(B)** Pooled OR (95% CrIs) for 1-year survival rate and 2-year survival rate in comparisons of all treatment strategies. Data in each cell are HR or (95% CrIs) for the comparison of row-defining treatment versus column-defining treatment. HR less than 1 and OR more than 1 favor upper-row treatment. Significant results are highlighted in red and bold. **(C)** Pooled OR (95% CrIs) for ORR and ≥3 AEs in comparisons of all treatment strategies. PEM, pembrolizumab; ATE, atezolizumab; NIV, nivolumab; CAM, camrelizumab; CEM, cemiplimab; BEV, bevacizumab; IPI, ipilimumab, CT, chemotherapy.

inhibitors or CT to further extend survival. Interestingly, the addition of AA improved 1ySR and final 2ySR in this population (although only IMpower150 data are available). However, we still need to identify and consider the small group of people with a high PD-L1 expression who fail to benefit from mono-ICI, especially those with hyper-progression, to give them individualized combination therapy such as a short course of CT at the beginning, to avoid rapid disease progression and poor prognosis.

To our knowledge, this is the first quantitative study to identify the optimal regimens for LS in patients with advanced wild-type NSCLC. By focusing on LS, we conducted NMA and SUCRA ranking of multidimensional survival indicators, such as mOS, 1ySR, and 2ySR, to comprehensively evaluate and identify the optimal treatments bringing LS for different populations with specific characteristics. Nevertheless, our study also has several limitations. First, several studies with moderate or high risk of bias are inevitably included, although most of them are phase 3 clinical trials. Second, the 1- or 2-year overall survival rate for which studies not directly presented were extracted through survival curve by software, especially the 2-year overall survival rate, might lead to some bias. Third, our idea for the definition of long-term survival is to simply define survival beyond the average overall OS level which is the result of the first integrated OS. Considering this method defining LS lacks the reference of statistical evidence, and we only use the integrated result as the standard to measure the pros and cons of various related treatment strategies, rather than promoting this definition as a rigorous statistical concept. In addition, the biomarkers associated with LS are only limited to high PD-L1 expression (33) or TMB (34) at present, so there are relatively few subgroup analyses. We found that the combination of immunotherapy with CT and AA is an effective mode to result in LS. The combined intervention targeting VEGF/VEGFR and

immune checkpoints upon the immunosuppressive tumor microenvironment may robustly lead to superior effect than either of them, which may represent the future direction of treatments. Therefore, it is necessary to carry out research on the combination of various ICIs and AA therapies, with or without CT, in the treatment of advanced NSCLC, and strive to explore solutions to bring longer LS to these patients.

CONCLUSIONS

In conclusion, the quantitative analysis of LS brought by immuno-related therapies to advanced wild-type NSCLC by integrated analysis and NMA will help expand the survival advantages of immunotherapy to the extreme and provide sufficient evidence for patients with different characteristics to choose individualized treatment regimens to obtain the maximum LS.

DATA AVAILABILITY STATEMENT

The raw data supporting the conclusions of this article will be made available by the authors, without undue reservation.

AUTHOR CONTRIBUTIONS

LL conceived and designed the study. XZ, QX, XY, MH, and XD independently assessed studies for possible inclusion and collected data. QX, XZ, LS, MH, SL, KH, JW, and XD analyzed the data. XZ and LL wrote the manuscript. LL is the guarantor of this study and accepts full responsibility for the work, had access to the data, and controlled the decision to publish. The corresponding authors attest that all listed authors meet the authorship criteria and that no other person meeting the criteria has been omitted. All authors contributed to the article and approved the submitted version.

ACKNOWLEDGMENTS

This manuscript was edited by Alexandra Marshall (Marshall Medical Communications).

SUPPLEMENTARY MATERIAL

The Supplementary Material for this article can be found online at: https://www.frontiersin.org/articles/10.3389/fimmu.2022.764643/full#supplementary-material

REFERENCES

1. Gadgeel S, Rodríguez-Abreu D, Speranza G, Esteban E, Felip E, Dómine M, et al. Updated Analysis From KEYNOTE-189: Pembrolizumab or Placebo Plus Pemetrexed and Platinum for Previously Untreated Metastatic Nonsquamous Non-Small-Cell Lung Cancer. *J Clin Oncol* (2020) 38:1505–17. doi: 10.1200/JCO.19.03136
2. Paz-Ares L, Vicente D, Tafreshi A, Robinson A, Soto Parra H, Mazières J, et al. A Randomized, Placebo-Controlled Trial of Pembrolizumab Plus Chemotherapy in Patients With Metastatic Squamous NSCLC: Protocol-Specified Final Analysis of KEYNOTE-407. *J Thorac Oncol* (2020) 15:1657–69. doi: 10.1016/j.jtho.2020.06.015
3. Herbst RS, Giaccone G, de Marinis F, Reinmuth N, Vergnenegre A, Barrios CH, et al. Atezolizumab for First-Line Treatment of PD-L1-Selected Patients With NSCLC. *N Engl J Med* (2020) 383:1328–39. doi: 10.1056/NEJMoa1917346
4. West H, McCleod M, Hussein M, Morabito A, Rittmeyer A, Conter HJ, et al. Atezolizumab in Combination With Carboplatin Plus Nab-Paclitaxel Chemotherapy Compared With Chemotherapy Alone as First-Line Treatment for Metastatic non-Squamous non-Small-Cell Lung Cancer (IMpower130): A Multicentre, Randomised, Open-Label, Phase 3 Trial. *Lancet Oncol* (2019) 20:924–37. doi: 10.1016/S1470-2045(19)30167-6
5. Nishio M, Barlesi F, Ball S, Bordoni R, Cobo M, Dubray-Longeras P, et al. 375o Final Efficacy Results From IMpower132: First-Line Atezolizumab + Chemotherapy in Patients With Stage IV non-Squamous NSCLC. *Ann Oncol Annals Oncol* (2020) 31:S1386. doi: 10.1016/j.annonc.2020.10.369
6. Hellmann MD, Paz-Ares L, Bernabe Caro R, Zurawski B, Kim SW, Carcereny Costa E, et al. Nivolumab Plus Ipilimumab in Advanced Non-Small-Cell Lung Cancer. *N Engl J Med* (2019) 381:2020–31. doi: 10.1056/NEJMoa1910231
7. Paz-Ares L, Ciuleanu TE, Yu X, Salman P, Pluzanski A, Nagrial A, et al. Nivolumab (NIVO) 1 Platinum-Doublet Chemotherapy (Chemo) vs Chemo as First-Line (1L) Treatment (Tx) for Advanced Non-Small Cell Lung Cancer (aNSCLC): CheckMate 227 - Part 2 Final Analysis. *Ann Oncol* (2019) 30xi67–67xi68. doi: 10.1093/annonc/mdz453.004
8. Brahmer JR, Rodriguez-Abreu D, Robinson AG, Hui R, Csőszi T, Fülöp A, et al. KEYNOTE-024 5-Year OS Update: First-Line (1L) Pembrolizumab (Pembro) vs Platinum-Based Chemotherapy (Chemo) in Patients (Pts) With Metastatic NSCLC and PD-L1 Tumour Proportion Score (TPS) ≥50%. *Ann Oncol Annals Oncol* (2020) 31:S1181. doi: 10.1016/j.annonc.2020.08.2284
9. Zhang Y, Zhang Z. The History and Advances in Cancer Immunotherapy: Understanding the Characteristics of Tumor-Infiltrating Immune Cells and Their Therapeutic Implications. *Cell Mol Immunol* (2020) 17:807–21. doi: 10.1038/s41423-020-0488-6
10. Rizvi NA, Cho BC, Reinmuth N, Lee KH, Luft A, Ahn MJ, et al. Durvalumab With or Without Tremelimumab vs Standard Chemotherapy in First-Line Treatment of Metastatic Non-Small Cell Lung Cancer: The MYSTIC Phase 3 Randomized Clinical Trial. *JAMA Oncol* (2020) 6:661–74. doi: 10.1001/jamaoncol.2020.0237
11. Hutton B, Salanti G, Caldwell DM, Chaimani A, Schmid CH, Cameron C, et al. The PRISMA Extension Statement for Reporting of Systematic Reviews Incorporating Network Meta-Analyses of Health Care Interventions: Checklist and Explanations. *Ann Intern Med* (2015) 162:777–84. doi: 10.7326/M14-2385
12. Nasser M. Cochrane Handbook for Systematic Reviews of Interventions. *Am J Public Health* (2020) 110:753–4. doi: 10.2105/AJPH.2020.305609
13. Schwarzer G, Chemaitelly H, Abu-Raddad LJ, Rücker G. Seriously Misleading Results Using Inverse of Freeman-Tukey Double Arcsine Transformation in Meta-Analysis of Single Proportions. *Res Synth Methods* (2019) 10:476–83. doi: 10.1002/jrsm.1348
14. Zhou C, Wu YL, Chen G, Liu X, Zhu Y, Lu S, et al. BEYOND: A Randomized, Double-Blind, Placebo-Controlled, Multicenter, Phase III Study of First-Line Carboplatin/Paclitaxel Plus Bevacizumab or Placebo in Chinese Patients With Advanced or Recurrent Nonsquamous Non-Small-Cell Lung Cancer. *J Clin Oncol* (2015) 33:2197–204. doi: 10.1200/JCO.2014.59.4424
15. Niho S, Kunitoh H, Nokihara H, Horai T, Ichinose Y, Hida T, et al. Randomized Phase II Study of First-Line Carboplatin-Paclitaxel With or Without Bevacizumab in Japanese Patients With Advanced non-Squamous non-Small-Cell Lung Cancer. *Lung Cancer* (2012) 76:362–7. doi: 10.1016/j.lungcan.2011.12.005
16. Leighl NB, Scott AL, Goss D, Gordon B, Stockler MR, Sound Tsao M, et al. CCTG BR.34 A Randomized Trial of Durvalumab and Tremelimumab Platinum Based Chemotherapy in Patients With Metastatic Squamous or Nonsquamous Non Small Cell Lung Cancer. *J Clin Oncol* (2020) 38:470S. doi: 10.1200/JCO.2020.38.15_suppl.9502

17. Zhou C, Chen G, Huang Y, Zhou J, Lin L, Feng J, et al. A Randomized Phase 3 Study of Camrelizumab Plus Chemotherapy as 1st Line Therapy for Advanced/Metastatic Non-Squamous Non-Small Cell Lung Cancer. *J Thorac Oncol* (2019) 14:S215–215S216. doi: 10.1016/S2213-2600(20)30365-9
18. Mok T, Wu YL, Kudaba I, Kowalski DM, Cho BC, Turna HZ, et al. Pembrolizumab Versus Chemotherapy for Previously Untreated, PD-L1-Expressing, Locally Advanced or Metastatic Non-Small-Cell Lung Cancer (KEYNOTE-042): A Randomised, Open-Label, Controlled, Phase 3 Trial. *Lancet* (2019) 393:1819–30. doi: 10.1016/S0140-6736(18)32409-7
19. Borghaei H, Langer CJ, Gadgeel S, Papadimitrakopoulou VA, Patnaik A, Powell SF, et al. 24-Month Overall Survival From KEYNOTE-021 Cohort G: Pemetrexed and Carboplatin With or Without Pembrolizumab as First-Line Therapy for Advanced Nonsquamous Non-Small Cell Lung Cancer. *J Thorac Oncol* (2019) 14:124–9. doi: 10.1016/j.jtho.2018.08.004
20. Chaimani A, Higgins JP, Mavridis D, Spyridonos P, Salanti G. Graphical Tools for Network Meta-Analysis in STATA. *PloS One* (2013) 8:e76654. doi: 10.1371/journal.pone.0076654
21. Brooks SP, Gelman A. General Methods for Monitoring Convergence of Iterative Simulations. *J Comput Graphical Stat* (1998) 7:434–55. doi: 10.1080/10618600.1998.10474787
22. Dias S, Welton NJ, Caldwell DM, Ades AE. Checking Consistency in Mixed Treatment Comparison Meta-Analysis. *Stat Med* (2010) 29:932–44. doi: 10.1002/sim.3767
23. Carbone DP, Reck M, Paz-Ares L, Creelan B, Horn L, Steins M, et al. First-Line Nivolumab in Stage IV or Recurrent Non-Small-Cell Lung Cancer. *N Engl J Med* (2017) 376:2415–26. doi: 10.1056/NEJMoa1613493
24. Sezer A, Kilickap S, Gümüş M, Bondarenko I, Özgüroğlu M, Gogishvili M, et al. EMPOWER-Lung 1: Phase III First-Line (1L) Cemiplimab Monotherapy vs Platinum-Doublet Chemotherapy (Chemo) in Advanced non-Small Cell Lung Cancer (NSCLC) With Programmed Cell Death-Ligand 1 (PD-L1) ≥50%. *Ann Oncol Annals Oncol* (2020) 31:S1182. doi: 10.1016/j.annonc.2020.08.2285
25. Jotte R, Cappuzzo F, Vynnychenko I, Stroyakovskiy D, Rodríguez-Abreu D, Hussein M, et al. Atezolizumab in Combination With Carboplatin and Nab-Paclitaxel in Advanced Squamous NSCLC (IMpower131): Results From a Randomized Phase III Trial. *J Thorac Oncol* (2020) 15:1351–60. doi: 10.1016/j.jtho.2020.03.028
26. Socinski MA, Jotte RM, Cappuzzo F, Orlandi F, Stroyakovskiy D, Nogami N, et al. Atezolizumab for First-Line Treatment of Metastatic Nonsquamous NSCLC. *N Engl J Med* (2018) 378:2288–301. doi: 10.1056/NEJMoa1716948
27. Govindan R, Szczesna A, Ahn MJ, Schneider CP, Gonzalez Mella PF, Barlesi F, et al. Phase III Trial of Ipilimumab Combined With Paclitaxel and Carboplatin in Advanced Squamous Non-Small-Cell Lung Cancer. *J Clin Oncol* (2017) 35:3449–57. doi: 10.1200/JCO.2016.71.7629
28. Lynch TJ, Bondarenko I, Luft A, Serwatowski P, Barlesi F, Chacko R, et al. Ipilimumab in Combination With Paclitaxel and Carboplatin as First-Line Treatment in Stage IIIB/IV non-Small-Cell Lung Cancer: Results From a Randomized, Double-Blind, Multicenter Phase II Study. *J Clin Oncol* (2012) 30:2046–54. doi: 10.1200/JCO.2011.38.4032
29. Reck M, Tudor-Eliade C, Cobo Dols M, Schenker M, Zurawski B, Menezes J, et al. Nivolumab + Ipilimumab + 2 Cycles of Platinum Doublet Chemotherapy vs 4 Cycles Chemo as First-Line Treatment Forstage IV non Small Cell Lung Cancer: CheckMate 9LA. *J Clin Oncol* (2020) 38:470S. doi: 10.1200/JCO.2020.38.15_suppl.9501
30. Lee J, Sugawara S, Kang JH, Kim HR, Inui N, Hida T, et al. Randomized Phase III Trial of Nivolumab in Combination With Carboplatin, Paclitaxel, and Bevacizumab as First-Line Treatment for Patients With Advanced or Recurrent non-Squamous NSCLC. *Ann Oncol Annals Oncol* (2020) 31:S1184. doi: 10.1016/j.annonc.2020.08.2287
31. Garon EB, Hellmann MD, Rizvi NA, Carcereny E, Leighl NB, Ahn MJ, et al. Five-Year Overall Survival for Patients With Advanced Non–Small-Cell Lung Cancer Treated With Pembrolizumab: Results From the Phase I KEYNOTE-001 Study. *J Clin Oncol* (2019) 37:2518–27. doi: 10.1200/JCO.19.00934
32. Sheng L, Gao J, Xu Q, Zhang X, Huang M, Dai X, et al. Selection of Optimal First-Line Immuno-Related Therapy Based on Specific Pathological Characteristics for Patients With Advanced Driver-Gene Wild-Type non-Small Cell Lung Cancer: A Systematic Review and Network Meta-Analysis. *Ther Adv Med Oncol* (2021) 13:17588359211018537. doi: 10.1177/17588359211018537
33. Gibney GT, Weiner LM, Atkins MB. Predictive Biomarkers for Checkpoint Inhibitor-Based Immunotherapy. *Lancet Oncol* (2016) 17:e542–542e551. doi: 10.1016/S1470-2045(16)30406-5
34. Yarchoan M, Hopkins A, Jaffee EM. Tumor Mutational Burden and Response Rate to PD-1 Inhibition. *N Engl J Med* (2017) 377:2500–1. doi: 10.1056/NEJMc1713444

Conflict of Interest: The authors declare that the research was conducted in the absence of any commercial or financial relationships that could be construed as a potential conflict of interest.

Publisher's Note: All claims expressed in this article are solely those of the authors and do not necessarily represent those of their affiliated organizations, or those of the publisher, the editors and the reviewers. Any product that may be evaluated in this article, or claim that may be made by its manufacturer, is not guaranteed or endorsed by the publisher.

Copyright © 2022 Zhang, Xu, Yu, Huang, Li, Sheng, Dai, Huang, Wang and Liu. This is an open-access article distributed under the terms of the Creative Commons Attribution License (CC BY). The use, distribution or reproduction in other forums is permitted, provided the original author(s) and the copyright owner(s) are credited and that the original publication in this journal is cited, in accordance with accepted academic practice. No use, distribution or reproduction is permitted which does not comply with these terms.

frontiers | Frontiers in Immunology

REVIEW
published: 07 April 2022
doi: 10.3389/fimmu.2022.830631

Checkpoint Inhibitor Pneumonitis Induced by Anti-PD-1/PD-L1 Therapy in Non-Small-Cell Lung Cancer: Occurrence and Mechanism

Jianqiong Yin[1†], *Yuanjun Wu*[1†], *Xue Yang*[1], *Lu Gan*[2] *and Jianxin Xue*[1,3,4*]

[1] Department of Thoracic Oncology, Cancer Center and State Key Laboratory of Biotherapy, West China Hospital, Sichuan University, Chengdu, China, [2] Research Laboratory of Emergency Medicine, Department of Emergency Medicine, National Clinical Research Center for Geriatrics, West China Hospital, Sichuan University, Chengdu, China, [3] Department of Radiation Oncology, Cancer Center, West China Hospital, Sichuan University, Chengdu, China, [4] Laboratory of Clinical Cell Therapy, West China Hospital, Sichuan University, Chengdu, China

OPEN ACCESS

Edited by:
Benjamin Frey,
University Hospital Erlangen, Germany

Reviewed by:
Rohimah Mohamud,
Universiti Sains Malaysia (USM), Malaysia
Jianchun Duan,
Peking Union Medical College (CAS), China

***Correspondence:**
Jianxin Xue
radjianxin@163.com

[†]These authors have contributed equally to this work and share first authorship

Specialty section:
This article was submitted to Cancer Immunity and Immunotherapy, a section of the journal Frontiers in Immunology

Received: 07 December 2021
Accepted: 16 March 2022
Published: 07 April 2022

Citation:
Yin J, Wu Y, Yang X, Gan L and Xue J (2022) Checkpoint Inhibitor Pneumonitis Induced by Anti-PD-1/PD-L1 Therapy in Non-Small-Cell Lung Cancer: Occurrence and Mechanism. Front. Immunol. 13:830631. doi: 10.3389/fimmu.2022.830631

Immune checkpointty inhibitors (ICIs), particularly those targeting programmed death 1 (PD-1) and anti-programmed death ligand 1 (PD-L1), enhance the antitumor effect by restoring the function of the inhibited effector T cells and produce durable responses in a large variety of metastatic and late patients with non-small-cell lung cancer. Although often well tolerated, the activation of the immune system results in side effects known as immune-related adverse events (irAEs), which can affect multiple organ systems, including the lungs. The occurrence of severe pulmonary irAEs, especially checkpoint inhibitor pneumonitis (CIP), is rare but has extremely high mortality and often overlaps with the respiratory symptoms and imaging of primary tumors. The development of CIP may be accompanied by radiation pneumonia and infectious pneumonia, leading to the simultaneous occurrence of a mixture of several types of inflammation in the lungs. However, there is a lack of authoritative diagnosis, grading criteria and clarified mechanisms of CIP. In this article, we review the incidence and median time to onset of CIP in patients with non-small-cell lung cancer treated with PD-1/PD-L1 blockade in clinical studies. We also summarize the clinical features, potential mechanisms, management and predictive biomarkers of CIP caused by PD-1/PD-L1 blockade in non-small-cell lung cancer treatment.

Keywords: programmed cell death 1, programmed cell death ligand 1, immune checkpoint inhibitors, immune-related adverse events, checkpoint inhibitor pneumonitis, non-small-cell lung cancer

1 INTRODUCTION

Although the incidence and mortality of lung cancer has shown a significant decline according to recent studies, it still exceeds the vast majority of cancer types (1). According to the International Agency for Research on Cancer, lung cancer is the most common malignant tumor with the highest mortality. Non-small-cell lung cancer (NSCLC) is the major histological subtype of lung cancer, accounting for approximately 85% of all lung cancers (2). Anti-programmed death 1 (PD-1) and

anti- programmed death ligand 1 (PD-L1) monoclonal antibodies (mAbs) have profoundly produced durable anticancer responses in patients with a variety of solid tumors, including NSCLC. The U.S. Food and Drug Administration has approved three PD-1 inhibitors (nivolumab, pembrolizumab and cemiplimab) and two PD-L1 inhibitors (atezolizumab and durvalumab) for the treatment of NSCLC with different stages (3–6).

However, accompanied by a promising survival advantage, PD-1/PD-L1 inhibitors are related to a broad spectrum of toxic effects known as immune-related adverse events (irAEs), including skin rash, colitis, hepatitis, endocrinopathies, and pneumonitis (7). In clinical trials, adverse events are reported and graded according to the Common Terminology Criteria for Adverse Events (CTCAE) from the U.S. National Cancer Institute, and immune-related pulmonary adverse events are graded from grade 1 to grade 5 depending on the symptoms from mild to serious (8). Most irAEs are mild and tolerable, while some of them can be fatal. In recent years, pulmonary adverse events caused by PD-1/PD-L1 inhibitors have been gradually reported, and some rare severe events even lead to death (9). It is worth noting that checkpoint inhibitor pneumonitis (CIP) accounts for 35% of PD-1 and PD-L1 inhibitor-related deaths (9). In addition, the incidence of CIP induced by anti-PD-1/PD-L1 is higher in patients with NSCLC than in patients with other cancers (3, 10). Pneumonitis can be mediated by various factors, such as radiotherapy, chemotherapy, targeted therapy, infection, and nonanticancer drugs (3). Thus, the diagnosis of CIP needs to be distinguished from hyperprogression, pseudoprogression, and other types of pneumonia (11). Further characterization of the unique clinical and radiographic features is needed to aid in the diagnosis of CIP. The incidence, risk, clinical characteristics and mechanism of CIP for anti-PD-1/PD-L1 monotherapy or a combination with other therapies (radiotherapy, chemotherapy or targeted therapy) may differ, which might influence the subsequent treatment options and prognosis of CIP (12). The clinical features and mechanisms of CIP induced by anti-PD-1/PD-L1 therapy in non-small-cell lung cancer have not been fully elaborated. In this review, we summarize recent discoveries on CIP introduced by anti-PD-1/PD-L1 treatment, especially in patients with NSCLC, and aim to provide a reference for clinical diagnosis and preclinical mechanistic research. We will also elucidate the incidence, time to onset and characteristic manifestations of CIP, as well as discuss the management and predictive biomarkers of CIP.

2 OCCURRENCE OF CIP DURING PD-1/PD-L1 BLOCKADE

2.1 Incidence and Timeline

Pulmonary irAEs are more common in patients with NSCLC than in patients with other cancers, with an incidence of 3% to 5% according to clinical trial data (3, 10, 13). Without the exclusion criteria of clinical trials, the incidence of CIP can be much higher in the real world. In a retrospective study of 205 patients with NSCLC, 19% of them encountered CIP during PD-1/PD-L1 blockade. PD-1/PD-L1 inhibitors show a higher incidence of CIP than other ICIs, including cytotoxic T-lymphocyte-associated protein 4 (CTLA-4) inhibitors, and are responsible for 35% of CIP-related deaths (9, 14). The incidence of CIP can vary when different PD-1/PD-L1 inhibitors are used (4, 10, 15–27) (**Table 1**). However, in general, PD-1 inhibitors account for a higher incidence of all-grade (3.6% vs. 1.3%) and high-grade (1.1% vs. 0.4%) CIP than PD-L1 inhibitors based on a clinical trial of NSCLC (28). A multicenter, open-label, global, phase 3 trial compared the effect and safety of cemiplimab single-agent therapy with platinum-doublet chemotherapy in the first-line treatment of advanced NSCLC patients with a PD-L1 expression level of 50% or higher. The results showed that the incidence of immune-related pneumonitis in NSCLC patients receiving cemiplimab therapy was 2.3% (22).

There is a lower incidence of pneumonitis in PD-1/PD-L1 inhibitor monotherapy than in concurrent or sequential chemotherapy (29), radiotherapy (30) or immunotherapy (3, 17, 27, 31). In a randomized phase III clinical trial, the incidences of any-grade and high-grade CIP in NSCLC patients receiving durvalumab plus tremelimumab, a CTLA-4 inhibitor, were higher than those with durvalumab monotherapy (6.7% vs. 2.2% for any-grade CIP and 2.2% vs. 1.1% for high-grade CIP) (27). This may be attributed to the overlapping pulmonary toxicity of different treatments. In addition, there are no reliable criteria to distinguish CIP from radiation pneumonitis and radiation recall pneumonitis, which may affect the diagnosis of CIP (32, 33). Concurrent or sequential combination therapy is common in the clinic and may account for the higher incidence of treatment-related pneumonitis in the real world (34–36).

The median time to onset of pulmonary adverse events can vary. A report showed that the median time to onset of pneumonitis was 2.8 months, with a wide range from 9 days to 19.2 months (3). The onset time may be affected by the selection of the ICI agent (15, 16, 18, 34–37) (**Table 2**). In a randomized, open-label, international phase 3 study, the median onset time to pneumonitis was 15.1 (2.6-85.1) weeks and 31.1 (11.7-56.9) weeks in patients with advanced squamous and nonsquamous NSCLC who received nivolumab, respectively (15, 16). In another randomized controlled trial, the median onset time was 8.1 (0.6-56.1) weeks in advanced NSCLC patients treated with pembrolizumab (18). The treatment strategy may also influence the onset time. A shorter median onset time was reported in patients with combination immunotherapy compared with monotherapy (2.7 months (9 days to 6.9 months) vs. 4.6 months (21 days-19.2 months), P=0.02) (3). In retrospective studies that enrolled only NSCLC patients, the onset of CIP occurred earlier when PD-1/PD-L1 inhibitors were combined with other treatments (**Table 2**). More high-grade CIP onset occurs within the first 100 to 200 days of immunotherapy (38). Naidoo et al. reported a type of CIP called chronic CIP, which refers to a kind of clinical pneumonitis persisting or worsening with steroid tapering and necessitating ≥12 weeks of immune suppression after ICI discontinuation. The incidence of chronic pneumonitis is

TABLE 1 | Important clinical trials that reported checkpoint inhibitor pneumonitis (CIP) in NSCLC patients with PD-1/PD-L1 blockade.

Registration number	Published year	Treatment	Enrollment [a]	Phage	NSCLC stage	Incidence, n (%)		Reference
						Any grade	High grade (≥3)	
PD-1 inhibitor								
NCT01642004	2015	Nivolumab	131	III	IIIB or IV	6 (5.0)	1 (1.0)	(15)
NCT01673867	2015	Nivolumab	287	III	IIIB or IV	8 (2.8)	3 (1.0)	(16)
NCT02477826	2018	Nivolumab	391	III	IV	9(2.3)	6 (1.5)	(17)
NCT02477826	2018	Nivolumab + Ipilimumab	576	III	IV	22 (3.8)	13 (2.3)	(17)
NCT01295827	2015	Pembrolizumab	550	III	IIIB or IV	21 (3.8)	11 (2.0)	(18)
NCT01905657	2016	Pembrolizumab	682	II/III	IIIB or IV	26 (3.8)	12 (1.8)	(19)
NCT02142738	2016	Pembrolizumab	154	III	IIIB or IV	9 (5.8)	4 (2.6)	(20)
NCT02220894	2019	Pembrolizumab	636	III	IIIB or IV	53 (8.3)	22 (3.5)	(21)
NCT02775435	2018	Pembrolizumab + Carboplatin+ (Nab-) Paclitaxel	278	III	IV	18 (6.5)	7 (2.5)	(10)
NCT03088540	2021	Cemiplimab	355	III	IIIB, IIIC or IV	8 (2.3)[b]	2 (0.6)[c]	(22)
PD-L1 inhibitor								
NCT02008227	2017	Atezolizumab	609	III	IIIB or IV	6 (1.0)	4 (0.7)	(4)
NCT02409342	2020	Atezolizumab	286	III	IV	11 (3.8)	2 (0.7)	(23)
NCT02657434	2021	Atezolizumab + Pemetrexed	291	III	IV	18 (6.2)	6 (2.1)	(24)
NCT02367781	2019	Atezolizumab + Carboplatin + Nab-paclitaxel	473	III	IV	25 (5.3)	2 (0.4)	(25)
NCT02125461	2017	Durvalumab	475	III	III	51 (10.7)	8 (1.7)	(26)
NCT02453282	2020	Durvalumab	369	III	IV	8 (2.2)	5 (1.4)	(27)
NCT02453282	2020	Durvalumab + Tremelimumab	371	III	IV	25 (6.7)	11 (3.0)	(27)

NSCLC, non-small-cell lung cancer; PD-1, programmed cell death 1; PD-L1, programmed cell death ligand 1.

[a]*Patients enrolled in and received ICI treatment.*

[b]*Includes 7 immune-related pneumonitis and 1 immune-mediated pneumonitis.*

[c]*Includes 1 immune-related pneumonitis and 1 immune-mediated pneumonitis.*

TABLE 2 | Study that reported the onset time of checkpoint inhibitor pneumonitis (CIP) in NSCLC patients with PD-1/PD-L1 blockade.

Published Year	Treatment	Study type	Enrollment [a]	NSCLC stage	Incidence, n (%)		Median time to onset, week(range)	Reference
					Any grade	High grade (≥3)		
2015	Nivolumab	Prospective, RCT	131	III	6 (5.0)	1 (1.0)	15.1 (2.6–85.1)	(15)
2015	Nivolumab	Prospective, RCT	287	III	10 (3.5) [b1]	4 (1.4) [b2]	31.1 (11.7-56.9)	(16)
2015	Pembrolizumab	Prospective, RCT	550	IIIB or IV	21 (3.8)	11 (2.0)	8.1 (0.6-56.1)	(18)
2017	Nivolumab (mono or combined with chemotherapy)	Retrospective	111	IV or recurrent	8 (7.2) [b3]	4 (3.6) [b3]	5.2 (2.3–24)	(34)
2018	Nivolumab/Pembrolizumab/ Durvalumab (mono or combined with other ICI/ chemotherapy)	Retrospective	205	all	39 (19.0)	24 (11.7)	11.7 (2.9–26.1) [c]	(35)
2020	Nivolumab (mono or combined with chemotherapy)	Retrospective	901	all	94 (10.4)	39 (4.3)	8.4 (0-75.1)	(36)
2020	Nivolumab/Ipilimumab/ Pembrolizumab (mono or combined with chemotherapy)	Retrospective [d]	205	all	5 (2.4) [e]	2 (1.0) [e]	52.9 (34-86.6)	(37)

NSCLC, non-small-cell lung cancer; PD-1, programmed cell death 1; PD-L1, programmed cell death ligand 1.

[a]*Patients enrolled in and received ICI treatment.*

[b]*Includes patients with interstitial lung disease (2 in a1, 1 in a2, all in a3).*

[c]*Interquartile range of onset time.*

[d]*A retrospective study on Chronic pneumonitis (clinical pneumonitis persisting or worsening with steroid tapering and necessitating ≥12 weeks of immune suppression after ICI discontinuation).*

[e]*Initial pneumonitis grade.*

approximately 2.4% in patients with NSCLC, and the onset time of chronic CIP is variable (range: 238–606 months) and occurs at a median time of 370 months after ICI start (37). In summary, the onset time of CIP shows various timespans and may be affected by many factors, including treatment regime (**Figure 1**).

2.2 Risk Factors

Checkpoint inhibitor pneumonitis may be the preferred attack in patients with features of lung deterioration conditions, including aging, smoking status, prior treatment, combinations with other drugs, primary tumor type, and previous lung disease. A previous study found that patients aged >70 years were more common in a CIP group than in a non-CIP group (54.5% vs. 30.3%; P = 0.025) (39), which may be due to decreased lung function and increased medical complications in the elderly. In a study by Suresh et al. (35), a higher incidence of CIP was observed in males than in females and in squamous cells than in other histological types. Notably, smoking may also play a role in the development of CIP. Former/current smokers were found to have a higher incidence of pneumonitis than nonsmokers (P=0.03) (40). The incidence of CIP is also influenced by treatment strategy. Currently, a significant number of patients with locally advanced unresectable or metastatic NSCLC receive treatment with radiotherapy alone or concurrent chemotherapy before receiving immunotherapy (41). Multiple clinical studies have shown that the incidence of CIP was numerically higher in patients receiving chest radiotherapy than in those receiving nonchest/no radiotherapy (40, 42–45). Some researchers consider this kind of pneumonitis radiation recall pneumonitis (RRP) introduced by immunotherapy, while the criteria for identifying CIP and RRP are still unclarified (33). However, radiation parameters did not correlate with the development of pneumonitis (40). As mentioned above, PD-1 inhibitors are related to a higher incidence of CIP both for any grade or ≥ grade 3 compared with PD-L1 inhibitors. PD-1/PD-L1 blockades are usually combined with chemotherapeutic drugs, tyrosine kinase inhibitors, or additional immune-targeted drugs. The combination of PD-1/PD-L1 inhibitors with a variety of different drugs was also associated with pneumonitis risk, indicating the superposition effect of multiple drugs on pulmonary toxicity (10, 17, 31, 45, 46). Patients with epidermal growth factor receptor (EGFR) mutations are more likely to undergo pneumonitis during the combination therapy of sequential PD-(L)1 blockade followed by later osimertinib (47). The risk of CIP was also closely associated with preexisting lung disease, including pulmonary infection (48), pulmonary emphysema (49), chronic obstructive pulmonary disease (COPD) (50), asthma (50), interstitial lung disease (ILD) (51), pulmonary fibrosis (52), pneumothorax, and pleural effusion (45). Interestingly, a recent study found that tumor invasion into the central airway was strongly associated with early-onset CIP in patients with NSCLC (53). The presence of extrathoracic metastasis was related to a lower incidence of ICI-related pneumonitis (39). In addition, according to a recent study, a high baseline absolute eosinophil count (≥0.125 $\times 10^9$ cells/L) was correlated with an increased risk of CIP and with a better clinical outcome (54). A higher baseline level of anti-CD74 autoantibody is also more likely to develop CIP (55). Taken together, the risk factors for CIP may include older age, history of smoking, squamous cell histological type, previous lung disease, prior thoracic irradiation and treatment combinations with other drugs (**Table 3**).

2.3 Effects of CIP on the Clinical Outcome of Patients With PD-1/PD-L1 Therapy

Several studies have indicated that melanoma patients with irAEs have a survival benefit (56–59), which suggests that the early occurrence of irAEs may predict better outcome of immune checkpoint inhibitor therapy, and appropriate management of these events is needed to maximize the therapeutic effect of these drugs. The mechanisms behind this association are not fully understood. It has been proposed that the shared antigens between melanoma cells and normal melanocytes may account for this association (57, 59, 60). Similarly, several studies have shown favorable treatment efficacy and survival in patients with NSCLC (2, 61, 62). However, whether there is a similar

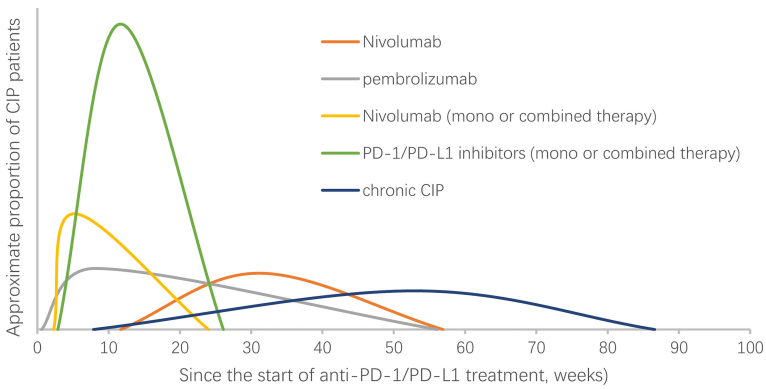

FIGURE 1 | Onset time of checkpoint inhibitor pneumonitis (CIP) in NSCLC patients receiving PD-1/PD-L1 treatment. NSCLC, non-small-cell lung cancer. The curve in the figure does not represent the change in the incidence of CIP over time. The abscissa of the highest point of the curve represents the median time of CIP reported in the studies (16, 18, 34, 35, 37).

TABLE 3 | Potential risk factors for checkpoint inhibitor pneumonitis (CIP) in NSCLC.

Potential risk factors	Details
Sex	Males have a higher incidence of CIP
Age of patients	·Patients aged >70 years ·The decreased lung function and increased medical complications in the elderly may be the cause of higher incidence of CIP
Tumor histologic type	A higher incidence of CIP in patients with squamous NSCLC
Smoking status	Patients with former or current smoking
Prior thoracic radiation therapy	The incidence of CIP is numerically higher in patients receiving chest-RT compared with non-chest/no RT ·Radiation parameters have no correlation with the development of pneumonitis ·The influence of radiotherapy courses, type and timing for development of CIP is still not clear ·T cells activated during ICIs treatment are more easily infiltrate into the damaged lung tissue by thoracic irradiation
PD-1 inhibitors	·The incidence of CIP with PD-1 inhibitors is higher than PD-L1 inhibitors ·PD-1/PD-L1 inhibitors are related to a higher incidence of CIP than anti-CTLA4 ·PD-1 inhibitors lead to increased risk through increasing the interaction of PD-L2- RGMb
Combination therapy	·Additional immune-targeted drugs, chemotherapeutic drugs and some specific tyrosine kinase inhibitors (TKIs) ·Combination of PD-1/PD-L1 inhibitors with other antitumor agents might mediate the superposition effect of multiple drugs on pulmonary toxicity
EGFR mutation	Patients with EGFR mutation are more likely to undergo pneumonitis during the combination therapy of ICIs with osimertinib
Sequences of drug administration	PD-(L)1 blockade followed by osimertinib is related to a higher incidence of pneumonitis
Preexisting lung disease	Pulmonary infection, pulmonary emphysema, COPD, asthma, ILD, pulmonary fibrosis, pneumothorax, and pleural effusion
Tumor invasion	·Tumor invades the central airway was strongly associated with early-onset CIP ·Extrathoracic metastasis was related to a lower incidence of CIP
Baseline peripheral-blood absolute eosinophil count (AEC)	A high level of baseline AEC($\geq 0.125\times10^9$cells/L) correlated with an increasing risk of CIP but a better clinical outcome
Baseline level of anti-CD74 autoantibody	A higher baseline level of anti-CD74 autoantibody is also more likely to develop CIP

NSCLC, non-small-cell lung cancer; CIP, checkpoint inhibitor pneumonitis; RT, radiation therapy; PD-1, programmed cell death protein 1; PD-L1, programmed cell death protein ligand-1; CTLA-4, cytotoxic T lymphocyte-associated protein 4; PD-L2, programmed cell death protein ligand-2; RGMb, repulsive guidance molecule b; TKIs, tyrosine kinase inhibitors; EGFR, epidermal growth factor receptor; COPD, chronic obstructive pulmonary disease; ILD, interstitial lung disease; AEC, absolute eosinophil count.

association between CIP and tumor response in patients with NSCLC remains controversial. Genova et al (62) have shown that the development of irAEs, including CIP, is a significantly positive predictor of survival outcomes in patients with NSCLC treated with nivolumab. However, in another study, the efficacy of ICI treatment was observably worse in patients with severe grade CIP than in those without severe grade CIP when patients were classified according to CIP severity (63). Thus, several challenges still need to be addressed in the future, and the association between the development of CIP and clinical efficacy in patients with NSCLC treated with ICIs still needs to be evaluated. In addition, although studies have shown that the occurrence of CIP is associated with a better response to ICI therapy, severe CIP can lead to interruption of ICI therapy and even fatality. In conclusion, the effects of CIP on the efficacy and prognosis of ICI therapy in NSCLC patients are still controversial, and more evidence is needed to clarify the relationship.

2.4 Overview of Manifestations

2.4.1 Common Symptoms

The most common clinical symptoms of CIP are dyspnea and cough. Fever and chest pain can also be observed but not often (3). However, it is difficult to distinguish these symptoms from infection or progression of malignancy, especially in patients with NSCLC. For individuals with suspected CIP, laboratory examinations are necessary to exclude infection, including culture of nasopharyngeal, sputum, and urine and sensitivity tests. In addition, some patients with subclinical CIP may experience no respiratory symptoms. Therefore, the diagnosis of CIP also depends on other auxiliary examinations (64).

2.4.2 Radiological Features

Radiological examination, especially chest CT, plays an important role in the diagnosis of CIP. Several radiographic patterns of CIP have been observed, including cryptogenic organizing pneumonia (COP), nonspecific interstitial pneumonia, hypersensitivity pneumonitis and pneumonitis not otherwise specified (3). The most predominant radiographic pattern is COP (65). Specific findings on chest CT include traction bronchiectasis, consolidation, reticular opacities, ground glass opacities (GGOs), centrilobular nodularity, and honeycombing, of which GGOs are present in the majority of patients (66). In addition, GGO was indicated as a significant predictor of worse overall survival (67). Clinically, the situation will be more complicated, and mixed patterns may be observed. In a case of a 73-year-old woman with NSCLC who received pembrolizumab treatment, organizing pneumonia with "air bronchogram" presented at the upper lung lobes and widespread thickening of the interlobular interstitium at the left lower lobe (68). The use of PET-CT in the diagnosis of immune-related pneumonia in patients with melanoma has been reported, but there were few specificities of the radiological images of pneumonia on PET/CT scans (69, 70). As mentioned above, there are several radiological patterns of CIP, and detailed analysis is needed when facing different patterns of CIP in the clinic.

2.4.3 Auxiliary Examinations

Bronchoalveolar lavage (BAL) is one of the most common invasive examinations of ICI-related pneumonitis. In general, lymphocytes elevated in bronchoalveolar lavage fluid (BALF). Nandoo et al. (37) found that lymphocytes, predominantly $CD4^+$ T cells, were increased in the BALF of CIP patients compared with the BALF from patients who received ICI treatment but had no evidence of CIP (n= 6) or suspected CIP patients (n= 14). Wang et al. found significantly elevated levels of interleukin-17A (IL-17A) and IL-35 in both serum and BALF (71). In addition, they also observed increased numbers of central memory T cells and decreased expression of CTLA-4 and PD-1 in regulatory T cells (Tregs). Enriched $IFNg^+IL\text{-}17\text{-}CD8^+T$ and $CXCR3^+CCR6^+$ Th17/Th1 cells were observed in the BALF of CIP compared with infection pneumonia in acute myeloid leukemia and myelodysplastic syndrome (67).

Transbronchial biopsy is seldom used in the auxiliary diagnosis of CIP. In the few cases of transbronchial biopsy, pneumonia tissue after ICI showed inflammation and lymphocyte infiltration (39). Nandoo et al. collected 11 tissue samples by transbronchial biopsy (8/11), core biopsy (2/11) and wedge resection (1/11), and the histopathological results included 4 cellular interstitial pneumonitis, 3 organizing pneumonia, 1 diffuse alveolar damage and 3 no abnormalities identified (3).

3 MECHANISMS OF PD-1/PD-L1 INHIBITOR-INDUCED PULMONARY TOXICITY

Due to the lack of effective preclinical studies, the mechanism of PD-1/PD-L1 inhibitor-induced CIP in NSCLC patients is still unclear. Here, we summarize the factors that may be involved in CIP based on existing studies (**Figure 2**).

3.1 Disordered T Cell Subsets

PD-1/PD-L1 inhibitors can enhance the antitumor function of T cells (72). There is some evidence that T cells may be involved in the development of immune-related pulmonary complications. Increased infiltration of highly proliferative $CD8^+$ T cells was observed in lung biopsy tissue from patients with NSCLC who developed chronic bronchiolitis obliterans organizing pneumonia after nivolumab treatment (37). Suresh et al. found that $CD4^+$ T cells were significantly increased in BAL samples of CIP patients (mainly with NSCLC) after receiving anti-PD-1/PD-L1 inhibitors (73). Suzuki et al. reported that the proportion of $CD8^+$ T cells with PD-1, Tim-3 and TIGHIT positivity in the BALF of patients with PD-1/PD-L1 inhibitor-induced ILD was significantly higher than that of patients with other types of ILD (74). All of these findings suggest dysregulated alveolar immunity in CIP patients. Kim et al. found significant elevation of Ki-67 (proliferation markers of $PD\text{-}1^+$ $CD8^+$ T cell) in metastatic NSCLC patients who received pembrolizumab or nivolumab. Various studies have shown that T cells are activated and infiltrate the lung tissue of CIP patients, which indicates the enhancement of antitumor effects. However, an excessive immune response may lead to damage to normal tissue.

When naïve T cells encounter antigens presented by antigen-presenting cells (APCs) in secondary lymphoid organs, they undergo differentiation/polarization processes according to cell division signals and become T helper 1 (Th1) cells, T helper 2 (Th2) cells, T helper 17 (Th17) cells or Tregs (72). Different T cell subsets may play different roles in irAEs.

3.1.1 Th1/Th2

A Th1/Th2 shift exists in tumor patients, and Th2 cells are often dominant (75). It has been suggested that the shift of Th1/Th2 cells may be related to the immune escape of tumors (76). Anti-PD-1/PD-L1 therapy can reverse Th1/Th2 in cancer patients by promoting the production of Th1 cells and inhibiting the production of Th2-related cytokines (77). However, Th1 cells may be the dominant response cell in the development of irAEs, as infiltration of Th1 cells has been observed in related tissues. Yoshino et al. reported nivolumab-related colitis in 2 patients with metastatic melanoma, whose pathological examinations of the colon showed infiltration of $CD8^+$ T cells and T-bet-expressing Th1 $CD4^+$ T cells (78). Kim et al. reported enrichment of $T\text{-}bet^+$ $POPGT^+$ (Th1) and $CXCR3^+$ $T\text{-}bet^+$ $CCR6^+$ $RORGT^+$ (Th17/Th1) cells in BAL $CD4^+$ T cells of leukemia patients with respiratory symptoms after ICI-based therapy. Interestingly, most Th17/Th1 cells express PD-1 (79). These studies indicated that Th1 cells may be involved in the formation and development of anti-PD-1-associated pneumonitis. In addition, Th1 cells are also associated with some autoimmune diseases (80), which may explain autoimmune symptoms after PD-1/PD-L1 blockade.

3.1.2 Treg

Tregs are an important factor in maintaining immune tolerance. Nedoszytko et al. reported that Tregs with high activity can lead to immunosuppression and decrease the number of Th1 cells (81). Tregs express both PD-1 and PD-L1 (82). Amarnath et al. found that human Th1 cells transform into Tregs through the involvement of the PD-1/PD-L1 axis (83). Francisco et al. reported that PD-L1 plays an important role in converting naïve $CD4^+$ T cells into induced Tregs (iTregs) as well as maintaining and strengthening their immunosuppressive function (82). When blocking the PD-1/PD-L1 axis, differentiation to Tregs may be prevented, and a decreased number of Tregs can be observed in the tumor microenvironment (TME) (84). This suggests that anti-PD-1/PD-L1 treatment could be a potential strategy to improve the anti-infective and antitumor immunity of T cells. However, immune-related damage occurs at the same time. In Francisco's study, fatal immune-mediated pulmonary damage and iTreg differentiation were observed *in vivo* in $PD\text{-}L1^{-/-}PD\text{-}L2^{-/-}Rag^{-/-}$recipients of naïve $CD4^+$T and $Rag^{-/-}$mice treated with a PD-L1 inhibitor (82). In addition, Suresh et al. found decreased expression of CTLA-4 and PD-1 on Tregs in the BALF of CIP patients, indicating the loss of the inhibitory phenotype of Tregs (73). Therefore, the lack and poor function of Tregs may lead to unchecked immune dysregulation, which may lead to irAEs such as CIP.

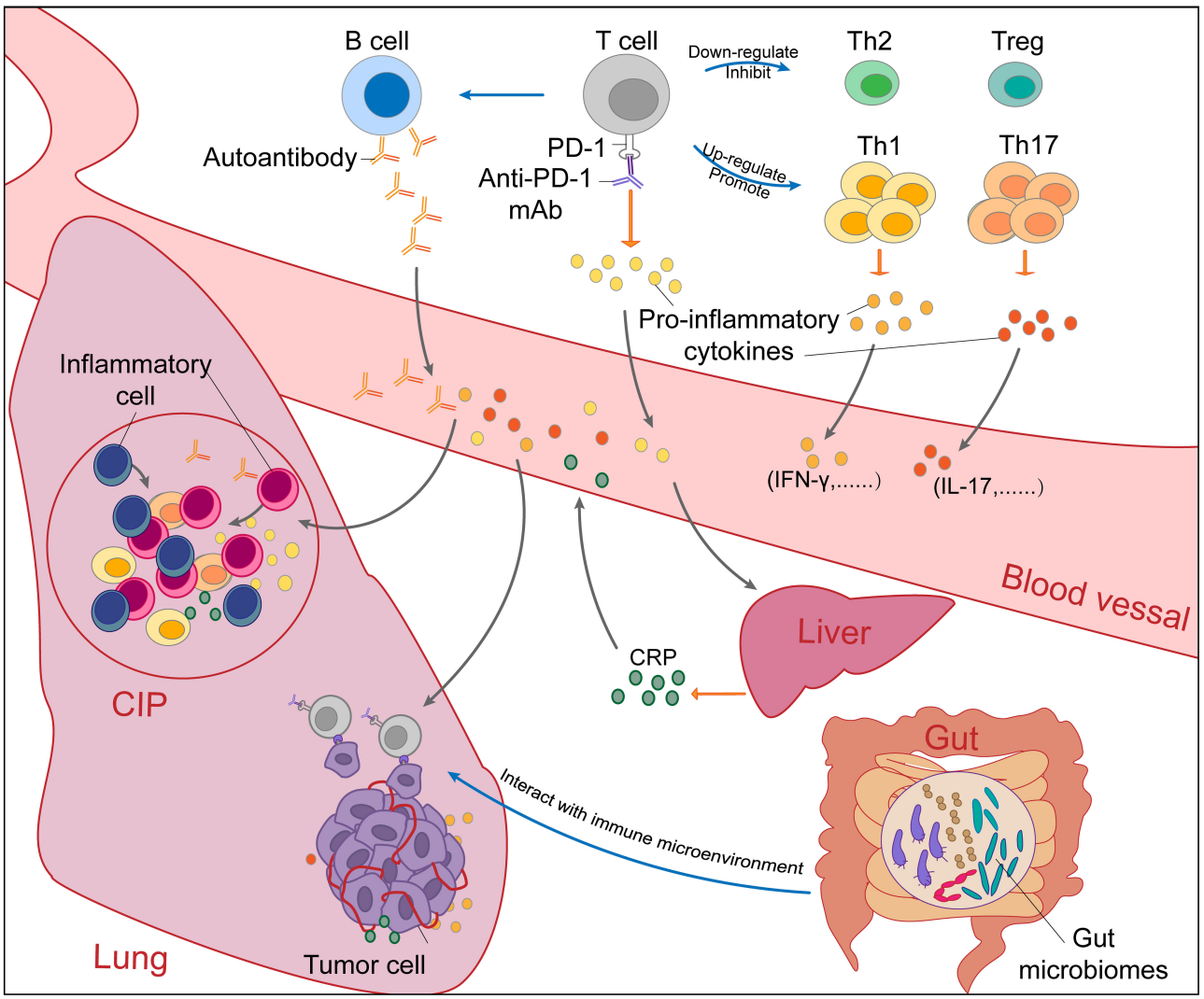

FIGURE 2 | The potential mechanisms of checkpoint inhibitor pneumonitis (CIP) in NSCLC patients receiving PD-1/PD-L1 inhibitor monotherapy. The occurrence of checkpoint inhibitor pneumonitis (CIP) in NSCLC is the result of a combination of many factors. Blockade of the PD-1-PD-L1 pathway by PD-1/PD-L1 mAbs (PD-1 mAb in the figure, for example) will upregulate and promote Th1 and Th17 cells and downregulate and inhibit Th2 cells and Tregs. Without immunosuppression of Th2 cells and Tregs, excessive immune responses and cytokine secretion of Th1 and Th17 cells will cause autoimmune damage in normal tissues such as the lung. In addition, autoantibodies increased after PD-1/PD-L1 blockade can also cause normal tissue lesions. Proinflammatory cytokines secreted by activated T cells promote the infiltration of inflammatory cells. Under the stimulation of IL-6, CRP produced by the liver will promote inflammation and strengthen autoimmunity. Through the "gut-lung axis", gut microbiomes can regulate the immune microenvironment in the lung. Overall, the immune dysregulation caused by PD-1/PD-L1 blockade leads to the occurrence and development of CIP. NSCLC, non-small cell cancer; CIP, checkpoint inhibitor pneumonitis; PD-1, programmed cell death protein 1; PD-L1, programmed cell death protein ligand-1; mAbs, monoclonal antibody; Th, helper T cell; IL, Interleukin; CRP, C-reactive protein.

3.1.3 Th17

Th17 cells are a subset of T cells that produce IL-17. Th17 lymphocytes exist in the anatomic barrier, mainly in the digestive system and lungs (85). In previous studies, the antitumor role of Th17 cells seems to be contradictory. On the one hand, Th17 cells can recruit $CD8^+$ cytotoxic T cells and promote their activation and expansion to inhibit the growth of tumors (86, 87). On the other hand, IL-17A produced by Th17 cells has been shown to enhance tumor angiogenesis (88). Jaclyn W. McAlees et al. found that the levels of Th1 and Th17 cells increased in naïve $PD\text{-}1^{-/-}$ mice, while the production of cytokines in polarized Th1 and Th17 cells *in vitro* was restricted in WT cells with PD-1 ligation (89). In this way, anti-PD-1 therapy may enhance the antitumor function of Th17 cells. Yun et al. found that under certain conditions, Th17 cells can transform into Th1 cells, lose the secretion of IL-17A, and then secrete interferon γ (IFN-γ), which plays a role in enhancing autoimmunity and antitumor activity (90). As mentioned above, Tregs can suppress the amplification of Th1 cells, but Tregs cannot inhibit the transformation of Th17 cells into Th1 cells (91). After blocking

PD-1/PD-L1, the decrease in Tregs may lead to an imbalance in Treg/Th17 cells. The dysregulation of Treg/Th17 cells is related to a variety of autoimmune diseases (92), which may lead to autoimmune adverse events after PD-1/PD-L1 inhibitor treatment. The pathological presence of Th17 lymphocytes has also been described in the TME of many cancers, including lung cancer (93). In lung cancer mouse models, Th17 and IL-17 have been proven to be involved in tumorigenesis through their proinflammatory effects, as well as the occurrence of toxic effects such as interstitial pneumonia (94).

3.2 Increased Preexisting and Emerging Autoantibodies

An increasing series of studies have shown that the occurrence of irAEs may be associated with increased preexisting and emerging autoantibodies in human immunity. PD-1-targeted therapy leads to the dysfunction of Tregs and mediates the production of pathological autoantibodies in both PD-1-knockout mice and patients (95, 96). A multivariate analysis indicated that the presence of preexisting antibodies, such as rheumatoid factor (RF), antinuclear antibody, antithyroglobulin, and antithyroid peroxidase, was independently associated with the development of irAEs in different organs. It can be concluded that increased preexisting and emerging autoantibodies are probably involved in the mechanism of CIP. Salahaldin A. Tahir et al. found a median 1.34-fold significant increase in autoantibodies against CD74 after immune checkpoint therapy in patients with immune-related pneumonia, which suggested that CD74 autoantibodies play a role in pneumonitis (55). CD74, an autoantibody active protein, can stimulate the release of inflammatory mediators (97) as an intracellular chaperone of major histocompatibility complex class II (MHC-II) but is expressed on the cell membrane of immune cells, including macrophages (55). Taken together, the above results suggest that elevated levels of preexisting or emerging autoantibodies play a role in the development of immune-related adverse events.

3.3 Unbalanced Inflammatory Cytokines

Cytokines, a class of small molecular proteins with a wide range of biological activities, are mainly synthesized and secreted by immune cells. Cytokines have multiple biological functions, such as regulating innate immunity and adaptive immunity, influencing tumor growth and participating in inflammation (98). The pathophysiological mechanisms of immune-related adverse events are also thought to be mediated *via* cytokines. Lim and colleagues analyzed the expression of 65 cytokines in longitudinal plasma samples collected prior to therapy and during treatment in melanoma patients treated with ICIs alone or in combination. Eleven circulating cytokines (G-CSF, GM-CSF, Fractalkine, FGF-2, IFNα2, IL-12p70, IL-1α, IL1, IL-1RA, IL-2 and IL-13) were significantly upregulated at baseline and early during treatment and were associated with the development of high-grade irAEs (99). In a similar study, 40 cytokines were assessed in plasma. Shaheen Khan et al. found that the upregulation of various cytokines, especially induced C-X-C motif chemokine ligand (CXCL) 9, 10, 11 and 13 after ICI treatment, was closely associated with the development of irAEs (100). CXCL9, CXCL10 and CXCL11 can activate T cells by binding to C-X-C motif chemokine receptor (CXCR) 3 and have been implicated in a variety of autoimmune diseases, including thyroiditis, systemic sclerosis, and inflammatory bowel disease (IBD) (101). ICIs can activate T cells, leading to excessive release of cytokines and powerful proinflammatory reactions, which promote the development of irAEs.

Although a large number of cytokines related to the occurrence of irAEs have been found, a considerable lack of data has been reported about CIP in NSCLC patients during anti-PD-1/PD-L1 treatment. At present, there are three main types of cytokines related to the occurrence of CIP: C-reactive protein (CRP), IL-6 and IL-17.

3.3.1 CRP and IL-6

CRP is an acute phase protein that is secreted by liver cells in response to inflammatory cytokines such as IL-6 and tumor necrosis factor-α (TNF-α) (102). A retrospective study reported that serum CRP levels were significantly elevated in patients with irAEs, such as pituitary inflammation, hepatitis, thyroiditis and autoimmune colitis (103). IL-6 has a proinflammatory effect in the TME (104) and plays an active role in innate and adaptive immunity, such as the activation of Th cells, inhibition of Tregs, and differentiation of B cells (105). Several studies have shown that elevated levels of IL-6 after ICI treatment are closely related to irAEs, such as psoriasiform (89) and Crohn's disease (106). Wussler, Kozhuharov et al. (107) have shown that IL-6 and CRP were significantly higher in patients with pneumonia. CRP and IL-6 levels are elevated in NSCLC patients who developed CIP after atezolizumab treatment compared with baseline levels (108). Therefore, the development of CIP may be attributed to the excessive activation of the immune system induced by CRP and IL-6 as well as its powerful pro-inflammatory properties. Taken together, the above results suggest that dysregulated immune activation and supraphysiological levels of CRP and IL-6 are involved in the mechanism of CIP in NSCLC patients.

3.3.2 IL-17

IL-17 is an important cytokine with diverse functions, playing an important role in autoimmune diseases and inflammation. IL-17 is expressed in $CD8^+$ T cells, natural immune γδ T cells, NK cells and ILC3s in the lungs. The abnormal expression of IL-17 is associated with the pathology of many lung diseases, including asthma, pneumonia and pulmonary fibrosis (109). In addition, IL-17 has been found to be associated with the development of some irAEs, such as colitis (110) and psoriasiform dermatologic toxicity (111). Lou et al. showed that the levels of IL-17 in serum significantly increased in NSCLC patients with CIP following ICI treatment (112). The underlying mechanism may be that blocking PD-1 and PD-L1 could destroy immune tolerance and increase the activation of T cells (113), including the increase in Th17 cells in peripheral blood (114). An increase in the percentages of Th1 and Th17 cells can induce higher levels of IL-17A in plasma and BALF (71). It is worth noting that the levels of IL-17A and IL-35 increased when CIP was diagnosed

and decreased during clinical recovery, indicating that IL-17A is related to the occurrence and development of CIP. Therefore, IL-17 may mediate off-target lung destruction in CIP.

3.4 Different Treatment Modes

A higher incidence and severity of CIP have been observed with anti-PD-1 therapy than PD-L1 inhibitors in patients with NSCLC, suggesting that the mechanisms of CIP induced by the two agents are not completely the same (28). The incidence and severity difference of CIP may be related to PD-1 ligands, including PD-L1 and PD-L2. It has been confirmed in animal models that the expression of programmed death ligand 2 (PD-L2) in tumor cells may inhibit antitumor immunity and may be involved in the resistance to monoanti-PD-L1 therapy (115). It is conceivable that the blockade of PD-L1 and PD-L2 with PD-1 inhibitors can reverse such resistance and enhance antitumor immunity. However, at the same time, the blockade of PD-1 triggers stronger T cell expansion and cytokine production without timely braking or clearing, which causes the occurrence of CIP (116). Cells expressing PD-L2 mainly include activated T cells, DCs, macrophages and Th2 cells (117). PD-L1 inhibitors do not influence the interaction between PD-L2 and its receptor PD-1, which is associated with immune tolerance in lung tissue. However, PD-1 inhibitors can not only block the interaction between PD-1 and its ligands PD-L1 and PD-L2 but also increase the binding of PD-L2 to repulsive guidance molecule b (RGMb). RGMb has been observed to be expressed in lung interstitial macrophages, alveolar epithelial cells and other cells of the immune system, such as CD4+ and CD8+ T cells (118). Blockade of PD-1-PD-L2 signaling has been observed to increase cytokine production and/or CD4+ T cell proliferation (119). Moreover, the increased interaction of RGMb–PD-L2 mediated by PD-1 inhibitors might disrupt the immune tolerance of lung tissue by increasing the vigorous clonal expansion of T cells that reside in the lung and then lead to the occurrence of pneumonitis (118) (**Figure 3**). Recently, the combination of radiotherapy and immunotherapy has attracted increasing attention. This combination therapy model has shown improved efficacy in patients with NSCLC (120). However, a history of previous radiotherapy may increase the incidence of CIP (42, 121). Myers and Lu found significantly elevated T cells in pulmonary tissues of C57BL/6 mice after combination therapy with anti-PD-1 and thoracic irradiation. They suggested that healthy tissue damaged by thoracic irradiation is more easily destroyed by T cells activated during ICI treatment, which may be the underlying mechanism of the increased incidence of CIP after radiotherapy (122). Furthermore, oxidative damage of DNA, overinfiltration of immune cells, upregulation of proinflammatory factors, and deposition of collagen induced by radiotherapy may alternate the immune microenvironment of the lung and make it more vulnerable to the stronger immune response caused by PD-1/L1 inhibitors (116, 123). A higher incidence of pneumonitis has been observed during the combination therapy of ICIs with other antitumor drugs, such as chemotherapeutic drugs (10) and EGFR tyrosine kinase inhibitors (TKIs) (124). The mechanisms underlying the increased risk of pneumonitis mediated by combination therapies are not clear. One of the reasons may be due to the additive effects of toxicities, and further preclinical studies are still needed to explore the exact mechanism.

3.5 Other Potential Mechanisms

The regulation of gut microbiomes on immunity may be related to the effect and toxicity of immunotherapy (125–127). Gut microbiome transplantation has been reported to treat CTLA-4-associated immune colitis (128). Hakozaki et al. observed differences in gut microbiomes in advanced NSCLC patients with low- and high-grade irAEs (129). The role of microbiomes in the "gut-lung axis" formed by releasing immune substances or migrating to interact with microbiota colonized in the respiratory system has also attracted increasing attention. Increasing attention has been given to the role of the "gut-lung axis" formed by the interaction between microbiomes colonized in the gut and respiratory system (130, 131). Further research is needed to determine whether microbiomes play a role in CIP. Compared with gut microbiomes, there are few studies on the relationship between respiratory microbiomes and immunotherapy in cancer patients. Studies have shown that anti-PD-1 treatment can increase the alpha diversity and abundance of specific microbes (132, 133). Zhang et al. (134) found that featured respiratory microbes such as enriched Streptococcus may enhance antitumor immune responses by increasing antigen presentation and effector T cell function, which may increase the incidence of irAEs, including CIP.

Noncoding RNAs may also be involved in the regulation of irAEs. Marschner and colleagues observed a higher incidence of severe irAEs in different organs, including the lung, in mice lacking microRNA-146a (miR-146a). They recently detected SNPs in the miR-146a gene in humans and found that reduced miR-146a expression caused by SNP rs2910164 was related to an increased risk of severe irAEs, reduced progression-free survival and increased neutrophil counts both at baseline and during ICI treatment (135). Further research is still needed to determine whether and how miR-146a affects the development of irAEs, especially CIP.

In addition, B cells, natural killer (NK) cells, and dendritic cells may also be involved in the development of CIP after PD-1 blockade (136–138). The expression of PD-1 on NK cells has been observed in cancer patients (138). Hsu et al. (139) found that NK cells expressing PD-1 may mediate immunosuppression in tumors by interacting with PD-L1$^+$ tumor cells. PD-1/PD-L1 blockade can activate the cytotoxicity of NK cells to tumors by releasing PD-1–imposed immune inhibition. When ICI treatment induces inflammation in nonmalignant lung tissue through various non-NK cell-mediated mechanisms, activated NK cells can directly kill infected cells and produce proinflammatory cytokines. Thus, NK cell activation mediated by PD-1/PD-L1 blockade may promote inflammation and aggravate damage to normal lung tissues.

4 MANAGEMENT OF CIP

The treatment of CIP varies among the clinical grades of CIP. Current treatment options mainly include interruption of ICI therapy, glucocorticoid administration, and immunosuppressive medications such as intravenous immunoglobulins (IVIG), infliximab, cyclophosphamide, and mycophenolate mofetil (7,

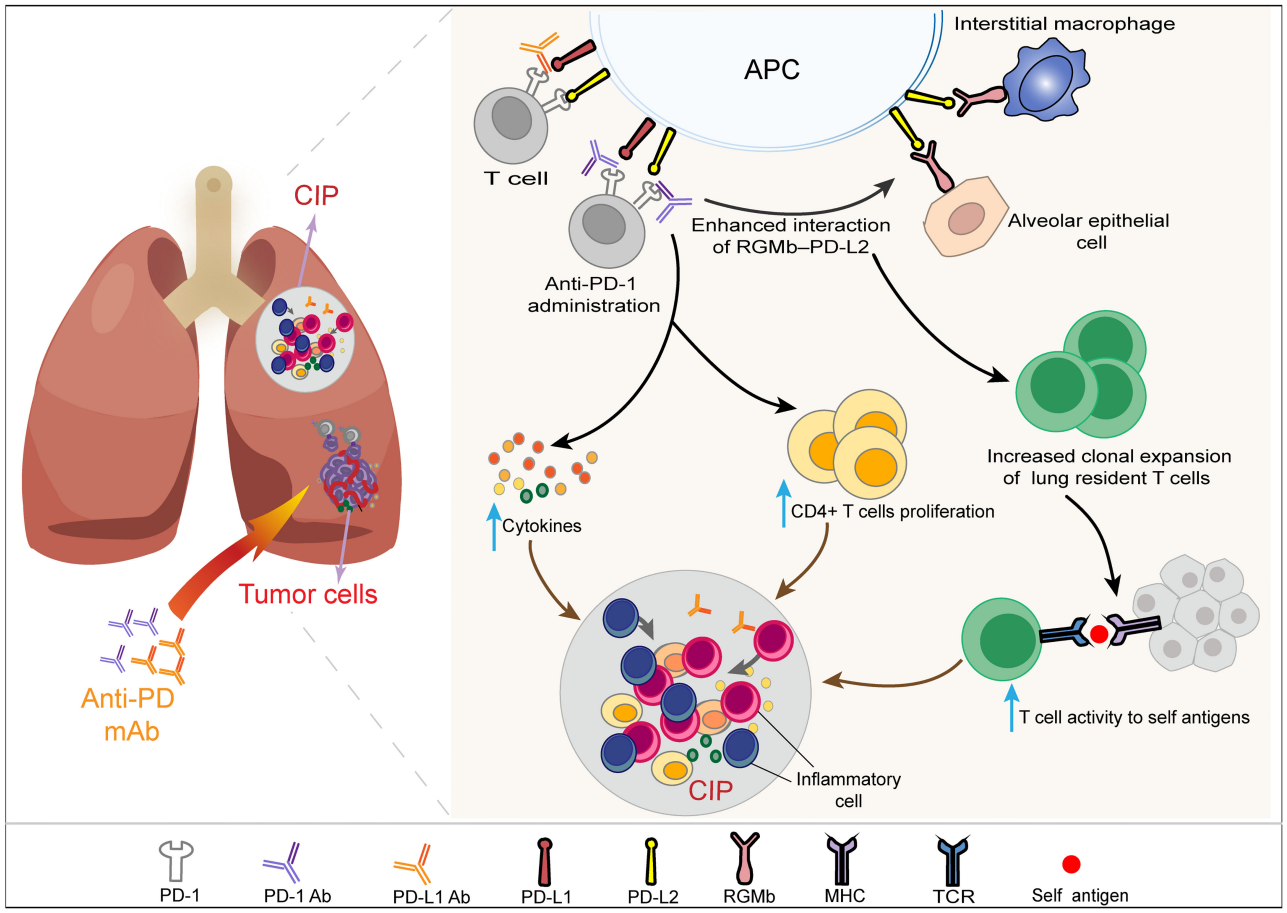

FIGURE 3 | Schematic diagram of the difference in the mechanism of CIP mediated by PD-L1 inhibitor and PD-1 inhibitor monotherapy. The mechanisms of checkpoint inhibitor pneumonitis (CIP) induced by PD-1 inhibitors and PD-L1 inhibitors in patients with NSCLC are not completely the same and may be related to PD-1 ligands, including PD-L1 and PD-L2. PD-L1 blockade does not influence the binding between PD-L2 and its receptor PD-1, which is associated with immune tolerance in lung tissue. PD-1 inhibitors can simultaneously block the interaction between PD-1 and its ligands, including PD-L1 and PD-L2. The blockade of PD-1-PD-L2 signaling by PD-1 inhibitors has been observed to increase cytokine production and/or CD4+ T cell proliferation, which can increase the incidence and severity of CIP compared with PD-L1 inhibitors. Moreover, the application of a PD-1 inhibitor can increase the binding of PD-L2 to repulsive guidance molecule b (RGMb). RGMb has been observed to be expressed in lung interstitial macrophages, alveolar epithelial cells and other cells of the immune system. The interaction of RGMb–PD-L2 can increase T cell activity to self-antigens by increasing the clonal expansion of T cells that reside in the lung and then damage normal lung tissue. NSCLC, non-small cell cancer; CIP, checkpoint inhibitor pneumonitis; PD-1, programmed cell death protein 1; PD-L1, programmed cell death protein ligand-1; PD-L2, programmed cell death protein ligand-2; RGMb, repulsive guidance molecule b.

14, 14, 139–142). There are several published guidelines that are involved in the management of CIP (14, 140, 143). These guidelines have issued different recommendations for patients with CIP according to their toxicity severity from grade 1 (mildest) to grade 5 (death associated with toxicity). For grade 1 CIP (asymptomatic), ICI might be considered holding while closely monitoring the symptoms of patients every 2–3 days with repeated chest CT scans and pulmonary function testing at least every 3 weeks. If any of the symptoms, radiographic testing or pulmonary function deteriorates, ICI therapy can be withdrawn, and systemic corticosteroid therapy should be initiated. Patients with grade 2 CIP need to withhold ICI therapy immediately and recommend systemic methylprednisolone treatment (0.5–1.0 mg/kg daily). Steroids can be administered orally or intravenously and taper over 4–6 weeks if symptoms improve after 48–72 h. Empiric treatment with antibiotics should start if infection is suspected. When no clinical improvement can be observed 48–72 hours after the beginning of steroid treatment, patients with CIP should be treated as grade 3–4. For grade 3–4 CIP, these patients should permanently discontinue ICI treatment and be hospitalized. Current guidelines recommend that methylprednisolone should be administered orally or intravenously at a dose of 2–4 mg/kg/day, along with empirical antibiotic therapy. If symptoms improve after 48–72 h, steroids should be tapered over 8 weeks. In contrast, if symptoms do not improve or deteriorate, additional immunosuppressive therapy should be considered. Currently, immunosuppressive agents mainly include IVIG, infliximab, cyclophosphamide, and

mycophenolate mofetil (MMF) (14, 140, 143). In addition, IL-6 blockade (tocilizumab) may be a potential second-line treatment for CIP without affecting the efficacy of immunotherapy (144, 145). However, the agent still lacks clear evidence of efficacy and safety, which needs further investigation.

5 POTENTIAL PREDICTIVE BIOMARKERS OF CIP

CIP is a life-threatening adverse event in some instances and possesses a higher rate in NSCLC than other tumor types. Thus, potential predictive biomarkers for CIP are necessary. The potential biomarkers reported to date mainly involve cell-based biomarkers, chemokines/cytokines, autoantibodies and genetics. In addition, there are some other emerging novel biomarkers on the rise, such as tumor genomics, microbiome and radiographic features (146). Recently, Lin et al. (147) conducted a real-world retrospective study to explore blood biomarkers related to the occurrence and prognosis of CIP in lung cancer patients. They found that increased levels of IL-6 and IL-10, neutrophil to lymphocyte ratio (NLR), platelet-to-lymphocyte ratio (PLR), and lactate dehydrogenase (LDH) or reduced absolute lymphocyte count (ALC) and albumin (ALB) levels during ICI treatment may act as biomarkers for the early diagnosis of CIP. Furthermore, squamous carcinoma may be related to an increased risk of CIP, and an increase in IL-6 levels along with a reduction in ALB levels at the onset of CIP were predictive of severe grade and poor prognosis of CIP. A case report has shown increased levels of several cytokines, including IL-1 receptor antagonist (IL-1 RA), IL2 RA and CXCL2, during radiation followed by ICI therapy, which indicates that these cytokines may be promising biomarkers for predicting the development of pneumonitis induced by combined therapy with radiation and ICIs (148). An increased level of anti-CD74 autoantibody pre- and posttreatment is considered a potential predictive biomarker for the development and timely treatment of CIP (55). Moreover, a high baseline absolute eosinophil count ($\geq 0.125 \times 10^9$ cells/L) can serve as a biomarker for predicting an increased risk of CIP (54). Hoefsmit et al. extensively explored the susceptible genetic loci likely to be related to irAEs. They found that several immune-related genes, including surfactant protein C (SP-C), autoimmune regulator (AIRE), telomerase reverse transcriptase (TERT) and mucin 5B oligomeric mucus/gel forming (MUC5B), might contribute to predicting the development of CIP (149).

6 DISCUSSION

CIP is rare but can be life threatening and accounts for 35% of PD-1 and PD-L1 inhibitor-related deaths. The incidence and onset time of CIP can vary due to different PD-1/PD-L1 agents. The excessive immune response caused by the extra blockade of PD-L2 with a PD-1 inhibitor may be involved in the onset of CIP. Combination therapy has a higher incidence of CIP than monotherapy, with a shorter median onset time. The possible mechanism is the overlap of pulmonary toxicity of different treatments.

In this article, we pay close attention to the clinical features of pulmonary irAEs during PD-1/PD-L1 blockade, implying that clinicians should monitor patients receiving anti-PD-1/PD-L1 therapy to optimize clinical safety and efficacy. The clinical symptoms of pulmonary toxicity, radiological examination, especially chest CT and BALF, play an important role in the diagnosis of CIP. Clinicians should be fully aware of the association between the presence of CIP and cancer outcomes in NSCLC, balancing the benefits and risks of immunotherapy and thereby identifying patients who would gain most from treatment.

There is growing evidence that several possible mechanisms are involved in the development of CIP, and it is clear that there are multiple factors at play, such as disordered T cell subsets, increased preexisting and emerging autoantibodies, unbalanced inflammatory cytokines, previous chest radiotherapy, previous lung disease and combined immunotherapy. Further prospective studies on the mechanisms of CIP are needed to provide a more comprehensive and robust management of CIP. Deep studies on the mechanism of CIP in NSCLC are still limited. Preclinical studies on the molecular and histopathology of irAEs are in progress. To better understand the mechanism, the establishment of animal models is necessary. At present, some models have been established (150, 151). However, there is still a lack of empirical evidence regarding whether the existing models can truly reproduce the complex tumor microenvironment in the human body and whether the models are repeatable. Furthermore, research on biomarkers is also underway (152–154), which will be instrumental in the prediction, diagnosis and monitoring of CIP. Further research should aim to explore a series of biomarkers that can efficiently and timely predict the development, diagnosis, treatment and prognosis of CIP to achieve early detection and diagnosis of CIP.

Immunotherapy has crossed the gap of cancer treatment. As the main immune checkpoint inhibitors for the treatment of NSCLC, the combined treatment of PD-1/PD-L1 and CTLA-4 inhibitors has a better response and long-term cancer control, but it increases the incidence of CIP (155, 156). The emergence of novel checkpoint inhibitors, such as LAG-3, TIM-3, TIGHT, VISTA inhibitors and dual immunomodulators (targeting PD-1 and LAG-3), may change the existing immunotherapy strategies (157, 158). However, when it brings possible synergy, it may also bring potential irAEs. More clinical trials on the efficacy and safety of novel immune checkpoint inhibitors and combination therapies are needed. As a new therapeutic method, chimeric antigen receptor T cell (CAR-T) immunotherapy has played an increasingly important role in cancer treatment. A recent study reported that the recruitment and infiltration of CAR-T cells in NSCLC tumors can be enhanced when combined with a PD-1 inhibitor and immunogenic chemotherapy (159). Whether the combination of immunotherapies will affect the incidence and severity of irAEs needs more clinical data. For the treatment of NSCLC, various new immunotherapy modes, such as new immune checkpoint inhibitors, CAR-T therapy, ICIs combined chemoradiotherapy and targeted therapy, still need to balance efficacy and safety to optimize the optimal treatment regimen.

Understanding the mechanism of CIP will help to better manage patients with adverse events. At present, glucocorticoids are the main

treatment, but some irAEs are insensitive to glucocorticoid. Mechanism-based therapy can improve symptoms, avoid treatment interruption or dose reduction due to irAEs, and finally prolong overall survival.

AUTHOR CONTRIBUTIONS

JY and YW collected information and wrote the manuscript. XY reviewed clinical studies and helped process the tables. LG provided language editing. JX conceived the idea for this review article. All authors contributed to the article and approved the submitted version.

FUNDING

This work was supported by National Natural Science Foundation of China (No. 81872478) and the Outstanding Youth Talent Foundation for Science and Technology of Sichuan Province (2022JDJQ0056).

REFERENCES

1. Siegel RL, Miller KD, Fuchs HE, Jemal A. Cancer Statistics, 2021. *CA Cancer J Clin* (2021) 71:7–33. doi: 10.3322/caac.21654
2. Toi Y, Sugawara S, Kawashima Y, Aiba T, Kawana S, Saito R, et al. Association of Immune-Related Adverse Events With Clinical Benefit in Patients With Advanced Non-Small-Cell Lung Cancer Treated With Nivolumab. *Oncologist* (2018) 23:1358–65. doi: 10.1634/theoncologist.2017-0384
3. Naidoo J, Wang X, Woo KM, Iyriboz T, Halpenny D, Cunningham J, et al. Pneumonitis in Patients Treated With Anti-Programmed Death-1/Programmed Death Ligand 1 Therapy. *J Clin Oncol* (2017) 35:709–17. doi: 10.1200/jco.2016.68.2005
4. Rittmeyer A, Barlesi F, Waterkamp D. Atezolizumab Versus Docetaxel in Patients With Previously Treated non-Small-Cell Lung Cancer (OAK): A Phase 3, Open-Label, Multicentre Randomised Controlled Trial. *Lancet* (2017) 389:255–65. doi: 10.1016/S0140-6736(16)32517-X
5. Antonia SJ, Villegas A, Daniel D, Vicente D, Murakami S, Hui R, et al. Durvalumab After Chemoradiotherapy in Stage III Non–Small-Cell Lung Cancer. *N Engl J Med* (2017) 377:1919–29. doi: 10.1056/NEJMoa1709937
6. *FDA Approves Cemiplimab-rwlc for Non-small Cell Lung Cancer With High PD-L1 Expression* (2021). Available at: https://www.fda.gov/drugs/resources-information-approved-drugs/fda-approves-cemiplimab-rwlc-non-small-cell-lung-cancer-high-pd-l1-expression.
7. Friedman CF, Proverbs-Singh TA, Postow MA. Treatment of the Immune-Related Adverse Effects of Immune Checkpoint Inhibitors: A Review. *JAMA Oncol* (2016) 2:1346–53. doi: 10.1001/jamaoncol.2016.1051
8. National Cancer Institute. *Common Terminology Criteria for Adverse Events (CTCAE)*. Version 4.0.(2010). Available at: http://ctep.cancer.gov/protocolDevelopment/electronic_applications/ctc.htm [Accessed November 25, 2021].).
9. Wang DY, Salem J-E, Cohen JV, Chandra S, Menzer C, Ye F, et al. Fatal Toxic Effects Associated With Immune Checkpoint Inhibitors A Systematic Review and Meta-Analysis. *JAMA Oncol* (2018) 4:1721–28. doi: 10.1001/jamaoncol.2018.3923
10. Paz-Ares L, Luft A, Vicente D, Tafreshi A, Gümüş M, Mazières J, et al. Pembrolizumab Plus Chemotherapy for Squamous Non-Small-Cell Lung Cancer. *N Engl J Med* (2018) 379:2040–51. doi: 10.1056/NEJMoa1810865
11. Ferrara R, Mezquita L, Texier M, Lahmar J, Audigier-Valette C, Tessonnier L, et al. Hyperprogressive Disease in Patients With Advanced Non-Small Cell Lung Cancer Treated With PD-1/PD-L1 Inhibitors or With Single-Agent Chemotherapy. *JAMA Oncol* (2018) 4:1543–52. doi: 10.1001/jamaoncol.2018.3676
12. Zhai X, Zhang J, Tian Y, Li J, Jing W, Guo H, et al. The Mechanism and Risk Factors for Immune Checkpoint Inhibitor Pneumonitis in non-Small Cell Lung Cancer Patients. *Cancer Biol Med* (2020) 17:599–611. doi: 10.20892/j.issn.2095-3941.2020.0102
13. Tong ZQ, Wu DY, Liu D, Dong M. Incidence Risk of PD-1/PD-L1-Related Pneumonia and Diarrhea in Non-Small Cell Lung Cancer (NSCLC) Patients: A Systematic Review and Meta-Analysis of Randomized Controlled Trials. *Eur J Clin Pharmacol* (2021) 77:1079–88. doi: 10.1007/s00228-020-03083-9
14. Haanen J, Carbonnel F, Robert C, Kerr KM, Peters S, Larkin J, et al. Management of Toxicities From Immunotherapy: ESMO Clinical Practice Guidelines for Diagnosis, Treatment and Follow-Up. *Ann Oncol* (2017) 28: iv119–42. doi: 10.1093/annonc/mdx225
15. Brahmer J, Reckamp KL, Baas P, Crino L, Eberhardt WEE, Poddubskaya E, et al. Nivolumab Versus Docetaxel in Advanced Squamous-Cell Non-Small-Cell Lung Cancer. *N Engl J Med* (2015) 373:123–35. doi: 10.1056/NEJMoa1504627
16. Borghaei H, Paz-Ares L, Horn L, Spigel DR, Steins M, Ready NE, et al. Nivolumab Versus Docetaxel in Advanced Nonsquamous Non-Small-Cell Lung Cancer. *N Engl J Med* (2015) 373:1627–39. doi: 10.1056/NEJMoa1507643
17. Hellmann MD, Ciuleanu TE, Pluzanski A, Lee JS, Otterson GA, Audigier-Valette C, et al. Nivolumab Plus Ipilimumab in Lung Cancer With a High Tumor Mutational Burden. *N Engl J Med* (2018) 378:2093–104. doi: 10.1056/NEJMoa1801946
18. Ahn MJ, Gandhi L, Hamid O, Hellmann MD, Garon EB, Ramalingam SS, et al. 459p Risk of Pneumonitis in Patients With Advanced NSCLC Treated With Pembrolizumab in KEYNOTE-001. *Ann Oncol* (2015) 26:ix125–47. doi: 10.1093/annonc/mdv532.43
19. Herbst RS, Baas P, Kim DW, Felip E, Pérez-Gracia JL, Han JY, et al. Pembrolizumab Versus Docetaxel for Previously Treated, PD-L1-Positive, Advanced Non-Small-Cell Lung Cancer (KEYNOTE-010): A Randomised Controlled Trial. *Lancet* (2016) 387:1540–50. doi: 10.1016/s0140-6736(15)01281-7
20. Reck M, Rodríguez-Abreu D, Robinson AG, Hui R, Csőszi T, Fülöp A, et al. Pembrolizumab Versus Chemotherapy for PD-L1-Positive Non-Small-Cell Lung Cancer. *N Engl J Med* (2016) 375:1823–33. doi: 10.1056/NEJMoa1606774
21. Mok TSK, Wu YL, Kudaba I, Kowalski DM, Cho BC, Turna HZ, et al. Pembrolizumab Versus Chemotherapy for Previously Untreated, PD-L1-Expressing, Locally Advanced or Metastatic non-Small-Cell Lung Cancer (KEYNOTE-042): A Randomised, Open-Label, Controlled, Phase 3 Trial. *Lancet* (2019) 393:1819–30. doi: 10.1016/s0140-6736(18)32409-7
22. Sezer A, Kilickap S, Gümüş M, Bondarenko I, Özgüroğlu M, Gogishvili M, et al. Cemiplimab Monotherapy for First-Line Treatment of Advanced non-Small-Cell Lung Cancer With PD-L1 of at Least 50%: A Multicentre, Open-Label, Global, Phase 3, Randomised, Controlled Trial. *Lancet* (2021) 397:592–604. doi: 10.1016/s0140-6736(21)00228-2
23. Herbst RS, Giaccone G, de Marinis F, Reinmuth N, Vergnenegre A, Barrios CH, et al. Atezolizumab for First-Line Treatment of PD-L1–Selected Patients With NSCLC. *N Engl J Med* (2020) 383:1328–39. doi: 10.1056/NEJMoa1917346
24. Nishio M, Barlesi F, West H, Ball S, Bordoni R, Cobo M, et al. Atezolizumab Plus Chemotherapy for First-Line Treatment of Nonsquamous NSCLC: Results From the Randomized Phase 3 IMpower132 Trial. *J Thorac Oncol* (2021) 16:653–64. doi: 10.1016/j.jtho.2020.11.025
25. West H, McCleod M, Hussein M, Morabito A, Rittmeyer A, Conter HJ, et al. Atezolizumab in Combination With Carboplatin Plus Nab-Paclitaxel Chemotherapy Compared With Chemotherapy Alone as First-Line Treatment for Metastatic non-Squamous non-Small-Cell Lung Cancer (IMpower130): A Multicentre, Randomised, Open-Label, Phase 3 Trial. *Lancet Oncol* (2019) 20:924–37. doi: 10.1016/s1470-2045(19)30167-6
26. Antonia SJ, Villegas A, Daniel D, Vicente D, Murakami S, Hui R, et al. Durvalumab After Chemoradiotherapy in Stage III Non-Small-Cell Lung Cancer. *N Engl J Med* (2017) 377:1919–29. doi: 10.1056/NEJMoa1709937

27. Rizvi NA, Cho BC, Reinmuth N, Lee KH, Luft A, Ahn MJ, et al. Durvalumab With or Without Tremelimumab vs Standard Chemotherapy in First-Line Treatment of Metastatic Non-Small Cell Lung Cancer: The MYSTIC Phase 3 Randomized Clinical Trial. *JAMA Oncol* (2020) 6:661–74. doi: 10.1001/jamaoncol.2020.0237
28. Khunger M, Rakshit S, Pasupuleti V, Hernandez AV, Mazzone P, Stevenson J, et al. Incidence of Pneumonitis With Use of Programmed Death 1 and Programmed Death-Ligand 1 Inhibitors in Non-Small Cell Lung Cancer: A Systematic Review and Meta-Analysis of Trials. *Chest* (2017) 152:271–81. doi: 10.1016/j.chest.2017.04.177
29. Durm GA, Jabbour SK, Althouse SK, Liu Z, Sadiq AA, Zon RT, et al. A Phase 2 Trial of Consolidation Pembrolizumab Following Concurrent Chemoradiation for Patients With Unresectable Stage III Non-Small Cell Lung Cancer: Hoosier Cancer Research Network LUN 14-179. *Cancer* (2020) 126:4353–61. doi: 10.1002/cncr.33083
30. Peters S, Felip E, Dafni U, Belka C, Guckenberger M, Irigoyen A, et al. Safety Evaluation of Nivolumab Added Concurrently to Radiotherapy in a Standard First Line Chemo-Radiotherapy Regimen in Stage III Non-Small Cell Lung Cancer-The ETOP NICOLAS Trial. *Lung Cancer* (2019) 133:83–7. doi: 10.1016/j.lungcan.2019.05.001
31. Nishino M, Giobbie-Hurder A, Hatabu H, Ramaiya NH, Hodi FS. Incidence of Programmed Cell Death 1 Inhibitor-Related Pneumonitis in Patients With Advanced Cancer: A Systematic Review and Meta-Analysis. *JAMA Oncol* (2016) 2:1607–16. doi: 10.1001/jamaoncol.2016.2453
32. Yang H, Jin T, Li M, Xue J, Lu BJPCM. Synergistic Effect of Immunotherapy and Radiotherapy in Non-Small Cell Lung Cancer: Current Clinical Trials and Prospective Challenges. *Precis Clin Med* (2019) 2:57–70. doi: 10.1093/pcmedi/pbz004
33. Cousin F, Desir C, Ben Mustapha S, Mievis C, Coucke P, Hustinx R. Incidence, Risk Factors, and CT Characteristics of Radiation Recall Pneumonitis Induced by Immune Checkpoint Inhibitor in Lung Cancer. *Radiother Oncol* (2021) 157:47–55. doi: 10.1016/j.radonc.2021.01.001
34. Kato T, Masuda N, Nakanishi Y, Takahashi M, Hida T, Sakai H, et al. Nivolumab-Induced Interstitial Lung Disease Analysis of Two Phase II Studies Patients With Recurrent or Advanced Non-Small-Cell Lung Cancer. *Lung Cancer* (2017) 104:111–8. doi: 10.1016/j.lungcan.2016.12.016
35. Suresh K, Voong KR, Shankar B, Forde PM, Ettinger DS, Marrone KA, et al. Pneumonitis in Non-Small Cell Lung Cancer Patients Receiving Immune Checkpoint Immunotherapy: Incidence and Risk Factors. *J Thorac Oncol* (2018) 13:1930–9. doi: 10.1016/j.jtho.2018.08.2035
36. Morita R, Okishio K, Shimizu J, Saito H, Sakai H, Kim YH, et al. Real-World Effectiveness and Safety of Nivolumab in Patients With non-Small Cell Lung Cancer: A Multicenter Retrospective Observational Study in Japan. *Lung Cancer* (2020) 140:8–18. doi: 10.1016/j.lungcan.2019.11.014
37. Naidoo J, Cottrell TR, Lipson EJ, Forde PM, Illei PB, Yarmus LB, et al. Chronic Immune Checkpoint Inhibitor Pneumonitis. *J Immunother Cancer* (2020) 8:e000840. doi: 10.1136/jitc-2020-000840
38. Suresh K, Naidoo J, Lin CT, Danoff S. Immune Checkpoint Immunotherapy for Non-Small Cell Lung Cancer: Benefits and Pulmonary Toxicities. *Chest* (2018) 154:1416–23. doi: 10.1016/j.chest.2018.08.1048
39. Cho JY, Kim J, Lee JS, Kim YJ, Kim SH, Lee YJ, et al. Characteristics, Incidence, and Risk Factors of Immune Checkpoint Inhibitor-Related Pneumonitis in Patients With Non-Small Cell Lung Cancer. *Lung Cancer* (2018) 125:150–6. doi: 10.1016/j.lungcan.2018.09.015
40. Voong KR, Hazell S, Hu C, Hayman J, Hales R, Marrone K, et al. MA 09.08 Receipt of Chest Radiation and Immune-Related Pneumonitis in Patients With NSCLC Treated With Anti-PD-1/PD-L1. *J Thorac Oncol* (2017) 12: S1837. doi: 10.1016/j.jtho.2017.09.529
41. Torre-Bouscoulet L, Arroyo-Hernandez M, Martinez-Briseno D, Munoz-Montano WR, Gochicoa-Rangel L, Bacon-Fonseca L, et al. Longitudinal Evaluation of Lung Function in Patients With Advanced Non-Small Cell Lung Cancer Treated With Concurrent Chemoradiation Therapy. *Int J Radiat Oncol Biol Phys* (2018) 101:910–8. doi: 10.1016/j.ijrobp.2018.04.014
42. Garon EB, Rizvi NA, Hui R, Leighl N, Balmanoukian AS, Eder JP, et al. Pembrolizumab for the Treatment of Non-Small-Cell Lung Cancer. *N Engl J Med* (2015) 372:2018–28. doi: 10.1056/NEJMoa1501824
43. Owen DH, Wei L, Bertino EM, Edd T, Villalona-Calero MA, He K, et al. Incidence, Risk Factors, and Effect on Survival of Immune-Related Adverse Events in Patients With Non-Small-Cell Lung Cancer. *Clin Lung Cancer* (2018) 19:e893–900. doi: 10.1016/j.cllc.2018.08.008
44. Barrón F, Sánchez R, Arroyo-Hernández M, Blanco C, Zatarain-Barrón ZL, Catalán R, et al. Risk of Developing Checkpoint Immune Pneumonitis and Its Effect on Overall Survival in Non-Small Cell Lung Cancer Patients Previously Treated With Radiotherapy. *Front Oncol* (2020) 10:570233. doi: 10.3389/fonc.2020.570233
45. Cui P, Liu Z, Wang G, Ma J, Qian Y, Zhang F, et al. Risk Factors for Pneumonitis in Patients Treated With Anti-Programmed Death-1 Therapy: A Case-Control Study. *Cancer Med* (2018) 7:4115–20. doi: 10.1002/cam4.1579
46. Ahn MJ, Yang J, Yu H, Saka H, Ramalingam S, Goto K, et al. 136o: Osimertinib Combined With Durvalumab in EGFR-Mutant Non-Small Cell Lung Cancer: Results From the TATTON Phase Ib Trial. *J Thorac Oncol* (2016) 11:S115. doi: 10.1016/s1556-0864(16)30246-5
47. Schoenfeld AJ, Arbour KC, Rizvi H, Iqbal AN, Gadgeel SM, Girshman J, et al. Severe Immune-Related Adverse Events Are Common With Sequential PD-(L)1 Blockade and Osimertinib. *Ann Oncol* (2019) 30:839–44. doi: 10.1093/annonc/mdz077
48. Lin X, Lu T, Li S, Xie X, Chen X, Jiang J, et al. Cytomegalovirus Infection as an Underestimated Trigger for Checkpoint Inhibitor-Related Pneumonitis in Lung Cancer: A Retrospective Study. *Clin Transl Oncol* (2021) 23:389–96. doi: 10.1007/s12094-020-02432-5
49. Shibata Y, Murakami S, Kato T. Overview of Checkpoint Inhibitor Pneumonitis: Incidence and Associated Risk Factors. *Expert Opin Drug Saf* (2021) 20:537–47. doi: 10.1080/14740338.2021.1898584
50. Sul J, Blumenthal GM, Jiang X, He K, Keegan P, Pazdur R. FDA Approval Summary: Pembrolizumab for the Treatment of Patients With Metastatic Non-Small Cell Lung Cancer Whose Tumors Express Programmed Death-Ligand 1. *Oncologist* (2016) 21:643–50. doi: 10.1634/theoncologist
51. Kanai O, Kim YH, Demura Y, Kanai M, Ito T, Fujita K, et al. Efficacy and Safety of Nivolumab in Non-Small Cell Lung Cancer With Preexisting Interstitial Lung Disease. *Thorac Cancer* (2018) 9:847–55. doi: 10.1111/1759-7714.12759
52. Yamaguchi T, Shimizu J, Hasegawa T, Horio Y, Inaba Y, Yatabe Y, et al. Pre-Existing Pulmonary Fibrosis Is a Risk Factor for Anti-PD-1-Related Pneumonitis in Patients With Non-Small Cell Lung Cancer: A Retrospective Analysis. *Lung Cancer* (2018) 125:212–7. doi: 10.1016/j.lungcan.2018.10.001
53. Moda M, Saito H, Kato T, Usui R, Kondo T, Nakahara Y, et al. Tumor Invasion in the Central Airway Is a Risk Factor for Early-Onset Checkpoint Inhibitor Pneumonitis in Patients With Non-Small Cell Lung Cancer. *Thorac Cancer* (2020) 11:3576–84. doi: 10.1111/1759-7714.13703
54. Chu X, Zhao J, Zhou J, Zhou F, Jiang T, Jiang S, et al. Association of Baseline Peripheral-Blood Eosinophil Count With Immune Checkpoint Inhibitor-Related Pneumonitis and Clinical Outcomes in Patients With Non-Small Cell Lung Cancer Receiving Immune Checkpoint Inhibitors. *Lung Cancer* (2020) 150:76–82. doi: 10.1016/j.lungcan.2020.08.015
55. Tahir SA, Gao J, Miura Y, Blando J, Tidwell RSS, Zhao H, et al. Autoimmune Antibodies Correlate With Immune Checkpoint Therapy-Induced Toxicities. *Proc Natl Acad Sci USA* (2019) 116:22246–51. doi: 10.1073/pnas.1908079116
56. Freeman-Keller M, Kim Y, Cronin H, Richards A, Gibney G, Weber JS. Nivolumab in Resected and Unresectable Metastatic Melanoma: Characteristics of Immune-Related Adverse Events and Association With Outcomes. *Clin Cancer Res* (2016) 22:886–94. doi: 10.1158/1078-0432.Ccr-15-1136
57. Hua C, Boussemart L, Mateus C, Routier E, Boutros C, Cazenave H, et al. Association of Vitiligo With Tumor Response in Patients With Metastatic Melanoma Treated With Pembrolizumab. *JAMA Dermatol* (2016) 152:45–51. doi: 10.1001/jamadermatol.2015.2707
58. Nakamura Y, Tanaka R, Asami Y, Teramoto Y, Imamura T, Sato S, et al. Correlation Between Vitiligo Occurrence and Clinical Benefit in Advanced Melanoma Patients Treated With Nivolumab: A Multi-Institutional Retrospective Study. *J Dermatol* (2017) 44:117–22. doi: 10.1111/1346-8138.13520
59. Sanlorenzo M, Vujic I, Daud A, Algazi A, Gubens M, Luna SA, et al. Pembrolizumab Cutaneous Adverse Events and Their Association With

Disease Progression. *JAMA Dermatol* (2015) 151:1206–12. doi: 10.1001/jamadermatol.2015.1916
60. Teulings H-E, Limpens J, Jansen SN, Zwinderman AH, Reitsma JB, Spuls PI, et al. Vitiligo-Like Depigmentation in Patients With Stage III-IV Melanoma Receiving Immunotherapy and Its Association With Survival: A Systematic Review and Meta-Analysis. *J Clin Oncol* (2015) 33:773–81. doi: 10.1200/jco.2014.57.4756
61. Haratani K, Hayashi H, Chiba Y, Kudo K, Yonesaka K, Kato R, et al. Association of Immune-Related Adverse Events With Nivolumab Efficacy in Non-Small-Cell Lung Cancer. *JAMA Oncol* (2018) 4:374–8. doi: 10.1001/jamaoncol.2017.2925
62. Ricciuti B, Genova C, De Giglio A, Bassanelli M, Dal Bello MG, Metro G, et al. Impact of Immune-Related Adverse Events on Survival in Patients With Advanced Non-Small Cell Lung Cancer Treated With Nivolumab: Long-Term Outcomes From a Multi-Institutional Analysis. *J Cancer Res Clin Oncol* (2019) 145:479–85. doi: 10.1007/s00432-018-2805-3
63. Tone M, Izumo T, Awano N, Kuse N, Inomata M, Jo T, et al. High Mortality and Poor Treatment Efficacy of Immune Checkpoint Inhibitors in Patients With Severe Grade Checkpoint Inhibitor Pneumonitis in non-Small Cell Lung Cancer. *Thorac Cancer* (2019) 10:2006–12. doi: 10.1111/1759-7714.13187
64. Brahmer JR, Lacchetti C, Thompson JA. Management of Immune-Related Adverse Events in Patients Treated With Immune Checkpoint Inhibitor Therapy: American Society of Clinical Oncology Clinical Practice Guideline Summary. *J Oncol Pract* (2018) 14:247–9. doi: 10.1200/JOP.18.00005
65. Nobashi TW, Nishimoto Y, Kawata Y, Yutani H, Nakamura M, Tsuji Y, et al. Clinical and Radiological Features of Immune Checkpoint Inhibitor-Related Pneumonitis in Lung Cancer and Non-Lung Cancers. *Br J Radiol* (2020) 93:20200409. doi: 10.1259/bjr.20200409
66. Nishino M, Ramaiya NH, Awad MM, Sholl LM, Maattala JA, Taibi M, et al. PD-1 Inhibitor-Related Pneumonitis in Advanced Cancer Patients: Radiographic Patterns and Clinical Course. *Clin Cancer Res* (2016) 22:6051–60. doi: 10.1158/1078-0432.ccr-16-1320
67. Watanabe S, Ota T, Hayashi M, Ishikawa H, Otsubo A, Shoji S, et al. Prognostic Significance of the Radiologic Features of Pneumonitis Induced by Anti-PD-1 Therapy. *Cancer Med* (2020) 9:3070–7. doi: 10.1002/cam4.2974
68. Marvisi M, Ramponi S, Balzarini L, Mancini C. A "Crazy Paving" Pattern on CT Scan in a Patient Treated With Pembrolizumab. *Curr Drug Saf* (2019) 14:242–5. doi: 10.2174/1574886314666190312115648
69. Bronstein Y, Ng CS, Hwu P, Hwu W-J. Radiologic Manifestations of Immune-Related Adverse Events in Patients With Metastatic Melanoma Undergoing Anti-CTLA-4 Antibody Therapy. *AJR Am J Roentgenol* (2011) 197:W992–1000. doi: 10.2214/ajr.10.6198
70. Raad RA, Kannan R, Madden K, Pavlick A. Ipilimumab-Induced Organizing Pneumonia on 18F-FDG PET/CT in a Patient With Malignant Melanoma. *Clin Nucl Med* (2017) 42:e345–6. doi: 10.1097/RLU.0000000000001673
71. Wang YN, Lou DF, Li DY, Jiang W, Dong JY, Gao W, et al. Elevated Levels of IL-17A and IL-35 in Plasma and Bronchoalveolar Lavage Fluid Are Associated With Checkpoint Inhibitor Pneumonitis in Patients With Non-Small Cell Lung Cancer. *Oncol Lett* (2020) 20:611–22. doi: 10.3892/ol.2020.11618
72. Ivanova EA. Orekhov AN. T Helper Lymphocyte Subsets and Plasticity in Autoimmunity and Cancer: An Overview. *BioMed Res Int* (2015) 2015:327470. doi: 10.1155/2015/327470
73. Suresh K, Naidoo J, Zhong Q, Xiong Y, Mammen J, de Flores MV, et al. The Alveolar Immune Cell Landscape Is Dysregulated in Checkpoint Inhibitor Pneumonitis. *J Clin Invest* (2019) 129:4305–15. doi: 10.1172/JCI128654
74. Suzuki K, Yanagihara T, Matsumoto K, Kusaba H, Yamauchi T, Ikematsu Y, et al. Immune-Checkpoint Profiles for T Cells in Bronchoalveolar Lavage Fluid of Patients With Immune-Checkpoint Inhibitor-Related Interstitial Lung Disease. *Int Immunol* (2020) 32:547–57. doi: 10.1093/intimm/dxaa022
75. Kharkevitch DD, Dai S, Balch GC, Maeda T, Balch CM, Itoh K. Characterization of Autologous Tumor-Specific T-Helper 2 Cells in Tumor-Infiltrating Lymphocytes From a Patient With Metastatic Melanoma. *Int J Cancer* (1994) 58:317–23. doi: 10.1002/ijc.2910580302
76. Najafi M, Farhood B, Mortezaee K. Contribution of Regulatory T Cells to Cancer: A Review. *J Cell Physiol* (2019) 234:7983–93. doi: 10.1002/jcp.27553
77. Dulos J, Carven GJ, van Boxtel SJ, Evers S, Driessen-Engels LJA, Hobo W, et al. PD-1 Blockade Augments Th1 and Th17 and Suppresses Th2 Responses in Peripheral Blood From Patients With Prostate and Advanced Melanoma Cancer. *J Immunother* (2012) 35:169–78. doi: 10.1097/CJI.0b013e318247a4e7
78. Yoshino K, Nakayama T, Ito A, Sato E, Kitano S. Severe Colitis After PD-1 Blockade With Nivolumab in Advanced Melanoma Patients: Potential Role of Th1-Dominant Immune Response in Immune-Related Adverse Events: Two Case Reports. *BMC Cancer* (2019) 19:1019. doi: 10.1186/s12885-019-6138-7
79. Kim ST, Sheshadri A, Shannon V, Kontoyiannis DP, Kantarjian H, Garcia-Manero G, et al. Distinct Immunophenotypes of T Cells in Bronchoalveolar Lavage Fluid From Leukemia Patients With Immune Checkpoint Inhibitors-Related Pulmonary Complications. *Front Immunol* (2021) 11:590494. doi: 10.3389/fimmu.2020.590494
80. Luger D, Silver PB, Tang J, Cua D, Chen Z, Iwakura Y, et al. Either a Th17 or a Th1 Effector Response can Drive Autoimmunity: Conditions of Disease Induction Affect Dominant Effector Category. *J Exp Med* (2008) 205:799–810. doi: 10.1084/jem.20071258
81. Nedoszytko B, Lange M, Sokołowska-Wojdyło M, Renke J, Trzonkowski P, Sobjanek M, et al. The Role of Regulatory T Cells and Genes Involved in Their Differentiation in Pathogenesis of Selected Inflammatory and Neoplastic Skin Diseases. Part I: Treg Properties and Functions. *Postepy Dermatol Alergol* (2017) 34:285–94. doi: 10.5114/ada.2017.69305
82. Francisco LM, Salinas VH, Brown KE, Vanguri VK, Freeman GJ, Kuchroo VK, et al. PD-L1 Regulates the Development, Maintenance, and Function of Induced Regulatory T Cells. *J Exp Med* (2009) 206:3015–29. doi: 10.1084/jem.20090847
83. Amarnath S, Mangus CW, Wang JC, Wei F, He A, Kapoor V, et al. The PDL1-PD1 Axis Converts Human TH1 Cells Into Regulatory T Cells. *Sci Transl Med* (2011) 3:111–20. doi: 10.1126/scitranslmed.3003130
84. Zhang L, Zhang M, Xu J, Li S, Gu M. The Role of the Programmed Cell Death Protein-1/Programmed Death-Ligand 1 Pathway, Regulatory T Cells and T Helper 17 Cells in Tumor Immunity: A Narrative Review. *Ann Transl Med* (2020) 8:1526. doi: 10.21037/atm-20-6719
85. Passat T, Touchefeu Y, Gervois N, Jarry A, Bossard C, Bennouna J. Physiopathological Mechanisms of Immune-Related Adverse Events Induced by Anti-CTLA-4, Anti-PD-1 and Anti-PD-L1 Antibodies in Cancer Treatment. *Bull Cancer* (2018) 105:1033–41. doi: 10.1016/j.bulcan.2018.07.005
86. Martin-Orozco N, Muranski P, Chung Y, Yang XO, Yamazaki T, Lu S, et al. T Helper 17 Cells Promote Cytotoxic T Cell Activation in Tumor Immunity. *Immunity* (2009) 31:787–98. doi: 10.1016/j.immuni.2009.09.014
87. Munegowda MA, Deng Y, Mulligan SJ, Xiang J. Th17 and Th17-Stimulated CD8 T Cells Play a Distinct Role in Th17-Induced Preventive and Therapeutic Antitumor Immunity. *Cancer Immunol Immunother* (2011) 60:1473–84. doi: 10.1007/s00262-011-1054-y
88. Numasaki M, Watanabe M, Suzuki T, Takahashi H, Nakamura A, Mcallister F, et al. IL-17 Enhances the Net Angiogenic Activity and *In Vivo* Growth of Human non-Small Cell Lung Cancer in SCID Mice Through Promoting CXCR-2-Dependent Angiogenesis. *J Immunol* (2005) 175:6177–89. doi: 10.4049/jimmunol.175.9.6177
89. McAlees JW, Lajoie S, Dienger K, Sproles AA, Richgels PK, Yang Y, et al. Differential Control of CD4(+) T-Cell Subsets by the PD-1/PD-L1 Axis in a Mouse Model of Allergic Asthma. *Eur J Immunol* (2015) 45:1019–29. doi: 10.1002/eji.201444778
90. Lee YK, Turner H, Maynard CL, Oliver JR, Chen D, Elson CO, et al. Late Developmental Plasticity in the T Helper 17 Lineage. *Immunity* (2009) 30:92–107. doi: 10.1016/j.immuni.2008.11.005
91. Basdeo SA, Cluxton D, Sulaimani J, Moran B, Canavan M, Orr C, et al. Ex-Th17 (Nonclassical Th1) Cells Are Functionally Distinct From Classical Th1 and Th17 Cells and Are Not Constrained by Regulatory T Cells. *J Immunol* (2017) 198:2249–59. doi: 10.4049/jimmunol.1600737
92. Knochelmann HM, Dwyer CJ, Bailey SR, Amaya SM, Paulos CM. When Worlds Collide: Th17 and Treg Cells in Cancer and Autoimmunity. *Cell Mol Immunol* (2018) 15:458–69. doi: 10.1038/s41423-018-0004-4
93. Kryczek I, Banerjee M, Cheng P, Vatan L, Zou W. Phenotype, Distribution, Generation, and Functional and Clinical Relevance of Th17 Cells in the

Human Tumor Environments. *Blood* (2009) 114:1141–9. doi: 10.1182/blood-2009-03-208249
94. Chang SH, Mirabolfathinejad SG, Katta H, Cumpian AM, Chen D. T Helper 17 Cells Play a Critical Pathogenic Role in Lung Cancer. *Proc Natl Acad Sci USA* (2014) 111:5664–9. doi: 10.1073/pnas.1319051111
95. Okazaki T, Tanaka Y, Nishio R, Mitsuiye T, Mizoguchi A, Wang J, et al. Autoantibodies Against Cardiac Troponin I are Responsible for Dilated Cardiomyopathy in PD-1-Deficient Mice. *Nat Med* (2003) 9:1477–83. doi: 10.1038/nm955
96. Kong YC, Flynn JC. Opportunistic Autoimmune Disorders Potentiated by Immune-Checkpoint Inhibitors Anti-CTLA-4 and Anti-PD-1. *Front Immunol* (2014) 5:206. doi: 10.3389/fimmu.2014.00206
97. Starlets D, Gore Y, Binsky I, Haran M, Harpaz N, Shvidel L, et al. Cell-Surface CD74 Initiates a Signaling Cascade Leading to Cell Proliferation and Survival. *Blood* (2006) 107:4807–16. doi: 10.1182/blood-2005-11-4334
98. Rotondi M, Chiovato L, Romagnani S, Serio M, Romagnani P. Role of Chemokines in Endocrine Autoimmune Diseases. *Endocr Rev* (2007) 28:492–520. doi: 10.1210/er.2006-0044
99. Lim SY, Lee JH, Gide TN, Menzies AM, Guminski A, Carlino MS, et al. Circulating Cytokines Predict Immune-Related Toxicity in Melanoma Patients Receiving Anti-PD-1-Based Immunotherapy. *Clin Cancer Res* (2019) 25:1557–63. doi: 10.1158/1078-0432.CCR-18-2795
100. Khan S, Khan SA, Luo X, Fattah FJ, Saltarski J, Gloria-McCutchen Y, et al. Immune Dysregulation in Cancer Patients Developing Immune-Related Adverse Events. *Br J Cancer* (2019) 120:63–8. doi: 10.1038/s41416-018-0155-1
101. Magliozzi R, Howell O, Vora A, Serafini B, Nicholas R, Puopolo M, et al. Meningeal B-Cell Follicles in Secondary Progressive Multiple Sclerosis Associate With Early Onset of Disease and Severe Cortical Pathology. *Brain* (2007) 130:1089–104. doi: 10.1093/brain/awm038
102. Pepys MB, Hirschfield GM. C-Reactive Protein: A Critical Update. *J Clin Invest* (2003) 111:1805–12. doi: 10.1172/JCI18921
103. Abolhassani AR, Schuler G, Kirchberger MC, Heinzerling L. C-Reactive Protein as an Early Marker of Immune-Related Adverse Events. *J Cancer Res Clin Oncol* (2019) 145:2625–31. doi: 10.1007/s00432-019-03002-1
104. Hunter CA, Jones SA. IL-6 as a Keystone Cytokine in Health and Disease. *Nat Immunol* (2015) 16:448–57. doi: 10.1038/ni.3153
105. Scheller J, Chalaris A, Schmidt-Arras D, Rose-John S. The Pro- and Anti-Inflammatory Properties of the Cytokine Interleukin-6. *Biochim Biophys Acta* (2011) 1813:878–88. doi: 10.1016/j.bbamcr.2011.01.034
106. Bettelli E, Carrier Y, Gao W, Korn T, Strom T, Oukka M, et al. Reciprocal Developmental Pathways for the Generation of Pathogenic Effector T(H)17 and Regulatory T Cells. *Nature* (2006) 441:235–8. doi: 10.1038/nature04753
107. Wussler D, Kozhuharov N, Tavares Oliveira M, Bossa A, Sabti Z, Nowak A, et al. Clinical Utility of Procalcitonin in the Diagnosis of Pneumonia. *Clin Chem* (2019) 65:1532–42. doi: 10.1373/clinchem.2019.306787
108. Zhang JJ, Dong X, Cao YY, Yuan YD, Yang YB, Yan YQ, et al. Clinical Characteristics of 140 Patients Infected With SARS-CoV-2 in Wuhan, China. *Allergy* (2020) 75:1730–41. doi: 10.1111/all.14238
109. Iwanaga N, Kolls JK. Updates on T Helper Type 17 Immunity in Respiratory Disease. *Immunology* (2019) 156:3–8. doi: 10.1111/imm.13006
110. Tarhini AA, Zahoor H, Lin Y, Malhotra U, Sander C, Butterfield LH, et al. Baseline Circulating IL-17 Predicts Toxicity While TGF-Beta1 and IL-10 Are Prognostic of Relapse in Ipilimumab Neoadjuvant Therapy of Melanoma. *J Immunother Cancer* (2015) 3:39. doi: 10.1186/s40425-015-0081-1
111. Johnson D, Patel AB, Uemura MI, Trinh VA, Jackson N, Zobniw CM, et al. IL17A Blockade Successfully Treated Psoriasiform Dermatologic Toxicity From Immunotherapy. *Cancer Immunol Res* (2019) 7:860–5. doi: 10.1158/2326-6066.CIR-18-0682
112. Luo W, Wang Z, Tian P, Li W. Safety and Tolerability of PD-1/PD-L1 Inhibitors in the Treatment of Non-Small Cell Lung Cancer: A Meta-Analysis of Randomized Controlled Trials. *J Cancer Res Clin Oncol* (2018) 144:1851–9. doi: 10.1007/s00432-018-2707-4
113. Makkouk A, Weiner GJ. Cancer Immunotherapy and Breaking Immune Tolerance: New Approaches to an Old Challenge. *Cancer Res* (2015) 75:5–10. doi: 10.1158/0008-5472
114. Citrin DE, Mitchell JB. Mechanisms of Normal Tissue Injury From Irradiation. *Semin Radiat Oncol* (2017) 27:316–24. doi: 10.1016/j.semradonc.2017.04.001
115. Tanegashima T, Togashi Y, Azuma K, Kawahara A, Ideguchi K, Sugiyama D, et al. Immune Suppression by PD-L2 Against Spontaneous and Treatment-Related Antitumor Immunity. *Clin Cancer Res* (2019) 25:4808–19. doi: 10.1158/1078-0432.CCR-18-3991
116. Li M, Gan L, Song A, Xue J, Lu Y. Rethinking Pulmonary Toxicity in Advanced Non-Small Cell Lung Cancer in the Era of Combining Anti-PD-1/PD-L1 Therapy With Thoracic Radiotherapy. *Biochim Biophys Acta Rev Cancer* (2019) 1871:323–30. doi: 10.1016/j.bbcan.2019.02.004
117. Greenwald RJ, Freeman GJ, Sharpe AH. The B7 Family Revisited. *Annu Rev Immunol* (2005) 23:515–48. doi: 10.1146/annurev.immunol.23.021704.115611
118. Xiao Y, Yu S, Zhu B, Bedoret D, Bu X, Francisco LM, et al. RGMb is a Novel Binding Partner for PD-L2 and its Engagement With PD-L2 Promotes Respiratory Tolerance. *J Exp Med* (2014) 211:943–59. doi: 10.1084/jem.20130790
119. Latchman Y, Wood CR, Chernova T, Chaudhary D, Borde M, Chernova I, et al. PD-L2 Is a Second Ligand for PD-1 and Inhibits T Cell Activation. *Nat Immunol* (2001) 2:261–8. doi: 10.1038/85330
120. Ko EC, Raben D, Formenti SC. The Integration of Radiotherapy With Immunotherapy for the Treatment of Non-Small Cell Lung Cancer. *Clin Cancer Res* (2018) 24:5792–806. doi: 10.1158/1078-0432.CCR-17-3620
121. Shaverdian N, Lisberg AE, Bornazyan K, Veruttipong D, Goldman JW, Formenti SC, et al. Previous Radiotherapy and the Clinical Activity and Toxicity of Pembrolizumab in the Treatment of Non-Small-Cell Lung Cancer: A Secondary Analysis of the KEYNOTE-001 Phase 1 Trial. *Lancet Oncol* (2017) 18:895–903. doi: 10.1016/S1470-2045(17)30380-7
122. Myers CJ, Lu B. Decreased Survival After Combining Thoracic Irradiation and an Anti-PD-1 Antibody Correlated With Increased T-Cell Infiltration Into Cardiac and Lung Tissues. *Int J Radiat Oncol Biol Phys* (2017) 99:1129–36. doi: 10.1016/j.ijrobp.2017.06.2452
123. Zhao J, Yorke ED, Li L, Kavanagh BD, Li XA, Das S, et al. Simple Factors Associated With Radiation-Induced Lung Toxicity After Stereotactic Body Radiation Therapy of the Thorax: A Pooled Analysis of 88 Studies. *Int J Radiat Oncol Biol Phys* (2016) 95:1357–66. doi: 10.1016/j.ijrobp.2016.03.024
124. Oshima Y, Tanimoto T, Yuji K, Tojo A. EGFR-TKI-Associated Interstitial Pneumonitis in Nivolumab-Treated Patients With Non-Small Cell Lung Cancer. *JAMA Oncol* (2018) 4:1112–5. doi: 10.1001/jamaoncol.2017.4526
125. Routy B, Le Chatelier E, Derosa L, Duong CPM, Alou MT, Daillère R, et al. Gut Microbiome Influences Efficacy of PD-1-Based Immunotherapy Against Epithelial Tumors. *Science* (2018) 359:91–7. doi: 10.1126/science.aan3706
126. Jin Y, Dong H, Xia L, Yang Y, Zhu Y, Shen Y, et al. The Diversity of Gut Microbiome is Associated With Favorable Responses to Anti-Programmed Death 1 Immunotherapy in Chinese Patients With NSCLC. *J Thorac Oncol* (2019) 14:1378–89. doi: 10.1016/j.jtho.2019.04.007
127. Chaput N, Lepage P, Coutzac C, Soularue E, Le Roux K, Monot C, et al. Baseline Gut Microbiota Predicts Clinical Response and Colitis in Metastatic Melanoma Patients Treated With Ipilimumab. *Ann Oncol* (2017) 28:1368–79. doi: 10.1093/annonc/mdx108
128. Wang Y, Wiesnoski DH, Helmink BA, Gopalakrishnan V, Choi K, Dupont HL, et al. Fecal Microbiota Transplantation for Refractory Immune Checkpoint Inhibitor-Associated Colitis. *Nat Med* (2018) 24:1804–8. doi: 10.1038/s41591-018-0238-9
129. Hakozaki T, Richard C, Elkrief A, Hosomi Y, Benlaïfaoui M, Mimpen I, et al. The Gut Microbiome Associates With Immune Checkpoint Inhibition Outcomes in Patients With Advanced Non-Small Cell Lung Cancer. *Cancer Immunol Res* (2020) 8:1243–50. doi: 10.1158/2326-6066.CIR-20-0196
130. Bingula R, Filaire M, Radosevic-Robin N, Bey M, Berthon JY, Bernalier-Donadille A, et al. Desired Turbulence? Gut-Lung Axis, Immunity, and Lung Cancer. *J Oncol* (2017) 2017:5035371. doi: 10.1155/2017/5035371
131. Zhang YB, Liu SJ, Hu ZD, Zhou JX, Wang YZ, Fang B, et al. Increased Th17 Activation and Gut Microbiota Diversity are Associated With Pembrolizumab-Triggered Tuberculosis. *Cancer Immunol Immunother* (2020) 69:2665–71. doi: 10.1007/s00262-020-02687-5
132. Gopalakrishnan V, Spencer CN, Nezi L, Reuben A, Andrews MC, Karpinets TV, et al. Gut Microbiome Modulates Response to Anti-PD-1 Immunotherapy in Melanoma Patients. *Science* (2018) 359:97–103. doi: 10.1126/science.aan4236

133. Sivan A, Corrales L, Hubert N, Williams JB, Aquino-Michaels K, Earley ZM, et al. Commensal Bifidobacterium Promotes Antitumor Immunity and Facilitates Anti-PD-L1 Efficacy. *Science* (2015) 350:1084–9. doi: 10.1126/science.aac4255
134. Zhang C, Wang J, Sun Z, Cao Y, Mu Z, Ji X. Commensal Microbiota Contributes to Predicting the Response to Immune Checkpoint Inhibitors in non-Small-Cell Lung Cancer Patients. *Cancer Sci* (2021) 112:3005–17. doi: 10.1111/cas.14979
135. Marschner D, Falk M, Javorniczky NR, Hanke-Muller K, Rawluk J, Schmitt-Graeff A, et al. MicroRNA-146a Regulates Immune-Related Adverse Events Caused by Immune Checkpoint Inhibitors. *JCI Insight* (2020) 5:e132334. doi: 10.1172/jci.insight.132334
136. Thibult ML, Mamessier E, Gertner-Dardenne J, Pastor S, Just-Landi S, Xerri L, et al. PD-1 Is a Novel Regulator of Human B-Cell Activation. *Int Immunol* (2013) 25:129–37. doi: 10.1093/intimm/dxs098
137. Garris CS, Arlauckas SP, Kohler RH, Trefny MP, Garren S, Piot C, et al. Successful Anti-PD-1 Cancer Immunotherapy Requires T Cell-Dendritic Cell Crosstalk Involving the Cytokines IFN-γ and IL-12. *Immunity* (2018) 49:1148–61. doi: 10.1016/j.immuni.2018.09.024
138. Sivori S, Pende D, Quatrini L, Pietra G, Della Chiesa M, Vacca P, et al. NK Cells and ILCs in Tumor Immunotherapy. *Mol Aspects Med* (2021) 80:100870. doi: 10.1016/j.mam.2020.100870
139. Hsu J, Hodgins JJ, Marathe M, Nicolai CJ, Bourgeois-Daigneault MC, Trevino TN, et al. Contribution of NK Cells to Immunotherapy Mediated by PD-1/PD-L1 Blockade. *J Clin Invest* (2018) 128:4654–68. doi: 10.1172/JCI99317
140. Brahmer JR, Lacchetti C, Schneider BJ, Atkins MB, Brassil KJ, Caterino JM, et al. Management of Immune-Related Adverse Events in Patients Treated With Immune Checkpoint Inhibitor Therapy: American Society of Clinical Oncology Clinical Practice Guideline. *J Clin Oncol* (2018) 36:1714–68. doi: 10.1200/JCO.2017.77.6385
141. Spain L, Diem S, Larkin J. Management of Toxicities of Immune Checkpoint Inhibitors. *Cancer Treat Rev* (2016) 44:51–60. doi: 10.1016/j.ctrv.2016.02.001
142. Howell M, Lee R, Bowyer S, Fusi A, Lorigan P. Optimal Management of Immune-Related Toxicities Associated With Checkpoint Inhibitors in Lung Cancer. *Lung Cancer* (2015) 88:117–23. doi: 10.1016/j.lungcan.2015.02.007
143. Puzanov I, Diab A, Abdallah K, Bingham CO3rd, Brogdon C, Dadu R, et al. Managing Toxicities Associated With Immune Checkpoint Inhibitors: Consensus Recommendations From the Society for Immunotherapy of Cancer (SITC) Toxicity Management Working Group. *J Immunother Cancer* (2017) 5:95. doi: 10.1186/s40425-017-0300-z
144. Naqash AR, Yang LV, Sanderlin EJ, Atwell DC, Walker PR. Interleukin-6 as One of the Potential Mediators of Immune-Related Adverse Events in Non-Small Cell Lung Cancer Patients Treated With Immune Checkpoint Blockade: Evidence From a Case Report. *Acta Oncol* (2018) 57:705–8. doi: 10.1080/0284186X.2017.1406668
145. Stroud CR, Hegde A, Cherry C, Naqash AR, Sharma N, Addepalli S, et al. Tocilizumab for the Management of Immune Mediated Adverse Events Secondary to PD-1 Blockade. *J Oncol Pharm Pract* (2019) 25:551–7. doi: 10.1177/1078155217745144
146. von Itzstein MS, Khan S, Gerber DE. Investigational Biomarkers for Checkpoint Inhibitor Immune-Related Adverse Event Prediction and Diagnosis. *Clin Chem* (2020) 66:779–93. doi: 10.1093/clinchem/hvaa081
147. Lin X, Deng H, Yang Y, Wu J, Qiu G, Li S, et al. Peripheral Blood Biomarkers for Early Diagnosis, Severity, and Prognosis of Checkpoint Inhibitor-Related Pneumonitis in Patients With Lung Cancer. *Front Oncol* (2021) 11:698832. doi: 10.3389/fonc.2021.698832
148. Schoenfeld JD, Nishino M, Severgnini M, Manos M, Mak RH, Hodi FS. Pneumonitis Resulting From Radiation and Immune Checkpoint Blockade Illustrates Characteristic Clinical, Radiologic and Circulating Biomarker Features. *J Immunother Cancer* (2019) 7:112. doi: 10.1186/s40425-019-0583-3
149. Hoefsmit EP, Rozeman EA, Haanen J, Blank CU. Susceptible Loci Associated With Autoimmune Disease as Potential Biomarkers for Checkpoint Inhibitor-Induced Immune-Related Adverse Events. *ESMO Open* (2019) 4:e000472. doi: 10.1136/esmoopen-2018-000472
150. Adam K, Iuga A, Tocheva AS, Mor A. A Novel Mouse Model for Checkpoint Inhibitor-Induced Adverse Events. *PloS One* (2021) 16:e0246168. doi: 10.1371/journal.pone.0246168
151. Guerin MV, Finisguerra V, Van den Eynde BJ, Bercovici N, Trautmann A. Preclinical Murine Tumor Models: A Structural and Functional Perspective. *Elife* (2020) 9:e50740. doi: 10.7554/eLife.50740
152. Jia XH, Geng LY, Jiang PP, Xu H, Nan KJ, Yao Y, et al. The Biomarkers Related to Immune Related Adverse Events Caused by Immune Checkpoint Inhibitors. *J Exp Clin Cancer Res* (2020) 39:284. doi: 10.1186/s13046-020-01749-x
153. Matsukane R, Watanabe H, Minami H, Hata K, Suetsugu K, Tsuji T, et al. Continuous Monitoring of Neutrophils to Lymphocytes Ratio for Estimating the Onset, Severity, and Subsequent Prognosis of Immune Related Adverse Events. *Sci Rep* (2021) 11:1324. doi: 10.1038/s41598-020-79397-6
154. Egami S, Kawazoe H, Hashimoto H, Uozumi R, Arami T, Sakiyama N, et al. Peripheral Blood Biomarkers Predict Immune-Related Adverse Events in Non-Small Cell Lung Cancer Patients Treated With Pembrolizumab: A Multicenter Retrospective Study. *J Cancer* (2021) 12:2105–12. doi: 10.7150/jca.53242
155. Paz-Ares LG, Ramalingam SS, Ciuleanu TE, Lee JS, Urban L, Caro RB, et al. First-Line Nivolumab Plus Ipilimumab in Advanced Non-Small Cell Lung Cancer: 4-Year Outcomes From the Randomized, Open-Label, Phase 3 CheckMate 227 Part 1 Trial. *J Thorac Oncol* (2022) 17:289–308. doi: 10.1016/j.jtho.2021.09.010
156. Chae YK, Arya A, Iams W, Cruz MR, Chandra S, Choi J, et al. Current Landscape and Future of Dual Anti-CTLA4 and PD-1/PD-L1 Blockade Immunotherapy in Cancer; Lessons Learned From Clinical Trials With Melanoma and Non-Small Cell Lung Cancer (NSCLC). *J Immunother Cancer* (2018) 6:39. doi: 10.1186/s40425-018-0349-3
157. Ramos-Casals M, Brahmer JR, Callahan MK, Flores-Chavez A, Keegan N, Khamashta MA, et al. Immune-Related Adverse Events of Checkpoint Inhibitors. *Nat Rev Dis Primers* (2020) 6:38. doi: 10.1038/s41572-020-0160-6
158. Kon E, Benhar I. Immune Checkpoint Inhibitor Combinations: Current Efforts and Important Aspects for Success. *Drug Resist Update* (2019) 45:13–29. doi: 10.1016/j.drup.2019.07.004
159. Srivastava S, Furlan SN, Jaeger-Ruckstuhl CA, Sarvothama M, Berger C, Smythe KS, et al. Immunogenic Chemotherapy Enhances Recruitment of CAR-T Cells to Lung Tumors and Improves Antitumor Efficacy When Combined With Checkpoint Blockade. *Cancer Cell* (2021) 39:193–208. doi: 10.1016/j.ccell.2020.11.005

Conflict of Interest: The authors declare that the research was conducted in the absence of any commercial or financial relationships that could be construed as a potential conflict of interest.

Publisher's Note: All claims expressed in this article are solely those of the authors and do not necessarily represent those of their affiliated organizations, or those of the publisher, the editors and the reviewers. Any product that may be evaluated in this article, or claim that may be made by its manufacturer, is not guaranteed or endorsed by the publisher.

Copyright © 2022 Yin, Wu, Yang, Gan and Xue. This is an open-access article distributed under the terms of the Creative Commons Attribution License (CC BY). The use, distribution or reproduction in other forums is permitted, provided the original author(s) and the copyright owner(s) are credited and that the original publication in this journal is cited, in accordance with accepted academic practice. No use, distribution or reproduction is permitted which does not comply with these terms.

frontiers | Frontiers in Immunology

ORIGINAL RESEARCH
published: 07 April 2022
doi: 10.3389/fimmu.2022.828560

Non-Invasive Measurement Using Deep Learning Algorithm Based on Multi-Source Features Fusion to Predict PD-L1 Expression and Survival in NSCLC

Chengdi Wang[1†], Jiechao Ma[2†], Jun Shao[1†], Shu Zhang[2], Jingwei Li[1], Junpeng Yan[2], Zhehao Zhao[3], Congchen Bai[4], Yizhou Yu[2,5*] and Weimin Li[1*]*

[1] Department of Respiratory and Critical Care Medicine, Med-X Center for Manufacturing, Frontiers Science Center for Disease-Related Molecular Network, West China Hospital, West China School of Medicine, Sichuan University, Chengdu, China, [2] AI Lab, Deepwise Healthcare, Beijing, China, [3] West China Hospital, West China School of Medicine, Sichuan University, Chengdu, China, [4] Department of Medical Informatics, West China Hospital, Sichuan University, Chengdu, China, [5] Department of Computer Science, The University of Hong Kong, Pokfulam, Hong Kong SAR, China

Background: Programmed death-ligand 1 (PD-L1) assessment of lung cancer in immunohistochemical assays was only approved diagnostic biomarker for immunotherapy. But the tumor proportion score (TPS) of PD-L1 was challenging owing to invasive sampling and intertumoral heterogeneity. There was a strong demand for the development of an artificial intelligence (AI) system to measure PD-L1 expression signature (ES) non-invasively.

Methods: We developed an AI system using deep learning (DL), radiomics and combination models based on computed tomography (CT) images of 1,135 non-small cell lung cancer (NSCLC) patients with PD-L1 status. The deep learning feature was obtained through a 3D ResNet as the feature map extractor and the specialized classifier was constructed for the prediction and evaluation tasks. Then, a Cox proportional-hazards model combined with clinical factors and PD-L1 ES was utilized to evaluate prognosis in survival cohort.

Results: The combination model achieved a robust high-performance with area under the receiver operating characteristic curves (AUCs) of 0.950 (95% CI, 0.938–0.960), 0.934 (95% CI, 0.906–0.964), and 0.946 (95% CI, 0.933–0.958), for predicting PD-L1ES <1%, 1–49%, and ≥50% in validation cohort, respectively. Additionally, when combination model was trained on multi-source features the performance of overall survival evaluation (C-index: 0.89) could be superior compared to these of the clinical model alone (C-index: 0.86).

Conclusion: A non-invasive measurement using deep learning was proposed to access PD-L1 expression and survival outcomes of NSCLC. This study also indicated that deep learning model combined with clinical characteristics improved prediction capabilities, which would assist physicians in making rapid decision on clinical treatment options.

Keywords: deep learning, PD-L1 expression, survival, lung cancer, radiomics

OPEN ACCESS

Edited by:
Udo S. Gaipl,
University Hospital Erlangen, Germany

Reviewed by:
Chengzhi Zhou,
National Respiratory Medical Center, China
Chengming Liu,
Chinese Academy of Medical Sciences and Peking Union Medical College, China

***Correspondence:**
Chengdi Wang
chengdi_wang@scu.edu.cn
Yizhou Yu
yizhouy@acm.org
Weimin Li
weimi003@scu.edu.cn

†These authors have contributed equally to this work

Specialty section:
This article was submitted to Cancer Immunity and Immunotherapy, a section of the journal Frontiers in Immunology

Received: *03 December 2021*
Accepted: *17 February 2022*
Published: *07 April 2022*

Citation:
Wang C, Ma J, Shao J, Zhang S, Li J, Yan J, Zhao Z, Bai C, Yu Y and Li W (2022) Non-Invasive Measurement Using Deep Learning Algorithm Based on Multi-Source Features Fusion to Predict PD-L1 Expression and Survival in NSCLC. Front. Immunol. 13:828560. doi: 10.3389/fimmu.2022.828560

INTRODUCTION

Lung cancer, one of the most common types of cancer, occupies the leading cause of malignant mortality (1). In China, only 17.3% of lung cancer patients were stage I at primary diagnosis and 5-year survival was under 20% (2). On the basis of its histological types, non-small cell lung cancer (NSCLC) accounts for about 85% of all cases (3). It is a critical trend to develop individualized therapeutic schemes based on comprehensive usage of multiple-modality data for NSCLC patients.

Programmed cell death-ligand 1 (PD-L1), a ligand of programmed cell death 1 (PD-1), frequently overexpressed on the surface of cancer cells to invade the anti-tumor immunity through PD-1/PD-L1 pathway (4). Thus, numerous clinical trials were conducted to evaluate the efficacy of immunotherapy targeted PD-1/PD-L1 pathway (5–7). However, the IMpower150 trial indicated high expression (≥50%) of PD-L1 showed a better outcome for NSCLC received atezolizumab than lower expression of PD-L1 (6). Furthermore, KEYNOTE-042 presented the similar results (7). Thus, National Comprehensive Cancer Network (NCCN) Guidelines proposed that immunohistochemistry should be applied to assess the expression of PD-L1 and further guide immunotherapy (8). Nevertheless, immunohistochemistry requires invasive procedure to obtain the samples of NSCLC, and sample quality influences the results of PD-L1 expression to a great extent (9). Thus, other alternative methods to measure the PD-L1 status would greatly assist clinical decision support, especially for insufficient available samples or immunohistochemistry failure.

Recently, state-of-the-art artificial intelligence (AI) methods such as deep learning have been applied to screen lung cancer, assist the drug efficacy and prognosis prediction (10–13). Previous study used deep learning on whole-slide images to assist pathologists in the precise assessment of immunotherapy-related biomarkers (14). However, it still remains a challenging issue of invasive, intertumoral heterogeneity and dynamic changes. As a convenience and one that is routinely available in clinical practice, CT images reflect the whole information of an entire tumor non-invasively. A recent study has constructed deep learning model to predict PD-L1 expression (≥50%) with high performance (area under the receiver operating characteristic curve, AUC ≥0.71), which could help to predict the efficacy of immunotherapy in patients with NSCLC and indicate a direction for molecular prediction utilizing deep learning (15). However, previous studies mainly classified binary patterns on basis of relatively small samples, and the prediction of detailed classification were warranted for further investigation.

Thus, we proposed a non-invasive deep learning model based on radiomic signature from pretreatment CT images to predict the PD-L1 status and overall survival (OS) in lung cancer, guiding the clinical practice.

METHODS

Patients' Cohort and Data Collection

This retrospective study was approved by the institutional research board of the West China Hospital of Sichuan University. A total of 1,274 non-small lung cancer patients diagnosed between January, 2016, and April, 2019 were enrolled in this study. Written informed consent was waived because the data used for system development were anonymized by removing personal information. All patients met the following inclusion criteria: 1) pathological analysis of tumor tissues confirmed non-small cell lung cancer; 2) chest CT examinations were available; and 3) PD-L1 expression signature (PD-L1ES) was detected (<1%, 1–49%, ≥50%) in immunohistochemical (IHC) assays performed on the Ventana Benchmark platform (SP142 antibody). Patients were excluded if: 1) basic clinical information (such as age, sex, and PD-L1ES) were missing; 2) preoperative treatment or the time between CT examination and subsequent surgery exceeded 1 month; 3) CT images were of low quality; and 4) molecular testing results were difficult to determine. After screening with the exclusion criteria, the PD-L1ES prediction cohort (n = 1,135) for classifying PD-L1 expression signature was built (**Supplementary Figure 1**). Moreover, the survival cohort was created to examine the association between various factors and prognosis prediction. The inclusion criteria for building the survival cohort were: 1) clear clinical information was provided including smoking history, family history, histopathology such as lung adenocarcinoma (LUAD), squamous cell carcinoma (LUSC), etc.; 2) treatment status (surgery, chemotherapy, radiation therapy, targeted therapy, immunotherapy etc.) and survival outcome were all gathered from medical records or telephone follow-up. Finally, the survival cohort included 811 patients who were admitted to the West China Hospital of Sichuan University and followed up to June 2021.

Data Pre-Processing

This study consisted of two datasets: the PD-L1ES prediction dataset (n = 1,135) and the survival dataset (n = 811). The PD-L1ES dataset was divided into three categories based on different levels of PD-L1ES, namely, low PD-L1ES <1%, medium PD-L1ES 1–49%, and high PD-L1ES ≥50%, aiming to predict molecular events based on PD-L1 expression status. The survival cohort was utilized to create an accessing model to investigate the association between survival risk factors and overall survival (OS). In this study, the training and testing cohorts from both datasets were randomly partitioned with a ratio of 4:1, and five-fold cross validations were used for model development and validation.

To address the imbalance of three PD-L1ES groups, we adopted a joint re-weight strategy and re-sampling approach, such as up-sampling the short-tail instances and down-sampling the long-tail ones. Moreover, in order to enhance the learning capacities of the developed models, we employed a combination of tactics (radiomics model: low-level feature; deep learning model: high-level feature, clinical model: semantic feature). Our combination model extracted CT-based deep learning features, CT-based radiomic features, and clinical record-based clinical data for each patient. Two groups of experienced radiologist specialists delineated the particular contour of the entire tumor and the region of interest (ROI) for that tumor was determined accordingly. All ROIs were resized to the same resolution of 36 ∗ 36 ∗ 36 cubes for deep feature extraction

using third-order spline interpolation and normalized to 0–255 using pre-computed windowing information of lung. To make the full use of the enrolled data for clinical information extraction, the k-nearest neighbor (KNN) technique was first utilized to impute missing clinical values.

Establishment of the Low-Level Feature Model

For each tumor cube and its paired segmentation mask, a dedicated open-source Python library called PyRadiomics (http://www.radiomics.io; v3.0.1) was applied to perform radiomic phenotypic feature extraction from the three-dimensional ROI. Our study used it to automatically extract 1,672 radiomic characteristics for each cube-mask pair, namely, first-order, size, shape, and texture features. The least absolute shrinkage and selection operator (LASSO) method was applied for feature dimensionality reduction to select radiomic features with high stability and repeatability of radiological properties. L1 penalty was used to shrink some regression coefficients to exactly zero. Following that, we calculated the partial probability deviation on each radiomic characteristics of that tumor, and removed radiomic characteristics with low variance (less than 0.6), yielding a total of 107 features for each cube-mask pair, comprising of first-order (18 features), shape (14 features), and texture (75 features).

We established a gradient boosting regressor on the extracted radiomic features for survival analysis. Gradient boosting was a traditional machine-learning approach used in high-dimensional data analysis for classification and regression applications. It was an ensemble model that comprised of numerous weak learners and output the sum of their results. Based on correcting the error of the predecessor learner, each weak prediction model approximated a feature screening function. The gradient descent approach gave guidance for the direction of the ensemble model's development, allowing the model to attain higher and more resilient performance. We utilized the coefficient of determination (R2) score as an assessment metric to determine the parameters of the model on our dataset. A higher R2 score (from 0 to 1) indicated greater consistency between the predictive value with the ground truth. Through a series of tests, hyper-parameter optimization was carried out in line with the assessment outcomes of both training and test set data. As a result, the generalization capability of the regressor could be ensured, and we finally acquired the radiomic features.

To comprehensively investigate the performance of several classifiers in the PD-L1ES prediction challenge, we also combined the aforementioned radiomic feature with other imaging features to predict the PD-L1ES. While the random survival forest machine-learning technique was used to generate the radiomics model and a radiomics score (Rad-score) for survival analysis and risk stratification. A higher Rad-score indicated a higher risk of progression or a shorter overall survival, representing the average projected number of events across all trees in the constructed forest.

Establishment of the High-Level Feature Model

In our study, the high-level feature model also had two components: a 3D ResNet model as the feature extractor to obtain deep learning features and the specialized classifier/regressor for the prediction task.

The deep learning feature extraction module received the ROI cubes of the CT image as input. Compared to general 2D image processing, 3D ResNet could take 3D context into consideration and capture more complementary information from various slices of the same tumor, and thus make better decision given the 3D features. Pertaining to the small-sized 3D tumor volume, we modified the traditional 3D ResNet by neglecting the sub-sample operation in the conv stem layers so as to retain as much detailed texture information as possible. Finally, ResNet totally sub-sample to 1/8 of the original input compared to 1/32 in the vanilla ResNet. Transfer learning was also applied in our deep feature extraction model, where model parameters learned from large scale data from another domain were used to aid our target learning tasks (prediction and evaluation tasks) in a new environment. Such an approach would minimize the number of training epochs, expedite model convergence, and, to some extent, prevent over-fitting. The deep learning features obtained from the PD-L1ES prediction task were also employed for the evaluation task afterwards.

We built a 3D ResNet to predict different levels of PD-L1 expression signature (low PD-L1ES, medium PD-L1ES, and high PD-L1ES). The 3D ResNet was composed of a feature extraction backbone and a classification head. The classification head used a binary cross-entropy loss function to back-propagate the loss error. All the layers in the 3D ResNet backbone were initialized with pre-trained weights, while other parameters were randomly initialized. We trained all models for 40 epochs. The learning rate was set to 0.02 and decayed by a factor of 10 after the 20th and 35th epochs respectively.

In addition, we used the trained 3D ResNet to extract deep learning features to retrieve the survival risk and integrated it with other mined features to create the combination model for the prognosis task. From these stable features, the deep learning features that contributed the most to OS were chosen to provide a deep learning score (DL-score), and an ideal score was cut-off using the X-tile software to distinguish between high and low progression risk.

Establishment of the Multi-Source Features Fusion Model

In this study, two tasks were performed: PD-L1ES prediction and the prognosis evaluation (**Figure 1**). Besides the extracted imaging features, the clinical features were employed to offer extra semantic information for both tasks. To identify potential important variables in the clinical feature, a Kaplan–Meier curve with log-rank test and a univariate Cox proportional-hazards model were used (clinical factors and PD-L1ES). Factors with a P-value <0.05 were included to format the clinical features. Factors were transferred to one-hot encoding into a high-dimensional vector space for the prediction task, and they were employed in the multivariate Cox proportional-hazards regression to build the clinical model for the survival analysis task.

We totally established two combination model (multi-source features model), one for the PD-L1ES identification task and the other for the survival analysis task. For the PD-L1ES prediction

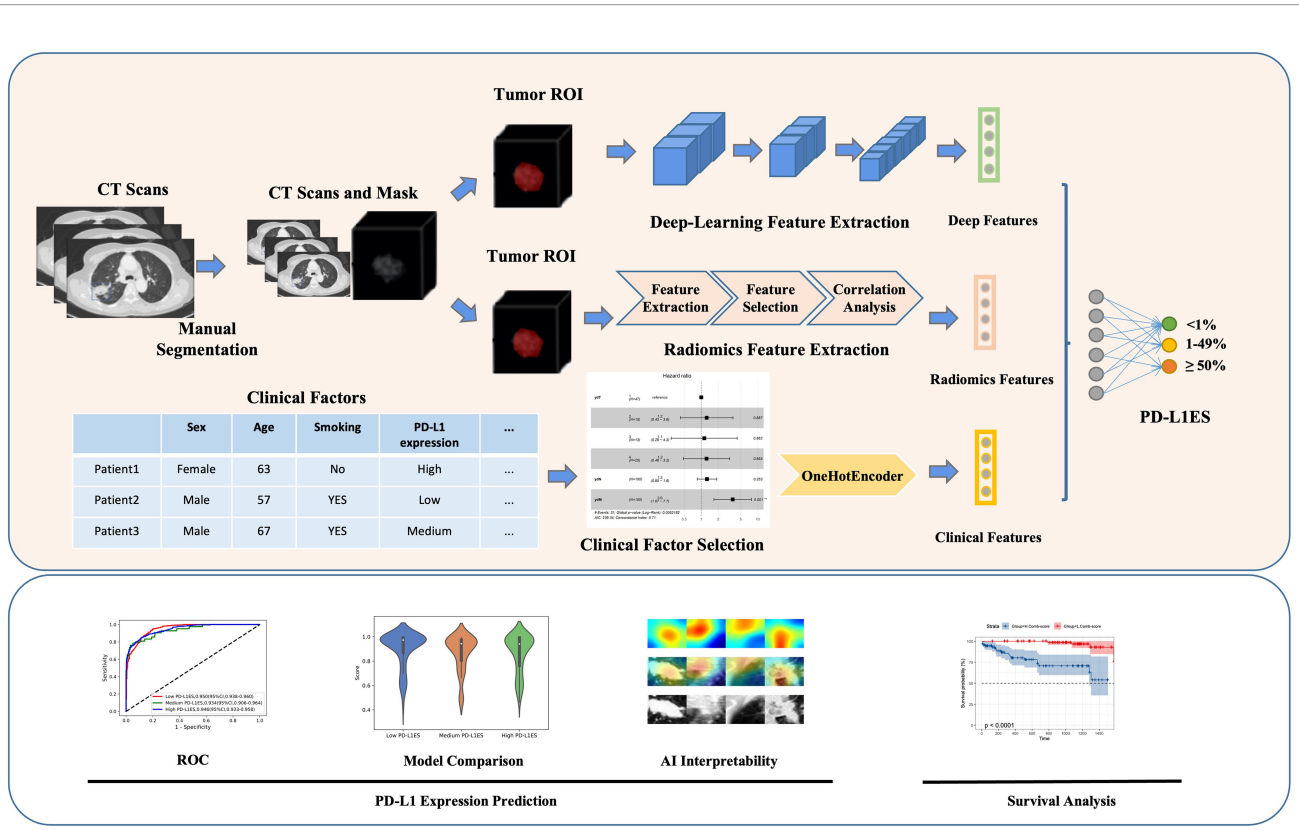

FIGURE 1 | Overall workflow of study design. The upper part showed the overall method of the study, while the lower part represented the analysis of the model. Original CT imaging data with manually labeled tumor images, comprehensive patient clinical information, overall survival, and PD-L1 expression signature were included in the data processing step. The deep learning, radiomics and clinical features were retrieved using the tumor ROI or clinical records during the feature extraction step. All features were utilized to predict PD-L1 expression signature and evaluate patient survival. PD-L1ES, PD-L1 expression signature; ROI, region of interest.

task based on the deep learning features, radiomic features and the one-hot clinical features were fused by a self-adapted fully-connected layer to generate the fusion embedding. For the prognosis prediction task, the deep learning features and the radiomic features were treated as Rad-score and DL-score to build the univariate for risk stratification. Then, to build the combination model, a multivariate Cox proportional-hazards model with the lowest Akaike information criteria was used to combine the Rad-score, DL-score, and high-relevance clinical risk variables.

Statistical Analysis

The following measures were used to assess the performance of classifiers: AUC, accuracy, sensitivity, and specificity. The DeLong technique was used to calculate the 95% confidence intervals (CIs) for the AUC. All statistical tests were two-tailed, with statistical significance set at P <0.05 was considered as significant. OS, measured from the diagnosis to death or the last follow-up, was generated using the Kaplan–Meier method, and differences in OS were examined using the log-rank test. Hazard ratios (HRs) were presented with their 95% CIs. The risk stratification capability was assessed by using the Kaplan–Meier survival curve and log-rank test. The optimal Rad-score and DL-score cut-off values were determined by X-tile software (version 3.6.1, Yale University).

RESULTS

Clinical Characteristics

After screening 1,274 patients with lung cancer who had molecular test, a total of 1,135 eligible patients who met the criteria were identified in prediction cohort, namely, 722 (63.6%) patients with PD-L1ES <1%, 50 (4.4%) patients with PD-L1ES 1–49%, and 363 (32.0%) patients with PD-L1ES ≥50% (**Supplementary Figure 1**). The mean age was 58.77 ± 10.66 years (**Table 1**). Women were predominant (582/1135, 51.3%), and more than 60% were never smokers. In terms of treatment, 784 patients (69.1%) received surgery, while 222 patients (19.6%) received radiation. Furthermore, 295 patients received chemotherapy and 386 patients receiving targeted treatment accounted for 26% and 34%, respectively. In terms of TNM stage, the majority of patients were in stage I (n = 498, 43.9%) and stage IV (n = 321, 28.3%), respectively. According to the data split strategy, 908 patients were utilized for training and internal validation, and 227 patients were used for external validation.

TABLE 1 | Clinical characteristics of patients used to measure PD-L1ES and survival analysis.

	Whole Cohort (n = 1,135)	Survival Cohort (n = 811)
Age (years)	58.77 ± 10.66	57.80 ± 11.03
Sex, N (%)		
Male	553 (48.7%)	371 (45.7%)
Female	582 (51.3%)	440 (54.3%)
Smoking status		
Current or former	403 (35.5%)	265 (32.7%)
Never	692 (61.0%)	517 (63.7%)
Unknown	40 (3.5%)	29 (3.6%)
Family history of cancer		
Yes	92 (8.1%)	94 (11.6%)
No	1,026 (90.4%)	715 (88.2%)
Unknown	17 (1.5%)	2 (0.2%)
Surgery		
Yes	784 (69.1%)	558 (68.8%)
No	351 (30.9%)	253 (31.2%)
Radiotherapy		
Yes	222 (19.6%)	161 (19.8%)
No	913 (80.4%)	650 (80.2%)
Chemotherapy		
Yes	295 (26.0%)	318 (39.2%)
No	508 (44.8%)	482 (59.4%)
Unknown	332 (29.2%)	11 (1.4%)
Targeted therapy		
Yes	386 (34.0%)	296 (36.5%)
No	749 (66.0%)	515 (63.5%)
Immunotherapy		
Yes	30 (2.6%)	27 (3.3%)
No	1,105 (97.4%)	784 (96.7%)
Histopathology		
LUAD	1,038 (91.4%)	755 (93.1%)
LUSC	36 (3.2%)	31 (3.8%)
Other	61 (5.4%)	25 (3.1%)
Stage T		
Tis	2 (0.2%)	3 (0.4%)
T1	440 (38.8%)	323 (39.8%)
T2	368 (32.4%)	258 (31.8%)
T3	100 (8.8%)	74 (9.1%)
T4	171 (15.1%)	118 (14.6%)
Tx	54 (4.7%)	35 (4.3%)
Stage N		
N0	603 (53.1%)	444 (54.7%)
N1	83 (7.3%)	59 (7.3%)
N2	240 (21.1%)	164 (20.2%)
N3	121 (10.7%)	84 (10.4%)
Nx	88 (7.8%)	60(7.4%)
Stage M		
M0	781 (68.8%)	559 (68.9%)
M1	300 (26.4%)	219 (27.0%)
Mx	54 (4.8%)	33 (4.1%)
Stage		
I	498 (43.9%)	363 (44.8%)
II	95 (8.3%)	63 (7.8%)
III	204 (18.0%)	142 (17.5%)
IV	321 (28.3%)	234 (28.8%)
Unknown	17 (1.5%)	9 (1.1%)
PD-L1 ES (%)		
<1%	722 (63.6%)	481 (59.3%)
1–49%	50 (4.4%)	49 (6.0%)
≥50%	363 (32.0%)	281 (34.7%)

LUAD, lung adenocarcinoma; LUSC, lung squamous cell carcinoma; ES, expression signature.

Meanwhile, PD-L1ES survival cohort included 811 patients with complete follow-up information (**Supplementary Figure 1** and **Table 1**).

Detection of PD-L1 Expression Status

The combination model achieved excellent performance to predict PD-L1 expression status than radiomics and deep learning methods (**Figure 2**). The ROC curve, confusion matrix and the model score distribution of PD-L1ES classification illustrated the performance of radiomics model with AUCs of low PD-L1ES 0.890 (95% CI, 0.871–0.916), medium PD-L1ES 0.851 (95% CI, 0.772–0.922), and high PD-L1ES 0.880 (95% CI, 0.858–0.908), respectively. Meanwhile, the deep learning model yielded AUCs of 0.902 (95% CI, 0.885–0.923), 0.863 (95% CI, 0.771–0.972), and 0.901 (95% CI, 0.881–0.927) for PD-L1ES <1%, 1–49%, and ≥50% in validation cohort, respectively. The AUC of the combination model also have the appreciable effect of low PD-L1ES 0.950 (95% CI, 0.938–0.960), medium PD-L1ES 0.934 (95% CI, 0.906–0.964), and high PD-L1ES 0.946 (95% CI, 0.933–0.958). The violin diagram of model score indicated that the predictive performance of deep learning was better than the performance of the radiomics model, and the combination model achieved the best predictive performance in terms of the PD-L1 ES identification.

Through the CAM visualization of the prediction model, the center of tumor region was identified as an important area for PD-L1 status classification with darker response color (**Figure 3**). It may provide clinicians with a biopsy position to as much as possible avoid misdiagnosis caused by intra-tumor heterogeneity.

Exploring Characteristics Associated With OS

According to the Kaplan–Meier survival analysis (**Supplementary Figure 2**), smoking history (P <0.001), surgery (P <0.001), chemotherapy (P <0.001), TMN stage (P <0.001), and cancer stage (P <0.001) were all significantly associated with OS. Patients with a smoking history had a considerably lower OS than those with no smoking history, and patients who had surgery had a significantly superior OS than those who did not. Then, taking into account the influence of clinical factors on OS, we built the clinical model using forest plots (**Figure 4A**) and selected the hazard ratio correlation with patient survival, followed by the multivariate analysis cox proportional-hazards regression (C-index of clinical model: 0.86). The clinical model was then verified using subgroup stratified analysis to see whether it could predict prognosis in individuals with various PD-L1ES. The patients in each group were classified by regression score as high or low risk of disease progression.

Validation of the PD-L1ES in Survival Analysis

Rad-score, DL-score, and clinical relevant features were used to create the combination model. We employed the multivariate Cox

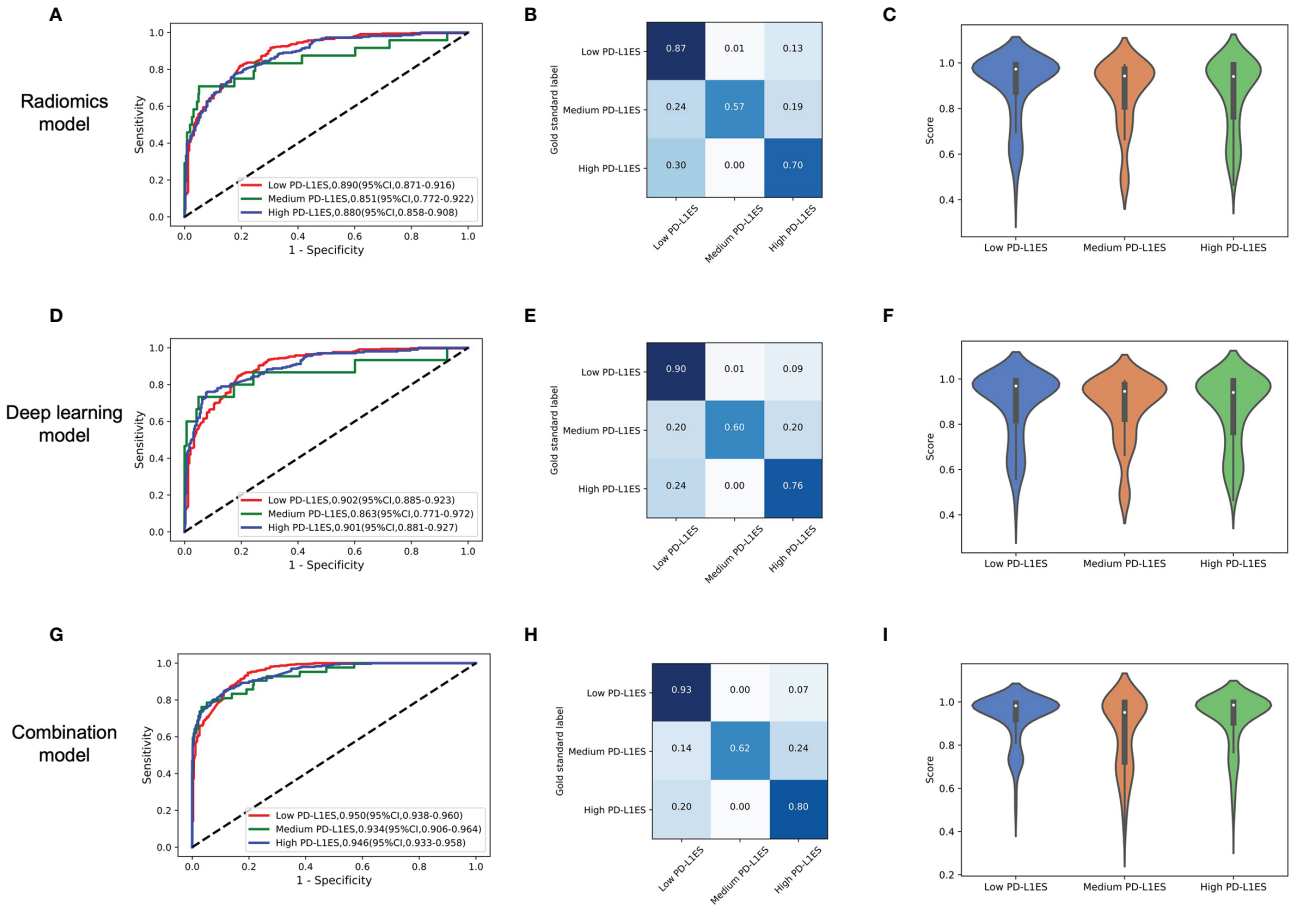

FIGURE 2 | The model performance in the prediction of PD-L1ES. The figure contained three groups of result analysis, including ROC curve, confusion matrix, and score distribution. The red line depicted low PD-L1 expression performance, the green line depicted medium PD-L1 expression performance, and the blue line depicted high PD-L1 expression performance. **(A–C)** The performance of the radiomics model. **(D–F)** The performance of the deep learning model. **(G–I)** The performance of the combination model. PD-L1ES, PD-L1 expression signature.

regression model to assess the importance of these characteristics in predicting OS. Furthermore, the forest plots of the combination model showed that cancer stage (HR = 26.18, $P = 0.017$), surgery (HR = 0.30, $P = 0.007$) and DL-score (HR = 0.23, $P = 0.006$) were independent predictors for OS. The performance of the combination model with a C-index of 0.89 was superior than the clinical model with a C-index of 0.86 (**Figures 4A, B**). Prognostic performance in different subgroups was compared by different models of low PD-L1ES <1%, medium PD-L1ES 1–49% and high PD-L1ES ≥50% to stratify the subgroup into low-risk and high-risk groups (**Figure 5**). The deep learning model score and combination model score achieved excellent discriminative ability regardless of three groups (all P <0.05).

DISCUSSION

According to the NCCN guidelines, PD-L1 expression levels of patients with lung cancer have a marked effect on clinical decision whether to use single-agent immunotherapy or interpretation chemotherapy (8). In this study, we constructed an alternative non-invasive measurement of accessing PD-L1 status and a prognostic model of predicting OS with high accuracy. It would be of paramount importance on clinical decision support, especially when tissues were not available.

The paradigm treatment of lung cancer patients varied according to different status of PD-L1 (16). The level of PD-L1 expression was presented as TPS given as <1%, 1–49%, and ≥50%. Atezolizumab single treatment was the preferred recommendation for patients with a PD-L1 expression status of ≥50% (17). While nivolumab combined with ipilimumab was first-line treatment for patients with PD-L1 expression status of ≥1% (18, 19). At the same time, PD-L1 expression status were useful for deciding whether to use single-agent immunotherapy or immunotherapy combinations as well (20, 21). Therefore, the study defined 1% and 50% as cut-off values. The predictive model could accurately evaluate the expression of three classifications, which was more in line with the clinical standard treatment needs.

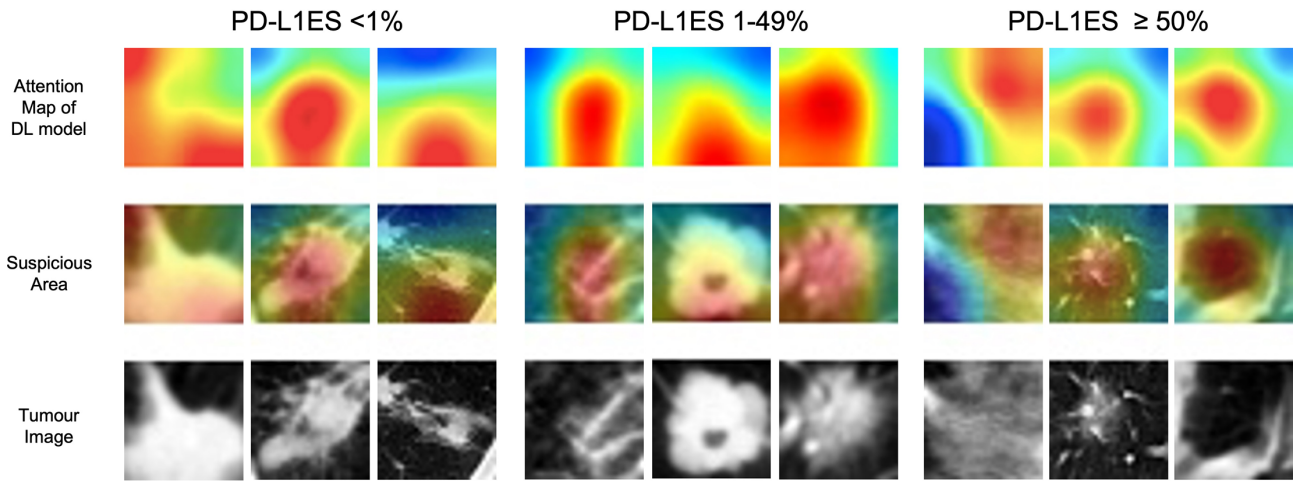

FIGURE 3 | The illustration of deep learning feature heatmap to predict PD-L1 expression. The first and second rows visualize the attention regions of a network for distinct mutant categories; the third row shows the origin tumor image in the 3D volume. PD-L1ES, PD-L1 expression signature.

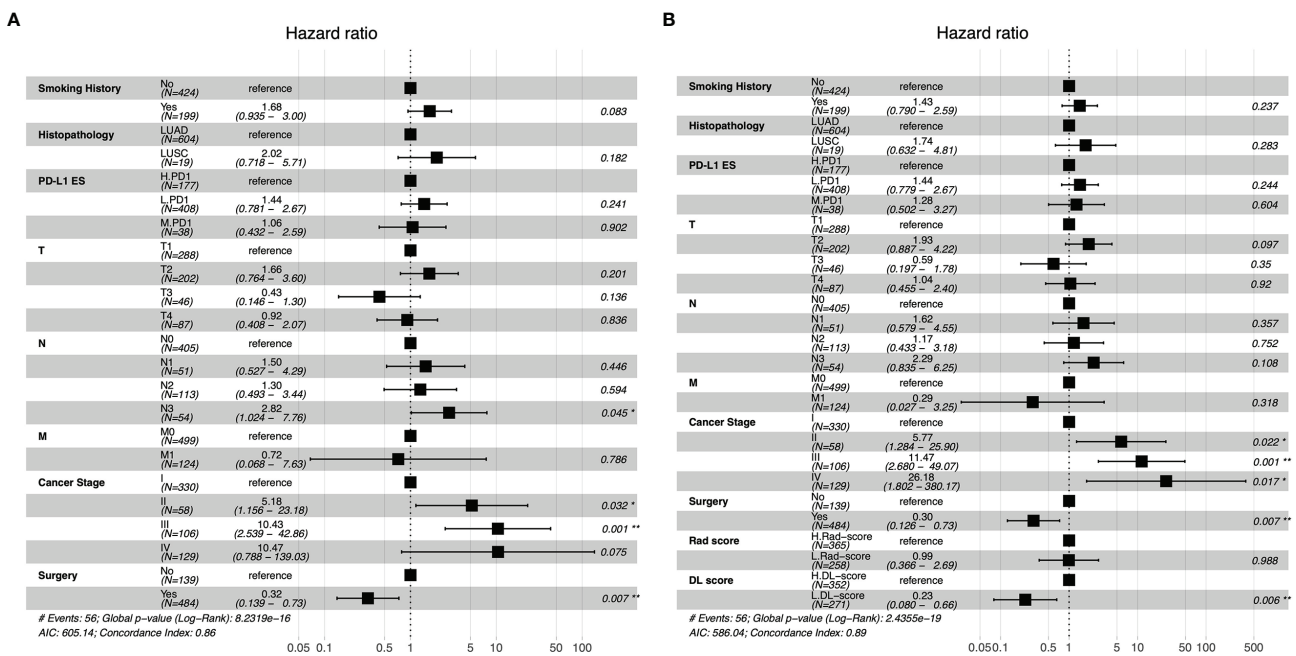

FIGURE 4 | Forest plots of clinical model **(A)**, the combination model with radiomics score and deep learning score **(B)**. PD-L1ES, PD-L1 expression signature; LUAD, lung adenocarcinoma; LUSC, lung squamous cell carcinoma; Rad, radiomics; DL, deep learning.

Conventional assessment of PD-L1 TPS was a time-consuming task due to intertumoral heterogeneity, inter-observer variability, and different antibodies with various possible staining properties (22, 23). As a non-invasive and repeatable method, deep learning based on CT images provided a novel solution. Previous studies have confirmed the application of radiomics and deep learning on accessing PD-L1 status (**Table 2**) (15, 24–31). The latest research proposed a small-residual-convolutional-network (SResCNN) of PET/CT images to discriminate between PD-L1 positive and negative patients (1% cut-off, Dako22C3 antibody) with AUC of ≥0.82 in the training, validation, and testing cohorts (24). The current work was the single largest study population of patients with NSCLC and achieved excellent performance of prediction.

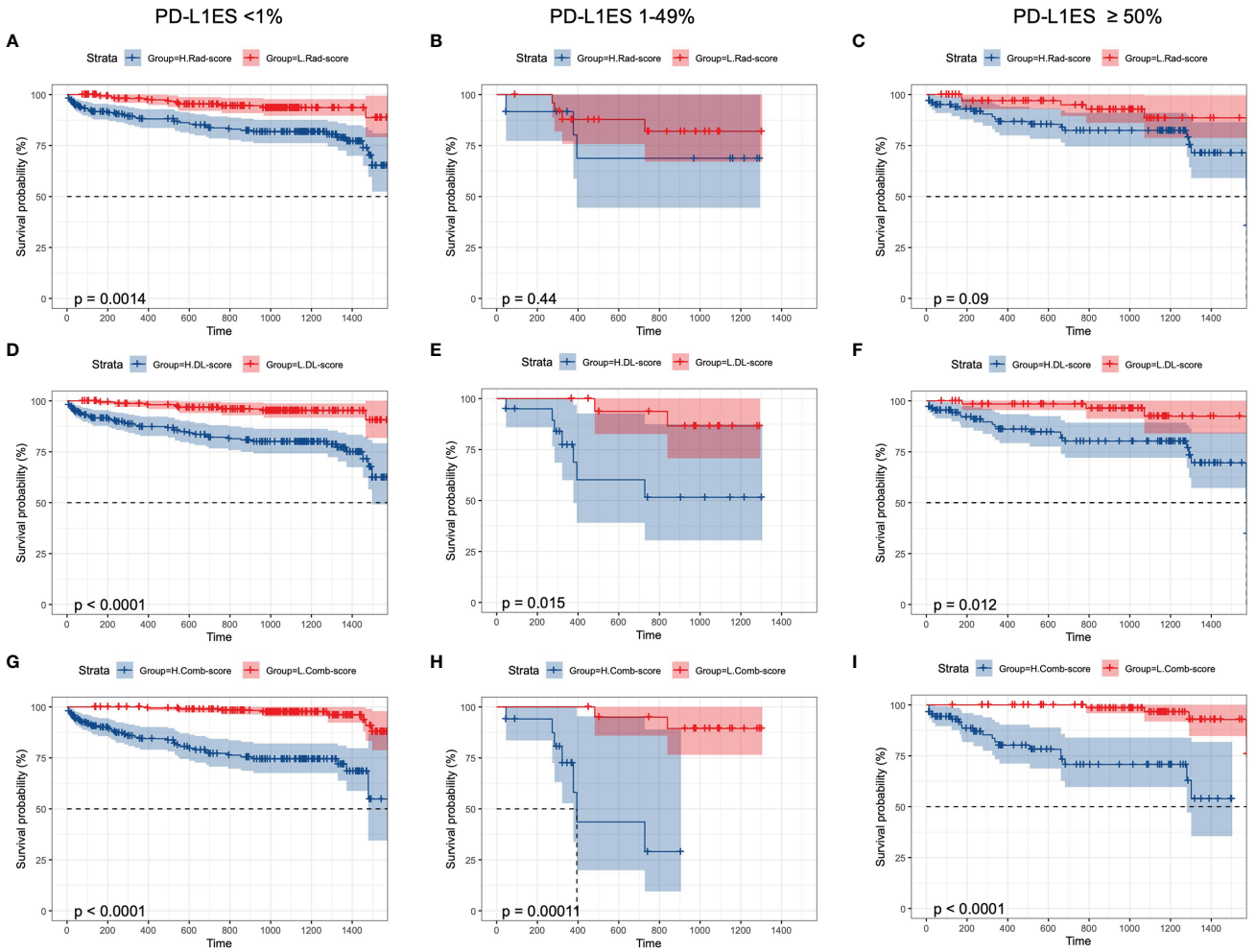

FIGURE 5 | Kaplan–Meier curves of overall survival prediction in different PD-L1 ES groups. K–M curves were stratified by **(A–C)** Rad-score, **(D–F)** DL-score, **(G–I)**: combination-score to identify high-risk and low-risk groups. PD-L1ES, PD-L1 expression signature; Rad, radiomics; DL, deep learning.

However, the challenges of AI faced on the path to clinical adoption cannot be ignored. For instance, the interpretability hindered the widespread of the models. In this study, we utilized heatmap for visualization of deep learning, but the principle of pathophysiology was still inexplicable. Several studies indicated high-response areas of deep learning model based on PET/CT images to predict PD-L1 ES could recognize the necrotic region of lung cancer (24, 32). One possible explanation was that hypoxia leaded cell necrosis while upregulating PD-L1 through hypoxia-inducible factor 1α (33). Therefore, continuous optimization and exploration were warranted for AI-based software to improve patient care ultimately.

Although PD-L1 expression level was widely used, it was not an ideal biomarker for treatment efficacy and prediction model. A phase III randomized trial suggested that TMB might be a useful immune biomarker for deciding whether to use immunotherapy in patients with metastatic NSCLC (18). Moreover, a radiomic signature for CD8 cells that included eight variable CD8 cell radiation signatures containing eight variables to infer clinical outcomes for patients with cancer who had been treated with anti-PD-1/PD-L1 (34). In this study, prognostic models based on usual clinical characteristics or deep learning features were established. Only the comprehensive model combined Rad-score, DL-score, and clinically relevant features achieved superior prediction performance. This indicated the complementarity of radiology image features and clinical variables, and potential of deep learning in precise prognostic assessment.

The current study has some limitations. First of all, this was a single-center study with patients tested with SP42. The model required more central data for verification. Second, this retrospective research cannot avoid the biases of patient selection and detection results. For example, the small number of PD-L1 ES 1-49% group may limit the performance of model. Unfortunately, due to the small number of immunotherapy treatments, we did not predict the efficacy of immune checkpoint inhibitors, which was the direction of our future

TABLE 2 | Recent studies of predicting PD-L1 status on CT images by radiomic or deep learning in lung cancer patients.

First author, Year	Model	Imaging modality	PD-L1 assays	Cut-off	Population,	Performance
Wei Mu (24)	DL small- residual-convolutional-network (SResCNN)	PET/CT	22C3	1%	485 NSCLCs to measure PD-L1 status, 284/116/85 for training validation/testing cohort	AUC of 0.89 (95% CI: 0.84 to 0.94), 0.84 (95% CI: 0.76 to 0.92);, and 0.82 in the training, validation, and testing cohorts, respectively
Panwen Tian (15)	DL KNN	CT	SP142	50%	939 NSCLCs, 750/93/96 for training validation/testing cohort	AUC of 0.78, 0.71, and 0.76 in the training, validation, and testing cohorts
Ying Zhu (25)	DL CNN 3D DenseNets	CT	SP263	1%, 50%	127 advanced LUADs, five-fold cross-validation	1%, AUC of 0.784; 50%, AUC of 0.765
Qiang Wen (26)	Radiomics	CT	SP263	50%	120 advanced NSCLCs	AUC of 0.730 based on radiomic signatures, AUC of 0.839 combined radiomic signatures with clinical and morphological factors
Zekun Jiang (27)	Radiomics	CT	NA	1%	125 NSCLC	AUC of 0.96, 0.85 in training, validation cohort
Stefano Bracci (28)	Radiomics	CT	SP263	50%	72 advanced NSCLCs	AUC of 0.811 and 0.789 in the training and validation cohort
Zongqiong Sun (29)	Radiomics	CT	22C3	50%	390 NSCLC, 260/130 for training/ validation cohort	AUC of 0.829 and 0.848 in the training and validation cohort
Jiyoung Yoon (30)	Radiomics	CT	SP263	50%	153 advanced LUADs	AUC of 0.661 (95% CI 0.580–0.735)
Mengmeng Jiang (31)	Radiomics	CT, PET/CT	SP142	1%, 50%	399 stage I–IV NSCLCs	1%, AUC of 0.97, 0.61, and 0.97 in the CT, the PET, and the PET/CT images respectively; 50% AUC of 0.80, 0.65, and 0.77
			28-8			1%, AUC of 0.86, 0.62, and 0.85; 50%, AUCs of 0.91, 0.75, and 0.88

DL, deep learning; AUC, area under the curve; LUAD, lung adenocarcinoma; NSCLC, Non-small cell lung cancer; CNN, convolutional neural network; KNN, k-nearest neighbor; NA, not applicable.

efforts. Thirdly, this study focused on multi-class prediction for PD-L1 expression, which was unable to cover all actionable biomarkers. Large-scale prospective samples from multi-centers are warranted for investigation in the future.

CONCLUSION

In conclusion, a non-invasive method to measure PD-L1 expression status and infer clinical outcomes was proposed. This deep learning model combined with clinical variables has showed excellent performance, which has potential to effectively manage the personalized treatment of NSCLC patients.

DATA AVAILABILITY STATEMENT

The original contributions presented in the study are included in the article/**Supplementary Material**. Further inquiries can be directed to the corresponding authors.

ETHICS STATEMENT

The studies involving human participants were reviewed and approved by the Ethics approval was obtained from the ethics committee of West China Hospital. The patients/participants provided their written informed consent to participate in this study.

AUTHOR CONTRIBUTIONS

WML and YZY were involved in the study design. CDW, JCM, and JS were involved in the organization of the entire project, data analysis with a clinical perspective, and manuscript writing. CDW, JS, JWL, ZHZ and CCB collected the imaging and clinical data. JCM, JPY, and SZ were involved in the establishment of the algorithm. All authors listed have made a substantial, direct, and intellectual contribution to the work and approved it for publication.

FUNDING

This study was supported by the National Natural Science Foundation of China (82100119, 92159302, 91859203, 81971616), the Science and Technology Project of Sichuan (2022ZDZX0018, 2020YFG0473), the Beijing Municipal Science and Technology Planning Project (Z201100005620008, Z201100005620002).

SUPPLEMENTARY MATERIAL

The Supplementary Material for this article can be found online at: https://www.frontiersin.org/articles/10.3389/fimmu.2022.828560/full#supplementary-material

Supplementary Figure 1 | The illustration of eligible patients enrolled in this study. **(A)** PD-L1 ES prediction (N=1135); **(B)** Survival cohort (N=811).

Supplementary Figure 2 | Kaplan-Meier curves of overall survival prediction based on clinical model. K-M curves were stratified by **(A)** age; **(B)** sex; **(C)** smoking history; **(D)** histopathology; **(E)** PD-L1 ES; **(F)** surgery; **(G)** chemotherapy; **(H)** immunotherapy; **(I)** T-categories; **(J)** N-categories; **(K)** M-categories; **(L)** stage.

REFERENCES

1. Sung H, Ferlay J, Siegel RL, Laversanne M, Soerjomataram I, Jemal A, et al. Global Cancer Statistics 2020: GLOBOCAN Estimates of Incidence and Mortality Worldwide for 36 Cancers in 185 Countries. *CA Cancer J Clin* (2021) 71(3):209–49. doi: 10.3322/caac.21660
2. Bagcchi S. Lung Cancer Survival Only Increases by A Small Amount Despite Recent Treatment Advances. *Lancet Respir Med* (2017) 5(3):169. doi: 10.1016/s2213-2600(17)30041-3
3. Oser MG, Niederst MJ, Sequist LV, Engelman JA. Transformation From Non-Small-Cell Lung Cancer to Small-Cell Lung Cancer: Molecular Drivers and Cells of Origin. *Lancet Oncol* (2015) 16(4):e165–72. doi: 10.1016/s1470-2045(14)71180-5
4. Kim JM, Chen DS. Immune Escape to PD-L1/PD-1 Blockade: Seven Steps to Success (or Failure). *Ann Oncol* (2016) 27(8):1492–504. doi: 10.1093/annonc/mdw217
5. Ribas A, Wolchok JD. Cancer Immunotherapy Using Checkpoint Blockade. *Science* (2018) 359(6382):1350–5. doi: 10.1126/science.aar4060
6. Socinski MA, Jotte RM, Cappuzzo F, Orlandi F, Stroyakovskiy D, Nogami N, et al. Atezolizumab for First-Line Treatment of Metastatic Nonsquamous NSCLC. *N Engl J Med* (2018) 378(24):2288–301. doi: 10.1056/NEJMoa1716948
7. Mok TSK, Wu YL, Kudaba I, Kowalski DM, Cho BC, Turna HZ, et al. Pembrolizumab Versus Chemotherapy for Previously Untreated, PD-L1-Expressing, Locally Advanced or Metastatic Non-Small-Cell Lung Cancer (KEYNOTE-042): A Randomised, Open-Label, Controlled, Phase 3 Trial. *Lancet (London England)* (2019) 393(10183):1819–30. doi: 10.1016/s0140-6736(18)32409-7
8. Ettinger DS, Wood DE, Aisner DL, Akerley W, Bauman JR, Bharat A, et al. NCCN Guidelines Insights: Non-Small Cell Lung Cancer, Version 2.2021. *J Natl Compr Canc Netw* (2021) 19(3):254–66. doi: 10.6004/jnccn.2021.0013
9. Tan WCC, Nerurkar SN, Cai HY, Ng HHM, Wu D, Wee YTF, et al. Overview of Multiplex Immunohistochemistry/Immunofluorescence Techniques in The Era of Cancer Immunotherapy. *Cancer Commun (Lond Engl)* (2020) 40(4):135–53. doi: 10.1002/cac2.12023
10. Li J, Wu J, Zhao Z, Zhang Q, Shao J, Wang C, et al. Artificial Intelligence-Assisted Decision Making for Prognosis and Drug Efficacy Prediction in Lung Cancer Patients: A Narrative Review. *J Thorac Dis* (2021) 13(12):7021–33. doi: 10.21037/jtd-21-864
11. Ardila D, Kiraly AP, Bharadwaj S, Choi B, Reicher JJ, Peng L, et al. End-To-End Lung Cancer Screening With Three-Dimensional Deep Learning on Low-Dose Chest Computed Tomography. *Nat Med* (2019) 25(6):954–61. doi: 10.1038/s41591-019-0447-x
12. Zhang K, Liu X, Shen J, Li Z, Sang Y, Wu X, et al. Clinically Applicable AI System for Accurate Diagnosis, Quantitative Measurements, and Prognosis of COVID-19 Pneumonia Using Computed Tomography. *Cell* (2020) 181(6):1423–33.e11. doi: 10.1016/j.cell.2020.04.045
13. Zhou Y, Xu X, Song L, Wang C, Guo J, Yi Z, et al. The Application of Artificial Intelligence and Radiomics in Lung Cancer. *Precis Clin Med* (2020) 3(3):214–27. doi: 10.1093/pcmedi/pbaa028
14. Wu J, Liu C, Liu X, Sun W, Li L, Gao N, et al. Artificial Intelligence-Assisted System for Precision Diagnosis of PD-L1 Expression in Non-Small Cell Lung Cancer. *Mod Pathol* (2021) 35(3):403–11. doi: 10.1038/s41379-021-00904-9
15. Tian P, He B, Mu W, Liu K, Liu L, Zeng H, et al. Assessing PD-L1 Expression in Non-Small Cell Lung Cancer and Predicting Responses to Immune Checkpoint Inhibitors Using Deep Learning on Computed Tomography Images. *Theranostics* (2021) 11(5):2098–107. doi: 10.7150/thno.48027
16. Wang C, Qiao W, Jiang Y, Zhu M, Shao J, Wang T, et al. The Landscape of Immune Checkpoint Inhibitor Plus Chemotherapy Versus Immunotherapy for Advanced Non-Small-Cell Lung Cancer: A Systematic Review and Meta-Analysis. *J Cell Physiol* (2020) 235(5):4913–27. doi: 10.1002/jcp.29371
17. Herbst RS, Giaccone G, de Marinis F, Reinmuth N, Vergnenegre A, Barrios CH, et al. Atezolizumab for First-Line Treatment of PD-L1-Selected Patients With NSCLC. *N Engl J Med* (2020) 383(14):1328–39. doi: 10.1056/NEJMoa1917346
18. Hellmann MD, Ciuleanu TE, Pluzanski A, Lee JS, Otterson GA, Audigier-Valette C, et al. Nivolumab Plus Ipilimumab in Lung Cancer With a High Tumor Mutational Burden. *N Engl J Med* (2018) 378(22):2093–104. doi: 10.1056/NEJMoa1801946
19. Hellmann MD, Paz-Ares L, Bernabe Caro R, Zurawski B, Kim SW, Carcereny Costa E, et al. Nivolumab Plus Ipilimumab in Advanced Non-Small-Cell Lung Cancer. *N Engl J Med* (2019) 381(21):2020–31. doi: 10.1056/NEJMoa1910231
20. Gandhi L, Rodríguez-Abreu D, Gadgeel S, Esteban E, Felip E, De Angelis F, et al. Pembrolizumab Plus Chemotherapy in Metastatic Non-Small-Cell Lung Cancer. *N Engl J Med* (2018) 378(22):2078–92. doi: 10.1056/NEJMoa1801005
21. Borghaei H, Langer CJ, Paz-Ares L, Rodríguez-Abreu D, Halmos B, Garassino MC, et al. Pembrolizumab Plus Chemotherapy Versus Chemotherapy Alone in Patients With Advanced Non-Small Cell Lung Cancer Without Tumor PD-L1 Expression: A Pooled Analysis of 3 Randomized Controlled Trials. *Cancer* (2020) 126(22):4867–77. doi: 10.1002/cncr.33142
22. McLaughlin J, Han G, Schalper KA, Carvajal-Hausdorf D, Pelekanou V, Rehman J, et al. Quantitative Assessment of the Heterogeneity of PD-L1 Expression in Non-Small-Cell Lung Cancer. *JAMA Oncol* (2016) 2(1):46–54. doi: 10.1001/jamaoncol.2015.3638
23. Cooper WA, Russell PA, Cherian M, Duhig EE, Godbolt D, Jessup PJ, et al. Intra- and Interobserver Reproducibility Assessment of PD-L1 Biomarker in Non-Small Cell Lung Cancer. *Clin Cancer Res* (2017) 23(16):4569–77. doi: 10.1158/1078-0432.Ccr-17-0151
24. Mu W, Jiang L, Shi Y, Tunali I, Gray JE, Katsoulakis E, et al. Non-Invasive Measurement of PD-L1 Status and Prediction of Immunotherapy Response Using Deep Learning of PET/CT Images. *J Immunother Cancer* (2021) 9(6):e002118. doi: 10.1136/jitc-2020-002118
25. Zhu Y, Liu YL, Feng Y, Yang XY, Zhang J, Chang DD, et al. A CT-Derived Deep Neural Network Predicts for Programmed Death Ligand-1 Expression Status in Advanced Lung Adenocarcinomas. *Ann Transl Med* (2020) 8(15):930. doi: 10.21037/atm-19-4690
26. Wen Q, Yang Z, Dai H, Feng A, Li Q. Radiomics Study for Predicting the Expression of PD-L1 and Tumor Mutation Burden in Non-Small Cell Lung Cancer Based on CT Images and Clinicopathological Features. *Front Oncol* (2021) 11:620246. doi: 10.3389/fonc.2021.620246
27. Jiang Z, Dong Y, Yang L, Lv Y, Dong S, Yuan S, et al. CT-Based Hand-Crafted Radiomic Signatures Can Predict PD-L1 Expression Levels in Non-Small Cell Lung Cancer: A Two-Center Study. *J Digit Imaging* (2021) 34(5):1073–85. doi: 10.1007/s10278-021-00484-9
28. Bracci S, Dolciami M, Trobiani C, Izzo A, Pernazza A, D'Amati G, et al. Quantitative CT Texture Analysis in Predicting PD-L1 Expression in Locally Advanced or Metastatic NSCLC Patients. *Radiol Med* (2021) 126(11):1425–33. doi: 10.1007/s11547-021-01399-9
29. Sun Z, Hu S, Ge Y, Wang J, Duan S, Song J, et al. Radiomics Study for Predicting The Expression of PD-L1 in Non-Small Cell Lung Cancer Based on CT Images and Clinicopathologic Features. *J Xray Sci Technol* (2020) 28(3):449–59. doi: 10.3233/xst-200642
30. Yoon J, Suh YJ, Han K, Cho H, Lee HJ, Hur J, et al. Utility of CT Radiomics for Prediction of PD-L1 Expression in Advanced Lung Adenocarcinomas. *Thorac Cancer* (2020) 11(4):993–1004. doi: 10.1111/1759-7714.13352
31. Jiang M, Sun D, Guo Y, Guo Y, Xiao J, Wang L, et al. Assessing PD-L1 Expression Level by Radiomic Features From PET/CT in Nonsmall Cell Lung Cancer Patients: An Initial Result. *Acad Radiol* (2020) 27(2):171–9. doi: 10.1016/j.acra.2019.04.016
32. Jreige M, Letovanec I, Chaba K, Renaud S, Rusakiewicz S, Cristina V, et al. (18)F-FDG PET Metabolic-To-Morphological Volume Ratio Predicts PD-L1 Tumour Expression and Response to PD-1 Blockade in Non-Small-Cell Lung Cancer. *Eur J Nucl Med Mol Imaging* (2019) 46(9):1859–68. doi: 10.1007/s00259-019-04348-x
33. Chang CH, Qiu J, O'Sullivan D, Buck MD, Noguchi T, Curtis JD, et al. Metabolic Competition in the Tumor Microenvironment Is a Driver of Cancer Progression. *Cell* (2015) 162(6):1229–41. doi: 10.1016/j.cell.2015.08.016
34. Sun R, Limkin EJ, Vakalopoulou M, Dercle L, Champiat S, Han SR, et al. A Radiomics Approach to Assess Tumour-Infiltrating CD8 Cells and Response to Anti-PD-1 or Anti-PD-L1 Immunotherapy: An Imaging Biomarker,

Retrospective Multicohort Study. *Lancet Oncol* (2018) 19(9):1180–91. doi: 10.1016/s1470-2045(18)30413-3

Conflict of Interest: The authors declare that the research was conducted in the absence of any commercial or financial relationships that could be construed as a potential conflict of interest.

Publisher's Note: All claims expressed in this article are solely those of the authors and do not necessarily represent those of their affiliated organizations, or those of the publisher, the editors and the reviewers. Any product that may be evaluated in this article, or claim that may be made by its manufacturer, is not guaranteed or endorsed by the publisher.

Copyright © 2022 Wang, Ma, Shao, Zhang, Li, Yan, Zhao, Bai, Yu and Li. This is an open-access article distributed under the terms of the Creative Commons Attribution License (CC BY). The use, distribution or reproduction in other forums is permitted, provided the original author(s) and the copyright owner(s) are credited and that the original publication in this journal is cited, in accordance with accepted academic practice. No use, distribution or reproduction is permitted which does not comply with these terms.

frontiers | Frontiers in Immunology

ORIGINAL RESEARCH
published: 14 April 2022
doi: 10.3389/fimmu.2022.811867

TNF-α-Secreting Lung Tumor-Infiltrated Monocytes Play a Pivotal Role During Anti-PD-L1 Immunotherapy

*Kirsten De Ridder[1], Hanne Locy[1], Elisa Piccioni[1], Miren Ibarra Zuazo[2], Robin Maximilian Awad[1], Stefaan Verhulst[3], Mathias Van Bulck[4], Yannick De Vlaeminck[1], Quentin Lecocq[1], Eva Reijmen[1], Wout De Mey[1], Lien De Beck[1], Thomas Ertveldt[1], Isabel Pintelon[5], Jean-Pierre Timmermans[5], David Escors[2,6], Marleen Keyaerts[7], Karine Breckpot[1] and Cleo Goyvaerts[1]**

[1] Laboratory for Molecular and Cellular Therapy, Department of Biomedical Sciences, Vrije Universiteit Brussel (VUB), Brussels, Belgium, [2] Immunomodulation Group, Navarrabiomed, Navarrabiomed-UPNA-IdISNA, Pamplona, Spain, [3] Liver Cell Biology Research Group, Vrije Universiteit Brussel (VUB), Brussels, Belgium, [4] Laboratory of Molecular and Medical Oncology, Department of Biomedical Sciences, Vrije Universiteit Brussel (VUB), Brussels, Belgium, [5] Laboratory of Cell Biology & Histology, Antwerp Centre for Advanced Microscopy (ACAM), University of Antwerp, Antwerp, Belgium, [6] Rayne Institute, Division of Infection and Immunity, University College London, London, United Kingdom, [7] In Vivo Cellular and Molecular Imaging laboratory, Vrije Universiteit Brussel (VUB), Brussels, Belgium

OPEN ACCESS

Edited by:
Udo S. Gaipl,
University Hospital Erlangen, Germany

Reviewed by:
Shohei Koyama,
Osaka University, Japan
Yaron Carmi,
Tel Aviv University, Israel

***Correspondence:**
Cleo Goyvaerts
cleo.goyvaerts@vub.be

Specialty section:
This article was submitted to Cancer Immunity and Immunotherapy, a section of the journal Frontiers in Immunology

Received: *09 November 2021*
Accepted: *03 March 2022*
Published: *14 April 2022*

Citation:
De Ridder K, Locy H, Piccioni E, Zuazo MI, Awad RM, Verhulst S, Van Bulck M, De Vlaeminck Y, Lecocq Q, Reijmen E, De Mey W, De Beck L, Ertveldt T, Pintelon I, Timmermans J-P, Escors D, Keyaerts M, Breckpot K and Goyvaerts C (2022) TNF-α-Secreting Lung Tumor-Infiltrated Monocytes Play a Pivotal Role During Anti-PD-L1 Immunotherapy. Front. Immunol. 13:811867. doi: 10.3389/fimmu.2022.811867

Immune checkpoint blockade (ICB) of the PD-1 pathway revolutionized the survival forecast for advanced non-small cell lung cancer (NSCLC). Yet, the majority of PD-L1$^+$ NSCLC patients are refractory to anti-PD-L1 therapy. Recent observations indicate a pivotal role for the PD-L1$^+$ tumor-infiltrating myeloid cells in therapy failure. As the latter comprise a heterogenous population in the lung tumor microenvironment, we applied an orthotopic Lewis Lung Carcinoma (LLC) model to evaluate 11 different tumor-residing myeloid subsets in response to anti-PD-L1 therapy. While we observed significantly reduced fractions of tumor-infiltrating MHC-II^{low} macrophages and monocytes, serological levels of TNF-α restored in lung tumor-bearing mice. Notably, we demonstrated *in vivo* and *in vitro* that anti-PD-L1 therapy mediated a monocyte-specific production of, and response to TNF-α, further accompanied by their significant upregulation of CD80, VISTA, LAG-3, SIRP-α and TIM-3. Nevertheless, co-blockade of PD-L1 and TNF-α did not reduce LLC tumor growth. A phenomenon that was partly explained by the observation that monocytes and TNF-α play a Janus-faced role in anti-PD-L1 therapy-mediated CTL stimulation. This was endorsed by the observation that monocytes appeared crucial to effectively boost T cell-mediated LLC killing *in vitro* upon

combined PD-L1 with LAG-3 or SIRP-α blockade. Hence, this study enlightens the biomarker potential of lung tumor-infiltrated monocytes to define more effective ICB combination strategies.

Keywords: anti-PD-L1 immunotherapy, non small cell lung cancer (NSCLC), tumor-infiltrating myeloid cells, TNF-α, immunotherapy resistance

INTRODUCTION

Clinical blockade of the Programmed Death-1 (PD-1, CD279) pathway using monoclonal antibodies (mAbs) was added to the first-line treatment arsenal for advanced non-small cell lung cancer (NSCLC) patients in 2016 (1). This is justified by unprecedented tumor regression and long-term survival benefit in patients upon immune checkpoint blockade (ICB) of PD-1 or its ligand PD-L1 (CD274, B7-H1). However, most patients do not benefit from ICB, while responders often relapse or suffer from immune-related adverse events (2). This highlights the need for continued research in resistance mechanisms to identify additional druggable targets that can embellish the overall survival outcome for NSCLC patients to anti-PD-(L)1 therapies (3).

Preclinical studies suggest that PD-(L)1$^+$ tumor-infiltrating myeloid cells, rather than tumor cells, determine the efficacy of ICB (4–12). In NSCLC, myeloid cells comprise a heterogeneous population of monocytic and granulocytic cells, including inflammatory, residential or Tie2$^+$ angiogenic monocytes; alveolar next to monocyte-derived macrophages with divergent degrees of MHC-II expression; conventional type 1 and 2 dendritic cells (DCs); granulocytes like neutrophils and eosinophils, but also platelets and mast cells. Moreover, they have been shown to express PD-1 and PD-L1, vary in numbers and associate with tumor progression, immunosuppression, and therapy resistance (9, 13–17). Notably, anti-PD-L1 therapy has been shown to improve the immunostimulatory properties of particular myeloid cell subsets (18–21). Moreover, two recent studies reported that anti-PD-L1 therapy induces a systemic alteration of the monocytic compartment in NSCLC patients (22, 23). Nevertheless, how treatment with anti-PD-L1 mAbs affects the composition and function of different lung tumor-infiltrating myeloid subsets in an orthotopic NSCLC model has not been addressed so far.

In search for druggable targets to combine with ICB, we investigated the hypothesis that anti-PD-L1 therapy can induce myeloid cell-mediated resistance mechanisms to ICB therapy. Therefore, we mapped the impact of anti-PD-L1 therapy on 11 different lung tumor-infiltrating myeloid subsets in an ICB-unresponsive tumor model. More specifically we used an orthotopic Firefly luciferase (Fluc)-expressing squamous Lewis Lung Carcinoma (LLC) model to demonstrate that anti-PD-L1 therapy specifically decreases the fraction of MHC-II^{low} macrophages and monocytes within the lung tumor microenvironment. We further demonstrate that anti-PD-L1 therapy stimulates TNF-α secretion *in vivo* as well as *in vitro* with a prominent role, as source and sentinel, for the tumor-infiltrating monocytes. Moreover, the latter rendered more immunosuppressive monocytes demonstrated by elevated expression levels of the alternative checkpoint molecules VISTA, LAG-3, SIRP-α and TIM-3. Importantly, *in vitro* co-blockade of PD-L1 with LAG-3 or SIRP-α strongly boosted cytotoxic T cell (CTL)-mediated LLC killing. As the latter phenomenon was completely abolished in the absence of monocytes, this suggests a crucial role for monocytes in ICB combination effectiveness.

MATERIALS AND METHODS

Mice, Cell Lines and Reagents

Six-week-old female C57BL/6J mice and transgenic OT-I mice were purchased from Charles River. All animals were handled according to the institutional guidelines, approved by the Ethical Committee Dierproeven (ECD) of the Vrije Universiteit Brussel for use of laboratory animals (ECD file numbers: 18-214-1, 18-281-9 and 20-214-12).

Lewis lung carcinoma (LLC) cells, kindly provided by Prof. Jo Van Ginderachter (VUB), were lentivirally transduced to express Firefly luciferase (LLC-Fluc) as described (24). For LLC-specific killing analysis, LLC cells were transduced with lentivectors encoding enhanced green fluorescent protein (eGFP) and ovalbumin (OVA), or Katushka (Kat) to generate LLC-eGFP/OVA or LLC-Kat, resp. Lentivector generation and cell line transductions are described in the **Supplementary Methods**. All LLC lines were maintained in DMEM$^+$ i.e., Dulbecco's-Modified-Eagle's-Medium supplemented with 10% fetal bovine serum (FBS, TICO Europe), 100 units/mL penicillin, 100 μg/mL streptomycin and 2 mM L-Glutamine (all Sigma-Aldrich) at 37°C, 5% CO_2, 21% O_2 and 95% humidity level.

In vivo and *in vitro* recombinant mAb treatments were performed with rat IgG2b, K anti-PD-L1 mAb (clone: 10F9G2), rat IgG1, K anti-TNF-α mAb (clone: MP6-XT22); Ultra-LEAF Purified rat IgG1, K anti-mouse CD223 (LAG-3) mAb (clone: C9B7W), Ultra-LEAF Purified Armenian Hamster IgG anti-mouse PD-1H (VISTA) mAb (clone: MH5A), Ultra-LEAF Purified rat IgG1, K anti-mouse CD172a (SIRP-α) mAb (clone:P84), all from Biolegend next to InVivoMAb rat IgG2a, K anti-mouse TIM-3 mAb (clone: RMT3-23) from BioXcell. The according isotype controls were: Ultra-LEAF^{TM} Purified rat IgG2b, K isotype control (Ctrl) mAb (clone: RTK4530) and rat IgG1, K Ctrl mAb (clone: RTK2071), both from Biolegend. All recombinant antibodies used to stain cells for flow cytometry are listed in **Supplementary Table 1**.

Murine Tumor Cell Transfer, Treatment, and Monitoring

Mice were injected intravenously with 5x1e5 LLC-Fluc cells dissolved in 200 μl phosphate-buffered saline (PBS, Sigma-

Aldrich). Control mice were challenged with 200 µl PBS only. Four days after LLC-Fluc challenge, mice were treated with four intraperitoneal injections of 200 µg anti-PD-L1 or rat IgG2b, K Ctrl mAb dissolved in 200 µl PBS given at 3-day intervals (days 4, 7, 10 and 13). To evaluate TNF-α blockade, 125 µg of anti-TNF-α or rat IgG1, K Ctrl mAb was administered on days 7, 10 and 13 instead. Tumor progression was monitored by body weight follow-up and *in vivo* bioluminescence imaging (BLI) as previously described (25). Briefly, mice were imaged for 7 min using the PhotonImager Optima (Biospace Lab), exactly 5 min after intravenous administration of 30 mg/kg substrate D-luciferin (Promega). Upon euthanasia, whole lungs were weighed and processed for whole-lung imaging or single-cell analysis.

Preparation of Single-Cell Suspensions

Upon cervical dislocation, murine lungs were perfused with 5 ml PBS and transferred to 1 ml Roswell-Park-Memorial-Institute-1640 medium (RPMI-1640, Sigma-Aldrich) with 300 U/ml collagenase-I (Sigma-Aldrich). Lungs were chopped, incubated at 37°C for 45 min, and further mechanically reduced using a 18G syringe until single-cell suspensions could be passed through a 40 µm strainer. Spleens were transferred to 1 ml PBS, tamped, and passed through a 40 µm strainer. Blood (200 µl) was collected submandibularly into 1.3 ml LH microtubes (Sarstedt) and centrifuged for 10 min at 2000g to separate cell pellets from plasma. Murine femurs were isolated to flush out bone marrow with a 25G syringe in 1 ml PBS. Cell pellets were resuspended in 1 ml red blood cell lysis buffer for 5 min, followed by a wash step with PBS before analysis.

Whole Lung Imaging

Lungs from 24 LLC tumor-bearing mice treated with Ctrl mAb and anti-TNF-α mAb or/and anti-PD-L1 mAb were isolated after perfusion with 5 ml PBS solution and fixed overnight at 4°C in 2 ml 0.05 M PBS containing 0.1 M L-lysine, 2 mg/ml NaIO4, and 10 mg/ml paraformaldehyde (PFA solution). The day after, lungs were rinsed in a 24-well plate (Costar) with PBS, consecutively immersed in a sucrose gradient (10%-20%-30%, 2 hrs at room temperature per gradient), embedded in optimal cutting temperature (OCT) compound and stored at -80°C. Frozen lungs were thawed in PFA solution and washed three times in PBS containing 0.5% Triton X-100 (washing buffer) at room temperature on a rotating shaker. For delipidation and antigenicity restoration after tissue fixation, lungs were submersed in FLASH buffer for overnight shaking (55 rpm) at 54°C, as described by Messal et al. (26). The following day, lungs were washed three times, be it with a first washing step in washing buffer with 1% H_2O_2 (Sigma). For nuclear staining, lungs were incubated with TO-PRO-3 (*Invitro*gen) diluted in ScaleCUBIC-1A buffer [as described by Susaki et al. (27)] at 37°C on a rotating shaker. Two days later, lungs were washed three times in PBS with 0.2% Tween 20 (Sigma) for 30 min on a rotating shaker. Subsequently, lungs were submersed in a 1:1 CUBIC-R: H_2O solution for at least 6 hrs [as described by Susaki et al. (27)] and in 100% CUBIC-R solution for overnight incubation at room temperature. The following day, samples were embedded in a CUBIC-R 2% low melting agarose solution and fitted in to a 3D-printed mold (dimensions 2x1x0.8cm). For complete gelation, agarose-embedded lungs were kept at 4°C for at least 2.5 hrs after which they were immersed in CUBIC-R solution. For dehydration, samples were treated with a 1-propanol dilution series (25% - 50% - 75% - 100%) on a rotating shaker at room temperature for 30 min per dilution, and subsequently immersed in 100% 1-propanol for overnight shaking. For optical clearing, a similar concentration gradient was executed with ethyl cinnamate (ECi, Sigma) for 30 min each prior to their imaging using a Lavision Ultramicroscope II. Therefore, samples were immersed in ECi within a quartz cuvette and excited with light sheets of wavelengths 488 and 640 nm to record autofluorescent and TO-PRO-3 staining, resp. Image acquisition was performed on 2x magnification, 0.63x zoom and Z-stack steps of 10 µm. Files were saved as OME.TIF stacks and converted to Imaris files (.ims) using ImarisFileConverter (version 9.5.0), while tiles were stitched using ImarisStitcher (version 9.5.0). Three-dimensional images and tumor volumes were obtained with Imaris and quantified using surface creation algorithms.

Flow Cytometry and Fluorescence-Activated Cell Sorting

Prior to staining, Fc-receptors were blocked using CD16/32 antibody (Biolegend) in cold FACS buffer i.e., PBS containing 1% bovine-serum-albumin and 0.02% sodium azide (Sigma-Aldrich). Next, staining was performed for 30 min at 4°C in FACS buffer. Fluorescently labelled cells were evaluated on a LSR Fortessa flow cytometer [Becton Dickinson (BD)], while analysis was performed using FlowJo_10.5.3 software. For myeloid subset sorts, the $CD45^+$ immune cell fraction was enriched from whole lung tissue using anti-mouse CD45 MicroBeads (Miltenyi Biotec), prior to staining and FACS with a BD FACSAriaIII.

LLC-Specific OT-I Killing Assay

Using the $CD8\alpha^+$ T-Cell-Isolation-Kit (Miltenyi Biotec), the $CD8^+$ T-cell fraction was enriched from an OT-I mouse-derived splenic single-cell suspension. Next, 1e6 OT-I cells were resuspended in 1 ml $RPMI\text{-}1640^+$ with 50 µmol/L β-mercaptoethanol and stimulated for two days with 20 µl Mouse T-Activator CD3/CD28 Dynabeads (Gibco). To evaluate target cell-specific killing, 6k LLC-eGFP/OVA cells were mixed with 6k LLC-Kat cells, 11k monocytes and 3k stimulated OT-I cells to obtain a target:effector ratio of 2:1 in 250 µl $DMEM^+$. The added monocytes were either *in vitro* differentiated from bone marrow cells or isolated and MACS enriched using the Monocyte Isolation Kit and CD45 microbeads (Miltenyi Biotec, #130-100-629 and 130-052-301 resp.). While supernatants were collected 72hrs later for TNF-α and IFN-γ ELISA, cells were detached with 50 µl Trypsine-EDTA (Sigma-Aldrich) for 5 min at 37°C. LLC target cell-specific OT-I killing was evaluated by comparing the ratio of LLC-eGFP/OVA (target) over LLC-Kat (non-target) cells *via* flow cytometry. The percentage of specific killing normalized for the ratio in the cultures without OT-I cells was calculated with the following equation: 1−(%LLC-eGFP/OVA/%LLC-Kat) with CTLs/(%LLC-eGFP/OVA/%LLC-Kat) without CTLs. For spatiotemporal

follow-up of target LLC-eGFP/OVA cell killing, eGFP intensity was monitored using Incucyte live cell imaging.

Cytokine and Chemokine Detection

Serological concentrations of 31 cytokines and chemokines were measured using the Bio-Plex Pro_Mouse_Chemokine_Panel_31-Plex (#12009159, Bio-Rad). Samples were prepared and analyzed according to the manufacturers' protocol using the Bioplex-200 instrument and Bio-Plex_Manager_6.0 software. Data points from standards that did not meet accuracy requirements were excluded prior to curve fitting. Standard curves obtained *via* 5PL logistic regression were used to determine the concentrations (pg/ml) for each analyte. Outliers were removed using the Interquartile Range method.

Protein levels of murine IFN-g and TNF-a were detected on supernatants collected from bone marrow-derived monocytes, splenocytes or the in vitro LLC-specific OT-I killing assay as described in the respective figure legends. Both ELISA kits (Invitrogen) were used according to the manufacturer's protocol.

Targeted Gene Expression Profiling

For each FACS-sorted lung-derived myeloid subset, 5x1e4 cells were collected in 500 µl Trizol and stored at -80°C. One to three weeks later, cell pellets were thawed, and RNA was isolated using the chloroform-isopropanol protocol. RNA recovery was quantified using fluorimetry (Qubit, LifeTechnologies) and qualified for purity and integrity using the nanophotometer (Implen) and Bioanalyzer Labchip (Agilent Technologies), resp. Due to low RNA concentrations, samples were pre-amplified using the nCounter Low-RNA-input kit (NanoString Technologies) with five amplification cycles. Sample hybridization was performed according to the manufacturers' recommendations using the nCounter_Myeloid_Innate_Immunity_Panel containing 770 genes. Hybridized samples were transferred to the nCounter Prep Station for further purification and immobilization to the sample cartridges. Absolute counts were quantified by the nCounter Digital Analyzer (nCounter MAX Analysis System, Brightcore, VUB). For quality control the nSolver_analysis_software_4.0 was used. Raw counts were processed in R and normalized using the RUVSeq method adjusted for NanoString analysis as described (28). Normalized counts were used to analyze differences between anti-PD-L1 and Ctrl mAb-treated samples. The DESeq R-package was used for differential expression analysis while gene-set-enrichment analysis (GSEA) was performed with settings: 1000 permutations, gene set selected as permutation type, and chip platform set to "Mouse_ENSEMBL_Gene_ID_Human_Orthologs_MsigDB.v7.2". For analysis, the Hallmark gene sets curated from the Molecular Signature Database (MSigDB) were used.

Generation and Evaluation of Bone Marrow-Derived Monocytes

Primary bone marrow-derived cells from healthy female C57BL/6J mice, were plated at 4x1e6 in 10 ml $DMEM^+$ supplemented with 20ng/ml macrophage colony-stimulating factor (M-CSF, Immunotools) in 100mmx15mm petri-dishes. Five days later, the non-adherent fraction was collected, representing a mixture of bone marrow-derived immature myeloid cells (**Figure 3C**). Next, 5x1e4 cells were plated per 200 µl $DMEM^+$ in flat-bottom 96-well plates and subjected to 5 µg/ml anti-PD-L1 or Ctrl mAb and/or 10 ng/ml TNF-α (PeproTech). While supernatants were collected 24hrs later for TNF-α ELISA, monocytes were detached 72 hrs later using Accutase (Sigma-Aldrich) for 30 min at 37°C prior to flow cytometric analysis.

Activation and Evaluation of Murine Splenocytes

Primary splenocytes from healthy female C57BL/6J mice were collected and plated at $2x10^5$ cells/200 µl $RPMI\text{-}1640^+$ with 50 µmol/L β-mercaptoethanol and 30 ng/ml IL-2 (Peprotech) per well of a U-bottom 96-well plate. After overnight stimulation with 20 µl/10^6 cells of Mouse T-Activator CD3/CD28 Dynabeads (Gibco), cells were treated for 72hrs with 1 µg/ml recombinant TNF-α (PeproTech), with or without 10 µg/ml Ctrl mAb or anti-PD-L1 mAb after which supernatants were collected for IFN-γ ELISA.

Statistics

The asterisk number in the figures indicates the level of statistical significance as follows: * for $p < 0.05$; ** for $p < 0.01$; *** for $p < 0.001$ and **** for $p < 0.0001$. The statistical test used to determine statistical significance is indicated in the figure legends. Statistical tests were performed using RStudio v1.3.1056 or Graphpad Prism v8.3.0. Heatmaps were constructed with the heatmap package in R. Serological concentrations are scaled by subtracting the mean and dividing by standard deviation for each sample. For GSEA, gene sets were identified as significant when nominal (NOM) p-value < 0.01, false discovery rate (FDR) < 0.25, and normalized enrichment score (NES) > 1.

RESULTS

Anti-PD-L1 Therapy Has No Therapeutic Benefit Despite PD-(L)1 Expression

Lewis Lung Carcinoma (LLC) represents a highly tumorigenic mesenchymal K-Ras mutant squamous lung cancer model, characterized by low tumor cell-specific PD-L1 expression with limited response to anti-PD-L1 therapy (5, 6). As $Fluc^+$ tumor lines have been shown to be more immunogenic (30), we first evaluated if LLC-Fluc tumors were similarly unresponsive to treatment with anti-PD-L1 or isotype control (Ctrl) mAbs (**Figure 1A**). Follow-up of body weights and tumor load (bioluminescent signals) over time demonstrated that anti-PD-L1 therapy does not reduce tumor progression (**Supplementary Figures 1A, B** resp.). Three weeks after engraftment, mice were sacrificed to isolate whole lungs. Similar lung weights (**Figures 1C**), tumor foci volumes (**Figures 1D, E**), numbers and average volumes (**Supplementary Figures 1B, C**), further confirmed the lack of therapeutic effect upon anti-PD-L1 therapy.

Anti-PD-L1 therapy can only lead to stimulation of antitumor immunity if the PD-1 pathway is exploited. Therefore, we evaluated whether absence of PD-1 and/or PD-L1 in the lung tumor microenvironment could account for therapy failure in

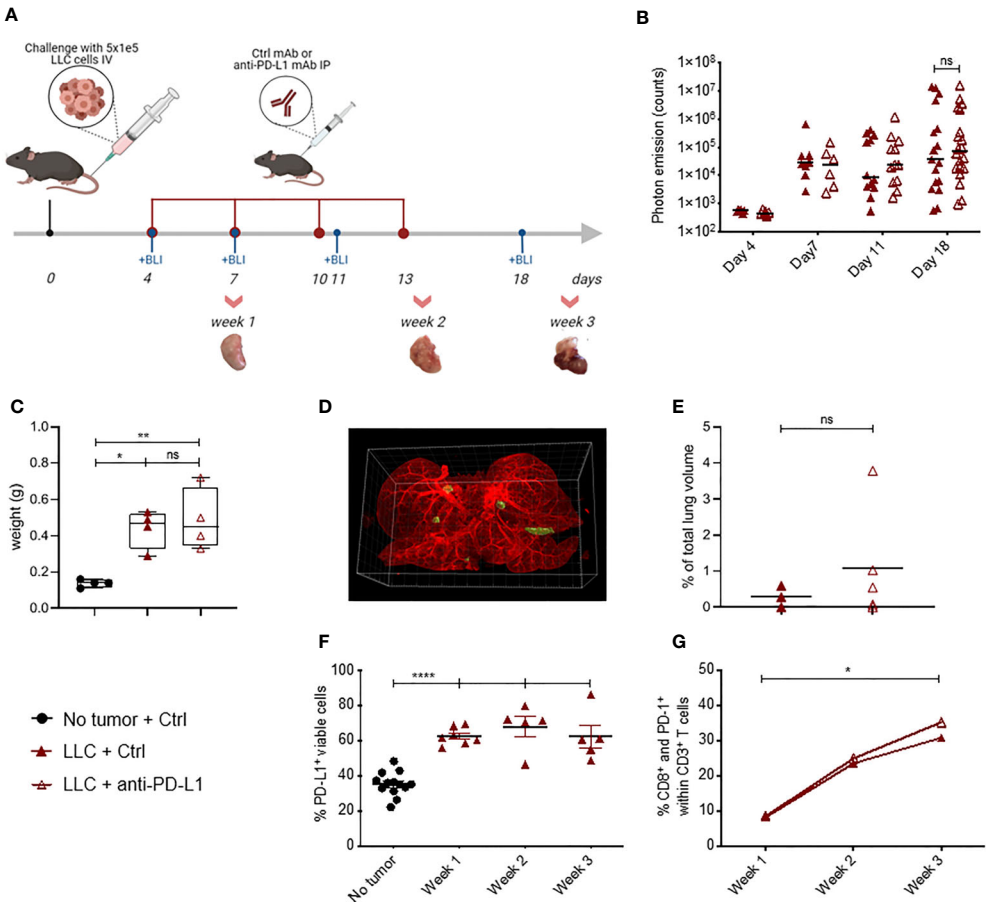

FIGURE 1 | Blockade of PD-L1 does not delay LLC-Fluc tumor progression, despite PD-(L)1 expression. **(A)** Schematic representation of the experimental set-up. Mice were challenged intravenously (IV) with LLC-Fluc cells and treated every 3 days with anti-PD-L1 or isotype control (Ctrl) mAbs for 4 times in total (red dots). LLC-Fluc engraftment was monitored using *in vivo* bioluminescence imaging (BLI) on the indicated time points (blue dots), while on weeks 1, 2 and 3, lungs were also isolated for flow cytometric evaluation. **(B)** Summary of photon counts collected upon BLI measurements. On a logarithmic scale, the absolute number of counts per analyzed day (on x-axis) are shown (n=3, 5 mice per condition [mpc]). A two-way ANOVA with Sidak's multiple comparisons test was performed to evaluate statistical significance. **(C)** Weights of whole lungs, isolated from healthy or tumor-bearing mice sacrificed three weeks after cancer initiation (n=1, 4-5 mpc). **(D)** A representative 3D image that is used for volumetric quantification of tumor volumes (green) in an Ctrl mAb-treated murine lung (autofluorescence, red), obtained with Imaris software. **(E)** Percentage of tumor volume over whole lung volume to compare LLC engraftment in mice treated with Ctrl mAbs or anti-PD-L1 mAbs (n=3-4). Statistical significance was measured using an unpaired t-test. **(F)** Graph representing the percentages of PD-L1$^+$ cells found upon flow cytometry analysis of the viable lung single-cell fraction, isolated from healthy or LLC-Fluc tumor-bearing mice on weeks 1-3 after tumor challenge (n=3, 1-3 mpc). **(G)** Percentage of lung tumor-infiltrated PD-1$^+$ CD8$^+$ T-cells within the CD3$^+$ T-cell population at 1, 2 and 3 weeks after LLC-Fluc inoculation analyzed *via* flow cytometry (n=3, 1-3 mpc). A two-way ANOVA with Tukey's multiple comparisons test was performed to determine statistical significance in panels **(C, F, G)**. ns, non-significant; * for $p < 0.05$; ** for $p < 0.01$; and **** for $p < 0.0001$.

the orthotopic LLC-Fluc model. Flow cytometric analysis of lungs, isolated 1, 2 and 3 weeks after LLC-Fluc challenge, showed that the overall percentage of PD-L1$^+$ pneumocytes increased during LLC-Fluc progression compared to healthy controls (**Figure 1F** with gating strategy in **Supplementary Figure 1D**). Also *in vitro*, flow cytometric analysis of LLC-Fluc cells endorsed their ability to express and upregulate PD-L1 upon exposure to IFN-γ (**Supplementary Figure 1E**). Moreover, we observed a significant increase in the percentage of PD1^{-+} CD8$^+$ T-cells over time irrespective of anti-PD-L1 therapy (**Figure 1G** with gating strategy in **Supplementary Figure 2A**). In parallel, while CD4$^+$ T- and B-cell fractions decreased upon tumor progression, their respective PD-1$^+$ portions also increased significantly (**Supplementary Figures 2B–E**). To conclude, despite significant PD-1 and PD-L1 expression in the orthotopic LLC-Fluc model, anti-PD-L1 therapy does not delay tumor progression.

LLC Progression Is Accompanied by a Local and Systemic Increase in Monocytes

In light of add-on therapies that can improve the response to anti-PD-L1 therapy, it is crucial to understand if, which and how PD-L1$^+$ cells respond *in vivo*. Therefore, we first deciphered which cells were PD-L1$^+$ and thus could act as potential targets

for anti-PD-L1 therapy. When the portions of $CD45^-$ (non-immune), $CD45^+$ (immune) or/and $CD11b^+$ (myeloid) cells were determined within the total PD-$L1^+$ fraction, a significant increase of myeloid cells was shown from week 1 onwards after LLC-Fluc challenge (**Figure 2A**). In accordance with recent reports on the negative impact of PD-1^+ myeloid cells on T-cell amplification responses (31, 32), PD-1 positivity was also evaluated, showing a similar five-fold increase for PD-1 and PD-L1 within the tumor-infiltrated $CD11b^+$ fraction upon LLC-Fluc progression (**Figure 2B**). Next, we assessed changes in abundance and PD-(L)1 expression level of 11 different myeloid subsets (gating strategy in **Supplementary Figure 3A**). Upon tumor progression, 6 lung-residing myeloid subsets increased compared to healthy mice: MHC-II^{high} and MHC-II^{low} tumor-associated macrophages (TAMs), inflammatory $Ly6C^+$ monocytes, residential $Ly6C^-$ monocytes and angiogenic $Tie2^+$ monocytes next to conventional type 2 dendritic cells (cDC2) (**Figure 2C**, upper row). Moreover, these subsets increased their PD-L1 expression over time, except for the MHC-II^{high} TAMs (**Figure 2C**, middle row). Further, cDC2s increased their PD-1 expression while the opposite was found for MHC-II^{high} TAMs (**Figure 2C**, lower row). In contrast, the fraction of alveolar macrophages and eosinophils decreased significantly during tumor progression, while mast cells, cDC1 and neutrophil portions remained status quo (**Supplementary Figure 3B**). The systemic impact of LLC-Fluc engraftment was evaluated by serological evaluation of 31 chemo- and cytokines next to determination of the myeloid composition in blood, spleen and bone marrow. In accordance with the increase in TAMs and monocytes linked to LLC-Fluc progression, macrophage chemoattracting protein-3 (MCP-3 or CCL7) circulated at a significantly higher level in LLC-bearing animals (**Figure 2D** and **Supplementary Table 2**). In contrast, the serological level of IFN-γ was significantly decreased in LLC-bearing mice compared to healthy controls. Finally, the lung-specific increase in monocytes (but not of TAMs nor cDC2s – data not shown), was reflected systemically by their significant rise in blood (**Figure 2E**) and bone marrow resp. (**Figure 2F**).

Anti-PD-L1 Therapy Abolishes the Rise in MHC-II^{low} TAMs and Monocytes Upon LLC Progression

The impact of anti-PD-L1 therapy on the local and peripheral myeloid cell distribution in LLC-bearing animals was evaluated using the experimental design shown in **Figure 1A**. Briefly, LLC-bearing mice were treated with Ctrl or anti-PD-L1 mAbs given 4 times at 3-day intervals. Lungs were isolated on weeks 1, 2 and 3 to evaluate the dynamics of 11 different lung-residing myeloid subsets. No significant differences were found for neutrophils, eosinophils, mast cells, alveolar macrophages, MHC-II^{high} TAMs, cDC1s or cDC2s (**Supplementary Figure 4**). In contrast, the elevation in MHC-II^{low} TAMs and monocytes linked to LLC progression was abolished by anti-PD-L1 therapy (**Figure 3A**). Also, anti-PD-L1 therapy resulted in a significantly reduced fraction of MHC-II^{low} macrophages residing in the bone marrow next to an insignificant trend towards reduced numbers of inflammatory and patrolling monocytes in blood and bone marrow (**Figure 3B**). To understand if this reduction was linked to a direct impact of anti-PD-L1 mAbs on macrophages and/or monocytes, we treated primary bone marrow-derived myeloid cells with anti-PD-L1 or Ctrl mAbs. In line with the *in vivo* data, co-cultivation with LLC cells resulted in a significant increase of the MHC-II^{low} $Ly6C^+$ monocyte fraction *in vitro*, while anti-PD-L1 mAb-treatment resulted in a significant decrease compared to the untreated monoculture (**Figure 3C**). In contrast, no significant changes were observed within the $F4/80^+$ macrophage populations. We further evaluated the ratio of MHC-II^{high} over MHC-II^{low} TAMs *in vivo* and only found an insignificant trend towards more MHC-II^{high} TAMs suggesting that anti-PD-L1 therapy in the LLC model was not able to install a pronounced immunostimulating environment (**Figure 3D**). Finally, we sorted the lung tumor-infiltrated MHC-II^{high} and MHC-II^{low} TAMs and $Ly6C^+$ inflammatory and $CX3CR1^+$ residential monocytes from 3-week LLC-engrafted mice to evaluate their capacity to boost LLC target cell-specific killing *ex vivo* (**Figures 3E, F**). We observed that anti-PD-L1 therapy only modestly improved the capacity of the MHC-II^{high} TAMs and residential monocytes to boost CTL-mediated LLC eradication.

Anti-PD-L1 Therapy Results in a Monocyte-Specific TNF-α Response

As anti-PD-L1 therapy does not result in LLC growth reduction while it modestly increases the immunostimulatory profile of TAMs and monocytes, we used the nCounter Myeloid_Innate_Immunity_Panel to uncover more subtle myeloid subset-specific transcriptional changes upon anti-PD-L1 therapy *in vivo*. While no significant differentially expressed genes were found within sorted $CX3CR1^+$ monocytes or MHC-II^{low} TAMs, *Dusp2* and *Stab1* were significantly up-and down-regulated resp., in inflammatory monocytes derived from anti-PD-L1 mAb-treated mice (**Supplementary Figure 5A**). Using Gene Set Enrichment Analysis (GSEA) with the hallmark gene-set collection of MSigDB, we found that MHC-II^{low} TAMs from anti-PD-L1-treated mice significantly decreased their expression of an IFN-γ response linked gene set, again suggesting that anti-PD-L1 therapy does not support stimulation of an IFN-γ-linked CTL response *in vivo* (**Supplementary Figure 5B**). In contrast, monocytes of anti-PD-L1-treated mice showed significant enrichment for a gene set that is regulated by NF-kB in response to TNF-α (**Figures 4A, B**). Accordingly, these monocytes showed a significantly increased level of intracytoplasmic TNF-α compared to healthy LLC-bearing Ctrl mAb-treated mice (**Figure 4C**). In contrast, we did not observe this TNF-α increase in the MHC-II^{high} nor ^{low} macrophages upon anti-PD-L1 therapy (**Supplementary Figures 5C, D** resp.). In congruence, anti-PD-L1 mAb treatment rectified the serological drop of TNF-α caused by LLC engraftment (**Figure 4D**). When bone marrow-derived immature myeloid cells were treated with anti-PD-L1 mAbs *in vitro*, we confirmed significantly elevated levels of TNF-α in these supernatants compared to Ctrl mAb treatment (**Figure 4E**). Encouraged by these data and previous reports on TNF-α blockade to improve anti-PD-1 therapy efficacy in a mouse model of melanoma and colon carcinoma (33, 34), we evaluated the therapeutic potential of TNF-α and PD-L1 co-blockade in the LLC-Fluc model. Mice were treated with anti-PD-L1 mAbs on

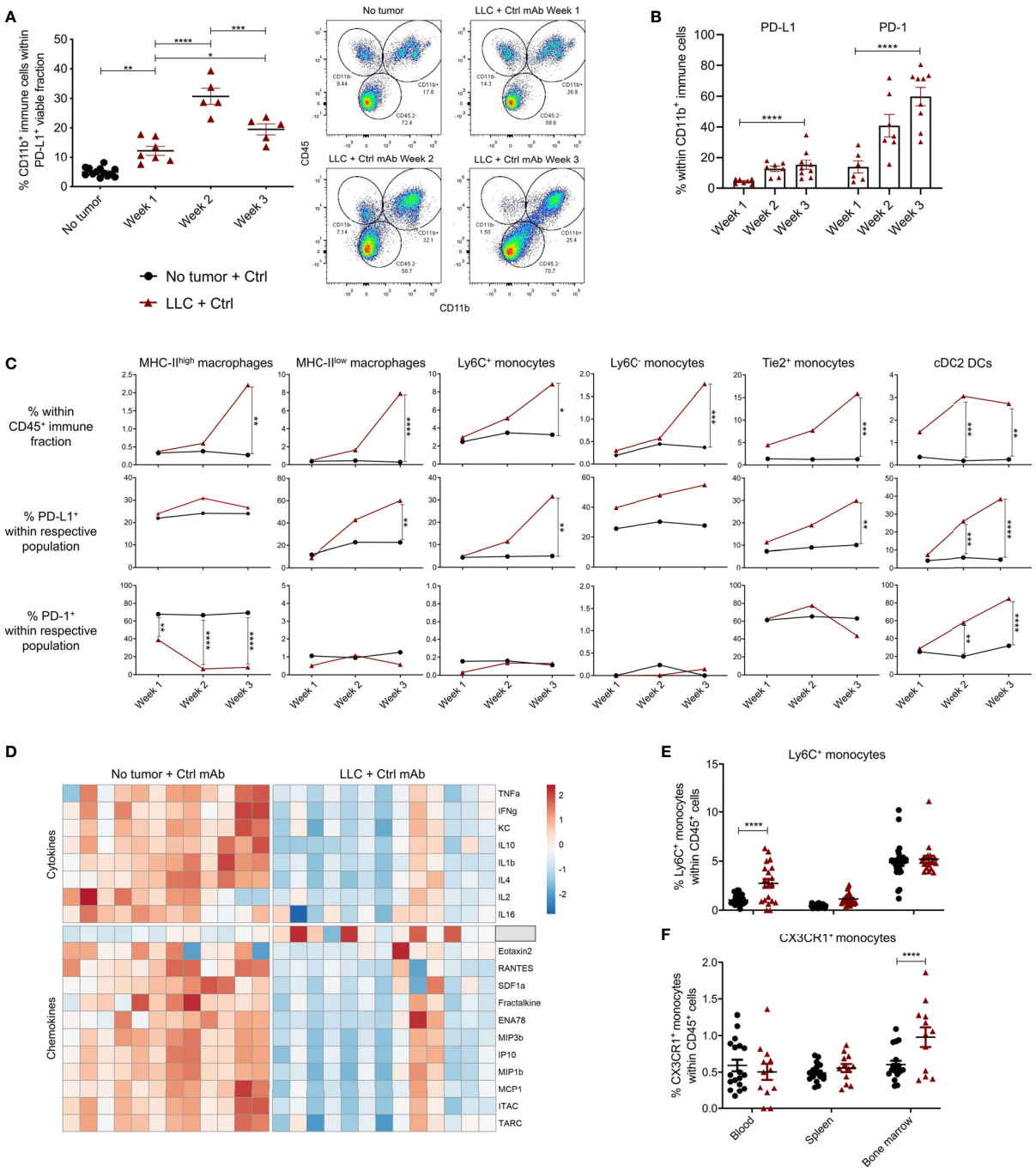

FIGURE 2 | PD-L1$^+$ and PD-1$^+$ myeloid cells in healthy and LLC-engrafted mice. Lungs of healthy and LLC-Fluc tumor-bearing mice were isolated on weeks 1, 2 and 3 after LLC-Fluc challenge to evaluate PD-L1 and PD-1 expression in flow cytometry. **(A)** Summary of percentages of CD45$^+$ CD11b$^+$ myeloid cells within the viable PD-L1$^+$ fraction (left panel) with representative dot plots (right panel, n=3, 1-3 mpc). **(B)** Evolution of myeloid cell-specific PD-L1 and PD-1 expression over time in lungs from LLC-bearing mice (n=3, 1-3 mpc). **(C)** Follow-up of MHC-II^{high} or MHC-II^{low} F4/80$^+$ macrophages; Ly6C$^+$, Ly6C$^-$ or Tie2$^+$ monocytes and CD11b$^+$ CD103$^-$ cDC2 within the CD45$^+$ immune fraction from healthy (no tumor) or LLC-engrafted lung tissue over the course of 3 weeks (upper row), next to their respective expression of PD-L1 (middle row) and PD-1 (lower row) (n=3, 1-3 mpc). **(D)** Heatmap of significantly altered cytokines and chemokines in serum of mice, collected 3 weeks after challenge with LLC-Fluc or PBS only. Per chemo-/cytokine, concentrations were centered and scaled resulting in a color scale ranging from blue to red for lowest to highest concentration values. Statistics were performed using one-way ANOVA followed by Tukey's multiple comparison test (F-value= 8.97, Df= 2) (n=2, 4-8 mpc). **(E, F)** Percentage of Ly6C$^+$ **(E)** and CX3CR1$^+$ **(F)** monocytes, within viable CD45$^+$ single-cells from blood, spleen and bone marrow collected from mice 3 weeks after inoculation with PBS or LLC-Fluc cells (n=3, 5-10 mpc). For panels **(A–C, E, F)** a two-way ANOVA with Sidak's multiple comparisons test was performed to evaluate statistical significance. ns, non-significant; * for $p < 0.05$; ** for $p < 0.01$; *** for $p < 0.001$; and **** for $p < 0.0001$.

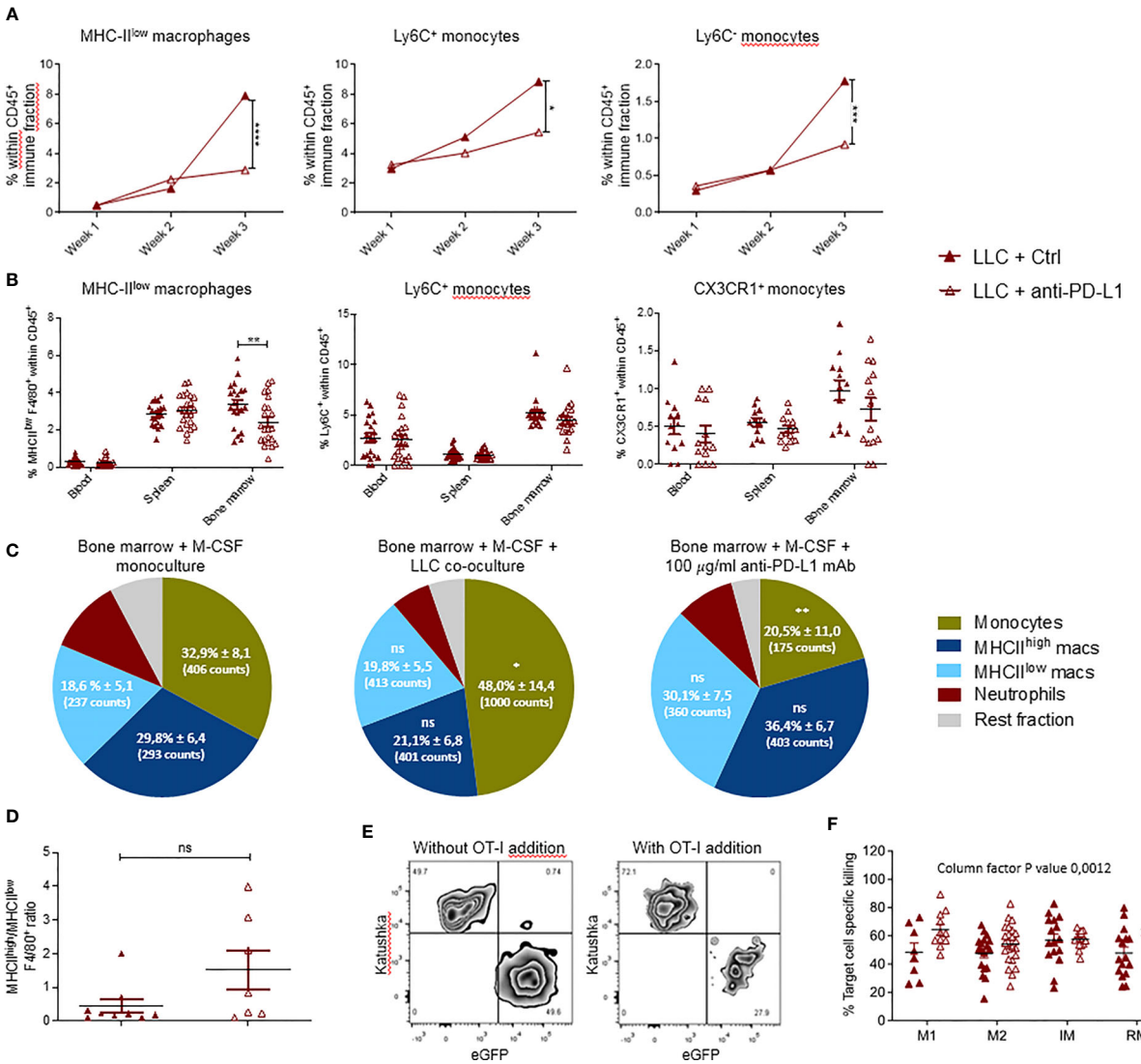

FIGURE 3 | Local and systemic impact of anti-PD-L1 therapy on myeloid cells. Mice were treated with Ctrl or anti-PD-L1 mAbs on days 4, 7, 10 and 13 after LLC-Fluc injection. On weeks 1, 2 and 3, mice of each group were sacrificed to isolate LLC-engrafted lungs. Blood, spleen and bone marrow were collected on week 3. **(A)** Graphs indicating changes in percentage of lung-infiltrated MHC-II^{low} macrophages (left), Ly6C^{+} monocytes (middle) and Ly6C^{-} monocytes (right) within the CD45^{+} immune cell fraction assessed using flow cytometry (n=3, 1-3 mpc). **(B)** Percentages of MHC-II^{low} macrophages (left), Ly6C^{+} monocytes (middle) and CX3CR1^{+} monocytes (right) in peripheral organs as depicted on the x-axis (n=3, mpc=5-10). Two-way ANOVA with Sidak's multiple comparisons test was performed to evaluate statistical significance. **(C)** Bone marrow-derived cells were cultivated with monocyte colony-stimulating factor (M-CSF) for 5 days. Next, cells were left untreated (left), co-cultured with LLC cells (middle) or 100μg/ml anti-PD-L1 mAb (right). One day later, alterations in myeloid subset composition were evaluated *via* flow cytometry. Percentages (± sd) from the total CD11b^{+} population are shown. Percentages are accompanied by the average counts for the surface markers MHC-II^{low}, MHC-II^{high} and Ly6C to describe the mean fluorescence intensity of MHC-II^{low} macrophages, MHC-II^{high} macrophages and monocytes resp. (n=5). **(D)** Graphical representation of the altered ratio of lung-residing MHC-II^{high} over MHC-II^{low} TAMs isolated from tumor-bearing mice treated with Ctrl or anti-PD-L1 mAbs. An unpaired t-test was performed to analyze statistical significance (n=3, 2-3 mpc). **(E)** Representative zebra plot of the LLC-specific OT-I killing assay with gating of target LLC-eGFP/OVA and non-target LLC-Kat cells, with or without pre-stimulated CD8^{+} OT-I T cells. **(F)** Percentage target cell-specific killing in the presence of MHC-II^{high} TAM, MHC-II^{low} TAM, Ly6C^{+} inflammatory (IM) and CX3CR1^{+} residential (RM) monocytes sorted from lung tumor-bearing mice, treated with Ctrl or anti-PD-L1 mAbs (n=5, ≧3 biological replicates). For determination of statistical analysis in **(A, C, F)**, a two-way ANOVA with Tukey's multiple comparisons test was performed. ns, non-significant; * for $p < 0.05$; ** for $p < 0.01$; *** for $p < 0.001$; and **** for $p < 0.0001$.

day 3 after LLC-Fluc cell injection and subsequently on days 7, 10 and 13 with anti-TNF-α mAbs, anti-PD-L1 mAbs or a combination thereof. Upon 3D whole lung tissue imaging 3 weeks later, no significant differences were found in terms of total tumor volume, number of foci or average foci volume (**Figures 4F, G** and **Supplementary Figures 5E, F**), showing no therapeutic benefit of TNF-α blockade in the anti-PD-L1-treated orthotopic LLC model.

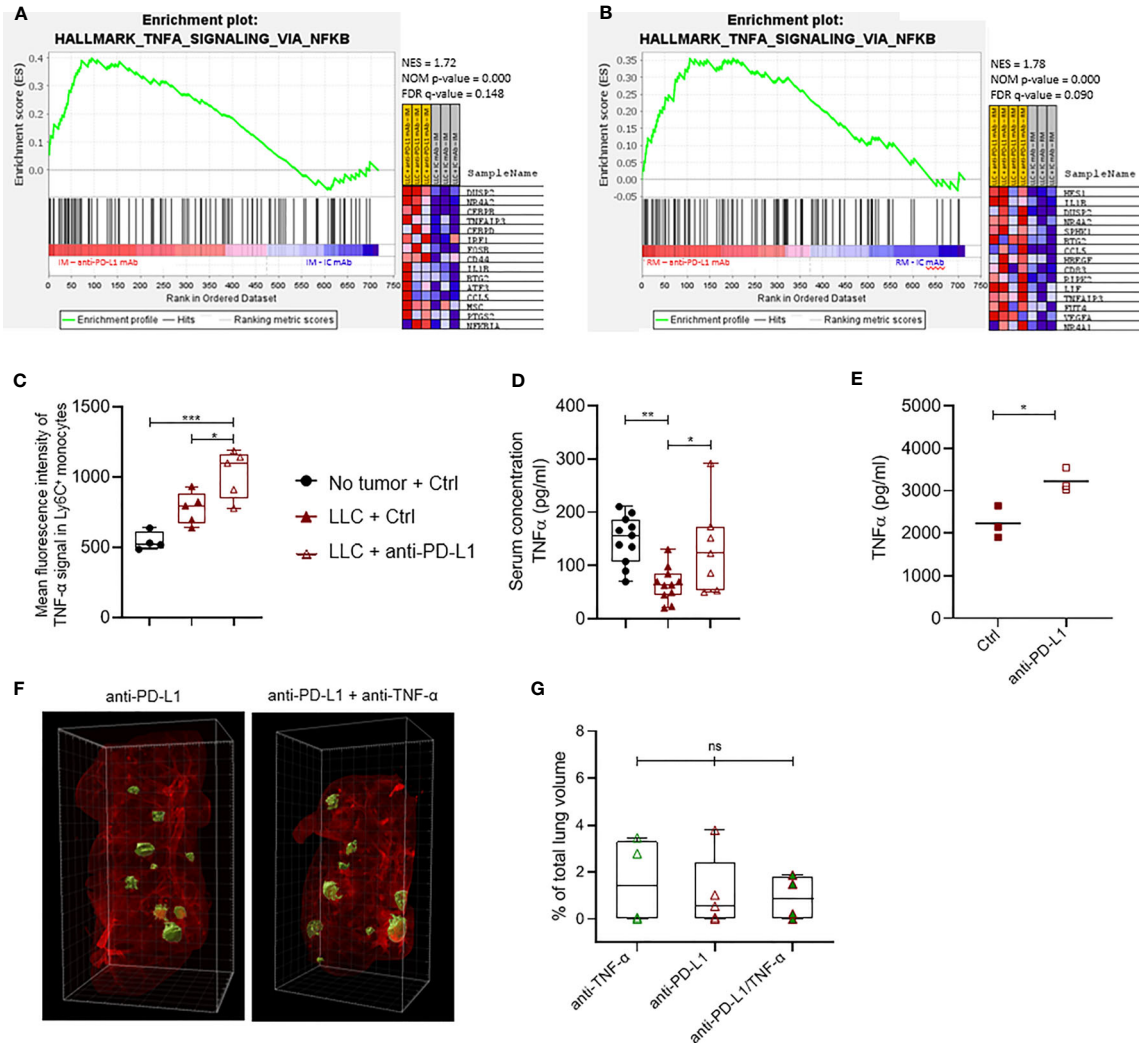

FIGURE 4 | Anti-PD-L1 therapy induces a TNF-α-linked response in monocytes. Three weeks after LLC engraftment, lungs from anti-PD-L1 or Ctrl mAb-treated mice were isolated and pooled to sort minimally 50k Ly6C$^+$ and CX3CR1$^+$ monocytes. Subsequently, RNA was isolated to perform targeted gene expression profiling using the Nanostring platform. **(A, B)** Gene set enrichment analysis ranking genes using the MSigDB Hallmark gene set collection for Ly6C$^+$ and CX3CR1$^+$ monocytes resp. with NES, NOM p-value and FDR q-value denoted on the graphs. On the right, the top 15 gene set members on the rank ordered list are depicted (n=1, mpc=3-4). **(C)** Mean fluorescence intensity of cytoplasmic TNF-α measured *via* flow cytometry in Ly6C$^+$ monocytes isolated from healthy, or LLC-bearing mice treated with Ctrl or anti-PD-L1 mAb (n=1, 4-5 mpc). **(D)** Boxplots representing the serological concentration of TNF-α in blood of healthy or LLC-bearing mice treated with Ctrl or anti-PD-L1 mAb resp. (n=2, mpc=4-8). **(E)** Dot plot depicts the concentration of TNF-α measured with ELISA in the supernatant of *in vitro* generated bone marrow-derived monocytes, treated with Ctrl or anti-PD-L1 mAbs for 24hrs. Statistical significance was measured with an unpaired t-test (n=3, 3 technical replicates). **(F)** Four days after LLC-Fluc inoculation, mice were treated with anti-PD-L1 mAb. On days 7, 10 and 13, mice received consistently one of the following 3 treatments: Ctrl + anti-TNF-α mAb; Ctrl + anti-PD-L1 mAb or anti-PD-L1 + anti-TNF-α mAb. Three weeks later, mice were euthanized, and perfused lungs were fixed for whole-tissue imaging. Representative 3D images obtained with lightsheet microscopy show the volumetric tumor foci (green) in lung tissue (red) of anti-PD-L1 mAb alone or anti-TNF-α + anti-PD-L1 mAb-treated mice. **(G)** Percentage of tumor volume over whole lung volume to compare LLC engraftment in mice treated with anti-TNF-α mAbs, anti-PD-L1 mAbs or a combination thereof (mpc = 4). Statistical significance in panels **(C, D, F)** were determined with a one-way ANOVA followed by a Tukey's multiple comparisons test. ns, non-significant; * for $p < 0.05$; ** for $p < 0.01$; and *** for $p < 0.001$.

TNF-α Fortifies the Upregulation of Checkpoint Molecules on Anti-PD-L1-Treated Monocytes

Although previous reports have shown that TNF-α blockade can elevate ICB effectiveness, we were unable to confirm this in the orthotopic LLC model. Since anti-PD-L1 therapy induces the secretion of TNF-α in monocytes *in vitro* and *in vivo*, we wondered what their combined immunological effect was on monocytes. Therefore, we treated *in vitro* generated bone marrow-derived monocytes with anti-PD-L1 mAbs and/or recombinant TNF-α. After 72 hrs, Ly6C$^+$ monocytes were analysed for their expression of the immunostimulatory

checkpoints CD80 (B7.1) and Inducible-T-Cell-Costimulator-Ligand (ICOSL) next to the immunosuppressive checkpoints: V-domain-Ig-suppressor-of-T-cell-activation (VISTA), Lymphocyte-Activating-3 (LAG-3), signal-regulatory-protein-α (SIRP-α), T-cell-immunoglobulin-and-mucin-domain-containing-3 (TIM-3), carcinoembryonic-antigen-related-cell-adhesion-molecule-1 (Ceacam1), T-Cell-Immuno-receptor-Ig-and-ITIM-domains (TIGIT), CD276 (B7-H3) and CD73. Flow cytometric analysis showed no alterations for ICOSL, Ceacam1, TIGIT, CD276 nor CD73 (data not shown) while an insignificant trend towards more expression of CD80 and VISTA was noted upon anti-PD-L1 treatment, especially in combination with TNF-α. More importantly, we observed a significant upregulation of LAG-3, SIRP-α and TIM-3 when monocytes were treated with recombinant TNF-α and/or anti-PD-L1 mAbs, especially when both were combined (**Figure 5A**). To validate these findings *in vivo*, we evaluated the expression levels of CD80, VISTA, LAG-3, SIRP-α and TIM-3 on freshly isolated Ly6C$^+$ monocytes, derived from healthy, Ctrl or anti-PD-L1 mAb treated tumor-bearing mice. We noticed that the expression levels of all checkpoints under investigation, except LAG-3, increased on monocytes derived from tumor-bearing lungs compared to healthy controls. What's more, anti-PD-L1 treatment fortified these elevations for CD80, VISTA, LAG-3 and TIM-3 (**Figure 5B**).

Monocytes Play a Key Role in the CTL-Stimulating Potential of ICB Combination Therapy

To understand the impact of TNF-α on anti-PD-L1 mAb treated CTLs, we evaluated the immune stimulatory impact of this treatment on freshly isolated splenocytes. Notably, anti-PD-L1 mAbs induced a significant drop of IFN-γ secretion (**Figure 6A**), in line with our previous *in vivo* finding that MHC-II^{low} TAMs display a decreased gene set enrichment for IFN-γ response upon anti-PD-L1 therapy (**Supplementary Figure 5B**). Yet, when prestimulated splenocytes were treated with anti-PD-L1 mAbs and TNF-α, their IFN-γ secretion profile remained unaffected by ICB, suggesting that splenocyte activation is improved by the combination of anti-PD-L1 mAbs and TNF-α.

These data suggest that anti-PD-L1-mediated TNF-α upregulation aids the stimulation of T cells directly and indirectly *via* upregulation of CD80 on monocytes, but that this stimulatory effect is most likely counterbalanced by the upregulation of VISTA, LAG-3, SIRP-α and TIM-3.

To investigate the latter, we first performed *in vitro* LLC-eGFP/OVA target cell-specific killing by OT-I cells with or without the addition of Ly6C$^+$ tumor-infiltrated monocytes, anti-PD-L1, -VISTA, -LAG-3, -SIRP-α or -TIM-3 mAbs or their combination with anti-PD-L1 (**Figures 6B-D**). When cell-specific percentages were calculated 3 days later, two important findings were observed: (1) killing dropped significantly in the presence of the Ly6C$^+$ monocytes and (2) only the combination of anti-PD-L1 with anti-SIRP-α mAb could fully revert the immunosuppressive impact of these Ly6C$^+$ monocytes (**Figure 6B**). Moreover, we evaluated the presence of TNF-α and IFN-γ in the supernatant of these killing assays (**Supplementary Figures 6A, B**). The respective cytokine profiles demonstrated (1) that presence of *in vivo* sorted Ly6C$^+$ monocytes increased the level of TNF-α and IFN-γ in all conditions, (2) a significant rise in TNF-α when anti-PD-L1 was combined with anti-LAG-3 mAb compared to anti-LAG-3 monotherapy and (3) significant rise in IFN-γ when anti-PD-L1 was combined with anti-VISTA, anti-LAG-3 or anti-TIM-3 mAbs. By monitoring the decrease of eGFP signal (LLC) from the same killing assays, we could additionally demonstrate that also anti-LAG-3 and anti-SIRP-α monotherapies enhanced OT-I-mediated killing 3 days after their addition (**Figure 6C**). Interestingly, the

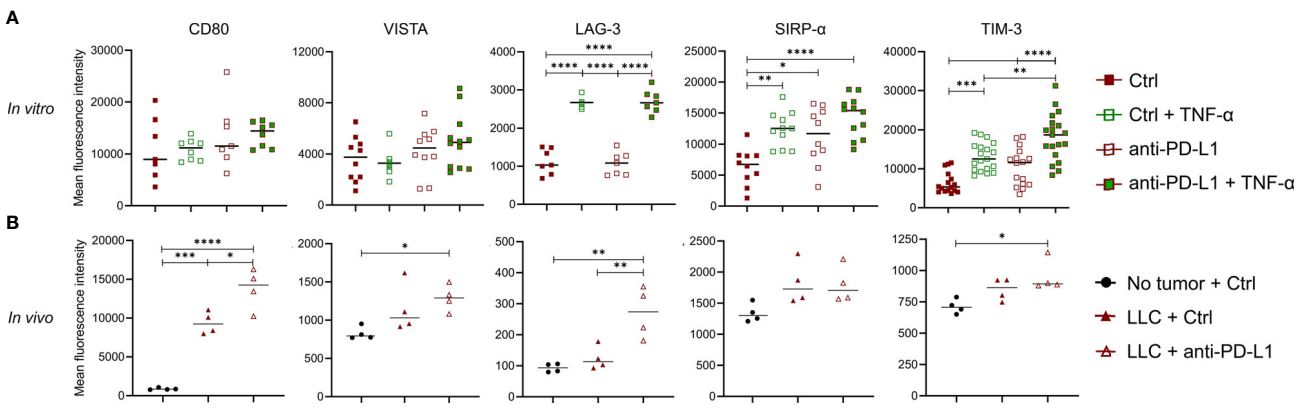

FIGURE 5 | Anti-PD-L1 therapy upregulates checkpoints on monocytes. **(A)** Bone marrow-derived monocytes were plated with LLC cells and treated with 5 µg/ml Ctrl or anti-PD-L1 mAb, with or without 10 ng/ml TNF-α. Three days later, mean fluorescence intensities were obtained *via* flow cytometry for CD80, VISTA, LAG-3, SIRP-α and TIM-3 (n=3, 4 technical replicates). **(B)** Three weeks after LLC engraftment, lungs from anti-PD-L1 or Ctrl mAb-treated mice were isolated to enrich the Ly6C$^+$ monocytes and evaluate their expression of the same checkpoints as described in panel **(A)** As internal reference, monocytes derived from healthy mice were taken along. A two-way panel **(A)** or one-way panel **(B)** ANOVA with Tukey's multiple comparisons test was performed to determine statistical significance. * for $p < 0.05$; ** for $p < 0.01$; *** for $p < 0.001$; and **** for $p < 0.0001$.

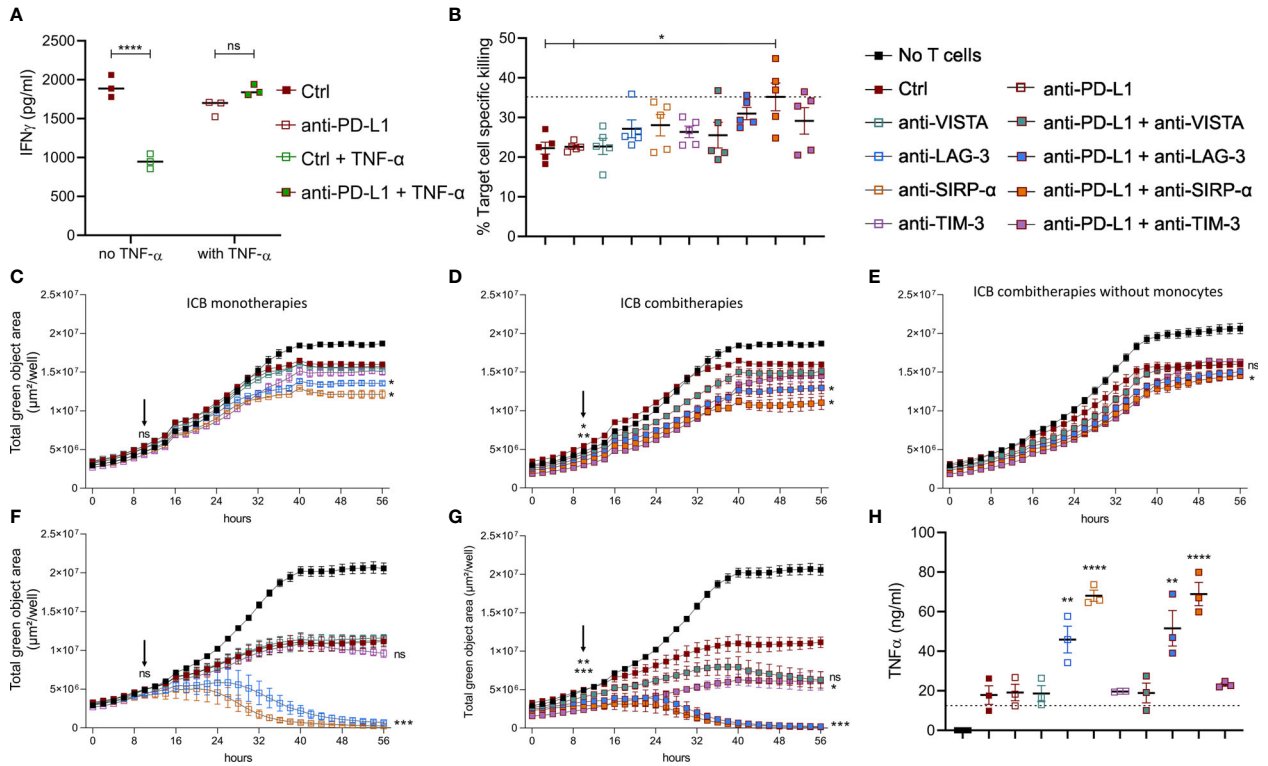

FIGURE 6 | Anti-PD-L1 therapy depends on monocytes to stimulate CTLs in combination with alternative ICBs. **(A)** Dot plot depicting IFN-γ concentrations in supernatants from splenocytes 72 hrs after their incubation with 10 µg/ml Ctrl or anti-PD-L1 mAbs, with or without 1 µg/ml recombinant TNF-α (n=3). **(B–H)** depict results from LLC specific OT-I killing assays, in the presence of Ly6C$^+$ monocytes sorted from lung tumor-bearing mice, no monocytes, or bone marrow derived monocytes resp. Moreover, the following conditions were compared: no monocytes + Ctrl mAb (dashed line in panels B and H), anti-PD-L1, -VISTA, -LAG-3, -SIRP-α, or -TIM-3 monotherapy **(C, F)** or their combination with anti-PD-L1 mAb **(D, E, G)**. **(B)** Percentages of cell-specific killing 3 days after experiment onset (n=1, 5 mpc). **(C–G)** Follow-up of target cell confluency *via* total green object area (µm²/well) during the respective LLC-specific OT-I killing assays over a time range of 56hrs. Images were obtained *via* Incucyte live cell imaging and statistical significances (on time points 10 and 56hrs) were calculated using a two-way ANOVA followed by a Dunnett's multiple comparison test compared to the Ctrl mAb condition. **(H)** Dot plot depicting TNF-α concentrations in supernatants from the LLC-specific OT-I killing assays shown in **(F, G)** at the 56hrs time point (n=3). Asterisks indicate significant differences between the marked conditions and the Ctrl mAb-treated condition. In panels **(A, B, H)** a one-way ANOVA with Tukey's multiple comparison test was used to test for statistical significance. ns, non-significant; * for $p < 0.05$; ** for $p < 0.01$; and **** for $p < 0.0001$.

addition of anti-PD-L1 mAb not only fortified but also accelerated the CTL stimulatory effect of anti-LAG-3 and - SIRP-α mAbs as a significant difference with anti-PD-L1 monotherapy was already shown 10hrs post-OT-I addition. In contrast, none of the ICB-mediated CTL-stimulating effects could be observed in the absence of monocytes, stressing the importance of monocytes for ICB mono and combi therapy effectiveness (**Figure 6E**).

Notably, very similar killing profiles were found when killing assays were repeated in the presence of *in vitro* generated bone marrow-derived monocytes (**Figures 6F–H**). As the latter showed more pronounced effects, the remarkable CTL-stimulating potential of anti-LAG-3 and anti-SIRP-α as mono- (**Figure 6F**) and combi- (**Figure 6G**) therapies was consolidated accompanied by significantly increased TNF-α secretion (**Figure 6H**). The latter killing assays further revealed that anti-VISTA and anti-TIM-3 mAbs also hold stimulatory effects when combined with anti-PD-L1 mAb on OT-I-mediated killing (**Figure 6G**) and IFN-γ secretion (**Supplementary Figure 5C**).

DISCUSSION

Sobering objective response rates of NSCLC patients to anti-PD-L1 therapy, stress the need for rationalized combinations to enhance therapeutic efficacy. In search for druggable targets to ameliorate ICB effectiveness, we investigated if the PD-(L)1$^+$ myeloid cell compartment hampers effective anti-PD-L1 therapy in a murine ICB-unresponsive squamous NSCLC model.

By monitoring the abundance of 11 different lung-infiltrating myeloid subsets during tumor progression, a specific increase in MHC-II^{high} and MHC-II^{low} TAMs, cDC2s, Ly6C$^+$, Ly6C$^-$ and Tie2$^+$ monocytes was shown. Moreover Ly6C$^+$ monocytes in blood and CX3CR1$^+$ monocytes in bone marrow showed a similar rise together with the serological level of CCL7. In line with clinical studies, the predominance of Ly6C$^+$ monocytes in blood samples of NSCLC patients has been described and linked to an attenuated anti-cancer response (35, 36). Also, monocyte mobilization from bone marrow was previously reported to be

managed by CCL7 (MCP-3) (37, 38) and recently found to be specifically upregulated in immature monocytes and neutrophils derived from NSCLC patient tumor parenchyma compared to adjacent non-neoplastic lung tissue (39). Previously Movahedi et al. found that Ly6C^{high} monocytes represent progenitors for TAMs in a subcutaneous LLC model (40), arguing that the rise in lung TAMs is likely preceded by an accompanying rise in peripheral Ly6C^{+} monocytes. Overall, these data suggest that the orthotopic LLC model represents a relevant squamous NSCLC model.

When LLC-bearing mice were treated with anti-PD-L1 therapy, flow cytometric analysis over time showed that the local and systemic rise in inflammatory and residential monocytes was completely abrogated. Notably, when we subjected bone marrow-derived myeloid cells to anti-PD-L1 treatment, we also observed a significant decrease in the fraction of Ly6C^{+} monocytes, suggestive of a direct, yet undetermined effect of anti-PD-L1 therapy on monocytes. These findings are further in line with a clinical case report in which it was shown that a stage III NSCLC patient undergoing durvalumab treatment (anti-PD-L1 mAb) showed a reduced number of circulating CD14^{+} and CD124^{+} myeloid cells (22).

In the assumption that most TAMs originated from Ly6C^{+} monocytes, it was not surprising that anti-PD-L1-treated mice also showed a significant decrease in their fraction of MHC-II^{low} (but not MHC-II^{high}) TAMs. Notably, while 26% ± 6,7 of MHC-II^{high} TAMs were PD-L1^{+} in 3-week-old LLC tumors, this percentage was about twice as high (60% ± 21,5) for MHC-II^{low} TAMs, making the latter more vulnerable for anti-PD-L1 mAb-mediated antibody dependent cellular cytotoxicity. Notably, a previous *in vitro* study demonstrated the induction of spontaneous macrophage proliferation upon *in vitro* PD-L1 blockade (41). While this contrasts our observed decrease in MHC-II^{low} TAMs, it might offer an additional rationale for the finding that the MHC-II^{high} TAM fraction was not altered upon anti-PD-L1 therapy in the LLC model.

Functional assessment of the sorted TAMs and monocytes from anti-PD-L1-treated mice showed only insignificant trends towards a more immunostimulatory phenotype. This could partly explain the lack of ICB effectiveness. Especially as effectiveness of anti-PD-L1 therapy was previously correlated to the presence of IFN-γ-secreting activated T-cells with favorable and significant TAM remodeling (19, 42, 43). Moreover, Boutsikou et al. recently reported that increased serological levels of IFN-γ and TNF-α next to IL-1β, IL-2, IL-4, IL-5, IL-6, IL-8, IL-10 and IL-12, resulted in better responses with longer survival upon anti-PD-1 therapy in NSCLC patients (29). However, we found that serological IFN-γ levels were significantly decreased in LLC-bearing animals compared to healthy controls, irrespective of anti-PD-L1 therapy. Moreover, sorted MHC-II^{low} TAMs from anti-PD-L1-treated mice were characterized by a significantly decreased expression of IFN-γ-responsive genes, while *in vitro* treated splenocytes with anti-PD-L1 treatment reduced their capacity to secrete IFN-γ.

Recently, various inflammation-associated genes have been reported to be rapidly upregulated in blood CD14^{+} monocytes, derived from anti-PD-L1-treated NSCLC patients (23). Accordingly, we found that the lung tumor-derived monocytes sorted from ICB-treated LLC-bearing mice upregulated a gene set that was linked to the inflammation-associated cytokine TNF-α. Interestingly, this corresponded to increased expression of TNF-α by Ly6C^{+} tumor-residing monocytes with a concomitant rise of serological TNF-α levels upon anti-PD-L1-treatment *in vivo*. *In vitro*, this effect seemed to be directly caused by the presence of anti-PD-L1 mAb, as we also observed increased TNF-α secretion in the supernatants of anti-PD-L1 treated bone marrow-derived monocytes. When Lin et al. previously treated mice with anti-PD-L1 therapy, they also showed an increase in TNF-α but, in contrast to our model, also of IFN-γ, which resulted in a therapeutic benefit in the MC38 colon carcinoma model (6). Notably, Hartley et al. showed that TNF-α administration could increase the expression level of PD-L1 in bone marrow-derived macrophages and monocytes *in vitro* (41). In contrast, it was recently shown that TNF-α-secreting TAMs found in subcutaneously LLC-engrafted mice as well as in NSCLC patients, were characterized by reduced PD-L1 expression and that their clodronate-mediated depletion led to a significant increase in PD-L1 expression in aerobic cancer cells, a higher infiltration of T cells and improved response to anti-PD-L1 therapy (44). In line with the negative impact of TNF-α-secreting TAMs, TNF-α has also been suggested to upregulate the alternative checkpoint molecule TIM-3 on lymphocytes *in vitro* and trigger activation-induced cell death of tumor-infiltrating CD8^{+} T cells in murine melanoma (33, 45). These findings rationalized at least two studies in which co-blockade of TNF-α and PD-1 was evaluated. While both studies demonstrated significant improvement of ICB efficacy in melanoma with reduced ICB-installed colitis (33, 34), we were unable to show any added benefit of TNF-α and PD-L1 co-blockade. To understand why TNF-α blockade did not ameliorate ICB effectiveness, we investigated the immunological impact of anti-PD-L1 mAb on Ly6C^{+} monocytes in the presence or absence of TNF-α. The presence of TNF-α made anti-PD-L1 mAb-treated bone marrow-derived monocytes express more CD80 (immune-stimulatory or suppressive when bound to CD28 or CTLA-4 expressed by T cells resp.) next to the alternative immunosuppressive checkpoint molecules VISTA, LAG-3, SIRP-α and TIM-3. A finding that was confirmed for each of these checkpoints in Ly6C^{+} tumor-infiltrated monocytes isolated from anti-PD-L1-treated mice, in which we previously demonstrated elevated levels of serological TNF-α. Moreover, the presence of monocytes markedly decreased the capacity of OT-I CTLs to kill LLC cells *in vitro*. Although these findings suggest the anti-PD-L1 mAb-mediated installation of immunosuppressive monocytes, their presence in the *in vitro* CTL-mediated LLC killing assays also significantly elevated the levels of IFN-γ and TNF-α, characteristic for an immunostimulatory profile. Additionally, TNF-α obliterated the anti-PD-L1 mAb-mediated decrease of IFN-γ secretion by *ex vivo* treated splenocytes. These data suggest that TNF-α plays a monocyte-associated Janus-faced role in the effectiveness of anti-PD-L1 therapy.

To investigate if we could push this see-saw profile to increased antitumor immunity upon anti-PD-L1 therapy, we finally tested the impact of VISTA, LAG-3, SIRP-α and TIM-3 co-blockade in the

presence of isolated lung tumor-infiltrated monocytes. Especially co-blockade of LAG-3 or SIRP-α and PD-L1, significantly enhanced OT-I-mediated LLC killing *in vitro*, accompanied by elevated levels of TNF-α and IFN-γ. An effect that was abrogated in the absence of monocytes, pointing out their crucial role in the CTL-stimulating effect of PD-L1-LAG-3 or -SIRP-α co-blockade. In the presence of bone-marrow derived monocytes, all CTL-stimulating effects of the investigated ICB combinations were more pronounced revealing that also the blockade of VISTA and TIM-3 could ameliorate the CTL-stimulating capacity of anti-PD-L1 mAbs. Strikingly, these combinations were only able to elevate the levels of IFN-γ and not TNF-α, again proving the importance of TNF-α and monocytes to boost CTL-mediated killing upon ICB combinations and providing an explanation for the ineffectiveness of TNF-α inhibition to increase anti-PD-L1 mAb effectiveness.

Today, numerous studies have described upregulation of alternative checkpoint molecules as important culprit for anti-PD-(L)1 therapy (46). In accordance with our study, VISTA, LAG-3, and TIM-3 have been demonstrated to increase in the NSCLC tumor microenvironment rationalizing their potential as targets for NSCLC immunotherapy (47–50). Especially the initial results from the ongoing phase II study TACTI-002 on the combination of pembrolizumab with soluble LAG-3 protein showing overall response rates of 47%, are very promising (51). While most studies revealed the suppressive role of VISTA, LAG-3, and TIM-3 role in the context of T cell exhaustion (52), we uncover their suppressive role on lung tumor-infiltrated monocytes as well. Moreover, we demonstrate their upregulation of 'don't eat me signal' SIRP-α too, previously shown to hamper phagocytosis upon ligation to CD47 on lung tumor cells (53–56).

In conclusion, this study divulges a Janus-faced role for monocytes upon anti-PD-L1 therapy. Hence, their biomarker potential should be considered to delineate more suited ICB combinations that increase the mediocre response rates observed in NSCLC patients today.

DATA AVAILABILITY STATEMENT

The datasets presented in this study can be found in online repositories. The names of the repository/repositories and accession number(s) can be found below: https://www.ncbi.nlm.nih.gov/geo/, GSE165517.

ETHICS STATEMENT

All animal experiments were reviewed and approved by the Ethical Committee for Animal Experiments of the Vrije Universiteit Brussel with ECD #: 18-214-1, 18-281-9 and 20-214-14.

AUTHOR CONTRIBUTIONS

KDR: designing research study, conducting experiments, acquiring data, analyzing data and writing the manuscript HL: conducting experiments, acquiring data, analyzing data and manuscript proof-reading EP: conducting experiments, acquiring data, analyzing data and manuscript proof-reading MIZ: conducting experiments, acquiring data, analyzing data and manuscript proof-reading RMA: conducting experiments, acquiring data and manuscript proof-reading SV: analyzing gene expression profiling data and manuscript proof-reading MVB: support with 3D whole tissue imaging procedure and manuscript proof-reading YDV: conducting experiments and manuscript proof-reading QL: conducting experiments and manuscript proof-reading ER: conducting experiments and manuscript proof-reading WDM: conducting experiments and manuscript proof-reading LDB: conducting experiments and manuscript proof-reading TE: conducting experiments and manuscript proof-reading IP: management of the ACAM imaging core, support with 3D whole tissue imaging procedure and manuscript proof-reading J-PT.: management of the ACAM imaging core, support with 3D whole tissue imaging procedure and manuscript proof-reading DE: obtaining funding and manuscript proof-reading MK: management of the small animal imaging core facility and manuscript proof-reading KB: obtaining funding, designing research studies, analyzing data and writing the manuscript CG: obtaining funding, designing research study, conducting experiments, acquiring data, analyzing data and writing the manuscript. All authors contributed to the article and approved the submitted version.

FUNDING

This research was performed with the financial support of the Research Foundation-Flanders (FWO-V, grant 1515718N, FWO-SBO, grant S004317N and FWO Junior Research, grant G041721N), Wetenschappelijk Fonds Willy Gepts of the UZ Brussel, and Kom op tegen Kanker, the Flemish Cancer Society. RMA, YDV and TE received an FWO-SB fellowship. LDB received an FWO-V fellowship. MK is senior clinical investigator at FWO-V. MIZ was funded by a PhD scholarship from Universidad Pública de Navarra, Pamplona (Spain) and DE is funded by Gobierno de Navarra (project BMED 050-2019), ISCIII (FEDER-PI17/02119, FEDER-PI20/00010) and AECC (PROYE16001ESCO). CG is funded by the Research Council of the Vrije Universiteit Brussel (OZR).

ACKNOWLEDGMENTS

The authors like to thank Petra Roman, Elsy Vaeremans, Angelo Willems and Yasmina Essam from the Laboratory of Molecular and Cellular Therapy for their technical and administrative support. The authors further thank Sofie Seghers and Elien Van de Velde from eTheRNA Immunotherapies for helping in large scale organ and cell isolation experiments. We further

thank Sofie Thys from ACAM, University of Antwerp for technical assistance with the LaVision light sheet microscope and Gunter Leuckx from the Vrije Universiteit Brussel for his help with whole lung tissue image analysis. Also the advice from Prof. Joeri Aerts was well appreciated.

SUPPLEMENTARY MATERIAL

The Supplementary Material for this article can be found online at: https://www.frontiersin.org/articles/10.3389/fimmu.2022.811867/full#supplementary-material

REFERENCES

1. Pai-Scherf L, Blumenthal GM, Li H, Subramaniam S, Mishra-Kalyani PS, He K, et al. FDA Approval Summary: Pembrolizumab for Treatment of Metastatic Non-Small Cell Lung Cancer: First-Line Therapy and Beyond. *Oncol* (2017) 22:1392–9. doi: 10.1634/THEONCOLOGIST.2017-0078
2. Memmott RM, Wolfe AR, Carbone DP, and Williams TM. Predictors of Response, Progression-Free Survival, and Overall Survival in Patients With Lung Cancer Treated With Immune Checkpoint Inhibitors. *J Thorac Oncol* (2021)16:1086-98. doi: 10.1016/j.jtho.2021.03.017
3. Remon J, Passiglia F, Ahn MJ, Barlesi F, Forde PM, Garon EB, et al. Immune Checkpoint Inhibitors in Thoracic Malignancies: Review of the Existing Evidence by an IASLC Expert Panel and Recommendations. *J Thorac Oncol* (2020)15:914-47. doi: 10.1016/j.jtho.2020.03.006
4. Bocanegra A, Fernandez-Hinojal G, Zuazo-Ibarra M, Arasanz H, Garcia-Granda M, Hernandez C, et al. PD-L1 Expression in Systemic Immune Cell Populations as a Potential Predictive Biomarker of Responses to PD-L1/PD-1 Blockade Therapy in Lung Cancer. *Int J Mol Sci* (2019) 20:1631. doi: 10.3390/ijms20071631
5. Li HY, McSharry M, Bullock B, Nguyen TT, Kwak J, Poczobutt JM, et al. The Tumor Microenvironment Regulates Sensitivity of Murine Lung Tumors to PD-1/PD-L1 Antibody Blockade. *Cancer Immunol Res* (2017) 5:767–77. doi: 10.1158/2326-6066.CIR-16-0365
6. Lin H, Wei S, Hurt EM, Green MD, Zhao L, Vatan L, et al. Host Expression of PD-L1 Determines Efficacy of PD-L1 Pathway Blockade–Mediated Tumor Regression. *J Clin Invest* (2018) 128:805–15. doi: 10.1172/JCI96113
7. Tang H, Liang Y, Anders RA, Taube JM, Qiu X, Mulgaonkar A, et al. PD-L1 on Host Cells is Essential for PD-L1 Blockade–Mediated Tumor Regression. *J Clin Invest* (2018) 128:580–8. doi: 10.1172/JCI96061
8. Kleinovink JW, Marijtg KA, Schoonderwoerd MJA, van Hall T, Ossendorp F, Fransen MF, et al. PD-L1 Expression on Malignant Cells is No Prerequisite for Checkpoint Therapy. *OncoImmunology* (2017) 6:e1294299. doi: 10.1080/2162402X.2017.1294299
9. Liu Y, Zugazagoitia J, Ahmed FS, Henick BS, Gettinger SN, Herbst RS, et al. Immune Cell PD-L1 Colocalizes With Macrophages and Is Associated With Outcome in PD-1 Pathway Blockade Therapy. *Clin Cancer Res* (2020) 26:970–7. doi: 10.1158/1078-0432.CCR-19-1040
10. Su S, Zhao J, Xing Y, Zhang X, Liu J, Ouyang Q, et al. Immune Checkpoint Inhibition Overcomes ADCP-Induced Immunosuppression by Macrophages. *Cell* (2018) 175:442–457.e23. doi: 10.1016/j.cell.2018.09.007
11. Petty AJ, Dai R, Lapalombella R, Baiocchi RA, Benson DM, Li Z, et al. Hedgehog-Induced PD-L1 on Tumor-Associated Macrophages Is Critical for Suppression of Tumor-Infiltrating CD8+ T Cell Function. *JCI Insight* (2021) 6:e146707. doi: 10.1172/JCI.INSIGHT.146707
12. Arlauckas SP, Garris CS, Kohler RH, Kitaoka M, Cuccarese MF, Yang KS, et al. *In Vivo* Imaging Reveals a Tumor-Associated Macrophage-Mediated Resistance Pathway in Anti-PD-1 Therapy. *Sci Trans Med* (2017) 9. doi: 10.1126/SCITRANSLMED.AAL3604
13. Kargl J, Busch SE, Yang GHY, Kim KH, Hanke ML, Metz HE, et al. Neutrophils Dominate the Immune Cell Composition in Non-Small Cell Lung Cancer. *Nat Commun* (2017) 8:1–11. doi: 10.1038/ncomms14381
14. Zhang S, Che D, Yang F, Chi C, Meng H, Shen J, et al. Tumor-Associated Macrophages Promote Tumor Metastasis *via* the TGF-β/SOX9 Axis in Non-Small Cell Lung Cancer. *Oncotarget* (2017) 8:99801–15. doi: 10.18632/oncotarget.21068
15. Altorki NK, Markowitz GJ, Gao D, Port JL, Saxena A, Stiles B, et al. The Lung Microenvironment: An Important Regulator of Tumour Growth and Metastasis. *Nat Rev Cancer* (2019) 19:9–31. doi: 10.1038/s41568-018-0081-9
16. Lavin Y, Kobayashi S, Leader A, Amir E ad D, Elefant N, Bigenwald C, et al. Innate Immune Landscape in Early Lung Adenocarcinoma by Paired Single-Cell Analyses. *Cell* (2017) 169:750–765.e17. doi: 10.1016/j.cell.2017.04.014
17. Lambrechts D, Wauters E, Boeckx B, Aibar S, Nittner D, Burton O, et al. Phenotype Molding of Stromal Cells in the Lung Tumor Microenvironment. *Nat Med* (2018) 24:1277–89. doi: 10.1038/s41591-018-0096-5
18. Hartley GP, Chow L, Ammons DT, Wheat WH, and Dow SW. Programmedcell Death Ligand 1 (PD-L1) Signaling Regulates Macrophage Proliferation and Activation. *Cancer Immunol Res* (2018) 6:1260–73. doi: 10.1158/2326-6066.CIR-17-0537
19. Xiong H, Mittman S, Rodriguez R, Moskalenko M, Pacheco-Sanchez P, Yang Y, et al. Anti-PD-L1 Treatment Results in Functional Remodeling of the Macrophage Compartment. *Cancer Res* (2019) 79:1493–506. doi: 10.1158/0008-5472.CAN-18-3208
20. Gordon SR, Maute RL, Dulken BW, Hutter G, George BM, McCracken MN, et al. PD-1 Expression by Tumour-Associated Macrophages Inhibits Phagocytosis and Tumour Immunity. *Nature* (2017) 545:495–9. doi: 10.1038/nature22396
21. Sun N-Y, Chen Y-L, Wu W-Y, Lin H-W, Chiang Y-C, Chang C-F, et al. Blockade of PD-L1 Enhances Cancer Immunotherapy by Regulating Dendritic Cell Maturation and Macrophage Polarization. *Cancers* (2019) 11:1400. doi: 10.3390/CANCERS11091400
22. Bertelli G, Trovato R, Ugel S, Bria E, Milella M, Bronte V, et al. Characterization of Myeloid-Derived Suppressor Cells in a Patient With Lung Adenocarcinoma Undergoing Durvalumab Treatment: A Case Report. *Clin Lung Cancer* (2019) 20:e514–6. doi: 10.1016/j.cllc.2019.04.013
23. Bar N, Costa F, Das R, Duffy A, Samur M, McCachren S, et al. Differential Effects of PD-L1 Versus PD-1 Blockade on Myeloid Inflammation in Human Cancer. *JCI Insight* (2020) 5:e129353. doi: 10.1172/jci.insight.129353
24. Hastir J-F, Delbauve S, Larbanoix L, Germanova D, Goyvaerts C, Allard J, et al. Hepatocarcinoma Induces a Tumor Necrosis Factor-Dependent Kupffer Cell Death Pathway That Favors Its Proliferation Upon Partial Hepatectomy. *Front Oncol* (2020) 10:547013:547013. doi: 10.3389/fonc.2020.547013
25. Reijmen E, de Mey S, de Mey W, Gevaert T, de Ridder K, Locy H, et al. Fractionated Radiation Severely Reduces the Number of CD8+ T Cells and Mature Antigen Presenting Cells Within Lung Tumors. *Int J Radiat OncologyBiologyPhys* (2021) 11:272–83. doi: 10.1016/j.ijrobp.2021.04.009
26. Messal HA, Almagro J, Zaw Thin M, Tedeschi A, Ciccarelli A, Blackie L, et al. Antigen Retrieval and Clearing for Whole-Organ Immunofluorescence by FLASH. *Nat Protoc* (2020) 16:239–62. doi: 10.1038/s41596-020-00414-z
27. Susaki EA, Shimizu C, Kuno A, Tainaka K, Li X, Nishi K, et al. Versatile Whole-Organ/Body Staining and Imaging Based on Electrolyte-Gel Properties of Biological Tissues. *Nat Commun* (2020) 11:1–22. doi: 10.1038/s41467-020-15906-5
28. Bhattacharya A, Hamilton AM, Furberg H, Pietzak E, Purdue MP, Troester MA, et al. An Approach for Normalization and Quality Control for NanoString RNA Expression Data. *Briefings Bioinf* (2020)22:bbaa163. doi: 10.1093/bib/bbaa163
29. Boutsikou E, Domvri K, Hardavella G, Tsiouda D, Zarogoulidis K, Kontakiotis T, et al. Tumour Necrosis Factor, Interferon-Gamma and Interleukins as Predictive Markers of Antiprogrammed Cell-Death Protein-1 Treatment in Advanced non-Small Cell Lung Cancer: A Pragmatic Approach in Clinical Practice. *Ther Adv Med Oncol* (2018) 10. doi: 10.1177/1758835918768238
30. Huang L, Bommireddy R, Munoz LE, Guin RN, Wei C, Ruggieri A, et al. Expression of Tdtomato and Luciferase in a Murine Lung Cancer Alters the Growth and Immune Microenvironment of the Tumor. *PloS One* (2021) 16:e0254125. doi: 10.1371/JOURNAL.PONE.0254125

31. Strauss L, Mahmoud MAA, Weaver JD, Tijaro-Ovalle NM, Christofides A, Wang Q, et al. Targeted Deletion of PD-1 in Myeloid Cells Induces Antitumor Immunity. *Sci Immunol* (2020) 5:eaay1863. doi: 10.1126/sciimmunol.aay1863
32. Chen L, Cao MF, Xiao JF, Ma QH, Zhang H, Cai RL, et al. Stromal PD-1+ Tumor-Associated Macrophages Predict Poor Prognosis in Lung Adenocarcinoma. *Hum Pathol* (2020) 97:68–79. doi: 10.1016/j.humpath.2019.12.007
33. Bertrand F, Montfort A, Marcheteau E, Imbert C, Gilhodes J, Filleron T, et al. Tnfα Blockade Overcomes Resistance to Anti-PD-1 in Experimental Melanoma. *Nat Commun* (2017) 8:1–13. doi: 10.1038/s41467-017-02358-7
34. Perez-Ruiz E, Minute L, Otano I, Alvarez M, Ochoa MC, Belsue V, et al. Prophylactic TNF Blockade Uncouples Efficacy and Toxicity in Dual CTLA-4 and PD-1 Immunotherapy. *Nature* (2019) 569:428–32. doi: 10.1038/s41586-019-1162-y
35. Kwiecień I, Rutkowska E, Polubiec-Kownacka M, Raniszewska A, Rzepecki P, and Domagała-Kulawik J. Blood Monocyte Subsets With Activation Markers in Relation With Macrophages in Non-Small Cell Lung Cancer. *Cancers* (2020) 12:2513. doi: 10.3390/cancers12092513
36. McCarthy FM, Ghirelli C, Zollinger R, Phillips M, Roshani R, Candido J, et al. Inflammatory Phenotype of Classical (CD14++CD16-) Monocytes in Patients With Advanced non-Small Cell Lung Cancer. *J Clin Oncol* (2013) 31:11071–1. doi: 10.1200/jco.2013.31.15_suppl.11071
37. Liu Y, Cai Y, Liu L, Wu Y, and Xiong X. Crucial Biological Functions of CCL7 in Cancer. *PeerJ* (2018) 2018:e4928. doi: 10.7717/peerj.4928
38. Han S, Wang T, Chen Y, Han Z, Guo L, Wu Z, et al. High CCL7 Expression is Associated With Migration, Invasion and Bone Metastasis of Non-Small Cell Lung Cancer Cells. *Am J Trans Res* (2019) 11:442–52.
39. Durrans A, Gao D, Gupta R, Fischer KR, Choi H, El Rayes T, et al. Identification of Reprogrammed Myeloid Cell Transcriptomes in NSCLC. (2015)10:e0129123. doi: 10.1371/journal.pone.0129123
40. Movahedi K, Laoui D, Gysemans C, Baeten M, Stangé G, van den Bossche J, et al. Different Tumor Microenvironments Contain Functionally Distinct Subsets of Macrophages Derived From Ly6C(high) Monocytes. *Cancer Res* (2010) 70:5728–39. doi: 10.1158/0008-5472.CAN-09-4672
41. Hartley G, Regan D, Guth A, and Dow S. Regulation of PD-L1 Expression on Murine Tumor-Associated Monocytes and Macrophages by Locally Produced TNF-α. *Cancer Immunol Immunother* (2017) 66:523–35. doi: 10.1007/s00262-017-1955-5
42. Gubin MM, Esaulova E, Ward JP, Malkova ON, Runci D, Wong P, et al. High-Dimensional Analysis Delineates Myeloid and Lymphoid Compartment Remodeling During Successful Immune-Checkpoint Cancer Therapy. *Cell* (2018) 175:1014–30.e19. doi: 10.1016/j.cell.2018.09.030
43. Lin H, Wei S, Hurt EM, Green MD, Zhao L, Vatan L, et al. Host Expression of PD-L1 Determines Efficacy of PD-L1 Pathway Blockade-Mediated Tumor Regression. *J Clin Invest* (2018) 128:805–15. doi: 10.1172/JCI96113
44. Jeong H, Kim S, Hong B-J, Lee C-J, Kim Y-E, Bok S, et al. Tumor-Associated Macrophages Enhance Tumor Hypoxia and Aerobic Glycolysis. *Cancer Res* (2019) 79:795–806. doi: 10.1158/0008-5472.CAN-18-2545
45. Bertrand F, Rochotte J, Colacios C, Montfort A, Tilkin-Mariamé A-F, Touriol C, et al. Blocking Tumor Necrosis Factor α Enhances CD8 T-Cell–Dependent Immunity in Experimental Melanoma. *Cancer Res* (2015) 75:2619–28. doi: 10.1158/0008-5472.CAN-14-2524
46. Koyama S, Akbay EA, Li YY, Herter-Sprie GS, Buczkowski KA, Richards WG, et al. Adaptive Resistance to Therapeutic PD-1 Blockade Is Associated With Upregulation of Alternative Immune Checkpoints. *Nat Commun* (2016) 7:10501. doi: 10.1038/ncomms10501
47. Hernandez-Martinez JM, Vergara E, Zatarain-Barrón ZL, Barrón-Barrón F, and Arrieta O. VISTA/PD-1H: A Potential Target for non-Small Cell Lung Cancer Immunotherapy. *J Thorac Dis* (2018) 10:6378. doi: 10.21037/JTD.2018.11.39
48. Datar I, Sanmamed MF, Wang J, Henick BS, Choi J, Badri T, et al. Expression Analysis and Significance of PD-1, LAG-3, and TIM-3 in Human Non-Small Cell Lung Cancer Using Spatially Resolved and Multiparametric Single-Cell Analysis. *Clin Cancer Res* (2019) 25:4663–73. doi: 10.1158/1078-0432.CCR-18-4142
49. Tu L, Guan R, Yang H, Zhou Y, Hong W, Ma L, et al. Assessment of the Expression of the Immune Checkpoint Molecules PD-1, CTLA4, TIM-3 and LAG-3 Across Different Cancers in Relation to Treatment Response, Tumor-Infiltrating Immune Cells and Survival. *Int J Cancer* (2019)147:423-38. doi: 10.1002/ijc.32785
50. Zuazo M, Arasanz H, Fernández-Hinojal G, García-Granda MJ, Gato M, Bocanegra A, et al. Functional Systemic CD 4 Immunity is Required for Clinical Responses to PD -L1/PD -1 Blockade Therapy. *EMBO Mol Med* (2019) 11:e10293. doi: 10.15252/emmm.201910293
51. Felip E, Doger B, Majem M, Carcereny E, Krebs M, Peguero JA, et al. Initial Results From a Phase II Study (TACTI-002) in Metastatic Non-Small Cell Lung or Head and Neck Carcinoma Patients Receiving Eftilagimod Alpha (Soluble LAG-3 Protein) and Pembrolizumab. *J Clin Oncol* (2020) 38:3100. doi: 10.1200/JCO.2020.38.15_SUPPL.3100.
52. Davar D, and Zarour HM. Immunological Targets for Immunotherapy: Inhibitory T Cell Receptors. *Methods Mol Biol (Clifton NJ)* (2020) 2055:23. doi: 10.1007/978-1-4939-9773-2_2
53. Zhao H, Wang J, Kong X, Li E, Liu Y, Du X, et al. CD47 Promotes Tumor Invasion and Metastasis in Non-Small Cell Lung Cancer. *Sci Rep* (2016) 6: e29719. doi: 10.1038/srep29719
54. Lian S, Xie R, Ye Y, Lu Y, Cheng Y, Xie X, et al. Dual Blockage of Both PD-L1 and CD47 Enhances Immunotherapy Against Circulating Tumor Cells. *Sci Rep* (2019) 9:e4532. doi: 10.1038/s41598-019-40241-1
55. Zhang X, Fan J, Wang S, Li Y, Wang Y, Li S, et al. Targeting CD47 and Autophagy Elicited Enhanced Antitumor Effects in Non-Small Cell Lung Cancer. *Cancer Immunol Res* (2017) 5. doi: 10.1158/2326-6066.CIR-16-0398
56. Chen SH, Dominik PK, Stanfield J, Ding S, Yang W, Kurd N, et al. Dual Checkpoint Blockade of CD47 and PD-L1 Using an Affinity-Tuned Bispecific Antibody Maximizes Antitumor Immunity. *J ImmunoTher Cancer* (2021) 9: e003464. doi: 10.1136/JITC-2021-003464

Conflict of Interest: MK, KB, and QL have a granted patent on "Human PD-L1 binding immunoglobulins" (WO2019166622A1). MK has patents on the use of nanobodies for imaging and therapy. MK received research funding from Precirix. MK has ownership in AbScint which leverages nanobody imaging tracers into clinical application.

The remaining authors declare that the research was conducted in the absence of any commercial or financial relationships that could be construed as a potential conflict of interest.

Publisher's Note: All claims expressed in this article are solely those of the authors and do not necessarily represent those of their affiliated organizations, or those of the publisher, the editors and the reviewers. Any product that may be evaluated in this article, or claim that may be made by its manufacturer, is not guaranteed or endorsed by the publisher.

Copyright © 2022 De Ridder, Locy, Piccioni, Zuazo, Awad, Verhulst, Van Bulck, De Vlaeminck, Lecocq, Reijmen, De Mey, De Beck, Ertveldt, Pintelon, Timmermans, Escors, Keyaerts, Breckpot and Goyvaerts. This is an open-access article distributed under the terms of the Creative Commons Attribution License (CC BY). The use, distribution or reproduction in other forums is permitted, provided the original author(s) and the copyright owner(s) are credited and that the original publication in this journal is cited, in accordance with accepted academic practice. No use, distribution or reproduction is permitted which does not comply with these terms.

frontiers | Frontiers in Immunology

ORIGINAL RESEARCH
published: 22 April 2022
doi: 10.3389/fimmu.2022.829634

Predicting Durable Responses to Immune Checkpoint Inhibitors in Non-Small-Cell Lung Cancer Using a Multi-Feature Model

Lei Wang[1†], Hongbing Zhang[2†], Chaohu Pan[3,4,5,6†], Jian Yi[3†], Xiaoli Cui[3], Na Li[3], Jiaqian Wang[3], Zhibo Gao[3], Dongfang Wu[3], Jun Chen[2*], Jizong Jiang[1*] and Qian Chu[1]*

[1] Department of Oncology, Tongji Hospital, Tongji Medical College, Huazhong University of Science and Technology, Wuhan, China, [2] Department of Lung Cancer Surgery, Tianjin Lung Cancer Institute, Tianjin Medical University General Hospital, Tianjin, China, [3] Department of Medicine, YuceBio Technology Co., Ltd, Shenzhen, China, [4] The First Affiliated Hospital, Jinan University, Guangzhou, China, [5] Zhuhai Institute of Translational Medicine, Zhuhai People's Hospital (Zhuhai Hospital Affiliated with Jinan University), Jinan University, Zhuhai, China, [6] The Biomedical Translational Research Institute, Faculty of Medical Science, Jinan University, Guangzhou, China

OPEN ACCESS

Edited by:
Udo S. Gaipl,
University Hospital Erlangen, Germany

Reviewed by:
Jun-Ling Li,
Chinese Academy of Medical Sciences and Peking Union Medical College, China
Vasyl Nagibin,
National Academy of Sciences of Ukraine, Ukraine

***Correspondence:**
Dongfang Wu
wudf@yucebio.com
Jun Chen
huntercj2004@qq.com
Jizong Jiang
solomon.hill.jiang@163.com

[†]These authors have contributed equally to this work

Specialty section:
This article was submitted to Cancer Immunity and Immunotherapy, a section of the journal Frontiers in Immunology

Received: 06 December 2021
Accepted: 22 March 2022
Published: 22 April 2022

Citation:
Wang L, Zhang H, Pan C, Yi J, Cui X, Li N, Wang J, Gao Z, Wu D, Chen J, Jiang J and Chu Q (2022) Predicting Durable Responses to Immune Checkpoint Inhibitors in Non-Small-Cell Lung Cancer Using a Multi-Feature Model. Front. Immunol. 13:829634. doi: 10.3389/fimmu.2022.829634

Due to the complex mechanisms affecting anti-tumor immune response, a single biomarker is insufficient to identify patients who will benefit from immune checkpoint inhibitors (ICIs) treatment. Therefore, a comprehensive predictive model is urgently required to predict the response to ICIs. A total of 162 non-small-cell lung cancer (NSCLC) patients undergoing ICIs treatment from three independent cohorts were enrolled and used as training and test cohorts (training cohort = 69, test cohort1 = 72, test cohort2 = 21). Eight genomic markers were extracted or calculated for each patient. Ten machine learning classifiers, such as the gaussian process classifier, random forest, and support vector machine (SVM), were evaluated. Three genomic biomarkers, namely tumor mutation burden, intratumoral heterogeneity, and loss of heterozygosity in human leukocyte antigen were screened out, and the SVM_poly method was adopted to construct a durable clinical benefit (DCB) prediction model. Compared with a single biomarker, the DCB multi-feature model exhibits better predictive value with the area under the curve values equal to 0.77 and 0.78 for test cohort1 and cohort2, respectively. The patients predicted to have DCB showed improved median progression-free survival (mPFS) and median overall survival (mOS) than those predicted to have non-durable clinical benefit.

Keywords: immune checkpoint inhibitors, durable responses, multi-feature model, genetic biomarkers, non-small cell lung cancer, cancer immunity and immunotherapy

1 INTRODUCTION

Lung cancer is one of the most commonly diagnosed malignant tumors, the majority of which are non-small-cell lung cancers (NSCLCs) (1). Among all cancer types, the incidence and mortality of lung cancer are ranked second and first, respectively (2). Immune checkpoint inhibitors (ICIs), including anti-cytotoxic T lymphocyte-associated antigen-4 (CTLA4) and anti-programmed cell death protein 1 (PD-1)/programmed death-ligand 1 (PD-L1), have dramatically altered the treatment landscape of

NSCLC (3–8). However, only a small subset of patients benefit from ICIs treatment, and some may even suffer from immune-related adverse events, requiring treatment discontinuation (9–12). Therefore, identification of more effective predictive biomarkers that can guide the treatment decision making with ICIs is significantly important and urgent.

Multiple clinical trials have verified that both PD-L1 expression level and tumor mutation burden (TMB) can predict the efficacy of ICIs in NSCLC (13–18). Recently, several novel genome-related biomarkers such as intratumoral heterogeneity (ITH), tumor neoantigen burden (TNB), loss of heterozygosity in human leukocyte antigen (HLA LOH), and HLA-I evolutionary divergence (HED), have been demonstrated to be associated with response to ICIs in patients (19–23). These single indicators can distinguish responders from non-responders to a certain extent, although their sensitivity and accuracy need to be further improved. For instance, some NSCLC patients with high TMB cannot benefit from immunotherapy (24).

Our objective was to construct a robust predictive model to predict durable response to ICIs in NSCLC patients based on multiple genomic features, and to assess its potential for clinical decision-making guidance in cancer treatment with ICIs.

2 MATERIALS AND METHODS

2.1 Study Cohorts

Genomic and clinical data of 69 and 72 NSCLC patients undergoing ICIs treatments were obtained from published cohorts, of which 69 NSCLC patients were used as the training cohort and 72 NSCLC patients were used as the test cohort1 (19, 25).

To further evaluate the accuracy and effectiveness of the multi-feature model, 21 patients treated with ICIs, collected from January 2018 to May 2020, were enrolled in this study and used as test cohort2.

Durable clinical benefit (DCB) was defined as complete response (CR), partial response (PR), or stable disease (SD) that lasted for ≥ 24 weeks, and non-durable benefit (NDB) was defined as progressive disease (PD) or SD that lasted for < 24 weeks.

Among the 162 NSCLC patients included in this study, 69% (111/162) were lung adenocarcinoma. The number of patients with DCB and NDB was 61 and 101, respectively. Detailed clinical information of patients is summarized in **Supplementary Tables 1**–**3**.

In addition, genomic and clinical data of 120 melanoma patients undergoing ICIs treatments were obtained from published cohort to further evaluate the accuracy and effectiveness of the multi-feature model (26). The patients with CR or PR were 55, and the patients with PD were 65. DCB was defined as CR and PR, and NDB was defined as PD. Detailed clinical information of patients is summarized in **Supplementary Table 4**.

2.2 Next-Generation Sequencing (NGS) and Mutation Analysis

Genomic profiling was performed on tumor tissues and matched peripheral blood samples. First, we used the GeneReadDNA FFPE kit (Qiagen) and Qiagen DNA blood mini kit (Qiagen) to extract DNA from tumor specimens and blood, respectively. Then, the extracted DNA was amplified, purified, and analyzed using an NGS panel (YuceOne™ Plus, Yucebio, China).

Sequencing reads with > 10% N rate and/or > 10% bases with a quality score < 20 were filtered using SOAPnuke (Version 1.5.6) (27). Somatic single nucleotide variants and insertions and deletions (indels) were detected using VarScan (Version 2.4) (28). Next, an in-house method was applied to filter possible false-positive mutations. Finally, SnpEff (Version 4.3) was used to functionally annotate the mutations detected in the tumor samples (29).

2.3 Evaluation of Genomic Biomarkers

2.3.1 Evaluation of Tumor Mutation Burden

TMB was determined as the number of all nonsynonymous mutations and indels per megabase of the genome examined, and the cut-off value for TMB-high and TMB-low was defined as the median TMB.

2.3.2 Evaluation of HLA Typing, HED, and Somatic HLA Loss

HLA typing of the paired peripheral blood and tumor samples was performed from whole-exome sequencing data using POLYSOLVER (v1.0) (30) and OptyType (v1.3.2) (31). A scoring algorithm was then used to integrate the results that were used for further analysis (32). HED was calculated as previously described (33). The mean HED of patients was calculated as the mean of divergences at HLA_A, HLA_B, and HLA_C, and the bioinformatic tool LOHHLA with the default program settings was used to determine their maintenance or loss in the tumor (21).

2.3.3 Evaluation of TNB

All nonsynonymous mutations and indels were translated into 21-mer peptide sequences using in-house software centered on the mutated amino acid. Then, the 21-mer peptide was used to create a 9- to 11-mer peptide *via* a sliding window approach for the prediction of MHC class I binding affinity. Next, NetMHCpan (v3.0) was used to predict the binding strength of the mutated peptides to patient-specific HLA alleles (34). A peptide with predicted binding affinity to any HLA allele with an IC50 < 500 nM was selected. If several selected peptides were generated from the same mutation, they were counted as one neoantigen. TNB was determined as the number of putative neoantigens per megabase of the genome.

2.3.4 Calculation of Copy Number Variants (CNV) and ITH

CNVs were called using CNVkit (v0.8.1) to compare the exome-wide profile between tumors and matched peripheral blood (35). Allele-specific copy number and tumor purity were assessed using the ascatNgs (v3.1.0). PyClone (v0.13.0) was used to infer the cancer cell fraction (CCF) of mutations in tumors. ITH was calculated using a previously developed method (19).

2.4 Construction of the Multi-Feature Model

Ten classifiers, including K-Nearest Neighbors (KNN), Logistic Regression (LR), Random Forest (RF), Gradient Boosting Classifier (GBC), Decision Tree Classifier (DTC), Extra Tree Classifier (ETC), Gaussian Process Classifier (GPC), support vector machine (SVM)_poly, SVM_rbf, and SVM_liner, were evaluated to construct a multi-feature model with three genomic biomarkers to predict the efficacy of ICIs in the training cohort. The GridSearchCV and cross_val_score packages in Sklearn (version 0.24.1.) were used to

iteratively optimize the RF, GBC, and DTC algorithms. The default parameters were adopted for the other algorithms. The predicted efficacy of these algorithms was calculated using the area under the receiver operating characteristic (ROC) curve. In addition, we evaluated the accuracy, specificity, sensitivity, positive predictive value, and negative predictive value of these algorithms in the training cohort.

2.5 Statistical Methods

An ROC curve was generated to evaluate diagnostic accuracy and the area under the curve was calculated to measure the discriminatory ability of potential biomarkers. Progression-free survival (PFS) was analyzed using the Kaplan–Meier method and log-rank test.

3 RESULTS

3.1 Single Biomarker Has Limited Ability to Distinguish the Responders From the Non-Responders

To evaluate the predictive ability of a single biomarker for ICIs response, eight genomic biomarkers (TMB, TNB, ITH, HLA LOH, HED, HED_A, HED_B and HED_C) were analyzed, respectively. First, we winsorized and normalized the data in the training cohort (**Supplementary Figure 1**). The receiver operating characteristic (ROC) curves of the individual biomarkers were plotted and their predictive ability was measured using the area under the curve (AUC) value. As shown in **Figures 1A–H**, the accuracy and effectiveness of TMB, TNB, and ITH (AUC = 0.70, 0.67, and 0.68, respectively) were higher than those of HLA LOH, HED, HED_A, HED_B, and HED_C (AUC = 0.58, 0.51, 0.54, 0.51, and 0.49, respectively); however, none of these values exceeded 0.7, suggesting that a single biomarker was not effective enough to precisely distinguish responders from non-responders treated with ICIs.

3.2 Feature Selection and Model Evaluation

Due to the limited predictive ability of a single biomarker, the predictive ability of the multi-feature model was further investigated and the detailed processes were shown in **Figure 2A**.

To avoid model overfitting, cross-validated recursive feature elimination was applied to select features from eight biomarkers (TMB, TNB, ITH, HLA LOH, HED, HED_A, HED_B, and HED_C). As shown in **Figure 2B** and **Table 1**, three of them, TMB, ITH, and HLA LOH, were screened to predict the efficacy of ICIs in the training cohort.

Based on the three selected features, the efficacy of different algorithms (KNN, LR, SVM_rbf, SVM_ linear, SVM_poly, RF, GBC, DTC, ETC, and GPC) were evaluated and compared. The best-performing hyperparameters were determined by 10-fold cross-validation in the training cohort. As shown in **Figure 2C** and **Table 2**, the top four algorithms for accuracy were GPC, DTC, SVM_rbf, and SVM_poly, while the top four algorithms for variance were KNN, SVM_rbf, SVM_poly, and GPC. After comprehensive consideration of the accuracy and variance, the GPC, SVM_rbf, and SVM_poly algorithms were selected for further analysis.

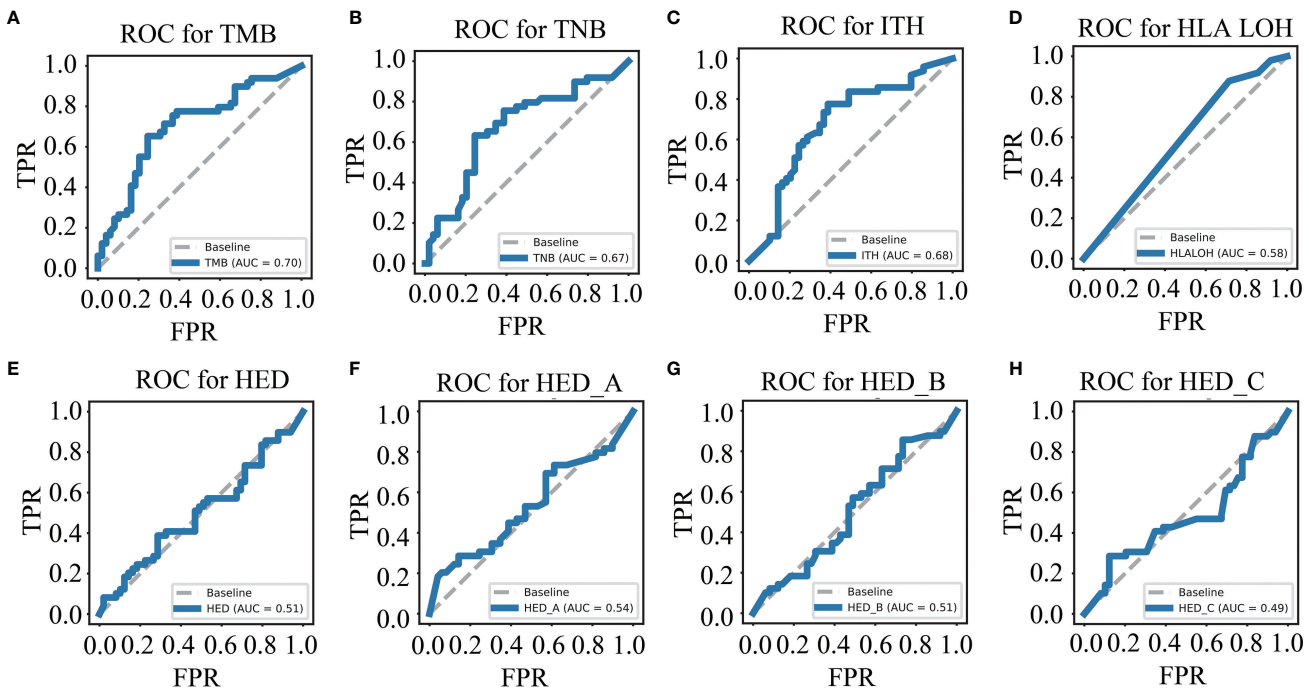

FIGURE 1 | Single biomarker has limited ability to distinguish the responders from the non-responders. ROC curves for TMB **(A)**, TNB **(B)**, ITH **(C)**, HLA LOH **(D)**, HED **(E)**, HED_A **(F)**, HED_B **(G)**, and HED_C **(H)** in the training cohort. TMB, tumor mutation burden; ITH, intratumoral heterogeneity; HLA LOH, loss of heterozygosity in human leukocyte antigen; HFD, HLA-I evolutionary divergence; ROC, receiver operating characteristic.

3.3 Algorithm Selection for Multi-Feature Model Construction

The algorithms of GPC, SVM_rbf, and SVM_poly were next assessed by their ability to predict the efficacy of patients with ICIs in the training cohort and test cohort1. As shown in **Figures 3A, B**, the AUC values of GPC, SVM_rbf, and SVM_poly algorithms were higher than those predicted by a single biomarker. Moreover, compared with the GPC and SVM_rbf algorithms, the SVM_poly algorithm was stabler in the training cohort and test cohort1, and thus was more suitable to be selected to construct the multi-feature model.

Next, the median progression-free survival (mPFS) and median overall survival (mOS) in the training cohort and test cohort1 were analyzed with the multi-feature model. The results showed that patients who were predicted to have durable clinical benefit (pDCB) had longer mPFS and mOS than those predicted to have no durable benefit (pNDB) (**Figures 3C–E**).

3.4 Validation of the Multi-Feature Model in Patients Enrolled in Test Cohort2

Twenty-one NSCLC patients treated with ICIs enrolled in this study were used for further validation of the multi-feature model. Consistent with the above results, the AUC value predicted by the multi-feature model was higher than those predicted by single biomarker (**Figure 4A**). Furthermore, the mPFS of the pDCB subgroup was significantly longer than that of the pNDB subgroup (**Figure 4B**). In conclusion, the multi-feature model is able to distinguish pDCB from pNDB.

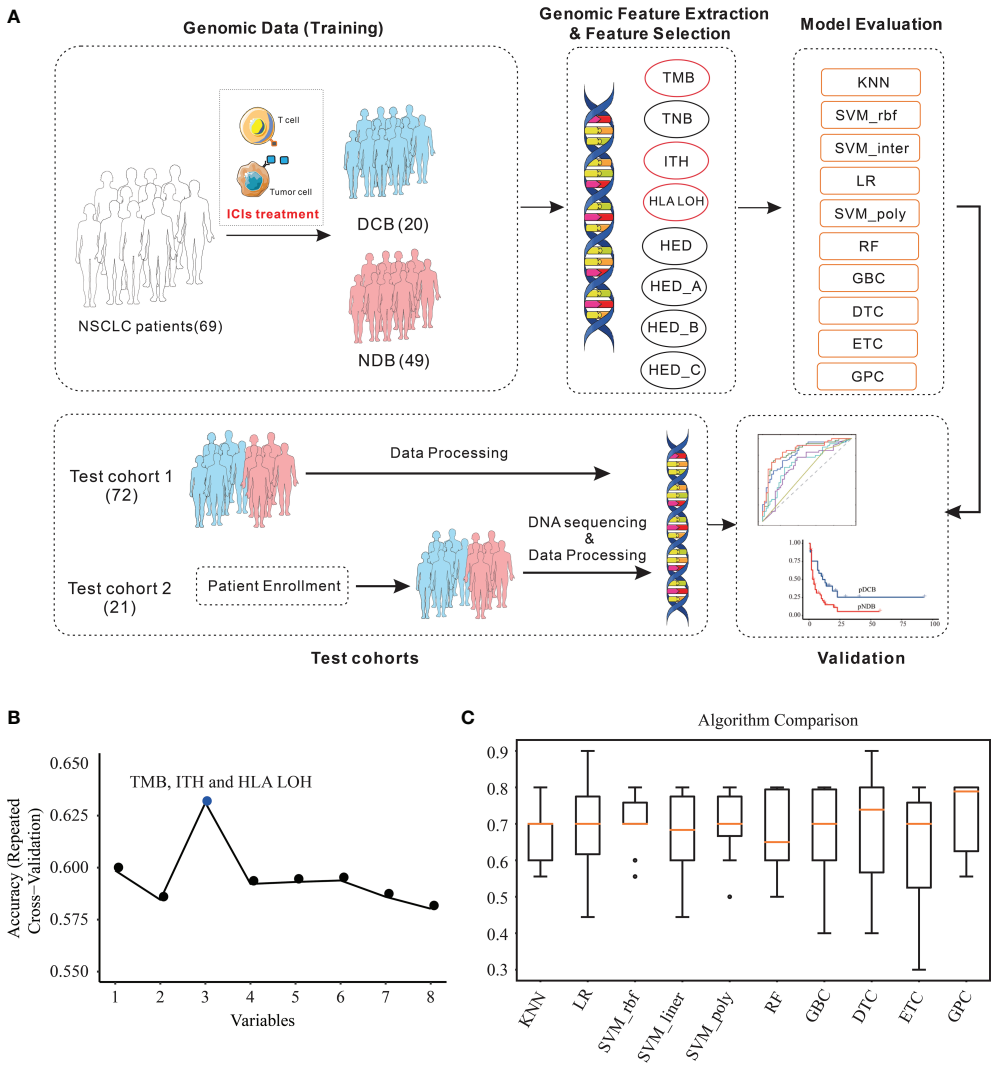

FIGURE 2 | Feature combination selection and performance evaluation. **(A)** Workflow of the study. **(B)** Feature combination selection with 10-fold cross-validation. **(C)** Comparison of the efficacy of different algorithms in the training cohort with the selected features. KNN, K-nearest neighbors; LR, logistic regression; RF, random forest; GBC, gradient boosting classifier; DTC, decision tree classifier; ETC, extra tree classifier; GPC, Gaussian process classifier; SVM, support vector machine.

TABLE 1 | List of the optimal combination from eight features.

Biomarker	Feature Selection	Ranking
TMB	True	1
ITH	True	1
HLA LOH	True	1
HED_C	False	2
TNB	False	3
HED_B	False	4
HED_A	False	5
HED	False	6

TABLE 2 | List of the accuracy and variance of different algorithms with 10-fold cross-validation in the training cohort.

Algorithm	Accuracy	Variance
KNN	0.66	0.08
LR	0.68	0.13
SVM_rbf	0.70	0.08
SVM_linear	0.66	0.12
SVM_poly	0.69	0.09
RF	0.67	0.11
GBC	0.67	0.13
DTC	0.70	0.14
ETC	0.65	0.16
GPC	0.72	0.10

4 DISCUSSION

ICIs have achieved great success in the treatment of NSCLC, and several biomarkers have been developed to help clinicians make treatment choices; however, the predictive accuracy of these biomarkers is finite (24, 36). In this study, a comprehensive analysis of NSCLC samples was carried out to investigate the role of a multi-feature model composed of TMB, ITH, and HLA LOH in determining the response to ICIs. Our study showed that the accuracy of this multi-feature model was higher than that of any single biomarker, and the mPFS and mOS of pDCB patients were longer than those of pNDB patients predicted by the multi-feature model. Finally, whole-exome sequencing data from 21 NSCLC patients treated with ICIs were applied to further validate the model, and the same results were obtained.

Several studies have integrated multiple indicators to predict the efficacy of ICIs in NSCLC patients. Shi et al. integrated genomic profiling, TMB, and the expression level of PD-L1 to predict the efficacy of ICIs and reported that *KMT2C/KRAS/TP53* co-mutation could serve as a biomarker to identify the best responders to ICIs therapy; however, the percentage of durable clinical benefit was only about 50% (37). Lin et al. also constructed a comprehensive predictive classifier model based on epidermal growth factor receptor and AT-

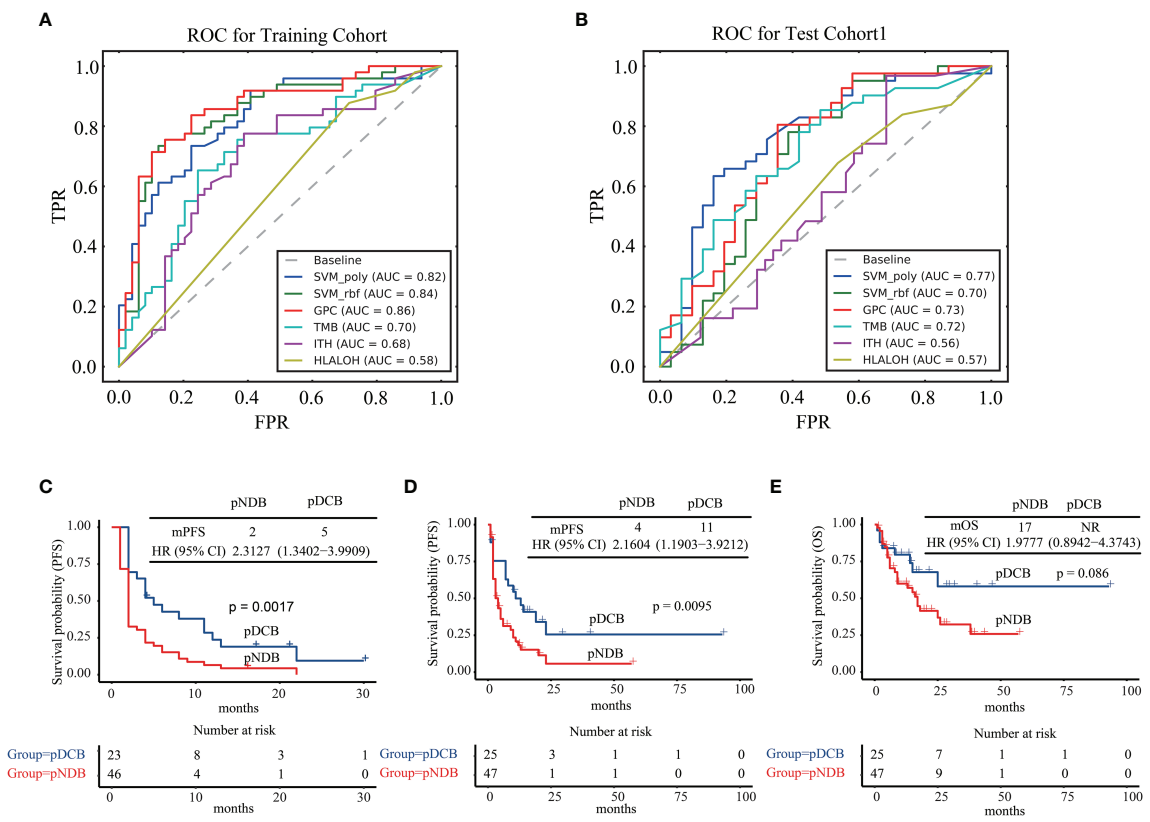

FIGURE 3 | Algorithm selection for multi-feature model construction. **(A)** ROC curves for SVM_poly, SVM_rbf, GPC, TMB, ITH, and HLA LOH in the training cohort. **(B)** ROC curves for SVM_poly, SVM_rbf, GPC, TMB, ITH, and HLA LOH in test cohort1. **(C)** Kaplan–Meier curves of PFS comparing pDCB with pNDB in the training cohort. **(D)** Kaplan–Meier curves of PFS comparing pDCB with pNDB in test cohort1. **(E)** Kaplan–Meier curves of OS comparing pDCB with pNDB in test cohort1. pDCB, patients predicted to have durable clinical benefit; pNDB, patients predicted to have no durable benefit; PFS, progression-free survival; OS, overall survival.

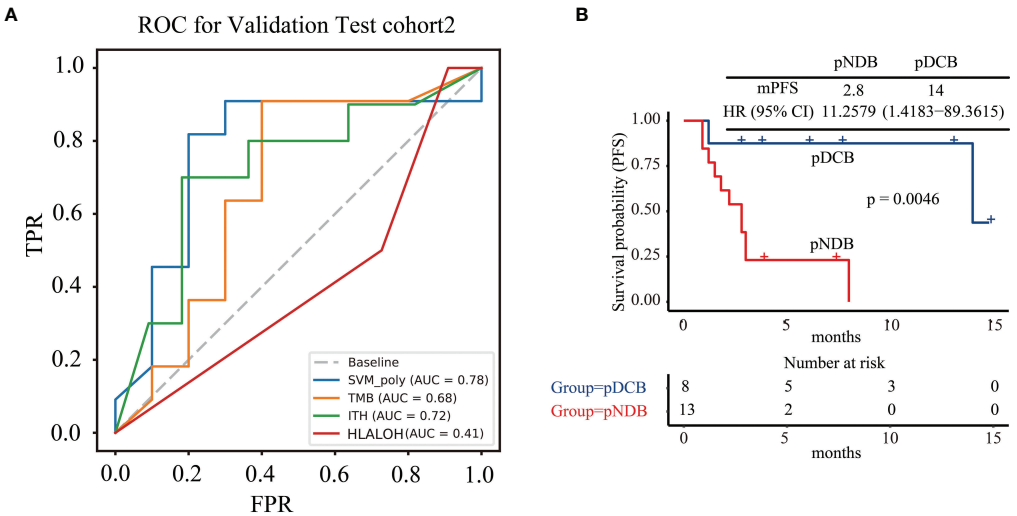

FIGURE 4 | The multi-feature model could effectively predict response to ICIs treatment in test cohort2. **(A)** ROC curves for multi-feature model, TMB, ITH, and HLA LOH in test cohort2. **(B)** Kaplan–Meier curves of PFS comparing pDCB with pNDB in test cohort2.

rich interaction domain 1B status, smoking history, treatment type, and PD-L1 score and found that patients with low-risk scores showed improved PFS compared to those with high-risk scores, while the AUC value of 6-month PFS was only 0.75 (38). In addition, these prediction models required multiple detection techniques, such as targeted panel sequencing and IHC of PD-L1, which need more tumor samples and costs. Therefore, in terms of the availability of clinical samples and the costs of treatment, we hoped that multiple features could be obtained through one detection technology. Targeted panel sequencing has been demonstrated in clinical application. As the costs of sequencing decreased, the clinical application of targeted panel sequencing gradually increased. More importantly, from targeted panel sequencing, multiple genomic features could be analyzed. Therefore, the multi-feature model based on genomic markers was developed. In our study, the AUC values of the multi-feature model in the training cohort, test cohort1 and test cohort2 were 0. 82, 0.77, and 0.78, respectively, which proved that our model is more effective in predicting the efficacy of NSCLC patients treated with ICIs. In order to further expand the application of this model, the predictive ability of this model in melanoma was also analyzed. As shown in **Figure S2**, the AUC value was 0.6, which indicated that the model may be unsuitable for melanoma.

In summary, we have constructed a multi-feature model that can effectively predict the efficacy of NSCLC patients treated with ICIs, which can help in clinical decision-making. In addition, patients with pDCB could be considered as more suitable candidates for treatment with ICIs. Ongoing intense work, especially prospective large cohorts, is needed to further validate and optimize our model.

DATA AVAILABILITY STATEMENT

The datasets presented in this study can be found in online repositories, *via* the following link: https://ngdc.cncb.ac.cn/gsa-human/browse/HRA001966.

ETHICS STATEMENT

The studies involving human participants were reviewed and approved by YuceBio Ethics Committee for research in health. The patients/participants provided their written informed consent to participate in this study.

AUTHOR CONTRIBUTIONS

Conceptualization, DW, JC, JJ, QC and ZG. Methodology, LW, HZ, CP, JY and JW. Data analysis, LW, HZ, CP, JY and XC. Wrote the manuscript, LW, HZ, CP, JY and XC. Revised the manuscript, LW, HZ, CP and NL. All authors contributed to the article and approved the submitted version.

FUNDING

This study was supported by Natural Science Foundation of China (NO. 62131009 and 82072597).

SUPPLEMENTARY MATERIAL

The Supplementary Material for this article can be found online at: https://www.frontiersin.org/articles/10.3389/fimmu.2022.829634/full#supplementary-material

Supplementary Figure 1 | Data winsorization and normalization in the training cohort. **(A)** Data of HED, HED_A, HED_B, HED_C, TMB, ITH and TNB before winsorization. **(B)** Data of HED, HED_A, HED_B, HED_C, TMB, ITH and TNB after winsorization. **(C)** Data of HED, HED_A, HED_B, HED_C, TMB, ITH and TNB after normalization.

Supplementary Figure 2 | ROC curves for multi-feature model, TMB, ITH, and HLA LOH in cohort of melanoma.

REFERENCES

1. Bodor JN, Boumber Y, Borghaei H. Biomarkers for Immune Checkpoint Inhibition in Non-Small Cell Lung Cancer (NSCLC). *Cancer* (2020) 126 (2):260–70. doi: 10.1002/cncr.32468
2. Bray F, Ferlay J, Soerjomataram I, Siegel RL, Torre LA, Jemal A. Global Cancer Statistics 2018: GLOBOCAN Estimates of Incidence and Mortality Worldwide for 36 Cancers in 185 Countries. *CA Cancer J Clin* (2018) 68 (6):394–424. doi: 10.3322/caac.21492
3. Sacher AG, Gandhi L. Biomarkers for the Clinical Use of PD-1/PD-L1 Inhibitors in Non-Small-Cell Lung Cancer: A Review. *JAMA Oncol* (2016) 2(9):1217–22. doi: 10.1001/jamaoncol.2016.0639
4. Perets R, Bar J, Rasco DW, Ahn MJ, Yoh K, Kim DW, et al. Safety and Efficacy of Quavonlimab, a Novel Anti-CTLA-4 Antibody (MK-1308), in Combination With Pembrolizumab in First-Line Advanced Non-Small-Cell Lung Cancer. *Ann Oncol* (2021) 32(3):395–403. doi: 10.1016/j.annonc.2020.11.020
5. Brahmer J, Reckamp KL, Baas P, Crino L, Eberhardt WE, Poddubskaya E, et al. Nivolumab Versus Docetaxel in Advanced Squamous-Cell Non-Small-Cell Lung Cancer. *N Engl J Med* (2015) 373(2):123–35. doi: 10.1056/NEJMoa1504627
6. Rittmeyer A, Barlesi F, Waterkamp D, Park K, Ciardiello F, von Pawel J, et al. Atezolizumab Versus Docetaxel in Patients With Previously Treated Non-Small-Cell Lung Cancer (OAK): A Phase 3, Open-Label, Multicentre Randomised Controlled Trial. *Lancet* (2017) 389(10066):255–65. doi: 10.1016/S0140-6736(16)32517-X
7. Herbst RS, Baas P, Kim DW, Felip E, Perez-Gracia JL, Han JY, et al. Pembrolizumab Versus Docetaxel for Previously Treated, PD-L1-Positive, Advanced Non-Small-Cell Lung Cancer (KEYNOTE-010): A Randomised Controlled Trial. *Lancet* (2016) 387(10027):1540–50. doi: 10.1016/S0140-6736(15)01281-7
8. Hellmann MD, Paz-Ares L, Bernabe Caro R, Zurawski B, Kim SW, Carcereny Costa E, et al. Nivolumab Plus Ipilimumab in Advanced Non-Small-Cell Lung Cancer. *N Engl J Med* (2019) 381(21):2020–31. doi: 10.1056/NEJMoa1910231
9. Khoja L, Day D, Wei-Wu Chen T, Siu LL, Hansen AR. Tumour- and Class-Specific Patterns of Immune-Related Adverse Events of Immune Checkpoint Inhibitors: A Systematic Review. *Ann Oncol* (2017) 28(10):2377–85. doi: 10.1093/annonc/mdx286
10. Weber JS, Kahler KC, Hauschild A. Management of Immune-Related Adverse Events and Kinetics of Response With Ipilimumab. *J Clin Oncol* (2012) 30 (21):2691–7. doi: 10.1200/JCO.2012.41.6750
11. Heinzerling L, Ott PA, Hodi FS, Husain AN, Tajmir-Riahi A, Tawbi H, et al. Cardiotoxicity Associated With CTLA4 and PD1 Blocking Immunotherapy. *J Immunother Cancer* (2016) 4:50. doi: 10.1186/s40425-016-0152-y
12. Topalian SL, Hodi FS, Brahmer JR, Gettinger SN, Smith DC, McDermott DF, et al. Safety, Activity, and Immune Correlates of Anti-PD-1 Antibody in Cancer. *N Engl J Med* (2012) 366(26):2443–54. doi: 10.1056/NEJMoa1200690
13. Giroux Leprieur E, Dumenil C, Julie C, Giraud V, Dumoulin J, Labrune S, et al. Immunotherapy Revolutionises Non-Small-Cell Lung Cancer Therapy: Results, Perspectives and New Challenges. *Eur J Cancer* (2017) 78:16–23. doi: 10.1016/j.ejca.2016.12.041
14. Tang J, Yu JX, Hubbard-Lucey VM, Neftelinov ST, Hodge JP, Lin Y. Trial Watch: The Clinical Trial Landscape for PD1/PDL1 Immune Checkpoint Inhibitors. *Nat Rev Drug Discov* (2018) 17(12):854–5. doi: 10.1038/nrd.2018.210
15. Samstein RM, Lee CH, Shoushtari AN, Hellmann MD, Shen R, Janjigian YY, et al. Tumor Mutational Load Predicts Survival After Immunotherapy Across Multiple Cancer Types. *Nat Genet* (2019) 51(2):202–6. doi: 10.1038/s41588-018-0312-8
16. Herbst RS, Giaccone G, de Marinis F, Reinmuth N, Vergnenegre A, Barrios CH, et al. Atezolizumab for First-Line Treatment of PD-L1-Selected Patients With NSCLC. *N Engl J Med* (2020) 383(14):1328–39. doi: 10.1056/NEJMoa1917346
17. Hellmann MD, Ciuleanu TE, Pluzanski A, Lee JS, Otterson GA, Audigier-Valette C, et al. Nivolumab Plus Ipilimumab in Lung Cancer With a High Tumor Mutational Burden. *N Engl J Med* (2018) 378(22):2093–104. doi: 10.1056/NEJMoa1801946
18. Montesion M, Murugesan K, Jin DX, Sharaf R, Sanchez N, Guria A, et al. Somatic HLA Class I Loss Is a Widespread Mechanism of Immune Evasion Which Refines the Use of Tumor Mutational Burden as a Biomarker of Checkpoint Inhibitor Response. *Cancer Discov* (2021) 11(2):282–92. doi: 10.1158/2159-8290.CD-20-0672
19. Fang W, Jin H, Zhou H, Hong S, Ma Y, Zhang Y, et al. Intratumoral Heterogeneity as a Predictive Biomarker in Anti-PD-(L)1 Therapies for Non-Small Cell Lung Cancer. *Mol Cancer* (2021) 20(1):37. doi: 10.1186/s12943-021-01331-9
20. Luksza M, Riaz N, Makarov V, Balachandran VP, Hellmann MD, Solovyov A, et al. A Neoantigen Fitness Model Predicts Tumour Response to Checkpoint Blockade Immunotherapy. *Nature* (2017) 551(7681):517–20. doi: 10.1038/nature24473
21. McGranahan N, Rosenthal R, Hiley CT, Rowan AJ, Watkins TBK, Wilson GA, et al. Allele-Specific HLA Loss and Immune Escape in Lung Cancer Evolution. *Cell* (2017) 171(6):1259–1.e1211. doi: 10.1016/j.cell.2017.10.001
22. Chowell D, Krishna C, Pierini F, Makarov V, Rizvi NA, Kuo F, et al. Evolutionary Divergence of HLA Class I Genotype Impacts Efficacy of Cancer Immunotherapy. *Nat Med* (2019) 25(11):1715–20. doi: 10.1038/s41591-019-0639-4
23. Wang Z, Zhao J, Wang G, Zhang F, Zhang Z, Zhang F, et al. Comutations in DNA Damage Response Pathways Serve as Potential Biomarkers for Immune Checkpoint Blockade. *Cancer Res* (2018) 78(22):6486–96. doi: 10.1158/0008-5472.CAN-18-1814
24. Hellmann MD, Nathanson T, Rizvi H, Creelan BC, Sanchez-Vega F, Ahuja A, et al. Genomic Features of Response to Combination Immunotherapy in Patients With Advanced Non-Small-Cell Lung Cancer. *Cancer Cell* (2018) 33 (5):843–52.e844. doi: 10.1016/j.ccell.2018.03.018
25. Anagnostou V, Niknafs N, Marrone K, Bruhm DC, White JR, Naidoo J, et al. Multimodal Genomic Features Predict Outcome of Immune Checkpoint Blockade in Non-Small-Cell Lung Cancer. *Nat Cancer* (2020) 1(1):99–111. doi: 10.1038/s43018-019-0008-8
26. Liu D, Schilling B, Liu D, Sucker A, Livingstone E, Jerby-Arnon L, et al. Integrative Molecular and Clinical Modeling of Clinical Outcomes to PD1 Blockade in Patients With Metastatic Melanoma. *Nat Med* (2019) 25 (12):1916–27. doi: 10.1038/s41591-019-0654-5
27. Chen Y, Chen Y, Shi C, Huang Z, Zhang Y, Li S, et al. SOAPnuke: A MapReduce Acceleration-Supported Software for Integrated Quality Control and Preprocessing of High-Throughput Sequencing Data. *Gigascience* (2018) 7(1):1–6. doi: 10.1093/gigascience/gix120
28. Koboldt DC, Zhang Q, Larson DE, Shen D, McLellan MD, Lin L, et al. VarScan 2: Somatic Mutation and Copy Number Alteration Discovery in Cancer by Exome Sequencing. *Genome Res* (2012) 22(3):568–76. doi: 10.1101/gr.129684.111
29. Cingolani P, Platts A, Wang le L, Coon M, Nguyen T, Wang L, et al. A Program for Annotating and Predicting the Effects of Single Nucleotide Polymorphisms, SnpEff: SNPs in the Genome of Drosophila Melanogaster Strain W1118; Iso-2; Iso-3. *Fly (Austin)* (2012) 6(2):80–92. doi: 10.4161/fly.19695
30. Shukla SA, Rooney MS, Rajasagi M, Tiao G, Dixon PM, Lawrence MS, et al. Comprehensive Analysis of Cancer-Associated Somatic Mutations in Class I HLA Genes. *Nat Biotechnol* (2015) 33(11):1152–8. doi: 10.1038/nbt.3344
31. Szolek A, Schubert B, Mohr C, Sturm M, Feldhahn M, Kohlbacher O. OptiType: Precision HLA Typing From Next-Generation Sequencing Data. *Bioinformatics* (2014) 30(23):3310–6. doi: 10.1093/bioinformatics/btu548
32. Yi J, Chen L, Xiao Y, Zhao Z, Su X. Investigations of Sequencing Data and Sample Type on HLA Class Ia Typing With Different Computational Tools. *Brief Bioinform* (2021) 22(3):bbaa143. doi: 10.1093/bib/bbaa143
33. Chowell D, Morris LGT, Grigg CM, Weber JK, Samstein RM, Makarov V, et al. Patient HLA Class I Genotype Influences Cancer Response to Checkpoint Blockade Immunotherapy. *Science* (2018) 359(6375):582–7. doi: 10.1126/science.aao4572
34. Nielsen M, Andreatta M. NetMHCpan-3.0; Improved Prediction of Binding to MHC Class I Molecules Integrating Information From Multiple Receptor and Peptide Length Datasets. *Genome Med* (2016) 8(1):33. doi: 10.1186/s13073-016-0288-x
35. Talevich E, Shain AH, Botton T, Bastian BC. CNVkit: Genome-Wide Copy Number Detection and Visualization From Targeted DNA Sequencing. *PloS Comput Biol* (2016) 12(4):e1004873. doi: 10.1371/journal.pcbi.1004873
36. Brueckl WM, Ficker JH, Zeitler G. Clinically Relevant Prognostic and Predictive Markers for Immune-Checkpoint-Inhibitor (ICI) Therapy in Non-Small Cell Lung Cancer (NSCLC). *BMC Cancer* (2020) 20(1):1185. doi: 10.1186/s12885-020-07690-8

37. Shi Y, Lei Y, Liu L, Zhang S, Wang W, Zhao J, et al. Integration of Comprehensive Genomic Profiling, Tumor Mutational Burden, and PD-L1 Expression to Identify Novel Biomarkers of Immunotherapy in Non-Small Cell Lung Cancer. *Cancer Med* (2021) 10(7):2216–31. doi: 10.1002/cam4.3649
38. Lin Z, Zhang Y, Zhang L. Construction of an Integrated Prognostic Classifier Model for Predicting the Efficacy of Immune Checkpoint Inhibitor Therapy in Non-Small Cell Lung Cancer. *Cancer Commun (Lond)* (2020) 40(8):370–3. doi: 10.1002/cac2.12070

Conflict of Interest: Author CP, JY, XC, NL, JW, ZG and DW were employed by the company YuceBio Technology Co., Ltd.

The remaining authors declare that the research was conducted in the absence of any commercial or financial relationships that could be construed as a potential conflict of interest.

Publisher's Note: All claims expressed in this article are solely those of the authors and do not necessarily represent those of their affiliated organizations, or those of the publisher, the editors and the reviewers. Any product that may be evaluated in this article, or claim that may be made by its manufacturer, is not guaranteed or endorsed by the publisher.

Copyright © 2022 Wang, Zhang, Pan, Yi, Cui, Li, Wang, Gao, Wu, Chen, Jiang and Chu. This is an open-access article distributed under the terms of the Creative Commons Attribution License (CC BY). The use, distribution or reproduction in other forums is permitted, provided the original author(s) and the copyright owner(s) are credited and that the original publication in this journal is cited, in accordance with accepted academic practice. No use, distribution or reproduction is permitted which does not comply with these terms.

frontiers | Frontiers in Immunology

ORIGINAL RESEARCH
published: 22 April 2022
doi: 10.3389/fimmu.2022.749241

The Comprehensive Analysis Identified an Autophagy Signature for the Prognosis and the Immunotherapy Efficiency Prediction in Lung Adenocarcinoma

Xizhe Li[1,2†], Ziyu Dai[3,4†], Xianning Wu[5], Nan Zhang[6], Hao Zhang[3,4], Zeyu Wang[3,4], Xun Zhang[3,4], Xisong Liang[3,4], Peng Luo[7], Jian Zhang[7], Zaoqu Liu[8], Yanwu Zhou[1,2,4], Quan Cheng[3,4] and Ruimin Chang[1,2,4*]*

[1] Department of Thoracic Surgery, Xiangya Hospital, Central South University, Changsha, China, [2] Hunan Engineering Research Center for Pulmonary Nodules Precise Diagnosis & Treatment, Changsha, China, [3] Department of Neurosurgery, Xiangya Hospital, Central South University, Changsha, China, [4] National Clinical Research Center for Geriatric Disorders, Changsha, China, [5] Department of Thoracic Surgery, The First Affiliated Hospital of University of Science and Technology of China (USTC), Division of Life Sciences and Medicine, University of Science and Technology of China, Hefei, China, [6] One-third Lab, College of Bioinformatics Science and Technology, Harbin Medical University, Harbin, China, [7] Department of Oncology, Zhujiang Hospital, Southern Medical University, Guangzhou, China, [8] Department of Interventional Radiology, The First Affiliated Hospital of Zhengzhou University, Zhengzhou, China

Background: Lung adenocarcinoma (LUAD) is a fatal malignancy in the world. Growing evidence demonstrated that autophagy-related genes regulated the immune cell infiltration and correlated with the prognosis of LUAD. However, the autophagy-based signature that can predict the prognosis and the efficiency of checkpoint immunotherapy in LUAD patients is yet to be discovered.

Methods: We used conventional autophagy-related genes to screen candidates for signature construction in TCGA cohort and 9 GEO datasets (tumor samples, n=2181; normal samples, n=419). An autophagy-based signature was constructed, its correlation with the prognosis and the immune infiltration of LUAD patients was explored. The prognostic value of the autophagy-based signature was validated in an independent cohort with 70 LUAD patients. Single-cell sequencing data was used to further characterize the various immunological patterns in tumors with different signature levels. Moreover, the predictive value of autophagy-based signature in PD-1 immunotherapy was explored in the IMvigor210 dataset. At last, the protective role of DRAM1 in LUAD was validated by *in vitro* experiments.

Results: After screening autophagy-related gene candidates, a signature composed by CCR2, ITGB1, and DRAM1 was established with the ATscore in each sample. Further analyses showed that the ATscore was significantly associated with immune cell infiltration

OPEN ACCESS

Edited by:
Udo S Gaipl,
University Hospital Erlangen, Germany

Reviewed by:
Jinhui Liu,
Nanjing Medical University, China
Katharina Hopp,
University of Colorado, United States

***Correspondence:**
Quan Cheng
chengquan@csu.edu.cn
Ruimin Chang
changruimin@csu.edu.cn

[†]These authors have contributed equally to this work and share first authorship

Specialty section:
This article was submitted to Cancer Immunity and Immunotherapy, a section of the journal Frontiers in Immunology

Received: *29 July 2021*
Accepted: *09 March 2022*
Published: *22 April 2022*

Citation:
Li X, Dai Z, Wu X, Zhang N, Zhang H, Wang Z, Zhang X, Liang X, Luo P, Zhang J, Liu Z, Zhou Y, Cheng Q and Chang R (2022) The Comprehensive Analysis Identified an Autophagy Signature for sthe Prognosis and the Immunotherapy Efficiency Prediction in Lung Adenocarcinoma. Front. Immunol. 13:749241. doi: 10.3389/fimmu.2022.749241

and low ATscore indicated poor prognosis. Meanwhile, the prognostic value of ATscore was validated in our independent LUAD cohort. GSEA analyses and single-cell sequencing analyses revealed that ATscore was associated with the immunological status of LUAD tumors, and ATscore could predict the efficacy of PD-1 immunotherapy. Moreover, *in vitro* experiments demonstrated that the inhibition of DRAM1 suppressed the proliferation and migration capacity of LUAD cells.

Conclusion: Our study identified a new autophagy-based signature that can predict the prognosis of LUAD patients, and this ATscore has potential applicative value in the checkpoint therapy efficiency prediction.

Keywords: lung adenocarcinoma, autophagy, gene signature, immune checkpoint therapy, TCGA, DRAM1

INTRODUCTION

Recent epidemiology studies have shown that lung cancer is the deadliest malignancy in the United States and China (1, 2). Lung adenocarcinoma (LUAD) is now holding the predominant position among all the pathological types of lung cancer. Although therapies of LUAD have achieved dramatic progress due to the innovation of surgery, chemotherapy, and targeted therapies, the prognosis of LUAD patients remains unsatisfactory (3). In the past decade, immune checkpoint blockade immunotherapies targeting PD-1 or other immune regulators are emerging as a new hope for LUAD patients (4, 5). However, few biomarkers can predict the efficacy of anti-PD-1 immunotherapy and stratify benefit population. Therefore, it is urgent to excavate more effective biomarkers to find appropriate patients that will benefit from anti-PD-1 immunotherapy.

Autophagy is a cellular process to degrade organelles and proteins by transporting them to the lysosomes, and its vital regulatory role in carcinogenesis is well known (6). During cancer development, autophagy may play tumor-promotor and tumor-suppressor roles in different cancers, and the specific function depends on the cancer type and development stage (7). Recent studies have shown that autophagy also has critical functions in tumor immunology (8). Like its double-edged sword functions in carcinogenesis, autophagy also plays a dual role in the anti-tumor immune response. On the one hand, autophagy activation may improve antigen presentation and immune recognition in dendritic cells (9, 10). On the other hand, autophagy can repress tumor-related antigen presentation by downregulation of MHC-I surface molecules (11). Meanwhile, pieces of evidence have revealed that autophagy in myeloid-derived suppressor cells (MDSCs) is associated with the M2 macrophage polarization and induces the immunosuppressive tumor microenvironment (12).

Since autophagy has a tight and elusive correlation with tumor immunology, researchers also pay attention to the potential association between autophagy and PD-1 blockade therapy. However, the effects of autophagy targeting drugs on PD-1 overexpressed cancer cells are controversial, and the interaction of autophagy regulators and PD-L1/PD-1 in LUAD is still to be revealed (13). Therefore, the investigation of a single regulator may not be enough to evaluate the full view of autophagy functions in LUAD. In comparison, the expression signature of autophagy-related genes may have the potential to predict the efficacy of anti-PD-1 immunotherapy in LUAD.

In this study, we selected 232 autophagy regulators and explored their expression in multiple datasets. Furthermore, we identified a signature (ATscore) composed of three autophagy-related genes, and this signature was correlated with the survival and tumor immunology factors of LUAD. Moreover, the prognostic predictive value of ATscores was validated in our independent LUAD cohort. The single-cell sequencing data analysis identified the potential relationship between this signature and the immune cell infiltration. And the ATscore could predict the therapeutic effects of the PD-1 blockade therapy. Therefore, our study provided a new predictive signature to evaluate the prognosis and possible effects of the PD-1 blockade therapy in LUAD.

Abbreviations: ANOVA, one-way analysis of variance; ATcluster, autophagy cluster; CCL2, chemokine MCP-1; CMP, common myeloid progenitor; CNV, copy number variation; CYT, cytotoxic activity; DEGs, differentially expressed genes; ERα, Estrogen receptor α; FDRs, False discovery rates; GEO, gene-expression omnibus; GEP, gene expression profile; GO, gene ontology; GSEA, gene set enrichment analysis; GSVA, gene set variation analysis; HADb, human autophagy database; IHC, Immunohistochemistry; lncRNAs, long non-coding RNAs; LUAD, lung adenocarcinoma; MDSCs, myeloid-derived suppressor cells; MHC-I, major histocompatibility complex-I; OS, overall survival; PCA, the principal component analysis; PD-1, Programmed cell death protein 1; PD-L1, Programmed death-ligand 1; TCGA, The Cancer Genome Atlas; TIDE, Tumor Immune Dysfunction and Exclusion; TME, The tumor microenvironment; t-SNE, t-distributed stochastic neighbor embedding.

MATERIALS AND METHODS

Dataset Source and Preprocessing

The workflow of our study was summarized in **Figure 1**. Open LUAD gene expression datasets and corresponding clinical information were obtained from The Cancer Genome Atlas (TCGA) and Gene-Expression Omnibus (GEO) databases. Patients with incomplete clinicopathological information were removed in further analyses. In total, TCGA-LUAD dataset and 9 eligible GEO datasets (GSE13213, GSE14814, GSE30219, GSE31210, GSE37745, GSE50081, GSE68465, GSE72094, and GSE81089) were enrolled for further evaluation. The RNA-sequencing data were downloaded from GDC portal, and the

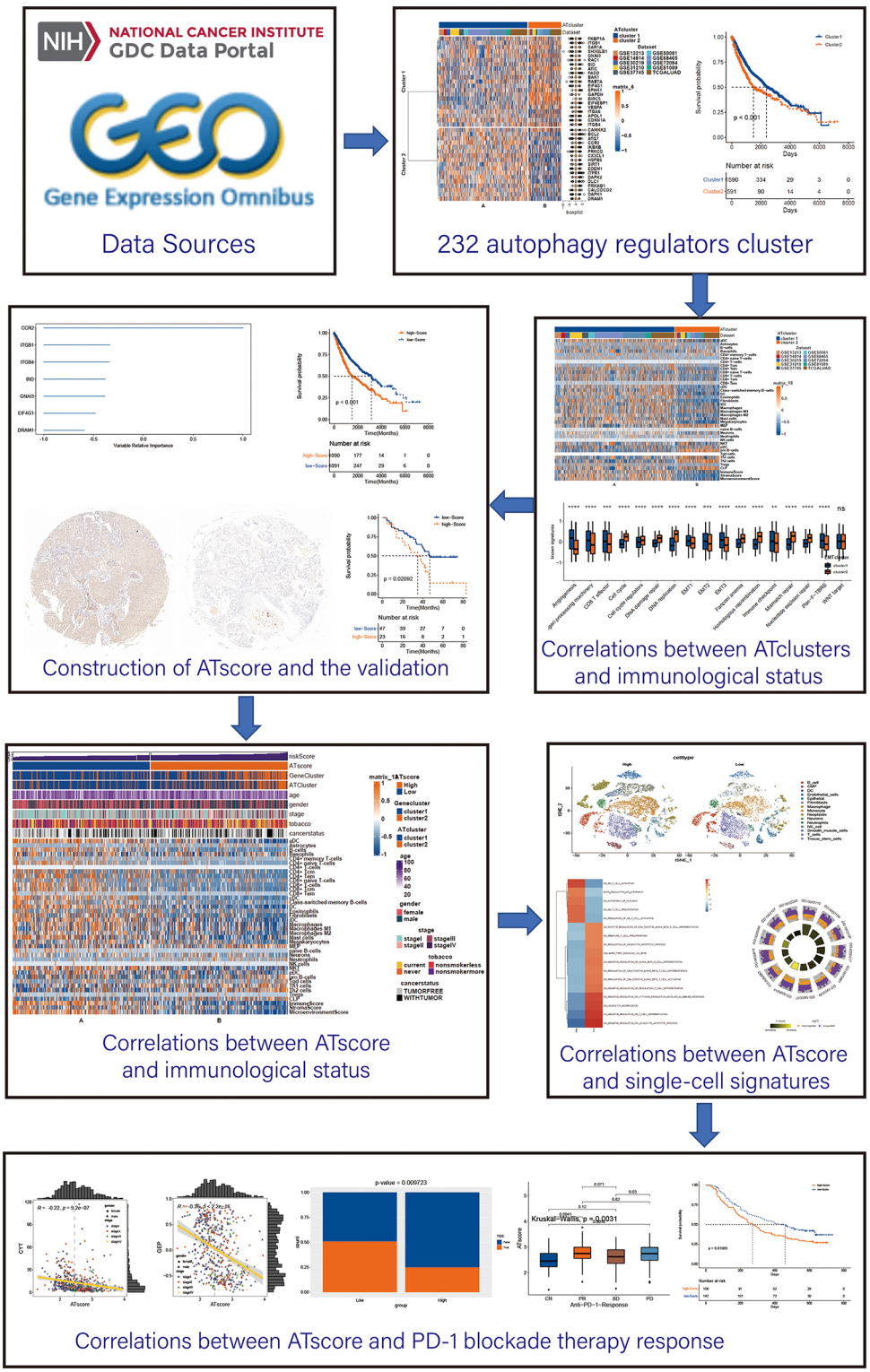

FIGURE 1 | The workflow of the bioinforamtic analysis. Datasets were obtained from TCGA and GEO databases, and Consensus clustering were performed using autophagy regulators. After identifying the correlation between the autophagy clustering and immunological status, ATscore was constructed and proven to be a prognostic predictor of LUAD patients. The correlation between ATscore and immunological status of tumor was confirmed in datasets and single-cell sequencing data. Moreover, the predictor value of ATscore in PD-1blockade therapy response was confirmed.

fragments per kilobase million (FPKM) values were transformed into transcripts per kilobase million (TPM), so the data can be comparable between samples (14). The raw data of microarray datasets were gererated by Affymetrix or Agilent platforms. We used the RMA algorithm of the Affy software to perform the quaintly normalization and background correction for Affymetrix raw data. The consensus median polish algorithm in the Affymetrix software was used for summarizing of oligonucleotides for each transcript. Meanwhile, the R package "limma" was used to process the Agilent raw data. The signal intensity of TPM values from TCGA was similar with RMA-standardized values from microarray datasets.

Consensus Clustering Analysis

We searched the canonical autophagy database HADb (Human Autophagy Database), and 232 autophagy regulators were identified to be autophagy signature clustering candidates (**Table S1**). Univariate COX analyses were performed to identify autophagy regulators for consensus clustering in the meta-cohort (P<0.001). Afterward, LUAD samples were grouped into clusters by consensus clustering analysis with the R package "ConsensusClusterPlus". Kaplan-Meier survival curves were created in each cluster, and log-rank tests were performed to compare the overall survival (OS) between subgroups. The "limma" package in R was used to investigate the differentially expressed genes (DEGs) between distinct autophagy clusters. The t-distributed stochastic neighbor embedding (t-SNE) analysis and the correlation analysis between autophagy regulators and DEGs were performed to validate the stability of the clustering.

Functional Annotation Enrichment and Immune Cells Infiltration Analyses

To determine the differences of biological functions between sample subgroups, Gene Set Variation Analysis (GSVA), Gene Set Enrichment Analysis (GSEA), and Gene Ontology (GO) enrichment analysis were performed. The functions and pathways with a strict cut of the value of $P < 0.05$ were selected. For immune cell infiltrating estimation, we performed an xCell algorithm to quantify the proportion of the infiltrating immune cells in LUAD samples (15). Total 64 cell signatures were calculated, and 40 immune cell-related signatures were selected for display (aDC, Astrocytes, B-cells, Basophils, CD4+ memory T-cells, CD4+ naive T-cells, CD4+ T-cells, CD4+ Tcm, CD4+ Tem, CD8+ naive T-cells, CD8+ T-cells, CD8+ Tcm, CD8+ Tem, cDC, Class-switched memory B-cells, DC, Eosinophils, Fibroblasts, iDC, Macrophages, Macrophages M1, Macrophages M2, Mast cells, Megakaryocytes, MEP, naive B-cells, Neurons, Neutrophils, NK cells, NKT, pDC, pro B-cells, Tgd cells, Th1 cells, Th2 cells, Tregs, CLP, ImmuneScore, StromaScore and).

Somatic Mutation Analyses

The copy number alterations (CNAs) and somastic mutations of LUAD patients was downloaded from the TCGA database. GSITIC analysis were applied to investigate the specific genomic event variations, and the threshold copy numbers at alteration peaks in different ATscore groups were illustrated. The somatic mutation analysis and mutation landscape delineation of TCGA was performed by the R package "maftool".

Generation of Autophagy Associated Signature

To construct the autophagy-based signature, the 38 autophagy regulators used for consensus clustering were subjected to univariate COX analysis in TCGA cohort., and those with P<0.05 were chosen as candidates for signature construction. To quantify the autophagy modification patterns of tumors, we use random survival forest analysis to perform dimension reduction to reduce noise or redundant genes among these prognostic autophagy regulators, and the relevant importance of each gene was calculated (14). Next, we conducted loop modeling to screen autophagy-based signatures based on the importance of each gene. The signature with the lowest P-value in Kaplan-Meier analysis was identified as the autophagy-based signature, and the ATscore was calculated as follows:

$$\begin{aligned} ATscore \quad &= \quad (-0.0923 * DRAM1 \quad (geneexpressionlevel)) \\ &+ \quad 0.4621 * ITGB1 \quad + \quad (-0.2977 * CCR2) \end{aligned}$$

The univariate and multivariate Cox regression analyses were used to investigate whether the ATscore can be an independent risk factor of OS for LUAD patients by R package "survival".

Single-Cell Characteristics Identification

For single-cell characteristics investigations, we obtained the single-cell RNA sequencing data of 49 clinical biopsies obtained from 30 patients (include 9 primary and 21 metastatic lung adenocarcinoma patients from an NCBI BioProject #PRJNA591860. The dataset was downloaded from ENA (European Nucleotide Archive (https://www.ebi.ac.uk/ena/browser/view/PRJNA591860). Follow genes were used as marker genes for the first clustering, immune (CD45+,*PTPRC*), epithelial/cancer (EpCAM+,*EPCAM*), stromal (CD10+,*MME*, fibo or CD31+,*PECAM1*,endo) (16). Cells previously annotated as epithelial cells were re-clustered using the following methods. We determined the single-cell copy number variation (CNV) through the "infercnv" package. We established an algorithm for the average expression of specific genes in each chromosome of all sample cells to distinguish between tumor and non-tumor epithelial cells (16). Infercnv searched cells with large copy number variations, sorted genes by chromosome position, and determined relative expression values by moving average method (17, 18). All epithelial cells as well as 300 fibroblasts and 300 endothelial cells were used as input. An additional 500 fibroblasts and 500 endothelial cells were used as reference controls. We scored the CNV degree for each cell and plotted the cells on a dendrogram, then cut at the highest point where all endothelial and fibroblasts belonged to a cluster (k = 6). All cells clustered with the spiked control were labelled as 'non-tumor', while the remaining two clusters were labelled as 'tumor'. The non-tumor cells were annotated by "scCATCH" package. We further performed the cell clustering and dimension reduction by R package "Seurat". Afterward, the principal component analysis

(PCA), "FindNeighbors" package, and "FindClusters" package were used to construct the cell clustering. "UMAP" was used to visualize the expression profiling, and the "SingleR" package was used to cluster the non-malignant cells. The "FindCluster" function in "Seurat" package was used to identify genes that differentially expressed between two ATscore groups. GSVA and GSEA were performed to determine the functional annotation of ATscore. Statistical significance was set at |correlation coefficient| > 0.5 for GSVA, and FDR < 0.05 for GSEA (19). Furthermore, we performed the cell-cell interaction analysis by the "CellChat" package (20). The various receptor-ligand signaling expression modules between the high and low ATscore groups and the roles of different ATscore groups in specific molecular pathways were visualized.

Immunotherapy and Molecular Therapy Response Prediction

To predict the potential immunotherapy response in patients with various levels of ATscores, T cell–inflamed gene expression profile (GEP), cytotoxic activity (CYT), and the Tumor Immune Dysfunction and Exclusion (TIDE) algorithm were performed in the TCGA cohort (21). To investigate the direct predictive value of ATscores on PD-1 therapy response, the IMvigor210 dataset was downloaded from http://research-pub.gene.com/IMvigor210CoreBiologies, and correlation between ATscore levels of patients and the anti-PD-1 therapy responses was calculated.

The chemotherapy response of LUAD patients from TCGA cohort was determined by the Genomics of Drug Sensitivity in Cancer database (GDSC, https://www. cancerrxgene.org). The IC50 values were calculated for the prediction of drug sensitivity by R package "pRRophetic".

Tissue Specimens and the Immunohistochemistry

The tissue sample collection in this study was approved by the ethics committee of Xiangya Hospital, Central South University (CSU; Changsha, China). Before the tumor sample collection, all patients were informed, and the written consent was obtained. From January 2011 to December 2012, 70 cases of LUAD tumor samples were collected from patients who underwent tumor resection at the Department of Thoracic Surgery, Xiangya Hospital, CSU. All patients did not receive radiotherapy or chemotherapy before the lung resection operation. The LUAD samples were collected from the edge of tumor lesions, and at least two experienced pathologists confirmed the pathological diagnosis. The collected samples were rapidly frozen in liquid nitrogen and transferred to a −80°C freezer for further assays. All patients were followed up every three months by telephone or a visit by our team for survival inquiry until death or the end of the follow-up.

IHC assays were performed for ATscore calculation in tissues. Paraffin-embedded tissues were cut into 4-μm sections. Sections were deparaffinized and boiled in 10 mM citrate buffer (pH 6.0) for antigen retrieval, and 3% H_2O_2 was used to block endogenous peroxidase activity. DRAM1 (sc-81713, Santacruz), CCR2 (ab203128, Abcam) and ITGB1 (ab134179, Abcam) antibodies were used as primary antibodies. The IHC staining scores were determined by combining staining intensity and the proportion of positively stained cells using histochemistry score (H-score). H-Score = (percentage of weak intensity cells ×1) + (percentage of moderate-intensity cells ×2) + (percentage of strong intensity cells ×3).

Cell Culture and Transfection

A549 and H1299 cell lines were obtained from the Chinese Academy of Science Cell Bank (Shanghai, China), and cultured in RPMI-1640 (Gibco) medium supplemented with 10% FBS (Gibco), 100 U/mL penicillin, and 100 μg/mL streptomycin (Gibco) in a humidified incubator with 5% CO2 at 37°C. The siRNA of DRAM1 (sense: CCUACAGUCCAUCAUCUCUUATT, antisense: UAAGAGAUGAUGGACUGUAGGTT) and the negative conthol (sense: UUCUCCGAACGUGUCACGUTT, antisense: ACGUGACACGUUCGGAGAATT) were obtained from Sangon Biotech (Shanghai, China), and transfected into cells by Lipofectamine 3000 (ThermoFisher) according to the manufacturer's protocol.

Western Blot Assays

The total protein of cell lines was extracted with RIPA lysis buffer (Beyotime) containing protease inhibitor for 20 min on ice. After the measurement of protein concentration by Bradford's reagent (Beyotime), protein samples were separated by sodium dodecyl sulfate polyacrylamide gel electrophoresis (SDS-PAGE) and transferred onto polyvinylidene fluoride (PVDF) membranes. After blocking with 5% nonfat milk in TBST for 60 min, membranes were incubated with primary antibodies at 4°C overnight. DRAM1 (sc-81713, Santacruz) and GAPDH (GB11002, Servicebio) were used as primary antibodies. Anti-rabbit or anti-mouse IgG conjugated to horseradish peroxidase (HRP) (Proteintech) was used as the secondary antibody. Bands were visualized by Bio-Rad Image Lab Software.

Cell Counting Kit-8 Assays

The proliferation ability of LUAD cells was monitored by cell counting kit-8 (Biosharp). A549 and H1299 cells ($3*10^3$/well) were seeded in the 96-well plates. The Optical Density (OD_{450}) were determined on 0, 24, 48, 72 and 96 h.

5-ETHYLNYL-2′-DEOXYURIDINE INCORPORATION ASSAY

EdU assays were performed by kFluor488 Click-iT EdU Kit (KeyGEN biotech). A549 and H1299 cells (3000/well) were incubated in 95-well plates after the siRNA transfection. The EdU marking and the Hoechst 33342 identification were performed according to the manufacturer's protocol.

Colony Formation Assays

A549 and H1299 cells (1000/well) were seeded in the 6-well plates after the transfection. After 14 days of incubation,

Paraformaldehyde fix solution (4% PFS) was used for the cells fixation, and 0.1% crystal violet (Beyotime Biotechnology) were used for identification of cell colonies.

Transwell Assays

Transwell assays were performed to examine the migratory and invasive capacity of LUAD cells. For the transwell migration assay, $4*10^4$ cells in serum-free media were placed into the upper chamber of an insert (8 μm pore size, Corning). For the transwell invasion assay, $8*10^4$ cells in serum-free media were seeded into the upper chamber, which was precoated with Matrigel (Corning). For both transwell migration and invasion assays, medium with 20% FBS was added to the lower chamber. Cells were incubated for 24 h at 37°C, and nonmigrating cells were removed with cotton swabs. Migrated or invaded cells on the bottom of the membrane were fixed with 4% paraformaldehyde for 15 min and stained with crystal violet for 15 min. Then, stained cells were assessed by counting 5 random fields per chamber under a microscope.

Statistical Analysis

R software (v3.6.3) was used for all statistical analyses. The normality of the variables was tested by the Shapiro-Wilk test. Differences between two normally distributed groups were determined by the Students' t-test, and the Wilcoxon test measured differences between two non-normally distributed variables. One-way analysis of variance (ANOVA) tests was used as a parametric method for multiple groups comparison, while Kruskal–Wallis tests were used as a nonparametric method. For correlation coefficients calculation, Pearson correlation and distance correlation analyses were performed. Chi-square contingency tests were used for contingency tables analyses. After the ATscore calculation, R package sva was used for reducing the computational batch effect. Data visualization was performed using the R package ggplot2. Benjamini–Hochberg method was used for P values to FDRs conversion in the DEG analysis (22). ROC curves and the area under the curve (AUC) calculation were performed by R package timeROC. Kaplan-Meier survival curves were created in each group, and log-rank tests were performed to compare the OS between subgroups. The univariate and multivariate Cox regression analyses were used to investigate the independent prognostic factor by R package survival. Survival curve visualization was performed by R package survminer. All heatmaps were generated by R package ComplexHeatmap. All the tests were two-sided, and $P < 0.05$ was considered statistically significant.

RESULTS

The Consensus Clustering of Autophagy Regulators Predicted the Prognosis of LUAD Patients

To explore the prognosis relevance of autophagy regulators, nine GEO datasets with available survival data (GSE13213, GSE14814, GSE30219, GSE31210, GSE37745, GSE50081, GSE68465, GSE72094, and GSE81089) and TCGA LUAD dataset were enrolled as the meta-cohort to construct the autophagy regulators consensus clustering. By the univariate COX analysis, 38 regulators with P<0.001 were selected for further analysis (**Table S2**). The R package ConsensusClusterPlus clusters the LUAD samples into subgroups based on the expression pattern of autophagy regulators (**Figure S1**). Our consensus matrix results showed that the LUAD meta-cohort could be distinctly divided into two subgroups, and these regulators exhibited different expression patterns in the meta-cohort and TCGA cohort (**Figures 2A, C**). Moreover, after we screening DEGs between clusters, the correlation analysis results showed that the clusters distinguished by autophagy regulators strongly correlated with identified DEGs (**Figure S2**).

Afterward, we examined whether the two subgroups of LUAD patients have different prognoses. The Kaplan-Meier analysis results showed that cluster2 had a worse prognosis than cluster1 in the meta-cohort and TCGA cohorts (**Figures 2B, D**). Furthermore, we performed t-SNE to validate the subgroup assignment. Our results showed that the two clusters were fine isolated, and these 38 autophagy regulators separated tumors from normal tissues remarkably (**Figures 2E, F**).

The Transcriptome Features of Autophagy Clusters

To determine the biological behavior differences between the two autophagy clusters (ATcluster), a GSVA enrichment analysis was performed to discover the potential function diversities. Interestingly, we found that plenty of immune-related and autophagy-associated pathways were enriched (**Figure 3A**). Therefore, we further investigated the unsupervised clustering of immune infiltrating cells in the meta-cohort. We found that the two ATclusters had different T cell-related infiltration clustering and significant discrepancy of tumor microenvironment scores (**Figure 3B**, **Figure S3A**), and these results were also confirmed in the TCGA cohort (**Figures S3B, C**). Moreover, the expression of immune-related genes in the two clusters had remarkable differences (**Figure S4**). Since T cells infiltration and the tumor microenvironment reshaping are the vital for PD-1 targeting therapies, these results suggested the potential association between our autophagy clustering and the response of PD-1 immune therapy. Moreover, the two autophagy clusters were associated with the well-known signatures in the meta-cohort and TCGA cohort (**Figure 3C**, **Figure S5A**). Apart from the immune infiltration, the autophagy clustering also correlates with proliferation-related genes and metabolic function of LUAD tumors (**Figures S5B, C** and **S6**).

The Construction of Autophagy Modification Patterns and its Correlation With Prognosis of LUAD Patients and Functional Annotations

The DEGs were acquired and adapted to investigate the comprehensive biological characteristics of two ATclusters (**Table S3**), and the consensus clustering by these DEGs was performed to construct the Geneclusters. Meanwhile, the 38 autophagy regulators used in the consensus clustering assay

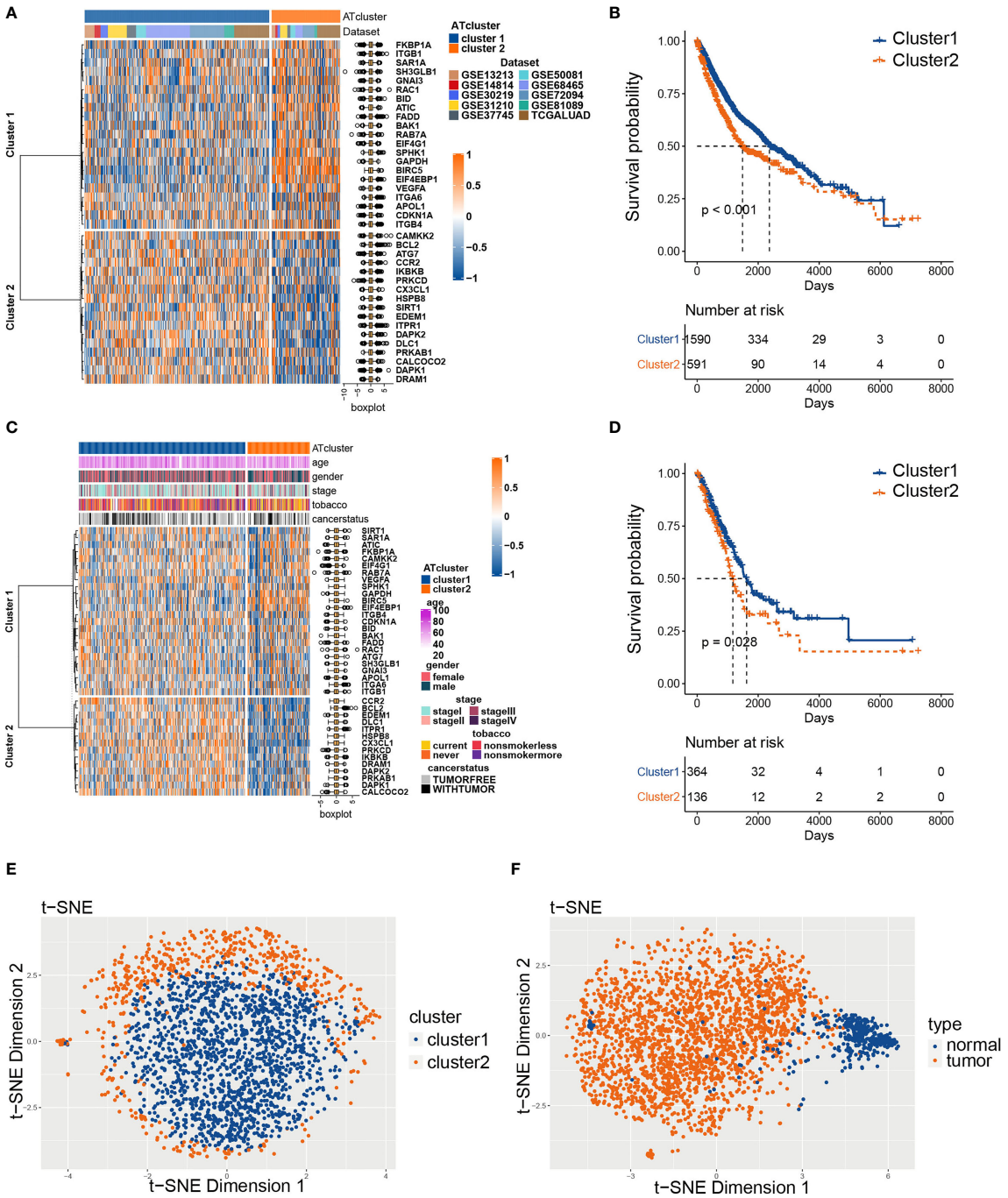

FIGURE 2 | The consensus clustering of autophagy regulators predicted the prognosis of LUAD patients. The expression pattern of 38 autophagy regulators in the meta-cohort **(A)** and TCGA cohort **(C)**. The heatmaps showed upregulated genes (red) and downregulated genes (blue) of autophagy regulators in subgroups. The Kaplan-Meier analysis showed that the clusters2 had worse prognosis than cluster1 in both meta-cohort **(B)** and TCGA cohort **(D)**. The t-SNE analyses showed that the two autophagy clusters were fine isolated **(E)**, and the autophagy-related regulators separated tumors from normal tissues noticeably **(F)**.

were selected for univariate COX analysis in TCGA cohort. The 20 regulators with P<0.05 were chosen as autophagy modification pattern candidates (**Table S4**). Furthermore, random survival forest analysis was used to explore the probability of autophagy modification pattern construction. After calculating the relative importance of 20 autophagy regulators, 7 genes were identified as the most critical factors (**Figure 4A**). Further log-rank analyses showed that the signature constructed by 3 genes (*CCR2*, *ITGB1*, and *DRAM1*) had the lowest P value and could predict LUAD patients' prognosis with

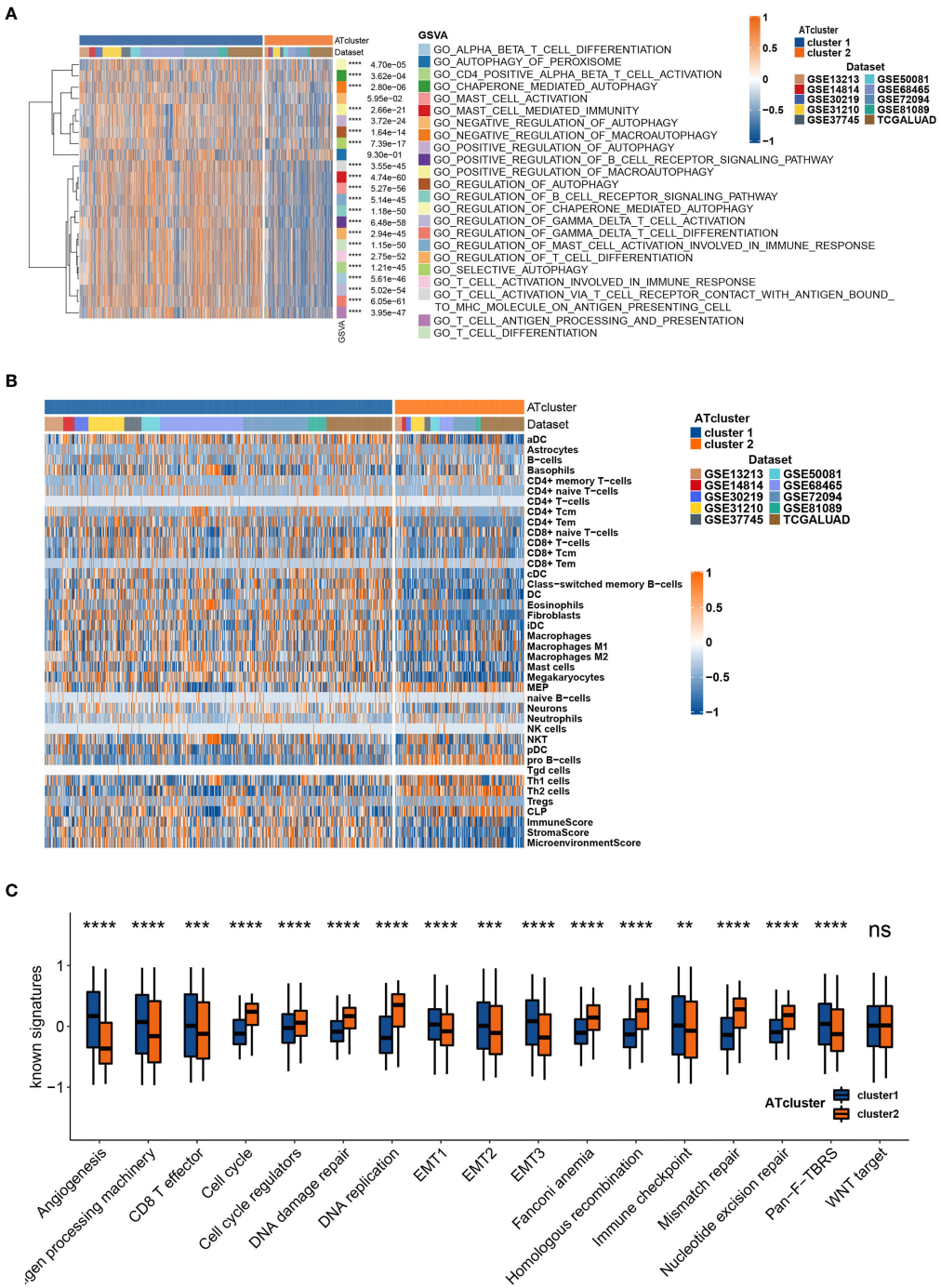

FIGURE 3 | The transcriptome features of autophagy clusters in the meta-cohort. Unsupervised clustering assays showed that immune and autophagy-related biological functions were enriched in meta-cohort samples **(A)**, and the two autophagy clusters (ATcluster) have different immune infiltrating cells patterns **(B)**. The two autophagy clusters had different well-known signature patterns in the meta-cohort **(C)**. **P<0.01, ***P<0.001, ****P<0.0001. "ns" means no significance.

highest efficiency (**Figure 4B**). Therefore, we name this gene signature as the ATscore. Unsurprisingly, LUAD patients with higher ATscore had noticeable worse overall survival in meta-cohort (**Figure 4C**, **Figure S7A**), and the Sankey plot showed the interconnection among the ATclusters, Geneclusters, ATscores, and patient survival (**Figure 4D**). The ROC curve showed that ATscore can be a sensitive marker for 3-years overall survival of LUAD patients. Meanwhile, the AUC of ATscore was bigger than other reported models (**Figure S7B**) (23, 24). Moreover, both the univariate and multivariate COX regression analyses

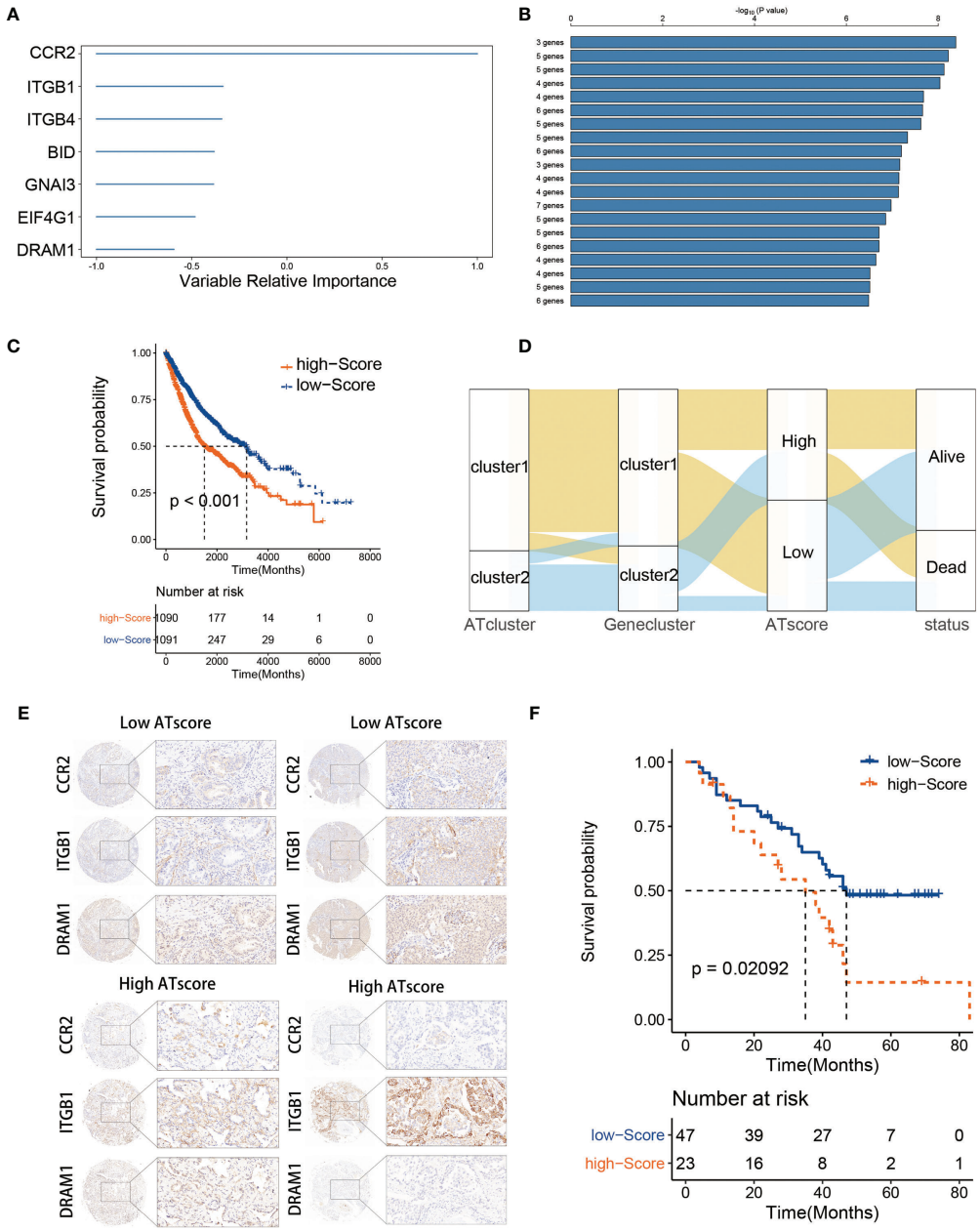

FIGURE 4 | The construction of ATscore and the validation of its prognostic predictive value. The relative importance of the 20 autophagy regulators was calculated by random survival forest analysis, and the 7 most critical ones were showed **(A)**. The log-rank analyses showed that ATscore constructed by 3 genes predicted LUAD patients' prognosis with a lowest P value **(B)**. LUAD patients with higher ATscore had noticeable worse overall survival in meta-cohort **(C)**. Sankey plot illustrating the interconnection among the ATclusters, Geneclusters, ATscores, and patient survival **(D)**. The representative IHC pictures of biopsies from independent cohort were showen **(E)**, and the prognostic predictive value of the ATscore was validated in independent cohort **(F)**.

revealed that ATscore was an independent risk factor of LUAD patients (**Figure S7C**). Besides the LUAD cohorts, we also investigated the pan-cancer cohorts to explore whether the autophagy signature score can predict the survival of patients in other cancers. Our results showed that the predicted value of ATscore could be confirmed in multiple cancer cohorts (**Figure S8**). Taken together, our analyses constructed a new signature called ATscore, and this signature was correlated with the prognosis of LUAD patients and could act as an independent prognostic marker for LUAD patients.

To confirm the survival predictive value of ATscores in LUAD patients, we verified the prognostic value of ATscore in an independent validation cohort composed by 70 LUAD tumor samples from the Thoracic surgery department of

Xiangya hospital. The IHC assays were performed to determine the expression levels of ATscore-related genes. Accordingly, the ATscores of these tumor samples were calculated. The samples with low expression levels of *CCR2* and *DRAM1* and high expression levels of *ITGB1* were classified into high ATscore group, vice versa (**Figure 4E**). The Kaplan-Meier analysis results showed that patients with higher ATscores had significantly wrose prognosis than those with lower ATscores (**Figure 4F**). These results validated the prognostic predictive value of the ATscore in our LUAD cohort.

To further investigate the functional traits of autophagy modification signature, transcriptome feature analyses were performed among patients with various ATscores. The GSVA analysis results showed that the ATscores were associated with T cell selection, T cell lineage commitment and other humoral immune-related pathways (**Figure 5A**). The further unsupervised clustering of immune infiltrating cells showed a more specific correlation of ATscores with checkpoints therapies-related immune cells (**Figure 5B**). Besides, we also found the relationship between the autophagy signature and the immune-related genes (**Figures S9**, **10**). Meanwhile, the results of CNA analysis revealed that patients with different ATscores had various copy number alterations (**Figure S11A**). Patients with high ATscore had higher levels of KRTAP9-9 (17q21.2) amplification and LCE3C (1q21.3) deletion, and those with low ATscore had higher levels of PLK2 (5q11.2) amplification. Somastic mutation analysis showed that patients with higher ATscore had higher mutation frequency of TP53 (55% vs. 41%), TTN (53% vs. 38%), MUC16 (45% vs. 34%), CSMD3 (44% vs. 30%) and RYR2 (43% vs. 29%) compared with those had lower ATscore (**Figure S11B**). Moreover, ATscores also presented a tight correlation with well-known signatures and carcinogenesis pathways (**Figures 5C, D**).

The Correlation of ATScores With the Single-Cell Characteristics

According to the potential correlation between T cell infiltrations of LUAD tumor and the autophagy signature, we further explored whether the ATscore could predict the single-cell characteristics by exploring the single-cell RNA sequencing data. We calculated the CNV of individual cells and the CNV score of each cell cluster by 'infercnv'. The cells were classified into malignant and non-malignant cells (**Figures S12A, B**). Furthermore, the statistical analysis results showed that the tumor samples with lower ATscores had a lower proportion of common myeloid progenitor (CMP), macrophage, and monocyte than those with higher scores (**Figures 6A–C**). These results suggested the remarkable immune microenvironment diversity between the two ATscore groups.

We next focused on malignant cells with different ATscore. By the DEGs between the different levels of ATscores (**Figure 6D**), GO enrichment and GSEA assays were further performed. At the same time, we compared the different pathways between the two groups by GSVA analysis. Our results identified a remarkable difference between the two ATscore groups on the autophagy and immune response-related cellular functions and signaling pathways (**Figures 7A–C**).

Further, we explored the interaction between tumor cells with different ATscore levels and microenvironmental cells, and the results also showed a diversity of communication patterns between tumor cells with different ATscore levels (**Figures S12C, D**). It is well known that each cell has its unique communication pattern as receivers, senders, mediators, and influencers. Our results showed that T cells in the LUAD tumor microenvironment may communicate with malignant cells at high ATscore levels *via* PARs, IFN-II and IL-4 pathways, thereby regulating tumor cell proliferation and invasive capacity (**Figures 7D–F**).

The Autophagy Modification Patterns Predicted Immunological Therapeutic Benefits

In the previous study, we have investigated the survival predictive role of ATscore in the LUAD cohort and explored the potential relationship between the ATscore and the immune escape of LUAD tumors. This section focused on the direct efficiency predictive value of ATscore in the PD-1 blockade therapy. Recently, T cell–inflamed GEP and CYT are emerging as predictive biomarkers for PD-1 blockade therapies (21). Therefore, we explored the correlation between ATscores and these well-known biomarkers. Our results showed that the patients with lower ATscore in the TCGA cohort had relatively higher GEP and CYT scores (**Figures 8A, B**). In addition, TIDE algorithm was also performed to evaluate the coherence of ATscores and the LUAD tumor immunotherapy response. Our results revealed that patients with higher ATscore in TCGA cohort might have poorer responses to immunotherapy (**Figure 8C**). These biomarker calculations suggested that the ATscores might have a negative correlation with the immunological therapy responses. Furthermore, we found that the levels of ATscores had a negative correlation with the PD-1 blockade therapy responses in the IMvigor210 cohort. In this cohort, patients with higher ATscores also had poorer anti-PD-1 response and prognosis than those with lower scores (**Figure 8D**). Moreover, we evaluated the chemotherapy response of LUAD patients with different ATscores. Our results showed that patients with higher ATscores had significantly higher IC50 value in many chemotherapy molecules compared with those with lower ATscore (**Figure S13**), especially in lung cancer sensitive AZD6244 and Gefitinib. These results indicated that patients with higher ATscores may also have poorer chemotherapy response than those with lower ATcores.

DRAM1 Suppressed the Proliferation and Migration of LUAD Cells

Among the three autophagy regulators that make up the ATscore, *CCR2* and *ITGB1* were well-discussed and considered as vital regulators in the development of LUAD. However, the biological functions of *DRAM1* remained controversial. For validation of our predicted tumor suppressor role of *DRAM1* in the ATscore, we used siRNA to inhibited the expression of *DRAM1* in A549 and H1299 cells (**Figure 9A**). The CCK-8 assays, EdU assays and colony formation assays demonstrated that the inhibition of *DRAM1* significantly promoted the proliferation and DNA duplication ability of LUAD cells (**Figures 9B–D**). Meanwhile, the results of Transwell assays and invasion assays showed that the repression of *DRAM1*

FIGURE 5 | The transcriptome features of patients with various ATscores in TCGA cohort. The GSVA analysis showed the different immune-related patterns of patients with various ATscores in TCGA cohort **(A)**. The diversity of immune cells infiltrating patterns between patients with various ATscores was identified by xCell algorithm, and our results showed a more specific correlation of ATscores with checkpoints therapies-related immune cells **(B)**. Patients with various ATscores also presented different states of well-known signaturesand carcinogenesis pathways **(C, D)**. *P<0.05, **P<0.01, ***P<0.001, ****P<0.0001. "ns" means no significance.

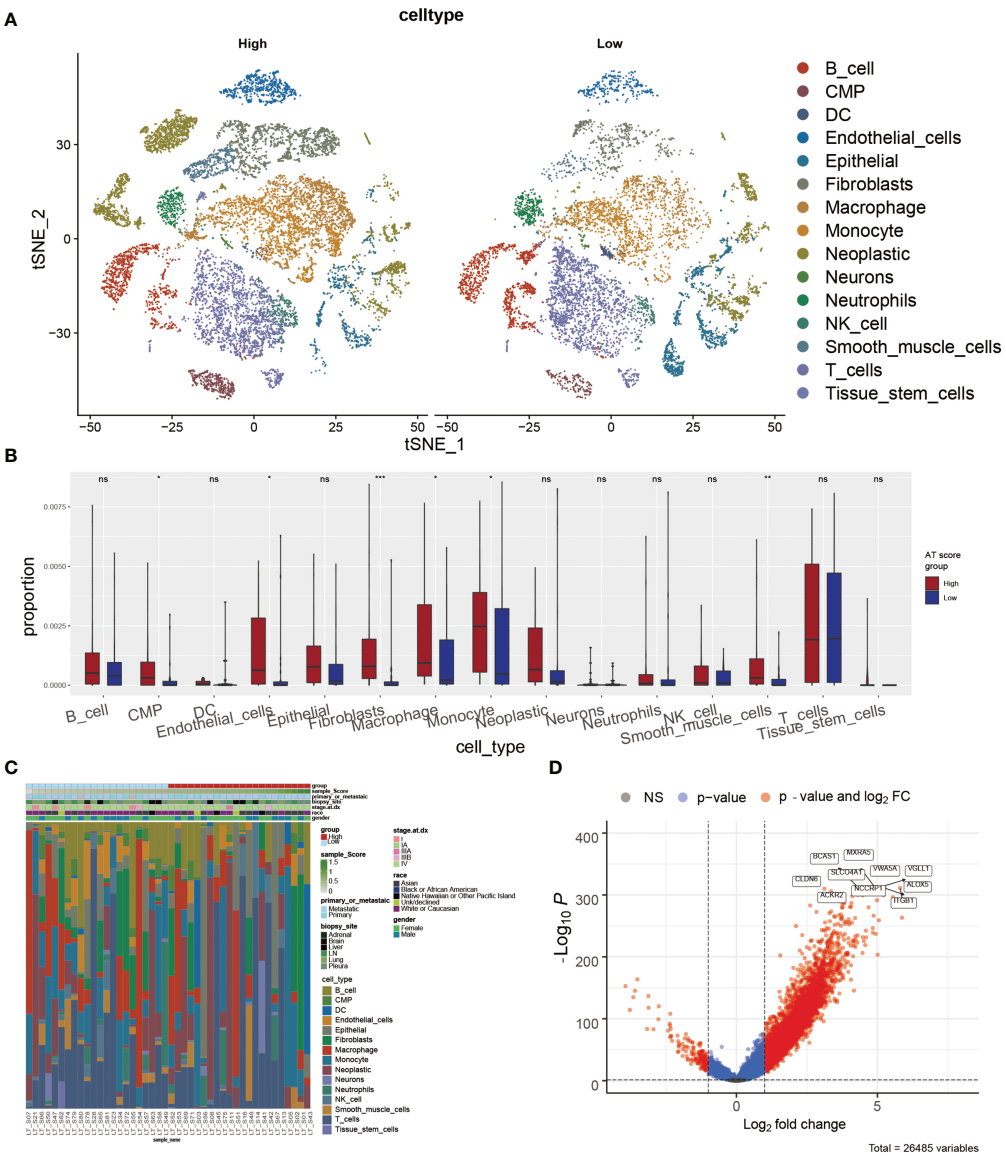

FIGURE 6 | The correlation of ATscores with the single-cell characteristics. The single-cell patterns showed that tumor samples with higher ATscore had significantly more Neoplastic cells compared with low ATscore group **(A)**. The statistical analysis results of immune cells diversity assay showed that the tumor samples with lower ATscores had a lower proportion of common myeloid progenitor (CMP), macrophage, and monocyte than those with higher scores **(B)**, and the immune cells diversity between two ATscore groups was remarkable **(C)**. The DEGs between the single-cell samples with different levels of ATscores were visualized, and the most remarkable genes were identified **(D)**. *P<0.05, **P<0.01, ***P<0.001, ****P<0.0001. "ns" means no significance.

expression remarkably enhanced the migration and invasive capacity of LUAD cells (**Figure 9E**). These results demonstrated that *DRAM1* played as a tumor suppressor in LUAD cells, and its protective role in the ATscore was validated.

DISCUSSION

LUAD is one of the fatal malignancies globally, and anti-PD-1 immunotherapy is the frontier domain in the LUAD treatment. At present, how to identify patients who can get the best response to anti-PD-1 immunotherapy remains a challenge. Gene signatures are a kind of biological function pattern constructed by the expression data of multiple genes and can be used for prognostic and progression prediction in many types of malignancies (25, 26). Therefore, a signature which can both predict the prognosis and the response of PD-1 therapy in LUAD patient is urgent to be discovered. Recent studies have demonstrated that autophagy is involved in the innate immune response as a critical mechanism of immune receptor regulation. Consequently, PD-1 therapy biomarkers consisted of autophagy-related genes can be a new research direction. In this work, we constructed an autophagy-related signature with only three

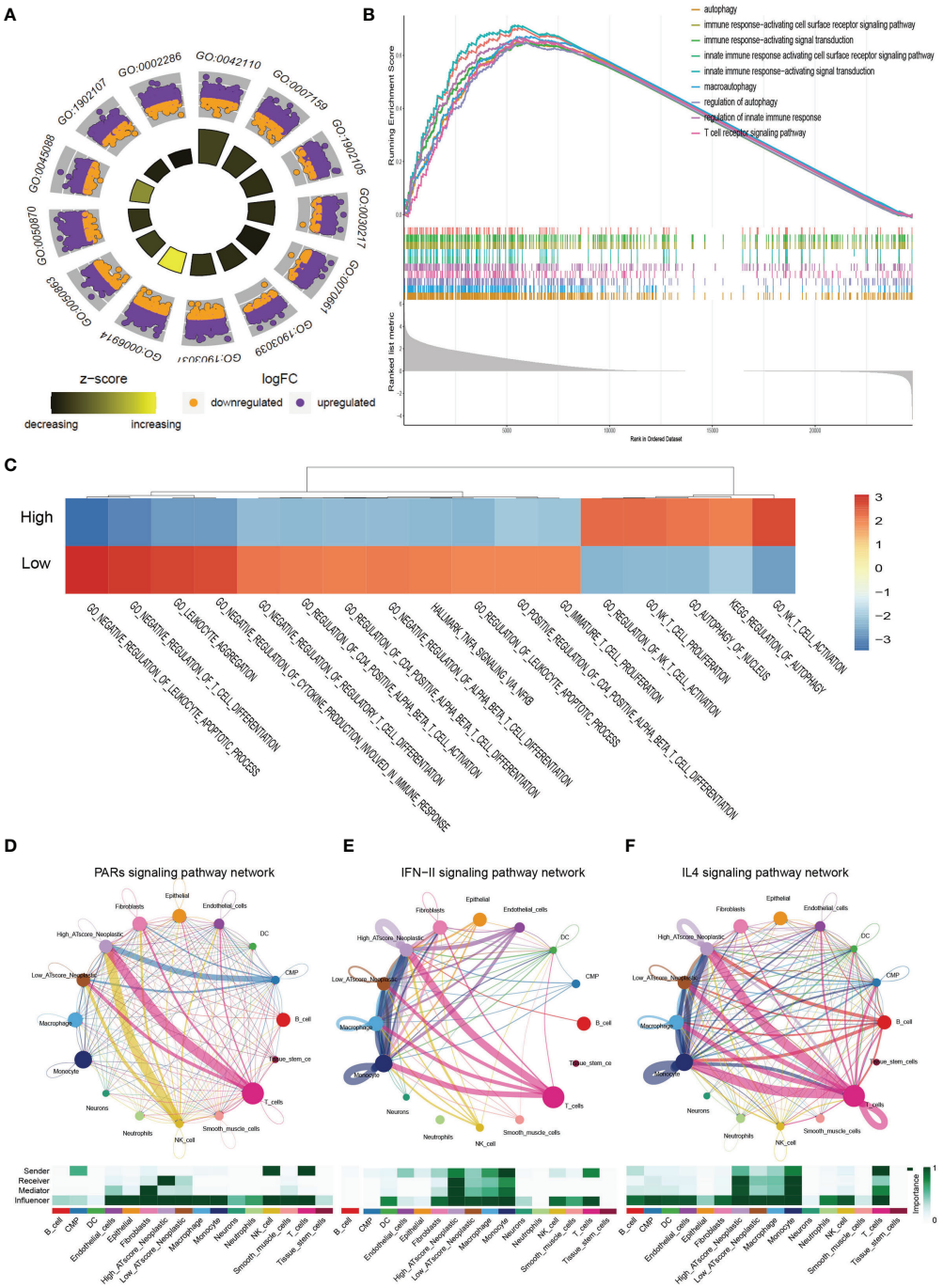

FIGURE 7 | The correlation of ATscores with immune cells infiltrating and the cellular communication patterns. GO enrichment analysis **(A)**, GSEA **(B)** and GSVA **(C)** revealed that two ATscore groups had different autophagy and immune response-related cellular functions and signaling pathways. The cells with various ATscore levels have diverse tumor-related (PARs signaling) and immune response-related signaling pathway (IFN-II signaling and IL4 signaling) patterns **(D–F)**. Tumor cells with different ATscore levels play different roles in cellular interactions with tumor microenvironment cells.

genes to predict the prognosis of LUAD patients and their response to PD-1 therapy, and the prognostic predictive value of this risk signature was validated in the independent LUAD cohort. A biomarker constructed with fewer genes in the clinical application means a lower cost and more accessible usage. Moreover, our results in pan-cancer cohorts inferred the potential application value of ATscore in other types of cancers. Therefore, the ATscore signature we constructed has good clinical application prospects in the future.

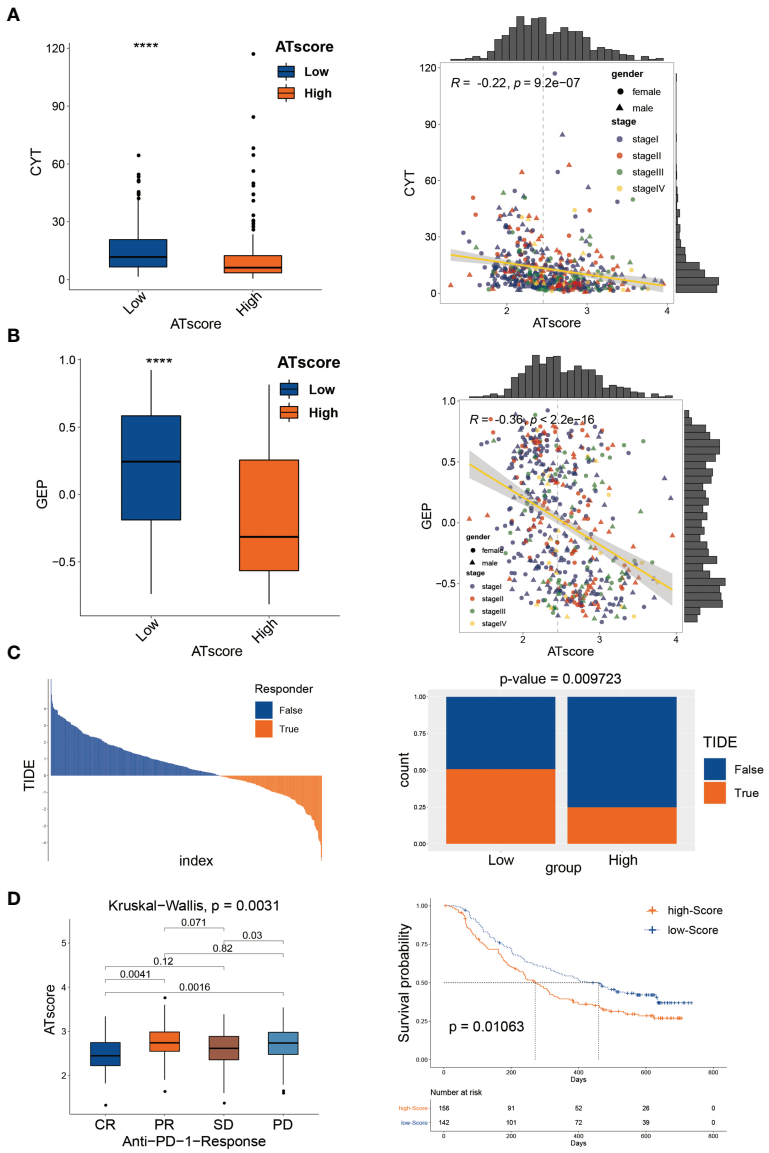

FIGURE 8 | The autophagy signature predicted immunological therapeutic benefits. The patients with lower ATscore in the TCGA cohort had relatively higher CYT **(A)** and GEP **(B)** scores compared with those had higher ATscore. The results of TIDE algorithm showed that patients with higher ATscore in TCGA cohort might get poorer immunotherapy response than patients with lower ATscore **(C)**. In IMvigor210 cohort, patients with higher ATscores also had poorer anti-PD-1 response and prognosis than those with lower scores **(D)**. ****P<0.0001.

The tumor microenvironment (TME) is an emerging concept in cancer research. The conventional TME consists of extracellular matrix, cancer-associated fibroblasts, vascular epithelial cells, and infiltrating immune cells (27). In recent years, immune cell infiltration in solid tumors is a pivotal factor in the TME-related carcinogenesis mechanisms. Among the numerous infiltrated immune cells, polarized macrophages including M1 and M2 subtypeswere reported to play critical roles in TME (28). However, the immune infiltration pattern in most malignancies cannot be portrayed by a single type of cells. Other immune cells such as CD4+ T cells and Tregs should also be considered (29). Thus, building a gene signature that reflects the overall situation of immune cell infiltration is indispensable for evaluating immune-related therapies. Autophagy is proven to be a vital cellular process in immune cell regulation (30). Accordingly, the determination of autophagy pattern in primary tumors is promising for assessing immune cell infiltration in LUAD TME.

Previous studies constructed the autophagy-related signature to predict the prognosis of LUAD patients, but they only built the signature in TCGA dataset (31, 32) and verified in a few GEO datasets. A few of them focused on the autophagy-related long non-coding RNAs (lncRNAs) (33, 34). In Jie Zhu's study, the

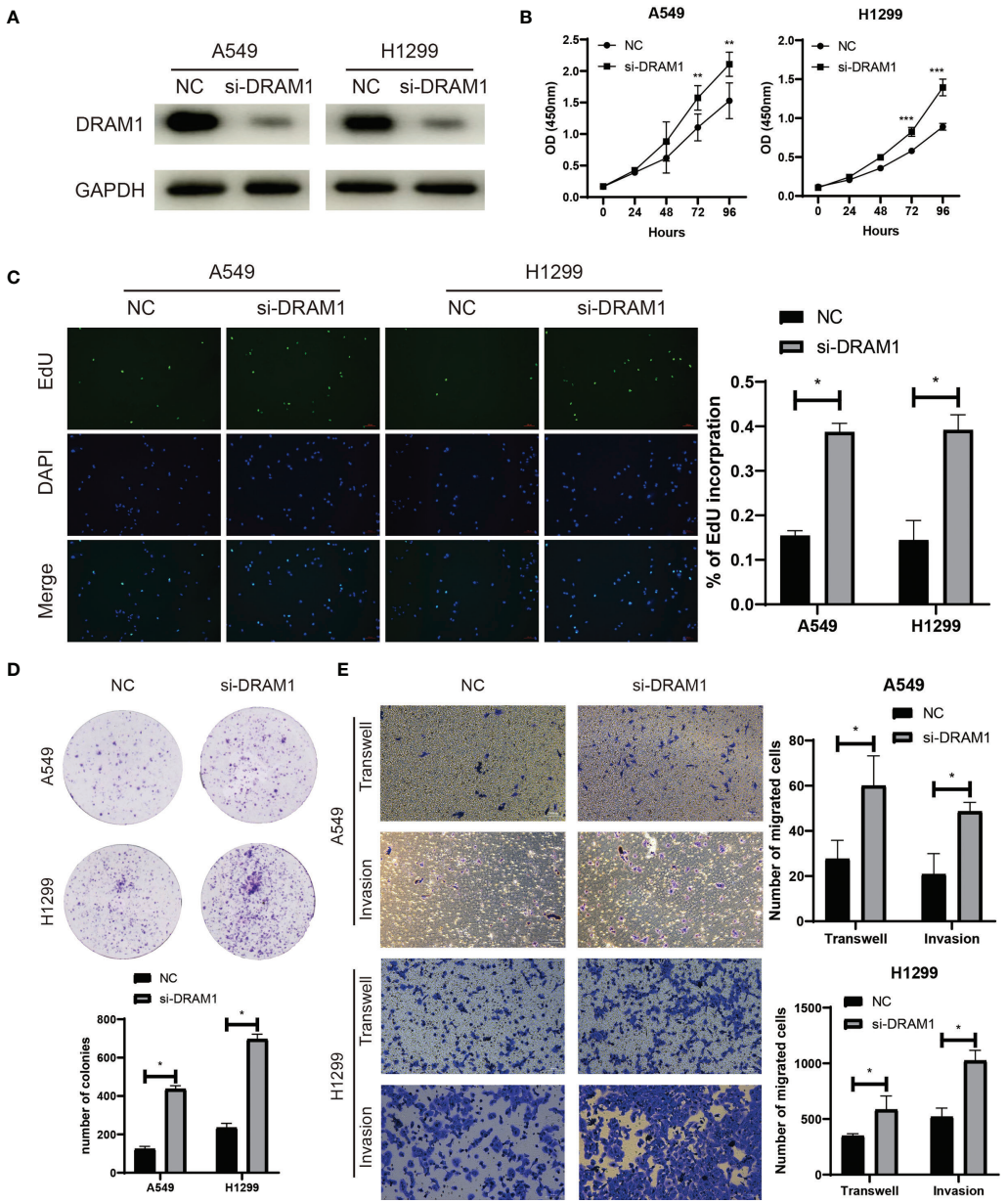

FIGURE 9 | DRAM1 suppressed the proliferation and migration capacity of LUAD cells. The siRNA of DRAM1 significantly inhibited the expression of DRAM1 in LUAD cells **(A)**. The results of CCK-8 assays **(B)**, EdU assays **(C)**, and colony formation assays **(D)** revealed that the inhibiton of DRAM1 expression remarkablely promoted the proliferation and the DNA duplication of LUAD cells. The results of Transwell assays and Invasion assays showed that the impairment of DRAM1 expression enhanced the migration and invasion capacity of LUAD cells **(E)**. *P<0.05, **P<0.01, ***P<0.001.

authors used one GEO dataset to validate the prognosis predictive value of their signature (35). Therefore, the autophagy signatures constructed by these studies need more patient samples to verify their predictive value. In our study, we used TCGA dataset and 9 GEO datasets to construct the autophagy ATscore and validate its prognostic value. More than that, the predictive value of ATscore was validated in our independent LUAD cohort, and proven to be more efficient than other preported signatures (23, 24). Thus, the reliability and repeatability of our signature are more stable compared with other signatures constructed by previous studies. Moreover, the correlation between autophagy-based signatures and the immune checkpoint therapy efficacy was barely characterized. Herein, we used single-cell sequencing data analysis to explore the potential correlation between ATscores and the immune cell patterns, and immune-related pathway differences between various levels of ATscore were also identified. To further determine predictive value of ATscore in immune checkpoint immunotherapy, well-known algorithms such as TIDE, GEP, and

CYT were used, and our results revealed remarkable correlations between ATscores and immunotherapy responses. Moreover, we used IMvigor210 dataset to directly confirm the PD-1 therapy response differences between patients with various ATscore levels, and the ATscores showed a noticeable negative correlation with the response of PD-1 therapy.

The biological role of three genes which were used in the ATscore calculation were well characterized in previous studies. CCR2 is a G protein-coupled receptor that binds the chemokine MCP-1 (CCL2) to recruit myeloid cells into the peripheral blood. Numerous studies have demonstrated that CCR2 participates in the development, especially the infiltration of the immune cells in lung cancer. It was demonstrated that CCR2 and CXCR1 signaling played a critical role in the cross-talk between tumor-associated macrophage and lung cancer cells (36). Recently, more studies revealed that CCR2 is involved in the ERα (Estrogen receptor α)-induced lung cancer cell invasion by macrophage infiltration mechanism and might be an essential component of cancer immunotherapy (37, 38). ITGB1 and DRAM1 were also abnormally expressed in many types of cancer including lung cancer (39–42). ITGB1 was a well-known oncogene and was found to have a critical role in the development of NSCLC. The expression of ITGB1 could be promoted by a long non-coding RNA ITGB1-DT, which was located in the opposite direction from the coding ITGB1 sequence (43). However, the biological functions of DRAM1 remained controversial. DRAM1 was found to be a p53 target gene and played a vital role in autophagy and apoptosis (44). Evidence revealed that DRAM1 could be a target of FTSJ1 and facilitate lung cancer progression (45). Interestingly, a few months later, another study showed that DRAM1 suppresses the development of lung cancer by promoting autophagy-related EGFR degradation (46). Herein, our *in vitro* experimental results showed that DRAM1 suppressed the proliferation and migration of LUAD cells. According to these data, the biological functions of component genes of ATscore were validated. Given the biological functions of these genes in lung cancer, they were also used to construct other tumor microenvironment-associated signatures (31, 32, 47, 48). These studies suggested the vital roles of these genes in developing cancers, and the specific biological functions of these genes should be identified in the future.

Taken together, we constructed a novel autophagy-based signature termed ATscore to predict the prognosis and anti-PD-1 immunotherapy efficacy in LUAD. Our study helps to elucidate the mechanism of LUAD progression and suggests a promising prognostic and therapeutic predictive model for LUAD patients.

DATA AVAILABILITY STATEMENT

The datasets presented in this study can be found in online repositories. The names of the repository/repositories and accession number(s) can be found in the article/**Supplementary Material**.

ETHICS STATEMENT

The studies involving human participants were reviewed and approved by the ethics committee of Xiangya Hospital, Central South University. The patients/participants provided their written informed consent to participate in this study.

AUTHOR CONTRIBUTIONS

Experimental performance and formal analysis, ZD, XW, NZ, HZ, ZW, XZ, XSL; funding acquisition, RC, YZ, XZL; project administration, QC; writing – original draft, XZL; writing – review & editing, QC, RC, PL, JZ, ZL. All authors contributed to the article and approved the submitted version.

FUNDING

This work was supported by grants from Hunan Science and Technology Innovation Talent Program-Excellent Postdoctoral Innovation Talent Project (2020RC2010, 2021RC2029), China Postdoctoral Science Foundation Funded Project (2021M693558), Outstanding Youth Fund of Natural Science Foundation of Hunan Province (2021JJ20092), and Innovation-Driven Project of Central South University (2020CX043), and Hunan Provincial Natural Science Foundation Youth Project (2019JJ50941).

ACKNOWLEDGMENTS

We acknowledge TCGA and GEO database for providing their platforms and contributors for uploading their meaningful datasets.

SUPPLEMENTARY MATERIAL

The Supplementary Material for this article can be found online at: https://www.frontiersin.org/articles/10.3389/fimmu.2022.749241/full#supplementary-material

REFERENCES

1. Siegel RL, Miller KD, Jemal A. Cancer Statistics, 2020. *CA Cancer J Clin* (2020) 70(1):7–30. doi: 10.3322/caac.21590
2. Zhang S, Sun K, Zheng R, Zeng H, Wang S, Chen R, et al. Cancer Incidence and Mortality in China, 2015. *J Natl Cancer Center* (2021) 1(1):2-11. doi: 10.1016/j.jncc.2020.12.001
3. Hirsch FR, Scagliotti GV, Mulshine JL, Kwon R, Curran WJ Jr, Wu YL, et al. Lung Cancer: Current Therapies and New Targeted Treatments. *Lancet* (2017) 389(10066):299–311. doi: 10.1016/S0140-6736(16)30958-8
4. Steven A, Fisher SA, Robinson BW. Immunotherapy for Lung Cancer. *Respirology* (2016) 21(5):821–33. doi: 10.1111/resp.12789
5. Zhang H, Dai Z, Wu W, Wang Z, Zhang N, Zhang L, et al. Regulatory Mechanisms of Immune Checkpoints PD-L1 and CTLA-4 in Cancer. *J Exp Clin Cancer Res* (2021) 40(1):184. doi: 10.1186/s13046-021-01987-7
6. Glick D, Barth S, Macleod KF. Autophagy: Cellular and Molecular Mechanisms. *J Pathol* (2010) 221(1):3–12. doi: 10.1002/path.2697
7. Li X, He S, Ma B. Autophagy and Autophagy-Related Proteins in Cancer. *Mol Cancer* (2020) 19(1):12. doi: 10.1186/s12943-020-1138-4

8. de Souza ASC, Goncalves LB, Lepique AP, de Araujo-Souza PS. The Role of Autophagy in Tumor Immunology-Complex Mechanisms That May Be Explored Therapeutically. *Front Oncol* (2020) 10:603661. doi: 10.3389/fonc.2020.603661
9. Ireland JM, Unanue ER. Autophagy in Antigen-Presenting Cells Results in Presentation of Citrullinated Peptides to CD4 T Cells. *J Exp Med* (2011) 208 (13):2625–32. doi: 10.1084/jem.20110640
10. Li Y, Hahn T, Garrison K, Cui ZH, Thorburn A, Thorburn J, et al. The Vitamin E Analogue Alpha-TEA Stimulates Tumor Autophagy and Enhances Antigen Cross-Presentation. *Cancer Res* (2012) 72(14):3535–45. doi: 10.1158/0008-5472.CAN-11-3103
11. Yamamoto K, Venida A, Yano J, Biancur DE, Kakiuchi M, Gupta S, et al. Autophagy Promotes Immune Evasion of Pancreatic Cancer by Degrading MHC-I. *Nature*. (2020) 581(7806):100–5. doi: 10.1038/s41586-020-2229-5
12. Rao S, Tortola L, Perlot T, Wirnsberger G, Novatchkova M, Nitsch R, et al. A Dual Role for Autophagy in a Murine Model of Lung Cancer. *Nat Commun* (2014) 5:3056. doi: 10.1038/ncomms4056
13. Robainas M, Otano R, Bueno S, Ait-Oudhia S. Understanding the Role of PD-L1/PD1 Pathway Blockade and Autophagy in Cancer Therapy. *Onco Targets Ther* (2017) 10:1803–7. doi: 10.2147/OTT.S132508
14. Wu XN, Su D, Mei YD, Xu MQ, Zhang H, Wang ZY, et al. Identified Lung Adenocarcinoma Metabolic Phenotypes and Their Association With Tumor Immune Microenvironment. *Cancer Immunol Immunother* (2021) 70 (10):2835–50. doi: 10.1007/s00262-021-02896-6
15. Aran D, Hu Z, Butte AJ. Xcell: Digitally Portraying the Tissue Cellular Heterogeneity Landscape. *Genome Biol* (2017) 18(1):220. doi: 10.1186/s13059-017-1349-1
16. Maynard A, McCoach CE, Rotow JK, Harris L, Haderk F, Kerr DL, et al. Therapy-Induced Evolution of Human Lung Cancer Revealed by Single-Cell RNA Sequencing. *Cell* (2020) 182(5):1232–51.e22. doi: 10.1016/j.cell.2020.07.017
17. Patel AP, Tirosh I, Trombetta JJ, Shalek AK, Gillespie SM, Wakimoto H, et al. Single-Cell RNA-Seq Highlights Intratumoral Heterogeneity in Primary Glioblastoma. *Science* (2014) 344(6190):1396–401. doi: 10.1126/science.1254257
18. Puram SV, Tirosh I, Parikh AS, Patel AP, Yizhak K, Gillespie S, et al. Single-Cell Transcriptomic Analysis of Primary and Metastatic Tumor Ecosystems in Head and Neck Cancer. *Cell* (2017) 171(7):1611–24.e24. doi: 10.1016/j.cell.2017.10.044
19. Hanzelmann S, Castelo R, Guinney J. GSVA: Gene Set Variation Analysis for Microarray and RNA-Seq Data. *BMC Bioinf* (2013) 14:7. doi: 10.1186/1471-2105-14-7
20. Jin S, Guerrero-Juarez CF, Zhang L, Chang I, Ramos R, Kuan CH, et al. Inference and Analysis of Cell-Cell Communication Using CellChat. *Nat Commun* (2021) 12(1):1088. doi: 10.1038/s41467-021-21246-9
21. Cristescu R, Mogg R, Ayers M, Albright A, Murphy E, Yearley J, et al. Pan-Tumor Genomic Biomarkers for PD-1 Checkpoint Blockade-Based Immunotherapy. *Science* (2018) 362(6411). doi: 10.1126/science.aar3593
22. Benjamini Y, Hochberg Y. Controlling the False Discovery Rate: A Practical and Powerful Approach to Multiple Testing. *J R Stat Soc Ser B (Methodol)* (1995) 57(1):289–300. doi: 10.1111/j.2517-6161.1995.tb02031.x
23. Al-Dherasi A, Huang QT, Liao Y, Al-Mosaib S, Hua R, Wang Y, et al. A Seven-Gene Prognostic Signature Predicts Overall Survival of Patients With Lung Adenocarcinoma (LUAD). *Cancer Cell Int* (2021) 21(1):294. doi: 10.1186/s12935-021-01975-z
24. Xie H, Xie C. A Six-Gene Signature Predicts Survival of Adenocarcinoma Type of Non-Small-Cell Lung Cancer Patients: A Comprehensive Study Based on Integrated Analysis and Weighted Gene Coexpression Network. *BioMed Res Int* (2019) 2019:4250613. doi: 10.1155/2019/4250613
25. Cheng Q, Huang C, Cao H, Lin J, Gong X, Li J, et al. A Novel Prognostic Signature of Transcription Factors for the Prediction in Patients With GBM. *Front Genet* (2019) 10:906. doi: 10.3389/fgene.2019.00906
26. Peng Z, Chen Y, Cao H, Zou H, Wan X, Zeng W, et al. Protein Disulfide Isomerases Are Promising Targets for Predicting the Survival and Tumor Progression in Glioma Patients. *Aging (Albany NY)* (2020) 12(3):2347-72. doi: 10.2139/ssrn.3449346
27. Wood SL, Pernemalm M, Crosbie PA, Whetton AD. The Role of the Tumor-Microenvironment in Lung Cancer-Metastasis and its Relationship to Potential Therapeutic Targets. *Cancer Treat Rev* (2014) 40(4):558–66. doi: 10.1016/j.ctrv.2013.10.001
28. Najafi M, Hashemi Goradel N, Farhood B, Salehi E, Nashtaei MS, Khanlarkhani N, et al. Macrophage Polarity in Cancer: A Review. *J Cell Biochem* (2019) 120(3):2756–65. doi: 10.1002/jcb.27646
29. Sasidharan Nair V, Elkord E. Immune Checkpoint Inhibitors in Cancer Therapy: A Focus on T-Regulatory Cells. *Immunol Cell Biol* (2018) 96 (1):21–33. doi: 10.1111/imcb.1003
30. Mgrditchian T, Arakelian T, Paggetti J, Noman MZ, Viry E, Moussay E, et al. Targeting Autophagy Inhibits Melanoma Growth by Enhancing NK Cells Infiltration in a CCL5-Dependent Manner. *Proc Natl Acad Sci* (2017) 114(44): E9271–E9. doi: 10.1073/pnas.1703921114
31. Liu Y, Wu L, Ao H, Zhao M, Leng X, Liu M, et al. Prognostic Implications of Autophagy-Associated Gene Signatures in Non-Small Cell Lung Cancer. *Aging (Albany NY)* (2019) 11(23):11440–62. doi: 10.18632/aging.102544
32. Zhang F, Xie S, Zhang Z, Zhao H, Zhao Z, Sun H, et al. A Novel Risk Model Based on Autophagy Pathway Related Genes for Survival Prediction in Lung Adenocarcinoma. *Med Sci Monit* (2020) 26:e924710. doi: 10.12659/MSM.924710
33. Zhou M, Shao W, Dai H, Zhu X. A Robust Signature Based on Autophagy-Associated LncRNAs for Predicting Prognosis in Lung Adenocarcinoma. *BioMed Res Int* (2020) 2020:3858373. doi: 10.1155/2020/3858373
34. Jiang A, Liu N, Bai S, Wang J, Gao H, Zheng X, et al. Identification and Validation of an Autophagy-Related Long Non-Coding RNA Signature as a Prognostic Biomarker for Patients With Lung Adenocarcinoma. *J Thorac Dis* (2021) 13(2):720–34. doi: 10.21037/jtd-20-2803
35. Zhu J, Wang M, Hu D. Development of an Autophagy-Related Gene Prognostic Signature in Lung Adenocarcinoma and Lung Squamous Cell Carcinoma. *PeerJ*. (2020) 8:e8288. doi: 10.7717/peerj.8288
36. Schmall A, Al-Tamari HM, Herold S, Kampschulte M, Weigert A, Wietelmann A, et al. Macrophage and Cancer Cell Cross-Talk *via* CCR2 and CX3CR1 Is a Fundamental Mechanism Driving Lung Cancer. *Am J Respir Crit Care Med* (2015) 191(4):437–47. doi: 10.1164/rccm.201406-1137OC
37. He M, Yu W, Chang C, Miyamoto H, Liu X, Jiang K, et al. Estrogen Receptor Alpha Promotes Lung Cancer Cell Invasion *via* Increase of and Cross-Talk With Infiltrated Macrophages Through the CCL2/CCR2/MMP9 and CXCL12/CXCR4 Signaling Pathways. *Mol Oncol* (2020) 14(8):1779–99. doi: 10.1002/1878-0261.12701
38. Mittal P, Wang L, Akimova T, Leach CA, Clemente JC, Sender MR, et al. The CCR2/MCP-1 Chemokine Pathway and Lung Adenocarcinoma. *Cancers (Basel)* (2020) 12(12). doi: 10.3390/cancers12123723
39. Yang X, Wang S, Yu W, Zheng Y, Wu Y. Inhibition of ITGB1 Enhance the Anti-Tumor Effect of Cetuximab in Colorectal Cancer Cell. *Med (Baltimore)* (2020) 99 (27):e20944. doi: 10.1097/MD.0000000000020944
40. Hu C, Ni Z, Li BS, Yong X, Yang X, Zhang JW, et al. hTERT Promotes the Invasion of Gastric Cancer Cells by Enhancing FOXO3a Ubiquitination and Subsequent ITGB1 Upregulation. *Gut* (2017) 66(1):31–42. doi: 10.1136/gutjnl-2015-309322
41. Zhang C, Wu S, Song R, Liu C. Long Noncoding RNA NR2F1-AS1 Promotes the Malignancy of Non-Small Cell Lung Cancer *via* Sponging microRNA-493-5p and Thereby Increasing ITGB1 Expression. *Aging (Albany NY)* (2020) 13(5):7660–75. doi: 10.18632/aging.103564
42. Ryan KM. P53 and Autophagy in Cancer: Guardian of the Genome Meets Guardian of the Proteome. *Eur J Cancer* (2011) 47(1):44–50. doi: 10.1016/j.ejca.2010.10.020
43. Chang R, Xiao X, Fu Y, Zhang C, Zhu X, Gao Y. ITGB1-DT Facilitates Lung Adenocarcinoma Progression *via* Forming a Positive Feedback Loop With ITGB1/Wnt/beta-Catenin/MYC. *Front Cell Dev Biol* (2021) 9:631259. doi: 10.3389/fcell.2021.631259
44. Crighton D, Wilkinson S, O'Prey J, Syed N, Smith P, Harrison PR, et al. DRAM, a P53-Induced Modulator of Autophagy, is Critical for Apoptosis. *Cell* (2006) 126(1):121–34. doi: 10.1016/j.cell.2006.05.034
45. He Q, Yang L, Gao K, Ding P, Chen Q, Xiong J, et al. FTSJ1 Regulates tRNA 2'-O-Methyladenosine Modification and Suppresses the Malignancy of NSCLC *via* Inhibiting DRAM1 Expression. *Cell Death Dis* (2020) 11(5):348. doi: 10.1038/s41419-020-2525-x

46. Geng J, Zhang R, Yuan X, Xu H, Zhu Z, Wang X, et al. DRAM1 Plays a Tumor Suppressor Role in NSCLC Cells by Promoting Lysosomal Degradation of EGFR. *Cell Death Dis* (2020) 11(9):768. doi: 10.1038/s41419-020-02979-9
47. Lu Y, Lemon W, Liu PY, Yi Y, Morrison C, Yang P, et al. A Gene Expression Signature Predicts Survival of Patients With Stage I Non-Small Cell Lung Cancer. *PloS Med* (2006) 3(12):e467. doi: 10.1371/journal.pmed.0030467
48. Fan T, Zhu M, Wang L, Liu Y, Tian H, Zheng Y, et al. Immune Profile of the Tumor Microenvironment and the Identification of a Four-Gene Signature for Lung Adenocarcinoma. *Aging (Albany NY)* (2020) 13(2):2397–417. doi: 10.18632/aging.202269

Conflict of Interest: The authors declare that the research was conducted in the absence of any commercial or financial relationships that could be construed as a potential conflict of interest.

Publisher's Note: All claims expressed in this article are solely those of the authors and do not necessarily represent those of their affiliated organizations, or those of the publisher, the editors and the reviewers. Any product that may be evaluated in this article, or claim that may be made by its manufacturer, is not guaranteed or endorsed by the publisher.

Copyright © 2022 Li, Dai, Wu, Zhang, Zhang, Wang, Zhang, Liang, Luo, Zhang, Liu, Zhou, Cheng and Chang. This is an open-access article distributed under the terms of the Creative Commons Attribution License (CC BY). The use, distribution or reproduction in other forums is permitted, provided the original author(s) and the copyright owner(s) are credited and that the original publication in this journal is cited, in accordance with accepted academic practice. No use, distribution or reproduction is permitted which does not comply with these terms.

frontiers | Frontiers in Immunology

ORIGINAL RESEARCH
published: 28 April 2022
doi: 10.3389/fimmu.2022.802665

Identification of a Novel Immune Landscape Signature for Predicting Prognosis and Response of Colon Cancer to Immunotherapy

Zheng Wang[1†], *Jingru Song*[1,2†], *Nisma Lena Bahaji Azami*[1,2] *and Mingyu Sun*[1,2*]

[1] *Shanghai University of Traditional Chinese Medicine, Shanghai, China,* [2] *Key Laboratory of Liver and Kidney Diseases, Institute of Liver Diseases, Shuguang Hospital Affiliated to Shanghai University of Traditional Chinese Medicine, Shanghai, China*

Purpose: To construct an immune-related gene prognostic index (IRGPI) for colon cancer and elucidate the molecular and immune characteristics as well as the benefit of immune checkpoint inhibitor (ICI) therapy in IRGPI-defined groups of colon cancer.

Experimental Design: Transcriptional and clinical data of colon cancer samples were obtained from The Cancer Genome Atlas (TCGA) (n = 521). Immune-related genes were obtained from ImmPort and InnateDB databases. 21 immune-related hub genes were identified byweighted gene co-expression network analysis (WGCNA). the Cox regression method was used to construct IRGPI and validated with Gene Expression Omnibus (GEO) dataset (n = 584). Finally, the molecular and immune profiles in the groups defined by IRGPI and the benefit of ICI treatment were analyzed.

Results: 8 genes were identified to construct IRGPI. IRGPI-low group had a better overall survival (OS) than IRGPI-high group. And this was well validated in the GEO cohort. Overall results showed that those with low IRGPI scores were enriched in antitumor metabolism, and collated with high infiltration of resting memory CD4 T cells and less aggressive phenotypes, benefiting more from ICI treatment. Conversely, high IRGPI scores were associated with cell adhesion molecules (CAMs) and chemokine signaling pathways, high infiltration of macrophage M1, suppressed immunity, more aggressive colon cancer phenotypes, as well as reduced therapeutic benefit from ICI treatment.

Conclusions: IRGPI is a promising biomarker to differentiate the prognostic and molecular profile of colon cancer, as well as the therapeutic benefits of ICI treatment.

Keywords: colon cancer, immune-related gene prognostic index, weighted gene co-expression network analysis (WGCNA), prognosis, signature

OPEN ACCESS

Edited by:
Udo S. Gaipl,
University Hospital Erlangen, Germany

Reviewed by:
Arantzazu Alfranca,
Hospital de la Princesa, Spain
Kang Xu,
Hubei University of Chinese Medicine, China

****Correspondence:***
Mingyu Sun
mysun248@hotmail.com

[†]These authors have contributed equally to this work

Specialty section:
This article was submitted to Cancer Immunity and Immunotherapy, a section of the journal Frontiers in Immunology

Received: *27 October 2021*
Accepted: *31 March 2022*
Published: *28 April 2022*

Citation:
Wang Z, Song J, Azami NLB and Sun M (2022) Identification of a Novel Immune Landscape Signature for Predicting Prognosis and Response of Colon Cancer to Immunotherapy. Front. Immunol. 13:802665. doi: 10.3389/fimmu.2022.802665

INTRODUCTION

Colon cancer, which is one of the major causes of death worldwide, has become the third most common cancer in men and the second most common cancer in women globally. Approximately 25% of colon cancer patients have been diagnosed with stage IV cancer. Another 25% of the patients with colon cancer are diagnosed in early stages, but their cancer still metasticizes (1). The five-year

survival rate for patients with stage IV tumors is less than 10% (2). It is estimated that by 2030, the incidence of colorectal cancer (CRC) will increase by 60%, with more than 2.2 million new cases worldwide, resulting in more than 1.1 million deaths (1). Over the past decades, immunotherapy drugs have been extensively used in the treatment of cancer and shown clinical efficacy. Immune checkpoint inhibitors (ICIs) targeting programmed cell death-1 (PD-1) or cytotoxic T lymphocyte-associated protein-4 (CTLA-4) have achieved tumor regression in several cancers, such as melanoma, lung cancers, and Hodgkin lymphoma (3, 4). Furthermore, PD-1 and programmed cell death-ligand 1 (PD-L1) blockers appear to be a promising option for patients with colon cancer (5). A major limitation, however, is the low response rate of patients with colon cancer to ICI therapy. The tumor immune microenvironment (TME) has gained increasing attention as an indispensable component of immunotherapy (6). In fact, TME may be used as a major prognostic indicator, which in turn can improve precision targeted therapy (7). Hence, Identifying potential prognostic markers associated with the therapeutic benefit of immunotherapy could allow patients with colon cancer to receive more individualized therapies.

In this study, we sought to develop an immune-related gene prognostic index (IRGPI) that is capable of predicting not only the prognosis of conventional therapy but also immunotherapy. We then assessed the molecular and immunological characteristics of IRGPI. Its reliability was validated with multiple datasets, and IRGPI was a promising prognostic biomarker for patients receiving conventional treatment and immunotherapy.

MATERIAL AND METHODS

The flow chart of the whole study is presented in **Figure 1**.

Collection of Sample Information

RNA-seq data of 521 colon cancer samples, including 480 cancer samples and 41 paracancerous tissue samples, and their clinicopathological information were downloaded from the TCGA database (https://portal.gdc.cancer.gov/projects/TCGA). RNA-seq data of 584 colon cancer samples (GSE39582) and the survival information were downloaded from the GEO database (https://www.ncbi.nlm.nih.gov/geo/) (8). The entire TCGA cohort and GSE cohort were used as the testing set and validation set, respectively. The lists of immune-related genes were downloaded from the ImmPort (https://www.immport.org/shared/home) and InnateDB (https://www.innatedbdb.com/) databases.

Differentially Expressed Immune-Related Genes (DEIRGs)

By analyzing RNA-seq data from colon cancer samples obtained through TCGA, a list of differentially expressed genes (DEGs) (false discovery rate (FDR) < 0.05, $|\log_2 FC| > 1$) for tumor and normal tissues was determined using the limma package (9). The DGEs were compared and crossed with immune-related genes (IRGs) to obtain DEIRGs. The heatmap of DEIRGs was generated using pheatmap package in R. After extracting the list of immune-related genes from ImmPort and InnateDB, DEIRGs were selected and analyzed by Gene Ontology (GO) and Kyoto Encyclopedia of Genes and Genomes (KEGG) analysis using clusterProfiler package of R (10).

We then constructed a co-expression network using the WGCNA package (11) to identify hub genes, as WGCNA analysis is biologically more significant compared with traditional methods (12). All crossover genes were reflected in the co-expression network. Scale-independent and average connectivity analyses were performed on modules with different power values to calculate the software threshold parameters. In this study, we set the scale irrelevance value to 0.9 to identify the hub genes. The adjacency matrix was transformed into a topological overlap matrix (TOM) describing the similarity of gene expression. 1-TOM represented the heterogeneity between genes. Based on the TOM-based similarity, a dynamic tree-cutting algorithm was used to group genes into different modules (clusters). Here, we set the cut height to 0.3 and the minimum module size to 30. The best cut-off value for overall survival (OS) was calculated for each hub gene using survminer and survival R packages (13). 21 immune-related hub genes significantly associated with survival were screened for further analysis ($P < 0.05$). To reveal relevant genetic alterations, somatic mutations of the 21 immune-related hub genes were analyzedusing maftools package in R (14).

Construction and Validation of the IRGPI

Among the 21 immune-related pivotal genes, those with significant effects on OS were identified. IRGPI was then constructed by multivariate Cox regression analysis. The risk score was calculated as below:

$$Risk \quad Score = \sum_{i=1}^{j} coeffient_i \times expression_i$$

IRGPI was calculated by multiplying the expression data of certain genes for each sample by their weights in the Cox model and then adding them together. The prognostic ability of IRGPI was assessed by Kaplan-Meier analysis in the TCGA and GEO cohorts, respectively. To further verify the prognostic value of IRGPI, univariate and multivariate Cox regression analyses were performed.

Molecular and Immunological Characterization of Different IRGPI Groups and Comprehensive Analysis of ICI Treatment

First, differential expression analysis of all genes was performed by limma package in R, and samples with high (n = 226) and low (n = 227) IRGPI scores were obtained. Enrichment analysis was then performed by clusterProfiler package in R using KEGG and genomic-based gene set enrichment analysis (GSEA) methods to identify the signaling pathways($P < 0.05$). Finally, gene mutations in the two IRGPI groups were analyzed using maftools package.

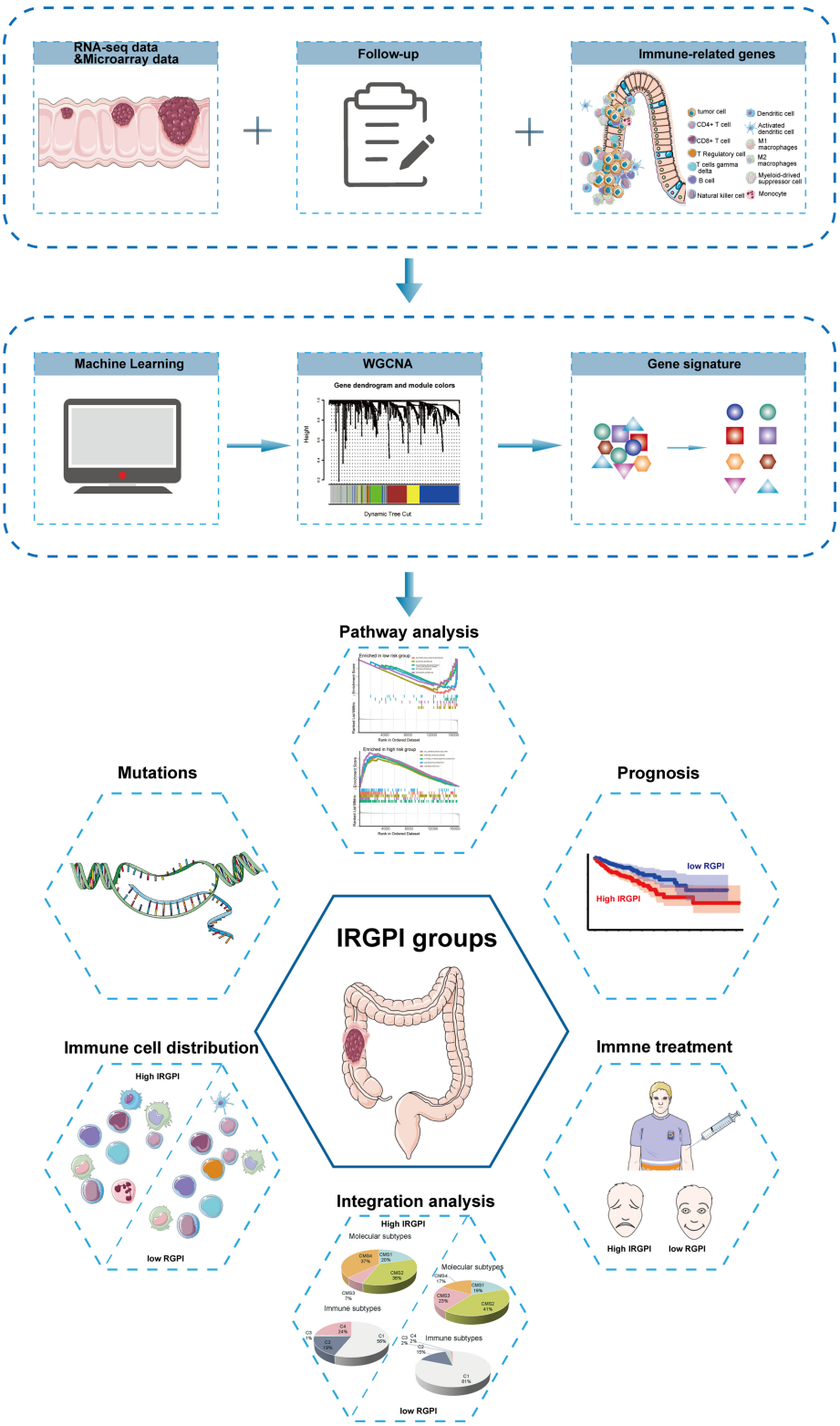

FIGURE 1 | Flow chart of the whole study.

To clarify the immune characteristics of the 480 colon cancer samples, expression data was imported into CIBERSORT (http://cibersort.stanford.edu/) and iterated 1000 times to estimate the relative proportions of 22 immune cell species. We then compared the relative proportions of the 22 immune cell species and clinicopathological factors between the two IRGPI groups, and the results were presented as landscape plots. Moreover, we performed GSEA on certain gene signatures and compared the score between two IRGPI groups in order to understand the immune and molecular functions (15–18).

Widely used biomarkers and other published immune-related signatures for cancer immunotherapy were evaluated to compare them with our IRGPI, in order to determine the prognostic value of IRGPI for patients with colon cancer. We compared the prognostic value among IRGPI, TIDE, and T cell-inflamed signature (TIS) using timeROC package (19) in R. The TIDE score, which can be calculated online (http://tide.dfci.harvard.edu/), predicted the prognosis of patients with tumors treated with first-line anti-PD1 or anti-CTLA4 therapy more accurately than other biomarkers such as PD-L1 levels and mutational load (20) The TIS score, which can be calculated as the mean of the $\log_2$-scale normalized expression of 18 signature genes (21), can enrich the clinical benefit of immune checkpoint blockade (22). We also selected immune prognostic models constructed in previous studies such as "Zhang signature" (23) and "Deng signature" (24). In addition, ROC curve analysis was performed to obtain the area under the curve (AUC).

Statistical Analysis

An independent *t*-test was performed for continuous variables between the two groups. Categorical data were tested using the chi-square test. TIDE score between groups was compared by the Wilcoxon test. Univariate survival analysis was performed by Kaplan-Meier survival analysis with the log-rank test. Multivariate survival analysis was performed using the Cox regression model. A two-sided $P < 0.05$ was considered significant.

RESULTS

Immune-Related Hub Genes

In differential expression analysis (480 tumors vs. 41 normal tissue samples), a total of 7762 DEGs were screened (**Figure 2A**). By crossing these genes with the list of immune-related genes, 651 differentially expressed immune-related genes were obtained. Compared with genes in normal tissue samples, 257 genes were upregulated and 394 downregulated in the tumor samples (**Figure 2B**).

The top 10 GO terms and 20 KEGG pathways were shown in **Figures 2C, D**. Functional enrichment analysis revealed that the most relevant signaling pathway for DEIRGs was "cytokine-cytokine receptor interaction". The most enriched term in biological process (BP), molecular function (MF), and cellular component (CC) was "humoral immune response", "receptor-ligand activity", and "immunoglobulin complex", respectively.

To extract immune-related hub genes, we performed WGCNA analysis on candidate genes. According to the scale-free network, the optimal soft-thresholding power was 5 (**Figures 3A, B**). A dendrogram of identified co-expressed genes in modules by using 651 DEGs (**Figure 3C**). Five modules were subsequently identified in terms of the average linkage hierarchical clustering and the optimal soft-thresholding power (**Figure 3D**). According to the Pearson correlation coefficient between a module and sample feature for each module, the yellow, brown, and blue modules closely correlated with colon cancer tumors. The genes in the yellow module were selected for further analysis. The network diagram showed the significant genes, and the two nodes were connected with lines to represent co-expression relationships. The genetic correlation in the yellow module was shown in **Figure 3E**. Two main clusters of genes exhibited good consistency in this module.

Survival Outcomes in Different IRGPI Groups

Kaplan-Meier survival analysis showed that the expression of 21 immune-related hub genes was strongly linked to OS in patients with colon cancer, as shown in **Figure 4A**. To select independent prognostic genes, multivariate Cox regression analysis for OS was performed among the 21 immune-related hub genes. As shown in **Figures 4A, B**, only eight genes (UCN, TRIM, RBCK1, TPM2, CD36, NMB, PPARGC1A, and LGALS4) significantly affected the OS in patients with colon cancer ($P < 0.05$). Following these results,we constructed a prognostic index for all cancer samples, with the following formula:

$$IRGPI = UCN * 0.775 + TRIM58 * 0.736 + RBCK1 * 0.304 + \text{TPM2} * 0.241 + \text{CD36} * 0.319 + \text{NMB} * 0.281 + \text{PPARGC1A} * (-0.359) + \text{LGALS4} * (-0.211)$$

The heatmap of the 8 genes presented well-distinguished clusters between the normal and tumor samples (**Figure 4C**). Age and stage were significantly associated with the prognosis of colon cancer as shown by univariate Cox regression analysis. Multivariate Cox regression analysis revealed that IRGPI was an independent prognostic factor, after being adjusted for other clinicopathologic factors (**Figure 4D**).

Taking the median IRGPI as the cutoff value, IRGPI-low group had a better OS than IRGPI-high group ($P = 0.002$). The role of IRGPI was then validated by the GSE39582 (n = 585) colon cancer dataset. Patients in the IRGPI-low group had a significantly better prognosis than those in the IRGPI-high group, which was consistent with the result of the TCGA dataset ($P = 0.022$; **Figure 4E**).

Molecular Characteristics of Different IRGPI Groups

GSEA analysis was carried out to explore the gene pathways enriched in different IRGPI groups. IRGPI-high group was enriched in cell adhesion molecules (CAMs) and chemokine signaling pathways, while IRGPI-low group was enriched in

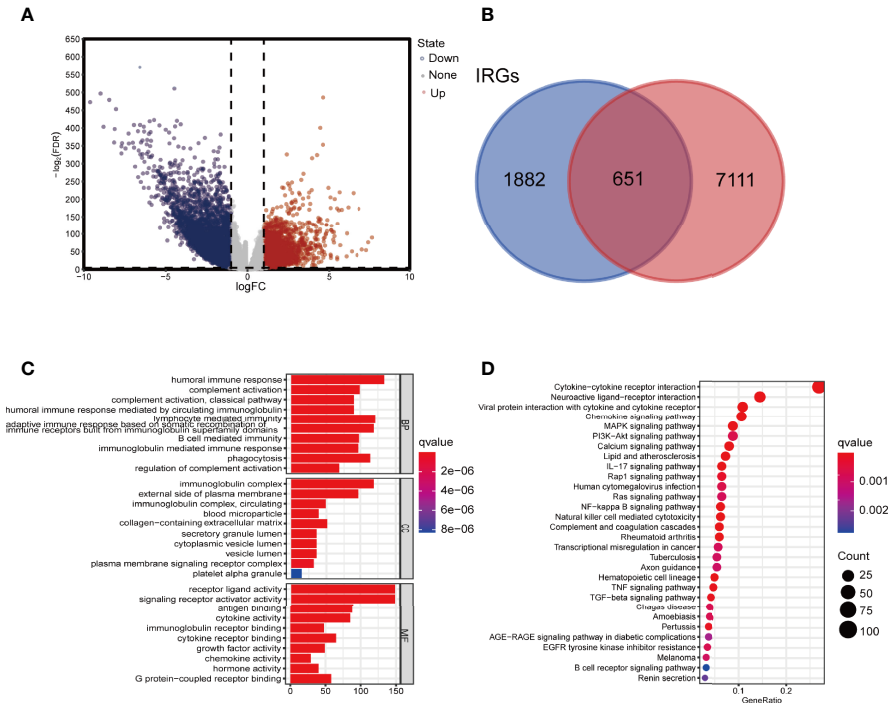

FIGURE 2 | Screening for DEGs and enrichment analysis. **(A)** Volcano map of DEIRGs. **(B)** Venn diagram showing the intersection of DEGs and IRGs. **(C)** GO enrichment analysis of DEIRGs for BP, CC, and MF, respectively. **(D)** KEGG enrichment analysis of DEIRGs. DEGs, differentially expressed genes; DEIRGs, differentially expressed immune-related genes; IRGs, immune-related genes; GO, Gene Ontology; BP, biological process; CC, cellular component; MF, molecular function; KEGG, Kyoto Encyclopedia of Genes and Genomes.

antitumor metabolisms, such as ascorbate and aldarate metabolism and butanoate metabolism ($P < 0.05$; **Figure 5A**).

Subsequently, we analyzed gene mutations to further understand the immunological nature of the IRGPI subpopulation (**Figure 5B**). To gain further biological insight into the immunological nature of the IRGPI groups. Missense variations were the most frequent mutation type. Most of the 21 immune-associated hub genes had missense mutations and frame shift mutation.In fact, mutations of APC, TTN, TP53, KRAS, and MUC16 were the 5 most prevalent mutations in the IRGPI-low group, whereas mutations of APC, TP53, TTN, KRAS, and SYNE1 were the 5 most prevalent mutations in IRGPI-high group.

Immune Characteristics of Different IRGPI Groups

The composition of immune cells in different IRGPI groups was analyzed using Wilcoxon test. The test compared the fraction of immune cells in different IRGPI groups. Here, we found that resting memory CD4 T cells and gammadelta T cells (γδ T cells) were more abundant in the IRGPI-low group, while neutrophils were more abundant in the IRGPI-high group (**Figure 6A**). The abundance ratios of 22 immune cells were displayed in **Figure 6B**. Consequently, the correlations between the abundance ratios of immune cells were analyzed using Kaplan-Meier survival analysis in overall survival. Seven immune cell types associated with survival were presented in the survival analysis performed on 22 immune cells. The relative proportion of naive B cells, plasma cells, resting memory CD4 T cells, regulatory T cells (Tregs), M1 macrophages, resting dendritic cells and activated mast cells were significantly related to OS ($P < 0.05$). Higher abundance ratios of M1 macrophages, naive B cells, plasma cells, resting memory CD4 T cells, and Tregs were associated with poorer OS, while a higher proportion of activated memory dendritic cells resting and activated mast cells were related to better OS (**Figure 6C**).

We then applied certain gene signatures to define the immune and molecular function between different IRGPI groups (19). We further investigated whether the prognostic value of IRGPI resulted from better immune control or less aggressive cancer growth. We found that patients with a lower score had a better outcome, with more resting memory CD4 T cells and γδ T cells infiltration. Less cytolytic activity, dendritic cells, plasmacytoid dendritic cells and plasmacytoid dendritic cells had a favorable prognosis. Therefore, we proposed that the prognostic value of IRGPI might result from both better immune control and less aggressive cancer growth. Collectively, IRGPI statistically correlated with the infiltration levels of most immune cells, implying that our IRGPI could potentially reflect the state of TME. In a nutshell, IRGPI was statistically associated with the levels of infiltration of immune cells, and immune function,

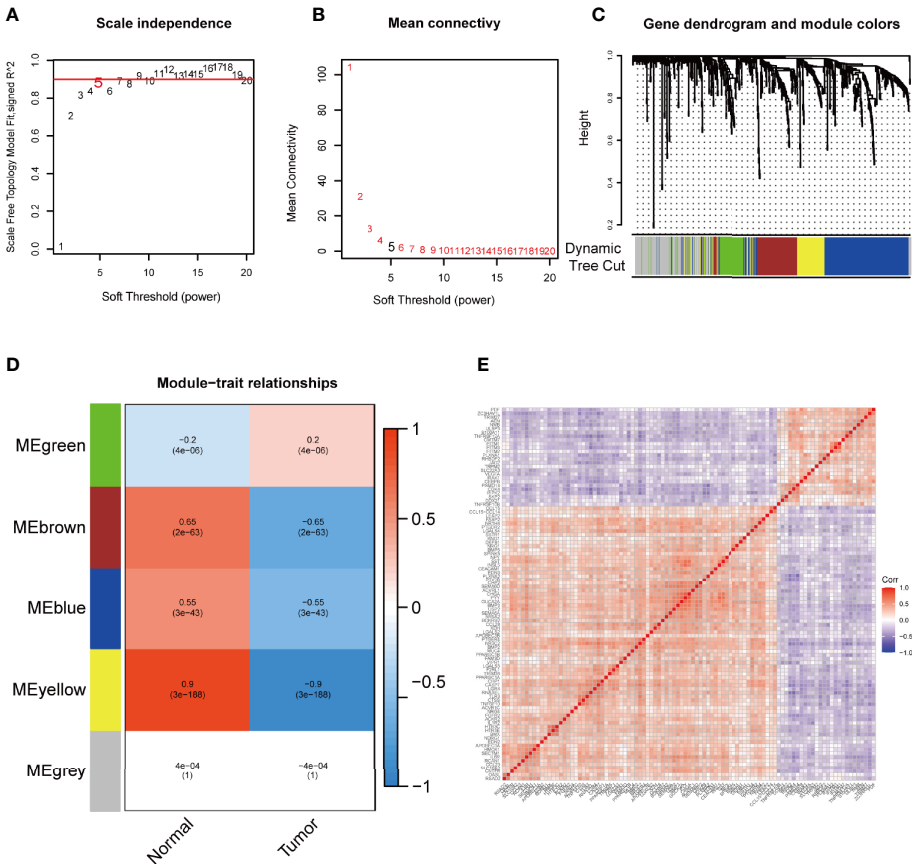

FIGURE 3 | WGCNA to mine differential immune gene modules. Analysis of IRGPI-related gene modules by WGCNA. **(A)** Analysis of the scale-independence of various soft-thresholding powers. **(B)** Mean connectivity analysis of various soft-thresholding powers. **(C)** Identification of co-expression modules. The branches of the tree diagram correspond to the five different gene modules. **(D)** Correlation of gene modules with tumor microenvironment correlation scores. Each cell contains the corresponding correlation coefficient and *P*-value. **(E)** Correlation analysis of each gene in the yellow module. WGCNA, weighted gene co-expression network analysis and IRGPI, immune-related gene prognostic index.

which means that our IRGPI could potentially reflect the status of TME.

Relationship Between IRGPI Groups and Other Immune and Molecular Subtypes

Features related to the immune landscape, including clinicopathological characteristics of different IRGPI groups, could be found in **Figure 7A**. The information about microsatellite instability (MSI) status of patients and chemotherapy were analyzed in relation to IRGPI (**Figure S1**). EGFR and KRAS status were analyzed in relation to IRGPI (**Table S1**). In conclusion, IRGPI was an independent prognostic factor for other clinicopathologic factors. Colon cancer immune subtype classification described the immune landscape according to the tumor and stromal compartments and summarized six immune subtypes: wound healing(C1), IFN-γ dominant(C2), inflammatory(C3), lymphocyte depleted(C4), immunologically quiet(C5) and TGF-β dominant(C6) (25, 26). The proportion of each group was approximately the same, with C2 being more in the high-risk group (**Figure 7B**). A unified transcriptomic classification identified four biologically distinct consensus molecular subtypes (CMSs) (27, 28): CMS1 (MSI immune subtype, 14%), characterized by BRAF mutation enriched, hypermutated and hypermethylated tumors, with a strong immune activation; CMS2(canonical subtype, 37%), commonly CIN tumors with upregulation of WNT and MYC signaling; CMS3 (metabolic subtype, 13%), encompassed epithelial tumors with metabolic deregulation, enriched in KRAS mutations; and CMS4 (mesenchymal subtype, 23%), defined by strong activation of epithelial-emesenchymal transition, angiogenesis, and stemness pathways (28). CMS4 was the subtype with the worst outcome (27).

As shown in **Figure 7B**, the IRGPI-low group included 79% of C1, 15% of C2, 2% of C3, and 4% of C4 samples in our study, whereas the group with high IRGPI score included 73% of C1, 24% of C2, 2% of C3, and 1% of C4 samples (P = 0.033). As shown in **Figure 7C**, the IRGPI-low group comprised 20% of CMS1, 41% of CMS2, 23% of CMS3, and 17% of CMS4 samples, while the IRGPI-high group comprised 20% of CMS1, 36% of CMS2, 7% of CMS3, and 37% of CMS4 samples. There were

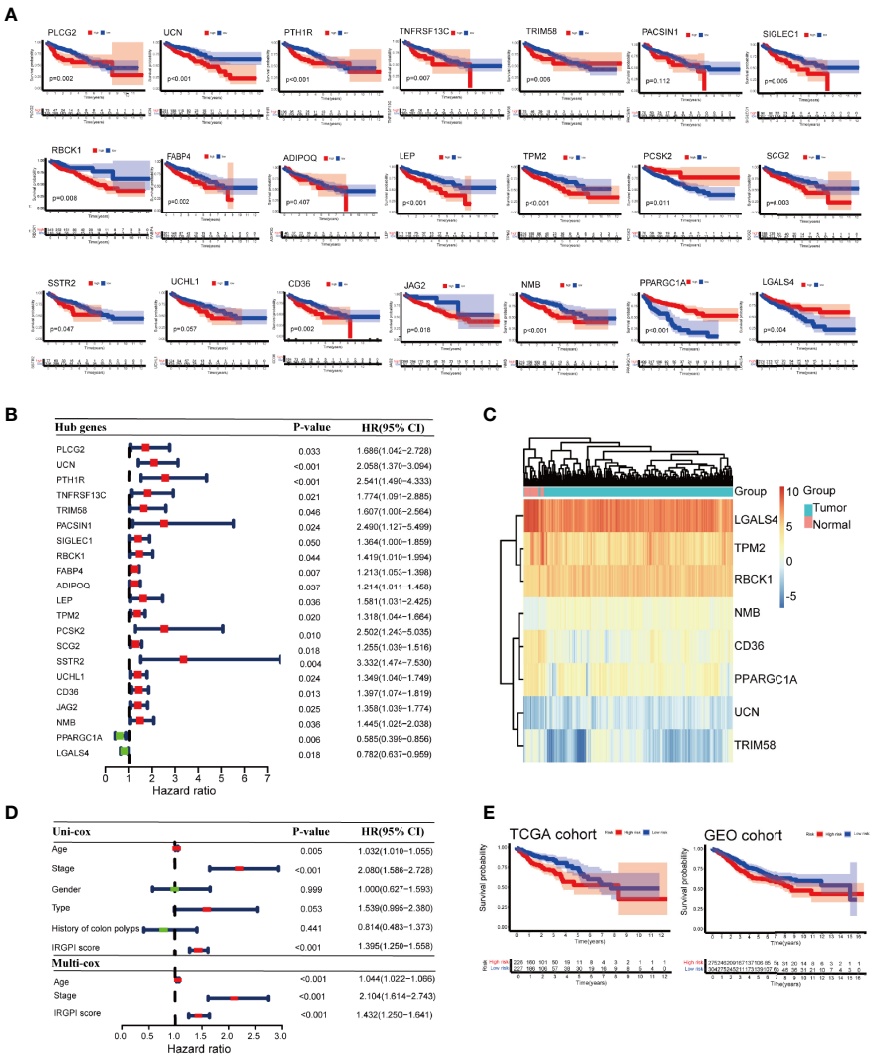

FIGURE 4 | Prognostic analysis of different colon cancer groups. **(A)** Kaplan-Meier survival analysis of the 21 immune-related hub genes. **(B)** Univariate Cox analysis of 21 immune-related hub genes. **(C)** Heat map of 8 genes in IRGPI score. **(D)** Univariate Cox analysis of clinicopathological factors and IRGPI scores, and multivariate Cox analysis of factors significant in univariate Cox analysis ($P < 0.05$). **(E)** Kaplan-Meier survival analysis of IRGPI groups in the TCGA cohort and the GEO cohort. IRGPI, immune-related gene prognostic index; TCGA, The Cancer Genome Atlas; and GEO, Gene Expression Omnibus.

more CMS2 and CMS3 samples in the IRGPI-low group, while more CMS4 subtypes in the IRGPI-high group ($P = 0.001$).

Benefits of ICI Treatment in Different IRGPI Groups

The potential efficacy ICI treatment in different IRGPI groups can be assessed with TIDE algorithm. A higher TIDE score indicated higher potential for immune evasion, meaning that patients were less likely to benefit from ICI treatment (29). In our results, the IRGPI-low group had a lower TIDE score than the IRGPI-high group, implying that IRGPI-low patients could benefit more from ICI therapy than IRGPI-high patients (**Figure 8A**). Furthermore, a higher TIDE score prediction score was associated with a worse outcome. Therefore, the IRGPI-low group with a low TIDE score might had a better outcome than the IRGPI-high group with a high TIDE score. We also found no difference in microsatellite instability (MSI) score between the two groups. The IRGPI-low group had a lower T cell exclusion score and T cell dysfunction compared with the IRGPI-high group.

In addition, the predictive performance of IRGPI was compared with other signatures through ROC curves. Here, the AUC at five-year of IRGPI was 0.722, compared with widely used biomarkers and other published immune-related features for cancer immunotherapy, achieving superior performance. (**Figure 8B**). The AUC was 0.696, 0.690, 0.684, 0.722 and 0.654 for 1-year, 2-year, 3-year, 5-year, and 7-year survival, respectively (**Figure 8C**). Overall, these results indicated that IRGPI was a highly reliable index and superior to other signatures.

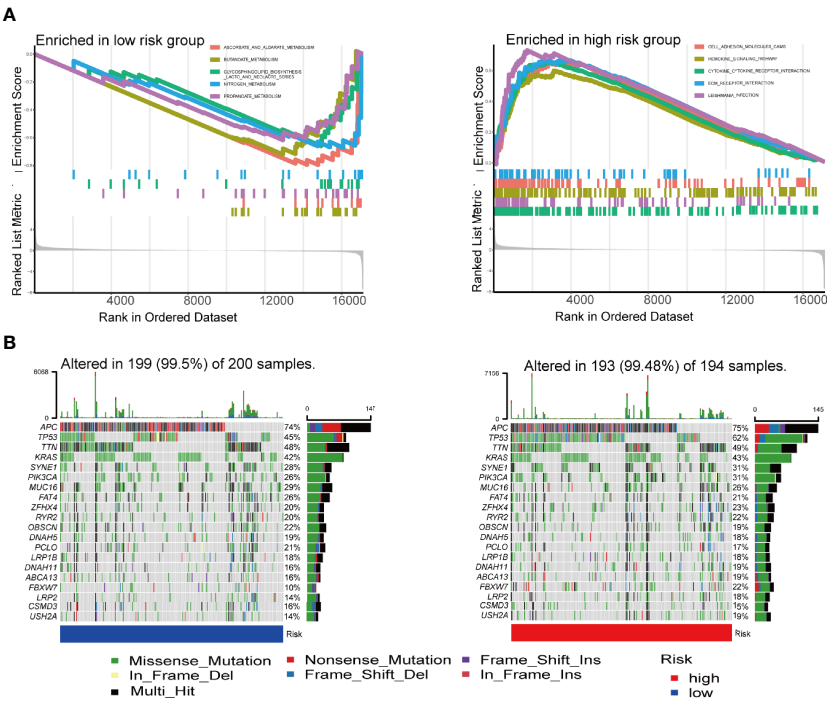

FIGURE 5 | GSEA analysis and mutation analysis of IRGPI groups. **(A)** Set of genes enriched in IRGPI groups ($P < 0.05$). **(B)** Significantly mutated genes in the colon cancer samples of different IRGPI groups. Mutated genes are sorted by mutation rate; the arrangement of samples (columns) emphasizes the mutual exclusivity between mutations. Mutation rates are shown on the right, and the total number of mutations is shown above. Color coding indicates mutation type. GSEA, genomic-based gene set enrichment analysis; IRGPI, immune-related gene prognostic index.

DISCUSSION

ICI therapy is an effective treatment for patients with colon cancer (30). Because the overall response rate to ICI therapy remains very low (31), it is critical to identify patients who can benefit the most from these treatments. Complex cellular and molecular interactions between the tumor and host immune system influence tumor progression and patient survival (32). After years of evaluating different prognostic markers in colon cancer, we still have not found validated biomarkers for predicting response to immunotherapy and OS. This highlights the need to identify prognostic biomarkers for use in immunotherapy in colon cancer.

There is growing evidence that cancer evolution is strongly dependent on the complex TME. The main immune parameters associated with survival are defined as the "immune environment" (32, 33), which is the type, functional localization, density, and location of adaptive immune cells in different tumor areas (32–35). Several soluble factors such as cytokines, chemokines, and cellular metabolites are also included (36). WGCNA can correlate modules with specific clinical features, from which genes performing key functions can be identified. In our study, based on the colon cancer immune gene datasets, we used WGCNA to identify 21 immune-related hub genes affecting patients' OS and constructed IRGPI based on 8 independent OS prognostic factors (UCN, TRIM58, RBCK1, TPM2, CD36, NMB, PPARGC1A, and LGALS4). IRGPI is a valid biomarker for predicting the prognosis of colon cancer. Patients with low IRGPI score had better survival, and patients with high IRGPI score had poorer survival in the TCGA and GEO cohorts.

IRGPI was composed of 8 genes UCN, TRIM58, RBCK1, TPM2, CD36, NMB, PPARGC1A, and LGALS4. Urocortins (UCNs) are adrenergic releasing factor-related peptides that regulate gastrointestinal motility and visceral pain in response to stress (37). UCNs can inhibit the growth of colon cancer tumor cells by inducing apoptosis through PUMA and p53 targets (38). TRIM58 expression was markedly inhibited in CRC and negatively related to CRC progression (39). Hypermethylation of TRIM58 down-regulation of its mRNA expression correlates with prognosis of various digestive tract tumors, suggesting that high expression is linked to bad outcome (40). RBCK1 is associated with the sensitivity and stemness of chemotherapeutic drugs in CRC (41). TPM2 (β -Tropomyosin), encoded tropomyosin β chain, was identified as a fibroblast-specific biomarker of poor prognosis in CRC (42). CD36 regulates cell-attachment-to-extracellular matrix attachment, stromal cell fate, TGFβ activation, and immune signaling, which is an early marker of cancer invasion and metastasis in breast, prostate, ovarian, liver, and colon cancer (43). PPARGC1A has an essential function in the modulation of mitochondrial biogenesis and metabolism and protects against tumorigenesis by regulating the fate enterocytes (44, 45). LGALS4 inhibits tumor cell infiltration (46), and LGALS4

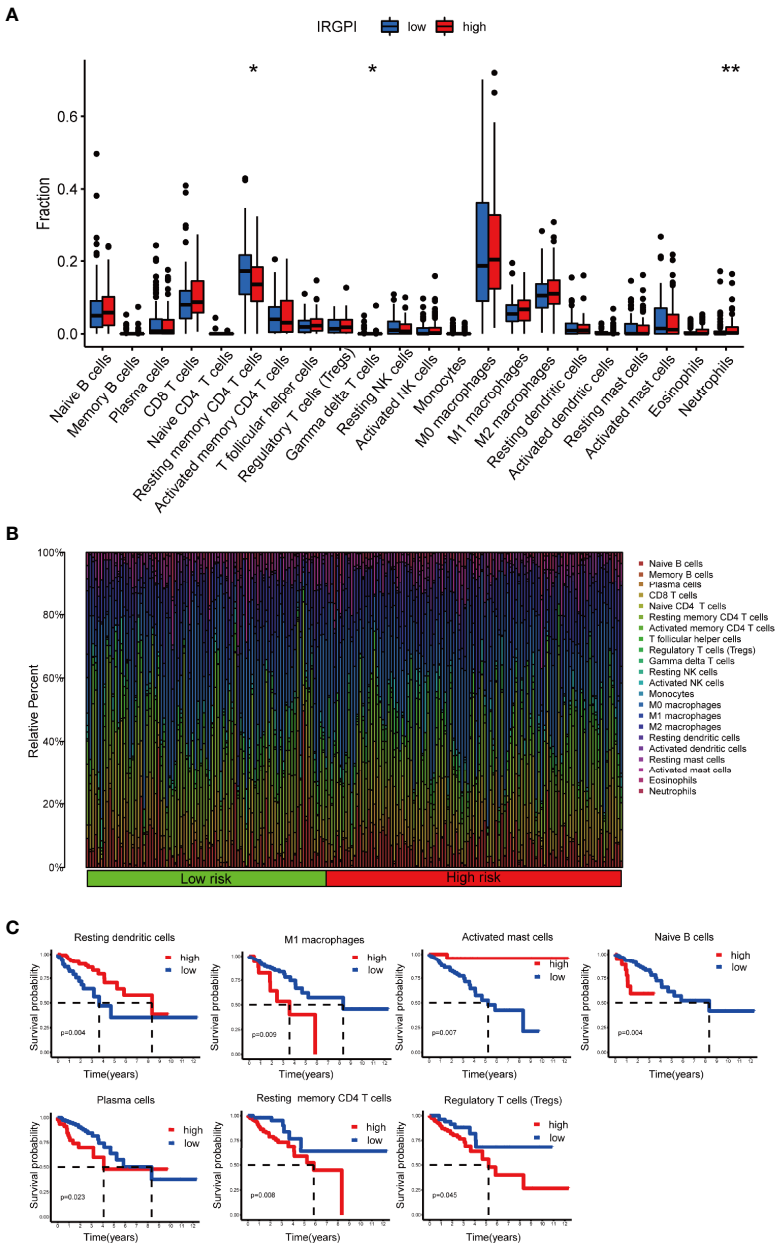

FIGURE 6 | TME landscape of colon cancer and characterization of different IRGPI groups. The proportions of TME cells in the high and low IRGPI groups. **(A)** The correlation of IRPGI scores with 22 immune cells. **(B)** Characteristics associated with the immune landscape. **(C)** Kaplan-Meier survival analysis of the correlation of immune cell abundance ratios in the IRGPI group. (*$P < 0.05$; **$P < 0.01$). TME, tumor immune microenvironment; IRGPI, immune-related gene prognostic index.

upregulation prolongs disease-free survival in CRC (47). Detailed links between these genes are yet to be elucidated. In addition, more research is warranted to uncover the mechanism of action of these genes in colon cancer.

To further understand the immunological nature of IRGPI groups, we investigated gene mutations in different IRGPI groups. The mutation landscape showed that APC and TP53 gene mutation were more frequent in both high and low risk groups, and the mutation rates were greater in the IRGPI-high group than in the IRGPI-low group for APC (74% vs 45%) and TP53 (62% vs 45%). Mutations in the tumor suppressor gene APC, found in approximately 80% of human colon cancer, disrupt intestinal stem cell (ISC) homeostasis and lead to unrestricted activation of the WNT pathway (48). TP53 mutation leads to loss of function, genome-wide ploidy, and local oncogene amplification in the colon (49). There is growing evidence that TP53 mutations affect the TME (50). Specific mutant p53 proteins are capable of producing non-cell-

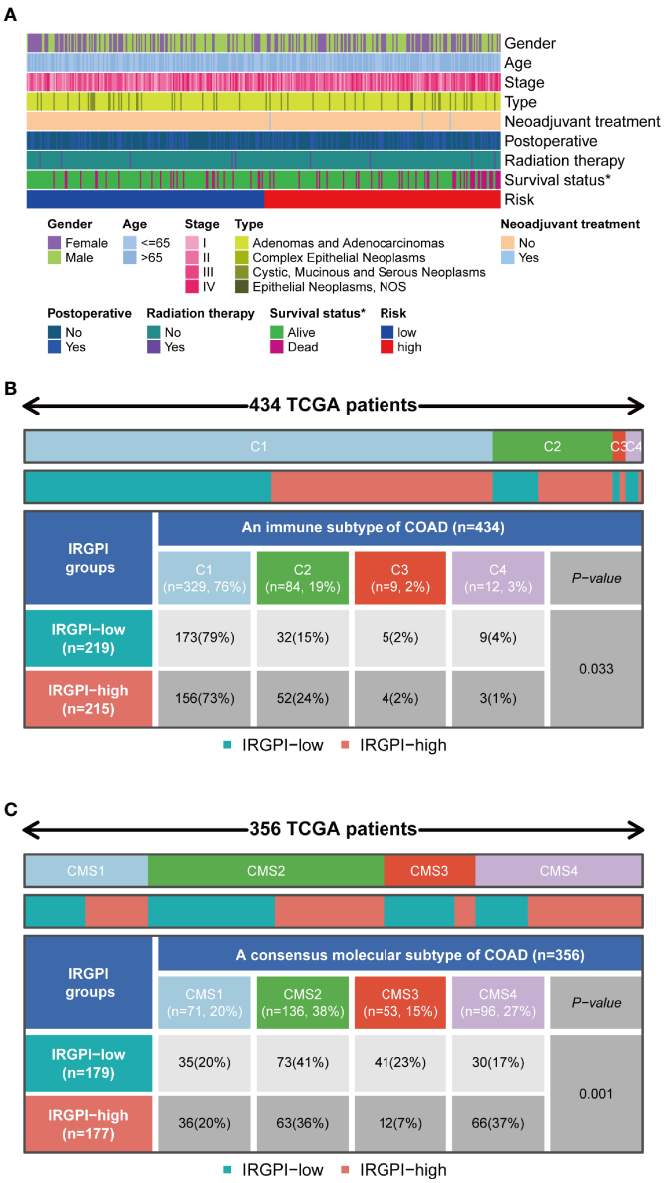

FIGURE 7 | Immunological and molecular subtype distribution of different IRGPI groups. **(A)** Heat map of IRGPI grouped clinical factors for colon cancer patients. **(B)** Heat map and table showing the distribution of colon cancer immune subtypes (C1, C2, C3, and C4) between the IRGPI groups. **(C)** Heat map and table showing the distribution of molecular subtypes (CMS1, CMS2, CMS3, and CMS4) between the IRGPI groups. IRGPI, immune-related gene prognostic index; CMS, consensus molecular subtypes. *P < 0.05.

autonomous effects, such as secreting higher levels of interferon-β (51), inducing paracrine effects, mediating the M1 polarization pattern in neighboring macrophages (52), and reprogramming neighboring macrophages (53). Thus, patients in the IRGPI-high group with high APC and TP53 mutations have a worse prognosis than patients in the IRGPI-low group with low APC and TP53 mutations, which is consistent with our survival results.

Considering the importance of immune cells in tumor immune infiltration, we further evaluated the relative proportion of 22 immune cells in each colon cancer specimen and assessed the immune function. Some evidence suggests that the interaction between tumor and microenvironment plays a crucial role in the progression of colon cancer and the probability of response to immunotherapy. Previous studies found an association between reduced resting memory CD4 T cell infiltration and poor prognosis (54). Indeed, γδ T cells are a subset of cytotoxic T cells that produce TNF-α, leading to tumor elimination through their powerful effector function. They can recruit other immune cells and increase the high antitumor activity in colon cancer. In addition, neutrophils play a key role in tumorigenesis and tumor promotion and metastasis by

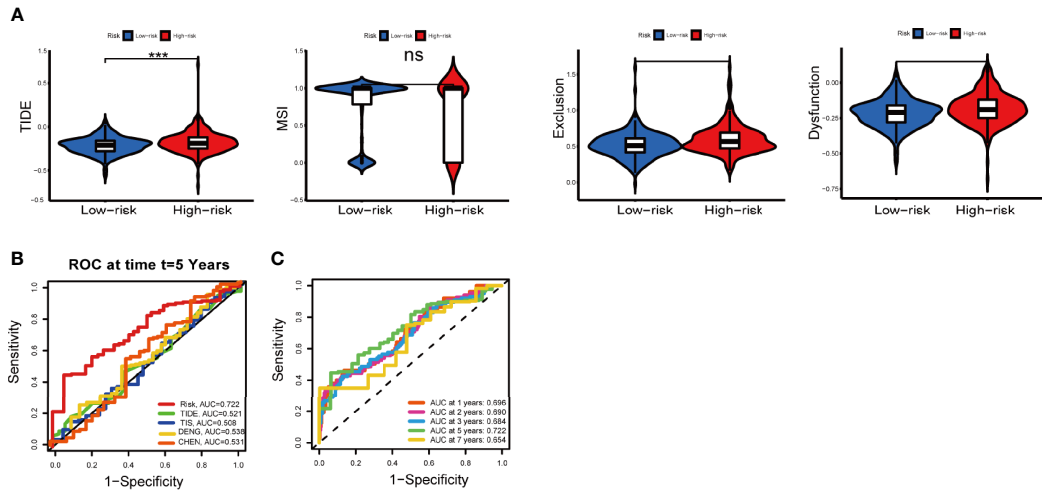

FIGURE 8 | Immune response to ICI therapy and the prognostic value. **(A)** TIDE, MSI, and T cell exclusion and dysfunction score for different IRGPI groups. Scores were compared between the two IRGPI groups (ns, not significant; ***$P < 0.001$). **(B)** Kaplan-Meier survival analysis of the IRGPI groups in TIDE, TIS, the colon cancer cohorts of Deng et al. and Chen et al. **(C)** Time-dependent ROC curve analysis. ICI, immune checkpoint inhibitor; MSI, microsatellite instability; TIS, T cell-inflamed signature; IRGPI, immune-related gene prognostic index; ROC, receiver operating characteristic.

increasing angiogenesis, cell motility, migration, and invasion. Neutrophils can amplify DNA damage in cancer cells through reactive oxygen species(ROC), promoting liver metastasis. M1 macrophages have pro-inflammatory and tumoricidal properties (55). However, the prognostic significance of macrophages in the microenvironment of CRC is not fully understood. Several studies have assessed the prognostic significance of macrophages in CRC, but the results are conflicting (56–65). Colon cancer progression is usually associated with a systemic inflammatory response, and multiple mechanisms of inflammatory mediators support tumor growth and spread (66, 67).Different tumor-associated macrophages (TAM) subpopulations have opposing functions and specific infiltration sites, hence the role of TAM in the prognosis of colon cancer has not been fully defined (68). Furthermore, IRGPI-low samples were enriched for stronger anti-tumor metabolism and inhibition of tumor metastasis, while IRGPI-high samples had more immunosuppressive cells and signals associated with tumor and metastasis, suggesting that the IRGPI-high group was characterized by immunosuppression and active tumor progression.

IRGPI groups could distinguish different molecular and immunological subtypes of colon cancer. Thorsson et al. developed a new worldwide immune classification of solid tumors from transcriptional profiles of more than 10,000 patients from all TCGAs (69). According to their classification, colon cancer immune subtypes were mainly composed of C1, C2, C3, and C4. Among them, colon cancer was dominated by C1, with increased expression of angiogenic genes associated with adaptive immune infiltration. In C1, the proportion of the IRGPI-low group was higher than the IRGPI-high group, suggesting that IRGPI was associated with adaptive immune infiltration. The International CRC Subtype Consortium has developed a unified transcript classification based on four biologically distinct CMS, which is widely accepted (27): CMS1, CMS2, CMS3, and CMS4. Among them, CMS2 was activated with WNT and MYC signaling with an intermediate prognosis. CMS3 epithelial cells had a marked metabolic disorder with an intermediate prognosis. CMS4 had prominent TNF-β activation and a poor prognosis. In our study, the proportion of CMS2 and CMS3 was higher in the IRGPI-low group than IRGPI-high group, respectively. Conversely, CMS4 was lower in the IRGPI-low group than IRGPI-high group. It was clarified that patients with low IRGPI scores had active immunity and a good prognosis, whereas patients with high IRGPI scores had immunosuppressive features and a poor prognosis, which was consistent with our previous findings.

To Assess the response to ICI therapy in patients with colon cancer, we forecasted the probability of the IRGPI model using TIDE and TIS scores. The TIDE score was a newly developed immunotherapy response prediction method for forecasting the effectiveness of anti-PD1 and anti-CTLA4 therapy more accurately than TMB or PD-L1 expression (70). A higher TIDE score indicated poorer tumor response to ICI therapy and a worse prognosis (20). In our study, TIDE scores were higher in the IRGPI-high group than the IRGPI-low group, suggesting a large immune escape and poor outcome with high IRGPI scores. This suggested that IRGPI was a valid biomarker for predicting response to immunotherapy. The low IRGPI score group may be more sensitive to immunotherapy. As for TIS score, it was described as a biomarker for predicting prognosis of patients with different types of cancer (21). The clinical trial assay, running on the nCounter Analysis System, contained genes associated with antigen presentation, chemokine

expression, cytotoxic activity, and adaptive immune resistance (71). Our IRGPI score was more sensitive compared to the TIDE and TIS scores, and hence better. In addition, we compared IRGPI score with Zhang's signature and Deng's signature in terms of predicting immune prognosis and consistently found that IRGPI score had a higher sensitivity. In conclusion, our study developed a reliable immune-related risk signature that could predict survival and response to ICI therapy in patients with colon cancer. To our knowledge, this is the first IRG prognostic model based on WGCNA to differentiate the prognostic, molecular, and immunological profile for colon cancer. It played an important role in differentiating immune and molecular features and predicting patient prognosis. However, the study still has some limitations. First, the data were based on retrospective datasets, and a prospective study of this IRGPI-based signature would be necessary. Second, all expression data were sequencing data downloaded from public databases, and the results need to be validated by new methods and external experiments with fresh specimens. Finally, indirect assessment of IRGPI's ability to predict response to immunotherapy would require further studies in large-scale multicenter studies.

DATA AVAILABILITY STATEMENT

The datasets presented in this study can be found in online repositories. The names of the repository/repositories and accession number(s) can be found in the article/**Supplementary Material**.

AUTHOR CONTRIBUTIONS

ZW and JS contributed to the methodology and formal analysis. JS and ZW contributed to write the manuscript. NA polished English writing of the manuscript. MS contributed to the funding, writing, review, and editing. All authors contributed to the article and approved the submitted version.

FUNDING

This work was supported by the major project of Shanghai Municipal S and T Commission (no. 19401972300), Shandong Province Key R&D Program (Major Science and Technology Innovation Project, 2021CXGC010509), Shanghai Key Laboratory of Traditional Chinese Clinical Medicine, Key Disciplines of Liver and Gall Bladder Diseases, and Key Laboratory of Chronic Deficiency Liver Disease of the State Administration of Traditional Chinese Medicine of the People's Republic of China (20DZ2272200). Shanghai University of Traditional Chinese Medicine Postgraduate Innovation Training Program (Y2021087).

SUPPLEMENTARY MATERIAL

The Supplementary Material for this article can be found online at: https://www.frontiersin.org/articles/10.3389/fimmu.2022.802665/full#supplementary-material

Supplementary Figure 1 | Relationship between MSI status, chemotherapy in IRGPI groups.**(A)** MSI status. **(B)** Chemotherapy. MSI, microsatellite instability.

REFERENCES

1. Arnold M, Sierra M, Laversanne M, Soerjomataram I, Jemal A, Bray FJG. Global Patterns and Trends in Colorectal Cancer Incidence and Mortality. *Gut* (2017) 66(4):683–91. doi: 10.1136/gutjnl-2015-310912
2. Labianca R, Nordlinger B, Beretta GD, Mosconi S, Mandalà M, Cervantes A, et al. Early Colon Cancer: Esmo Clinical Practice Guidelines for Diagnosis, Treatment and Follow-Up. *Ann Oncol* (2013) (24 Suppl 6):vi64–72. doi: 10.1093/annonc/mdt354
3. Zhang T, Xie J, Arai S, Wang L, Shi X, Shi N, et al. The Efficacy and Safety of Anti-Pd-1/Pd-L1 Antibodies for Treatment of Advanced or Refractory Cancers: A Meta-Analysis. *Oncotarget* (2016) 7(45):73068–79. doi: 10.18632/oncotarget.12230
4. D'Angelo SP, Larkin J, Sosman JA, Lebbé C, Brady B, Neyns B, et al. Efficacy and Safety of Nivolumab Alone or in Combination With Ipilimumab in Patients With Mucosal Melanoma: A Pooled Analysis. *J Clin Oncol Off J Am Soc Clin Oncol* (2017) 35(2):226–35. doi: 10.1200/jco.2016.67.9258
5. Binnewies M, Roberts EW, Kersten K, Chan V, Fearon DF, Merad M, et al. Understanding the Tumor Immune Microenvironment (Time) for Effective Therapy. *Nat Med* (2018) 24(5):541–50. doi: 10.1038/s41591-018-0014-x
6. Nishino M, Ramaiya NH, Hatabu H, Hodi FS. Monitoring Immune-Checkpoint Blockade: Response Evaluation and Biomarker Development. *Nat Rev Clin Oncol* (2017) 14(11):655–68. doi: 10.1038/nrclinonc.2017.88
7. Taube JM, Galon J, Sholl LM, Rodig SJ, Cottrell TR, Giraldo NA, et al. Implications of the Tumor Immune Microenvironment for Staging and Therapeutics. *Mod Pathol an Off J United States Can Acad Pathol Inc* (2018) 31(2):214–34. doi: 10.1038/modpathol.2017.156
8. Marisa L, de Reyniès A, Duval A, Selves J, Gaub M, Vescovo L, et al. Gene Expression Classification of Colon Cancer Into Molecular Subtypes: Characterization, Validation, and Prognostic Value. *PloS Med* (2013) 10(5): e1001453. doi: 10.1371/journal.pmed.1001453
9. Ritchie M, Phipson B, Wu D, Hu Y, Law C, Shi W, et al. Limma Powers Differential Expression Analyses for Rna-Sequencing and Microarray Studies. *Nucleic Acids Res* (2015) 43(7):e47. doi: 10.1093/nar/gkv007
10. Yu G, Wang LG, Han Y, He QY. Clusterprofiler: An R Package for Comparing Biological Themes Among Gene Clusters. *Omics J Integr Biol* (2012) 16 (5):284–7. doi: 10.1089/omi.2011.0118
11. Zhang B, Horvath S. A General Framework for Weighted Gene Co-Expression Network Analysis. *Stat Appl Genet Mol Biol* (2005) 4:Article17. doi: 10.2202/1544-6115.1128
12. Niemira M, Collin F, Szalkowska A, Bielska A, Chwialkowska K, Reszec J, et al. Molecular Signature of Subtypes of Non-Small-Cell Lung Cancer by Large-Scale Transcriptional Profiling: Identification of Key Modules and Genes by Weighted Gene Co-Expression Network Analysis (Wgcna). *Cancers* (2019) 12 (1):37. doi: 10.3390/cancers12010037
13. Lorent M, Giral M, Foucher Y. Net Time-Dependent Roc Curves: A Solution for Evaluating the Accuracy of a Marker to Predict Disease-Related Mortality. *Stat Med* (2014) 33(14):2379–89. doi: 10.1002/sim.6079
14. Mayakonda A, Lin DC, Assenov Y, Plass C, Koeffler HP. Maftools: Efficient and Comprehensive Analysis of Somatic Variants in Cancer. *Genome Res* (2018) 28(11):1747–56. doi: 10.1101/gr.239244.118
15. He Y, Jiang Z, Chen C, Wang X. Classification of Triple-Negative Breast Cancers Based on Immunogenomic Profiling. *J Exp Clin Cancer Res CR* (2018) 37(1):327. doi: 10.1186/s13046-018-1002-1
16. Zeng D, Ye Z, Wu J, Zhou R, Fan X, Wang G, et al. Macrophage Correlates With Immunophenotype and Predicts Anti-Pd-L1 Response of Urothelial Cancer. *Theranostics* (2020) 10(15):7002–14. doi: 10.7150/thno.46176
17. Hwang S, Kwon AY, Jeong JY, Kim S, Kang H, Park J, et al. Immune Gene Signatures for Predicting Durable Clinical Benefit of Anti-Pd-1

Immunotherapy in Patients With Non-Small Cell Lung Cancer. *Sci Rep* (2020) 10(1):643. doi: 10.1038/s41598-019-57218-9
18. Tirosh I, Izar B, Prakadan SM, Wadsworth MH2nd, Treacy D, Trombetta JJ, et al. Dissecting the Multicellular Ecosystem of Metastatic Melanoma by Single-Cell Rna-Seq. *Sci (New York NY)* (2016) 352(6282):189–96. doi: 10.1126/science.aad0501
19. Blanche P, Dartigues JF, Jacqmin-Gadda H. Estimating and Comparing Time-Dependent Areas Under Receiver Operating Characteristic Curves for Censored Event Times With Competing Risks. *Stat Med* (2013) 32 (30):5381–97. doi: 10.1002/sim.5958
20. Jiang P, Gu S, Pan D, Fu J, Sahu A, Hu X, et al. Signatures of T Cell Dysfunction and Exclusion Predict Cancer Immunotherapy Response. *Nat Med* (2018) 24(10):1550–8. doi: 10.1038/s41591-018-0136-1
21. Ayers M, Lunceford J, Nebozhyn M, Murphy E, Loboda A, Kaufman D, et al. Ifn-Γ-Related Mrna Profile Predicts Clinical Response to Pd-1 Blockade. *J Clin Invest* (2017) 127(8):2930–40. doi: 10.1172/jci91190
22. Damotte D, Warren S, Arrondeau J, Boudou-Rouquette P, Mansuet-Lupo A, Biton J, et al. The Tumor Inflammation Signature (Tis) Is Associated With Anti-Pd-1 Treatment Benefit in the Certim Pan-Cancer Cohort. *J Trans Med* (2019) 17(1):357. doi: 10.1186/s12967-019-2100-3
23. Chen W, Huang J, Xiong J, Fu P, Chen C, Liu Y, et al. Identification of a Tumor Microenvironment-Related Gene Signature Indicative of Disease Prognosis and Treatment Response in Colon Cancer. *Oxid Med Cell Longev* (2021) 2021:6290261. doi: 10.1155/2021/6290261
24. Deng D, Luo X, Zhang S, Xu ZJA. Immune Cell Infiltration-Associated Signature in Colon Cancer and Its Prognostic Implications. *Aging (Albany NY)* (2021) 13(15):19696–709. doi: 10.18632/aging.203380
25. Thorsson V, Gibbs DL, Brown SD, Wolf D, Bortone DS, Ou Yang T-H, et al. The Immune Landscape of Cancer. *Immunity* (2018). 48(4):812–30. doi: 10.1016/j.immuni.2018.03.023
26. Xu Y, Li D, Liu Z, Gibbs DL, Xie L, Qin G. Intrinsic Genetic and Transcriptomic Patterns Reflect Tumor Immune Subtypes Facilitating Exploring Possible Combinatory Therapy. *Front Mol Biosci* (2020) 7:53. doi: 10.3389/fmolb.2020.00053
27. Guinney J, Dienstmann R, Wang X, de Reyniès A, Schlicker A, Soneson C, et al. The Consensus Molecular Subtypes of Colorectal Cancer. *Nat Med* (2015) 21(11):1350–6. doi: 10.1038/nm.3967
28. Soldevilla B, Carretero-Puche C, Gomez-Lopez G, Al-Shahrour F, Riesco MC, Gil-Calderon B, et al. The Correlation Between Immune Subtypes and Consensus Molecular Subtypes in Colorectal Cancer Identifies Novel Tumour Microenvironment Profiles, With Prognostic and Therapeutic Implications. *Eur J Cancer (Oxford Engl 1990)* (2019) 123:118–29. doi: 10.1016/j.ejca.2019.09.008
29. Li D, Lin X, Chen B, Ma Z, Zeng Y, Wang H. Identification and Validation of Emt-Related Lncrna Prognostic Signature for Colorectal Cancer. *Front Genet* (2021) 12:723802. doi: 10.3389/fgene.2021.723802
30. Lichtenstern CR, Ngu RK, Shalapour S, Karin M. Immunotherapy, Inflammation and Colorectal Cancer. *Cells* (2020) 9(3):618. doi: 10.3390/cells9030618
31. Xiao W, Ibrahim ML, Redd PS, Klement JD, Lu C, Yang D, et al. Loss of Fas Expression and Function Is Coupled With Colon Cancer Resistance to Immune Checkpoint Inhibitor Immunotherapy. *Mol Cancer Res MCR* (2019) 17(2):420–30. doi: 10.1158/1541-7786.Mcr-18-0455
32. Galon J, Angell HK, Bedognetti D, Marincola FM. The Continuum of Cancer Immunosurveillance: Prognostic, Predictive, and Mechanistic Signatures. *Immunity* (2013) 39(1):11–26. doi: 10.1016/j.immuni.2013.07.008
33. Galon J, Fridman W, Pagès F. The Adaptive Immunologic Microenvironment in Colorectal Cancer: A Novel Perspective. *Cancer Res* (2007) 67(5):1883–6. doi: 10.1158/0008-5472.Can-06-4806
34. Angell H, Galon J. From the Immune Contexture to the Immunoscore: The Role of Prognostic and Predictive Immune Markers in Cancer. *Curr Opin Immunol* (2013) 25(2):261–7. doi: 10.1016/j.coi.2013.03.004
35. Fridman WH, Pagès F, Sautès-Fridman C, Galon J. The Immune Contexture in Human Tumours: Impact on Clinical Outcome. *Nat Rev Cancer* (2012) 12 (4):298–306. doi: 10.1038/nrc3245
36. Bao X, Shi R, Zhao T, Wang Y. Mast Cell-Based Molecular Subtypes and Signature Associated With Clinical Outcome in Early-Stage Lung Adenocarcinoma. *Mol Oncol* (2020) 14(5):917–32. doi: 10.1002/1878-0261.12670
37. Martinez V, Wang L, Million M, Rivier J, Taché YJP. Urocortins and the Regulation of Gastrointestinal Motor Function and Visceral Pain. *Peptides* (2004) 25(10):1733–44. doi: 10.1016/j.peptides.2004.05.025
38. Dudgeon C, Wang P, Sun X, Peng R, Sun Q, Yu J, et al. Puma Induction by Foxo3a Mediates the Anticancer Activities of the Broad-Range Kinase Inhibitor Ucn-01. *Mol Cancer Ther* (2010) 9(11):2893–902. doi: 10.1158/1535-7163.Mct-10-0635
39. Liu M, Zhang X, Cai J, Li Y, Luo Q, Wu H, et al. Downregulation of Trim58 Expression Is Associated With a Poor Patient Outcome and Enhances Colorectal Cancer Cell Invasion. *Oncol Rep* (2018) 40(3):1251–60. doi: 10.3892/or.2018.6525
40. Qiu X, Huang Y, Zhou Y, Zheng F. Aberrant Methylation of Trim58 in Hepatocellular Carcinoma and Its Potential Clinical Implication. *Oncol Rep* (2016) 36(2):811–8. doi: 10.3892/or.2016.4871
41. Liu M, Zang F, Zhang SJB. Biomedecine P, Pharmacotherapie. Rbck1 Contributes to Chemoresistance and Stemness in Colorectal Cancer (Crc). *BioMed Pharmacother* (2019) 118:109250. doi: 10.1016/j.biopha.2019.109250
42. Zhou Y, Bian S, Zhou X, Cui Y, Wang W, Wen L, et al. Single-Cell Multiomics Sequencing Reveals Prevalent Genomic Alterations in Tumor Stromal Cells of Human Colorectal Cancer. *Cancer Cell* (2020) 38(6):818–28.e5. doi: 10.1016/j.ccell.2020.09.015
43. Enciu AM, Radu E, Popescu ID, Hinescu ME, Ceafalan LC. Targeting Cd36 as Biomarker for Metastasis Prognostic: How Far From Translation Into Clinical Practice? *BioMed Res Int* (2018) 2018:7801202. doi: 10.1155/2018/7801202
44. D'Errico I, Salvatore L, Murzilli S, Lo Sasso G, Latorre D, Martelli N, et al. Peroxisome Proliferator-Activated Receptor-Gamma Coactivator 1-Alpha (Pgc1alpha) Is a Metabolic Regulator of Intestinal Epithelial Cell Fate. *Proc Natl Acad Sci United States America* (2011) 108(16):6603–8. doi: 10.1073/pnas.1016354108
45. Cho YA, Lee J, Oh JH, Chang HJ, Sohn DK, Shin A, et al. Genetic Variation in Ppargc1a May Affect the Role of Diet-Associated Inflammation in Colorectal Carcinogenesis. *Oncotarget* (2017) 8(5):8550–8. doi: 10.18632/oncotarget.14347
46. Long M, Campbell MJT. Integrative Genomic Approaches to Dissect Clinically-Significant Relationships Between the Vdr Cistrome and Gene Expression in Primary Colon Cancer. *J Steroid Biochem Mol Biol* (2017) 173:130–8. doi: 10.1016/j.jsbmb.2016.12.013. Josb, Biology M.
47. Long MD, Campbell MJ. Integrative Genomic Approaches to Dissect Clinically-Significant Relationships Between the Vdr Cistrome and Gene Expression in Primary Colon Cancer. *J Steroid Biochem Mol Biol* (2017) 173:130–8. doi: 10.1016/j.jsbmb.2016.12.013
48. van Neerven S, de Groot N, Nijman L, Scicluna B, van Driel M, Lecca M, et al. Apc-Mutant Cells Act as Supercompetitors in Intestinal Tumour Initiation. *Nature* (2021) 594(7863):436–41. doi: 10.1038/s41586-021-03558-4
49. Kim JE, Choi J, Sung CO, Hong YS, Kim SY, Lee H, et al. High Prevalence of Tp53 Loss and Whole-Genome Doubling in Early-Onset Colorectal Cancer. *Exp Mol Med* (2021) 53(3):446–56. doi: 10.1038/s12276-021-00583-1
50. Muller PA, Vousden KH. Mutant P53 in Cancer: New Functions and Therapeutic Opportunities. *Cancer Cell* (2014) 25(3):304–17. doi: 10.1016/j.ccr.2014.01.021
51. Madar S, Harel E, Goldstein I, Stein Y, Kogan-Sakin I, Kamer I, et al. Mutant P53 Attenuates the Anti-Tumorigenic Activity of Fibroblasts-Secreted Interferon Beta. *PloS One* (2013) 8(4):e61353. doi: 10.1371/journal.pone.0061353
52. Trivedi M, Talekar M, Shah P, Ouyang Q, Amiji M. Modification of Tumor Cell Exosome Content by Transfection With Wt-P53 and Microrna-125b Expressing Plasmid DNA and Its Effect on Macrophage Polarization. *Oncogenesis* (2016) 5(8):e250. doi: 10.1038/oncsis.2016.52
53. Cooks T, Pateras IS, Jenkins LM, Patel KM, Robles AI, Morris J, et al. Mutant P53 Cancers Reprogram Macrophages to Tumor Supporting Macrophages *Via* Exosomal Mir-1246. *Nat Commun* (2018) 9(1):771. doi: 10.1038/s41467-018-03224-w
54. Song J, Wu L. Friend or Foe: Prognostic and Immunotherapy Roles of Btla in Colorectal Cancer. *Front Mol Biosci* (2020) 7:148. doi: 10.3389/fmolb.2020.00148

55. López-Janeiro Á, Padilla-Ansala C, de Andrea CE, Hardisson D, Melero I. Prognostic Value of Macrophage Polarization Markers in Epithelial Neoplasms and Melanoma. *A Syst Rev Meta-Analysis. Mod Pathol* (2020) 33(8):1458–65. doi: 10.1038/s41379-020-0534-z
56. Herrera M, Herrera A, Domínguez G, Silva J, García V, García JM, et al. Cancer-Associated Fibroblast and M2 Macrophage Markers Together Predict Outcome in Colorectal Cancer Patients. *Cancer Sci* (2013) 104(4):437–44. doi: 10.1111/cas.12096
57. Feng Q, Chang W, Mao Y, He G, Zheng P, Tang W, et al. Tumor-Associated Macrophages as Prognostic and Predictive Biomarkers for Postoperative Adjuvant Chemotherapy in Patients With Stage Ii Colon Cancer. *Clin Cancer Res* (2019) 25(13):3896–907. doi: 10.1158/1078-0432.Ccr-18-2076
58. Kim Y, Wen X, Bae JM, Kim JH, Cho NY, Kang GH. The Distribution of Intratumoral Macrophages Correlates With Molecular Phenotypes and Impacts Prognosis in Colorectal Carcinoma. *Histopathology* (2018) 73 (4):663–71. doi: 10.1111/his.13674
59. Edin S, Wikberg ML, Dahlin AM, Rutegård J, Öberg Å, Oldenborg PA, et al. The Distribution of Macrophages With a M1 or M2 Phenotype in Relation to Prognosis and the Molecular Characteristics of Colorectal Cancer. *PloS One* (2012) 7(10):e47045. doi: 10.1371/journal.pone.0047045
60. Forssell J, Oberg A, Henriksson ML, Stenling R, Jung A, Palmqvist R. High Macrophage Infiltration Along the Tumor Front Correlates With Improved Survival in Colon Cancer. *Clin Cancer Res* (2007) 13(5):1472–9. doi: 10.1158/1078-0432.Ccr-06-2073
61. Koelzer VH, Canonica K, Dawson H, Sokol L, Karamitopoulou-Diamantis E, Lugli A, et al. Phenotyping of Tumor-Associated Macrophages in Colorectal Cancer: Impact on Single Cell Invasion (Tumor Budding) and Clinicopathological Outcome. *Oncoimmunology* (2016) 5(4):e1106677. doi: 10.1080/2162402x.2015.1106677
62. Chaput N, Svrcek M, Aupérin A, Locher C, Drusch F, Malka D, et al. Tumour-Infiltrating Cd68+ and Cd57+ Cells Predict Patient Outcome in Stage Ii-Iii Colorectal Cancer. *Br J Cancer* (2013) 109(4):1013–22. doi: 10.1038/bjc.2013.362
63. Algars A, Irjala H, Vaittinen S, Huhtinen H, Sundström J, Salmi M, et al. Type and Location of Tumor-Infiltrating Macrophages and Lymphatic Vessels Predict Survival of Colorectal Cancer Patients. *Int J Cancer* (2012) 131 (4):864–73. doi: 10.1002/ijc.26457
64. Väyrynen JP, Haruki K, Lau MC, Väyrynen SA, Zhong R, Dias Costa A, et al. The Prognostic Role of Macrophage Polarization in the Colorectal Cancer Microenvironment. *Cancer Immunol Res* (2021) 9(1):8–19. doi: 10.1158/2326-6066.Cir-20-0527
65. Zhang QW, Liu L, Gong CY, Shi HS, Zeng YH, Wang XZ, et al. Prognostic Significance of Tumor-Associated Macrophages in Solid Tumor: A Meta-Analysis of the Literature. *PloS One* (2012) 7(12):e50946. doi: 10.1371/journal.pone.0050946
66. Tuomisto AE, Mäkinen MJ, Väyrynen JP. Systemic Inflammation in Colorectal Cancer: Underlying Factors, Effects, and Prognostic Significance. *World J Gastroenterol* (2019) 25(31):4383–404. doi: 10.3748/wjg.v25.i31.4383
67. Dolan RD, Lim J, McSorley ST, Horgan PG, McMillan DC. The Role of the Systemic Inflammatory Response in Predicting Outcomes in Patients With Operable Cancer: Systematic Review and Meta-Analysis. *Sci Rep* (2017) 7 (1):16717. doi: 10.1038/s41598-017-16955-5
68. Li J, Li L, Li Y, Long Y, Zhao Q, Ouyang Y, et al. Tumor-Associated Macrophage Infiltration and Prognosis in Colorectal Cancer: Systematic Review and Meta-Analysis. *Int J colorectal Dis* (2020) 35(7):1203–10. doi: 10.1007/s00384-020-03593-z
69. Huang TX, Fu L. The Immune Landscape of Esophageal Cancer. *Cancer Commun (London England)* (2019) 39(1):79. doi: 10.1186/s40880-019-0427-z
70. Becht E, Giraldo NA, Lacroix L, Buttard B, Elarouci N, Petitprez F, et al. Estimating The Population Abundance of Tissue-Infiltrating Immune and Stromal Cell Populations Using Gene Expression. *Genome Biol* (2016) 17 (1):218. doi: 10.1186/s13059-016-1070-5
71. Danaher P, Warren S, Lu R, Samayoa J, Sullivan A, Pekker I, et al. Pan-Cancer Adaptive Immune Resistance as Defined by the Tumor Inflammation Signature (Tis): Results From the Cancer Genome Atlas (Tcga). *J immunother Cancer* (2018) 6(1):63. doi: 10.1186/s40425-018-0367-1

Conflict of Interest: The authors declare that the research was conducted in the absence of any commercial or financial relationships that could be construed as a potential conflict of interest.

Publisher's Note: All claims expressed in this article are solely those of the authors and do not necessarily represent those of their affiliated organizations, or those of the publisher, the editors and the reviewers. Any product that may be evaluated in this article, or claim that may be made by its manufacturer, is not guaranteed or endorsed by the publisher.

Copyright © 2022 Wang, Song, Azami and Sun. This is an open-access article distributed under the terms of the Creative Commons Attribution License (CC BY). The use, distribution or reproduction in other forums is permitted, provided the original author(s) and the copyright owner(s) are credited and that the original publication in this journal is cited, in accordance with accepted academic practice. No use, distribution or reproduction is permitted which does not comply with these terms.

frontiers | Frontiers in Immunology

CASE REPORT
published: 03 June 2022
doi: 10.3389/fimmu.2022.840916

Upper Gastrointestinal Tract IrAEs: A Case Report About Sintilimab-Induced Acute Erosive Hemorrhagic Gastritis

Qi Ai[†], *Wen Chen*[†], *Yonggui Li and Guoqing Li*[*]

The Second Affiliated Hospital, Department of Digestive Internal Medicine, Hengyang Medical School, University of South China, Hengyang, China

OPEN ACCESS

Edited by:
Hubing Shi,
Sichuan University, China

Reviewed by:
Yinghong Wang,
University of Texas MD Anderson Cancer Center, United States
Noa Gordon,
Ben-Gurion University of the Negev, Israel

***Correspondence:**
Guoqing Li
ligq1970@163.com

[†]*These authors have contributed equally to this work and share first authorship*

Specialty section:
This article was submitted to Cancer Immunity and Immunotherapy, a section of the journal Frontiers in Immunology

Received: *21 December 2021*
Accepted: *06 May 2022*
Published: *03 June 2022*

Citation:
Ai Q, Chen W, Li Y and Li G (2022) Upper Gastrointestinal Tract IrAEs: A Case Report About Sintilimab-Induced Acute Erosive Hemorrhagic Gastritis. Front. Immunol. 13:840916. doi: 10.3389/fimmu.2022.840916

Introduction: Immune checkpoint inhibitors (ICIs) have now become the standard therapy for malignancies like non-small cell lung cancer and classical Hodgkin's lymphoma. ICIs are associated with unique immune-related adverse events (irAEs) caused by dysregulated immune activation. Treatment of lower gastrointestinal (GI) tract irAEs, such as colitis, is more common. However, for upper gastrointestinal tract irAEs, there is a lack of consensus in terms of globally standardized disease classification and treatment guidelines. Here, we report a case of sintilimab-induced acute erosive hemorrhagic gastritis.

Case Presentation: A 54-year-old man with metastatic NSCLC (PT2N2M1 stage IV) underwent treatment with eight courses of sintilimab + bevacizumab, followed by maintenance therapy with sintilimab alone. However, he presented with epigastric pain and melena at the end of the first sintilimab treatment, and the symptoms occurred repeatedly after regular treatment with acute erosive hemorrhagic gastritis. Repeat esophagogastroduodenoscopy (EGD) showed severe hemorrhagic gastritis; symptomatic relief and improvement in EGD images were noted for as long as he was being treated with steroids, methylprednisolone sodium.

Conclusion: As far as we are aware, we here describe the first case of sintilimab-associated acute erosive hemorrhagic gastritis, an upper gastrointestinal toxicity event. Throughout the treatment progression, differential diagnosis, multidisciplinary discussion, and the use of immunosuppressants were instrumental in clarifying the diagnosis and were crucial to the prognosis of the patient and continued treatment with ICIs.

Keywords: sintilimab, immune checkpoint inhibitor, acute erosive hemorrhagic gastritis, immune-related adverse event, upper gastrointestinal tract irAE

INTRODUCTION

Currently, immune checkpoint inhibitors (ICIs) are a hot topic in the field of oncology research and the mainstay of metastatic malignancies because immunotherapy of malignancies improves the survival of patients in whom conventional therapy has failed (1, 2). Immune checkpoint blockade enhances antitumor immunity by blocking immune innate downregulatory factors such as cytotoxic T-lymphocyte antigen 4 (CTLA-4) and programmed cell death 1 (PD-1) or its ligand (PD-L1). Sintilimab, a recombinant and fully human immunoglobulin G4 (IgG4)-type anti-programmed cell death receptor-1 (PD-1) monoclonal antibody, activates T-cell function by binding with PD-1 and blocking the binding of PD-1 to PD-L1 and PD-L2, thus relieving the immunosuppressive effect, enhancing the immunosurveillance and killing ability of T cells against tumors, and generating an immune response against the tumor (2, 3). ICIs have revolutionized the treatment of metastatic cancer, and although their unique immune-related adverse events (irAEs) in the lower GI tract, such as colitis, are commonly discussed, irAEs in the upper GI tract are discussed sparingly. Furthermore, the clinical manifestations of upper GI toxicity are less well described in the previous literature, and currently, there is no uniform classification standard for ICI-associated gastritis (2, 4–6).

As treatment with sintilimab is becoming more common in immune therapy, cases of sintilimab-induced **upper gastrointestinal tract** irAE are limited. While sintilimab-associated **upper gastrointestinal toxicity events** are rarely recognized, here we report a case **due to sintilimab**-induced acute erosive hemorrhagic gastritis.

CASE PRESENTATION

A 54-year-old male was diagnosed as having lung cancer. He underwent video-assisted thoracoscopic surgery for left upper lung cancer in the Second Affiliated Hospital of the University of South China, and his postoperative diagnosis was polymorphic adenocarcinoma of the left upper lung (T2aN2M0 stage IIIA). Immunohistochemical staining showed the following: CK (+), CK7 (+), TTF1 (+), Napsin A (part+), Vim (+), Syn (−), CgA (−), CD56 (−), P40 (−), CK5/6 (−), and Ki67 (50%+). After the surgery, he was started on the TP chemotherapy regimen, which included the administration of carboplatin (40 mg, days 1–3) + paclitaxel (400 mg, day 1). Four cycles of this TP chemotherapy regimen were administered, with each cycle lasting about 21 days. However, about 178 days postoperatively, he was diagnosed with brain metastases [pT2N2M1 stage IV, epidermal growth factor receptor/anaplastic large-cell lymphoma kinase/ROS1 negative, Kirsten rat sarcoma virus (KRAS) mutation 71.8%, KRAS amplification 2.4, cyclin D1 gene amplification 2.6, cyclin-dependent kinase inhibitor 2A mutation 9.1%, and PD-L1 tumor proportion score 60%], after which he received eight courses (approximately 21 days per course) of bevacizumab (1,100 mg) + sintilimab (200 mg) from 2020 to 2021. In April 2021, he was started on sintilimab maintenance therapy. Bevacizumab was discontinued. About 10 days later, he soon visited our hospital for epigastric pain. He underwent gastroscopy on day 419, which showed squamocolumnar junction (SCJ) blurred, local mucosal hyperemia edema with erosion and opaque white mucus covering the mucosal surface, and localized hemorrhage. A large amount of opaque white mucus was attached to the mucosal surface of the gastric antrum and body, and the gastric mucosa was diffusely hyperemic with spontaneous hemorrhage (**Supplementary Figure 1**). Colonoscopy showed no abnormalities. The patient was treated with oral ilaprazole (5 mg, once daily) and gastric protection with sucralfate oral suspension (1 packet, twice daily). Repeat esophagogastroduodenoscopy (EGD) performed in May showed improvements, and repeat colonoscopy still showed no abnormalities. Then, he stopped the oral drug treatment without permission from the doctors after the symptoms subsided (**Supplementary Figure 2**).

After treatment with three courses of sintilimab alone, he had recurrent epigastric pain and black tarry stools, which were worse than before. Repeat EGD showed that the entire gastric mucosa was evidently edematous and hyperemic and showed adhesion of opaque mucus, diffuse erosion of the white moss, and active localized hemorrhaging was extensively observed. The gastric antrum was found to have a necrotic mucosa with exfoliation of large flakes (**Figure 1**). The Carbon 14 breath test was negative, and tests for cytomegalovirus and Epstein–Barr virus revealed a previous infection, but not a current infection. The patient was also negative for tuberculosis immunoglobulin G (IgG) antibodies, HBV, HCV, syphilis antibodies, and HIV (**Supplementary Table 1**). Initially, he was treated with esomeprazole (40 mg every 6 h *via* an intravenous pump), oral rebamipide (100 mg, thrice daily), sucralfate oral suspension (10 ml, twice daily), and rehabilitative new liquid (10 ml, thrice daily, taken orally). However, the symptoms of the patient did not subside and were aggravated even with consuming a small amount of water or other fluids. After regular treatment for acute erosive hemorrhagic gastritis, his fecal occult blood test was still positive, indicating that the upper GI lesion still existed.

After three days of the abovementioned regular treatment for acute gastritis, his EGD revealed that the whole gastric mucosa was hyperemic and edematous, with erosion of the attached diffuse white moss and active oozing of blood. Small flaps of mucosal necrosis and stripping could be visualized at the posterior wall of the gastric antrum, indicating a relatively healed mucosa compared with previous EGD findings (**Figure 2**). Pathologic findings of the biopsy specimens from the gastric antrum showed severe atrophic gastritis with erosion, atrophy, and loss of intrinsic glands; focal aggregation of lymphocytes in the lamina propria and mucosal muscular layer; multiple neutrophil infiltration; and the formation of small abscesses (**Figure 3**). Considering that bevacizumab has already been discontinued for almost 2 months, it can be concluded that the current presentation was not an effect of bevacizumab; we confirmed that his gastritis was associated with the immune checkpoint inhibitor sintilimab.

We suspended sintilimab administration and simultaneously changed the regimen to steroid therapy as follows: intravenous

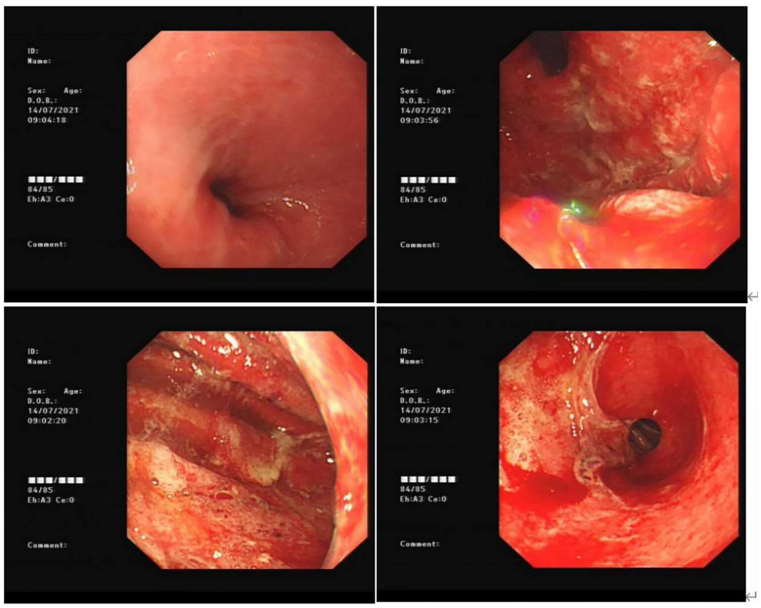

FIGURE 1 | Gastroscopy of acute erosive hemorrhagic gastritis for the first time (day 502). The esophageal mucosa was smooth with good contraction; the whole gastric mucosa was evidently edematous and hyperemic with opaque mucous adhesions on the surface. Diffuse erosion of white moss was seen, and active oozing of blood was extensively observed. The gastric antrum was found to have a necrotic mucosa with exfoliation of large flakes.

methylprednisolone sodium succinate drip (100 mg, once daily for 4 days; 70 mg, once daily for 3 days; and 40 mg, once daily for 3 days), followed by oral methylprednisolone tablets as maintenance therapy (32 mg once daily for a week; **Supplementary Figure 3**). His symptoms gradually subsided after this treatment. Re-examination of EGD on day 526 showed markedly relieved edematous and hyperemic gastric mucosa and no signs of active oozing of blood compared to previous EGD findings (**Figure 4**). The patient began to resume the next course of sintilimab treatment (200 mg, 42 days per cycle) starting in October (day 598). Approximately half a

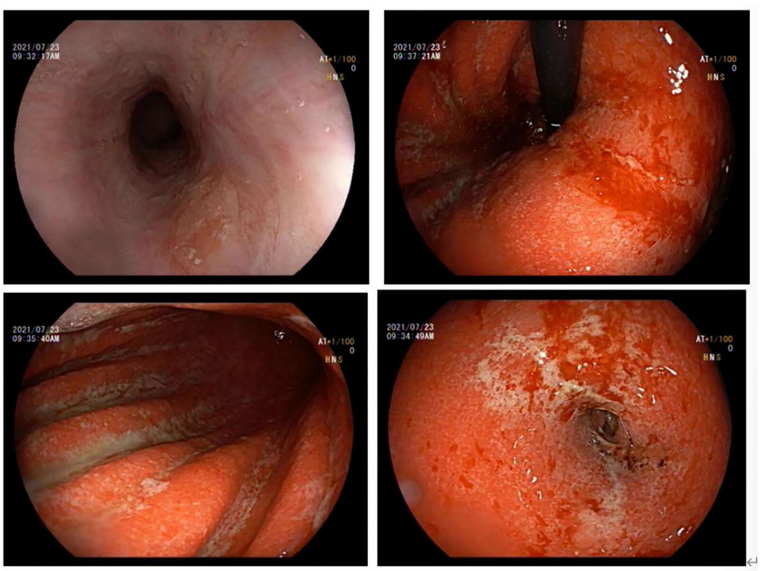

FIGURE 2 | Gastroscopy of acute erosive hemorrhagic gastritis after regular treatment (day 511). The esophageal mucosa was smooth with good contraction, and his EGD showed the whole gastric mucosa was hypermic and edematous, with diffuse erosion of white moss and active oozing of blood. Small flaps of mucosal necrosis and stripping could be seen at the posterior wall of the gastric antrum, which showed a relatively more healed condition than seen in the previous EGD.

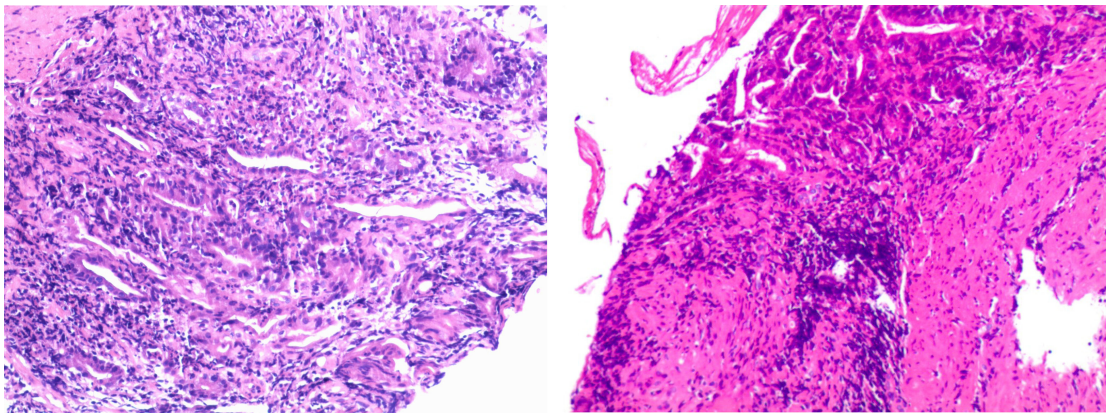

FIGURE 3 | Pathologic findings of the biopsy specimen showed severe atrophic gastritis with erosion, atrophy, and loss of intrinsic glands; focal aggregation of lymphocytes in the lamina propria and mucosal muscular layer; multiple neutrophil infiltration; and the formation of small abscesses.

month later (day 613), his EGD revealed that the entire gastric mucosa was hyperemic and edematous with white opaque mucus attachment; however, no erosion, ulcer, or mass was identified (**Supplementary Figure 5**).

DISCUSSION

Notably, ICIs are becoming an important component in treating metastatic malignancies. However, there are various organ-specific irAEs associated with the administration of ICIs that limit their widespread use, and in patients with severe irAEs, treatment with ICIs needs to be suspended or permanently discontinued; this greatly hampers the continuity of the treatment. Adverse events associated with ICIs are considered to arise after the inhibition of auto-regulatory signals, which leads to autoimmune-like events. There are grading criteria for ICI-associated colitis and diarrhea; although their diagnosis, disease classification, and treatment have already been established, patients with a certain severity may even require ICIs to be permanently discontinued. Thus far, there are no uniform criteria for grading the severity of ICI-associated gastritis, and the reports on ICI-associated gastritis are not only few but also lacking in terms of indications for therapy.

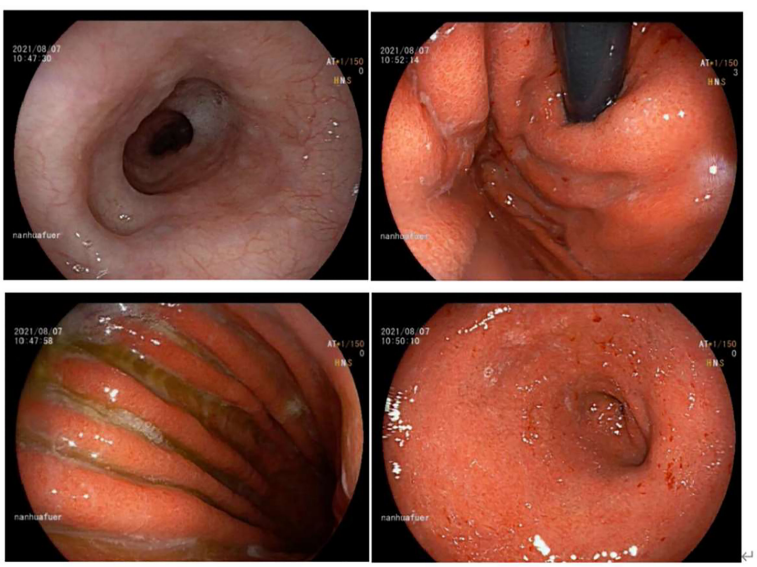

FIGURE 4 | Gastroscopy of acute erosive hemorrhagic gastritis after steriod treatment (day 526) showed marked improvements. The esophageal mucosa was smooth with good contraction. The whole gastric mucosa was hyperemic and edematous, with scattered flaky erosion (particularly in the gastric antrum) and partial bleeding. The gastric mucosa showed yellow–green bile and some white opaque mucus. Compared with the previous EGD findings, the mucosa as seen in this EGD was basically healed.

According to the 2021 guidelines of the Chinese Society of Clinical Oncology, the combination of PD-1/PD-L1 inhibitor and platinum-based chemotherapy is the first-line treatment regardless of PD-L1 expression in squamous and non-squamous NSCLC without mutational cancer drive genes. Administering a single PD-1/PD-L1 inhibitor has become the standard second-line option in patients with a PD-L1 tumor proportion score of ≥50% (7). The combination of Sintilimab + pemetrexed or carboplatin has been approved by the Chinese National Medical Products Administration as the first-line treatment of EFGR/ALK-negative, advanced non-squamous NSCLC. The ORIENT-11 study, which was a Chinese phase III study, showed that compared with the chemotherapy group patients, the sintilimab + chemotherapy group patients had significantly longer PFS (median 8.9 months vs. 5.0 months, P <0.00001) and improved ORR (51.9% vs. 29.8%, P = 0.00003). The supplementation of standard chemotherapy (pemetrexed and a platinum-based drug) with sintilimab in Chinese patients having previously untreated locally advanced or metastatic non-squamous NSCLC markedly prolonged their PFS with a manageable safety profile (7, 8). Additionally, the combination of anti-vascular endothelial growth factor (VEGF) agents and immune checkpoint blockade could have synergistic antitumor activity along with favorable tolerance in the tumor microenvironment, and notably, clinical evidence supports that a combination of an antiangiogenic agent and immunotherapy offers increased efficacy (9–11). Herbst et al. evaluated the safety and tolerability of pembrolizumab + ramucirumab in patients with advanced NSCLC and reported that the objective response rate was 30% and the disease control rate was 85% (12). In the IMpower150 clinical trial, the addition of atezolizumab to bevacizumab + chemotherapy significantly improved PFS and OS in patients with metastatic non-squamous NSCLC, and this outcome was unaffected by PD-L1 expression and EGFR or ALK genetic alteration status of the patients (13).

Bevacizumab is a recombinant humanized monoclonal antibody that binds to human VEGF and blocks its biological activity as an inhibitor of tumor angiogenesis. The adverse effects of bevacizumab affecting the digestive system typically manifest as diarrhea, nausea, vomiting, and abdominal pain. When the patient was first diagnosed with acute erosive hemorrhagic gastritis in April, we considered that bevacizumab may have induced the condition. Then, bevacizumab was discontinued, and the patient was treated with **sintilimab** alone as maintenance therapy. However, he was again diagnosed with acute erosive hemorrhagic gastritis two months later, and considering that it had already been two months since bevacizumab was stopped, bevacizumab was not considered to have caused this complication. Notably, the diagnostic process of ICI-related acute erosive hemorrhagic gastritis has exclusiveness; the patient's colonoscopy showed no abnormalities, which did not support the diagnosis of ICI-related colitis or inflammatory bowel disease (IBD). Additionally, the patient did not have a history of *Helicobacter pylori* infection or non-steroidal anti-inflammatory drug use, and his histopathology findings showed inflammatory cell infiltration, which was identified on the basis of the presence of lymphocytes in the lamina propria. Combined with the strong immunogenicity of PD-1, we hypothesized that his gastritis was triggered by **sintilimab**.

After the diagnosis of irAEs was clarified, the patient was advised to withhold ICI therapy and was started on periodic steroid de-escalation therapy (2, 14, 15). In most cases, acute erosive hemorrhagic gastritis can heal and the bleeding can stop without any intervention. However, in some cases, mucosal erosion may develop into ulcers, which usually respond well to drug therapy. During treatment progression, our patient responded well to steroids instead of regular drug therapy, which can further support **our diagnosis to be correct.**

Previous studies have suggested that the histopathological patterns of ICI-associated gastritis can be divided into three types: chronic active gastritis, lymphocytic gastritis, and focal enhancing gastritis (5, 16, 17). The pathological finding**s** of the gastric antrum in our case show severe atrophy of the gastric sinus mucosa with lymphocytic and neutrophil infiltration, with visibly evident local abscess formation but no signs of apoptotic bodies. Immunostaining identified these lymphocytes as predominantly CD3-positive T cells, CD4-positive helper T cells, and CD8-positive cytotoxic T cells, which is consistent with the pathological findings of ICI-associated gastritis (**Supplementary Figure 4**). Given that EGD images have features nonspecific to ICI-associated gastritis, immunostaining may greatly help diagnose upper GI disorders induced by ICIs. Interestingly, the spectrum of clinical presentations of ICI-related gastritis is limited and nonspecific, and endoscopic features range from mild inflammation to severe hemorrhagic gastritis.

Although checkpoint inhibitor-induced gastritis has been reported with PD-1 like nivolumab (18–20) and pembrolizumab (21), to our knowledge, the effects of sintilimab on the upper GI tract have not been described so far. We reported here a rare case of acute erosive hemorrhagic gastritis induced by sintilimab, suggesting a presentation consistent with the potent immunogenic effects shown by other ICIs. A few cases of acute erosive hemorrhagic gastritis caused by ICIs have been reported till date, and our case had more extensive and severe lesions than similar cases reported previously (18, 20–22). Therefore, we believe that this case report not only makes a case for adding a new subtype of ICI-associated gastritis but also provides a reference for future grading and treatment guidelines for ICI-associated gastritis.

Of course, this study has certain limitations: (1) interleukin-17 has been reported to be elevated in the serum of patients with ipilimumab-induced colitis, suggesting that cytokines may be involved in the pathophysiological process of immune-related adverse events; however, we did not perform the interleukin-17 relevant tests for in this case (23) (2). Patients with genetic polymorphisms associated with IBD may be more prone to ICI-associated, gastrointestinal tract-related immune adverse reactions, and it is believed that patients with IBD susceptibility genes should be considered for use in helping diagnosis as early as possible, in which case we did not refine the relevant tests (3). Although early administration of infliximab can improve the prognosi**s** of patients with ICI-related colitis, it has been suggested that the addition of infliximab in patients with severe ICI-related colitis should be considered only when the effect of glucocorticoids is poor at 48 h

after administration (15), and furthermore, it has also been suggested that diffuse lesions of ICI-associated colitis should be treated with biologics as early as possible (2, 14). Treatment with infliximab was not considered given the high price of infliximab, the lack of consensus guidelines for ICI-associated gastritis, and the fact that the clinical symptoms gradually resolved with glucocorticoids in this study.

CONCLUDING REMARKS

Taken together, early detection, early diagnosis, and early treatment are critical for irAEs to avoid the associated complications and enable the patient to continue ICIs. Early diagnosis and early use of immunosuppressive agents, such as glucocorticoids and infliximab, in treatment can be beneficial for patients. This case report will help standardize the treatment of ICI-associated gastritis, deepen our understanding of various types of irAEs, and help clinicians make the correct diagnosis and administer treatment promptly.

DATA AVAILABILITY STATEMENT

The original contributions presented in the study are included in the article/**Supplementary Material**. Further inquiries can be directed to the corresponding author.

ETHICS STATEMENT

Written informed consent was obtained from the individual(s) for the publication of any potentially identifiable images or data included in this article.

AUTHOR CONTRIBUTIONS

QA and WC wrote the paper, they have contributed equally to this work. YL provided technical or material support. GL designed the paper. All authors listed have made a substantial, direct, and intellectual contribution to the work and approved it for publication.

ACKNOWLEDGMENTS

The authors are grateful to the patient for consenting to share the medical information. We thank Medjaden Inc. for the scientific editing of this manuscript.

SUPPLEMENTARY MATERIAL

The Supplementary Material for this article can be found online at: https://www.frontiersin.org/articles/10.3389/fimmu.2022.840916/full#supplementary-material

Supplementary Figure 1 | Gastroscopy (day419) showed squamocolumnar junction blurred. Local mucosa was hyperemic and edematous. Flaky erosion was noted, and the surface was covered with white mucus. Oozing of blood was noted. A large amount of white opaque mucus was attached to the mucosal surface of the gastric antrum and body, and the gastric mucosa was diffusely hyperemic with spontaneous hemorrhaging.

Supplementary Figure 2 | Gastroscopy (day 449) showed an improved condition than seen on day 419.

Supplementary Figure 3 | Timeline of hospitalization and agents used. **(A)** Immunostaining shows CD3 positivity **(B)** CD4+ **(C)** CD8+ **(D)** HE4x10 **(E)** HE10X10 **(F)** HE20X10.

Supplementary Figure 4 | IHC **(A–C)** Immunostaining shows mainly CD3-positive **(A)** and CD4-positive **(B)** lymphocytes with CD8-positive cells **(C–F)** Histopathology shows inflammatory cell infiltration based on lymphocytes in the lamina propria. **(D)** Stomach (hematoxylin–eosin, 4x10, bar 100 μm). **(E)** Stomach (haematoxylin–eosin, 10x10, bar 100 μm). **(F)** Stomach (haematoxylin–eosin, 20x10, bar 100 μm).

Supplementary Figure 5 | Gastroscopy (day 613): Esophageal mucosa was smooth with good contraction. The whole gastric mucosa was hyperemic and edematous, with white opaque mucous attachments but no erosion, ulcer, or mass.

Supplementary Table 1 | Laboratory data Carbon 14 breath test was negative, and cytomegalovirus and Epstein–Barr virus detection showed previous infection, not current infection. Tuberculosis IgG antibody,HBC, HCV, syphilis antibody, and HIV were also negative.

REFERENCES

1. Ramos-Casals M, Brahmer JR, Callahan MK, Flores-Chavez A, Keegan N, Khamashta MA, et al. Immune-Related Adverse Events of Checkpoint Inhibitors. *Nat Rev Dis Primers* (2020) 6:38. doi: 10.1038/s41572-020-0160-6
2. Brahmer JR, Abu-Sbeih H, Ascierto PA, Brufsky J, Cappelli LC, Cortazar FB, et al. Society for Immunotherapy of Cancer (SITC) Clinical Practice Guideline on Immune Checkpoint Inhibitor-Related Adverse Events. *J Immunother Cancer* (2021) 9(6):e002435. doi: 10.1136/jitc-2021-002435
3. Shi Y, Su H, Song Y, Jiang W, Sun X, Qian W, et al. Safety and Activity of Sintilimab in Patients With Relapsed or Refractory Classical Hodgkin Lymphoma (ORIENT-1): A Multicentre, Single-Arm, Phase 2 Trial. *Lancet Haematol* (2019) 6:e12–9. doi: 10.1016/S2352-3026(18)30192-3
4. Tang T, Abu-Sbeih H, Luo W, Lum P, Qiao W, Bresalier RS, et al. Upper Gastrointestinal Symptoms and Associated Endoscopic and Histological Features in Patients Receiving Immune Checkpoint Inhibitors. *Scand J Gastroenterol* (2019) 54:538–45. doi: 10.1080/00365521.2019.1594356
5. Patil PA, Zhang X. Pathologic Manifestations of Gastrointestinal and Hepatobiliary Injury in Immune Checkpoint Inhibitor Therapy. *Arch Pathol Lab Med* (2021) 145:571–82. doi: 10.5858/arpa.2020-0070-RA
6. Martins F, Sofiya L, Sykiotis GP, Lamine F, Maillard M, Fraga M, et al. Adverse Effects of Immune-Checkpoint Inhibitors: Epidemiology, Management and Surveillance. *Nat Rev Clin Oncol* (2019) 16:563–80. doi: 10.1038/s41571-019-0218-0
7. Proto C, Ferrara R, Signorelli D, Lo Russo G, Galli G, Imbimbo M, et al. Choosing Wisely First Line Immunotherapy in Non-Small Cell Lung Cancer (NSCLC): What to Add and What to Leave Out. *Cancer Treat Rev* (2019) 75:39–51. doi: 10.1016/j.ctrv.2019.03.004
8. Yang Y, Wang Z, Fang J, Yu Q, Han B, Cang S, et al. Efficacy and Safety of Sintilimab Plus Pemetrexed and Platinum as First-Line Treatment for Locally

Advanced or Metastatic Nonsquamous NSCLC: A Randomized, Double-Blind, Phase 3 Study (Oncology Program by InnovENT Anti-PD-1-11). *J Thorac Oncol* (2020) 15:1636–46. doi: 10.1016/j.jtho.2020.07.014
9. Manegold C, Dingemans AC, Gray JE, Nakagawa K, Nicolson M, Peters S, et al. The Potential of Combined Immunotherapy and Antiangiogenesis for the Synergistic Treatment of Advanced NSCLC. *J Thorac Oncol* (2017) 12:194–207. doi: 10.1016/j.jtho.2016.10.003
10. Jenks S. New Therapy Targets Resistant Non-Small-Cell Lung Cancers. *J Natl Cancer Inst 106* (2014) 106(11):dju393. doi: 10.1093/jnci/dju393
11. Zhang Y, Zhao M, Cao S, Zhang X, Du Y. Unexpected Favorable Outcome to Sintilimab Plus Bevacizumab in an EGFR-Mutated Non-Small Cell Lung Cancer Patient: A Case Report. *Thorac Cancer* (2020) 11:2717–22. doi: 10.1111/1759-7714.13569
12. Bendell J, Herbst RS, Isambert N. A Phase 1 Study of Ramucirumab (R) Plus Pembrolizumab (P) in Patients (Pts) With Advanced Gastric or Gastroesophageal Junction (G/GEJ) Adenocarcinoma, Non-Small Cell Lung Cancer (NSCLC), or Urothelial Carcinoma (UC): Phase 1a Results. *J Clin Oncol* (2016) 34(15_suppl):3056–6. doi: 10.1200/JCO.2016.34.15_suppl.3056
13. Socinski MA, Jotte RM, Cappuzzo F, Orlandi F, Stroyakovskiy D, Nogami N, et al. Atezolizumab for First-Line Treatment of Metastatic Nonsquamous NSCLC. *N Engl J Med* (2018) 378:2288–301. doi: 10.1056/NEJMoa1716948
14. Postow MA, Sidlow R, Hellmann MD. Immune-Related Adverse Events Associated With Immune Checkpoint Blockade. *N Engl J Med* (2018) 378:158–68. doi: 10.1056/NEJMra1703481
15. Li Y, Wang H, Guo X, Zhou J, Duan L, Si X, et al. Clinical Diagnosis and Treatment of Immune-Related Adverse Events in Digestive System Related to Immune Checkpoint Inhibitors. *Zhongguo Fei Ai Za Zhi* (2019) 22:661–5. doi: 10.3779/j.issn.1009-3419.2019.10.10
16. Johncilla M, Grover S, Zhang X, Jain D, Srivastava A. Morphological Spectrum of Immune Check-Point Inhibitor Therapy-Associated Gastritis. *Histopathology* (2020) 76:531–9. doi: 10.1111/his.14029
17. Zhang ML, Neyaz A, Patil D, Chen J, Dougan M, Deshpande V. Immune-Related Adverse Events in the Gastrointestinal Tract: Diagnostic Utility of Upper Gastrointestinal Biopsies. *Histopathology* (2020) 76:233–43. doi: 10.1111/his.13963
18. Kobayashi M, Yamaguchi O, Nagata K, Nonaka K, Ryozawa S. Acute Hemorrhagic Gastritis After Nivolumab Treatment. *Gastrointest Endosc* (2017) 86:915–6. doi: 10.1016/j.gie.2017.04.033
19. Shi Y, Lin P, Ho EY, Nock CJ. Nivolumab-Associated Nausea and Vomiting as an Immune Adverse Event. *Eur J Cancer* (2017) 84:367–9. doi: 10.1016/j.ejca.2017.07.029
20. Boike J, Dejulio T. Severe Esophagitis and Gastritis From Nivolumab Therapy. *ACG Case Rep J* (2017) 4:e57. doi: 10.14309/crj.2017.57
21. Onuki T, Morita E, Sakamoto N, Nagai Y, Sata M, Hagiwara K. Severe Upper Gastrointestinal Disorders in Pembrolizumab-Treated Non-Small Cell Lung Cancer Patient. *Respirol Case Rep* (2018) 6:e00334. doi: 10.1002/rcr2.334
22. Nishimura Y, Yasuda M, Ocho K, Iwamuro M, Yamasaki O, Tanaka T, et al. Severe Gastritis After Administration of Nivolumab and Ipilimumab. *Case Rep Oncol* (2018) 11:549–56. doi: 10.1159/000491862
23. Harbour SN, Maynard CL, Zindl CL, Schoeb TR, Weaver CT. Th17 Cells Give Rise to Th1 Cells That Are Required for the Pathogenesis of Colitis. *Proc Natl Acad Sci USA* (2015) 112:7061–6. doi: 10.1073/pnas.1415675112

Conflict of Interest: The authors declare that the research was conducted in the absence of any commercial or financial relationships that could be construed as a potential conflict of interest.

Publisher's Note: All claims expressed in this article are solely those of the authors and do not necessarily represent those of their affiliated organizations, or those of the publisher, the editors and the reviewers. Any product that may be evaluated in this article, or claim that may be made by its manufacturer, is not guaranteed or endorsed by the publisher.

Copyright © 2022 Ai, Chen, Li and Li. This is an open-access article distributed under the terms of the Creative Commons Attribution License (CC BY). The use, distribution or reproduction in other forums is permitted, provided the original author(s) and the copyright owner(s) are credited and that the original publication in this journal is cited, in accordance with accepted academic practice. No use, distribution or reproduction is permitted which does not comply with these terms.

frontiers | Frontiers in Immunology

ORIGINAL RESEARCH
published: 03 June 2022
doi: 10.3389/fimmu.2022.829640

ASCL2 Affects the Efficacy of Immunotherapy in Colon Adenocarcinoma Based on Single-Cell RNA Sequencing Analysis

Lei Wu[1,2,3], Shengnan Sun[1,2], Fei Qu[4], Xiuxiu Liu[1,2], Meili Sun[3], Ying Pan[5], Yan Zheng[1] and Guohai Su[1,2]**

[1] Research Center of Translational Medicine, Central Hospital Affiliated to Shandong First Medical University, Jinan, China, [2] Research Center of Translational Medicine, Jinan Central Hospital, Shandong University, Jinan, China, [3] Department of Oncology, Central Hospital Affiliated to Shandong First Medical University, Zhuhai, China, [4] Department of Pathology, Central Hospital Affiliated to Shandong First Medical University, Jinan, China, [5] Department of Oncology, Zhuhai People's Hospital (Zhuhai Hospital Affiliated With Jinan University), Zhuhai, China

OPEN ACCESS

Edited by:
Hubing Shi,
Sichuan University, China

Reviewed by:
Guanyu Yan,
China Medical University, China
Huanwen Wu,
Peking Union Medical College Hospital (CAMS), China

***Correspondence:**
Yan Zheng
8793822@qq.com
Guohai Su
gttstg@163.com

Specialty section:
This article was submitted to Cancer Immunity and Immunotherapy, a section of the journal Frontiers in Immunology

Received: *06 December 2021*
Accepted: *06 May 2022*
Published: *03 June 2022*

Citation:
Wu L, Sun S, Qu F, Liu X, Sun M, Pan Y, Zheng Y and Su G (2022) ASCL2 Affects the Efficacy of Immunotherapy in Colon Adenocarcinoma Based on Single-Cell RNA Sequencing Analysis. Front. Immunol. 13:829640. doi: 10.3389/fimmu.2022.829640

Colon adenocarcinoma (COAD) is one of the leading causes of cancer-associated deaths worldwide. Patients with microsatellite instability-high (MSI-H) tumors were shown to highly benefit from immune checkpoint inhibitors (ICIs) than patients with microsatellite stable (MSS) tumors. Furthermore, the infiltration of immune cells and the expression of cancer stem cells (CSCs) in COAD were associated with the anti-tumor immune response. However, the potential mechanisms showing the relationship between microsatellite instability and CSCs or tumor-infiltrating immune cells (TIICs) have not been elucidated. Accumulating evidence reveals that achaete-scute family bHLH transcription factor 2 (ASCL2) plays a crucial role in the initiation and progression of COAD and drug resistance. However, the specific biological functions of ASCL2 in COAD remain unknown. In this study, we performed weighted gene co-expression network analysis (WGCNA) between MSS and MSI-H subsets of COAD. The results revealed that ASCL2 was a potential key candidate in COAD. Subsequently, the single-cell RNA-seq revealed that ASCL2 was positively associated with CSCs. Further, ASCL2 was shown to indirectly affect tumor immune cell infiltration by negatively regulating the expression of DUSP4. Finally, we inferred that the immunotherapy-sensitive role of ASCL2/DUSP4 axis on COAD is partly attributed to the activation of WNT/β-catenin pathway. In conclusion, this study revealed that ASCL2 was positively correlated to CSCs and tumor immune infiltration in COAD. Therefore, ASCL2 is a promising predictor of clinical responsiveness to anti-PD-1/PD-L1 therapy in COAD.

Keywords: colon adenocarcinoma, single-cell RNA-seq, microsatellite stable, microsatellite instability-high, immunotherapy

INTRODUCTION

Colon adenocarcinoma (COAD) is one of the leading causes of cancer-associated deaths worldwide (1). Conventional therapy for COAD includes surgery, targeted therapy, and chemotherapy. Despite progress in the treatment of COAD, the prognosis remains poor (2). Therefore, novel therapeutic strategies with high efficacy are urgently required.

An increasing number of new effective anti-tumor therapies have been developed (3). The activation of anti-tumor immune surveillance by immune checkpoint inhibitors is an attractive strategy (4). Immune checkpoint inhibitors (ICIs) such as programmed cell death-1 (PD-1) and programmed death-ligand 1 (PD-L1) inhibitors have made a significant breakthrough in COAD treatment (5).

Microsatellites are highly polymorphic DNA sequences located throughout the human genome. They display a high degree of inter-individual variation (6). Microsatellite instability (MSI) may occur due to mutations or epigenetic changes in DNA mismatch repair (MMR) genes, thus impairing the function of the DNA MMR system (7). High microsatellite instability (MSI-H) is the hallmark of tumors with a mismatch DNA repair deficiency (dMMR) (8). Immune checkpoint inhibitors were shown to be effective in dMMR/MSI-H subsets of COAD. However, ICIs were ineffective in microsatellite instability-low or microsatellite stable (MSI-L/MSS) and mismatch repair proficient (pMMR) subsets (9). However, the specific mechanism by which MSI-H/dMMR influences the efficacy of ICIs in COAD remains unknown.

Achaete-scute family bHLH transcription factor 2 (ASCL2) is a transcription factor that is over-expressed in colon cancer. Previous studies have shown that ASCL2 can affect anti-tumor drug sensitivity (10). Furthermore, recent studies have revealed that ASCL2 is associated with immune infiltration in colorectal cancer. Microsatellite stable colorectal cancer samples overexpressing ASCL2 were shown to have low $CD8^+$ T cell infiltration (11). Moreover, a vaccine targeting ASCL2 was shown to affect the efficacy of anti-PD-1 in colorectal cancer (12). Nevertheless, the potential mechanism behind the association of ASCL2 with immune infiltration and immunotherapy in COAD remains unknown.

In this study, we performed multiple methods between dMMR/MSI-H and pMMR/MSS of COAD. Meanwhile, ASCL2 might have an effect on tumor immune cell infiltration through an indirect mechanism by negatively regulating the expression of DUSP4. Finally, we inferred that immunotherapy-sensitive role of ASCL2/DUSP4 axis on COAD is attributed, at least partly, to the activation of WNT/β-catenin pathway. In brief, our findings elucidated that ASCL2 correlated with CSCs and tumor immune infiltration in COAD. ASCL2 might serve as a promising predictor of clinical responsiveness to anti-PD-1/PD-L1 therapy in COAD.

MATERIALS AND METHODS

Cell Culture

Human colon cancer cell line, HCT116 cells, were cultured in RPMI-1640 medium supplemented with 10% fetal bovine serum (FBS). The cells were grown in a humidified atmosphere supplemented with 5% CO_2 at 37°C.

Plasmid and siRNA Transfection

Two different small interfering RNAs (siRNAs) for specific inhibition of ASCL2 expression and a negative control siRNA were synthesized by Research cloud biology Co., Ltd. (Shandong, China). The ASCL2 gene was inserted into pcDNA3.1 by Boshang Biotechnology (Shandong, China). The empty vector was used as the negative control. Subsequently, exponentially growing untreated cells were plated 24 h before transfection. ASCL2-specific siRNA and pcDNA3.1-ASCL2 were transiently transfected with HCT116 cells using lipofectamine 2000 (Invitrogen, USA), and the cells were subsequently cultured for 48 hours. After that, total proteins were extracted for western blot analysis.

Western Blotting

Total protein was extracted from the HCT116 cells using RIPA buffer (Beyotime, China). Total proteins were separated in SDS-PAGE and then transferred onto PVDF membranes. After blocking with 5% nonfat milk for two hours at room temperature, the membranes were incubated overnight with the primary antibodies ASCL2 (1:1000, Abways Technology), DUSP4 (1:1000, ABclonal) and c-myc(1:1000, Proteintech) at 4°C. Subsequently, the membranes were incubated with the corresponding secondary antibodies, and visualization was done using enhanced chemiluminescence (ECL, Thermo Fisher Scientific).

Immunohistochemistry Analysis

For IHC analysis, the COAD and adjacent tissue paraffin-embedded slides were deparaffinized and rehydrated using xylene and a graded series of ethanol (100%, 95%, 80%, 75%), then washed with PBS three times for 5 minutes each time. Then, EDTA antigen restore solution was used to repair antigens on slices in a microwave oven at the condition of high heat for 5 min, heat preservation for 10 min, and high heat for 5 min followed by natural cooling, and washed with PBS three times for 5 minutes each time. Then immersed in 3% H_2O_2 solution at room temperature to abrogate endogenous peroxidase activity. The slides were incubated in 5% BSA to block non-specific binding of antibody for 1 hour, then incubated in a humidified chamber overnight at 4°C with the primary antibodies anti-ASCL2 (1:200 dilution; Bioss, Beijing, China). After PBS washes, the slides were subsequently incubated with goat anti-rabbit HRP secondary antibody for 60 min at room temperature, followed by PBS washes again. For a color reaction, slides were incubated with the DAB solution (Biyuntian Biotechnology Co., Ltd.). Subsequently, the slides were then counterstained with hematoxylin, dehydrated with graded alcohol series, covered-slipped with neutral balsam.

Data Acquisition and Selection

The transcriptome profiles of COAD were acquired from the TCGA database (https://portal.gdc.cancer.gov/), containing 473 COAD tissues and 41 non-tumor tissues. Microarray dataset GSE39582 was downloaded from the gene expression omnibus (GEO) database (https://www.ncbi.nlm.nih.gov/geo/).

The GPL570 dataset contained 519 samples, including 444 COAD tissues with pMMR and 75 COAD tissues with dMMR. The single-cell RNA sequencing data of human colon cancer samples (accession number GSE166555) were generated using 10× genomics. For accurate results, we used MSI patient as a benchmark, selected data source of C18.9 without lymph node metastasis samples for subsequent analysis.

Construction of Weighted Gene Co-Expression Network Analysis

The raw microarray data, GSE39582, were processed and normalized using R software (version 4.0.5) to identify significant mRNAs associated with the MMR status of COAD. The genes were ranked by SD values from large to small, and the top 25% genes were chosen for WGCNA analysis using R package "WGCNA" (13). $\beta = 3$ was selected as the soft threshold. After that, the minimum number of genes in a module was set at 100, with a total of six modules. Then, the Pearson correlation coefficient was calculated to determine the degree of association between the MMR status and the module. In general, the module with the absolute correlation coefficient ranked first among all the selected modules was considered related to the clinical trait. Finally, 736 genes that were most relevant to MSS/pMMR and MSI-H/dMMR were identified in the blue module.

Identification of Differentially Expressed Genes Between MSS/pMMR COAD and MSI-H/dMMR COAD

Differentially expressed genes (DEGs) were identified by comparing MSI-H/dMMR COAD tissues with MSS/pMMR COAD tissues using the R software. Adjusted P value < 0.05 and $|\log FC| > 1$ were set as the cut-off values. The analysis revealed 179 DEGs, including 91 upregulated and 88 downregulated DEGs.

Functional and Pathway Enrichment Analysis

Kyoto Encyclopedia of Genes and Genomes (KEGG) analysis was performed to annotate pathways in the KEGG pathway database and identify the potential biological mechanism of hub genes,. KEGG pathway enrichment was performed using R package "clusterProfiler" with $P < 0.05$ (R version 4.0.5) (14).

Identification of Hub Genes From Protein–Protein Interaction Network

The STRING database is a functional protein association database for forecasting protein-protein interactions (15). Cytoscape (version 3.8.2) was used to display the PPI network after the DEGs were uploaded to STRING (16). CytoHubba (version 0.1) was used to detect candidate hub genes based on the density of the maximum neighborhood component (DMNC) algorithm (17).

Processing of Single-Cell RNA-Seq Data

Single-cell RNA (scRNA) sequencing data was extracted from the human derived COAD with MSI and MSS group. For accurate results, we used MSI patient as a benchmark, selected data source of C18.9 without lymph node metastasis samples for subsequent analysis. The Seurat package in R software was used to organize and analyze the scRNA-seq data (18). Quality control was carried out as follows: 1) Genes expressed in less than ten cells were excluded; 2) cells expressing less than 200 unique gene counts were excluded. After that, the top 1000 highly variable genes were selected using "vst" of Seurat. Dimensionality reduction of scRNA-seq data was performed using the t-distributed stochastic neighbor embedding (tSNE) algorithm (19). An adjusted P value < 0.05, | log FC | > 0.5, pct 1≥0.5 and pct 2 < 0.5 were considered the cut-off values for identifying marker genes. In addition, different cell clusters were annotated using the SingleR algorithm (20).. Finally, the CellMarker database was used for manual verification and correction (21).

Correlation Analysis of ASCL2/DUSP4 With MSI and Immune Infiltration Cells in Pan-Cancer

The correlation between ASCL2/DUSP4 and MSI score and immune cells in several cancer types were analyzed in "Gene+" module of Sangerbox. In terms of colon cancer, to make reliable immune infiltration estimations, we utilized the immunedeconv, an R package which integrates TIMER algorithms. It mainly calculated the infiltration scores of six immune infiltration cells: CD4+ T cell, CD8+T cell, neutrophil, dendritic cell, B cell and macrophage.

Data Acquisition of Spatial Transcriptomic Dataset

The spatial transcriptomics dataset for colon cancer was obtained from the 10X Genomics website. The Visium Gene Expression Library (T1T2-E8) was prepared as described in the Visium Spatial Reagent Kits User Guide (CG000239 Rev D). Sequencing data were processed using Space Ranger.

Gene Set Enrichment Analysis

The GSEA was performed using the GSEA v4.1.0 software. COAD samples were classified into high-and low-expression groups using the median expression values of ASCL2 and DUSP4 as the cut-off values. The procedure followed the detailed protocol from the Broad Institute Gene Set Enrichment Analysis website (22). A gene set was considered significantly enriched at NOM p-value less than 0.05 and FDR q-value less than or equal to 0.1 (23).

Wnt/β-Catenin Pathway Inhibitor Response Predictions

To predict drug-sensitivity of ASCL2 and DUSP4, the pRRophetic package of R software was implemented to extrapolate half-maximal inhibitory concentration (IC50) values by building ridge regression model with ten-fold cross-validation. Wnt/β-catenin pathway inhibitor drug XAV939 and its genetic profiles were obtained from the Genomics of Drug Sensitivity in Cancer (GDSC).

Statistical Analyses

The boxplots for the two groups were analyzed using Wilcoxon test. Further, correlation analysis was carried out using Spearman

correlation test. For RNAseq data of Pan-cancer, expression levels were TPM-normalized. The statistical analyses were performed using R software (version 4.0.5). A p-value <0.05 was considered statistically significant.

RESULTS

Weighted Co-Expression Network Construction

Data obtained from the GSE39582 were preprocessed using R to obtain 21,654 genes used to construct the WGCNA networks. A total of 5,414 genes were used for cluster analysis using the WGCNA package. β = 3 was set as the soft threshold power (**Figures 1A, B**). The cluster dendrogram constructed based on the selected threshold identified nine color modules (**Figures 1C, D**). There were 195 genes in the black module, 736 genes in the blue module, 527 genes in the brown module, 278 genes in the green module, seven genes in the grey module, 187 genes in the pink module, 229 genes in the red module, 2196 genes in the turquoise module, and 419 genes in the yellow module. Finally, the mRNAs in the nine color modules were used to analyze the relationship between the modules and the traits (pMMR status and dMMR status). The blue module showed a high correlation with the pMMR and dMMR status compared with other modules (**Figure 1E**), indicating that genes in the blue module play significant roles in the treatment of COAD patients with PD-1/PD-L1 inhibitors. Details of specific gene names in blue module can be found in **Supplementary Table 1**.

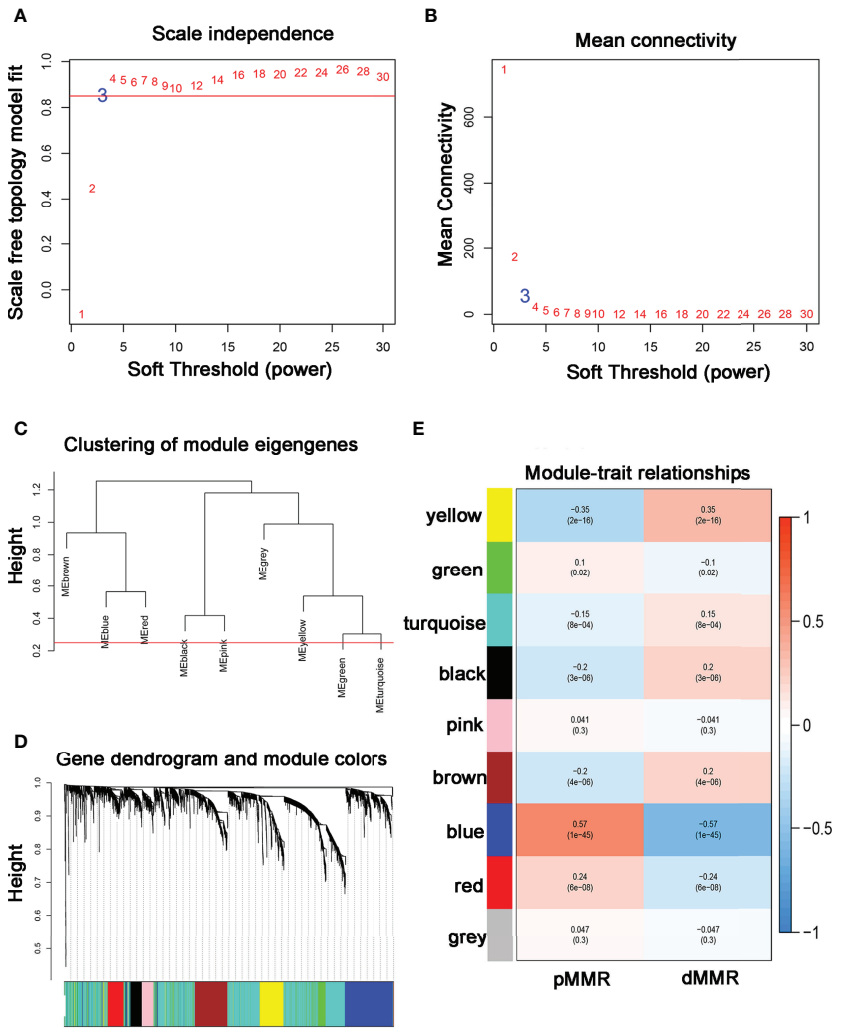

FIGURE 1 | Construction of co-expression modules using WGCNA **(A, B)** The most fit soft-thresholding power of WGCNA was 3. **(C)** Hierarchical clustering tree showing co-expression modules. **(D)** The cluster dendrogram of genes in GSE39582. **(E)** Heatmap showing the correlation between 9 modules and MMR status of COAD. The blue module showed the strongest correlation with pMMR and dMMR status ($p = 1\times10^{-45}$, r = -0.57).

Identification of Hub Genes and Functional Enrichment Analysis

The microarray dataset, GSE39582, revealed 179 DEGs (**Figure 2A**; **Supplementary Table 2**). After that, the 736 genes identified in the blue module were intersected with the 179 DEGs. In total, 92 common genes were identified through a comprehensive analysis of the two datasets (**Figure 2B**). Further, the KEGG pathway analysis revealed 18 signaling pathways that were concentrated on the overlapped 92 DEGs. The genes were mainly enriched in the Wnt signaling pathway, protein processing in the endoplasmic reticulum, chemokine signaling pathway, and colorectal cancer-related pathways (**Figure 2C**).

PPI Network Construction, Hub Gene Selection, and Hub Gene Expression in Pan-Cancer

The PPI network of the hub genes, including 33 nodes and 64 edges was constructed. Subsequently, the top ten hub genes (HOXC6, APCDD1, ASCL2, ZIC2, RNF43, FOXD1, OSR2, MLH1, AMFR, and WIF1) were selected based on the DMNC scores *via* the cytoHubba (**Figure 3A**). The scoring file is detailed in **Supplementary Table 3**. Immediately, we analyzed the expression of the top three genes, which tie for first place (HOXC6, APCDD1, and ASCL2) in multiple cancer types to explore possible roles of the genes in carcinogenesis. The results revealed that HOXC6, APCDD1, and ASCL2 were significantly upregulated in COAD compared with the adjacent non-tumor tissues, as shown in **Figures 3B–D**. Moreover, ASCL2 was highly expressed in COAD compared with HOXC6 and APCDD1 in multiple tumor types. As shown in **Supplementary Figures 4A, B**, high mRNA expression of ASCL2 was detected in human colon cancer cell lines and colon cancer tissues. Meanwhile, by immunohistochemistry, colon cancer tissues were found to express stronger ASCL2 than normal colon tissues (**Supplementary Figures 4C, D**). Taken together, ASCL2 may be a crucial regulator of carcinogenesis in COAD.

Single-Cell RNA-Seq Profiling of the Microsatellite Status

The single-cell RNA sequencing data of human colon cancer samples were generated using 10× genomics. For accurate results, we used MSI patient as a benchmark, selected data source of C18.9 without lymph node metastasis samples for subsequent analysis. The pathological stage and grade of the MSI patient were pT1 N0 and G2, respectively. The pathological stage and grade of the MSS patient were pT3 N0 and G2. Microsatellite status was determined by immunohistology for mismatch repair protein deficiency. We analyzed the single-cell RNA-seq data to identify the molecular features in the microsatellite status of colon cancer. A total of 4196 cell samples were acquired from two groups consisting of MSS-COAD and MSI-COAD. The number of detected genes and the sequencing count of each cell were illustrated in a quality control chart, as shown in **Figure 4A**. The number of genes detected was positive

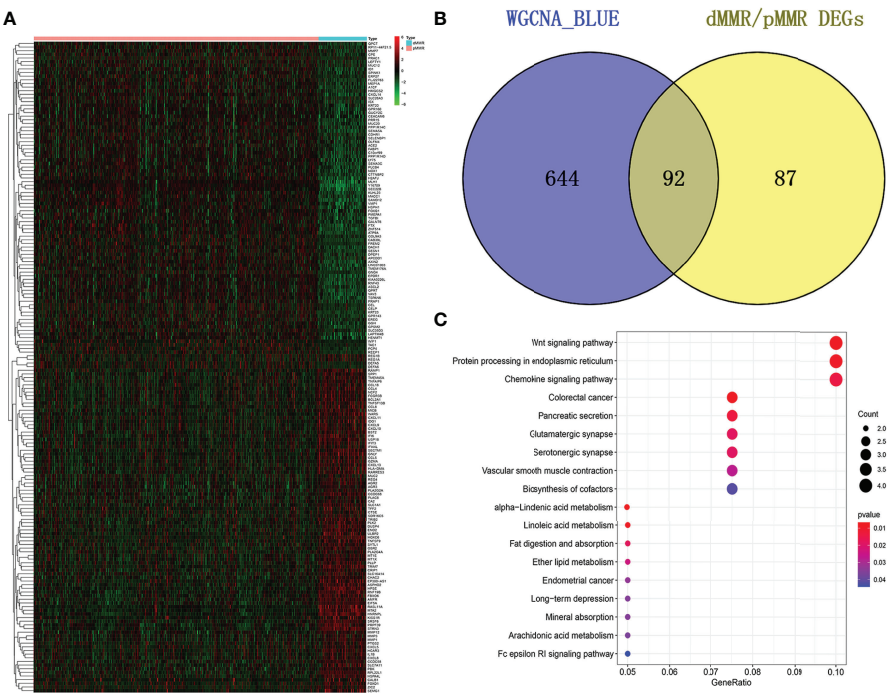

FIGURE 2 | Overlapping genes and enrichment analysis. **(A)** Heatmap of DEGs in the GSE39582 dataset. **(B)** A Venn diagram showing overlapping genes between dMMR/pMMR DEGs and WGCNA-MEblue genes. **(C)** The 18 significantly enriched pathways associated with the overlapping genes as determined through KEGG enrichment analysis.

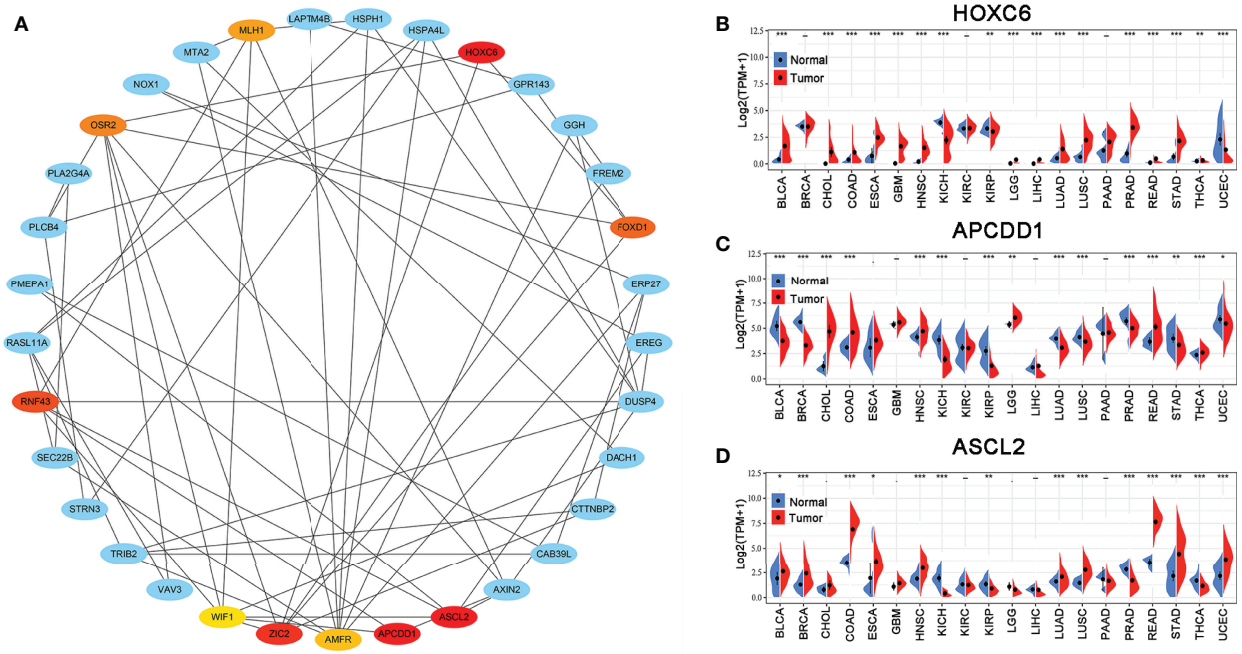

FIGURE 3 | PPI network and hub gene selection. **(A)** Top ten hub genes identified using the cytoHubba from Cytoscape based on DMNC scores. The darker the color, the higher the score. The expression levels of **(B)** HOXC6, **(C)** APCDD1, and **(D)** ASCL2 in multiple human cancers based on TCGA cancer and normal data. *p < 0.05, **p < 0.01, and ***p < 0.001.

correlated with the sequencing depth using Pearson's R = 0.67 (**Figure 4B**). In addition, the cells were mapped into two dimensions based on PC_1 and PC_2 components. The two correct independent cell subpopulations indicated the preferable clustering efficiency during the principal component analysis (PCA) procedure (**Figure 4C**). A total of 50 principal components (PCs) were selected for subsequent analysis (**Figure 4D**). Afterward, the tSNE algorithm was applied, and cells in COAD with MSS or MSI were classified into 17 separate clusters (**Figure 4E**). There were significant differences between the two groups in terms of the distribution of cells (**Figures 4F, G**).

Single-Cell RNA-Seq Screening of Microsatellite Status-Associated Marker Genes

Further, a total of 3911 unique marker genes from all 17 clusters were identified. Then, the adjusted P-value < 0.05, | log FC] | > 0.5, pct 1≥0.5 and pct 2 < 0.5 were considered the cut-off criteria for further screening to identify relevant marker genes. Ultimately, a total of 3166 marker genes (1968 unique genes) were identified for further analysis. The clusters were annotated using singleR and CellMarker according to the expression patterns of the marker genes. Cluster 0, containing 951 cells, was annotated as $CD4^+$ T cells, clusters 1 and 14, containing 728 cells, were annotated as $CD8^+$ T cells, cluster 2, containing 436 cells, was annotated as enterocytes, cluster 3, containing 385 cells, was annotated as B cells, cluster 4, containing 287 cells, was annotated as cancer stem cells, cluster 5, containing 284 cells, was annotated as monocytes, cluster 6, containing 246 cells, was annotated as epithelial cells, clusters 7, 8, 10, 12 and 13, containing 575 cells, were annotated as plasma cells, cluster 9, containing 111 cells, was annotated as fibroblasts, cluster 11, containing 98 cells, was annotated as goblet cells, cluster 15, containing 51 cells, was annotated as endothelial cells, while cluster 16, containing 44 cells, was annotated as mast cells (**Figure 5A**). The cells, especially the $CD4^+$ T cells, $CD8^+$ T cells, B cells, cancer stem cells, and enterocytes, were significantly altered in the MSI group compared to the MSS group. Then, we examined the expression of ASCL2 in the above 17 different cell types. As illustrated in **Figure 5B**, ASCL2 was highly expressed in cancer stem cells (cluster 4). mRNA expression-based stemness index (mRNAsi) is involved in maintaining cancer stem-like properties in specific tumor types. The OCLR algorithm constructed by Malta et al. (24) revealed that mRNAsi in the ASCL2-high expression group was significantly higher than that of the ASCL2-low expression group (**Figure 5C**). In previously **Figures 4F, G**, we identified that the cancer stem cells in the MSS group were significantly increased compared with the MSI group. This implies that ASCL2-related cancer stem cell signature could affect the efficacy of colon cancer immunotherapy.

Identification of DEGs in COAD

The genes were annotated based on Ensembl and the TCGA databases. Based on the given threshold (|log FC| >2 and adjust P -value < 0.05), 1570 differentially expressed genes

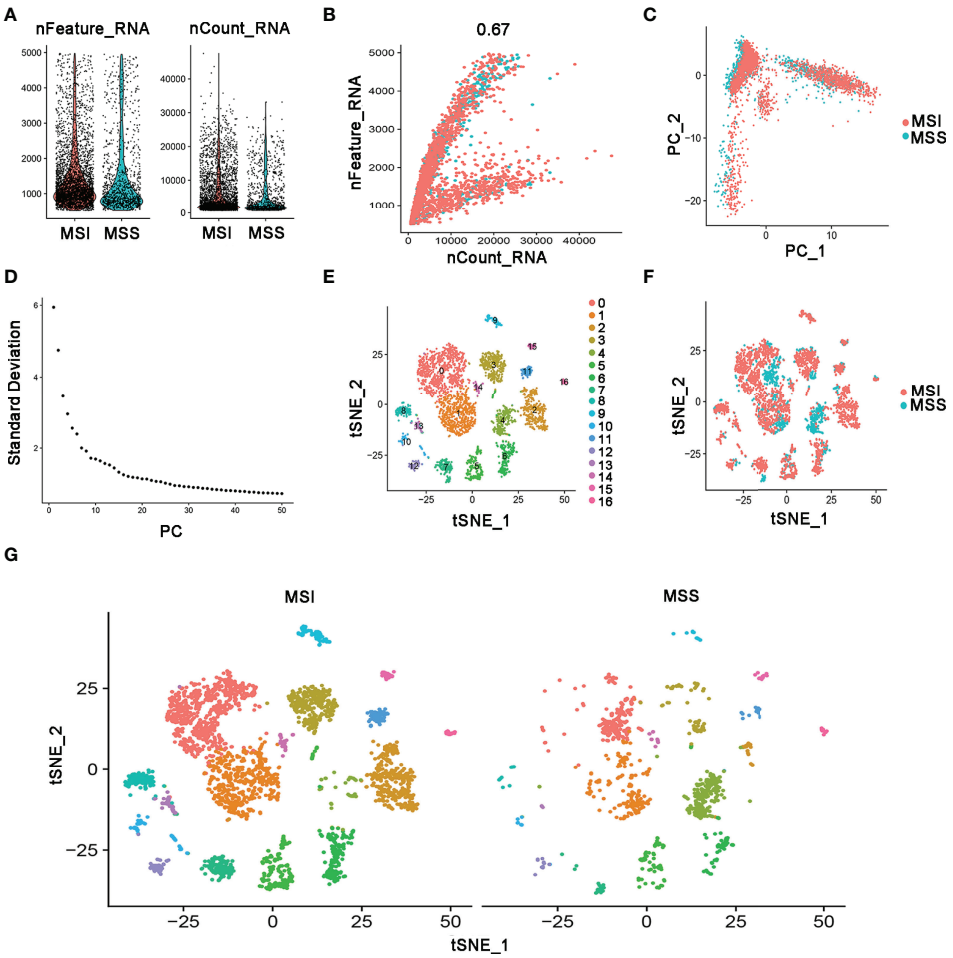

FIGURE 4 | Identification of 17 cell clusters in COAD by single-cell sequencing analysis. **(A)** A total of 4,196 cells identified after quality control. **(B)** Genes correlated with sequencing depth, with a Pearson's correlation coefficient of 0.67. **(C)** Comparison of batch effects between groups. **(D)** The 50 PCs with P value < 0.05 identified using PCA. **(E)** The 17 cell clusters classified using the tSNE algorithm. **(F, G)** The distribution of cells between MSS and MSI in COAD patients.

(DEGs) were identified between 473 COAD tissues and 41 normal tissues, of which 582 DEGs were upregulated and 988 DEGs were downregulated (**Supplementary Figure 1**; **Supplementary Table 4**).

The Enrichment of Candidate Genes in T Cells

The persistence of T cells *in vivo* may play a paramount role in the efficacy of immunotherapy with anti-PD-1/PD-L1. The Venn diagram identified five common genes (ASCL2, DUSP4, MT1E, RNF43, and TGFBI) in the four different gene expression datasets obtained by diverse data analysis methods, such as WGCNA, differential gene expression analysis, and single-cell sequencing analysis (**Figure 6A**). As shown in **Figures 6B–E**, only DUSP4 was highly expressed in CD4+ T cells (cluster 0) and CD8+ T cells (clusters 1 and 14). Based on this finding, we hypothesized that DUSP4 could enhance T cell expression, thus improving immunotherapy with anti-PD-1/PD-L1.

Correlation Between the Expression of ASCL2 and DUSP4 With MSI and Immune Landscape in Pan-Cancer

Microsatellite instability occurs in multiple cancer types and acts as a predictive biomarker for immunotherapy efficacy. Therefore, we determined the correlation between the expression of ASCL2 and DUSP4 with MSI in 32 cancer types. As shown in **Figure 7A**, the expression of ASCL2 was negatively correlated with MSI in COAD. In contrast, the expression of DUSP4 was positively correlated to MSI in COAD (**Figure 7B**). Notably, ASCL2 and DUSP4 had the highest association with MSI in COAD compared to the other cancer types. On the other hand, tumor-infiltrating immune cells (TIICs) are components of the tumor microenvironment that influence sensitivity to immunotherapy in multiple cancers. Hence, we explored the correlation between the expression of ASCL2 and DUSP4 with TIICs in Pan-cancer. The results revealed that ASCL2 was highly correlated to the infiltration levels of $CD4^+$ T cells, $CD8^+$ T cells,

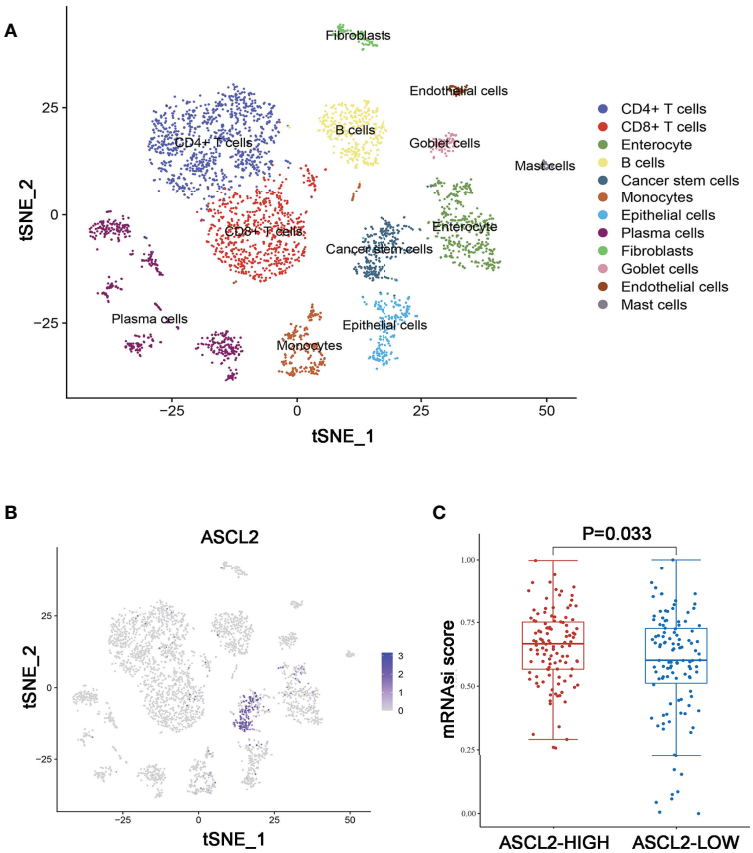

FIGURE 5 | Annotation of MSS/MSI COAD single-cell data set. **(A)** The 17 cell clusters were annotated into major types using singleR and CellMarker. **(B)** t-SNE plots of single-cell sequencing results showing that ASCL2 was expressed in cancer stem cells. **(C)** The distribution of mRNAsi in different groups, where the abscissa represents samples from different groups, and the ordinate represents the distribution of mRNAsi scores. The red dots represent the group with high expression of ASCL2, while blue dots represent the group with low expression of ASCL2.

B cells, neutrophils, and dendritic cells in the vast majority of cancer types. Furthermore, the expression of ASCL2 was inversely correlated to the immune cell infiltration level of $CD4^+$ T cells, $CD8^+$ T cells, B cells, neutrophils, and dendritic cells in COAD (**Figure 7C**). However, data from DUSP4 with diametrically opposed results in COAD (**Figure 7D**). Hence, the above results suggested that ASCL2 and DUSP4 expression were closely related to the extent of immune infiltration in multiple cancer types, including COAD. Moreover, there might be a mutually antagonistic effect between ASCL2 and DUSP4 in COAD.

Relationship Between the Immune Cell Infiltrates and the Expression of ASCL2 and DUSP4 in COAD Patients

The expression of six main infiltrating immune cell types, ($CD8^+$ T cells, $CD4^+$ T cells, B cells, neutrophils, dendritic cells, and macrophages) was determined and compared between ASCL2 and DUSP4 in COAD patients. The ASCL2 low expression group contained a higher proportion of $CD8^+$ T cells (P = 5.06e-10), neutrophils (P = 1.08e-13), dendritic cells (P =5.74e-13), B cells (P=1.67e-02), $CD4^+$ T cells (P = 4.89e-03), and macrophages (P = 4.89e-02) compared with the ASCL2 high expression group (**Figure 8A**). Conversely, the DUSP4 high expression group had a higher proportion of $CD8^+$ T cells (P = 9.75e-10), neutrophils (P = 3.31e-16), dendritic cells (P =5.36e-15), B cells (P=4.89e-03), and $CD4^+$ T cells (P = 3.03e-02) compared with the DUSP4 low expression group. However, there were no significant differences observed in the expression of macrophages (P = 5.89e-01) (**Figure 8B**).

Transcription Factor ASCL2 Regulated the Expression Level of DUSP4

The scRNA-seq analysis showed no significant enrichment of ASCL2 in $CD4^+$ T cells and $CD8^+$ T cells. However, the expression of ASCL2 was highly associated with the infiltration levels of CD4+ T cells and CD8+ T cells in various tumors, including COAD. JASPAR is a database for eukaryotic transcription factor binding profiles (25). The JASPAR database predicted six potential binding motifs on the promoter region of DUSP4 for binding the transcription factor ASCL2 (**Figure 9A**). Correlation analysis of ASCL2 and DUSP4 showed

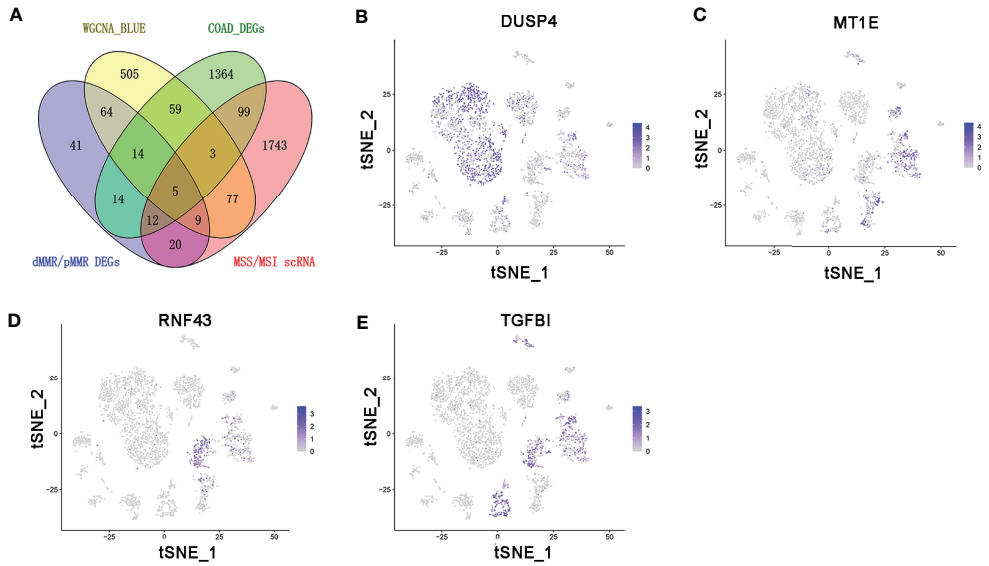

FIGURE 6 | The expression profile of DUSP4, MT1E, RNF43, and TGFBI is displayed on tSNE projection. **(A)** The Venn diagram showing the top 5 common genes (ASCL2, DUSP4, MT1E, RNF43 and TGFBI) included in 4 different gene expression datasets. **(B)** t-SNE plots of single-cell sequencing results showing that DUSP4 was expressed in CD4+ T cells (cluster 0) and CD8+ T cells (cluster 1 and 14). **(C)** t-SNE plots of single-cell sequencing results demonstrating that MT1E was expressed in enterocyte (cluster 2), epithelial cells (cluster 6), fibroblasts (cluster 9) and goblet cells (cluster 11). **(D)** t-SNE plots of single-cell sequencing results indicating that RNF43 was expressed in enterocyte (cluster 2) and cancer stem cells (cluster 4). **(E)** t-SNE plots of single-cell sequencing results demonstrating that TGFBI was expressed in enterocyte (cluster 2), cancer stem cells (cluster 4), monocytes (cluster 5), fibroblasts (cluster 9) and goblet cells (cluster 11).

a negative correlation between ASCL2 and DUSP4 (r = -0.520, p<0.001) (**Figure 9B**). Further, we knocked down the expression or elevated expression of ASCL2 using siRNA or pcDNA3.1-ASCL2 transfection into HCT116 cells to validate the results. As shown in **Figure 9C**, ASCL2 inhibition by siRNA or overexpression using a pcDNA3.1-ASCL2 plasmid was shown to increase or decrease the expression of DUSP4, respectively. These results suggested that ASCL2 negatively regulates DUSP4. Next, we carried out spatial transcriptomics analysis for the colon cancer tissues (**Figure 9D**). The results showed the enrichment of ASCL2 in colon cancer tissue is higher, while enrichment of DUSP4 is lower (**Figures 9E, F**). The gene expression patterns of ASCL2 and DUSP4 revealed by the spatial transcriptomics were consistent with the gene microarrays.

GSEA and Drug IC50 Values Analysis of ASCL2 and DUSP4 in COAD

We performed GSEA comparing colon cancer samples with high expression and low expression of ASCL2 and DUSP4 using TCGA dataset to identify pathways correlated with ASCL2 and DUSP4. The GSEA results revealed that ASCL2 and DUSP4 were all enriched in the WNT/β-catenin pathway. Further, as shown in **Figure 10A**, ASCL2 was positively associated with the WNT/β-catenin pathway. However, DUSP4 was negatively associated with the WNT/β-catenin pathway (**Figure 10B**). In addition, DUSP4 was positively correlated with the T cell receptor signaling pathways (**Figure 10C**). XAV939 is an inhibitor of WNT/β-catenin pathway, to investigate the effect of ASCL2 and DUSP4 in WNT/β-catenin pathway, the IC_{50} values of XAV939 on ASCL2 and DUSP4 were calculated. The prediction process was implemented by R package "pRRophetic" where the samples' half-maximal inhibitory concentration (IC50) was estimated by ridge regression and the prediction accuracy. The results of the IC_{50} values indicated a significant increase in the drug sensitivity of both ASCL2-LOW and DUSP4-HIGH to WNT pathway inhibitor in colon cancer (**Figures 10D, E**). Finally, we transfected ASCL2 over-expression and siRNA plasmids in colon cancer cells, and found ASCL2 positively regulates the expression of c-Myc expression, which is a key gene of the Wnt signaling pathway by western blot (**Supplementary Figure 3**). These results showed that the ASCL2 and DUSP4 were essential effectors in the WNT/β-catenin pathway.

DISCUSSION

Colon adenocarcinoma patients, especially those with dMMR/MSI-H, show significantly higher sensitivity to ICIs than COAD patients with pMMR/MSS (26, 27). However, metastatic colon cancer patients with MSI-H/dMMR treated with anti-PD-1 show an overall response rate (ORR) of about 33% (28). Therefore, it is important to investigate the underlying molecular mechanisms behind immunotherapy sensitivity. In this study, the differential gene expression and WGCNA analysis conducted between dMMR/MSS and pMMR/MSI-H of COAD revealed 92 hub genes. Furthemore, the PPI network and contrast analysis of the hub genes revealed that ASCL2 was highly correlated with the microsatellite status and abnormal expression of the hub genes.

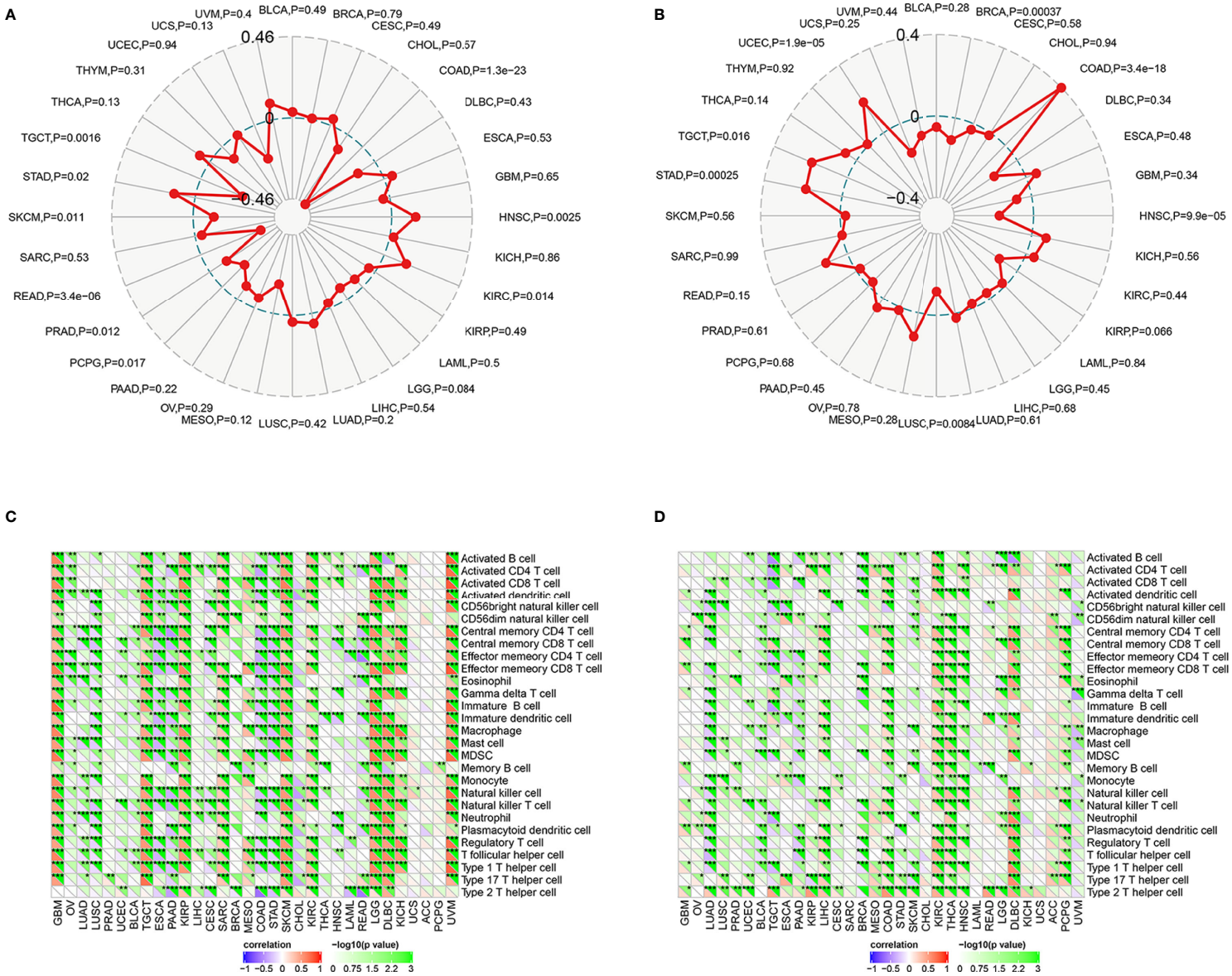

FIGURE 7 | Association of ASCL2 and DUSP4 expression with MSI and immune infiltration in Pan-cancer. Radar plots showing the association of **(A)** ASCL2 and **(B)** DUSP4 expression with MSI across 32 different cancer types. The red curve indicates the correlation coefficient. **(C)** Association of immune infiltration with ASCL2. **(D)** Association of immune infiltration with DUSP4. Positive correlations are shown in red, whereas negative correlations are shown bluish violet. *p < 0.05, **p < 0.01, and ***p < 0.001.

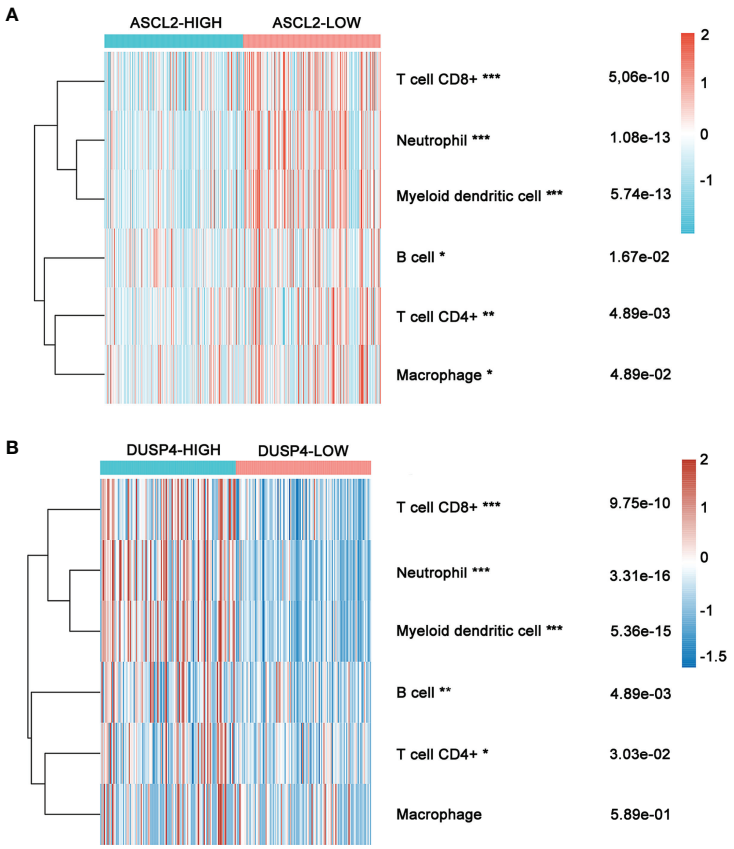

FIGURE 8 | Heatmap showing immune cell infiltration in COAD patients with high or low ASCL2 and DUSP4 expression. **(A)** Comparison of immune infiltration between the high-and low-expression of ASCL2 in COAD patients. **(B)** Comparison of immune infiltration between the high-and low-expression of DUSP4 in COAD patients. *p < 0.05, **p < 0.01, and ***p < 0.001.

Therefore, we hypothesized that ASCL2 might serve an important role in regulating microsatellite instability status and immunotherapy sensitivity in COAD.

The single-cell RNA-seq analysis revealed that the number of CD4+ T cells, CD8+ T cells, B cells, and cancer stem cells (CSCs) were altered significantly in the MSI group compared with the MSS group. Moreover, ASCL2 was highly expressed in CSCs. Accumulating evidence reveals that CSCs in tumors contributes to chemo and radio-resistance, metastasis, and tumor invasion (29, 30). The PD-1/PD-L1 signaling plays a crucial function in stemness maintenance of CSCs (31). On the other hand, T cell activity can be suppressed by CSCs (32). A previous study revealed that blockade of the PD-1/PD-L1 pathway with PD-1 orPD-L1 antibodies could inhibit the tumorigenic effect of colon cancer stem cells (33). Therefore, targeting CSCs with anti-PD-1/anti-PD-L1 shows promising therapeutic value. This study revealed that ASCL2 was highly expressed in colon cancer stem cells. In addition, mRNAsi showed higher expression in the ASCL2-high expression group than in the ASCL2-low expression group. Therefore, we inferred that an ASCL2-related cancer stem cell signature was likely to affect the efficacy of colon cancer immunotherapy.

Tumor-infiltrating immune cells (TIICs) are a part of the complex tumor microenvironment (TME). They can be effectively targeted by drugs and are correlated with clinical outcomes (34, 35). Colon adenocarcinoma is infiltrated by various TIICs, including T cells, B cells, NK cells, macrophages, and neutrophils. Previous studies have demonstrated that the density and type of TIICs within COAD affect treatment response and correlate to the prognosistic value (36–38). Several studies reveal that the tumor immune environment influences response to immunotherapeutics (39, 40). A previous study showed that an increased $CD8^+$ T cell density in post-treatment serial biopsies from responding melanoma patients treated with pembrolizumab (41). Further, the number of tumor-infiltrating $CD4^+$ and $CD8^+$ T cells in patients with MSI-H colorectal cancer who benefit from pembrolizumab immunotherapy was significantly higher than in the MSS colorectal cancer (42). Although TIICs and MSI play vital roles in the efficacy of immunotherapy with ICIs, the potential correlation between TIICs and MSI in COAD immunotherapy remains poorly understood. In the present study, ASCL2 expression was significantly correlated with the infiltration levels of CD4+ T cells, CD8+ T cells, B cells,

A

Table 1 Six potential binding motifs were obtained via JASPAR database on the promoter region of DUSP4 towards transcription factor ASCL2

Matrix ID	Name	Relative score	Sequence ID	Start	End	Strand	Predicted sequence
MA0816.1	Ascl2	0.851286671	NC_000008.11:c29352684-29350585	1380	1389	-	CGCTGCTGCC
MA0816.1	Ascl2	0.820274702	NC_000008.11:c29352684-29350585	1552	1561	-	GGCACCTGTG
MA0816.1	Ascl2	0.819934881	NC_000008.11:c29352684-29350585	864	873	+	CAGAGCTGCT
MA0816.1	Ascl2	0.811625697	NC_000008.11:c29352684-29350585	1552	1561	+	CACAGGTGCC
MA0816.1	Ascl2	0.810729706	NC_000008.11:c29352684-29350585	864	873	-	AGCAGCTCTG
MA0816.1	Ascl2	0.808417655	NC_000008.11:c29352684-29350585	1380	1389	+	GGCAGCAGCG

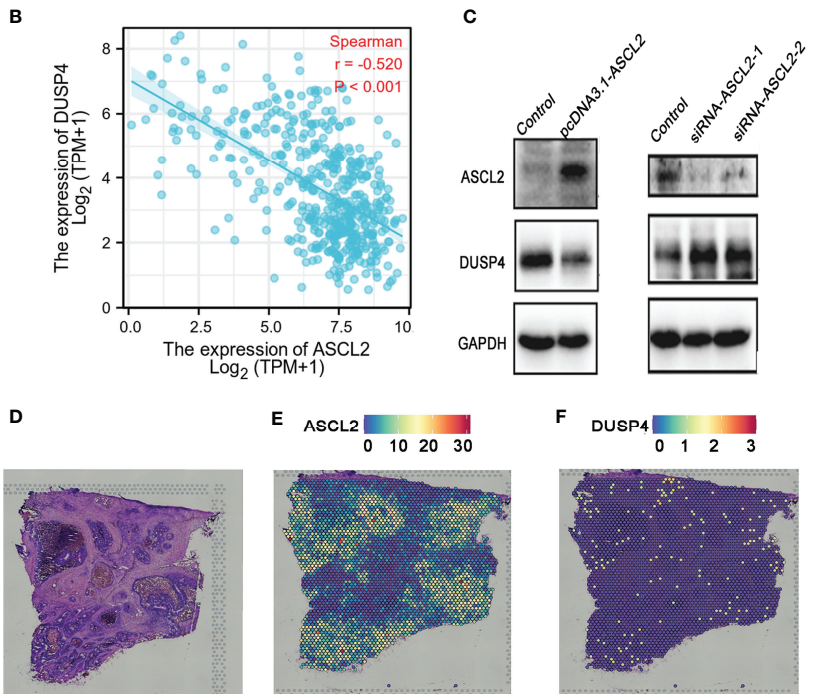

FIGURE 9 | DUSP4 expression was negatively regulated by ASCL2 in COAD samples. **(A)** Predicted ASCL2 binding sites within the region of DUSP4 promoter. **(B)** A scatter plot showing the association of ASCL2 with DUSP4 in COAD. **(C)** ASCL2 was upregulated in pcDNA3.1-ASCL2 group. DUSP4 expression was lower in pcDNA3.1-ASCL2 group than in the control group. ASCL2 expression was lower in si-ASCL2-1 and si-ASCL2-2 groups compared to control group. The decrease in ASCL2 expression was accompanied an increase in DUSP4 expression. **(D)** HE staining of colorectal cancer sections. Spatial transcriptomics expression of **(E)** ASCL2 and **(F)** DUSP4 in cancer tissue. Each dot represents a different locus at which gene expression was profiled.

neutrophils, and dendritic cells in various cancer types, including COAD. We revealed potential binding motifs on the promoter region of dual-specificity protein phosphatase 4 (DUSP4) towards transcription factor ASCL2. Moreover, the expression of ASCL2 was negatively associated with DUSP4 in COAD. In other words, ASCL2 could negatively regulate the expression of DUSP4 by binding specifically to the DUSP4 promoter region.

DUSP4 is involved in multiple cellular processes such as cell proliferation and immune response (43). Research shows that DUSP4 is a vital regulator of tumor development. However, it is not clear how DUSP4 affects the clinical and biological effects of tumors. Different tumor types showed different results (44–46). Previous studies revealed that the expression of DUSP4 was negatively associated with distant metastases in colorectal cancer (47). On the other hand, DUSP4 was highly in MSI-H than in MSS tumors (48). In this study, the single-cell RNA sequencing analysis revealed that DUSP4 was highly expressed in $CD4^+$ T cells and $CD8^+$ T cells. Moreover, DUSP4 expression was significantly correlated with the infiltration levels of $CD4^+$ T cells, $CD8^+$ T cells, B cells, neutrophils, and dendritic cells in various cancer types. The expression of ASCL2 was significantly correlated with the infiltration levels of CD4+ T cells, CD8+ T cells, B cells, neutrophils, and dendritic cells in various cancer types, including COAD. This implies that ASCL2 can indirectly

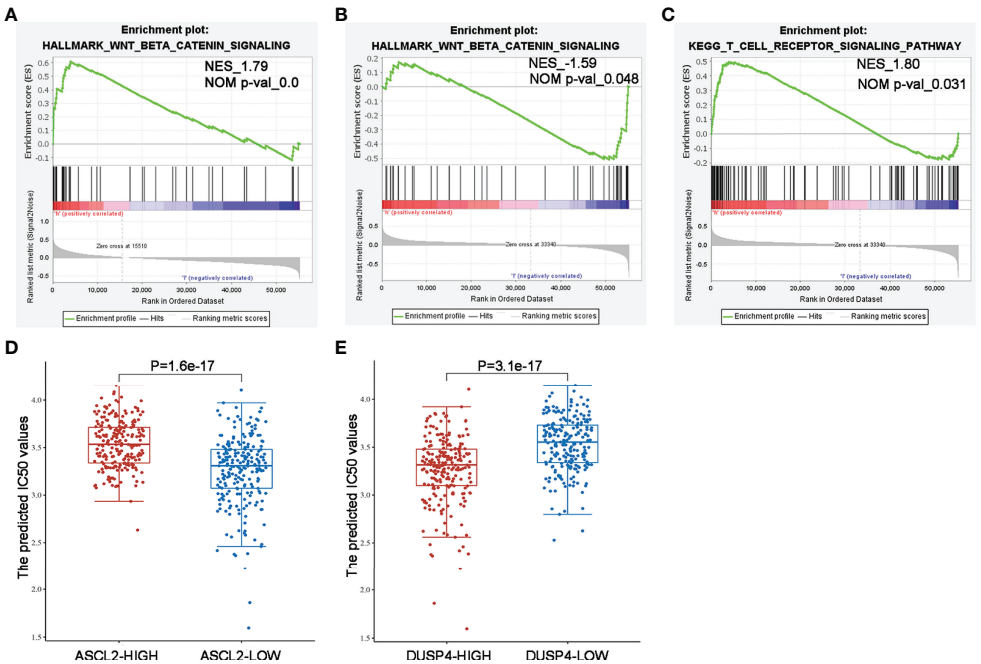

FIGURE 10 | GSEA enrichment and drug IC50 values analysis of ASCL2 and DUSP4 in COAD **(A)** WNT/β-catenin pathway was enriched in ASCL2-related COAD in the Hallmark category. **(B, C)** WNT/β-catenin pathway and T cell receptor signaling were differentially enriched in DUSP4-related COAD in the Hallmark/KEGG category. NES, normalized enrichment score. **(D)** IC_{50} values of Wnt pathway inhibitor was lower in ASCL2 low expression group compared to ASCL2 high expression group. **(E)** IC_{50} values of Wnt pathway inhibitor was higher in DUSP4 low expression group compared to DUSP4 high expression group.

affect the tumor immune microenvironment by regulating the expression of downstream target gene DUSP4. This revealed that the ASCL2 could affect immunotherapy response by direct regulation of colon cancer stem cells and indirect regulation of tumor-infiltrating immune cells.

The WNT/β-catenin signaling pathway is a tightly controlled pathway that regulates homeostasis and embryogenesis. Dysregulation of the WNT/β-catenin pathway is associated with several cancer types (49, 50). Previous studies revealed that the WNT/β-catenin pathway was aberrantly activated in colon cancer stem cells. Inhibition of the target proteins can block the signaling pathways, thereby affecting the stemness and proliferation of CSCs (51). Meanwhile, a recent study revealed that activation of the WNT/β-catenin pathway in colon cancer stem cells contributes to chemoresistance (52). Furthermore, the WNT/β-catenin pathway might play a vital role in the immunoregulation of the tumor microenvironment (53). Spranger et al. (54) found that overactivation of the WNT/β-catenin pathway reduced infiltration of T cells into tumor-immune microenvironment in a mouse model of primary melanoma, which subsequently decreased the efficacy of the ICIs. In addition, another study reported that overactivation of the WNT/β-catenin pathway could reduce the levels of interferon-γ (IFN-γ), thus suppressing the cytotoxic function of T lymphocytes (55). These findings indicate that the WNT/β-catenin pathway could be involved in immunosuppression and anti-tumor immune responses. Further, this study revealed that ASCL2 and DUSP4 were enriched in the WNT/β-catenin pathway. In addition, ASCL2 was positively correlated with the WNT/β-catenin pathway. However, DUSP4 was negatively regulated with the WNT/β-catenin pathway. Therefore, it was deduced that the immunotherapy-sensitive role of the ASCL2/DUSP4 axis on COAD is partly attributed to the activation of the WNT/β-catenin signaling.

CONCLUSION

In conclusion, ASCL2 was highly expressed in COAD. In addition, ASCL2 plays a significant role in microsatellite instability status, cancer stemness, and immune cell infiltration of COAD. Furthermore, the ASCL2/DUSP4 axis was identified as a downstream regulator of COAD. The ASCL2 could be used as a predictor of therapeutic response to anti-PD1/PD-L1 therapy in COAD. However, these results need to be validated in large clinical trials.

DATA AVAILABILITY STATEMENT

The original contributions presented in the study are included in the article/**Supplementary Material**. Further inquiries can be directed to the corresponding authors.

AUTHOR CONTRIBUTIONS

LW and, YZ, and GS conceived and designed the study. LW, SS and XL analyzed the data and revised the images. FQ performed the immunohistochemistry analysis. LW drafted the manuscript. MS and YP revised the manuscript. All authors contributed to the article and approved the submitted version.

FUNDING

This work was supported by the Scientific Research Foundation for the Introduced Talents of Jinan Central Hospital (YJRC2021011).

ACKNOWLEDGMENTS

The authors wish to thank everyone who has been of assistance in this study.

SUPPLEMENTARY MATERIAL

The Supplementary Material for this article can be found online at: https://www.frontiersin.org/articles/10.3389/fimmu.2022.829640/full#supplementary-material

REFERENCES

1. Sung H, Ferlay J, Siegel RL, Laversanne M, Soerjomataram I, Jemal A, et al. Global Cancer Statistics 2020: GLOBOCAN Estimates of Incidence and Mortality Worldwide for 36 Cancers in 185 Countries. *CA Cancer J Clin* (2021) 71(3):209–49. doi: 10.3322/caac.21660
2. Wu C. Systemic Therapy for Colon Cancer. *Surg Oncol Clin N Am* (2018) 27 (2):235–42. doi: 10.1016/j.soc.2017.11.001
3. Tabchi S, Kassouf E, Florescu M, Tehfe M, Blais N. Factors Influencing Treatment Selection and Survival in Advanced Lung Cancer. *Curr Oncol* (2017) 24(2):e115–22. doi: 10.3747/co.24.3355
4. Chen TT. Milestone Survival: A Potential Intermediate Endpoint for Immune Checkpoint Inhibitors. *J Natl Cancer Inst* (2015) 107(9). doi: 10.1093/jnci/djv156
5. Yaghoubi N, Soltani A, Ghazvini K, Hassanian SM, Hashemy SI. PD-1/ PD-L1 Blockade as a Novel Treatment for Colorectal Cancer. *BioMed Pharmacother* (2019) 110:312–8. doi: 10.1016/j.biopha.2018.11.105
6. De' Angelis GL, Bottarelli L, Azzoni C, De' Angelis N, Leandro G, Di Mario F, et al. Microsatellite Instability in Colorectal Cancer. *Acta BioMed* (2018) 89(9-S):97–101. doi: 10.23750/abm.v89i9-S.7960
7. Yang G, Zheng RY, Jin ZS. Correlations Between Microsatellite Instability and the Biological Behaviour of Tumours. *J Cancer Res Clin Oncol* (2019) 145 (12):2891–9. doi: 10.1007/s00432-019-03053-4
8. Lichtenstern CR, Ngu RK, Shalapour S, Karin M. Immunotherapy, Inflammation and Colorectal Cancer. *Cells* (2020) 9(3). doi: 10.3390/cells9030618
9. Ganesh K, Stadler ZK, Cercek A, Mendelsohn RB, Shia J, Segal NH, et al. Immunotherapy in Colorectal Cancer: Rationale, Challenges and Potential. *Nat Rev Gastroenterol Hepatol* (2019) 16(6):361–75. doi: 10.1038/s41575-019-0126-x
10. Tanaka T, Yamashita K. ASO Author Reflections: ASCL2, a Marker of Dynamic Colon Stem Cell, Involved in Wnt Pathway Activation Reflects Anti-Cancer Drug Resistance in Primary Colorectal Cancer. *Ann Surg Oncol* (2019) 26(Suppl 3):634. doi: 10.1245/s10434-019-07469-7
11. Yang Q, Huang G, Li L, Li E, Xu L. Potential Mechanism of Immune Evasion Associated With the Master Regulator ASCL2 in Microsatellite Stability in Colorectal Cancer. *J Immunol Res* (2021) 2021:5964752. doi: 10.1155/2021/5964752
12. Belnoue E, Leystra AA, Carboni S, Cooper HS, Macedo RT, Harvey KN, et al. Novel Protein-Based Vaccine Against Self-Antigen Reduces the Formation of Sporadic Colon Adenomas in Mice. *Cancers (Basel)* (2021) 13(4). doi: 10.3390/cancers13040845
13. Langfelder P, Horvath S. WGCNA: An R Package for Weighted Correlation Network Analysis. *BMC Bioinf* (2008) 9:559. doi: 10.1186/1471-2105-9-559
14. Yu G, Wang LG, Han Y, He QY. Clusterprofiler: An R Package for Comparing Biological Themes Among Gene Clusters. *OMICS* (2012) 16(5):284–7. doi: 10.1089/omi.2011.0118
15. Szklarczyk D, Gable AL, Nastou KC, Lyon D, Kirsch R, Pyysalo S, et al. The STRING Database in 2021: Customizable Protein-Protein Networks, and Functional Characterization of User-Uploaded Gene/Measurement Sets. *Nucleic Acids Res* (2021) 49(D1):D605–12. doi: 10.1093/nar/gkaa1074
16. Shannon P, Markiel A, Ozier O, Baliga NS, Wang JT, Ramage D, et al. Cytoscape: A Software Environment for Integrated Models of Biomolecular Interaction Networks. *Genome Res* (2003) 13(11):2498–504. doi: 10.1101/gr.1239303
17. Chin CH, Chen SH, Wu HH, Ho CW, Ko MT, Lin CY. Cytohubba: Identifying Hub Objects and Sub-Networks From Complex Interactome. *BMC Syst Biol* (2014) 8 Suppl 4(Suppl 4):S11. doi: 10.1186/1752-0509-8-S4-S11
18. Stuart T, Butler A, Hoffman P, Hafemeister C, Papalexi E, Mauck WM3rd, et al. Comprehensive Integration of Single-Cell Data. *Cell* (2019) 177(7):1888–1902.e21. doi: 10.1016/j.cell.2019.05.031
19. Satija R, Farrell JA, Gennert D, Schier AF, Regev A. Spatial Reconstruction of Single-Cell Gene Expression Data. *Nat Biotechnol* (2015) 33(5):495–502. doi: 10.1038/nbt.3192
20. Aran D, Looney AP, Liu L, Wu E, Fong V, Hsu A, et al. Reference-Based Analysis of Lung Single-Cell Sequencing Reveals a Transitional Profibrotic Macrophage. *Nat Immunol* (2019) 20(2):163–72. doi: 10.1038/s41590-018-0276-y
21. Zhang X, Lan Y, Xu J, Quan F, Zhao E, Deng C, et al. CellMarker: A Manually Curated Resource of Cell Markers in Human and Mouse. *Nucleic Acids Res* (2019) 47(D1):D721–8. doi: 10.1093/nar/gky900
22. Subramanian A, Tamayo P, Mootha VK, Mukherjee S, Ebert BL, Gillette MA, et al. Gene Set Enrichment Analysis: A Knowledge-Based Approach for Interpreting Genome-Wide Expression Profiles. *Proc Natl Acad Sci U.S.A.* (2005) 102(43):15545–50. doi: 10.1073/pnas.0506580102
23. Subramanian A, Kuehn H, Gould J, Tamayo P, Mesirov JP. GSEA-P: A Desktop Application for Gene Set Enrichment Analysis. *Bioinformatics* (2007) 23(23):3251–3. doi: 10.1093/bioinformatics/btm369
24. Malta TM, Sokolov A, Gentles AJ, Burzykowski T, Poisson L, Weinstein JN, et al. Machine Learning Identifies Stemness Features Associated With Oncogenic Dedifferentiation. *Cell* (2018) 173(2):338–354.e15. doi: 10.1016/j.cell.2018.03.034
25. Fornes O, Castro-Mondragon JA, Khan A, van der Lee R, Zhang X, Richmond PA, et al. JASPAR 2020: Update of the Open-Access Database of Transcription Factor Binding Profiles. *Nucleic Acids Res* (2020) 48(D1): D87–92. doi: 10.1093/nar/gkz1001
26. Overman MJ, McDermott R, Leach JL, Lonardi S, Lenz HJ, Morse MA, et al. Nivolumab in Patients With Metastatic DNA Mismatch Repair-Deficient or Microsatellite Instability-High Colorectal Cancer (CheckMate 142): An Open-Label, Multicentre, Phase 2 Study. *Lancet Oncol* (2017) 18(9):1182–91. doi: 10.1016/S1470-2045(17)30422-9
27. Bao X, Zhang H, Wu W, Cheng S, Dai X, Zhu X, et al. Analysis of the Molecular Nature Associated With Microsatellite Status in Colon Cancer Identifies Clinical Implications for Immunotherapy. *J Immunother Cancer* (2020) 8(2). doi: 10.1136/jitc-2020-001437
28. Le DT, Kim TW, Van Cutsem E, Geva R, Jäger D, Hara H, et al. Phase II Open-Label Study of Pembrolizumab in Treatment-Refractory, Microsatellite Instability-High/Mismatch Repair-Deficient Metastatic Colorectal Cancer: KEYNOTE-164. *J Clin Oncol* (2020) 38(1):11–9. doi: 10.1200/JCO.19.02107
29. Batlle E, Clevers H. Cancer Stem Cells Revisited. *Nat Med* (2017) 23 (10):1124–34. doi: 10.1038/nm.4409
30. Walcher L, Kistenmacher AK, Suo H, Kitte R, Dluczek S, Strauß A, et al. Cancer Stem Cells-Origins and Biomarkers: Perspectives for Targeted Personalized Therapies. *Front Immunol* (2020) 11:1280. doi: 10.3389/fimmu.2020.01280

31. Pan Q, Li Q, Liu S, Ning N, Zhang X, Xu Y, et al. Concise Review: Targeting Cancer Stem Cells Using Immunologic Approaches. *Stem Cells* (2015) 33 (7):2085–92. doi: 10.1002/stem.2039
32. Schatton T, Schütte U, Frank NY, Zhan Q, Hoerning A, Robles SC, et al. Modulation of T-Cell Activation by Malignant Melanoma Initiating Cells. *Cancer Res* (2010) 70(2):697–708. doi: 10.1158/0008-5472.CAN-09-1592
33. Seow HF, Yip WK, Fifis T. Advances in Targeted and Immunobased Therapies for Colorectal Cancer in the Genomic Era. *Onco Targets Ther* (2016) 9:1899–920. doi: 10.2147/OTT.S95101
34. Xiong Y, Wang Z, Zhou Q, Zeng H, Zhang H, Liu Z, et al. Identification and Validation of Dichotomous Immune Subtypes Based on Intratumoral Immune Cells Infiltration in Clear Cell Renal Cell Carcinoma Patients. *J Immunother Cancer* (2020) 8(1). doi: 10.1136/jitc-2019-000447
35. Shibutani M, Maeda K, Nagahara H, Fukuoka T, Iseki Y, Matsutani S, et al. Tumor-Infiltrating Lymphocytes Predict the Chemotherapeutic Outcomes in Patients With Stage IV Colorectal Cancer. *In Vivo* (2018) 32(1):151–8. doi: 10.21873/invivo.11218
36. Saito T, Nishikawa H, Wada H, Nagano Y, Sugiyama D, Atarashi K, et al. Two FOXP3(+)CD4(+) T Cell Subpopulations Distinctly Control the Prognosis of Colorectal Cancers. *Nat Med* (2016) 22(6):679–84. doi: 10.1038/nm.4086
37. Galon J, Costes A, Sanchez-Cabo F, Kirilovsky A, Mlecnik B, Lagorce-Pagès C, et al. Type, Density, and Location of Immune Cells Within Human Colorectal Tumors Predict Clinical Outcome. *Science* (2006) 313(5795):1960–4. doi: 10.1126/science.1129139
38. Peng D, Wang L, Li H, Cai C, Tan Y, Xu B, et al. An Immune Infiltration Signature to Predict the Overall Survival of Patients With Colon Cancer. *IUBMB Life* (2019) 71(11):1760–70. doi: 10.1002/iub.2124
39. Fridman WH, Pagès F, Sautès-Fridman C, Galon J. The Immune Contexture in Human Tumours: Impact on Clinical Outcome. *Nat Rev Cancer* (2012) 12 (4):298–306. doi: 10.1038/nrc3245
40. Gnjatic S, Bronte V, Brunet LR, Butler MO, Disis ML, Galon J, et al. Identifying Baseline Immune-Related Biomarkers to Predict Clinical Outcome of Immunotherapy. *J Immunother Cancer* (2017) 5:44. doi: 10.1186/s40425-017-0243-4
41. Tumeh PC, Harview CL, Yearley JH, Shintaku IP, Taylor EJ, Robert L, et al. PD-1 Blockade Induces Responses by Inhibiting Adaptive Immune Resistance. *Nature* (2014) 515(7528):568–71. doi: 10.1038/nature13954
42. De Smedt L, Lemahieu J, Palmans S, Govaere O, Tousseyn T, Van Cutsem E, et al. Microsatellite Instable vs Stable Colon Carcinomas: Analysis of Tumour Heterogeneity, Inflammation and Angiogenesis. *Br J Cancer* (2015) 113 (3):500–9. doi: 10.1038/bjc.2015.213
43. Seternes OM, Kidger AM, Keyse SM. Dual-Specificity MAP Kinase Phosphatases in Health and Disease. *Biochim Biophys Acta Mol Cell Res* (2019) 1866(1):124–43. doi: 10.1016/j.bbamcr.2018.09.002
44. Waha A, Felsberg J, Hartmann W, von dem Knesebeck A, Mikeska T, Joos S, et al. Epigenetic Downregulation of Mitogen-Activated Protein Kinase Phosphatase MKP-2 Relieves Its Growth Suppressive Activity in Glioma Cells. *Cancer Res* (2010) 70(4):1689–99. doi: 10.1158/0008-5472.CAN-09-3218
45. Bang S, Jee S, Kim H, Jang K, Park H, Myung JK, et al. Low DUSP4 Expression Is Associated With Aggressive Phenotypes and Poor Prognosis in Gastric Cancer. *In Vivo* (2021) 35(1):131–40. doi: 10.21873/invivo.12240
46. Ratsada P, Hijiya N, Hidano S, Tsukamoto Y, Nakada C, Uchida T, et al. DUSP4 is Involved in the Enhanced Proliferation and Survival of DUSP4-Overexpressing Cancer Cells. *Biochem Biophys Res Commun* (2020) 528 (3):586–93. doi: 10.1016/j.bbrc.2020.05.140
47. Saigusa S, Inoue Y, Tanaka K, Toiyama Y, Okugawa Y, Shimura T, et al. Decreased Expression of DUSP4 Is Associated With Liver and Lung Metastases in Colorectal Cancer. *Med Oncol* (2013) 30(3):620. doi: 10.1007/s12032-013-0620-x
48. Gröschl B, Bettstetter M, Giedl C, Woenckhaus M, Edmonston T, Hofstädter F, et al. Expression of the MAP Kinase Phosphatase DUSP4 Is Associated With Microsatellite Instability in Colorectal Cancer (CRC) and Causes Increased Cell Proliferation. *Int J Cancer* (2013) 132(7):1537–46. doi: 10.1002/ijc.27834
49. Bian J, Dannappel M, Wan C, Firestein R. Transcriptional Regulation of Wnt/β-Catenin Pathway in Colorectal Cancer. *Cells* (2020) 9(9). doi: 10.3390/cells9092125
50. Yu J, Li S, Guo J, Xu Z, Zheng J, Sun X. Farnesoid X Receptor Antagonizes Wnt/β-Catenin Signaling in Colorectal Tumorigenesis. *Cell Death Dis* (2020) 11(8):640. doi: 10.1038/s41419-020-02819-w
51. Gupta R, Bhatt LK, Johnston TP, Prabhavalkar KS. Colon Cancer Stem Cells: Potential Target for the Treatment of Colorectal Cancer. *Cancer Biol Ther* (2019) 20(8):1068–82. doi: 10.1080/15384047.2019.1599660
52. Wu X, Luo F, Li J, Zhong X, Liu K. Tankyrase 1 Inhibitior XAV939 Increases Chemosensitivity in Colon Cancer Cell Lines *via* Inhibition of the Wnt Signaling Pathway. *Int J Oncol* (2016) 48(4):1333–40. doi: 10.3892/ijo.2016.3360
53. Pai SG, Carneiro BA, Mota JM, Costa R, Leite CA, Barroso-Sousa R, et al. Wnt/beta-Catenin Pathway: Modulating Anticancer Immune Response. *J Hematol Oncol* (2017) 10(1):101. doi: 10.1186/s13045-017-0471-6
54. Spranger S, Bao R, Gajewski TF. Melanoma-Intrinsic β-Catenin Signalling Prevents Anti-Tumour Immunity. *Nature* (2015) 523(7559):231–5. doi: 10.1038/nature14404
55. Yaguchi T, Goto Y, Kido K, Mochimaru H, Sakurai T, Tsukamoto N, et al. Immune Suppression and Resistance Mediated by Constitutive Activation of Wnt/β-Catenin Signaling in Human Melanoma Cells. *J Immunol* (2012) 189 (5):2110–7. doi: 10.4049/jimmunol.1102282

Conflict of Interest: The authors declare that the research was conducted in the absence of any commercial or financial relationships that could be construed as a potential conflict of interest.

Publisher's Note: All claims expressed in this article are solely those of the authors and do not necessarily represent those of their affiliated organizations, or those of the publisher, the editors and the reviewers. Any product that may be evaluated in this article, or claim that may be made by its manufacturer, is not guaranteed or endorsed by the publisher.

Copyright © 2022 Wu, Sun, Qu, Liu, Sun, Pan, Zheng and Su. This is an open-access article distributed under the terms of the Creative Commons Attribution License (CC BY). The use, distribution or reproduction in other forums is permitted, provided the original author(s) and the copyright owner(s) are credited and that the original publication in this journal is cited, in accordance with accepted academic practice. No use, distribution or reproduction is permitted which does not comply with these terms.

frontiers | Frontiers in Oncology

ORIGINAL RESEARCH
published: 22 July 2022
doi: 10.3389/fonc.2022.746526

Cost-Utility Analysis of Camrelizumab Plus Chemotherapy Versus Chemotherapy Alone as a First-Line Treatment for Advanced Nonsquamous Non-Small Cell Lung Cancer in China

Ting Chen[1], *Ruixiang Xie*[1], *Qiuling Zhao*[1], *Hongfu Cai*[2] *and Lin Yang*[1]*

[1] Department of Pharmacy, Fujian Medical University Cancer Hospital, Fujian Cancer Hospital, Fuzhou, China,
[2] Department of Pharmacy, Fujian Medical University Union Hospital, Fuzhou, China

OPEN ACCESS

Edited by:
Benjamin Frey,
University Hospital Erlangen, Germany

Reviewed by:
Erdem Goker,
Ege University, Turkey
Angel Artal,
Hospital Universitario Miguel Servet, Spain

***Correspondence:**
Lin Yang
apera@163.com

Specialty section:
This article was submitted to Cancer Immunity and Immunotherapy, a section of the journal Frontiers in Oncology

Received: *24 July 2021*
Accepted: *06 June 2022*
Published: *22 July 2022*

Citation:
Chen T, Xie R, Zhao Q, Cai H and Yang L (2022) Cost-Utility Analysis of Camrelizumab Plus Chemotherapy Versus Chemotherapy Alone as a First-Line Treatment for Advanced Nonsquamous Non-Small Cell Lung Cancer in China. Front. Oncol. 12:746526. doi: 10.3389/fonc.2022.746526

Purpose: To evaluate the cost utility of camrelizumab plus standard chemotherapy versus standard chemotherapy alone as a first-line treatment for advanced nonsquamous non-small cell lung cancer (NSCLC) from the perspective of the Chinese health care system and to provide a reference for health decision-making.

Methods: A Markov model consisting of three health states was designed to evaluate the cost utility of these two treatment regimens for NSCLC patients with the incremental cost-effectiveness ratio (ICER) as the primary output indicator. Clinical data were derived from a published phase III clinical trial (CameL; ClinicalTrials.gov; NCT03134872). One-way sensitivity analysis and probabilistic sensitivity analysis were performed to assess the model uncertainty.

Results: Base case analysis showed that the ICER of camrelizumab plus chemotherapy compared with chemotherapy alone was $43,275.43 per QALY. It was higher than the willingness-to-pay (WTP) threshold of $31,510.57 per QALY in China, which has a standard of three times the GDP per capita recommended by the WHO. One-way sensitivity analysis showed that the utility value of PFS had the greatest influence on the results, and the other sensitive parameters were the cost of subsequent second-line therapy in the two group, the pemetrexed price, the cost of adverse event management and the utility value of PD. The probability sensitivity analysis showed that the probabilities of the cost-effectiveness of camrelizumab plus standard chemotherapy were 27.1%, 66.7% and 88.0% when the WTP values were $40,000, $50,000 and $60,000 per QALY, respectively.

Conclusions: Taking three times the GDP per capita in China as the WTP threshold, the camrelizumab plus standard chemotherapy regimen does not have a cost-effectiveness advantage compared with the standard chemotherapy regimen alone as a first-line treatment for advanced NSCLC.

Keywords: nonsquamous NSCLC, camrelizumab, chemotherapy, first-line treatment, cost-utility analysis

INTRODUCTION

Lung cancer is a kind of malignant tumor that seriously endangers human health, ranking first in incidence and mortality among malignant tumors in China (1). Non-small cell lung cancer (NSCLC) is the most common type of lung cancer, accounting for 85% to 90% of cases in China (2, 3). Most cases of lung cancer are found in an advanced stage when they are first diagnosed, and they lose the opportunity for surgery. From 2012 to 2014, the proportion of stage IIIA-IV lung cancer in China was 64.6% (2, 3). Over the past decade, the treatment of NSCLC has focused on systemic chemotherapy to extend the survival and improve the quality of life of advanced-stage patients. For example, based on histology, pemetrexed combined with platinum-based chemotherapy and maintenance therapy with pemetrexed is often used. With the development of molecular biology, lung cancer has ushered in the era of targeted therapy. Moreover, the development of immune checkpoint inhibitors (ICIs) in recent years has become a new milestone in cancer treatment, allowing untreated or multiline NSCLC patients to benefit from this treatment (4).

As a humanized immunoglobulin G4 monoclonal antibody, camrelizumab binds to the programmed cell death 1 (PD-1) receptor, blocks the binding of PD-1 and its ligand to reactivate T cells, and plays an antitumor role (5–8). Based on the results of CameL (9), camrelizumab has been approved in addition to pemetrexed and carboplatin as a first-line treatment for advanced or metastatic nonsquamous NSCLC and has been included in the Chinese Society of Clinical Oncology NSCLC guidelines for first-line treatment recommendations. The CameL study showed that the median overall survival (mOS) of camrelizumab plus chemotherapy as first-line treatment for advanced nonsquamous NSCLC was 27.9 months. Although the success of breaking through the two-year mark will bring good survival benefits to patients, high prices may bring a heavy socioeconomic burden to patients and the healthcare system. There is no uniform conclusion about its economic impact at present (10, 11), and the systematic review showed that checkpoint inhibitors as a first-line treatment for NSCLC has no economic advantage versus conventional chemotherapy regardless of PD-L1 level (12). Therefore, a cost-utility evaluation was performed to compare camrelizumab plus standard chemotherapy with standard chemotherapy alone as a first-line treatment for advanced nonsquamous NSCLC from the perspective of the Chinese health care system in this study. Information on these factors is required by healthcare decision makers to choose more reasonable treatments (13, 14).

MATERIALS AND METHODS

Clinical Data

Data were derived from CameL (9), which was a randomized, open-label, multicenter, phase III clinical trial conducted in 52 hospitals in China. The inclusion criteria were as follows: patients histologically or cytologically diagnosed with stage IIIB-V NSCLC, with measurable lesions, without prior systemic antitumor therapy, without epidermal growth factor receptor (EGFR) and anaplastic lymphoma kinase (ALK) alterations, without active brain metastasis, and with an Eastern Cooperative Oncology Group (ECOG) performance status of 0 or 1. A total of 412 patients were randomly divided (1:1) into a camrelizumab (200 mg) plus pemetrexed (500 mg/m^2) with carboplatin (area under curve [AUC], 5 mg/mL per min) group (n=205) or a pemetrexed (500 mg/m^2) with carboplatin (AUC 5 mg/mL per min) group (n=207), with a treatment cycle every 21 days. Patients in the two groups received 4-6 cycles of the above treatment and then maintenance therapy. The total camrelizumab exposure was up to a maximum of 34 cycles. The median progression-free survival (mPFS) was 11.3 months vs 8.3 months (hazard ratio [HR] =0.6, 95% confidence interval [CI]: 0.45-0.79, P =0.0001), and the mOS was 27.9 months vs 20.5 months in the camrelizumab plus chemotherapy group vs the chemotherapy alone group (HR=0.73, 95% CI: 0.55-0.96, P = 0.0117). Severe treatment-related adverse events occurred in 74 (36%) patients in the camrelizumab plus chemotherapy group and in 27 (13%) patients in the chemotherapy alone group.

Model Structure

In this study, cost-utility analysis was carried out by constructing and simulating a Markov model run in TreeAge Pro 2011 (TreeAge Software Inc, Williamstown, MA, USA). According to the progression of the tumor, the structure of the model was composed of three independent states: PFS state, progression survival state, and death. All patients were in a progression-free state when they were enrolled, and the death state was an absorbed state, as shown in **Figure 1**. The cycle period of the model was 21 days. The model simulation showed that almost all patients in the two groups died after 10 years. Therefore, the time limit of this study was set at 10 years (15–17). The output indicators of the model were the cost and quality-adjusted life years (QALYs) of the two groups, and then the incremental cost-effectiveness ratio (ICER) was calculated.

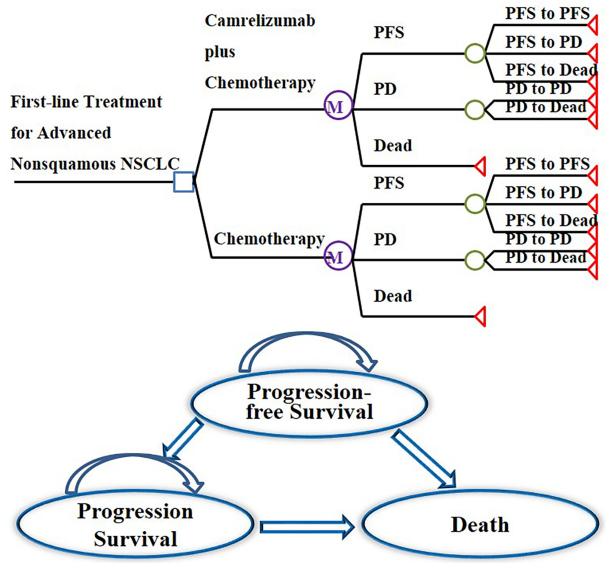

FIGURE 1 | Markov model structure of camrelizumab plus chemotherapy versus chemotherapy alone as first-line treatment for advanced nonsquamous NSCLC and bubble diagram for NSCLC.

Transition Probability

Engauge Digitizer software (version 12.1, https://github.com/markummitchell/engauge-digitizer/releases) was used to extract the PFS and OS curve data from the CameL study, a Weibull distribution was used to fit and extrapolate the Kaplan-Meier (KM) curves of the two groups, and R software (version 4.1.0, https://cran.r-project.org/mirrors.html) was used to obtain the scale parameter (λ) and shape parameter (γ) of the function, as shown in **Table 1**. The transition probability was calculated according to the principle of DEALE ($p = 1 - e^{-rt}$) (18). We assumed that the probability of transitioning from the PFS state to death was the local natural death rate.

Utility

Since the CameL study did not collect utility data, this study quoted the utility value of Chinese patients with metastatic nonsquamous NSCLC from published literature. The utility of PFS was 0.804, and the utility of progressive disease (PD) was 0.321 (19, 20).

Cost Inputs

From the perspective of the Chinese health care system, this study considered only direct medical costs, including drug costs, drug management costs, disease management costs, and the cost of handling adverse events of level 3 and above. The adverse event processing cost was equal to the incidence of grade 3 and above adverse reactions times the processing cost of a single event. **Table 2** shows the grade 3 or more treatment-related adverse events in CameL with an incidence greater than 3% (9). Reactive cutaneous capillary hyperplasia (RCCEP) was the most common immune-related adverse event of camrelizumab, but most of the cases were grade 1, with only 2 cases of grade 3 (<1%) and no grade 4-5 adverse events. The incidence was reported; therefore, the cost calculation was not included in this article.

The price of the drug in this study is the median value of the bid-winning price of each province (21), and other costs come from the charging standard of a tertiary hospital in Fujian Province in China. The price of camrelizumab is the latest price after medical insurance negotiations in 2020. Based on the actual situation, there is no room for further increase, so only the impact of the decline in the price of camrelizumab on the results is considered. According to the "Guidelines for the Evaluation of Chinese Pharmacoeconomics (2020)", all costs and output are discounted at an annual discount rate of 5% (22). The average exchange rate of Chinese Yuan renminbi for the entire year of 2020 is 6.8974 yuan per US dollar. It is assumed that the corresponding cost is incurred when the treatment is started in each cycle; therefore, the cost is not adjusted for the half cycle. The average body surface area is 1.71 m^2, which was calculated from the average height and weight data of Chinese adults obtained in the "Report on Nutrition and Chronic Disease Status of Chinese Residents (2020)" (23) and the sex ratio of patients in the CameL study according to Xu Wensheng's formula. The dose range and the lower limit of the treatment course were selected for the drug dosage and course of treatment. Referring to the other studies, it is assumed that docetaxel was used as the subsequent second-line chemotherapy, and nivolumab and camrelizumab as the immunotherapy, which is commonly used in China (10). The drug management cost was equal to the hospitalization cost plus the chemotherapy drug preparation injection cost. The two groups of patients were hospitalized for 3 days per cycle, the hospitalization cost per cycle was $55.67, and the chemotherapy drug preparation injection cost was different. The cost of drug administration in the chemotherapy alone group in the PFS state (>4 cycles) was the same as the cost of drug administration in the camrelizumab plus chemotherapy

TABLE 1 | Parameters for Weibull survival curve fitting.

Survival Curve-Fitting	Scale (λ)	Shape (γ)
Survival Curve Fitting of PFS of Camrelizumab plus Chemotherapy	0.021350	1.210605
Survival Curve Fitting of OS of Camrelizumab plus Chemotherapy	0.006578	1.263333
Survival Curve Fitting of PFS of Chemotherapy	0.057642	1.019433
Survival Curve Fitting of OS of Chemotherapy	0.010970	1.216254

TABLE 2 | Incidence rate of TRAEs.

	Camrelizumab plus Chemotherapy (n = 205)	Chemotherapy (n = 207)
Neutrophil count decreased	78 (38%)	63 (30%)
White blood cell count decreased	40 (20%)	30 (14%)
Anemia	38 (19%)	23 (11%)
Platelet count decreased	34 (17%)	24 (12%)
Lymphocyte count decreased	8 (4%)	5 (2%)
Alanine aminotransferase increased	10 (5%)	5 (2%)
Asthenia	7 (3%)	3 (1%)
Gamma-glutamyltransferase increased	6 (3%)	1 (<1%)

group in the PFS state (>34 cycles) (24, 25). The cost details are shown in **Table 3**.

Sensitivity Analysis

One-way sensitivity and probabilistic sensitivity analyses were used to evaluate the stability of the model results. One-way sensitivity analysis is used to analyze the influence of different parameters on ICERs in a certain range, and the results are presented by a tornado diagram. When the value range of the parameter can not be obtained, the variation range is ±25%. Considering the actual situation, the price of camrelizumab does not have the possibility of increasing, so only the impact of the price decline on ICER was analyzed. The probabilistic sensitivity analysis was performed using a bivalent Monte Carlo simulation. Assuming that each parameter follows a certain probability distribution, 1,000 repeated samples were taken, and ICER values of different treatment regimens were calculated based on each sample. The results of probabilistic sensitivity analysis are presented as an incremental cost-effectiveness scatter plot and an acceptability curve (26–28).

RESULTS

Base Case Analysis

The analysis results of the Markov model established in this study showed that within the 10-year study period, both camrelizumab plus chemotherapy and first-line chemotherapy alone had clinical benefits in the treatment of advanced NSCLC. Compared with chemotherapy alone, camrelizumab plus

TABLE 3 | Model parameters and distribution.

Parameters	Base value	Low	High	Distribution	Source
Cost					
Cost of camrelizumab, US$	424.51	318.38	424.51	Gamma	(21)
Cost of pemetrexed, US$	393.99	187.78	402.11	Gamma	(21)
Cost of carboplatin, US$	11.96	3.84	22.91	Gamma	(21)
Cost of chemotherapy pretreatment, US$	1.52	1.14	1.89	Gamma	Local charge
Cost of subsequent second-line therapy in the camrelizumab plus chemotherapy group, US$	392.61	294.46	490.76	Gamma	(10)
Cost of subsequent second-line therapy in the chemotherapy alone group, US$	698.77	524.08	873.46	Gamma	(10)
Cost of drug administration in the camrelizumab plus chemotherapy group in the progression-free survival state (≤4 cycles), US$	72.54	54.40	90.67	Gamma	Local charge
Cost of drug administration in the camrelizumab plus chemotherapy group in the progression-free survival state (>4 cycles and ≤34 cycles), US$	66.27	49.70	82.84	Gamma	Local charge
Cost of drug administration in the camrelizumab plus chemotherapy group in the progression-free survival state (>34 cycles), US$	65.58	49.19	81.98	Gamma	Local charge
Cost of drug administration in the chemotherapy alone group in the progression-free survival state (≤4 cycles), US$	71.85	53.89	89.82	Gamma	Local charge
Cost of drug administration in the chemotherapy alone group in the progression survival state (≤34 cycles), US$	56.36	42.27	70.45	Gamma	Local charge
Cost of disease management in the first 18 cycles, US$	60.64	45.48	75.80	Gamma	Local charge
Cost of disease management after 18 cycles, US$	48.68	36.51	60.85	Gamma	Local charge
Cost of adverse reactions in the camrelizumab plus chemotherapy group, US$	120.06	90.05	150.08	Gamma	Local charge
Cost of adverse reactions in the chemotherapy alone group, US$	80.32	60.24	100.40	Gamma	Local charge
Utility values					
Utility of PFS	0.804	0.536	0.883	Beta	(19, 20)
Utility of PD	0.321	0.05	0.473	Beta	(19, 20)
Discount rate (%)	5	0	8		(22)

TABLE 4 | Basic analysis results.

	Costs, US$	ΔCosts, US$	QALYs	ΔQALYs	ICER, US$/QALY
Chemotherapy	30,575.23	0	1.10	0	0
Camrelizumab plus Chemotherapy	45,393.28	14,818.05	1.44	0.34	43,275.43

chemotherapy could add 0.34 QALYs, with an incremental cost of $14,818.05 and a calculated ICER of $43,275.43 per QALY, as shown in **Table 4**. In 2020, the Chinese per capita GDP was $10,503.52 (29), so the willingness-to-pay (WTP), which is three times the per capita GDP according to the WHO, was $31,510.57. The ICER value was higher than the WTP, indicating that chemotherapy combined with camrelizumab was not economical compared with chemotherapy alone.

Sensitivity Analysis

One-Way Sensitivity Analysis

The results of one-way sensitivity analysis showed that the utility of PFS had the greatest influence on the results, and the other sensitive parameters were the cost of subsequent second-line therapy in the two group, the pemetrexed price, the cost of adverse event management and the utility value of PD. However, ICER generated when all parameters change within a certain range does not intersect with WTP, so the model is robust. The analysis results are shown in **Figure 2**.

Probabilistic Sensitivity Analysis

The bivalent Monte Carlo simulation was used for probabilistic sensitivity analysis, as shown in **Figures 3**, **4**. The scatter points are in the first quadrant of the coordinate axis, indicating that camrelizumab combined with chemotherapy can result in more QALYs but at a higher cost. As shown in **Figure 4**, when the WTP values were $40,000, $50,000 and $60,000 per QALY, the probabilities of the cost-effectiveness of camrelizumab combined with chemotherapy were 27.1%, 66.7% and 88.0%, respectively.

DISCUSSION

The main research and development direction of new antitumor drugs in the world is the development of drugs with strong targeting and few side effects. In recent years, tumor immunotherapy represented by ICIs has been the most eye-catching among the many approved new antitumor drugs, in addition to the targeted drugs of various small molecule tyrosine kinase inhibitors and large molecule monoclonal antibodies. Camrelizumab, a PD-1 inhibitor independently developed in China, was approved in June 2020 in combination with pemetrexed and carboplatin for the first-line treatment of unresectable locally advanced or metastatic nonsquamous NSCLC without EGFR and ALK alterations and was included

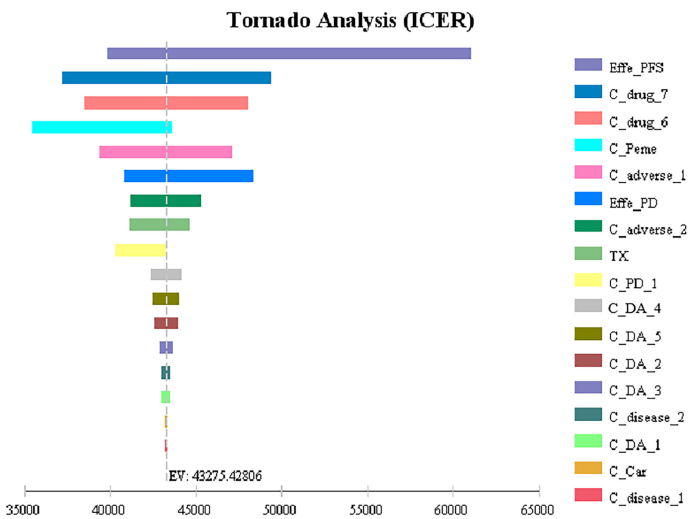

FIGURE 2 | Tornado diagrams for one-way sensitivity analysis Effe_PD, utility of PD; Effe_PFS, utility of PFS; C_Peme, cost of pemetrexed; C_drug_6, cost of subsequent second-line therapy in the chemotherapy group; C _drug_7, cost of subsequent second-line therapy in the camrelizumab plus chemotherapy group; C_adverse_2, cost of adverse reactions in the chemotherapy alone group; C_adverse_1, cost of adverse reactions in the camrelizumab plus chemotherapy group; C_PD_1, cost of the PD-1 inhibitor camrelizumab; TX, discount rate (%); C_Car, cost of carboplatin; C_disease_1, cost of disease management in the first 18 cycles; C_disease_2, cost of disease management after 18 cycles; C_pretreat, cost of chemotherapy pretreatment; C_DA_5, cost of drug administration in the chemotherapy alone group in the progression survival state (≤34 cycles); C_DA_4, cost of drug administration in the chemotherapy alone group in the progression-free survival state (≤4 cycles); C_DA_3, cost of drug administration in the camrelizumab plus chemotherapy group in the progression-free survival state (>34 cycles); C_DA_2, cost of drug administration in the camrelizumab plus chemotherapy group in the progression-free survival state (>4 cycles and ≤34 cycles); C_DA_1, cost of drug administration in the camrelizumab plus chemotherapy group in the progression-free survival state (≤4 cycles).

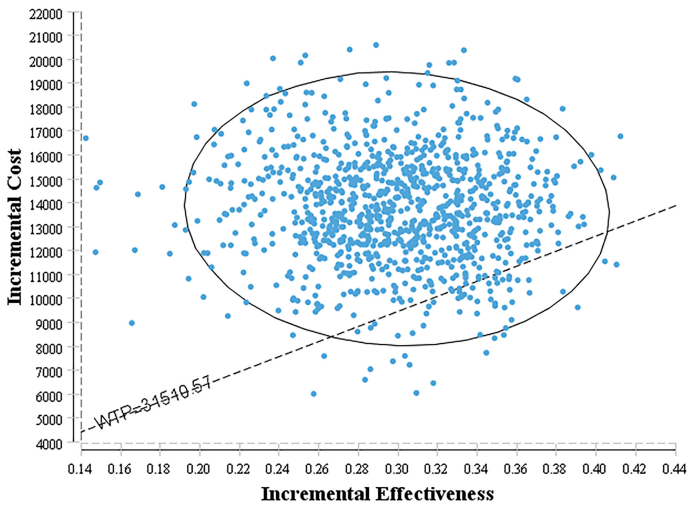

FIGURE 3 | Cost-effectiveness scatter plot.

in the first-line treatment recommendation of NSCLC and treatment guidelines of the Chinese Society of Clinical Oncology. On December 28, 2020, it was officially included in the medical insurance drug list with a price reduction of more than 80%. So far, the economic evaluations of camrelizumab have been inconsistent (10, 11), in order to determine the economic efficiency, we established a Markov model to evaluate the two treatment schemes from the aspects of cost and effectiveness.

The results of the basic analysis showed that compared with chemotherapy alone, the ICER of camrelizumab combined with chemotherapy was $43,275.43 per QALY, which was higher than the WTP of $31,510.57 and meant that camrelizumab combined with chemotherapy was not economic. This is different from the previous study which established a partitioned survival model (PSM) for patients and found that the ICER of camrelizumab plus chemotherapy compared with chemotherapy was $-7,382.72 per QALY (10). This may be related to the structural assumption adopted by PSM that the survival functions (i.e. PFS and OS) is independent, resulting in inaccurate predictions of PFS and OS. We established a Markov model which is classic in the economic evaluation of antitumor drugs. Our results are consistent with that of another study based on the same clinical trial (11). And the conclusion is consistent with the systematic review, which showed that ICIs as a first-line treatment for NSCLC has no economic advantage versus chemotherapy regardless of PD-L1 level, but they may be economic in developed countries (12). Of course, the WTP varies from country to country. In European

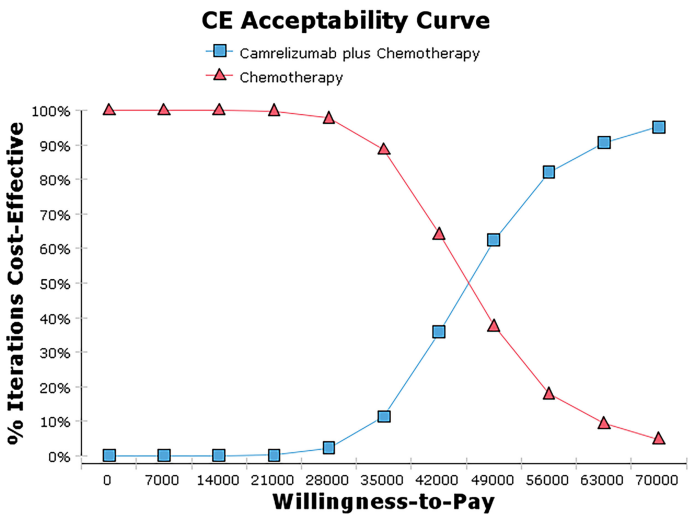

FIGURE 4 | Cost-effectiveness acceptability curve.

and American countries, the WTP for oncology drugs is significantly higher than that for general drugs and can reach $180,000.

One-Way sensitivity analysis showed that all parameters within the floating range would not reverse the result and the utility value of PFS had the greatest influence on the ICER. The cost of subsequent second-line therapy in the two group also had a significant impact on the results which might be related to the longer duration of the progressive state in terms of the OS of patients. The probability sensitivity analysis results showed that when the WTP values were $40,000, $50,000 and $60,000 per QALY, the probabilities of the cost-effectiveness of camrelizumab combined with chemotherapy were 27.1%, 66.7% and 88.0%, respectively. Considering the uneven regional economic development levels in China, if the WTP is set separately based on the per capita GDP of each province in 2020, then camrelizumab plus chemotherapy can be economical compared with chemotherapy alone in economically developed areas, including Beijing, Shanghai, Jiangsu, Fujian, Tianjin and Zhejiang (29). In addition, the survival time of patients in the final stages of life is more valuable to the patients themselves and society. Therefore, the choice of threshold is also an important factor affecting the economy of the result. It can be questioned whether accepting a higher ICER should be considered in antitumor drugs.

In the CameL study, the PFS times of PD-1-positive patients in the camrelizumab plus chemotherapy group and the chemotherapy alone group were 15.4 and 9.9 months, respectively (HR=0.56, 95% CI 0.39-0.82, one-sided P =0.0011). As of January 2021, the OS was 23.7 months in the chemotherapy group and not yet mature in the camrelizumab plus chemotherapy group. The better survival benefit of camrelizumab in PD-1-positive patients than in all patients may increase the probability of the cost-effectiveness of camrelizumab plus chemotherapy, and further studies may be conducted to determine whether PD-1 testing can help patients choose more cost-effective treatment options.

There are some limitations to this study. First, the survival data were derived from a phase III clinical trial rather than from a prospective real-world study. Second, according to the individual patient, the follow-up treatment plan is different in reality. Third, the utility values of this study were derived from a study of the utility values of NSCLC in the Chinese population, but the difference in the utility values caused by different treatment methods was not reflected. However, the one-way sensitivity analysis results of this study showed that the utility values in the PFS states had the most significant impact on the ICER results. Therefore, it is necessary to refine and measure the effectiveness value of different treatment methods and different states in Chinese patients with NSCLC in the future.

This study may be biased when it comes to real-world decision-making, we look forward to combining the Chinese economic development level with the social average WTP and starting real-world trials of NSCLC as soon as possible to improve the accessibility of new drugs to help cancer patients in the future.

CONCLUSIONS

From the perspective of the Chinese health care system, the camrelizumab plus standard chemotherapy regimen was unable to be cost-effective compared with the standard chemotherapy regimen alone as a first-line treatment for advanced NSCLC if three times the GDP per capita in China is taken as the WTP threshold. However, if the WTP is set separately based on the per capita GDP of each province in 2020, the camrelizumab plus standard chemotherapy regimen can be economical compared with chemotherapy alone in economically developed areas, including Beijing, Shanghai, Jiangsu, Fujian, Tianjin and Zhejiang.

DATA AVAILABILITY STATEMENT

The original contributions presented in the study are included in the article/supplementary material. Further inquiries can be directed to the corresponding author.

AUTHOR CONTRIBUTIONS

TC, HC and LY made substantial contributions to conception and design of the study. TC and QZ performed the data extraction, statistical analysis and drafted the article. RX revised manuscript of important intellectual content. LY reviewed and edited the manuscript. All authors contributed to the article and approved the submitted version.

FUNDING

This project was supported by Beijing Health Alliance Charitable Foundation (grant yxky-TQ20210), and Joint Funds for the innovation of science and Technology, Fujian province (2019Y9040).

REFERENCES

1. He J, Li N, Chen W, Wu N, Shen H, Jiang Y, et al. Guidelines for Screening, Early Diagnosis and Early Treatment of Lung Cancer in China (Beijing, 2021). *Chin J Oncol* (2021) 43:243–68. doi: 10.11735/j.issn.1004-0242.2021.02.A001
2. Shi J, Wang L, Wu N, Li J, Hui Z, Liu S, et al. Clinical Characteristics and Medical Service Utilization of Lung Cancer in China, 2005-2014: Overall Design and Results From a Multicenter Retrospective Epidemiologic Survey. *Lung Cancer* (2019) 128:91–100. doi: 10.1016/j.lungcan.2018.11.031
3. Zang R, Shi J, Lerut T, Wang L, Liu C, Brunelli A, et al. Ten-Year Trends of Clinicopathologic Features and Surgical Treatment of Lung Cancer in China. *Ann Thorac Surg* (2020) 109:389–95. doi: 10.1016/j.athoracsur.2019.08.017

4. Ettinger DS, Wood DE, Aggarwal C, Aisner DL, Akerley W, Bauman JR, et al. NCCN Guidelines Insights: Non-Small Cell Lung Cancer, Version 1. 2020. *J Natl Compr Canc Netw* (2019) 17:1464–72. doi: 10.6004/jnccn.2019.0059
5. Markham A, Keam SJ. Camrelizumab: First Global Approval. *Drugs* (2019) 79:1355–61. doi: 10.1007/s40265-019-01167-0
6. Song H, Liu X, Jiang L, Li F, Zhang R, Wang P. Current Status and Prospects of Camrelizumab, A Humanized Antibody Against Programmed Cell Death Receptor 1. *Recent Pat Anticancer Drug Discovery* (2021) 16:312-32. doi: 10.2174/1574892816666210208231744
7. Wang C, Sheng C, Ma G, Xu D, Liu X, Wang Y, et al. Population Pharmacokinetics of the Anti-PD-1 Antibody Camrelizumab in Patients With Multiple Tumor Types and Model-Informed Dosing Strategy. *Acta Pharmacol Sin* (2020) 42:1368–75. doi: 10.1038/s41401-020-00550-y
8. Shan Q, Wang H, Han X, Guo J, Wang Z. Duration of Immunotherapy in Patients With Advanced Lung Adenocarcinoma With Negative Driver Genes: Case Report and Literature Review. *Thorac Cancer* (2020) 11:3001–6. doi: 10.1111/1759-7714.13600
9. Zhou C, Chen G, Huang Y, Zhou J, Lin L, Feng J, et al. Camrelizumab Plus Carboplatin and Pemetrexed Versus Chemotherapy Alone in Chemotherapy-Naive Patients With Advanced non-Squamous non-Small-Cell Lung Cancer (CameL): A Randomised, Open-Label, Multicentre, Phase 3 Trial. *Lancet Respir Med* (2021) 9:305–14. doi: 10.1016/S2213-2600(20)30365-9
10. Zhu C, Xing X, Wu B, Liang G, Han G, Lin C, et al. Cost-Effectiveness Analysis of Camrelizumab Plus Chemotherapy vs. Chemotherapy Alone as the First-Line Treatment in Patients With IIIB-IV Non-Squamous Non-Small Cell Lung Cancer (NSCLC) Without EGFR and ALK Alteration From a Perspective of Health-Care System in China. *Front Pharmacol* (2021) 24:735536. doi: 10.3389/fphar.2021.735536
11. Xiang G, Gu L, Chen X, Wang F, Chen B, Zhao J, et al. Economic Evaluation of First-Line Camrelizumab for Advanced Non-Small-Cell Lung Cancer in China. *Front Public Health* (2021) 10:2021.743558. doi: 10.3389/fpubh.2021.743558
12. Li N, Zheng H, Zheng B, Chen C, Cai H, Liu M, et al. Economic Evaluations of Immune Checkpoint Inhibitors for Patients With Non-Small Cell Lung Cancer: A Systematic Review. *Cancer Manag Res* (2020) 12:4503–18. doi: 10.2147/CMAR.S248020
13. Aziz M, Tan LE, Tan W, Toh CK, Loke LPY, Pearce F, et al. Cost-Effectiveness Analysis of Pembrolizumab Monotherapy Versus Chemotherapy for Previously Untreated Advanced non-Small Cell Lung Cancer. *J Med Econ* (2020) 23:952–60. doi: 10.1080/13696998.2020.1775620
14. Ding H, Xin W, Tong Y, Sun J, Xu G, Ye Z, et al. Cost Effectiveness of Immune Checkpoint Inhibitors for Treatment of Non-Small Cell Lung Cancer: A Systematic Review. *PLos One* (2020) 15:e238536. doi: 10.1371/journal.pone.0238536
15. Cai H, Zhang L, Li N, Chen S, Zheng B, Yang J, et al. Cost-Effectiveness of Osimertinib as First-Line Treatment and Sequential Therapy for EGFR Mutation-Positive Non-Small Cell Lung Cancer in China. *Clin Ther* (2019) 41:280–90. doi: 10.1016/j.clinthera.2018.12.007
16. Weng X, Luo S, Lin S, Zhong L, Li M, Xin R, et al. Cost-Utility Analysis of Pembrolizumab Versus Chemotherapy as First-Line Treatment for Metastatic Non-Small Cell Lung Cancer With Different PD-L1 Expression Levels. *Oncol Res* (2020) 28:117–25. doi: 10.3727/096504019X15707883083132
17. Liu Q, Luo X, Peng L, Yi L, Wan X, Zeng X, et al. Nivolumab Versus Docetaxel for Previously Treated Advanced Non-Small Cell Lung Cancer in China: A Cost-Effectiveness Analysis. *Clin Drug Investig* (2020) 40:129–37. doi: 10.1007/s40261-019-00869-3
18. Olariu E, Cadwell K, Hancock E, Trueman D, Chevrou-Severac H. Current Recommendations on the Estimation of Transition Probabilities in Markov Cohort Models for Use in Health Care Decision-Making: A Targeted Literature Review. *Clinicoecon Outcomes Res* (2017) 1:537–46. doi: 10.2147/CEOR.S135445
19. Nafees B, Stafford M, Gavriel S, Bhalla S, Watkins J. Health State Utilities for Non Small Cell Lung Cancer. *Health Qual Life Outcomes* (2008) 6:84. doi: 10.1186/1477-7525-6-84
20. Nafees B, Lloyd AJ, Dewilde S, Rajan N, Lorenzo M. Health State Utilities in non-Small Cell Lung Cancer: An International Study. *Asia Pac J Clin Oncol* (2017) 13:e195–203. doi: 10.1111/ajco.12477
21. *Winning Price of Drugs in Each Province* . Available at: https://www.yaozh.com (Accessed May 5, 2021).
22. Wang L, Peng L, Peng Y, Li S, Wan X, Zeng X, et al. Comparative Analysis Between 2020 Version and 2011 Version on China Guidelines for Pharmacoeconomic Evaluation. *China J Pharm Economics* (2021) 16:5–8. doi: 10.12010/j.issn.1673-5846.2021.03.001
23. *Report on Nutrition and Chronic Diseases in China* (2020). Available at: https://www.nhc.gov.cn (Accessed June 10, 2021).
24. Wan N, Zhang T, Hua S, Lu Z, Ji B, Li L, et al. Cost-Effectiveness Analysis of Pembrolizumab Plus Chemotherapy With PD-L1 Test for the First-Line Treatment of NSCLC. *Cancer Med* (2020) 9:1683–93. doi: 10.1002/cam4.2793
25. Georgieva M, Da SNLJ, Aguiar PJ, De LLGJ, Haaland B. Cost-Effectiveness of Pembrolizumab as First-Line Therapy for Advanced non-Small Cell Lung Cancer. *Lung Cancer* (2018) 124:248–54. doi: 10.1016/j.lungcan.2018.08.018
26. Wu B, Zhang Q, Sun J. Cost-Effectiveness of Nivolumab Plus Ipilimumab as First-Line Therapy in Advanced Renal-Cell Carcinoma. *J Immunother Cancer* (2018) 6:124. doi: 10.1186/s40425-018-0440-9
27. Shay R, Nicklawsky A, Gao D, Lam ET. A Cost-Effectiveness Analysis of Nivolumab Plus Ipilimumab Versus Pembrolizumab Plus Axitinib and Versus Avelumab Plus Axitinib in First-Line Treatment of Advanced Renal Cell Carcinoma. *Clin Genitourin Cancer* (2021) 19:370-370.e7. doi: 10.1016/j.clgc.2021.01.009
28. Lin S, Luo S, Zhong L, Lai S, Zeng D, Rao X, et al. Cost-Effectiveness of Atezolizumab Plus Chemotherapy for Advanced Non-Small-Cell Lung Cancer. *Int J Clin Pharm* (2020) 42:1175–83. doi: 10.1007/s11096-020-01076-3
29. *Statistical Communique of the People's Republic of China on the 2020 National Economic and Social Development* (Accessed May 7, 2021).

Conflict of Interest: The authors declare that the research was conducted in the absence of any commercial or financial relationships that could be construed as a potential conflict of interest.

Publisher's Note: All claims expressed in this article are solely those of the authors and do not necessarily represent those of their affiliated organizations, or those of the publisher, the editors and the reviewers. Any product that may be evaluated in this article, or claim that may be made by its manufacturer, is not guaranteed or endorsed by the publisher.

Copyright © 2022 Chen, Xie, Zhao, Cai and Yang. This is an open-access article distributed under the terms of the Creative Commons Attribution License (CC BY). The use, distribution or reproduction in other forums is permitted, provided the original author(s) and the copyright owner(s) are credited and that the original publication in this journal is cited, in accordance with accepted academic practice. No use, distribution or reproduction is permitted which does not comply with these terms.

Frontiers in Immunology

Explores novel approaches and diagnoses to treat immune disorders.

The official journal of the International Union of Immunological Societies (IUIS) and the most cited in its field, leading the way for research across basic, translational and clinical immunology.

Discover the latest Research Topics

See more →

Frontiers

Avenue du Tribunal-Fédéral 34
1005 Lausanne, Switzerland
frontiersin.org

Contact us

+41 (0)21 510 17 00
frontiersin.org/about/contact